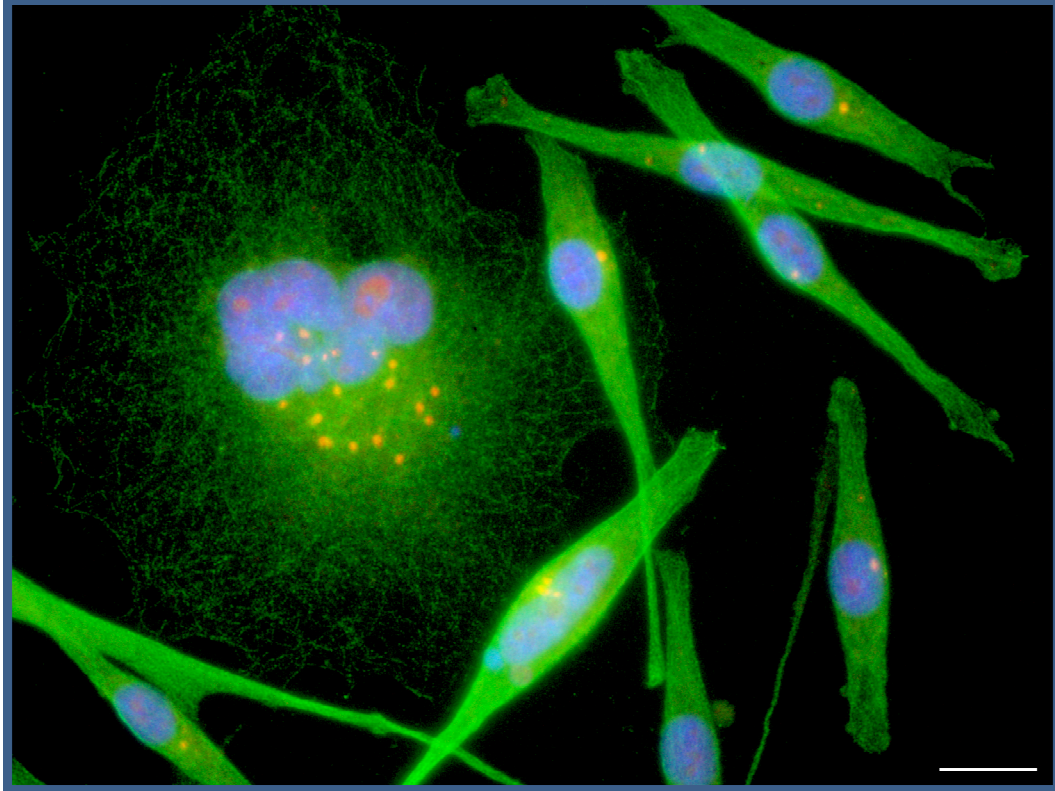


# **Human metastatic melanoma in vitro**



### *Constellation*

This fluorescence microscope image demonstrates that centrosomes (orange), which play a critical role in maintaining the integrity of the genome, are not always correctly regulated in human melanoma. Each cell should contain either one, or two, yet here is a cell with four, and another with at least seventeen.

Loss of regulation of centrosome number causes instability in the inheritance of genes as cells divide. Although many cells that result may have so many flaws that they never divide again, or may even simply die, some may survive. Among these may be some that grow faster than before, no longer need signals from other cells in order to divide, or no longer respond to signals that tell them not to. They may begin to send out their own signals that will promote the growth of blood vessels to supply nutrients, the process of angiogenesis, or they may even launch themselves into circulation to form a tumour at a distant site, the process of metastasis. Very importantly, the changes that occur may have given them ways to evade entire classes of therapeutic drugs, contributing to the difficulties encountered in treating metastatic melanoma. Understanding how the process of centrosome regulation works, and how it fails, may lead to new therapies for melanoma.

The cells illustrated here, NZM2, were derived from material donated by a New Zealand melanoma patient to the Auckland Cancer Society Research Centre for research purposes. DNA is shown in blue,  $\alpha$ -tubulin in green, and pericentrin, a marker of centrosomes, in red. The scale bar represents a length of 20  $\mu\text{m}$ . This image received the Biomedical Imaging Research Unit's award for the best light microscopy image of 2006, and the trophy for the best image overall.

# **Human metastatic melanoma in vitro:**

**Ploidy**

**Centrosomal integrity**

**Serum dependency**

**Chromosome 9p21 genetic status**

**Tumour-suppressor expression**

*Third Edition (amended)*

*A thesis submitted in partial fulfilment of the requirements for the degree of  
Doctor of Philosophy*

*Geoffrey A. Charters*

*The University of Auckland, New Zealand  
2007*



---

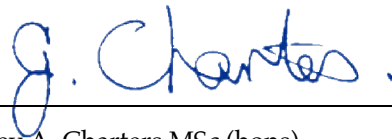
# Candidate's attestation

---

**In satisfaction of clause 6(c) of the University of Auckland Statute for the Degree of Doctor of Philosophy (PhD):**

I, Geoffrey Alan Charters, attest that:

- the work contained herein, except where otherwise specifically attributed, is my own;
- neither this work, nor any part of it, has been submitted or accepted for any other Degree or Diploma.



---

Geoffrey A. Charters MSc (hons)

Doctoral Candidate

The Auckland Cancer Society Research Centre



---

# Dedication

---

This work is dedicated to the memory of those who have fought and lost,  
to the courage of those who are still fighting, and  
to the strength of those who must look on.

Susan Byrne

John L. Charters

Ruth Charters

Joyce Ewen

Terry Housby

Suellen McIlroy

Janet Waters

Alan Anderson

Lex Anderson

Wendy Davis

Betty Charters

Helen Charters

Judith Mollot

---

# Acknowledgements

---

The author acknowledges and thanks the following for their assistance:

- Financial support: The Auckland Division of the Cancer Society of New Zealand Inc.  
The Department of Molecular Medicine and Pathology
- Supervision: Prof. Bruce Baguley, Assoc. Prof. Andrew Shelling, and Dr Graeme Finlay
- NZM cell-lines: Mrs Elaine Marshall
- Technical support: Ms Pamela Turner, Ms Cynthia van Ee, Mr Wayne Joseph, and Jacqueline Ross (BIRU)
- Administrative support: Ellen Semb, Mary Spellman, and Leigh-Anne Wadley
- Resource donation: Bristol-Myers Squibb: for the generous gift of paclitaxel  
Kodak (NZ) Ltd: for the gift of a gelatin filter
- Statistical consultancy: Dr Steve J. Black
- Information services: The staffs of the Philson and Biological Sciences libraries at the University of Auckland  
The National Institutes of Health, The United States of America
- Software support: *www.mvps.org*
- Use of copyright material: Esther Biconvy, Dr John Everson, Dr Laura Hale, Dr John Hammer, and Dr Art Huntley {See 'Trademarks, copyright, and intellectual property provisions', below}.

The publishers of journals who have demonstrated a willingness to support the scientific community by making freely available online full-text versions of published material, among others, the journals: *American Journal of Pathology, Biochemical Journal, Blood, Cancer Research, Cell Growth and Differentiation, Current Biology (for a time), Development, EMBO Journal, European Journal of Biochemistry, FASEB Journal, Genes and Development, Human Mutation, Journal of Biological Chemistry, Journal of Cell Science, Journal of General Virology, Journal of Virology, Laboratory Investigation, Molecular and Cellular Biology, Neurosignals, Proceedings of the National Academy of Sciences of the USA, and Progress in Cell Cycle Research.*



---

# Abstract

---

Metastatic melanoma cells frequently have flaws in the proliferative control mediated by the retinoblastoma-associated protein (pRB), normally operative at the G<sub>1</sub>-S cell-cycle phase transition. Functional and molecular aspects of this were investigated in seventeen human metastatic melanoma cell-lines (NZMs).

Flow-cytometry revealed aneuploidy and heteroploidy in many NZMs that were unstable over time. This plasticity may contribute to melanoma's therapeutic resistance. A potential cause of this, dysregulation of centrosomal numerical control, was demonstrated by immunofluorescence microscopy, apparently for the first time in melanoma cell-lines.

Pericentrin was found to accumulate in nucleolar reservoirs, previously unreported, and release from these on nuclear envelope breakdown may trigger mitotic spindle formation. Dysregulation of pericentrin may be particularly important in melanoma, and could represent a therapeutic target.

To test the integrity of pRB-mediated proliferative regulation, NZM cells were grown under conditions of serum deprivation that in normal cells would cause arrest via pRB. Cell-cycle phase analysis revealed three classes of response: accumulation in G<sub>1</sub>, accumulation in G<sub>2</sub> or mitosis, or stimulation to enter S phase. G<sub>1</sub> arrest indicates that proliferative regulation in response to serum deprivation may be normal in some melanomas, implying that the pRB subsystem may not be the sole regulator of this, or that it is not defective in all melanomas.

Using PCR deletion analysis, an investigation was undertaken into the integrity of the tandem 9p21 *CDKN2A* and *CDKN2B* genes that encode tumour-suppressors implicated in melanoma tumorigenesis. Homozygous deletions affecting only *CDKN2A* were found in two cell-lines, and affecting both genes in six. In the case of NZM7, where different sub-clones exist, heterogeneity was found by microsatellite analysis. DNA sequencing revealed a known *CDKN2A* G500C polymorphism in the NZM7 group, also heterogeneous among sub-clones. A *CDKN2B* G411A polymorphism was found in NZM14, but it is predicted not to affect the amino acid sequence of the encoded protein.

Protein analysis revealed that all NZMs express pRB, but in some, this was in the inhibitory unphosphorylated state, despite their being proliferative. This correlated with strong p16 expression and known *BRAF* mutations, suggesting that proliferation of *BRAF* mutants may require compromised function of the pRB subsystem.



---

# Contents

---

---

## Prologue

---

Candidate's attestation.....	v
Dedication.....	vii
Acknowledgements .....	viii
Abstract.....	ix
Contents.....	xi
Figures.....	xiii
Equations.....	xvii
Tables.....	xvii
Abbreviations and symbols.....	xix
Gene and protein nomenclature .....	xxi
Preface to the third edition (V3).....	xxxiii
Preface.....	xxxvii

---

## Basis

---

1 .....	Melanoma
2 .....	Melanocyte biology
3 .....	The NZM cell-lines
4 .....	Experimental rationale and strategy

---

## Thesis

---

5 .....	Ploidy
6 .....	Centrosomal integrity
7 .....	The effect of serum-deprivation
8 .....	9p21 status
9 .....	Tumour-suppressor expression

---

## Synthesis

---

10 .....	Summary of experimental results
11.....	Conclusion

---

---

## Technical appendices

---

A.....	Methodological foundations
B.....	Methodology
C.....	Solutions
D.....	PCR primers
E.....	Apparatus, materials, and suppliers

---

---

## Reviews and supplementary material

---

F.....	Cancer
G.....	Immunodeficiency and cancer
H.....	The pRB subsystem
I.....	BRCA1 super-complexes
J.....	Genome partitioning
K.....	DNA replication licensing
L.....	Synchronisation of cytokinesis
M.....	The autocrine effect

---

---

## References and bibliography

---

---

# Figures

---

---

## Prologue

---

Figure i.....	Post-submission timeline
Figure ii.....	Diagrammatic symbology

---

## Basis

---

Figure 1-1 .....	Melanoma lesion
Figure 2-1 .....	Cross-section of the epidermis
Figure 2-2 .....	Stem cell factor signal transduction
Figure 2-3 .....	G-protein-coupled receptor signal transduction
Figure 2-4 .....	MITF influences net proliferation via TBX2
Figure 2-5 .....	Biosynthesis of melanin
Figure 2-6 .....	Melanosome distribution
Figure 3-1 .....	NZM cell-lines studied as imaged by phase contrast microscopy

---

## Thesis

---

Figure 5-1 .....	Region placement
Figure 5-2 .....	Melanoma cell-line DNA profiles
Figure 5-3 .....	Ploidy correlation
Figure 5-4 .....	NZM10 population components
Figure 5-5 .....	The core centrosome regulation network
Figure 5-6 .....	Effect of paclitaxel on NZM10 cell-cycle phase distribution
Figure 5-7 .....	Melanoma cell-line DNA profiles (V3)
Figure 6-1 .....	Examples of normal mitotic phases
Figure 6-2 .....	Examples of slightly abnormal mitotic cells
Figure 6-3 .....	Examples of grossly abnormal mitotic cells
Figure 6-4 .....	Centrosome morphology class examples
Figure 6-5 .....	Pericentrin labelling class examples
Figure 6-6 .....	Symmetry class examples
Figure 6-7 .....	Null image
Figure 6-8 .....	Immunofluorescent labelling control results
Figure 6-9 .....	Positive labelling control composite image
Figure 6-10 .....	Effects of cytospinning
Figure 6-11 .....	Irregular centrosome structure
Figure 6-12 .....	Extended pericentrin in NZM9
Figure 6-13 .....	Polar pericentrin structures
Figure 6-14 .....	NZM13 pericentrin and $\alpha$ -tubulin detail
Figure 6-15 .....	Cooperative and bystander centrosomes
Figure 6-16 .....	Representative hypodicentrosomal mitotic cells
Figure 6-17 .....	NZM5 prometaphases
Figure 6-18 .....	NZM5 [c] pericentrin
Figure 6-19 .....	Normal mitoses
Figure 6-20 .....	Chromosomal bridges in dicentrosomal cells
Figure 6-21 .....	Remaining grossly abnormal dicentrosomal cells

---

---

Figure 6–22 .....	Tricentrosomal NZM2 prophase
Figure 6–23 .....	Tricentrosomal NZM2 anaphase
Figure 6–24 .....	Lagging chromosome
Figure 6–25 .....	Tricentrosomal NZM2 prometaphase
Figure 6–26 .....	Tetracentrosomal tetrahedral metaphases
Figure 6–27 .....	Quadripolar NZM6 telophase
Figure 6–28 .....	Tetracentrosomal tripolar mitoses
Figure 6–29 .....	Tetracentrosomal quasibipolar mitoses
Figure 6–30 .....	Representative polycentrosomal mitoses
Figure 6–31 .....	Polycentrosomal ternary telophases
Figure 6–32 .....	Mitotic pericentrin elevation
Figure 6–33 .....	Nucleolar pericentrin reservoirs in NZM9 cells
Figure 6–34 .....	Confocal imagery of nucleolar pericentrin in NZM2 cells
Figure 6–35 .....	$\alpha$ -tubulin nests in NZM1 cells
Figure 6–36 .....	$\alpha$ -tubulin-negative NZM2 cell
Figure 6–37 .....	Asynchronous mitoses in bi- and tri-nuclear cells
Figure 6–38 .....	Asynchronous apoptosis in NZM10 nuclei?
Figure 6–39 .....	Tubulin void in NZM1
Figure 6–40 .....	Giant NZM10 cells
Figure 6–41 .....	Anomalous nucleic acid bodies
Figure 6–42 .....	Colour reassignment example
Figure 6–43 .....	Fluorescence ratio test image
Figure 6–44 .....	Green:blue Hoechst fluorescence ratio for nuclear and ANAB labelling
Figure 6–45 .....	ANAB confocal imagery
Figure 6–46 .....	Apoptotic NZM10 cells
Figure 6–47 .....	NZM10 nuclei
Figure 6–48 .....	Ternary cytokinesis in NZM12
Figure 7–1 .....	Effect of serum-deprivation on TLM1 cells
Figure 7–2 .....	Key to interpretation of graphs for serum-deprivation results
Figure 7–3 .....	Serum-deprivation results
Figure 7–4 .....	Spontaneous cell-cycle phase redistribution in control cultures
Figure 7–5 .....	IPR as a function of time
Figure 7–6 .....	Rate of IPR decrease vs initial rate
Figure 7–7 .....	IPR vs cell-cycle phase contribution
Figure 7–8 .....	Distribution of Q
Figure 7–9 .....	Effect of serum-deprivation on cell-cycle phasing
Figure 7–10 .....	Results for NZM2 replication
Figure 7–11.....	Results for NZM12 replication
Figure 7–12 .....	NZM12 growth curve
Figure 7–13 .....	Results for NZM6 replication
Figure 7–14 .....	NZM6 growth curve
Figure 7–15 .....	NZM6 serum-deprived growth concordance
Figure 7–16 .....	NZM6 serum-deprived growth concordance (scaled)

---

Figure 7–17 .....	NZM6 serum-deprived phasing concordance
Figure 7–18 .....	NZM12 serum deprivation results comparison
Figure 7–19 .....	NZM2 serum deprivation results comparison
Figure 7–20 .....	NZM6 serum deprivation results comparison
Figure 8–1 .....	The <i>CDKN2A/B</i> locus and its encoded proteins
Figure 8–2 .....	9p12–9p23 PCR results
Figure 8–3 .....	Silver-stained SSCP gels
Figure 8–4 .....	DNA sequences corresponding to the <i>CDKN2A</i> 3' UTR of NZM7.2 and NZM7.4
Figure 8–5 .....	DNA sequence from <i>CDKN2A</i> exon 2 of NZM12
Figure 8–6 .....	NZM14 <i>CDKN2B</i> exon 2 sequence variation
Figure 8–7 .....	NZM7.2/7.4 <i>CDKN2A</i> 3' UTR sequence variations
Figure 8–8 .....	NZM12 <i>CDKN2A</i> exon 2 sequence variations
Figure 8–9 .....	NZM14 <i>CDKN2B</i> exon 2 sequence variation
Figure 8–10 .....	V2 figure for DNA sequence from <i>CDKN2A</i> exon 2 of NZM12
Figure 8–11 .....	Quantitative real-time PCR results for <i>CDKN2A</i> and <i>CDKN2B</i>
Figure 8–12 .....	Initial V3 genomic DNA extracts
Figure 8–13 .....	Discord between fluorometric and spectrophotometric assessment of DNA
Figure 8–14 .....	RNase A treatment
Figure 8–15 .....	RNase treatment variations
Figure 8–16 .....	DNase-free RNase treatment of NZM genomic DNA extracts
Figure 8–17 .....	Detecting heterogeneity
Figure 8–18 .....	NZM5 DNA pellet
Figure 8–19 .....	Amplification of <i>HBB</i>
Figure 8–20 .....	NZM5 PCR target trials
Figure 8–21 .....	NZM5 nuclease test
Figure 8–22 .....	NZM5 short time in culture DNA
Figure 8–23 .....	NZM5 inhibitor test
Figure 8–24 .....	NZM5 BSA gradient
Figure 8–25 .....	NZM panel with BSA
Figure 8–26 .....	Fargnoli primer hairpin
Figure 8–27 .....	<i>CDKN2A</i> exon 2 non-specificity
Figure 8–28 .....	Non-specific product from 12q
Figure 8–29 .....	<i>CDKN2A</i> exon 2 specificity
Figure 8–30 .....	Standardised genomic DNA used in experimentation
Figure 8–31 .....	9p12–9p23 PCR results (V3)
Figure 8–32 .....	Genotyping examples (D9S974)
Figure 8–33 .....	<i>CDKN2A</i> exon 3 heterozygosity
Figure 8–34 .....	<i>CDKN2B</i> exon 2 G411A transition in NZM14
Figure 9–1 .....	Western analysis of pRB expression by NZM cell-lines
Figure 9–2 .....	Western analysis of p15 expression by NZM cell-lines
Figure 9–3 .....	Western analysis of p16 expression by NZM cell-lines
Figure 9–4 .....	Effect of genomic demethylation on p16 expression
Figure 9–5 .....	Western analysis of ARF expression by NZM cell-lines

---

Figure 9–6 .....	Trial pRB Western blot
Figure 9–7 .....	Untrimmed V1 pRB Western blot
Figure 9–8 .....	GAPDH Western blot
Figure 9–9 .....	Representative Ponceau S stained membranes as used in pRB Western blots
Figure 9–10 .....	Ponceau S stained membranes used in p16 Western blots
Figure 9–11.....	pRB Western blots
Figure 9–12 .....	p16 Western blots

---

### Technical appendices

Figure A–1 .....	Example histogram plot
Figure A–2 .....	Example density plot
Figure A–3 .....	Singlet selection
Figure B–1.....	ANABs
Figure B–2.....	Colour reassignment process
Figure B–3.....	Colour reassigned Figure 6–41
Figure B–4.....	Image registration using difference blending
Figure B–5.....	Z-projection of images

---

### Reviews and supplementary material

Figure H–1 .....	Salient pRB features
Figure H–2 .....	The pRB small A/B pocket
Figure I–1.....	Model for DNA mismatch repair initiation
Figure I–2.....	Replication factor C interactions
Figure J–1 .....	Centrosome structure
Figure J–2.....	The centrosome in interphase
Figure J–3.....	The centrosome at S-phase entry
Figure J–4.....	Centriole component delivery
Figure J–5.....	Centrosomal regulatory phosphorylations
Figure J–6.....	Centrosomes in G <sub>2</sub>
Figure J–7.....	Generation of inter-centrosome force
Figure J–8.....	Centrosome separation
Figure J–9.....	Centriole peregrination
Figure J–10.....	CDK2 phosphorylation states
Figure J–11.....	Complex of cyclin-A, CDK2, and p27
Figure J–12.....	Mechanism of CDK2 inhibition by p27
Figure J–13.....	p27 function and degradations
Figure J–14.....	Activation and effect of p53 pertaining to centrosome regulation
Figure K–1 .....	Enabling DNA replication at anaphase
Figure K–2 .....	Disabling DNA replication at G <sub>1</sub> –S
Figure L–1 .....	Initiation of cytokinesis
Figure M–1 .....	Anti-proliferative reflexive effect
Figure M–2 .....	Theoretical growth rate deviation due to a reflexive anti-proliferative effect
Figure M–3 .....	Measured deviation from exponential growth in exemplar NZM cell-lines

---



---

---

# Equations

---

Equation 7-1 .....	Derivation of retardation quotient (Q)
Equation M-1 .....	Independent growth
Equation M-2 .....	Theoretical growth with reflexive influence

---

---

# Tables

---

---

## Prologue

---

Table i .....	Abbreviations and symbols
Table ii .....	Symbols for human genes
Table iii .....	Generic gene and protein symbols
Table iv .....	Copyright material used in this document

---

## Basis

---

Table 1-1 .....	Clark's melanoma stages
Table 1-2 .....	Staging by Breslow thickness
Table 1-3 .....	AJCC melanoma staging
Table 2-1 .....	Melanocyte cytokines
Table 2-2 .....	Genes implicated in melanomagenesis
Table 3-1 .....	ACSRC metastatic melanoma cell-lines studied

---

## Thesis

---

Table 5-1 .....	Melanoma cell-line DNA ploidy
Table 5-2 .....	Centrosome abnormalities in cancer
Table 5-3 .....	Centrosomal regulators implicated in the aetiology of melanoma
Table 5-4 .....	Melanoma cell-line DNA ploidy (V3)
Table 5-5 .....	Ploidy analyses of cutaneous melanoma tumours
Table 6-1 .....	Immunofluorescent labelling controls
Table 6-2 .....	Fluorescence microscope filter blocks used
Table 6-3 .....	Mitotic survey results
Table 6-4 .....	Statistical analysis of mitotic survey results
Table 6-5 .....	Tricentrosomal survey results
Table 7-1 .....	Proliferation rates with and without serum
Table 7-2 .....	Serum-deprivation response types
Table 7-3 .....	Serum-deprivation experimental series parameters
Table 8-1 .....	Deletion map of 9p12-9p23 region based on PCR
Table 8-2 .....	V3 PCR primers and conditions
Table 8-3 .....	Deletion map of 9p12-9p23 region based on PCR (V3)
Table 8-4 .....	Microsatellite allele grouping
Table 8-5 .....	NZM 9p12-9p23 microsatellite allelotypes
Table 8-6 .....	NZM 9p12-9p23 microsatellite allelotype groupings
Table 9-1 .....	Microsatellite allelotype for putative SAOS-2 cell-line

---

---

## Synthesis

---

Table 10-1 .....	Summary of experimental results
Table 10-2 .....	Summary of experimental results (V3)

---

## Technical appendices

---

Table D-1 .....	PCR primers, products, and references
Table E-1 .....	Apparatus
Table E-2 .....	Commercial kits
Table E-3 .....	Antibodies
Table E-4 .....	Enzymes
Table E-5 .....	Standards
Table E-6 .....	General reagents
Table E-7 .....	Sundries
Table E-8 .....	Supplier data
Table E-9 .....	Software
Table E-10 .....	Additional apparatus (V3)
Table E-11 .....	Additional commercial kits (V3)
Table E-12 .....	Additional antibodies (V3)
Table E-13 .....	Additional enzyme (V3)
Table E-14 .....	Additional standards (V3)
Table E-15 .....	Additional general reagents (V3)
Table E-16 .....	Additional sundries (V3)
Table E-17 .....	Additional supplier data (V3)
Table E-18 .....	Additional software (V3)

---

## Reviews and supplementary material

---

Table F-1 .....	Cancer incidence and survival rates in the USA (1950-1997/8)
Table F-2 .....	Cancer mortality rates in the USA (1950-1998)
Table F-3 .....	Hereditary conditions that predispose toward cancer
Table G-1 .....	Genes implicated in hereditary immunodeficiency
Table G-2 .....	Cancer risks associated with therapeutic immunosuppressive agents
Table H-1 .....	pRB protein sequence conservation
Table H-2 .....	Human proteins similar to pRB
Table H-3 .....	Selected pRB-interacting proteins
Table H-4 .....	Competition matrix for pRB binding
Table H-5 .....	pRB phosphorylation summary
Table I-1 .....	Diseases associated with failure of BASC components
Table J-1 .....	Proteins implicated in centrosomal regulation
Table J-2 .....	Conservation of CDK regulatory phosphorylation sites

---

# Abbreviations and symbols

5aza-dC	5-aza-2'-deoxycytidine
6-FAM	6-carboxyfluorescein
$\alpha$ MEM	Alpha minimal essential medium
ABC	Avidin-biotinylated-HRP conjugate
AC	Adenylyl cyclase
ACSRC	Auckland Cancer Society Research Centre
AHB	Alanylhydroxybenzothiazine
AJCC	American Joint Committee on Cancer
ALM	Acral lentiginous melanoma
ANABs	Anomalous nucleic acid bodies
APS	Ammonium persulphate
AT	Ataxia telangiectasia
BASC	BRCA1-associated genome surveillance complex
BCC	Basal cell carcinoma
BCL	B-cell lymphoma
BrdU	5-bromo-2'-deoxyuridine
BS	Bloom's syndrome
BSA	Bovine serum albumin
CDK(s)	Cyclin-dependent kinase(s)
cDNA	Complementary deoxyribonucleic acid (DNA)
CKI(s)	CDK inhibitor(s)
CRE	cAMP response element
CVID	Common variable immune deficiency
DAG	Diacylglyceride
DAPI	4',6-Diamidino-2-phenylindole
DHI	5,6-dihydroxyindole
DHICA	5,6-dihydroxyindole-2-carboxylic acid
DMSO	Dimethylsulphoxide
DNA	Deoxyribonucleic acid
DNase(s)	Deoxyribonuclease(s)
DOPA	3,4-dihydroxyphenylalanine
ECL	Enhanced chemiluminescence
EDTA	Ethylenediaminetetraacetic acid
EGTA	Ethylene glycol-bis(2-aminoethyl ether)-N,N,N',N'-tetraacetic acid
ER	Endoplasmic reticulum
FA	Fanconi anaemia
FCS	Fetal calf serum
FISH	Fluorescence in situ hybridisation
FL2	Detector in a flow cytometer for red-orange fluorescence (often used for DNA detection)
FL2-A	FL2 signal integral
FL2-W	FL2 signal event duration, alias width
FSC	Forward light scatter; a detector for this in a flow cytometer
GPCR	G-protein-coupled receptor
HIV	Human immunodeficiency virus
HNPCC	Hereditary non-polyposis colorectal cancer
HPV	Human papillomavirus
HRP	Horseradish peroxidase
IBP	Inhibin binding protein
IF	Intermediate filament
IP <sub>3</sub>	Inositol-1,4,5-triphosphate
IPR	Instantaneous proliferation rate
IQ	5,6-indolequinone
IQCA	5,6-indolequinone-2-carboxylic acid
KS	Kaposi's sarcoma
LFS	Li-Fraumeni syndrome
LMM	Lentigo maligna melanoma
LOH	Loss of heterozygosity
MCM	Mini-chromosome maintenance (used for elements of the DNA licensing complex)
MMR	DNA mismatch repair
mRNA	Messenger ribonucleic acid (RNA)
NBS	Nijmegen breakage syndrome
NEB	Nuclear envelope breakdown
NGF	Nerve growth factor (referring to the hexameric holoprotein)
NHL	Non-Hodgkin's lymphoma
NIH	National Institutes of Health (USA)
NK	Natural killer cell(s)

**Table i: Abbreviations and symbols (continues overleaf)**

---

NLS	Nuclear localisation signal
NM	Nodular melanoma
NZM	NZ melanoma cell-line
ORC	Origin recognition complex
PBL(s)	Peripheral blood leukocytes (human)
PCR	Polymerase chain reaction
PDF	Portable document format
PI	Propidium iodide
PIPES	Piperazine-N,N'-bis(2-ethanesulfonic acid)
PKA	The protein kinase A holoenzyme
PNG	Portable Network Graphic
PP1	Type I protein phosphatase complex
PVDF	Polyvinylidene fluoride
Q	Retardation quotient
qPCR	Quantitative real-time polymerase chain reaction (PCR)
qRTPCR	Quantitative real-time reverse-transcriptase PCR (RTPCR)
R	Proliferation rate, the reciprocal of tD
RFC	Replication factor C (referring to the heteropentamer)
RTK	Receptor tyrosine kinase
RNA	Ribonucleic acid
RNase(s)	Ribonuclease(s)
RTPCR	Reverse-transcriptase PCR
SCC	Squamous cell carcinoma
SCFC	SKP1-cullin-F-box complex
SCID	Severe combined immunodeficiency
SNP	Single nucleotide polymorphism
SSC	Sideways light scatter; a detector for this in a flow cytometer
SSCP	Single-strand conformation polymorphism
SSM	Superficial spreading melanoma
Ta	Annealing temperature
tD	Doubling time of a population of cells, the reciprocal of R
TD-PCR	Touch-down PCR
TEMED	1,2-bis(dimethylamino)ethane
TGN	Trans-Golgi network
Tris	Tris(hydroxymethyl)aminomethane
UTR	Untranslated region of messenger ribonucleic acid (mRNA), or the corresponding genomic sequence
UV	Ultraviolet
UVR	Ultraviolet radiation
WAS	Wiskott-Aldrich syndrome
XLA	X-linked agammaglobulinaemia
§	Data from a non-human model, generality uncertain
®	Reference thus tagged is a review article

**Table i (concluded): Abbreviations and symbols**

# Gene and protein nomenclature

Wherever possible, the symbol recommended in the HUGO Nomenclature Database<sup>554</sup> has been used.

Where a symbol for a protein has been used in the text that differs from its gene symbol to the extent that it would be unlikely to be found by inspection, the protein symbol is listed with a cross-reference to the gene.

Symbol	Full name	Locus	Protein name(s)
14-3-3 $\gamma$	See <i>YWHAG</i>		
$\alpha$ -MSH	See <i>POMC</i>		
<i>AATF</i>	Apoptosis antagonising transcription factor	17q11.2–q12	← (alias CHE-1, DED)
<i>ABL1</i>	v-abl Abelson murine leukaemia viral oncogene homologue 1	9q34.1	ABL(-x) Multiple isoforms
<i>ACTB</i>	Actin, beta	7p15–p12	$\beta$ -actin
<i>ACTH</i>	See <i>POMC</i>		
<i>ADA</i>	Adenosine deaminase	20q12–q13.11	←
<i>ADPRT</i>	ADP-ribosyltransferase (NAD <sup>+</sup> ; poly (ADP-ribose) polymerase)	1q41–q42	PARP
<i>AHR</i>	Aryl hydrocarbon receptor	7p15	←
<i>AKAP9</i>	A kinase (PRKA) anchor protein (yotiao) 9	7q21–q22	←
<i>AKT1</i>	v-akt murine thymoma viral oncogene homologue 1	14q32.32	←
<i>AP-2</i>	See <i>TFAP2A</i>		
<i>APC</i>	Adenomatosis polyposis coli	5q21–q22	←
<i>AR</i>	Androgen receptor (dihydrotestosterone receptor; testicular feminisation; spinal and bulbar muscular atrophy; Kennedy disease)	Xq11.2–q12	←
<i>ARF</i>	See <i>CDKN2A</i>		
<i>ARHA</i>	Ras homologue gene family, member A	3p21.3	rhoA
<i>ARID3B</i>	Dead ringer ( <i>Drosophila</i> )-like 2 (bright and dead ringer)	15q24	← (alias Bdp, DRIL2)
<i>ASIP</i>	Agouti (mouse)-signalling protein	20q11.2–q12	←
<i>ASK</i>	See <i>DBF4</i>		
<i>ATF2</i>	Activating transcription factor 2	2q32	←
<i>ATM</i>	Ataxia telangiectasia mutated	11q22–q23	←
<i>ATR</i>	Ataxia telangiectasia and Rad3 related	3q22–q24	←
$\beta$ -actin	See <i>ACTB</i>		
$\beta$ -catenin	See <i>CTNNB1</i>		
$\beta$ -globin	See <i>HBB</i>		
<i>B2M</i>	Beta-2-microglobulin	15q21–q22.2	$\beta$ 2-microglobulin
<i>BAD</i>	BCL2-antagonist of cell death	11	←
<i>BAX</i>	BCL2-associated X protein	19q13.3–q13.4	←
<i>BCL2</i>	B-cell CLL/lymphoma 2	18q21.3	←
<i>BCL2L1</i>	BCL2-like 1	20q11.1	BCL-XL BCL-XS
<i>BCR</i>	Breakpoint cluster region	22q11	←
<i>BIRC5</i>	Baculoviral IAP repeat-containing 5 (survivin)	17q25	survivin
<i>BLM</i>	Bloom syndrome (alias <i>REQL3</i> )	15q26.1	←
<i>BMP2</i>	Bone morphogenetic protein 2	20p12	←
<i>BRAF</i>	v-raf murine sarcoma viral oncogene homolog B1	7q34	B-RAF
<i>BRCA1</i>	Breast cancer 1, early onset	17q21–q24	←
<i>BRCA2</i>	Breast cancer 2, early onset	13q12.3	←
<i>BTK</i>	Bruton agammaglobulinaemia tyrosine kinase	Xq21.33–q22	←
<i>C3</i>	Complement component 3	19p13.3–p13.2	←
<i>C4A</i>	Complement component 4A	6p21.3	←
<i>C4B</i>	Complement component 4B	6p21.3	←
<i>C5R1</i>	Complement component 5 receptor 1 (C5a ligand)	19q13.3–q13.4	←
<i>CASP3</i>	Caspase 3, apoptosis-related cysteine protease	4q34	←
<i>CASP8</i>	Caspase 8, apoptosis-related cysteine protease	2q33–q34	←
<i>CBP</i>	See <i>CREBBP</i>		
<i>CCNA1</i>	Cyclin A1	13q12.3–q13	Cyclin-A1
<i>CCNA2</i>	Cyclin A2	4q25–q31	Cyclin-A2
<i>CCNB1</i>	Cyclin B1	5q12	Cyclin-B1

Table ii: Symbols for human genes (continues overleaf)

Symbol	Full name	Locus	Protein name(s)
<b>CCND1</b>	Cyclin D1	11q13	Cyclin-D1
<b>CCND2</b>	Cyclin D2	12p13	Cyclin-D2
<b>CCND3</b>	Cyclin D3	6p21	Cyclin-D3
<b>CCNE1</b>	Cyclin E1	19q12	Cyclin-E1
<b>CCNE2</b>	Cyclin E2	8p22	Cyclin-E2
<b>CD14</b>	CD14 antigen	5q31.1	←
<b>CD19</b>	CD19 antigen	16p11.2	←
<b>CD2</b>	CD2 antigen (p50), sheep red blood cell receptor	1p13	←
<b>CD28</b>	CD28 antigen (Tp44)	2q33	←
<b>CD3E</b>	CD3E antigen, epsilon polypeptide (TiT3 complex)	11q23	CD3ε
<b>CD4</b>	CD4 antigen (p55)	12pter-p12	←
<b>CD5</b>	CD5 antigen (p56-62)	11q13	←
<b>CD74</b>	CD74 antigen (invariant polypeptide of major histocompatibility complex, class II antigen-associated)	5q32	←
<b>CD80</b>	CD80 antigen (CD28 antigen ligand 1, B7-1 antigen)	3q13.3-q21	← (alias B7-1)
<b>CD8A</b>	CD8 antigen, alpha polypeptide (p32)	2p12	←
<b>CD8B1</b>	CD8 antigen, beta polypeptide 1 (p37)	2p12	←
<b>CDC16</b>	Cell division cycle 16 homologue ( <i>Saccharomyces cerevisiae</i> )	13q34	←
<b>CDC2</b>	Cell division cycle 2, G <sub>1</sub> to S and G <sub>2</sub> to M	10q21.1	← (alias CDK1)
<b>CDC20</b>	Cell division cycle 20 homologue ( <i>Saccharomyces cerevisiae</i> )	1p34.1	←
<b>CDC25A</b>	Cell division cycle 25A	3p21	←
<b>CDC25B</b>	Cell division cycle 25B	20p13	←
<b>CDC25C</b>	Cell division cycle 25C	5q31	←
<b>CDC27</b>	Cell division cycle 27	17q12-17q23.2	←
<b>CDC2L1</b>	Cell division cycle 2-like 1 (PITSLRE proteins)	1p36	←
<b>CDC34</b>	Cell division cycle 34	19p13.3	← (alias UBC3)
<b>CDC42</b>	Cell division cycle 42 (GTP binding protein, 25kD)	1p36.1	←
<b>CDC6</b>	CDC6 (cell division cycle 6, <i>Saccharomyces cerevisiae</i> ) homologue	17q21.3	←
<b>CDC7L1</b>	CDC7 (cell division cycle 7, <i>Saccharomyces cerevisiae</i> , homologue)-like 1	1p22	←
<b>CDH1</b>	Cadherin 1, type 1, E-cadherin (epithelial)	16q22.1	E-cadherin
<b>CDH13</b>	Cadherin, type 13, H-cadherin (heart)	16q24.2	H-cadherin
<b>CDH3</b>	Cadherin 3, type 1, P-cadherin (placental)	16q22.1	P-cadherin
<b>CDK2</b>	Cyclin-dependent kinase 2	12q13	←
<b>CDK4</b>	Cyclin-dependent kinase 4	12q13	←
<b>CDK5R1</b>	Cyclin-dependent kinase 5, regulatory subunit 1 (p35)	17q11.2	← Multiple isoforms
<b>CDK6</b>	Cyclin-dependent kinase 6	7q21-q22	←
<b>CDKN1A</b>	Cyclin-dependent kinase inhibitor 1A (alias <i>CIP1</i> , <i>SDI1</i> , <i>WAF1</i> )	6p21.1	p21
<b>CDKN1B</b>	Cyclin-dependent kinase inhibitor 1B (alias <i>KIP1</i> )	12p13.1-p12	p27
<b>CDKN1C</b>	Cyclin-dependent kinase inhibitor 1C (p57, Kip2)	11p15.5	p57
<b>CDKN2A</b>	Cyclin-dependent kinase inhibitor 2A (alias <i>INK4A</i> )	9p21	p16 ARF
<b>CDKN2B</b>	Cyclin-dependent kinase inhibitor 2B (alias <i>INK4B</i> )	9p21	p15
<b>CDKN2C</b>	Cyclin-dependent kinase inhibitor 2C (p18, inhibits CDK4)	1p32	p18
<b>CDKN2D</b>	Cyclin-dependent kinase inhibitor 2D (p19, inhibits CDK4)	19p13	p19
<b>CDKN3</b>	Cyclin-dependent kinase inhibitor 3 (CDK2-associated dual specificity phosphatase)	14q22	KAP
<b>CDT1</b>	Chromatin licensing and DNA replication factor 1	16q24	←
<b>CEBPB</b>	CCAAT/enhancer binding protein (C/EBP), beta	20q13.1	C/EBPβ
<b>Centrin</b>	See <i>CETN1</i>		
<b>CETN1</b>	Centrin, EF-hand protein, 1	18p11.32	centrin
<b>CEP2</b>	Centrosomal protein 2	20pter-q12	←
<b>CGA</b>	Glycoprotein hormones, alpha polypeptide	6q12-q21	←
<b>CHEK1</b>	<i>CHK1</i> (checkpoint, <i>Schizosaccharomyces pombe</i> ) homologue (alias <i>CHK1</i> )	11q24	CHK1

Table ii: (continued)

Symbol	Full name	Locus	Protein name(s)
<b>CHEK2</b>	CHK2 (checkpoint, <i>Schizosaccharomyces pombe</i> ) homologue	22q11	CHK2
<b>CHK1</b>	See <i>CHEK1</i>		
<b>CHK2</b>	See <i>CHEK2</i>		
<b>CHS1</b>	Chediak-Higashi syndrome 1	1q42.1–q42.2	← (alias LYST)
<b>CIT</b>	Citron (rho-interacting, serine/threonine kinase 21)	12q	citron
<b>CKS1</b>	CDC28 protein kinase 1	1q21.2	←
<b>CR2</b>	Complement component (3d/Epstein Barr virus) receptor 2	1q32	←
<b>CREBBP</b>	CREB binding protein (Rubinstein-Taybi syndrome)	16p13.3	CBP
<b>CSF2</b>	Colony stimulating factor 2 (granulocyte-macrophage)	5q31.1	GM-CSF
<b>CSF2RB</b>	Colony stimulating factor 2 receptor, beta, low-affinity (granulocyte-macrophage)	22q13.1	←
<b>CSK</b>	c-src tyrosine kinase	15q23–q25	c-src
<b>CTLA4</b>	Cytotoxic T-lymphocyte-associated protein 4	2q33	←
<b>CTNNB1</b>	Catenin (cadherin-associated protein), beta 1 (88kD)	3p21	β-catenin
<b>CTNNBIP1</b>	Catenin, beta interacting protein 1	1pter–p36.31	ICAT
<b>CUL1</b>	Cullin 1	7q34–q35	←
<b>CUL3</b>	Cullin 3	2q37.1	←
<b>DCT</b>	Dopachrome tautomerase (dopachrome delta-isomerase, tyrosine-related protein 2) (alias TYRP2)	13q32	←
<b>DCTN1</b>	Dynactin 1 (p150, glued homologue, <i>Drosophila</i> )	2p13	p150
<b>DDB2</b>	Damage-specific DNA binding protein 2 (48 kD) (alias XPE)	11p12–p11	←
<b>DBF4</b>	DBF4 homolog ( <i>Saccharomyces cerevisiae</i> ) Activator of S phase kinase	7q21.3	ASK
<b>DDEF1</b>	Development and differentiation enhancing factor 1	8q24.1–q24.2	←
<b>DHFR</b>	Dihydrofolate reductase	5q11.2–q13.2	←
<b>DMD</b>	Dystrophin (muscular dystrophy, Duchenne and Becker types)	Xp21.2	Dystrophin
<b>DNA pol-α</b>	See <i>POLA</i>		
<b>DNA pol-δ1</b>	See <i>POLD1</i>		
<b>DNTT</b>	Deoxynucleotidyltransferase, terminal	10q23–q24	TdT
<b>Dystrophin</b>	See <i>DMD</i>		
<b>E-cadherin</b>	See <i>CDH1</i>		
<b>E2F1</b>	E2F transcription factor 1	20q11.2	←
<b>E2F2</b>	E2F transcription factor 2	1p36	←
<b>E2F3</b>	E2F transcription factor 3	6p22	←
<b>E2F4</b>	E2F transcription factor 4, p107/p130-binding	16q21–q22	←
<b>E2F5</b>	E2F transcription factor 5, p130-binding	8p22–q21.3	←
<b>E2F6</b>	E2F transcription factor 6	22q11	←
<b>ECT2</b>	Epithelial cell transforming sequence 2 oncogene	3q26.1–q26.2	←
<b>EDN1</b>	Endothelin 1	6p23–p24	ET1
<b>EDN2</b>	Endothelin 2	1p34	ET2
<b>EDN3</b>	Endothelin 3	20q13.2–q13.3	ET3
<b>EDNRB</b>	Endothelin receptor type B	13q22	←
<b>EG5</b>	See <i>KNSL1</i>		
<b>EGF</b>	Epidermal growth factor (beta-urogastrone)	4q25	←
<b>EGFR</b>	Epidermal growth factor receptor (erythroblastic leukaemia viral (v-erb-b) oncogene homologue, avian)	7p12	←
<b>ELF1</b>	E74-like factor 1 (ets domain transcription factor)	13q13	←
<b>ENC1</b>	Ectodermal-neural cortex (with BTB-like domain)	5q12–q13.3	← (alias NRP/B)
<b>EP300</b>	E1A binding protein p300	22q13.2	p300
<b>ERCC1</b>	Excision repair cross-complementing rodent repair deficiency, complementation group 1 (includes overlapping antisense sequence)	19q13.32	←
<b>ERCC2</b>	Excision repair cross-complementing rodent repair deficiency, complementation group 2 (alias XPD)	19q13.3	←
<b>ERCC3</b>	Excision repair cross-complementing rodent repair deficiency, complementation group 3 (alias XPB)	2q21	←
<b>ERCC4</b>	Excision repair cross-complementing rodent repair deficiency, complementation group 4 (alias XPF)	16p13.3–p13.11	←
<b>ERCC5</b>	Excision repair cross-complementing rodent repair deficiency, complementation group 5 (alias XPG)	13q22–q34	←

Table ii: (continued)

Symbol	Full name	Locus	Protein name(s)
<b>ERCC6</b>	Excision repair cross-complementing rodent repair deficiency, complementation group 6 (alias <i>CSB</i> )	10q11	←
<b>ET1</b>	See <i>EDN1</i>		
<b>ET2</b>	See <i>EDN2</i>		
<b>ET3</b>	See <i>EDN3</i>		
<b>ETS1</b>	v-ets erythroblastosis virus E26 oncogene homologue 1 (avian)	11q23.3	←
<b>F2RL1</b>	Coagulation factor II (thrombin) receptor-like 1	5q13	← (alias <i>PAR2</i> )
<b>FAK</b>	See <i>PTK2</i>		
<b>FANCA</b>	Fanconi anaemia, complementation group A	16q24.3	←
<b>FANCB</b>	Fanconi anaemia, complementation group B	Xp22.2	←
<b>FANCC</b>	Fanconi anaemia, complementation group C	9q22.3	←
<b>FANCD2</b>	Fanconi anaemia, complementation group D2 (alias <i>FANCD</i> )	3p25.3	←
<b>FANCE</b>	Fanconi anaemia, complementation group E	6p21–p22	←
<b>FANCF</b>	Fanconi anaemia, complementation group F	11p15	←
<b>FANCG</b>	Fanconi anaemia, complementation group G (alias <i>XRCC9</i> )	9p13	←
<b>FAS</b>	Tumour necrosis factor receptor super-family, member 6	10q24.1	←
<b>FASLG</b>	Tumour necrosis factor (ligand) super-family, member 6	1q23	FasL
<b>FCER2</b>	Fc fragment of IgE, low affinity II, receptor for (CD23A)	19p13.3	CD23
<b>FCGR2A</b>	Fc fragment of IgG, low affinity IIa, receptor for (CD32)	1q23	←
<b>FCGR2B</b>	Fc fragment of IgG, low affinity IIb, receptor for (CD32)	1q32	←
<b>FCGR3A</b>	Fc fragment of IgG, low affinity IIIa, receptor for (CD16)	1q23	←
<b>FCGR3B</b>	Fc fragment of IgG, low affinity IIIb, receptor for (CD16)	1q23	←
<b>FHIT</b>	Fragile histidine triad gene	3p14.2	←
<b>FLT3</b>	fms-related tyrosine kinase 3	13q12	← (alias <i>FLK-2</i> )
<b>FOS</b>	v-fos FBJ murine osteosarcoma viral oncogene homologue	14q24.3	←
<b>FOXO3A</b>	Forkhead box O3A	6q21	←
<b>FSHB</b>	Follicle stimulating hormone, beta polypeptide	11p13	←
<b>FYN</b>	FYN oncogene related to SRC, FGR, YES	6q21	←
<b>FZR1</b>	Fizzy / cell division cycle 20 related 1 ( <i>Drosophila</i> )	19p13.3	← (alias <i>HCDH1</i> )
<b>GABPB1</b>	GA-binding protein transcription factor, beta subunit 1 (53 kD)	7q11.2	← (alias <i>RBF-1</i> )
<b>GADD45A</b>	Growth arrest and DNA-damage-inducible, alpha	1p34–p12	GADD45 $\alpha$
<b>GADD45B</b>	Growth arrest and DNA-damage-inducible, beta	19p13.3	GADD45 $\beta$
<b>GADD45G</b>	Growth arrest and DNA-damage-inducible, gamma	9q22.1–q22.2	GADD45 $\gamma$
<b>GATA2</b>	GATA binding protein 2	3q21	←
<b>geminin</b>	See <i>GMNN</i>		
<b>GM-CSF</b>	See <i>CSF2</i>		
<b>GMNN</b>	Geminin, DNA replication inhibitor	6pter–p21.32	geminin
<b>GRB2</b>	Growth factor receptor-bound protein 2	17q24–q25	←
<b>GRO1</b>	GRO1 oncogene (melanoma growth stimulating activity, alpha)	4q21	←
<b>GSK3B</b>	Glycogen synthase kinase 3 beta	3q13.3	GSK3 $\beta$
<b>GSTM1</b>	Glutathione S-transferase M 1	1p13.3	←
<b>GSTP1</b>	Glutathione S-transferase pi	11q13–qter	←
<b>GSTT1</b>	Glutathione S-transferase theta 1	22q11.2	GST $\theta$ 1
<b>GZMA</b>	Granzyme A (granzyme 1, cytotoxic T-lymphocyte-associated serine esterase 3)	5q11–q12	Granzyme-A
<b>HBB</b>	Haemoglobin, beta	11p15.5	$\beta$ -globin
<b>HBP1</b>	HMG-box containing protein 1	7q31.1	←
<b>HCDH1</b>	See <i>FZR1</i>		
<b>HDAC1</b>	Histone deacetylase 1	1p34	←
<b>HDAC2</b>	Histone deacetylase 2	6q21	←
<b>HDAC3</b>	Histone deacetylase 3	5q31	←
<b>HDAC4</b>	Histone deacetylase 4	2q37.2	←
<b>HEC</b>	See <i>NDC80</i>		
<b>HGF</b>	Hepatocyte growth factor (hepapoietin A; scatter factor)	7q21.1	←
<b>HMOX1</b>	Heme oxygenase (decycling) 1	22q12	HO-1
<b>HOX11</b>	Homeobox 11 (T-cell lymphoma 3-associated breakpoint)	10q24	←

Table ii: (continued)



Symbol	Full name	Locus	Protein name(s)
<b>HRAS</b>	v-Ha-ras Harvey rat sarcoma viral oncogene homologue	11p15.4	H-RAS
<b>HSET</b>	See <i>KNSL2</i>		
<b>HSP73</b>	See <i>HSPA8</i>		
<b>HSP75</b>	See <i>TRAP1</i>		
<b>HSPA8</b>	Heat shock 70kD protein 8	11q23.3–q25	HSP73
<b>ICAM1</b>	Intercellular adhesion molecule 1 (CD54), human rhinovirus receptor	19p13.3–p13.2	←
<b>ICAT</b>	See <i>CTNNB1P1</i>		
<b>ID1</b>	Inhibitor of DNA binding 1, dominant negative helix-loop-helix protein	2q11	←
<b>ID2</b>	Inhibitor of DNA binding 2, dominant negative helix-loop-helix protein	2p25	←
<b>IFNG</b>	Interferon, gamma	12q14	IFN $\gamma$
<b>IFNGR1</b>	Interferon gamma receptor 1	6p23–q24	IFN $\gamma$ R1
<b>IGF1</b>	Insulin-like growth factor 1 (somatomedin C)	12q22–q23	←
<b>IGF2</b>	Insulin-like growth factor 2 (somatomedin A)	11p15.5	←
<b>IGKC</b>	Immunoglobulin kappa constant	2p12	←
<b>IGSF1</b>	Immunoglobulin superfamily, member 1	Xq25	InhBP
<b>IL10</b>	Interleukin 10	1q31–q32	←
<b>IL12B</b>	Interleukin 12B (natural killer cell stimulatory factor 2, cytotoxic lymphocyte maturation factor 2, p40)	5q31.1–q33.1	←
<b>IL1A</b>	Interleukin 1, alpha	2q14	IL1 $\alpha$
<b>IL1B</b>	Interleukin 1, beta	2q14	IL1 $\beta$
<b>IL2</b>	Interleukin 2	4q26–q27	←
<b>IL2RA</b>	Interleukin 2 receptor, alpha	10p15–p14	IL2R $\alpha$
<b>IL2RB</b>	Interleukin 2 receptor, beta	22q13.1	IL2R $\beta$
<b>IL2RG</b>	Interleukin 2 receptor, gamma	Xq13.1	IL2R $\gamma$
<b>IL3</b>	Interleukin 3 (colony-stimulating factor, multiple)	5q31.1	←
<b>IL4</b>	Interleukin 4	5q31.1	←
<b>IL5</b>	Interleukin 5 (colony-stimulating factor, eosinophil)	5q31.1	←
<b>IL5RA</b>	Interleukin 5 receptor, alpha	3p26–p24	IL5R $\alpha$
<b>IL6</b>	Interleukin 6 (interferon, beta 2)	7p21	←
<b>IL7</b>	Interleukin 7	8q12–q13	←
<b>IL7R</b>	Interleukin 7 receptor	5p13	←
<b>IL8</b>	Interleukin 8	4q13–q21	←
<b>IL8RA</b>	Interleukin 8 receptor, alpha	2q35	IL8R $\alpha$
<b>IL8RB</b>	Interleukin 8 receptor, beta	2q35	IL8R $\beta$
<b>INCENP</b>	Inner centromere protein antigens (135 kD, 155 kD)	11q12–q13	←
<b>ING1</b>	Inhibitor of growth family, member 1	13q34	←
<b>INS</b>	Insulin	11p15.5	insulin
<b>IRF1</b>	Interferon regulatory factor 21	5q31.1	←
<b>IRF2</b>	Interferon regulatory factor 2	4q34.1–q35.1	←
<b>ITGB2</b>	Integrin, beta 2 (antigen CD18 (p95), lymphocyte function-associated antigen 1; macrophage antigen 1 (mac-1) beta subunit)	21q22.3	integrin- $\beta$ 2 (alias CD18)
<b>ITGB7</b>	Integrin, beta 7	12q13.13	integrin- $\beta$ 7
<b>ITK</b>	IL2-inducible T-cell kinase	5q31–q32	←
<b>JAK2</b>	Janus kinase 2 (a protein tyrosine kinase)	9p24	←
<b>JAK3</b>	Janus kinase 3 (a protein tyrosine kinase, leukocyte)	19p13.1	←
<b>JUN</b>	v-jun avian sarcoma virus 17 oncogene homologue	1p32–p31	← (alias c-jun)
<b>JUND</b>	jun D proto-oncogene	19p13.2	←
<b>KAP</b>	See <i>CDKN3</i>		
<b>KIT</b>	v-kit Hardy-Zuckerman 4 feline sarcoma viral oncogene homologue	4q11–q12	←
<b>KITLG</b>	KIT ligand (alias <i>SLC</i> , <i>STEEL</i> )	12q22	←
<b>KNSL1</b>	Kinesin-like 1	10q24.1	Eg5
<b>KNSL2</b>	Kinesin-like 2	6p21.3	HSET
<b>KRAS2</b>	v-Ki-ras2 Kirsten rat sarcoma 2 viral oncogene homologue	12p12.1	K-RAS
<b>LAG3</b>	Lymphocyte-activation gene 3	12p13.32	←
<b>lamin A/C</b>	See <i>LMNA</i>		
<b>LCK</b>	Lymphocyte-specific protein tyrosine kinase	1p34.3	←
<b>LEF1</b>	Lymphoid enhancer-binding factor 1	4q23–q25	←
<b>LMNA</b>	Lamin A/C	1q21.2–q21.3	lamin A/C
<b>LTA</b>	Lymphotoxin alpha (TNF super-family, member 1)	6p21.3	TNF $\beta$

Table ii: (continued)

Symbol	Full name	Locus	Protein name(s)
<i>LYN</i>	v-yes-1 Yamaguchi sarcoma viral related oncogene homologue	8q13	←
<i>MAP2K1</i>	Mitogen-activated protein kinase kinase 1	15q22.1–q22.33	MEK1
<i>MAPK1</i>	Mitogen-activated protein kinase 1 (alias <i>ERK2</i> )	22q11.2	←
<i>MAPK12</i>	Mitogen-activated protein kinase 12 (alias <i>ERK6</i> )	22q13.3	←
<i>MAPK14</i>	Mitogen-activated protein kinase 14 (alias <i>SAPK2A</i> )	6p21.3–p21.2	p38MAPK
<i>MAPK3</i>	Mitogen-activated protein kinase 3 (alias <i>ERK1</i> )	16p12–p11.2	←
<i>MAPK8</i>	Mitogen-activated protein kinase 8 (alias <i>JNK1</i> , <i>SAPK1</i> )	10	← (alias JNK)
<i>MATK</i>	Megakaryocyte-associated tyrosine kinase	19p13.3	←
<i>MC1R</i>	Melanocortin 1 receptor (alpha melanocyte stimulating hormone receptor)	16q24.3	←
<i>MCM2</i>	Mini-chromosome maintenance deficient ( <i>Saccharomyces cerevisiae</i> ) 2 (mitotin)	3q21	←
<i>MCM3</i>	Mini-chromosome maintenance deficient ( <i>Saccharomyces cerevisiae</i> ) 3	6p12	←
<i>MCM4</i>	Mini-chromosome maintenance deficient ( <i>Saccharomyces cerevisiae</i> ) 4	8q12–q13	←
<i>MCM5</i>	Mini-chromosome maintenance deficient ( <i>Saccharomyces cerevisiae</i> ) 5 (cell division cycle 46)	22q13.1–q13.2	←
<i>MCM6</i>	Mini-chromosome maintenance deficient ( <i>Saccharomyces cerevisiae</i> ) (mis5, <i>Schizosaccharomyces pombe</i> ) 6	2q14–q21	←
<i>MCM7</i>	Mini-chromosome maintenance deficient ( <i>Saccharomyces cerevisiae</i> ) 7	7q21.3–q22.1	←
<i>MDM2</i>	Mouse double minute 2, human homologue of; p53-binding protein	12q13–q14	←
<b>MEK1</b>	See <i>MAP2K1</i>		
<b>melanophilin</b>	See <i>MLPH</i>		
<i>MEN1</i>	Multiple endocrine neoplasia type 1	11q13	menin
<i>MET</i>	met proto-oncogene (hepatocyte growth factor receptor)	7q31	←
<i>MHC2TA</i>	MHC class II transactivator	16p13	←
<i>MIA</i>	Melanoma inhibitory activity	19q13.32–q13.33	←
<i>MITF</i>	Microphthalmia-associated transcription factor	3p14.1–p12.3	←
<i>MLH1</i>	mutL ( <i>Escherichia coli</i> ) homologue 1	3p21.3	←
<i>MLPH</i>	Melanophilin	2q37.3	melanophilin
<i>MRE11A</i>	Meiotic recombination 11, <i>Saccharomyces cerevisiae</i> homologue of, A	11q21	←
<i>MSH2</i>	mutS ( <i>Escherichia coli</i> ) homologue 2	2p16	←
<i>MSH6</i>	mutS ( <i>Escherichia coli</i> ) homologue 6 (alias <i>GTBP</i> )	2p16	←
<i>MYB</i>	v-myb myeloblastosis viral oncogene homologue (avian)	6q22–q23	←
<i>MYC</i>	v-myc avian myelocytomatosis viral oncogene homologue	8q24.12–q24.13	←
<i>MYCN</i>	v-myc avian myelocytomatosis viral related oncogene, neuroblastoma derived	2p24.1	←
<i>MYOD1</i>	Myogenic factor 3	11p15.4	MYOD
<b>MYT1</b>	See <i>PKMYT1</i>		
<i>NBN</i>	Nijmegen breakage syndrome 1	8q21–q24	nibrin
<i>NDC80</i>	NDC80 homolog, kinetochore complex component ( <i>S. cerevisiae</i> )	18p11.31	HEC
<i>NEDD8</i>	Neural precursor cell expressed, developmentally down-regulated 8	14q11.2	←
<i>NEDD9</i>	Neural precursor cell expressed, developmentally down-regulated 9	6p25–p24	←
<i>NEK2</i>	NIMA (never in mitosis gene a)-related kinase 2	1q32.2–q41	←
<b>neurofibromin</b>	See <i>NF1</i>		
<i>NF1</i>	Neurofibromin 1	17q11.2	neurofibromin
<i>NF2</i>	Neurofibromin 2	22q12.2	merlin I/II
<i>NFKB1</i>	Nuclear factor of kappa light polypeptide gene enhancer in B-cells 1 (p105)	4q24	NF $\kappa$ <sub>B</sub> p105 NF $\kappa$ <sub>B</sub> p50
<b>nibrin</b>	See <i>NBN</i>		
<i>NPM1</i>	Nucleophosmin (nucleolar phosphoprotein B23, numatrin)	5q35	←
<i>NME2</i>	Non-metastatic cells 2, protein (NM23B) expressed in	17q21.33	NM23-H2
<i>NOS1</i>	Nitric oxide synthase 1 (neuronal)	12q14–qter	nNOS
<i>NRAS</i>	Neuroblastoma RAS viral (v-ras) oncogene homologue	1p13	N-RAS
<i>NUMA1</i>	Nuclear mitotic apparatus protein 1	11q13	←

Table ii: (continued)

Symbol	Full name	Locus	Protein name(s)
<i>OCA2</i>	Oculocutaneous albinism II (pink-eye dilution homologue, mouse)	15q11.2–q12	←
<i>ODC1</i>	Ornithine decarboxylase 1	2p25	←
<b>P-cadherin</b>	See <i>CDH3</i>		
<b>p107</b>	See <i>RBL1</i>		
<b>p130</b>	See <i>RBL2</i>		
<b>p15</b>	See <i>CDKN2B</i>		
<b>p150</b>	See <i>DCTN1</i>		
<b>p16</b>	See <i>CDKN2A</i>		
<b>p18</b>	See <i>CDKN2C</i>		
<b>p19</b>	See <i>CDKN2D</i>		
<b>p21</b>	See <i>CDKN1A</i>		
<b>p27</b>	See <i>CDKN1B</i>		
<b>p300</b>	See <i>EP300</i>		
<b>p38MAPK</b>	See <i>MAPK14</i>		
<b>p53</b>	See <i>TP53</i>		
<b>p57</b>	See <i>CDKN1C</i>		
<b>p73</b>	See <i>TP73</i>		
<i>PA2G4</i>	Proliferation-associated 2G4, 38 kD	12q13	← (alias EBP1)
<b>PARP</b>	See <i>ADPRT</i>		
<i>PAX3</i>	Paired box gene 3 (Waardenburg syndrome 1)	2q35–q37	←
<i>PAX5</i>	Paired box gene 5 (B-cell lineage specific activator protein)	9p13	←
<i>PAX6</i>	Paired box gene 6 (aniridia, keratitis)	11p13	←
<i>PCM1</i>	Pericentriolar material 1	8p22–p21.3	←
<i>PCNA</i>	Proliferating cell nuclear antigen	20pter–p12	←
<i>PCNT</i>	Pericentrin (kendrin)	21q22.3	Multiple isoforms pericentrin (alias PCNT1), kendrin.
<i>PDPK1</i>	3-phosphoinositide dependent protein kinase-1	16p13.3	←
<i>PGR</i>	Progesterone receptor	11q22–q23	PGR(-x) Multiple isoforms
<i>PHB</i>	Prohibitin	17q21	prohibitin
<i>PIAS3</i>	Protein inhibitor of activated STAT3	1q21	←
<i>PIM1</i>	pim-1 oncogene	6p21.2	←
<i>PINK1</i>	PTEN induced putative kinase 1	1p36	←
<i>PKMYT1</i>	Membrane-associated tyrosine- and threonine-specific cdc2-inhibitory kinase	16p13.11	← (alias MYT1)
<i>PLK</i>	Polo-like kinase ( <i>Drosophila</i> )	16p11	←
<i>PMS1</i>	Post-meiotic segregation increased ( <i>Saccharomyces cerevisiae</i> ) 1	2q31–q33	←
<i>PMS2</i>	Post-meiotic segregation increased ( <i>Saccharomyces cerevisiae</i> ) 2	7p22	←
<i>POLA</i>	Polymerase (DNA directed), alpha	Xp22.1–p21.3	DNA pol-α
<i>POLB</i>	Polymerase (DNA directed), beta	8p11.2	DNA pol-β
<i>POLD1</i>	Polymerase (DNA directed), delta 1, catalytic subunit (125 kD)	19q13.3	DNA pol-δ1
<i>POLH</i>	Polymerase (DNA directed), eta (alias <i>XPV</i> )	6pter–p24.1	DNA pol-η
<i>POMC</i>	Proopiomelanocortin	2p23	ACTH β-lipotropin α-MSH β-MSH β-endorphin
<i>POU2F2</i>	POU domain, class 2, transcription factor 2	19q13.31	← (alias OCT-2)
<i>PPP1CA</i>	Protein phosphatase 1, catalytic subunit, alpha isoform	11q13	PPP1CA(-x) Multiple isoforms
<i>PPP1CB</i>	Protein phosphatase 1, catalytic subunit, beta isoform	2p23	←
<i>PPP1CC</i>	Protein phosphatase 1, catalytic subunit, gamma isoform	12q24.1–q24.2	←
<i>PPP1R12A</i>	Protein phosphatase 1, regulatory (inhibitor) subunit 12A	12q15–q21	←
<i>PPP1R12B</i>	Protein phosphatase 1, regulatory (inhibitor) subunit 12B	1q32.1	← M20
<i>PPP2R1A</i>	Protein phosphatase 2 (formerly 2A), regulatory subunit A, alpha isoform	19q13	←

Table ii: (continued)

Symbol	Full name	Locus	Protein name(s)
<b>pRB</b>	See <i>RB1</i>		
<b>PRDM2</b>	PR domain containing 2, with ZNF domain	1p36	← (alias RIZ)
<b>PRF1</b>	Perforin 1 (pore forming protein)	10q22	perforin
<b>PRKCB1</b>	Protein kinase C, beta 1	16p11.2	PKCβ1
<b>PRKDC</b>	Protein kinase, DNA-activated, catalytic polypeptide	8q11	DNA-PK
<b>prohibitin</b>	See <i>PHB</i>		
<b>PSMB8</b>	Proteasome (prosome, macropain) subunit, beta type, 8 (large multifunctional protease 7)	6p21.3	← (alias LMP-7)
<b>PSMB9</b>	Proteasome (prosome, macropain) subunit, beta type, 9 (large multifunctional protease 2)	6p21.3	← (alias LMP-2)
<b>PTCH</b>	Patched ( <i>Drosophila</i> ) homologue	9q22.3	←
<b>PTEN</b>	Phosphatase and tensin homologue (mutated in multiple advanced cancers 1) (alias <i>MMAC1</i> )	10q23	←
<b>PTGS2</b>	Prostaglandin-endoperoxide synthase 2 (prostaglandin G/H synthase and cyclooxygenase) (alias <i>COX2</i> )	1q25.2–q25.3	COX-2
<b>PTK2</b>	PTK2 protein tyrosine kinase 2 (alias <i>FAK</i> )	8q24–qter	FAK
<b>PTK2B</b>	Protein tyrosine kinase 2 beta	8p21.1	PYK2
<b>PTPRC</b>	Protein tyrosine phosphatase, receptor type, C	1q31–q32	CD45
<b>PTPRD</b>	Protein tyrosine phosphatase, receptor type, D	9p23–p24.3	←
<b>PYK2</b>	See <i>PTK2B</i>		
<b>RAB27A</b>	RAB27A, member RAS oncogene family	15q15–21.1	←
<b>RAB7</b>	RAB7, member RAS oncogene family	3q22.1	←
<b>RAC1</b>	RAS-related C3 botulinum toxin substrate 1 (rho family, small GTP binding protein Rac1)	7p22	←
<b>RAD50</b>	RAD50 ( <i>Saccharomyces cerevisiae</i> ) homologue	5q31	←
<b>RAD51</b>	RAD51 ( <i>Saccharomyces cerevisiae</i> ) homologue ( <i>Escherichia coli</i> RecA homologue)	15q15.1	←
<b>RAF1</b>	v-raf-1 murine leukaemia viral oncogene homologue 1	3p25	RAF
<b>RAG1</b>	Recombination activating gene 1	11p13	←
<b>RAG2</b>	Recombination activating gene 2	11p13	←
<b>RARB</b>	Retinoic acid receptor, beta	3p24	RARB(-x) Multiple isoforms
<b>RASSF1</b>	Ras association (RalGDS/AF-6) domain family 1	3p21.3	RASSF1(-x) Multiple isoforms
<b>RB1</b>	Retinoblastoma 1	13q14.2	pRB
<b>RBBP1</b>	Retinoblastoma-binding protein 1	14q22.1–q22.3	← Multiple isoforms
<b>RBBP2</b>	Retinoblastoma-binding protein 2	12p11	←
<b>RBBP4</b>	Retinoblastoma-binding protein 4	1	← (alias RbAp48)
<b>RBBP5</b>	Retinoblastoma-binding protein 5	1q32	←
<b>RBBP6</b>	Retinoblastoma-binding protein 6	16p12–p11.2	← PACT <sup>1228</sup>
<b>RBBP7</b>	Retinoblastoma-binding protein 7	Xp22.1	← (alias RbAp46)
<b>RBBP8</b>	Retinoblastoma-binding protein 8	18q11.2	←
<b>RBBP9</b>	Retinoblastoma-binding protein 9	20p11.2	←
<b>RBL1</b>	Retinoblastoma-like 1 (p107)	20q11.2	p107
<b>RBL2</b>	Retinoblastoma-like 2 (p130)	16q12.2	p130
<b>RELA</b>	v-rel reticuloendotheliosis viral oncogene homologue A, nuclear factor of kappa light polypeptide gene enhancer in B-cells 3, p65 (avian)	11q13	NFκ <sub>B</sub> p65
<b>RFC1</b>	Replication factor C (activator 1) 1 (145kD)	4p14–p13	←
<b>RFX5</b>	Regulatory factor X, 5 (influences HLA class II expression)	1q21	←
<b>RFXANK</b>	Regulatory factor X-associated ankyrin-containing protein	19p12	←
<b>RFXAP</b>	Regulatory factor X-associated protein	13q14	←
<b>rhoA</b>	See <i>ARHA</i>		
<b>ROCK1</b>	Rho-associated, coiled-coil containing protein kinase 1	18	←
<b>SCIDA</b>	Severe combined immunodeficiency, type a (Athabascan)	10p13	←
<b>SDF1</b>	Stromal cell-derived factor 1	10q11.1	←
<b>SELE</b>	Selectin E (endothelial adhesion molecule 1)	1q22–q25	E-selectin
<b>SELL</b>	Selectin L (lymphocyte adhesion molecule 1)	1q23–q25	L-selectin
<b>SFN</b>	Stratifin	1p	stratifin

Table ii: (continued)

Symbol	Full name	Locus	Protein name(s)
<i>SH2D1A</i>	SH2 domain protein 1A, Duncan's disease (lymphoproliferative syndrome)	Xq25–q26	←
<i>SHH</i>	Sonic hedgehog ( <i>Drosophila</i> ) homologue	7q36	sonic hedgehog
<i>SILV</i>	Silver homologue (mouse)	12q13–q14	←
<i>SKP2</i>	S-phase kinase-associated protein 2 (p45)	5p13	←
<i>SMARCA2</i>	SWI/SNF related, matrix associated, actin dependent regulator of chromatin, subfamily a, member 2 (alias <i>HBRM</i> )	9p24–p23	← (alias <i>HBRM</i> )
<i>SMARCA4</i>	SWI/SNF related, matrix associated, actin dependent regulator of chromatin, subfamily a, member 4 (alias <i>BRG1</i> )	19p13.2	← (alias <i>BRG1</i> )
<i>SMOH</i>	Smoothened ( <i>Drosophila</i> ) homologue	7q31–q32	smoothened
<i>SOCS1</i>	Suppressor of cytokine signalling 1 (alias <i>JAB</i> )	16p13.13	←
<b>sonic hedgehog</b>	See <i>SHH</i>		
<i>SOS1</i>	Son of sevenless ( <i>Drosophila</i> ) homologue 1	2p22–p21	←
<i>SOX10</i>	SRY (sex determining region Y)-box 10	22q13	←
<i>SOX4</i>	SRY (sex determining region Y)-box 4	6p22.3	←
<i>SP1</i>	Sp1 transcription factor	12q13.1	←
<i>SPI1</i>	Spleen focus forming virus (SFFV) proviral integration oncogene <i>spi1</i>	11p11.2	PU.1
<i>SPN</i>	Sialophorin (gpL115, leukosialin, CD43)	16p11.2	← (alias <i>CD43</i> )
<i>STAT1</i>	Signal transducer and activator of transcription 1, 91kD	2q32.2	←
<i>STAT3</i>	Signal transducer and activator of transcription 3 (acute-phase response factor)	17q21	←
<i>STAT6</i>	Signal transducer and activator of transcription 6, interleukin-4 induced	12q13	←
<i>STK11</i>	Serine/threonine kinase 11 (Peutz-Jeghers syndrome) (alias <i>LKB1</i> )	19p13.3	←
<i>STK12</i>	Serine/threonine kinase 12 (alias <i>AIM1</i> , <i>AIR2</i> , <i>AIK2</i> , <i>AIRK2</i> )	17p13.1	←
<i>STK15</i>	Serine/threonine kinase 15	20q13.2–q13.3	←
<b>stratifin</b>	See <i>SFN</i>		
<i>STX8</i>	Syntaxin 8	17p12	←
<b>survivin</b>	See <i>BIRC5</i>		
<i>SYK</i>	Spleen tyrosine kinase	9q22	←
<i>TACR1</i>	Tachykinin receptor 1	2p12	←
<i>TAF1</i>	TAF1 RNA polymerase II, TATA box binding protein (TBP)-associated factor, 250 kD	Xq13.1	←
<i>TAF2A</i>	TATA box binding protein (TBP)-associated factor, RNA polymerase II, A, 250 kD	Xq13.1	← (alias <i>TAF<sub>II</sub>250</i> )
<i>TAP1</i>	Transporter 1, ATP-binding cassette, sub-family B (MDR/TAP)	6p21.3	←
<i>TAP2</i>	Transporter 2, ATP-binding cassette, sub-family B (MDR/TAP)	6p21.3	←
<i>TBX2</i>	T-box 2	17q23	←
<i>TCF3</i>	transcription factor 3 (E2A immunoglobulin enhancer binding factors E12/E47)	19p13.3	← (alias <i>E2A</i> )
<i>TCF4</i>	Transcription factor 4	18q21.1	←
<i>TCF7</i>	Transcription factor 7 (T-cell specific, HMG-box)	5q31.1	← (alias <i>TCF-1</i> )
<b>TdT</b>	See <i>DNTT</i>		
<i>TERT</i>	Telomerase reverse transcriptase	5p15.33	←
<i>TFAP2A</i>	Transcription factor AP-2 alpha (activating enhancer binding protein 2 alpha)	6pter–p22.3	AP-2
<i>TGFA</i>	Transforming growth factor, alpha	2p13	TGF $\alpha$
<i>TGFB1</i>	Transforming growth factor, beta 1 (Camurati-Engelmann disease)	19q13.2	TGF $\beta$ 1
<i>TGFBR2</i>	Transforming growth factor, beta receptor II (70–80 kD)	3p22	TGF $\beta$ RII
<i>THBS1</i>	Thrombospondin 1	15q15	←
<i>TIMP3</i>	Tissue inhibitor of metalloproteinase 3 (Sorsby fundus dystrophy, pseudoinflammatory)	22q12.1–q13.2	←
<i>TNF</i>	Tumour necrosis factor (TNF superfamily, member 2)	6p21.3	←
<i>TNFRSF1A</i>	Tumour necrosis factor receptor super-family, member 1A	12p13.2	TNFRp55a
<i>TNFRSF5</i>	Tumour necrosis factor receptor super-family, member 5	20q12–q13.2	CD40
<i>TNFRSF8</i>	Tumour necrosis factor receptor super-family, member 8	1p36	CD30

Table ii: (continued)

Symbol	Full name	Locus	Protein name(s)
<i>TNFSF5</i>	Tumour necrosis factor (ligand) super-family, member 5 (hyper-IgM syndrome)	Xq26	←
<i>TOP1</i>	Topoisomerase (DNA) I	20q12-q13.1	topo-I
<i>TP53</i>	Tumour protein p53	17p3.1	p53
<i>TP73</i>	Tumour protein p73	1p36	p73
<i>TRAP1</i>	Heat shock protein 75 (alias <i>HSP75</i> )	16	HSP75
<i>TRIP11</i>	Thyroid hormone receptor interactor 11	14q31-q32	←
<i>TTK</i>	TTK protein kinase	6q13-q21	← (Mps1p in mice)
<i>TYMS</i>	Thymidylate synthetase	18p11.32	TS
<i>TYR</i>	Tyrosinase (oculocutaneous albinism IA)	11q14-q21	←
<i>TYRP1</i>	Tyrosinase-related protein 1	9p23	←
<i>UBC12</i>	See <i>UBE2M</i>		
<i>UBC4</i>	See <i>UBE2D2</i>		
<i>UBE2D2</i>	Ubiquitin-conjugating enzyme E2D 2 (UBC4/5 homologue, yeast)	5q31.3	UBC4
<i>UBE2M</i>	Ubiquitin-conjugating enzyme E2M (UBC12 homologue, yeast)	19q13.43	UBC12
<i>UBTF</i>	Upstream binding transcription factor, RNA polymerase I	17q21.3	←
<i>VAV1</i>	vav 1 oncogene	19p13.2	←
<i>VDR</i>	Vitamin D (1,25-dihydroxyvitamin D3) receptor	12q12-q14	←
<i>VEGFA</i>	Vascular endothelial growth factor A	6p12	VEGF
<i>VHL</i>	von Hippel-Lindau syndrome	3p26-p25	VHLp18 VHLp24
<i>VIM</i>	Vimentin	10p13	vimentin
<i>WAS</i>	Wiskott-Aldrich syndrome (eczema-thrombocytopenia)	Xp11.23-p11.22	WASP
<i>WRN</i>	Werner syndrome	8p	←
<i>WT1</i>	Wilms' tumour 1	11p13	WT1(-x) Multiple isoforms <sup>1149</sup>
<i>XPA</i>	Xeroderma pigmentosum, complementation group A	9q22.3	←
<i>XPC</i>	Xeroderma pigmentosum, complementation group C	3p25	←
<i>XRCC2</i>	X-ray repair complementing defective repair in Chinese hamster cells 2	7q36.1	←
<i>XRCC3</i>	X-ray repair complementing defective repair in Chinese hamster cells 3	14q32.3	←
<i>XRCC5</i>	X-ray repair complementing defective repair in Chinese hamster cells 5 (double-strand-break rejoining; Ku autoantigen, 80kD)	2q35	Ku80
<i>YWHAG</i>	Tyrosine 3-monooxygenase/tryptophan 5-monooxygenase activation protein, gamma polypeptide	7q11.23	14-3-3γ
<i>ZAP70</i>	Zeta-chain (TCR) associated protein kinase (70 kDa)	2q12	←
<i>ZNFN1A1</i>	Zinc finger protein, subfamily 1A, 1 (Ikaros)	7p13-p11.1	Ikaros

Key: ← = protein is referred to by the gene abbreviation.

**Table ii (concluded): Symbols for human genes**

Gene	Protein	Unifying characteristics	Human variants
	14-3-3	Non-enzymatic proteins conserved from yeast to mammals.	>6 14-3-3 proteins
<i>ARRB</i>	$\beta$ -arrestin	Involved in agonist-specific receptor desensitisation	>1 $\beta$ -arrestin
	CaM	The calmodulins. Calcium binding results in a conformational change that may influence the function of bound enzymes.	>2 CaMs
	CaMDK	The CaM-dependent kinases.	>6 CaMDKs
<i>CCNA</i>	Cyclin-A	The A-cyclins. These are involved in regulating the cell-cycle from S-phase into mitosis.	>1 cyclin-A
<i>CCNB</i>	Cyclin-B	The B-cyclins. These are involved in regulating the progression of mitosis.	>1 cyclin-B
<i>CCND</i>	Cyclin-D	The D-cyclins. These are involved in regulating entry into S-phase of the cell-cycle, particularly from a state of quiescence.	>2 cyclin-Ds
<i>CCNE</i>	Cyclin-E	The E-cyclins. These are involved in regulating entry and progression of S-phase of the cell-cycle.	>1 cyclin-E
<i>CDC25</i>	CDC25	The CDC25 protein phosphatases are involved in the regulation of the cell-cycle by contributing to the activation of CDKs.	>2 CDC25s
	CREB	cAMP response element binding transcription factors	>2 CREBs
<i>E2F</i>	E2F	The E2F transcription factors. In conjunction with their DP dimerisation partners, these regulate many of the genes involved in DNA replication and apoptosis.	>5 E2Fs >2 DPs
	$\gamma$ -tubulin	Centrosome-specific tubulins.	>1 $\gamma$ -tubulin
<i>GADD45</i>	GADD45	<i>GADD45</i> genes are induced by p53 as part of the response to genetic damage.	>2 GADD45s
<i>HSPC</i>	HSP90	Heat-shock induced proteins.	>1 HSP90
<i>IFNA</i>	IFN $\alpha$	The type I interferons with genes clustered at 9p22.	>12 IFN $\alpha$ s
<i>IFNB</i>	IFN $\beta$	The type II interferons. IL6 is closely related.	>1 IFN $\beta$
	MAPK	The mitogen-induced protein kinases. These are broadly divided into the extra-cellular-signal regulated kinases (ERKs), and the stress-activated protein kinases (SAPKs).	>11 MAPKs
	PDGF	Platelet-derived growth factors.	>3 PDGFs
	PI3K	The phosphatidylinositol-3-kinases. These heteromeric complexes contain both catalytic and regulatory subunits.	> 11 PI3K components
	PKC	Protein kinase C. Most are regulated by diacylglyceride, and some are also calcium-dependent.	>9 PKCs
	PLC	Phospholipase C. These enzymes are involved in the modification of phosphatidylinositol derivatives.	>9 PLCs
	PMS	Proteins involved in DNA mismatch repair.	> 1 PMS
	RAB3	Members of the RAS family.	>2 RAB3s
	RAL	Members of the RAS family.	>1 RAL
<i>RAS</i>	RAS	The RAS-family of small GTP-dependent GTPases.	> 2 RASs
<i>RPS6KA</i>	p90RSK	Ribosomal protein S6 kinases.	>5 p90RSKs
<i>RPS6KB</i>	p70RSK	Ribosomal protein S6 kinases.	>1 p70RSK
	SHC	SRC homology 2 containing adaptor proteins.	>1 SHC
	SKP1	Components of the SCF ubiquitin ligase complex.	>1 SKP1
	SMAD	A conserved protein family involved in the signalling of TGF $\beta$ type cytokines.	>6 SMADs
	SNARE	Golgi SNAP-receptor. Involved Golgi and ER protein trafficking.	>1 SNAREs
	STAT	Signal transducer and activator of transcription proteins.	>6 STATs
	TGF $\beta$	TGF $\beta$ cytokines are involved in morphogenesis and regulation of proliferation, in general being strongly inhibitory for cells of epithelial lineage. There is an extremely large super-family of similar proteins, including the bone morphogenic proteins and the activins.	>2 TGF $\beta$ s
	WNT	The wingless-family of conserved secreted signalling proteins. Involved in embryogenesis, and cellular differentiation.	> 18 WNTs

Table iii: Generic gene and protein symbols





---

# Preface to the third edition (V3)

---

## Timeline

In December of 2002, the first edition of this thesis (V1) was submitted. An oral examination was required, and this was held on 16 June, 2003. The result of this, communicated on 8 August 2003, was that the thesis must be amended and resubmitted. Revision thought to be satisfactory was made and the thesis (V2) was resubmitted on 26 March 2004. A letter from the University of Auckland dated 29 November 2004 contained the advice that the Board of Graduate Studies had resolved not to award the doctorate. Advice from the Acting Postgraduate Dean resulted in an appeal to the Vice-chancellor being lodged on 5 January 2005, and notification that this appeal had been upheld was given by letter dated 16 February 2005. That decision provided for the further submission of the thesis, amended again on the basis of the report made after the 2003 oral examination. There ensued a period of negotiation culminating in a resumption of work in October 2005, with a view to submission of a revised thesis within 12 months, this time subsequently being extended until 1 May 2007. This, the third edition, or V3, is the result.

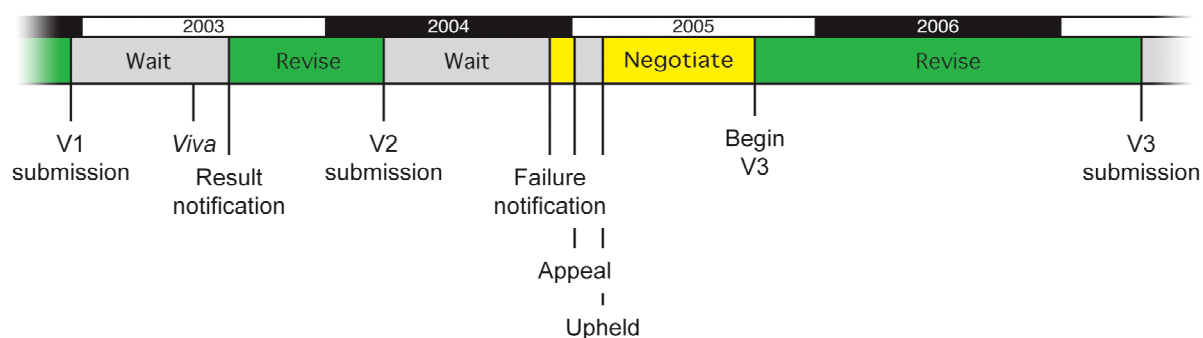


Figure i: Post-submission timeline

## A dilemma in presentation mode

The particular circumstances surrounding these events are complex, extraordinary, and controversial. To describe them in detail would dilute the essential content of the thesis and would not be in keeping with the traditionally dispassionate presentation of such work. Herein lies a dilemma: with the contextual information included, the thesis would not be in a form likely to be considered to "meet internationally recognised standards for such work", as required by the University of Auckland's Ph.D statute, yet without it, it is not a "systematic exposition of a coherent piece of advanced research work", as is also required, as it would omit very significant factors that dictated the execution of that work, and further, reduced its coherence.

This dilemma has been addressed by adopting a dispassionate objective approach, and in keeping with this, as far as possible, details of the context of this revision are omitted. That means that in places apparent non sequiturs may occur, the rationale for some procedures or interpretation of some results may appear weak, apparently unnecessary detail may be provided, or seeming irrelevancies may be introduced. The reader should consider that these may be present, or expected material absent, due to compelling circumstance.

---

## Structure of the V3 thesis

### General retention of the substance of the first edition

Two alternative approaches to the incorporation of the necessary revisions to the V1 work were considered. In the first, deletions, additions, and amendments would be made in place in the V1 work, with the whole having the semblance of a thesis submitted for the first time. In the second, only minor changes would be made to the original material with clarifications and additions presented as addenda to the affected sections. The first would have the advantage of producing a somewhat more efficient presentation of the ultimate content, but would exacerbate the issues brought about by the historical progression of the work. The second would allow the extent of the revision made to be better appreciated and would compartmentalise these revisions to reduce the impact of the historical issues, but would produce a longer document containing superseded material. If the revision required had been relatively minor, and the time between original submission and resubmission reasonably short, then the first approach would seem best, and that was the course adopted for V2. However, three cogent reasons exist that make the second approach better for V3: the revisions made are quite substantial and not easily integrated by interpolation; many of the references would now seem quite dated in a thesis combining new work with old, but in the semblance of something newly produced; and the retention of the V1 material as a record of the work originally done is intrinsically valuable, regardless of the quality of that work. It was this second approach that was adopted.

### Incorporation of substantial new material

New material to be incorporated as the result of revision is predominantly contained in addenda to each chapter of the thesis. These may contain a section in which the material presented in V1 is critiqued, clarified, expanded, or retracted, as need be, without introducing any new experimental data gathered during V3. However, in one instance, early V3 experimentation revealed a very significant error in the V1 interpretation of some Western blots, and sufficient new information is presented in advance to describe the discovery of this error. For experimental chapters, any clarification section may be followed by the description of new investigations undertaken during V3, and the results presented, discussed, and integrated with the V1 results.

One of the key inferences drawn from the V1 research was that centrosomal dysregulation could well be occurring in the NZM cell-lines, and this was investigated further during V3. This proved to be especially rewarding, and the scale of the results obtained demanded chapter status, rather than inclusion as an addendum to the chapter devoted to the study of ploidy. A new chapter has therefore been introduced to accommodate this.

To maintain consistent reference numbering between versions, new citations are listed in an addendum to the references and bibliography section, rather than being merged with the old. As before, ordering within this is alphabetical by first author, but reference is by number to minimise intrusion into the text.

### Alterations to the substance of the first edition

While maintaining the substance of the V1 work as much as possible, some modifications were made, and these included:

- correction of spelling and grammar;
- minor clarification of text not involving more than one paragraph;
- expansion of some figure legends;
- incorporation of new entries in tables in the prologue section, including tables of contents, abbreviations, and gene and protein symbols;

- renumbering of chapters, pages, figures, tables and the like, and cross-references thereto, as a result of the amendment of existing material or the incorporation of new, most notably the interpolation of the new chapter on centrosomal integrity;
- consolidation of three small concluding chapters into one;
- replacement of the symbol denoting a review article with ® due to a change in typeface support;
- identification of retracted material by the use of *grey text*. This is also marked by a marginal note;
- minor formatting or other typographical changes, usually pursuant to the above.

The V1 and V2 theses are available on the companion DVD-ROM, and can be consulted for comparative purposes if desired.

### **The companion DVD-ROM computer disk**

The inclusion of nearly 200 high-resolution fluorescence microscopy images has taken the total size of associated data files beyond the capacity of a CD-ROM disk. As a result, the disk included with the thesis is now a DVD-ROM: This disk contains the following:

- A folder with the contents of the V1 CD-ROM;
- A folder containing material for V2:
  - the thesis document in hyperlinked Microsoft Word format ("Thesis V2");
  - the linked figures in a separate folder;
  - the linked Microsoft Word document with abstracts for cited literature ("Abstracts");
  - PDF versions of the thesis suitable for:
    - printing a high quality document ("Thesis V2 (print).pdf");
    - routine computer-based access ("Thesis V2 (eBook).pdf").
- A folder containing material for V3a:
  - the thesis document in hyperlinked Microsoft Word format ("Thesis V3a");
  - the linked figures in a separate folder ("Figures");
  - the linked Microsoft Word document with abstracts for cited literature ("Abstracts");
  - PDF versions of the thesis with:
    - uncompressed full-size images ("Thesis V3a (max).pdf");
    - images resampled to 300 dpi, but not compressed ("Thesis V3a (print).pdf");
    - images resampled to 100 dpi and compressed ("Thesis V3a (screen).pdf");
  - a PDF version of the DVD-ROM label ("V3a disk label.pdf").

The disk itself, the PDF files, and the individual image files should all be platform-independent, however, owing to shoddy software engineering by Microsoft, the Word documents for V2 and V3a will not display the included figures when accessed under a Microsoft Windows operating system, the most egregious of three faults involved being the corruption of the file names in links by the replacement of most spaces with underscores, meaning that the linked files cannot be found. This fault has not been addressed by Microsoft despite the passage of 5 years and the release of several major revisions to Windows, Word for Windows, and Word for Mac OS. In V1, time was available to undertake the laborious task of working around these faults to produce a second file, with embedded rather than linked images, however there was no such opportunity for the V2 or V3a files. In most cases, the PDF files should suffice. If access to the Word document should be required for some reason, it would be faster and simpler to use the Apple Mac OS X operating system than to seek a solution from Microsoft.

---

## **Caveats over content**

### **Doubt over the identity of NZM10.1**

During the execution of the V3 experimental work, doubt arose over the authenticity of the NZM10.1 cell-line, and this doubt was not resolved. It is a possibility that the cell-line designated NZM10.1 was at its inception, actually NZM4, or that at some later time it was contaminated with, and possibly supplanted by NZM4 due to an error in handling. This may have occurred at any time, even during the V1 work, so all data relating to NZM10.1 from both the V1 and V3 experimental work must be considered provisional only {See '*Doubt over NZM10.1 authenticity*', on page 8–36}.

### **Tumour-suppressor expression**

As noted above, a very significant error was made in the interpretation of some V1 Western blotting results. In consequence, a very large part of the chapter on tumour-suppressor expression has been invalidated, and the reader should be aware of this when reading the V1 part of the relevant chapter. The chapter addendum describes this in detail.

### **V3 post-examination amendments**

The third edition of this thesis was examined and found to be satisfactory, with the proviso that a small amount of material be added to enumerate the hypotheses and objectives of the research undertaken. This has been added as Sections 4.5 and 4.6.

The opportunity was taken to proofread the thesis in its entirety once again, and a number of typographic, formatting, spelling, and grammatical errors were uncovered and corrected. Some text was very slightly altered to clarify meaning or readability. This amended version is designated V3a.

All changes made were with the approval of the project supervisor.

---

# Preface

---

## Formal requirements

- c. The PhD thesis is a formal and systematic exposition of a coherent piece of advanced research work carried out over the period of registration for the Degree and is required to satisfy the examiners and the Postgraduate Committee on all of the following criteria:
- (i) to be an original contribution to knowledge in its field, and to meet internationally recognised standards for such work
  - (ii) to demonstrate a knowledge of the literature relevant to the subject and the field or fields to which the subject belongs, and the ability to exercise critical and analytical judgment [sic] of it
  - (iii) to be satisfactory in its methodology, in the quality and coherence of its written expression, and in its scholarly presentation and format (including adequate references and bibliography).

Clause 1, Statute for the Degree of Doctor of Philosophy  
The University of Auckland

The 'internationally recognised standards' are nowhere defined, and so conformance to them is problematical. Indeed, while the University makes available 'Guidelines' for the presentation of theses, there are very few specific regulations, and in general, it refers Candidates to their Supervisors for direction. In the preparation of this thesis, this guidance was sought, and this, the 'Examination Edition', has been edited to conform strictly to the consensus view of the Supervisors.

## Document structure

### The Prologue section

This section contains material pertinent to the presentation and efficient utilisation of this document.

### The Basis, Thesis, and Synthesis sections

In the Basis section, a general introduction to the area of study is presented and the experimental rationale and objectives are explained in broad terms. The Thesis section provides a description of the experimental work undertaken. To facilitate conciseness and aid readability, details of materials and methods are relegated to Appendices, but these are extensively cross-referenced. The results obtained are reported and an interpretation of their meaning in isolation is presented. In the Synthesis section, these results are interpreted as a whole with the hope of uncovering any clues that may lead to the development of an effective therapy for metastatic melanoma. These three sections are the mainstream of the document and provide a self-consistent exposition of the work undertaken.

### The technical appendices

In these appendices are presented detailed descriptions of the methods, materials, solutions, apparatus and suppliers. In addition, the theoretical basis for many of the techniques employed is described.

### Reviews and supplementary material

A great deal of literature exists that, while relevant to the subject of this thesis, is too general, too specialised, or not sufficiently apposite to warrant inclusion in the mainstream of the thesis. Instead, it has been presented as a small number of independent focussed reviews whose scope and detail are dictated by the bearing they have on the main subject.

### References and bibliography

A comprehensive listing of cited literature is provided.

---

## CD-ROM contents

This thesis is accompanied by a cross-platform compatible CD-ROM that contains the following:

- This document as a compact PDF file suitable for routine computer-based access;
- This document as a high quality PDF file suitable for printing;
- This document in hyperlinked Microsoft Word format. Two files are provided: one with the images linked; and one with them embedded, intended for non-Macintosh users;
- An ancillary Microsoft Word document containing the abstracts for the literature cited;
- Experimental data including SSCP gel images, sequencing electropherograms, serum-deprivation results and analysis, and flow cytometry files for cell-cycle phasing and ploidy analyses;
- Figures from the thesis, generally at a resolution of 600 dpi, in PNG, JPEG, or MPEG format;
- PDF files for two posters based on this work presented at conferences;
- Several Microsoft PowerPoint presentations derived from this work;
- PDF files of the material associated with the CD-ROM case.

## Typographic conventions

### Protein and nucleic acid sequences

Individual amino acid and nucleotide symbols, and sequences of these, are rendered with a distinctive typeface, for example: GCAT, Y15. Where a reference must be made to a particular amino acid that shares a common function between very similar proteins, but differs in type or location, this is enclosed by angle brackets, that is '<', and '>'. For example, <T160> in the context of the protein CDK2 refers to T160, but in the context of the related CDC2, it refers to T161, the functional equivalent.

### Gene and protein nomenclature

#### *Specific*

All human genes referred to in this work, their HUGO names, where allocated, their full names, their cytogenetic loci, and their protein products are listed in Table ii. Genes and proteins for other species are not listed, and are presented in their generally accepted typographical form.

#### *Generic*

A central theme of molecular biology is that any gene or protein is likely to have a number of close relatives, and the concept of molecular families has emerged. Often, the differences among family members are unclear, and the extent to which an observation made about one applies to all is uncertain. In this work, generic gene and protein names are used under these circumstances. Typographically, these are indistinguishable from the specific forms, but rather than being listed in Table ii, they are given in Table iii, together with a brief description of the unifying characteristics of the family.

As examples, the term 'RAS' represents an unspecified member of the family of genes for small GTPases that includes *HRAS*, *KRAS2*, and *NRAS*; and the term 'CDC25' represents an unspecified member of the family of protein phosphatases implicated in the regulation of cell-cycle progression that includes *CDC25A*, *CDC25B*, and *CDC25C*.

#### *Trans-specific*

In an analogous manner to the use of angle brackets to denote functionally related amino acids in similar proteins of one organism, they are also used to indicate homologous genes or proteins in different organisms. Thus, <TP53> in the human context refers to the gene *TP53*, but in the mouse context, it refers to *Trp53*.

## Units

The SI system of units is used preferentially throughout, but where non-SI units are in common use, they do appear. These include the minute (min), the hour (h), the day (d), the litre (L), the gravity (G), the dalton (D), the Morgan (M), and the Svedberg (S). The reference body consulted in this regard was the National Institute of Standards and Technology of the United States of America<sup>939</sup>.

## Data and statistical conventions

### Statistics reference

The primary reference work for statistical matters was Pagano and Gauvreau, *Principles of Biostatistics*<sup>992</sup>.

### Uncertainty

In quantifying the dispersion of a distribution, standard deviation and coefficient of variation are used. Standard error is not employed in this context as its common usage is at odds with its strict definition<sup>180</sup>. It is used, however, to indicate the degree of uncertainty in regressions, along with the square of the regression coefficient. Unless otherwise noted, where numerical results are given in the form ' $m \pm s$ ',  $m$  is the arithmetic mean of all experimentally determined values and  $s$  is the sample standard deviation.

## Diagrammatic conventions

### Symbology

A common symbology has been employed in the diagrams depicting molecular processes and a key to this is given in Figure ii.

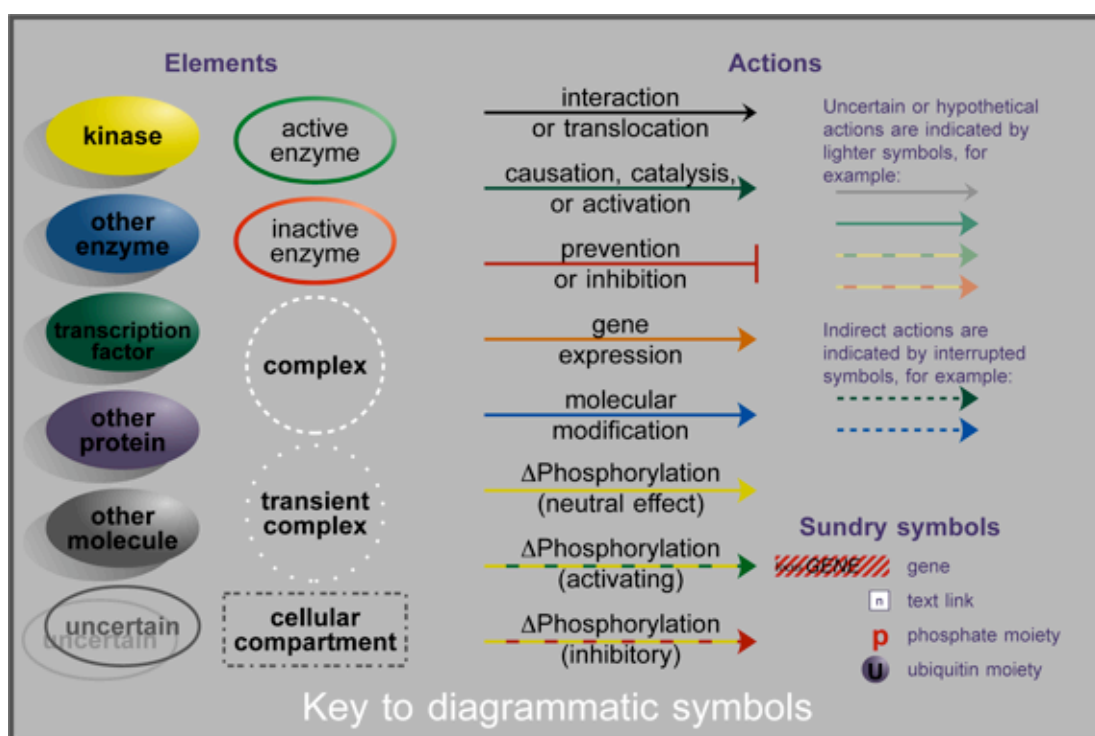


Figure ii: Diagrammatic symbology

### Graphical data representation

Where data are presented graphically, unless otherwise noted, points given correspond to  $m$  and error bars to  $\pm s$ . Any regression or trend line shown is the linear or exponential least-squares line of best fit, as is appropriate for the circumstances. In some graphs, the complete data set is shown in addition to  $m \pm s$ . Where this is done, the individual points are displayed in smaller, lighter symbols, while means are displayed in larger, darker symbols.

---

## Internal and external referencing

References to text within this document are enclosed by braces, that is '{', and '}'. The enclosed reference may be to a named section, for example '{See "Topic", below}', to a numbered element, for example '{1.1}', '{Method 3}', '{Appendix F}', '{Table 6-1}', or to a page number, for example '{2-3}'. References to parts of a figure or table are numbers enclosed by square brackets, for example '[4]'. The particular figure or table is the one most recently presented or referenced. Where possible, in versions of this document intended for computer-based access, internal references, both direct and parenthetical, references to cited literature, and references to internet resources are hyperlinks. Similarly, in the citation listing, hyperlinks are provided to article abstracts contained in an ancillary file ('*Abstract*').

## Trademarks, copyright, and intellectual property provisions

The ownership of all registered brand names, trademarks, logos, and the like used herein is acknowledged. Some included material is the intellectual property of others and may be protected by copyright. This is itemised in Table iv.

Item	Source	Proprietor	Use permitted by
Figure 1-1	University of California Davis <a href="http://matrix.ucdavis.edu/tumors/new/tutorial-intro.html">http://matrix.ucdavis.edu/tumors/new/tutorial-intro.html</a>	Art Huntley, MD.	Published conditions that permit educational use
Figure 2-1	Department of Pathology Duke University Medical Center, USA. <a href="http://pathology.mc.duke.edu/research/Histo_course/epi3.jpg">http://pathology.mc.duke.edu/research/Histo_course/epi3.jpg</a>	Duke University	Dr. Laura Hale <a href="mailto:hale0004@mc.duke.edu">hale0004@mc.duke.edu</a>
Figure 2-6	National Heart, Lung, and Blood Institute National Institutes of Health, USA. <a href="http://www.nhlbi.nih.gov/labs/cellbiology/9a.mov">http://www.nhlbi.nih.gov/labs/cellbiology/9a.mov</a>	NHLBI/NIH	Dr. John Hammer <a href="mailto:HammerJ@NHLBI.NIH.GOV">HammerJ@NHLBI.NIH.GOV</a>
Figure 7-1	Figure 1B from Modiano et al. <i>DNA and Cell Biology</i> 18:357-67 (1999) <sup>901</sup>	Mary Anne Liebert Inc.	Esther Bicozny <a href="mailto:ebicozny@liebertpub.com">ebicozny@liebertpub.com</a>

Table iv: Copyright material used in this document

This thesis and the companion computer disk and its contents are protected by copyright. Except where specifically attributed to others, this work is the intellectual product and property of the author, and all rights to it are reserved.

## Disclaimer

While all due care and diligence were exercised in the execution of the work described herein and in its presentation, the author accepts no responsibility for any adverse consequences, direct or indirect, of any event or non-event arising from the content of this thesis or any accompanying material or any omission from them.



---

## **Basis**

---



*While melanoma is not common, its global incidence is rising dramatically. Nowhere is this rate higher than in New Zealand. If detected prior to metastasis, surgical excision is curative in almost all cases. However, once a melanoma has reached a thickness of 750  $\mu\text{m}$ , it is likely to have metastasised, and the prognosis then is extremely bleak. Malignant melanoma is notoriously difficult to treat effectively, as it is very often resistant to chemotherapy. The five-year survival rate where distant metastasis has occurred is below 12%.*

An overview of the nature of cancer, its origins, attributes, and treatment, is given in Appendix F.

## 1.1 The nature of melanoma

### Definition

Melanoma is the name given to a carcinoma that has arisen from cells of melanocytic lineage. Whether it arises in fully mature melanocytes, or less differentiated melanoblasts, or both, is not known. Most commonly, it is cutaneous, but intra-ocular tumours can arise from melanocytes in the uvea, and abdominal, pulmonary, and other internal primary tumours do occur.

### Sub-types

Multiple sub-types of melanoma are recognised based on their origin, morphology, and progression<sup>1086</sup>. The four most common are superficial spreading (SSM), nodular (NM), acral lentiginous (ALM), and lentigo maligna (LMM).

SSM accounts for about 70% of melanomas and is the most common form seen in the young. It begins as an irregular, dark, often multi-hued skin blemish, usually on a sun-exposed area. In its initial radial growth phase, it may increase in area over a period of months or years, but during this time it remains either flat or only slightly raised, being a carcinoma in situ. It will then enter a vertical growth phase in which it becomes vascularised and begins to invade the dermis. The cause/effect relationship between this vascularisation and the onset of vertical growth is unclear. Once vertical growth has commenced, it is extremely likely that metastasis has occurred. This event effectively delineates SSM that is curable from that which is not.

NM accounts for 15–20% of melanomas and is seen mostly in persons of middle-age. It appears as a skin nodule, generally uniform and often black in colour. Unlike SSM, it has no initial radial growth phase, but grows vertically from its outset. In consequence, this form is



Image © Art Huntley, MD, 1994. {Table iv}

**Figure 1–1: Melanoma lesion**

particularly pernicious as it rarely presents prior to metastasis. It is possible that SSM and NM differ only in the timing of acquisition of angiogenic capacity.

ALM is the form most commonly seen in persons of dark skin and is predominantly palmar, plantar, or associated with nails, often appearing very similar to subungual haematoma. Lesions are usually multi-hued, with black and brown predominating. Early tumours often go unnoticed, resulting in late presentation and poor prognosis.

LMM usually affects people in their 70s and generally involves the nose or cheeks. Most often, it retains its superficial character, with the tumour frequently reaching 60 mm in diameter. LMM only rarely becomes metastatic, and so it is one of the less dangerous forms of melanoma.

### Symptomatology

A useful mnemonic for the most common symptoms of melanoma is 'ABCD'. Any cutaneous mole should be considered suspicious and investigated further if its appearance changes, or it is: asymmetrical (A); its border is irregular (B); its colour is not uniform (C); or its diameter is greater than 6 mm (D).

### Incidence

By most measures, melanoma is rare, accounting for ~4% of cancers and ~1.5% of cancer deaths in the USA. However, its incidence is increasing at a rate second only to that of lung cancer among women {See Table F-1}. It is of particular concern that Auckland, New Zealand, was recently identified as having the highest incidence of melanoma in the world<sup>620</sup>.

## 1.2 The cause of melanoma

A number of hereditary syndromes include a predisposition toward the development of melanoma {See Table F-3}. Notable is the involvement of the genes *CDKN2A* and *CDK4*, whose protein products are involved in the regulation of proliferation, and also the genes associated with xeroderma pigmentosum, whose products participate in DNA repair. Significantly, these syndromes entail only a predisposition toward melanoma, and its spontaneous development from infancy has not been reported. Indeed, individuals homozygous for mutated *CDKN2A* are known who did not develop early melanoma<sup>442</sup>. Clearly, there is at least one more factor: an initiating event that is inconsequential in a normal genetic context.

Epidemiological studies provide some insight into what this event may be, and the weight of opinion is that it is exposure to sunlight, and more particularly, its ultraviolet component. While the mutagenicity of ultraviolet radiation (UVR) is well established, this interpretation is not without its difficulties. In multi-factorial studies of incidence of skin cancers in general, there was very strong support for a major carcinogenic effect of sun exposure in squamous cell carcinoma (SCC) and basal cell carcinoma (BCC), but the data for melanoma were equivocal<sup>254</sup>. Furthermore, a significant number of melanomas arise at sites not normally exposed to the sun, being internal, or plantar. Among the proponents of UVR as a cause of melanoma there is also discord. Many are of the opinion that the causative component is the shorter wavelength UVB radiation<sup>804</sup>, known to be responsible for sunburn, and which is blocked by topical



sunscreens<sup>1152</sup>. In support of this contention, the point mutations seen in sporadic melanoma are often consistent with UVB causation<sup>1251</sup>. However, doubt exists over the relevance of this finding since this type of lesion has been seen in primary melanoma tumours when it is absent from metastases, suggesting that it is a late event and may not be causal<sup>1506</sup>. Others hold that it is the longer wavelength UVA component<sup>1401</sup>, and if this is indeed the case, there are serious implications. By preventing sunburn, and thereby giving a semblance of protection, a sunscreen may actually promote increased exposure to the damaging UVA, contributing to, rather than defending against the development of melanoma. Ironically, such sunscreens may protect against SCC, while rendering the user at greater risk of a much more serious disease<sup>1357</sup>. This has been addressed by the introduction of sunscreens that block both UVA and UVB.

There are suggestions that sunburn at an early age may predispose toward the development of melanoma later in life. Several large studies have not borne this out, and it appears to be the number of sunburn episodes, rather than their timing, that is correlated with incidence<sup>1023 1425</sup>.

An alternative interpretation of the epidemiological data, particularly the associations between melanoma and geographical latitude, socio-economic status, and age, is that it is elevated skin temperature, possibly in consequence of sun exposure, that is causative<sup>199</sup>. Several intriguing observations lend weight to this possibility. Firstly, heat and UVB have been shown independently to have similar effects on melanocyte function<sup>937</sup>, reducing the need to invoke UVR as a basis for the changes seen in response to sun exposure. Secondly, the germ-line mutation of *CDKN2A* seen in some melanoma predisposition kindreds is temperature sensitive<sup>1005</sup>. At physiological temperatures, the resultant protein is functional, but at elevated temperatures, it is not. Thirdly, immortalised human keratinocytes can be rendered tumorigenic solely by culture at an elevated temperature<sup>123</sup>. It is noteworthy also that the normal skin temperature is 34 °C, and for purely thermodynamic reasons, an increase of 3 °C can be imposed quite readily before any further increase is limited by the regulation of core body temperature. An increase of this magnitude could well have physiological implications.

### 1.3 Clinical assessment of melanoma

#### Clark levels

Wallace Clark<sup>869</sup> proposed a melanoma staging system based on the degree of skin penetration by the tumour {Table 1–1}. This correlates well with clinical outcome and is widely employed.

Clark level	Description
1	In situ melanoma; superficial, involving only the epidermis
2	The tumour extends into the papillary layer of the dermis
3	The tumour has reached the bottom of the dermal papillary layer
4	The tumour has penetrated into the dermal reticular layer
5	The tumour has penetrated into subcutaneous tissue

Table 1–1: Clark’s melanoma stages

#### Breslow thickness

A second classification system {Table 1–2} relates tumour thickness to 5-year survival and was proposed in 1975 by Alexander Breslow<sup>133</sup>.

Breslow thickness (mm)	5-year survival (%)
less than 0.76	97
0.76 – 1.50	92
1.51 – 2.50	76
2.51 – 4.0	62
4.1 – 8.0	52
greater than 8.0	32

Table 1–2: Staging by Breslow thickness

### American Joint Committee on Cancer staging system

The American Joint Committee on Cancer (AJCC) has developed a three-parameter staging system based on Breslow thickness (T), and the degree of local lymph node (N), and distant (M) metastasis. From these parameters, an overall stage number is defined, ranging from 0, for relatively early stage disease, to IV, for very advanced disease {Table 1–3}. Recently, this system has been revised to put more weight on ulceration as a prognostic feature, to use integral thickness boundaries, and to include serum enzyme data<sup>670</sup>.

Stage	TNM	Clark level	Description
0	–	1	In situ melanoma (superficial)
IA	T1N0M0	2	Invasion to upper dermis (less than 750 $\mu$ m thick)
IB	T2N0M0	3	Upper dermis entirely involved (750 $\mu$ m – 1.5 mm thick)
IIA	T3N0M0	4	Invasion into lower dermis (1.5 mm – 4 mm thick)
IIB	T4N0M0	5	Invasion beyond dermis
III	TnN1M0	–	Local lymph node involvement or in transit metastases
IV	TnNnM1 or TnNnM2	–	Distant metastasis

Table 1–3: AJCC melanoma staging

## 1.4 The treatment of melanoma

For melanoma in situ, excision of the tumour with margins of ~1 cm is usually curative<sup>1372</sup>. Thicker tumours require wider margins, and sentinel node biopsies should be performed to determine if there is nodal involvement. If so, complete lymph node dissection is indicated. Where the tumour is more than 4 mm thick, adjuvant high-dosage interferon- $\alpha$  therapy may be considered<sup>435</sup>, but this has potentially severe side effects. Where distant metastasis has occurred, the prognosis can be very poor, as melanomas are notoriously resistant to systemic cytotoxic therapy<sup>1182</sup>. Dacarbazine<sup>553</sup>, or the related temozolomide<sup>17</sup>, elicit responses in ~20% of cases, but these are generally of short duration and cure is rare. Combination therapy with platinum compounds, nitrosoureas, microtubule toxins, and cytokines can increase this response rate to some degree<sup>48</sup>; in particular, high-dosage interleukin-2 adjuvant therapy holds some promise<sup>49</sup>. Tamoxifen and thalidomide have also been included in treatment regimens with a degree of success<sup>561</sup>, and experimental tumour vaccines have been developed<sup>840</sup>.

Despite this array of therapeutic options, metastatic melanoma remains essentially incurable. Median survival time is about six months<sup>201</sup>, and five-year survival is about 12%<sup>1092</sup>. Hopefully, a greater understanding of its molecular biology will pave the way for the introduction of new and effective therapies. A prerequisite for this is an understanding of the biology of the cell-type that underlies melanoma, the melanocyte.

*Melanin is a dark pigment that occurs in a vast variety of organisms and its production and distribution are the duties of a single class of cell: the melanocyte. While its absorbance at visible wavelengths makes it an important adjunct to communication between animals ranging from camouflage to bold display, absorbance at infrared wavelengths makes it an excellent basis for thermal regulation in poikilothermic animals. The extension of this to the near ultraviolet makes melanin an ideal sink for solar radiation that might otherwise be damaging. This role in photoprotection is underscored by the increased production of melanin in response to ultraviolet irradiation. To achieve this, the melanocyte must survive in an environment that would likely cause the self-destruction of other types of cell. Melanocytes are therefore particularly hardy, but this may come at a price. By enduring genetic damage in order to prevent other cells from sustaining it themselves, melanocytes are uniquely prone to the fruit of such damage, an increased risk of tumorigenic transformation, possibly culminating in melanoma.*

## 2.1 Definition, ontogenesis, morphology, and ultrastructure

The skin of all mammals is pigmented, and while the intensity and hue of this pigmentation may vary with genetic and environmental factors, in all cases it results from the accumulation of heterogeneous polycyclic polymers known as melanins. The capacity to synthesise these compounds is restricted to ~5% of skin cells that have a common embryological origin and a distinct morphology and are thus considered to be a unique cell-type: the melanocyte<sup>@112 @1364</sup>.

Melanocytes differentiate from melanoblasts within the neural crest. By week eight *in utero*, human melanocytes begin to migrate first to the dermis, and thence, the stratum basale of the epidermis. Alternative paths also lead them to hair follicles or to the uveal tract of the eye and the retina. Molecular aspects of the regulation of melanocyte differentiation and migration are discussed below.

Melanocytes are relatively large, clear, dendritic cells that lack tonofilaments and desmosomes. They are distinguishable by their many dense, membrane-bound, spherical or ovoid organelles called melanosomes, occurring throughout the cytoplasm and associated with a microtubule network extending into the dendritic arms.

## 2.2 Melanocytes in situ

The body of the epidermal melanocyte lies among the columnar basal keratinocytes and, like them, has one

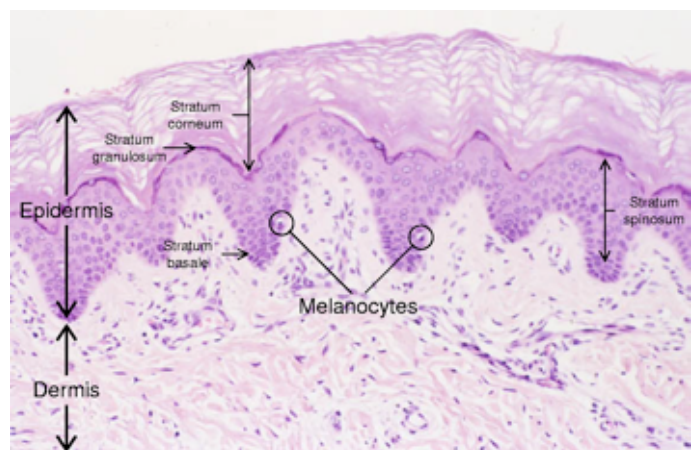


Image © Duke University {See Table iv}. Labels added.

Figure 2–1: Cross-section of the epidermis

face in contact with the dermis. Lacking the strong inter-cellular attachment afforded by desmosomes, they usually appear in histological photomicrographs to be surrounded by a clear margin {Figure 2–1}. Via its dendritic arms, each melanocyte forms intimate contact with ~36 surrounding keratinocytes, both within the stratum basale, and in the adjoining stratum spinosum. This serves to maximise the volume of tissue to which the melanocyte can supply melanin, and defines the epidermal melanin unit.

## 2.3 Molecular biology

### Sensitivity to external stimuli

#### Cytokines

##### Introduction

A *sine qua non* for the existence of multicellular organisms with differentiated tissues is the ability of cells to influence one another's phenotype, for without this, there could be no regulation of the roles of individual cells, and hence, no true organism. In general, the mediators of this communication operate by interaction with specific receptors at the cell surface, and a great many of these fall into one of two classes: the receptor tyrosine kinases (RTKs)<sup>①354</sup>, and the heptahelical G-protein-coupled receptors (GPCRs)<sup>①608 ①852</sup>. There are however significant exceptions, particularly among the interferons and interleukins. In melanocytes, many cytokines that influence survival, proliferation, differentiation, and function have been identified<sup>①464</sup>, and all receptor classes are represented {Table 2–1}.

Cytokine	Receptor class	Effects
ACTH	GPCR	Proliferation; eumelanogenesis <sup>4</sup>
ASIP	GPCR	Suppression of melanogenesis <sup>4</sup>
CGA+FSHB	GPCR	Proliferation <sup>507</sup> Dendricity <sup>827</sup>
EGF/TGF $\alpha$	RTK	Proliferation in low density cultures <sup>717</sup>
ET1	GPCR	Proliferation; melanogenesis <sup>s526 576 1472</sup> Enhances migration <sup>1163</sup> Modulates UVR response <sup>1289</sup>
ET2	GPCR	Proliferation; melanogenesis <sup>s526 1472</sup>
ET3	GPCR	Proliferation of melanocyte precursors; differentiation <sup>s526</sup> ; increases sensitivity to $\alpha$ -MSH <sup>1088</sup> Melanogenesis <sup>1472</sup>
FGF2	RTK	Proliferation <sup>717</sup>
GM-CSF	other	Proliferation; melanogenesis <sup>579</sup>
GRO1	GPCR	Proliferation <sup>118</sup>
HGF	RTK	Proliferation, motility, melanogenesis <sup>467 712</sup>
IFN $\alpha$	other	Mild growth inhibition <sup>717</sup>
IFN $\beta$ /IL6	other	Strong growth inhibition <sup>717</sup>
IFN $\gamma$	other	Mild growth inhibition <sup>717</sup>
IL1 $\alpha/\beta$	other	Growth inhibition <sup>717</sup>
IL8	GPCR	Proliferation <sup>717</sup>
Insulin/IGF1	RTK	Survival <sup>507</sup>
$\alpha$ -MSH	GPCR	Proliferation <sup>4</sup> Eumelanogenesis <sup>4</sup>
NGF	RTK	Proliferation <sup>717</sup> Chemotaxis <sup>1470</sup>
SCF	RTK	Survival; melanogenesis <sup>458</sup>
TGF $\beta$ 1	RTK	Strong growth inhibition of melanocytes, but may stimulate some melanomas <sup>717</sup>
TNF	other	Strong growth inhibition <sup>717</sup>

Table 2–1: Melanocyte cytokines





In vivo, many of these are produced locally within the skin by fibroblasts<sup>580</sup> and keratinocytes<sup>466</sup>. This provides the communication basis for a functional epidermal melanin unit by allowing the distribution of environmental sensitivity and cellular response among different specialised cell-types. Consistent with this, co-culture of melanocytes with keratinocytes satisfies the growth factor requirements of the former, and immunogold electron-microscopy reveals keratinocyte-derived FGF2 adorning melanocytes<sup>574</sup>. The frequently observed production of FGF2 by melanomas<sup>644</sup> and results from in vitro tissue reconstruction experiments<sup>874</sup> strongly suggest that this autocrine production is an important step in tumour progression. Beyond the assessment of gross phenotypic effect, melanocyte cytokine response is in general poorly understood. The best studied are probably SCF (stem cell factor)<sup>794</sup>, the related adrenocorticotrophic hormones ACTH, ASIP and  $\alpha$ -MSH, and the endothelins<sup>653</sup>, and these are the foci of the discussion below. Information on other cytokines is available in the references cited in Table 2–1.

### **Stem cell factor and the KIT receptor tyrosine kinase**

#### *Receptor activation*

Current opinion on the mode of SCF action has it that homodimers form<sup>1028</sup> {Figure 2–2} [1] prior to, or at the time of binding to its specific receptor, KIT, probably facilitating the dimerisation and activation of the latter [2]. As with most RTKs, KIT includes itself among its substrates [3], undergoing auto-phosphorylation on Y703<sup>1325</sup>, Y823, Y936<sup>1325</sup>, and possibly other tyrosines. Y568<sup>769</sup>, Y570<sup>769</sup>, and Y721 are phosphorylated, but it is not clear if this is by auto-phosphorylation or the action of another kinase.

#### *The PI3K channel*

Phosphorylated Y721 is bound by the SH2 domain of the regulatory sub-unit of PI3K<sup>81183</sup>, causing its activation [4]. This results in the phosphorylation of the membrane-associated lipid phosphatidylinositol-4',5'-diphosphate to become phosphatidylinositol-3',4',5'-triphosphate [5], a reaction opposed principally by the PTEN phosphatase, a recognised tumour-suppressor<sup>1231</sup>. The triphosphate, or its derivative 3',4'-diphosphate, have strong affinity for pleckstrin homology domains, and in consequence of this, the kinases PDPK1 and AKT1 are recruited to the inner surface of the plasma membrane<sup>105</sup> [6].

PDPK1, a constitutively active kinase, phosphorylates and thereby contributes to the activation of PKC isoforms<sup>303</sup> [7], which in turn have been shown to phosphorylate S741 and S746 of KIT, events thought to diminish its kinase activity<sup>106</sup> or lead to proteolytic cleavage<sup>1484</sup> [8]. This provides a negative feedback mechanism triggered by membrane-association of PDPK1 that is capable of governing receptor activation. PDPK1 also phosphorylates AKT1 on a regulatory threonine, T308, causing its kinase activation<sup>27</sup> [9] and the consequent inhibitory phosphorylation of GSK3 $\beta$  on S9<sup>232</sup> [10]. As a result, GSK3 $\beta$  is no longer able to phosphorylate  $\beta$ -catenin [11], required for its ubiquitin-directed degradation<sup>7</sup> [12]. This allows it to associate with the LEF1 transcription factor [13], whose activity it dramatically enhances<sup>960</sup>.

Transcription of the  $\beta$ -catenin–LEF1 target *CCND1*<sup>1216</sup> [14] results in increased production of cyclin-D1 [15]. This effect is augmented by the diminution of ubiquitin-directed proteolysis of cyclin-D1<sup>275</sup> [16] that would otherwise be triggered by phosphorylation of T286 by GSK3 $\beta$ <sup>274</sup> [17], were this not inhibited. Other circumstances permitting, this allows the activation of CDK4 and the consequent abatement of pRB-mediated proliferative inhibition.

See Appendix H for a review of the pRB subsystem.

A second target of  $\beta$ -catenin–LEF1 is *MITF*<sup>1207</sup> [18], the gene for a melanocyte-specific transcription factor critical to the expression of several genes whose protein products significantly contribute to melanocyte phenotype. The *MITF* promoter also contains cAMP response element (CRE) sequences through which the CREB transcription factor can contribute to gene expression<sup>1207</sup> [19]. CREB is phosphorylated directly by AKT1<sup>295</sup> [20] and also in a GSK3 $\beta$ -dependent manner<sup>441</sup> [21]. In the first case, phosphorylation of S133 promotes recruitment of CBP [22], while in the second, phosphorylation, were the kinase not inhibited, would prevent its interaction with DNA. S298 of the MITF protein itself is a substrate for GSK3 $\beta$  [23], and phosphorylation here, again if the kinase were active, would reduce its transactivation capacity<sup>1293</sup>. While two independent mechanisms cooperate to enhance cyclin-D1 expression, there are multiple mechanisms operative at both the transcriptional and post-transcriptional level that contribute to the increased expression of MITF. However, it has been shown that the presence of MITF is not of itself sufficient to promote increased expression of its target genes<sup>537</sup>. Phosphorylation of MITF S409 by p90RSK [24], and on S73 by MAPK1 [25] contribute synergistically to its activation [26] by promoting interaction with the p300 co-activator [27]<sup>498 1454</sup>. Since p90RSK is itself activated by PDPK1<sup>605</sup> [28], this requirement is already partially met. Co-stimulation by activators of the MAPK cascade, such as that described below, will confer on MITF the ability to contribute significantly to the expression of genes critical for the phenotype and function of the mature melanocyte, including two essential for melanogenesis: *TYR* and *TYRP1*<sup>1482</sup> [29]. While MITF–p300 is necessary for the induction of DCT, it is not sufficient<sup>1482</sup>, and co-activation by the transcription factor SOX10 appears to be required<sup>S1050</sup> [30]. Significantly, the duration of MITF contribution is constrained, as the same phosphorylation events that promote its activity, also promote its degradation<sup>498</sup> [31].

SCF signalling will also influence melanocyte survival by modulating the cellular apoptotic response. Firstly, activated CREB contributes to the expression of the anti-apoptotic protein BCL2<sup>1062</sup> [32]. Secondly, BAD is phosphorylated on S136<sup>104</sup> and S155<sup>1301</sup> by AKT1 [33], and S112 by p90RSK<sup>1151</sup> [34]. This promotes its association with a member of the 14-3-3 family of proteins<sup>1301</sup> and prevents its dimerisation with BCL-XL<sup>342</sup> inhibiting its pro-apoptotic function<sup>1214</sup>. Finally, the forkhead transcription factor FOXO3A is phosphorylated by AKT1, again contributing to 14-3-3 association and consequent nuclear exclusion. This will contribute to the diminution of apoptosis by reducing the expression of pro-apoptotic target genes such as *FASLG*<sup>140</sup>.

See J-17 for more about 14-3-3 proteins.

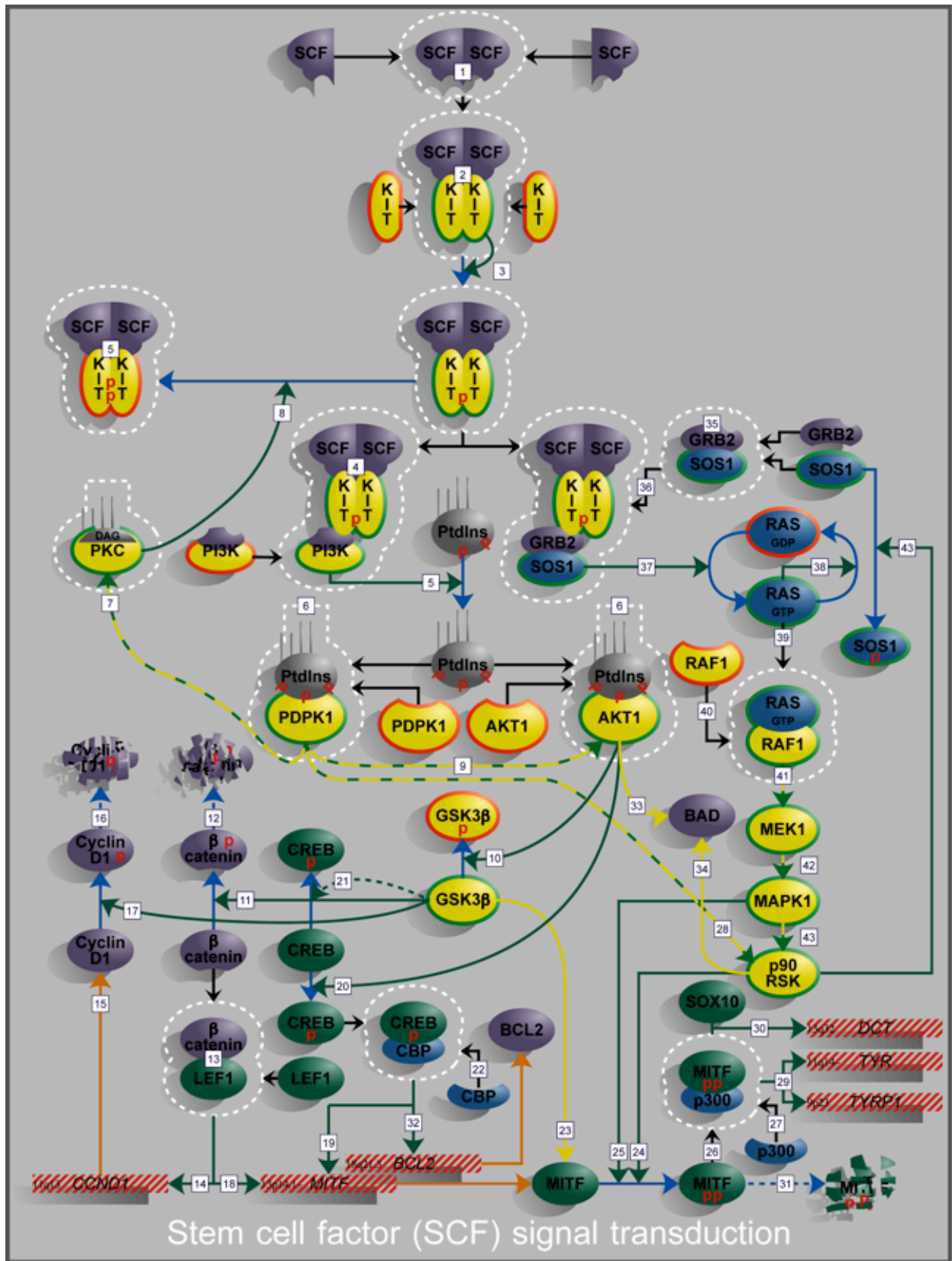


Figure 2-2: Stem cell factor signal transduction

*The RAS-MAPK channel*

The cytoplasmic GRB2 protein, and its relatives, contain little more than protein linkage domains and serve as adaptors that perform molecular matchmaking functions<sup>6289</sup>. In particular, GRB2 associates with the RAS guanine nucleotide exchange factor SOS1<sup>311</sup> [35]. Upon activation of KIT and the consequent phosphorylation of Y703, GRB2 is able to bind the

receptor complex via an SH2 domain<sup>1325</sup> [36], and in so doing, recruits SOS1 to the plasma membrane. This brings the enzyme into proximity with its substrate RAS, enabling it to facilitate the exchange of GTP for the GDP associated with the latter [37]. This places RAS into its active conformation until its inherent GTPase activity hydrolyses the bound GTP [38]. While in its active state, RAS–GTP binds [39] and activates the RAF1 kinase [40], which then precipitates the sequential phosphorylation and activation of MEK1 [41], MAPK1 [42], and p90RSK [43]<sup>@704</sup>. This serves to reinforce the activation of p90RSK that occurs via the PI3K channel already described. Finally, negative feedback regulation is implemented by the phosphorylation of SOS1 by p90RSK, which disrupts its association with GRB2<sup>287</sup> [44].

### *Other SCF signalling channels*

The PI3K and RAS-MAPK channels are the best characterised of those stimulated by the binding of SCF to KIT, but branches of these, and the possibility of entirely independent channels have been reported. For example, RAS, operating through MAPK3, and either via, or in parallel with JUN, contributes to the activation of *CCND1* transcription dependent on an AP-1 binding site at nucleotide –954 relative to the initiation codon<sup>23</sup>.

Also, soon after stimulation by SCF, the adaptor protein SHC becomes phosphorylated in a manner that depends on the association of the SRC kinase with phosphorylated KIT<sup>769</sup>. In consequence of this, the binding of SHC to GRB2, and any associated protein, is greatly enhanced. This has the effect of priming the channel used by receptors that employ SHC to signal, such as the G-protein-coupled receptors described below. Cross-channel reinforcement such as this provides a molecular basis for the synergistic effects often reported with simultaneous stimulation by multiple cytokines<sup>575</sup>.

A close relative of p90RSK, p70RSK, is also activated by AKT1 phosphorylation<sup>1063</sup>. A likely consequence of this is that the ribosomal S6 protein will be phosphorylated, resulting in enhanced protein synthesis, particularly from mRNAs that contain an oligo-pyrimidine domain in their 5' region<sup>@1383</sup>. Many of these encode proteins that are themselves elements of the cellular protein synthesis subsystem<sup>@298</sup>. Such a stimulus is a useful adjunct to the enhancement of gene transcription mediated by cytokine binding, whether to promote proliferation or phenotypic modulation. Other p70RSK substrates may exist.

Evidence is mounting that the JAK-STAT channel<sup>@572</sup> is involved in the signal transduction of RTKs, including KIT<sup>795</sup>. JAK2<sup>1418</sup> and several STAT proteins<sup>137</sup> associate with KIT and become phosphorylated after stimulation by SCF. The functional consequences of this have not been reported in detail.

Jhun et al.<sup>607</sup> cloned a cytoplasmic tyrosine kinase that they found to associate with activated KIT in megakaryocytes. This kinase, MATK, has more recently been implicated in the phosphorylation and inhibition of SRC-related kinases such as FYN<sup>1055</sup> and LYN<sup>1054</sup>. A role in the biology of melanocytes has not been reported.



### G-protein-coupled receptor mediated signalling

For some time it was thought that the most significant, and perhaps only mode of signal transduction employed by GPCRs was the release of their coupled  $G\alpha$  proteins with the simultaneous activation of their latent GTPase function, leading to activation of PKC and PLC channels. The residual beta-gamma dimer was not considered particularly significant, other than as an inhibitor of  $G\alpha$  function. Even had this been true, the situation would already have been inordinately complex due to the multiplicity of isoforms of many of the molecular intermediaries, with ten or more each of  $G\alpha$ , adenylyl cyclase (AC), PLC, and PKC. In the last case, differences in  $Ca^{2+}$  dependency of PKC variants adds to the difficulty as it can create a functional association between PLC and PKC activity. The realisation that signalling can also propagate via the detached beta-gamma dimer, and by means entirely independent of G-protein coupling added more levels of complexity. This is compounded still further by the ability of GPCRs to activate MAPK and other channels via multiple cross-links. Together, these aspects render the dissection of the particular signalling mechanism employed in a particular cell-type under particular conditions among the most formidable facing molecular biologists. A thorough review of the current state of scientific knowledge of this subject is beyond the scope of this thesis, and the interested reader is referred to a number of recent excellent reviews that attempt to consolidate the complex and often conflicting data <sup>83 447 556 1030</sup>.

As a basis for the discussion of G-protein-coupled receptor activity in melanocytes, a greatly simplified and generic signal transduction scheme is given in Figure 2–3. Binding of the ligand to its receptor results in a conformational change that allows the receptor to act as a guanine-nucleotide exchange factor for the alpha subunit of a heterotrimeric G-protein complex [1]. The effects of this are twofold: it causes the alpha subunit to dissociate from both the receptor complex and from the beta-gamma dimer, while simultaneously it is activated as a GTPase [2]. The liberated dimer remains associated with the plasma membrane due to the hydrophobicity of the isoprenylated beta subunit [3]. As occurs with the archetypal G-protein, RAS, autohydrolysis of the GTP associated with the alpha subunit allows its spontaneous reversion to an inactive conformation and re-association with the beta-gamma complex. The net result is that upon ligand binding  $G\alpha$ -GTP subunits appear transiently, and, when present, they are able to bind and thereby activate either AC or PLC [4]. AC then catalyses the conversion of ATP to cAMP [5], which activates the protein kinase A holoenzyme (PKA) by causing the regulatory subunits to dissociate from the complex [6].

Among PKA's substrates is S133 of CREB [7], which as described above, facilitates association with CBP [8], promoting transcription of target genes. Activation of PLC by  $G\alpha$ -GTP allows the conversion of phosphatidylinositol-4,5-bisphosphate to inositol-1,4,5-triphosphate ( $IP_3$ ) [9], soluble in the cytoplasm, and diacylglyceride (DAG) [10], which remains membrane-associated.  $IP_3$  stimulates the release of  $Ca^{2+}$  ions [11] from the endoplasmic reticulum (ER) by direct association with components of the ion channel structures in the ER membrane. Calcium thus liberated associates with CaM promoting a conformational change that renders stable the

otherwise transient association of CaM with its many binding partners, among them, the CaMDKs, causing their activation [12]. This too leads to the activating phosphorylation of CREB S133<sup>@222</sup> [13]. Simultaneously with this, the DAG that remains at the plasma membrane recruits and activates PKC [14], some isoforms of which are also Ca<sup>2+</sup>-dependent. It seems likely that PKC represents one of the crossover points between the PI3K and MAPK signalling channels since PKC-dependent activation of RAF1 has been demonstrated<sup>S148</sup>, and probably occurs via direct serine phosphorylation by PKC<sup>S158 S705</sup> [15].

The membrane-associated Gβ–Gγ dimer generated upon ligand fusion is free to participate in further molecular interactions, many mediated by pleckstrin-homology domains in its binding partners<sup>1334</sup>. Such association may be sufficient to activate latent enzymatic potential in them<sup>1402</sup>, suggesting a role in signal transduction<sup>@582</sup>. Notable among these are isoforms of PLC [16]<sup>1082</sup>, raising the possibility of independent regulation of PLC substrate specificity between the cytosolic fraction, activated by Gα, and the membrane-associated fraction, activated by Gβ–Gγ. Complexes comprising Gβ–Gγ, pleckstrin, and enzymatically active PI3K [17] have been detected at the membrane of natural killer cells after stimulation by chemokines<sup>22</sup>. This has the potential to link GPCR activation to PDPK1/AKT1 signalling as described above<sup>S1275</sup>.

Less well understood is the mechanism accounting for the observed activation of SRC-related kinases after ligand binding [18]. An intriguing scenario has been suggested wherein activation of the GPCR causes the rapid release of an autocrine factor that then stimulates its specific RTK with resultant SRC activation and downstream consequences<sup>@1030</sup>. More direct paths to SRC activation may involve the formation of complexes containing β-arrestin<sup>@819</sup>, and associations with focal adhesion kinases such as FAK<sup>@1497</sup> and PYK2<sup>278</sup> have also been implicated [19]. However produced, activated SRC will cause the phosphorylation of SHC [20], promoting its recruitment of GRB2–SOS1 to the membrane [21] where it can initiate RAS signalling [22]. Additionally, FAK may contribute directly to SHC phosphorylation<sup>1153</sup> [23], and there is also a PKC-dependent mechanism<sup>894</sup> [24]. SRC activation after GPCR ligand binding can also lead to phosphorylation of STAT3 [25] and its consequent dimerisation [26] and nuclear accumulation, where it contributes to transcriptional control<sup>@1074</sup>.

### *Mechanical stretch*

When subjected to mechanical stretching, as may occur during the retraction of attached keratinocytes<sup>683</sup> (See 'Dendritic', below), both MAPK1 and MAPK8 (JNK) kinases are activated<sup>685</sup>. Cyclic stretching results in increased expression of HSP90<sup>684</sup>, a protein known to enhance the activity of PDPK1<sup>383</sup>, and both consequently and independently, AKT1<sup>1140</sup>. The biological significance of these effects is unclear, but roles in regulating both proliferation and dendritic may be expected.

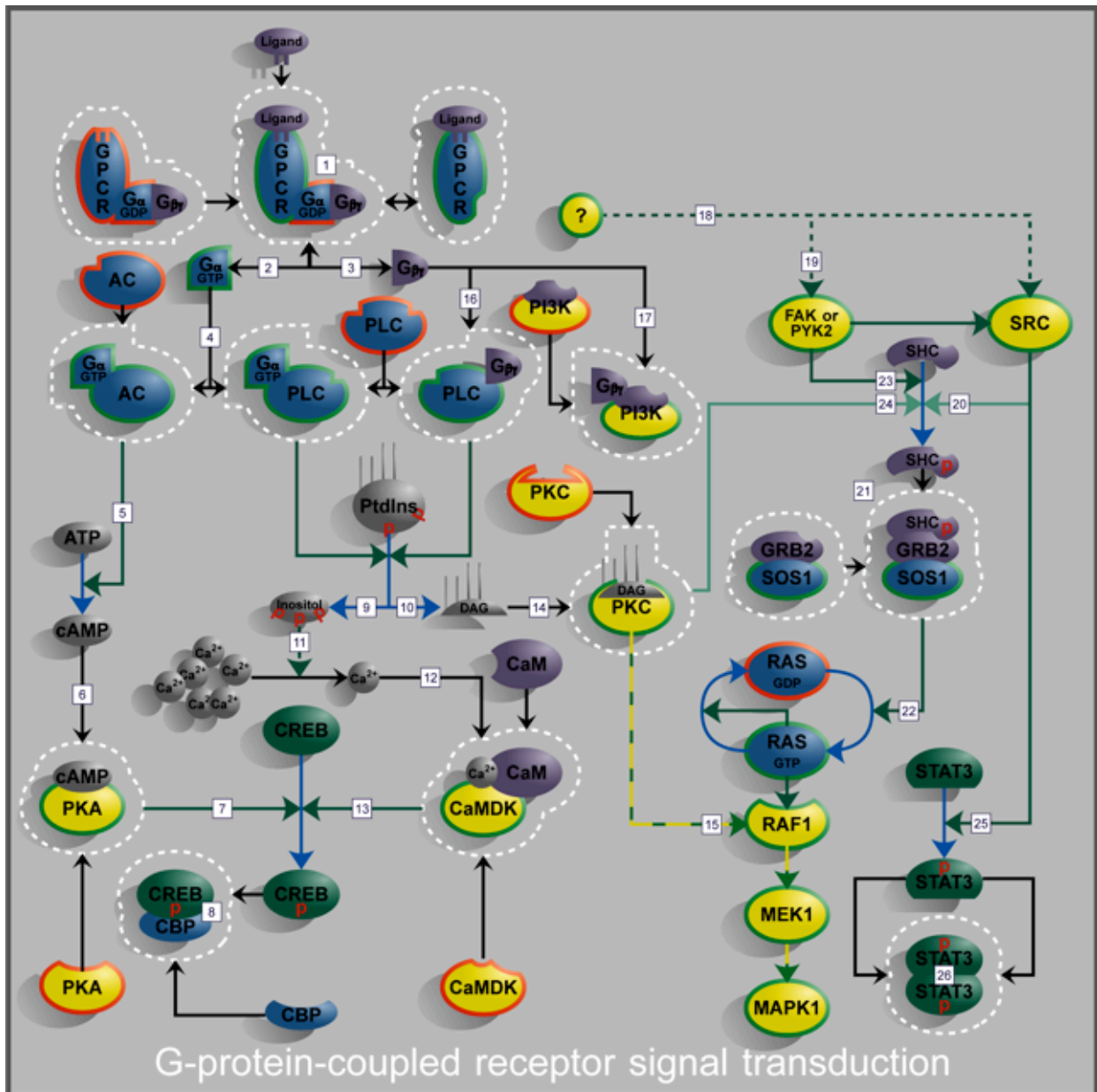


Figure 2-3: G-protein-coupled receptor signal transduction

### Sensitivity to intracellular stimuli

#### *Replicative senescence*

Melanocytes do not normally express telomerase, and it is thought that as in many other cell-types, telomere shortening below a critical length precipitates their replicative senescence<sup>68</sup>. In support of this, melanocytes engineered to express ectopic telomerase have increased proliferative capacity in vitro and do not display the characteristic senescent phenotype of flattening, enlargement, and increased melanisation. While the exact means by which telomere shortening translates into senescence remains enigmatic, the ability to induce an indistinguishable phenotype by stimulation with  $\alpha$ -MSH or treatment with cholera toxin suggests that signalling via cAMP may be involved<sup>67 460</sup>.

### *Genomic damage and ultraviolet radiation*

#### *Introduction*

The literature pertaining to melanocytic sensitivity to DNA damage is surprisingly sparse, and what exists is overwhelmingly dominated by studies relating to the effects of ultraviolet radiation. That brought about by oxidation, free radicals, ionising radiation, and alkylating agents is all but neglected. By way of example, a search of the National Institutes of Health (NIH) PubMed database with the query phrase '(melanocyte\*[ti] AND (p53 OR BRCA1 OR ATM OR ataxia OR GADD45\* OR ERCC\* OR DNA repair[mesh]))' identified only thirty articles, and of these, all but six pertained to UVR. This may prove to be an embarrassment if it is ultimately shown that it is an altered response to generic DNA damage, rather than UVR, that contributes to the tumorigenesis of melanoma. Perforce then, any review of melanocyte sensitivity to genomic damage is largely limited to that caused by ultraviolet radiation.

This sensitivity can be viewed as having two components, the first, where the initial detection of genomic damage occurs within the melanocyte, and the second, where the detection occurs in an adjoining cell, but a response is elicited from the melanocyte via paracrine messaging.

#### *Direct sensitivity*

The molecular biology of the cellular response to UVR-induced damage is incompletely understood, and while a number of signal transduction channels are activated, details of their temporal sequencing, interactions, and consequences are unclear. The postulated existence of a specific UVR sensor in melanocytes, while superficially plausible given the dramatic effect UVR has on their phenotype, may be unnecessary. By most measures, early cellular responses to genomic damage are very similar, irrespective of the cause of the damage or the type of the cell. For example, the early response of a melanocyte to UVR does not differ radically from that of a fibroblast to ionising radiation. In both cases, multiple signalling channels are activated, cell-cycle arrest occurs, DNA repair is initiated, and apoptosis may ensue. The major difference with melanocytes is that it also stimulates melanogenesis. Arguably, if other cell lineages had the capacity to respond in this way, they would, but lacking expression of the melanocyte specific transcription factor MITE, they cannot. The melanocyte response may properly be considered an extension of an underlying generic one.

Current understanding of the early response to generic DNA damage centres on the BRCA1-associated genome surveillance complex (BASC), but the precise mechanism of its activation is yet to be elucidated. The most fundamental input to this subsystem yet recognised is the activation of ATM. This is known to associate preferentially with damaged DNA<sup>34 1278</sup>, and if its activity were enhanced thereby, it may well represent the initial event. Both ATM<sup>192</sup>, and its relative, ATR<sup>1328</sup>, are activated soon after UV irradiation, in all likelihood leading to stimulation of BASC. Once triggered, this can mediate proliferative arrest, DNA repair, and apoptosis via numerous effectors, including p53. Additional responses, perhaps dependent on the precise nature of the DNA lesion, may be mediated by phosphorylation of ATM/ATR substrates not intimately associated with BASC.





At this point, the notion of a UVR sensor arises again, because while in general, the response to UVR is similar to that to other genotoxic stresses, there are significant variations. The basis for these must be explained, requiring an intracellular means of distinguishing types of DNA damage. The logical place to commence a search for such a sensor is therefore at the level of the nucleotide. Eller et al.<sup>316</sup> found that the mere presence of thymidine dimers (pT<sub>p</sub>T), typical excision products of the repair of UVR damaged DNA, evoked a melanocytic response identical to that caused by UVR itself: expression of TYR, increased melanogenesis, stimulation of DNA repair enzymes, and a cell-cycle arrest. Longer DNA fragments, up to 19 bp, were found to elicit a greater response and the presence of a 5'-phosphate group was found to be an important factor. There is an element of circularity here though as the fragments excised as a consequence of DNA repair cannot be the stimulus for the expression of the repair enzymes themselves. However, this is not an issue if the melanocyte response is considered to be an extension of a generic response as described above. It simply represents the first point at which the nature of the damage is recognisable. In this context, the sensor would be the enzyme or enzymes whose activity was modified by the presence of the excised fragments. These are unknown.

#### *Indirect sensitivity*

In response to UVR, keratinocytes produce larger amounts of ET1<sup>475</sup>,  $\alpha$ -MSH<sup>1150</sup>, and nitric oxide (NO)<sup>139</sup>. The first stimulates nearby melanocytes to proliferate, and all stimulate melanogenesis<sup>979 1137 1276</sup>. NO reduces the adhesion of melanocytes to the extracellular matrix, an effect that may bear on the increased dendriticity seen, and may also have implications for melanoma metastasis<sup>595</sup>. One puzzling aspect of the effect NO has on melanocytes is that it opposes the stimulus to proliferate provided by ET1<sup>1106</sup>. Macrophages also produce a dendrite elongation factor in response to UV<sup>1280</sup>, but the nature of this, and whether the effect is direct or mediated by another cell-type, such as the keratinocyte, remain to be determined. Possible mechanisms may involve interleukin 1<sup>§639</sup>, GM-CSF<sup>§961</sup>, or NO<sup>§1486</sup>.

### **Melanocytic responses to stimulation**

#### *Differentiation*

The establishment of epidermal melanocytes depends on their differentiation from neural crest precursors and their migration to the epidermis during embryogenesis. Two significant events in this progression are the expression of the receptor KIT and of the melanocyte-specific basic helix-loop-helix (bHLH) transcription factor, MITF<sup>§419 537 979 1056</sup>. There is, however, a degree of controversy over their relative timing and interdependence.

The importance of MITF in determining cellular fate is evident from the assumption of a melanocytic phenotype by fibroblasts engineered to express it ectopically<sup>§1288</sup>. It is also required for the survival of neural crest melanocyte precursors until they reach the migration staging area<sup>§536</sup>. MITF {Figure 2–4} has as target genes several whose protein products are essential for establishment and maintenance of the melanocyte phenotype, including *TYR*, *TYRP1*, and *DCT*<sup>§537</sup> [1]. It induces expression of the transcriptional repressor *Tbx2*<sup>§157</sup> [2], and via this may

## Human metastatic melanoma in vitro

regulate genes that carry the T-box motif. One such is *TYRP1*<sup>S156</sup> [3], a direct target of MITF, leading to a paradoxical situation wherein its expression is both enhanced and repressed via different transcription factors responding to the same stimulus. Clearly, our understanding of this regulation is incomplete. Tbx2 is also a repressor of *Cdkn2a-β* transcription [4] leading to a reduction in the levels of ARF protein<sup>S601</sup> [5]. In consequence of this, there will be an increase in

See J-21 for more on the regulation of E2F1 and p53 by ARF.

E2F1, as it will not be targeted for degradation by binding ARF [6]. This increase in E2F1 will stimulate S-phase entry. Simultaneously there will be a reduction in p53 levels [7] due to increased degradation [8] directed by increased levels of MDM2 arising from reduced ARF-mediated degradation [9]. This decrease in p53 level will reduce the propensity of the cell to undergo apoptosis, and this will be reinforced by the expression of the anti-apoptotic protein DCT {See 'Apoptosis', below}.

The transcription factor SOX10, in addition to co-activating the DCT promoter as described, binds the *MITF* promoter<sup>1369</sup> and causes a 100-fold enhancement of transcription, and this is further enhanced by PAX3<sup>1049 1407</sup>.

Furthermore, PAX3 is required for the expansion of committed melanocyte precursors during embryonic migration<sup>S536</sup>. This suggests that these transcription factors may be critical regulators of *MITF* expression early in melanocyte differentiation. The functional association among these three is confirmed by the close similarity of phenotype that results from the mutation of each, manifesting in humans as Waardenburg syndrome<sup>S114</sup>. Interestingly, mutation of *EDNRB* or *EDN3* also results in a very similar phenotype, and ET3 stimulation, by itself, may be<sup>S990</sup> sufficient to cause *MITF* expression<sup>S537</sup>. While this may in part be due to signalling through cAMP, PKA, and CREB, the activation of SOX10 or PAX3 may also occur. In combination, these findings suggest that endothelins may be the primary stimulus that sets a precursor cell on the path to becoming a melanocyte. This would suffice to stimulate proliferation and the expression of DCT and TYRP1, and there are also strong indications that MITF contributes to the expression of KIT in melanocyte precursors<sup>S979</sup> as it does in mast cells<sup>S1346</sup>.

Expression of KIT allows responsiveness to SCF, supporting at least two independent functions during melanocyte differentiation<sup>@1487</sup>. By using KIT inhibitory antibodies, Ito et al. showed

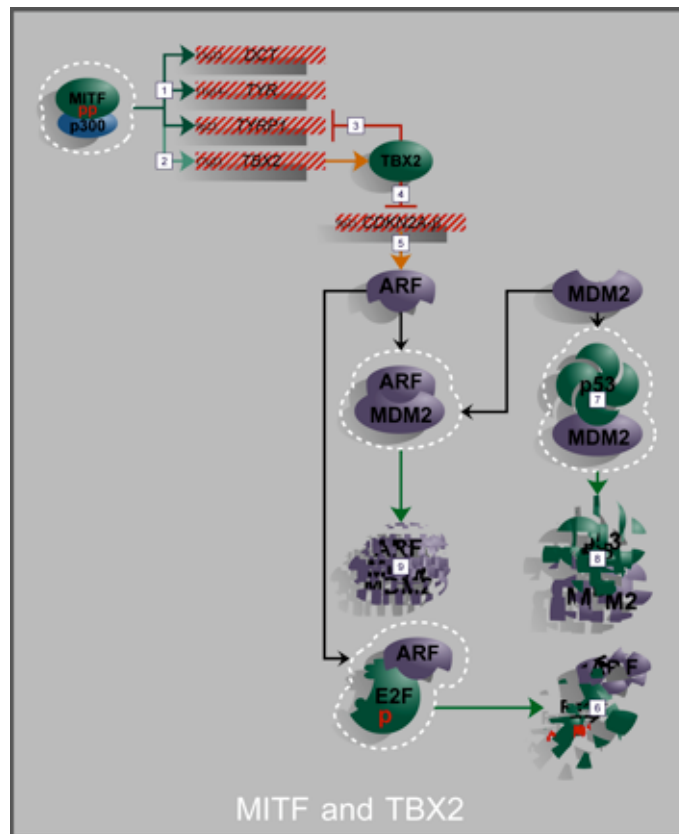


Figure 2-4: MITF influences net proliferation via TBX2



that the absence of SCF stimulation during critical periods of melanocyte differentiation resulted in their death through apoptosis<sup>588</sup> {See 'Apoptosis', below}. SCF is therefore essential to the survival of melanocyte precursors. It may also play a less obvious, but equally important role: that of rendering irreversible the differentiation process. This is achieved firstly by the contribution SCF stimulation can make to the expression of MITF via AKT1, CREB, and LEF1, and secondly, post-transcriptionally {Figure 2–2}. SCF dramatically increases MITF activity by sponsoring p300 recruitment<sup>1056</sup> via MAPK1-dependent phosphorylation<sup>498</sup>, but at the same time reduces its stability by promoting its ubiquitin-directed proteolysis<sup>1454</sup>. Thus while SCF may be insufficient to instigate the expression of MITF, it may well serve to maintain, amplify, and regulate this once it has begun. As a last step, SCF stimulation is required in parallel with MITF activity for the production of TYR, and hence the culmination of the melanocytic phenotype.

This cannot be the complete description of melanocyte differentiation however, as it omits a number of observations, particularly with respect to modes of inhibition of MITF activity. The transcription factor TCF4 inhibits *MITF* transcription {See 'Regulation of melanin type', below} and the STAT3 inhibitor PIAS3<sup>5773</sup>, and the transcription factor PAX6 both bind MITF and repress its transactivation function. In the case of PAX6, this inhibition is reciprocal<sup>1032</sup>. Finally, MITF is the subject of regulation in a manner akin to that of another bHLH transcription factor involved in differentiation, MYOD. Both are bound by pRB, the result being stimulation of its transactivation function in the case of MYOD<sup>1176</sup>, and its inhibition in the case of MITF<sup>1483</sup>.

### ***Embryogenic migration***

While SCF stimulates melanocyte precursor migration<sup>535</sup>, whether or not it directs it is unclear. Investigation of this role is hampered by the necessity of SCF stimulation for melanocyte precursor survival, hence simply ablating its function can shed no light on its role in migration since the cells do not survive. Nevertheless, Wehrle-Haller et al. have attempted to circumvent this by using mice that lack neurofibromin function and so have constitutively active RAS, alleviating the dependency of survival on SCF stimulation<sup>51415</sup>. Melanocyte precursors of these mice migrated normally, unless they were also lacking SCF, in which case, they remained in the migration staging area. Based on the normal expression of SCF at some distance ahead of the advancing melanocytes, they suggested that SCF acts to direct this migration. However, doubt has been cast on this conclusion by Jordan and Jackson who reported that the implantation of beads that release SCF increased the rapidity with which melanocytes colonised hair follicles, but did not themselves act as foci<sup>5623</sup>. They proposed that SCF acts merely to stimulate general motility, but plays no part in its direction. The driving force behind directed melanocyte migration along the dorsolateral pathway is as yet unknown. Factors such as FGF2 and ET1, both known to be chemotactic for melanocytes<sup>535</sup>, and nerve growth factor (NGF)<sup>1470</sup> may also prove to have their place.

More is known about the disposition of melanocytes once they have reached the dermis, and here, members of the cadherin family of proteins are implicated. Nishimura et al.<sup>953</sup> showed

that melanocyte precursors express neither E-, nor P-cadherin until they arrive in the dermis, but immediately prior to entry into the epidermis, E-cadherin begins to be expressed at high levels. Subsequently, P-cadherin is expressed by those that become follicular. If the expression pattern of different cadherins regulates melanocyte tissue targeting, then the possibility exists that aberrant expression may play a role in melanoma metastasis<sup>506 1306</sup>. Indeed, loss of E-cadherin expression is frequently observed in melanoma<sup>238 1132</sup> perhaps as the result of autocrine production of HGF<sup>777</sup>. Simultaneously, N-cadherin, not normally seen in melanocytes, is frequently expressed<sup>544</sup>. This may well contribute to increased migration across dermal fibroblasts, and serve to protect melanocytes from apoptosis by influencing BAD function via AKT1<sup>776</sup>.

### **Proliferation control**

#### **General**

Melanocytes do not differ dramatically from the mainstream with respect to the regulation of proliferation<sup>463</sup> and the retinoblastoma-associated protein and its functional associates form the basis for this. There are a number of specific nuances associated with melanocytes however. Among the D-cyclins, they express only cyclin-D1 and -D3<sup>73</sup>. Proliferative stimuli may stem from the binding of cytokines such as the keratinocyte-derived endothelins<sup>577 578</sup>, which induce *CCND1* expression via PI3K, and stimulate CDK2 activity via PKC<sup>1275</sup>. They may also derive from intercellular contacts mediated by integrins and FAK. The full gamut of signal transduction channels is implicated, including RAS-MAPK, WNT, and PI3K, and the primary *CCND1* transcription factors implicated are CREB and LEF1. The principal G<sub>1</sub> cyclin-dependent kinases (CDKs) are CDK4, CDK6, and CDK2. Inhibitory effectors include p15<sup>CDKN2B</sup>, p16<sup>CDKN2A</sup>, p21<sup>CDKN1A</sup>, and p27<sup>CDKN1B</sup>.

#### **Replicative senescence**

The irreversible cell-cycle arrest associated with replicative senescence in general occurs in G<sub>1</sub> phase and here too, pRB plays a vital role. In the general case, this arrest is associated with a reduction in the levels of cyclin-E, and a sustained increase in levels of cyclin-dependent kinase inhibitors (CKIs). The CKIs involved in implementing senescence may differ among cell-types, with p16<sup>CDKN2A</sup>, p21<sup>CDKN1A</sup>, and p27<sup>CDKN1B</sup> variously implicated.

In senescent melanocytes, p21 and p27 are present only at low levels, while p16 is elevated<sup>67</sup>, specifically implicating this CKI. This model is supported by the observation that melanocytes from *Cdkn2a*-null mice do not senesce in vitro in parallel with control cells<sup>1284</sup>. The senescent phenotype is however immediately restored upon enforced expression of p16, but not ARF. The effect appears to be dependent on gene dosage as cells from *Cdkn2a* +/- mice display an intermediate response. If, as believed, cAMP is involved in the initiation of senescence, how this may lead to enhanced *CDKN2A* expression is unclear, as the *CDKN2A* promoter does not contain a recognisable CREB binding domain. It does however contain one predicted to bind p300, a recognised CREB co-factor, so a direct role for cAMP via activation of PKA and phosphorylation of CREB seems unlikely, but not impossible. This apparent dependence of



melanocytes on p16 for the implementation of replicative senescence is particularly noteworthy in light of the very frequent loss of p16 expression seen in melanoma.

### **Arrest in response to genomic damage**

Activation of ATM and in consequence, BASC, plays a major role in causing cell-cycle arrest in response to genomic damage. In broad terms, similar responses are evoked after UV irradiation, but there are a number of distinctions. Early in the generic response, activated ATM phosphorylates the proteins CHK2, BRCA1, nibrin, and PLK. These are also phosphorylated after UV irradiation, and even though ATM is activated under these circumstances, it is not the responsible kinase<sup>858 1362 1458</sup>. In the case of BRCA1<sup>1328</sup> and PLK<sup>1362</sup>, and possibly other targets, it is ATR. In consequence, the substrate specificity or activity of these targets may be subtly altered. ATR also leads to phosphorylation of CHK1 on S345<sup>800</sup>, probably directly<sup>8452</sup>. Those means of instigating a cell-cycle arrest that depend on ATM, CHK2, and BRCA1 may still operate in response to UVR, but irrespective of this, a parallel mechanism operative via ATR and CHK1 exists. CDC25C, phosphorylated by CHK2 in the generic response, is phosphorylated by CHK1 in response to UVR<sup>47</sup>. Simultaneously, in a process that depends on p38MAPK, phosphorylations of CDC25B T309 and S361 occur<sup>143</sup>. In each case, the consequence is sequestration of CDC25 by 14-3-3, the prevention of CDC2 activation, and the imposition of a constraint to passage through G<sub>2</sub>. CHK1 activation also leads to the degradation of CDC25A<sup>832</sup>, probably influencing progression through G<sub>1</sub>.

None of these responses is at all dependent on the presence of functional p53, but the work of Eller et al.<sup>316</sup> described above demonstrated that transcriptional targets of p53 are indeed expressed in response to UVR, in particular, p21 and GADD45. These have the capacity to contribute to a cell-cycle arrest in both G<sub>1</sub> and G<sub>2</sub>. This may be due in part to activity of ATM, but ATR also phosphorylates p53 S15<sup>1327</sup>, promoting apoptosis, and, via an unidentified kinase, S20<sup>184</sup>, enhancing p53 stability.

### **Apoptosis**

Apoptosis is a phenomenon peculiar to multicellular differentiated organisms as it is only in this context that the process of cellular suicide can be an evolutionary asset, enhancing the possibility that the genes a cell contains will be transmitted. Three critical roles are performed by apoptosis. During embryogenesis, it is instrumental in the morphogenesis of organs and body structures, for example in the deletion of the webbing between human fingers. In what may be considered an extension of this process into adult life, it is immensely important in the negative selection of self-reactive lymphocytes, an absolutely essential function. In its third role, it is the agency by which cells that sustain irreparable genetic damage are destroyed. In the study of cancer, this aspect takes on great importance.

The regulation of melanocyte apoptosis has been all but ignored by the scientific community, with NIH PubMed returning only 31 references when queried with the phrase 'melanocyte\*[ti] AND apoptosis'. This is surprising since the melanocyte may constitute a unique apoptotic context. In contrast to every other cell-type, the sustaining and detection of genomic damage

Additional discussion of the generic response to genomic damage begins on page J-17.

Additional discussion of the role of p53 in response to genomic damage begins on page J-22.

must not lead to immediate apoptosis in the melanocyte. If it did, the cell would have no opportunity to carry out its biological function, the manufacture and export of melanin. In melanocytes, the apoptotic response must be dampened in order to allow this to occur. When apoptosis is viewed as a means of protection against cancer, it is clear that the melanocyte may be uniquely prone to tumorigenic transformation. Furthermore, this inherent resistance to apoptosis may contribute significantly to the generally poor outcome of the treatment of melanoma by cytotoxic agents including radiation, which may depend on eliciting just such a response. This is clearly an area that warrants much closer scrutiny.

Some molecular aspects of this raised apoptotic threshold have been uncovered. In cultures of normal human melanocytes supported by the addition of phorbol ester, its removal results in increased rates of apoptosis associated with a decrease in the expression<sup>692</sup> of the anti-apoptotic protein BCL2<sup>43</sup>. Phorbol esters are best known as stimulators of some PKC isozymes, but signalling mediated by other proteins is known, including the chimaerins and RAS guanyl-releasing proteins<sup>651</sup>, so the meaning of this finding is not obvious. As noted above, stimulation by SCF is necessary during melanocyte differentiation to prevent cell death from apoptosis and this effect is also mediated, at least in part, by enhancing BCL2 expression via AKT1 and CREB [Figure 2–2]. Kim et al.<sup>678</sup> reported that human melanocytes exposed to UVR in vitro express increased amounts of p53 and BAX, but BCL2 levels remained unchanged. They suggested that the high constitutive level of BCL2 protects melanocytes from apoptosis, and it may therefore represent the molecular basis for the raised threshold. A further component may be the MITF and Tbx2-mediated repression of ARF expression noted above. A reduction in ARF will promote the accumulation of MDM2, with a resultant reduction in p53 levels, also serving to dampen any apoptotic response. Finally, DCT, another melanocyte-specific enzyme, while it plays a critical role in melanogenesis {See 'Melanin biosynthesis', below}, also has anti-apoptotic properties<sup>954</sup>. Nevertheless, if this threshold is passed, UV irradiation can lead to melanocyte apoptosis, and this is mediated by ATM, p53, and MAPK8<sup>1512</sup>.

This reduced emphasis on p53 responses to genomic damage may resolve another enigma: the basis for the importance of p16 in the prevention of melanoma. In a cell predisposed to resist apoptosis, the propagation of cells that are genetically flawed must be based on the prevention of proliferation. One such means, induction of p21 by p53, is already weakened. The constraint to growth will therefore rest more heavily on the CDC25 family, and on the pRB subsystem, particularly p16, the apparent basis for replicative senescence in melanocytes.

### *Dendritic*

In an apparent recapitulation of their neural lineage, melanocytes possess numerous dendritic processes, but recent in vitro studies of melanocyte cultures and melanocyte/keratinocyte co-cultures have shown that lineage alone may not account for dendrite formation. Keratinocytes, by strongly binding the melanocyte cell membrane and then contracting, may actively draw out dendrites<sup>683</sup>. This may trigger activation of the MAPK signalling channel as a consequence of the mechanical stretching involved. In addition to this direct role, keratinocytes can promote



melanocyte dendritic through the release of substances to which melanocytes are receptive<sup>1358</sup>. These include the cytokines endothelin-1<sup>475</sup> and NGF<sup>1471</sup>, and also nitric oxide<sup>1106</sup>, particularly after UV irradiation. UVR can act directly on melanocytes to stimulate dendrite outgrowth via the RAS-related GTPase Rac1<sup>81167</sup>, which also mediates the dendrite-promoting effect of the cytokine  $\alpha$ -MSH<sup>1167</sup>. Since Rac1 enhances expression of cyclin-D1<sup>8624</sup>, proliferation and dendritic are both linked to UV irradiation.

There is evidence for UV-tropism influencing the orientation of dendrite outgrowth, perhaps as a means of directing delivery of melanin to the region where it is most useful. Other subtle effects of this UV-tropism may also occur since UVR biophotons are produced intracellularly during TYR catalysis in the production of melanin<sup>1236</sup>, potentially amplifying the melanisation response. As mitotic and S-phase cells are also a source of UV biophotons<sup>597</sup> such stimulation may be greater in tissues with a higher proliferative index. What part this may play in tumour pathology is unknown.

Components of the cytoskeleton are functionally linked to dendrite formation, with actin polymerisation<sup>81167</sup> being an absolute requirement, and myosin Va being required for their formation, but not their stability<sup>8310</sup>. The cytokine SCF may be influential here as it affects actin cytoskeletal structure and cellular adhesion<sup>1165</sup>.

### *Melanogenesis*

#### **Melanin**

Melanin is a pigment ubiquitous in nature, present in species of all phylogenetic kingdoms<sup>1094</sup>. It serves variously as photoprotection, camouflage, thermal regulator, and in the provision of visual cues among animals. It is a random co-polymer of aromatic bicyclic units, and consequently has no fixed structural formula or molecular weight. Based on the predominant monomer, two classes of melanin are recognised: eumelanin, derived from indoles and being dark in colour, and pheomelanin, derived from alanylhydroxybenzothiazine (AHB), being yellow or red. There is variety among the eumelanin class, as it can be derived from either 5,6-dihydroxyindole (DHI) or 5,6-dihydroxyindole-2-carboxylic acid (DHICA). That derived from DHI is black, that from DHICA is brown, and co-polymers are of intermediate shade.

#### **Melanin biosynthesis**

The principal ingredient for the synthesis of all melanins {Figure 2–5} is the amino acid tyrosine, with cysteine also being required for the production of pheomelanin. Synthesis begins with the hydroxylation of tyrosine to form 3,4-dihydroxyphenylalanine (DOPA) [1] catalysed by the enzymes TYR<sup>606</sup> and TYRP1<sup>1515</sup>. DOPA is then oxidised to form DOPAquinone [2], a reaction also catalysed by TYR in humans<sup>606 1515</sup>. DOPAquinone may be produced in one step by direct oxidation of tyrosine mediated by TYR [3]. These reactions are rate-limiting for the overall synthesis, establishing TYR as an important regulatory target.

In the presence of cysteine, DOPAquinone is rapidly reduced to form cysteinylDOPA [4], probably via a cysteinylDOPAquinone intermediate<sup>743</sup>, leading to the generation of AHB [5] and thence, presumably spontaneous polymerisation<sup>940</sup> to form pheomelanin [6]. The

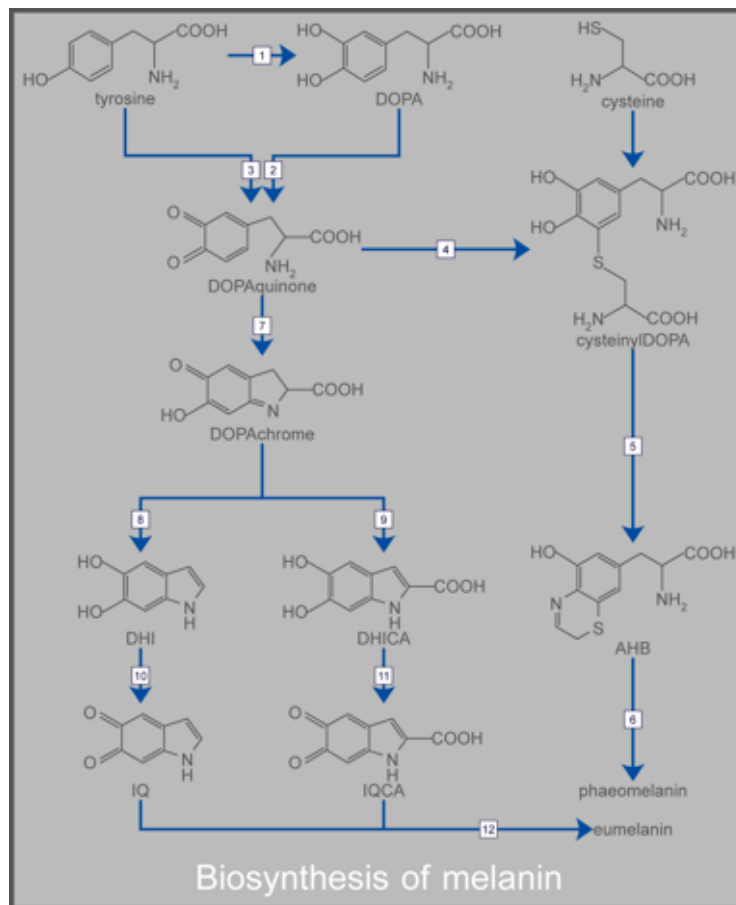


**Figure 2–5: Biosynthesis of melanin**

availability of cysteine therefore dictates the class of melanin produced<sup>743</sup>. In the absence of cysteine or another reducing thiol such as glutathione<sup>88</sup>, DOPAquinone will undergo a spontaneous ring closure to form DOPAchrome [7]. Slow, non-enzymatic decarboxylation may yield DHI [8], but in the presence of DCT, DHICA is the predominant product [9]. Further oxidation of these leads to 5,6-indolequinone (IQ) [10], and 5,6-indolequinone-2-carboxylic acid (IQCA) [11], respectively. In the first case, the reaction is catalysed by <TYR><sup>112 493</sup>, but there are inter-species differences in the catalysis of the second, with involvement of TYR in humans<sup>111 989</sup>, but Tyrp1 in mice<sup>698</sup>. Both IQ and IQCA are then incorporated into eumelanin [12]. This polymerisation may be spontaneous, catalysed by the protein silver<sup>173</sup>, or its rate subject to active regulation either directly by melanosomal proteins<sup>1187</sup>, or indirectly via melanosomal pH<sup>1385</sup>.

## Melanosomes

### Formation

The melanosome, the organelle in which the synthesis of melanin occurs, has many features of formation and structure in common with the lysosome, being membrane-bound with an acidic internal environment, and containing lysosome-associated membrane proteins (LAMPs)<sup>260</sup>. The ultimate origin of the lysosome and related organelles is still not entirely clear, but is likely to involve budding from the trans-Golgi network (TGN) as a vesicle containing matrix proteins. Subsequently, melanosome-specific enzymes such as TYR and DCT are delivered from the TGN via endosomes. In this regard, AP-3 (adaptor-protein-3) may be important in the





correct consignment of melanosomal proteins, relying on the presence of a leucine-leucine dimer motif in their cytoplasmic tails<sup>612</sup>. This is probably true for TYR, and perhaps DCT, but is not so for TYRP1 since correct consignment occurs even where AP-3 is defective<sup>552</sup>. The possibility of separate regulation of TYRP1 delivery is reinforced by the findings that it is dependent both on PI3K<sup>188</sup> and on the GTP-binding protein Rab7<sup>5423</sup>.

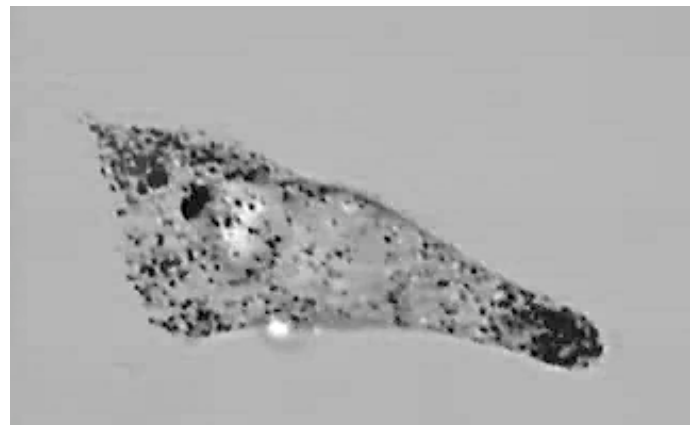
There are some structural differences between melanosomes that produce eumelanin and those that produce pheomelanin. The former are ovoid and contain a lamellar matrix, while the latter are spherical and do not<sup>611</sup>. Both types may be present within the same cell<sup>581</sup>, and they may be interconvertible.

#### *Maturation*

Melanosomes undergo a process of maturation that has been arbitrarily divided into four stages. The first is reached with the delivery of its characteristic enzymes. At this point, the melanosome is approximately spherical, and has neither TYR activity nor melanin. Stage II begins with the onset of detectable TYR activity and such melanosomes, where they are destined to produce eumelanin, are characterised by having an ovoid shape with evident longitudinal matrix elements carrying some deposition of melanin. Stage III melanosomes have high TYR activity and are moderately melanised, while in stage IV, melanin content is maximal and TYR activity abates.

#### *Transport*

Time-lapse video-microscopic studies (Figure 2–6) have revealed that melanosomes are highly mobile, moving bi-directionally between the perinuclear region and the dendrite tips at the relatively rapid rate of  $\sim 1 \mu\text{m}/\text{s}$ <sup>51457</sup>, allowing traversal of an extended dendrite structure in under 1 min. Once at the tip, melanosomes have a tendency to linger, resulting in their accumulation prior to transfer to the adjacent keratinocyte. These motions are



This is the key frame from a video illustrating melanosome movement.

© NHLBI/NIH {Table iv}

consistent with a model in which melanosomes carry both kinesin-related<sup>476</sup> plus-end-directed, and dynein-related<sup>1363</sup> minus-end-directed motor proteins and travel on the microtubule core of the dendrite. Assuming random attachment by either motor, the distribution of melanosomes under such a system would depend on the relative translational speed of the two motors, and apical accumulation would be favoured if kinesin-mediated anterograde motion were the faster. However, these translational speeds are not significantly different<sup>51457</sup>, so another mechanism must operate. A clue to the basis for this comes from the phenotype of the ‘dilute’ mutant mouse, deficient in production of myosin Va, and hence a model for the human disease

GrisCELLI syndrome<sup>1006</sup>. Here, although bi-directional shuttling occurs normally<sup>S1457</sup>, melanosomes do not accumulate at dendrite tips. This, and immunocytochemical studies<sup>742</sup> that show an association between melanosomes and myosin Va, strongly implicate it in apical accumulation. The nature of this association became much clearer with the identification of mutations in *RAB27A*, which encodes a RAS-related GTPase, as another basis for GrisCELLI syndrome<sup>875</sup>, causing similar melanosomal displacement<sup>56</sup>. Inexplicably, *MYO5A*, the myosin Va gene, and *RAB27A* are closely linked, being less than 7.3 cM apart at chromosomal locus 15q21. *RAB27A* was found to mediate the recruitment of myosin Va to the melanosome<sup>S1459</sup> via the intermediary protein melanophilin<sup>S1268</sup>. Upon arrival of a kinesin-transported melanosome at a dendrite tip, it disengages from the microtubule core, whereupon it may reassociate via its dynein motor and return toward the nucleus. Alternatively, it may become coupled to the sub-cortical actin network via the myosin Va motor protein, and begin to move upon it. Since the actin network is spatially random, the melanosome will tend to be found at a distance proportional to the square root of the time since detachment, following a 'drunkard's walk'. This accounts for the lingering and accumulation of melanosomes seen at dendrite apices.

See J-7 for more on microtubule motors as they relate to centrosomal movement.

Further regulation of the transfer from the microtubule core to the actin network may occur, since kinesin and myosin Va interact directly<sup>@246</sup>, but this aspect remains to be explored in detail.

### *Transfer*

Ultimately, mature melanosomes are transferred to the adjacent keratinocyte. Mechanisms proposed for this include the merging of keratinocyte and melanocyte membranes, the pinching-off of a dendrite tip by a keratinocyte, active inoculation by the melanocyte, and coupled melanocytic exocytosis and keratinocytic phagocytosis. Ultrastructural studies have not been able to exclude any of these, and tend to support dendritic pinching<sup>973 1475</sup>. Nevertheless, information from molecular biological and genetic studies has suggested that exocytosis/phagocytosis may be the predominant mechanism.

Stimulation of melanocytes by  $\alpha$ -MSH leads to increased membrane-ruffling and exocytosis of melanosome-containing vesicles<sup>S1378</sup>, rendering them available for keratinocyte ingestion. This phagocytotic process appears to be non-specific, with melanosomes and latex beads being taken up equally<sup>S1378</sup>. Any process that enhances general keratinocyte phagocytosis will therefore contribute to increased melanosome transfer. Particularly implicated is F2RL1, normally expressed superficially by keratinocytes and not by melanocytes<sup>@1172 1173</sup>. Experimental activation of F2RL1 results in enhanced melanosome uptake, while inhibition prevents it<sup>1173 1191</sup>. Consistent with a role in photoprotection, after UVR exposure, F2RL1 is expressed at higher levels, and within keratinocytes further removed from the stratum basale<sup>1164</sup>. Melanosomal expression of RAB3 and SNARE has also been implicated in melanosomal membrane association and transfer<sup>1166</sup>, but the significance of this remains to be determined.



Finally, melanin may not be the sole significant cargo delivered to the keratinocyte within the melanosome. The protein, PCNA, extremely important in the repair of DNA, is also transferred from melanocytes to mature keratinocytes, which, being non-replicative, they do not express themselves<sup>598</sup>.

#### *Degradation*

As the keratinocyte advances from the stratum basale through the stratum spinosum and differentiates into a squamous cell, the melanosomes within it are degraded by lysosomal enzymes. The melanin released accumulates in the nuclear membrane affording protection against UVR-induced mutation, both by absorbing the radiation directly, and by acting as a sink for oxidative molecular species that may be formed. Indeed the brown colour characteristic of eumelanin is a consequence of its oxidation. This protection is particularly important, as it is in this region that progenitor cells responsible for the continuous renewal of the epidermis reside.

#### **Regulation of melanogenesis**

The coarsest control of melanogenesis is the limited availability of the means of production: melanin is produced only by melanocytes. The basis for this is discussed above, and appears to rest critically on the initial endothelin-induced expression of MITF. Once this is present, melanocytes are poised to fulfil their biological function, and thereafter, melanogenic regulation reduces to the control of just two variables: the rate at which melanin is synthesised, and its type.

#### *Rate regulation*

A crucial aspect of MITF molecular biology is that, by itself, it is not competent to induce transcription. Association with the p300 co-factor is necessary, and this requires the prior phosphorylation of MITF. The total cellular transcriptional activity of MITF is therefore a function both of its level of expression and the extent of its phosphorylation. These may be subject to separate regulation, with the first serving to define the maximum level of activity possible, and the second, the actual level within the range so defined. As a concomitant of this, the rate of melanogenesis is also subject to this regulation since TYR is induced by MITF and is rate-limiting for melanin biosynthesis. The promoter of *MITF* contains a CRE, and consequently, its transcription is regulated by the CRE binding protein CREB. Hence, the rate of melanogenesis is affected by intracellular levels of cAMP. As described above, this links melanogenesis to extracellular influences that are mediated by GPCRs (Figure 2–3).

One such receptor that is extremely important in melanocyte regulation is MC1R, a melanocortin receptor<sup>®1147</sup>. This interacts with the cytokines ACTH, its cleavage product  $\alpha$ -MSH<sup>®166</sup>, and the related protein ASIP {See 'Regulation of melanin type', below}. The effects of  $\alpha$ -MSH and ACTH binding are indistinguishable<sup>4</sup> and include an increase in the production of melanin. This effect indeed derives from a cAMP-dependent increase in the rate of transcription of *MITF*<sup>92 1057</sup>. However,  $\alpha$ -MSH stimulation may not of itself promote the activation of this additional MITF. This aspect does not appear to have been addressed directly,

but can be inferred from the longevity of MITF produced after  $\alpha$ -MSH stimulation<sup>1057</sup> and the established coupling of MITF activation with its degradation<sup>1454</sup>. This absence of activation, together with the existence of polymorphic human MC1R receptors<sup>1270</sup> with varying efficacy, may have contributed to the many early reports suggesting that human melanocytes were refractory to  $\alpha$ -MSH<sup>374 385</sup>.

Similar discord exists over the matter of pituitary production of  $\alpha$ -MSH in post-natal, including adult, humans<sup>1324</sup>, but it seems likely that it is indeed produced. In a comprehensive study of peripheral blood  $\alpha$ -MSH levels of healthy donors<sup>166</sup>, a remarkable stability over time was seen for each individual, but wide variability was seen among them. Functionally, this means that when and if melanogenesis is triggered, it proceeds with a specific minimum rate that is determined systemically by each person's pituitary gland. This would form the basis for the differences in individual tanning response seen, and may contribute to the range of pigmentation present among human sub-populations. This minimum rate may be modified by local  $\alpha$ -MSH produced within the skin, in particular, by keratinocytes in response to UVR<sup>1150</sup>.

Whatever level of MITF is present due to stimulation by systemically and locally produced  $\alpha$ -MSH, melanogenesis will not proceed at all until MITF is activated via phosphorylation by MAPK1 or a related kinase, enabling its association with p300. This implicates signalling via RAS and PI3K, and therefore RTKs, including KIT and its ligand SCF {Figure 2–2}. The importance of this is that human keratinocytes produce SCF<sup>907</sup>, and there is very strong evidence from studies of keratinocyte/melanocyte co-cultures and intact human skin that this production increases after UVB exposure<sup>458</sup>. Furthermore, sub-epidermal injection of KIT neutralising antibodies prevented post-exposure skin melanisation of guinea-pig skin<sup>5458</sup>, consistent with paracrine stimulation. A similar role has been proposed for GM-CSF in response to UVA exposure<sup>579</sup>. This effect is in addition to the increased keratinocyte production of ET1,  $\alpha$ -MSH, and NO described above. It is noteworthy also that ET1 stimulation of melanocytes increases expression of MC1R<sup>1289</sup>, enhancing the influence of  $\alpha$ -MSH and thereby raising the maximum rate of melanogenesis. By analogy, what occurs after UV irradiation is a request by keratinocytes, in the form of SCF, for greater availability of melanin within the epidermal melanin unit. With the infrastructure for melanogenesis in place in the melanocyte, and a pool of MITF awaiting activation whose size is regulated by  $\alpha$ -MSH, the melanocyte can respond very rapidly with synthesis of TYR and the production of fully melanised melanosomes.

Since GPCRs may engage the RAS signalling channel {Figure 2–3}, the question of the failure of  $\alpha$ -MSH to activate MITF via MAPK1 phosphorylation arises. The explanation is remarkably simple. While ET1, acting via the EDNRB receptor<sup>308 575</sup> activates FAK, causing the phosphorylation of SHC and therefore RAS,  $\alpha$ -MSH, signalling via MC1R does not<sup>1163</sup>.

In addition to these external stimuli, the intrinsic UV sensitivity of melanocytes contributes to increased melanogenesis. Exposure to UVB or pTpT increases expression<sup>389</sup> and activity<sup>316</sup> of



MC1R by melanocytes independently of the paracrine effect of keratinocyte-derived ET1. UVR exposure results in phosphorylation of AKT1 T308, and S473, and GSK3 $\beta$  S9<sup>1308</sup>, enhancing the activity of the former<sup>1340</sup>, while diminishing that of the latter<sup>1195</sup>. Through CREB and  $\beta$ -catenin, this increases transcription of MITF. Simultaneously, UVR activates the MAPK channel, and via this, p90RSK<sup>882</sup>, leading to MITF activation.

The production of melanin is not without its dangers since it does produce very reactive molecular species<sup>182</sup>. The pros and cons have been weighed in the evolutionary balance with the benefits of melanin production outweighing the risks. However, this is only true while the threat of UVR exists, and were the melanogenic response to be in essence a final, irreversible step in melanocyte differentiation, the result may well be different. To avoid this, the activation of MITF is intrinsically coupled to its degradation via ubiquitin-directed proteolysis<sup>1454</sup>, ensuring that the melanocyte reverts to a state of preparedness, rather than remaining fully active.

#### *Regulation of melanin type*

The archetypal regulator of melanin type is the mouse agouti protein<sup>5</sup>, so named because it is required for the presence of a sub-apical yellow band on each hair caused by the transient change from eumelanogenesis to phaeomelanogenesis within the follicle. Agouti was found to bind to the Mc1r receptor in competition with  $\alpha$ -Msh, and antagonise its stimulus of eumelanogenesis<sup>809</sup>. It soon transpired that agouti did more than deny  $\alpha$ -Msh access to Mc1r, since in the absence of  $\alpha$ -Msh it reduces the basal rate of melanogenesis, but only in cells with functional Mc1r<sup>8434 8976</sup>. The corresponding situation was subsequently found also to apply in human cells<sup>4 1277</sup>, and one basis for this effect was found to be a reduction in the activity of TYR<sup>5</sup>. Ultimately, the importance of agouti as a modifier of melanocyte phenotype was rendered unequivocal by the discovery that it can prevent the differentiation of precursor cells into melanocytes by inhibiting the expression of *Mitf*<sup>86</sup>.

Using a method based on differential mRNA expression, Furumura et al.<sup>395</sup> identified three genes with elevated, and six with reduced expression after treatment of mouse melanocytes with agouti. Among those seen to decrease were, not surprisingly, Tyr and Dct. Among those with increased expression, they identified the bHLH transcription factor *Tcf4*. Further study<sup>394</sup> revealed that while the binding of agouti to Mc1r increases *Tcf4* expression, binding of  $\alpha$ -Msh decreases it, and furthermore, that expression of *Tcf4* reduces expression of *Mitf*. The mechanism of *Mitf* repression is likely to involve competition between *Tcf4* and *Lef1* for binding to  $\beta$ -catenin<sup>982</sup>, an important regulator of *Mitf* transcription. Many of the mysteries of agouti signalling have thus been resolved, including the bases for the reductions in *Mitf*, Tyr, and Dct seen, and of the prevention of melanocyte precursor differentiation. The loss of TYRP1 expression seen during phaeomelanogenesis<sup>256</sup> could also be explained by this mechanism, although such a reduction does not appear to have been documented as a specific response to agouti.

The consensus view appears to be that while TYRP1 and DCT expression is eliminated during phaeomelanogenesis, that of TYR is only reduced. This is as it should be considering that TYR activity is rate limiting for phaeomelanogenesis, and therefore, total elimination of expression cannot occur. The basis for the retention of TYR expression may involve MITF-independent transcription of *TYR*, such as is known to occur in response to BMP2<sup>897</sup>. Further nuances of regulation may involve denial of the necessary co-activation of the DCT promoter by SOX10, and differential protein trafficking to melanosomes, particularly in the case of TYRP1.

While these changes in melanogenic enzyme expression may account for a decrease in the rate of production, it is not immediately obvious how it could account for a change in the type of melanin produced. Consideration of the synthesis reaction kinetics offers one possibility. In the presence of cysteine, the formation of phaeomelanin monomers from DOPAquinone is favoured. With low or zero levels of DCT, DOPACHROME will not be converted to DHICA, increasing the probability of its reaction with cysteine. Similarly, with limiting TYR, the irreversible step from DHI to IQ will be less likely to occur. Such an argument is not particularly convincing, however.

Two other aspects of melanogenesis are likely to play more significant roles in mediating this change. The first is the regulation of intra-melanosomal cysteine, which, more than any other factor, influences the nature of the melanin produced<sup>743</sup>. This is attested to by the increase in phaeomelanogenesis seen following the addition of cysteine to the culture medium of melanocytes in vitro<sup>1238</sup>. Transport of cysteine across the melanosomal membrane occurs by an active mechanism<sup>89 §1051</sup>, but how this is regulated is unknown. Agouti may be involved here as it reduces both systemic and follicular cysteine levels<sup>§437</sup>.

The second potential mediator is the OCA2 protein, predicted to be a 12-transmembrane anion-transporter, consistent with its melanosomal membrane location<sup>136</sup>. OCA2 regulates intramelanosomal pH, and this in turn can affect melanin type<sup>33</sup>. One way in which an anion-transporter could assist in the maintenance of a low internal pH would be by transporting a suitable counter-ion to maintain a trans-membrane charge balance. It remains to be seen if this is actually the case, and there are some who advocate a role for OCA2 as a transporter of tyrosine<sup>764</sup>.

Whether agouti signalling does regulate phaeomelanogenesis via cysteine levels, via OCA2, or by an as yet unknown mechanism remains to be determined. What is clear is that there are aspects of agouti signalling yet to be elucidated, its ability to stimulate an influx of Ca<sup>2+</sup>, for one<sup>673</sup>.

## 2.4 Summary

The morphology and biochemical activities of the melanocyte have evolved to enable it to perform a specific function with great efficiency: the regulated production and distribution of melanin within the epidermis. While melanin is photoprotective, it and its precursors are also chemically reactive molecules, so melanogenesis carries a degree of risk of cellular damage. By



---

encapsulating melanogenesis within a specific cell-type and exporting only the final product, the majority of cells need not be exposed to this risk. This exposure is further diminished by regulation of melanogenesis so that melanin is produced only during times when its protective advantage outweighs the inherent risk.

While the melanocyte may contain intrinsic sensors of melanin demand, it is exquisitely sensitive to changes in local context as signalled by cytokines produced by adjacent fibroblasts and keratinocytes. These profoundly influence both the level of melanin production and the proliferation rate of the melanocyte. This enhancement of proliferation is coupled with an inherently high threshold to apoptosis, necessary to provide melanocytes with the durability to survive and function in what of necessity is a harsh environment. Furthermore, the enzyme DCT, essential in melanogenesis, also has anti-apoptotic properties, accentuating this characteristic.

The melanocyte therefore leads a precarious existence, being highly responsive to proliferative cytokines, having a reduced propensity for apoptosis, and existing in an environment where genomic damage is not only extremely likely, but indeed, is a prerequisite of its function. Given these characteristics, the surprising feature is not that neoplastic transformation of melanocytes occurs, but that it is so rare. The study of cell-lines derived from melanoma may lead to a greater understanding of the mechanisms that prevent this change, and the ways in which these fail. This in turn may lead to the development of new and better therapies for melanoma.

# Melanocyte biology (V3)

---

## 2.5 The genetic basis of melanoma

### Introduction

V1 dealt with melanocyte molecular biology quite comprehensively, but the discussion of melanomagenesis was decentralised, and only those aspects relevant to interpretation of experimental results were dealt with in any depth. The very brief review that follows is intended to address this by presenting recent data from the study of melanoma genetics, and by providing cross-referencing to other parts of the thesis where particular aspects are discussed more fully.

### Background

All biological processes are the result of interaction between the expression products of an organism's genome and its environment, in its broadest sense. Thus any change of phenotype implies a change in one or both of these. When phenotypic changes occur without environmental cause, and when these changes are inherited by descendants of a cell or organism, changes to the content or expression of the genome are very strongly implied.

This process is vital in embryogenesis as it allows the creation of differentiated tissues and organ structures. This operates by the successive elimination of expression of parts of the genome. This can have cascading effects since the mechanisms for genetic transcription are themselves encoded by the genome, and are subject to the same selective alterations. Through the modification of expression of such transcription factors, entire suites of genes may have their levels of expression altered or eliminated. Ultimately, just those genes that are required to provide the products necessary to perform functions beneficial to the organism as a whole remain enabled, and their basal level of expression and the potential ways in which this may be modified by changes in the environment are determined. In this way, differentiation is the implementation of the lessons learned by evolution. Different types of cells may have subtly or distinctly different molecular bases for the performance of even core functions, as differences in these may be necessary for them to perform their basic roles, or to respond correctly to their particular environments. In consequence, each type of cell may have a different spectrum of intrinsic vulnerabilities that may upset these finely tuned mechanisms.

As with embryogenesis and tissue differentiation, tumorigenesis involves a heritable change in phenotype, and alterations of genomic content and expression are a virtual certainty. Here, changes to core regulatory processes occur within cells causing them to deviate from their differentiated state. Since the molecular bases for these, and their vulnerabilities, may vary with cell lineage, each tissue or cell type may have its own set of potential paths for tumorigenesis. The ultimate goal of molecular oncopathology is to identify and understand these paths to disease, and hopefully, armed with that knowledge, develop means to detect, prevent, arrest, and correct the effects of these aberrant processes.





The most fundamental source of information available to achieve this is the genetic analysis of naturally occurring tumours and cell-lines derived from them, as this can provide insight into tumorigenesis as it has actually occurred. Coupled with functional knowledge gained from the results of research into cellular molecular physiology, new candidates for involvement may be identified, and using the tools of molecular biology, hypotheses can be tested in model systems, where a specific molecular mechanism is disrupted or otherwise modified on the basis of its involvement being known or suspected. However, artificial systems may well produce artificial results that may have little bearing on, or application to, the natural progression of tumorigenesis. For this reason, greater weight must be placed on the analysis of tumours and derived cell-lines.

### Genes implicated in melanomagenesis

Genes implicated by recent genetic studies of melanoma patients, predisposed kindreds, tumours, and cell-lines are given in Table 2–2. Brief notes on the genes implicated by the strongest evidence follow, broadly organised by the functions of the encoded proteins, as far as these are known.

Gene	Lead author	Year	Observations
APC	Reifenberger <sup>1643</sup>	2002	Exon 15 missense mutation in 1/15 primary melanomas
	Worm <sup>1692</sup>	2004	Truncating mutation with loss of heterozygosity (LOH) in 1/40 cell-lines. Hypermethylation of APC promoter 1A in 5/40 cell-lines and 9/54 biopsies
ATM	Ramsay <sup>1075</sup>	1998	Mutation in radiosensitive melanoma cell-line
BRAF	<i>BRAF</i> codon 600 mutation is perhaps the most common somatic mutation seen in melanoma, but it does not appear to be a melanoma predisposition gene <sup>1564</sup> .		
	Casula <sup>1545</sup>	2004	Mutation in 59% of tumours, but only 0.7% were germ-line (n = 569); in a second series, germ-line mutations were seen in 0.29% of 358 consecutive patients
	Libra <sup>1606</sup>	2005	Mutation in 15/23 primary tumours and 7/12 metastases
	Willmore-Payne <sup>1688</sup>	2005	Mutation in 43/90 melanomas
	James <sup>1580</sup>	2006	No germ-line codon 600 variations in 1 082 melanoma patients, 154 unaffected relatives, and 2 744 controls
	Stark <sup>1666</sup>	2007	Amplification in 3/76 cell-lines
BRCA2	Houlston <sup>540</sup>	1999	Ocular melanoma predisposition among <i>BRCA2</i> families
	Sinilnikova <sup>1661</sup>	1999	Germ-line mutation in 7/62 ocular melanomas
	The Breast Cancer Linkage Consortium <sup>1673</sup>	1999	Relative risk of melanoma in <i>BRCA2</i> carriers or first-degree relatives is 2.6 (n = 3 728)
	Iscovich <sup>1578</sup>	2002	Marginally significant association found between ocular melanoma and 6174 del T mutation
CCND1	Sauter <sup>1650</sup>	2002	Amplification in ALM (8/18), LMM (2/19), and SSM (4/71)
	Yamaura <sup>1694</sup>	2005	Amplification in 6/17 melanomas seen by fluorescence in situ hybridisation (FISH)
	Stark <sup>1666</sup>	2007	Amplification in 3/76 cell-lines
CDC2L1	Candidate gene for 1p36 linked melanoma predisposition.		
	Feng <sup>1560</sup>	2002	Mutation in 1/20 cell-lines and 6/11 1p36 linked melanomas; four polymorphisms found in conserved transcription factor binding sites in promoter
CDK4	<i>CDK4</i> is a recognised minor melanoma predisposition gene.		
	Molgen <sup>1618</sup>	2005	Linkage in only 3 families known; all are R24H
	Goldstein <sup>1568</sup>	2006	Mutation in 5/466 families (2 137 patients) with familial melanoma
CDKN1B	Muthusamy <sup>1624</sup>	2006	Amplification in 3/55 melanomas
	Worm <sup>1452</sup>	2000	Mono-allelic silencing through promoter methylation
	Woenckhaus <sup>1690</sup>	2004	Mutation in 2/53 tumours

Table 2–2: Genes implicated in melanomagenesis (continues overleaf)

## Human metastatic melanoma in vitro

Gene	Lead author	Year	Observations
CDKN2A	CDKN2A is the major known melanoma tumour-suppressor gene. It encodes two proteins that are each tumour-suppressors in their own right <sup>1655</sup> .		
	<i>p16</i>		
	Casula <sup>1545</sup>	2004	Germ-line mutations were seen in 2.5% of 358 consecutive melanoma patients
	Begg <sup>1535</sup>	2005	A large international study of melanoma patients (n = 3 550) indicates a lifetime risk of melanoma for mutation carriers of 28%. Interestingly, while 18 of the probands had 3 or more first-degree relations with melanoma, only 1 carried a CDKN2A mutation.
	Goldstein <sup>1568</sup>	2006	Mutation in 178/466 families (2 137 patients) with familial melanoma
	<i>ARF</i>		
	Randerson-Moor <sup>1076</sup>	2001	Germ-line deletion of exon 1β affecting ARF, but not p16 in melanoma-astrocytoma
	Rizos <sup>1096</sup>	2001	Germ-line 16 bp insertion in exon 1β in melanoma
	Hewitt <sup>1574</sup>	2002	Germ-line mutation resulting in haploinsufficiency
	Goldstein <sup>1568</sup>	2006	Mutation in 7/466 families (2 137 patients) with familial melanoma
CTNNB1	Rubinfeld <sup>1648</sup>	1997	Splice or missense mutations in 6/26 cell-lines increasing protein stability
	Reifenberger <sup>1643</sup>	2002	Mutations in 1/15 primary tumours and 1/22 metastases
	Worm <sup>1692</sup>	2004	Missense mutation in 1/40 cell-lines
CTNNBIP1	Candidate gene for 1p36-linked melanoma predisposition.		
	Reifenberger <sup>1643</sup>	2002	Point mutation altering translation start codon in 1/22 metastases; reduced transcription seen
DDEF1	Ehlers <sup>1556</sup>	2005	Correlation with amplification in uveal melanoma (n = 25); a role in motility suggested
DMD	Korner <sup>1592</sup>	2007	Homozygous and hemizygous partial deletions in 2/55 and 1/55 melanoma cell-lines, respectively; sequence variations in 6/37 cell-lines; knock-down of dystrophin enhanced migration and invasiveness
E2F1	Nelson <sup>1627</sup>	2006	Amplification in 12/12 cell-lines and 9/12 metastases; increased expression in 8/9 cell-lines
EDNRB	Soufir <sup>1664</sup>	2005	Germ-line mutation in 15/137 melanoma patients, statistically significant with odds ratio of ~20
EGF	Amend <sup>1531</sup>	2004	No association between A61G polymorphism and cancer risk (n = 330)
	Okamoto <sup>1629</sup>	2006	A61G polymorphism correlates with disease-free period (n = 130)
EGFR	Udart <sup>1676</sup>	2001	mRNA expression and FISH suggests increased copy number
	Chin <sup>1547</sup>	2006	Mutation in melanoma not reported
ERCC1	Povey <sup>1640</sup>	2007	Polymorphism associated with melanoma (n = 596)
ERCC2	Han <sup>1573</sup>	2005	D312N and K751Q associated with melanoma (n = 219)
	Debniak <sup>1550</sup>	2006	K751Q/G156G genotype over-represented in late-onset melanoma
	Li <sup>1602</sup>	2006	Polymorphisms associated with increased melanoma risk (n = 602)
	Millikan <sup>1615</sup>	2006	N312N and Q751Q genotypes associated with melanoma (n = 2 485 primary melanomas; n = 1 238 secondary or higher order melanomas)
ERCC4	Povey <sup>1640</sup>	2007	Polymorphism associated with melanoma (n = 596)
FAS	Li <sup>1603</sup>	2006	Increased melanoma risk associated with some promoter polymorphisms
FASLG	Li <sup>1603</sup>	2006	Increased melanoma risk associated with some polymorphisms
HDAC4	Stark <sup>1666</sup>	2007	Deletion in 3/76 cell-lines
HMOX1	Okamoto <sup>1628</sup>	2006	~2-fold increase in risk of melanoma associated with short microsatellite repeat in promoter thought to modulate level of transcription
ICAM1	Howell <sup>1576</sup>	2005	No association between codon 241 status and risk found
	Vinceti <sup>1682</sup>	2006	R241 allele associated with ~4-fold increased risk of melanoma
ING1	Campos <sup>1543</sup>	2004	Missense mutations in 9/46 melanoma biopsies
	Stark <sup>1667</sup>	2006	Mutation in 0/83 primary melanomas and 0/55 cell-lines
KIT	Willmore-Payne <sup>1688</sup>	2005	Activating mutation in 2/74 metastatic melanomas
	Curtin <sup>1548</sup>	2006	Amplification or mutation in ~30% of primary tumours (n = 102)

Table 2-2: (continued)



Gene	Lead author	Year	Observations
MC1R	Palmer <sup>1633</sup>	2000	Variant alleles more prevalent in those with melanoma (n = 460)
	Kennedy <sup>1587</sup>	2001	Carriers of any of four variants investigated had relative risk for melanoma of 2.7. Those with D84E had relative risk of 16 (n = 123)
	Landi <sup>1595</sup>	2005	Carriers of variant alleles have 2-4-fold increased risk of melanoma (n = 267)
	Mossner <sup>1621</sup>	2007	Polymorphisms associated with melanoma (n = 422)
MDM2	Muthusamy <sup>1624</sup>	2006	Amplification in 3/55 melanomas
MET	Puri <sup>1641</sup>	2007	N948S mutation found in 3/5 cell-lines; R988C mutation in 1/14 melanomas
MITF	Garraway <sup>1565</sup>	2005	Amplification seen by FISH in 2/19 primary and 27/160 metastatic tumours after identification as candidate by high-density single nucleotide polymorphism (SNP) array analysis
	Stark <sup>1666</sup>	2007	Amplification in 9/76 cell-lines
MLH1	Castiglia <sup>1544</sup>	2003	Biallelic inactivation in one melanoma
	Korabiowska <sup>1591</sup>	2006	Deletion of exon 15 in 22/86 and exon 16 in 24/86 melanomas
MSH2	Korabiowska <sup>1591</sup>	2006	Deletion of exon 12 in 26/86 and exon 13 in 25/86 melanomas
MYC	Kraehn <sup>714</sup>	2001	Gene amplification associated with advanced cutaneous melanoma
	Koynova <sup>1593</sup>	2007	Amplification associated with lower metastatic potential in patients with CDKN2A deletion
NBN	Debniak <sup>1549</sup>	2003	NBS founder mutation found in 2/80 consecutive melanoma patients and 3/530 controls; this was not statistically significant, but both melanomas had lost the normal allele
NEDD9	Kim <sup>1589</sup>	2006	Amplified in 23/63 metastatic melanomas and 12/35 cell-lines. Increased expression in metastatic melanoma shown by qRT-PCR and protein analysis.
NF1	Guillot <sup>1571</sup>	2004	Review of 11 cases of melanoma/neurofibromatosis type 1
	Rubben <sup>1647</sup>	2006	Loss of normal allele in melanoma from person with hereditary neurofibromatosis
NME2	Hamby <sup>1572</sup>	1995	Mutation identified in one of a pair of autologous melanoma cell-lines; the mutation was in the cell-line with the higher metastatic potential
NOS1	Li <sup>1601</sup>	2007	Marginally significant association between two promoter polymorphisms and risk of melanoma (n= 602)
NRAS	Demunter <sup>1551</sup>	2001	Mutation in 23/69 primary and 9/35 metastatic tumours
	Stark <sup>1666</sup>	2007	Amplification in 3/76 cell-lines
OCA2	Jannot <sup>1581</sup>	2005	Polymorphism associated with melanoma (n = 113)
PPP2R1A	Calin <sup>1542</sup>	2000	Mutation found in 1/14 cell-lines
PTEN	Boni <sup>115</sup>	1998	No LOH or aberrant SSCP pattern in 23 primary and 17 metastatic melanomas
	Celebi <sup>170</sup>	2000	LOH in 7/21 and sequence alterations in 4/21 metastatic melanomas
	Poetsch <sup>1038</sup>	2001	Some intronic alterations, and two amino acid changes, but only in late-stage melanoma
	Mirmohammadsadegh <sup>1616</sup>	2006	Promoter methylation in 62% of circulating DNA from metastatic melanoma patients (n = 37), correlated with low expression in corresponding tumours (n = 21)
	Stark <sup>1666</sup>	2007	Deletion in 8/76 cell-lines
PTPRD	Stark <sup>1666</sup>	2007	Deletion in 7/76 cell-lines
RB1	Bartkova <sup>73</sup>	1996	Hemizygous deletion and mutation in melanoma cell-lines
	Moll <sup>903</sup>	1997	Of the 243 second tumours seen among 5 856 retinoblastoma survivors, 18 were melanoma
STK11	Guldberg <sup>451</sup>	1999	Two somatic mutations in 35 sporadic melanoma patients
	Rowan <sup>1114</sup>	1999	Mutations in 2/50 cell-lines, primary, and metastatic tumours
TFAP2A	Woenckhaus <sup>1691</sup>	2003	Mutations in 4/50 tumours
TP53	Akslen <sup>21</sup>	1998	Mutation in 7/46 nodular melanomas
	Zerp <sup>1506</sup>	1999	Mutation in 17/81 melanomas; frequency in metastases lower than in primaries, and only in skin and not internal metastases
	Parmar <sup>1002</sup>	2000	Non-conservative mutation in 2/15 melanoma cell-lines
	Shen <sup>1657</sup>	2003	Increased risk in codon R72R homozygotes (n = 289)
	Soto Martinez <sup>1663</sup>	2005	Variations seen in 8/39 tumours

Table 2-2: (continued)

## Human metastatic melanoma in vitro

Gene	Lead author	Year	Observations
TP73	Candidate gene for 1p36 linked melanoma predisposition.		
	Tuve <sup>1675</sup>	2004	Splice variants giving rise to dominant-negative proteins found significantly more frequently in metastases (n = 19)
VDR	Povey <sup>1640</sup>	2007	Polymorphism associated with melanoma (n = 596)
VEGFA	Howell <sup>1575</sup>	2002	Promoter variations associated with melanoma, but also with early stage disease (n = 152)
WRN	Shibuya <sup>1638</sup>	2005	Three primary melanomas in a woman with Werner Syndrome
XPA	Sidwell <sup>1660</sup>	2006	Spindle cell melanoma in xeroderma pigmentosum patient with XPA mutation
XPC	Blankenburg <sup>1541</sup>	2005	Intron 9 poly-AT polymorphism, intron 11 -6A, and exon 15 2920C variants associated with melanoma (n=294)
XRCC3	Winsey <sup>1689</sup>	2000	Exon 7 T allele associated with melanoma (n = 211)
	Bertram <sup>1537</sup>	2004	Exon 7 T allele study not corroborated

The genes listed are those implicated by the discovery of deletion, mutation, transcriptional silencing, haplotype association, or amplification in studies using melanoma patients, members of familial melanoma kindreds, or human melanoma cell-lines. Studies involving changed protein expression only, or from animal models alone are not included. Where evidence is equivocal studies showing lack of involvement are also listed. "Associated" implies statistical significance.

**Table 2–2 (concluded): Genes implicated in melanomagenesis**

### Genomic integrity

The melanocyte's primary recognised function is to produce melanin. One evolutionary advantage for this is that it appears to provide surrounding cells with protection against genomic damage resulting principally from solar radiation. Since melanin itself is a reactive molecule capable of causing genetic damage, the system for its production is inducible upon detection of the type of genetic damage against which it offers protection. This places the melanocyte in a precarious situation in that it must both experience, and survive genetic damage in order to carry out its primary function. This implies that as a result of its heritage, mechanisms in melanocytes promoting apoptosis in response to genetic damage must be attenuated, and thus melanocytes may be uniquely prone to mutation.

When compared with tumours from other tissues, melanomas might be expected to harbour a greater number of genetic defects relating to DNA repair mechanisms, particularly nucleotide excision repair, since the effects of their failure would closely simulate the melanogenic trigger, and thus must not result in apoptosis.

In Table 2–2, are listed the genes *ERCC1*, *ERCC2*, *ERCC4*, *WRN*, *XPA*, *XPC*, and *XRCC3*, encoding proteins involved in nucleotide excision repair, and in addition, *MLH1*, *MSH2*, *BRCA2*, *NBN*, whose products participate in DNA mismatch repair and the detection and repair of double-stranded DNA breaks. *ATM*, which encodes a kinase linking DNA repair with cell-cycle arrest as part of the BASC also appears in the list.

Maintenance of the integrity of the cellular genome as a whole, rather than at the DNA level, is chiefly the province of the centrosome. The work to be described in Chapter 5 led to a prediction that centrosomal dysregulation may be important in the generation of the aneuploidy and heteroploidy that is often seen in melanoma, and the validity of this was established by the work described in Chapter 6. Several genes encoding proteins known or suspected to play a role in centrosome regulation are listed in Table 2–2: *BRCA2*, *CDKN1B*, *CDKN2A*, *HRAS*, *MDM2*, *TP53*, and *XRCC3*. Notes and references relating to evidence for

See Appendix I for a brief review of BASC, the BRCA1-associated genome surveillance complex.

A substantial review of centrosomal function and regulation is given in Appendix J.



involvement of the encoded proteins in centrosomal regulation are given in Table J–1, with the exception of *CDKN2A*, as its involvement was not known at the time of writing. McDermott et al.<sup>1610</sup> have shown that p16 may play a very significant role in centrosomal regulation, with supernumerary centrosomes and aneuploidy resulting from its functional loss. The significance of this for melanoma in particular does not appear to have been reported.

### Concerted changes of gene expression

In a fashion similar to the programming of cell fate during differentiation, when entire suites of genes can be disabled by changes in transcription factor expression, so can multiple coordinated changes be brought about during tumorigenesis by the modification of transcription factor expression or function. Several of the genes listed in Table 2–2 encode transcription factors.

#### CTNNB1

The  $\beta$ -catenin transcription factor has several target genes that, if expressed, tend to promote proliferation. Perhaps most notable among these are *CCND1*, the gene for Cyclin-D1, a key regulator of environmentally determined cellular proliferation and arrest, and *MYC*, a well-known oncogenic transcription factor. The ability for  $\beta$ -catenin to activate transcription is regulated by the binding of an inhibitory protein, ICAT, encoded by *CTNNBIP1*. An additional transcriptional target very important in melanocytes, and with growing relevance to melanoma is *MITF*<sup>1597</sup>. All of these genes appear in Table 2–2, but in some cases the functional significance of the findings listed is not yet known.

#### MITF

*MITF* encodes a melanocyte specific transcription factor that is a major determinant of phenotype<sup>1600</sup>. Its effects are more wide-ranging, however, and include suppressing apoptosis through induction of the genes for the transcriptional repressor *TBX2*, the anti-apoptotic protein *BCL2*, and the gene for the melanocyte-specific enzyme *DCT*, which has anti-apoptotic properties {2–11}. *MITF* also regulates *MET*<sup>1611</sup>, the gene for the HGF receptor, normally expressed by melanocytes (see below). Finally, *MITF* activation can reduce E-cadherin expression and thereby lessen the cell's requirements for substrate adhesion, also aiding metastasis<sup>777</sup>.

#### MYC

*MYC*, a transcriptional target of *MITF*, itself encodes a transcription factor, and among its targets are very many genes with potential roles in tumorigenesis. These include *BRCA1*<sup>1612</sup>, *CDC2*<sup>1612</sup>, *CDC2L1*<sup>1612</sup>, *CCNA1*<sup>1582</sup>, *CCND2*<sup>124</sup>, *CCNE1*<sup>1635</sup>, *ODC1*<sup>1536</sup>, *CDC25A*<sup>1563</sup>, *E2F*<sup>1598</sup>, *TERT*<sup>1693</sup>, and *TP53*<sup>1646</sup>. It also binds the *CDK4*<sup>1612</sup> promoter, but the functional significance of this appears unknown. It can function as a transcriptional repressor<sup>1684</sup>, and in this capacity can prevent p53-mediated transcription of *CDKN1A* and the production of the p21 CKI, effectively constraining p53 to initiate apoptosis rather than cell-cycle arrest<sup>1653</sup>; and SMAD-mediated induction of *CDKN2B*, preventing cell-cycle arrest in response to TGF $\beta$ <sup>1179 1559</sup>. *MYC* and some of

its functional targets are to be found in Table 2–2: *CDC2*, *CDC2L1*, *CDK4*, *CDKN2A*, *E2F1*, and *TP53*. Also present is its repressor<sup>492</sup>, *APC*.

### TP53

The transcription factor encoded by *TP53*, p53, is a crucial component of the apoptotic response in most cells, and the need to disable it for tumorigenesis to occur has led to it being perhaps the most commonly mutated gene in all cancer types<sup>®1669</sup>. Due to the specific functional requirements of the melanocyte, discussed above, the generic apoptotic mechanisms that operate in most cell types are probably significantly modified in them. This is perhaps most clearly illustrated with *TP53*, which, in contrast to most other cancers, is only rarely mutated in melanoma. This may indicate that p53-mediated apoptosis is less of a barrier to tumorigenesis in melanocytes, or that mechanisms other than mutation of *TP53* operate to overcome it. In addition to *TP53* itself, Table 2–2 contains several genes whose encoded proteins modify p53 activity: *CDKN2A*, in its second role encoding ARF, *ING1*, *MDM2*, and *TP73*.

In the ARF, MDM2, p53 group, a common theme is proteolytic regulation. MDM2, whose gene is itself a transcriptional target of p53, binds p53 and promotes its destruction by proteolysis. In this way, amplification of *MDM2*, as has been reported in melanoma {Table 2–2}, could reduce the levels of p53 present in the cell and so attenuate the apoptotic process. However, MDM2 is similarly targeted by ARF, so mutation, deletion, or transcriptional silencing of its gene, *CDKN2A*, would have the same effect. As noted in the table, *CDKN2A* is a melanoma tumour-suppressor gene of the first order, primarily, it is thought, because of its encoding of the CKI p16. However, due to the dual encoding property of *CDKN2A*, rare, if not unique in humans, what affects the production of p16 and enhances proliferation is also very likely to affect production of ARF, and attenuate apoptosis. This may in part explain why p53 mutation is relatively rare in melanoma: the function that would be achieved by this is already very often served by the loss of ARF.

See 'Inferred characteristics of p53' on page J–21 for more on p53 function and regulation.

While the data concerning the status of *ING1* in melanoma are sparse and equivocal, if alterations do prove to be occurring, then p53 functions, including those governing apoptosis, may be abnormal due to changes in its acetylation<sup>®1558</sup>.

### TP73

This gene encodes a set of alternatively spliced transcription factors, similar to p53, but with significant differences<sup>®1608</sup>. One feature is the production of dominant negative splice variants with the capacity to inhibit p53. The molecular biology of p73 is very complex, and while modification of the apoptotic mechanisms orchestrated by p53 may be occurring, alterations to  $\beta$ -catenin channel signalling may prove to be more significant. The observations that *TP53* mutation is less frequent in metastases, while the expression of dominant negative p73 splice variants is greater are interesting, but their joint significance is unclear.



Further discussion on E2F transcription factors can be found on pages H-12 and H-24.

## E2F1

E2F family transcription factors regulate genes involved in cellular proliferation and apoptosis, and in particular, E2F1 is a functional target of repression by pRB through which cell-cycle arrest may be imposed. Amplification of *E2F1* in melanoma has been reported {Table 2-2}, but there appear to have been no reports of mutational analysis of this gene in melanoma. More broadly, mutation seems rare, as none was found in a panel of 406 human tumours, not including melanoma<sup>932</sup>. In theory though, mutations affecting binding with pRB might be expected, and an examination in melanoma is warranted. E2F1 binds pRB through the latter's large pocket domain, and while E2F proteins do not contain the LXCXE motif associated with this binding mode, E2F1 and E2F4 both contain the similar LXSXE motif thought to be functionally similar<sup>301</sup>, and the corresponding coding part of the *E2F1* gene would make a sensible initial subject for investigation {See 'LXCXE relatives' on page H-5}. Additionally, the 18 amino acid region identified by Shan et al.<sup>1654</sup> could be explored.

## TFAP2A

This gene encodes the AP-2 transcription factor that is implicated in the regulation of several genes with possible significance to melanomagenesis<sup>1533</sup>. These include *CDH1*, *CDKN1A*, *FAS*, *KIT* and *VEGFA*. This set of targets suggests an important role in the processes of proliferation control, apoptosis, angiogenesis, and metastasis.

## Altered environmental responses

Direct alteration of transcription factors can have multiple effects, but this can also occur when the regulation of intact transcription factors is altered, by the interactions among ARF, MDM2, and p53, for example. Dysregulation of transcription factors can also result from alterations to the signal transduction channels that lead to them and implement cellular responses to both internal and external events. Genes for many of the components of these channels occur in Table 2-2.

### *Growth factors and their receptors*

Of chief importance in the melanocytic context are *KIT* and *EDNRB*, which encode respectively a receptor tyrosine kinase and a G-protein-coupled receptor. The effects of activation of these receptors and their modes of signal transduction are described in Section 2.3.

The significance of alterations to *KIT* is not clear, and they may play different roles in different tumours or in different stages of tumorigenesis. *KIT* signalling in melanocytes can contribute to survival and initiate melanogenesis, but it can also cause apoptosis. Most often, *KIT* expression is lost in advanced tumours, but there seems to be a subset, perhaps where the apoptotic aspect is disabled by another means, where *KIT* expression remains high or constitutive activation through mutation is seen.

Endothelin signalling through *EDNRB* can contribute to proliferation and cellular migration, giving altered activation a potential role in invasion. It also enhances the cell's sensitivity to  $\alpha$ -MSH, an adrenocorticotrophic hormone that binds the MC1R receptor.

Signal transduction channels are illustrated in Figure 2-2 (RTKs) and Figure 2-3 (GPCRs). The associated notes give more detail.

Activation of the MC1R receptor causes increased transcription of MITF, and carriage of variant receptors appears to increase risk of *BRAF* mutation<sup>1594</sup> (see below), although the mechanism for this is not known<sup>1552</sup>. Further studies into the functional significance of the polymorphic receptors are warranted.

Vitamin D is produced in the skin, and so local levels around melanocytes may be high. The receptor for this, encoded by *VDR*, is a transcription factor whose targets are implicated in the regulation of many processes. Signalling can reduce proliferation through effects on Cyclin-D and CKIs, such as p21 and p27, and it can also induce apoptosis. Involvement in cell adhesion is also known, giving it a possible role in the regulation of metastasis. Certainly it is a plausible candidate as a significant contributor to melanomagenesis, but as yet the data are too sparse to allow any conclusions to be drawn<sup>1631</sup>.

The growth factor EGF is implicated in melanocyte proliferation, so the reports relating to this and its receptor EGFR are interesting, but equivocal, and their significance is yet to be established. The role played by other EGFR ligands, such as TGF $\alpha$  is also worthy of investigation.

*MET* is the gene for the receptor for the growth factor HGF<sup>1667</sup> and is a transcriptional target of MITF<sup>1538</sup>. *MET* signalling promotes proliferation in melanocytes<sup>1083</sup> and this is usually achieved through paracrine interactions, but melanomas frequently produce HGF<sup>1611</sup>, thus establishing autocrine stimulation<sup>777</sup>. This may have implications not just for proliferation, but also for metastasis<sup>1561 1632</sup>, as any dependence on adjacent tissues for stimulatory HGF will be removed, and such a role would be consistent with the higher levels of *MET* expression seen in later stage tumours<sup>1625</sup>. It has also been suggested to play a role in protection against apoptosis<sup>1538</sup>.

### **Signal transduction elements**

Aberrant constitutive activation of the RAS/RAF/MAPK signalling channel is a common feature of many types of cancer<sup>1696</sup>, principally as a means of driving cellular proliferation. Perhaps the most significant advance in the understanding of melanomagenesis in recent years has been the recognition of *BRAF* as a key target for somatic mutation, with constitutive signalling being the typical result. Its significance is at least two-fold in that it can cause elevation of Cyclin-D1 levels even in the absence of cellular adhesion<sup>1539</sup>, and by promoting the phosphorylation of the MITF transcription factor, which enables it to bind its p300 cofactor and become active.

The *MITF* gene and its protein product MITF are both targets of another major signal transduction channel. Signalling via PI3K/AKT1 results in activation of genes containing the CRE motif, and these include *MITF*. Simultaneously, the GSK3 $\beta$  kinase is phosphorylated and disabled, preventing it from phosphorylating and inactivating the MITF that is produced. Thus constitutive activation of both the RAS/RAF channel and the PI3K channel will ensure that any MITF present is competent both to bind DNA by virtue of not having been phosphorylated by GSK3 $\beta$ , and to bind its cofactor p300, by virtue of phosphorylation by AKT1. Furthermore,

Figure 2-2 illustrates these events, and the associated notes give more detail.





See Appendix H for a review of the pRB subsystem.

See H.6 for more about pRB and melanoma.

See 'Regulation by inhibition' on page J-15 for more on p27 function and regulation.

inhibition of GSK3 $\beta$  will increase the stability of  $\beta$ -catenin elevating transcription of *MITF* and thus increasing the amount of MITF available to be activated. Simultaneously, the levels of Cyclin-D1 will rise both from increased  $\beta$ -catenin-mediated transcription of *CCND1*, and also from increased protein stability due to the inhibition of GSK3 $\beta$ .

In Table 2–2 the genes for several elements of these signal transduction channels are listed: *BRAF*, *NRAS*, and *PTEN*. When functional, the first two operate to activate RAS/RAF channel signalling, while the PTEN phosphatase opposes PI3K and dampens signalling through that channel. Consistent with the tumorigenic advantage to be had by unconstrained signalling through both channels, activating mutations and amplification are seen for the first pair, while deletion or loss of expression are seen for *PTEN*.

### Regulation of proliferation

The critical regulator of proliferation that appears to be lost in melanoma, like many cancers, is the pRB-mediated subsystem<sup>®1604</sup>, wherein unphosphorylated pRB is able to bind and hold inactive a host of proteins including members of the E2F family, whose targets are genes that initiate and maintain progression through the cell-cycle. Table 2–2 lists the gene for pRB itself, *RB1*, the gene for the kinase responsible for its phosphorylation, and thus the release of cells from proliferative inhibition, *CDK4*<sup>1529</sup>, and *CDKN2A*<sup>355</sup>, which encodes p16, a specific inhibitor of CDK4. These three constitute the known melanoma predisposition genes, and by far the most important is *CDKN2A*. Also present in Table 2–2 are *CCND1* and *CDKN1B*, whose encoded proteins also regulate the cell-cycle primarily through pRB. The first encodes Cyclin-D1, the activating partner of CDK4, so the amplification seen is consistent with pRB being the functional target. *CDKN1B* encodes the CKI p27 that has specificity for CDK2. In conjunction with its activating Cyclin-A or Cyclin-E partner, this kinase phosphorylates pRB during S-phase, but it also has other targets that drive cell-cycle progression.

### Regulation of apoptosis

Hyperplasia is an essential aspect of tumorigenesis, for without it, there could be no tumour. Traditionally, hyperplasia has been considered to result from aberrant proliferation of cells, and indeed this is a very significant contributor to it, but failure of cells to die by apoptosis can also contribute to hyperplasia. More importantly perhaps, many mechanisms intended to remove aberrant cells do so by initiating an apoptotic programme in the cell. These may be purely internal, for example in response to the detection of irreparable DNA damage, may be triggered by an inappropriate cellular context, a process termed anoikis, or initiated from outside the cell via signal transduction, as occurs through operation of immune system surveillance. Given the magnitude of the derangements that must occur in a cell during tumorigenesis, an intact apoptotic mechanism would very likely be triggered and the cell would die, so aberrations in genes whose products participate in the apoptotic process are virtually universal in tumours. Genes encoding proteins involved in apoptosis listed in Table 2–2 include *TP53*, *CDKN2A*, *FAS*, *FASLG*, *ING1*, *MDM2*, and *TP73*. All but *FAS* and *FASLG* were discussed above.

The FAS/FASLG system implements apoptosis directed from outside the cell, typically in conjunction with T-lymphocytes, and the mechanism is independent of p53. The role these play in melanomagenesis is currently unclear, as is the significance of any polymorphisms affecting their genes.

### **Promotion of angiogenesis**

Very little is known concerning how melanoma promotes angiogenesis. This is a critical area since connection of the tumour to the vasculature provides a channel for metastasis, and melanoma tumours appear to gain metastatic potential very early in their development. Given the very much poorer prognosis for metastatic melanoma as opposed to melanoma in situ, therapy directed at preventing angiogenesis may be helpful, but there are practical limitations to this. At presentation, either a tumour has metastasised or it has not. If it has not, and is excised, angiogenesis becomes irrelevant; if it has metastasised, then the damage is already done. A thin opportunity for an anti-angiogenic agent exists by way of prophylaxis. If a specific and safe agent were developed, it could be routinely used by those thought to be at most risk through genetic predisposition or environmental exposure. This might prevent any melanoma that does occur from metastasising before it can be detected and removed.

Of the genes listed in Table 2–2 only one is strongly implicated in angiogenesis, *VEGFA*<sup>1670</sup>. Ectopic expression of *AKT1* in experimental melanomas can result in increased production of VEGF and this correlates with a transition from radial to vertical growth of tumours<sup>1569</sup>. As *AKT1* is on the signal transduction path for *KIT*, the receptor for the major melanocyte cytokine *SCF*, alterations in receptor expression or activation may lead to increased VEGF production, and such changes do occur (see above).

### **Metastatic progression**

A large measure of the seriousness of cancer is that it can become a disseminated disease and affect bodily functions in tissues both distant from its point of origin and different in type. For melanoma, the progression to metastasis tends to occur quite rapidly, and from primary tumours of only small size. Given the poor prognosis for metastatic melanoma, any advances in the understanding of this process have significant therapeutic potential.

The implication in melanomagenesis of *ICAM1*, which encodes an adhesion protein, and *DDEF1*, whose encoded protein may have a role in cellular motility, offer small increments of knowledge. In contrast, the study of Kim et al.<sup>1589</sup> is a brilliant example of the application of modern techniques to addressing this poorly understood area, and their results may have very significant implications for therapy. After selecting for metastatic phenotype in an inducible mouse melanoma model, the *Nedd9* gene was identified as a candidate metastasis regulatory gene by comparative genomic hybridisation analysis. Investigation of the corresponding human locus revealed it to be amplified in 23 of 63 metastatic melanomas and 12 of 35 cell-lines, and increased expression in metastatic melanoma was shown by qRT-PCR and protein analysis. Finally, gene knock-down experiments were able to attenuate the metastatic potential of the original selected cell-line, and ectopic expression of *NEDD9* conferred a metastatic



potential on primary melanocytes. This extraordinary study has all the hallmarks of a breakthrough, and offers promise for the targeted development of an antimetastatic therapy for melanoma.

### **Conclusion**

The principal drivers of melanomagenesis are constitutive signalling through RAS/RAF and PI3K channels leading to activation of AP-2,  $\beta$ -catenin, MITF, and MYC transcription factors and the aberrant expression of their target genes. These changes must be coupled with suppression of regulation on proliferation, typically by disrupting the pRB subsystem, and attenuation of the apoptotic response that generally follows from continuous stimulation.

The dual-encoding *CDKN2A* gene is quite clearly the most significant melanoma tumour-suppressor gene. Its protein products function independently in two of the key subsystems whose disruption is essential in tumorigenesis: proliferation and apoptosis. The discovery of a functional role for p16 in centrosome regulation raises the importance of *CDKN2A* even further, as it provides a partial explanation for the high level of genomic heterogeneity that is seen in melanoma, and this is something thought to contribute both to the accumulation of genetic changes that allow tumorigenesis to proceed, and the resistance these tumours have to conventional therapies.

The gene responsible for 1p36-linked melanoma predisposition kindreds has not been identified, although several plausible candidates exist. The 2005 study of Begg et al.<sup>1535</sup>, in which it was found that only 1/18 melanoma patients with three or more affected first-degree relatives carried a *CDKN2A* mutation, certainly implies that one or more important melanoma predisposition genes remain to be identified. Their discovery may well shed more light on the molecular processes involved and offer new directions for therapeutic intervention, as exemplified by Kim et al.<sup>1589</sup> in their identification of NEDD9 as a potential target of great promise.



### 3.1 Establishment

For many years, the Auckland Cancer Society Research Centre (ACSRC) has been establishing cell-lines from tumour material excised during surgical resection, including many derived from metastatic melanoma. These were designated NZM 1 to NZM15 in the order of their establishment. Table 3–1 gives general data about the origin of each cell-line, and includes chromosome counts obtained during initial karyotyping, and an indication of whether the cell-line produces readily discernible quantities of melanin in culture. NZM8 is omitted, as it is no longer extant. To date, these have been characterised in terms of their in vitro response to irradiation<sup>846</sup> and chemotherapeutic agents<sup>844 845</sup>, karyotype<sup>846 966</sup>, and *TP53* status<sup>1002</sup>. They are an obvious resource for the furtherance of our understanding of the commonalities among melanomas with a view to developing an effective therapy.

Cell-line	Patient age (sex)	Tumour site	Chromosome number	Melanotic
NZM1	47 (M)	Obturator lymph node	71–78 <sup>846</sup>	No
NZM2		Deep iliac lymph node	71–78 <sup>846</sup>	No
NZM3	69 (M)	Cervical lymph node	78–95 <sup>846</sup>	No
NZM4	56 (M)	Malignant ascites	110–120 <sup>846</sup>	No
NZM5	79 (M)	Axillary lymph node	40–43 <sup>846</sup>	Yes
NZM6	72 (F)	Small intestine	79–88 <sup>846</sup>	No
NZM7	36 (M)	Cervical lymph node	55–59 <sup>846</sup>	Yes
NZM7.2	Sub-clone of NZM7		n.a.	Yes
NZM7.4	Sub-clone of NZM7		n.a.	No
NZM9	80 (M)	Axillary lymph node	~84 <sup>966</sup>	No
NZM10	52 (M)	Lung	n.a.	No
NZM10.1	Sub-clone of NZM10		n.a.	No
NZM11	74 (M)	Subcutaneous lesion	~78 <sup>966</sup>	No
NZM12	19 (M)	Small intestine	~49, ~108 <sup>966</sup>	No
NZM13	81 (F)	Neck nodule	~88 <sup>966</sup>	No
NZM14	72 (M)	Thigh skeletal muscle	~51 <sup>966</sup>	No
NZM15	63 (M)	Subcutaneous neck nodule	~76 <sup>966</sup>	No

Table 3–1: ACSRC metastatic melanoma cell-lines studied

### 3.2 Lack of primary tumour material and paired normal tissue

Early stage melanoma usually presents as an atypical mole, and in the New Zealand context is often simply excised by a General Practitioner. Where melanoma is suspected, the tissue is fixed and sent for histological analysis. Therefore, without enlisting the cooperation of General Practitioners, and, bearing in mind that melanoma is rare and most excised lesions will be benign, it is a difficult task to obtain primary material. It is also the practice of the hospitals with which the ACSRC collaborates to send resected primary melanomas for histological study in their entirety, preventing development of cell-lines from such material. Consequently, all of the melanoma cell-lines developed at the ACSRC are from metastases. One implication of this is that they may have limited value in the study of early melanoma development.

The commencement of the drive to establish tumour cell-lines predated the boom that has occurred in the field of molecular biology, particularly molecular genetics, and the protocols in

place did not anticipate the great value that matched normal tissue or DNA from blood might provide; consequently, no such material is available. It is therefore not possible to state whether a DNA sequence variation found in a cell-line is an insignificant polymorphism present in normal tissue, and similarly, the utility of microsatellite markers for genetic analysis is reduced. Now, wherever possible, a blood sample is also obtained from the patient.

### **3.3 The relationship between NZM1 and NZM2**

These two cell-lines were derived from the same patient, with NZM1 being established first, and NZM2 being established from material resected four weeks later. As such, they form a useful resource for the investigation of tumour diversity and of on-going changes in late-stage disease.

### **3.4 Sub-cloning**

Cytogenetic studies of these cell-lines have shown them to be highly heterogeneous in terms of chromosomal content {Table 3-1}, with this being reported as a range. As part of their initial characterisation, cellular DNA content was assessed by flow cytometry, the results of this investigation being reported in Chapter 5. To explain fully the cell-line nomenclature used here necessitates the early presentation of some data from that chapter.

Previous flow cytometric analysis of NZM7<sup>180</sup> brought to light the fact that it contained multiple populations differing in base DNA content, a phenomenon known as heteroploidy, rendering mathematical modelling of cell-cycle phasing impossible without the imposition of artificial constraints, a facility not present in the available Modfit LT software in any case. Since such an analysis was to be required in the determination of the integrity of the G<sub>1</sub> restriction point, firstly, NZM7 was excluded from the experimental panel as unsuitable, and secondly, sub-clones of NZM7 were isolated by the propagation of individual cells in a quest to obtain a cell-line of uniform ploidy for use. Ultimately nine were established and these were designated NZM7.1 to NZM7.9. Of these, two have been the subject of further investigation and are included in this study, namely NZM7.2 and NZM7.4. While they have very similar cellular DNA content, they differ markedly in the production of melanin.

Similarly, during the course of this work, NZM10 was found to be heteroploid, leading to the establishment of NZM10.1, however in this case, since the work had been commenced with the parental NZM10 cell-line in the subject panel, it was retained.

The further investigation of the extent of heteroploidy within the NZM cell-lines, together with the quest for a molecular explanation for this, form significant parts of the work at hand.



---

# The NZM cell-lines (V3)

---

## 3.5 Extension of the existing material

### The NZM cell-lines in culture

#### *General characteristics*

The NZM cell-lines are diverse in many respects but do have a number of common characteristics, albeit with variation in these too. Generally, they are easy to maintain in culture {Method 2} and grow well in alpha minimal essential medium ( $\alpha$ MEM) supplemented by fetal calf serum (FCS). For the work described here, FCS is used at 10% v/v, but more recent practice in the ACSRC has been to use 5% v/v, with supplemental insulin, transferrin, and selenium. The NZM cell-lines are adherent, and passaging is by trypsinisation for 5 min {Method 4} with reseeding of approximately 10% of the cells. Weekly inspection to determine if passaging is required is satisfactory, and where not required, medium replacement is undertaken.

Morphologically, the predominant cell shape among the NZM cell-lines is the bipolar spindle, but there is considerable variation in the length of the cells. Other morphologies exist including round cells, those with a large cell body and a few dendritic processes, and polygonal cells that form a dense tiling. Multiple morphologies can exist in some cell-lines either simultaneously, or appearing after increased time in culture or at higher cell density.

Cell pellets tend to be off-white in colour, with some notable exceptions: where there is a high level of melanin production by the cells, brown to black pellets are seen.

Standard cryopreservation techniques are suitable for the NZMs {Method 5}. Storage involves the addition of dimethylsulphoxide (DMSO)-containing medium followed by slow cooling to  $-80^{\circ}\text{C}$ , and then submersion in liquid nitrogen. Recovery is by rapid warming to  $37^{\circ}\text{C}$  and washing in fresh medium before seeding {Method 6}.

#### *Idiosyncrasies of NZM cell-lines in culture*

In keeping with their common origin, NZM1 and NZM2 are indistinguishable in culture. Both are relatively slow growing with large cell bodies and several relatively long dendritic processes that are often branched once, or rarely twice. The cells maintain contact with one another through these processes and tend not to crowd together. Consequently, density at confluence is initially quite low, but does increase as cells pack more closely with continuing culture.

NZM3 cells are predominantly bipolar spindles, but tripolar spindles are seen frequently. Cultures grow as a network of interconnected dense islands of cells leaving voids on the substrate, suggestive of limited mobility.

NZM4 grows particularly uniformly and cleanly in culture, arresting at confluence and being able to survive in that state for weeks, provided that the culture medium is replaced weekly.

Cultures adopt a network growth pattern like NZM3, with interconnected islands of densely packed cells. The cells are almost entirely bipolar spindles with a large central cell body that appears very bright by phase contrast microscopy.

NZM5 has an appearance unique within the panel of cell-lines studied here. It has very small, very poorly adherent cells that typically appear by phase contrast microscopy as very bright round cells with a frilled margin. The occasional spindle-shaped cell is to be seen, but whether this indicates natural phenotypic variability, or low-level cross-contamination with a cell-line of practically equal proliferative potential is unknown. Sub-cloning of NZM5 may be warranted to investigate this. NZM5 cultures will grow to very high density, easily ten times that of any of the other cell-lines, and at high density, spherical clumps of several hundred cells each form and detach from the substrate. NZM5 is a producer of copious melanin, and its cell pellets are virtually black, and, uniquely among the cell-line panel, DNA extracted from NZM5 is also nearly black as a result of this high melanin content. No method of DNA extraction yet attempted has produced DNA not heavily contaminated with melanin. This is more than a cosmetic issue as melanin can interfere with downstream applications such as PCR (*See 'PCR amplification of NZM5 DNA', beginning on page 8–21*). One approach not yet tried is to isolate nuclei first and then extract DNA from these in the hope that the melanin present in the cells is predominantly in cytoplasmic melanosomes, and can be eliminated before release of the DNA into solution by nuclear lysis.

NZM6 cells are generally bipolar, extended spindles, although tri- and higher order symmetries occur. Cells pack well and cultures achieve a high confluent density. NZM6 produces considerable debris in culture suggestive of a high rate of cell death. Despite this, NZM6 is particularly reliable in culture and has been adopted by other workers as a research tool.

NZM7, NZM7.2, and NZM7.4 are similar in all respects in culture except one: NZM7 and NZM7.2 produce significant quantities of melanin and when harvested, cell pellets are of a mid-brown colour; in contrast, NZM7.4 is amelanotic, and cell pellets are the usual off-white colour. The NZM7 group is relatively homogeneous in morphology, having spindle-shaped cells, but these are notable for their short, blunt ends. Cultures expand quickly and to high density, but the cells will quickly die off if cultures are not passaged at or before confluence.

NZM9 cells generally have variably sized, flattened cell bodies, with two or three processes of moderate length. Occasional giant cells are to be seen. Cultures proliferate a little more slowly than average, and maintain uniform density across the substrate, implying cellular mobility. Moderate levels of subcellular debris are generated.

NZM10 is notoriously difficult to maintain, and quite variable in culture. Morphologies range from greatly extended spindles, often binuclear, to giant, multinuclear cells that may contain many apparent voids. When recovered from cryogenic storage, it can take many weeks for a culture to approach confluence, even in the smallest flask routinely used. Seeding of too few cells during passaging can result in a culture that stalls. At very high density, local variations





in cell morphology develop that raise concerns about the possibility of cross-contamination, concerns that prove to be unfounded when explored by DNA sequencing or microsatellite analysis. In an attempt to address this, variations in culture medium were tried including differing concentrations of FCS, from 5 to 15%, and the inclusion of supplemental glutamine, insulin, transferrin, and selenium. None yielded more consistent growth than the standard  $\alpha$ MEM/10% FCS/antibiotics medium. It is quite plausible that this variability is an effect of the genomic instability found in this cell-line, described in this work.

The authenticity of NZM10.1 is in doubt as a result of the microsatellite analysis undertaken during V3. By this measure, it seems likely that at some point, possibly even as early as during its sub-cloning, it has been contaminated with NZM4 and may have been supplanted by this faster growing cell-line. However, the data are internally inconsistent and the issue remains unresolved. This situation is described more fully elsewhere {See '*Doubt over NZM10.1 authenticity*', on page 8–36}. With that proviso, NZM10.1 presents as cells with very large cell bodies and usually bi- or -tripolar spindle morphology. Giant cells, often free-floating are seen not infrequently, and triplets of free-floating apparently telophase cells are to be seen.

The morphology of NZM11 is unique among the cell-lines studied here. The cells are small and appear star-like with two to twelve short points when at low density. This changes at high density to create a closely fitting tiling of polygonal cells. Cells are very strongly adhering and can require trypsinisation for 15 min, or replacement of trypsin, before detaching from the substrate. Cultures expand quite slowly, but due to the small size of the cells and efficient substrate tiling, will grow to high density. The cells are also remarkable for their relatively low refractility when observed by phase contrast microscopy.

NZM12 cells have long processes, typically two, that extend from an oval cell body. Cultures grow as a loose mesh, implying good mobility, and to high density with no tendency to cluster. A low level of variably sized subcellular debris is generated.

NZM13 cells are of mixed morphology, being typically bi- or tripolar spindles, but with triangular cells also being seen, especially when growing at low density. Very large cells are also not uncommon. NZM13 cells disperse across the plastic substrate during growth, implying a high degree of mobility. It is among the more slowly growing cell-lines.

NZM14 cells are very elongated bipolar spindles that at high density form intricate, swirling patterns as the cells mutually align themselves. It is more strongly adhering than most cell-lines, and extended trypsinisation is sometimes required.

NZM15 cultures expand quickly. The cells are remarkable for their variability in shape and for their relatively large cell bodies. Cultures produce subcellular debris in a variety of sizes, but not to the extent of NZM6. By phase contrast microscopy, cells appear to be of generally low refractility, but with a granular cytoplasm. The general appearance of cultures might best be described as "untidy".

*Phase contrast microscopy*

The developments in digital photography since the V1 work have made the acquisition and processing of photomicrographs a very much less complex undertaking, and the inclusion of a set of images for the cell-lines under investigation as they appear during culture is an appropriate addition to this brief chapter.

The methodology is trivial, with the exception of the image processing step using Photoshop software. In this, captured images were subjected to automatic level assignment and desaturated to convert them to greyscale. To make the brightness uniform across all images, the "levels" tool was used to adjust the gamma for each image until the median pixel brightness was 100, as determined by the histogram display. Scale bars were then added, their size being determined from images of a haemocytometer grid captured during each session in order to account for different camera zoom settings.

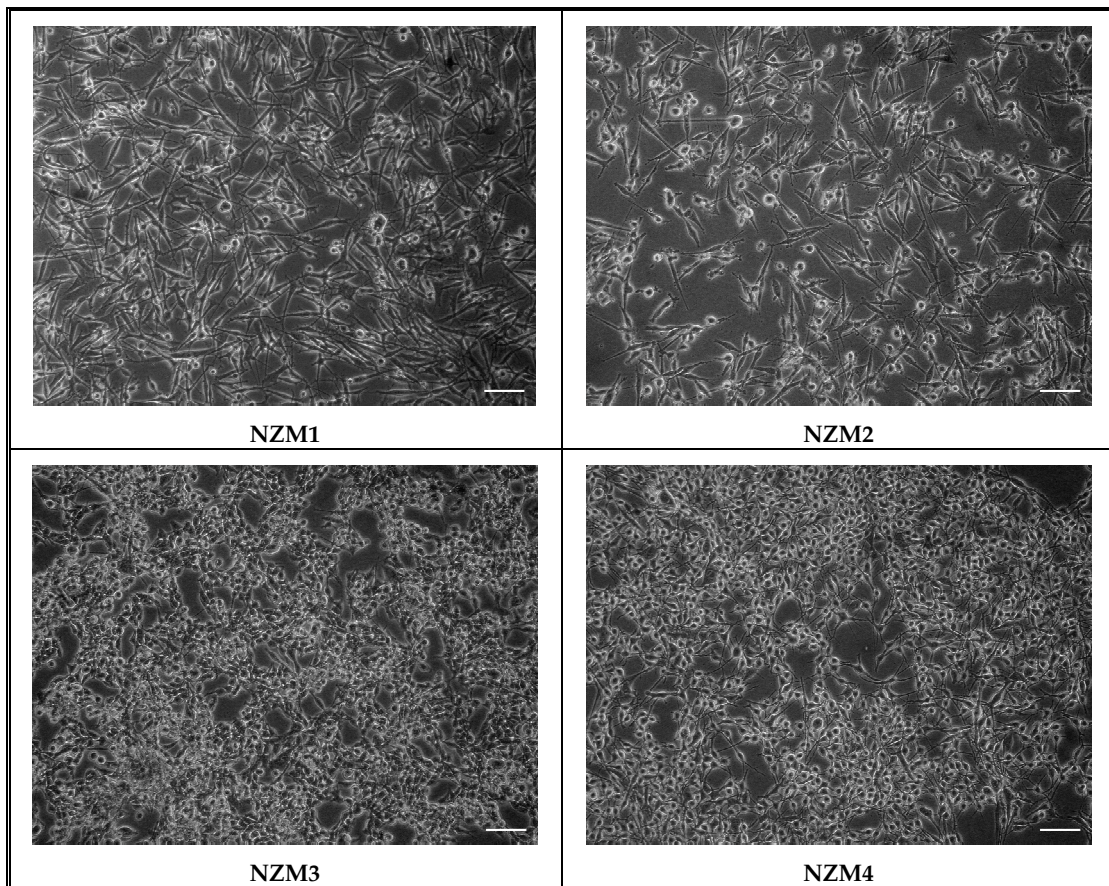


Figure 3-1: NZM cell-lines studied as imaged by phase contrast microscopy (continues overleaf)

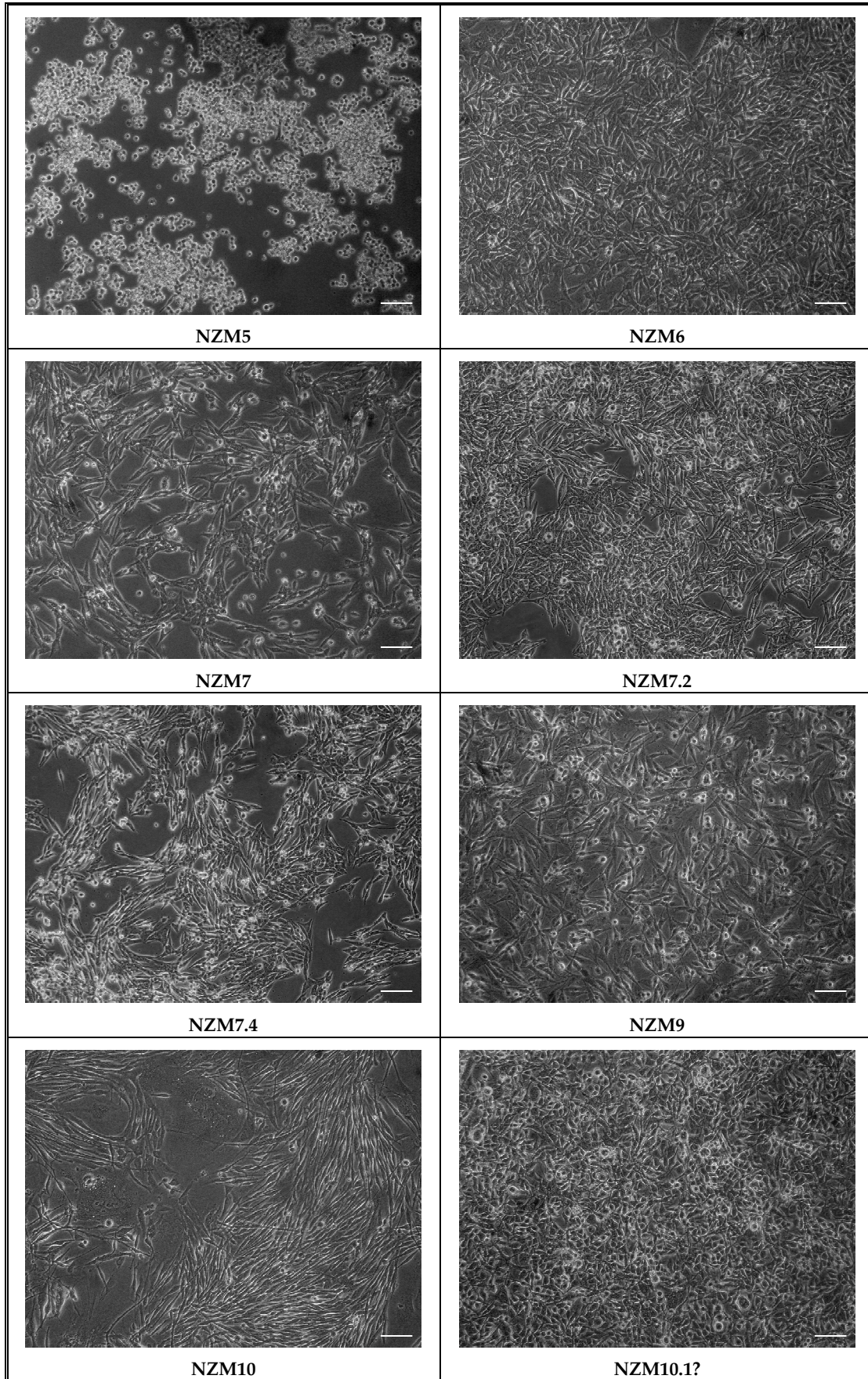
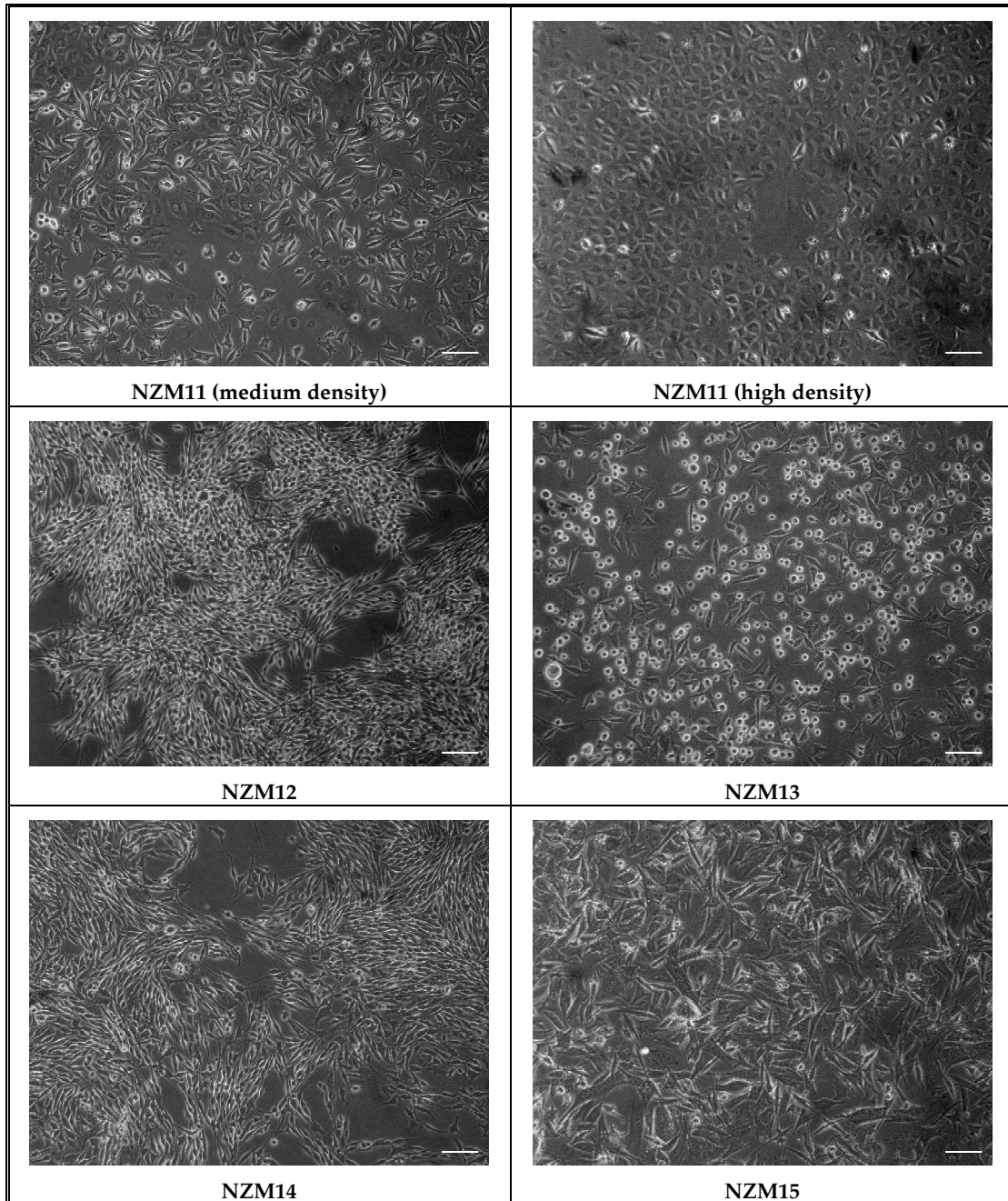


Figure 3-1: (continued)



The morphology of NZM11 cells alters significantly at high density, and cultures adopt a polygonal tiling of translucent cells. Two images are therefore shown for this cell-line. Scale bars = 100  $\mu$ m.

**Figure 3–1 (concluded): NZM cell-lines studied as imaged by phase contrast microscopy**

---

# 4 Experimental rationale and strategy

---

## 4.1 Rationale

Altered cellular proliferation is a hallmark of cancer. One major molecular subsystem that regulates this has at its core the retinoblastoma-associated protein, pRB. It has no known inherent catalytic activity and acts by sequestering or modifying the function of other proteins. This it does in a phosphorylation-dependent manner. Broadly, when hypophosphorylated it binds proteins and constrains proliferation, and when hyperphosphorylated, it releases them allowing cell division to proceed. Its degree of phosphorylation changes in synchrony with the cell division cycle, increasing late in the  $G_1$  phase, and decreasing during mitosis. The principal kinase involved in this phosphorylation is CDK4, which is activated by D-class cyclins. These cyclins are themselves induced by mitogens, linking cellular proliferation to the extra-cellular context via pRB. CDK4 kinase activity is influenced by members of two classes of inhibitors (CKIs), among them p15, p16, p21, and p27. Their expression is also subject to regulation both by extracellular and intracellular events. The pRB protein acts to integrate diverse positive and negative growth signals, ultimately determining if the cell proceeds into S-phase of the cell-cycle, or arrests in  $G_1$ . It has been found that in melanoma tumours, and in cell-lines derived from them, elements of this subsystem, particularly p16 and pRB, may be defective in all cases. The study at hand had its origins in the quest to discover if this was true of the NZM cell-lines.

An extensive review of the pRB subsystem is presented in Appendix H.

## 4.2 Strategy

The experimental strategy employed comprised two parts. In the first, a functional analysis of subsystem integrity was made based on cell-cycle phase perturbation after withdrawal of serum growth factors. The principal tool employed was flow cytometric determination of cellular DNA distribution in experimental cultures. As a prelude to this, a comprehensive study of the DNA content, or ploidy, of the cell-lines was needed, providing additional characterising information about the NZM cell-lines that is valuable in its own right. In the second, a molecular and genetic survey of subsystem components was made, with emphasis on pRB and p16. The tools employed were PCR, single-strand conformation polymorphism (SSCP) analysis, DNA sequencing, and Western protein analysis.

---

## Experimental rationale and strategy (V3)

---

### 4.3 Rationale

Few changes were required to the experimental designs in place for V1, and the thrust of the new experimental work was to improve the techniques developed where necessary, and replicate earlier results.

The V1 9p21 integrity study was based on PCR, and the results were at best counterintuitive, and at worst, technically badly flawed. There was a need to revisit this work to determine if unknown factors may have contributed to the variations in amplification seen, and to confirm or disprove these results. Reduced DNA sequencing costs have meant that a preliminary mutation screening tool such as SSCP is no longer economically required, and given that it suffers from a false negative detection rate of ~20%, the move to direct sequencing of all exonic PCR products was justified for V3. Since no matching normal DNA is available for the NZM cell-lines, results of loss of heterozygosity studies based on microsatellite analysis cannot be informative in the general case, and an exhaustive survey of all such loci involved in V1 was not warranted. However, investigation of microsatellite allele length for loci in and around 9p21 does have the potential to establish that two alleles are present, and that information is potentially useful. In addition, such an analysis would serve to characterise these cell-lines further. Hence, there was a case for undertaking a study of microsatellite allele length variation for a small number of loci.

The results of Western blotting experiments in V1 were not of good quality, despite the investment of a great deal of time. This needed to be addressed in V3, and firm results obtained, with particular attention being paid to the analysis of pRB. Furthermore, rather than simply seeking to determine if pRB is expressed or not in each cell-line, information about its phosphorylation status under different conditions was to be gathered, as it may reveal more about the integrity, or otherwise, of this molecular mechanism, an important aim of this thesis.

One of the outcomes of V1 was the establishment of a strong case, albeit circumstantial and largely theoretical, for numerical dysregulation of centrosomes in the NZM cell-lines as a cause of the heteroploidy and ongoing genomic instability observed. This was thought important enough to warrant the inclusion in V3 of preliminary investigations to determine if this hypothetical defect was indeed present.

### 4.4 Strategy

At the heart of the PCR strategy for V1 was the development of a touch-down thermal cycling program that allowed the amplification of a variety of targets and avoided the time-consuming optimisation step. The primary change in strategy for V3 was to optimise individual cycling conditions, something made much easier with the advent of thermal gradient cycling machines. As will be described, other possible ways of improving the reliability and reproducibility of PCR were developed as V3 progressed.



Given the lack of matched normal DNA, a survey of all the microsatellite loci involved in V1 was not warranted, and virtually the same degree of information was likely to be obtained by the inspection of just three: one between the *CDKN2A* and *CDKN2B* genes at 9p21, and one in each of the flanking regions thought from the V1 work to be intact in all cell-lines. The most expeditious methodology available was the separation of fluorescently tagged PCR products by capillary electrophoresis, performed by the Genomics Unit of the School of Biological Sciences as a contract service, and this approach was adopted.

Efforts toward improving the results of Western analysis centred on the use of different antibodies, mostly in an attempt to resolve an outstanding issue relating to an apparently non-specific band in the pRB blots. This turned out to be a rather larger issue than had been anticipated, and revealed that the V1 pRB blots may have been wrongly interpreted, as will be described in the relevant chapter addendum. To allow a qualitative study of pRB phosphorylation to be made, phosphatase inhibitors were included in the protein extraction buffer for V3, something unnecessary in V1 where only pRB presence or absence was being investigated. Concentration of protein extracts by centrifugally driven ultrafiltration units replaced the problematical vacuum sublimation method and facilitated the loading of greater amounts of protein. The basis for loading equivalency was changed from equal cell numbers to equal total protein, and in conjunction with this, more stringent protein quantitation methods were employed. The efficacy of this approach was established by reversible membrane staining. A move was made to nitrocellulose membranes rather than polyvinylidene fluoride (PVDF), trading off reduced protein retention against reduced background. Use was made of a new digital gel documentation system, greatly facilitating image capture in comparison to traditional film-based systems.

The study of centrosomal regulation was effected by immunofluorescence microscopy of cells simultaneously labelled for DNA,  $\alpha$ -tubulin as a marker of the mitotic spindle, and pericentrin, as a marker of centrosomes. Laser scanning confocal microscopy was available on a limited basis to explore this further. The experimental strategy was to inspect mitotic cells to determine the prevalence of incorrect centrosome numbers, and their degree of involvement in events likely to lead to genomic instability and the generation of aneuploidy and heteroploidy. The best control for these experiments would probably have been normal melanocytes, however the risk that these might take too long to procure and establish was not taken. Instead, tumour-associated fibroblasts, readily available in the ACSRC as a by-product of cell-line establishment, offered a solution, albeit not an ideal one.

#### **4.5 Hypotheses to be explored**

It was hypothesised that in the NZM cell-lines the following are occurring:

- functional failure of the pRB-mediated  $G_1$  arrest mechanism;
- centrosomal numerical dysregulation.

## 4.6 Specific objectives

### Developmental objectives

Objectives to be met in order to establish an effective experimental system included:

- to establish methods for the extraction and accurate quantitation of very high quality DNA from the NZM cell-lines;
- to establish optimal PCR conditions for the gene and microsatellite targets of interest;
- to establish methods for the extraction, concentration, and accurate quantitation of soluble protein from the NZM cell-lines, preserving protein integrity and phosphorylation status;
- to characterise and validate the NZM cell-lines by ploidy and microsatellite allelotype;
- to establish optimal methods of Western blotting to detect proteins of interest, and variation in the phosphorylation status of pRB;
- to establish methods for the immunofluorescent study of centrosomal regulation in the NZM cell-lines, including cell culture, labelling, and image processing.

### Experimental objectives

Objectives to be met in order to investigate the hypotheses above included:

- to assay the functional integrity of the pRB-mediated G<sub>1</sub> arrest mechanism;
- to explore the genetic integrity of the tumour-suppressor genes *CDKN2A* and *CDKN2B*, and the structural integrity of their chromosome 9p21 locus;
- to explore the expression of pRB and the 9p21 encoded tumour-suppressors;
- to explore aspects of the phosphorylation of pRB under different cultural stresses;
- to explore the integrity of centrosomal number and structure, and to describe the nature of any aberrations identified.



---

# Thesis

---



---

*It was found by flow cytometric analysis that the NZM cell-lines all have aberrant DNA content, ranging from near diploidy to dodecaploidy. Some were composed of multiple populations of differing ploidy, suggesting that such genetic instability is a dynamic process, rather than a consequence of a single event in the development of the tumour. In most cases, the measured ploidy was close to, but not exactly, an integral multiple of diploidy, or in some, triploidy. The simplest mechanism able to account for all of these defect classes is failure of centrosome numerical control.*

*These observations led to the recognition of a core centrosome regulation network, overlapping in composition with that governing the nuclear cell-cycle. Additionally, a close link between the cellular stress response and centrosome dysregulation was established. The majority of the cell-lines are known to contain defects in elements of this network, explaining the aberrant ploidy observed.*

*The evolution of centrosomal regulation and its coupling to genome replication is discussed briefly, and it is argued that the location and biological function of the melanocyte render it particularly vulnerable to centrosomal dysregulation and thence, genomic instability.*

---

## 5.1 Introduction

During work investigating the effects of TGF $\beta$  on cell-cycle progression<sup>180</sup>, it was found that at least some of the melanoma cell-lines under study were heterogeneous in terms of cellular DNA content. As a significant part of this work will entail flow cytometric determination of cell-cycle phasing, the presence of such populations would hamper the analysis of the resultant data. Furthermore, determining the underlying DNA ploidy of the cell-lines, and of any heterogeneity in this, contributes important information toward their characterisation. It also provides a benchmark for each cell-line against which any further genomic instability in vitro can be compared.

## 5.2 Experimental design

Flow cytometry provides a rapid, sensitive, and simple technique for the evaluation of cellular DNA content for large populations of cells. While being insensitive to subtle variations of chromosomal structure, it is entirely adequate for the detection of gross genomic derangements such as aneuploidy, hyperploidy, and heteroploidy. To obtain a measure of absolute ploidy for a cell-line, its measured modal DNA fluorescence must be related to that of normal human cells, and peripheral blood leukocytes (PBLs) provide an ideal standard. Exactly how to compare the two values is not a trivial matter. The interactions between DNA content, propidium iodide concentration, cell number, sample volume, multiple populations, and variable proliferation rates, as they relate to measured propidium iodide fluorescence, are poorly understood. The incorporation of normal human PBLs into the samples for analysis<sup>141</sup> provides an internal standard, and coupled with a relatively high propidium iodide concentration, many of these uncertainties can be eliminated. The utility of flow cytometry is

See A.5 for background information about flow cytometry.

such that the data for the standard can be isolated and analysed separately from the remainder of the sample.

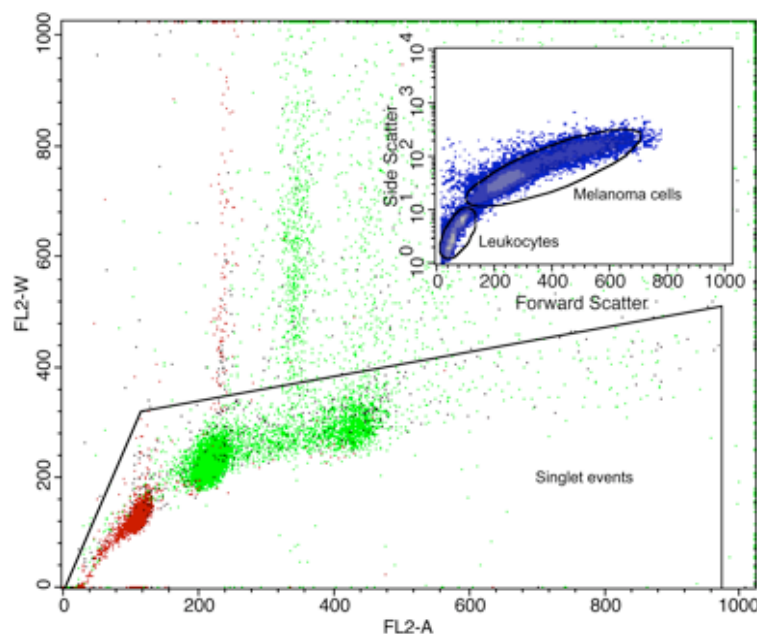
### 5.3 Methods in brief

Melanoma cells were seeded into P100 tissue culture plates at a density of  $\sim 100$  cells/mm<sup>2</sup> in Alpha minimal essential medium ( $\alpha$ MEM) supplemented with 10% v/v FCS and antibiotics {Solution 11}. When approaching confluence, the cells were harvested by trypsinisation {Method 4} and fixed in methanol {Method 30}. For each melanoma cell-line, equal quantities ( $5 \times 10^5$ ) of fixed cells and of previously methanol-fixed PBLs were combined, stained with propidium iodide (final concentration 50 mg/L) {Method 31}, and analysed for DNA content by flow cytometry {B.11}.

### 5.4 Results

#### Data acquisition

Instrument settings were established such that modal DNA fluorescence peak amplitude (FL2-H) and signal integral (FL2-A) both occurred near channel 100, except in the case of NZM10, where 50 was found to be more appropriate. Regions corresponding to the PBLs and melanoma cell components were constructed based upon the differing light scatter characteristics of the two cell-types, and corresponding to singlet events based on propidium iodide fluorescence {Figure 5–1}. Gating on combinations of these regions allowed the separate analysis of the leukocyte standard and the melanoma cells. Data for a minimum of 5 000, but generally 20 000 events of interest were collected for analysis.



The inset density plot shows the positioning of regions to isolate the different cell-types within a sample. Key: X-axis = forward scatter channel number; Y-axis (logarithmic) = side scatter channel number; point colour gives the relative frequency of occurrence of the event type (blue = low; white = high).

The enclosing dot plot shows the positioning of a region to isolate singlet events. Key: X-axis = event DNA fluorescence integral (FL2-A); Y-axis = DNA fluorescence signal width (FL2-W); point colour indicates the region in the inset plot to which each event belongs: green represents events in the 'Melanoma cells' region; red, those in the 'Leukocytes' region.

Figure 5–1: Region placement



## Cellular DNA distributions

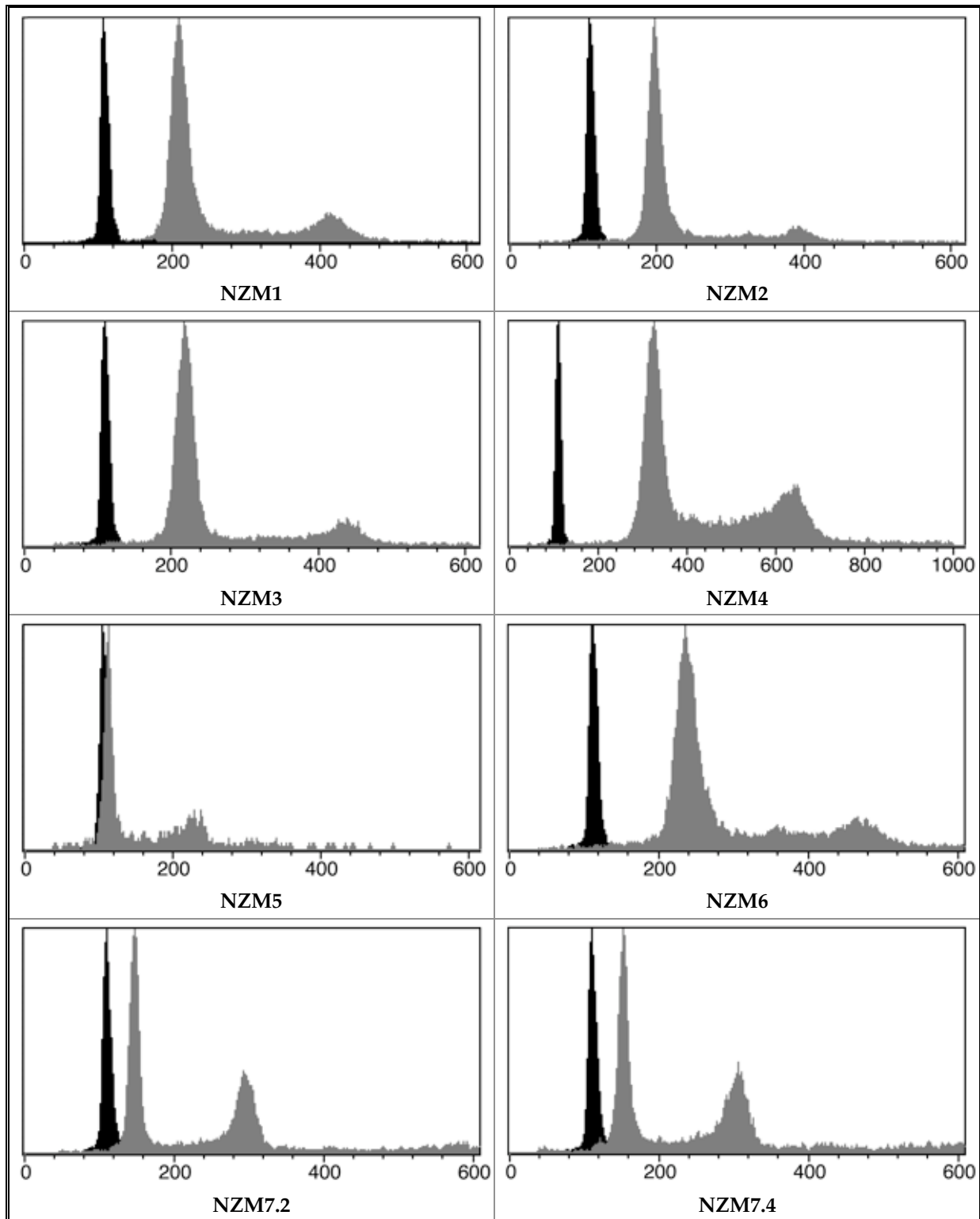


Figure 5-2: Melanoma cell-line DNA profiles (continues overleaf)

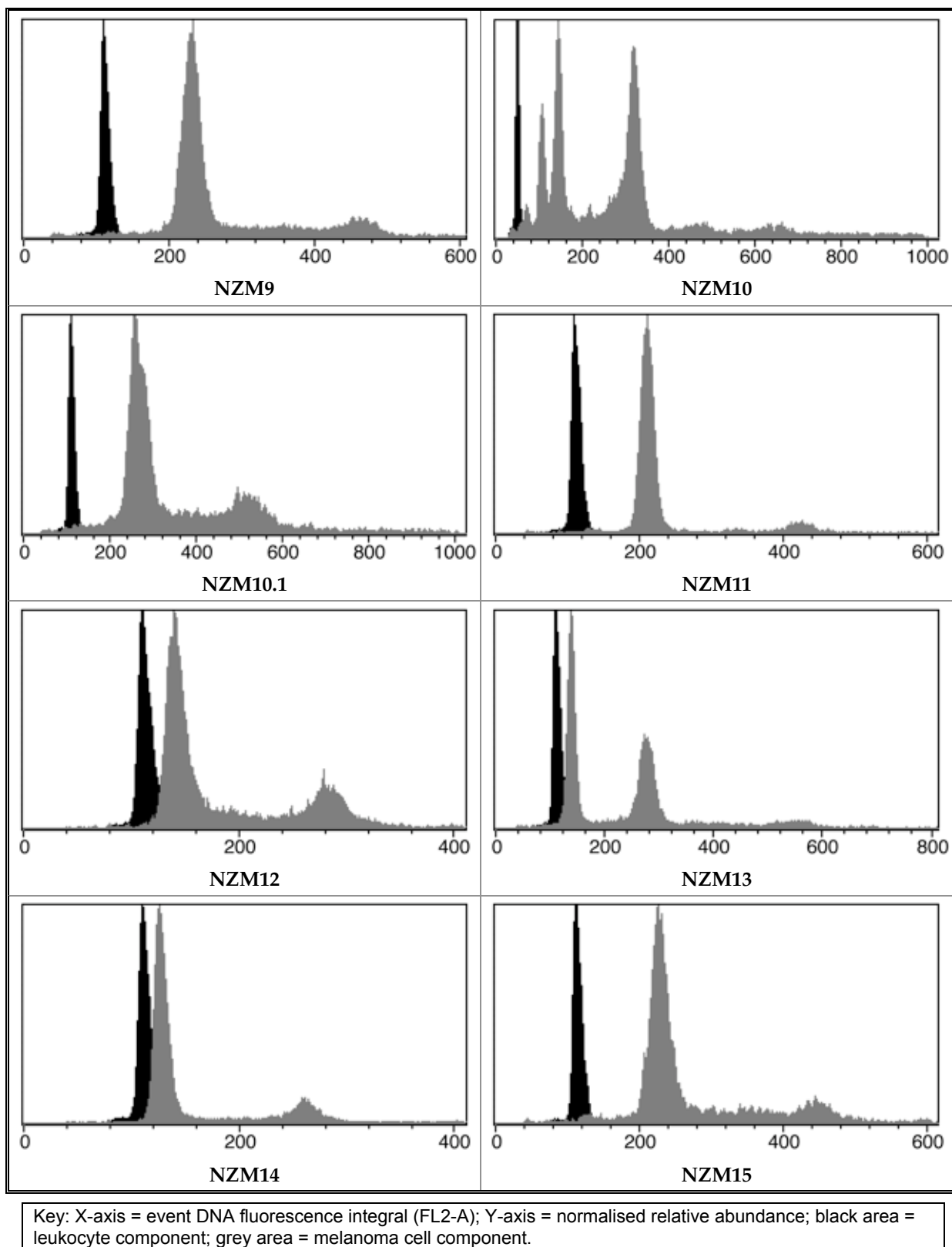


Figure 5-2 (concluded): Melanoma cell-line DNA profiles

### Uniformity of PBL staining

The distribution of modal channel numbers for DNA in PBL populations among all samples had a coefficient of variation of 1.6% indicating that there was very little variability in staining among experiments. In light of this, with the concentration of propidium iodide used here, the incorporation of PBLs within each sample was probably unnecessary, and a single separate PBL sample would have sufficed.

### Abnormal absolute ploidy

In the case of NZM10, where classification of peaks as  $G_1$  and  $G_2$  was not possible by inspection, a separate similar experiment was performed with cells cultured in the presence of the mitotic inhibitor, paclitaxel (data not shown). This caused an accumulation of cells with a  $G_2$  DNA content at the expense of  $G_1$ , allowing the unambiguous classification of peaks. For each sample, the maximum channel number for the  $G_1$  peak of each component was determined, and absolute ploidy calculated by reference to the PBL component {Table 5–1}. All melanoma cell-lines displayed abnormal absolute ploidy.

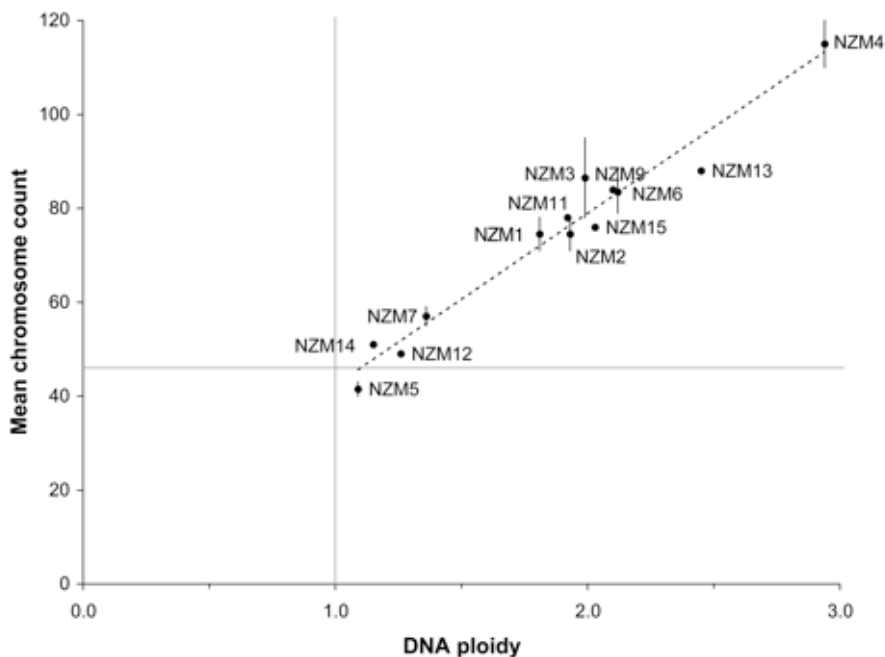
Cell-line (component)	PBL $G_1$ peak	Melanoma $G_1$ peak	DNA ploidy
NZM1	106	210	1.98
NZM2	108	196	1.81
NZM3	109	217	1.99
NZM4	110	323	2.94
NZM5	105	114	1.09
NZM6	111	235	2.12
NZM7.2 (1)	109	146	1.34
NZM7.2 (2)	109	299	2.74
NZM7.4 (1)	109	151	1.39
NZM7.4 (2)	109	304	2.79
NZM9	111	233	2.10
NZM10 (1)	51	107	2.10
NZM10 (2)	51	144	2.82
NZM10 (3)	51	233	4.57
NZM10 (4)	51	320	6.27
NZM10.1	111	256	2.31
NZM11	110	211	1.92
NZM12	111	138	1.26
NZM13 (1)	111	138	1.24
NZM13 (2)	111	272	2.45
NZM14	110	126	1.15
NZM15	112	227	2.03

Parentthesised numbers following cell-line designations denote different identifiable sub-populations. The inset graph shows the ploidy for each component (X-axis) relative to diploidy.

Table 5–1: Melanoma cell-line DNA ploidy

The measured cellular DNA contents were in accord with cytogenetic data available for some cell-lines<sup>846 966</sup>, and there is a high level of correlation ( $R^2 = 0.96$ ) between the mean reported chromosome count {Table 3–1}, and the DNA ploidy {Figure 5–3}. Most appeared to have DNA

ploidies close to  $2^I \times$  diploid ( $I$ , a non-negative integer), suggesting a process acting on a genome-wide basis. Other mechanisms are implied by the presence of  $2^I \times$  triploid lines, and minor departures from both types.



Bars are the count range; lines  $x = 1.0$  and  $y = 46$  indicate normal diploid content. NZM7 ploidy has been inferred from that of NZM7.2 and NZM7.4 by taking their mean. No cytogenetic data exist for NZM7.2 and NZM7.4 and these are therefore omitted. The NZM13 data point reflects the ploidy of the second sub-population detected by flow cytometry.

Figure 5–3: Ploidy correlation

### Heterogeneity of ploidy within cell-lines

Several of the cell-lines contain multiple sub-populations with differing base DNA content.

This is most obvious in the NZM10 cell-line, and, being noted early in experimentation, led to the isolation and establishment of the NZM10.1 sub-clone. A similar observation had previously been made for the NZM7 cell-line, also leading to the establishment of sub-clones of pure ploidy [3.4]. In other cell-lines, the effect was more subtle, with additional peaks being visible in NZM6 and NZM13, and disproportionately high  $G_2$  peaks coupled with evidence of high DNA content cells in NZM7.2 and NZM7.4. Interestingly, these NZM7 sub-clones were again displaying evidence of heteroploidy, and in the newer NZM10.1 sub-clone, the presence of a shoulder on the  $G_1$  peak suggests that it too is inherently genomically unstable.

The presence of the heteroploidy seen here, together with similar reports by others<sup>61 245</sup>, raises the possibility that this may be a general characteristic of melanoma. In this regard, the results from NZM1 and NZM2 warrant consideration as these were derived from the same patient at different times. While no distinction in chromosome count was made, there was a discernible difference in DNA ploidy. Furthermore, the populations appeared to be relatively pure by this criterion. Perhaps the best explanation of this observation is that the underlying primary tumour was itself genomically unstable and in all likelihood heteroploid, and that the different metastatic tumours used in the establishment of the cell-lines developed from cells of differing



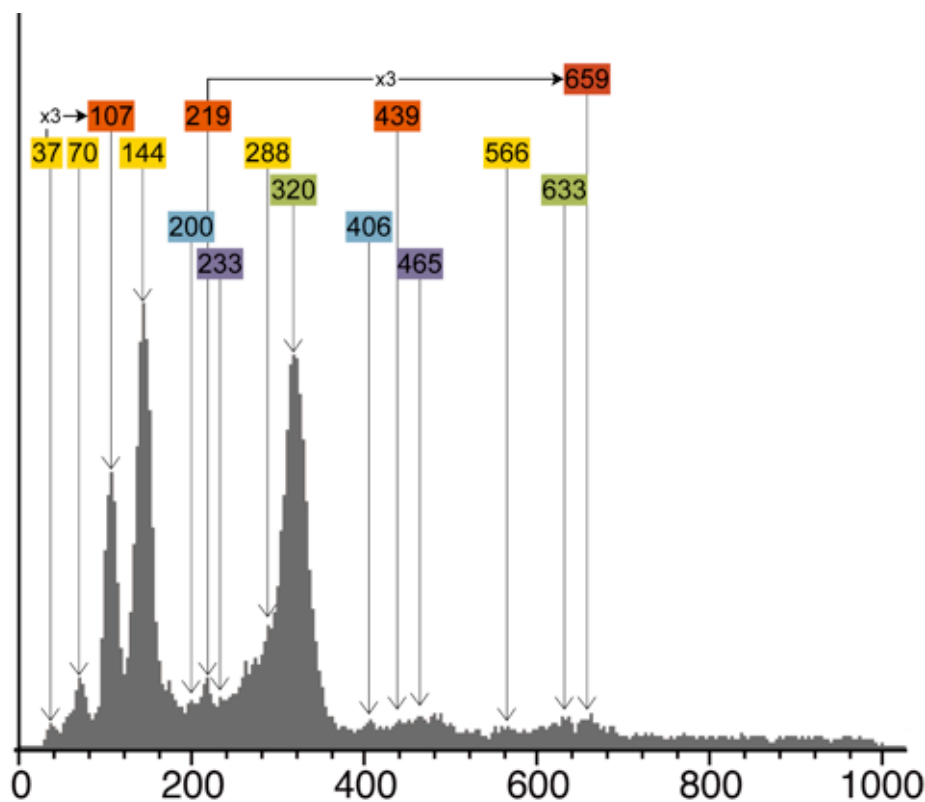
ploidy. Two implications arise from this. The first is not unexpected: that **genomic instability in the primary tumour can continue after metastatic potential has been achieved**. The second is that it is the presence of genomic instability that is associated with tumorigenesis, not its magnitude.

## 5.5 Discussion

### NZM10 as a model

These static measurements of DNA content confirm for melanoma the general observation that genomic derangement is associated with tumorigenesis. Among the cell-lines, NZM10 stands out as having the most complex ploidy pattern [Figure 5–4]. As such, it potentially offers the greatest scope for investigating the underlying causes of melanoma ploidy defects and is therefore the subject of greater scrutiny.

The major NZM10 component has a  $G_1$  peak at channel 144, making it nominally hexaploid. The peak at 320 is both too intense and at too high a channel number to be attributable to the  $G_2$  phase of this component. Its breadth and the presence of a minor peak at the expected channel 288 suggest that it may be the overlap of the corresponding  $G_2$  phase, and the  $G_1$  phase of a component with higher base DNA content, being nominally dodecaploid. To explore this further, use was made of the mitotic inhibitor paclitaxel in a separate experiment. In its presence, cells arrest in mitosis with the consequent elimination of  $G_1$  and S populations. When this was performed, the 288–320 peak was much smaller, establishing that  $G_1$  cells of higher



Key: X-axis = Event DNA fluorescence integral; Y-axis = relative abundance; boxed numbers are the channel numbers for the local maxima. Members of each separately coloured horizontal series differ by a factor of ~2 from each neighbour. In two pairs of series, base DNA content is related by a factor of ~3. The peak for normal leukocytes, not shown, was at 51.

Figure 5–4: NZM10 population components

ploidy were indeed a major constituent of it (data not shown). This is further supported by the presence of a small, but discernible peak at 566, possibly corresponding to G<sub>2</sub> cells. The difficulty of maintaining genome integrity can be appreciated on considering that in these cells, approximately 140 pairs of chromosomes are being managed by a system evolved to deal with only 23.

The hexaploid and dodecaploid components are part of an ordered series in which adjacent members differ in base DNA content by a factor of approximately two. The G<sub>1</sub> peaks of this series, overlapping with the G<sub>2</sub> peak of the lower ploidy component, can be seen at 37, 70, 144, 288, and 566. Other similar series with initial peaks at 107, 200, 233, and 320 are discernible. There is also evidence of components with ploidies differing by factors of three, as illustrated by the DNA peak pairs 37/107, and 219/659. The presence of cells with even greater DNA content implies that higher-order components exist.

The derivation of each of these populations cannot be certain, but a representative progression might be as follows. Cells with a normal DNA content, corresponding to channel 51, undergo an imperfect polyploidisation, yielding the population with a G<sub>1</sub> peak at channel 107. Subsequently, erroneous genome partitioning during division results in the generation of populations with one third, and two thirds of the polyploid DNA content, yielding the peaks at 37 and 70. G<sub>2</sub> cells derived from the G<sub>1</sub> peak at 37 may also contribute to the peak at 70. NZM10 encompasses all of the ploidy anomalies seen throughout the entire panel, and so represents a useful model for future investigation of genomic instability in melanoma.

### **The molecular basis of genomic instability**

#### *Potential causes*

For the base DNA content of a cell to differ from its progenitor implies that DNA synthesis was not confined to exact doubling during the cell-cycle, that the DNA was not evenly distributed among daughter cells, or that there were not exactly two such daughter cells produced after genome doubling. This analysis implicates the processes of replicated genome segregation {Appendix J}, DNA replication licensing {Appendices K}, and cytokinesis {Appendix L}. After considering the likely effect on maintenance of ploidy of failure of each, the most probable explanation for the patterns observed here appears to be a failure of centrosome numerical control, able to account for both multiplication and fractionation of the genome by integral factors and minor departures from these.

See Appendix J for a review of genome segregation regulation.

See Appendix K for a review of DNA licensing regulation.

See Appendix L for a review of cytokinesis regulation.

#### *Centrosomes and cancer*

This theoretical analysis is supported by the frequent reporting of aberrations of centrosomal morphology and number in diverse cancers, very often being associated with aneuploidy, hyperploidy, and chromosome missegregation {Table 5–2}.



Cancer type	Observations
Biliary tract	Atypical centrosome size, shape and number, particularly in late-stage disease <sup>728</sup>
Breast	Excess, misplaced, disrupted, extended centrioles <sup>792 1521</sup>
Cervical	Excess centrosomes, aneuploidy, tetraploidy <sup>1235</sup>
Colorectal	Excess centrosomes in aneuploid cell-lines <sup>414 1521</sup>
Neuroectodermal	Excess centrosomes and chromosome missegregation in <i>TP53</i> mutant tumours <sup>1413</sup>
Ovarian	Excess centrosomes, aneuploidy <sup>1521</sup>
Pancreatic	Atypical centrosome size, shape and number, chromosome missegregation <sup>1139</sup>
Prostatic	Excess centrosomes, aneuploidy <sup>1521</sup>
Squamous cell	Excess centrosomes <sup>159</sup>

**Table 5-2: Centrosome abnormalities in cancer**

### *Centrosomes and melanoma*

Given that melanoma is the tumour type of concern here, it is interesting that it is not represented in Table 5-2. This may not be because melanomas do not contain aberrant centrosomes; more likely, it is because this has not been investigated. A recent search of the more than 11 million items indexed in the NIH PubMed database using the query phrase ‘centrosom\* AND (melanoma OR melanocyt\*)’ returned only nine records, none relevant to this discussion. A search of over 3 billion internet web-pages using the ‘Google’ engine found no instances of ‘melanoma’ and ‘centrosome’ in the same phrase.

### **The molecular basis of genomic instability in melanoma**

Consideration of the proteins associated with centrosomal regulation {Table J-1} and their functional associates allows the formulation of a list of candidates potentially involved in melanoma genomic instability. If any are in fact involved, there should be indications in the scientific literature of an association between their dysfunction and melanoma, even if centrosomal abnormality has not been reported, per se. Unfortunately, in many of the cases, no data exist, notably for *BRCA1*, *WEE1*, *CDC25C*, *PKMYT1*, *NBN*, and *SNF*. Nor have components of the SKP1-cullin-F-box complex (SCFC) ubiquitin ligase, or its substrate designators been investigated. Such a study would be particularly interesting in the situation where cyclin-E and p27 were found to be coordinately over-expressed<sup>65</sup>.

The available data are also deficient in another respect. Predominantly, they derive from studies of protein expression, and while these can be indicative, particularly where a protein is found to be absent, since levels of expression are invariably determined by multiple factors, no specific causal information can be obtained. For example, over-expression of cyclin-E may result from E2F dysregulation, which may result from pRB dysregulation, which may result from p21 dysregulation, which may result from p53 dysregulation, which may result from CHK2 dysregulation, which may result from ATM mutation. At each step, multiple causative branches may exist. Ultimately, protein expression is determined by the interaction of the genome and the environment within the bounds of physical laws. The key to understanding centrosome dysregulation, or any biological process for that matter, will not be uncovered by studies of protein expression alone, but by the more fundamental study of molecular genetics.

A summary of published data is given in Table 5-3. On the basis that data from genetic analysis may provide greater insight than those based on protein expression, the salient

observations are: a mutation in *ATM*; promoter methylation in *CDKN1B*; germ-line mutations affecting *ARF*; amplification of *MYC*; deletion and mutation of *RB1*; mutation of *TP53*; possible involvement of *PTEN*; and the association of ocular melanoma with *BRCA2* mutation. The common feature of all of these is their contribution to the regulation of CDK2 and CDC2. Consistent with the model of centrosomal regulation presented in Appendix J, these can be logically divided into two classes, those affecting normal cell-cycle progression, and those pertaining to a delayed or interrupted cell-cycle. Defects of p27, MYC, pRB, and PTEN function would fall into the first class, while those of ATM, p53, ARF, and BRCA2 would fall into the second. Arguably, the first class should be more frequent than the second since no unusual additional stimulus would be required for any defect to become relevant. This may not be the case for the melanocyte however {See 'Conclusion', below}.

See Appendix I for a brief review of BASC, the BRCA1-associated genome surveillance complex.

With these critical components identified by genetic analysis, the protein expression data {Table 5–3} can now be considered, and overwhelmingly, it is in support of this model, with over-expression of cyclins, CDKs, CDK activating phosphatases, and transcription factors; and under-expression of CDK inhibitors (CKIs) and elements of the BRCA1-associated genome surveillance complex (BASC). This set of candidates was reached solely based on their involvement in centrosomal regulation and with only passing consideration given to any role they may have in mediating the nuclear cell-cycle. That the set identified is critical for the latter in no way detracts from the candidature of its members as regulators of the former; rather, it adds to their importance as oncoproteins or tumour-suppressors.

The available data contain some conflicting or puzzling observations. While CDK2 has been identified as a strong candidate centrosome regulator, no activating mutations were found in a panel of 60 melanoma cell-lines<sup>1390</sup>. This study sought mutations only in a region conserved between CDK4 and CDK2 and implicated in inhibition of the former by p16. Since p16 is considered to be a specific inhibitor of CDK4 and the very similar CDK6, the absence of mutations in this region is not surprising; nevertheless, the basis for the sequence conservation between CDK2 and CDK4 remains unexplained. Of much greater interest would be the results of a quest for mutations affecting the binding of p27. On a more general note, mutations rendering CDK2 constitutively active would seem to be improbable since both the T14/Y15 and T160 phosphorylation controls would need to be simultaneously abrogated to achieve this.

Expression of MDM2 and p53 have been reported to be both increased and diminished, and that of p21 to be anomalously high in light of its inhibitory role. The caveat concerning the significance of protein expression data applies here. Without knowledge of the underlying cause of the altered expression, conclusive interpretation is impossible. Both MDM2 and p21 are transcriptional targets of p53 and all are degraded by the proteasome. Where p53 is defective, MDM2 and p21 may be diminished; where proteasomal processing or targeting is defective, all may be abundant. In either case, a supervening explanation for centrosome dysregulation exists.



Gene	Observations
<i>ATM</i>	<i>ATM</i> mutation in radiosensitive melanoma cell-line <sup>1075</sup>
<i>BRCA2</i>	Ocular melanoma predisposition among <i>BRCA2</i> families <sup>540</sup>
<i>CCNA</i>	Greater expression in melanoma than in benign naevi <sup>1307 1338</sup> Greater expression in melanoma cell-lines than in melanocytes <sup>1307</sup>
<i>CCNB</i>	Greater expression in melanoma than in benign naevi <sup>1338</sup> Greater expression of cyclin-B1 in mouse melanoma cells with high ploidy <sup>870</sup>
<i>CCNE</i>	Greater expression in melanoma than in benign naevi <sup>411 1307</sup>
<i>CDC2</i>	Greater expression in melanoma than in benign naevi <sup>1338</sup>
<i>CDC25A</i>	Greater expression in melanoma than in benign naevi <sup>1307</sup>
<i>CDK2</i>	Greater expression in melanoma than in benign naevi <sup>411 1307</sup> No activating mutations found <sup>1390</sup>
<i>CDKN1A</i>	Over-expression seen in 7/23 primary and 4/12 metastatic melanomas <sup>1340</sup>
<i>CDKN1B</i>	Expressed at high levels in primary melanomas in association with high cyclin-E expression <sup>65</sup> Reduced expression in melanoma versus benign naevi <sup>634</sup> Expression inversely correlated with disease-free survival in melanoma <sup>359</sup> Mono-allelic silencing through promoter methylation <sup>1452</sup>
<i>CDKN2A-β</i>	Germ-line deletion of exon 1β affecting ARF, but not p16 in melanoma-astrocytoma <sup>1076</sup> Germ-line 16 bp insertion in exon 1β in melanoma <sup>1096</sup>
<i>E2F</i>	Greater expression in melanoma cells than melanocytes, and altered levels of free versus bound E2F <sup>465</sup>
<i>GADD45A</i>	Reduced expression seen in primary melanoma <sup>710</sup>
<i>MDM2</i>	Expression seen in only 1/8 melanoma cell-lines <sup>1508</sup> Over-expression commonly seen in large melanoma panel, especially in invasive and metastatic tumours <sup>1043</sup>
<i>MLH1</i>	Reduced expression seen in primary melanoma <sup>710</sup>
<i>MSH2</i>	Reduced expression seen in primary melanoma <sup>710</sup>
<i>MYC</i>	Gene amplification associated with advanced cutaneous melanoma <sup>714</sup>
<i>PTEN</i>	LOH in 7/21 and sequence alterations in 4/21 metastatic melanomas <sup>170</sup> Some intronic alterations, and two amino acid changes, but only in late-stage melanoma <sup>1038</sup> No LOH or aberrant SSCP pattern in 23 primary and 17 metastatic melanomas <sup>115</sup>
<i>RB1</i>	Hemizygous deletion and mutation in melanoma cell-lines <sup>73</sup>
<i>TP53</i>	Non-conservative mutation in 2/15 melanoma cell-lines <sup>1002</sup> Expression seen in 15/20 tumours versus 0/20 matched normal tissues <sup>1071</sup> Mutation in 17/81 melanomas <sup>1506</sup> Mutation frequency in metastases lower than in primaries, and only in skin and not internal metastases <sup>1506</sup> Abnormally high expression in 22/121 tumours <sup>1432</sup> Mutation in 7/46 nodular melanomas, over-expression in 4/31 primary tumours <sup>21</sup> Expression in 41/50 melanomas versus 0/10 benign naevi <sup>1108</sup> Level of expression correlated with tumour stage, patient age, and inversely with disease-free survival <sup>1108</sup>

Table 5–3: Centrosomal regulators implicated in the aetiology of melanoma

### The core melanoma centrosome regulation network

The culmination of the analysis above is the identification of a core regulation network, failure of any component of which is likely to lead to centrosome dysregulation and thence aneuploidy, hyperploidy, and heteroploidy. The elements of this network and their principal interactions are summarised in Figure 5–5.

### The basis of heteroploidy in the NZM cell-lines

In the case of the particular melanoma cell-lines under investigation here, NZM4 has been reported to be a *TP53* mutant<sup>1002</sup>, and as will be described in following chapters, NZM6, NZM7.2, NZM7.4, and NZM10.1 do not express pRB; NZM1, NZM2, NZM3, NZM9, NZM11, and NZM13 are homozygously deleted for all or part of *CDKN2A*; and NZM12 is a *CDKN2A* (ARF) mutant. Of the remaining four, it is noteworthy that NZM5 and NZM14 display the smallest departures from diploidy of any of the cell-lines.

See Appendix J, and particularly Figure J-14, for a full description of the interactions depicted here.

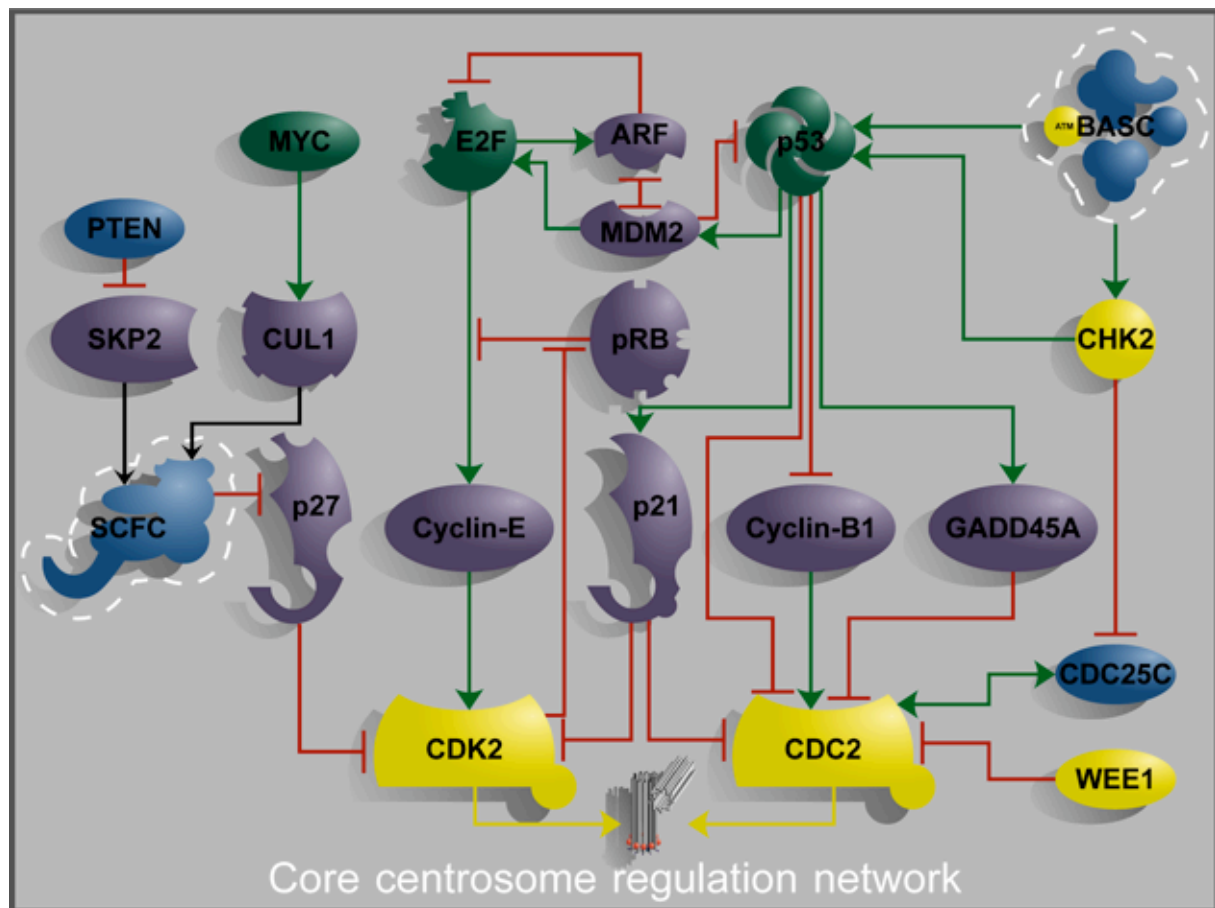


Figure 5-5: The core centrosome regulation network

## 5.6 Conclusion

The evidence from the cell-lines studied here is that major abnormalities in ploidy are very common, if not universal in melanoma. The simplest explanation for the types of abnormality seen is the failure of centrosome regulation; there is however no significant literature on the role of such regulation in melanoma. Indeed, in the broader literature, the detection of centrosomal regulators such as p21, p53, and CDC2 in the cytoplasm, rather than the nucleus, is considered a novelty<sup>1439</sup>.

Any analysis must therefore be partly speculative. From a consideration of the molecular basis of centrosomal regulation and known aberrations of components of this in melanoma, a core centrosome regulation network can be identified. It substantially overlaps the network that governs the nuclear cell-cycle, not surprisingly in view of the need for close coupling between the two. In consequence of this overlap, failure of any common component may deregulate both cycles, and it is by no means clear which event would contribute more to tumorigenesis.

Furthermore, there is a direct link between the cellular stress response, including the response to genetic damage, and the centrosome cycle. This stems from BASC and is mediated via p53 and CHK2. Melanocytes, by virtue of their location, are under constant genomic assault from ultraviolet radiation. For them, the triggering of the DNA damage response is not an abnormal event, but rather, a necessary concomitant, and possibly a crucial part, of their biological function, the production of photoprotective melanin. In melanocytes therefore, much more



---

than in any other cell-type, there is a dependency on the integrity of DNA-damage responsive centrosome cycle control, and it is in melanocytes that any vulnerabilities in this control will first make themselves known.

Ironically, the very act of responding to genomic damage by cell-cycle arrest could be self-defeating. Numerical control of centrosomes is not robust and centrosome re-duplication can occur simply as a consequence of S-phase prolongation. While evolution has provided a rudimentary mechanism to delay the centrosome cycle under these circumstances, it is not infallible, particularly in the context of the melanocyte. Its failure will ultimately lead to the most profound genomic instability, a hallmark of cancer.

Ultrastructural studies of melanoma must be conducted to determine the status of centrosome regulation. Other components of the core centrosome regulatory network must be screened for mutation and altered expression.

## Ploidy (V3)

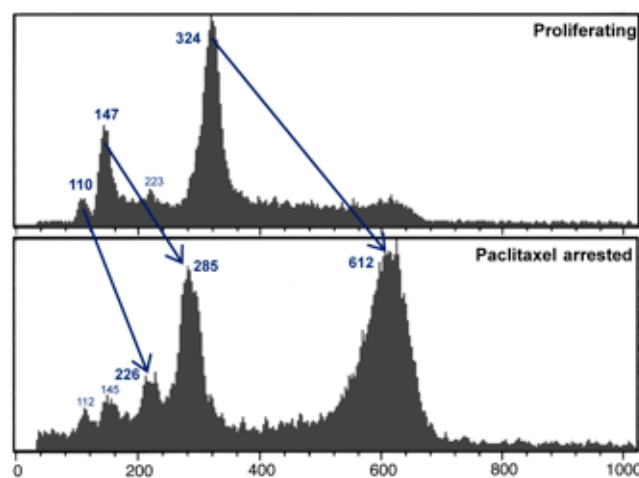
### 5.7 Clarification of the existing material

#### Correlation between ploidy and cytogenetic studies

There is an anomaly present in the ploidy correlation graph {Figure 5–3} with respect to NZM13. The information for the NZM cell-lines numerically less than 9 derived from the survey of Marshall et al.<sup>846</sup> and comprised chromosome count ranges, while that for the remaining cell-lines included was obtained from a study being conducted by Dr Paul Oei<sup>966</sup>, and comprised karyograms for a few mitoses from each. From these, a single representative figure for chromosome number was derived. This accounts for the presence of range bars in the graph for the data derived from Marshall et al., but only points for that from Oei. It transpired that the limited cytogenetic data available for NZM13 were far more consistent with the near tetraploid sub-population detected by flow cytometry than with the predominant near-diploid sub-population. It was, therefore, the DNA ploidy for the former that was used as the abscissa value for the NZM13 data point. In consequence, there is a potentially confusing disparity between the tabulated values for ploidy {Table 3–1} and those used for the graph. To clarify this, the legend for Figure 5–3 has been modified.

#### Additional data not shown in the original work

Visible peaks in the DNA fluorescence histogram for NZM10 could not be assigned to cell-cycle phases by inspection due to its very complex nature, and this prevented the identification of discrete sub-populations of differing ploidy. To address this, an experiment where NZM10 cells were arrested by treatment with paclitaxel was undertaken so that peaks corresponding to a  $G_2$  DNA content would be enriched at the expense of those of  $G_1$  and S content, thus allowing their unambiguous identification. This proved successful, and while the implications of this result were used as the basis of discussion, the results themselves were not presented. These data are now given in Figure 5–6.



Key: X-axis = event DNA fluorescence integral (FL2-A); Y-axis = normalised relative abundance. Numbers show FL2-A values for peaks. Arrows indicate transfer of events for a sub-population from  $G_1$  to M as a consequence of paclitaxel treatment.

Figure 5–6: Effect of paclitaxel on NZM10 cell-cycle phase distribution





## 5.8 Extension of the existing material

### Rationale

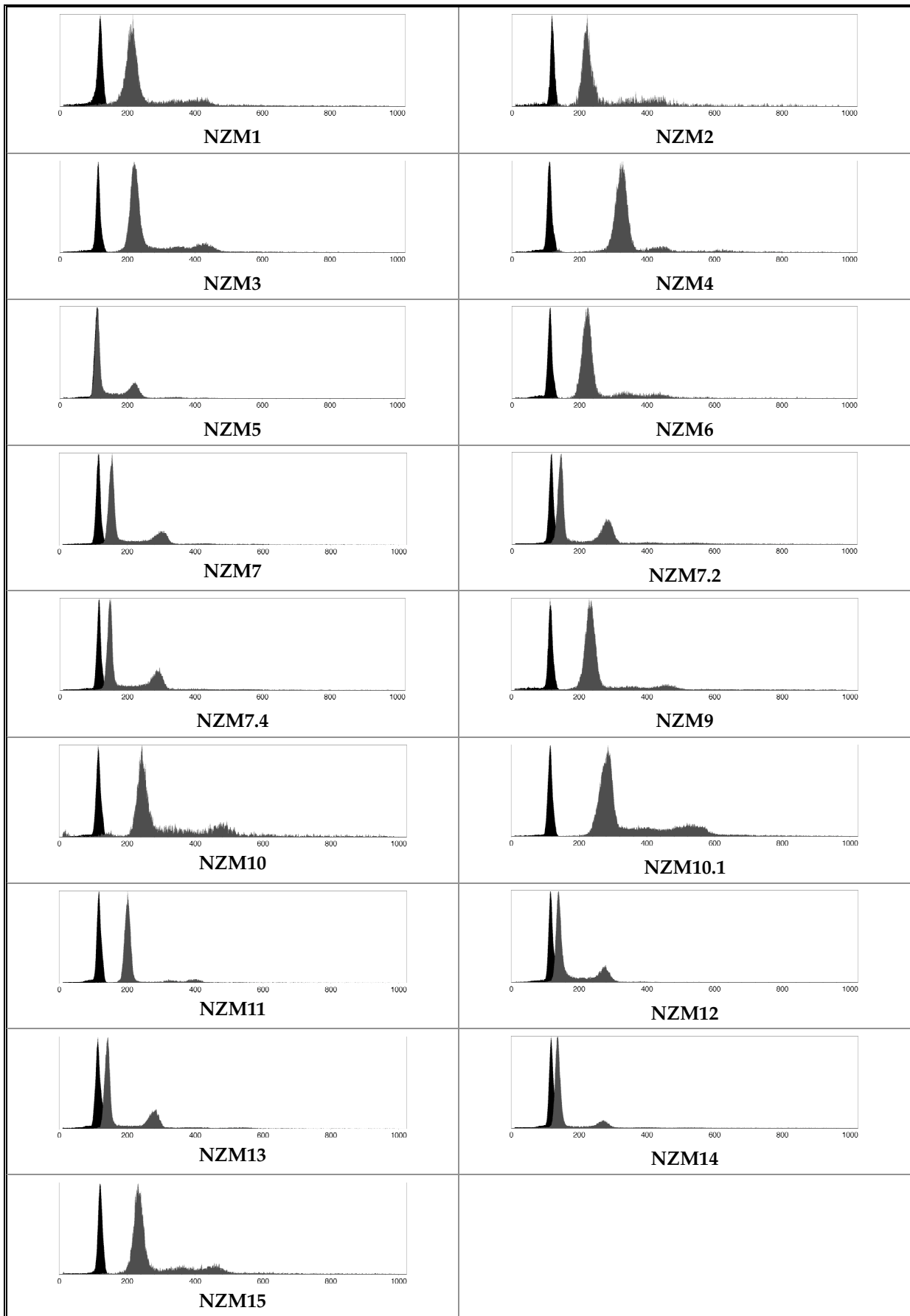
Partly to seek to replicate the original data, and partly to confirm the identity of the cells recovered from cryogenic storage to some degree, the DNA ploidies for the cell-lines included in the original study were measured again by flow cytometry. For the V3 work, the original NZM panel was extended to include the parental NZM7 cell-line from which NZM7.2 and NZM7.4 were derived. This had been intentionally omitted from V1, as it was already known to be heteroploid and so, unsuitable for use in experiments where cell-cycle analyses by mathematical model fitting were intended, as is the case here. Its inclusion in the panel represents little additional work and has the potential to provide useful information.

### Methods

The methods described for the original work were employed essentially unaltered. On this occasion however, the same cytometer settings were used for all cell-lines with the PBL  $G_1$  reference peak being set to approximately channel number 100 for both the FL-2 height and FL-2 area parameters. This is in contrast to the original work where NZM10 was treated as an exception due to the many high ploidy peaks present, with the reference peak being set to approximately 50. Due to changes seen in the DNA profile for NZM10 in preliminary work this was not required on this occasion. Additionally, wherever possible, 50 000 gated events were saved for each analysis.

### Results

The DNA profiles obtained are given in Figure 5–7, and the peak fluorescence channel numbers for control PBLs and NZM cells, together with the derived figures for DNA ploidy, are given in Table 5–4. Also given are the original figures for ploidy and a comparison of those with the new data.



Key: X-axis = event DNA fluorescence integral (FL2-A); Y-axis = normalised relative abundance; black area = leukocyte component; grey area = melanoma cell component.

Figure 5-7: Melanoma cell-line DNA profiles (V3)

Cell-line	PBL G <sub>1</sub> peak	Melanoma G <sub>1</sub> peak	DNA ploidy (V3)	DNA ploidy (V1)	% difference
NZM1	119	216	1.82	1.98	-8.1
NZM2	118	223	1.89	1.81	4.4
NZM3	113	220	1.95	1.99	-2.0
NZM4	110	329	2.99	2.94	1.7
NZM5	109	110	1.01	1.09	-7.3
NZM6	113	226	2.00	2.12	-5.7
NZM7	114	155	1.36	n.d.	n.d.
NZM7.2	117	146	1.25	1.34	-6.7
NZM7.4	116	147	1.27	1.39	-8.6
NZM9	114	230	2.02	2.10	-3.8
NZM10	114	244	2.14	2.10	1.9
NZM10.1	114	285	2.50	2.31	8.23
NZM11	116	201	1.73	1.92	-9.9
NZM12	114	139	1.23	1.26	-2.4
NZM13	113	143	1.27	1.24	2.4
NZM14	117	137	1.17	1.15	1.7
NZM15	119	232	1.95	2.03	-3.9

Peak values are DNA fluorescence integral local maxima; ploidy figures are the ratio of melanoma to PBL peak values; the difference is calculated as (V3 ploidy - V1 ploidy) / V1 ploidy expressed as a percentage. n.d. = no data.

Table 5-4: Melanoma cell-line DNA ploidy (V3)

## Discussion

### *The DNA ploidy of NZM7*

A datum absent from the original work due to the exclusion of NZM7 from the experimental panel is now available: the DNA ploidy of the parental NZM7 cell-line is 1.36. Since this is identical to the value inferred from the measured ploidies of NZM7.2 and NZM7.4 at the time of the creation of Figure 5-3, no replacement figure is necessary.

### *Evidence for heteroploidy*

There was much less evidence of heteroploidy present on this occasion to the extent that only a single population could confidently be identified in each cell-line. Many cell-lines displayed a small broad peak in the S-phase region, and while this could denote an additional G<sub>1</sub> population of higher base ploidy than the major component present, corresponding G<sub>2</sub> peaks were not conspicuous. Possibly some or all of these small peaks represent pulses of cells passing through S-phase as a result of unintentional partial cell-cycle synchronisation during culture. Nevertheless, there are small indications of heteroploidy. In several cases, there are more events with greater than a G<sub>2</sub> DNA content than would be expected in cells of pure ploidy. The NZM10.1 profile has anomalously broad peaks suggestive of aneuploidy. In NZM7.2, the unusually high G<sub>2</sub> peak relative to G<sub>1</sub>, combined with the small peak at the relatively tetraploid position are good indications of the presence of an additional sub-population.

Most interestingly, NZM10 displayed a very much more conventional DNA profile than in the initial work, and had not the earlier complex profile been observed repeatedly at the time, as evidenced by the paclitaxel data shown above, then its validity might be in question. Subtle cues to genomic instability do exist in the current profile however, in particular, the number of events with higher than base G<sub>2</sub> DNA content, and the barely discernible increase in this at twice the DNA content of the small peak in the S-phase region.

NZM10 is notoriously difficult and variable in culture {See '*Idiosyncrasies of NZM cell-lines in culture*' beginning on page 3–3}. Given the plasticity of the cell-line, and the potential for unanticipated selection due to culture stress, it is possible that at times a culture may be reasonably uniform in ploidy, even if it remains genomically heterogeneous, since equality of DNA content by no means guarantees genomic equality. A further possibility has been uncovered, described more fully in Chapter 6. By fluorescence microscopy using Hoechst 33342 as a nuclear label, NZM10 cells have been found to develop a variable size and number of anomalous subnuclear nucleic acid bodies. The incidence of these varies from cell to cell and from culture to culture. Their origins are unknown, and consequently, so is the basis for this variation. What influence these would have on ploidy measured by propidium intercalation is uncertain, but it could reasonably be expected to result in a more complex than usual DNA profile. It is quite possible that the cells used for the initial ploidy analysis were experiencing a high level of this phenomenon while those used in the current work were not.

### ***Replicability and identity***

With respect to the concordance of measured ploidy between the original and V3 assays, paired assessments are within 10%, comparable to the variation present among the reference PBL peaks. The mean divergence between V1 and V3 data is 3.4%, and the standard deviation 2.6%. This mean is not significantly different from zero (Student's t-test;  $p < 0.001$ ). The values for NZM7.4 and NZM11 fall further than two standard deviations from the mean and might be considered outliers. NZM11's morphology is unique within the subject panel and the possibility of misidentification is remote {See '*Phase contrast microscopy*' in Section 3.5}. In the case of NZM7.4, a genetic feature unique within the subject panel confirms its identity {See '*DNA sequencing*' in Section 8.4}.

### **Supplementary literature review**

#### ***Aneuploidy***

Genomic derangement of one type or another is a hallmark of all cancers, but the nature and extent of this derangement is to a degree tumour-type dependent. For example, near one end of the spectrum of derangement lies chronic myelogenous leukaemia, where a well-defined t(9;22) translocation that serves to activate the *ABL* oncogene is seen in the great majority of tumours, but little other derangement is found<sup>1579</sup>. Melanoma lies at or near the opposite extreme of this spectrum. While similarities in chromosomal aberrations found in cytogenetic studies have suggested the presence of a number of genes critical in the tumorigenesis of melanoma, or its prevention<sup>1626</sup>, overall, the karyotypes observed are heterogeneous not only



among tumours from different patients<sup>1674</sup>, but also between primary tumours and metastases<sup>1532</sup>, and among different metastases from the same patient<sup>1620 1634</sup>. Such cytogenetic studies as these also reveal derangements that go beyond the structural, and involve changes in the total chromosomal content of cells through the complete loss of some chromosomes, to the gain of additional copies of apparently structurally normal chromosomes, to the appearance of marker chromosomes of sometimes obscure origin; changes collectively known as aneuploidy: the departure from normal diploidy. As is the case with structural abnormalities, heterogeneity of ploidy between and among tumours and metastases is also seen when investigated with techniques that measure the distribution of DNA content in populations of cells, such as flow cytometry and image analysis<sup>1652</sup>.

A summary of some representative ploidy studies of cutaneous melanoma tumours is given in Table 5–5. While the frequency with which aneuploidy was detected varied considerably among studies, perhaps due to the inclusion criteria used in the study or the therapeutic interventions taken prior to sample collection<sup>1681</sup>, it is clearly a common feature of melanoma.

Lead author	Year	Method	Type	n	Diploid	Aneuploid	Heteroploid
Barlogie <sup>1534</sup>	1978	FCM	met	7	0%	100%	–
Wass <sup>1685</sup>	1985	FCM	pri	14	36%	43%	21%
Wass <sup>1685</sup>	1985	FCM	met	115	33%	52%	15%
van Roenn <sup>1683</sup>	1986	FCM	pri	53	–	25%	4%
Kamino <sup>1584</sup>	1990	FCM	pri	22	55%	45%	–
Björnhagen <sup>1540</sup>	1991	IA	pri	23	61%	39%	–
Björnhagen <sup>1540</sup>	1991	IA	met	35	54%	46%	–
Slater <sup>1662</sup>	1991	FCM	pri	12	75%	25%	–
Rode <sup>1644</sup>	1991	IA	pri	26	27%	73%	–
Muhonen <sup>1622</sup>	1991	FCM	met	107	31%	46%	12%
van Oven <sup>1681</sup>	1992	FCM	pri	25	52%	44%	4%
Karlsson <sup>1585</sup>	1993	FCM	pri	82	44%	56%	–
Schmidt <sup>1651</sup>	1994	IA	pri	12	67%	33%	–
Talve <sup>1672</sup>	1997	IA	pri	66	32%	68%	–
Kheir <sup>1588</sup>	1998	FCM	pri	172	72%	22%	–
Korabiowska <sup>1590</sup>	2000	IA	pri	106	6%	94%	–
Pilch <sup>1638</sup>	2000	IA	pri	58	14%	86%	–
Pilch <sup>1638</sup>	2000	IA	met	11	19%	81%	–

FCM = flow cytometry; IA = image analysis; met = metastases; pri = primary; n = dataset size; – = not reported. Note: aneuploid includes tetraploid.

**Table 5–5: Ploidy analyses of cutaneous melanoma tumours**

### *Diversity*

The flow cytometric study of Wass et al.<sup>1685</sup> is of particular note. Biopsy samples were obtained from 14 patients with primary, and 86 with metastatic disease. While no matched primary/metastatic material was available, in five patients, samples were taken from multiple metastatic tumours concurrently, in 14 patients samples were available from metastases occurring at different times, and in four patients, multiple samples were available from discrete areas of differing pigmentation within individual metastases. The authors reported discordance in the measured ploidy in three of the five cases of concurrent biopsies from different metastases, in ten of the fourteen cases of biopsies taken at different times, and in one of the four cases of biopsies from differently pigmented areas. Similar results have also been

seen using the method of image analysis. Björnhagen et al.<sup>1540</sup> found differences in the DNA histograms associated with tissue from histopathologically distinct parts of a single primary tumour. Clearly, primary melanoma can be genomically diverse.

The Björnhagen et al. study could also address a question unanswered by that of Wass et al.<sup>1685</sup>, as matched material from primary tumours and subsequent metastases was available. In six of fourteen cases where the primary tumour was predominantly diploid, the metastases were predominantly aneuploid, and in four of nine cases primary tumours were predominantly aneuploid while the metastases were predominantly diploid. This was also seen in the study of Rode et al.<sup>1644</sup> who reported three of seven cases where aneuploid metastases arose from diploid primaries, and one of thirteen cases where a diploid metastasis arose from an aneuploid primary. The conclusion to be drawn from these observations is that there is no correlation between the transition to aneuploidy, as inferred from DNA content, and metastasis.

### *Heterogeneity*

The results of the studies so far described primarily deal with the relationship between samples where they have each been classified simply as diploid, aneuploid, and possibly tetraploid, the thrust of the studies being to seek to correlate these classes with disease progression, drug responsiveness, or some other clinical measure. However, in some studies<sup>1534 1622 1681 1683 1685</sup> where flow cytometry was employed, the increased resolution of ploidy data available, due to the greater number of cells analysed when compared to image analysis, led to the discovery that even within tumours without histopathologically distinct regions, several aneuploid populations with differing ploidy may be present.

Studies of ploidy variation in melanoma cell-lines are more sparse in the literature. Among karyotypic analyses, Liao et al.<sup>1605</sup>, and subsequently McCulloch et al.<sup>1609</sup>, reported on a panel of seven cell-lines. All displayed gross aneuploidy with a range of chromosome numbers present in each. One cell-line, M-6, had what was termed a random or diffuse distribution of chromosome numbers in which no clear modal value was present. Pope et al.<sup>1639</sup> studied ten cell-lines through metaphase spreads, and all were aneuploid by chromosome count, with a range of counts being found in 20 spreads, including one with bimodal chromosome count distribution. The same panel was further studied<sup>1623</sup>, and again all cell-lines exhibited a range of chromosome numbers, with some being clearly bimodal. In the latter study, four of the cell-lines were analysed again after a year or more, and small changes in ploidy were detected.

There appears to be a single report of a flow cytometric study of human melanoma cell-line ploidy<sup>1659</sup>, and this was for a single cell-line, MeWo, which was found to contain two populations of differing ploidy.

### **The current work in perspective**

While the work described in this thesis pertains only to the flow cytometric study of ploidy in human metastatic melanoma cell-lines, it is consistent with the published literature relating to the analysis of human primary and metastatic melanoma tumours and short-term cultures



---

therefrom, and with the published findings relating to human melanoma cell-lines when explored with other techniques. The current work describes what appears to have been the only flow cytometric study of ploidy for a panel of human metastatic melanoma cell-lines undertaken.

Since the genomic diversity seen *in vivo* is also seen *in vitro*, this suggests firstly that this diversity is not merely an artefact of cell-line establishment or an adaptation to passage culture, and secondly, that *in vitro* studies of genomic instability in cell-lines may well have relevance in the context of tumours *in vivo*, and hence in the possible development of new therapies.

### **Remaining questions**

None of the published studies attempts to elucidate the causes for this genomic instability, or even speculates in any depth as to what these causes might be. The causal relationship between genomic instability and tumorigenesis in melanoma remains an open question: is it that a failure of genomic regulation allows melanocytes to develop into melanoma, or is this derangement simply an incidental consequence of a more fundamental flaw that also leads to tumorigenesis?





---

# 6

## Centrosomal integrity (V3)

---

*The possibility that centrosomal numerical dysregulation may be contributing to unstable ploidy in the NZM cell-lines was investigated by an immunofluorescence microscopic study of mitotic cells in which  $\alpha$ -tubulin, the centrosomal marker protein pericentrin, and DNA were differentially fluorescently labelled.*

*Evidence of dysregulation was abundant, and aberrant mitoses were present in all cell-lines studied. Pericentrin accumulated in nucleoli, and its release from these reservoirs at prometaphase entry suggests this may be a means of initiating spindle formation.*

*The results of this study prove that the loss of centrosome numerical regulation deduced from the consideration of heteroploidy exists in reality, and further, that events of the types necessary to account for this heteroploidy are indeed occurring in the NZM cell-lines. The possibility that pericentrin regulation is defective in melanoma has arisen, and if this is so, it could lead to the development of new therapies.*

---

### 6.1 Introduction

The study of ploidy through flow cytometric analysis of cellular DNA content, described in the previous chapter, has led to the proposal that failure of centrosomal numerical control is the likely cause of the abnormal and unstable ploidy detected in many of the NZM cell-lines. Before embarking on a screening process to determine the integrity of molecular targets that might be involved in such dysregulation, a reasonable first step is to undertake a microscopic study to determine if the hypothesised dysregulation is indeed occurring. To do this, it is necessary to count centrosomes in their cellular context. Cells should either have one centrosome if they are in the G<sub>1</sub> or early S phases, or two, if they are in late S phase, G<sub>2</sub>, or mitosis; any other number would represent an anomaly. To determine if any numerical aberrations that may be occurring are likely to lead to changes in ploidy, it is necessary to observe the centrosomes during their critical period of activity, that is, when they are orchestrating the segregation of the newly duplicated cellular genome during mitosis. To achieve these goals, the centrosomes themselves, the mitotic spindle apparatus that mediates their organisational influence on the cellular genome, and the genome itself must be visualised simultaneously in mitotic cells. While ideally this should be done in live cells and events followed in real time, the developmental effort required to achieve this degree of analysis would only be warranted once definitive proof of the suspected dysregulation was available.

The method of immunofluorescence microscopic examination of fixed monolayer cell cultures lends itself particularly well to the task of seeking to obtain this definitive proof. Antibodies to  $\alpha$ -tubulin, a major component of both centrioles and the mitotic spindle, are commercially available from many suppliers, but unfortunately, antibodies to core centrosomal components, such as centrin, that are recommended by their manufacturer as suitable for immunofluorescent studies are not, and many researchers use a mouse monoclonal anti-centrin

---

antibody gifted by Professor Jeffrey Salisbury of the Mayo Clinic. There is some inconsistency in its nomenclature in the literature. While it is most recently and commonly referred to as clone 20H5, the citation given in the first such published usage<sup>S1680</sup> refers to the isolation of a mouse monoclonal dubbed 17E10<sup>S1649</sup>. It seems probable that it was renamed to avoid confusion with an anti-catalase antibody developed by Wiemer et al. also named 17E10<sup>1686</sup>. To ensure ongoing availability of antibody, both in this work and for any who may seek to replicate or extend it, the decision was taken to use a commercially available antibody to pericentrin {E.12}, a centrosome-associated protein<sup>1554</sup>. Work published using this antibody<sup>1697</sup> and examples present in the manufacturer's data indicate that it should provide clear focal labelling of centrosomes. It must be noted that this antibody was raised against a synthetic peptide that is also present in a related protein, kendrin. For simplicity, the labelled protein will be referred to as pericentrin for the purposes of discussion, but it must be borne in mind that any conclusion drawn may apply equally well, or indeed only, to kendrin. Since the purpose intended for this antibody is simply to provide a centrosomal marker, which it does, this ambiguity is of little consequence. While bona fide centrosomes, that is, those that contain centrioles, should show focal pericentrin labelling, the converse may not necessarily be true. A focus of pericentrin labelling may or may not contain centrioles and interpretation of any such foci as centrosomes can therefore only be tentative, particularly where differences in focal size are evident. Nevertheless, since it has been shown that acentriolar pericentrin foci can also nucleate microtubule growth<sup>1636</sup>, there may be no functional distinction between these and true centrosomes. Visualisation of the genome is relatively simply achieved through counterstaining of cellular DNA using the conditionally fluorescent minor groove binding bisbenzimidazole derivative 2'-(4-ethoxyphenyl)-5-(4-methyl-1-piperazinyl)-2,5'-bis-1H-benzimidazole, also known as Hoechst 33342, or 4',6-diamidino-2-phenylindole (DAPI). Selection of fluorescent secondary antibodies without significant overlap in their emission spectra, or with that of Hoechst 33342 or DAPI, allows the simultaneous unambiguous assignment of fluorescent signals to the specific targets under investigation, and, where instrumentation permits, simultaneous capture of data for each.

## 6.2 Methods in brief

### Cell culture

NZM cells, or early passage tumour-associated fibroblasts, were seeded in quadruplicate at low density (~50 cells/mm<sup>2</sup>) in  $\alpha$ MEM supplemented with 10% v/v FCS and antibiotics into 35 mm diameter tissue culture plates, into each of which a sterile 22 mm x 22 mm glass coverslip had previously been placed [Method 35]. After ~3d, when phase contrast microscopy confirmed that the cells had become adherent, had adopted their normal in vitro morphology, and appeared to be proliferating as evidenced by the presence of detached, rounded, highly refractile, presumably mitotic cells, one pair of coverslips for each cell-line was fixed in 3.5% paraformaldehyde for 15 min and stored in PBS with added antibiotics at 4 °C until processed [Method 36]. After a further ~3 d, when cell density was somewhat higher, the remaining pair of coverslips for each cell-line was similarly fixed and stored.

## Slide preparation

Working in reduced light as necessary, coverslips with fixed monolayer cells were treated with Hoechst 33342, if this was the DNA stain to be employed, permeabilised with Triton X-100 detergent, blocked with BSA, incubated with primary antibodies against  $\alpha$ -tubulin and pericentrin, washed, incubated with an Alexa Fluor 488 conjugated secondary antibody specific for the  $\alpha$ -tubulin primary antibody and an Alexa Fluor 594 conjugated secondary antibody specific for the pericentrin primary antibody, washed four times, dried, mounted with Prolong Gold Anti-fade reagent, with or without DAPI as appropriate, cured, sealed, and stored at 4 °C [Method 44]. One slide of each pair was designated for fluorescent microscopic examination, and one reserved for inspection by laser scanning confocal microscopy if this proved warranted.

## Controls

One set of control slides {Table 6–1} using NZM6 was prepared to validate the specificity of antibody binding and explore the level of autofluorescence.

Control	Anti-pericentrin	Anti- $\alpha$ -tubulin	Alexa Fluor 488	Alexa Fluor 594
Autofluorescence	omitted	omitted	omitted	omitted
594 non-specificity	omitted	omitted	omitted	included
488 non-specificity	omitted	omitted	included	omitted
594 cross-reactivity	omitted	included	omitted	included
488 cross-reactivity	included	omitted	included	omitted
Positive control	included	included	included	included

**Table 6–1: Immunofluorescent labelling controls**

## Fluorescence microscopy and photography

Prepared slides were viewed by fluorescence microscopy using a Zeiss Axioskop 2 microscope equipped with filter blocks suitable for the detection of the individual fluorophores employed [Table 6–2]. Separate images were captured with each relevant filter block at 2560 × 1920 pixel resolution with an attached Sony DXC-S500 digital camera and image capture system and saved as losslessly compressed PNG files for post-processing. Image scale was determined by comparison to images of the rulings of a standard haemocytometer grid taken with each objective used.

Label	Block ID	Excitation filter	Dichroic	Barrier filter
DAPI or Hoechst 33342	48-79-02 (FS02)	G365	FT395	LP420
Alexa Fluor 488	48-79-09 (FS09)	BP450–490	FT510	LP520
Alexa Fluor 594	48-79-00 (FS00)	BP530–585	FT600	LP615

**Table 6–2: Fluorescence microscope filter blocks used**

A small amount of laser scanning confocal microscopy was performed with expertise provided by the Biomedical Imaging Research Unit of the Faculty of Medical and Health Sciences.

## Image processing

Selected image files were processed using Photoshop, ImageJ, and GraphicConverter software [E.9, E.18]. Typically, the individual fluorophore images were imported into a Photoshop document as separate layers, were constrained to discrete colour channels [Method 45], adjusted for brightness and contrast [Method 46], spatially registered [Method 47], exported to ImageJ as greyscale files and z-projected [Method 48] if necessary, before being merged into a

composite image {Method 49}. Rarely, slight image enhancement was performed, but this was limited to noise-reduction and sharpening {Method 50}. Scale bars were added and images cropped as required in Photoshop. Images intended for low-resolution usage were resampled, compressed, or converted to other file formats with GraphicConverter or ImageReady {E.18} as required. At all points in the workflow prior to down-sampling, if any, the files were maintained in a lossless format, typically TIFF or PNG.

### Mitotic cell survey

For each cell-line under investigation, mitotic cells were sought by systematically scanning a slide while observing the DNA staining under 200x magnification. The first one hundred cells where chromatin condensation was observed were scored according to the criteria described below. If fewer than 100 mitoses were found on one slide, the other slide for the cell-line designated for fluorescence microscopy, with cells at a different density, was used as well.

### Mitotic phase

The major divisions of mitosis, prophase, prometaphase, metaphase, anaphase, and telophase were identified by observing the condensation state of the chromatin and its spatial arrangement, together with the nature of any tubulin structures present, usually in association with centrosomes. Where chromatin condensation was observed in cells not obviously part of a post-mitotic pair, and where this chromatin was apparently constrained to an approximately spherical region, the cell was assigned to prophase. Assignment to prometaphase was made on the basis that this condensed chromatin did not appear to be constrained to such a region, implying that nuclear envelope breakdown had occurred. Where it appeared that chromosomes were being organised into a metaphase plate or corresponding aberrant structure, the cells were classed as metaphase. Anaphase was inferred if chromatids appeared to be being partitioned in association with centrosomally organised tubulin structures. If the chromatin had begun to disperse and an intercellular bridge was evident, but daughter cells were still clearly attached, the cell was classed as being in telophase. This definition of telophase is rather broad and includes cells up to the point of abscission in cytokinesis. Such advanced cells are still suitable for inclusion in this survey.

Representative images of cells in each phase of mitosis are given in Figure 6–1.

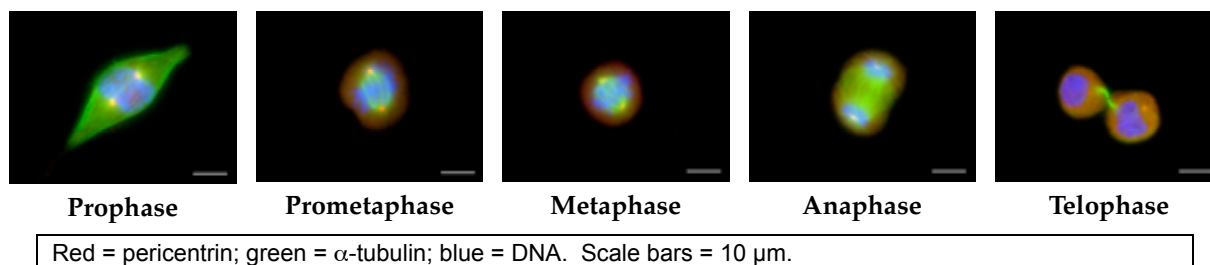


**Figure 6–1: Examples of normal mitotic phases**

Even in apparently normal mitoses, the divisions between mitotic phases were not always clear-cut. For example, the difference between the prometaphase and metaphase images in Figure 6–1 is subtle, the distinction depending on the greater constraint of the condensed

chromosomes to the metaphase plate seen in the latter. In aberrant mitoses, assignment to a mitotic phase was sometimes not possible at all due to the chaotic nature or conflicting implications of the structures present. In these cases, the cell was scored either in the phase that it most plausibly resembled, or as indeterminate if no reasonable placement could be made.

### *General aspect*

An initial overall subjective assessment of cellular normality was made for each cell to be included in the mitotic survey. The cell was classed as normal if no unusual aspects were immediately obvious. It was classed as slightly abnormal if an unusual feature was observed, but not obviously so severe as to interfere with the proper execution of mitosis. Examples include: the presence of micronuclei; a lagging chromosome during anaphase; a presumably non-centrosomal pericentrin focus not influencing  $\alpha$ -tubulin structure; centrosomes with an extended or overly granular appearance; and an unusual chromatid arrangement during metaphase. It is almost certain that many cells classed as slightly abnormal would be found to be within the range of normal variation if a larger study were undertaken; conversely, many, particularly early mitotic cells, may have strayed further from normality if they had had the opportunity. Inclusion in this class is therefore indicative, rather than definitive.

Some examples of this class are shown in Figure 6–2.

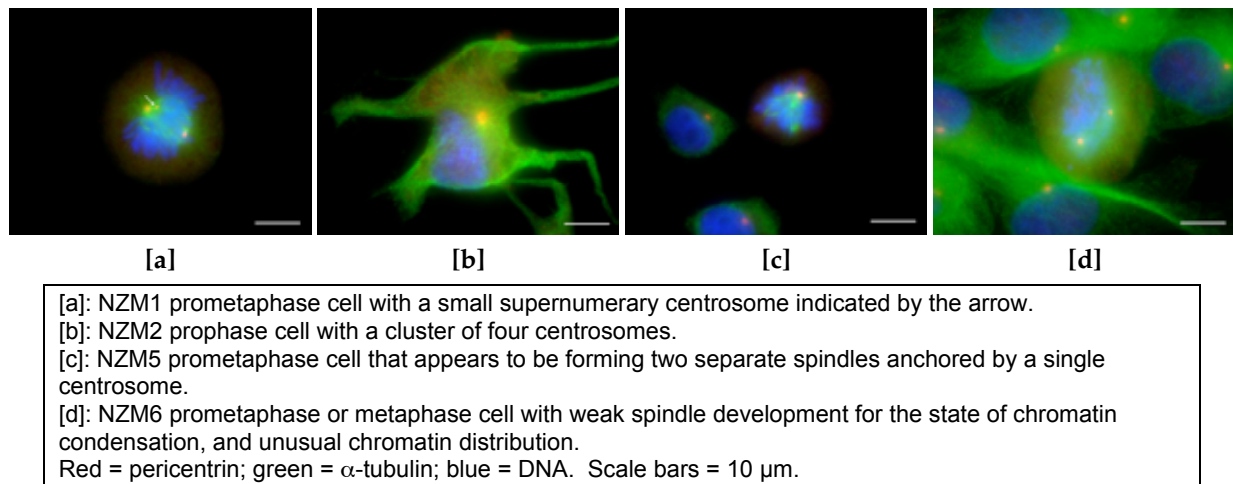


**Figure 6–2: Examples of slightly abnormal mitotic cells**

A cell was classed as grossly abnormal if features were seen that seemed likely to result in an aberrant mitosis, such as supernumerary centrosomes directing the formation of a multipolar spindle, multi-nuclear cells, gross missegregation of chromatids, or other than binary anaphase or telophase.

Some examples of this class are shown in Figure 6–3.

### *Centrosome number*

For the majority of cells examined, identification of centrosomes by pericentrin staining was unambiguous, and centrosomal number could be ascertained with a very high degree of confidence. This was not always the case, however. There were many instances where

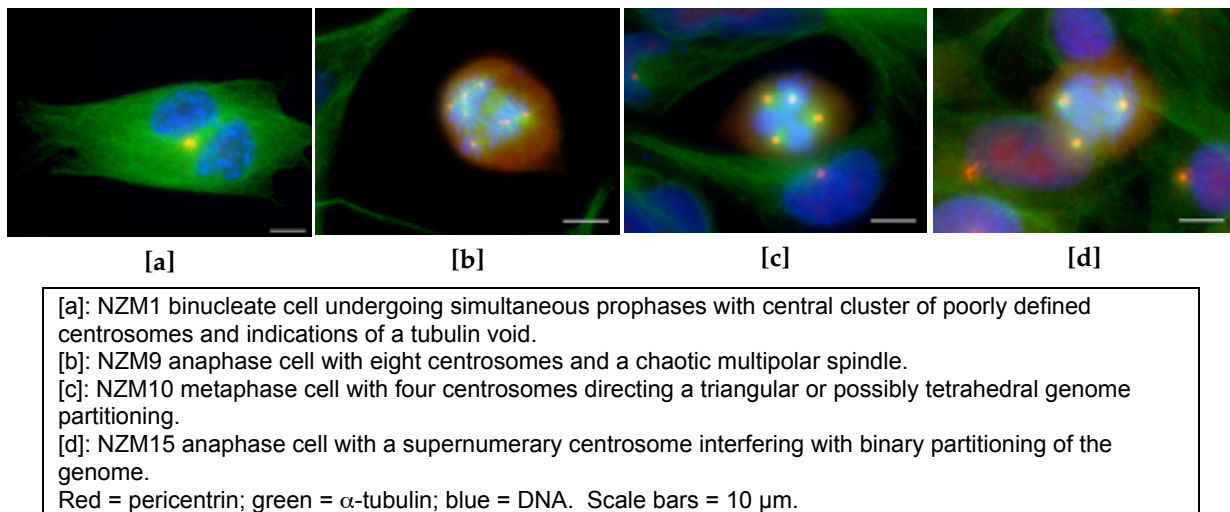


**Figure 6-3: Examples of grossly abnormal mitotic cells**

punctate pericentrin labelling occurred and the threshold beyond which a pericentrin focus was classified as a centrosome was necessarily subjective. In other cases, it was not always clear if a particularly large-seeming centrosome was actually one, or two in close association or optically aligned. It was observed that telophase cells almost invariably had reduced centrosomal pericentrin labelling, and in some cases fewer than two pericentrin foci ascribable to centrosomes were observed. Such cells contributed to the count of those with abnormal centrosomal number, and if this phenomenon is actually normal, the consolidated data may overstate numerical abnormalities slightly.

### *Centrosome morphology*

An attempt was made to infer basic centrosome morphology from pericentrin labelling. Intensity of labelling was taken as an indication of centrosome size, although it could equally well indicate levels of pericentrin expression or centrosomal localisation. Centrosomes were classed as of normal size, smaller, or larger than usual for the mitotic phase of the cell-line. Due to the reduced pericentrin labelling of centrosomes in telophase cells {6-30}, these were not classed as having smaller than normal centrosomes. Individual cells, particularly when they contained an abnormal number of centrosomes, could contain centrosomes of differing sizes, thus the cell could be scored in multiple classes. In addition, if the presumed centrosome-associated pericentrin labelling was other than a distinct point, the cell was scored as having additional centrosomal structure. If this structure was particularly evident, the cell was classed as having a slightly abnormal general aspect. The types of structure seen ranged from granular patches of labelling at  $\alpha$ -tubulin foci to the presence of pericentrin bars, arcs, or spurs emanating from a central focus.

Examples of cells containing centrosomes of the various classes are given in Figure 6-4.

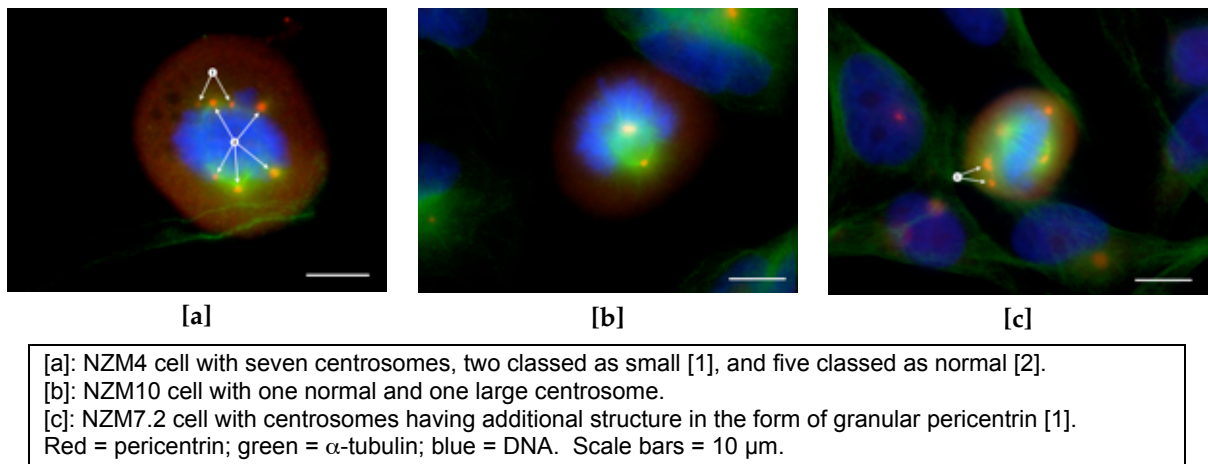


**Figure 6-4: Centrosome morphology class examples**

### *Centrosome positioning*

The spatial arrangement of centrosomes was characterised as clustered or distributed depending on their proximity. Where only one centrosome was present, this was inapplicable, and where more than two were present it was possible for centrosomes to be arranged in separated clusters, hence some cells were scored in both classes.

### *Pericentrin distribution*

Pericentrin distribution was categorised in terms of the following non-mutually exclusive classes: centrosomal, where very intense uniform globular labelling was seen, particularly when associated with the intersection of numerous  $\alpha$ -tubulin filaments; diffuse, where amorphous or somewhat granular labelling was seen throughout the cell; punctate, where small pericentrin foci were seen, generally not associated with  $\alpha$ -tubulin structures; patched, where areas of labelling greater than the diffuse background were seen; and structured, where extended pericentrin structures were visible. Examples of these labelling patterns are given in Figure 6-5.

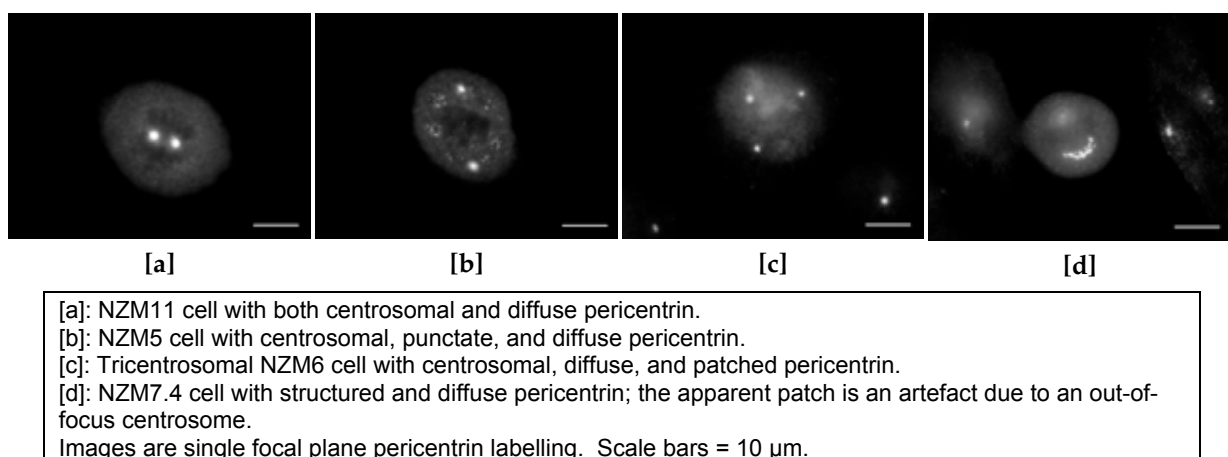


**Figure 6-5: Pericentrin labelling class examples**

### *Symmetry*

During mitosis, the normal cell moves from a state of asymmetry in early prophase to one of axial symmetry beginning in late prophase or prometaphase once the centrosomes have separated fully. The state of cellular symmetry was assessed primarily with reference to the

mitotic spindle prior to telophase, and then with respect to the spatial distribution of the nascent daughter cells. Spindle symmetry was categorised as absent, unipolar, normal bipolar, abnormal bipolar, tripolar, quadripolar, or multipolar. In early mitotic phases, absence of a spindle, or the presence of a unipolar spindle may not constitute an abnormality, but beyond late prometaphase, they would, and such cells would be scored with a general aspect of slightly abnormal. In some cell-lines, such as NZM6, where the initial production of unipolar spindles is common, the transition from unipolar to bipolar produces a conformation that cannot easily be assigned to either class. These cases were categorised as indeterminate. The distinction between a normal and an abnormal bipolar spindle lies in the number of centrosomes involved. In the normal case there is a single centrosome at each pole; in the latter, supernumerary centrosomes may be present, at the poles or otherwise, but a strong bipolar spindle exists in spite of this. This need not be the case when supernumerary centrosomes are present however, and rather than clustering to form two functional poles and a bipolar spindle, other symmetries can occur. For example, three equally strong and mutually equidistant centrosomes can direct the formation of a tripolar spindle, which can ultimately result in a ternary anaphase and cytokinesis. While the geometry of this can only be planar, for higher numbers other geometries are possible. In the case of tetracentrosomal cells where no centrosomal clustering occurs, one geometry is planar quadripolar and another is tetrahedral quadripolar, and in these cases correct segregation seems very unlikely to result. Visually distinguishing between these two geometries can be difficult since it depends on the interpretation of different focal plane views to place the centrosomes in three dimensions, and scoring of these quadripolar geometries is therefore somewhat subjective. Beyond four centrosomes, no attempt is made to categorise symmetries, as all must be chaotic to some extent. This follows directly from the fact that more than four points cannot be mutually equidistant in only three spatial dimensions.

Example images for these classes are given in Figure 6–6.

### *Segregation anomalies*

Where the arrangement of condensed chromosomes observed in prometaphase or metaphase appeared unusual due to asymmetry or apparent disconnection from the mitotic spindle, the cell was classed as either slightly or grossly abnormal as warranted. In anaphase, cells were scored for the presence of lagging chromosomes, and in anaphase and telophase, for the presence of chromatin bridges connecting the separating chromatid masses. Additionally, if micronuclei were observed, or thought to be forming in telophase cells, this too was recorded.

### *Additional observations*

In addition to the systematic survey of mitotic cells, random visual tours of each slide were performed using all filter blocks, and images of cells displaying unusual labelling irrespective of cell-cycle phase were captured.



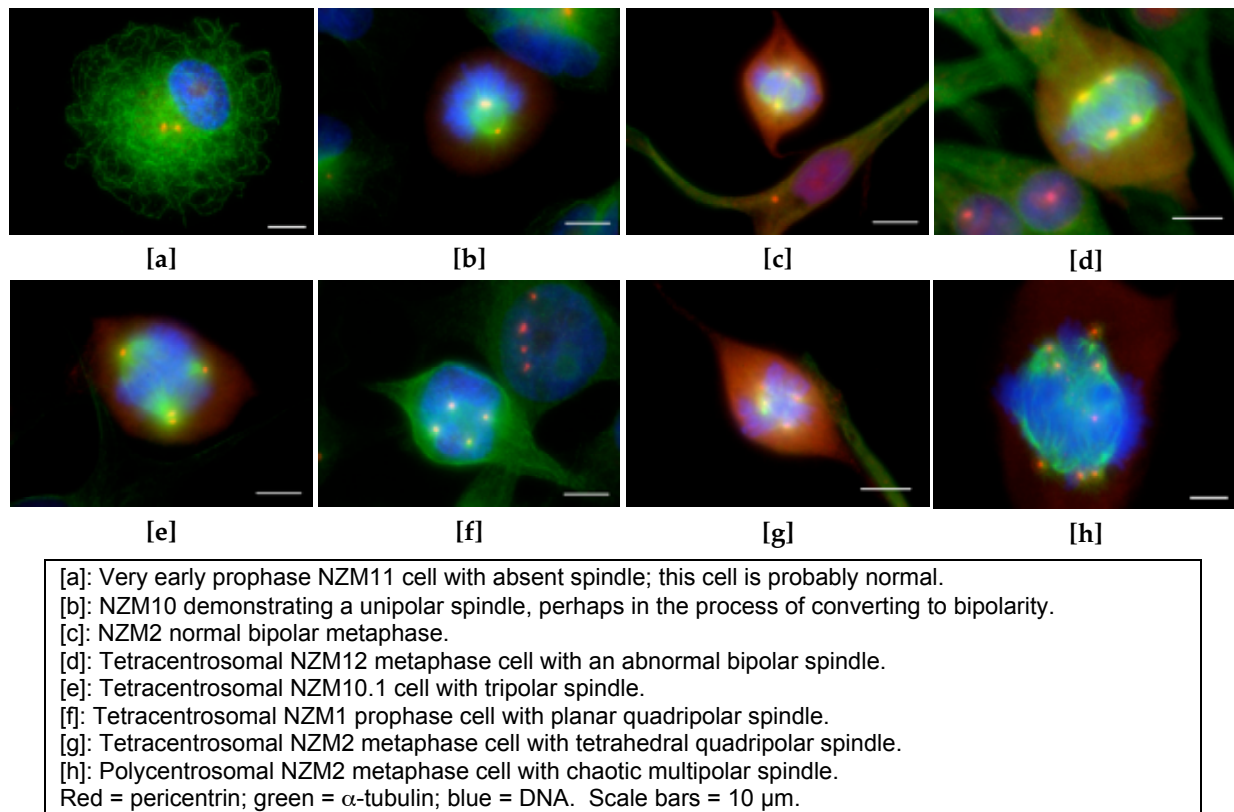


Figure 6-6: Symmetry class examples

## 6.3 Results and discussion

### Magnitude of endeavour

Cell culture time was a minor component of total effort. Slide preparation required approximately 35 h. Fluorescent microscopic examination in order to score the required 100 mitotic cells per cell-line, and capturing images of representative normal and abnormal cells typically took approximately six hours. For the 17 cell types examined this entailed approximately 100 h of microscopy, during which nearly 30 gigabytes of image data were captured comprising over 5 000 component images. Image processing for each composite image produced typically took 40 min, the majority of this time being spent in registering the component images. Approximately 200 images were produced, making the total image processing time in excess of 130 h. Confocal data capture required about eight hours, and image processing approximately 30 h. Total time invested was in excess of 300 h.

### Inherent system flaws

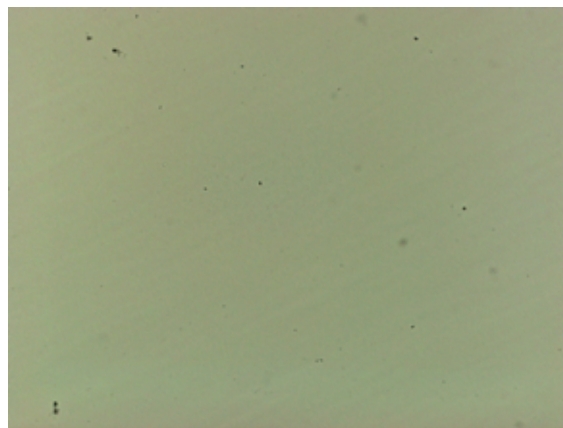
#### *Filter block misregistration*

Initial attempts to assemble images captured using different filter blocks revealed a mutual misregistration among these, and this did not appear to be consistent over time, thus a computer-assisted manual method was necessary for each image {Method 47}, approximately tripling the image processing time required.

#### *Camera sensor defects*

An enhanced version of an image captured by the digital camera system using transmitted white light with no slide in place is shown in Figure 6-7. The most significant inherent defect present is the loss of signal from some parts of the image. As these defects are in focus and are

independent of the objective in use, they most likely corresponds to dirt on the camera's sensor. This may have been removable by professional servicing, but to have done so would have significantly delayed the execution of this work. In practice, it caused little problem of interpretation of the captured images, however, in combination with the slight mutual misregistration of the filter blocks in the microscope, these specks could suggest a focus of labelling, or a labelling void where none existed. Usually, these could be recognised for what they were by the close proximity of identical artefacts for several colours, corresponding to the misregistration of different filter blocks. It was also sometimes possible to reduce the impact of these defects by making small adjustments to the microscope stage position prior to image capture to prevent coincidence of a defect with a structure of interest. That was often a time-consuming exercise, as tiny adjustments to position are not easily made, particularly with an image refresh rate of half a second or more.



Null image captured by the digital camera employed. Colour and contrast are enhanced to accentuate small variations.

**Figure 6–7: Null image**

While these defects could easily have been eliminated by retouching for cosmetic purposes during image processing, this was not performed as it would have constituted subjective manipulation of the captured data.

The other artefacts present, the zone of minute circular marks near the centre, the diagonal smearing, and the slight marginal colour variation, particularly at the bottom of the field, have been intentionally exaggerated in the figure, and while reducing resolution and signal uniformity very slightly, they were inconsequential in practice.

### **Controls**

Optimal exposure times for each fluorophore were determined from the positive control to be 500 ms for the 488 nm fluorophore, and 267 ms for the 594 nm fluorophore. Exposures of these durations for the corresponding fluorophores for each control were made in order to assess the relative strength of any non-specific signal produced. Longer exposures, of 4 s duration, were also made in order that the spatial labelling characteristics of the low levels of non-specific signal present could be assessed. The resultant images, with no adjustments to brightness, contrast, or other image processing having been performed upon them, are given in Figure 6–8.

Control	488 nm fluorophore		594 nm fluorophore	
	500 ms exposure	4 s exposure	267 ms exposure	4 s exposure
Autofluorescence				
594 non-specificity				
488 non-specificity				
594 cross-reactivity				
488 cross-reactivity				
Positive control				

Figure 6–8: Immunofluorescent labelling control results

For the exposure times required to capture the specific signal from the fluorophore-conjugated secondary antibodies, noise from non-specific and cross-reactive antibody binding, and from autofluorescence is negligible. The somewhat better performance of the 594 nm fluorophore may be due to the higher grade of this reagent, it being “highly cross-adsorbed” during manufacture to deplete non-specific interactions beyond that of the normal grade, to which the 488 nm fluorophore conjugated antibody belongs. From these controls, it can be concluded that the fluorescent signals obtained from experimental slides can confidently be interpreted as specific for their respective primary antibody targets.

A processed composite image from the positive control slide, including the DNA counterstain, is given in Figure 6–9. This shows that the cells have been fluorescently labelled in accord with expectation. Nuclei are well defined, and variations in staining indicative of chromatin structure are visible. Alpha-tubulin labelling shows the cytoskeletal microtubule meshwork well, with stronger labelling evident where bundles have formed. Pericentrin labelling is generally focal, with one or two perinuclear foci visible per cell, consistent with centrosomal

association. The yellow-orange colouration of these foci indicates spatial coincidence of pericentrin and  $\alpha$ -tubulin, consistent with known centrosomal structure and nucleation of microtubules by pericentrin<sup>1636</sup>.

### Exclusion of NZM14

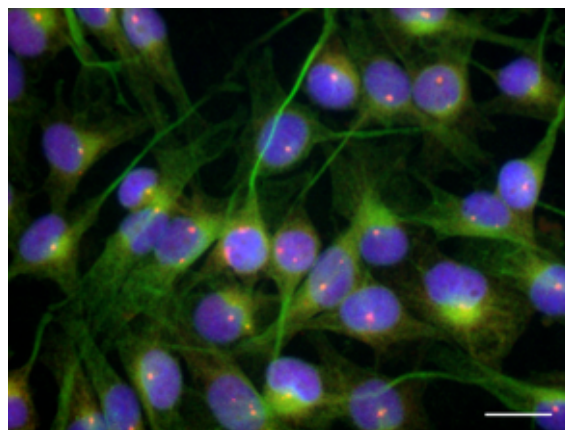
Despite repeated attempts to produce slides containing adequate numbers of mitotic cells to allow scoring, none could be produced for the NZM14 cell-line. Only a very few mitotic cells, exclusively in prophase, were observed among the hundreds of thousands of cells scanned. Since this cell-line was clearly proliferating in culture on coverslips, it was concluded that the failure to observe significant numbers of mitotic cells was due to their being selectively lost during preparation. This was probably as a result of an early loss of adhesion and late restoration of adhesion during mitosis in this cell-line leading to the loss of mitotic cells during the many wash steps involved.

Earlier attempts to enrich the proportion of mitotic cells present on a slide by harvesting the culture supernatant and cytopinning the recovered cells onto slides before labelling had met with only partial success. While the cells then present on the slide were highly enriched for mitotic cells, as intended, the damage sustained by  $\alpha$ -tubulin structures during centrifugation, together with the uncertainty introduced over the relationship, if any, between cells found in close proximity, led to the abandonment of this approach (Figure 6–10). Consequently, attempts were not made to obtain data in this way for NZM14, nor would any data thus obtained have been comparable to that for the other cell-lines due to the difference in methodology, and NZM14 was therefore excluded from the survey of mitotic cells.

### General observations

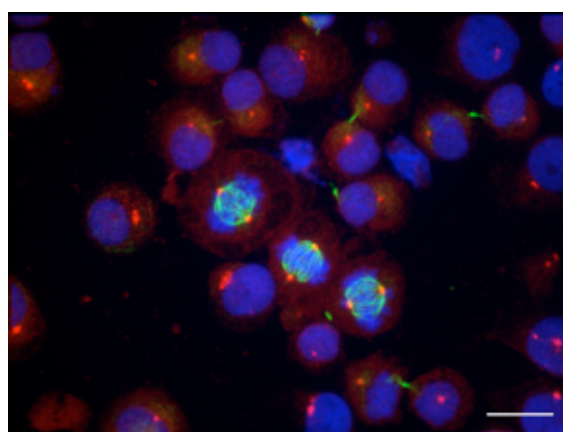
#### *Pericentrin structure*

The preconception of the appearance of pericentrin labelled centrosomes was that they would appear as discrete points exhibiting no discernible structure. In most cases, particularly when observed at low to moderate magnification, this seemed to be the case. However, as more



Red = pericentrin; green =  $\alpha$ -tubulin; blue = DNA. Scale bar = 25  $\mu$ m.

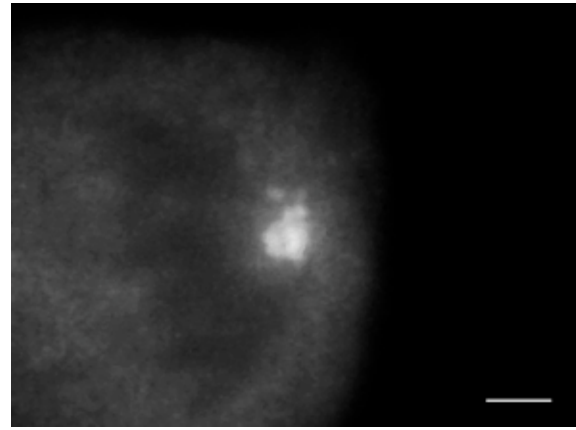
**Figure 6–9: Positive labelling control composite image**



Mitotic enrichment of NZM6 cells by cytopinning culture supernatants is successful, but results in destruction of all but the strongest tubulin structures.  
Red = pericentrin; green =  $\alpha$ -tubulin; blue = DNA. Scale bar = 25  $\mu$ m.

**Figure 6–10: Effects of cytopinning**

centrosomes were observed under high magnification it became clear that centrosome pericentrin labelling was often not strictly focal, with a granular appearance being very common {Figure 6–11}. Owing to its prevalence, and the otherwise normal mitotic structures usually present, this was accepted as being within the range of normality. In their initial characterisation of pericentrin, Doxsey et al.<sup>§1554</sup> reported strong focal pericentrin labelling associated with centrosomes, but also more diffuse

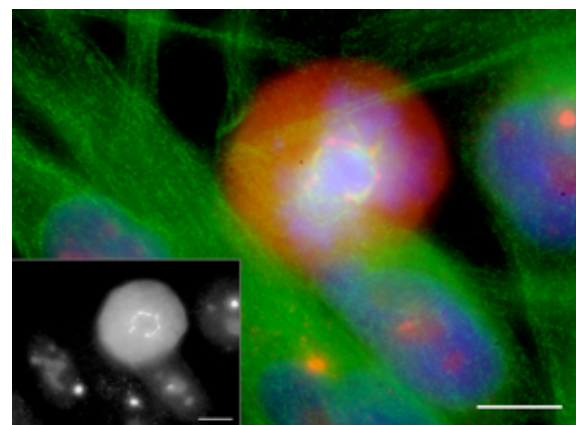


Pericentrin labelling. Scale bar = 2  $\mu\text{m}$ .

**Figure 6–11: Irregular centrosome structure**

centrosomal labelling, and multiple punctae in addition to centrosomal foci, so this interpretation of normality seems reasonable. Figure 6–11 bears a striking resemblance to the unprocessed images shown by Dichtenberg et al.<sup>1553</sup>, where a pericentrin lattice structure surrounding centrosomes was identified based on mathematical image deconvolution. While no specific study was made, the impression gained in the current work was that the irregularity of centrosomal pericentrin structure was at a minimum in prophase, and increased to a maximum during metaphase or anaphase, suggesting a regulated process of lattice formation.

In some cases, commonly in NZM9, centrosomal pericentrin structure was much more extensive {Figure 6–12}. There seemed to be an association between these spur structures and mitotic plates that were particularly broad {Figure 6–13 [a]}, but it is not possible to assign causality in either direction. Their frequent apparently supportive involvement in the organisation of polar tubulin in metaphase and anaphase suggests that they may be beneficial in maintaining spindle stability. However, quite exaggerated structures were also seen, as in the NZM7.4 cell illustrated {Figure 6–13 [b]}, and it seems likely that at the end of this spectrum may lie a disruption of genome partitioning.



Red = pericentrin; green =  $\alpha$ -tubulin; blue = DNA. Inset image: pericentrin only. Scale bars = 10  $\mu\text{m}$ .

**Figure 6–12: Extended pericentrin in NZM9**

Instances were seen where it seemed that an extended centrosomal pericentrin structure may have fractured, possibly as a result of tension along kinetochore fibres {Figure 6–13 [c]}. While the independent foci for microtubule nucleation that result remain in proximity, there should be little adverse effect on spindle structure or the process of genome segregation. However, increasing separation runs an increasing risk of distorting spindle bipolarity and may result in chromosome collisions during anaphase if kinetochore fibres cross.

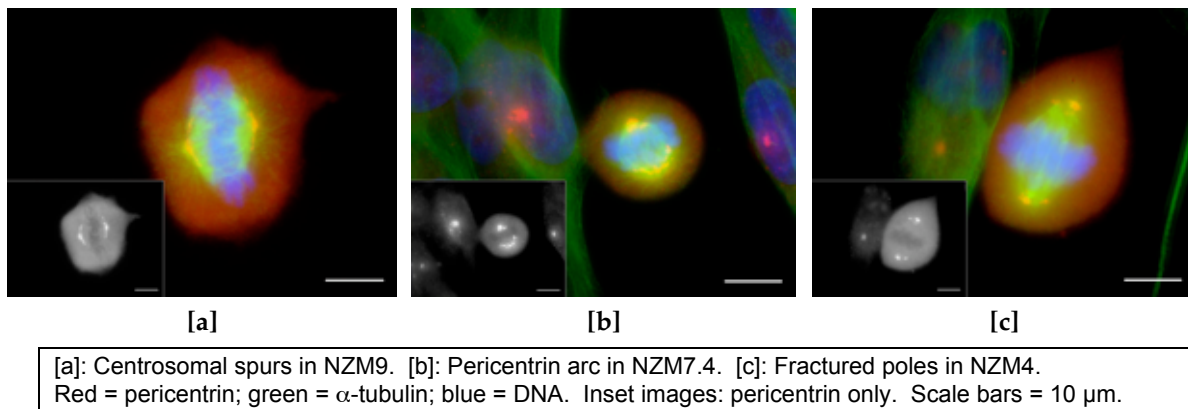


**Figure 6–13: Polar pericentrin structures**

#### *Non-centrosomal pericentrin structures*

In addition to extended pericentrin structures associated with centrosomes, others were found that had no discernible centrosomal association. The NZM13 prometaphase cell illustrated in Figure 6–14 exhibits multiple abnormalities. Only one pericentrin labelling focus is sufficiently large and bright to warrant interpretation as being centrosomal, and thus this cell appears to be monocentrosomal. The centrosomal pericentrin has rather more structure than was normally observed in prometaphase centrosomes, and in addition, both small foci and extended non-centrosomal pericentrin structures are present. The extent to which these are influencing tubulin structure can be assessed by reference to the image given in the right panel that shows a z-projection of a subset of  $\alpha$ -tubulin and pericentrin component images only.

It appears that all but the smallest pericentrin foci are associated with higher densities of tubulin labelling, but no well-defined asters are present, nor any sign of protospindle formation. Were this cell to have continued through mitosis, its destiny would most likely have been a chaotic multipolar metaphase and anaphase followed by a potentially non-binary telophase resulting in aneuploidy and micronucleus generation. Similar structures were reported by Pihan et al.<sup>1636</sup> in their survey of centrosomes in solid tumours and cell-lines, and there they were also considered abnormal and likely to contribute to aneuploidy.

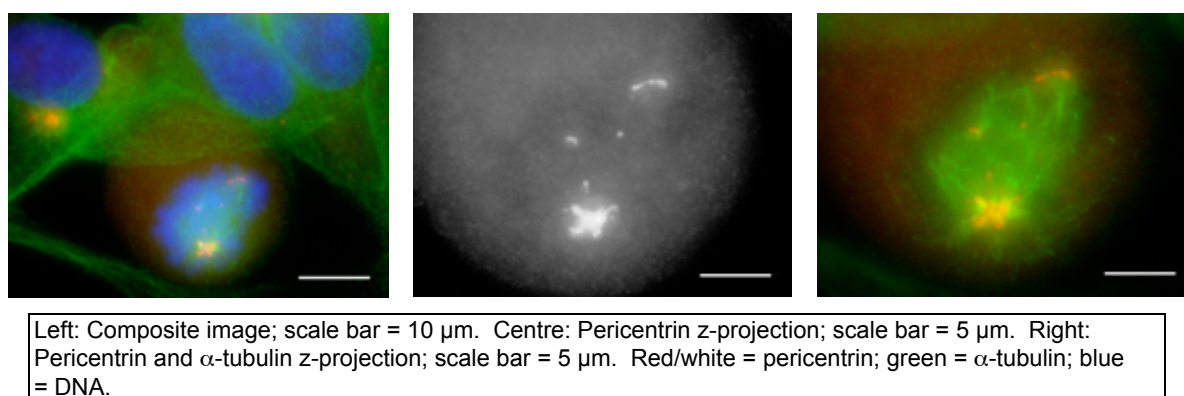
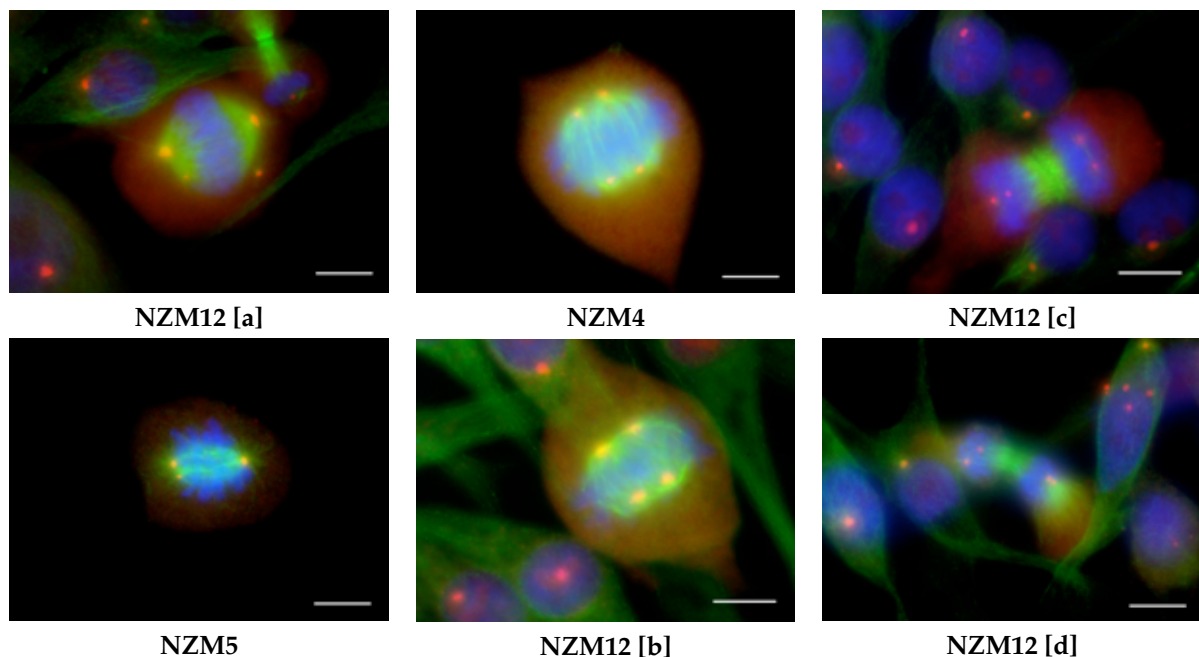


**Figure 6–14: NZM13 pericentrin and  $\alpha$ -tubulin detail**

### *Cooperative and bystander supernumerary centrosomes*

The success of centrosomes in enhancing the fidelity of mitosis hinges on their forming two diametrically opposed poles to impose a strict alignment on the spindle axis with respect to the plane of cytokinesis. To do otherwise would be to destabilise the very process they evolved to enhance. Implicit in this is the notion of bipolarity, something that in the normal course of events is ensured by the strict regulation of centrosome duplication. However, the need for bipolarity can be met by any number of centrosomes greater than one, provided either that some centrosomes cooperate to form a single pole, or that some exert no significant influence over the mitotic spindle. Examples consistent with each of these possibilities were found during the survey, with cooperation among multiple centrosomes being quite common among cells with supernumerary centrosomes {Figure 6–15}. Variability in pericentrin labelling suggests that the participating centrosomes may not always be equivalent, and functional poles formed by cooperating centriolar centrosomes are not always easily distinguishable from those formed by pole fracturing. However, enough examples were seen with strongly and equally labelled centrosomes to suggest that correct genome partitioning may sometimes still eventuate despite the presence of supernumerary centrosomes. Possibly, this is the result of a fortuitous positioning of centrosomes when they become stabilised by the mitotic spindle, but it could also be a regulated process, as cooperation of centrosome pairs to promote bipolar mitosis is seen in the terminal differentiation of hepatocytes<sup>1570</sup>.



Cell NZM12 [a] contains one bystander centrosome not contributing to spindle symmetry, and one weak pericentrin focus, possibly a centrosome, which is either cooperating in the stability of the pole or is another bystander. The NZM5 cell appears to contain a cooperative centrosome at the left hand pole, although this may be a pericentrin fragment arising from pole fracturing. The NZM4 cell and cell NZM12 [b] contain pairs of cooperating centrosomes allowing the formation of a broad quasibipolar spindle. Cells NZM12 [c] and [d] each contain cooperative centrosome pairs. All cases may well have resulted in correct genome partitioning despite the presence of supernumerary centrosomes. Red = pericentrin; green =  $\alpha$ -tubulin; blue = DNA. Scale bars = 10  $\mu$ m.

**Figure 6–15: Cooperative and bystander centrosomes**

**Mitotic survey proper**

*Summary of results*

The results of the formal survey of mitotic cells are summarised in Table 6–3. It is evident from these figures that centrosomal numerical dysregulation is indeed occurring in NZM cells, as are errors of mitotic symmetry.

%	Fibroblasts	NZM1	NZM2	NZM3	NZM4	NZM5	NZM6	NZM7	NZM7.2	NZM7.4	NZM9	NZM10	NZM10.1	NZM11	NZM12	NZM13	NZM15
<b>Mitotic phase</b>																	
Indeterminate	0	0	0	0	1	1	0	0	0	0	0	3	0	0	0	0	0
Prophase	6	7	5	5	1	3	22	8	12	10	2	3	1	9	0	2	8
Prometaphase	13	38	11	74	7	42	18	17	26	38	28	28	6	26	3	57	52
Metaphase	49	35	59	8	64	24	38	56	39	39	45	30	76	7	59	17	22
Anaphase	7	7	7	4	2	14	6	5	3	1	9	3	5	4	11	6	9
Telophase	25	13	18	9	25	16	16	14	20	12	16	33	12	54	27	18	9
<b>General aspect</b>																	
Normal	87	76	82	95	79	75	90	83	88	83	78	67	64	89	85	94	85
Slightly abnormal	11	11	12	2	13	19	10	12	8	10	14	20	19	10	4	3	10
Grossly abnormal	2	13	6	3	8	8	0	5	4	7	8	13	17	1	11	3	5
<b>Centrosome number</b>																	
Indeterminate	1	3	2	0	0	3	1	8	3	2	5	2	0	0	1	1	0
0	0	0	1	0	0	1	0	0	0	0	0	0	0	0	1	0	0
1	0	2	0	0	1	5	0	1	1	0	1	1	0	0	0	1	0
2	92	82	88	98	87	79	98	84	90	89	84	80	73	95	83	96	90
3	6	7	4	0	3	10	0	1	0	2	5	3	4	3	2	0	5
4	0	4	4	2	2	1	1	6	5	3	4	8	11	2	9	2	4
5	1	2	1	0	0	0	0	0	1	2	0	2	6	0	2	0	0
6 – 9	0	0	0	0	6	1	0	0	0	2	1	4	5	0	2	0	1
10 – 15	0	0	0	0	1	0	0	0	0	0	0	0	0	0	0	0	0
>15	0	0	0	0	0	0	0	0	0	0	0	0	1	0	0	0	0
<b>Centrosome morphology</b>																	
Indeterminate	1	4	0	0	0	2	2	3	3	2	0	2	0	0	2	0	0
Normal size	99	96	95	100	100	97	97	90	94	96	98	98	100	99	98	99	100
Too small	5	8	6	1	5	14	3	3	2	4	5	13	7	4	8	0	3
Too large	0	2	0	0	0	0	1	1	4	3	2	3	3	4	0	0	11
Structured	15	7	5	3	5	13	4	42	14	9	35	4	4	5	3	1	11
<b>Centrosome positioning</b>																	
Indeterminate	1	2	7	0	13	5	1	3	1	1	1	2	6	0	5	0	0
Dispersed	91	73	88	77	87	85	94	89	87	91	84	80	94	78	93	78	92
Clustered	15	28	6	23	0	14	5	3	10	9	16	24	4	25	0	25	23
<b>Pericentrin distribution</b>																	
Indeterminate	0	0	0	0	0	0	0	0	0	0	0	1	0	0	0	0	0
Centrosomal	100	98	98	100	100	99	99	94	97	98	98	98	100	100	98	100	100
Diffuse	100	100	99	100	100	99	100	99	99	100	98	99	100	100	100	100	100
Punctate	13	1	5	0	3	15	0	3	8	2	9	3	1	3	3	4	1
Patched	2	0	0	0	7	1	27	2	4	5	14	7	3	16	0	0	0
Structured	1	1	2	0	1	2	2	7	2	6	6	0	3	0	0	1	1
<b>Symmetry</b>																	
Indeterminate	0	2	2	6	1	9	20	2	0	1	4	5	6	2	4	13	16
Absent	0	2	6	0	1	0	0	0	4	2	0	0	0	7	1	2	2
Unipolar	9	26	7	15	13	4	5	6	10	11	14	14	0	16	0	11	7
Normal bipolar	84	59	76	77	69	74	74	84	81	77	70	65	64	70	82	72	67
Abnormal bipolar	7	2	4	0	5	7	0	1	1	3	5	6	12	4	4	0	4
Tripolar	0	3	2	0	1	3	1	0	0	2	2	3	6	1	4	0	1
Quadripolar(planar)	0	1	0	1	0	0	0	0	0	0	0	0	0	0	2	0	0
(tetrahedral)	0	0	1	0	0	0	0	2	2	1	2	2	4	0	2	2	2
Multipolar	0	5	2	1	9	3	0	5	2	3	3	5	8	0	1	0	1
<b>Segregation errors</b>																	
Lagging chromosome	1	1	4	0	1	1	1	0	0	0	3	0	2	0	0	0	0
Chromosomal bridge	0	2	0	4	4	1	0	0	0	1	5	5	0	0	0	1	0
Micronucleation	0	1	0	0	2	0	0	0	0	2	3	0	0	2	0	0	1

**Table 6–3: Mitotic survey results**





### Statistical analysis

Statistical tests were performed following the methods described by Jarrold H. Zar<sup>1695</sup> using the summary data given in Table 6–3. As a first step, a standard chi-squared test at a significance level of  $p < 0.01$  was performed to detect variation among the cell-lines for each of several characteristics of interest: abnormal centrosome number, slightly abnormal general aspect, grossly abnormal general aspect, abnormal centrosome morphology, abnormal symmetry, and rate of segregation errors. All showed significant overall differences between observed and expected frequencies.

To explore this variation further, an analysis was undertaken using Dunnett's procedure. This compares each NZM cell-line to the control tumour-associated fibroblasts in a structured way so as to set an "experimentwise" error rate of  $p < 0.01$ . The results of this analysis are given in Table 6–4.

	Grossly abnormal	Slightly abnormal	Centrosome number	Centrosome morphology	Symmetry	Segregation errors
NZM1	↓		↓	↓	↓	
NZM2	↓			↓	↓	
NZM3		↑	↑	↓		
NZM4	↓			↓	↓	↓
NZM5	↓	↓	↓		↓	
NZM6	↓		↑	↓	↓	
NZM7	↓		↓	↑		
NZM7.2						
NZM7.4	↓			↓	↓	
NZM9	↓		↓	↑	↓	↓
NZM10	↓	↓	↓	↓	↓	↓
NZM10.1	↓	↓	↓	↓	↓	
NZM11				↓	↓	
NZM12	↓	↑	↓	↓		
NZM13		↑		↓	↓	
NZM15	↓				↓	

↓ = NZM cell-line is significantly worse than control in this characteristic;  
 ↑ = NZM cell-line is significantly better than control in this characteristic; blank = no significant difference.  
 Tests used Dunnett's procedure at a significance level of  $p < 0.01$ . Note: NZM14 was not surveyed.

**Table 6–4: Statistical analysis of mitotic survey results**

In considering these data, it must be taken into account that the control used was one of expediency in the absence of cultured human melanocytes, and that tumour-associated fibroblasts may themselves be abnormal in some respects. Additionally, at passage number 2, as these were, the possibility of a residue of tumour cells in the culture cannot be excluded.

NZM3 appears to be the best regulated of all of the cell-types investigated, including the controls. This cell-line also had a very much higher proportion of cells in prophase or prometaphase than any other cell-line surveyed, at 79%, and this was more than four times the corresponding proportion in the control fibroblasts. NZM15, with the next highest proportion of early phase mitotic cells, also appeared to fare better than most.

This is an area where the sampling methodology may have been at fault, in that some classes of characteristic being sought are more likely to appear the further through mitosis a cell progresses. Indeed, some, such as segregation errors, cannot occur at all prior to anaphase.

Others, such as centrosome number should be independent of mitotic phase, except perhaps for telophase, where they become difficult or impossible to identify by pericentrin labelling in most cases. Resampling of the existing data, where feasible, or acquisition of new data with equal sample size for each mitotic phase, could be used to address this, but as can be seen from the table above, and as occurred with NZM14, obtaining slides with adequate numbers of cells in particular phases of mitosis may not prove easy to accomplish, nor would it necessarily add much to the important conclusions to be drawn from this experiment.

Not surprisingly, NZM10, the cell-line which prompted this investigation more than any other with its complex pattern of heteroploidy, appears to be the most poorly regulated, being significantly worse than the control fibroblasts in every category considered. This was closely followed by NZM10.1, worse in five of six categories.

The characteristics of greatest interest here are centrosome numerical abnormality and mitotic or cytokinetic asymmetry. Among the mitotic NZM cells surveyed where centrosome number could be established, 11% contained other than the expected two centrosomes, and centrosomal numerical regulation was worse in 7/9 cell-lines where a significant difference from the control fibroblasts existed {Table 6–4}. Centrosome number ranged from seemingly zero, observed in some cells from NZM2, NZM5, and NZM12, to as many as 17, seen in NZM10.1. Even higher numbers were seen incidentally in cells not forming part of the formal survey. Among the cells surveyed where symmetry could be assessed, 11% had abnormal bipolar, tripolar, or higher order symmetry, and symmetry other than normal bipolar was more prevalent in 12/12 cell-lines where a significant difference from the control fibroblasts existed {Table 6–4}.

Overall, characteristics likely to result from or contribute to aneuploidy and heteroploidy appear to be more prevalent in the NZM cell-lines than in the control fibroblasts.

### *Mitotic cells with fewer than two centrosomes*

A total of sixteen mitotic NZM cells were seen that appeared to contain fewer than two centrosomes: three were acentrosomal and thirteen monocentrosomal. NZM5 appears to be over-represented in this class, as it contributed 6/16 cells, suggesting that this cell-line may be prone to centrosome loss. No such cells were seen among the control fibroblasts. There are several ways that these observations may be artefactual and it cannot be stated with certainty that two centrosomes were not actually present in these cells. Cells gauged as being in prophase may not have fully completed centrosome duplication, or the centrosomes may not have separated sufficiently or may be optically aligned giving the impression of just one centrosome, and one monocentrosomal cell fell into this category. In telophase cells, pericentrin labelling of centrosomes is generally weak, and sometimes absent, and two of the monocentrosomal cells fell into this category. One or both centrosomes may be masked due to positioning behind opaque structures, such as condensed chromatin. No assessment of how likely this is can be made, and to explore this further would be difficult. Confocal microscopy could not be used since the pseudo-three-dimensional imaging offered still depends on transmission of light through the specimen. Physical serial sectioning of samples, or perhaps

immunogold labelling of centrosomes and X-ray tomographic microscopy would serve, but the results are very unlikely to justify the effort.

Representative images of these cells hypodictrosomal cells are shown in Figure 6–16.

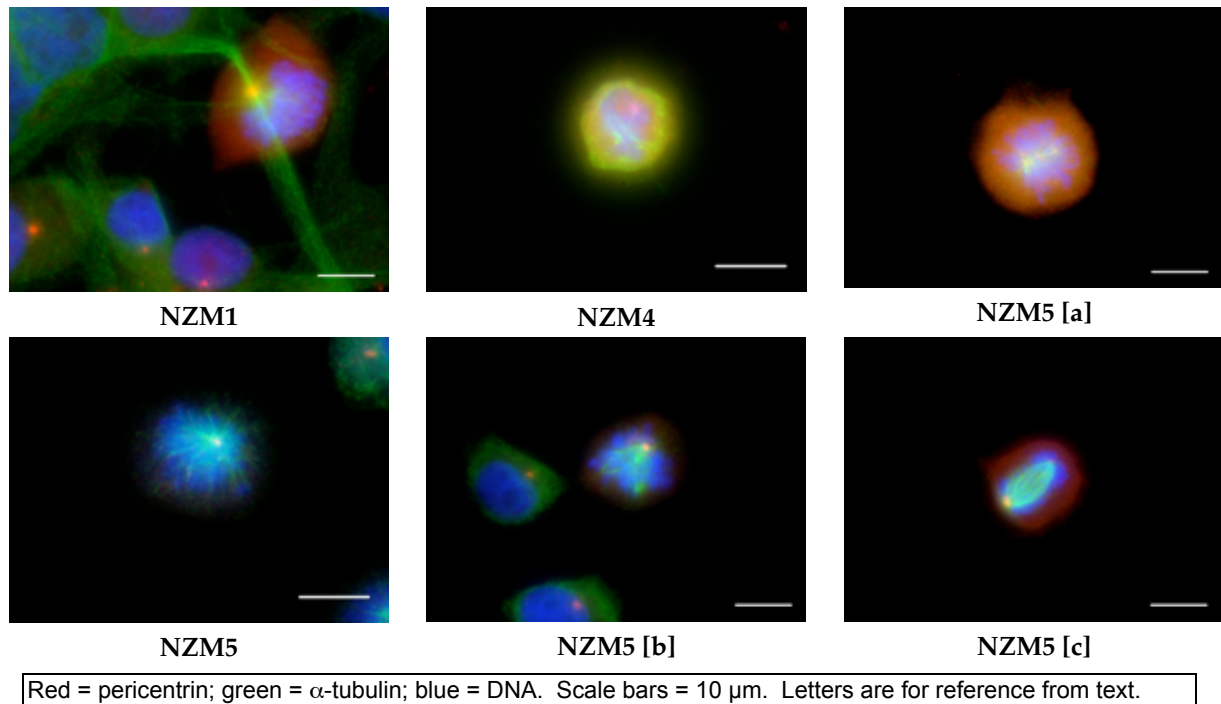
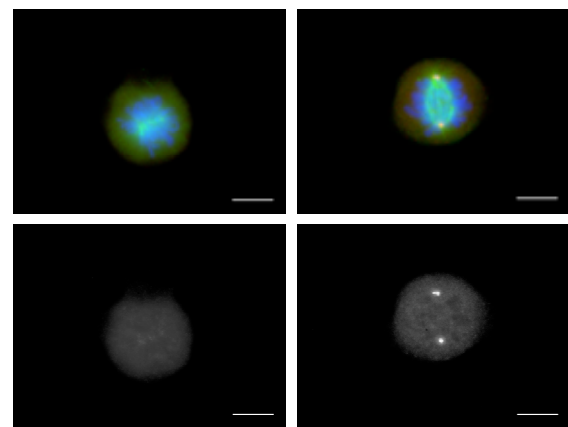


**Figure 6–16: Representative hypodictrosomal mitotic cells**

Cell NZM5 [a] in Figure 6–16 was one scored as being acentrosomal, despite focal pericentrin labelling with associated  $\alpha$ -tubulin. This was because of the very weak nature of the focal labelling, something not immediately evident in this image due to the adjustment of brightness levels during image processing {Method 46}. It is clearer when this cell and a near-normal prometaphase NZM5 cell are compared directly, with the brightness of the NZM5 [a] cell adjusted so that the diffuse background pericentrin labelling of the two cells is approximately equal {Figure 6–17}. It is also possible that centrosomes are present, but masked by the condensed chromatin mass.

Cell NZM5 [b] is an aberrant prometaphase wherein a single centrosome is anchoring two independent bipolar spindles. Possibly the two free poles will coalesce during metaphase and a quasinormal anaphase, telophase, and cytokinesis may follow, but the degree of independence shown and the similar apparent strengths of the two spindles would seem to

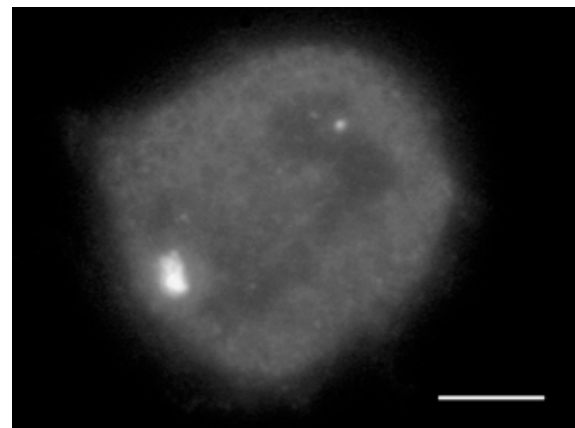


Top left: Image of cell NZM5 [a] from Figure 6–16, reprocessed to match diffuse background pericentrin labelling intensity with the reference cell at right.  
 Top right: Near-normal NZM5 prometaphase image for comparison.  
 Bottom: Corresponding pericentrin component images.  
 Red/white = pericentrin; green =  $\alpha$ -tubulin; blue = DNA. Scale bars = 10  $\mu$ m.

**Figure 6–17: NZM5 prometaphases**

make this unlikely. The best-case scenario for a cell in this state would probably be a binary cytokinesis, but with the generation of aneuploidy and micronuclei as a result of improper chromosomal segregation and reformation of nuclear membranes around isolated chromosomes. There seems little likelihood that centrosome masking has occurred during the capture of this image.

Cell NZM5 [c] seems to be involved in a normal anaphase, despite only a small pericentrin focus being visible at one pole. The disparity in pericentrin content between the two poles is more readily discernible in Figure 6–18, but as with cell NZM5 [a], a bona fide centrosome may be present, but masked. Even if no centrosome is present at one pole, the inherent microtubule nucleation capacity of the small pericentrin focus, in combination with the self-organising capacity of the mitotic spindle and the anchor provided by the bona fide centrosome at the other pole, appear to have given rise to an anaphase structure that has correctly segregated the duplicated genome. Were it not for fixation, this cell may have continued through telophase and cytokinesis correctly, but if in fact only one centrosome were present, only the daughter cell that inherited it would be able to continue to cycle normally; the future of the acentrosomal daughter cell would be less certain, with  $G_1$  arrest, or repeated polyploidisation through future failed mitoses being the likely outcomes.



Pericentrin maximum intensity z-projection for cell NZM5 [c] from Figure 6–16.  
Scale bar = 5  $\mu\text{m}$ .

**Figure 6–18: NZM5 [c] pericentrin**

### *Potential causes of hypodicentrosomalism*

Three possibilities seem to exist to account for how these cells reached their hypodicentrosomal states. Least likely is that centriole loss has occurred, perhaps through aberrant proteolysis. This cannot be completely discounted, but it does seem unlikely given the overall integrity of the cell observed. Loss of centrioles through a process of cellular export is conceivable, given that due to their melanocytic lineage, these cells at one time had as their principal function the export of organelles, namely melanosomes. While it is perhaps possible that centrioles could become entrained in this process and similarly exported, this theoretical event must be ascribed a very low probability. Infection by a pathogen which carries with it either an enzyme destructive of centrioles or a gene for such is possible, but none is known, and to carry such an agent would seem to be of dubious benefit to the pathogen. More likely, one or more centrioles may be present in the cells, but there may be a flaw in the trafficking of pericentrin to the centrosome, thus interfering with both their detection by focal labelling, and their microtubule nucleation function by preventing the recruitment of  $\gamma$ -tubulin<sup>S1619 1699</sup>.

The most likely cause for the presence of a single centrosome in a cell would seem to be a failure of centriole duplication or severance. Genetic or epigenetic events affecting the



production of centrosomal components or their delivery for use in construction of the daughter centriole could account for this, as could a similar flaw in the mechanisms that signal or perform the severance function. Most likely to account for acentrosomal cells would seem to be their failure to receive a centrosome at inception owing to a flawed cytokinesis. In support of this, it is known that cells with just a single centrosome can proceed completely through mitosis and cytokinesis yielding an acentrosomal daughter cell<sup>S664</sup>. Furthermore, given the many examples encountered in this survey of aberrant mitoses involving supernumerary centrosomes, multipolar spindles, and non-binary anaphases and telophases, the possibility of an aberrant daughter cell being produced without inheriting a centrosome seems quite likely.

Although Khodjakov<sup>S664</sup> found that acentrosomal cells arrested in G<sub>1</sub>, the two putatively acentrosomal cells found here had progressed to prometaphase. The resolution of this discord may lie in the nature of the cells: Khodjakov's work used transfected, but otherwise normal, rat kangaroo and green monkey epithelial cells, but here the cells are derived from melanoma, and the disruption of a growth-suppressive mechanism should not be unexpected. The molecular basis for acentrosomal arrest does not appear to have been fully elucidated, and NZM5, for example, may have utility in furthering this investigation. Whatever the mechanism may be, it must be distinct from that implementing the post-mitotic arrest occurring in cells experimentally depleted of centrosomal proteins<sup>1614</sup> mediated through p38MAPK, p53, and p21 since this arrest was found to require recruitment of p53 to the centrosome, something not possible in acentrosomal cells. A plausible hypothesis would be that the absence of a centrosome renders impossible the initial activating dephosphorylation of Y15 of CDC2<sup>248</sup> thus preventing the onset of mitosis. Deregulation of phosphatase activity, perhaps involving CDC25C, or of CDC2 itself or a downstream effector would obviate the need for a centrosome, eliminating this arrest mechanism. In so doing it would give the tumour cell a proliferative advantage while simultaneously allowing the propagation of a genomically unstable cell lineage.

### *Normal dicentrosomal mitoses*

The class of mitotic cells containing two centrosomes, which includes normal mitoses, was by far the largest class in each of the cell types studied. However, dicentrosomal cells were less common in 7/9 cell-lines where a significant difference with control fibroblasts could be established {Table 6-4}.

The most typical mitotic progression involves a pair of closely associated centrosomes in prophase that separate to opposite poles of the nucleus and begin to develop interconnecting microtubules that will become a symmetrical bipolar, uniaxial spindle. During this time the interphase cytoplasmic tubulin network is dismantled. In a variation, unipolar development, separation of centrosomes does not occur until after nuclear envelope breakdown, but in either case, bipolarity is established by the end of prometaphase. In metaphase, chromosomes are aligned within a well-defined metaphase plate. In anaphase, chromosome segregation is balanced with no lagging chromosomes. In telophase, two nascent daughter cells of equal

## Human metastatic melanoma in vitro

volume form. Images of normal mitoses for each mitotic phase for each cell-line and for tumour-associated fibroblasts are given in Figure 6–19 where available. With the emphasis on the recording of abnormalities, in many cases no representative normal image was made.

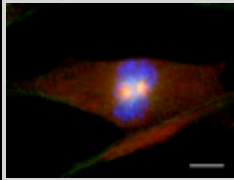
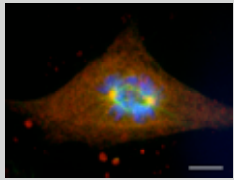
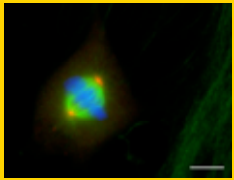
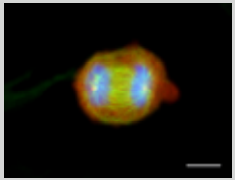
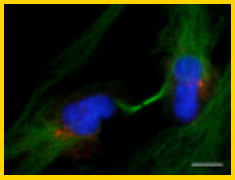
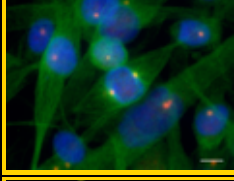
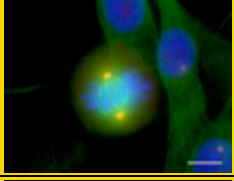
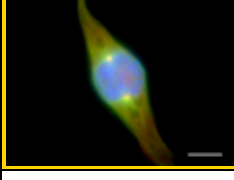
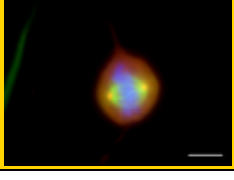
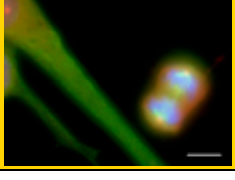
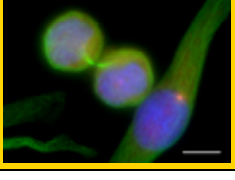
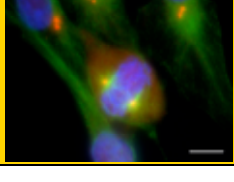
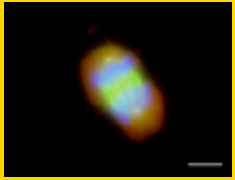
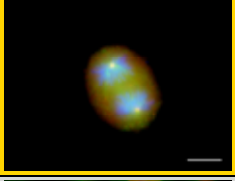
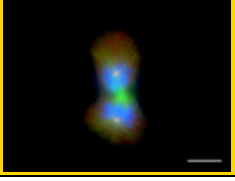
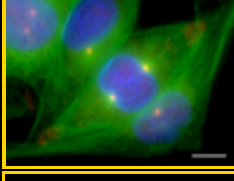
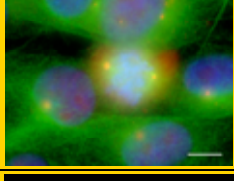
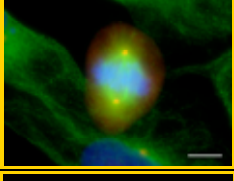
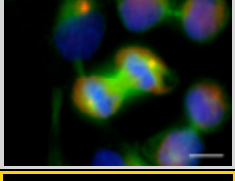
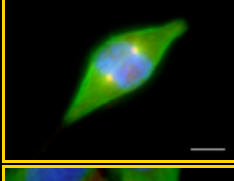
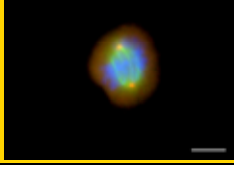
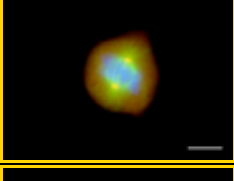
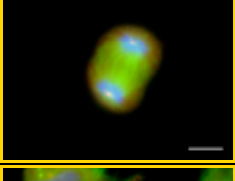
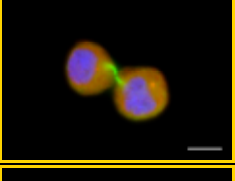
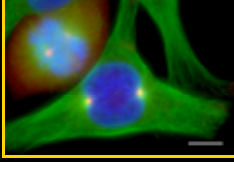
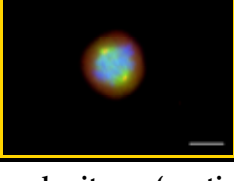
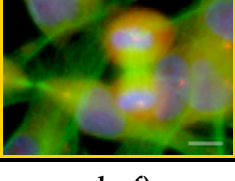
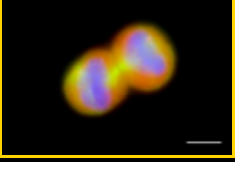
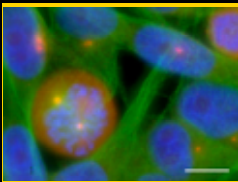
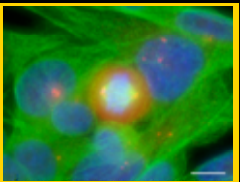
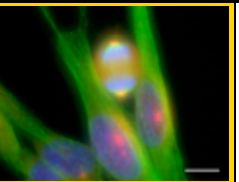
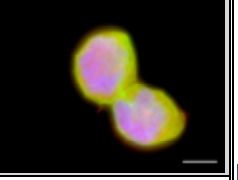
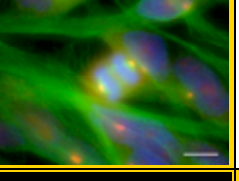
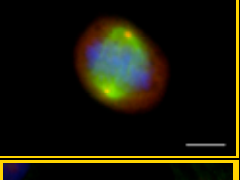
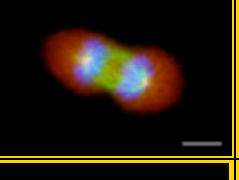
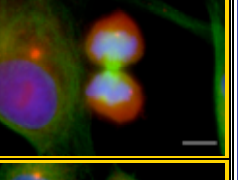
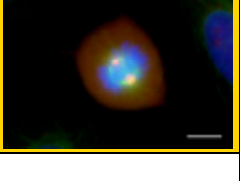
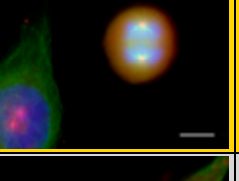
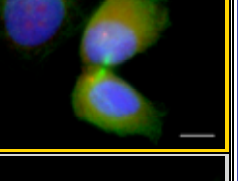
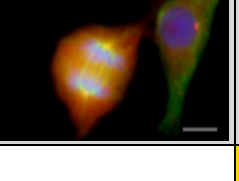
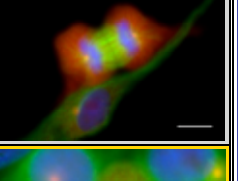
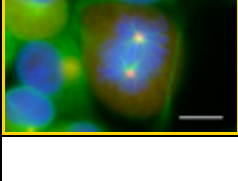
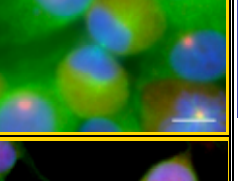
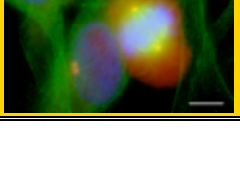
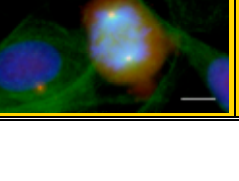
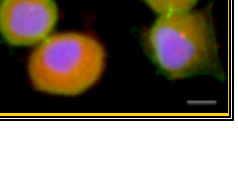
	Prophase	Prometaphase	Metaphase	Anaphase	Telophase
FB					
NZM1		no image available		no image available	no image available
NZM2		no image available			
NZM3	no image available		no image available	no image available	no image available
NZM4	no image available	no image available	no image available		no image available
NZM5	no image available	no image available	no image available		
NZM6					no image available
NZM7					
NZM7.2		no image available			

Figure 6–19: Normal mitoses (continues overleaf)

	Prophase	Prometaphase	Metaphase	Anaphase	Telophase
NZM7.4	no image available				no image available
NZM9	no image available	no image available	no image available	no image available	
NZM10	no image available	no image available	no image available		no image available
NZM10.1	no image available	no image available			
NZM11	no image available	no image available			
NZM12	no image available	no image available	no image available		
NZM13	no image available		no image available	no image available	
NZM15	no image available	no image available			

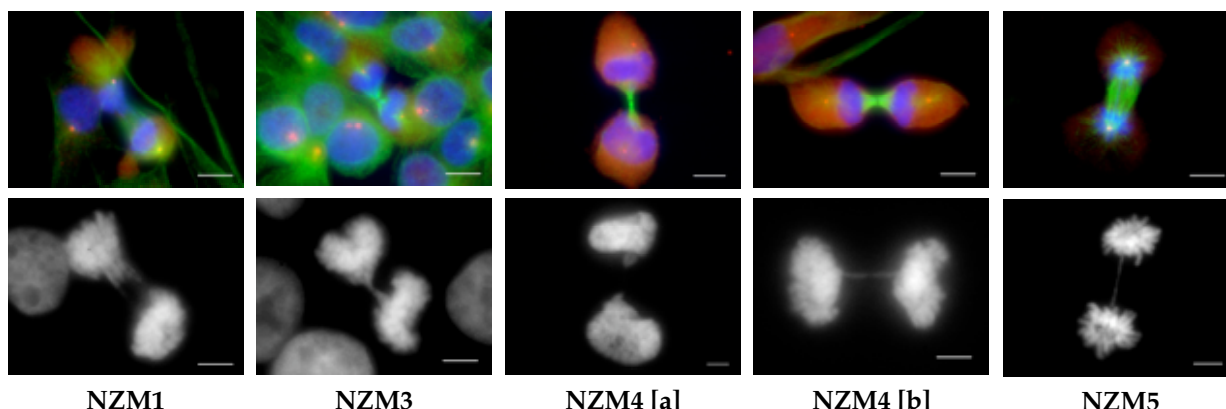
**6: Centrosomal integrity**

Shown are representative images of normal mitoses for early passage tumour-associated fibroblasts (FB) and each of the NZM cell-lines studied. Images are not available in all cases as not all cell-lines had normal cells in all phases, and priority was given to capturing images of abnormal cells. NZM14 was not surveyed. Supplementary images not from the formal survey are included where these are available. Gold border = image from formal survey; grey border = supplementary image. Red = pericentrin; green =  $\alpha$ -tubulin; blue = DNA. Scale bars = 10  $\mu$ m.

**Figure 6–19 (concluded): Normal mitoses**

*Abnormal dicentrosomal mitoses*

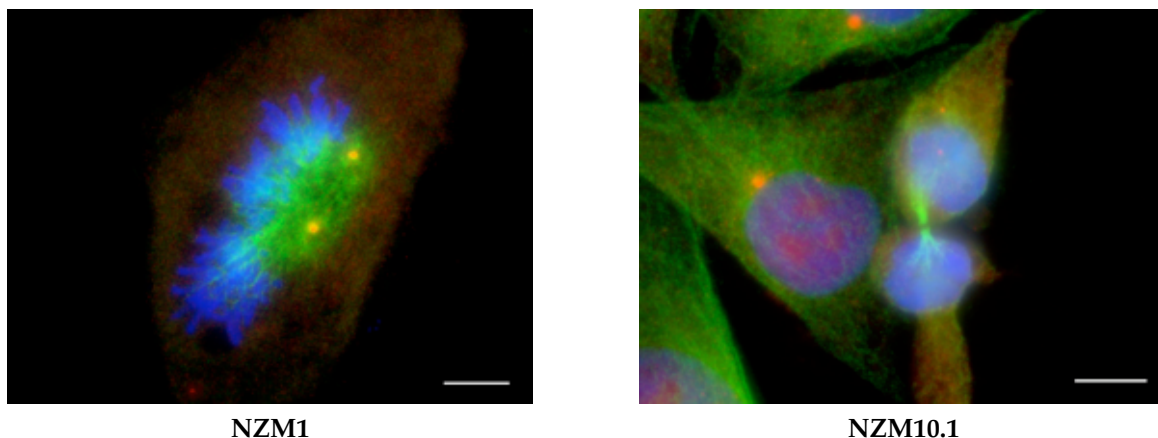
Of all cells surveyed, just seven were scored as being both dicentrosomal and grossly abnormal. In one anaphase and four telophases the gross anomaly was a chromosomal bridge between separating replicated genomes. These are illustrated in Figure 6–20.



Corresponding composite (upper) and DNA only (lower) images for dicentrosomal cells surveyed where chromosomal bridging was observed. Upper images: red = pericentrin; green =  $\alpha$ -tubulin; blue = DNA. Scale bars = 10  $\mu$ m. Lower images: white = DNA. Scale bars = 5  $\mu$ m.

**Figure 6–20: Chromosomal bridges in dicentrosomal cells**

The two remaining cells included a dysmorphic metaphase in NzM1, and a binary telophase in NzM10.1 with incorrect centrosomal distribution between the nascent daughter cells. These are illustrated in Figure 6–21. No grossly abnormal dicentrosomal mitoses were found among the tumour-associated fibroblasts surveyed.



Red = pericentrin; green =  $\alpha$ -tubulin; blue = DNA. Scale bars = 10  $\mu$ m.

**Figure 6–21: Remaining grossly abnormal dicentrosomal cells**

*Tricentrosomal mitoses*

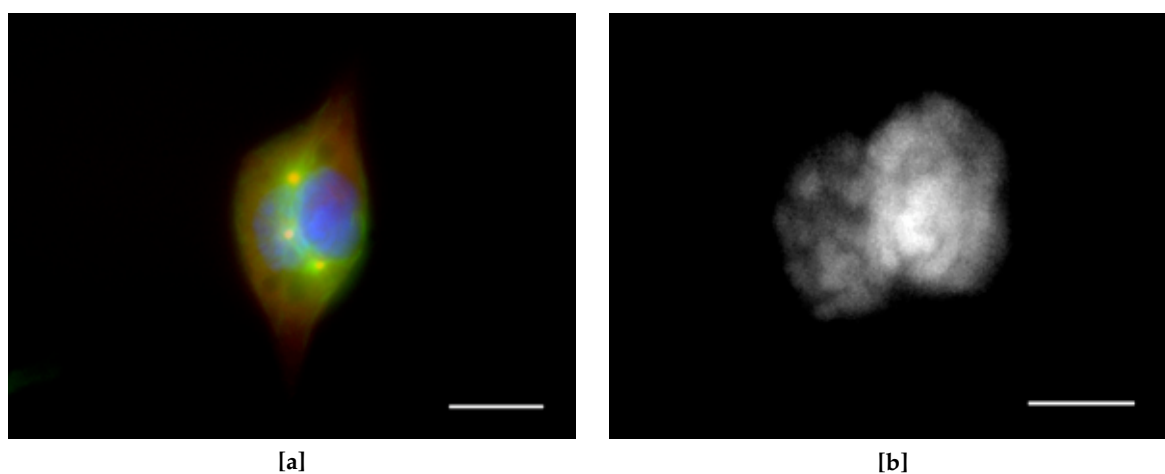
Approximately 3% (49/1 570) of the mitotic NzM cells surveyed where centrosome number was assessable had three centrosomes, the modal cell-line being NzM5, with ten instances recorded. They were observed in 12 of 16 NzM cell-lines, the exceptions being NzM3, NzM6, NzM7.2 and NzM13. Since there are very few normal circumstances under which an animal cell should have more than two centrosomes, megakaryocytes being the principal exception, this observation alone confirms the hypothesis under test that [centrosome numerical dysregulation is occurring in metastatic melanoma cells in vitro](#).



Numerical results for tricentrosomal mitotic cells are given in Table 6–5, but the absolute numbers are too low to allow separate analysis using Dunnett's procedure.

Number of cells	Fibroblasts	NZM1	NZM2	NZM3	NZM4	NZM5	NZM6	NZM7	NZM7.2	NZM7.4	NZM9	NZM10	NZM10.1	NZM11	NZM12	NZM13	NZM15
<b>Mitotic phase</b>																	
Indeterminate	0	0	0		0	1		0		0	0	0	0	0	0		0
Prophase	0	0	1		0	0		0		0	0	0	0	0	0		0
Prometaphase	0	5	0		0	4		1		2	2	1	0	2	0		3
Metaphase	4	2	1		2	3		0		0	2	0	3	0	1		0
Anaphase	1	0	1		0	1		0		0	1	0	0	0	1		1
Telophase	1	0	1		1	1		0		0	0	2	1	1	0		1
<b>General aspect</b>																	
Normal	0	0	1		0	0		0		0	0	0	0	0	1		0
Slightly abnormal	5	2	1		3	6		0		1	2	2	3	2	0		4
Grossly abnormal	1	5	2		0	4		1		1	3	1	1	1	1		1
<b>Symmetry</b>																	
Indeterminate	0	1	0		0	1		0		0	0	1	0	0	0		0
Absent	0	0	0		0	0		0		0	0	0	0	0	0		0
Unipolar	0	2	0		0	0		0		0	0	0	0	0	0		0
Normal bipolar	6	1	2		2	6		0		1	3	2	3	1	1		3
Abnormal bipolar	0	0	0		0	0		0		0	0	0	0	0	0		0
Tripolar	0	3	2		1	2		0		1	2	0	1	1	1		2
Quadripolar(planar)	0	0	0		0	0		0		0	0	0	0	0	0		0
" (tetrahedral)	0	0	0		0	0		0		0	0	0	0	0	0		0
Multipolar	0	0	0		0	1		1		0	0	0	0	0	0		0

Table 6–5: Tricentrosomal survey results

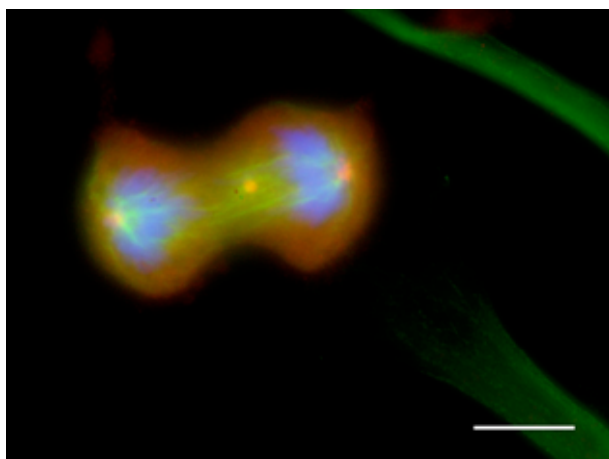


[a]: Red = pericentrin; green =  $\alpha$ -tubulin; blue = DNA. Scale bar = 10  $\mu$ m.  
 [b]: DNA labelling only. Scale bar = 5  $\mu$ m.

Figure 6–22: Tricentrosomal NZM2 prophase

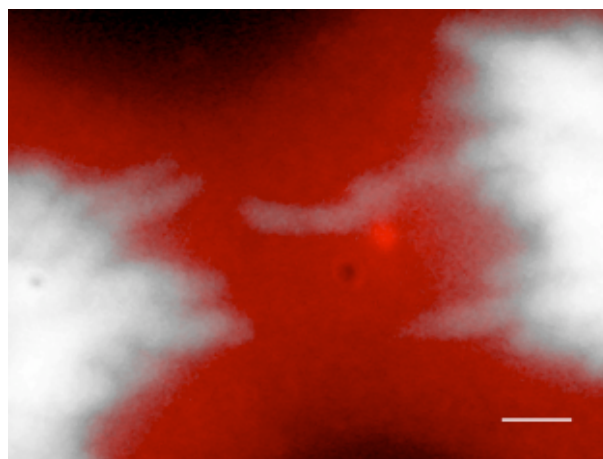
NZM2 provided the only example of a tricentrosomal prophase cell in the survey {Figure 6–22}. It contains three bright foci of pericentrin labelling likely to correspond to true centriolar centrosomes. Each of these is at the nexus of set of radial tubulin astral filaments, and those emanating from the central centrosome overlap with those from each of the others. Each overlap region forms the basis of a mitotic spindle, and together these protospindles partially girdle the nucleus constricting the condensed chromatin into two lobes, as is more readily discernible in the image of the chromatin alone.

It is difficult to predict the fate of this cell had it not been fixed, but improper chromosomal segregation would seem to be very likely. Operation of motor proteins upon adjacent antiparallel microtubules emanating from different centrosomes will tend to drive the centrosomes apart. If the tubulin ring linking the centrosomes is not closed, or the symmetry is less than perfect, then the initial triangular geometry will tend to linearise into a bipolar spindle, but with a third centrosome occupying a central position. NZM2 also provided an example cell with this configuration {Figure 6–23}.



Red = pericentrin; green =  $\alpha$ -tubulin; blue = DNA. Scale bar = 10  $\mu$ m.

**Figure 6–23: Tricentrosomal NZM2 anaphase**



Red = pericentrin; white = DNA  
Scale bar = 2  $\mu$ m.

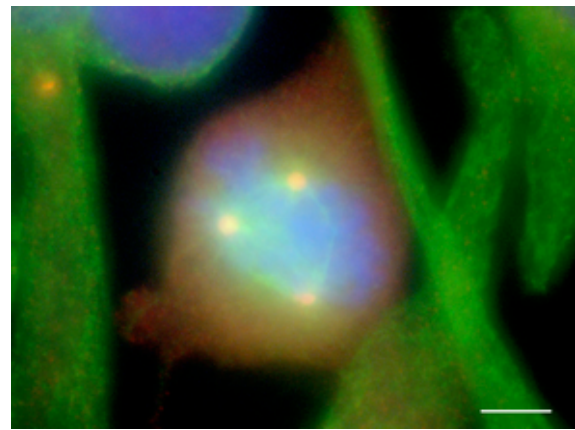
**Figure 6–24: Lagging chromosome**

Consistent with the scenario of non-uniform overlap microtubule density, the central centrosome in this cell appears not to be a strong focus for microtubule network formation, and astral microtubules are not well defined. Nevertheless, its presence appears to be interfering with correct chromosomal segregation, as illustrated in Figure 6–24. It seems plausible that the kinetochore of this lagging chromosome is attached to the central centrosome, rather than either of the polar centrosomes, and its segregation along the main spindle axis has thereby been either prevented or retarded. The likely future for this cell would have been the severance of this chromosome during cytokinesis followed by micronucleus formation, and both daughter cells would almost certainly have become more aneuploid as a result.

Alternatively, if the three centrosomes formed a ring with similar microtubule overlap between adjacent members, an expanding triangle of spindles would tend to develop. During prometaphase, mutual competition among the spindles for attachment to kinetochores would ensue, and a triaxial metaphase plate could develop, the degree of its symmetry depending mainly on the relative density of microtubules in each of the spindles. Another tricentrosomal NZM2 cell found in the survey demonstrates this type of development {Figure 6–25}.

With three centrosomes, correct chromosomal segregation and the provision of a single centrosome to daughter cells are mutually exclusive events. The only way each could receive a single centrosome is if the cytokinesis were ternary, not binary, and that would essentially guarantee partitioning of the genome into three, with aneuploidy being unavoidable.

Conversely, the only way correct segregation could occur is if the cytokinesis were binary, possibly due to centrosome cooperation at one pole. In this case, at best one daughter cell will receive a single centrosome and be essentially normal, but the other must receive two, likely leading to an abnormal tetracentrosomal mitosis on its next division. It follows then that the presence of three centrosomes in a cell will invariably lead to aneuploidy eventually. Thus, centrosomal numerical dysregulation of this type must lead to aneuploidy.

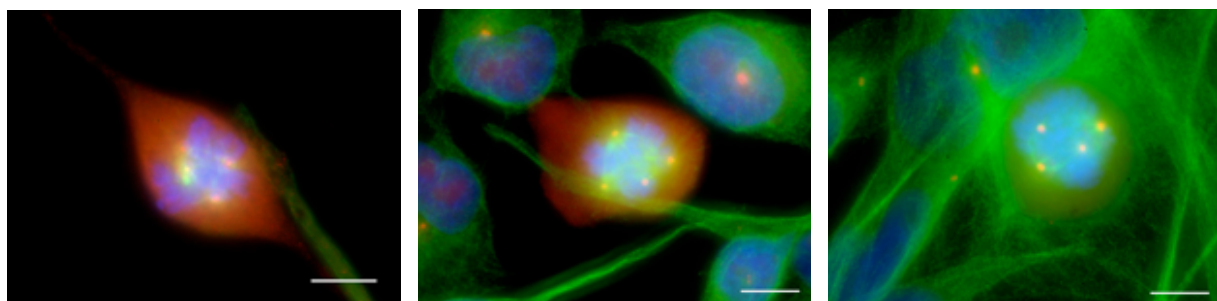


Red = pericentrin; green =  $\alpha$ -tubulin; blue = DNA. Scale bar = 5  $\mu$ m.

**Figure 6–25: Tricentrosomal NZM2 prometaphase**

### *Tetracentrosomal mitoses*

Where four centrosomes have equivalent microtubule nucleation potential, as might be expected in most cases, a similar degree of overlap of antiparallel microtubules would tend to exist among all. Cross-linkage of these by motor proteins and their translation relative to the microtubules will result in the production of forces tending to drive each centrosome away from every other centrosome. The distance between each would be both maximised within the confines of the cell, and equalised since microtubule crossings, and hence motive force, would reduce as centrosomes separated. The result of this would be a regular tetrahedral arrangement of centrosomes, and metaphase cells in this configuration were seen {Figure 6–26}.



NZM2

NZM9

NZM10

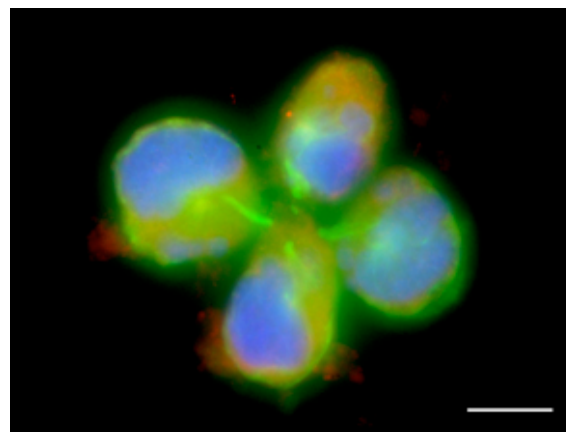
Red = pericentrin; green =  $\alpha$ -tubulin; blue = DNA. Scale bars = 10  $\mu$ m.

**Figure 6–26: Tetracentrosomal tetrahedral metaphases**

Mitotic progression beyond this point is largely conjectural. Kinetochore attachment could see chromosome pairs aligned on the edges of the tetrahedron formed, and the analogue to the metaphase plate that forms might consist of four planar structures orthogonal to the edges. Hints of these structures are seen in the cells illustrated. Anaphase could proceed with the accumulation at each centrosome of half of the chromosomes present on each of its adjacent edges, and telophase could result in the coalescence of the tetrahedron edges into a higher order midbody. Cytokinesis would be extremely problematical however, if only a single contractile ring were to form. While theory at least allows speculation that such quadripolar mitoses could occur, only one candidate for such an event was seen at a late mitotic stage

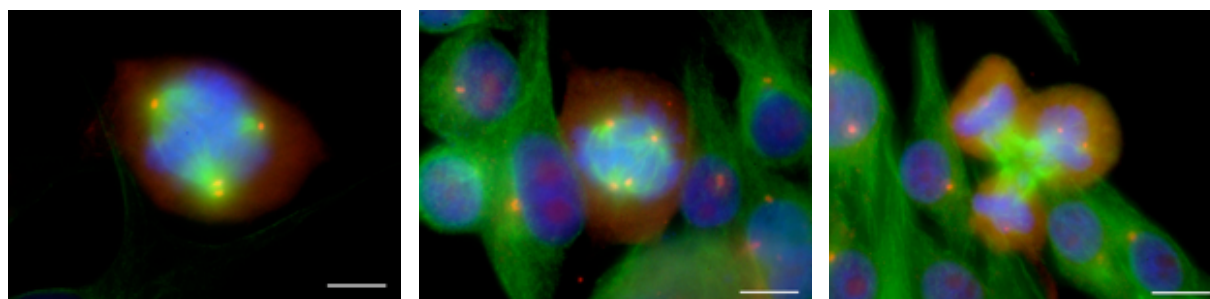
{Figure 6–27}. The specific cell was not part of the formal survey and the technical quality is poor, but although the number of centrosomes involved cannot be determined, it does appear to be a quadripolar telophase. Not surprisingly, this mitosis appears to have resulted in the formation of many micronuclei.

Centrosomal cooperation where a pair of centrosomes formed one functional pole while two others operated independently sometimes resulted in a planar triaxial mitotic symmetry, similar to that seen in some tricentrosomal mitoses. Cells in this state were seen to have progressed beyond metaphase {Figure 6–28}.



Red = pericentrin; green =  $\alpha$ -tubulin; blue = DNA. Scale bar = 10  $\mu$ m.

Figure 6–27: Quadripolar NZM6 telophase



NZM10.1 metaphase

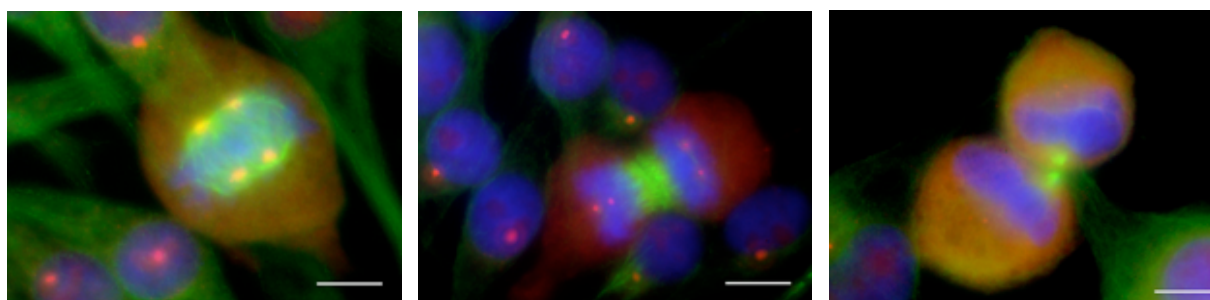
NZM12 metaphase

NZM12 anaphase

Red = pericentrin; green =  $\alpha$ -tubulin; blue = DNA. Scale bars = 10  $\mu$ m.

Figure 6–28: Tetracentrosomal tripolar mitoses

When the four centrosomes formed two cooperative pairs, quasibipolar spindles were seen to form, and well defined metaphase plates developed. Normal anaphases and telophases, at least with respect to chromosomal segregation, were seen and it appears that this configuration could potentially preserve mitotic integrity {Figure 6–29}. Whether a planar or tetrahedral geometry forms may simply depend on the chance arrangement of the centrosomes when spindle formation begins as whichever is in place then is likely to be stabilised by the formation of kinetochore fibres {See 'Cooperative and bystander supernumerary centrosomes' on page 6–15}.



NZM12 metaphase

NZM12 late anaphase

NZM4 telophase

Red = pericentrin; green =  $\alpha$ -tubulin; blue = DNA. Scale bars = 10  $\mu$ m.

Figure 6–29: Tetracentrosomal quasibipolar mitoses

### Higher order mitoses

Forty-one mitoses with more than four centrosomes were found, with only one being seen in the control fibroblasts. Images of some of these are given in Figure 6–30. The most extreme case surveyed was an NZM10.1 metaphase with at least 12 centrosomes. Other, non-mitotic cells with many more centrosomes were seen incidentally, including that presented as the frontispiece to this thesis, an interphase NZM2 cell with at least 17 centrosomes.

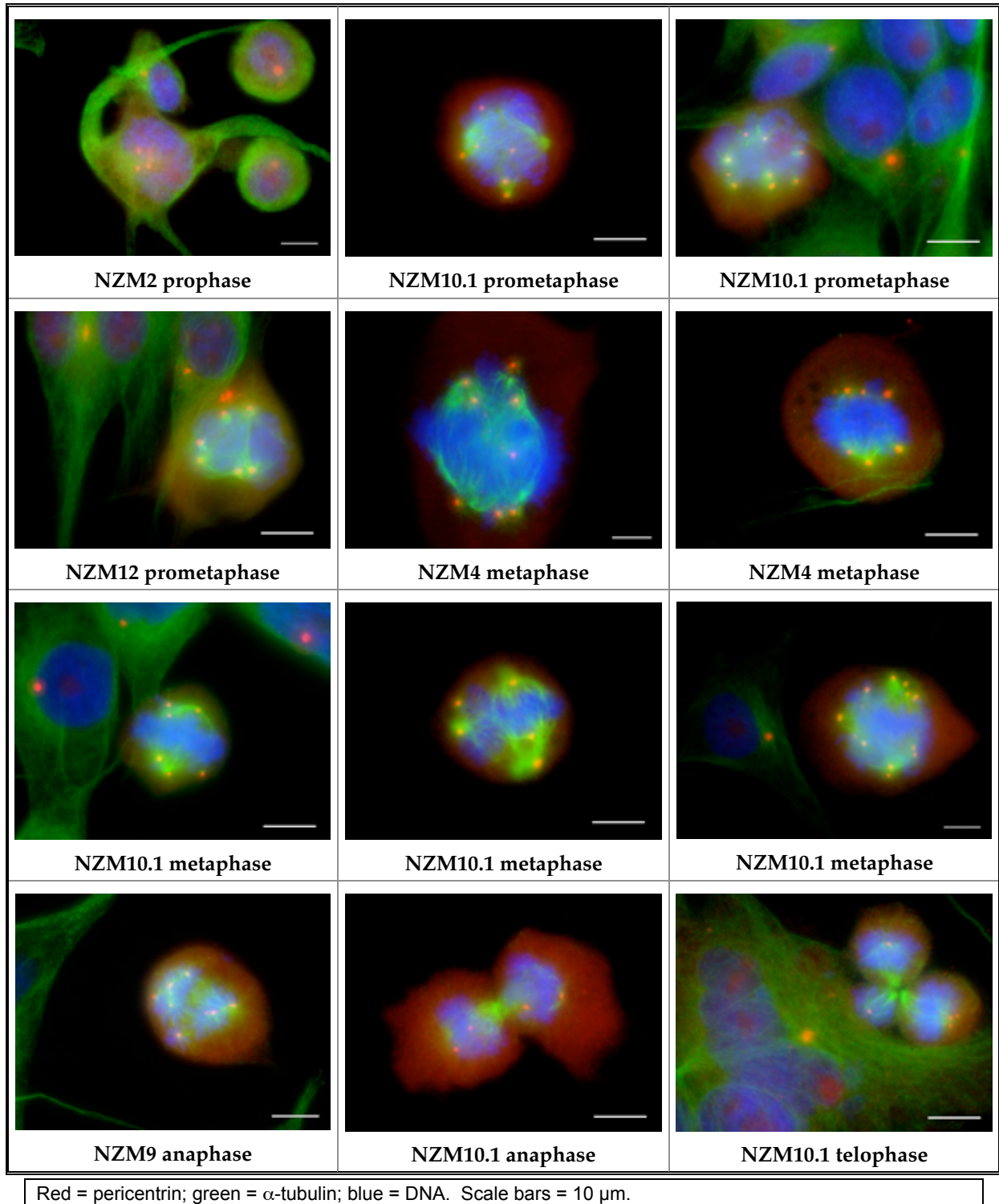


Figure 6–30: Representative polycentrosomal mitoses

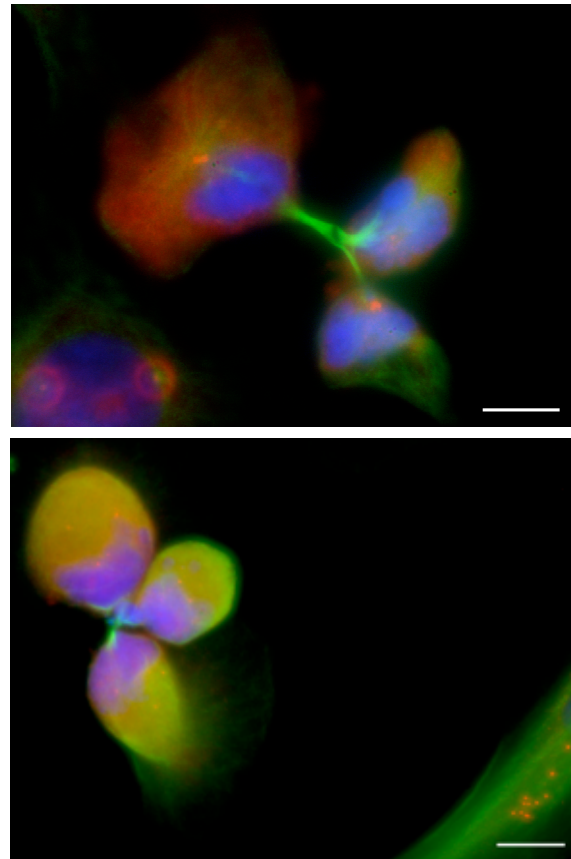
## Human metastatic melanoma in vitro

The mechanism that leads to the production of a stable arrangement for two, three, or four centrosomes, wherein every centrosome is equidistant from every other, cannot exist for higher numbers as no such figures are possible in only three spatial dimensions. Therefore, in the general case, it will only be where cooperative and bystander centrosomes have reduced the number of functional poles to fewer than five that stability in polycentrosomal mitoses will be achieved. Instances of this are illustrated in Figure 6–31. Where five or more poles remain, the mitosis will be inherently dynamic and probably chaotic. This instability may account for the observation of very few multipolar cells at a mitotic phase recognisable as being beyond a distorted metaphase. If true, there are at least two possible outcomes: first, they may remain locked in this state indefinitely, perhaps ultimately undergoing cellular necrosis as essential proteins are degraded but not replaced since gene transcription will be delayed by the condensed chromatin state; or second, the multipolar pseudospindle may be dismantled, the chromatin decondense, a nuclear envelope form, and a polyploid, possibly multinuclear cell survive with its complete complement of supernumerary centrosomes. In that latter case, should a further cycle of division occur, it is likely to begin with duplication of the existing centrosomes, leading to the even more complex situation of mitosis orchestrated by yet more centrosomes. Indeed, the very existence of such polycentrosomal cells implies that this does occur, and that multiple rounds of polyploidisation and centrosome numerical amplification are not inherently lethal. Occasionally, a chance alignment may result in centrosome cooperation that allows a cytokinesis to complete, and with each such event the aneuploidy of the progeny cells will increase, and so will the genomic heterogeneity of the culture of which the cell is a part.

### Additional observations

#### *Cell-cycle dependency of pericentrin expression*

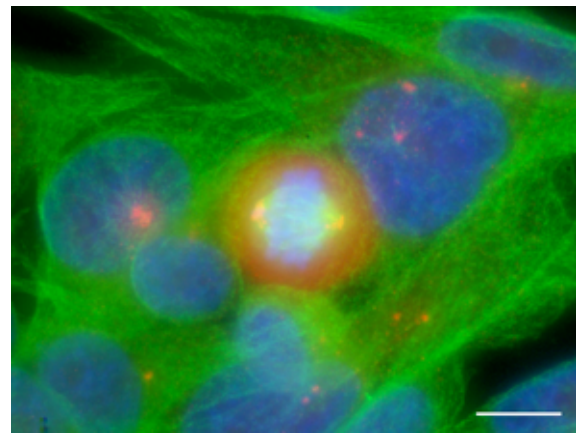
The search for mitotic cells was undertaken on the basis of chromatin condensation, but it soon became evident that another marker of these cells was available: [the level of diffuse cytoplasmic pericentrin labelling was quite obviously higher in mitotic cells from the beginning of prometaphase to late telophase.](#)



Top image: NZM6; scale bar = 10  $\mu\text{m}$ .  
Bottom image: NZM10; scale bar = 20  $\mu\text{m}$ .  
Red = pericentrin; green =  $\alpha$ -tubulin; blue = DNA.

**Figure 6–31: Polycentrosomal ternary telophases**

This elevation of pericentrin is clear in many of the images presented in this chapter, for example in this image of NZM7.4 cells where a cell in metaphase is surrounded by cells in interphase [Figure 6–32]. One has only to compare the red/orange of the metaphase cell with the bright green  $\alpha$ -tubulin labelling in the cytoplasm of interphase cells to appreciate the difference in pericentrin levels present.



Red = pericentrin; green =  $\alpha$ -tubulin; blue = DNA. Scale bar = 10  $\mu$ m.

**Figure 6–32: Mitotic pericentrin elevation**

The images captured during the survey had the primary purpose of demonstrating characteristics of mitotic cells, and to obtain

the clearest images possible, isolated cells were generally chosen as photographic subjects. During image processing, brightness levels were adjusted to make use of the full dynamic range available. The combination of these factors means that no quantitative comparison between cells from different images is possible, and so no comprehensive quantitative data concerning pericentrin as a function of mitotic phase can be extracted from these images. A further experiment to investigate this as a primary goal could be undertaken, and one approach to quantitation would be to ensure that for each subject mitotic cell in the image, one or more interphase cells are also present to act as internal standards against which a relative measurement of pericentrin levels could be made, thereby allowing comparison between images. Another approach would be to use a more advanced instrument capable of absolute quantitation of signal levels.

A further observation made was that focal centrosomal pericentrin labelling diminished markedly in telophase, very often to the point that the centrosomes could not be readily detected by this means. Perhaps this is related to a change in microtubule nucleation mode needed with the change from mitosis to interphase, but from the observations made here, it appears to be a short-lived state. The very great majority of interphase cells observed in passing contained one bright centrosomal focus of pericentrin, so at some point soon after cytokinesis, pericentrin must again localise to the centrosome.

Little is known about the regulation of pericentrin transcription and protein turnover, and since it is a requirement for centrosomal microtubule nucleation and thus for mitosis, to discover that it was regulated in synchrony with the cell-cycle would not be surprising. The coincidence of increase in pericentrin with the end of prophase is interesting in two respects. Firstly, this is the time when microtubule nucleation begins in earnest for the production of the mitotic spindle, and secondly, as will now be described, nuclear envelope breakdown at the end of prophase may serve to release a pool of pericentrin maintained within the nucleus to bring this about.

### *Nucleolar pericentrin reservoirs*

Hoechst or DAPI stained nuclei usually contain voids corresponding to nucleoli, and these were routinely seen in the NZM cells, frequently several per nucleus. An unexpected observation was that these voids very often coincided exactly with areas of pericentrin labelling noticeably higher than the diffuse background (Figure 6–33).

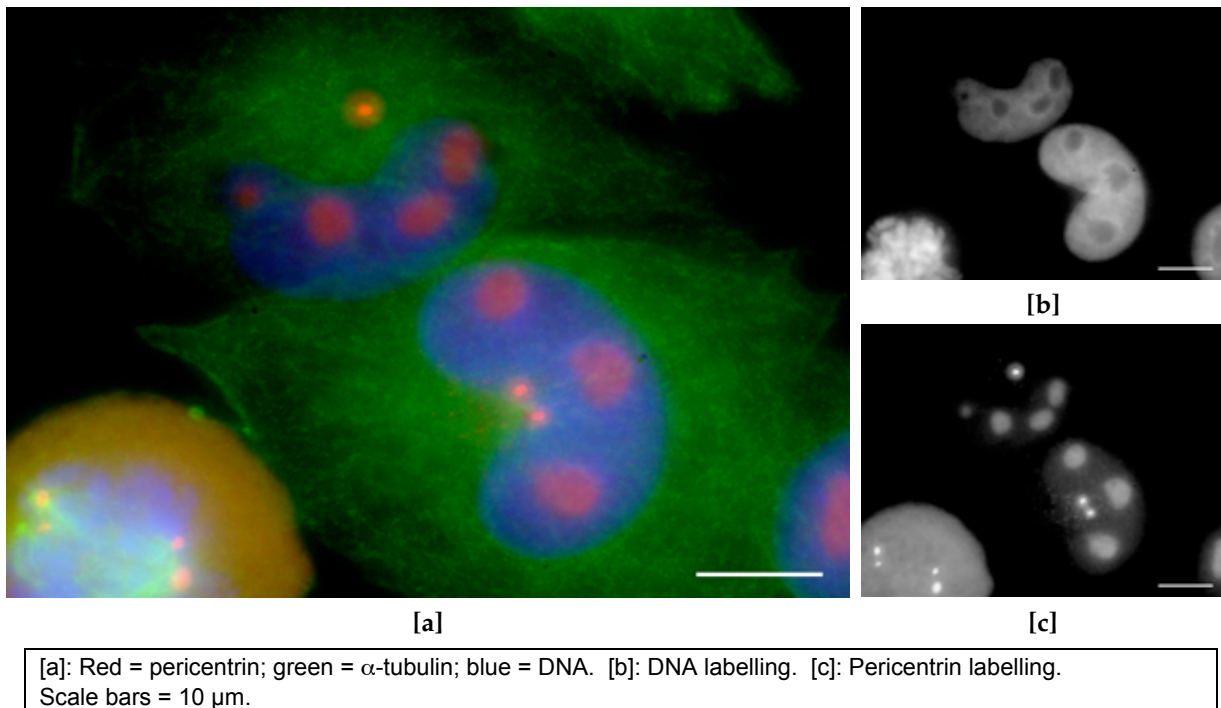


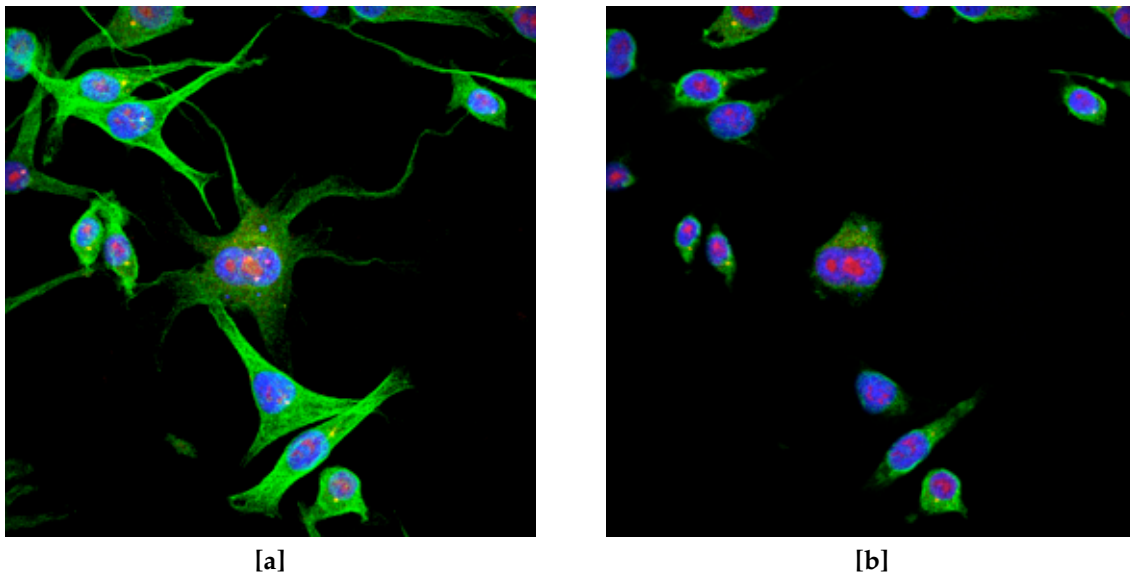
**Figure 6–33: Nucleolar pericentrin reservoirs in NZM9 cells**

This was observed in many of the cell-lines, although there did seem to be variability in this: NZM6 and NZM9 exhibited the phenomenon particularly well.

While by direct observation and inspection of merged images the clear impression to be had was of a pool of pericentrin within the nucleus, fluorescent microscopy could not exclude the possibility that an opaque patch in the nuclear membrane containing pericentrin was interfering either with the excitation of Hoechst below it, or with the transmission of the resultant fluorescence. This was addressed by a limited confocal microscopy study. Figure 6–34 [a] shows the z-projection of the image stack captured and is similar to the fluorescent microscopy images with both focal centrosomal pericentrin labelling and the putatively nucleolar pericentrin pools visible. Figure 6–34 [b] is an optical slice through the cells clearly illustrating that this diffuse pericentrin is within the nucleus, rather than being external to it.

This raises the interesting possibility that **the nucleolus acts as a reservoir for pericentrin, being filled during interphase, and emptied upon nuclear envelope breakdown at the boundary between prophase and prometaphase.** This could form the basis for synchronising the commencement of construction of the mitotic spindle, as released pericentrin translocating to the centrosomes would enhance their microtubule nucleation capacity.



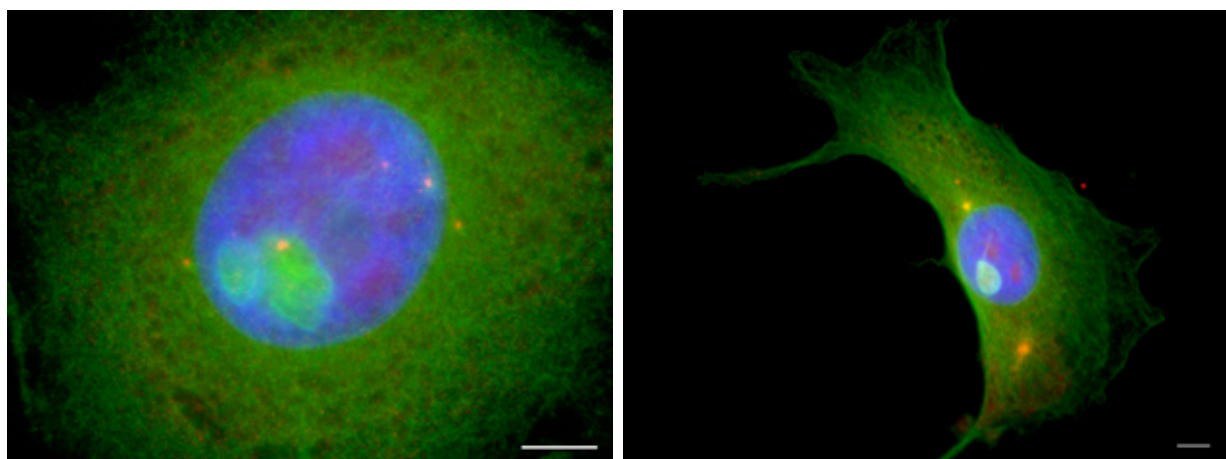


[a]: z-projection. [b]: optical slice. Red = pericentrin; green =  $\alpha$ -tubulin; blue = DNA.

Figure 6-34: Confocal imagery of nucleolar pericentrin in NZM2 cells

### *Tubulin "nests"*

A small number of cells, fewer than ten in total, were observed to contain unusual tubulin structures resembling eggs in a nest. These were most notably in NZM1 (Figure 6-35).



Red = pericentrin; green =  $\alpha$ -tubulin; blue = DNA. Scale bars = 10  $\mu$ m.

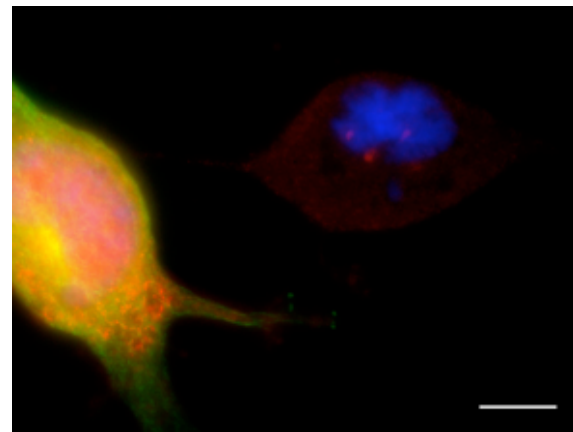
Figure 6-35:  $\alpha$ -tubulin nests in NZM1 cells

These manifested as dense knots of tubulin and appeared to be intranuclear as they coincided with areas not labelled by Hoechst. Often, pericentrin levels were elevated in these regions, similar to the elevation seen in the nucleolar reservoirs. The origin of these is unknown, but conceivably they represent tubulin trapped during reformation of the nuclear membrane in telophase. Their significance, if any, is also unknown. Confocal microscopy studies could be undertaken as the next step in their study.

### *Mitotic cells apparently lacking $\alpha$ -tubulin*

During the early stages of the mitotic survey, an occasional cell was seen that lacked any fluorescence attributable to  $\alpha$ -tubulin labelling. This seemed so unlikely to be genuine that such cells were initially dismissed as probable artefacts of flawed labelling during slide

preparation, perhaps due to edge effects where reagents had not been fully dispersed across the coverslip. With continuation of the survey however, these cells were found in contexts that rendered this an interpretation unlikely to be correct {Figure 6–36}. It is clear from the cell at the left of the image that both  $\alpha$ -tubulin and pericentrin labelling are functioning correctly. Furthermore, since the primary antibodies for both targets were added simultaneously as a mixture, as were their respective secondaries, the presence of



Red = pericentrin; green =  $\alpha$ -tubulin; blue = DNA. Scale bar = 10  $\mu$ m.

Figure 6–36:  $\alpha$ -tubulin-negative NZM2 cell

pericentrin labelling in the abnormal cell implies that had any normal  $\alpha$ -tubulin been present, it too would have been labelled. This cell was scored as acentrosomal based on its very weak focal pericentrin labelling. If it does indeed lack  $\alpha$ -tubulin, this could be readily explained, since without tubulin there can be no centrioles, and without centrioles there can be no centrosomes. Absence of microtubules would also prevent delivery of centrosomal components, such as pericentrin, since the dynein/dynactin transport system conveys cargo along paths defined by microtubules.

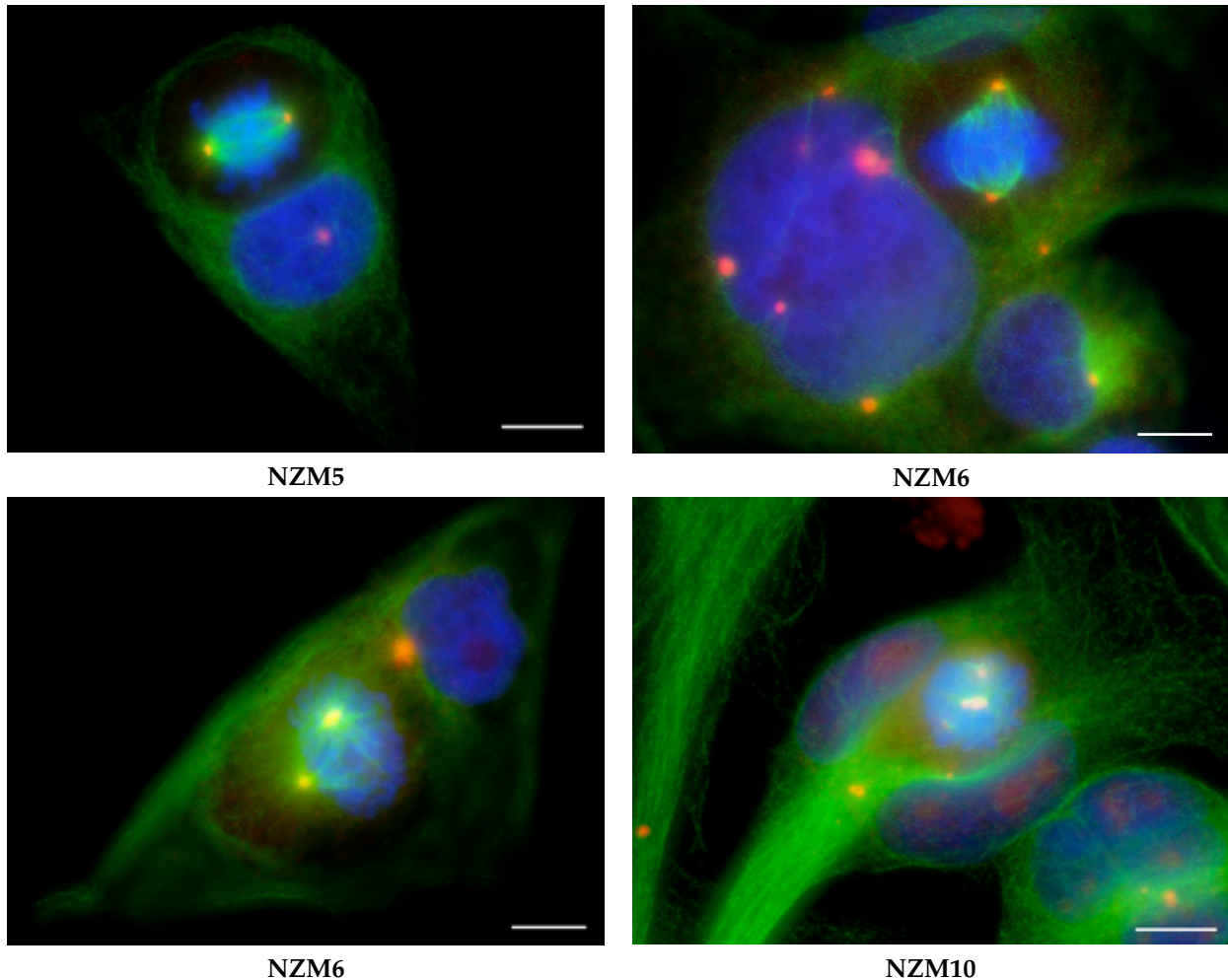
See J.4 for more on the centrosome cycle, including component delivery systems.

Nothing is known concerning which of the several genes for  $\alpha$ -tubulin are being transcribed in these cell-lines. If a single gene is active, then it is conceivable that  $\alpha$ -tubulin is being produced which is functional, but which no longer contains in recognisable form the epitope against which the antibody used in the experiment was raised. Given that the epitope is in a region that is highly conserved among both human paralogues and homologues, this seems to be an unlikely scenario. Even were it so, it would of itself indicate a major disruption of tubulin molecular biology hardly less significant than an outright loss of protein expression. Overall, it is difficult not to conclude that these cells contain no  $\alpha$ -tubulin, and if it were borne out by further study that entry into prometaphase does indeed occur in such cells, as seems to be the case here, then the inference would be that neither the presence of  $\alpha$ -tubulin nor the existence of centrosomes is a prerequisite for the commencement of mitosis.

### *Independent mitoses in multinuclear cells*

The observation of binuclear, or even multinuclear cells was not surprising, but the discovery of such cells where a single nucleus was undergoing mitosis was. This type of event was seen in several cell-lines, most notably in NZM6, and representative images are given in Figure 6–37.

This is an extraordinary result with significant ramifications for the study of the regulation of mitosis. It strongly implies that [the commitment to undergo mitosis does not occur on a global cellular level, but on a nuclear level](#), a distinction not able to be recognised, or for that matter, studied, in normal uninuclear cells.



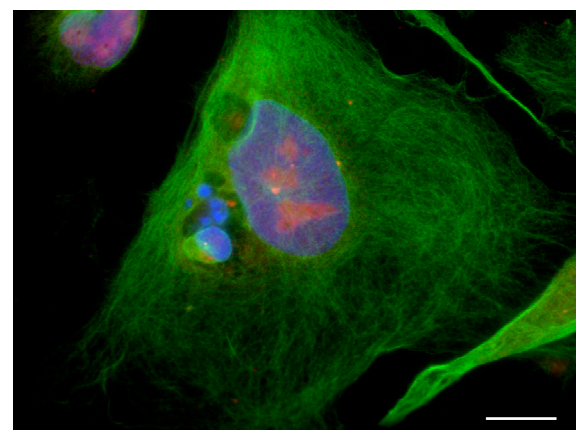
Red = pericentrin; green =  $\alpha$ -tubulin; blue = DNA. Scale bars = 10  $\mu$ m.

**Figure 6-37: Asynchronous mitoses in bi- and tri-nuclear cells**

Significantly for the study of the generation of heteroploidy being undertaken here, it provides an unanticipated mechanism for the production of relative hexaploidy, something otherwise difficult to explain without invoking cell fusion, and yet a feature of the complex NZM10 heteroploidy spectrum.

***Independent apoptoses in multinuclear cells?***

Cellular perversity may not end there. Most of the cell-lines exhibited a very low proportion of apoptotic cells, noticeable by their distinctive Hoechst labelling due to the formation of very dense apoptotic bodies. One such collection of objects found in NZM10 proved not to be an apoptotic cell at all, but had every appearance of having formed from the apoptotic fragmentation of a single nucleus of a multinuclear cell {Figure 6-38}. These objects did not have the appearance of



Red = pericentrin; green =  $\alpha$ -tubulin; blue = DNA. Non-linear contrast enhancement of DNA signal used owing to the brightness of the putative apoptotic bodies present relative to the nuclei, this being ~4-fold. Scale bar = 25  $\mu$ m.

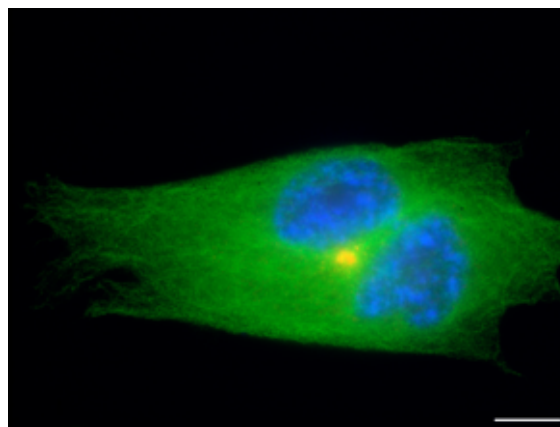
**Figure 6-38: Asynchronous apoptosis in NZM10 nuclei?**

micronuclei: they were very much brighter, and appeared in a tubulin void such as might have been recently occupied by an intact nucleus. Interestingly, another such void is present in this cell, and this may mark the position occupied until recently by another nucleus that has met the same fate.

If independent apoptoses are indeed occurring, then clearly the regulation of apoptosis also occurs on a per-nucleus, not per-cell basis, as seems to be the case with mitosis. This also provides another mechanism for increasing aneuploidy and heteroploidy.

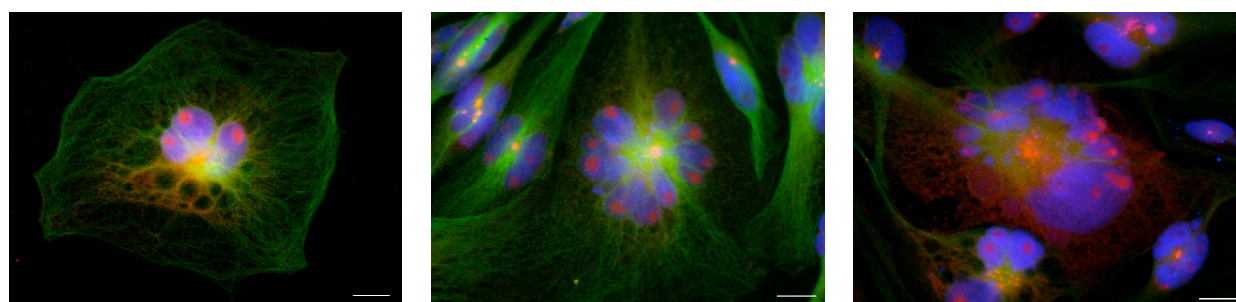
### *Tubulin voids*

Voids in the tubulin network were very commonly observed in all cell-lines, but in the vast majority of cases, once the DNA image was merged the void was neatly filled by a nucleus. Many instances of tubulin voids that were not occupied by nuclei were seen in NZM10, but they were also seen in NZM1 {Figure 6–39}. These were found serendipitously during the mitotic survey, and had they been being actively sought, they may have proven to be more widespread. Non-mitotic NZM10 cells did fall under closer scrutiny than those of other cell-lines because of the rich and fascinating complexity of nuclear and cell morphologies displayed by the cell-line {Figure 6–40}, and this may be why more voids were detected there. Where they were seen, these voids were indistinguishable in appearance from those that would normally contain nuclei. A mechanism involving an antiparallel set of elongating microtubules anchored at both ends and bulging due to the action of cross-linking motor proteins was considered, but compared to the simplicity of the disappearance of a nucleus by apoptosis, it seems unnecessarily cumbersome.



Simultaneous binuclear prophase with clustered centrosomes and a tubulin void seen in outline.  
Red = pericentrin; green =  $\alpha$ -tubulin; blue = DNA.  
Scale bar = 10  $\mu$ m.

**Figure 6–39: Tubulin void in NZM1**

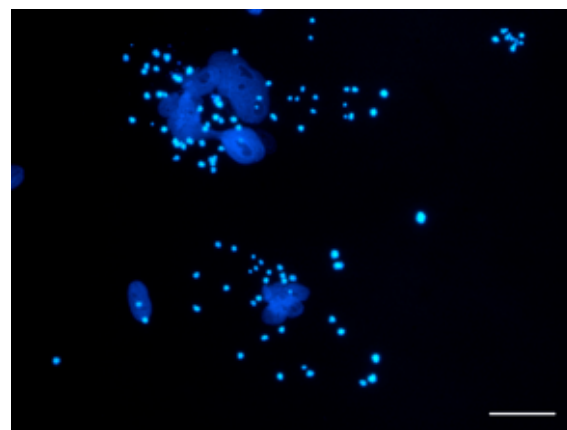


Red = pericentrin; green =  $\alpha$ -tubulin; blue = DNA. Scale bars = 20  $\mu$ m.

**Figure 6–40: Giant NZM10 cells**

### *Anomalous nucleic acid bodies*

During the survey, it was found that some NZM10 and NZM10.1 cells exhibited an unusual phenomenon for which no explanation has been found. It manifests as a variable size and number of globular bodies that fluoresce when excited by the 365 nm ultraviolet light used for the nuclear DAPI and Hoechst dyes {Figure 6–41}. This fluorescence is conditional upon the presence of either of these dyes, and is therefore not an autofluorescence phenomenon. Moreover, given the dependence on nucleic acid binding for fluorescence of these dyes, it is inferred that these bodies most probably are composed of DNA, or possibly RNA. In light of the specificity of Hoechst 33342 and DAPI for nucleic acids, and the uncertainty over the exact identity of the nucleic acid involved, these objects have been termed anomalous nucleic acid bodies (ANABs).

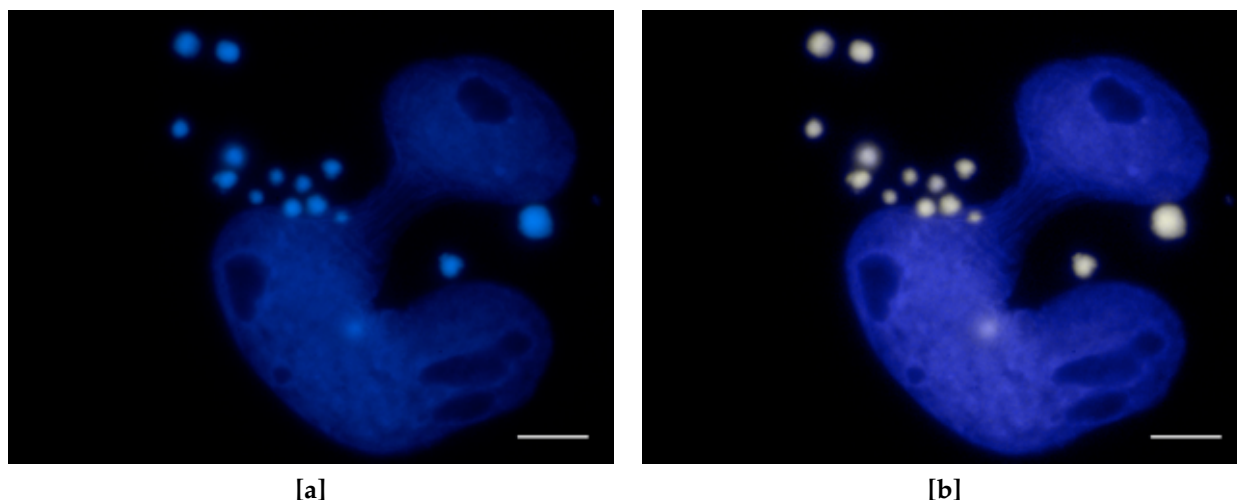


Hoechst 33342 labelling. Scale bar = 50  $\mu\text{m}$ .

**Figure 6–41: Anomalous nucleic acid bodies**

One thing about ANABs is obvious when they are viewed directly: the colour of their fluorescence appears quite distinct from that of chromatin or chromosomal DNA, being much yellower. Both Hoechst 33342 and DAPI have significant emission in the range of wavelengths perceived as green, and similarly recorded as a green component of any captured image. Here, what seems to be occurring is that some difference in nucleic acid composition or configuration, dye binding mode or chemical environment is causing a greater Stokes shift when the dye is in the ANAB context than in the nuclear context, moving more of the fluorescence into the green and altering the perceived and recorded images. Put another way, the ratio of green to blue fluorescence appears higher in ANABs than in nuclei.

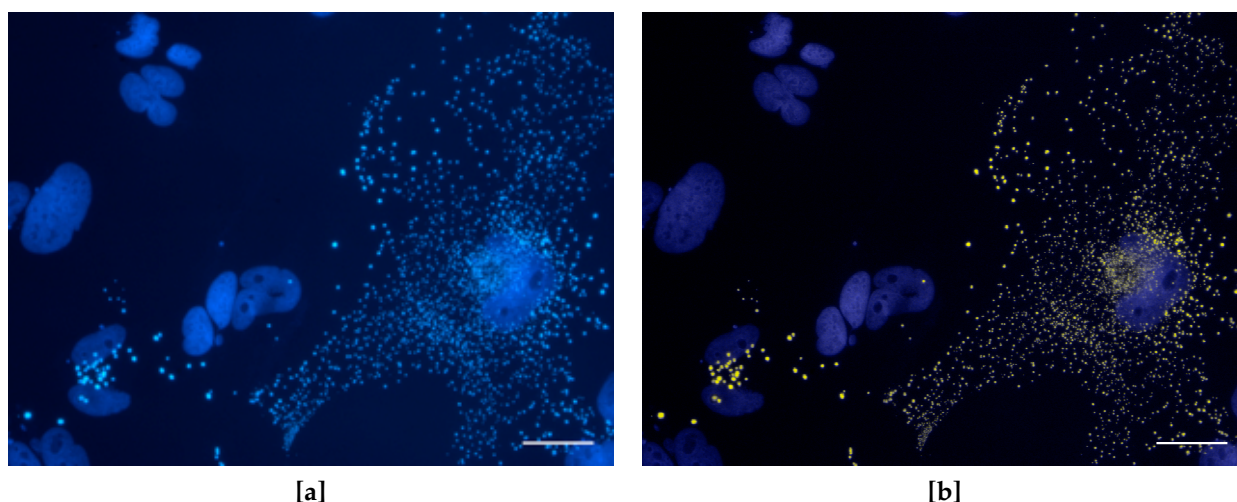
It proved to be very difficult to capture images demonstrating this clearly, as can be seen from the minimal variations in colour visible in Figure 6–41. To address this, digital colour reassignment was undertaken using Photoshop software. The effect of this is demonstrated in Figure 6–42, while the process itself is described fully as part of Method 45. The improvement is dramatic, assisted in this case by the original nuclear labelling having an overall green:blue ratio of less than the nominal 1:2, resulting in nuclei that retain a blue hue, while the ANABs take on a less than saturated yellow.



[a]: Contrast enhanced, but otherwise unadjusted Hoechst image of an NZM10 nucleus and ANABs.  
 [b]: Corresponding image after colour reassignment. Scale bars = 10  $\mu\text{m}$ .

**Figure 6-42: Colour reassignment example**

To determine if the perceived and recorded effect was real, or artefactual resulting from sensor saturation, be it electronic or organic, an image was chosen that contained cells both with and without ANABs {Figure 6-43}.



[a]: Uncorrected image used as data source.  
 [b]: Corresponding colour reassigned image. Scale bars = 50  $\mu\text{m}$ .

**Figure 6-43: Fluorescence ratio test image**

From the uncorrected image, fifty pixels were chosen from within ANABs and fifty from within uninvolved nuclei. This was done without conscious selection, other than with the proviso that the blue level was on scale and hence the green:blue ratio would not be subject to artefactual alteration. The intensity of green and blue was recorded for each pixel, and the results are graphed in Figure 6-44.

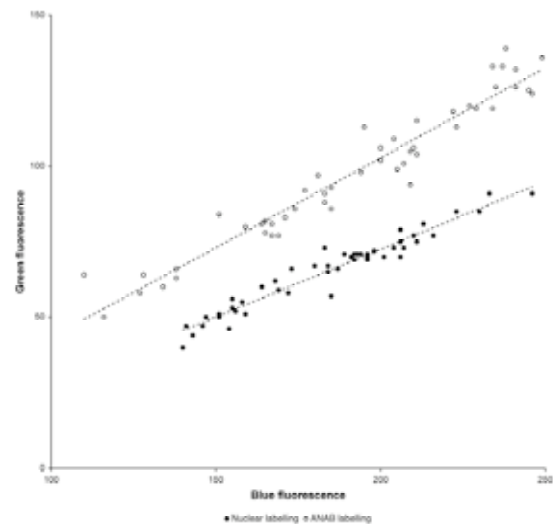
Correlation coefficients are high for both sets of data indicating that the expected linear relationship between green and blue fluorescence exists. When the mean ratios of green to blue fluorescence intensity for pixels in ANABs was compared to the mean for pixels in nuclei by two-tailed heteroscedastic Student's t-test, the probability that they were actually drawn from the same population was  $\sim 10^{-40}$ , confirming what is evident from the clear separation of the two

datasets in the figure. To confirm that this separation is not due to a systematic bias, the slopes of the regression lines for the two contexts were compared. The 99.9% confidence interval for the slope for nuclear labelling is [0.39, 0.51] and for ANAB labelling it is [0.52, 0.67]. As these intervals do not overlap it can be concluded with a high degree of confidence that the slopes differ, further verification that the ratios are different.

Clearly, the fluorescence characteristics of Hoechst 33342 differ in the two contexts. Furthermore, while overexposure may lead to the semblance of the ANAB context in nuclei or condensed chromatin, this can be discounted as an artefact not affecting the validity of the underlying observation.

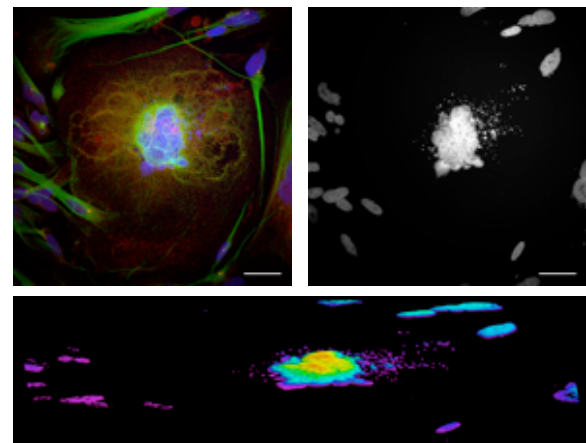
Initially, it was thought that ANABs might simply represent culture contamination, perhaps by mycoplasma, as this was present in the laboratory at the time. This hypothesis was rejected for several reasons. Within a culture, some cells may have ANABs, while others, even those immediately adjacent, may not. Figure 6–43, the test image above, serves to illustrate this. The incidence of affected cells varies from place to place on a slide, and also between preparations, even when these have been grown and

processed in parallel as duplicates. ANAB size is quite variable among cells, but reasonably uniform within any one cell. Shape, while globular, is also variable; it is not the flask-shape said to be characteristic of mycoplasma. Again, these characteristics can be discerned in Figure 6–43. ANABs continued to be detected in cultures derived from cells recently tested to be negative for mycoplasma, but which were nevertheless treated with ciprofloxacin. For confirmation of this conclusion, representative images of Hoechst labelled cells displaying ANABs were sent to Prof. H. G. Drexler, an eminent authority in the field. A response from his colleague, Dr. C. C. Uphoff<sup>1678</sup>, confirmed that this phenomenon was quite



Axes are green and blue brightness levels of sampled pixels in Figure 6–43. Correlation coefficients are 0.937 for the nuclear data and 0.935 for the ANAB data.

**Figure 6–44: Green:blue Hoechst fluorescence ratio for nuclear and ANAB labelling**



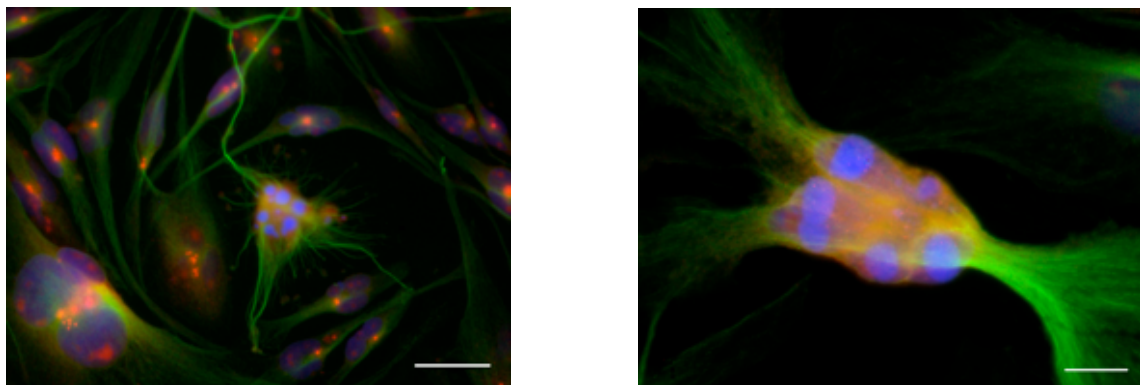
Top panel: Left image is a maximum intensity z-projection of a 63-slice confocal image stack of a giant NZM10 cell with ANABs. Right image is the DNA labelling alone. Red = pericentrin; green =  $\alpha$ -tubulin; blue/white = DNA. Scale bars = 50  $\mu$ m. Bottom panel: Volume-rendered oblique projection from 15° above the bottom edge of the x-y plane of the DNA of the cell in the upper panel. Colours indicate distance from base plane.

**Figure 6–45: ANAB confocal imagery**

uncharacteristic of mycoplasma contamination, or of bacterial contamination in general. Finally, laser-scanning confocal microscopy showed that ANABs were intracellular [Figure 6–45]. Taken together, these observations lead to the conclusion that these objects were not mycoplasma or other contaminant, but rather resulted from an endogenous process.

In general, the number of ANABs and their size seemed to be inversely correlated: cells contained relatively few large ANABs, or many more very small ANABs. Again, Figure 6–43 serves to illustrate this. In itself, this suggests a degradative process where a constant mass is being repeatedly subdivided.

ANABs do not correspond to DNA fragmented due to apoptosis as these are much brighter, generally larger, and are accompanied by changes in tubulin structure not seen in association with ANABs [Figure 6–46]. Furthermore, ANABs exist in cells where the nucleus remains essentially intact. This would seem to exclude apoptosis as a possible source of ANABs, although the possibility that apoptosis may occur in a subset of nuclei in multinuclear cells leaves room for some doubt. ANABs do not have the typical appearance of micronuclei, as these have the same fluorescence colour and structure as nuclei, simply on a smaller scale, therefore even if micronucleation plays a role in the formation of ANABs, it is not the complete explanation.



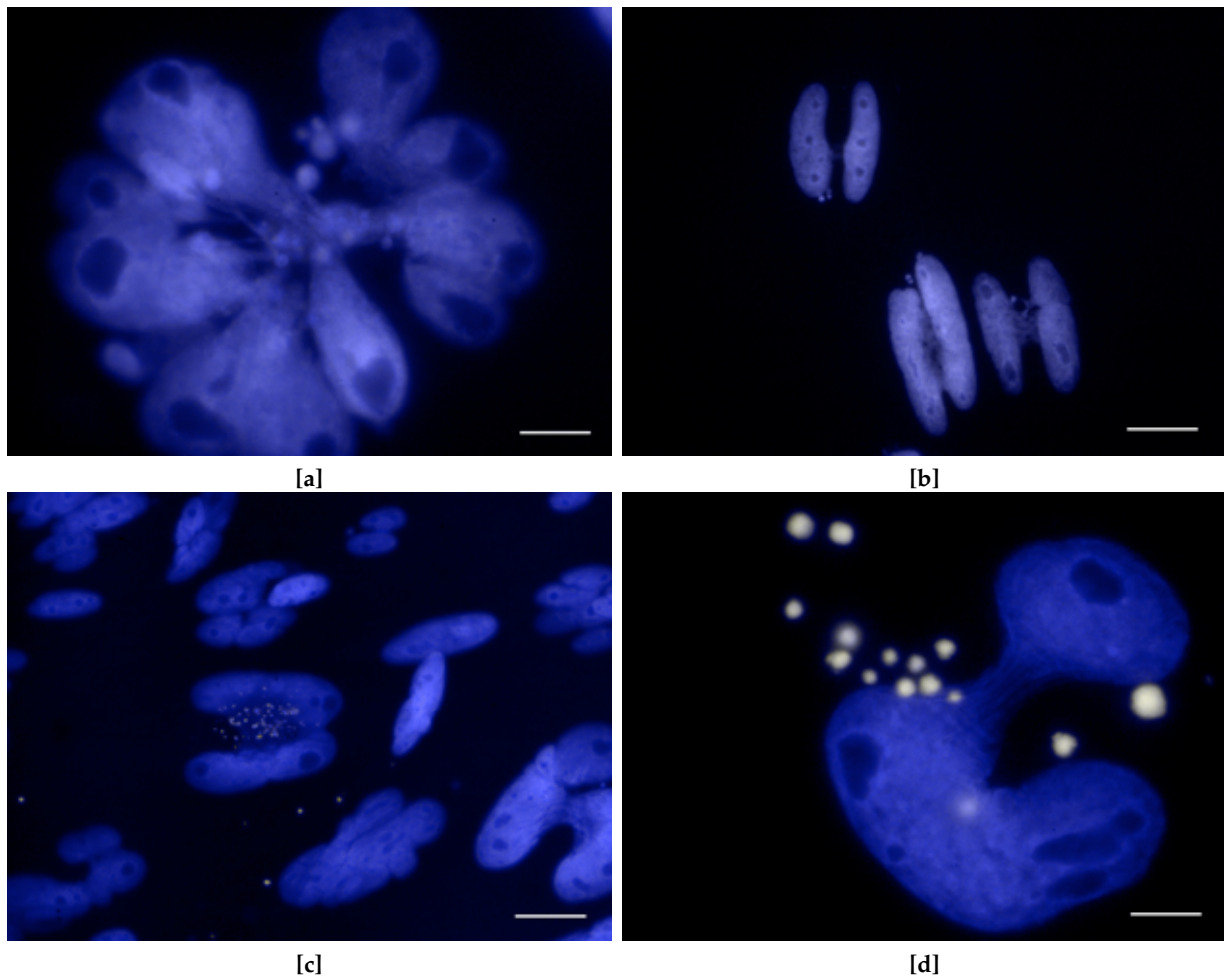
Red = pericentrin; green =  $\alpha$ -tubulin; blue = DNA. Scale bars = 25  $\mu\text{m}$  (left), 10  $\mu\text{m}$  (right).

**Figure 6–46: Apoptotic NZM10 cells**

NZM10 nuclei are usually multilobed, often bizarrely so [Figure 6–47 [a]], and a frequent observation was the presence of a ribbon of DNA stretching between lobes of a nucleus [Figure 6–47 [b]]. It was observed that ANABs were often present between the lobes of a nucleus [Figure 6–47 [c]], suggesting that ANAB formation may involve the degradation of the interlobe ribbons. However, the data are equivocal, with many cells being observed with a few large ANABs beyond the immediate vicinity of the interlobe region [Figure 6–47 [d]].

Exactly what ANABs are, how they form, and whether this process is an actively regulated metabolic or catabolic one, or just a physical result of the process that leads to multilobed nuclei, or something else entirely, remain open questions. Their resolution must wait, as while this is a fascinating observation that warrants further investigation, the research required was well beyond the scope of the current work.





Interlobe DNA ribbons may or may not be the source of ANABs.  
Colour reassigned Hoechst labelling. Scale bars = 10  $\mu$ m.

Figure 6-47: NZM10 nuclei

## 6.4 Perspective

### Results from similar studies

#### *Centrosomal dysregulation in cancer*

Studies similar to this have been carried out for other solid tumours, and the results seen here are in accord with these. Perhaps the most comprehensive study has been that of Pihan et al.<sup>1636</sup>, who examined archival and fresh breast, lung, prostate, colon, and brain tumour tissue, and colon, breast, and kidney tumour cell-lines. They found supernumerary centrosomes, acentriolar pericentrin foci nucleating microtubules, extended centrosomal and non-centrosomal pericentrin structures, cooperative centrosomes, and non-bipolar spindles and cytokineses. They proposed that aberrations such as these could easily contribute to aneuploidy and the tumorigenic process. They further suggested that elevated pericentrin levels might contribute to this by allowing the formation of acentriolar microtubule nucleating centres and aberrant mitotic spindles. Other studies have explored the centrosomal status of bladder<sup>1586</sup>, prostate<sup>1637</sup>, hepatic<sup>728</sup>, and pancreatic<sup>1665</sup> tumours with similar results. Supernumerary and abnormally large centrosomes were the most common findings.

### *Regulation of pericentrin*

On the subject of pericentrin regulation, the literature is virtually silent. Doxsey et al.<sup>§1554</sup> does mention that "Pericentrin staining intensity changed with the nucleating capacity of the centrosome during the cell cycle, being highest at metaphase and lowest at telophase", but no data are presented, and it is not clear from the context whether this refers to centrosomal pericentrin, cytoplasmic pericentrin, or both. This comment is certainly consistent with two of the findings here: that cytoplasmic pericentrin increases at prometaphase, and that centrosomal pericentrin labelling diminishes in telophase.

### *Asynchronous mitosis and apoptosis in multinuclear cells*

Asynchronous mitosis of nuclei in multinuclear tumour cells has been reported, although there has been very little published on this: in a tritiated thymidine tracer study, Sheehy et al. found independent mitoses in human ovarian ascitic tumour cells in vivo<sup>1656</sup>. Both asynchronous mitosis and apoptosis have been reported to occur following colcemid-induced polyploidisation of Chinese hamster ovary cells<sup>§1562</sup>. It was hypothesised that failure of the cell to bring the independent mitotic cycles into synchrony triggers apoptosis in some nuclei, consistent with the results of much earlier work based on virus-mediated fusion of cells<sup>1642</sup>.

### **Novel findings**

#### *ANABs and tubulin nests*

Neither of these features appears to have been reported previously. It is possible that each has a mundane explanation, but their significance cannot be discounted while these remain unknown. ANABs would seem to be the easier to study, as they are readily found in the affected cell-lines, and furthermore, as they appear to involve a novel nucleic acid degradation mechanism, they may have a broad significance.

#### *Centrosomal dysregulation in melanoma*

There seems to have been no published study of centrosomal status in melanoma, either in tumours or cell-lines, so the bulk of the work described here appears to be novel. From the extent of the anomalies found, there can be little doubt that in melanoma, as in the other solid tumours studied, centrosomal dysregulation plays a major role in the generation of tumour diversity, influencing both the progression of tumorigenesis, and the response to therapy. It may not even be too radical to suggest that this dysregulation may be the initiating event in melanomagenesis. Doubtless a great deal of interest will soon be focussed on this area with the recent recognition that p16, so commonly lost in melanoma, has a role in centrosomal regulation<sup>1610</sup>. The results of these studies, and the insights they will bring, are eagerly awaited.

#### *Nucleolar pericentrin reservoirs*

The existence of nucleolar pericentrin reservoirs does not appear to have been reported previously, although nucleolar sequestration of other proteins, for example ARF, MDM2, and p53 is known. Observations such as these are currently promoting a re-evaluation of nucleolar function<sup>®1599</sup>. The suggestion made here that nucleolar sequestration and release of pericentrin may synchronise the initiation of mitotic spindle formation with nuclear envelope breakdown

appears novel. If it transpires that the situation in melanoma reflects an aberration of a normal process, then this may lead to new understandings of regulation and dysregulation of mitosis.

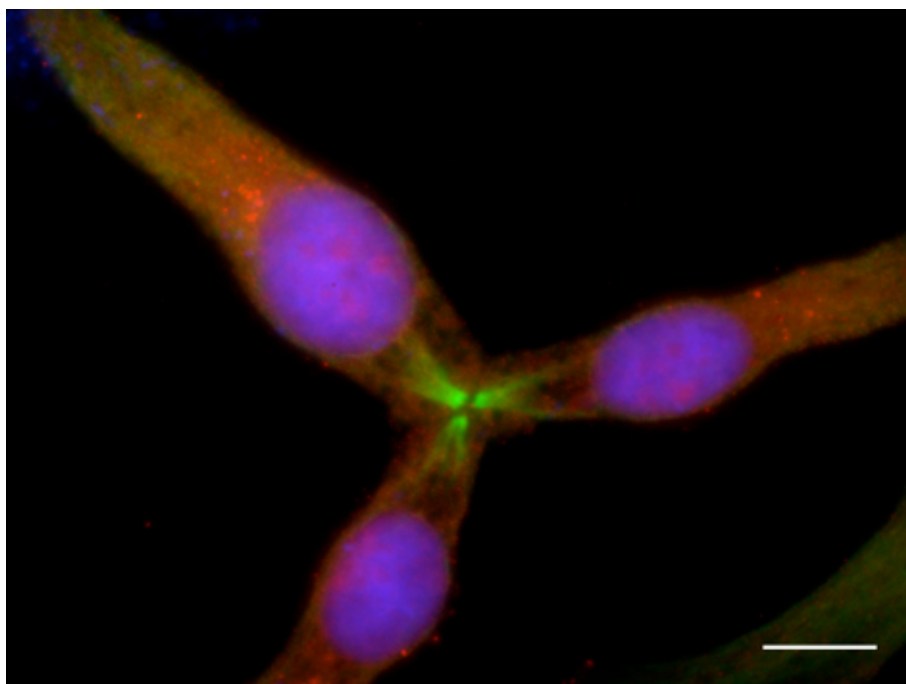
### *Regulation of pericentrin*

Nucleolar pericentrin reservoirs were immediately obvious on observation of appropriately labelled NZM cells, and so was the potentially related upsurge in cytoplasmic pericentrin at prometaphase entry. It seems very improbable that these things can have been observed in similar studies in other tumour types without having been reported, so perhaps they have special relevance to melanoma. If so, then given the growing evidence of the importance of centrosomal regulation in genome stability, and the role of pericentrin aberrations in upsetting this, *PCNT* may prove to be one of the missing melanoma predisposition genes, and pericentrin would become a potential therapeutic target.

## 6.5 Conclusion

The primary objective of the experimental work described in this chapter was to seek to determine if the numerical control of centrosomes was dysregulated in the NZM cell-lines, and if so, whether this was a plausible mechanism for the genomic instability indicated as present by studies of cellular DNA content. If this chapter had to be condensed to a single image, it would be the one shown below {Figure 6–48}. It contains uncountable centrosomes, and can only be interpreted as a ternary cytokinesis. It is simply impossible for such a situation to occur where euploidy is being maintained.

Centrosomal numerical dysregulation occurred in all of the NZM cell-lines studied and the production of malformed mitotic spindles incapable of mediating correct genome segregation was a frequent concomitant of this.



Red = pericentrin; green =  $\alpha$ -tubulin; blue = DNA. Scale bar = 10  $\mu$ m.

Figure 6–48: Ternary cytokinesis in NZM12

## 6.6 Summary

- Aberrations of centrosome structure, number, and function are widespread in the human metastatic melanoma cell-lines investigated;
- There is a strong association between these and the generation of flaws in mitotic and cytokinetic symmetry, establishing this dysregulation as a likely source of aneuploidy and heteroploidy;
- Pericentrin accumulates in the nucleolus and its release with nuclear envelope breakdown at the prophase/prometaphase boundary may trigger spindle formation;
- Pericentrin expression may be cell-cycle regulated, or the operation of nucleolar reservoirs may give this impression;
- Regulation of pericentrin may be particularly significant in melanoma, and its dysregulation may represent an opportunity for therapeutic intervention;
- Centrosomes with extended pericentrin structures were seen that may either help or hinder mitotic fidelity;
- Cooperative and bystander centrosomes may allow normal mitosis despite the presence of supernumerary centrosomes;
- Anomalous nucleic acid bodies of unknown origin and significance were discovered;
- Mitosis may be regulated on a per-nucleus, not a per-cell basis, a simple path to relative hexaploidy;
- Apoptosis may also be regulated in this way and contribute to aneuploidy and heteroploidy;
- Neither  $\alpha$ -tubulin nor centrosomes may be required for entry into prometaphase;
- Tubulin nests of unknown origin and significance were found.

---

# 7

## The effect of serum-deprivation

---

*Entry of cells into S-phase of the cell-cycle is governed by a molecular checkpoint in late G<sub>1</sub> in which the retinoblastoma-associated protein, pRB, is a crucial component. There is considerable evidence supporting the hypothesis that defects in this subsystem may be a hallmark of melanoma. One function thought to be regulated through this mechanism is entry by a cell into a state of proliferative quiescence in the absence of mitogens. By depriving cell cultures of serum and examining their subsequent proliferation rates and the distribution of cells among cell-cycle phases, it is possible to determine if this checkpoint is grossly intact.*

*It was found that all of the melanoma cell-lines responded to serum withdrawal with an immediate and drastic reduction in proliferation rate, but cell-cycle analysis revealed that the basis for this was not always through arrest in G<sub>1</sub>. While some responded by displaying a sustained increase in G<sub>1</sub>-phase fraction at the expense of S-phase, others responded with an immediate, dramatic, and sustained increase in transit time through G<sub>2</sub>/M-phases, demonstrating the existence of a previously unsuspected serum dependency of G<sub>2</sub> transit. Yet others responded with a cohort of cells leaving G<sub>1</sub> and continuing through the cell-cycle. These observations essentially refute the model of a 'restriction point' late in G<sub>1</sub> beyond which progression through the cell-cycle is assured.*

*In the control cultures for some cell-lines, spontaneous changes in cell-cycle phasing were seen that increased with time in culture. These were not due to the effects of confluence, but rather, suggested the production of an inhibitory autocrine/paracrine factor.*

---

### 7.1 Introduction

#### The late-G<sub>1</sub> checkpoint in melanoma

As in the quest to understand the causes of cancer in general, the study of hereditary melanoma predisposition syndromes has revealed important insights into the molecular basis of this disease. Two well-studied syndromes involve germ-line aberrations in *CDK4* and *CDKN2A*<sup>422</sup>. The first encodes a CDK that, in conjunction with its mitogen-induced activating partner, cyclin-D, is important in promoting proliferation. The second encodes p16, a specific inhibitor of the first. The most common mutation found in *CDK4* is one that has been shown to prevent its interaction and consequent inhibition by p16, and the alteration in *CDKN2A* is variously homozygous deletion, hemizygoty with mutation of the remaining allele, and transcriptional silencing, probably via methylation. Added to this is the observation that the incidence of melanoma is abnormally high in survivors of hereditary retinoblastoma<sup>903</sup>, where a germ-line *RB1* mutation exists. The protein encoded by this gene, pRB, is a known substrate for activated CDK4, and such phosphorylation is a critical step in the inhibition of its proliferation-suppressive function, serving to cause the release of E2F-family transcription factors, which can then sponsor entry into S-phase. Thus, pRB operates to implement a checkpoint in late G<sub>1</sub>. The coincidence of timing and character make pRB a strong candidate to form the crux of the 'restriction point' postulated by Pardee<sup>999</sup>.

See H-15 and J-12 for more on CDK activation.

See Appendix H for a review of the pRB subsystem.

Pardee's work is discussed on page H-16.

---

In many cases, mutations, deletions, or other anomalies in *CDKN2A*, *CDK4*, or *RB1* have been documented in sporadic melanoma, and in melanoma cell-lines. The relevance of the cyclin-D-CDK4-pRB-E2F subsystem to melanoma is therefore well supported. Attention was focussed particularly on pRB and p16 as it appeared that dysfunction of these proteins was mutually exclusive in melanoma<sup>73 1391</sup>. The proliferation-suppressive role of pRB was considered to be the likely target of such flaws, in particular, its role in mediation of a G<sub>1</sub> restriction point. However, many signalling channels converge at pRB, and not all are subject to modulation by p16. For example, pRB is also a substrate for other CDKs, notably CDK2 in conjunction with cyclin-E, and CDK2 is not inhibited by p16. Therefore, the possibility remains that cells may derive some additional growth advantage if the function of both pRB and p16 were lost.

As a precursor to a molecular characterisation of components of this key subsystem in the NZM cell-lines, an assessment of its gross functionality was made. Since mitogen-dependency is mediated via pRB<sup>285 487</sup>, and this is readily measured experimentally, this was selected as the basis for the functional assessment, an approach used by Pardee<sup>999</sup>. The assumption is that it is the growth factors present in the serum that influence cell proliferation, but the effects of other components, such as anti-oxidants, cannot be formally excluded. Cells were deprived of serum and their response measured in terms of proliferation rate and cell-cycle phasing. At the outset, the expectation was that none would arrest in G<sub>1</sub>, in accordance with the hypothesis that this checkpoint is defective in all melanomas.

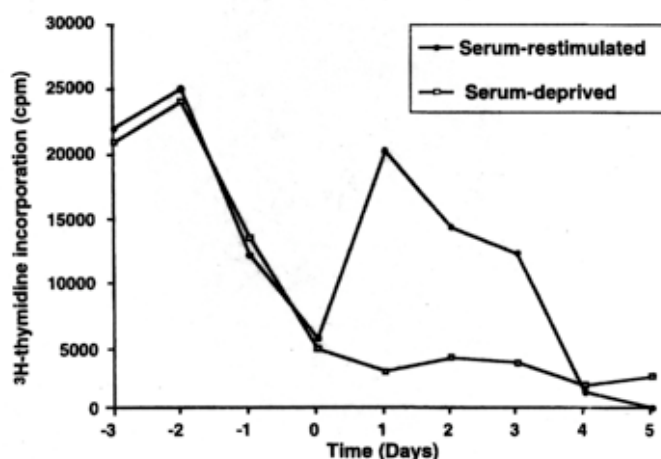
### **Serum-deprivation of melanoma cell-lines: the literature**

The literature pertaining to the effects of serum-deprivation on the proliferation of melanoma in vitro is surprisingly sparse. A search of NIH PubMed disclosed only three studies of relevance. Each assessed a single cell-line, and in only one case was this of human origin.

In 1986, Sauvaigo et al.<sup>1142</sup> published the results of their study of variants of the human MeWo melanoma cell-line. They reported that both the parental line, and a variant of higher metastatic potential in xenograft models (MeWo-LCI), failed to arrest in G<sub>0</sub> upon serum withdrawal. Since conditioned medium from these cultures was able to stimulate proliferation, both of autologous cultures, and of the unrelated SK-MEL-28 melanoma cell-line, they proposed that this was due to the production of autocrine growth factors.

In attempting to dissect the molecular difference, if any, between growth arrest due to confluence, and that due to serum-deprivation, Modiano et al.<sup>901</sup> investigated the canine melanoma cell-line TLM1. The focus of their work was the possible roles of p53 and p21 in mediating these effects. Their procedure involved the seeding of cells from a sub-confluent culture into medium containing 0.5% serum. After three days, the medium of the experimental cultures was replaced with medium containing 20% FCS. At that time, the medium of the control cultures was also replaced<sup>900</sup>. Daily thereafter for five days, some control and treated cultures were assayed for the uptake of <sup>3</sup>H-thymidine, a marker of S-phase progression, while others were harvested for flow cytometric determination of DNA content.

They found {Figure 7-1} that after seeding actively proliferating cells into low-serum medium, the rate of incorporation of  $^3\text{H}$ -thymidine began to drop after one day, reaching ~25% of the initial value after three days. Upon serum stimulation, the rate of incorporation for the previously serum-deprived cultures immediately returned to its initial level and again declined over three days. Simultaneously, they found by flow cytometry that the  $G_0/G_1$  content of cultures fell from 89% at the time of serum addition to 44% the following day, and then rose to over 70%. This was construed as evidence for a serum-dependent release from  $G_1$ .



© Mary Anne Liebert Inc. {Table iv}. As published.

Figure 7-1: Effect of serum-deprivation on TLM1 cells

Rodriguez and Smith<sup>S1102</sup> performed a limited study involving the B16F10 murine melanoma cell-line, and reported that while complete withdrawal of serum for 48 h resulted in cell death, levels of serum between 0.1% and 0.5% resulted in arrest of proliferation in a manner they described as a 'cell cycle freeze'. They found that subsequent addition of serum did not result in cycle synchrony, implying that no reversible arrest had occurred at any particular point.

## 7.2 Experimental objectives

To:

- determine the effect of serum withdrawal on growth rate;
- determine the effect of serum withdrawal on cell-cycle phasing;
- measure the overall integrity of the late  $G_1$  restriction point.

## 7.3 Methods in brief

For each cell-line, 60 P60 tissue culture plates were each seeded with  $\sim 2.5 \times 10^5$  cells in 5 mL of medium and incubated. After one day, by which time the cells had become adherent, the medium of half of the plates was replaced with medium containing 0.1% v/v FCS, rather than the usual 10% v/v. For the NZM5 cell-line, which is poorly adhering, cells in the supernatant medium were collected by centrifugation and returned to the cultures during medium replacement. Daily thereafter for six days, quadruplicate plates for control and serum-deprived cultures were harvested with retention of the culture supernatant, and the cell number was assessed by electronic particle counter {E.1}. In cases where the rate of growth was slow, later time points were more widely spaced. Replicates were pooled, fixed in methanol/PBS, and subsequently analysed for DNA content by flow cytometry {B.11}. The resulting data were processed to determine the contribution of each distinguishable cell-cycle phase to the overall fluorescence intensity distribution.

## 7.4 Results

Graphs summarising the experimental results are given in Figure 7–3. Owing to the great amount of data gathered, the graphs are necessarily complex. A visual key to their interpretation is given in Figure 7–2. For each time point in each series, control, or serum-deprived, cell counts for each replicate are given, together with their mean and a bar representing the standard deviation of their distribution. For each series, the exponential line of best fit to these means is given, the assumption being that all cells in each replicate behave similarly and independently {but see below}. Above each time point are given vertically paired column charts that show the partitioning of cells among cell-cycle phases as determined from flow cytometric analysis and model-fitting of pooled replicates. The upper graph shows the results for the control point, and the lower, the serum-deprived point. The red column denotes cells in  $G_0/G_1$ , green, those in S-phase, and blue, those in  $G_2/M$  phases. Markers are given indicating 20% intervals.

This manner of presentation allows a rapid visual assessment of the effect of serum-deprivation on cell-cycle phase partitioning over time, while also allowing this to be viewed in the context of the simultaneous effect of deprivation on proliferation rate.

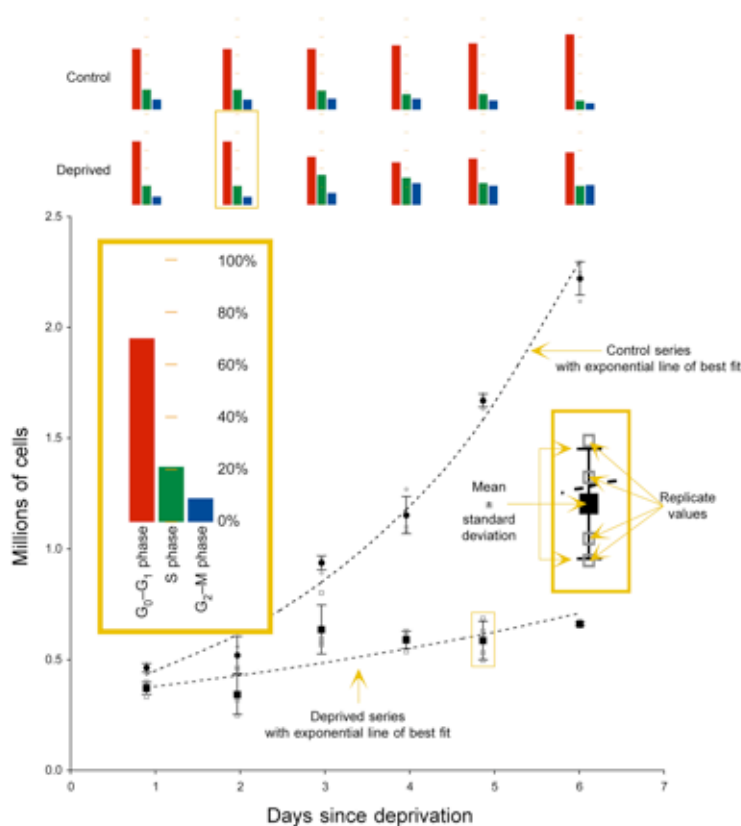


Figure 7–2: Key to interpretation of graphs for serum-deprivation results



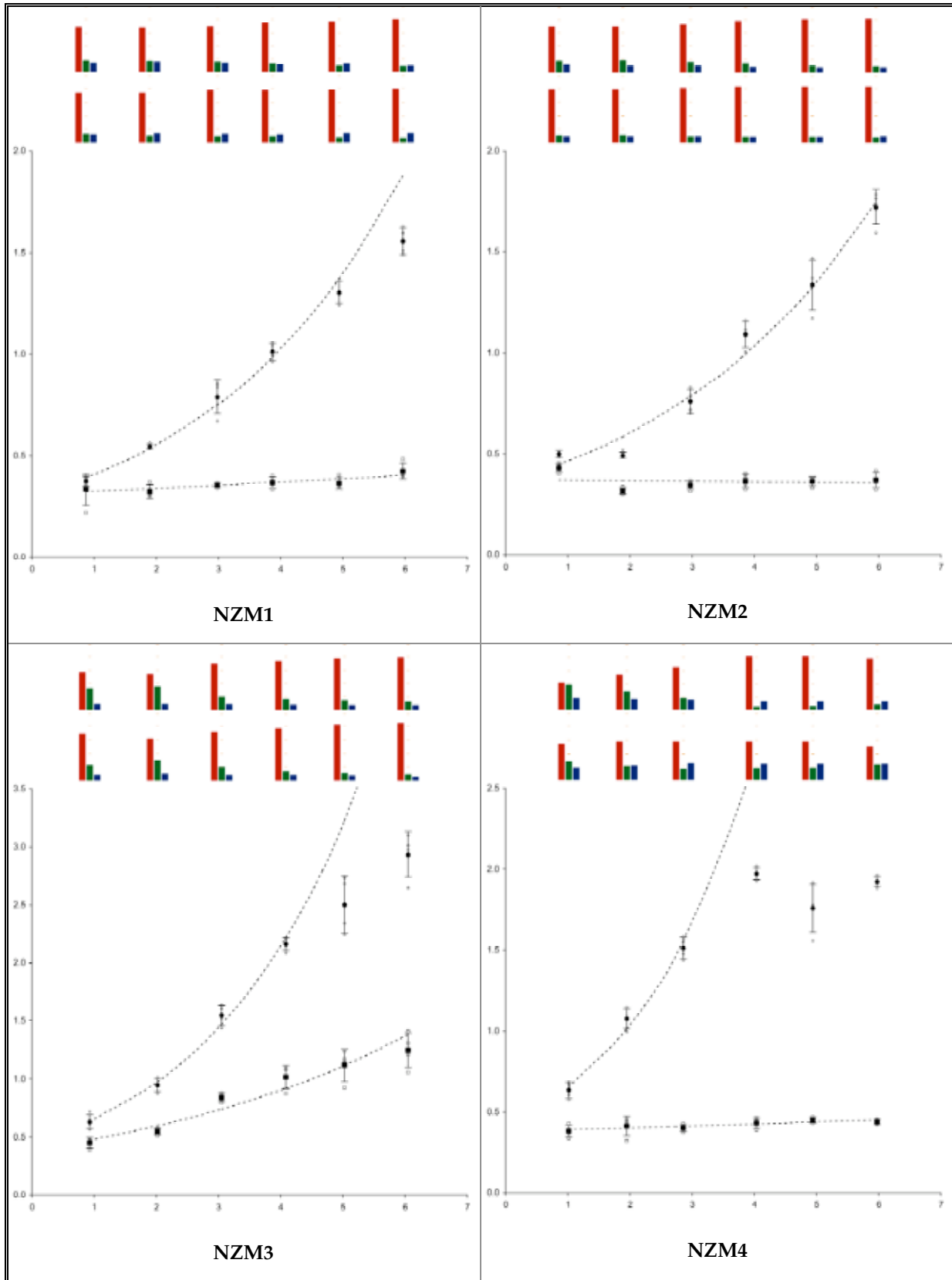


Figure 7-3: Serum-deprivation results (continues overleaf)

7: Serum-deprivation

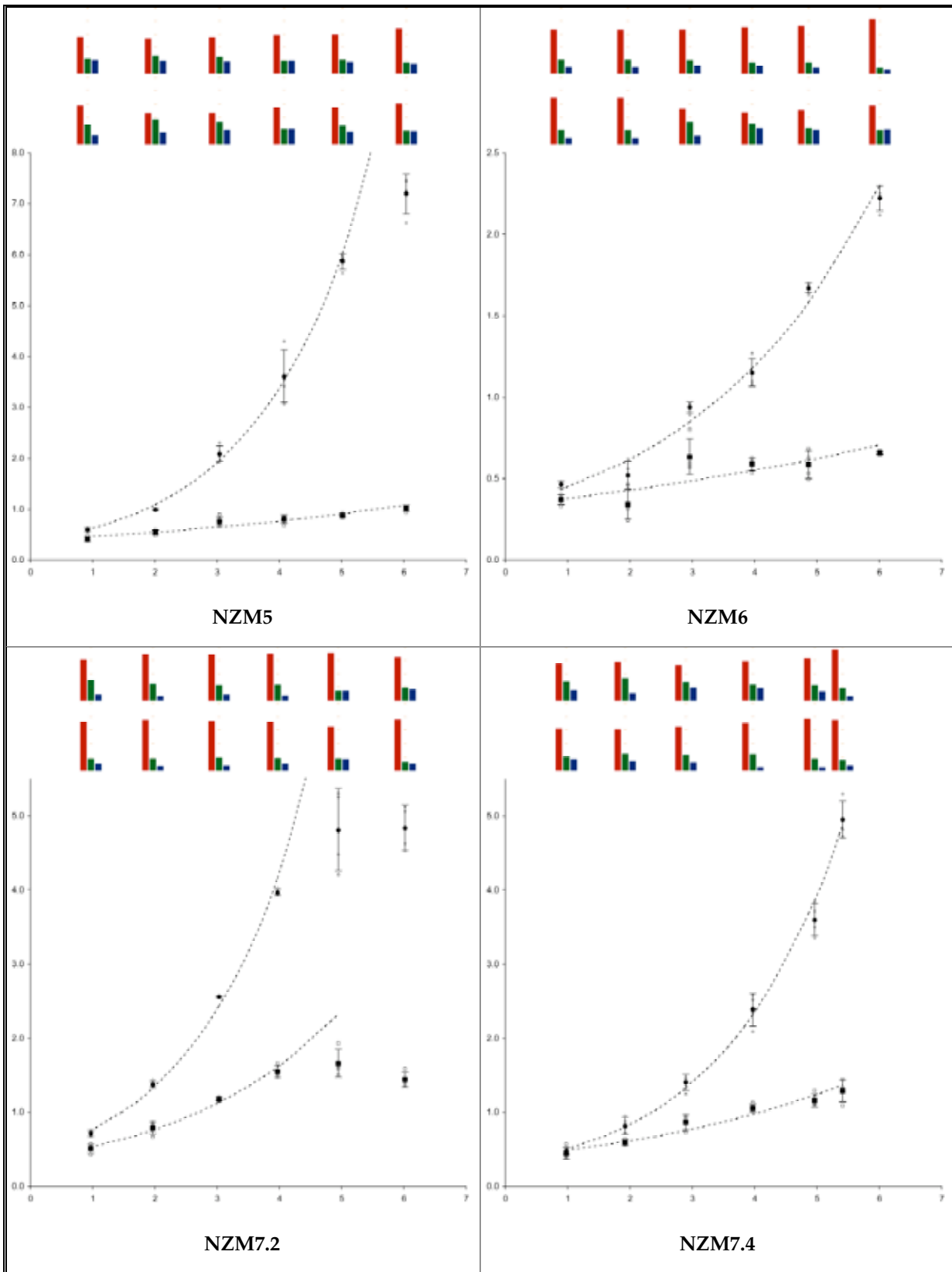


Figure 7-3 (continued)

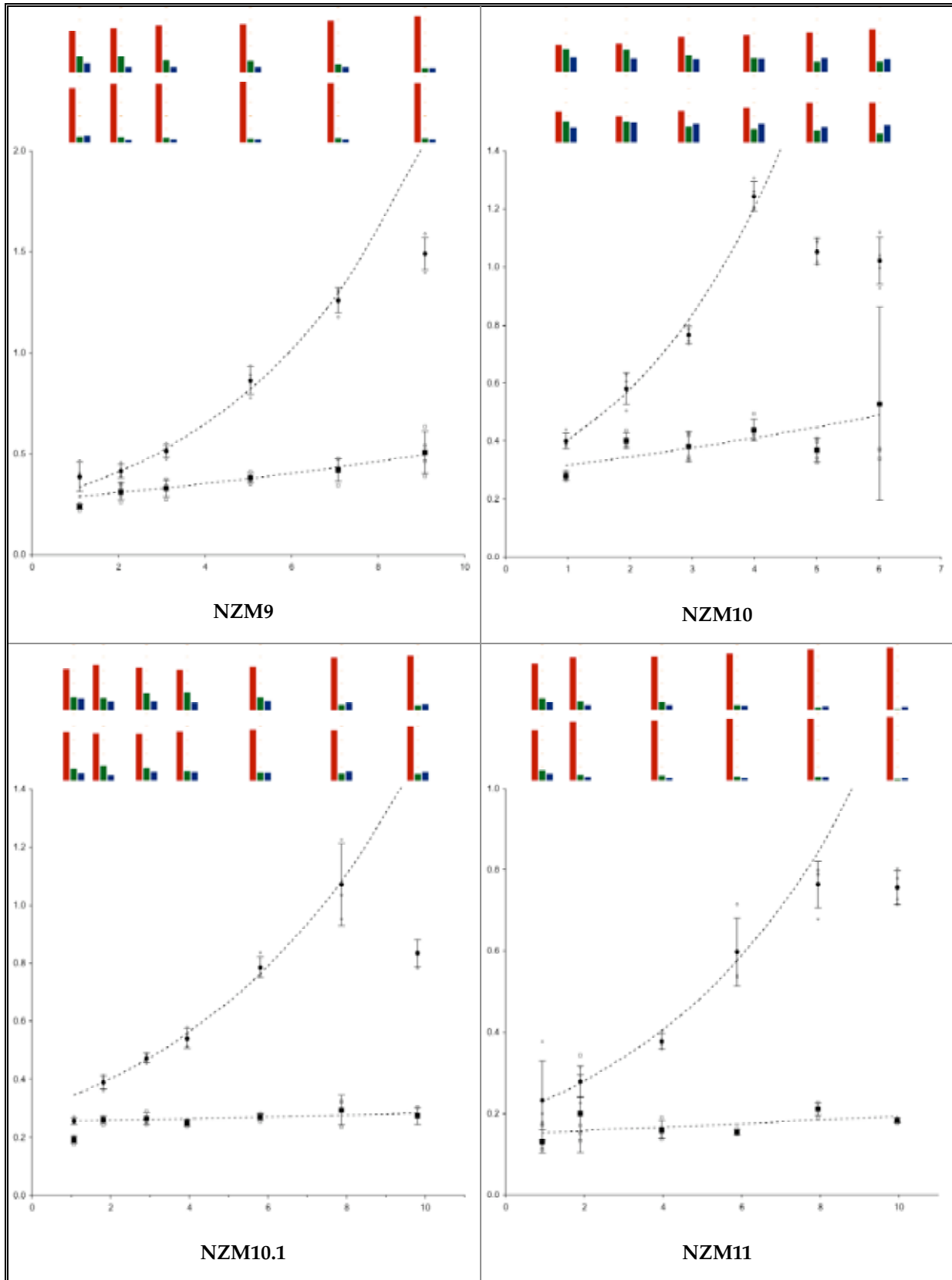
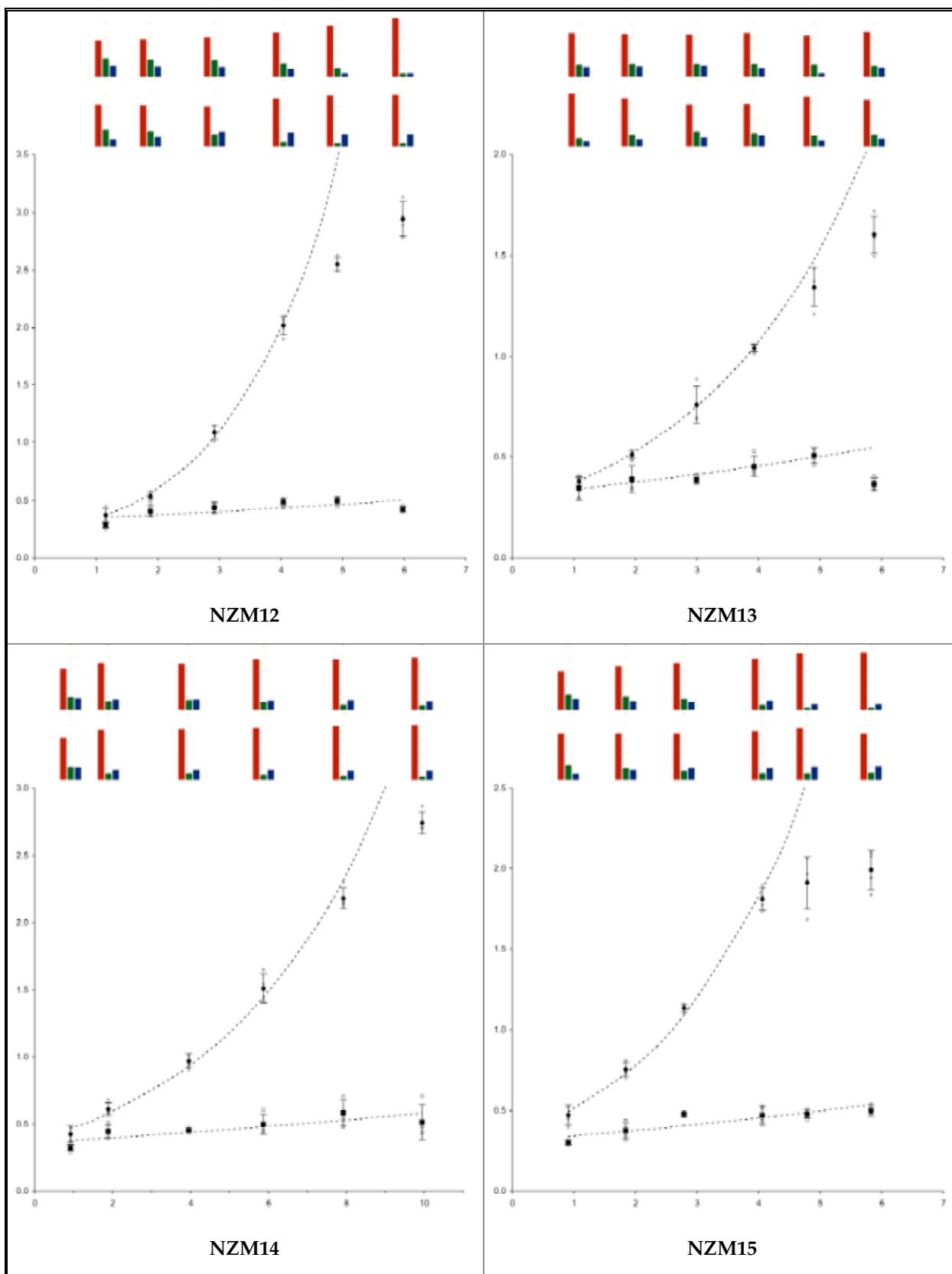


Figure 7-3 (continued)



These graphs show the effect of serum-deprivation on proliferation and cell-cycle phasing for the melanoma cell-lines under investigation. See Figure 7-2 for a visual key to their interpretation. See Figure 7-9 for a different rendering of the flow cytometry data.

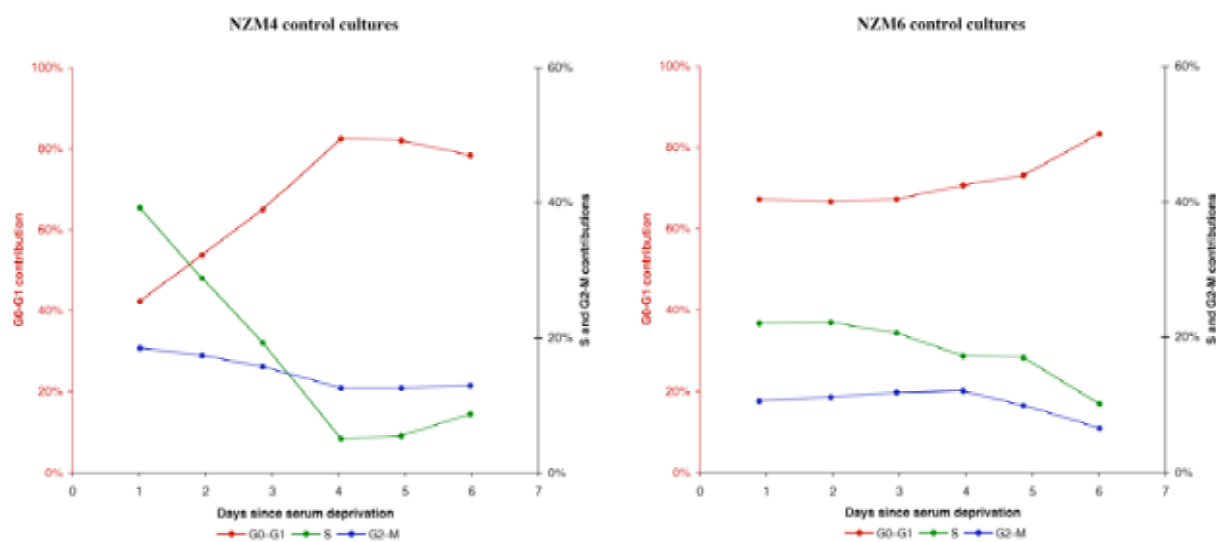
Figure 7-3 (concluded): Serum-deprivation results

## 7.5 Discussion

### Spontaneous phasing changes in many control cultures

In the control cultures for many of the cell-lines, there was a spontaneous redistribution of cells among cell-cycle phases, with a growth in  $G_0/G_1$ -phase and a concomitant decline in S-phase.

This is best exemplified by NZM4 where  $G_0/G_1$  content doubled over three days while S-phase decreased by nearly 90%, in marked contrast to the situation with, for example, NZM6 {Figure 7–4}.



X-axis: days since serum-deprivation; Y-axes: contribution of phase to total population; left axis:  $G_0/G_1$ -phase; right axis: S and  $G_2/M$ -phases.  
Key: ● =  $G_0/G_1$ ; ● = S; ● =  $G_2/M$ .

Figure 7–4: Spontaneous cell-cycle phase redistribution in control cultures

Culture cell density can be ruled out as a cause of this phenomenon since the effect is immediate and progressive from low initial density. Cellular senescence can also be excluded as the effect occurs over a time period corresponding to only one or two population doublings. Furthermore, the cell-lines have diverse passage numbers and all are immortal in culture. Rather, we must look to some element of the cultural context that has changed with time, the only reasonable candidate being the composition of the medium, and the only source of such variation being the cells themselves. Thus, we arrive at the inference that during growth in culture, many of the cell-lines either produce something that favours retention in  $G_0/G_1$ -phase, or consume something that favours passage into S-phase. The production of autocrine growth factors represents a strong candidate mechanism for such a reflexive influence.

If this were the case, the rate of proliferation should also change in concert with the phasing changes, or equivalently, with time in culture. To investigate this possibility, an instantaneous proliferation rate (IPR) can be derived. The IPR is the number of doublings per day calculated from the exponential curve that best fits the proliferation data for the time point in question and the two points immediately adjacent to it. Conceptually, this is similar to the derivative with respect to time of the proliferation function. As this redistribution effect was unexpected, and hence not considered in the experimental design, the conditions and sampling intervals

used were not optimal for the assessment of IPR with a high order of precision. Nevertheless, the data suffice to determine if the correlation implied exists. This is demonstrated for the exemplars NZM4 and NZM6 {Figure 7-5}. In NZM4, where a large spontaneous redistribution occurred, the IPR decreased with time in culture (null hypothesis: slope = 0;  $P = 0.08$ ; 95% confidence level), while in NZM6 where this effect is minor, if present at all, the IPR does not vary significantly with time in culture (null hypothesis: slope = 0;  $P=0.51$ ; 95% confidence level). This is consistent with a common cause for the changed phasing and proliferation rate, or a causal linkage between them.

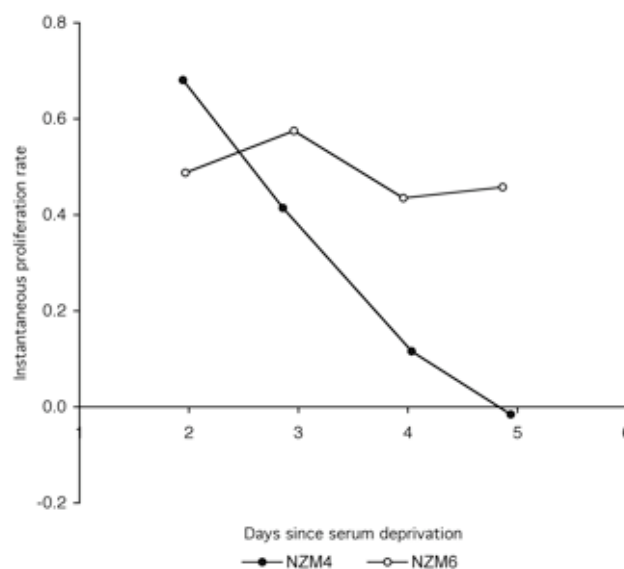
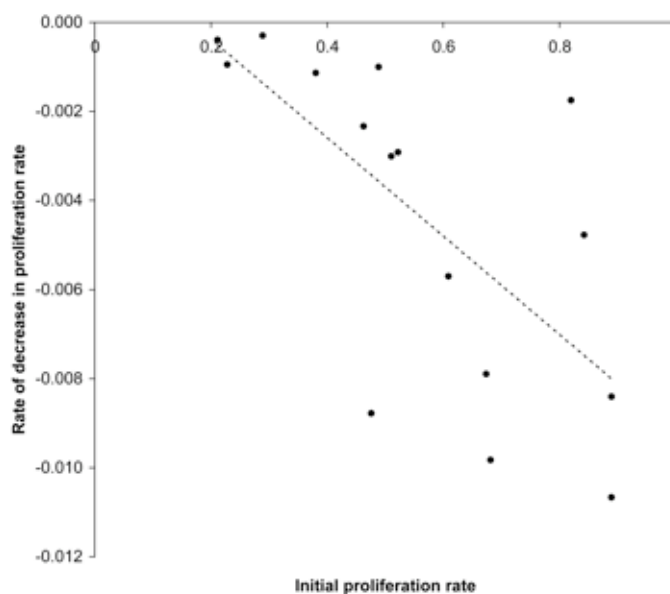


Figure 7-5: IPR as a function of time

When a similar analysis for all cell-lines is performed, an additional pattern can be recognised {Figure 7-6}. There is a correlation between absolute initial proliferation rate and the rate at which this declines with time. Linear regression bears this out, yielding  $R^2 = 0.46$ . Phrased another way, the more rapidly a cell-line proliferates when unconstrained, the more rapidly this rate slows when it is deprived of serum. The significance of this association is unclear.



Each point represents the first measurable IPR and its rate of decrease over time for a single cell-line.

Figure 7-6: Rate of IPR decrease vs initial rate

The relationship between IPR and cell-cycle phasing can be further explored. An analysis of the consolidated data for all cell-lines and time points is presented

in Figure 7-7. While the correlation coefficients are modest, they do suggest that an increase in  $G_1$ -phase is associated with a reduction in growth rate, while increases in either S or  $G_2/M$  are associated with accelerated growth. Surprisingly, while the highest correlation might have been expected to be with S-phase, it is in fact the  $G_2/M$  contribution that is the best indicator of instantaneous proliferation rate. This may be because whatever the final checkpoint is before mitosis becomes inevitable, it must necessarily be in this phase.

Earlier work<sup>180</sup> characterising the NZM4 cell-line provides a basis for understanding the observations made here. This line is particularly sensitive to the inhibitory effects of TGFβ1, a characteristic shared by many human melanoma cell-lines<sup>1359</sup>, and TGFβ1-treated cells were found by flow cytometry to arrest in G<sub>1</sub><sup>180</sup>. It was also shown that conditioned medium from NZM4 cultures contained a substance which was growth-inhibitory with respect to freshly seeded cultures.

Somewhat paradoxically, the conditioned medium also inhibited NZM7 growth, a cell-line known to be resistant to TGFβ1. This is explicable considering the existence of multiple TGFβ isoforms.

TGFβ2 and TGFβ3 are widely expressed in human melanomas, particularly in advanced cases<sup>1359</sup>. While TGFβ1 was excluded from playing a part in density-dependent arrest of NZM4 through the use of a neutralising antibody, this technique was not extended to the treatment of conditioned medium. One plausible cause of the spontaneous cell-cycle redistribution seen in NZM4, and conceivably other cell-lines, is therefore the production of one or more TGFβ isoforms, resulting in autocrine growth inhibition. It is possible however that an entirely different cytokine is involved, and only further investigation could clarify the situation. In this regard, the discussion of MIA below is of some relevance. [This finding disproves the widely held belief that cell cultures invariably grow exponentially until a plateau is reached.](#) This basic tendency may be modified by the production of stimulatory or inhibitory autocrine factors that may accumulate during culture.

### Cell-cycle phasing in the confluent control cultures

The commonly observed phenomenon that human cells in culture grow to form a confluent monolayer and then cease proliferation has been described as 'density-dependent arrest', or 'confluent arrest'. One finding of the work cited earlier<sup>180</sup> was that confluence is not always sufficient to cause cell-cycle arrest, since replacement of the medium of NZM4 and NZM7 cultures which had been grown to post-confluence resulted in a temporary resurgence of proliferation. The results just described extend this by showing that confluence, as well as not always being sufficient to cause arrest, is not always necessary either. If it were, then no departure from exponential growth would be seen prior to its advent. This is in distinct contrast to the progressive slowing of proliferation seen here. Again, NZM4 provides a relevant example. Examination of the growth curve {Figure 7-3}, which demonstrates a clear plateau at the time the cultures were becoming confluent, coupled with the low S-phase

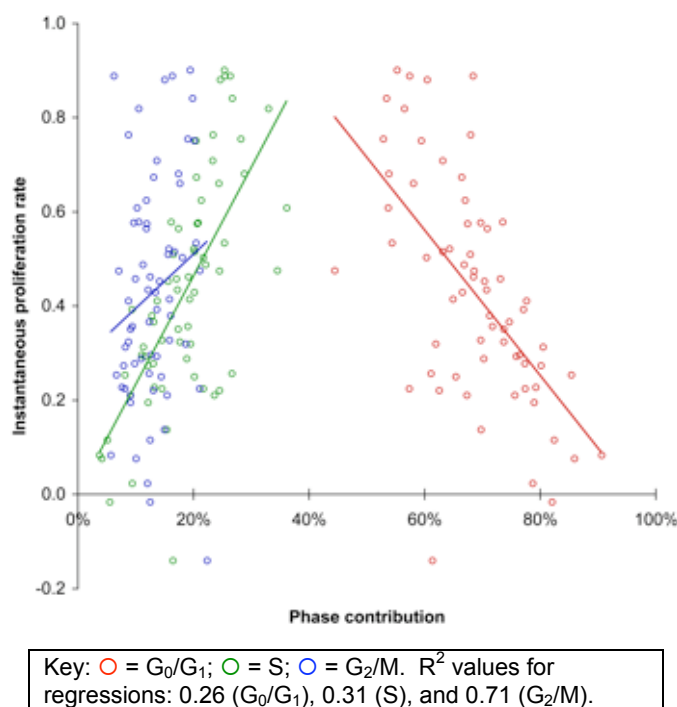


Figure 7-7: IPR vs cell-cycle phase contribution

fraction seen during this time, suggest the existence of a confluence-dependent arrest mechanism in these cells. That this is not the case becomes clear when it is appreciated that both the decline in S-phase and the departure from exponential growth began immediately after the establishment of the cultures. Clearly, **confluence, per se, is not always necessary to cause a cell-cycle arrest after time in culture, and the operation of an autocrine inhibitor may produce superficially indistinguishable results.**

**The effect of serum-deprivation on proliferation rate**

Cursory examination of Figure 7-3 reveals that **serum-deprivation has an immediate and drastic effect on net proliferation rate for all cell-lines studied.** This fulfils the first experimental objective. The magnitude of this effect can be quantitated by comparing the IPRs of control and deprived cultures. From the equation of the exponential line of best fit for each series, the in vitro doubling time (tD) can be calculated, and the reciprocal of this is the proliferation rate (R). The retardation quotient (Q) is then derived according to Equation 7-1.

$$Q = 1 - \frac{R_{Deprived}}{R_{Control}}$$

**Equation 7-1: Derivation of retardation quotient (Q)**

A Q value of zero indicates that removal of serum has no effect on proliferation rate, and a value of 1 (100%), that it completely inhibits proliferation. Calculated values for tD, R and Q are given in Table 7-1.

Cell-line	Control tD (h)	R <sub>Control</sub> (doublings/d)	Deprived tD (h)	R <sub>Deprived</sub> (doublings/d)	Q (%)
NZM1	54	0.4442	362	0.0663	85
NZM2	62	0.3864	-2078	-0.0116	103
NZM3	42	0.5743	80	0.3013	48
NZM4	35	0.6811	541	0.0443	93
NZM5	29	0.8197	100	0.2400	71
NZM6	51	0.4713	133	0.1807	62
NZM7.2	29	0.8245	45	0.5395	35
NZM7.4	32	0.7452	71	0.3398	54
NZM9	74	0.3262	248	0.0969	70
NZM10	46	0.5274	195	0.1233	77
NZM10.1	99	0.2433	1391	0.0172	93
NZM11	90	0.2675	661	0.0363	86
NZM12	28	0.8633	217	0.1106	87
NZM13	47	0.5129	174	0.1381	73
NZM14	73	0.3306	356	0.0674	80
NZM15	39	0.6118	181	0.1326	78

**Table 7-1: Proliferation rates with and without serum**

While a marked effect was evident for all cell-lines, there was variability in Q {Figure 7-8}. Its distribution had a coefficient of variation of 24%, and was skewed toward higher Q values, with three times as many cell-lines having values above 70% as below. With the exception of NZM7.2, all values fell within 1.6 s of the mean. NZM7.2, an outlier at m - 2.2 s, is worthy of future investigation.

Over the entire duration of the experiment, only NZM3, NZM5, NZM7.2, NZM7.4, and NZM9 were able to support a single population doubling in the absence of serum, and no cell-line



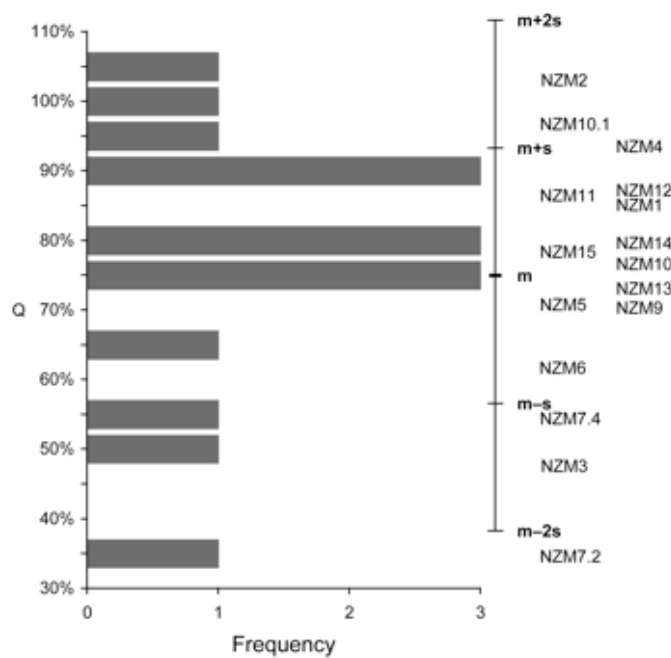
doubled twice. The last time point for the NZM10 experiment is noteworthy for the extremely wide variability among the replicate cultures, with one having achieved a growth comparable to the controls. This may reflect a technical error, or it may be an indication that in one culture, a variant arose with increased proliferation rate in the absence of serum. In contrast to the general restriction of growth seen in the serum-deprived cultures, all of the controls doubled at least once, the mean doubling time being 2.2 d.

For net proliferation rate to change, the rate of cell division, the rate of cell death, or both must change. The objectives of this experiment focus on determining if it is the former that takes place, and if so, if this is due to a cell-cycle arrest, in particular, in  $G_1$ . To determine if cell-cycle transit time increased without altering phase partitioning would require a different approach. Pulse-labelling of proliferating cultures with bromodeoxyuridine (BrdU) would allow a cohort of cells to be followed from S-phase by flow cytometry [A-6]. Blockade of passage through mitosis with an agent such as paclitaxel would provide complementary data. To determine if it was the rate of cell death that had altered, perhaps due to the removal of survival factors, studies into the activation of apoptosis, perhaps by end-labelling of cleaved DNA with terminal deoxynucleotidyl transferase and flow cytometric assessment, would be an appropriate experimental approach.

### The effect of serum-deprivation on cell-cycle phasing

The second experimental objective calls for the determination of the effect of serum-deprivation on cell-cycle phasing. To facilitate this, the flow cytometry results given as bar-charts in Figure 7-3, are presented again in a different format [Figure 7-9].

Unfortunately, the spontaneous departure from exponential growth seen in control cultures for some cell-lines defeats the traditional approach of reporting results as a function of the control value, since the controls themselves are subject to variation during the experiment. In effect, the control culture at the time of serum-deprivation, and the samples from the early time points for serum-deprived cultures must serve as controls. The analysis undertaken here then is to compare the cell-cycle phasing changes seen with lengthening deprivation, with an emphasis on any early effects. To systematise this, each cell-line can be assigned a response type based



Q values are grouped in 5% bins. Cell-line names are placed corresponding to their respective Q value; their horizontal placement is arbitrary. A mean and standard deviation scale is given.

Figure 7-8: Distribution of Q

## Human metastatic melanoma in vitro

on the changes that occur in each cell-cycle phase {Table 7-2}. This assignment is necessarily subjective, given the unknown importance of minor deviations within the data.

Excluding the possible response types that were not seen, a further subjective categorisation can be made into classes. In Class 0 (type 0), no alteration is seen. In Class 1 (types +2, +3, and +5),  $G_1$  alone increases. In Class 2 (types -6, -5, and +4), an increase in  $G_2/M$ , and possibly  $G_1$ , is seen. In Class 3 (type -2), the primary characteristic is an increase in S-phase, and possibly  $G_2/M$ -phases.

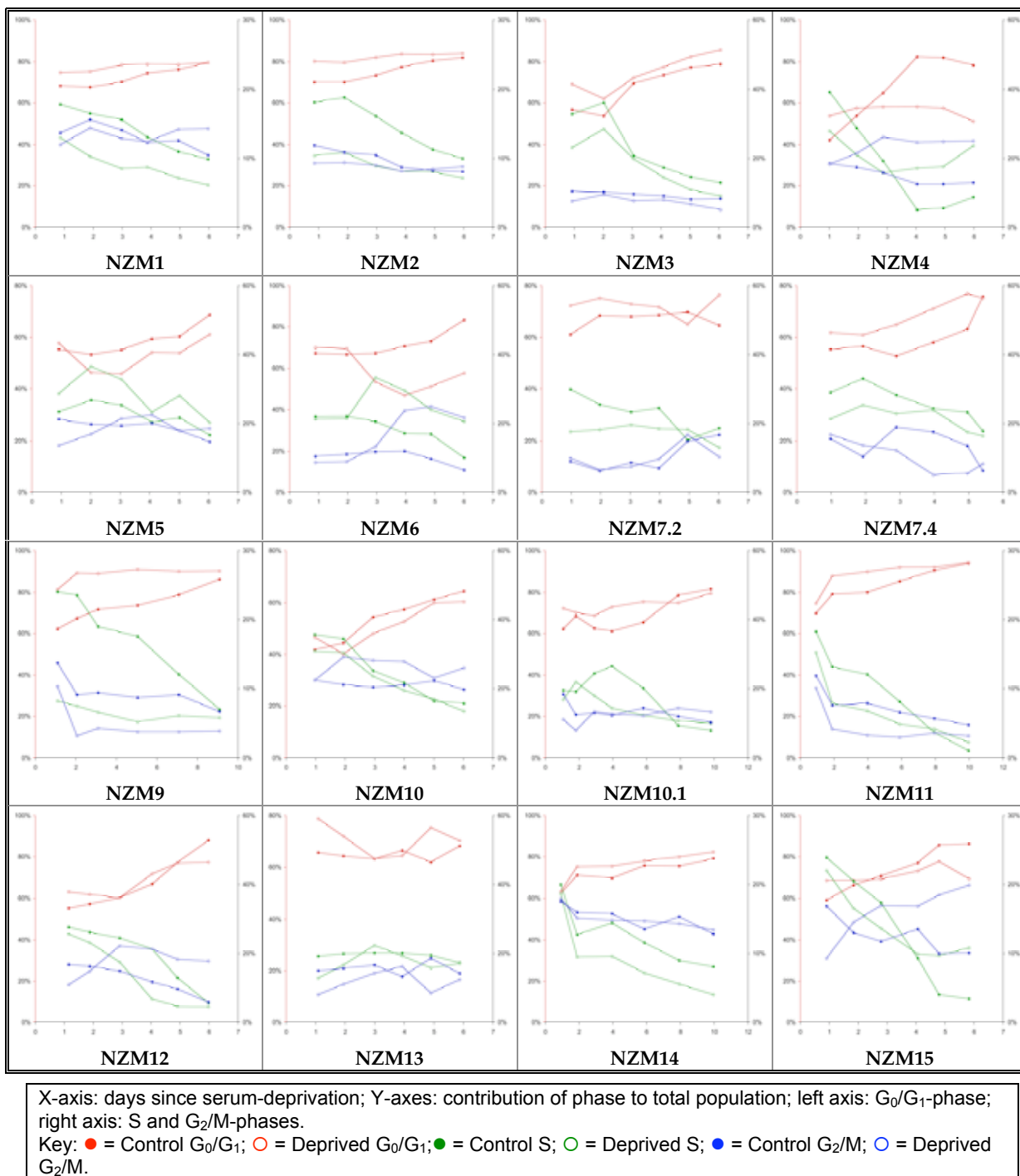


Figure 7-9: Effect of serum-deprivation on cell-cycle phasing



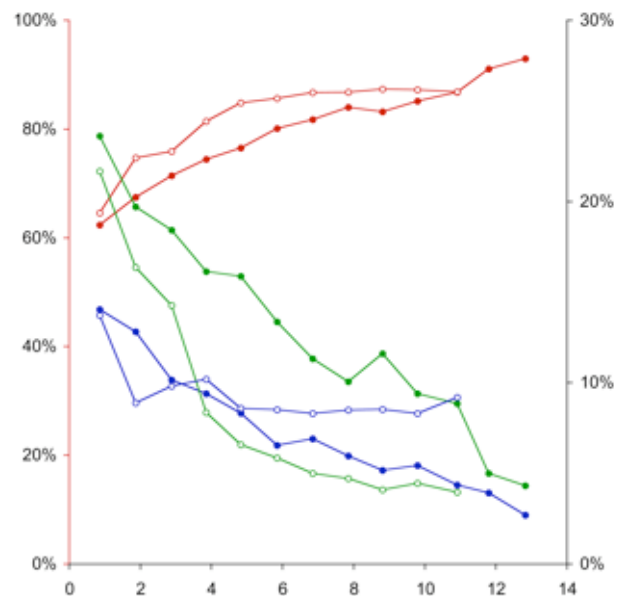
Response type	$\Delta G_1$	$\Delta S$	$\Delta G_2/M$	NZM cell-lines
-6	-	-	+	NZM4
-5	-	0	+	NZM15
-4	-	+	-	nil
-3	-	+	0	nil
-2	-	+	+	NZM5, NZM6, NZM13
-1	0	-	+	nil
0	0	0	0	NZM7.2
+1	0	+	-	nil
+2	+	-	-	NZM1, NZM2, NZM3, NZM7.4, NZM11
+3	+	-	0	NZM10.1, NZM14
+4	+	-	+	NZM10, NZM12
+5	+	0	-	NZM9
+6	+	+	-	nil

This table characterises the response to serum-deprivation exhibited by the cell-lines. Different response types are grouped into classes as described in the text. Key to highlighting: **Class 1**; **Class 2**; **Class 3**.

Table 7-2: Serum-deprivation response types

**Class 1: The classical  $G_1$  arrest**

This class conforms to the predictions made for the effect of a functional serum-sensitive restriction point, with NZM2 being the exemplar. The experiment was repeated for this cell-line over a longer period from a lower starting cell density with broadly concordant results (Figure 7-10). With the extended time line however a further facet emerged. Beyond d5, the  $G_2/M$  fraction remained essentially static, but at a higher level than seen in the controls. The continued growth of the  $G_1$ -phase at the expense of S implies that while passage through  $G_2/M$  was occurring, it was at a reduced rate. Possibly, the  $G_2/M$  control point better demonstrated in the Class 2 response, described below, was operative here, but subservient to the  $G_1$  arrest. It is also possible that cells were being selectively lost from S or  $G_2/M$  phases.



X-axis: days since serum-deprivation.  
 Y-axes: contribution of phase to total population; left axis:  $G_0/G_1$ -phase; right axis: S and  $G_2/M$ -phases.  
 Key: ● = Control  $G_0/G_1$ ; ○ = Deprived  $G_0/G_1$ ; ● = Control S; ○ = Deprived S; ● = Control  $G_2/M$ ; ○ = Deprived  $G_2/M$ .

Figure 7-10: Results for NZM2 replication

The presence of a functional serum-sensitive  $G_1$  checkpoint in many melanoma cell-lines proves that either the cyclin D-CDK4-pRB-E2F subsystem is not defective in all melanomas, or it does not mediate the putative  $G_1$  restriction point. Either possibility could be considered a novel finding. Further clarification of this must await the presentation of the results of the molecular characterisation of these cell-lines, the subject of later chapters.

7: Serum-deprivation

**Class 2: A serum-sensitive G<sub>2</sub>/M checkpoint**

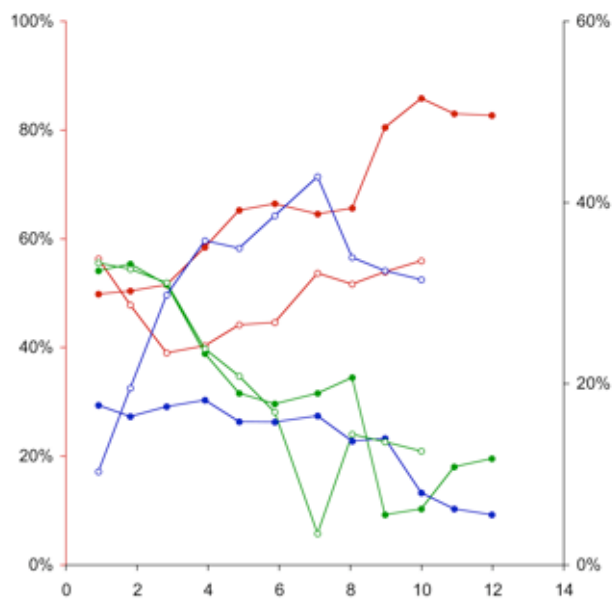
As NZM2 was selected as exemplar for Class 1 and re-examined experimentally, so was NZM12 selected for Class 2. The results for the replication are given in Figure 7–11. NZM12’s response to serum-deprivation can be divided into three stages.

In the first, running from inception to about d3, G<sub>1</sub> and S fell while G<sub>2</sub>/M rose dramatically. The fall in G<sub>1</sub> implies that progression to S was still possible, and when coupled with the rise in G<sub>2</sub>/M component, strongly suggests that transit through these latter phases was restricted.

In the second stage, from d3 to d7, G<sub>1</sub> began to climb, while the increase in G<sub>2</sub>/M continued to its maximum, but at a reduced rate. The growth in G<sub>1</sub> implies that no absolute restriction to passage through mitosis existed, confirmed by the continued climb in cell numbers [Figure 7–12]. The decline in S phase was a flow-on effect of reduced entry to G<sub>1</sub> caused by the restriction in G<sub>2</sub>/M.

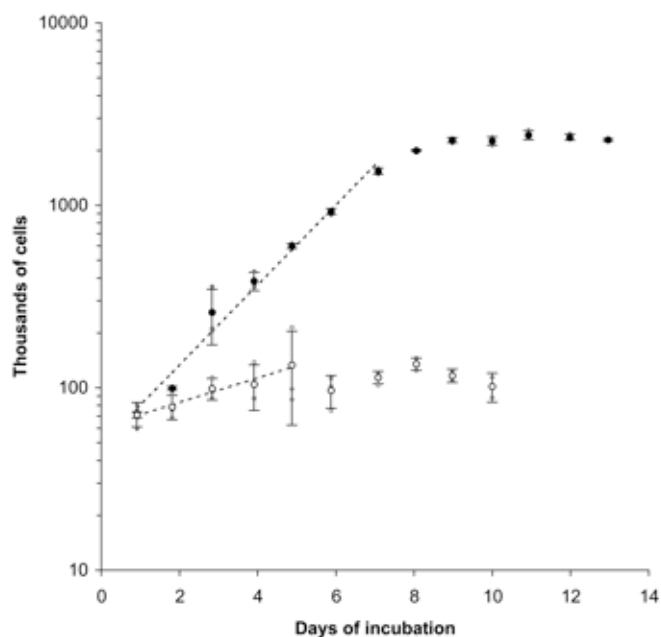
In the third stage, beyond d7, G<sub>2</sub>/M declined from its peak, while S and G<sub>1</sub> increased. Superficially, this would imply that cells were passing both into, and out of G<sub>1</sub>. However, by this late stage of culture without serum, cell numbers had begun to decline. Here too, selective loss of G<sub>2</sub>/M cells may have contributed to the alteration in cell-cycle phasing seen.

G<sub>2</sub> arrest due to DNA damage<sup>965</sup> and microtubule malformation<sup>873</sup> are well documented, and an association with cell size is known in yeast<sup>S1283</sup>. There is also a small body of literature



X-axis: days since serum-deprivation.  
 Y-axes: contribution of phase to total population; left axis: G<sub>0</sub>/G<sub>1</sub>-phase; right axis: S and G<sub>2</sub>/M-phases.  
 Key: ● = Control G<sub>0</sub>/G<sub>1</sub>; ○ = Deprived G<sub>0</sub>/G<sub>1</sub>; ● = Control S; ○ = Deprived S; ● = Control G<sub>2</sub>/M; ○ = Deprived G<sub>2</sub>/M.

**Figure 7–11: Results for NZM12 replication**



Key: ● = with serum; ○ = serum-deprived.  
 See Figure 7–2 for further information on symbols.

**Figure 7–12: NZM12 growth curve**



et al.<sup>S1498</sup> reported a study of temperature-sensitive rat fibroblast cells where an arrest was seen in either  $G_1$  or  $G_2$  at the non-permissive temperature that could be relieved by the addition of fresh serum. They concluded, *inter alia*, that 'the commitment to DNA synthesis is not necessarily a commitment to cell division.' Kinzel et al.<sup>682</sup> reported that HeLa cells were inhibited by EGF in a receptor-dependent manner, and that the basis for this was a transient inhibition of the  $G_2$ -M transition. Later work showed that this process involved the modulation of CDC2 activity<sup>72</sup> via CDC25C<sup>71</sup>. Another growth factor with activity in  $G_2$  is FGF2, able to cause arrest in SK-N-MC neuroepithelioma cells<sup>1243</sup>. On a broader front, cAMP, a commonly activated second-messenger molecule, has been implicated in the  $G_2$  arrest seen in mouse macrophages<sup>S729</sup>. Lazebnik et al.<sup>755</sup> discovered that the addition of ascites fluid to the medium of Ehrlich ascites carcinoma cells inhibited their growth by causing a block in progression through  $G_2$ . In this case however, the addition of serum could not relieve the arrest. They postulated 'that ascites fluid contains a factor(s) which potently interrupts the  $G_2$ -phase of the cell-cycle'.

Of significance here is the work of Bogdahn et al.<sup>109</sup>, who isolated three melanoma supernatant fractions with growth-suppressive properties against melanoma and glioblastoma, but not against normal fibroblasts. The protein responsible, MIA (melanoma inhibitory activity), is an autocrine factor produced by many melanomas, and normally by cartilage. It was found that inhibition of sensitive cells required exposure to MIA at the  $G_1$ -S boundary, but that the effect was a prolongation of S-phase and an arrest in  $G_2$ <sup>1417</sup>. After the identification of the active components of some fractions<sup>38</sup>, MIA was cloned in 1994<sup>103</sup>, and assigned to 19q13.32-q13.33 by fluorescence in situ hybridisation<sup>700</sup>. The primary product is a 131 amino acid precursor that gives rise to a mature protein of 107 amino acids and molecular weight of ~11 kD. The crystal structure for MIA was solved in 2001<sup>808</sup>. Interestingly, it contains an SH3 domain, the first secreted protein known to contain this. However, it is thought that due to changes in otherwise conserved residues, this domain is unlikely to bind polyproline helices. Little is yet known about the control of expression of this gene, its role in normal chondrocytes, or what part it plays in melanoma. There does appear to be a correlation between expression and metastasis<sup>121</sup> and the significance of this is under active investigation. Yet to be addressed is the question of whether MIA is playing a role in the NZM cell-lines. It may help explain the spontaneous reduction in proliferation rate seen in the control cultures.

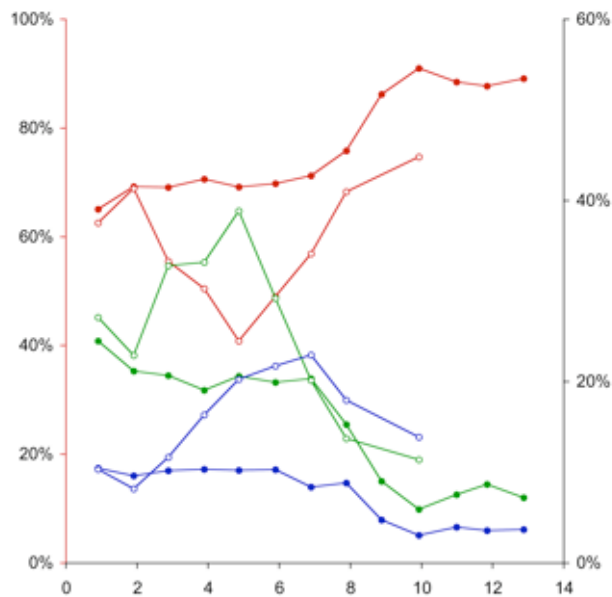
While growth factor inhibition in  $G_2$  has received some attention, the existence of a serum dependency in  $G_2$  or M-phase is all but unreported in the literature. A relevant paper suggests that IGF1 may be necessary for  $G_2$  progression in the response of mouse uterine cells to the mitogen oestradiol<sup>S14</sup>.

The existence of a Class 2 response, wherein there is restriction of passage of cells through  $G_2$  in response to serum-deprivation, is a significant discovery in its own right. Furthermore, it directly contradicts the notion of a restriction point in  $G_1$  being the point of commitment to divide.

**Class 3: Disinhibition at the G<sub>1</sub>-S boundary**

If the existence of a Class 2 response was surprising, that of Class 3 was even more so. In this case, NZM6 was selected as the exemplar and the experiment repeated {Figure 7–13}.

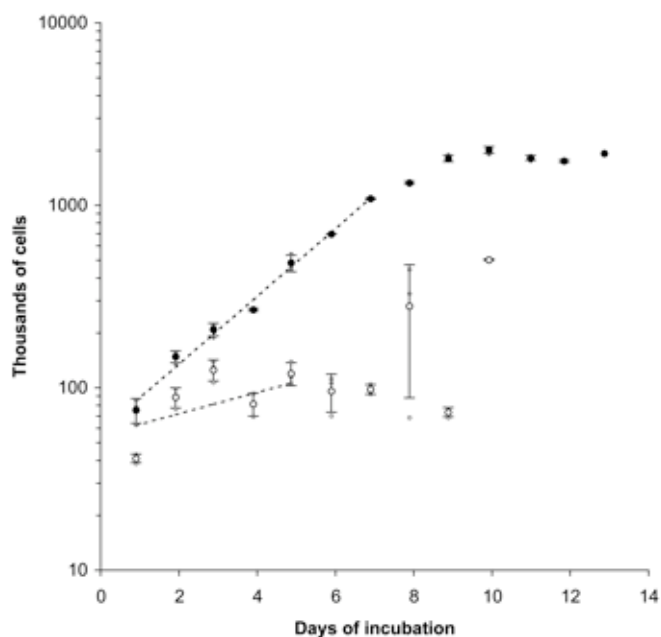
The existence and magnitude of the pulse of cells leaving G<sub>1</sub> upon serum-deprivation was quite evident. One reason for the time line extension in the replicate experiment was to determine if this cohort of cells would continue to pass through G<sub>2</sub> and mitosis. It seems that they did, as there was clear evidence of a continued decline of G<sub>2</sub>/M associated with an increase in G<sub>1</sub> beginning at d7. The experiment would have to be extended further to determine if they continued to cycle or arrested in G<sub>1</sub>.



X-axis: days since serum-deprivation.  
 Y-axes: contribution of phase to total population; left axis: G<sub>0</sub>/G<sub>1</sub>-phase; right axis: S and G<sub>2</sub>/M-phases.  
 Key: ● = Control G<sub>0</sub>/G<sub>1</sub>; ○ = Deprived G<sub>0</sub>/G<sub>1</sub>; ● = Control S; ○ = Deprived S; ● = Control G<sub>2</sub>/M; ○ = Deprived G<sub>2</sub>/M.

**Figure 7–13: Results for NZM6 replication**

Some insight is available from the growth curve for the replication {Figure 7–14}. Data for d8 showed wide dispersion, and it was clear from the examination of the replicate cultures that one of three was not proliferating, while the other two appeared to be thriving. D9 saw all three cultures in decline, while d10 saw all three growing actively and concordantly. The inference is that a minor component present in the original population has the ability to thrive in the absence of serum, while the major component cannot. In effect, serum reduction has acted as a selection mechanism. While it was clear that this was occurring, the decision was made to continue pooling cultures prior to flow cytometry analysis in accordance with the experimental protocol, principally because there would be too few cells for analysis from a single culture. Indeed, there were too few cells to allow analysis



Key: ● = with serum; ○ = serum-deprived.  
 See Figure 7–2 for further information on symbols.

**Figure 7–14: NZM6 growth curve**



of the pooled serum-deprived cultures from d9. Among the implications of such selection having occurred is the likelihood that the cells would continue to cycle, but also the raising of doubt as to exactly what the subject of analysis would actually be at late time points in an experiment extended even further.

The basis for the stimulus to entry of S-phase is unknown. Most probably, fetal calf serum contains a growth factor that causes a partial  $G_1$  arrest in some melanoma cell-lines. It is unlikely to be TGF $\beta$ 1 since NZM4, known to be inhibited by this, demonstrated a marked reduction in S-phase in response to serum-deprivation.

Interestingly, all of the cell-lines with Q values below the mean, with the exception of NZM9, displayed initial increases in S-phase upon serum-deprivation. Conversely, all with Q values above the mean, with the exception of NZM10.1, displayed an initial decrease. The relevance of this is unknown.

Despite this release of cells from  $G_0/G_1$ , the net proliferation rate was still constrained. The nature of this constraint is not clear from the data presented here: retardation in  $G_1$ ,  $G_2$ , or both, could have been occurring. It seems likely that it was the rate of progression that controlled proliferation, rather than the imposition of an impediment to progression at any point. It is also possible that the alternative processes mentioned above, such as increased incidence of apoptosis, may have been operative.

## 7.6 Summary

While not addressing the molecular integrity of pRB-mediated control of proliferation in melanoma cell-lines, this work effectively excludes the removal of growth factor dependence as the functional target of the reported alterations to this subsystem. The presence of a previously unsuspected serum-sensitive control point in  $G_2/M$  has been established. This casts doubt on the existence, or universality, of a 'restriction point' in  $G_1$  as a point of commitment to cellular division. The results presented here are consistent with the limited literature on the subject. The reduction in S-phase content seen upon serum withdrawal in canine TLM1 melanoma cells<sup>S901</sup> corresponds to a Class 1 response. The failure of MeWo human melanoma cells to arrest in  $G_0$  upon serum withdrawal<sup>1142</sup> corresponds to either a Class 2 or Class 3 response. The cell-cycle 'freeze' seen in murine B16F10 cells<sup>S1102</sup> was not observed.

Nevertheless, the association between melanoma and pRB and its functional associates is well supported, and further characterisation of these molecules is warranted if this is to be explained. The following chapters describe investigations into the status of some key molecular components of the pRB subsystem in the NZM cell-lines.

# The effect of serum-deprivation (V3)

---

## 7.7 Clarification of the existing material

### Experimental procedure

To achieve the objectives for this chapter required the measurement of growth rate and cell-cycle phase distribution as a function of time, serum concentration, and cell-line. These were addressed by cell counts and flow cytometry of cultures harvested at multiple time points after serum deprivation. Given the likely growth rates of the cell-lines, the effects were expected to take several days to appear.

A pilot investigation was performed on a subset of cell-lines to establish the feasibility of the proposed method, with NZM5, NZM9, and NZM10.1 being selected as representing a broad range of growth rates. For each cell-line, 16 P60 tissue culture plates were each seeded with  $\sim 5 \times 10^5$  cells in 5 mL of medium and incubated. After 1 d, the medium of half of the plates was replaced with medium containing 0.1% v/v FCS, rather than the usual 10% v/v. Daily thereafter for 4 d, duplicate plates for control and serum-deprived cultures were harvested with retention of the culture supernatant, and the cell number was assessed by electronic particle counter. Replicates were pooled, fixed in methanol/PBS, and subsequently analysed for DNA content by flow cytometry. The resulting data were processed to determine the contribution of each distinguishable cell-cycle phase to the overall DNA fluorescence intensity distribution through use of Modfit LT software.

This experiment was not reported in V1, but from the results it was concluded that a time course of 7–10 d would be needed to yield meaningful data; that seeding at a lower density would be needed to avoid problems of over-growth at late time points; and that within-experiment replication would ensure adequate cell numbers for flow cytometric analysis, while simultaneously improving the quality of the data obtained. The main investigation encompassing the entire NZM panel was implemented based on these conclusions, and was reported in V1. A single experiment was performed for each cell-line in which control and serum-deprived cultures were each sampled in quadruplicate at each time point, and cell counts obtained for each replicate individually, as described [7.3] and illustrated in Figure 7–2. Within-treatment quadruplicate samples were pooled as described [7.3] to provide sufficient cells for flow cytometric analysis, essential at early time points in both arms of the experiment, and at later time points in the cell-lines deprived of serum, where numbers remained low, or even declined. The entire experiment was not repeated owing primarily to its very substantial scale, and secondarily to the high degree of replication already present within the experiment.

The analysis of the results of these experiments led to the identification of three response classes, and a further set of experiments seeking to confirm this was performed using exemplar cell-lines from each response class: NZM2, NZM6, and NZM12. These experiments were described in V1. The Class 3 response, modelled by NZM6, involved a release of cells from  $G_1$  upon serum withdrawal, a very interesting counter-intuitive result. The question of the fate of



this cohort of cells arose, and in order that more information could be gleaned about this during the confirmatory experiment, a longer time course was required. To achieve that without risking distorting cell-cycle partitioning by high cell density effects in control cultures late in the time course, either a lower starting cell density, or a much larger scale experiment was necessary. The former option was selected, and cultures were seeded at  $\sim 5 \times 10^4$  cells/5 mL, rather than  $\sim 2.5 \times 10^5$  cells/5 mL, as was the case in the survey of the entire NZM panel.

This was not a direct replication of the comprehensive experiment even for these cell-lines as the experimental conditions were different with respect to seeding density, duration, and within-experiment replication. However, the concordance of the results obtained, and illustrated below for the case of NZM6, strongly indicate that these variables did not affect the key observations made, and so, at least for the exemplar cell-lines investigated, the findings with respect to the effects of serum deprivation were reproducible.

### Concordance of results

The growth data obtained for the serum-deprived NZM6 cultures on the two occasions (Figure 7–15) are far from ideal, and superficially may appear disparate.

The high variability within replicate groups in many cases is unfortunate, and may reflect the technical difficulty involved in obtaining accurate cell counts for cultures under stress by electronic particle counter. Since these can contain cells with a wide range of sizes, and also subcellular debris, the setting of particle volumes to be counted electronically is somewhat arbitrary. However, as discussed in the original text {7–18}, the variability seen may be, at least in part, a true portrayal of an inherent variability among the replicate cultures, as differences in cell density among replicates were visible microscopically. This variability has resulted in the presence of data outliers, particularly for two of the final three time points for the confirmatory experiment.

The disparity that immediately presents itself upon examination of Figure 7–15 is the difference in the absolute number of cells, but this is due simply to the difference in seeding density and can be discounted. A better comparison of the results of the two experiments is possible if the datasets are separately scaled and presented with the outliers omitted (Figure 7–16). When the overall pattern and the relative changes and trends displayed in each dataset are compared, the differences are not particularly remarkable. In essence, both rise to plateaux by day three and

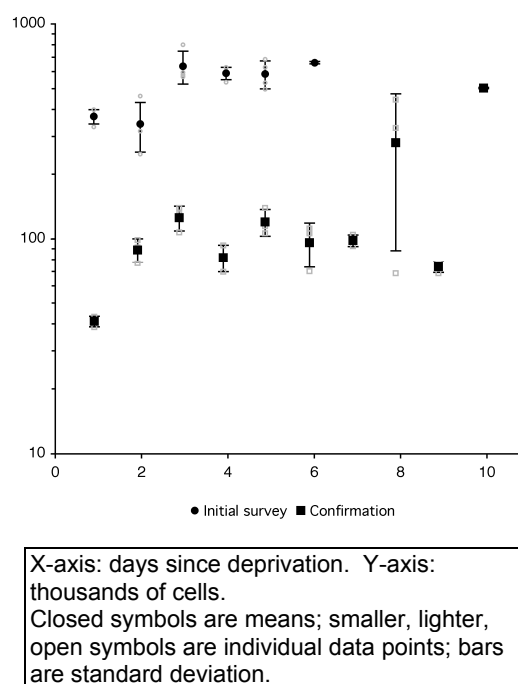


Figure 7–15: NZM6 serum-deprived growth concordance

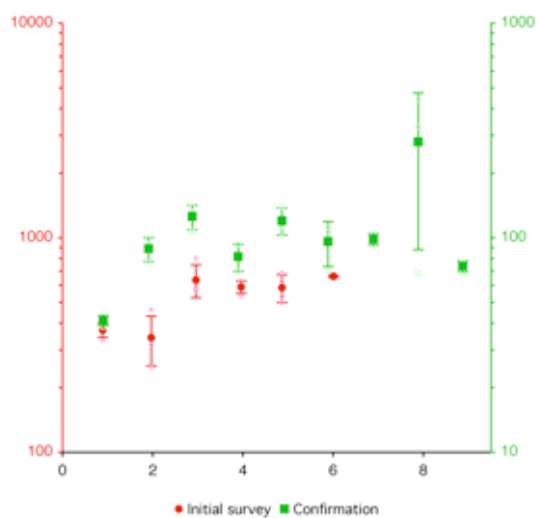
## Human metastatic melanoma in vitro

remain there or decline. While imperfect, the data from both experiments are concordant in demonstrating that serum deprivation severely constrains NZM6 proliferation.

Turning now to the results for the assessment of the effect of serum deprivation on cell-cycle phasing, the high degree of concordance between the two experiments is immediately obvious when both sets of data are compared directly (Figure 7–17). The overall pattern is very clear: a cohort of cells is released from  $G_1$  in response to serum deprivation, passes through S, and into  $G_2/M$ ; the only difference is in the timing. This difference is likely to be a consequence of the difference in seeding density. Cellular growth can be accelerated through interaction among cells by juxtacrine and autocrine mechanisms. If this is occurring in NZM6, higher cell density will result in more direct interactions among cells, augmenting juxtacrine effects. If a soluble factor is involved, at higher densities more of it will be secreted into the medium. While the amount of growth factor per cell will not be different, its concentration will be since the volume of medium is the same in both cases. The higher the concentration is, the greater the chance of interaction between the factor and a receptive cell, again stimulating growth of high density cultures more than low.

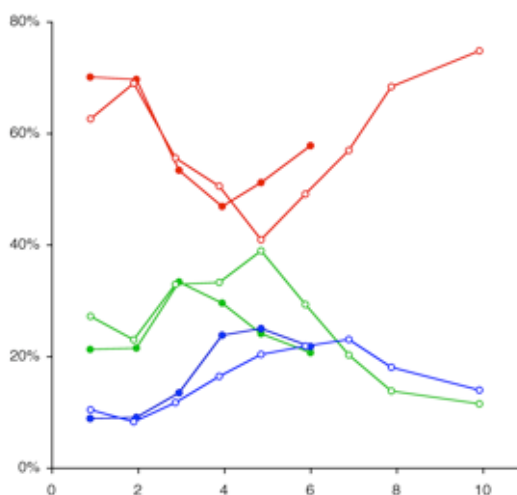
Interestingly, in some cell-lines exactly the opposite effect was revealed in that the existence of a growth suppressive effect was

found among control cultures {See '*Spontaneous phasing changes in many control cultures*' in Section 7.5}. Notably, this inhibitory effect was absent from NZM6 (Figure 7–4), leaving the way clear for the hypothesised stimulatory effect to operate. The subtle difference in timing revealed here indicates new avenues for exploration: a series of experiments tracking cell-cycle phasing for cultures seeded at a range of densities would be expected to show a trend in stimulation; and if a soluble factor is involved, conditioned medium from a high density culture would be expected to accelerate the growth of a low density culture. While the clear



X-axis: days since deprivation.  
Y-axes: thousands of cells; left axis for initial survey; right axis for confirmation.  
Closed symbols are means; smaller, lighter, open symbols are individual data points; bars are standard deviation.

Figure 7–16: NZM6 serum-deprived growth concordance (scaled)



X-axis: days since deprivation.  
Y-axis: cell-cycle phase proportion.  
Closed symbols: results from initial survey.  
Open symbols: results from confirmation.  
Red =  $G_0/G_1$ ; green = S; blue =  $G_2/M$ .

Figure 7–17: NZM6 serum-deprived phasing concordance



similarities in the two results attest to the reliability and reproducibility of the method, the minor differences present between them attest to its sensitivity.

### **Differing plateau densities**

Markedly different plateau cell densities were observed among the cell-lines. The NZM cell-lines exhibit a wide spectrum of morphological and physiological characteristics, to the extent that many are immediately distinguishable in culture at a glance {See '*Idiosyncrasies of NZM cell-lines in culture*' beginning on page 3–3}. One feature that is highly variable among the cell-lines is cell size, with NZM5 being minute, and NZM10 capable of producing enormous cells, so to observe differences in confluent density was unsurprising. While perhaps significant for the study of cell size regulation and contact interactions, it is less so in the context of a discussion of serum deprivation, particularly since the serum-deprived cultures invariably arrested or died well before reaching high density. Nevertheless, observations that may have some bearing on this were made, specifically, the serendipitous discovery of a spontaneous cell-cycle phase redistribution and increasing departure from exponential growth occurring in some control cultures beginning immediately upon seeding {See '*Spontaneous phasing changes in many control cultures*' in Section 7.5}. This brings into question whether arrest at high density is a function of confluence at all, or instead, is merely the result of the production of an inhibitory autocrine factor {See '*Cell-cycle phasing in the confluent control cultures*' in Section 7.5}.

## **7.8 Extension of the existing material**

### **Rationale**

To further elucidate the effect of serum-deprivation on human metastatic melanoma cell-lines and to seek to confirm the earlier findings, the exemplar cell-lines exhibiting the different classes of response to serum-deprivation were again examined to determine the effect this deprivation has on proliferation and cell-cycle phasing.

### **Methods**

To explore this comprehensively, a large-scale extended time course experiment was performed, but it was subsequently found that the NZM12 cells used were both of questionable identity {8–26}, and were from mycoplasma-contaminated stock {Method 33}, rendering the results for this cell-line invalid. In contrast, the stocks from which the NZM2 and NZM6 cells were drawn were subsequently found to be negative for mycoplasma and were confirmed as to identity {See '*Discrimination among the cell-lines*' on page 8–35}. While the study is incomplete for lack of valid NZM12 data, the data for NZM2 and NZM6 are probably valid.

The problem of mycoplasma contamination was addressed by recovering early passage cells for all lines, testing them for mycoplasma contamination, treating them with ciprofloxacin {Method 34} regardless of their status, and using the resultant stock for all future experiments. Given the loss of the NZM12 data, this included a further investigation of serum-deprivation in the exemplar cell-lines on a more modest scale, one similar to that employed in the initial V1 survey of the complete NZM panel. The methods employed for this were essentially as described in the original chapter, and these are repeated below with changes noted.

For each of the exemplar cell-lines, 60 P60 tissue culture plates were each seeded with  $\sim 2.5 \times 10^5$  cells in 5 mL of medium and incubated. After 1 d, by which time the cells had become adherent, the medium of half of the plates was replaced with medium containing 0.1% v/v FCS, rather than the usual 10% v/v. Between removal of the existing medium and addition of the new, each plate was rinsed twice with PBS to remove any traces of serum that may have remained (Changed from V1: see point 1 below). Daily thereafter for 7 d (Changed from V1: see point 2 below), quadruplicate (Changed from V1: see point 3 below) plates for control and serum-deprived cultures were harvested, and the cell number assessed using a standard haemocytometer slide (Changed from V1: see point 4 below). Replicates were pooled, fixed in methanol/PBS, and subsequently analysed for DNA content by flow cytometry. The resulting data were processed to determine the contribution of each distinguishable cell-cycle phase to the overall fluorescence intensity distribution using Modfit LT software.

### *Changes to the method formerly used*

1. In V1 no rinse step was performed and in consequence, as much as 200  $\mu$ L of the original medium may have remained in a plate. This could correspond to increasing the serum concentration after replacement to 0.5% v/v. This is still in the range used in published deprivation experiments, so does not invalidate the original experimental series. However, with this issue having been recognised, the decision was made to improve the experimental procedure by incorporating a rinse step, even though this reduces the fidelity of experimental replication.
2. The duration of the experiment was increased from six days to seven.
3. Supernatants were not retained. This step was only included originally because of the poor adherence of NZM5. The exemplar cell-lines are all strongly adherent rendering this step superfluous. It may result in a small depletion of mitotic cells, but this was judged to be less important than the improvement in control over serum concentration.
4. The Coulter Counter Z1 used in the original experiments had been retired prior to resumption of this work. A Z2 model was available, and was used in the incomplete large-scale experiment described above, however because of the issues noted concerning instrument settings, in this experiment cell counts were assessed by digitally photographing cells on a haemocytometer slide and subsequently counting cells from the images. This has the advantages of greatly reducing counting errors due to inadvertent omission or double counting of cells, something difficult to avoid with a direct count of adequate cell numbers, and also providing a permanent record; it has a small disadvantage of reducing the ability to discriminate viable from non-viable cells.

### **Results**

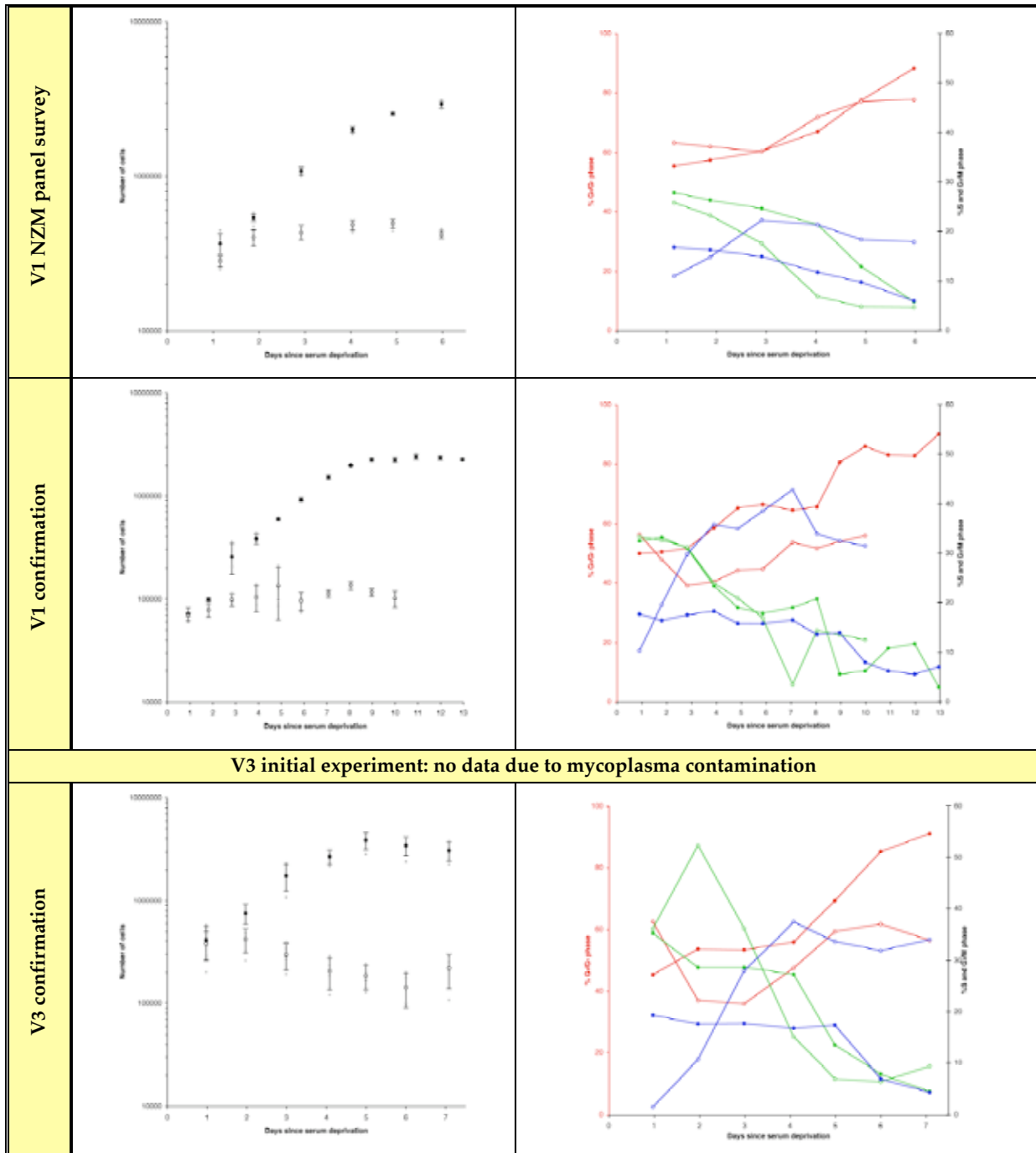
Growth and cell-cycle phasing data from both the incomplete large-scale experiment and the smaller-scale confirmatory experiment are presented below in Figure 7–18 to Figure 7–20. These figures also contain the results obtained in the original work for the purposes of comparison. To aid in interpretation of these results, a summary of salient experimental parameters for each series is given in Table 7–3.



Experimental series	Cell-lines	Seeding density	Replication	Duration	Rinse step	Counting method
V1 NZM survey	NZM panel	$2.5 \times 10^5$ /plate	Quadruplicate	6 – 10 d	No	Z1
V1 confirmation	M2, M6, M12	$5 \times 10^4$ /plate	Triplicate	13 d	No	Z1
V3 large-scale	M2, M6	$5 \times 10^4$ /plate	Triplicate	11 – 12 d	No	Z2
V3 confirmation	M2, M6, M12	$2.5 \times 10^5$ /plate	Quadruplicate	7 d	Yes	Haemo.

NZM panel = all cell-lines included in V1 study. M2 = NZM2; M6 = NZM6; M12 = NZM12. Replication specifies plates per treatment per time point. Duration is days from deprivation. The rinse step is as described in the text. Z1/Z2 = Coulter electronic particle counter model Z1 or Z2; Haemo = haemocytometer.

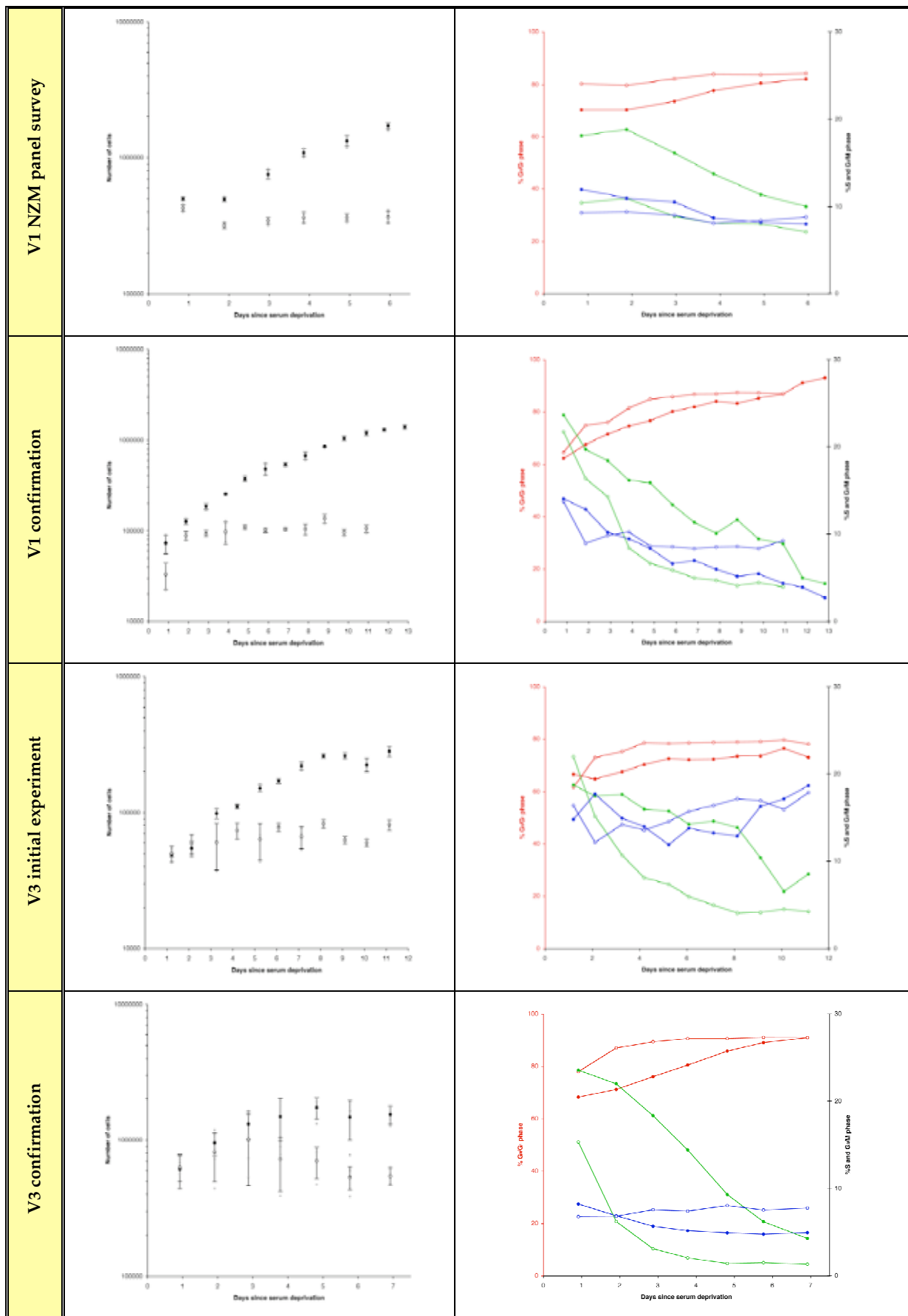
Table 7-3: Serum-deprivation experimental series parameters



Closed symbols: control. Open symbols: serum-deprived. Red = G<sub>0</sub>/G<sub>1</sub>; green = S; blue = G<sub>2</sub>/M. For left panels, large symbols and bars are mean and standard deviation; small symbols are replicate data.

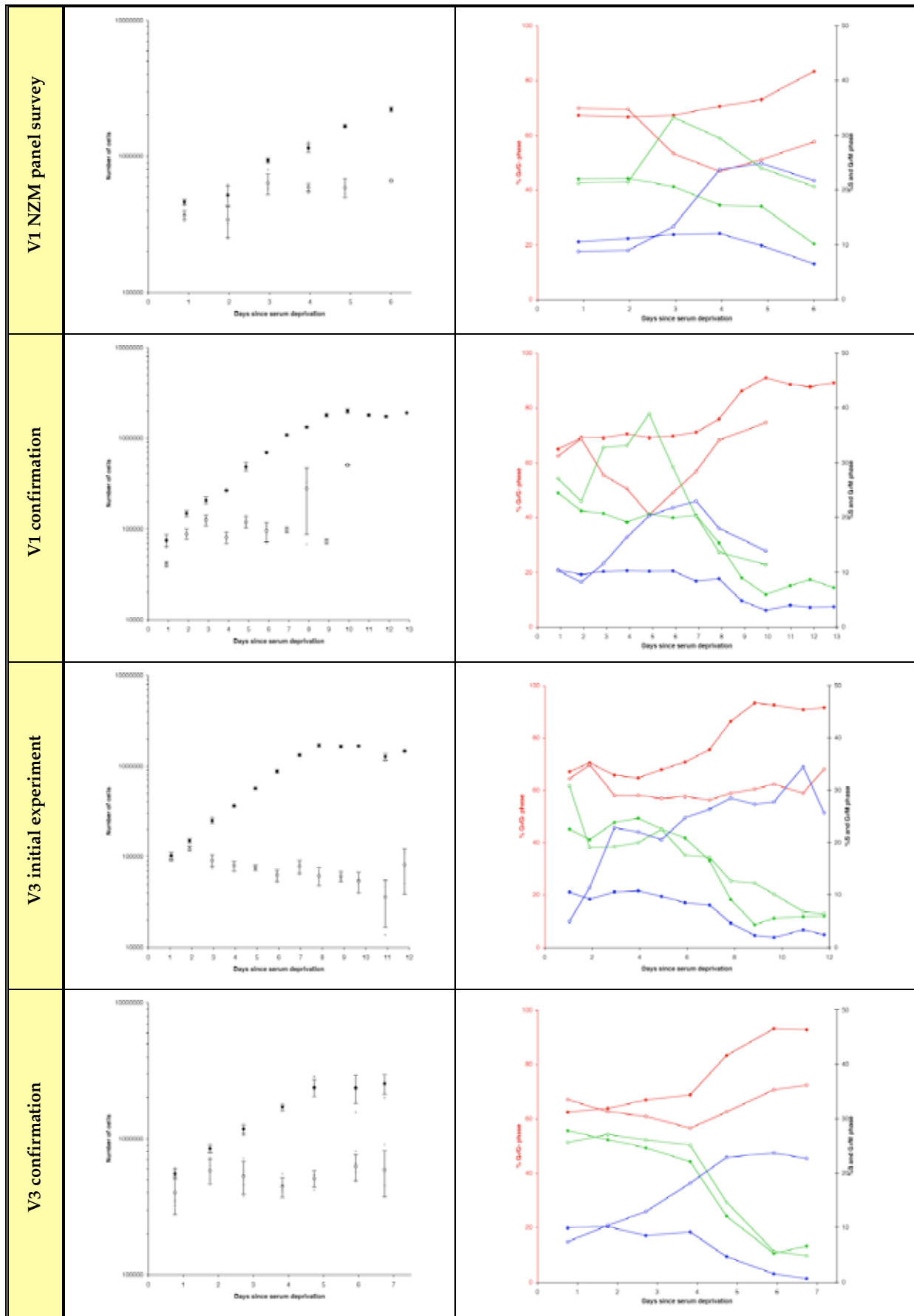
Figure 7-18: NZM12 serum deprivation results comparison

7: Serum-deprivation



Closed symbols: control. Open symbols: serum-deprived. Red = G<sub>0</sub>/G<sub>1</sub>; green = S; blue = G<sub>2</sub>/M. For left panels, large symbols and bars are mean and standard deviation; small symbols are replicate data.

Figure 7-19: NZM2 serum deprivation results comparison



Closed symbols: control. Open symbols: serum-deprived. Red = G<sub>0</sub>/G<sub>1</sub>; green = S; blue = G<sub>2</sub>/M.  
 For left panels, large symbols and bars are mean and standard deviation; small symbols are replicate data.

Figure 7–20: NZM6 serum deprivation results comparison

7: Serum-deprivation

### Discussion

The high variability in the cell counts seen in the original work persisted in V3, and was greatest in the confirmation experiment where counting was done with a haemocytometer slide as opposed to electronic particle counter; the lower cell numbers counted with this technique probably contributed to this. Despite its superficial simplicity, the concept of counting viable melanoma cells quickly and reliably does not yet seem to have a technical solution.

The new data gathered continue to support the conclusion drawn from the earlier work: in the exemplar cell-lines, the absence of serum greatly restricts proliferation.

The results for the cell-cycle phasing analysis are interesting in two ways: firstly for the similarities shown on re-examination, and secondly for the differences.

For NZM2, the exemplar cell-line for the classic  $G_1$  arrest response class, the result in each case confirmed this, with an immediate increase in  $G_1$  proportion above control levels and a concomitant decrease in S-phase, with  $G_2$  remaining constant or increasing slightly. The more gradual increase in  $G_1$  and decrease in S associated with spontaneous departure from exponential growth were also confirmed in the control cultures. The difference in the relative proportions of  $G_1$  to  $G_2$  seen between the two V3 experiments is puzzling. In the initial experiment, the ratio is ~4:1, but in the confirmatory experiment it is ~8:1. At early time points this effect was also observed in the V1 experiments, however there was a more pronounced early decline in  $G_2$  proportion in both control and serum-deprived cultures which brought the ratio back to ~9:1 by day 3. The difference in seeding density may play some part in this as the more usual ~8:1 ratio was seen at low density in both the V1 and V3 experimental series. While no explanation for this is available, its presence does not detract from the observation of changes in proportion in each of the phases, and these are consistent across all experiments. To reiterate the conclusion drawn in the original work: the presence of a  $G_1$  block in response to serum-deprivation implies either that the cyclin-D–CDK4–pRB–E2F subsystem is not defective in all melanomas, or that it is not the sole mediator of the  $G_1$  restriction point.

NZM6, for which the V1 results were considered more closely above, provided a surprise during V3. The very pronounced stimulus to enter S-phase in response to serum-deprivation that was seen twice in V1, was essentially absent in V3, and the decline in S-phase very closely followed that of the control cells. This was seen both in the initial V3 experiment and the later confirmatory experiment. However, whereas in the controls the proportion of  $G_2$  cells remained static and then declined, in the serum-deprived cultures it increased to a constant proportion; instead of there being a net transfer from S to  $G_1$  as there was in the controls and consistent with proliferation, there was a transfer only to  $G_2$  initially, implying a block there. At later times there was an increase in  $G_1$  proportion at the expense of S, implying that this  $G_2$  block was not perfect. These are now the characteristics of the Class 2 response, a serum-dependent  $G_2$ /M checkpoint, for which NZM12 was the exemplar.





What then can be learnt from NZM12's behaviour when re-examined? Here, owing to the issues of misidentification and mycoplasma, no data are available for the initial V3 experiment, but in the confirmatory experimental series, remarkably, NZM12 displayed the Class 3 response expected but missing from NZM6. There was a dramatic rise in S-phase proportion at the expense of  $G_1$  immediately upon serum deprivation, followed over the next few days with a surge in  $G_2$  and an increase in  $G_1$  slightly after that. However, between days 3 and 5, total cell numbers may or may not have been increasing; the growth data variance prevents certainty in assessing this. If they were, a degree of proliferation was still occurring; if not, then the alteration in proportion in favour of  $G_1$  phase must have been due to selective loss from S and  $G_2/M$ , possibly coupled with a  $G_2$  block as was seen in the initial investigation of NZM12.

The upshot of this is that [the three response classes reported in V1 have been confirmed to exist, but apparently they are not wholly determined by cell-line](#). Possibly all cells are capable of exhibiting all classes of response, or some potential responses may be lost due to the genetic or epigenetic status of the cells as imposed by differentiation and mutation. Of those that remain, which actually occurs upon deprivation may depend on the exact composition of the medium in which the cells had been growing, and the exact extent to which serum factors were removed.

The first, medium composition, is something that cannot be rigidly controlled without the use of totally synthetic medium including defined growth factors. In the typical experimental scenario, this would be addressed by the use of the same batch of serum throughout, and so provide consistency, if not precise definition. However, that has not been the case here. The V1 NZM survey took place between July and December 2000, and the confirmation between June and August 2001; the V3 initial experiment was conducted in June 2006, and the confirmation between August and September 2006. Thus, over five years had elapsed between the original experimentation and the re-examination, and a change in serum supply is a virtual certainty. This variability could not be controlled for without the foreknowledge that additional work would be required and the reservation of serum for subsequent use.

The second, the extent of deprivation, was altered by the introduction of the rinse step during serum deprivation in V3. The difference was considered to be of minimal significance, as the concentrations achieved in either case were within the range used in such experiments. However, it is quite possible that cells exhibit one class of response when restricted to 0.1% serum, and a different class when provided with five times that, 0.5%. Variability in behaviour at such low serum levels is an area that could be investigated further.

There may also be random factors involved. Removal of serum proteins may lead to a greater degree of oxidative damage being experienced by cells, or may lead to changes in epigenetic status, and these may be exacerbated by variation in serum composition and the actual degree of deprivation achieved. Changes of this type could also contribute to the response class switching that was seen.

Biological systems are inherently variable and perfect replication of results can often be elusive. Nowhere is this likely to be more apparent than in the study of genomically unstable tumour cell-lines, where the characteristics of the subject may alter even during the course of an experiment, never mind between attempted replications conducted years apart.

### **Summary**

Further analysis of the data gathered in V1 has shown internal consistency between the results of the two experimental series undertaken. The existence of the three classes of response to serum deprivation has been confirmed, but that exhibited by a cell-line has been shown to be at least partly, if not wholly, context dependent, rather than being an intrinsic property of that cell-line. The occurrence of spontaneous departure from exponential growth and cell-cycle phase changes in control cultures commencing immediately after seeding was confirmed. The problems associated with obtaining accurate cell counts have become apparent, as have the difficulties in attempting to replicate results after an extended interval.

The human 9p21 chromosomal locus contains the genes *CDKN2A* and *CDKN2B* that encode three proteins, p15, p16, and ARF, each capable of causing cellular growth arrest. Aberrations of expression of these genes, or of their functional associates, are widely reported in many tumour types, notably melanoma. Using PCR, single-strand conformation polymorphism analysis, and DNA sequencing, the genetic integrity of the 9p21 region was investigated in sixteen human metastatic melanoma cell-lines.

Seven cell-lines were found to have deletions affecting *CDKN2A*, and in five of these, *CDKN2B* was also affected. Two related cell-lines contained sequence polymorphisms in the 3'-untranslated region of *CDKN2A*, and one, in addition to being partially deleted, also contained a sequence variation expected to alter ARF. One cell-line contained a sequence variation in *CDKN2B*, probably an inconsequential polymorphism. In two cases, there was evidence of a deletion telomeric to the 9p21 locus.

In addition, compelling evidence of genetic heterogeneity within individual cell-lines was found, reinforcing the conclusions drawn from the analysis of ploidy.

Retracted material.  
See section addendum for details

## 8.1 Introduction

Cytogenetic studies of melanoma have implicated the human 9p chromosomal region in tumorigenesis<sup>369</sup>, and there is a great deal of evidence that a melanoma tumour-suppressor gene resides within 9p21<sup>322</sup>. Here, two closely related genes have been identified: *CDKN2A* and *CDKN2B* {Figure 8–1}.

In a manner extremely rare in eukaryotes, the first gives rise to two distinct protein products. Two promoter sites direct the transcription of different initial exons, termed 1 $\alpha$  and 1 $\beta$ . In either case, the first exon is spliced to common exons 2 and 3, but as the alternative first exons differ in length, the common exons are appended in differing reading frames<sup>839</sup>. This eliminates any similarity of sequence, and by extension, function, between the two resultant

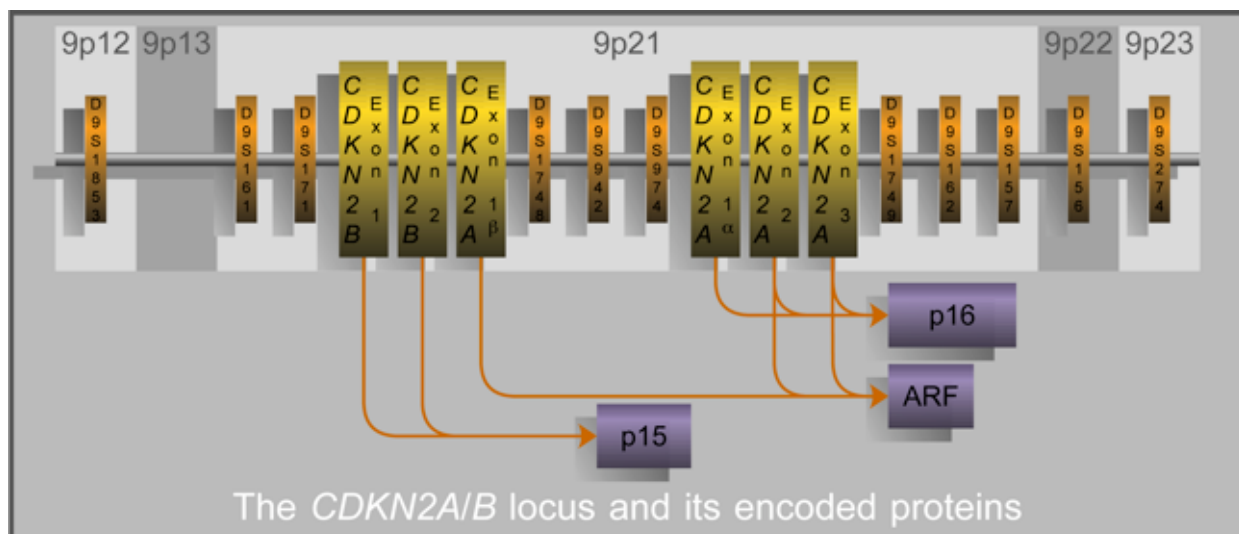


Figure 8–1: The *CDKN2A/B* locus and its encoded proteins

See H-22 for more on p16.

See J-21 for more on ARF.

A review of the pRB subsystem is given in Appendix H.

proteins, p16 and ARF. Nevertheless, both are inhibitors of cellular proliferation. The first is a CKI for CDK4 and CDK6, and when expressed, prevents phosphorylation of pRB, thereby allowing it to retain its growth-suppressive function, even in the presence of mitogens<sup>816 1181</sup>.

This typically results in a cell-cycle arrest late in G<sub>1</sub>. ARF functions by binding the MDM2 protein, translocating it to the nucleolus<sup>1412</sup>, and targeting it for destruction<sup>533 1513</sup>. Thus, it shields p53 from the direct inhibitory effects of MDM2, and from degradation as a consequence of ubiquitinylation by it<sup>737</sup>. Expression products of p53 transcriptional targets, such as p21<sup>CDKN1A</sup><sup>1389</sup> and the 14-3-3 protein<sup>1350</sup>, stratifin<sup>511</sup>, are likely effectors of ARF function, causing arrest both in G<sub>1</sub> and in G<sub>2</sub>.

For more on p15, see H-20 and H-22.

*CDKN2B* has close sequence similarity to *CDKN2A*, and while it does not have an alternate first exon, several mRNA splice variants are known. It lacks the final exon of *CDKN2A*, but shares a conserved intron, suggesting a past gene duplication event. Its best-characterised protein product, p15, is structurally and functionally very similar to p16, and it is probably in the manner of their respective transcriptional control that their biological roles diverge. In this respect it is particularly noteworthy that p15 is dramatically induced after treatment of epithelial cells with the inhibitory cytokine TGFβ<sup>471 1089 1134</sup>.

*CDKN2A* and *CDKN2B* therefore represent plausible candidates for the 9p21-linked melanoma tumour-suppressor gene. The evidence is very strong that p16 is a significant contributor to this tumour suppression, but the statuses of ARF and p15 are less clear. In particular, the relative importance of control of cellular proliferation via p15, p16, and pRB, versus the maintenance of genomic integrity and regulation of apoptosis via ARF and p53, are still to be determined. In seeking to address this issue, the genetic integrity of the putative 9p21 tumour-suppressor genes was assessed in a panel of sixteen human metastatic melanoma cell-lines. This chapter describes this survey and its results.

## 8.2 Experimental design

### Controls

DNA isolated from peripheral blood leukocytes from a healthy volunteer was included as a putatively normal reference for PCR/SSCP experiments. To detect DNA contamination, each series included a PCR reaction to which no template DNA was added. Template DNA quality was assessed by amplification of an irrelevant target within the gene for β-globin, *HBB*. The human HL60 promyelocytic leukaemia cell-line was grown as a control for SSCP as it is known to contain sequence variations in *CDKN2A*<sup>1225</sup>.

### 9p12–9p23 marker selection

Numerous sources were consulted<sup>96 165 361 407 408 418 494 558 676 839 871 881 1019 1084 1118 1211 1376</sup> and markers were selected from among those where there was the greatest concordance of opinion over ordering. As microsatellites offer the potential to yield heterozygosity information they were accorded priority, particularly where high levels of heterozygosity had been reported. The relative positions of these markers are shown in Figure 8–1.



## PCR primers

PCR primer sequences were taken from published sources or public databases. These, together with the expected product sizes, are detailed in Table D-1.

## SSCP considerations

Two of the intended target exons exceed the size that can be assayed reliably by SSCP. For exon 2 of *CDKN2A*, this had been addressed by the developers of the PCR primers<sup>559</sup>, who had designed three pairs that amplify the exon in overlapping segments of suitable sizes, here designated 2A, 2B, and 2C. For the 440 bp PCR product encompassing *CDKN2A* exon 1 $\beta$ , examination of the published sequence data with MapDraw software {E.9} revealed that it could be cut with the restriction enzyme *Bst*N1 into fragments of size 82, 126, 81, and 151. While the use of multiplex SSCP is not common, it has been used with success<sup>318</sup>, and it may increase mutation detection sensitivity, with the greater number of intra- and inter-fragment interactions resulting in an SSCP 'fingerprint'. This course was adopted.

See A.3 for a discussion of the principles of the SSCP assay.

## 8.3 Methods in brief

Cultures of the NZM and HL60 cell-lines were established in vitro {Method 2}. Mean passage number for all NZM cell-lines was ~18. DNA was extracted {Method 7}, the selected markers and coding targets amplified by touch-down PCR {Method 10}, and examined by 3% agarose electrophoresis {Method 11} with ethidium bromide staining {Method 12}. The *CDKN2A* exon 1 $\beta$  product was cut with the restriction enzyme *Bst*N1 {Method 9}. All exonic PCR products where no gross genetic alteration was detected were examined by SSCP {A.3} and silver staining {B.9}. Where SSCP band patterns differed from control, the PCR reaction mixture was purified using a resin spin-column {E.2} and sequenced bi-directionally using the PCR primers {Method 32}.

## 8.4 Results

### PCR amplification of targets from the chromosome 9p12–9p23 region

Images of ethidium bromide stained agarose gels of PCR products are given in Figure 8-2.

#### *Controls*

PCR amplification with *HBB* primers demonstrated that template DNA loading and quality was practically equal for all cell-lines. The absence of detectable product in every control lacking template DNA demonstrated that no contamination of PCR reaction mixtures had occurred. For all primer pairs used, a single product of the expected size was obtained from the normal template DNA. The thermal cycling parameters employed were satisfactory for all primer pairs.

#### *Melanoma cell-lines*

In many cases, the intensity of ethidium bromide staining of bands was of an intermediate level, being clearly greater than background, but also distinctly less than control. This effect was reproducible, never seen in *HBB* controls, and inconsistent with genomic DNA contamination.



Markers are given in physical order {See Figure 8-1}. Expected product sizes are given. For microsatellites, this is indicative only.

Lanes: M = 100 bp marker, ø = control without template DNA, N = normal DNA, 1-15 = corresponding NZM DNA. HL60 data not shown.

Figure 8-2: 9p12-9p23 PCR results

These intermediate bands may be an indication of differences in target prevalence within DNA extracts from different cell-lines. Numerical densitometry of the band intensities was performed, but such precision is needless and confuses, rather than elucidates, the underlying observation. To reflect the presence of this variability, amplification was scored subjectively {Table 8–1}.

Marker	1	2	3	4	5	6	7.2	7.4	9	10	10.1	11	12	13	14	15
D9S1853	++	++	++	++	++	++	++	++	++	++	++	++	++	++	++	++
D9S161	-	-	++	++	++	++	++	++	++	++	++	++	++	++	++	++
D9S171	-	-	+	++	++	++	++	++	-	++	+	++	++	+	++	+
CDKN2B exon 1	±	-	±	++	++	++	++	++	-	++	++	±	++	+	++	++
CDKN2B exon 2	-	-	±	++	++	++	++	++	-	++	++	-	++	+	++	++
CDKN2A exon 1β	-	-	-	++	++	+	++	++	-	++	++	+	++	+	++	++
D9S1748	±	-	±	++	++	++	++	++	-	++	++	-	++	±	++	++
D9S942	-	-	-	++	++	++	++	++	-	++	++	-	++	±	++	++
D9S974	-	-	-	++	++	++	++	++	-	++	++	-	++	±	++	++
CDKN2A exon 1	-	-	-	++	+	++	++	++	-	++	++	-	++	+	++	++
CDKN2A exon 2A	-	-	±	++	++	++	++	++	+	++	++	±	±	+	++	++
CDKN2A exon 2B	+	-	±	++	++	++	++	++	-	++	++	-	±	-	++	++
CDKN2A exon 2C	-	-	-	++	++	++	++	++	-	++	++	-	-	±	++	++
CDKN2A exon 3	±	-	±	++	++	++	++	++	-	++	+	+	+	+	±	++
D9S1749	-	-	++	++	+	+	++	++	-	+	++	++	+	+	+	+
D9S162	+	+	+	+	+	+	+	++	++	++	++	++	++	±	++	+
D9S157	++	++	+	+	++	++	+	++	++	++	++	++	++	+	+	++
D9S156	-	-	±	+	++	++	++	++	+	±	++	++	++	++	++	-
D9S274	++	++	++	++	+	++	++	++	++	+	-	+	++	+	+	-

Subjective assessment of intensity of amplification of PCR targets. Column headings denote NZM cell-line. Row headings denote PCR target sequence. ++ = indistinguishable from control; + = marginally less than control; ± = clearly less than control; - = weak, but readily discernible amplification; - = no visible product.

Table 8–1: Deletion map of 9p12–9p23 region based on PCR

### SSCP analysis

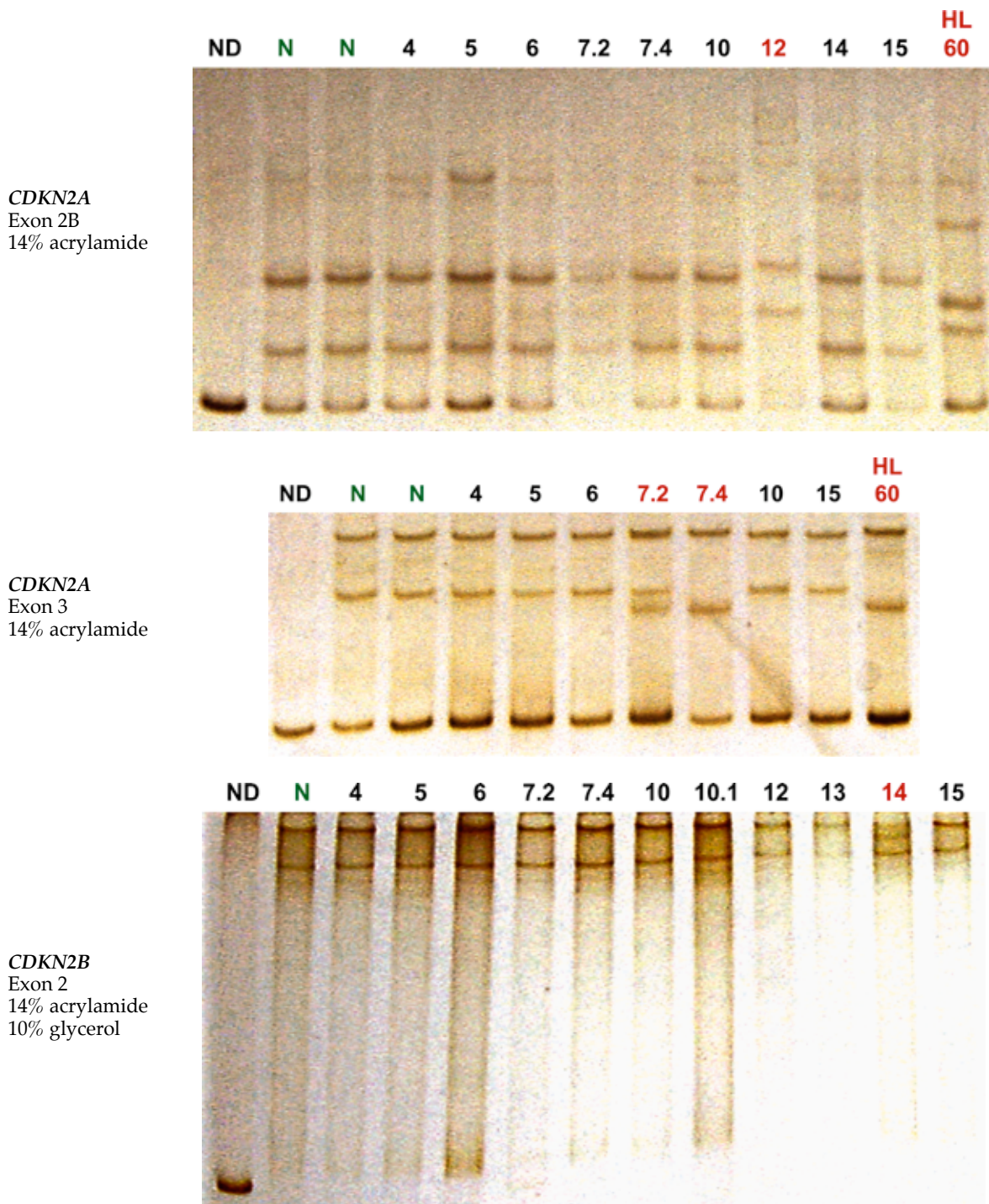
Images of silver-stained acrylamide gels from SSCP experiments are given in Figure 8–3.

#### Controls

Non-denatured DNA controls invariably produced a single strong band after silver staining. Putatively normal DNA reliably produced two strong bands corresponding to self-annealing single-stranded DNA, and, depending on the experimental conditions, a band corresponding to renatured duplex DNA. HL60 DNA, known to harbour two sequence variations, produced the expected band mobility shifts in the *CDKN2A* exon 2 PCR products, confirming that the SSCP assay was functioning. In addition, HL60 also displayed anomalous banding for the *CDKN2A* exon 3 PCR product. This does not appear to have been reported previously, but was not explored further.

#### Melanoma cell-lines

Anomalous banding patterns were seen for *CDKN2A* exon 2B of NZM12; *CDKN2A* exon 3 for NZM7.2 and NZM7.4; and exon 2 of *CDKN2B* for NZM14 {Figure 8–3}.



Lanes: ND = non-denatured DNA; N = normal DNA; others = DNA from indicated cell-line.  
 Note the anomalous banding for N7M7.2, N7M7.4, N7M12, N7M14, and HL60.

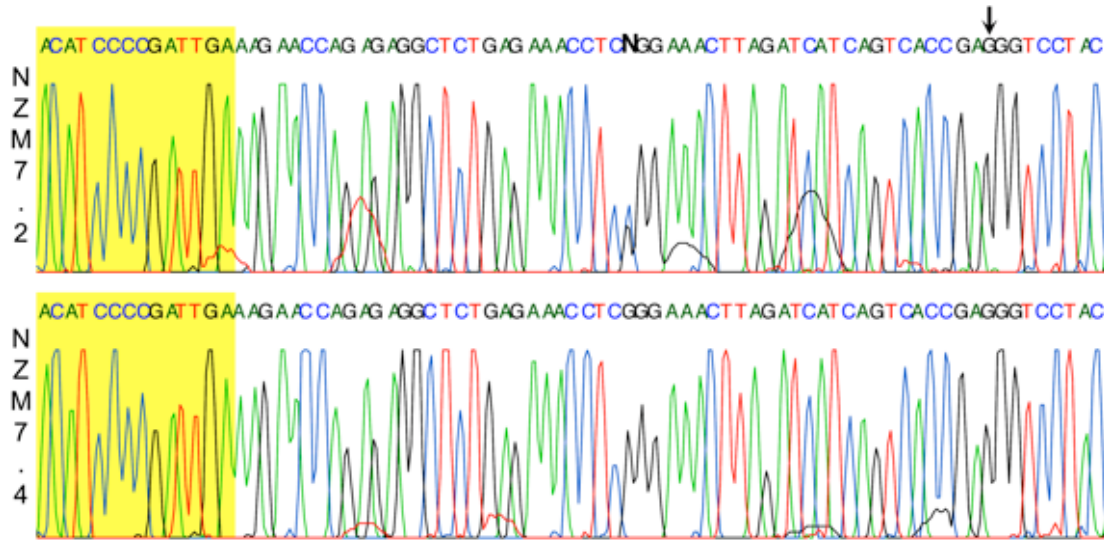
Figure 8-3: Silver-stained SSCP gels

**DNA sequencing**

The genomic sequence corresponding to the 3' untranslated region of *CDKN2A* harboured two sequence variations in the related N7M7.2 and N7M7.4 cell-lines. The first, G500C, was apparently heterozygous in N7M7.2, while only the G variant was seen in N7M7.4 (Figure 8-4). This is consistent with the additional SSCP band seen for N7M7.2. In the second case, A526G, only the G variant was detected, suggesting hemizyosity or homozygosity. The latter seems the more likely in N7M7.2 given the heterozygosity seen at G500C.

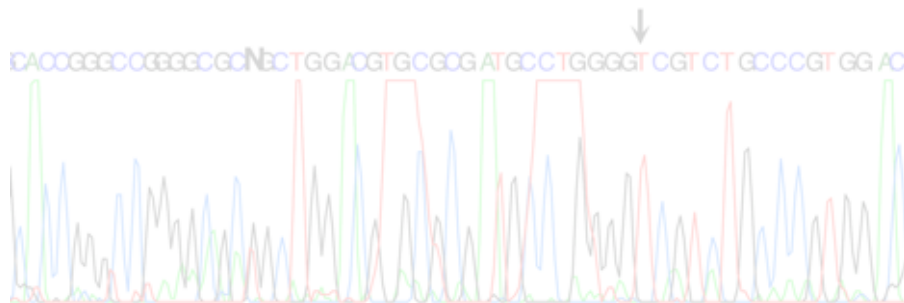
Retracted material. See section addendum for details





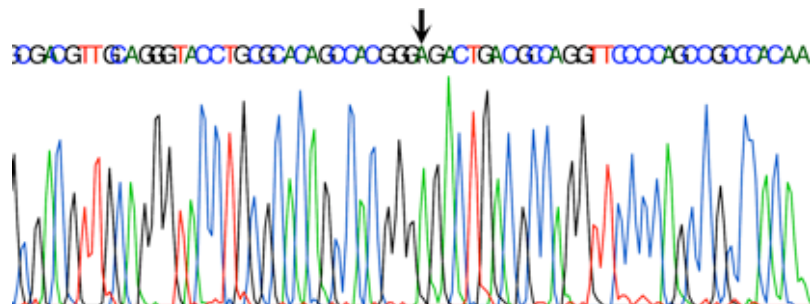
The highlighted regions indicate exon 3. The 'N' denotes the heterozygosity at position 500; the arrow, the variation at position 526.

**Figure 8-4: DNA sequences corresponding to the *CDKN2A* 3' UTR of NZM7.2 and NZM7.4**  
 NZM12 *CDKN2A* exon 2B differed in two places from the reference sequence: G308T, heterozygous; and C333T. The electropherogram (Figure 8-5) is not technically perfect, with cross talk from an adjacent gel lane giving a low level of spurious signal for the A bases, but these are readily distinguishable from the intense peaks seen for bona fide signals. Anomalous broad T peaks are also present, but consideration of peak spacing allows the correct interpretation to be made.



The 'N' denotes the heterozygosity at position 308; the arrow, the variation at position 333.

**Figure 8-5: DNA sequence from *CDKN2A* exon 2 of NZM12**  
 NZM14 *CDKN2B* exon 2 displayed a novel G411A transition (Figure 8-6).



The arrow indicates the variation at position 411.

**Figure 8-6: NZM14 *CDKN2B* exon 2 sequence variation**

## 8.5 Discussion

### Heterogeneity

A cursory examination of the results of the electrophoresis of PCR products would probably conclude that many were technically badly flawed, with suspicion being aroused chiefly by the non-uniformity of amplification among cell-lines in many cases. Indeed, this is how they were first interpreted, and considerable effort was expended in searching for the source of this variation. Likely candidate causes were differing reagent or template DNA concentrations. To exclude these, a bulk mixture of all reagents including primers was prepared, thoroughly mixed, and distributed among PCR tubes. The final step involved the addition of scrupulously quantitated template DNA, and repetitions were performed with DNA extracted using several different techniques. The equivalence of reaction conditions and template DNA addition is demonstrated by the uniformity of amplification using the *HBB* primers. Although the efficiency of amplification with different primer pairs was variable, in all cases, a single band of the expected size was seen in the normal control, and the intensity of this was similar to the maximum seen for any cell-line amplified in parallel. Ultimately, it was accepted that the variability seen among cell-lines for some targets was not a technical artefact.

One interpretation of these data is that every cell in any cell-line contains the same number of copies of each marker, but no relationship exists between the number of copies of different markers. In this way, the *HBB* target may be uniformly represented across all cell-lines, but for example, the number of copies of D9S1748 may differ from the number of copies of D9S157. This seems implausible for a number of reasons. Firstly, to obtain the range, and seemingly continuously variable levels of amplification intensity seen, there would need to be a wide difference in copy number of different markers. If these were present at their normal loci as tandem repeats of closely-linked markers, separate amplification events would be needed to account for each, and this would need to be achieved without any significant disruption to the *HBB* gene. If the copies were present on separate pseudo-chromosomal structures and therefore unlinked, they would need to be faithfully replicated during mitosis. Secondly, such a mechanism would in some cases require simultaneous non-contiguous deletions, a seemingly unlikely event.

Alternatively, and, in the context of the heterogeneity of ploidy reported in Chapter 5, the ability to isolate sub-clones of differing phenotype<sup>180</sup>, and the presence of multiple karyotypes within a culture<sup>60 966</sup>, the preferred interpretation is that **NZM cultures contain multiple sub-populations with differing genotype**, and the disparate amplification seen is a result of the relative abundance of cells that contain the target sequence versus those that do not.

Only two possibilities exist to account for this genetic heterogeneity: either it was present in the original tumour and has been maintained during serial passage, or the divergence occurred in vitro. These are not entirely disjoint, since if the tumour cells were able to generate diversity in vivo, it is difficult to see how they would lose this capacity in vitro. Since studies with fluorescence in situ hybridisation and immunohistochemistry routinely reveal just such

heterogeneity in genetic markers or expressed proteins in tumours<sup>391 654 1085</sup>, it seems probable that the first is the correct interpretation, and the situation in vitro accurately reflects this. While it is possible that extended serial culture may result in the purification of a favoured clone, it is also possible that the divergence continues. This is a surprising result, particularly in light of the widespread use made of cell-lines on the basis that their intrinsic homogeneity and stability facilitate experimental replicability.

### Specific anomalies detected

#### DNA sequence variations

#### NZM7.2/7.4 CDKN2A 3' untranslated region

	500	
Reference	ACATCCCCGATTGAAAGAACCAGAGAGGCTCTGAGAAACCTC	GGAAACTTAGATCATCAGTCACCGAAGGTCCTAC
NZM7.2	ACATCCCCGATTGAAAGAACCAGAGAGGCTCTGAGAAACCTC	SGAAACTTAGATCATCAGTCACCGAGGGTCCTAC
NZM7.4	ACATCCCCGATTGAAAGAACCAGAGAGGCTCTGAGAAACCTC	GGAAACTTAGATCATCAGTCACCGAGGGTCCTAC

The shading at left denotes the end of exon 3; other shaded bases are sites of sequence variation. S = G and C. Nucleotide numbering is with respect to the initiating ATG codon in the p16 reading frame. Nucleotide reference was NT\_008410.

Figure 8–7: NZM7.2/7.4 CDKN2A 3' UTR sequence variations

The G500C variation found {Figure 8–7} is a well-known polymorphism<sup>119</sup>, but probably unimportant in the aetiology of melanoma as neither allele occurs with significantly higher incidence in melanoma than in normal controls<sup>726</sup>. The presence of both alleles in NZM7.2 but not NZM7.4 is of interest given that these cell-lines were derived from the same parental culture by sub-cloning. The progenitor cells for each sub-clone may have differed in their genotype at this locus, indicating heterogeneity within the parental culture, something already suspected based on the results of ploidy analysis and PCR. Alternatively, NZM7.4 may have suffered LOH, or NZM7.2 suffered a mutation in vitro. Irrespective of the actual cause, genetic instability within the NZM7 family is suggested.

The A526G variation appears to be novel. Whether it is involved in the aetiology of melanoma will only become clear after a much more extensive study.

#### NZM12 CDKN2A exon 2B

	308										333														
Reference	TGGACACGCTGGTGGT	TGCTGCACCGGGCCGGGGCGC	GGCTGGACGTGCGCGATGCCTGGGG	CCGTCTGCCCGTGGAC																					
NZM12	TGGACACGCTGGTGGT	TGCTGCACCGGGCCGGGGCGC	KGCTGGACGTGCGCGATGCCTGGGG	TCGTCTGCCCGTGGAC																					
Ref. p16	L	D	T	L	V	V	L	H	R	A	G	A	R	L	D	V	R	D	A	W	G	R	L	P	V
p16	L	D	T	L	V	V	L	H	R	A	G	A	R	L	D	V	R	D	A	W	G	R	L	P	V
Ref. ARF	G	H	A	G	G	A	A	P	G	R	G	A	A	G	R	A	R	C	L	G	P	S	A	R	G
ARF	G	H	A	G	G	A	A	P	G	R	G	A/A	A	G	R	A	R	C	L	G	S	S	A	R	G

Shaded bases or amino acids denote sites of sequence variation. K = G and T. Nucleotide numbering is with respect to the initiating ATG codon in the p16 reading frame. Nucleotide reference was NT\_008410; p16 reference was XP\_027621; ARF reference was XP\_027622.

Figure 8–8: NZM12 CDKN2A exon 2 sequence variations

The presence of T308, rather than G308, should cause a non-conservative ARG103LEU mutation in p16, but not affect ALA117 in ARF {Figure 8–8}. As G308 is conserved among human, mouse, rat, opossum, and pig, this mutation probably affects functionality. The interaction between the proteins encoded by the two alleles is unknown. The mutant protein may be non-functional and unimportant in the presence of the normal protein or some dosage

effect may exist. Conceivably, it may act in a dominant-negative manner, but this seems unlikely, as self-association of p16 has not been reported.

While no evidence of heterozygosity for the C333T variation was seen, hemizyosity cannot be excluded. This alteration should not affect the GLY111 in p16, but should cause a PRO126SER mutation in ARF. Since the functionality of ARF lies principally in the N-terminal region implicated in MDM2 interaction<sup>1513</sup>, and secondarily between residues 83 and 100, implicated in nucleolar localisation<sup>1201</sup>, this change may be inconsequential, despite a significant effect on protein conformation being likely. The normal occurrence of T333 in mouse, rat, and opossum supports this.

**NZM12 CDKN2A exon 2C**

The inability to amplify the NZM12 CDKN2A exon 2C product suggests that NZM12 has a further genomic disruption beyond those described above, possibly a small deletion affecting a primer binding site. If so, a frame shift may have occurred, potentially altering the sequence and length of the resultant protein. From the portion of the gene known to be intact, it can be deduced that the minimum molecular weight for such a protein would be ~10.8 kD. As will be described, a variant p16 protein is indeed produced by this cell-line {9-7}.

**NZM14 CDKN2B exon 2**

	411
<b>Reference</b>	AGGAGCGGGGCCACCGCGACGTTGCAGGGTACCTGCGCACAGCCACGGGGGACTGACGCCAGGTTCCCCAGCCGCC
<b>NZM14</b>	AGGAGCGGGGCCACCGCGACGTTGCAGGGTACCTGCGCACAGCCACGGGAAGACTGACGCCAGGTTCCCCAGCCGCC
<b>Ref. p15</b>	E E R G H R D V A G Y L R T A T G D .
<b>p15</b>	E E R G H R D V A G Y L R T A T G D .

Shaded bases denote sites of sequence variation. Nucleotide numbering is with respect to the initiating ATG. Nucleotide reference was NM\_004936; p15 reference was NP\_004927.

**Figure 8-9: NZM14 CDKN2B exon 2 sequence variation**

The G411A variation found should not alter the encoded GLY137 amino acid {Figure 8-9}. The homologous genes for mouse and pig also carry A411, suggesting that this is a polymorphism normally present among humans. There appears to have been no prior report of this polymorphism.

**Deletions telomeric to 9p21**

The inability to amplify the D9S274 (NZM10.1 and NZM15) and D9S156 (NZM15) microsatellites by PCR raises the possibility that a further tumour-suppressor gene may reside telomeric to the CDKN2A/B locus. Other studies have postulated such a 9p21-pter tumour-suppressor gene in melanoma<sup>1042</sup>, BCC<sup>1135</sup>, and non-small-cell lung cancer<sup>841</sup>.

**8.6 Summary and conclusion**

Of the sixteen cell-lines investigated, seven showed clear evidence of genomic disruption within the 9p21 locus of the CDKN2A/B tumour-suppressor genes, one (NZM14) gave indications of a disruption here, and a further three cell-lines contained disruptions telomeric to 9p21. The remaining five cell-lines appeared to be substantially genomically intact in the region investigated.



---

The possibility that heterogeneity may be an intrinsic attribute of melanoma, and possibly other solid tumours, rather than a consequence of lingering remnants of out-competed clones may have profound implications, both for our understanding of tumour biology and in the development of new therapies. These aspects are explored further in Chapter 11.

## 9p21 status (V3)

### 8.7 Retraction of existing material

#### Sequence variations reported

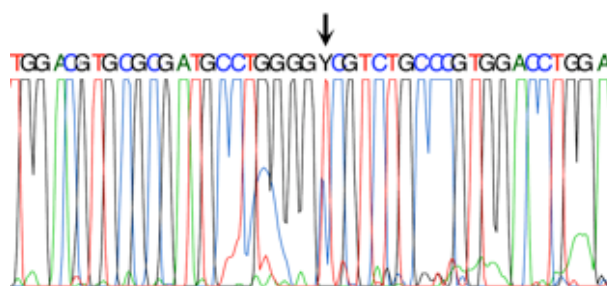
##### *NZM7.2/7.4 CDKN2A 3' untranslated region*

A novel A526G transition was reported as present in NZM7.2 and NZM7.4. Further inspection led to the realisation that the 526 position is actually within the reverse PCR primer used during amplification and so this change is entirely artefactual. The ultimate source of this error is that the published primer used contains this departure from the reference sequence. While this was noted in Table D–1, the list of PCR primers for V1, this fact was overlooked when the data were analysed. The finding is retracted and the affected portions of the text should be considered deleted.

It is interesting to note that had all PCR products been sequenced, rather than relying on SSCP as a screening tool, this error may have come to light sooner, since all cell-lines would have been found to contain A526G, something that would have aroused suspicion. As it was, it was only the presence of the G500C polymorphism in NZM7.2 and NZM7.4 that led to a distinct SSCP pattern and resulted in their being sequenced, leading to the erroneous discovery of A526G.

##### *NZM12 CDKN2A exon 2*

The quality of the electropherograms produced during V1 was not ideal, and in the case of NZM12 *CDKN2A* exon 2B, not acceptable. During the revision for V2, the PCR and sequencing for this target were repeated and a new electropherogram was produced to replace the substandard one {Figure 8–10}.



The arrow indicates the variation at position 333.

Figure 8–10: V2 figure for DNA sequence from *CDKN2A* exon 2 of NZM12

While this was an improvement, it was still not technically perfect. Nevertheless, it did seem to confirm the C333T variation, albeit now apparently heterozygous; the G308T heterozygosity was not found and should be attributed to misinterpretation of the original poor data.

A significant word in the previous sentence is "seem", as all is still not well with this interpretation<sup>1687</sup>. A combination of factors has very likely resulted in the amplification of a target similar to, but distinct from that intended, specifically, the corresponding region of the homologous *CDKN2B* gene. The PCR primers used, although they were from a published



source<sup>559</sup>, each differs in one non-critical base from the *CDKN2B* sequence, and so together offer little inherent specificity relative to *CDKN2A*, and furthermore, the alternative products are of identical length. In these circumstances, amplifying only the intended product depends strongly on the stringency of the thermal cycling programme, but while the generic touch-down PCR programme used supported amplification for all sets of primers, it was probably optimal for none. It is also likely that at least one of the primer binding sites for the *CDKN2A* target is absent from NZM12. In combination, these factors may have allowed the amplification of the non-specific *CDKN2B* product in the guise of that from *CDKN2A*, and because of the close homology, the results of sequencing, with a single anomalous base, were entirely plausible. This analysis means in essence that the results obtained for this target in *CDKN2A* must be interpreted with great care, and in the case of NZM12, are probably invalid.

As will be described below, attempts to amplify NZM12 *CDKN2A* exon 2 in its entirety using intronic primers failed, while succeeding for other cell-lines. This, together with the failure to amplify the 2C segment of exon 2 described in the original work, suggest that there is homozygous deletion in this region rather than a primer site mutation. A mystery does still remain however: if this region is deleted, what is the source of the *CDKN2A* C333 allele seen here? Candidate causes include: a variant NZM12 sub-population existing that contains this; cross-contamination of cell-lines during culture; and cross-contamination of template DNA or amplified products during PCR.

In summary then, no defensible evidence was found to support the presence of *CDKN2A* exon 2B in the NZM12 cell-line and so the questionable results and related discussion are retracted and should be considered deleted from the chapter.

## 8.8 Clarification of existing material

### Anomalous PCR results

The PCR results obtained in the initial work displayed several anomalies stemming for the most part from the desire to find a single set of PCR cycling conditions satisfactory for the many target sequences to be amplified, rather than having to optimise the conditions for each target individually, a significant issue since thermal gradient cyclers were not then available. Apart from offering a considerable time-saving, this also had the advantage of allowing the amplification of different targets in separate reactions in one thermal cycling run. The issues that arose included the presence of primer artefacts and non-specific products, particularly in the absence of the intended target. Most puzzling was the reliable production of electrophoretic bands for some target/cell-line combinations that were clearly present, but always much lower in intensity than those for other cell-lines or the control *HBB* target. This was taken to suggest that differences in target prevalence within DNA extracts from different cell-lines existed. This interpretation was awkward, but was consistent with other evidence of genomic heterogeneity, and the observed variation was fully replicable. One consequence was that for some cell-lines, some targets were detected at apparently higher prevalence than flanking markers, and in the extreme case, this could suggest that a target existed where

flanking markers were homozygously deleted. While this seems implausible, it is not impossible. PCR, of itself, gives no indication of where in the genome a target was found and it is quite possible for chromosomal rearrangements, common in cancer, to place a target in a new context, unlinking it from normally adjacent markers. If those markers were then homozygously deleted, the results of PCR would be as they were seen here. Since this and genomic heterogeneity within cultures are both viable hypotheses to account for the variation seen, the data could not simply be rejected as invalid. As will be described below {8.9}, this issue was revisited during the V3 work, and to a large extent, was resolved.

### **Available quantitative real-time PCR (qPCR) data**

During V1, a request was made by Dr Ian Morison for DNA from the NZM cell-lines to be made available to the Cancer Genetics Laboratory at Otago University, where a project investigating 9p21 alterations in childhood acute lymphoblastic leukaemia using qPCR was underway. This was supplied, and in July of 2000 Dr Morison kindly provided graphical results for three loci, one within *CDKN2B*, one within exon 1 $\beta$  of *CDKN2A*, and a third in a different, unspecified exon of *CDKN2A*. These are given in Figure 8–11.

In the cell-lines NZM1, NZM2, NZM3, NZM9, and NZM11, where PCR revealed strong evidence of deletion, qPCR also failed to amplify any of the target sequences. In NZM13, where the PCR evidence for deletion was present, but less strong, the interpretation made is confirmed by the lack of amplification seen during qPCR.

In NZM4, NZM5, NZM6, NZM10, NZM14, and NZM15, both PCR and qPCR demonstrated the presence of the sequences assayed by both techniques. For these cell-lines, the qPCR results would typically be interpreted as suggesting hemizyosity for these markers, however, the substantial departure of many of these cell-lines from diploidy renders this interpretation moot. For example, NZM14 is hyperdiploid {Table 5–1}, and there is no certainty that it is not an additional copy of the control marker on chromosome 2 that makes the target loci appear hemizygous.

In NZM7.2 and NZM7.4, qPCR confirms the presence of the target loci. Further discussion on the import of these results appears below {See '*Loss of heterozygosity*' on page 8–36}.

Finally, NZM12, by PCR, appeared to be substantially intact across the 9p21 region, with the exception of exon 2 of *CDKN2A*. Quantitative real-time PCR confirms these PCR results by successfully amplifying the targets from *CDKN2B* and exon 1 $\beta$  of *CDKN2A*, but not that from the remainder of the *CDKN2A* gene.



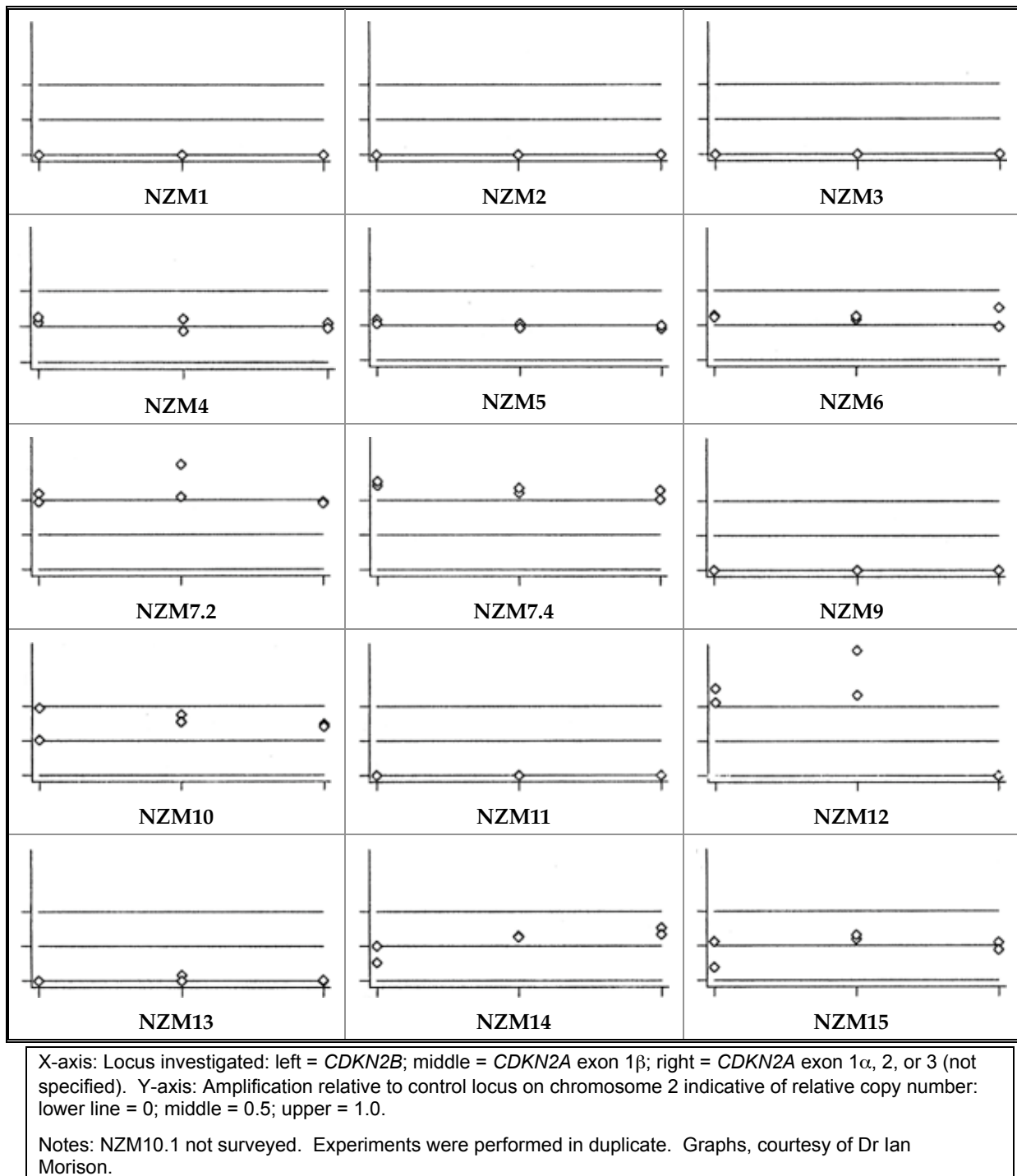


**Figure 8–11: Quantitative real-time PCR results for *CDKN2A* and *CDKN2B***

Interpretation of qPCR data in terms of copy number has the inherent assumption that all cells present in the culture from which the DNA to be assayed was extracted have identical genotype, and that any result based on culture population data applies to all cells equally. While this assumption may not hold for these melanoma cell-lines, given the evidence of genetic heterogeneity, the results from qPCR are in complete accord with the PCR results presented here, providing independent support for their validity.

## 8.9 Extension of existing material

### Rationale

PCR forms the very basis for the work reported in this chapter, and yet it was poorly executed in V1, and left open many areas of doubt when it came to interpretation. The key problem was the false parsimony of seeking a single set of thermal cycling conditions suitable for all targets in order to eliminate the often very time-consuming optimisation process. It was successful in that respect, but often yielded artefacts or poor amplification that presented downstream problems. To elucidate the status of the 9p21 region without interference from these issues, PCR conditions were to be individually optimised for each target for use in the V3 experiments. This was greatly facilitated by the advent of thermal gradient PCR machines.

The fall in the costs of DNA sequencing over recent years has meant that a screening process such as that based on SSCP is now no longer warranted, particularly in light of SSCP's known failure to detect sequence variations in all cases. Consequently, for V3 it was decided to omit this step and proceed directly to sequencing of all PCR products obtained. As a result of this decision, there would no longer be a need to amplify *CDKN2A* exon 2 in three segments and new primers would be required.

Microsatellite loci were originally selected for use as markers primarily because of their well-defined relative positions. While their generally high levels of heterozygosity with respect to allele length could not be used to determine allele loss, since no matched normal DNA for the NZM cell-lines was available, known maximum heterozygosity values for the potential markers were considered as a secondary selection criterion in case a future use should arise. However, notwithstanding the lack of matched normal DNA, it was suggested<sup>1687</sup> that microsatellite allele length analysis might still provide some useful information, and this was to be included in the V3 revision.

### Developmental issues

#### *Introduction to a narrative*

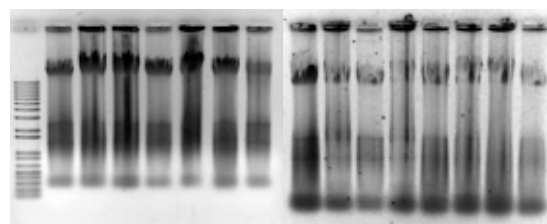
The undertaking of this work was an example of the distinction that must often be drawn between strategy and tactics. The strategy was very simple: grow cells, extract DNA, obtain new primers, optimise them, carry out the PCR, and do the sequencing; obtain fluorescently labelled primers, amplify the designated microsatellites and do the allele analysis. In practice, many of these steps proved to be non-trivial, and several unexpected events occurred that resulted in significant departures from the anticipated course of the research being made, often leading to rewarding discoveries. As a result, the execution of the work is best described as a narrative before embarking on the more traditional methods, results, and discussion format, in which some of the following will be reiterated.

#### *DNA extraction, quality assessment, and quantitation*

It had been hoped that DNA samples stored upon completion of V1 would provide the material necessary to undertake the work required for this revision. To assess the feasibility of this, samples from the available DNA stocks were analysed by agarose electrophoresis and

ethidium bromide staining. Many were of very poor quality, with substantial degradation, or indeed a total absence of genomic DNA in some cases. Since all relevant cell-lines were again in culture to address other aspects of the revision, these would provide a source of new DNA. As cells became available, genomic DNA was extracted according to the method used formerly: trypsinisation, lysis, guanidine denaturation, proteolysis, extraction, ethanol precipitation, dissolution in water, heating to inactivate deoxyribonucleases (DNases), and storage at 4 °C. DNA concentration was determined by spectrophotometry and the ratio of absorbance at 260 nm to that at 280 nm was taken as a measure of DNA quality, as had been the method in V1.

Newly extracted DNA from a number of cell-lines displayed typical OD260/OD280 values of 1.89 or more, better than the 1.8 value considered acceptable. The DNA was standardised to 100 mg/L based on OD260 and was run on 0.8% agarose gels to assess quality [Figure 8–12]. Although the gels were badly overloaded, they showed that high molecular weight DNA was present with little degradation. Substantial amounts of low molecular weight material were present, and its size and banding strongly suggested that this was contaminating RNA. Also of interest was the apparent difference in quantity of genomic DNA present, despite all samples having been standardised.



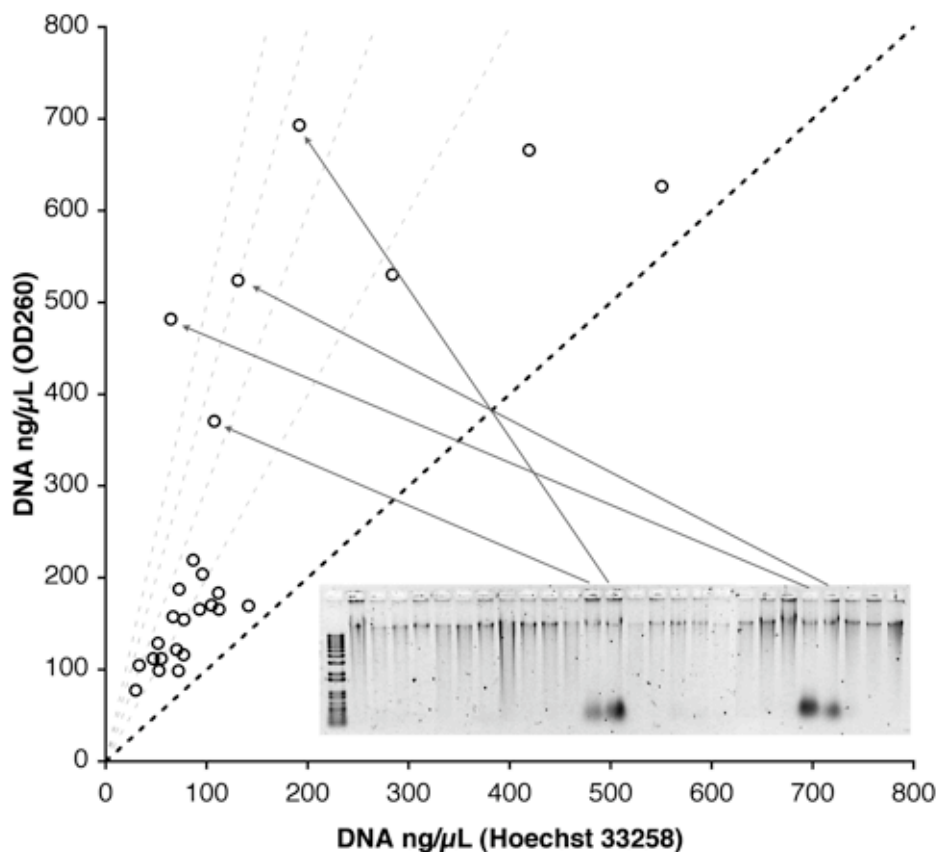
Two ethidium bromide stained 0.8% agarose gels. Lane 1 = 1 kb+ ladder; other lanes are genomic NZM DNA. Cell-line identities are unimportant in the context.

Figure 8–12: Initial V3 genomic DNA extracts

The question arose as to whether the presence of contaminating RNA and the variation in genomic DNA amount seen were related, and there was every reason to think that they might have been. RNA, being a nucleic acid, also absorbs ultraviolet light strongly at 260 nm, so contaminating RNA would cause an inflated figure for DNA concentration to be derived from spectrophotometry. That in turn would result in the standardisation process producing lower than intended stock DNA concentrations.

The reality of this problem was demonstrated when all available genomic DNA extracts were assessed for DNA content both by the OD260 method and by fluorometry using the bisbenzimidazole dye Hoechst 33258, an assay impervious to RNA presence. These extracts were also examined by 0.8% agarose electrophoresis and ethidium bromide staining. The combined results of this study are shown in Figure 8–13.

In all cases, DNA concentration as assessed by spectrophotometry was greater than that assessed by fluorometry, with the spectrophotometric value being ~7.5 times the fluorometric value in the worst case. Samples with the greatest quantity of RNA present, as indicated by ethidium bromide staining, had the greatest discord in values. In three of the four cases of very high RNA concentration, the cell-line was NZM10 or NZ10.1, the other being NZM11. These cell-lines appear to be generators of prodigious RNA.



Main graph: Points show correlation of DNA concentrations as measured by fluorometry and spectrophotometry for NZM genomic DNA extracts. Dashed lines show constant ratios of 1:1 (heavy line), 2:1, 3:1, 4:1, and 5:1  
 Inset figure: Ethidium bromide stained 0.8% agarose gel for these extracts.  
 Arrows show association between gel lanes and points where the measured DNA concentrations are in greater than 4:1 discord.

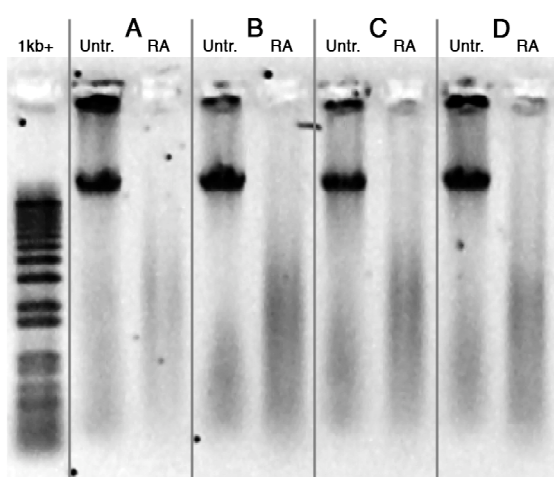
**Figure 8-13: Discord between fluorometric and spectrophotometric assessment of DNA**

There is a lesson here concerning the use of spectrophotometry in quantitating DNA: **OD260 does not give a measure of DNA content at all, it gives a measure of nucleic acid content, and that will include any RNA that is present.** Even where RNA is not detectable by ethidium bromide staining, spectrophotometry can overstate DNA content by 2- or 3-fold. It is suitable only where either the extract is known to be free of RNA, or where only the most approximate of values is satisfactory. For the purposes of standardisation of extracts where RNA contamination may exist, it is manifestly unsuitable.

This raises a very significant point. In V1, all DNA used was extracted with the method above, which does not exclude RNA contamination, and standardised to 100 mg/L by the accepted OD260 method. As a result, stock DNA solutions thought to have been at 100 mg/L concentration almost certainly were lower, and were very probably of concentrations differing from one another. This means that in the PCR reactions that were performed, the amount of DNA template added was uncontrolled, and this may well have contributed to the variability in product band intensities that was reproducibly seen. This casts great doubt over the significance of those observations and the inferences drawn therefrom. The resolution of the status of those earlier results now depends on repetition of the experiments with more

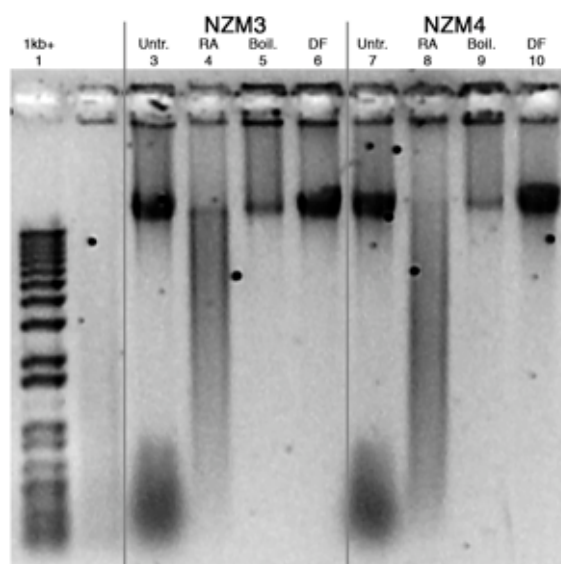
stringently quantitated DNA, whether this is achieved by eliminating the RNA contamination prior to spectrophotometric assay, or the use of a technique such as the Hoechst fluorometric assay that is insensitive to the presence of RNA. In the event, both approaches were adopted.

As a test of the efficacy of removing RNA by enzymatic means, 50  $\mu$ L samples of nominally 100 mg/L DNA from four representative NZM cell-lines were incubated with 500 nL of 20 g/L ribonuclease (RNase) A for 10 min at 65  $^{\circ}$ C, and pairs of untreated and treated DNAs run in adjacent wells on a 0.8% agarose gel {Figure 8–14}. Unexpectedly, the genomic DNA was destroyed. The RNase used was a general laboratory grade product, and clearly retained significant DNase activity. The usual method to rectify this is to boil the enzyme to denature any DNase present, RNase being extremely heat-stable. A further experiment comparing the effects of untreated general grade RNase, boiled (15 min; 100  $^{\circ}$ C) general grade RNase, and a certified DNase-free RNase was performed for DNA from NZM3 and NZM4 {Figure 8–15}.



Ethidium bromide stained 0.8% agarose gel.  
Untr. = untreated; RA = RNase A treated  
A–D = different NZM genomic DNA extracts.

**Figure 8–14: RNase A treatment**



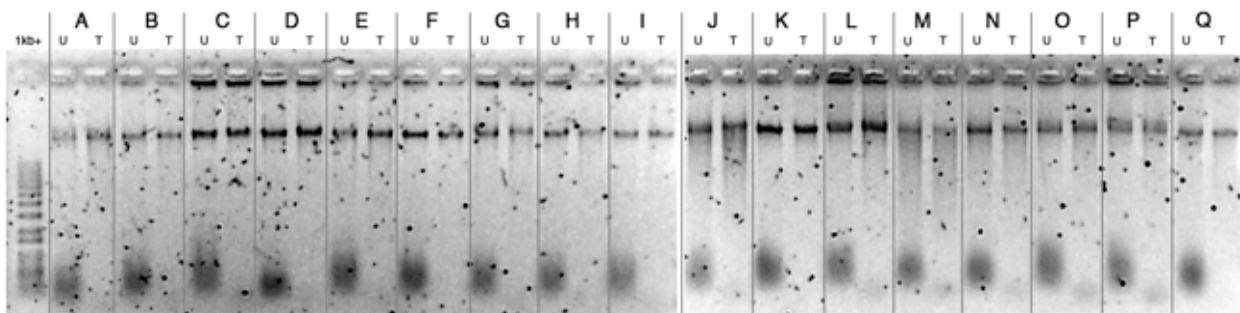
Ethidium bromide stained 0.8% agarose gel.  
Untr. = untreated; RA = RNase A;  
Boil. = boiled RNase A; DF = DNase-free RNase.

**Figure 8–15: RNase treatment variations**

Untreated general grade RNase degraded the genomic DNA from both cell-lines (lanes 4 and 8), while that which had been boiled eliminated the RNA contaminant, but at the expense of a considerable reduction in DNA content (lanes 5 and 9). The proprietary RNase product eliminated the RNA without any discernible effect on DNA quantity (lanes 6 and 10). On the basis of this result a certified DNase-free RNase was purchased {E.13}.

Suitability of this was verified on its arrival by treating 200  $\mu$ L samples of the available nominally 100 mg/L genomic NZM DNA extracts with RNase (500 nL; 65  $^{\circ}$ C; 15 min) and examining pre- and post-treatment samples on 0.8% agarose gels {Figure 8–16}. In all cases, the RNA evident in the pre-treatment samples was rendered virtually undetectable by the treatment without undue degradation of the genomic DNA or reduction in its quantity.

**8: 9p21 status**



Composite of two ethidium bromide stained 0.8% agarose gels.  
 U = Untreated; T = treated with certified DNase-free RNase.  
 A – Q = Different NZM genomic DNA extracts; their identities are unimportant in the context.

**Figure 8-16: DNase-free RNase treatment of NZM genomic DNA extracts**

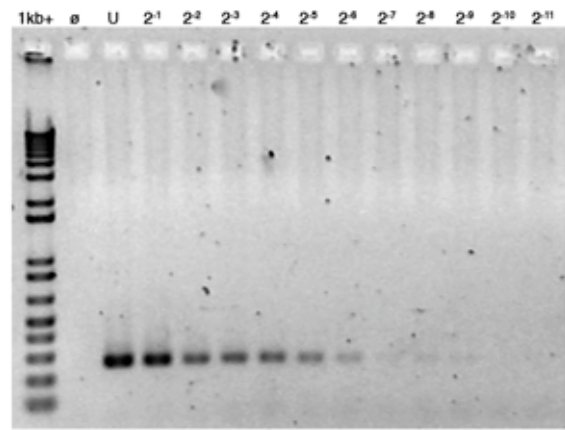
This would seem to be an ideal method to resolve the problem of RNA interference with DNA concentration determination, but caution is still required. While the action of the RNase has eliminated regions of double-strandedness to which the ethidium binds by intercalation, the ribonucleotides produced remain in solution, and with them, their ability to absorb ultraviolet light and interfere with spectrophotometric assessment of concentration. Unless these are removed, the improvement to be had by this treatment is purely cosmetic. The first-line method for purification of nucleic acids once extracted is reprecipitation, but this may not be of assistance here as the monomeric nucleotides that result from ribonuclease treatment are insoluble in the alcohols typically used, and would coprecipitate with the genomic DNA. Gel purification or ultrafiltration or a similar molecular weight dependant method could be employed, after which concentration assessment by spectrophotometry might be reliable. An additional complication is that a highly stable active ribonuclease has been introduced into the extracts, and this could interfere with downstream applications such as reverse-transcriptase-PCR, if such were to be undertaken.

In consequence of these investigations, the method of DNA extraction was altered to incorporate DNase-free RNase digestion and an additional chloroform extraction step. Quantitation was by Hoechst-based fluorometry {See 'DNA extraction, quantitation, standardisation, and storage', below}.

#### ***Sensitivity of agarose gels in detecting template heterogeneity***

Analysis of the V1 results depended strongly on the interpretation of intermediate levels of amplification being indicative of altered target prevalence, as might occur with altered copy number or the presence of multiple sub-populations differing in their possession of the target. Without the modifications associated with quantitative real-time analysis, PCR is generally considered to be non-quantitative, and ethidium bromide stained agarose gels inadequate for detection of differences in product quantity. To determine if there was any justification in the basis for the interpretation of the PCR results made in V1, an experiment was performed involving an attempt to amplify a target from DNA templates comprising differing proportions of DNA from a cell-line known to contain the target and from one where it was known to be absent. Given the exponential amplification inherent in PCR, an exponential dilution gradient

was employed. The resulting ethidium bromide stained agarose gel is shown in Figure 8–17. While the relationship is non-linear, possibly due to the departure from exponential amplification that occurs during PCR cycling, this experiment demonstrates that if genomic DNA were extracted from a culture where 98% of cells were deleted for the target, but 2% retained it, a definite band with intensity markedly less than control levels would still be observed. While the presence of a weak bands would not prove heterogeneity within the population from which the genomic DNA was extracted, it is entirely consistent with it, and to that extent the basis for interpretation of the intermediate levels of amplification seen in V1 appears justified.



Ethidium bromide stained 1.5% agarose gel. ø = no template; U = undiluted NZM4 template (intact *CDKN2A* exon 1β target); Lanes 4 – 14 = serial 2-fold dilution of NZM4 DNA with NZM1 DNA (deleted for target).

**Figure 8–17: Detecting heterogeneity**

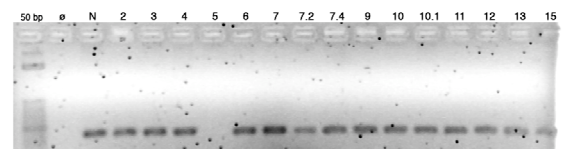
#### PCR amplification of NZM5 DNA

Simultaneously with progress toward producing high quality DNA for analysis, experiments were performed to begin deletion mapping of the 9p12 – 9p23 region by PCR. The first such experiment for *CDKN2A* exon 1 brought to light an inconsistency with earlier results in that no product was seen for NZM5, whereas it had been during V1. NZM5 DNA had proved to be very difficult to use as a PCR template during V1, and this had been ascribed to the considerable amount of melanin that co-purified with the DNA (Figure 8–18). Many different extraction techniques were tried with the intention of isolating purer DNA, but none met with success; all NZM5 DNA ever extracted has been very dark in colour. By chance alone, one extraction during V1 yielded NZM5 DNA that supported PCR, and that formed the basis for the investigations undertaken. Beyond establishing that NZM5 DNA contained something that inhibited the PCR, nothing further was done.



**Figure 8–18: NZM5 DNA pellet**

The ability of the available panel of NZM DNA extracts to support PCR was tested using primers for part of the *HBB* gene, routinely used as a positive reaction control (Figure 8–19). It seemed that again, NZM5 DNA was not supporting PCR amplification, but now the issue would need to be resolved.



Ethidium bromide stained 1.5% agarose gel. ø = no template; N = control template; 2 – 15 = various NZM templates as labelled. Note: No product seen for NZM5.

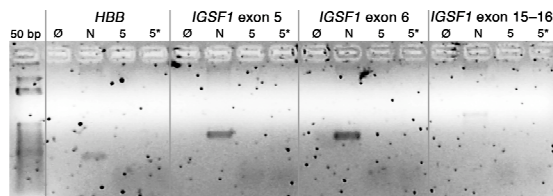
**Figure 8–19: Amplification of *HBB***

## Human metastatic melanoma in vitro

To test for the possibility that the newly extracted NZM5 DNA was deleted for the *HBB* gene, an experiment was performed using primers from an unrelated project whose subject was the inhibin binding protein gene, *IGSF1*. Also included was newly isolated NZM5 DNA that had been further processed with three phenol and two chloroform extractions in an attempt to improve its purity and restore PCR function [Figure 8–20]. No amplification for the NZM5 DNA extracts was seen for any target, despite amplification of all targets from normal DNA, albeit weakly in one case. The failure of NZM5 DNA to support PCR is not target specific.

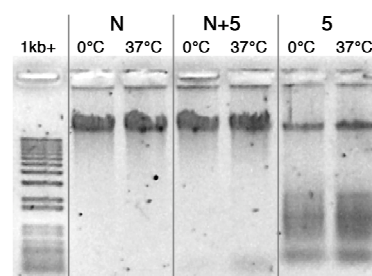
To explore the possibility that extracted NZM5 DNA contains a nuclease that may degrade template or primers, an experiment was performed wherein normal DNA was incubated, on ice and at 37 °C, for 20 minutes in the presence of 10% NZM5 DNA [Figure 8–21]. While the amount of low molecular weight material did increase in the 37 °C treated sample, it was not consistent with the presence of a nuclease of sufficient activity to interfere with PCR, nor was the amount of genomic DNA remaining noticeably diminished. Furthermore, autodigestion of NZM5 extracts had never been observed. These facts essentially ruled out the possibility of a nuclease activity in extracted NZM5 DNA as a cause of non-amplification.

Since DNA was normally extracted from near confluent cultures, an experiment was performed to determine if DNA from actively proliferating NZM5 cultures would support PCR. Simultaneously, different extraction methods were tested: phenol/chloroform extraction, the standard guanidine and chloroform method, and a genomic DNA isolation kit from Promega based on salt precipitation of proteins [Figure 8–22]. Only the control DNA template supported PCR. The issue with NZM5 is not dependent on either time in culture or mode of extraction.



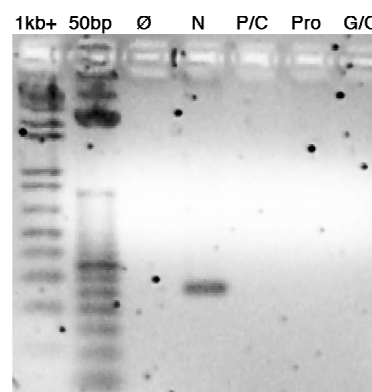
Ethidium bromide stained 1.5% agarose gel. Primer sets for *HBB*, and *IGSF1* exons; Ø = no template; N = control template; 5 = normally extracted NZM5 DNA template; 5\* = re-extracted NZM5 DNA template.

**Figure 8–20: NZM5 PCR target trials**



Ethidium bromide stained 1.5% agarose gel. N = control DNA; 5 = NZM5 DNA; N+5 = control DNA + 10% v/v NZM5 DNA.

**Figure 8–21: NZM5 nuclease test**

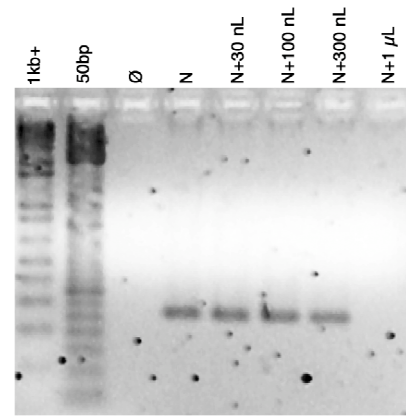


Ethidium bromide stained 1.5% agarose gel. PCR with *HBB* primer set. Lane 1 = 1kb+ ladder; lane 2 = 50 bp ladder; Ø = no template; N = control template; P/C = phenol/chloroform extraction; Pro = Promega kit extraction; G/C = guanidine/chloroform extraction.

**Figure 8–22 : NZM5 short time in culture DNA**



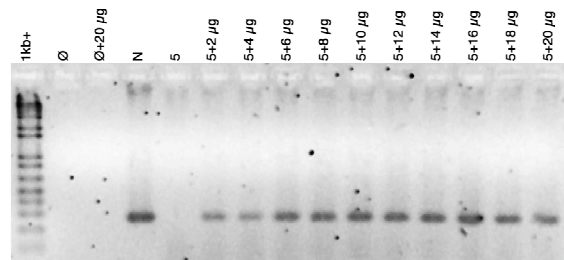
To determine if NZM5 DNA extracts contain an inhibitor of PCR, rather than the failure of amplification being due to the nature of NZM5 DNA itself, an experiment was undertaken where increasing amounts of NZM5 DNA extract were used to attempt to poison a working reaction involving control DNA and *HBB* primers [Figure 8–23]. Addition of up to 100 nL of nominally 100 mg/L NZM5 DNA extract did not appear to affect amplification of the target; addition of 300 nL reduced it visibly; addition of 1  $\mu$ L eliminated it. It can be concluded that NZM5 DNA extracts contain a titratable inhibitor of the PCR.



Ethidium bromide stained 1.5% agarose gel. PCR with *HBB* primer set. Ø = no template; N = control template; N + x = control template spiked with stated volume of NZM5 DNA extract.

Figure 8–23: NZM5 inhibitor test

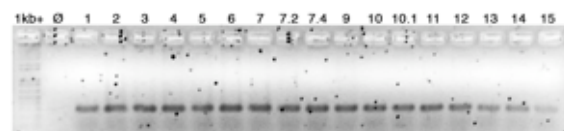
A search of the literature revealed a paper that was in press during V1 in which Eckhart et al.<sup>1555</sup> reported that melanin reversibly binds *Taq* polymerase, inhibiting its activity at concentrations no greater than 200  $\mu$ g/L, and further, that it co-purifies with DNA. Melanin had long been considered a likely cause of the problem with NZM5, and here was an explanation consistent with observations. The remedy found by Eckhart was to include BSA in the PCR reaction to compete with *Taq* for binding to melanin, and so protect it from inhibition. An experiment was performed to determine if the addition of BSA to NZM5 PCR reactions would restore amplification [Figure 8–24]. With no addition of BSA, the reaction was inhibited as expected, but with the addition of even the smallest amount of BSA tested, 2  $\mu$ g, the reaction was rescued. No enhancement was seen with additions above 6  $\mu$ g.



Ethidium bromide stained 1.5% agarose gel. PCR with *HBB* primer set. Ø = no template; N = control template; 5 = NZM5 template; template+x = stated mass of BSA included.

Figure 8–24: NZM5 BSA gradient

To confirm that the addition of BSA would not adversely affect PCR using DNA from the other NZM cell-lines, an experiment seeking to amplify the *HBB* target from each NZM was performed with 5  $\mu$ g of BSA included in each 25  $\mu$ L reaction [Figure 8–25]. Amplification was successful in all cases, although it was weak in NZM15. At the time this experiment was performed the DNA in use was still quantitated by the OD260 method, and the variable amplification seen may be attributable to different template concentrations.



Ethidium bromide stained 1.5% agarose gel. PCR with *HBB* primer set. Ø = no template; 1 – 15 = NZM templates as stated.

Figure 8–25: NZM panel with BSA

This then would seem to be the resolution of the problem with NZM5 DNA and PCR amplification. The addition of 5  $\mu$ g, and ultimately 10  $\mu$ g of BSA per 25  $\mu$ L reaction was adopted for all subsequent reactions.

There is a tremendous irony here: the many attempts made to obtain ever purer NZM5 DNA extracts seeking to enable PCR amplification probably served only to eliminate more and more contaminating protein, while the melanin present continued to co-purify with the DNA. Each "improvement" would have resulted in less protein remaining to sequester the melanin and greater subsequent inhibition of the *Taq* polymerase: the purer the DNA was made, the less well it would support PCR. In all probability, it was a technically poor DNA extraction, with significant protein contamination, that fortuitously allowed NZM5 PCR during the V1 experimentation.

This discovery raises another question over the V1 PCR work, however. Several NZM cell-lines apart from NZM5 produce discernible melanin, particularly NZM7 and NZM7.2, and others may do so to a less obvious degree. Extracts from these cell-lines therefore contain an unknown concentration of an inhibitor of *Taq* polymerase, and this too may have contributed to the reproducible differences in amplification seen among cell-lines. The inclusion of BSA in the definitive V3 work should eliminate this source of uncertainty.

### *Primer issues*

#### **Review of primer suitability**

With the move to direct sequencing of PCR products and the abandonment of SSCP came a need for primers to amplify exon 2 of *CDKN2A* in its entirety, rather than as small overlapping segments. While investigating possible primers for this, consideration was given to the locations of the other published exonic primers used in V1 with respect to known regions of interest in their target genes. The V1 primers for *CDKN2A* exon 3 were satisfactory, but in addition to a new set being needed for exon 2, those for exon 1 and 1 $\beta$  needed attention. While the V1 primers for *CDKN2B* exon 2 were acceptable, those for exon 1 were thought to be poor. Attempts to address these issues by designing new primers using the Primer3 application met with variable success.

#### ***CDKN2B* exon 1**

While the V1 primer pair for *CDKN2B* exon 1 bracket the start codon and the normal splice junction, it does not encompass either the entire 5' region from the start of the exon to the ATG start codon, or an alternative splice site. A new pair of primers was designed using the Primer3 application and purchased. Once the annealing temperature had been optimised, PCR performed using these primers was very successful.

#### ***CDKN2A* exon 1 $\beta$**

The V1 *CDKN2A* exon 1 $\beta$  forward primer is placed 23 nucleotides 3' of the initiating ATG codon, and so the resulting amplicon does not span the entire coding region of the exon. The importance of obtaining sequence information for this region was well understood, but despite exhaustive attempts to optimise reagent and cycling conditions for two alternative pairs of

computer-designed primers, no successful PCR was achieved. Reluctantly, the work for the V3 revision proceeded using the original primers, and the status of the 5' end this gene remains unknown.

#### **CDKN2A exon 1**

The V1 *CDKN2A* exon 1 forward primer overlaps the ATG start codon, and the amplicon produced by this and its reverse primer does not encompass the normal splice site or the TGA terminator used in a splice variant. New primers were designed and these yielded good results during optimisation. However, when applied to the NZM panel several inconsistencies appeared. Firstly, DNA from some cell-lines that could readily be amplified with the V1 primers, could not with the new primers. Secondly, the same type of consistent variation in band intensity on agarose gels as was widespread in the V1 work was again seen, despite the use of rigorously standardised, high quality DNA and the addition of BSA. Thirdly, inexplicably, it proved impossible to replicate the PCR for the NZM panel that had been successful in most cell-lines immediately after optimisation. It is thought that a primer site polymorphism in some cell-lines may be responsible for the discord and weak amplification seen, but with limited time available to pursue this, and the larger problem presented by the failure of the primers on attempted replication, the definitive work for this locus in V3 was performed using the V1 primers, after specific optimisation of reaction conditions.

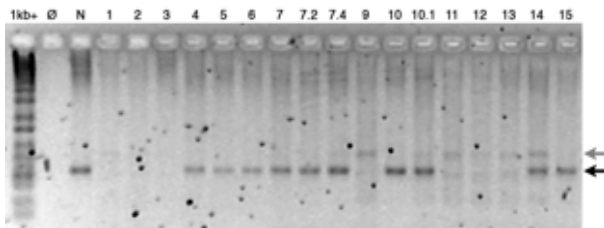
#### **CDKN2A exon 2**

The search for suitable primers for *CDKN2A* exon 2 began in the literature, where a paper from Fagnoli et al.<sup>343</sup> appeared to offer a solution as the primers they had used spanned the region of interest. These were purchased and optimisation attempted, but no combination of additional magnesium, the proprietary 'Q' PCR enhancement reagent (thought to be predominantly betaine), or annealing temperatures from 56 °C to 66 °C produced even the faintest product. The sequence of their primers was inspected more closely and a serious flaw was found in the design of the reverse primer in that it contains a very stable hairpin {Figure 8–26}. This was corroborated as potentially problematical by use of the Primer3 program, which, when constrained to consider this primer, rejected it for multiple reasons. A further experiment was conducted seeking to replicate the PCR conditions of Fagnoli et al. Their protocol included 5% DMSO in the reaction mixture, so that, 1.5 mol/L betaine, 'Q', and water as an additive control were tested in conjunction with their thermal cycling programme: 95 °C x 10 min; 35 x {95 °C x 30 s; 61 °C x 1 min; 72 °C x 1 min}; 72 °C x 10 min (; 15 °C x ∞) The surprising result was that only for the water additive control was amplification seen. Further use of this primer was abandoned, and Primer3 was used to search for an alternative set. A highly rated primer pair was found that shared the forward primer of the Fagnoli pair but replaced the questionable one, and this pair delimited a suitable 491 bp amplicon. The optimisation process revealed that an addition of DMSO facilitated amplification, probably due to the high G : C content of the promoter region.



Figure 8–26: Fagnoli primer hairpin

When DNA from the NZM panel was amplified using the conditions found optimal for control DNA, the need for further optimisation was revealed {Figure 8–27}: apparently non-specific products were present, particularly where the intended target was thought to be deleted. The ~700 bp product from NZM9 was sequenced and identified as coming from chromosome 12q, and an inspection of the adjacent areas revealed the likely false primer binding sites {Figure 8–28}. The band is therefore non-specific.



Ethidium bromide stained 1.5% agarose gel. Ø = no template; N = control template; 1 – 15 = NZM templates as stated. Black arrow shows position of specific product; grey arrow shows position of non-specific product.

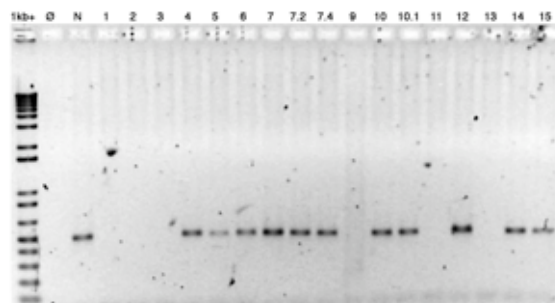
Figure 8–27: *CDKN2A* exon 2 non-specificity

```
TGCACACAGCCTTAGGAAACTGGAAAGGGAGGGAGGGTGTACTGAAGGAGGGGGA
GAGAAATACTGAGTGGGCGTTAGGAGGGAGAGGGCTTCACACAGGCCCTCAATGC
TTGGGCAGGAACCTGACAGACAGGACAGGAGACAGCCCTTCTAGACCAGAGTGAT
GTGAGCTCTGACGGTAAGTTCATGAAGACAGGTCGACTGTCTTGTTTAATCT
GAATCCCCGGGGCCCGACAGAGGATCTGGCAAACCTAGGCATCATGGAGAATC
ACAGAAGAGTGGTTGGAAATGACAGAAACGAGGCCCTGCTGCTTGAAGGCATC
GACTCCTCAGAGCAAGCCTGTGAGTGGACAGCATGGTTCCCTTTACAGATGAG
GACACTGAGGCAGCCGACGTAATGACTGCCACCACCATGCAGCTGGCGAGAG
GCAGGGCTGGGGCTGACCCGTGATGGCCCTGCTACAGCAGCAAGCATGTATTC
AGCACCTACTGTGCACCATGCACGGAAGTCTCATTGCAGTGGGGAAGCGGGTGA
TGAAACAAAGACGTGGATGTGTAACCGTGAATAAATACCTAAGGCTGCCAGTGC
GTGTTGATGAGGCTGTGATGGAACACACAGGGGCGGTGGCGGAGGTGACTGCA
GAGGGAAGAGGGATGGTGGCCCTCACACGGCCAAGATCTGAGAAAAGGCCCTGAC
```

Region of chromosome 12q erroneously amplified by *CDKN2A* exon 2 revision 2 primers in the absence of the intended target. Highlighted areas are the likely false primer binding sites. The distance spanned is 679 nucleotides, consistent with the product size seen by electrophoresis.

Figure 8–28: Non-specific product from 12q

This type of issue is not something that is detectable in the normal optimisation process since the target must be present to allow the optimisation to be undertaken. There was clearly a need to refine the PCR conditions further, and the approach taken was to seek an annealing temperature high enough to prevent primer binding to the 12q region when the intended target was absent, but not so high as to prevent correct binding when the target was present. This trial employed as templates normal DNA, NZM9 DNA, where only the non-specific product had been seen, NZM14 DNA, with both specific and non-specific products, and NZM15 DNA, with only the intended product. It was determined that an annealing temperature of 56 °C would provide the specific amplification required, and this proved to be successful when applied to the complete NZM panel {Figure 8–29}.



SYBR-green stained 1.5% agarose gel. Ø = no template; N = control template; 1 – 15 = NZM templates as stated.

Figure 8–29: *CDKN2A* exon 2 specificity

This experiment was performed some months after the issue of non-specificity in the absence of the target was identified. It demonstrated an alarming discord with respect to the NZM12 result, as although this cell-line was believed to have a deletion in this region, a product was seen. Ultimately, by surveying NZM12 DNA from all earlier extractions, and that from a different researcher, and with the microsatellite allele length analyses then becoming available, it was determined that what was thought to have been NZM12 DNA, was not. This prompted a very careful investigation to ensure that wherever possible, some distinction could be drawn



between each cell-line in culture and every other, be it phenotypic, DNA sequence variation, deletion pattern, ploidy, or microsatellite allele length {See 'Discrimination among the cell-lines' on page 8–35}. New DNA was then extracted from all such verified lines and used subsequently.

One potentially positive outcome of this was the very strong recommendation being made that all cell-lines currently maintained by the ACSRC be genotyped, and that this be done as a matter of course during the establishment of any new cell-line. This information would then provide a reference against which any cells in culture could be compared at any future time to determine their identity unambiguously. In the particular case of NZM12, once the bona fide cell-line was established, the expected deletion was again found.

### **Microsatellite primers**

Although many of the primers used for the microsatellite targets were designed before the advent of software tools and could possibly be improved upon, no attempt was made to do so. PCR conditions were optimised for their use in the V3 work, but in some cases issues such as poor amplification and primer artefacts remained. Even so, the levels of amplification achieved allowed a good assessment of target presence, and products obtained using fluorescently labelled variants of these primers were satisfactory for the genotyping that was performed.

### **Methods in brief**

#### *Cell culture*

NZM cell-lines were recovered from cryogenic storage and brought into passage culture as described in the original work. In addition, before definitive experimental work was undertaken, all were tested for mycoplasma contamination {Method 33} and confirmed to be negative, but notwithstanding this, were treated with ciprofloxacin {Method 34}. During the course of the experimentation, it was determined that with one exception, each cell-line in culture apart from those with a known common genetic origin, differed in some reproducibly measurable respect from all others. While this does not confirm absolute identity, it does indicate that each is unique within the panel. The exception is the cell-line NZM10.1, and doubt exists over its authenticity. While the results obtained for this cell-line are included, they should be considered provisional at best, and may well be invalid. This is discussed more fully elsewhere {See 'Doubt over NZM10.1 authenticity', on page 8–36}.

#### *DNA extraction, quantitation, standardisation, and storage*

The methods for genomic DNA processing used in the original work were modified in light of the discovery of the high level of contaminating RNA that these produced and the consequences for DNA quantitation that this has. The following modifications were made:

1. Genomic DNA was always maintained in TE buffer (Solution 20), never water, to mitigate double-strand breakage catalysed by magnesium ions.
2. DNase-free RNase (E.13, 2  $\mu$ L) was added to the DNA suspension made after washing of the DNA pellet.
3. This DNA suspension was incubated (50 °C, 1 h) to denature any endogenous DNases as before, but also to allow the added RNase to digest any contaminating RNA.

4. After this incubation, a further chloroform extraction was performed, followed by sodium acetate/isopropanol precipitation {Method 37}, washing in ethanol (80% v/v, 1 mL), drying, resuspension in an appropriate volume of TE buffer {Solution 20}, and incubation (50 °C, 1 h) to dissolve.
5. DNA quantitation was always achieved by fluorometry {E.10} in duplicate using a commercial kit based on Hoechst 33258 {E.11}. A duplicated 7 point calibration curve was established on each occasion using the supplied standard concentration calf thymus DNA.
6. Standardisation was with TE buffer to 50 mg/L.

### **PCR**

Optimisation of thermal cycling parameters for individual primer pairs was performed using a gradient thermal cycler {E.10}, and wherever possible experimental reactions were carried out in the same or an identical model machine. All 25  $\mu$ L reactions used materials from a Qiagen kit {E.11}, supplemented with magnesium chloride (3 mmol/L final concentration), 10  $\mu$ g of BSA {E.15} and, in one instance DMSO. The details of primers, thermal cycling programs and additives for each reaction are given in Table 8–2, as they are more properly considered results of experimentation rather than methods defined in advance.

### **DNA sequencing**

Purification of PCR products prior to sequencing was performed as in the original work with resin spin-columns. All PCR products from *CDKN2A* and *CDKN2B* were sequenced without prior screening by SSCP. Initially, this was done in one direction only, but where an anomaly was detected, it was confirmed by reverse sequencing, if possible. Where reverse sequencing was not practicable due to the proximity of the reverse primer to the anomaly, forward sequencing was repeated using newly amplified template. All steps beyond preparation of template DNA and sequencing primer were performed either by the Genomics Unit at the University of Auckland, or by the Allan Wilson Centre Genome Service at Massey University.

### **Microsatellite analysis**

Forward PCR primers of identical sequence to those used in the amplification of the microsatellites D9S1853, D9S974, and D9S157 for the purposes of deletion analysis, but with the addition of a 5' fluorescent 6-carboxyfluorescein (6-FAM) tag, were purchased. These were used to amplify NZM genomic DNA in conjunction with their respective unlabelled reverse primers for cell-lines where the target had previously been determined to be present. These were purified with resin spin-columns and quantitated by spectrophotometry. Samples of each in several dilutions were despatched to the Genomics Unit, University of Auckland, for separation by capillary electrophoresis and analysis for allele length by the inclusion of labelled standards in each sample.

## **Results**

### ***Optimal PCR conditions***

The primer sequences and optimal thermal cycling conditions used in the V3 work are summarised in Table 8–2.

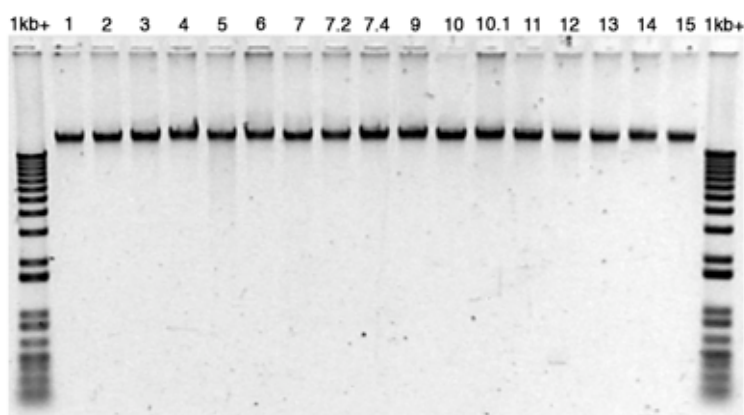
Target	Primers (5' → 3')	Size	Cycling
D9S1853	GAT CCA GCC TCA CTG AA TTG GGC ATA GAA TTT TTA CTT T	~253	94 °C x 3 min; 30 x {94 °C x 15 s; 54 °C x 15 s; 72 °C x 30 s}; 72 °C x 5 min; 15 °C x ∞
D9S161	GCT GCA TAA CAA ATT ACC ACA ATC CCC GGA AAC AGA TAA TA	~104	94 °C x 3 min; 30 x {94 °C x 15 s; 56.5 °C x 15 s; 72 °C x 30 s}; 72 °C x 5 min; 15 °C x ∞
D9S171	AGC TAA GTG AAC CTC ATC TCT GTC T ACC CTA GCA CTG ATG GTA TAG TCT	~159	94 °C x 3 min; 30 x {94 °C x 15 s; 57 °C x 15 s; 72 °C x 30 s}; 72 °C x 5 min; 15 °C x ∞
CDKN2B Exon 1*	ATG CGT CCT AGC ATC TTT GG TTT GCT GGG TAA AAG CCT GT	835	94 °C x 3 min; 32 x {94 °C x 30 s; 55 °C x 15 s; 72 °C x 1 min}; 72 °C x 5 min; 15 °C x ∞
CDKN2B Exon 2	GGC CGG CAT CTC CCA TAC CTG TGT GGG CGG CTG GGG AAC CTG	345	94 °C x 3 min; 30 x {94 °C x 15 s; 64 °C x 15 s; 72 °C x 30 s}; 72 °C x 5 min; 15 °C x ∞
CDKN2A Exon 1β	TCC CAG TCT GCA GTT AAG G GTC TAA GTC GTT GTA ACC CG	440	94 °C x 3 min; 30 x {94 °C x 15 s; 57 °C x 15 s; 72 °C x 30 s}; 72 °C x 5 min; 15 °C x ∞
D9S1748	CAC CTC AGA AGT CAG TGA GT GTG CTT GAA ATA CAC CTT TCC	~140	94 °C x 3 min; 30 x {94 °C x 15 s; 57 °C x 15 s; 72 °C x 30 s}; 72 °C x 5 min; 15 °C x ∞
D9S942	GCA AGA TTC CAA ACA GTA CTC ATC CTG CGG AAA CCA TT	~115	94 °C x 3 min; 30 x {94 °C x 15 s; 56 °C x 15 s; 72 °C x 30 s}; 72 °C x 5 min; 15 °C x ∞
D9S974	GAG CCT GGT CTG GAT CAT AA AAG CTT ACA GAA CCA GAC AG	~200	94 °C x 3 min; 30 x {94 °C x 15 s; 57 °C x 15 s; 72 °C x 30 s}; 72 °C x 5 min; 15 °C x ∞
CDKN2A Exon 1	GGG AGC AGC ATG GAG CCG AGT CGC CCG CCA TCC CCT	203	94 °C x 3 min; 30 x {94 °C x 15 s; 67 °C x 15 s; 72 °C x 30 s}; 72 °C x 5 min; 15 °C x ∞
CDKN2A Exon 1*	AGT CCT CCT TCC TTG CCA AC ACT CCC TTT TTA TCC CAA ACG	814	94 °C x 3 min; 30 x {94 °C x 15 s; 58 °C x 15 s; 72 °C x 30 s}; 72 °C x 5 min; 15 °C x ∞
CDKN2A Exon 2*	GGA AAT TGG AAA CTG GAA GC TCA GGG TAC AAA TTC TCA GAT CA	491	94 °C x 3 min; 32 x {94 °C x 30 s; 55 °C x 15 s; 72 °C x 1 min}; 72 °C x 5 min; 15 °C x ∞
CDKN2A Exon 3	CCG GTA GGG ACG GCA AGA GA CTG TAG GAC CCT CGG TGA CTG ATG A	169	94 °C x 3 min; 32 x {94 °C x 30 s; 54 °C x 30 s; 72 °C x 30 s}; 72 °C x 5 min; 15 °C x ∞
D9S1749	AGG AGA GGG TAC GCT TGC AA TAC AGG GTG CGG GTG CAG ATA A	~140	94 °C x 3 min; 30 x {94 °C x 15 s; 63 °C x 15 s; 72 °C x 30 s}; 72 °C x 5 min; 15 °C x ∞
D9S162	TGA CCA GTT AAG GTT CCT TTC ATT CCC ACA ACA AAT CTC CT	~181	94 °C x 3 min; 30 x {94 °C x 15 s; 55 °C x 15 s; 72 °C x 30 s}; 72 °C x 5 min; 15 °C x ∞
D9S157	CAT TTC ATC TGG TAG ACC CA TTT GAT TGG CTG GAA GTA GA	~205	94 °C x 3 min; 32 x {94 °C x 15 s; 55 °C x 15 s; 72 °C x 30 s}; 72 °C x 5 min; 15 °C x ∞
D9S156	ATC ACT TTT AAC TGA GGC GG AGA TGG TGG TGA ATA GAG GG	~134	94 °C x 3 min; 30 x {94 °C x 15 s; 56 °C x 15 s; 72 °C x 30 s}; 72 °C x 5 min; 15 °C x ∞
D9S274	TTG CTG TTC AAG TGA TCC TT TAC CTC ATG GCA ATT TCT TC	~141	94 °C x 3 min; 30 x {94 °C x 15 s; 55 °C x 15 s; 72 °C x 30 s}; 72 °C x 5 min; 15 °C x ∞
HBB	GAA GAG CCA AGG ACA GGT AC CAA CTT CAT CCA CGT TCA CC	268	94 °C x 3 min; 30 x {94 °C x 15 s; 56 °C x 15 s; 72 °C x 30 s}; 72 °C x 5 min; 15 °C x ∞

\* = primers developed for V3 work; other primers are as for V1. All reaction mixtures included additional magnesium to a final concentration of 3 mmol/L. All except for *CDKN2A* exon 2\* included 'Q' PCR enhancer, and that included 5% v/v DMSO. Conditions for *CDKN2A* exon 1\* are included although these primers were not used for definitive work owing to unresolved problems of inconsistent amplification between experiments.

Table 8–2: V3 PCR primers and conditions

### Genomic DNA preparation

Figure 8–30 shows samples of the standardised 50 mg/L NZM genomic DNA working stocks used for the definitive V3 PCR, sequencing, and microsatellite experiments, and attests to the efficacy of the new methods of extraction and quantitation adopted.



SYBR-green stained 0.8% agarose gel. 1 – 15 = NZM templates as stated.

Figure 8–30: Standardised genomic DNA used in experimentation

PCR

The use of SYBR-green DNA stain was found to provide superior detection with lower backgrounds than ethidium bromide. In addition, it is believed to be of lower toxicity, reducing both the exposure risk and safe disposal requirements.

Images of SYBR-green stained 1.5% or 3% agarose gels of the results of PCR for all NZM templates and all 9p12 – 9p23 targets are shown in Figure 8–31. In general, the level and specificity of amplification seen and distinction visible between intact and deleted loci is excellent, but in some cases there appears to be variability in amplification among cell-lines. With the exception of the D9S1749 result, primer artefacts were negligible. This was also seen in the V1 work and could not be eliminated by optimisation of PCR conditions; it is thought to represent an inherent deficiency in the published primers used.

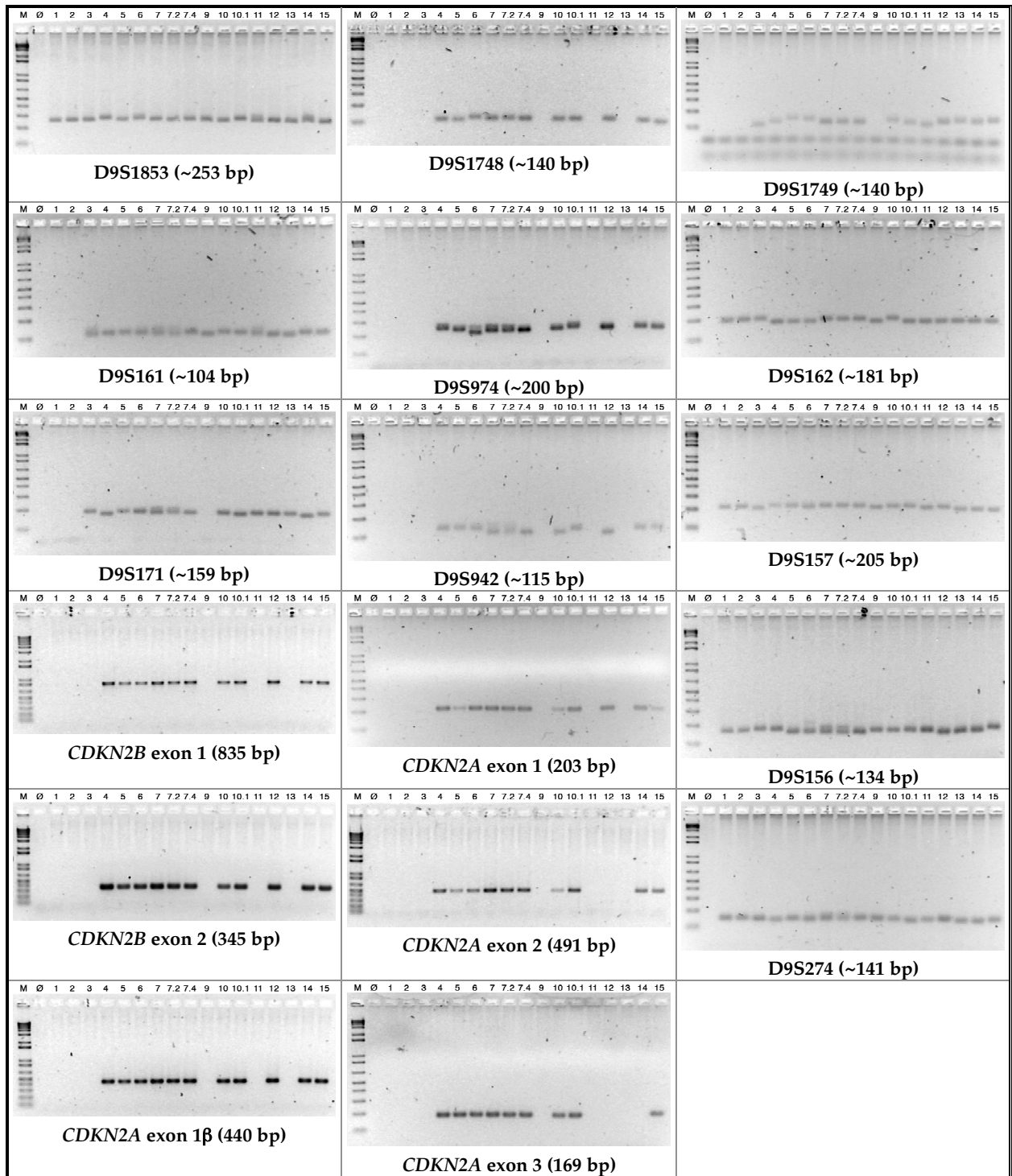
The deletion map derived from these data is shown in Table 8–3.

	1	2	3	4	5	6	7	7.2	7.4	9	10	10.1	11	12	13	14	15
D9S1853	+	+	+	+	+	h	+	+	+	+	+	+	h	+	+	h	+
D9S161	-	-	h	+	+	h	h	h	+	+	+	+	+	+	+	+	+
D9S171	-	-	+	+	+	h	h	h	+	-	+	+	+	+	+	+	+
CDKN2B exon 1	-	-	-	+	+	+	+	+	+	-	+	+	-	+	-	+	+
CDKN2B exon 2	-	-	-	+	+	+	+	+	+	-	+	+	-	+	-	+	+
CDKN2A exon 1β	-	-	-	+	+	+	+	+	+	-	+	+	-	+	-	+	+
D9S1748	-	-	-	+	+	+	+	+	+	-	+	+	-	+	-	+	+
D9S942	-	-	-	+	+	+	+	h	h	-	+	h	-	+	-	+	+
D9S974	-	-	-	h	+	h	h	h	+	-	+	h	-	+	-	+	+
CDKN2A exon 1	-	-	-	+	±	+	+	+	+	-	±	+	-	+	-	+	±
CDKN2A exon 2	-	-	-	+	±	+	+	+	+	-	±	+	-	-	-	+	+
CDKN2A exon 3	-	-	-	+	+	+	+	+	+	-	+	+	-	-	-	-	+
D9S1749	-	-	-	+	+	+	+	+	+	-	+	+	+	+	+	+	+
D9S162	+	+	+	+	+	+	+	+	+	+	+	+	+	+	+	+	+
D9S157	+	+	+	+	+	+	+	+	+	+	+	+	+	+	+	+	+
D9S156	+	+	+	+	+	h	h	h	+	+	+	+	+	+	+	+	+
D9S274	+	+	+	+	+	+	+	+	+	+	+	+	+	+	+	+	+

Column headings denote NZM cell-line. Row headings denote PCR target sequences in physical order. + = present, ± = present but reproducibly weak amplification; h = present and heterozygosity suggested; - = probable homozygous deletion of target locus. Note: microsatellites shown as + may be homo-, hemi-, or heterozygous.

Table 8–3: Deletion map of 9p12–9p23 region based on PCR (V3)





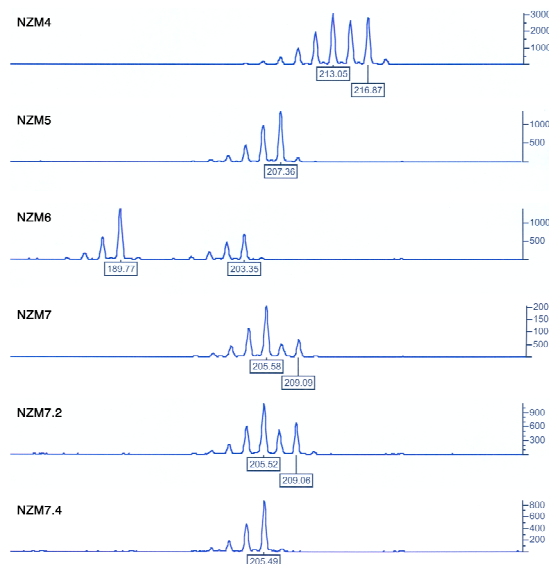
SYBR-green stained agarose gels. Lanes: M = 1 kb+ marker;  $\emptyset$  = control without template DNA; 1–15 = corresponding NZM DNA template. Expected amplicon sizes are given in captions, approximate only for microsatellites.

Figure 8–31: 9p12–9p23 PCR results (V3)

8: 9p21 status

**Microsatellite analysis**

PCR using 5'-6-FAM labelled forward primers proceeded with results of similar quality to those seen with unlabelled primers when inspected by agarose gel electrophoresis and SYBR-green staining. Examples of the quality of the electropherograms typically produced by capillary separation are shown in Figure 8–32. Concordant results were obtained with differing template dilutions, and between repeated analyses of separately amplified templates. No analyses contained more than two distinct identifiable allele lengths, suggesting that cross-contamination and unintentional co-culturing of cell-lines was not occurring on a significant scale. Present in the analyses were stutter banding and "plus-A" artefacts caused by the addition of an untemplated A nucleotide during PCR. These are typical of this type of analysis and in no instance did these features prevent a confident assignment of allele size.



Boxed figures are the amplicon lengths calculated by interpolation from differently labelled internal size standards. Note the allele loss in NZM7.4 with respect to the parental NZM7 cell-line and the NZM7.2 co-sub-clone.

**Figure 8–32: Genotyping examples (D9S974)**

Inferred amplicon lengths were consolidated into allele groups as shown in Table 8–4. The results of the microsatellite analysis of NZM cell-lines are shown in Table 8–5.

Label	D9S1853			D9S974			D9S157		
	n	l	range	n	l	range	n	l	range
A	13	249	249.59 – 250.09	10	189	189.67	14	197	196.40 – 196.57
B	14	251	251.62	11	191		15	199	198.39 – 198.49
C	15	253		12	193		16	201	200.33 – 200.56
D	16	255		13	195		17	203	
E	17	257	257.27	14	197		18	205	
F	18	259	259.44	15	199		19	207	207.87 – 208.14
G	19	261	261.13 – 261.37	16	201		20	209	209.91 – 210.00
H				17	203	203.20 – 203.42			
I				18	205	205.42 – 205.69			
J				19	207	207.02 – 207.19			
K				20	209	208.98 – 209.14			
L				21	211				
M				22	213	212.72 – 212.75			
N				23	215				
O				24	217	216.56 – 216.58			
P				25	219				
Q				26	221	220.65			

The label is the code used for an allele contained in the group range for the microsatellite. n = number of dinucleotide repeats present in amplicon; l = theoretical amplicon length; range = value or range of inferred amplicon lengths actually seen that were assigned to the group. Alleles from non-NZM cell-lines assayed are also included. A blank indicates that no allele in this potential group was seen.

**Table 8–4: Microsatellite allele grouping**



	D9S1853		D9S974		D9S157	
	Allele 1	Allele 2	Allele 1	Allele 2	Allele 1	Allele 2
NZM1	250.00 (A)	–	Deleted		208.09 (F)	–
NZM2	249.97 (A)	–	Deleted		208.07 (F)	–
NZM3	249.81 (A)	–	Deleted		196.51 (A)	–
NZM4	261.37 (G)	–	212.72 (M)	216.56 (O)	210.00 (G)	–
NZM5	249.77 (A)	–	207.02 (J)	–	207.97 (F)	–
NZM6	249.92 (A)	259.44 (F)	189.67 (A)	203.42 (H)	200.33 (C)	208.04 (F)
NZM7	250.09 (A)	–	205.43 (I)	209.14 (K)	208.03 (F)	–
NZM7.2	249.73 (A)	–	205.53 (I)	209.10 (K)	208.14 (F)	–
NZM7.4	249.72 (A)	–	205.61 (I)	–	207.87 (F)	–
NZM9	249.68 (A)	–	Deleted		198.49 (B)	–
NZM10	251.62 (B)	–	207.06 (J)	–	207.94 (F)	–
NZM10.1	261.19 (G)	–	212.75 (M)	216.58 (O)	209.91 (G)	–
NZM11	249.63 (A)	261.13 (G)	Deleted		200.49 (C)	–
NZM12	249.59 (A)	–	205.69 (I)	–	208.01 (F)	–
NZM13	249.68 (A)	–	Deleted		196.45 (A)	–
NZM14	249.68 (A)	257.27 (E)	208.98 (K)	–	198.39 (B)	–
NZM15	249.77 (A)	–	207.19 (J)	–	196.40 (A)	–

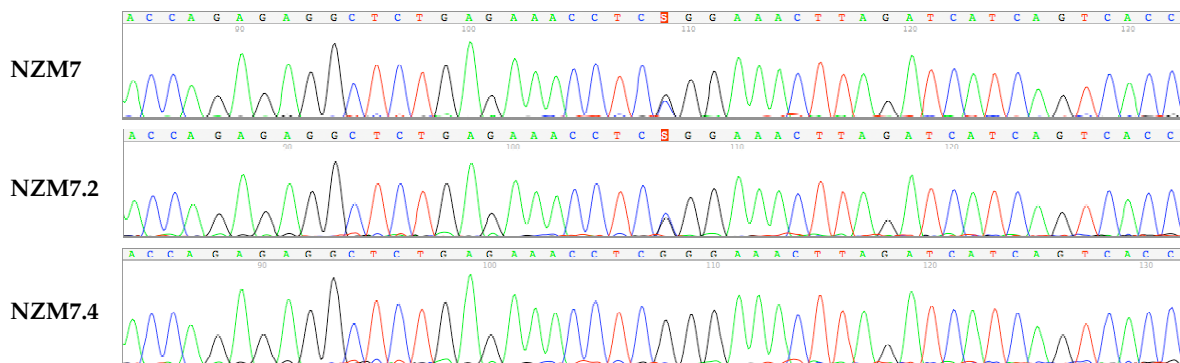
Entries give the one or two distinct lengths of amplicon found after PCR as inferred from capillary electrophoresis. Parenthetical letters identify the allele group to which this amplicon length was assigned {Table 8–4}. Deleted = not surveyed as no PCR product formed; – = no second allele length found.

Table 8–5: NZM 9p12–9p23 microsatellite allelotypes

### DNA sequencing

Unidirectional sequencing of all *CDKN2A* and *CDKN2B* PCR products yielded sequences identical to the appropriate reference sequence in all but three cases.

In exon 3 of NZM7 and NZM7.2 an identical G500C heterozygosity was found that was absent from the related NZM7.4 {Figure 8–33}. This was confirmed by repeating the sequencing with newly amplified PCR products, as the location of the heterozygosity was too close to the reverse primer site to permit reverse sequencing.



These electropherograms show part of *CDKN2A* exon 3. Note the G500C heterozygosity (S) present in NZM7 and NZM7.2, but absent from NZM7.4.

Figure 8–33: *CDKN2A* exon 3 heterozygosity

In exon 2 of *CDKN2B* amplified from NZM14 a homo- or hemizygous G411A transition was found {Figure 8–34}. This was verified by reverse sequencing.

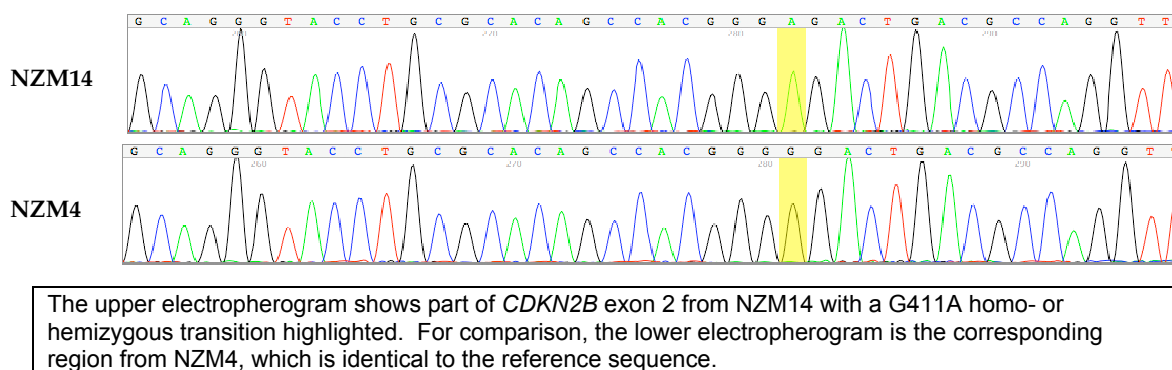


Figure 8–34: *CDKN2B* exon 2 G411A transition in NZM14

## Discussion

### PCR

Results for PCR were of a very much higher quality than those achieved in V1, and for the most part, the variability of amplification among cell-lines for some targets was not observed. The rectification of DNA standardisation procedures and the incorporation of BSA doubtless contributed greatly to this. However, despite this, some variability was still seen reproducibly, in particular, for *CDKN2A* exons 1 and 2 of NZM5, NZM10, and NZM15, and this was not alleviated by doubling the amount of BSA added to the reactions to address *Taq* inhibition by melanin. In the case of exon 1, similar effects were seen for these cell-lines during preliminary work with new PCR primers intended to span a greater region of *CDKN2A* exon 1 than those used in V1. However, these data cannot be considered more than suggestive, as the template DNA used at the time had not been rigidly quantitated. It does leave open the possibility that it is heterogeneity rather than primer site sequence variation that is responsible for the differences in amplification levels, especially since such effects have been shown to be detectable by ethidium bromide stained agarose gels {See 'Sensitivity of agarose gels in detecting template heterogeneity', above}.

### Deletion mapping

The question of heterogeneity aside, the PCR results obtained allow a much more definitive statement to be made concerning the integrity of the 9p21 chromosomal region in the NZM cell-lines, specifically, that NZM1, NZM2, NZM3, NZM9, NZM11, and NZM13 have substantial stretches of homozygous deletion affecting both *CDKN2A* and *CDKN2B*, and NZM12 has a smaller deletions affecting exons 2 and 3 of *CDKN2A* and not involving *CDKN2B*. These deletions were foreshadowed by the V1 results.

There is evidence for a deletion affecting exon 3 of *CDKN2A* in NZM14, and this too was seen in the V1 work. However, this conclusion derives from assessment using only a single pair of PCR primers on both occasions, and so the possibility of a primer binding site polymorphism

affecting amplification efficiency must be considered, and verification sought with an alternative set before the existence of a deletion should be considered proven.

These new data continue to be concordant with those from qPCR provided by courtesy of Dr Ian Morison {Figure 8–11}.

### *DNA sequencing*

Other than the errors discussed above concerning interpretation of substandard electrophoretic data and the erroneous introduction of a base change in *CDKN2A* exon 3 PCR products for NZM7.2 and NZM7.4, the new sequencing results confirm those reported in V1, specifically, the G500C heterozygosity in NZM7.2 *CDKN2A* exon 3 absent from NZM7.4, and the G411A transition in NZM14 *CDKN2B* exon 2.

The inclusion of NZM7 in the panel extends the V1 findings by establishing that the G500C heterozygosity also exists in the parental cell-line, and so the possibility of an in vitro mutation introducing the C allele into NZM7.2 can be discounted.

### *Microsatellite analysis*

#### **Discrimination among the cell-lines**

The microsatellite analysis proved to be very robust, with excellent agreement in size data for presumably identical alleles in different cell-lines, and in repeated analyses. By this analysis the cell-lines fall into the allelotype groups shown in Table 8–6.

D9S1853	D9S974	D9S157	NZM cell-lines
A	I	F	NZM7.4, NZM12
A	IK	F	NZM7, NZM7.2
A	J	A	NZM15
A	J	F	NZM5
A	Deleted	A	NZM3, NZM13
A	Deleted	B	NZM9
A	Deleted	F	NZM1, NZM2
AE	K	B	NZM14
AF	AH	CF	NZM6
AG	Deleted	C	NZM11
B	J	F	NZM10
G	MO	G	NZM4, NZM10.1

Entries give the allele(s) detected for each microsatellite locus investigated as defined in Table 8–4. Deleted = no PCR product to analyse.

**Table 8–6: NZM 9p12–9p23 microsatellite allelotype groupings**

Those cell-lines that share microsatellite allelotypes are in most cases distinguishable by other means. NZM12 has the *CDKN2A* deletions described above which NZM7.4 does not. Although the deletion pattern and microsatellite allelotypes of NZM3 and NZM13 are identical, and morphologically they are not dissimilar, the absolute ploidy of NZM3 is 1.95, while that of NZM13 is 1.27 {Table 5–4}. In some cases, it would not be expected that a distinction would be easy to draw. NZM1 and NZM2 by all measures are identical, in keeping with their origins being the same person, and similarly, the characteristics of NZM7 and NZM7.2 are indistinguishable.

### **Doubt over NZM10.1 authenticity**

There is one serious anomaly, and that is the issue of the identical microsatellite allelotypes of NZM4 and NZM10.1. This might be considered coincidence, except that NZM10.1 was developed as a sub-clone of NZM10, and yet it shares no microsatellite alleles with it, and further, the D9S974 M and O alleles it carries exist in no other cell-line tested except NZM4. This would seem to be incontrovertible evidence that NZM4 cells have been misidentified as NZM10.1 at some point, due perhaps to an error of handling or labelling during passage culture, or that a cross-contamination has occurred followed by the supplanting of the relatively slow growing NZM10.1 cells by NZM4. To seek further clarification, DNA sequence analysis for exon 2 of *NRAS* was carried out as it is known that NZM4 differs from NZM10 at this locus, the former having the prevalent C434 allele, while the latter has the A434 allele, expected to produce a Q61K protein mutation<sup>1668</sup>. The suspect NZM10.1 cell-line was found to carry the C434 allele, again making derivation from NZM10 very improbable. However the situation is more complex than this. The measured ploidies of NZM4 and NZM10.1 are each consistent with their V1 values, and appear distinct from each other; the morphology of NZM10.1 and its behaviour in culture are more consistent with NZM10 than NZM4; the anomalous subnuclear bodies reported in Chapter 6 were seen to occur in NZM10 and NZM10.1, but not in NZM4; and the pRB and p16 protein expression seen in NZM10.1 differed from both NZM4 and NZM10 {See 'Results', beginning on page 9–22}. This issue remains unresolved at the time of writing. On the basis of the microsatellite data it seems probable that NZM4 is genuine, since apart from NZM10.1, its allelotype is unique, and results reported for NZM4 should therefore be robust. However doubt remains over the origin and status of the cell-line designated NZM10.1, and consequently all results pertaining to this cell-line must be considered provisional only. Furthermore, it cannot be entirely sure when the cross-contamination or other error occurred. It remains a possibility that this predated the sub-cloning of NZM10, and that it was in this process that an NZM4 cell was isolated and expanded to become what is now known as NZM10.1. The original results for NZM10.1 must also be considered suspect.

### **Loss of heterozygosity**

There is little information to be gleaned with respect to loss of heterozygosity in the general case owing to the lack of matched normal DNA; nor can a statistical approach be taken since the allele frequencies for these microsatellites are not known with certainty, not least because the ethnicity of the original tissue donors is not known. It can be said with certainty that NZM4, NZM6, NZM7, NZM7.2, NZM11, and NZM14 have not suffered loss of heterozygosity over the entire region surveyed as they are heterozygous at one or more of the microsatellite loci investigated. Further, it can be inferred with reasonable confidence that NZM6 has not suffered loss of heterozygosity at any part of the region surveyed as it retains heterozygosity at all of the loci.

The microsatellite results for NZM7 and its sub-clones allow a definitive statement to be made concerning the *CDKN2A* G500C heterozygosity that was found. From the sequencing data the



possibility of an in vitro mutation in NZM7.2 to create the C allele could be discounted, and while a reasonable inference was that the progenitor cell that formed NZM7.4 had lost the C allele, it can now be stated with confidence that **NZM7.4 has suffered a loss of heterozygosity in this region** as it has also lost the K allele of D9S974, and is therefore hemizygous at nucleotide 500. Since the parental NZM7 is presumably homozygous at the D9S1853 and D9S157 loci, as it is heterozygous between them at nucleotide 500, nothing more can be learnt about the extent of the chromosome loss.

There is a minor discord between the NZM7.4 microsatellite allelotype and the qPCR data available in that the former shows a loss of heterozygosity while the latter suggests a copy number of two at the *CDKN2A* locus. However, this may be an indication that the region of chromosome loss that resulted in the hemizygosity did not extend as far as the location of the marker used in the qPCR, something that was not disclosed.

No further information about whether the *CDKN2B* G411A transition is homozygous or hemizygous is available from the microsatellite analysis. At best, it could have been shown to be likely to be homozygous for this if it had been heterozygous, and therefore biallelic, at D9S157 in addition to D9S1853, however it was not. Again, there is a minor discord with the qPCR data: NZM14 is heterozygous at D9S1853, yet the qPCR data suggests a copy number of one for *CDKN2B*, exon 1 $\beta$  of *CDKN2A*, and *CDKN2A* proper. As it was with the similar situation regarding NZM7.4, this may be an indication that the chromosome loss begins at a point between D9S1853 at 9p12, and *CDKN2B* at 9p21.

#### **Microsatellite instability not seen**

No evidence of microsatellite instability was seen in any of the NZM cell-lines investigated.

While such instability has been reported in metastatic melanoma, it is not considered a general feature of melanoma tumorigenesis, and when it does occur it is predominantly of a low level<sup>1577</sup>. The absence of detection here does not add significantly to this knowledge.

#### ***Future research directions***

Some work is still required here. The extent of the deletion in NZM12 needs to be established, and as a first step, optimisation of the three sets of *CDKN2A* exon 2 primers that produce overlapping amplicons could be undertaken. It is worth exploring the feasibility of producing and sequencing a complementary DNA (cDNA) to determine if a variant mRNA is being transcribed and assess what impact this might have for protein structure, particularly in light of the short p16 protein detected in V1. The possibility of primer site polymorphisms should be explored as potential reasons for the inability to amplify *CDKN2A* exon 3 from NZM14, and the variability of amplification seen in NZM5, NZM10, and NZM15. Further sets of primers could be designed, or variations in reagents or methodology investigated, to attempt to obtain material to sequence for the areas of interest not yet studied.

### **Summary**

Revisiting the work performed on chromosome 9p21 status during V1 has been very rewarding. Important errors of interpretation have been discovered and corrected, key findings have been confirmed, and new data have been gathered in the shape of microsatellite allelotypes. The mystery of NZM5 DNA's erratic performance as a PCR template has been resolved, something that is now benefiting others undertaking genetic research into the NZM cell-lines. An excellent protocol for the preparation of genomic DNA of the highest quality and rigidly standardised has been developed. The importance of establishing a genotype database for cell-lines developed at the ACSRC has been demonstrated, and an alert over mycoplasma contamination was raised that minimised the loss of data that might otherwise have occurred throughout the research group. On the negative side, the allelotype work that was done has raised doubt over the authenticity of the NZM10.1 cell-line, something which was not able to be resolved in the available time.



# 9

## Tumour-suppressor expression

*While some of the melanoma cell-lines show clear evidence of genomic derangement at the 9p21 locus that contains CDKN2A and CDKN2B, some appear to be intact. In order to determine if the tumour-suppressor proteins encoded by these genes are actually expressed, Western analysis of cell lysates using specific antibodies was undertaken. In addition, the retinoblastoma-associated protein, pRB, was analysed since it is a major functional target of these proteins. Where CDKN2A appeared to be intact, but no p16 protein was found, genomic demethylation was attempted, and the demethylated cells assayed to determine if there was re-expression of p16.*

*Expression of pRB was seen in all cell-lines except NZM6, NZM7.2, NZM7.4, and NZM10.1. Little, if any, p15 was found in any cell-line, but it was induced by TGF $\beta$ 1 in NZM4, known to be proliferatively inhibited by this cytokine. Generally, high levels of p16 expression were seen in cell-lines that did not express pRB, and little, if any, in those that did. A form of p16 with aberrantly high electrophoretic mobility was detected in NZM12, consistent with the genetic defect revealed by PCR. ARF expression was detected in all cell-lines, apparently at odds with the genomic status in some cases. Demethylation was not found to enhance p16 expression in any of the cell-lines investigated. No correlation was found between pRB expression and the ability of cell-lines to arrest in G<sub>1</sub> in the absence of serum as previously determined, weakening the case for a pRB-dependent G<sub>1</sub> restriction point.*

*Finally, the intriguing observation was made that while the parental NZM10 cell-line expresses pRB, the derivative NZM10.1 does not. Of itself, this strengthens the growing case for heterogeneity within melanoma cell-lines, but when combined with data obtained during the sub-cloning process, a hypothesis develops that the survival of the parental cell-line in vitro, and perhaps some melanoma tumours in vivo, may critically depend on this heterogeneity.*

Retracted material.  
See section addendum for details

### 9.1 Introduction

A major functional target of the 9p21-encoded tumour-suppressors is the retinoblastoma-associated protein, pRB. The gene encoding pRB, *RB1*, comprises 28 exons, making genetic analysis expensive and time-consuming. Furthermore, PCR amplification of exon 1 has proven to be problematical, apparently due to a high G:C content, and few studies report data for it. To address the first issue, an attempt was made to reverse-transcribe the ~4.6 kb *RB1* mRNA to facilitate analysis of the coding region and detection of splice variations. This attempt did not meet with success, and no full-length cDNA was produced. The likely reason for this failure is the same G:C-rich region in exon 1 that renders PCR difficult. The current availability of reagent systems intended to obviate such problems could make this approach worth revisiting.

Even without complete genetic information, much useful data can be obtained by an analysis of pRB protein expression, especially when coupled with similar analyses of p15, p16, and ARF. In particular, it has been reported that p16 expression is often elevated where functional pRB is not expressed, and conversely, that where functional pRB is present, p16 expression is weak<sup>1125</sup>. It is also reported that p16 is sometimes not expressed even when there is no apparent 9p21

See Appendix H for a more about pRB, p15, and p16.

genetic defect. One mechanism known to account for this is transcriptional silencing of *CDKN2A* through DNA methylation<sup>986</sup>, the same means by which genetic imprinting and X chromosome inactivation occur.

Aberrant methylation had been implicated in a number of diseases, perhaps most notably, Fragile-X syndrome. It has been recognised as an aspect of neoplastic transformation, initially as a means of generation of tumour heterogeneity<sup>618</sup>, and later as an inherent cause of mutation due to the spontaneous deamination of 5-methylcytosine<sup>619 738</sup>. A much more direct role was appreciated with the publication of a series of papers from Johns Hopkins University School of Medicine implicating methylation in the silencing of the gene for the oestrogen receptor in breast<sup>985</sup> and colon carcinoma<sup>587</sup>, *VHL* in renal carcinoma<sup>510</sup>, and then, for *CDKN2A-α* in multiple cancer types<sup>883</sup>. Now, transcriptional silencing through methylation<sup>1112</sup> has been found for *APC*<sup>325</sup>, *AR*<sup>681</sup>, *BRCA1*<sup>167</sup>, *CASP8*<sup>1317</sup>, *CCND2*<sup>330</sup>, *CDH1*<sup>1491</sup>, *CDH13*<sup>1335</sup>, *CDKN1B*<sup>1065</sup>, *CDKN2A-β*<sup>326</sup>, *CDKN2B*<sup>37</sup>, *FHIT*<sup>1525</sup>, *GSTP1*<sup>1232</sup>, *MLH1*<sup>1229</sup>, *PGR-B*<sup>1136</sup>, *POMC*<sup>943</sup>, *PTGS2*<sup>1247</sup>, *RARB-2*<sup>1434</sup>, *RASSF1-A*<sup>237</sup>, *RBI*<sup>1230</sup>, *SOCS1*<sup>1489</sup>, *SFN*<sup>348</sup>, *THBS1*<sup>781</sup>, *TIMP3*<sup>54</sup>, *TOP1*<sup>382</sup>, *TP73*<sup>224</sup>, and *WT1*<sup>752</sup>. In addition, aberrant re-expression due to demethylation of an imprinted gene has been seen with *HOX11*<sup>1411</sup>. Recognition of this silencing mechanism effectively allayed doubts over the authenticity of p16 as a tumour-suppressor based on the higher rates of mutation seen in vitro when compared to primary tumours. While some in vitro selection may occur, a large number of primary tumours with genetically intact *CDKN2A* did not express p16 due to methylation.

Of the sixteen cell-lines under investigation, six were found to have major genetic anomalies in the 9p21 region likely to prevent production of the tumour-suppressor proteins encoded there. To confirm this, and to determine if the apparently genetically intact cell-lines do indeed produce these, a survey of protein expression is required. Furthermore, should some appear genetically intact, but not express p16, an assessment of any role for DNA methylation is required. This chapter describes such analyses and their results.

## 9.2 Experimental design

### Protein expression analysis

Two readily available techniques for the analysis of protein expression are Western analysis {A.4} and flow cytometry {A.5}. Both depend on the recognition of the target protein by an antibody and its subsequent detection. They differ in several important ways, but one often overlooked is that unless the primary antibody used is truly specific for the protein of interest, results from flow cytometry will be at best ambiguous. This is because of the difficulty in controlling for the relative contribution of specific and non-specific signals to overall fluorescence. On the other hand, in Western analysis, the distinction is often possible due to differences in protein mobility during electrophoresis. It must also be remembered that flow cytometry yields data about the distribution of protein expression within a population of cells, while Western analysis can determine only the mean expression.



As proving the suitability of the primary antibody for use in flow cytometry requires that Western analysis be performed as a first step, the decision as to which was the more appropriate technique was moot. It transpired that the primary pRB antibody to be used did indeed recognise an additional protein, and is therefore of dubious value for flow cytometry. The situation was complicated further by the similarity of mobility between pRB and the non-specific target which was such that identification based solely on molecular weight markers was not possible. To resolve this, two controls were added, lysate from MOLT-4 human lymphoblastic leukaemia cells, known to express pRB, and from SAOS-2 human osteosarcoma cells, that express a truncated pRB<sup>1205</sup> lacking the epitope recognised by the antibody used.

There is a further technical aspect that requires discussion that relates to ensuring equivalence of loading among samples. The rationale is that if this is achieved, then the data ultimately obtained may be considered quantitatively. Common practice is to perform a total protein determination of each extract and load equal protein masses. For experiments intended to study the expression of a generic structural protein after different treatments of a single cell-line, this may be satisfactory. The work described here has neither of these attributes. Firstly, it involves regulatory proteins, and their expression levels may not be proportional to total cellular protein content. Consider the case of core histones: as the amount of chromosomal DNA in a cell is not determined by the cell size, the amount of histone present need not be proportional to, for example,  $\beta$ -actin. Similarly, the same quantity of pRB can regulate the division of a cell of any size. Secondly, the melanoma cell-lines being studied here differ widely in cell volume: NZM5 is particularly small, while NZM10 is very large. Loading equal masses of total protein under these circumstances would cause the under-representation of regulatory proteins for larger cells. In consequence of this, the experiments described here use equivalent cell number as the criterion for uniformity of loading, and no loading control, such as analysis with an irrelevant antibody to a ubiquitous protein, is performed.

#### Assessing transcriptional silencing from DNA methylation

There are several possible approaches available to elucidate what role, if any, genomic methylation is having on the expression of a protein. At the genetic level, the use of methylation-status sensitive restriction enzymes, methylation-specific PCR, and bisulphite-modified DNA sequencing can all be informative<sup>962</sup>, but do not address whether any methylation so discovered is of functional significance for protein expression. While a correlation between methylation of an otherwise normal sequence and non-expression of the encoded protein would certainly be a good indication, it would not be conclusive. In this work, cell-lines that are not seen to express p16 in spite of an apparently normal gene are cultured in the presence of the demethylating DNA base analogue 5-aza-2'-deoxycytidine (5aza-dC) over a period many times greater than the population doubling time. Under these conditions, each time the population doubles, the proportion of cells with methylated DNA is halved. Cells from such substantially demethylated cultures are then subjected to analysis for re-expression of the protein of interest. This technique also has limitations. If re-expression is

Retracted material.  
See section addendum for details

## 9: Tumour-suppressor expression

Retracted material.  
See section addendum for details

not seen, it can be concluded that genomic methylation is not the cause of loss of expression. However, if re-expression does occur, it does not prove that the demethylation event directly involved the gene of interest. Any gene whose protein product is required for the expression of the gene of interest may have been the critical element, for example, that for a transcription factor. Proving that genomic demethylation has indeed occurred after treatment is also problematical, and reliance has been placed on the use of an established protocol<sup>1986</sup>.

### 9.3 Methods in brief

Cultures of the NZM, MOLT-4, SK-MEL-28, and SAOS-2 cell-lines were established in vitro [Method 2] in  $\alpha$ MEM supplemented with antibiotics and 15% v/v (SAOS-2) or 10% v/v (other cell-lines) FCS (Solution 11). Mean passage number for all NZM lines was ~18. NZM4 was also grown in the presence of recombinant human TGF $\beta$ 1 (1.0  $\mu$ g/L) for 5 d as a potential positive control for p15 expression<sup>180</sup>. Cell-lines to be demethylated were grown in medium supplemented with 5aza-dC (1  $\mu$ mol/L) for about eight doublings; harvested and passaged into 5aza-dC-supplemented medium for a further eight doublings; passaged into normal medium; and maintained therein. Actively proliferating cells ( $\sim 10^7$ ) were lysed in protein sample loading buffer containing protease inhibitors [Method 8]. The tubes were vortexed vigorously to disperse cell pellets and stored at  $-70^\circ\text{C}$  until required. The level of each protein of interest present in 50 000 – 100 000 cell equivalents was determined for each cell-line by Western analysis [Method 16] using 6% v/v (pRB) or 15% v/v (other proteins) acrylamide separating gels, PVDF membranes, primary antibodies as specified {E.3}, and either a commercial tagging kit {E.2} in the case of pRB, or a horseradish peroxidase conjugated secondary antibody in the other cases, followed by enhanced-chemiluminescent (ECL) {E.2} exposure of autoradiography film.

Retracted material.  
See section addendum for details

### 9.4 Results

#### Expression of pRB

There was strong pRB expression in all NZM cell-lines except NZM6, NZM7.2, NZM7.4, and NZM10.1 {Figure 9–1}. Where there was expression, multiple bands were present, usually attributed to differences in pRB phosphorylation state.



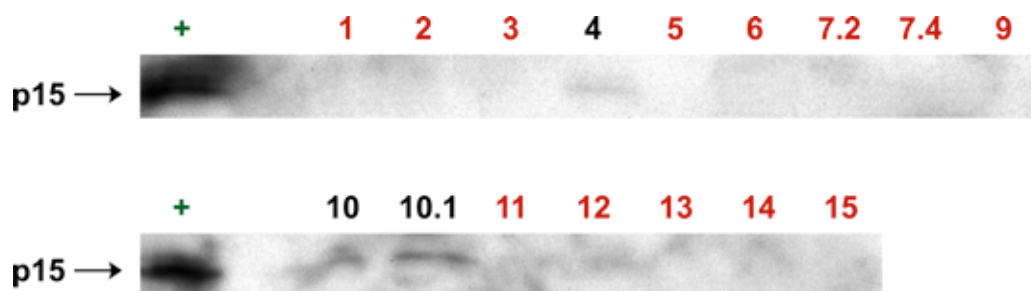
M = marker lane; + = positive control (MOLT-4); - = negative control (SAOS-2); 1–15 = corresponding NZM cell-line lysate.

Upper band is non-specific. Note weak or absent expression for NZM6, NZM7.2, NZM7.4, and NZM10.1.

Figure 9–1: Western analysis of pRB expression by NZM cell-lines

### Expression of p15

Clear expression of p15 was seen in the TGFβ1 treated NZM4 cells, and a low level in NZM4, NZM10, and NZM10.1. While no expression was discernible for any other line, the possibility of very low levels cannot be excluded, as overall sensitivity appeared to be low {Figure 9–2}.



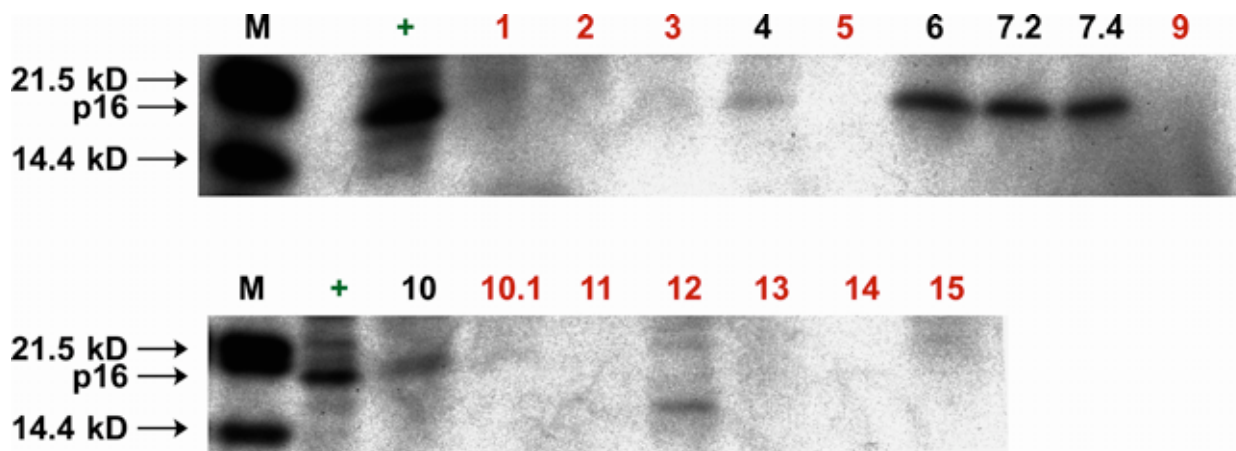
+ = positive control (NZM4 in the presence of TGFβ1); 1–15 = corresponding NZM cell-line. Mobility of the detected positive control band was assessed by reference to dye-conjugated molecular weight markers transferred to the membrane and was consistent with the detection of p15. These are not detectable by the visualisation reagents used and hence are not shown.

Note weak expression only for NZM4, NZM10, and NZM10.1.

Figure 9–2: Western analysis of p15 expression by NZM cell-lines

### Expression of p16

Strong p16 expression was seen in NZM6, NZM7.2, and NZM7.4, with weak expression detectable for NZM4, NZM10, and possibly NZM10.1 and NZM12. In addition, there was weak expression by NZM12 of a product of aberrantly high mobility.



M = marker lane; + = positive control (SK-MEL-28); 1–15 = corresponding NZM cell-line.

Note strong expression in NZM6, NZM7.2, and NZM7.4; weak expression in NZM4, NZM10, and possibly NZM12; aberrant band in NZM12.

Figure 9–3: Western analysis of p16 expression by NZM cell-lines

For cell-lines with no apparent genetic anomaly, but without expression of p16, genomic demethylation was attempted, and protein extracts of demethylated cells analysed {Figure 9–4}.

Although this analysis is marred by the presence of a strong non-specific band and a number of extraneous patches, particularly in the NZM15 lanes, there is no evidence of increased p16 expression among the demethylated cell-lines. Surprisingly, both the control and demethylated NZM10.1 cells expressed p16, whereas during the initial survey this had been very weak {See 'Discussion', below}.



Lane labels specify cell-line; green label is untreated; black label is demethylated. Upper band is non-specific. Reference to dye-conjugated molecular weight markers transferred to the membrane allowed identification of the p16 band. These are not detectable by the visualisation reagents used and hence are not shown.

Figure 9-4: Effect of genomic demethylation on p16 expression

### Expression of ARF

There was evidence of strong expression of ARF in the NZM2, NZM3, NZM5, NZM6, NZM7.2, NZM7.4 and NZM15 cell-lines, and weaker expression in the others {Figure 9-5}.



+ = positive control (supplied with antibody); 1–15 = corresponding NZM cell-line. Mobility of the detected positive control band was assessed by reference to dye-conjugated molecular weight markers transferred to the membrane and was consistent with the detection of ARF. These are not detectable by the visualisation reagents used and hence are not shown.

Figure 9-5: Western analysis of ARF expression by NZM cell-lines

## 9.5 Discussion

### pRB expression

While pRB protein was detected in most lysates, NZM6, NZM7.2, NZM7.4, and NZM10.1 did not express pRB. Possible causes of this include the loss of *RB1* alleles, defective regulation of gene transcription, reduced mRNA stability or other translational defect, and reduced protein half-life. In melanoma, among these possibilities, homozygous deletion of *RB1* alleles has been reported only rarely<sup>774</sup>, although LOH at the 13q14 *RB1* locus is known in uveal melanoma<sup>1158</sup>. Transcriptional silencing of *RB1* via DNA methylation has been reported in some non-melanoma tumours {H-2}. Further investigation will be required to determine if either of these possibilities applies in each of the non-expressing NZM cell-lines, or if another cause exists. This would include reverse transcription PCR of a target spanning an *RB1* intron in order to assess transcription, Northern analysis, and demethylation studies similar to that undertaken for p16.

### p16 expression

Failure to detect p16 expression in the NZM1, NZM2, NZM3, NZM9, NZM11, NZM12, and NZM13 cell-lines was consistent with the presence of genomic anomalies in the 9p21 region {Table 8-1}. However, no p16 was detected in lysates from NZM5, NZM14, or NZM15, cell-lines with ostensibly intact *CDKN2A*. While gene methylation can transcriptionally silence



*CDKN2A*<sup>883</sup>, this was excluded, as expression was not seen after demethylation. Other possibilities, including changes in mRNA or protein stability, remain to be explored. As a first step, reverse transcription PCR or Northern analysis could be used to verify mRNA expression. Protein stability is somewhat harder to investigate, but the use of protease inhibitors may provide further information.

NZM4 and NZM10 express both pRB and, apparently normal, p16, but without a genetic analysis of *RB1* no conclusive interpretation is possible. The pRB produced may be non-functional, or another essential element of the pRB subsystem may be altered, such as CDK4<sup>1343</sup>. Of course, since the presence of functional pRB in normal cells in no way precludes their expression of p16, this subsystem may be intact. The conclusive evidence that the NZM10 cell-line is not genetically or phenotypically homogeneous [5.5], and that Western analysis provides population-average data together make further interpretation subject to ambiguity.

The p16 expression data presented here contain an inconsistency: while NZM10.1 was found to express only low levels of protein in the first analysis, when assayed to determine if the cause of this was demethylation, significant p16 was detected in both control and demethylated cells. No clear explanation for this is available. Expression of p16 is to a degree cell-cycle dependent, and it may be that an element of cycle synchronisation had inadvertently been incorporated during culture. This may have resulted either from the use of cultures seeded at relatively high density that were grown for only a few days and then harvested, or from the exhaustion of a required serum factor due to poor culture practice. As has been shown, NZM10.1 will arrest in G<sub>1</sub> in response to serum-deprivation, and a similar situation may have arisen in culture. Under these conditions, variation in p16 expression may also be a direct consequence of such stress. While unresolved, this is in reality a minor matter. NZM10.1 was seen to express p16 in both experiments and hence, methylation is not an issue.

Analysis of 9p21 genomic status revealed that the NZM12 cell-line contains an anomaly within exon 2 of *CDKN2A*, or the following intron, that prevented PCR-amplification of the exon 2C target [8–10], and implies the possible production of a truncated protein of minimum molecular weight ~10.8 kD. Figure 9–3 shows that **NZM12 expresses a protein with anomalously high electrophoretic mobility** that is recognised by the monoclonal anti-p16 antibody employed. This provides strong corroboratory evidence that the inferred genomic alteration was indeed present.

### **p15 expression**

While *CDKN2A* and *CDKN2B* are very similar structurally, their transcriptional control differs substantially. Generally, *CDKN2B* is induced dramatically by TGFβ in what is thought to be a major component of its anti-proliferative effect<sup>471</sup>, but no such induction of *CDKN2A* is seen. TGFβ production and sensitivity occur in melanoma cells<sup>1101</sup>, but little is known about the involvement of p15. Indeed, any role may be minor, as melanoma cells can arrest in response to TGFβ despite lacking *CDKN2B*, with p21<sup>CDKN1A</sup> being the likely mediator<sup>358</sup>. Modulation of

Retracted material.  
See section addendum for details

## **9: Tumour-suppressor expression**

CDC25A, a phosphatase important in G<sub>1</sub> CDK activation, has also been implicated<sup>566</sup>. Insofar as expression of *CDKN2B* in melanoma is concerned, mRNA has been detected in 8 of 23 cell-lines<sup>1099</sup>, but there appear to have been no protein studies. Consistent with this paucity of data is the view held widely, but not universally<sup>418</sup>, that deletion of *CDKN2B* may simply be a consequence of its proximity to *CDKN2A*, rather than it being a target in its own right. While the results presented here do not suggest any unusual role for p15 in melanoma, they do confirm that **TGFβ1 can induce p15 expression in a sensitive melanoma cell-line**, as demonstrated by the NZM4 positive control {Figure 9–2}.

### ARF expression

The results from Western analysis show detectable, and in many cases strong, expression of ARF in all NZM cell-lines. This is difficult to reconcile with the results of the genetic analysis of the 9p21 region {Chapter 8}, particularly in the case of NZM2, where no *CDKN2A* exon 1β PCR product was detectable. It is possible that the genetic sequence is present, but a mutation in a PCR primer binding site may have prevented amplification, but this appears unlikely given the lack of amplification of flanking targets. For all other cell-lines there was discernible PCR product, and in many cases there is a correlation between the strength of PCR amplification and the level of ARF expression seen. As examples, NZM1 and NZM9 showed weak amplification and low expression; and NZM5, NZM7.2, NZM7.4, and NZM15 showed both strong amplification and expression. However, neither Western analysis nor PCR is rigorously quantitative. Although a recombinant protein positive control was employed, no true negative control was available, so the possibility of antibody cross-reactivity with a different antigen exists. This is unlikely, as the primary antibody used was monoclonal and, according to its manufacturer, specific. Without verification of these findings, the data for ARF expression should not be considered robust.

Retracted material.  
See section addendum for details

### Relationship between p16 and pRB expression

Dysfunction of individual elements of the pRB subsystem is widely reported among melanoma cell-lines<sup>1391</sup> suggesting that they operate sequentially, rather than in parallel, and are each critical in the suppression of melanoma<sup>73</sup>. Consistent with this, an apparent inverse correlation between pRB and p16 function has been reported, and this is broadly supported by these results. In NZM6, NZM7.2, and NZM7.4, where pRB was absent, very high levels of p16 expression were seen, and conversely in the other cell-lines, where pRB was abundant, p16 expression was weak or absent.

These data are equally consistent with inhibition of *CDKN2A*–α transcription by functional pRB. This would provide negative feedback whereby the phosphorylation of pRB by CDK4/6 would be self-limiting through the induction of p16. Where pRB function was defective, levels of p16 would increase in a futile attempt to constrain proliferation. To date, no such pRB-controlled element has been identified, but the transcription of *CDKN2A*–α is known to be regulated by members of the ETS<sup>972</sup> family, and inhibited by ID1<sup>1044</sup>. The retinoblastoma protein





binds ELF1<sup>1393</sup>, an ETS protein, and ID2<sup>567</sup>, a helix-loop-helix protein related to ID1, so a link may yet be forged.

In addition to this uncertainty over the dynamic relationship between pRB and p16, doubt exists over the biological importance of their joint function. The focus has tended to be on the regulation of mitogen responsiveness since: p16 is an inhibitor of CDK4/6<sup>1181</sup>; CDK4/6 activation requires a cyclin-D partner<sup>332</sup>; cyclin-D transcription is enhanced by mitogens<sup>236</sup>; and the formation of cyclin-D–CDK4 complexes is mitogen-dependent<sup>196</sup>. This view is strengthened by the involvement of the related p15 in growth inhibition by TGFβ. Notwithstanding this, evidence is mounting that the role of p16 in cellular senescence<sup>25</sup> may be at least as important. Accumulation of p16 with continuing culture has been demonstrated<sup>474</sup>, and prolonged expression can lead to an irreversible cell-cycle arrest<sup>235</sup>. One implication of control of *CDKN2A*–α transcription by pRB would be a molecular basis for this accumulation. Under these circumstances, p16 would be produced only during the brief period between the release of sequestered proteins from pRB upon its phosphorylation by activated CDK4/6, and their subsequent re-sequestration, either through the activity of phosphatases, or, as has recently been suggested, by further phosphorylation of pRB by activated CDK2<sup>336 480</sup>. Little is known about the mode and timing of p16 degradation. If p16, or its mRNA, has a very long half-life, it may accumulate with successive cell divisions, raising the threshold level of activated CDK necessary to defeat the growth suppressive function of pRB. It may be this role in melanocyte senescence that makes the pRB subsystem critical in the suppression of melanoma, rather than its putative role in maintaining mitogen-dependency {See Chapter 7, and ‘Replicative senescence’, 2–14}.

#### **No correlation between pRB expression and serum-deprivation response class.**

The work described in Chapter 7 established that in both NZM7.4 and NZM10.1, the immediate effect of serum withdrawal was an accumulation of cells in G<sub>1</sub> phase. It is now clear that this redistribution was achieved in the absence of pRB. Therefore, the scenario of unrestrained E2F activity must be contemplated and an explanation sought for G<sub>1</sub> accumulation despite this. One consequence of erroneous disinhibition of E2F1 would be an increase in the expression of ARF, leading to a reduction in MDM2 levels, and so to a reduction in E2F1-dependent transcriptional activity and increased p53 levels {J–21}. The ARF expression seen in NZM7.4 supports this interpretation, but only weak expression was seen for NZM10.1, and furthermore, the ARF data may not be robust. Elevated ARF expression would provide a basis for the well established phenomena that inappropriate E2F1 expression, while leading to S-phase entry, also promotes p53-dependent apoptosis<sup>1068</sup>, and that absence of pRB is sufficient to bring this about<sup>29</sup>. It is in this capacity that p53 earned the epithet ‘Guardian of Rb’<sup>1430</sup>. With elevated levels of activated p53 present, induction of p21 is probable, and with this will come inhibition of CDK2, irrespective of the levels of cyclin-E induced by unconstrained E2F. Therefore, even without pRB, if the E2F/ARF/MDM2/p53/p21 chain is intact, a slowing or arrest of G<sub>1</sub> passage can still be implemented. This proviso is of particular interest since the

NZM7.2 cell-line, ultimately derived from the same tumour as NZM7.4, did not manifest any delay in G<sub>1</sub> progression after serum-deprivation, and unlike NZM7.4, is a *TP53* mutant<sup>1002</sup>.

The converse situation also exists: NZM4, NZM5, NZM13, and NZM15 do not display an immediate reduction in G<sub>1</sub> content after serum withdrawal despite expressing pRB. For NZM13 and NZM15, this may be explicable by their failure to express p16, as in its absence, CDK4/6 activity will in general be unopposed, and pRB may be rendered ineffectual through aberrant phosphorylation.

Retracted material.  
See section addendum for details

Without a complete genetic analysis of *RB1*, or functional studies with protein isolated from the remaining cell-lines, nothing is known or can be deduced about the functional status of any pRB present. Nevertheless, as discussed above, even where pRB is defective, arrest can still occur via p21-mediated inhibition of CDK2. Since this did not occur in these cell-lines, the possibility exists that both the pRB and p53/p21 subsystems are defective; indeed, like NZM7.2, NZM4 has been reported to be a *TP53* mutant<sup>1002</sup>. Further experimentation will be necessary to explore this, particularly since the production of autocrine growth factors may mask the effects of serum-deprivation.

In summary, there is no correlation between pRB status and the integrity of the late-G<sub>1</sub> serum-dependent checkpoint: expression of pRB does not guarantee it, nor absence, preclude it. However, the correlation improves if pRB and p16 are considered as a functional unit.

### A proposed mechanism for melanoma protection by p16

While p16 abnormalities have been found in many tumour types, melanoma is by far the predominant cancer seen where a *CDKN2A* defect is inherited. The explanation for this must lie in some particular importance of p16 in controlling the net proliferation of cells of melanocytic lineage. In this regard, one unique aspect of melanocyte biology must be considered: their response to DNA damage. The essential function of melanocytes is the export of melanin as a defence against UV-induced damage, and there is strong evidence that the presence of excised UV-induced DNA lesions drives melanogenesis<sup>316 1012</sup>. Therefore, melanocytes must endure genomic damage that in other cell-types may lead to apoptosis. While p53-sponsored activation of p21<sup>CDKN1A</sup> in response to UVB causes G<sub>1</sub> arrest of melanocytes<sup>872</sup>, any potential apoptotic response must be dampened. This may be through the melanocyte-specific enzyme DCT, necessary for the production of eumelanin, but also having anti-apoptotic properties<sup>954</sup>. With a reduced apoptotic propensity, a greater dependence on cellular senescence as a mechanism for proliferative control may exist, perhaps accounting for the mutant *CDKN2A* phenotype {See 'Replicative senescence', 2–14}. A reduced dependence on apoptosis may also explain the relatively low incidence of *TP53* mutation seen in melanoma<sup>1506</sup>. As noted above, NZM4, which expresses p16 and pRB and thus may have an intact senescence mechanism, is a *TP53* mutant<sup>1002</sup>.

Further information about the function of p53 is available in Appendix J.



### NZM10 provides yet more clues

An intriguing observation made during this work relates to the pRB status of the NZM10 cell-line and its derivative NZM10.1. In consequence of the heteroploidy detected in NZM10 (Figure 5–4), sub-clones were prepared by individual cell propagation in an attempt to isolate the differing ploidy components. While ~20 individual cells began to proliferate and reached populations of ~100, only two such colonies grew beyond this and could be maintained by serial passage (data not shown). Of these, one was lost to contamination, leaving only NZM10.1. From its ploidy (Table 5–1), it was known to be only a minor component of the parental NZM10.

It is unlikely that cells inherently incapable of surviving beyond a few replications would represent the majority of cells in a mixed population, even after a relatively few passages in vitro. The alternative is to postulate that this incapacity is not inherent to the cell, but is a consequence of their isolation during sub-cloning. From this it follows that such cells depend for survival upon the presence of other components of the mixed population. Since during routine passaging, seeding density is such that few cells are in physical contact, and yet the cultures are readily established, a soluble factor, rather than physical association is implicated. This is a functional definition of the production and operation of a paracrine growth factor, a phenomenon frequently seen in melanoma cells<sup>464</sup>.

The situation in the parental NZM10 then is that the majority of cells depend critically on the production of a cytokine by a relative minority, and are therefore incapable of survival in isolation. Those few cells that can survive must either produce this factor, and respond to it in an autocrine manner, or not require it at all. NZM10.1 must have one or both of these attributes. In this regard, it is most interesting that while the lysate from the parental NZM10 culture contained pRB, that from NZM10.1 did not (Figure 9–1). Given its central role in the cellular response to growth factor stimulation (See Appendix H), the loss of pRB may well account for the survival of NZM10.1.

It may be thought that any clone within the parental culture that lacked the growth-suppressive influence of pRB would rapidly expand to displace its pRB-expressing relations. This need not be the case, since the same deregulation of E2F that allows cell-cycle progression also engenders apoptosis. The combination of an increased propensity to divide and an increased likelihood of apoptosis could easily result in a net clonal expansion rate slower than that of the bulk culture. This is confirmed by the results presented in Chapter 7, where the proliferation rate of NZM10.1 in isolation was shown to be approximately half that of its NZM10 parent.

The correlation, if any, between production of this hypothetical growth factor and pRB status is unknown. While the two characteristics may be independent, it is also possible that they are linked. Such would be the case for the cytokine IL8, as its expression is repressed by pRB<sup>1508</sup>, it is an important autocrine growth factor in melanoma<sup>1146</sup>, and it is implicated in metastasis<sup>1234</sup>. IL8 is therefore an attractive candidate.

To pursue this further, additional sub-clones of NZM10 should be isolated and characterised for pRB expression. This should also be undertaken for any abortive sub-clones, and here, immunocytochemistry offers the greatest prospect of success since too little material will be available for Western analysis. If paracrine support by a minority of cells is proven to be taking place, the implications for the treatment of melanoma may be profound, particularly if it is linked to non-expression of functional pRB {*See Chapter 11*}.



---

# Tumour-suppressor expression (V3)

---

## 9.6 Retraction of existing material

### General

This chapter was arguably the weakest in the initial version of this thesis. A very great effort was put into developing satisfactory methods for Western blotting during V1, but unremitting failure over more than a year ultimately led to the acceptance of substandard results as being the best practicable. The strategy adopted in V2 was very conservative, and no additional work was carried out to address these deficiencies, largely because it was thought that all options that could be attempted in the time available for revision had already been explored.

Some V1 results, particularly the study into the expression of ARF, and the possibility of re-expression of p16 after genomic demethylation, were inherently flawed and ought never to have been part of the submitted thesis. They were, however, reluctantly included, as they formed a part of the record of the work undertaken. While the V3 work did not address these questions anew, at least resubmission of this thesis provides the opportunity to retract the unacceptably weak material.

For what were considered the key areas though, V3, with the benefit of a longer time-scale, has allowed further development to be performed and the adoption of some newer methodologies. This was for the most part very successful, but as a result, further shortcomings of the V1 work on pRB expression came to light, rendering interpretation of those results unreliable. This is discussed fully below.

### Retraction of ARF expression results and discussion

The results of the Western analysis of ARF expression in V1 are clearly at odds with the *CDKN2A* deletion analysis undertaken, and while the V1 text discusses this and possible reasons for it, as they stand, the data gathered have very little credibility, and so the results and discussion pursuant to the V1 study of ARF expression are retracted.

### Retraction of *CDKN2A* demethylation results and discussion

Obtaining meaningful results for this study required robust genetic data and a robust protein assay, and neither was achieved in V1. The experimental design did not include proper controls, and the entire approach of addressing this question by Western analysis without prior inspection of the methylation status of the *CDKN2A* gene is questionable. Even if it had been shown that global genomic demethylation resulted in re-expression of p16, there would have been no way of determining if this was in consequence of demethylation of *CDKN2A*; demethylation may have enabled transcription of a gene encoding a protein necessary for the production of p16, perhaps a transcription factor or an element of a signal transduction channel, or it may have resulted in the down-regulation of a degradative mechanism that targets p16. Ultimately, the results obtained were internally inconsistent and of dubious value. They and their dependent discussion are retracted.

### Retraction of retinoblastoma-associated protein expression results and discussion

The worst technical flaw with the V1 pRB expression data was the presence of an apparently non-specific band with markedly lower mobility than the expected multiple bands of differently phosphorylated pRB species. To determine if this genuinely was a non-specific band, or instead represented a mutated or modified form of pRB, a negative control cell-line, SAOS-2, was introduced. This had been reported to produce only a truncated 95 kD pRB variant that lacks amino acids 703–928<sup>1205</sup>, a region including the amino acid 914–928 immunogen against which the polyclonal antibody in use was raised. Any band detected by this antibody in an SAOS-2 protein extract was therefore very unlikely to be pRB, and the corresponding bands for extracts from other cell-lines could be dismissed from consideration. This led to the conclusion made in V1 that some of the cell-lines investigated did not express the pRB protein.

In an effort to avoid this problem in V3, a different antibody was selected, but in order to ensure the availability of a negative control should a similar problem arise, an antibody recognising an epitope also missing from SAOS-2 was selected, specifically, amino acids 703–722. To aid specificity further, a monoclonal antibody was selected.

As new protein extracts became available during V3, a preliminary Western analysis was undertaken to begin the process of optimising antibody dilutions and blocking conditions. It produced technically excellent results immediately {Figure 9–6}, with good signal strength against a negligible background, no non-specific signal at any molecular weight and, particularly in the MOLT-4 positive control, clear multiple banding, presumably due to differences in phosphorylation. It also presented a conundrum: [the SAOS-2 extract included as a negative control displayed a band that could only be interpreted as pRB](#).

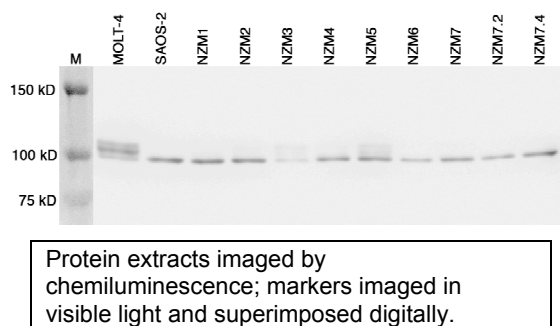


Figure 9–6: Trial pRB Western blot

This immediately raised a number of questions. Is the cell-line thought to be SAOS-2 actually something else? Was the wrong cell-line supplied by the ATCC when SAOS-2 was ordered? Does SAOS-2 actually produce full-length pRB despite the report to the contrary<sup>1205</sup>? Was the cell-line used as the basis of that report in fact not SAOS-2? Most importantly, if the cell-line that was used as a negative control during V1 was actually expressing detectable pRB, what does this mean for the interpretation of the results obtained?

With the microsatellite genotyping assay developed for V3 available, part of this mystery could be unravelled. The results of analysis of nominally SAOS-2 DNA for D9S974 and D9S157 allele type are given in Table 9–1.



	D9S974		D9S157	
	Allele 1	Allele 2	Allele 1	Allele 2
SAOS-2 (?)	203.20 (H)	220.65 (Q)	196.57 (A)	200.56 (C)

Column headings denote target microsatellite. Entries give the two distinct sizes of amplicon present after PCR as deduced from capillary electrophoresis with internal size standards. Parenthetical letters identify the allele group to which each amplicon was assigned, according to Table 8–4.

**Table 9–1: Microsatellite allelotype for putative SAOS-2 cell-line**

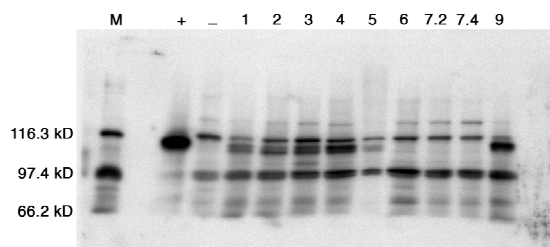
This allele pattern is unique among the cell-lines cultured during this research, including NZM cell-lines and others grown for control purposes. Analysis of either microsatellite alone suffices to distinguish this cell-line, as it includes the D9S974 Q allele seen nowhere else, and it contains a D9S157 allele not present in NZM6, the only other cell-line heterozygous at this locus. Handling, labelling, and cross-contamination errors can be ruled out, as there is no apparent source for cells with this allelotype. **The very strong implication is that the root cause of the use of an erroneous negative control lies externally to the execution of this research.**

In light of this new information, specifically, that the putative negative control actually expresses the target protein, can anything be salvaged from the original pRB Westerns by reinterpretation? The most obvious approach is to interpret the bands that appear at ~116 kD as phosphorylated pRB, implying that all of the NZM cell-lines express the protein of interest. This concurs with the expression data obtained in V3, as will be described below, although it effectively demolishes the bulk of the V1 discussion. However, a problem arises with this interpretation when consideration is given to the pRB phosphorylation states to be inferred.

From the V1 data, it appears that all but perhaps a trace of the pRB in NZM6, NZM7.2, and NZM7.4 is in the phosphorylated form with lower mobility, but from the V3 data, for example that shown in Figure 9–6, it appears that it is only in the unphosphorylated form. This apparent difference in phosphorylation state cannot reasonably be ascribed to differences in culture conditions since, in the V3 experimentation, four actively proliferating control cultures that would be expected to contain phosphorylated pRB were sampled for each cell-line, and none contained any indication of phosphorylated pRB. The possibility that the V3 results have been misinterpreted due to the lack of a specific reference for phosphorylated pRB can be discounted since in the preliminary work, where extracts from the cell-lines in question were run in parallel with others {Figure 9–6}, the sole band present for members of the NZM6/NZM7 group had mobility equivalent to the unphosphorylated form seen in other cell-lines. Furthermore, mistakes in cell-line identity can be excluded on genetic grounds.

Another possibility is that the ~116 kD bands genuinely are non-specific. This may seem very unlikely given the V3 discovery that the putative SAOS-2 cell-line expresses pRB, for if it does, and the ~116 kD band is non-specific, then where is its band for pRB in the V1 blots, and where are the corresponding bands for NZM6, NZM7.2, and NZM7.4? To understand how this might be, it is important to appreciate the technical limitations of the V1 blots. The ~116 kD band was not the only troubling one present, and other very strong bands existed, but with mobilities that eliminated them as possible pRB. Once it had been determined, erroneously perhaps, that

the ~116 kD band was non-specific, the image of the membrane was cropped to eliminate as many non-specific bands as possible, even to the extent of deleting the bracketing 97.4 kD marker; the ~116 kD band was simply too close to crop out, and so remained. The uncropped image for one of the V1 membranes is shown in Figure 9–7. Two things become clear from this: first, despite being the best achievable at the time, the absolute quality is very poor; and second, the ready acceptance of the ~116 kD band as non-specific is understandable given the number and strength of other clearly non-specific bands. The puzzle of the missing pRB bands for the spurious SAOS-2 and NZM6, NZM7.2, and NZM7.4 may be resolved by observing that in their respective lanes a faint band is visible at the position of unphosphorylated pRB. Issues of loading equivalency and inherent expression levels may have played a part here.



M = markers; + = MOLT-4 positive control; - = SAOS-2 negative control; other lanes NZM cell-line indicated. The marker lane was digitally moved in the creation of Figure 9–1.

Figure 9–7: Untrimmed V1 pRB Western blot

This is not an entirely satisfactory explanation of the discord between the V1 and V3 results with respect to phosphorylation of pRB, but the exploration of phosphorylation was never an objective of V1 so only incidental data are available. The mysteries over the ~116 kD band and the true bands for pRB in various states of phosphorylation in these blots remain, but to delve further into them would require a return to the original antibody and the continuation of methodological optimisation that did not achieve an acceptable standard after many months of effort. When a working assay is available based on a new antibody that produces exemplary results, there is little justification for expending resources to solve a five year old riddle posed by a poor Western blot.

Whether the interpretation of the V1 pRB Westerns was flawed because a spurious negative control led to erroneous conclusions of non-expression, or whether that conclusion was reached because of differences in loading or poor signal to noise ratio preventing detection, the effect is the same: the V1 pRB results must be treated as dubious and they and the V1 discussion that depended on them are retracted.

## 9.7 Extension of existing material

### Rationale

The primary objective of the work to be undertaken during the V3 revision was to obtain robust data concerning the expression of the retinoblastoma-associated protein in the NZM panel through Western blotting. In addition, by ensuring the preservation of phosphorylation state through the inclusion of phosphatase inhibitors in the extraction buffer, differences in phosphorylation, as assessed by alterations in mobility in acrylamide gels, were to be sought in extracts from cells that were actively proliferating early in culture, that were at high density after extended culture, and that had been deprived of serum. It was hoped that this would





elucidate the role such phosphorylation may play in the regulation of proliferation, and whether this is altered in any or all of the NZM cell-lines.

Secondarily, a renewed attempt was to be made to obtain more robust data concerning the expression of p16<sup>CDKN2A</sup> in the NZM cell-lines. Studies of ARF<sup>CDKN2A</sup>, p15<sup>CDKN2B</sup>, and the effects of genomic demethylation were not to be undertaken.

## Developmental work

### *Protein loading equivalency*

The most common method for implementing equivalency of protein loading among samples for electrophoresis and Western blotting is to load equal masses of total protein into each well, but where the analysis of regulatory proteins whose principal function is the direct or indirect regulation of gene expression in a panel of cell-lines of diverse mean cell mass is intended, this may not be the most appropriate method. In V1, to avoid this pitfall, extracts from equivalent cell numbers were used, but in the event, the data obtained were too poor to allow comparison among cell-lines.

In V3, the goal was not a quantitative comparison of expression levels among cell-lines, but were first, to distinguish between expression and non-expression, and second, in the case of pRB, to make a qualitative assessment of changes in phosphorylation under different conditions of culture. In this context, loading of equal total protein was justifiable, and even preferable, given the difficulty of obtaining accurate cell counts {See 'Discussion', on page 7–28}.

Numerous methods are available for protein concentration determination, and among these perhaps the most highly respected and widely used is the colourimetric bicinchoninic acid (BCA) assay. While specific for protein, it has the deficiency that the reduction of Cu<sup>2+</sup> to Cu<sup>+</sup> ions that forms the basis of the assay is caused not just by peptide bonds, but also by cysteine, tryptophan, and tyrosine amino acids present in the protein, and therefore the composition of the protein or protein mixture being assayed, not just its concentration, dictates the measurement. This raises the further complication of selecting a standard by which to calibrate the assay, since values deduced for unknown proteins will only be accurate if they have the same proportion of reactive amino acids as the chosen standard. While the relative concentrations of homogeneous mixtures of proteins could be deduced, determination of their absolute concentration can only be approximate. This is analogous to the difficulty of simply using spectrophotometry to determine protein concentration, since this too depends upon composition, not merely concentration. Common practice in this case is to use BSA as a standard, since it is widely available, and its composition and characteristics are well known.

The conditions for cell culture to be used here are specifically intended to provoke changes in cellular metabolism, and so are very likely to result in changes to protein expression, both in terms of quantity and composition, and furthermore, these changes may be cell-line dependent. When this is coupled with the limitations of the BCA assay and the use of a BSA standard that may well differ in composition from control extracts, experimental extracts, or both, it is clear

## Human metastatic melanoma in vitro

that any standardisation of extracts performed may be neither accurate, nor consistent. At best, one can hope that standardised extracts contain approximately the same amount of protein, and consequently, approximately the same amount is loaded in each well for electrophoresis. It must be remembered that in experiments of this type apparent differences in target protein expression observed after Western blotting may not be significant.

If protein loading equivalency cannot be guaranteed by standardisation in advance, can it at least be verified after protein transfer? Here, two methods are often used: reversible membrane stains and reprobing with an antibody to a "house-keeper" protein, such as GAPDH. These approaches suffer from the same sorts of problems as were described above: the degree of dye binding may depend on protein composition, not merely concentration, or it may differ among cell-lines or change with experimental treatment, the level of the "house-keeper" protein may not always be proportional to that of regulatory proteins, or even total protein, or its expression may be altered by experimental conditions. The reality of this situation became apparent in an early V3 trial of p16 Westerns, where a

Ponceau S stained membrane was subsequently reprobed with a GAPDH antibody {Figure 9–8}: while protein loading is reasonably uniform, as assessed by Ponceau S staining, there is very marked variability in the levels of GAPDH detected, and no obvious correlation between the variations in each.

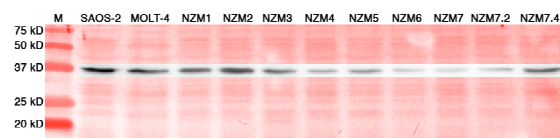


Image of a Ponceau S stained membrane with GAPDH immunodetection signal superimposed.

Figure 9–8: GAPDH Western blot

The pragmatic approach taken here was to standardise protein extracts using the BCA assay against a BSA standard, to load equal masses of protein per well based on that assessment, and to stain membranes after transfer to ensure that there had been no gross discrepancy in apparent loading. Given the result just described, no reprobing for "house-keeper" proteins was carried out.

### Methods in brief

#### *Sample preparation summary*

Duplicate soluble protein extracts were made, using buffer containing protease and phosphatase inhibitors, from each of the seventeen NZM cell-lines in the panel, at early and late times in culture, and with and without serum deprivation. These were standardised to 4 g/L and stored at  $-80^{\circ}\text{C}$ . In total, 136 extracts were produced.

#### *Cell culture*

All cell-lines in the NZM panel were used in these experiments: NZM1, NZM2, NZM3, NZM4, NZM5, NZM6, NZM7, NZM7.2, NZM7.4, NZM9, NZM10, NZM10.1, NZM11, NZM12, NZM13, NZM14, and NZM15; no additional control cell-lines were required. Cell stocks were derived from cultures recently tested for mycoplasma contamination and found negative [Method 33], but treated with ciprofloxacin regardless [Method 34]. Aside from the NZM1 and NZM2 pair, and the NZM7 and NZM7.2 pair, all cell-lines used had been proven to be unique



within the panel, with the exception of NZM10.1, which may have been accidentally supplanted by NZM4 {See 'Doubt over NZM10.1 authenticity', on page 8–36}.

For each cell-line, four P100 plates were each seeded with  $7.5 \times 10^5$  cells for use in the extended culture experiment, and four P100 plates were each seeded with  $1.5 \times 10^6$  cells for use in the serum deprivation experiment. All cultures were in 15 mL of  $\alpha$ MEM supplemented with 10% v/v FCS and antibiotics {Solution 11}. Plates were incubated as for passage culture {Method 2}.

When the cultures intended for serum deprivation had reached ~25% confluence, typically after 2 d, the medium from all such plates was removed by aspiration, with particular care being taken with the poorly adhering NZM5 cultures, and the plates were rinsed gently twice with PBS, this being removed by aspiration. Fresh medium (15 mL) containing either 10% v/v FCS as normal, or only 0.1% v/v FCS instead, was introduced into pairs of plates for each cell-line, and the plates were returned to incubation. After ~24 h, protein from every plate was separately extracted.

For the extended culture experiment, on the second and eighth days after seeding, protein was separately extracted from one pair of cultures for each cell-line.

#### ***Protein extraction, concentration, quantitation, standardisation, and storage***

Protein extraction {Method 39} using buffer containing both protease {E.16} and phosphatase inhibitors {Solution 66} was carried out on ice, with retention of the soluble fraction only. In order to obtain relatively high protein concentrations, only 500  $\mu$ L of extraction buffer was used in total for each short culture time plate, while 1 mL was used for the others. Extracts were stored at  $-80^\circ\text{C}$  and thawed and held on ice when they were needed.

Five hundred microlitres of each sample was concentrated with centrifugally-driven ultrafiltration units having membranes with a 3 kD cut-off {E.16}. Earlier trials had shown that an increase of up to five-fold in concentration could be achieved with no detectable loss of low molecular weight protein, as assessed by acrylamide electrophoresis of eluates followed by amido-black staining of gels.

The concentration of protein in these samples was determined by the BCA method in a 96-well plate format {Method 41} using triplicate samples against a calibration curve from a duplicate dilution series derived from a commercial BSA standard {E.14}.

Working stocks were standardised to 4 g/L concentration by the addition of the appropriate volumes of extraction buffer including phosphatase and protease inhibitors.

#### ***Western analysis***

For each analysis, stock protein extract (4 g/L, 13  $\mu$ L) was added to Laemmli loading buffer (13  $\mu$ L) {E.16} containing 2-mercaptoethanol in a microcentrifuge tube (1.5 mL capacity), heated ( $98^\circ\text{C}$ , 5 min), centrifuged briefly (16 000 G, 30 s) to settle the tube contents, and held at ambient temperature until loaded for electrophoresis.

Discontinuous acrylamide gels of 1 mm thickness were used comprising a separating gel of pH 8.8, whose concentration is given below, topped with a 4% v/v stacking gel of pH 6.8 {Solution 38} in which 10 wells were formed. Dye-conjugated molecular weight standards (5  $\mu$ L) {E.14} were loaded into the first well of each gel, and 25  $\mu$ L of sample, equivalent to 50  $\mu$ g of protein, was loaded into each experimental well. Unused wells were filled with loading buffer alone to reduce gel distortion. Electrophoresis using tris/glycine running buffer {Solution 32} was performed at a constant voltage, given below, and running buffer was reused at most once.

Transfer to 450 nm pore size nitrocellulose membranes {E.16} was effected by electrotransfer using tris/glycine/methanol buffer {Solution 78}. After transfer, membranes were stained with Ponceau S {Method 42}, dried, and imaged to record protein loading, then trimmed to retain only the relevant section based on the molecular weight markers, and imaged again. They were then destained in TBS {Solution 61}, dried, and stored at 4 °C until immunolabelling was performed, as described below.

Detection was by chemiluminescence and image capture performed digitally {Method 43}. Without intervening movement of the membranes, images were also made in visible light to record the relative positions of the dye-conjugated molecular weight markers. After detection, membranes were rinsed in TBS {Solution 61}, stripped using a proprietary solution (10 min, ambient temperature, moderate (~300 mHz) rocking agitation) {E.16}, rinsed in TBS {Solution 61}, dried, and stored at 4 °C in case of further need.

Specific variations for each protein being investigated follow.

### **Analysis of pRB**

Separating gels for pRB analysis were 5% v/v acrylamide {Solution 77}. Samples from duplicate cultures for short culture time, long culture time, normal serum culture, and reduced serum culture were loaded into successive pairs of wells. Electrophoresis was at 150 V for 65 min and electrotransfer for 1 h at a constant 100 V. Membrane blocking was in TBS {Solution 61} supplemented with 2% w/v BSA and 0.1% v/v Tween-20, and was for 1 h at ambient temperature with moderate (~300 mHz) rocking agitation. Incubation with the monoclonal mouse anti-human retinoblastoma protein primary antibody {E.12} was at a dilution of 1:100 in blocking buffer at ambient temperature for 1 h with gentle (~150 mHz) rocking agitation. The antibody solution was recovered, stored at 4 °C, and reused up to five times with no apparent loss of sensitivity or increase in background signal. Membranes were rinsed briefly once, and then washed for 5 min three times in TBS {Solution 61} supplemented with 0.05% v/v Tween-20 with vigorous (~850 mHz) rocking agitation. Incubation with the HRP-conjugated rabbit polyclonal anti-mouse secondary antibody {E.12} was at a dilution of 1:5 000 in blocking buffer at ambient temperature for 1 h with gentle (~150 mHz) rocking agitation. Membranes were rinsed briefly once, and then washed for 5 min three times in TBS {Solution 61} with vigorous (~850 mHz) rocking agitation, after which they were drained, detection reagents were applied, and the membrane images captured as above.



### Analysis of p16

Separating gels for p16 analysis were 20% v/v acrylamide {Solution 37}. Two gels were required to survey the full panel, and a slight variation in layout was necessary for them. In the first, samples of the long culture time extracts from NZM1 to NZM7.4 were loaded into the available wells. It transpired that none of the remaining cell-lines expressed significant amounts of p16, making the inclusion of a positive control necessary for the gel that contained them. As a result, in addition to samples of long culture time extracts from NZM9 to NZM15 being loaded, in the last well of the second gel a sample of NZM7 was also loaded, as this expressed significant p16 and would provide the necessary positive control. Ideally, both gels should have used the same layout, but to do so would have meant either a move to 15 well gels with a consequential reduction in the amount of protein that could be loaded, or increasing the number of gels to three in order to have sufficient wells available. The essentially cosmetic issue of different gel formats was considered to be the least significant. Electrophoresis was at 100 V for 155 min, the relatively low voltage, and resulting slow electrophoresis being helpful in resolving this small protein. Electrotransfer took place in two stages: first at 30 V for 15 min, immediately followed by 100 V for 45 min. The rationale for this was that small proteins such as p16 tend to migrate from the gel soon after the application of current. By operating at a reduced voltage during this initial phase, the rate of migration of the proteins is reduced, allowing them more time to interact with the membrane and be bound by it. Although the reduction in time at 100 V meant a reduced transfer of high molecular weight proteins, this was no hindrance, indeed, it may have helped reduce non-specific binding by non-target proteins. Optimal membrane blocking requirements proved to be very mild indeed: TBS {Solution 61} containing 1% w/v non-fat milk powder without added detergent for only 15 min at ambient temperature with moderate (~300 mHz) rocking agitation. Anything more stringent prevented detection; indeed reasonable results were initially obtained with no blocking whatsoever. After blocking, membranes were rinsed briefly twice with TBS {Solution 61} containing 0.05% v/v Tween-20 to remove unbound milk proteins. Incubation with fresh monoclonal mouse anti-human p16 primary antibody {E.12} was at a dilution of 1:100 in TBS {Solution 61} containing 0.05% v/v Tween-20, but no blocking agent, at ambient temperature for 1 h with gentle (~150 mHz) rocking agitation. It was found that the antibody solution could not be reused satisfactorily. Membranes were rinsed briefly once, and then washed for 5 min three times in TBS {Solution 61} containing 0.05% v/v Tween-20 with vigorous (~850 mHz) rocking agitation. Incubation with the HRP-conjugated rabbit polyclonal anti-mouse secondary antibody {E.12} was at a dilution of 1:5 000 in TBS {Solution 61} containing 0.05% v/v Tween-20, but no blocking agent, at ambient temperature for 1 h with gentle (~150 mHz) rocking agitation. Membranes were rinsed briefly once, and then washed for 5 min three times in TBS {Solution 61} containing 0.05% v/v Tween-20 with vigorous (~850 mHz) rocking agitation, after which they were drained, detection reagents were applied, and the membrane images captured as above.

**Results**

*Ponceau S staining*

Contrast-enhanced images of the Ponceau S stained NZM2 and NZM3 membranes prior to physical trimming are shown in Figure 9–9 as being representative of those for the extended culture and serum-deprivation investigation of pRB. Similar images for both membranes from a p16 expression experiment are shown in Figure 9–10.

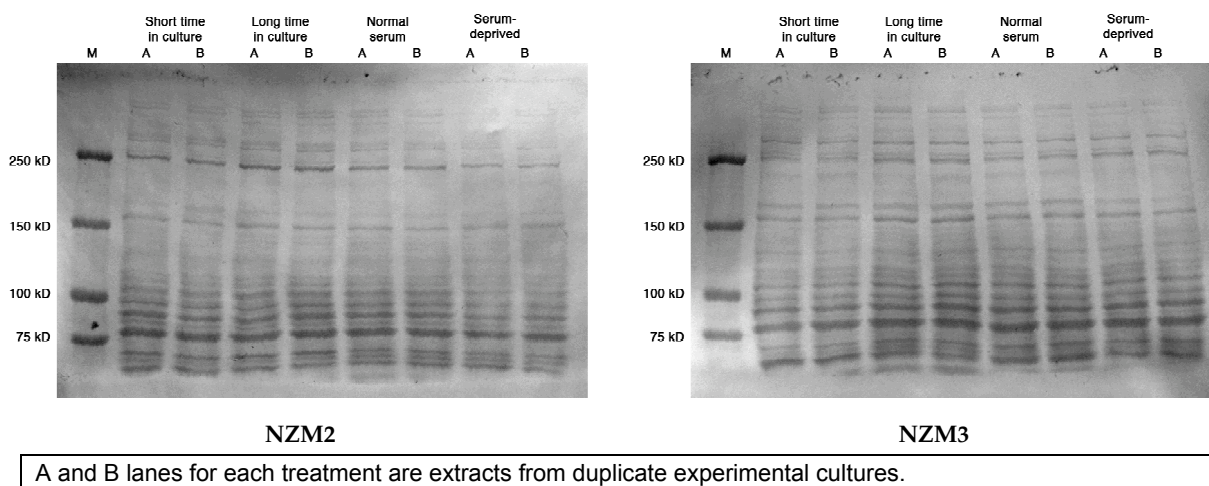


**Figure 9–9: Representative Ponceau S stained membranes as used in pRB Western blots**

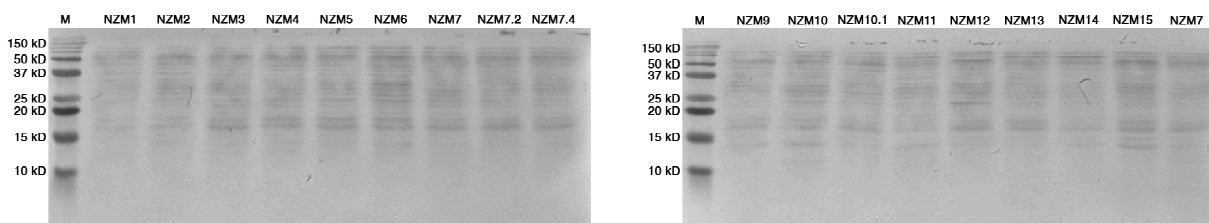


**Figure 9–10: Ponceau S stained membranes used in p16 Western blots**

### Retinoblastoma associated protein expression

The results for the detection of pRB expression in the extended culture and serum-deprivation experiments are shown in Figure 9–11.

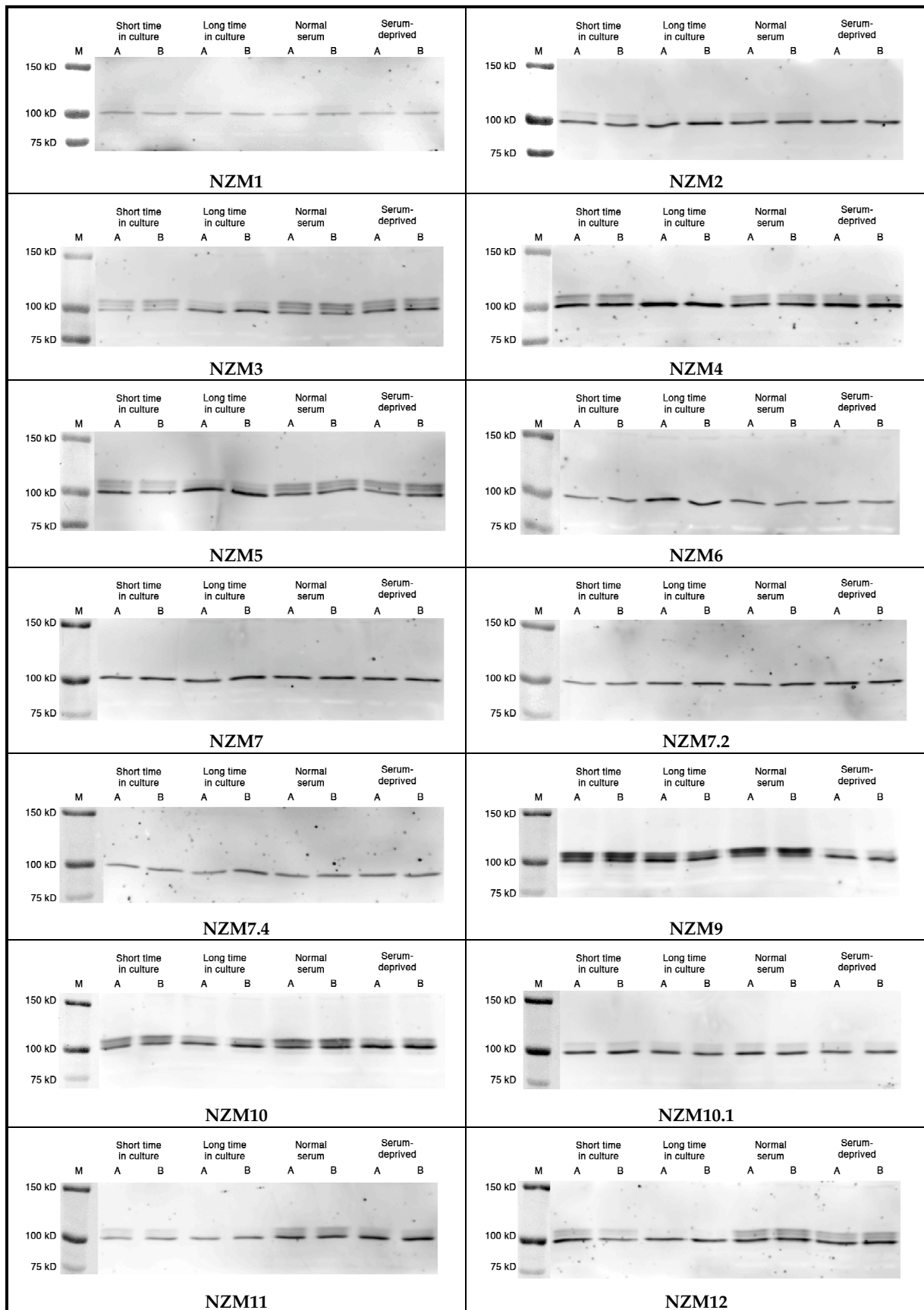


Figure 9–11: pRB Western blots (continues overleaf)

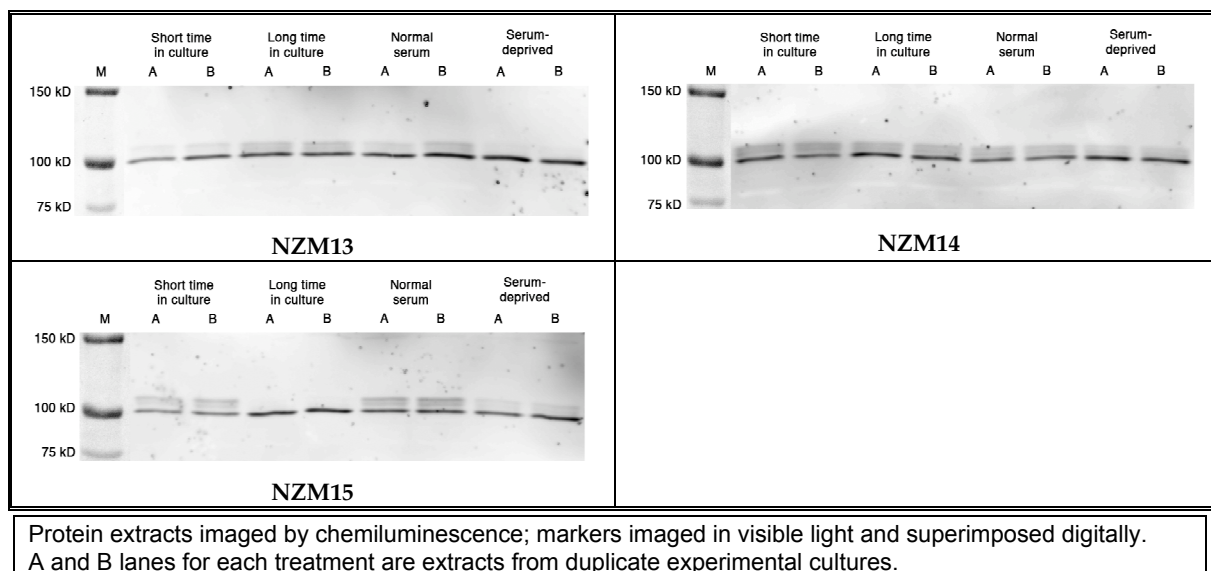
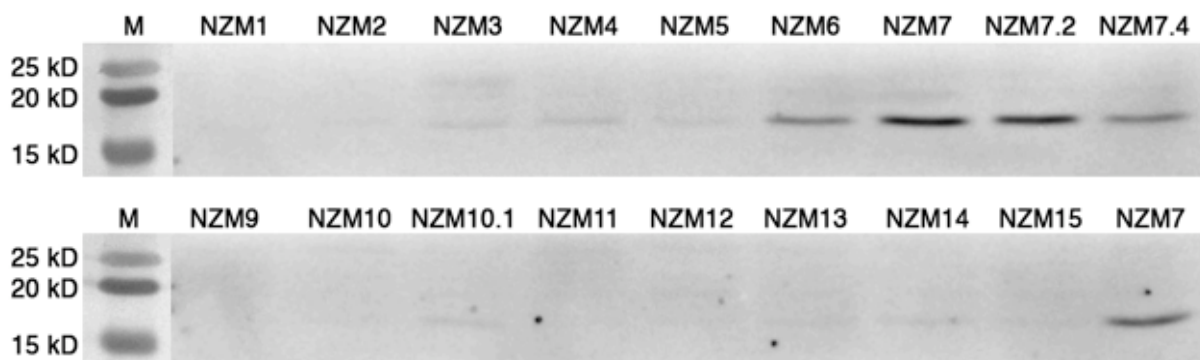


Figure 9–11 (concluded): pRB Western blots

*p16<sup>CDKN2A</sup> expression*

The results from the survey of p16 expression for the NZM cell-line panel are shown in Figure 9–12.



Protein extracts imaged by chemiluminescence; markers imaged in visible light and superimposed digitally.

Figure 9–12: p16 Western blots

**Discussion**

*Quality of results*

Artefacts such as those discussed {See 'Developmental work', above} relating to the difficulties in ensuring equivalent protein loading presented themselves in the course of these experiments. In Figure 9–9, there may seem to be differences in the amount of total protein present in extracts made after different treatments, yet there is a high degree of concordance between experimental replicates, despite these being derived from different cultures and being standardised independently, processes during which potential errors are most likely to occur. Differences in the relative intensities of some individual protein bands are also evident between cell-lines, visible in Figure 9–10. While the quantities of protein present in each lane seem to be similar, differences do exist, but given the uncertainties discussed these were not considered so great as to imply the occurrence of errors of standardisation or loading. Broad qualitative statements about relative target protein expression would seem to be justifiable.





Overall, the quality of the pRB Western blots was excellent, with good levels of signal strength obtained, no non-specific signal present, and usually very clear delineation of multiple phosphorylation states. An extremely high degree of concordance is evident when comparing the replicate samples, not only in the amount of the protein detected, but also in the degree to which this was phosphorylated.

For the p16 Westerns, quality was greatly improved over that achieved in V1, but the combination of apparently low target prevalence resulting in low signal strength, and the need for the mildest blocking to avoid complete loss of signal, meant that some non-specific bands remained, including in the region of interest. Cautious interpretation is required of the faint bands present for some cell-lines at the position where p16 would be expected to appear, as these may be non-specific.

### ***Retinoblastoma associated protein expression***

These findings establish that pRB is expressed by all of the cell-lines examined, consistent with the generally low rate of expression failure seen in melanoma<sup>®1604</sup>. No comparison in the levels of expression among cell-lines was intended, nor can any be made from these data since each cell-line was analysed separately, and detection efficiency may not have been uniform. Without a validated basis for loading equivalency, anything more than broad qualitative comparison of expression levels among treatments is not justified.

### ***Phosphorylation status of pRB***

These experiments have produced some very useful data concerning pRB phosphorylation changes in response to conditions intended to restrict cellular proliferation. The various NZM cell-lines can be grouped into five classes. The largest, comprising NZM2, NZM3, NZM9, NZM10, NZM11, NZM12, and NZM15, includes those in which pRB was phosphorylated in control extracts, but the proportion of phosphorylated pRB declined, or it was eliminated entirely, after either serum-deprivation or prolonged culture. This is the expected behaviour for cells that respond correctly to inhibitory signals by cell-cycle arrest<sup>®1617</sup>. It implies that the kinases and phosphatases that have pRB as a substrate are functioning, and probably doing so normally, but gives no information on whether the change in pRB to its growth inhibitory, unphosphorylated form is actually translating into cell-cycle arrest. It may be mutated in such a way that while it is unphosphorylated, it is unable to bind and regulate its downstream effectors, such as E2F transcription factors, or these themselves may be aberrantly constitutively active. The remaining classes involve a departure from this apparently normal regulation of phosphorylation.

In the second class, comprising NZM4, and NZM5, pRB was phosphorylated as expected in the actively proliferating controls, and the proportion of this was reduced after prolonged culture, but there was no clear reduction in the proportion of phosphorylated pRB after deprivation of serum for 24 h. In the case of NZM4 however, there were indications of an increase in the total amount of pRB present, even if the amount of phosphorylated pRB did not change, but the caveat concerning quantitative inferences applies in full force here. It is possible that cells from

See H.4 for a discussion on the regulation of pRB proliferative control by phosphorylation.

these cell-lines take longer to respond to serum-deprivation than do those of the first class. The 24 h interval between deprivation and sampling was chosen on the basis that in the absence of mitogens, genes for D-cyclins are not transcribed and the half-life of cyclin-D proteins decreases to the order of 10 minutes<sup>274 412</sup>. This means that by the time of sampling, there should have been no active CDK4 in the cells for some time for lack of an activating cyclin partner. Of itself, that would not have reduced the level of pRB phosphorylation, but it would have reduced competition with phosphatases that do. The retention of phosphorylated pRB after serum-deprivation may indicate a delay in operation or failure of phosphatase activity, aberrantly high stability of cyclin-A, -D, or -E, constitutively active CDK2 or CDK4, or problems with CKIs such as p21 and p27. Whatever the cause, there must be a distinction between the response to high density culture and the response to serum-deprivation, and this may provide a clue as to the molecular mechanisms involved.

The third class of behaviour includes only NZM14. Here, phosphorylated pRB was present at virtually equal levels in control cultures, after prolonged culture, and after serum deprivation. As with NZM4 and NZM5 above, there were suggestions of greater total amounts of pRB in the stressed cultures, but the quantitation caveat applies. NZM14 cultures grow to very high density in good health, with cells packing together very closely with large areas of intercellular contact due to their extended bipolar spindle morphology. It is possible that despite having been in culture for eight days, and being near-confluent, they were not yet under high-density stress.

In the fourth class, containing only NZM13, there may have been an increase in the amount of phosphorylated pRB after prolonged culture, while after serum-deprivation phosphorylated pRB was absent, as expected. These data are not incontrovertible with respect to the prolonged culture outcome, however. Differences in total pRB in the control and experimental extract were suggested, but these may be artefactual, if, for instance, after prolonged culture NZM13 cells have lower total protein content while retaining constant quantities of regulatory proteins. If that is so, the ratio of phosphorylated to total pRB may not have altered.

The fifth, final, and perhaps most intriguing class, comprises NZM6, NZM7, NZM7.2, NZM7.4, and perhaps NZM1; the data for NZM1 were not clear, however. In this class there was **no evidence of any phosphorylated pRB whatsoever, even in the control cultures that were actively proliferating**. This presents two anomalous behaviours: pRB existed in its growth-repressive unphosphorylated state even at low density in the presence of serum mitogens; and, despite it being in this state, these cells proliferated, did so rapidly, and are known to fail to arrest at confluence, at least in the case of the NZM7 group. This appears to be an unusual mode of failure of pRB regulation, as it is far more typical for unconstrained proliferation to be associated with pRB being aberrantly placed in a growth-permissive hyperphosphorylated state<sup>1604</sup>.



Perhaps the most parsimonious explanation for this would be a mutation in pRB that prevents binding of cyclin-CDK complexes, and hence phosphorylation, and simultaneously, binding of its downstream targets whose repression mediates its antiproliferative effects, such as E2F-family transcription factors. In a variation on this, pRB mutation may allow proliferation, while simultaneous dysregulation of pRB kinases or phosphatases maintains it in an unphosphorylated state. An alternative hypothesis is that there have simultaneously been dysregulation of kinases or phosphatases with pRB as a substrate, and a change to pRB-insensitivity of critical downstream regulators of proliferation. Since this involves two independent flaws, it would seem to be an unlikely prospect, but it cannot be discounted. Strong support for such a possibility comes from the work of Leone et al.<sup>1593</sup>, who showed that deregulated RAS and MYC activity can together drive proliferation in quiescent cells by the expression of E2F1 and Cyclin-E. This occurred while pRB remained in its unphosphorylated state, consistent with prior phosphorylation by Cyclin-D-CDK4 being necessary to permit this.

A further, much less attractive possibility is that a hemi- or homozygous partial *RB1* deletion resulting in constitutive pRB phosphorylation has occurred that simultaneously increases its electrophoretic mobility to coincide fortuitously with that of unphosphorylated normal pRB.

#### ***p16<sup>CDKN2A</sup>* protein expression**

Clear expression of p16 was detected in the cell-lines NZM6, NZM7, NZM7.2, and NZM7.4.

While faint bands exist at the appropriate position for p16 in extracts for most other cell-lines, these cannot be interpreted as evidence for the presence of p16. The chief reason for this exclusion is the occurrence of these bands in cell-lines in which *CDKN2A* is homozygously deleted, most notably NZM3 and NZM13. Since non-specific banding of similar intensity is present at other places, these are very likely also to be non-specific, and so too are the corresponding bands for cell-lines with intact *CDKN2A*. However, this absence of clear expression of p16 may be informative. If the amounts of p16 seen in NZM6 and the NZM7 group are taken as a basis for comparison, then the vanishingly low levels seen in cell-lines where *CDKN2A* is known to be intact must imply down-regulation of expression, something very common in melanoma cell-lines<sup>1604</sup>. This may be at the gene level via transcriptional silencing, at the translational level, implying alterations in mRNA processing or stability, or at the post-translational level, implying increased degradation. These are all avenues for further experimentation.

It is also possible that the levels of p16 expression seen in the NZM6/NZM7 group were aberrantly high. It has long been conjectured that one regulatory target of pRB is *CDKN2A*. This is plausible as a means for ensuring that, once phosphorylated, pRB sets in motion a mechanism by which this phosphorylation is disabled. This would constitute a monostable system that should spontaneously revert to pRB being unphosphorylated. In combination with the timely destruction of cyclins, this would act to prevent immediate entry into S phase after mitosis. It may also be a senescence timer, where pRB-mediated induction of *CDKN2A* causes increasing levels of p16 with each cell division, raising the required threshold of CDK4

activation by cyclin D to a point where cells cannot proceed into S phase. Despite these theoretical grounds, proof of this induction has not yet been obtained<sup>1567</sup>, but if such regulation did exist and pRB's repressive function were defective in the NZM6/NZM7 group, then elevated p16 would be a natural consequence.

### *p16 expression and pRB non-phosphorylation*

This raises perhaps the most striking observation concerning p16 expression made in the current work: the cell-lines in which p16 was clearly expressed are exactly those in which there was an absence of pRB phosphorylation in proliferating cells, NZM6 and the NZM7 group, so it seems that pRB function is indeed abrogated in these cell-lines. A scenario for these cells then could be that deregulated pRB permits unconstrained proliferation, and along with it the production of copious p16. Since no mutation or deletion affecting the coding region of *CDKN2A* was found in either NZM6 or the NZM7 group, it can reasonably be inferred that the p16 produced is functional, and this could easily account for the lack of phosphorylated pRB seen through the inhibition of the Cyclin-D–CDK4 complex. If the putative regulation of p16 expression by pRB does not in fact exist, then the cycle may be more indirect. Unconstrained activity of the downstream effectors of pRB may have been detected by a molecular surveillance system, perhaps related to that which operates to induce apoptosis when E2F1 activity is deregulated<sup>1607</sup>, and as a result, *CDKN2A* may have been induced in an attempt to correct this by preventing CDK4 phosphorylation of pRB, futile in this case because of the downstream fault that triggered the response in the first place.

Consideration of known mechanisms for elevation of p16 levels raises other possibilities that have many very appealing features. Aberrant signalling through the RAS–RAF channel is a common feature of many tumour types<sup>1546</sup><sup>1566</sup>, and is known to be important in melanoma, where approximately 70% of tumours carry mutations in *BRAF* that typically activate signalling<sup>1552</sup>. RAS-RAF signalling can cause the induction of *CDKN2A* transcription<sup>1698</sup>, and it has been shown that a constitutively active mutant form of B-RAF is associated with high levels of p16<sup>1613</sup>. Rather than facilitating proliferation, as might be expected for a tumour-associated mutation, this results in a withdrawal from the cell-cycle and the adoption of a senescent phenotype, most probably through inhibition of pRB phosphorylation. Since this presents a barrier to proliferation, any advantage that a *BRAF* mutation may offer to a tumour depends on this barrier being inoperative in the cells that carry it, specifically, that the growth-suppressive function mediated by pRB is compromised.

Studies suggest that *BRAF* mutation is a very early event in melanomagenesis<sup>1630</sup>, and in consequence, the initial phases of melanoma may involve cells with an apparently senescent phenotype. However, it is likely that senescence is an actively maintained state, by virtue of protein turnover if nothing else, and so its continuation depends upon the ongoing genomic integrity of the cell. Mutation of genes can still occur in non-proliferative cells, and ongoing transcription from these can result in phenotypic changes due to the loss of protein function that may result. Mutation in a gene encoding a protein vital to the maintenance of senescence



may act to reverse that phenotype, and the cell may once again be able to proliferate, but with whatever advantages the carriage of a *BRAF* mutation bestows. Alternatively, if the senescence mechanism in the cell is already defective at the time of *BRAF* mutation, no such delay will occur. Under these scenarios, *BRAF* mutants may lie dormant until mutation and protein turnover release the cell from senescence, or prior failure of this senescence mechanism may provide an environment permissive of *BRAF* mutant proliferation.

There are several ways this could occur, including deletion, transcriptional silencing or mutation of *CDKN2A* or *RB1*, and mutation of *CDK4* to a form immune to inhibition. In a study of 47 melanoma cell-lines, Jönsson et al.<sup>1583</sup> found 41 to contain activating *BRAF* mutations. Of these, 37 also were deficient in p16 production due to deletion, mutation, or transcriptional silencing, and one more carried a mutant *CDK4* producing an uninhibitable kinase. The genetic evidence gathered in the current work has demonstrated deletions of *CDKN2A* in many cell-lines and the study of pRB phosphorylation has led to a very plausible case for *RB1* mutation, or its functional equivalent, in NZM6/NZM7 group. The failure to detect p16 in the other cell-lines may not be a deficiency of the assay, but could be a genuine indication that there is none to be detected, but for reasons other than deletion, for example, by transcriptional silencing.

At this point the genetic study of the NZM cell-lines by Stones<sup>1668</sup> becomes very relevant. Investigation of the NZM6 and NZM7 cell-lines, potentially *RB1* mutants based on their incongruous phosphorylation, revealed them to contain the archetypal V600E B-RAF activating mutation. In the cell-lines NZM3 and NZM11, where *CDKN2A* is deleted, this mutation was also found. It was found in NZM12, a *CDKN2A* mutant in which it is thought a truncated and probably defective p16 protein is produced, one that may be undetectable by the antibody used. In NZM14, where exon 3 of *CDKN2A* could not be amplified by PCR, a similar B-RAF mutation, V600K, also thought to be activating, was found. Of the other cell-lines for which pRB and p16 data are available, only one other B-RAF mutant was found: NZM4. This has intact *CDKN2A*, and exhibits a normal pRB phosphorylation response to prolonged culture if not serum deprivation, but elevated levels of p16 were not seen. Here the possibility of transcriptional silencing of *CDKN2A* via promoter methylation must be considered<sup>986</sup>, something that may also apply to NZM14 should the anomaly present there not account for its apparent absence by removal of the necessary epitope.

The situation then is that a correlation appears to exist among B-RAF activating mutation, abundant p16 expression, and a pRB phosphorylation state inconsistent with proliferative status, and the *RB1* mutation inferred from the phosphorylation data fits very neatly into this model. Perhaps more significantly though, if activation of B-RAF is functionally equivalent to activation of RAS, then only the presence of activated MYC would be required in these cells to account for proliferation in the presence of unphosphorylated pRB<sup>1593</sup>, thus given the presence of the *BRAF* mutation, MYC activation is now just as plausible as *RB1* mutation as an explanation for pRB's anomalous phosphorylation status.

This appears to be a relatively unexplored phenomenon, as a literature search using the query phrase ' ("retinoblastoma protein"[mesh] OR pRB) AND (CDKN2A OR p16 OR INK4A) AND (B-RAF OR BRAF) ' retrieved just two publications, only one of which was of any real relevance. Rotolo et al.<sup>1645</sup> explored the effects of exogenous expression of normal p16 or a *BRAF* interference RNA construct in the *CDKN2A/BRAF* (B-RAF V600E), double mutant melanoma cell-line 624Mel. While they found that expression of either resulted in growth inhibition, this was accompanied by a decrease in the phosphorylation of pRB, as determined by the use of phosphospecific pRB antibodies in Western blotting experiments. Hence, their situation differs from that found here in that in their untreated cells, pRB was in the hyperphosphorylated, growth-permissive state. The particular combination of circumstances that exists in the NZM6/NZM7 group appears to be novel.

### *Centrosomal dysregulation and p16*

The recent finding<sup>1610</sup> that loss of p16 function in human mammary epithelial cells is associated with the presence of supernumerary centrosomes and the generation of aneuploidy raises the question of whether any link can be drawn between the status of p16 and centrosomal regulation in the NZM cell-lines. This can be considered for two situations: those where *CDKN2A* is known to be deleted, and those where p16 expression was seen; the remaining cases are indeterminate, as the data for non-expression of p16 are not robust.

The first group comprises NZM1, NZM2, NZM3, NZM9, NZM11, NZM13, which are homozygously deleted for *CDKN2A*, and possibly NZM12, which retains it only in part. NZM14 cannot be considered, as no centrosomal data are available. Here, the mean number of normal bipolar mitoses seen was 72%. The second group comprises NZM6, NZM7, NZM7.2, and possibly NZM7.4, which has lost one *CDKN2A* allele, but expresses p16. In this group, the mean number of normal bipolar mitoses seen was 79%. Although very close, these means are significantly different, but the distinction is not strong (one-tailed heteroscedastic Student's t-test,  $p = 0.045$ ). When the mean numbers of dicentrosomal cells are compared for the two groups, the difference is not significant (two-tailed heteroscedastic Student's t-test,  $p = 0.84$ ).

No firm conclusion can be drawn from this analysis, and it may also not be a reasonable comparison: the NZM6/NZM7 group, even if they do express p16, clearly have a flaw in the pRB subsystem, and it is possible, perhaps probable, that the effect that loss of p16 has on centrosomal regulation is mediated via pRB. The same flaw that allows proliferation in these cells in the presence of unphosphorylated pRB may also cause centrosomal dysregulation in the presence of p16.

### **Integration with V1 results**

The only work remaining from V1 after retractions that was explored further in V3 related to the expression of p16. Where this was seen in the NZM6/NZM7 group with one antibody during V1, it was also seen with a different antibody during V3, and should be considered confirmed. Other p16 results from V1 are not further elucidated here, but nor are they contradicted. The weak expression by NZM4, NZM10, and NZM12 seen in V1 may be



occurring here, but this cannot be confirmed because of the issue of non-specific banding in V3. V1 also provided evidence for a high mobility variant being produced in NZM12. This was not seen here, but that may be a consequence of the use of a different antibody. If, as is suspected from the deletion analysis of NZM12, a truncated p16 is being produced, then it is quite possible that the epitope recognised by the antibody now in use is missing. While both antibodies are monoclonals raised against recombinant human p16, no information appears to be available concerning where their epitopes lie in the protein<sup>1557</sup>, so this cannot be confirmed.

The situation regarding the possibility of *RB1* mutation or *MYC* activation in the NZM6/NZM7 group leading to abrogation of pRB-mediated proliferative control does gain some support from a V1 result. In the V1 study of serum deprivation, a numerical measure of the strength of the G<sub>1</sub> block imposed in response to this was derived, the retardation coefficient, Q {See 'The effect of serum-deprivation on proliferation rate', on page 7–12}. Three of the four lowest strength blocks were seen in NZM6, NZM7.2, and NZM7.4, with Q values of 62%, 35%, and 54% respectively; NZM7 was not surveyed in V1. Although these were based on growth rates determined from cell counts that had high variability, this association may be causal, rather than coincidental. It was found, however, that cultures of these cell-lines also ceased numerical proliferation within four days of serum deprivation, and it may be that it was a lack of survival factors that was the limitation for them, rather than a lack of mitogens, and their proliferation may have been regulated by cell death, rather than arrest.

#### **Follow-up studies indicated**

Information concerning differences in total pRB present in different cell-lines, or after different treatments, would complement these data, but for this to be explored through Western blotting would require a return to the V1 method of loading equal cell numbers, rather than total protein, and the vagaries of obtaining meaningful cell counts make this difficult. A more robust and much more informative technique could be based on flow cytometry now that the specificity of the antibody used has been established. It is marketed as being suitable for immunofluorescence, so presumably the epitope would not be altered beyond recognition by the fixation of cells required in preparation for flow cytometry. Triple labelling, with a pRB phosphospecific antibody and propidium iodide, in addition to the current antibody, would have the potential to reveal a wealth of information about regulation of pRB levels and phosphorylation status as the cell-cycle proceeds normally, or under circumstances such as those imposed experimentally here.

To explore further the apparent failure of some cell-lines to exhibit decreased levels of pRB phosphorylation after serum-deprivation, a time course experiment could be undertaken to determine if the expected reduction in phosphorylation was genuinely absent, or merely delayed. Such a time course was initially considered for the investigation of the NZM panel reported here, but to have surveyed seventeen cell-lines at perhaps six time points with controls and serum-deprived treatments in duplicate would have involved over 400 cultures and analyses, and the scale was simply too great. With the additional knowledge that

regulation appears intact in many cell-lines, the scope of the experiment is now reduced to more manageable proportions. A similar approach could be taken with NZM14 to explore pRB phosphorylation after more extended culture to determine if it eventually decreases.

The observation that in NZM13 pRB phosphorylation appears to increase after extended culture requires confirmation, and if thereby justified, a multiple-labelling flow-cytometric time course experiment would be very informative. Investigation of the possible production of a stimulatory autocrine factor would seem appropriate, and studies of the effects of NZM13 conditioned medium on cellular proliferation rate may be useful in this regard.

The data gathered from the study of NZM6 and the NZM7 group are sufficient to warrant a study of *RB1* genetic integrity in these cell-lines. This is a complex gene that contains a high level of G:C base-pairs in the promoter region that can make PCR difficult. On the basis of the known relationship between structure and function of pRB {Appendix H}, and the nature of the observations for which an explanatory mutation is being sought, a reasonable plan would be to examine just those portions of the gene that define the pocket binding domain of pRB. PCR-based deletion or sequencing studies complemented by reverse-transcriptase PCR experiments would seem to be suitable methods to employ. The alternative possibility that activated MYC is present should also be explored. This might entail FISH studies to determine if *MYC* gene copy number has increased, qRT-PCR to determine if expression is higher, and transfection with a suitable reporter construct to determine if MYC-directed transcription is elevated.

The cursory examination of p16 expression undertaken here has had its basis in the analysis of extracts made after prolonged culture, the intention being to maximise the chances of detecting a growth-inhibitory factor such as p16. While it is clear that proliferation is not constrained by unphosphorylated pRB in the cell-lines with high levels of p16, it would be interesting to know if the p16 that is being observed is produced constitutively, as might be expected if induction is due to B-RAF mutation, or just in response to antiproliferative stimuli, as was tested here. This is relatively easily achieved through the use of the existing short culture time control extracts, but a time course experiment might be more informative. If it were found that the expression is dependent on antiproliferative stimulation and there is little p16 to be seen in the control extracts, then the non-expression of p16 by the other cell-lines with intact *CDKN2A* when under stress would take on more significance. It may be that there was actually nothing there to be found, and the quest for increased sensitivity in an attempt to find this absent protein through the use of very mild blocking conditions may have led to undesirably high numbers of non-specific bands that were avoidable. If total absence of p16, rather than just very low levels, seems more plausible, it may be possible to improve on this protocol.

Irrespective of that outcome, studies should be made into the *CDKN2A* methylation status of those cell-lines with an intact gene, but no appreciable expression of p16. This is particularly relevant for NZM4 and NZM14, where promoter methylation may account for the failure to produce p16 under the stimulus of an activating B-RAF mutation. These studies should not





---

use demethylation and Western blotting as was attempted in V1 without further development to reduce the level of non-specific signal being produced. Should that not be possible, other methods such as methylation-sensitive PCR and bisulphite modification sequencing are available, and these could be more informative in any event.

More work is required on verifying the existence of a truncated p16 protein in NZM12, something that may be assisted by the B-RAF status of this cell-line, as this should stimulate high levels of production. A return to the earlier antibody that appeared to detect this would seem to be a logical starting point.

### **Summary**

All NZM cell-lines expressed pRB, but some displayed anomalous pRB phosphorylation patterns. Most unusual were the cell-lines NZM6, NZM7, NZM7.2, and NZM7.4, which proliferated freely even though they did not contain phosphorylated pRB. This suggests a flaw in pRB structure or function, or that of its downstream effectors. Deregulated MYC activity is a candidate cause for this since where this occurs in conjunction with *BRAF* mutation, pRB regulation can be bypassed, and these cell-lines are *BRAF* mutants. In addition, these cell-lines expressed abundant p16, and this is also probably causally related to their *BRAF* mutation status, with failure of pRB mediated growth arrest being permissive of the proliferation of *BRAF* mutants. There was no clear evidence of p16 expression in the other cell-lines studied, including those with intact *CDKN2A*. Further studies are warranted to seek to understand why this should be.



---

# Synthesis

---



# 10 Summary of experimental results

## 10.1 Summary table

The results from the analysis of ploidy, serum-deprivation response, 9p21 genetic status, and tumour-suppressor gene expression are summarised in Table 10–1.

Cell-line	Ploidy	Serum deprivation		9p12–p23 status			Tumour-suppressor expression			
		Q (%)	Class	Deletions	H	Δ DNA	pRB	p15	p16	ARF
NZM1	1.98	85	1	CDKN2A CDKN2B	+	–	++	–	–	+
NZM2	1.81	103	1	CDKN2A CDKN2B	+	–	++	–	–	++
NZM3	1.99	48	1	CDKN2A CDKN2B	+	–	++	–	–	++
NZM4	2.94	93	2	–	–	–	++	+	+	+
NZM5	1.09	71	3	–	–	–	++	–	–	++
NZM6	2.12 Ins	62	3	–	–	–	–	–	++	++
NZM7.2	1.34 2.74	35	0	–	–	CDKN2A	–	–	++	++
NZM7.4	1.39 2.79	54	1	–	–	CDKN2A	–	–	++	++
NZM9	2.10	70	1	CDKN2A CDKN2B	+	–	++	–	–	+
NZM10	2.10 2.82 4.57 6.27	77	2	–	–	–	++	+	+	++
NZM10.1	2.31 Ins	93	1	D9S274	–	–	–	+	+	+
NZM11	1.92 Ins	86	1	CDKN2A CDKN2B	+	–	++	–	–	+
NZM12	1.26 Ins	87	2	CDKN2A	+	CDKN2A	++	–	+	+
NZM13	1.24 2.45	73	3	CDKN2A	+	–	++	–	–	+
NZM14	1.15	80	1	–	+	CDKN2B	++	–	–	+
NZM15	2.03 Ins	78	2	D9S274 D9S156	–	–	++	–	–	++

Ploidy is relative to diploidy; multiple populations may be present; Ins = instability seen but not characterised. Q = retardation coefficient {Equation 7–1}; class 0 = no effect, class 1 = G<sub>1</sub> arrest, class 2 = G<sub>2</sub> arrest, class 3 = stimulation. + = seen; – = not seen. H = heterogeneity. Δ DNA = sequence variant. ++ = abundant.

Table 10–1: Summary of experimental results

## 10.2 Ploidy

All of the melanoma cell-lines investigated displayed aneuploidy as determined by flow cytometry, and the measured ploidy was concordant with the results of earlier cytogenetic studies. The cell-lines NZM1 and NZM2, derived from the same patient at different times, while differing in ploidy, were essentially homogeneous by this criterion. This strongly suggests that instability of ploidy was an attribute of this melanoma in vivo.

There was clear evidence of heteroploidy in many cases. Often, the ploidy of two populations within a cell-line was related by a factor of very nearly two, suggesting imprecise polyploidisation as a mechanism. Instances where this factor was approximately three were also seen, suggesting that flawed chromosome segregation or cytokinesis may also be

occurring. Taken together, these inferences further suggest that centrosome numerical control may be defective in a subset of melanomas, consistent with the sparse existing literature.

### 10.3 Serum deprivation

In the serum-supplemented control cultures for many cell-lines, there was clear evidence of a spontaneous and immediate reduction in proliferation rate after seeding, the magnitude of which increased with time in culture. This was most probably due to the production of an inhibitory growth factor that operated via an autocrine/paracrine mechanism. One consequence of this is that the assumption that cells in culture grow exponentially cannot be considered universally applicable. Furthermore, this effect is superficially indistinguishable from an arrest due to confluence, differing only in its timing. These observations show that conventional interpretations of even well established cellular phenomena may not always be valid.

When deprived of serum, all of the cell-lines responded with a reduction in net proliferation rate. From flow cytometric study of cell-cycle distribution of serum-deprived cultures, three broad response classes were identified. In the first, an immediate and sustained cell-cycle arrest in  $G_1$  was seen. This occurred in the cell-lines NZM1, NZM2, NZM3, NZM9, and NZM11, subsequently shown to harbour major genetic disruption of the *CDKN2A* gene encoding p16; in NZM14, which did not express p16 protein; and in NZM7.4, and NZM10.1, which were found not to express pRB. The intact  $G_1$  arrest seen in these cell-lines strongly suggests that the disruption of the pRB subsystem frequently found in melanoma is not primarily a means of escape from serum-dependency.

In the second response class, while an initial accumulation in  $G_1$  was seen, this was quickly superseded by an impediment to progression through  $G_2$  or M phases. The existence of such a serum-sensitive regulatory point is not widely reported, and warrants greater investigation. Furthermore, it belies the proposition that any irreversible commitment to cell division based on extra-cellular influence is made in the  $G_1$  phase.

In the third class, an immediate stimulus to enter S phase was observed upon serum-withdrawal. This strongly suggests that fetal calf serum contains an inhibitory growth factor that constrains entry into S-phase in some cell-lines. The identity of this and its significance in vivo are unknown.

### 10.4 9p21 status

The 9p21 chromosomal locus, which contains the genes encoding three candidate tumour-suppressors, was found to be significantly disrupted in nearly half of the cell-lines investigated. In all of these cases, the *CDKN2A* gene was affected, and in all but two of these, *CDKN2B* was also involved. These findings are consistent with literature reports. In two cell-lines, apparently intact throughout 9p21, there was evidence of a deletion telomeric to this locus, suggesting that a further tumour-suppressor gene significant in the development of some melanomas may exist there, as has been suggested by others.



DNA sequence analysis of PCR products that displayed abnormal SSCP banding revealed two polymorphisms in the related NZM7.2 and NZM7.4 cell-lines. Interestingly, the G500C polymorphism was heterozygous only in NZM7.2, suggesting that the parental cell-line, NZM7, was heterogeneous. The A526G polymorphism appears to be a novel finding. In addition to displaying evidence of an intragenic deletion in *CDKN2A*, NZM12 exon 2 contained two sequence variations, of which one might reasonably be expected to affect the function of any p16 protein produced. Finally, an apparently novel G411A variation in *CDKN2B* exon 2 was found in NZM14. It is unlikely to be of functional significance.

In some cell-lines the PCR amplification seen for some targets was clearly greater than background, but distinctly less than for the normal control. When combined with the evidence of multiple populations within individual cell-lines as determined during ploidy analysis, the conclusion was drawn that this was a result of heterogeneity of genotype.

## 10.5 Tumour-suppressor expression

Reproducible, clear, and unambiguous results are often difficult to achieve with Western analysis. The number of variable factors is very large, and the underlying causes of technical artefacts can be difficult to identify, and hence, rectify. Even when data of an acceptable quality are obtained, their interpretation is not always easy. In particular, where multiple populations of cells may be represented in a lysate, no distinction is possible between a low level of target protein expression by every cell, and a high level of expression by relatively few. From the results described above, just this situation may apply to the NZM cell-lines. A further aspect of protein analysis is that it elucidates a biological level between the genetic and the phenotypic. Results may help to explain some molecular mechanisms, but little information can be gained about ultimate causes, as any alteration in protein expression seen may be a consequence of innumerable antecedent steps.

In the investigation of the expression of selected tumour-suppressor proteins in the NZM cell-lines, it was found that all expressed pRB, except NZM6, NZM7.2, NZM7.4, and NZM10.1. Of these, the first three, and possibly all, produced abundant p16. This was in agreement with the widely reported reciprocal expression levels seen for these proteins, and with the hypothesis that pRB may mediate repression of p16. These data are all consistent with the apparent integrity of the 9p21 locus in these cell-lines as determined by PCR. There was evidence of production of a low molecular weight p16 variant by NZM12, also consistent with the genetic anomaly found by PCR. In three other cell-lines, apparently intact at 9p21, no p16 was detected. No evidence that this was due to transcriptional silencing by genomic methylation was found, but this possibility could not be entirely discounted. Low levels of ARF expression were detected in all cell-lines, apparently at odds with the 9p21 data in the cases of NZM1, NZM2, NZM3, NZM9, and NZM11. This may be a further manifestation of the presence of multiple sub-populations, and additional investigation would be required to determine this. Expression of p15 was in general absent or weak in all cell-lines, but it was induced by treatment of NZM4 with TGF $\beta$ 1.

Retracted material.  
See section addendum for details

10: Summary of experimental results

# Summary of experimental results (V3)

## 10.6 Retraction of some V1 results

The *CDKN2A* A526G variation in NZM7.2 and NZM7.4 reported proved on review to be a phantom: it was a variation unwittingly introduced during PCR through the use of published primers that did not match the reference sequence. The *CDKN2A* C333T variation in NZM12 was not confirmed, but neither was it disproved, as the use of primers amplifying *CDKN2A* exon 2 in one segment in V3 resulted in no product for NZM12. On review, it appears likely that the product seen in V1 was actually the homologous *CDKN2B* target being amplified in the absence of the intended one. The interpretation of the pRB Westerns in V1 was flawed as a result of the use of a spurious negative control, and the conclusion drawn about non-expression in some cell-lines was wrong. The V1 results for *CDKN2A* demethylation and ARF expression were of unacceptable quality.

## 10.7 Summary table

A summary of the main experimental results of the V3 work is presented in Table 10–2.

	Ploidy	CND	9p12–9p23 integrity	Microsatellites			DNA sequence variations	Protein expression		
				D9S1853	D9S974	D9S157		pRB SD	pRB EC	p16
NZM1	1.82	Yes		A	del	F	–	+??	+??	–
NZM2	1.89	Yes		A	del	F	–	+B↓	+B↓	±
NZM3	1.95	Yes		A	del	A	–	+B–	+B↓	±
NZM4	2.99	Yes		G	MO	G	–	+B–	+B↓	±
NZM5	1.01	Yes		A	J	F	–	+B–	+B↓	±
NZM6	2.00	Yes		AF	AH	CF	–	+U–	+U–	+
NZM7	1.36	Yes		A	IK	F	2A G500C (het)	+U–	+U–	+
NZM7.2	1.25	Yes		A	IK	F	2A G500C (het)	+U–	+U–	+
NZM7.4	1.27	Yes		A	I	F	–	+U–	+U–	+
NZM9	2.02	Yes		A	del	B	–	+B↓	+B↓	–
NZM10	2.14	Yes		B	J	F	–	+B↓	+B↓	–
NZM10.1	2.50	Yes		G	MO	G	–	+B–	+B–	±
NZM11	1.73	Yes		AG	del	C	–	+B↓	+B↓	–
NZM12	1.23	Yes		A	I	F	–	+B↓	+B↓	–
NZM13	1.27	Yes		A	del	A	–	+B↑	+B↓	±
NZM14	1.17	n.d.		AE	K	B	2B G411A (–het)	+B–	+B–	±
NZM15	1.95	Yes		A	J	A	–	+B↓	+B↓	±

Ploidy is relative to diploidy. CND = centrosomal numerical dysregulation; n.d. = no data. 9p12–9p23 image is unscaled map of loci inspected; green = intact, orange = microsatellite not detected, red = exon not detected; *CDKN2A* is to the right. Microsatellite letters denote alleles found {Table 8–4}; del = deleted. DNA variations are with respect to the reference sequence; 2A = *CDKN2A*; 2B = *CDKN2B*; – = none found; het = heterozygous; –het = not heterozygous. For pRB: SD = serum deprivation experiment; EC = extended culture experiment; + = detected, U = only unphosphorylated pRB present in control; B = both phosphorylated and unphosphorylated pRB present in control; ↑ = phosphorylated proportion increases on treatment; – = no change on treatment; ↓ = phosphorylated proportion decreases on treatment; ?? = data uncertain. For p16: + = detected; – = not detected; ± = data uncertain, weak expression possible where *CDKN2A* not deleted.

Table 10–2: Summary of experimental results (V3)



## 10.8 Concordance with V1 results

The ploidy results obtained in V1 and V3 were in broad agreement, diverging by a mean of 3.4% and by less than 10% in the worst case. Evidence of heteroploidy was not as marked, but signs were still present.

Repetition of the serum deprivation time course confirmed the existence of the three classes of response reported in V1. However, the type of response seen on repetition was different in two of the three exemplar cell-lines investigated. This shows that the response to serum-deprivation is not dictated purely by the cell-line, and may well depend upon the exact constitution of the FCS used in culture. Given that, no attempt was made to evaluate values for Q for the three cell-lines.

Deletion mapping of the 9p12–9p23 region was generally concordant in that with very few exceptions, where a deletion was detected with high confidence using refined PCR procedures in V3, clear indications of this were found during V1. With improved standardisation of DNA and the addition of BSA to the PCR reaction to counteract the inhibitory effects of melanin, most of the variations in product band intensity seen in V1 vanished, although some differences did remain. The original hypothesis of differences in target prevalence is still viable in these cases, but primer binding site mutation is an equally viable alternative explanation.

The *CDKN2A* G500C sequence variation in NZM7.2 was confirmed, as was its heterozygous nature; the presence of only the G allele in NZM7.4 was confirmed. The *CDKN2B* G411A variation in NZM14 was confirmed.

The expression of p16 in NZM6, NZM7.2, and NZM7.4 reported in V1 was confirmed in V3. Of those cell-lines reported as having weak p16 expression in V1, consistent data were obtained in V3 for NZM4, but not for NZM10. While a faint band was seen for NZM10 in V3, it was similar in strength to those seen in *CDKN2A* null cell-lines, and so cannot be interpreted as evidence of p16 presence. The production of a short p16 by NZM12 reported in V1 was not confirmed, but the possibility that this is a consequence of the loss of a C-terminal epitope recognised by the V3 antibody cannot be excluded, as the actual epitope has not been characterised. Overall, the quality of the p16 Westerns still has room for improvement.

V3 did not encompass further studies into demethylation as a potential means of recovering p16 expression, nor expression of p15 or ARF.

## 10.9 New findings

The principal new findings in V3 relate to centrosomal integrity and anomalous pRB phosphorylation in some cell-lines. It is now very clear that centrosomal numerical dysregulation is a common, possibly ubiquitous, feature of metastatic melanoma cell-lines, and from the evidence gathered showing multipolar mitotic spindles and non-binary cytokineses mediated by supernumerary centrosomes, the role hypothesised in V1 for centrosomal involvement in genome instability should be considered proven.

The discovery of aberrant phosphorylation of pRB in cell-lines that concomitantly have high p16 expression is intriguing and warrants further investigation, directed in the first instance at the mutational status of other components of the mechanism for the regulation of cellular proliferation mediated by pRB, and the status of *MYC* and its encoded protein.

Novel secondary observations stemming from the centrosomal study include: nucleolar pericentrin reservoirs, cell-cycle dependent variation in cytoplasmic pericentrin, tubulin nests, and anomalous nucleic acid bodies. The finding of independent mitosis and possibly apoptosis in multinuclear cells was surprising, but there have been rare reports of both of these phenomena. All of these are significant initial findings and certainly warrant further study.

## 11.1 Centrosomes and melanoma

### Justification for further study

When it is considered that the centrosome ranks with the nucleus in terms of the stringency of its regulation, and that a clear association exists between its dysfunction and tumorigenesis in general, centrosomal molecular biology appears not to have received the level of scientific scrutiny it warrants, and so, is poorly understood. The data presented here, primarily from the analysis of ploidy, but supported by the 9p21 integrity and tumour-suppressor gene expression studies, provide a case, albeit circumstantial, that centrosomal dysregulation may play a significant role in the pathogenesis of many melanomas.

With metastatic melanoma being essentially incurable at present, no aspect of its molecular biology can be ignored without the risk of overlooking an opportunity for the development of new therapies. There are more than sufficient grounds to justify a rigorous examination of the association between centrosomes and melanoma.

### Plausible research directions

With such a limited existing body of work, the scope for further investigation is vast. Perhaps the simplest starting point would be an ultrastructural study of centrosome number and morphology in melanoma tumours and cell-lines, utilising techniques of immunocytochemistry, and confocal and electron microscopy. These could be extended in vitro by following the lead of Khodjakov et al.<sup>564</sup>, who incorporated green fluorescent protein into the centrosomal structure. Rather than being targets for laser micro-surgical ablation, centrosomes so tagged could be followed readily with time-lapse fluorescent video-microscopy<sup>1029</sup>. By allowing time-resolved visualisation of the centrosome cycle in concert with cytokinesis, this approach should rapidly provide answers to the most pressing questions raised here.

At the molecular and genetic level, many candidate centrosomal regulators could be screened for mutation, expression, and dynamic distribution. The focus for this research should be CDK2, and it should encompass mechanisms of regulation including phosphorylation state maintenance, and inhibitor activity. High on the priority list for study would therefore be the cyclin-E isoforms, the WEE1 and PKMYT1 kinases, the CDC25 phosphatases, p27, and elements of the proteasomal degradation subsystem that targets p27, including SKP1, SKP2, and CUL1. Additional molecules of interest would include the p53 associates or transcriptional targets BRCA1, p21, and the GADD45 isoforms, as these may participate in centrosomal regulation after genomic damage.

### Potential therapeutic implications

Even while this research is being carried out, existing therapies may be reconsidered from new perspectives. For example, the role of microtubule modulating agents such as paclitaxel should be evaluated in terms of their effect on centrosomal function, rather than on microtubules in isolation. There are signs that this is taking place, with a recent study reporting that fluorescent taxoids accumulate in the centrosome before engendering apoptotic death of tumour cells<sup>3</sup>.

Should a causal role for centrosome dysregulation in the development of melanoma be verified, a new therapeutic target will have been defined. However, it is not one that readily lends itself to manipulation. Since centrosomes are critical for the faithful replication of all cell-types, agents acting directly on them, or on components of their regulatory subsystem, are unlikely to be more selective than traditional cytotoxic drugs. Complete specificity would require a therapeutic mechanism that targets only mitotic cells without exactly two centrosomes. Short of a counting mechanism based on nanotechnology, this may not be possible. Some assistance may be available from the inherent block to further propagation that occurs in acentrosomal cells [J-2], assuming that this has remained intact in the tumour, which is by no means a certainty. Then, only cells with supernumerary centrosomes need be targeted. This could provide a very slender therapeutic opportunity through the use of a hypothetical set of ternary agents. Each would target a single centrosome, but their joint cytotoxicity would depend on the presence of three distinct types in the same cell. A greater understanding of the molecular basis by which centrosomes officiate at the last step of cytokinesis may lead to opportunities for intervention there. Finally, if the hurdles that currently hinder effective gene therapy can be surmounted, problems of centrosome regulation that stem from a genetic cause may also become tractable.

## 11.2 Heterogeneity and melanoma

### Introduction

During the execution of this work, one finding arose repeatedly: heterogeneity within individual melanoma cell-lines. It was seen in the heteroploidy of NZM10 {Figure 5-4}; in the intermediate levels of PCR amplification of 9p21 targets {Figure 8-2}; in the heterozygosity of a genetic marker in NZM7.2 that was lost from the related NZM7.4 {Figure 8-4}; in the survival of only very few NZM10 sub-clones {9-11}; in the disparate growth of nominally replicate cultures after serum-deprivation in NZM10 {Figure 7-3} and NZM6 {Figure 7-14}; and in the absence of pRB expression in NZM10.1, despite its expression in the parental cell-line, NZM10 {Figure 9-1}. It has previously been reported as a difference in *TP53* mutation status between NZM7.2 and NZM7.4<sup>1002</sup>, as heteroploidy in NZM7<sup>180</sup>, and in the karyotypes of the NZM cell-lines<sup>966</sup>. Wherever the characteristics of individual cells, or sub-clones was investigated, heterogeneity was found; wherever semiquantitative procedures were used to investigate total cell culture extracts, it was found. What is the cause of this heterogeneity, and what, if anything, might it portend?

Retracted material.  
See section addendum for details

### **The source of heterogeneity**

Diversity of character among descendants of a single cell can arise from genetic, epigenetic, and contextual variations. In the NZM cell-lines, genetic variation was a frequent finding, and of itself, is sufficient to explain the diversity seen. As for the underlying cause of this genetic variation, no specific basis has been established, but genomic instability brought about by centrosomal dysfunction presents a very plausible explanation, as discussed above. An alternative might be the existence of an inherently high rate of mutation due, perhaps, to errors in genomic repair, but this could not account directly for the integral changes in ploidy seen. It is also conceivable that during a single tumour-wide event, multiple variants came into existence, and what is being observed in these early passage cell-lines is a transitional state during which remnants of less-favoured clones remain, possibly only by virtue of the relatively permissive in vitro context. However, this would not account for the production of new variants as detected in the NZM7.2, NZM7.4, and NZM10.1 sub-clones. The most probable explanation therefore seems to be that genomic instability is an attribute of some melanoma tumours {8–8}, and that this is perpetuated in vitro.

This produces a paradox when the role of these melanoma cell-lines in research is considered. On the one hand, their heterogeneity detracts from their usefulness since they are intrinsically unstable, making reproducibility problematical. On the other, they may accurately reflect what has been occurring in vivo for precisely the same reason. The question of whether this makes them more, or less valuable as research tools in the quest to understand the dynamic molecular biology of tumours remains open.

### **The biological significance of heterogeneity**

#### *A new model of tumorigenesis?*

Many of these tumours, and hence their derivative cell-lines, may therefore be in a state of continuous genomic flux. By its essential nature, this flux precludes the out-growth of favoured sub-clones, since they themselves would be unstable. This is quite contrary to the traditional view of multi-step tumorigenesis. Instead, it can be viewed as a vastly accelerated process of cellular evolution, wherein countless variations on a central theme occur simultaneously. Many will prove to be inviable, contributing to the necrosis seen in tumours. Some may have a borderline viability, being dependent upon external support through growth factors or similar mechanisms, as proposed here for NZM10 {9–11}. Some may be entirely self-sufficient, but since their ability to bequeath this attribute to their descendants is compromised by their inherent genetic instability, this can only be a transient state. They serve simply to alter the current theme on which the next variations will be based. Conceivably, this random process may lead to a situation where no independently viable cells exist, perhaps accounting for the rare spontaneous regressions seen in individual melanoma tumours.

#### *A means of escape from therapy?*

In this model of tumorigenesis, the heterogeneity and dynamic variability of tumour cells present major obstacles to the complete therapeutic eradication of a tumour. Among the

variants that exist at the time of treatment may well be a subset that is immune to the agent used. This may account for the observed phenomena of supra-additive effects of multi-agent therapies, the development of resistance to agents with common modes of action, and the overall poor therapeutic response of metastatic melanoma. It also casts doubt on the viability of any therapy based solely on a 'magic bullet', since such a strategy depends on uniformity and constancy within the tumour. Variations wherein a bystander effect is incorporated may still hold promise, however.

The heterogeneity seen at the locus of an implicated tumour-suppressor gene, *CDKN2A* {8–8}, implies that human tumours cannot simply be described as expressing or lacking any particular molecular marker. Nevertheless, characterisation of just this type has been a driving force behind the design of novel anti-cancer agents that target signal transduction channels, such as oestrogen receptor antagonists and epidermal growth factor receptor inhibitors, and it is being used to an increasing extent as a guide to therapeutic decisions.

### *A basis for tumour survival?*

This model includes the possibility that marginally viable variants may be supported by the heterogeneous tumour population as a whole, but the converse situation may also occur: that the majority of tumour cells may be inviable but for the existence of a supportive minority. The difficulty in establishing sub-clones of NZM10 by individual cell propagation is consistent with this {9–11}, and the subsequent finding that while the parental heterogeneous cell-line expresses pRB, the viable sub-clone NZM10.1 does not, provides a possible molecular basis.

If this were so, and for some reason this supportive minority was lost, the tumour may simply die out. This too may contribute to spontaneous regression, particularly when the rigours of growth in the solid tumour environment are considered.

### *New therapeutic targets in metastatic melanoma?*

More importantly, such a distinct sub-population may be susceptible to selective targeting allowing tumour regression to be triggered therapeutically, and this would be as true for disseminated metastases as for primary tumours. It may seem that this presents a daunting problem of cellular discrimination, much harder than finding the elusive 'magic bullet' needed for tumour selectivity, but this need not be so. Much depends on the molecular basis for this supportive effect. Identification of the growth factor involved may lead to the development of agents interfering with its production or activity, severing the link between supportive and dependent cells. However, as discussed above, the very heterogeneity that allows this co-dependency also contains the seeds of drug-resistance.

If the lack of pRB expression seen in the independently viable NZM10.1 sub-clone proves to be inextricably linked to the production of the required growth factor {9–11}, a somewhat different situation would exist: the lack of pRB, not the production of the cytokine could serve as the distinguishing characteristic. This begs the question of how a therapeutic agent could be selective for cells that *do not* possess the critical molecular target. In the case of pRB, the answer



to this could have its basis in the enormously important role it plays in regulating DNA synthesis. Its potency is such that DNA-viruses, which may have genomes of only a few tens of genes, often contain one with the sole function of disabling pRB {See 'Viral infection', H-19}. This allows viral genome replication to proceed and may contribute to the survival of the host cell until it is ultimately lysed, releasing the viral progeny. Where this gene is defective, the virus cannot replicate, unless the host cell lacks functional pRB. It follows that a virus of this type, engineered to be defective in its anti-pRB gene, would selectively replicate in, and ultimately destroy, only cells that lack pRB, precisely what may be required therapeutically.

#### *An existing therapy for metastatic melanoma?*

Onyx Pharmaceuticals of Richmond, California, have developed such an engineered replication-competent adenovirus, ONYX-411. It was created in parallel with their more widely known construct ONYX-015, a similar adenovirus that replicates only in cells lacking functional p53. While the latter is in clinical trials for treatment of various cancers<sup>686</sup>, ONYX-411 has not yet advanced to this stage. Nor is it clear if Onyx perceive that ONYX-411 may have particular application to metastatic melanoma, since while known, pRB defect is not considered a major contributor to melanoma tumorigenesis, particularly in comparison to p16 defect. The selection of patients for any ONYX-411 trial may be based on tumour type, and be biased in favour of those where pRB involvement is more overt, retinoblastoma, osteosarcoma, and bladder carcinoma being the most obvious candidates. Alternatively, it may encompass a broad range, on the basis that some 25% of cancers do have pRB defects. Without the information that pRB-deficient sub-populations may support pRB-expressing melanoma tumours, there is a risk that too few melanoma patients may be enrolled to allow a statistically significant finding to be made. This is particularly true since melanoma is a not a common cancer.

There may be pitfalls inherent in this approach, one being that it includes the delivery of a gene, which if expressed, disables cellular p53 function. While in pRB-expressing cells, ONYX-411 is unlikely to expand to a high copy-number<sup>360</sup>, the risk exists that a pseudo-Li-Fraumeni syndrome phenotype may be engendered to some degree. This prospect may be avoidable by further engineering the virus such that expression of the p53 antagonist is inducible, and co-administering the inducer with the virus. Subsequent removal of the inducer would disable expression of the antagonist, reversing any effect.

These observations, inferences, and implications are extremely important and must be pursued with vigour. The correlations between pRB-deficiency, independent survival, and paracrine support must be confirmed. If they are, in vitro assessment of ONYX-411, or a similar virus, against melanoma cell-lines should be carried out. Lacking such a virus, but having identified the cytokine involved, proof of principle experiments could still be performed through antibody neutralisation or antisense technology. Efforts must be made to ensure that metastatic melanoma is included in any clinical trial of ONYX-411.

## Conclusion (V3)

---

### 11.3 Retraction of some V1 results

The V1 results for the analysis of pRB were misinterpreted in consequence of a spurious negative control having been used, and it now seems very likely that all NZMs express the protein. Additionally, doubt over the authenticity of the NZM10.1 cell-line has arisen as a result of the analysis of microsatellite allele length {See '*Doubt over NZM10.1 authenticity*', on page 8–36}.

### 11.4 As one door closes...

#### Heterogeneity and melanoma

The case for genomic heterogeneity in melanoma made in V1 has been weakened by the near disappearance of heteroploidy as assessed by flow cytometry, the very marked reduction in the variability of PCR amplification of 9p12–9p23 targets seen, and the invalidation of the pRB non-expression data for NZM10.1. Nevertheless, the confirmed DNA sequence variations in the NZM7 group, and the new data showing loss of a microsatellite allele in NZM7.4 attest to the presence of multiple populations in the parental line. Even on this reduced evidence, especially when the case is bolstered by the results of the centrosomal study, the arguments that genomic heterogeneity exists in melanoma and may play a role in therapeutic evasion remain justified, and the bulk of the earlier discussion remains valid.

The greatest casualty of the V3 work has been the invalidation of the conclusion that while the parental NZM10 cell-line produced pRB, the NZM10.1 sub-clone did not, with this falling under the twin blows of the very greatly improved pRB Western blotting results, and the doubt over the authenticity of NZM10.1. Of course, this doubt may also work the other way. It is possible, if improbable, that the pRB result for NZM10.1 obtained in V1 was valid: the cells used may have been genuine NZM10.1 cells, and the mysterious 116 kD band on the Western blot may have been non-specific; while in V3, the cells assayed were very probably not NZM10.1, so the V1 result should not be invalidated just on that basis. The truth is unlikely ever to be known.

Without confirmation of that disparity between NZM10 and NZM10.1, there would seem to be no foundation for the suggestion that an effective therapy could be based on targeting cells that do not express pRB through the use of an agent like the ONYX-411 virus. Nevertheless, there are still valid reasons for thinking that this approach is worth pursuing. Defects in pRB-mediated proliferation control occur in very many melanomas, even where pRB itself is intact, notably through inactivation of p16, and it is pRB functional failure, not pRB absence itself, that gives ONYX-411 selectivity. It follows then that ONYX-411, or a similar agent, may have therapeutic value in a subset of melanomas, and perhaps even in the majority. Unfortunately, Onyx Pharmaceuticals ceased development of viral products in 2003 for lack of collaborators.





---

## 11.5 ...another often opens

### Centrosomes and melanoma

The first step in investigating whether centrosomal dysregulation could form a basis for genomic instability in melanoma has now been taken {See Chapter 6}, and it has been graphically demonstrated that it could. An appreciation of the scale and consequences of this may prove to be the most significant result of this research.

Three very significant challenges exist on the path to converting this finding into one of practical application in the treatment of melanoma. First, it must be established that what is being seen in vitro is not a cultural artefact, and is indeed occurring in vivo. Second, it must be established that this phenomenon does significantly contribute to the poor response melanoma has to therapy, for if it does not, any further development along these lines may be of little benefit. Third, and by far the most daunting task, a means of selectively targeting cells with this flaw for remedial therapy or destruction must be found.

Creation of a therapeutic mechanism that could count centrosomes in cells, and where that number was found to be more than two, set about destroying either the supernumerary centrosomes, or the cells themselves, would seem to be in the realm of nanotechnology, if not science fiction. However, if pericentrin regulation does prove to be disturbed in melanoma, and this leads to centrosomal irregularities, then the prospects are much more realistic. Once more is known of the structure and function of pericentrin, it may prove possible to develop drugs that either prevent it from exerting its disturbing influence, or that target cells that over-express the protein.

There is much still to be done.

---

### Envoi

---

What began as a relatively mundane molecular survey of cell-lines has led to the recognition of a novel basis for melanoma tumorigenesis, perhaps also applicable to other tumour types. Avenues for further exploration have been identified, the results of which may allow both the refinement of existing therapy, and the development of new therapies for what is currently an intractable disease.

This success is a testament to the far-sightedness of those who sought to establish the NZM cell-lines and who sponsored this work. The saddest aspect is that the very generous people who literally give of themselves to make this possible could not themselves benefit from it. Their gifts were to the future. We must not squander them.



---

## **Technical appendices**

---



---

# A

# Methodological foundations

---

## A.1 Principles of restriction enzyme digestion

Restriction enzymes are endonucleases that recognise specific base sequences within double-stranded DNA and cleave it there. The cut site can be within or adjacent to the recognition site, and the resultant cut can be either blunt-ended or staggered. In some cases, cleavage is dependent upon the methylation status of the DNA.

Such enzymes are thought to form the basis for the immunity bacteria may have against infection by bacteriophages in that they express a restriction enzyme that degrades invading DNA, while leaving the host's DNA intact. This selectivity may be by virtue differences of DNA sequence or methylation status between the host and the bacteriophage. In this way, they restrict the host range of bacteriophages, hence the name. Several hundred such enzymes are known and are commercially available, usually as recombinant proteins.

Molecular biologists have seized upon these enzymes as powerful tools for the manipulation of DNA, nowhere more so than in the practice of cloning. Other applications include restriction fragment length polymorphism (RFLP) analysis, single-strand conformation polymorphism (SSCP) analysis, and DNA quality assessment.

Each has particular optimal reaction conditions, with typical variable parameters being pH, temperature, incubation time, and buffer composition. Information concerning these is usually provided with the commercial product.

## A.2 The polymerase chain-reaction

### Principles of PCR

The basic theory and practice of PCR are well established and many excellent reference works are available<sup>273</sup>.

### Traditional primer optimisation

In establishing optimal amplification conditions, two potentially conflicting requirements must be addressed: while the primers used must bind tightly to their specific sequences, they must not bind to any other. Most conditions which favour one disfavour the other. Difficulties also arise from primers that homo- or heterodimerise, form loop or hairpin structures, or have poor 3' binding strength. In addition, if the melting temperatures ( $T_m$ ) of the primers are not close, then asymmetrical binding can result in poor amplification. Consequently, a tedious and generally undirected process of optimisation usually must be performed, with the varying of such parameters as the annealing temperature ( $T_a$ ),  $Mg^{2+}$  and primer concentrations, and the use of PCR enhancers.

Most problems can be substantially alleviated by rational primer design, usually with the assistance of specialised computer software. This can provide stable primers with matched predicted  $T_m$ . However, there is often a discrepancy between the calculated primer  $T_m$  and the optimal  $T_a$  for PCR. The technique of touch-down PCR (TD-PCR) was developed to address this issue.

---

### Touch-down PCR

In TD-PCR, rather than successive amplification cycles using the same  $T_a$ , cycling begins at a  $T_a$  some 5 °C above the calculated  $T_m$ , and decreases by 0.5 °C per cycle until it is some 5 °C below the calculated  $T_m$ . In the early cycles, it is unlikely that either primer will bind anywhere, but as cycling proceeds, this becomes more likely. The key is that the first place that the primers bind will be their specific site, as with properly designed primers, this will have the highest stability. This gives amplification from these sites priority, essentially performing more cycles at the specific site than at non-specific sites, greatly reducing the production of artefacts.

It is usual in TD-PCR to follow this first phase with a second in which the  $T_a$  is held constant, and is set to be about  $T_m - 10$  °C. This provides for amplification of all species present, but the proportion of specific to non-specific products will be essentially unchanged.

### Reducing the risk of contamination

A remaining obstacle to reliable PCR is the possible presence of contaminating DNA. Several measures can be taken to minimise this risk, including:

- use of a PCR-dedicated, physically separated, nucleic acid-free, work-space;
- use of certified nuclease-free, filtered pipette tips;
- dedication of a set of pipettes solely for PCR work;
- UVR-irradiation of all tubes, racks, pipettes, tips, and reagents to be used, except those that contain nucleic acids, dNTPs, or enzymes;
- final addition of template DNA in a separate physical location.

### A.3 The single-strand conformation polymorphism assay (SSCP)

In the SSCP assay, the two strands of DNA are separated by heat denaturation and are then quickly chilled, causing rapid reannealing. If the DNA concentration is low, a high proportion of strands will undergo intra-molecular annealing. The exact conformation adopted by a strand is highly dependent upon its primary sequence<sup>938</sup>. Two sequences differing in only a single nucleotide can have vastly different folding outcomes. Once formed, the self-annealed strands are separated by high-resolution PAGE and visualised by a sensitive detection system, such as silver staining. Typically, three bands will be seen, corresponding to the two separated strands which have self-annealed, and reformed duplex DNA. Additional bands may be present resulting from alternate conformations being adopted, or where multiple sequence species exist, as in heterozygosity.

It is usual to run putatively normal DNA alongside as a control. Where banding differences are seen, the variant DNA is further characterised by sequencing of the PCR product, or by cloning followed by sequencing.

The ability of SSCP to detect sequence polymorphisms is approximately 80%, however this can be increased by the utilisation of several different electrophoresis conditions. Parameters commonly varied are:

- acrylamide concentration;
- degree of gel cross-linking;
- buffer ionic strength;
- buffer pH;
- electrophoresis running temperature;
- the use of gel additives, such as glycerol, formamide, or urea.



Based on the work of Teschauer<sup>1321</sup>, conditions of 14% acrylamide, with and without the addition of 10% glycerol, were selected for routine use in this research.

## A.4 Fundamentals of Western blotting

### Principles

Western blotting uses the specificity of antibodies to detect a protein of interest among a host of irrelevant ones. It comprises the following major steps:

1. Extraction of protein from the source material;
2. Heat denaturation of the extracted proteins in the presence of SDS and a reducing agent;
3. SDS-PAGE to separate the proteins by molecular weight;
4. Transfer of the proteins from the gel to a suitable membrane, where they are immobilised;
5. Blocking of the membrane to eliminate non-specific binding of antibodies;
6. Exposure to an antibody specific for the protein of interest;
7. Detection of the bound antibody.

There are possible variations on all steps.

### Variations

The source material may be tissue, cultured cells, or sub-cellular fractions.

Extraction may be into a specialised lysis buffer containing multiple protease inhibitors, or merely into sample loading buffer. Several reducing agents are in common use, notably 2-mercaptoethanol and dithiothreitol.

The gel concentration is often selected based on the expected MW of the target protein. This may range from 6% for large, to 20% for small proteins. In addition, use has been made of gels with concentration gradients, both linear and non-linear.

Membranes may be nylon, nitrocellulose or PVDF, and transfer by capillary action or electrotransfer.

Various materials are commonly used in blocking solutions, including non-fat milk, bovine serum albumin (BSA), and gelatine. However, care must be taken with this selection, as cross-reactivity between any antibody used and a component of the blocking solution will result in a very high background signal. Blocking agent concentration, blocking time and temperature are all variable. Higher concentration, longer duration, and higher temperature all favour more stringent blocking. It is usual to include a detergent such as Tween-20, and the concentration of this may also be varied. A low concentration, such as 0.01% v/v would increase binding at the expense of specificity. A high concentration, such as 1% v/v would have the opposite effect.

The primary antibody working concentration is usually determined empirically and depends upon such factors as the target abundance, the antibody affinity, and the sensitivity of the detection system to be used. It is conventionally specified as a dilution factor, but this can be subject to misinterpretation if antibodies are supplied at different concentrations. Working dilutions usually range from 1:100 for a low-affinity antibody used with a detection system with low sensitivity, to 1:10 000 at the other extreme. Duration and temperature of attachment may be varied with increases in each resulting in increased specificity, but possibly decreased total binding. Attachment may also be in the presence of blocking agents to reduce non-specific binding further.

Finally, the manner of detection of the bound antibody is open to great variation. The antibody could be labelled directly with a radioactive or fluorescent tag, or with an enzyme or other catalyst, but it is much

more common and cost-effective to use a tagged secondary antibody specific for the immunoglobulin type and species of origin of the primary antibody. In this way the same 2° antibody can be used for many different primaries. The use of a catalytic tag allows amplification of the signal, increasing the sensitivity of detection. Perhaps the most common detection system relies on the attachment of an enzyme to the 2° antibody, typically alkaline phosphatase or horseradish peroxidase. A substrate is then applied to the membrane as a whole that, upon reaction catalysed by the tag, produces a detectable signal, often the creation of a coloured product, or the emission of light through chemiluminescence.

### A.5 Fundamentals of flow cytometry

#### Principles and terminology

The essence of flow cytometry is the analysis of the effects produced by the passage of a particle of interest through a beam of light, termed an event. Typically, the particle will be a cell, the beam of light will be from a laser, and the effects measured those of light scattering and fluorescence.

Within the cytometer, a continuous non-turbulent flow of sheath fluid is maintained through the flow cell. Into the axis of this is introduced the sample to be analysed. The laminar flow of the sheath fluid restricts the sample to the central core of the flow cell without the need for any physical constraint, facilitating the passage of light to and from the sample. Usually, the rate of sample injection, the flow rate, is under operator control and may be varied either continuously, or in discrete steps {See 'Flow rate', below}.

Light emanating from the particle under scrutiny encounters a series of optical components, including beam-splitters that redirect a proportion of incident photons, and filters that selectively block and pass particular wavelengths of light. These serve to distribute the light produced among multiple detectors. Each detector produces an output voltage that depends upon the intensity of the light falling upon it. This dependency can be either linear or logarithmic allowing the reporting of intensities that differ by several orders of magnitude, and the mode of operation is under operator control. Typically, a detector is based on a photomultiplier tube. In this device, incident photons dislodge electrons from a metallic target, and these are accelerated by an applied electric field. In turn, these electrons strike a second target, where, by virtue of the energy they have gained by being accelerated, they dislodge a greater number of electrons. This multiplication effect is repeated several times in each tube resulting in a geometrical increase in output voltage with each stage. In addition to being dependent upon the intensity of the incident light, the output is also dependent upon the voltage difference applied between photomultiplier stages that imparts the acceleration to the electrons. This voltage is under the control of the instrument operator and represents the primary means of adjusting the detector sensitivity. It must be borne in mind that because of the multiplicative nature of the amplification, a small increase in this voltage can result in a very large increase in the output voltage. For signals that are particularly weak, such as fluorescence, a further linear amplification stage is added. This is controlled by adjusting amplifier gain, providing a finer degree of sensitivity control. In summary, for each detector there is usually:

- The possibility of a restricted wavelength window;
- A choice between linear and logarithmic detector response modes;
- A coarse geometric sensitivity adjustment through the photomultiplier tube voltage;
- A fine linear sensitivity adjustment through the amplifier gain.



### What can be detected?

The intensity of light detected on the opposite side of the particle from the light source, forward scatter (FSC), is strongly dependent upon particle size, with larger particles giving greater intensity. At first glance, this may seem counter-intuitive as one may expect a larger particle to block more light. The key is that FSC is not light that has passed unhindered through the particle, but rather light that has been scattered at a very low angle. This arises from lensing or diffraction effects that are increased by particle size. FSC is relatively bright and so there is often no amplifier stage associated with this detector. Furthermore, photomultiplier voltage settings may be constrained to orders of magnitude only, with no finer adjustment possible, or indeed necessary.

The intensity of light scattered perpendicularly to the beam path, side scatter (SSC), is strongly dependent upon particle internal reflectivity or granularity, and more weakly dependent upon particle size, with large, granular particles giving the strongest signal.

Fluorescence can also be detected. This can result from the excitation of substances either normally present in the particle, auto-fluorescence, or ectopically expressed, such as green fluorescent protein. Of much greater utility is the detection of signals from dyes that have by some means been attached to a target of interest, such as DNA or proteins.

The output from the amplification stage may be fed into an electronic signal processing subsystem. Typically, this calculates three derived values for each event: the height, proportional to the maximum signal level; the area, proportional to the total light emitted during the event; and the width, proportional to the duration of the event. Often, the width is derived from the time between the input signal exceeding half of what its ultimate peak will be, and when it subsequently falls below this level. Clearly, since the maximum value cannot be known in advance, such post-processing is required. The information obtained this way may be extremely valuable, and is worth the cost of the complex instrumentation necessary to obtain it {See 'Singlet event selection', below}. Ultimately, the instrument reports a set of numbers for each event in arbitrary units that, for historical reasons, are called channel numbers.

### Data capture and processing

In the analysis of a single sample lasting just a few minutes, data from multiple detectors for each of 10 000 events may be recorded. The volume and rate of data produced are such that its acquisition by a dedicated computer is practically indispensable. Once captured, the data can be analysed at leisure. Since presentation of this data numerically would be so voluminous as to obscure any underlying meaning, extensive use is made of graphical data representation and statistical summarisation.

### Graphical data representation

#### Histogram plots

The simplest type of graph used is the histogram plot, which shows the distribution of reported light intensities for a single detector {Figure A-1}. From this, target prevalence can be visualised and quantified in terms of central tendency (mean, median, and modal channel) and spread (CV).

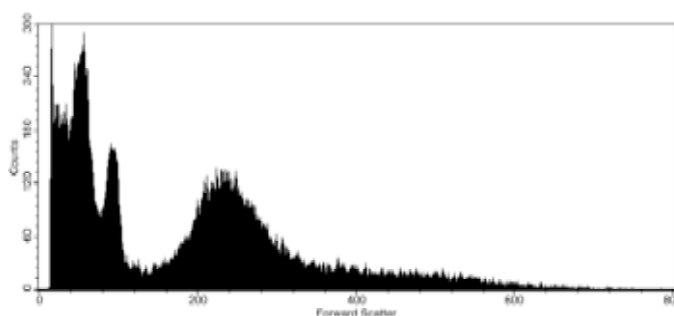
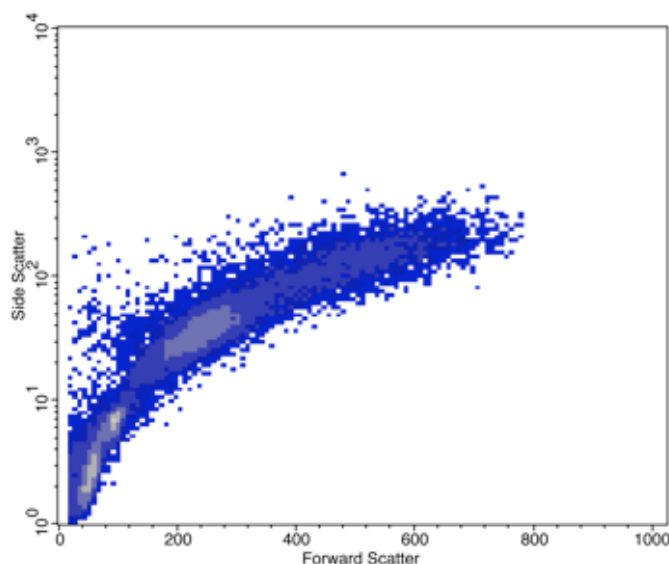


Figure A-1: Example histogram plot

Multiple differing sub-populations within a sample can be seen as multiple peaks on the histogram.

### *Dot, density, and contour plots*

Two-dimensional graphs are used to display data from two detectors simultaneously by assigning one detector to each of two Cartesian axes. In the dot plot, the existence of an event with a particular combination of signal intensity for each detector is indicated by a point at the corresponding position in the graph. An extremely useful variation introduces a third dimension to the graph, that of event frequency. Rather than overlapping events obscuring one another as occurs in the dot plot, the number of events with a particular combination of intensities is indicated by colour, yielding the density plot (Figure A-2). A further variation is the



**Figure A-2: Example density plot**

contour plot where rather than illustrating the points themselves, line segments are drawn between adjacent points with equal density. Such representations allow the visual discrimination of differing components within the sample, as they will appear as disjoint islands of points.

### *Regions and gating*

If a component of interest is identified graphically, this can be labelled and isolated for further analysis by defining a region that encompasses it, but excludes irrelevant points. This definition is performed by drawing a bounding polygon or ellipse directly on the plot with the analysis software.

Multiple regions can be defined on multiple plots that use any detector signals. These region definitions can be logically combined to create more complex event filters, termed gates. These gates can be used to restrict the data displayed on any analysis graph and so provide an extremely powerful tool for dissecting interactions and analysing minor, but important classes of event. Examples of gating appear in Figure 5-1 and Figure A-3.

## **Flow cytometric analysis of DNA**

### *DNA staining*

To analyse DNA by flow cytometry, it must first be rendered detectable. Several techniques exist with different strengths and weaknesses.

Where data concerning DNA synthesis are required, it is common to expose growing cells to a DNA base analogue, typically bromodeoxyuridine (BrdU), which can subsequently be detected with a dye-conjugated antibody. An exposure to BrdU of short duration compared to the cellular doubling time allows the identification and independent analysis of the S-phase component, while a long exposure allows this for the proliferating component, not necessarily the same thing. Another, but less common technique, is to incorporate nucleotide analogues that have appropriate fluorophores attached via linkers, rendering newly synthesised DNA inherently fluorescent and obviating the need for antibody labelling.

For gross assessment of cellular or nuclear DNA content, perhaps the most common method is the use of the DNA intercalator propidium iodide (PI). When bound to DNA it has a red-orange fluorescence



markedly stronger than when it is in solution. It does also bind RNA with a different, but overlapping, fluorescence spectrum. This characteristic can be used to gather further information if sufficiently discriminating detectors are available on the instrument. Where only information concerning DNA is desired and such discrimination is not possible, or simply as an expedient, it is common practice to digest RNA prior to analysis to reduce the non-specific signal generated.

### ***Ploidy analysis***

Two techniques that exist for the determination of gross cellular genomic complement are cytogenetic karyotyping and flow cytometric cellular DNA analysis. In the former, a slow and painstaking process yields a great deal of information about chromosomal identity, number and structure, but for relatively few cells. In the latter, a rapid, reasonably simple process yields information about the distribution of cellular DNA content among many thousands of cells. Despite the distinct types of the information derived, there is some overlap in terminology, with ploidy referring to the chromosomal content of individual cells in one case, and to modal population DNA content in the other. Thus, to a cytogeneticist, diploid implies a cell that contains two instances of each chromosome, but to a flow cytometrist, it implies a population that has the usual modal DNA content. For normal cells, the two are equivalent, but in cancer, changes in chromosomal structure and cellular DNA content are the norm, rather than the exception. Similarly, the terms tetraploid, aneuploid, and the like, have different nuances of meaning.

### ***Cell-cycle phase distribution***

Since the amount of nuclear DNA doubles during S-phase of the cell division cycle, some information about the replicative state of each cell can be inferred from DNA content. Cells with DNA equivalent to  $2n$  for their ploidy are in  $G_0$  or  $G_1$ -phase, those with the equivalent of  $4n$  are in  $G_2$  or M-phase, and those with an intermediate content are in S-phase. Study of the distribution of cells among these phases can shed light on what effect an experimental treatment has had on proliferation. By fitting a mathematical model to the observed distribution, generally with the aid of appropriate computer software, these effects can be quantified.

Staining with PI alone cannot distinguish between cells arrested at any point in the cell-cycle, and those in transit through it. It represents only a 'snap-shot' of the population. Often though, the dynamics of the situation can be explored with time course experiments. Additionally, BrdU could be employed to mark active DNA synthesis as outlined above.

### ***The need for high PI concentration***

Most flow cytometry references suggest the use of 5 – 20  $\mu\text{g}/\text{mL}$  of PI to stain a sample containing  $10^6$  cells. Where PI is limiting, the amount taken up by each cell is not only proportional to the DNA content, but also to the PI concentration. While this is entirely satisfactory for investigation of cell-cycle phasing, it can present problems for the quantitation of ploidy. Minor variation of cell number per sample and indeed variations in the cell-cycle phasing itself can alter the effective dose of PI encountered by each cell. This can lead to high between-sample variance of fluorescence integral for any given DNA content. Where the determination of sample ploidy depends upon the comparison of independent measurements of sample and standard DNA fluorescence, error may be introduced. Two solutions to this problem are available. Firstly, by raising the PI concentration to a level sufficient to saturate the DNA ( $\sim 50 \mu\text{g}/\text{mL}$  containing  $10^6$  cells), the resulting fluorescence will again be independent of PI concentration. This has the added advantage of improving the linearity of fluorescence integral versus DNA content within each sample. Secondly, and perhaps better, where possible, a ploidy standard can

be used within each sample. As an example, each experimental sample may be laced with normal peripheral blood leukocytes prior to staining. The DNA signals emanating from the different cell-types may be isolable by differences in forward and side scatter characteristics by the creation of appropriate gates. Where such a distinction is not possible, it may be necessary to employ a second fluorophore coupled to a marker specific for either the standard or the sample cell-type.

### *Singlet event selection*

One difficulty that arises in DNA analysis is the identity of DNA content in a singlet event where just one G<sub>2</sub> or M-phase cell is sampled, and in a doublet event consisting of two joined G<sub>0</sub> or G<sub>1</sub> cells. It is here that the derived data produced by the signal processing subsystem justifies itself. It allows singlet events to be distinguished from cluster events by their shorter signal duration for any given DNA content. This is illustrated in Figure A-3, a density plot of fluorescence detector 2 signal width (FL2-W), versus fluorescence detector 2 signal integral (FL2-A) for a set of PI-stained cells. The singlet events are readily distinguishable from clusters, which are at the top of the graph. In this way, a gate can be defined which can be used to exclude cluster events from further analysis.

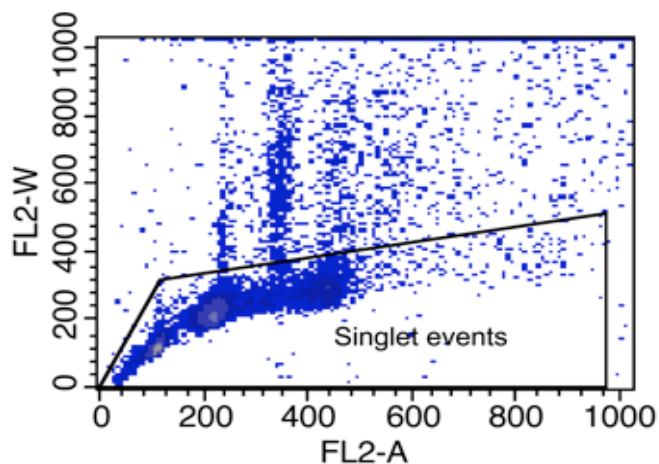


Figure A-3: Singlet selection

### *Peak versus integral fluorescence intensity as measures of cellular DNA content*

During the analysis of DNA, the typical flow cytometer produces two values for each event that have valid claim to represent the DNA content: the fluorescence height, and the fluorescence integral. Unfortunately, there are circumstances where these can be discordant and the question arises as to which is the more reliable measure. The case that proves the point is that where the particle size is larger than the effective illumination area of the activating light source. Here, the peak fluorescence is a measure only of the DNA present in the largest area illuminable, not the entire particle. The use of the fluorescence integral eliminates this problem, as all light emitted by the particle will contribute to the derived signal. Proponents of the use of peak fluorescence would argue that in most cases, this is not an issue, and the height parameter tends to have lower variability.

### *Flow rate*

The final practical aspect of flow cytometry to be discussed here is the effect of sample flow rate on the information captured. The essential difference is that by injecting a greater volume of sample per unit time into the sheath fluid column, the diameter of the central core must be increased. This increases the volume in which a particle can move during its passage through the flow cell, particularly if small particles, such as isolated nuclei, are being examined. Where the illumination is not uniform, or does not fully encompass the central core, variation in fluorescence may occur. Ultimately this shows as a slight increase in the breadth of the peaks seen in the DNA histograms. The effect is minor, but samples for DNA analysis should be run at the lowest flow rate consistent with a reasonable run time per sample.

**B.1 General considerations**

Principles of safe laboratory practice were respected at all times.

Unless otherwise indicated:

- 'Water' means high purity water such as 'Nano-pure' or 'Milli-Q';
- Solutions were in water;
- 'Medium' means sterile  $\alpha$ MEM with 10% v/v FCS and antibiotics (Solution 11);
- Incubations were performed at 37 °C;
- Procedures, other than incubation and refrigeration, were performed at ambient temperature, typically ~22 °C;
- Reagents were at ambient temperature, typically ~22 °C;
- Reagents were of molecular biological or reagent purity or better;
- Cells were assumed to have zero volume in calculations of cell suspension density;
- No adjustment was made in the preparation of solutions for any mutual solubility of one liquid in another, as with ethanol and water. All such v/v concentrations given are therefore only approximate.

**B.2 Methods for cell culture****General methods****Method 1**

Sterility was maintained for all reagents. This was achieved by autoclaving, sterile-filtration, or simply by the inherent characteristics of the particular reagent, as in the case of DMSO, which will not support microbial life.

Level-2 biohazard containment facilities were employed for all cell culture procedures involving human-derived material.

**Passage culture in vitro****Method 2**

Cell-lines were maintained by serial passage in  $\alpha$ MEM supplemented with penicillin-G ( $10^5$  units/L), streptomycin sulphate (100 mg/L) and 10% v/v FCS (Solution 11), unless otherwise noted. Incubation was in water-jacketed, temperature-controlled incubators in an atmosphere of 5% v/v carbon dioxide in air, with saturating humidity. For adherent cell-lines, passage was by trypsinisation (Method 4) and replating, and for non-adherent cell-lines, by simple division and medium replenishment.

**Washing of cells****Method 3**

1. If necessary, pellet the cells by centrifugation (~200 G, 5 min) and discard the supernatant.
2. Resuspend the cell pellet in a large excess of washing solution, usually PBS.
3. Centrifuge (~200 G, 5 min).
4. Discard the supernatant.

**Trypsinisation of adherent cells****Method 4**

1. Remove, and if appropriate, retain the supernatant medium.
  2. Rinse the vessel with PBS (Solution 6) to remove any remaining medium that may inhibit the action of trypsin. Optionally, this liquid may be retained.
-

3. Add trypsin {Solution 13} in sufficient volume to cover the growth surface of the vessel. For a well of a 96-well plate this may be as little as 50  $\mu\text{L}$ . For a T75 tissue culture flask, it may be as much as 5 mL.
4. Incubate until the cells begin to lift from the growth surface. The time required depends on the cell-line and typically ranges from 2 – 10 min, with 3 min being a good first approximation. After this time, the lifting of cells can be encouraged by applying several sharp taps to the vessel. Cell detachment should be assessed visually, and microscopically if necessary.
5. To arrest trypsinisation, add a volume of  $\alpha\text{MEM}$  containing 10% v/v FCS {Solution 11} equal to the volume of trypsin used.
6. Remove the cell suspension and transfer it to a centrifuge tube.
7. Optionally, the vessel can be rinsed with a suitable volume of PBS {Solution 6} and this liquid added to the suspension.
8. Centrifuge the recovered suspension (~200 G, 5 min) and discard the supernatant.
9. Optionally, the cells may be washed once or twice with PBS to remove traces of trypsin {Method 3}.

### Long-term cryogenic cell storage

Method 5

This procedure is scaled for the freezing of  $\sim 10^6$  cells.

1. Wash the cells {Method 3} in medium.
2. Resuspend the cell pellet in medium (800  $\mu\text{L}$ ).
3. Add DMSO freezing solution (800  $\mu\text{L}$ ; 4 °C) {Solution 19} slowly with gentle agitation.
4. Transfer the suspension to a cryotube.
5. Freeze overnight to -70 °C in an insulated box to reduce the freezing rate.

**Caution:** *Cryotubes may shatter upon warming.  
Use a full-face mask and gloves when accessing liquid nitrogen storage.*

6. Transfer the frozen tube to liquid nitrogen storage.

### Recovery of cells from cryogenic storage

Method 6

1. Incubate medium (5 mL) for 10 min in a loosely stoppered tube for pH and temperature equilibration.

**Caution:** *Cryotubes may shatter upon warming.  
Use a full-face mask and gloves when accessing liquid nitrogen storage.*

2. Recover the required cryotube from liquid nitrogen storage.
3. Rapidly thaw and warm the tube to 37 °C in a water bath.
4. Decontaminate the exterior of the cryotube with 70% v/v ethanol {Solution 4}.
5. Transfer the cryotube contents to the equilibrated medium.
6. Centrifuge (~200 G, 5 min) and discard the supernatant.
7. Wash the cells {Method 3} in medium (5 mL).
8. Resuspend the cell pellet in medium (5 mL).
9. Transfer the suspension to a suitable tissue culture vessel and incubate.

## B.3 Methods for extraction

### Extraction of genomic DNA (guanidine hydrochloride/chloroform method)

Method 7

1. Wash  $\sim 2 \times 10^7$  cells {Method 3} in PBS (6 mL {Solution 6}) in a chloroform-resistant tube (for example, polypropylene).



**Caution:** *Guanidine hydrochloride is a strong denaturant. Suitable handling procedures must be used.*

2. Resuspend the pellet in guanidine hydrochloride (6 mol/L, 3.5 mL {Solution 15}) and mix by vigorous vortexing.
3. Add ammonium acetate solution (7.5 mol/L, 250  $\mu$ L {Solution 14}), proteinase-K (20 g/L, 25  $\mu$ L {Solution 17}) and sodium sarcosyl solution (20% w/v, 250  $\mu$ L {Solution 18}).
4. Incubate, preferably overnight at 37 °C, for 2 h at 55 °C, or for 1 h at 60 °C.
5. Cool to room temperature.
6. Add chloroform (2 mL, -20 °C) and mix by vortexing or shaking.
7. Allow to stand for 1 min.
8. Centrifuge (500 G, 3 min) to separate the phases.
9. Carefully recover the upper layer, avoiding the phase interface, and gently add it to a tube containing ethanol (10 mL, -20 °C).
10. Invert the tube gently several times to cause DNA precipitation.
11. Transfer the precipitated DNA to a 1.5 mL capacity microcentrifuge tube.
12. Add ethanol (80% v/v, 1 mL {Solution 5}) and allow to stand for 10 min to wash.
13. Transfer the washed DNA to a 1.5 mL capacity microcentrifuge tube.
14. Add sterile water (200  $\mu$ L) or TE buffer (200  $\mu$ L, pH 8.0 {Solution 20}).
15. Flick the tube repeatedly until the DNA dissolves.
16. If necessary, incubate (50 °C; 1 – 2 h) to facilitate dissolution.
17. Optionally, quantitate DNA concentration by fluorometry using Hoechst 33258, by agarose electrophoresis with appropriate mass standards, or, together with assessing purity, by UV spectrophotometry at 260 and 280 nm.
18. Optionally, dilute the DNA to a suitable standard concentration, such as 100 mg/L.
19. Store working solutions at 4 °C, and stocks at -20 °C or -70 °C.

#### Extraction of protein

#### Method 8

1. Harvest cells, by trypsinisation {Method 4} in the case of adherent cells.
2. Wash the cells {Method 3} three times in PBS (10 mL {Solution 6}) to remove any protease traces.
3. Resuspend the cells in PBS {Solution 6} at a density of greater than  $5 \times 10^9$  cells/L.
4. Count the cells by electronic particle counter {E.1} or haemocytometer.
5. Calculate the volume of cell suspension that contains  $5 \times 10^6$  cells. This should be less than 1 mL.
6. Divide the cell suspension into portions of this volume and transfer these to 1.5 mL microcentrifuge tubes.
7. Centrifuge (~200 G, 5 min) to pellet the cells, and discard the supernatant(s).
8. Add protease inhibitors (100  $\times$ , 10  $\mu$ L {Solution 16}) to each tube.
9. Add protein sample loading buffer (1.0 mL {Solution 31}) to each tube.
10. Mix by vigorous vortexing.
11. Store the tube(s) at -70 °C. The protein should be stable for months.

#### B.4 Digestion of PCR products with *Bst*N1 to facilitate SSCP

#### Method 9

1. Place 10  $\mu$ L of each completed PCR reaction solution into labelled PCR tubes.
2. Add 1 unit of *Bst*N1 enzyme {E.4} in the supplied buffer to each tube.
3. Add 2.5  $\mu$ g (final concentration 100 mg/L) of BSA (supplied with the enzyme) to each tube.
4. Add PCR-quality water to make final reaction volumes of 25  $\mu$ L.

5. Incubate in a PCR machine at 60 °C for 1 h.
6. Hold at 4 °C until required.

### B.5 Touch-down PCR

Method 10

#### General

See A.2 for background information.

Anti-contamination measures {A.2} should be employed. All reagents and tubes should be held on ice for the duration of the preparation.

1. Ensure the thermal cycler {E.1} is turned on and the correct program entered, as follows:

Initial denaturation:	95 °C x 5 min
Touch-down cycling:	30x(94 °C x 30 s; 65 °C – 0.5 °C/cycle x 30 s; 72 °C x 30 s)
Constant Ta cycling:	15x(94 °C x 30 s; 50 °C x 30 s; 72 °C x 30 s + 2 s/cycle)
Final extension:	72 °C x 10 min
Hold:	4 °C x indefinite
2. Label the reaction tubes on their sides where it will not be rubbed off by the lid of the thermal cycler.
3. Prepare a master mix comprising the reagents common to all reactions being performed {Solution 50}. This reduces pipetting error and contamination risk by minimising transfers. Prepare slightly more than the calculated amount to allow for minor pipette setting variation.
4. Divide the master mix among the reaction tubes.
5. Add any reagents unique to each reaction, for example, primers.
6. Move from the genomic DNA-free preparation area and add the template DNA to the appropriate tubes.
7. Start the thermal cycler program and pause it when it reaches the initial denaturing temperature. This preheating represents a minimal 'hot-start' procedure.
8. Mix the tube contents by brief vortexing, and settle them by brief centrifugation.
9. Place the tubes in the thermal cycler and allow the program to proceed.
10. When the program has reached the final 'Hold' step, the tubes can be removed and held at 4 °C until required.
11. Allow any condensation formed in the thermal cycler to evaporate.

### B.6 Agarose electrophoresis

Method 11

1. Microwave heat 0.8% – 3% w/v agarose in TAE buffer, diluted from Solution 29, in a loosely stoppered vessel until completely melted. Allow to cool to ~50 °C.
2. Assemble the gel casting apparatus {E.1} with appropriate well-combs in place.
3. When cooled, but before solidification begins, pour the agarose solution into the gel mould to a suitable depth, taking care to avoid the formation of air bubbles.
4. Allow the gel to set. This will take ~15 min.
5. Once set, carefully remove the well-comb and other mould components.
6. Submerge the gel in TAE running buffer, diluted from Solution 29, in the electrophoresis tank.
7. Load the samples and DNA length standards {E.5}. An effective method for this is to spot ~1 µL volumes of 5x TAE loading buffer {Solution 28} onto a strip of laboratory film and to mix ~5 µL of each sample with one such before loading into a gel well.
8. Connect the electrodes to a power supply and apply current at 80 – 100 V until the dye front has advanced an appropriate distance. Note that the loading buffer employed here includes only xylene cyanol dye as bromophenol blue was too often found to obscure the region of interest.

### B.7 Ethidium bromide staining

Method 12

1. Recover the gel from the electrophoresis apparatus and place it in a suitably sized shallow dish.





2. Cover the gel to approximately twice its thickness in ethidium bromide stain {Solution 26}.
3. Stain for 10 – 20 minutes at 50 °C with gentle agitation.
4. Recover the stain, which can be reused many times.
5. Destain in two changes of 1x TAE buffer, diluted from Solution 29, at 50 °C with gentle agitation.  
**Note:** Ethidium bromide waste must be rendered non-toxic before disposal.
6. Visualise bands by UV trans-illumination and optionally, record a photographic or digital image.

## **B.8 Single-strand conformation polymorphism assay**

**Method 13**

### **Method in brief**

Completed PCR reaction solutions are diluted 1:9 with TE buffer {Solution 20}, combined with an equal volume of 2x formamide loading buffer {Solution 27}, denatured for 3 min at 90 °C, and held on ice. 5  $\mu$ L of each sample is run through a 14% acrylamide gel, made with or without the addition of 10% glycerol {Solution 36}, in 0.5x TBE buffer, diluted from Solution 30, at 200V for from 90 min to 4 h, with experience being the best guide as to time. Gels are recovered, silver stained {Method 15}, digitally imaged and dried onto a paper backing for permanent storage.

### **Method in detail**

#### *Gel preparation*

**Method 14**

1. Scrupulously clean the glass plates used in forming the gels: first in water, and then in 100% ethanol. Allow them to air-dry.
2. Prepare a suitable gel solution {Solution 36}, withholding the 1,2-bis[dimethylamino]ethane (TEMED) and ammonium persulphate (APS).
3. Degas the gel solution under vacuum (5 min), and assemble the gel-casting apparatus {E.1}.
4. Add the TEMED and APS to the gel solution and mix by gentle swirling.
5. Pour the gel(s) taking care to avoid the incorporation of air bubbles that may interfere with polymerisation.
6. Insert the well-comb(s) and allow the gel(s) to polymerise (~10 min).
7. When polymerised, transfer the gel modules to the electrophoresis tank and assemble the core.
8. Fill the inner chamber with 0.5x TBE buffer, diluted from Solution 30.
9. Remove the well-comb(s) and carefully flush the wells to remove unpolymerised acrylamide.
10. If, by this time, there has been no leakage of buffer from the inner to the outer chamber, the latter can now be filled to an appropriate level. Otherwise, dismantle and reassemble the central core to rectify the leakage problem. Particular attention should be paid to the seating of the seals, and their correct alignment with the tops of the gel modules.

#### *Sample preparation*

1. Preheat a heating block for 1.5 mL microcentrifuge tubes to 90 °C.
2. Dilute at least 500 nL of each completed PCR reaction solution 1:9 with TE buffer {Solution 20}.
3. Transfer 3  $\mu$ L of each diluted reaction solution to separate 1.5 mL microcentrifuge tubes.
4. Add 3  $\mu$ L of 2x formamide loading buffer {Solution 27} to each tube.
5. Denature the DNA by placing the tubes into the preheated heating block for 3 min.
6. After denaturing, immediately place the tubes on ice and hold them there until loading.
7. Load 5  $\mu$ L per well.

#### *Electrophoresis*

Electrophoresis is carried out at a constant 200 V for a period dependent on the particulars of the experiment. High gel concentration, incorporation of glycerol, or a lengthy product all necessitate longer runs. Typical times range from 90 min to 4 h.

## B.9 Silver staining

Method 15

### Method in brief

After electrophoresis, gels are recovered, fixed in ethanol/acetic acid, oxidised, washed scrupulously, stained with silver nitrate, washed briefly, and developed. They are imaged by trans-illumination with white light and digital photography and then dried onto a paper backing under vacuum.

### Method in detail

The achievement of clear bands against a low background critically depends upon the scrupulous cleanliness of the implements used to manipulate the gels and the purity of the reagents, particularly the water used in rinsing. It is important that gloves be worn, not solely to protect from traces of unpolymerised acrylamide, but also to prevent proteins from the skin being transferred to the gel resulting in blemishes.

1. Recover the gels from the electrophoresis apparatus.
2. Fix in a combination of fixer A (200 mL {Solution 39}) and fixer B (200 mL {Solution 40}), for at least 30 min.
3. Fix in a combination of fixer A (50 mL {Solution 39}), fixer B (100 mL {Solution 40}) and water (250 mL) for 15 min.
4. Repeat the previous step.
5. Oxidise in oxidiser (1x, 200 mL, diluted from Solution 41) for 15 min.
6. Wash thoroughly (5 x 5 min) in water with gentle agitation. The importance of water purity at this point is critical.
7. Stain with silver stain solution (1x, 200 mL, diluted from Solution 42) in the dark for 20 min.
8. Rinse briefly (1 min) in water.
9. Develop in three 200 mL changes of freshly prepared developer {Solution 43}. The first development is brief, ~30 s, by which time the developer will have become discoloured. The second development should proceed until bands are discernible, ~3 min, and the third, until the contrast between bands and background is subjectively optimal, ~3 min. If, in general, the development reaction proceeds too quickly, it can be slowed by chilling the developer prior to use.
10. Stop development in 5% acetic acid (fixer B (100 mL {Solution 40}) and water (300 mL)) for 5 min.
11. Wash twice in water for 30 min each time.
12. Optionally, photograph the gels by trans-illumination and dry them as a permanent record.

## B.10 Western blotting

### Method in brief

Method 16

Protein is extracted from stringently washed {Method 3} trypsinised {Method 4} cultured cells directly into protein sample loading buffer {Solution 31} with added protease inhibitors {Solution 16} at a density of  $5 \times 10^9$  cells/L. After electrophoresis, protein is transferred to PVDF membranes by high current electrotransfer. Optionally, membranes may be stained with amido black {Method 21} to monitor loading. Membranes are blocked in 10% non-fat milk powder in TTBS with 0.05% Tween-20 {Solution 46} for 1 h. Attachment of the 1° antibodies is in blocking solution for 1 – 2 h {E.3}. After stringent rinsing with TTBS {Solution 49}, the detection reagents are applied. In general, this is a horseradish peroxidase (HRP)-conjugated 2° antibody {E.3}, but for detection of pRB, a commercial avidin/biotin tagging kit {E.2} is used, with a protocol modified from the manufacturer's instructions {Method 25}. In

See A.4 for background information.



either case, detection is by exposure of X-ray film {E.7} using an enhanced chemiluminescent (ECL) substrate {E.2}, optionally followed by digital imaging of the film.

### **Method in detail**

#### ***Gel preparation***

**Method 17**

The same apparatus {E.1} is used for the polyacrylamide electrophoresis of proteins as for DNA. Consequently, gel preparation is very similar, and reference should be made to the appropriate section {Method 14} for general guidance. Unlike DNA gels however, gels for protein analysis have two components: the main separating gel, and, above it, a small, low acrylamide concentration, more acidic stacking gel that forms the wells. The procedure for gel preparation is:

1. Clean and assemble the gel casting apparatus.
2. Prepare and optionally degas the separating gel solution and add the TEMED and APS.
3. Pour the contents between the glass plates up to a level ~5 mm below where the bottom of the well-comb will be when installed.
4. Gently overlay the solution with water to provide a sharp boundary.
5. Allow the gel to set (~10 min).
6. Decant the water layer. A paper tissue may be used to draw out the last of the water.
7. Prepare and optionally degas the stacking gel solution and add the TEMED and APS.
8. Insert the well-comb.
9. With the aid of a pipette, introduce the stacking gel solution into the mould.
10. Dispel any bubbles and rearrange the well-comb if necessary.
11. Allow the stacking gel to set (~10 min).
12. Transfer the gel to the electrophoresis tank.
13. Fill the inner chamber with electrophoresis buffer {Solution 32}.
14. Remove the well-comb.
15. Carefully flush the wells with buffer to expel unpolymerised acrylamide.
16. If no leakage is evident, fill the outer chamber with buffer to an appropriate level.

#### ***Standards***

Two lanes per gel are usually reserved for protein standards {E.5}. The first is for dye-conjugated proteins to allow for monitoring of electrophoresis progress and protein transfer, and the second for biotinylated proteins to allow for molecular weight estimation and as a positive control for the detection reagents. In addition, one lane should be reserved for a positive control for protein detection, either purified target protein, or an extract from a source known to express it. A known negative control may also be of benefit, particularly where non-specific banding is present.

#### ***Sample preparation and loading***

**Method 18**

Maximum sample volume is dictated by the well-comb in use, being ~20  $\mu\text{L}$  for fifteen well combs and ~30  $\mu\text{L}$  for ten well combs. Usually the two outer wells are not used, as protein mobility is often irregular at the gel edges. With the lanes reserved for standards, this reduces the effective number of lanes available for experimental samples to five or ten, depending on the comb used.

1. Thaw frozen protein extracts.
2. Transfer an appropriate volume (10 – 30  $\mu\text{L}$ ) of each extract to microcentrifuge tubes.
3. If the extract is not already in loading buffer, add sample loading buffer (5 x {Solution 31}) in the appropriate proportion.
4. Return the protein extracts to the freezer.

5. If being used, dilute an appropriate volume (1 – 2  $\mu\text{L}$ ) of biotinylated protein standard stock {E.5} 1:99 with sample loading buffer {Solution 31}. Do not dilute the dye-conjugated standard: it is used neat.
6. Heat the samples and the diluted biotinylated protein standard, if any, in a heating block or water-bath at 100 °C for 5 min. Do not heat the dye-conjugated standard.
7. Place the samples on ice until they are loaded. Opinion as to the validity of this step is divided, with some workers feeling that the risk of SDS precipitation outweighs the benefits of protein stability.
8. Load 10 – 30  $\mu\text{L}$  of sample, 10 – 30  $\mu\text{L}$  of biotinylated standard, or 5 – 10  $\mu\text{L}$  of dye-conjugated standard per well. If two gels are being run simultaneously, loading a second well of one gel with biotinylated standard, even if it is an edge well, will reduce the possibility of confusion between gels.

### *Electrophoresis*

### *Method 19*

Generally, electrophoresis is carried out at a constant 200 V. Note should be taken of the maximum power dissipation of the apparatus in use, and if possible, the power supply should be set to limit the current supplied so that this is not exceeded. The formula to use is  $I = P / V$ , where  $I$  is the current limit to set in amperes,  $P$  is the maximum power dissipation in watts, and  $V$  is the electrophoresis voltage. For the equipment used in this work, this value is 200 mA. In practice, this current would only be reached under fault conditions, such as a short circuit or wildly inappropriate buffer concentration, but it is a simple precaution to take which may prevent equipment damage and possible fire.

Duration of electrophoresis depends upon gel concentration and running temperature. By observing the mobility of the dye in the loading buffer, and more importantly, the dye-conjugated standards, electrophoresis can be terminated when a protein of the expected MW of the target has travelled a suitable distance. By way of an example, electrophoresis with p16<sup>CDKN2A</sup> as target and 15% gel concentration at ambient temperature takes ~30 min.

### *Protein transfer*

### *Method 20*

The apparatus used here employs an ice pack to absorb the heat generated during the transfer. This must be frozen prior to commencement. Once electrophoresis has completed, the apparatus is dismantled and the gel or gels recovered. One of the glass plates is removed leaving the other as a support for the gel. Handle the membrane as little as possible, and use both gloves and forceps. Any extraneous protein transferred to the membrane will mar the final result.

For each gel:

1. Cut away and discard the stacking gel.
2. Place the gel, still on its plate, in transfer buffer {Solution 47} to equilibrate for at least 10 min.
3. Cut to the size of the gel a piece of PVDF membrane {E.7} and two pieces of filter paper.
4. Briefly wet the hydrophobic PVDF membrane in methanol, then allow to equilibrate in transfer buffer {Solution 47} for at least 10 min.
5. Soak the support pads in transfer buffer {Solution 47} for 10 min. Do not soak the filter paper, as it will lose its integrity.
6. Once all components have equilibrated, assemble the transfer cell. By virtue of the negative charge carried by the SDS bound to the protein, it will migrate in an electric field from the cathode (negative terminal, black) to the anode (positive terminal, red). The order of components is critical and must be: cathode, black transfer cell plate, support pad, filter paper,



gel, membrane, filter paper, support pad, white transfer cell plate, anode. Transfer of the gel from its support plate to the filter paper is somewhat awkward. Either the filter paper can be placed on the support pad and the gel floated into place, or the filter paper can be placed directly onto the gel, the glass support plate inverted, and the gel encouraged to fall onto the filter paper. It can then be placed on the support pad. At all stages, care should be taken to avoid the incorporation of air bubbles between layers, as this will interfere with the uniform transfer of protein. Once the layers are in place, the assembly is secured by locking the hinged transfer cell plates together.

7. Install the assembled transfer cell into its frame. Care must be taken to ensure its correct orientation. The black transfer cell plate must be closer to the black side of the frame, as this will become the cathode.

To commence the transfer:

1. Put a magnetic stir-bar into the transfer tank, the frozen ice pack into the frame, and the frame into the transfer tank.
2. Fill the transfer tank to capacity with transfer buffer {Solution 47}.
3. Place the tank in a dish as there will be some overflow as the buffer heats. Place the dish and tank on a magnetic stirrer and begin stirring the buffer. This is essential as it ensures uniform heat distribution within the apparatus. If a magnetic stirrer with an integral heating element is used, ensure this is turned off.
4. Connect the power supply and electrotransfer for 1 h at 100 V. As with the electrophoresis step, the power supply should be set to limit the current supplied. For the equipment used here the current limit should be 400 mA.

After transfer:

1. Dismantle the apparatus and recover the membrane(s). Discard the used buffer.
2. Confirm that the dye-conjugated standards have transferred successfully.
3. Note the orientation of the membrane with respect to the position of the standards. The surface that was in intimate contact with the gel will carry the greatest quantities of protein, and this will need to be identified later.
4. If further processing will be delayed by more than a day, the membranes(s) should be dehydrated briefly in methanol, air-dried and stored at 4 °C until further processed. Otherwise, they may be stored in TTBS {Solution 49} at 4 °C.

#### ***Amido black membrane staining/destaining***

***Method 21***

1. Membranes are rinsed briefly in TTBS {Solution 49} and stained in sufficient amido black stain {Solution 44} to cover them fully for ~5 min with agitation.
2. Once stained, the excess amido black solution can be saved for reuse and the membranes destained briefly in two or three changes of amido black destain solution {Solution 45} until the protein banding is sufficiently clear.
3. Optionally, the stained membranes can be digitally imaged.

#### ***Blocking***

***Method 22***

1. If necessary, wet the membrane(s) briefly in methanol, and rehydrate in TTBS {Solution 49}.
2. Make 10 mL of blocking solution {Solution 46} per gel.
3. Transfer the membrane(s), protein side up, to the blocking solution. Block for 1 h at ambient temperature with moderate agitation, or overnight at 4 °C.

### **Primary antibody attachment**

**Method 23**

1. Discard the bulk of blocking solution, retaining a measured quantity sufficient to submerge the membrane(s) fully (2 – 5 mL per membrane).
2. Add stock primary antibody to the retained blocking solution to yield the working concentration {E.3}.
3. Soak the membrane(s) for 1 – 2 h {E.3} with moderate agitation.
4. It may be possible to reuse the antibody solution a few times. Experience is the best guide here. If it is to be stored, do so at 4 °C, otherwise, discard.
5. Wash twice briefly with TTBS (5 – 10 mL per membrane {Solution 49}).
6. Wash three times with TTBS (5 – 10 mL per membrane {Solution 49}) for 5 min each time with moderate agitation.

### **Secondary antibody complex attachment (HRP-conjugated antibody)**

**Method 24**

1. Wash twice briefly with TTBS (5 – 10 mL per membrane {Solution 49}).
2. Wash three times with TTBS (5 – 10 mL per membrane {Solution 49}) for 5 min each time with moderate agitation.
3. Add a measured volume of TTBS {Solution 49} sufficient to submerge the membrane(s) fully.
4. Add 2° antibody to give the required working concentration {E.3}.
5. Soak the membrane(s) for 1 h with moderate agitation.

### **Secondary antibody complex incubation (avidin/biotin kit {E.2})**

**Method 25**

The protocol departs here from the manufacturer's recommendations in order to reduce non-specific binding. Whereas the recommendation is to apply the biotinylated secondary antibody in the presence of normal serum, better results are obtained if these steps are separated. Furthermore, the amounts of 2° antibody can be reduced dramatically, also improving the signal to noise ratio.

1. Soak the membrane(s) in TTBS (10 mL per membrane {Solution 49}), to which normal serum (300 µL per membrane) has been added, for 1 h with gentle agitation.
2. Add the biotinylated 2° antibody (5 µL per membrane) and continue soaking for 45 min.
3. After 30 min of this soaking time, prepare the avidin-biotinylated-HRP conjugate (ABC) according to the manufacturer's instructions by adding two drops each of the 'A' solution (avidin) and the 'B' solution (biotinylated-HRP) to TTBS (5 mL per membrane {Solution 49}). Mix by inversion and allow to stand for 30 min.
4. After the attachment of the 2° antibody is complete, wash the membrane(s) in TTBS as described above.
5. When this is complete, the ABC complex will have formed. Add TTBS (5 mL per membrane {Solution 49}) to the ABC.
6. Soak the membrane(s) in the ABC solution for 45 min with moderate agitation.
7. Wash the membrane(s) as described above.

### **Detection**

**Method 26**

1. Gather together the following: the membrane(s) in their last TTBS wash; ECL reagents (2 mL per membrane of each {E.2}, in separate tubes); X-ray film; timer; two sheets of plastic such as overhead projection transparencies; forceps; paper towels; a tube for waste liquid; a shallow dish in which the membrane(s) can be laid flat without overlapping; and a suitable working surface such as an autoradiography film cassette.
2. Proceed to a darkroom equipped with an X-ray film developer.
3. Set up the working surface and place one of the sheets of plastic on it.



4. Using the forceps, remove the membrane(s) from their TTBS wash and drain by briefly placing one edge onto a paper towel. Discard the TTBS into the waste tube.
5. Arrange the membrane(s) protein side up in the shallow dish without overlapping them.
6. Set the timer for one minute, but do not activate it.
7. Pour one of the ECL reagents into the other and mix by inversion.
8. Pour equal amounts of the mixed ECL reagents into the centre of each membrane and carefully disperse it across the surface(s). Start the one-minute timer.
9. At the expiry of the one minute, drain each membrane thoroughly, as above, to reduce background signal, and place it, protein side up, on the plastic sheet.
10. Use the second plastic sheet to cover the membrane(s).
11. In darkness, remove a piece of X-ray film from its packet and lay it on top of the enclosed membrane(s) to be exposed. Initial exposure time should be ~5 s for avidin/biotin based detection, and 5 min for direct-conjugated HRP detection.
12. Develop and inspect the film. If necessary, perform additional exposures for different times to obtain the optimal result. If the initial signal is too strong, wait for a time and try again as the light output of the ECL reaction peaks at about 1 min and declines over a period of ~1 h.
13. Discard the spent ECL reagents into the waste tube.

#### *Membrane storage*

*Method 27*

Membranes may be rinsed in TTBS (Solution 49), dehydrated briefly in methanol, air-dried, and stored at 4 °C for further analysis if required.

#### *Reuse of membranes*

*Method 28*

It is possible to strip primary antibodies and detection reagents from membranes to allow sequential re-probing. This can be done a number of times, but some sensitivity is lost.

1. If necessary, rewet the membrane in methanol followed by TTBS (Solution 49).
2. Incubate the membrane in a large volume of membrane stripping buffer (10 – 20 mL (Solution 48)) at 50 °C for 1 h with gentle agitation.
3. Wash thoroughly with TTBS (Solution 49) and proceed to the 1° antibody attachment step.

### **B.11 Flow cytometric analysis of cellular DNA content**

#### **Method in brief**

**Method 29**

Cells are harvested, by trypsinisation in the case of adherent cells, washed, counted and fixed at a density of  $5 \times 10^8$  cells/L in 90% v/v methanol at -20 °C for more than 8 h. For each analysis  $10^6$  cells (2 mL) are taken in suspension, gradually rehydrated, and washed. They are treated with RNase A, and stained with propidium iodide (PI). They are then run on a flow cytometer.

For the quantitative analysis of DNA ploidy, human peripheral blood leukocytes are processed similarly and run, either in parallel, or internally, as a standard.

#### **Method in detail**

##### *Fixation of cells*

*Method 30*

1. Harvest cells by trypsinisation (Method 4).
2. Wash (Method 3) in PBS (Solution 6).
3. Count cells by haemocytometer or electronic particle counter (E.1).
4. Centrifuge (~200 G, 5 min), and discard the supernatant.
5. Resuspend the cell pellet in PBS (200  $\mu$ L per  $10^6$  cells, 4 °C (Solution 6)).

6. Add methanol (1.8 mL per  $10^6$  cells,  $-20\text{ }^{\circ}\text{C}$ ) drop-wise with vigorous vortexing. The correct execution of this step is essential for the minimisation of cell clumping.
7. Hold at  $-20\text{ }^{\circ}\text{C}$  for at least 8 h. There is no practical upper limit to storage time in this state.

### *Propidium iodide staining*

*Method 31*

**Caution:** *Propidium iodide is a mutagen.  
Suitable handling procedures must be used.*

This procedure is appropriate for the treatment of  $10^6$  cells fixed in 2 mL of methanol/PBS. The key to success here is the sequential rehydration of the cells. Simply pelleting the cells and resuspending in PBS leads to major cell losses through the strong adhesion of cells to the tube walls, and to the formation of cellular aggregates not suitable for flow cytometric analysis. The inclusion of FCS also assists in preventing these problems.

Some authorities recommend a prolonged (~30 min) staining with propidium iodide. This is unnecessary as the PI binds the DNA after just a few seconds (data not shown). Where cell-cycle analysis is intended, a lower PI concentration may be used. Where ploidy analysis is the goal, a higher concentration must be used.

For each sample of  $10^6$  cells in 2 mL of methanol/PBS:

1. Add FCS/PBS (2% v/v, 1 mL {Solution 22}).
2. Allow to stand for 5 min to rehydrate partially.
3. Add FCS/PBS (2% v/v, 1 mL {Solution 22}).
4. Allow to stand for 5 min to rehydrate further.
5. Centrifuge (~200 G, 5 min) and discard the supernatant.
6. Wash the cells {Method 3} in FCS/PBS (2% v/v, 4 mL {Solution 22}).
7. Resuspend in FCS/PBS (2% v/v, 200  $\mu\text{L}$  {Solution 22}).
8. Add RNase A (5 g/L, 10  $\mu\text{L}$  {Solution 24}).
9. Incubate (20 min).
10. Add FCS/PBS (2% v/v, 2 mL {Solution 22}).
11. Centrifuge (~200 G, 5 min), and discard the supernatant.
12. Resuspend in EDTA/PBS (100  $\mu\text{mol/L}$ , 500  $\mu\text{L}$  {Solution 21}).
13. Add propidium iodide solution (1 g/L, 5 – 25  $\mu\text{L}$  {Solution 23}).

### **DNA sequencing**

**Method 32**

Completed PCR reaction solutions are purified with commercial resin spin-columns {E.2} according to the manufacturer's instructions, DNA concentration assessed either spectrophotometrically or by electrophoresis with mass standards, adjusted to a suitable value by dilution with DNase-free water, and sequenced bi-directionally {E.1} using the PCR primers. The resultant electropherograms are inspected with Editview software {E.9} and sequence data adjusted, where necessary, with Editseq {E.9}. Sequence alignments are performed with Megalign {E.9}.





# Methodology (V3)

## B.12 Methods for cell culture

### Detection of mycoplasma contamination in cell cultures

Method 33

Mycoplasma contamination is a relatively common occurrence in cell culture<sup>1596</sup>, and it has been estimated that perhaps 30% of cultures may be thus contaminated, generally without the experimenter's knowledge, as this contamination is not obvious under routine phase contrast inspection of cultures. Suspicion may be aroused by observing changes in proliferation rate or cellular morphology, or by an increase in cell death resulting in the accumulation of debris in cultures; however contamination may also be cryptic. Since such contamination can have significant effects on cellular metabolism, the presence of mycoplasma can render the conclusions of many experiments undertaken with contaminated cells invalid. When contamination is suspected, or as a matter of routine, specific testing must be undertaken.

1. Establish cells in  $\alpha$ MEM supplemented with 10% v/v FCS, but unsupplemented by any antibiotics.
2. Maintain in culture for two weeks, passaging {Method 2} as necessary.
3. After this time, conditioned supernatant medium from the culture can be assayed by PCR using mycoplasma specific primers<sup>1671 @1677</sup>, or with a commercial kit, such as that from Roche {E.11}. If testing is delayed, the supernatant may be stored at  $-20^{\circ}\text{C}$  until required.

It must be borne in mind that mycoplasma can be insidious, and a lingering infection can occur at a level below that detectable by some methods. In addition, not all strains of mycoplasma are necessarily detected by all testing procedures. Retesting, perhaps with multiple methods, may be necessary where a high degree of confidence is required, or where anomalous growth continues to be observed in putatively clear cell-lines.

### Elimination of mycoplasma contamination from cell cultures

Method 34

If detected, mycoplasma can generally be eliminated through the use of appropriate antibiotics, although this can prove difficult, and cultures may have to be discarded. The method adopted here is to treat with the antibiotic ciprofloxacin. This is reported to be 70% effective in eliminating mycoplasma contamination<sup>1679</sup>.

1. Establish cells in  $\alpha$ MEM supplemented with 10% v/v FCS and ciprofloxacin (20 mg/L {Solution 63}).
2. Maintain in culture for two weeks, passaging {Method 2} as necessary.
3. On the first passage after this time, establish two parallel cultures, one in  $\alpha$ MEM supplemented with 10% v/v FCS and normal antibiotics (Solution 11), and one in  $\alpha$ MEM supplemented with 10% v/v FCS, but unsupplemented by any antibiotics {Solution 62}. The intention of establishing the first culture is to protect against loss of the hopefully successfully treated culture to other bacterial contamination; that for the second is to encourage any residual contamination to develop further so that it can then be detected, and treatment can be shown to have failed.
4. Maintain each in their respective media, passaging {Method 2} as necessary.
5. After two weeks, test the supernatant medium from the culture maintained in the absence of antibiotics for contaminating mycoplasma {Method 33}. If it is clear, either of the cultures can be used as the basis for experimental work. If the result is positive for contamination, either culture

may form the basis for treatment by other procedures, or both may be discarded and a new source for the cell-line found, or in the worst case, experimental work on that line abandoned.

### **Growth of adherent cells on glass coverslips**

**Method 35**

1. Store 22 mm x 22 mm coverslips in 70% v/v ethanol {Solution 4}.
2. Using a forceps, remove a coverslip and place it into a sterile 35 mm diameter plastic culture dish.
3. Rinse the coverslip twice with sterile PBS {Solution 6}.
4. Seed the dish with cells at a relatively low density,  $\sim 5 \times 10^4$  cells in 2 mL of  $\alpha$ MEM supplemented with FCS and antibiotics {Solution 11}.
5. Incubate. The cells should adhere and adopt a normal morphology within a day.

### **B.13 Methods for cell fixation**

#### **Fixation of adherent cells on glass coverslips**

**Method 36**

1. Remove the supernatant medium from the coverslip by aspiration.
2. Rinse gently with PBS (1 mL {Solution 6}) to remove debris and serum proteins. Remove the PBS by aspiration.
3. Carefully add buffered formaldehyde fixative (100  $\mu$ L {Solution 64}) to the coverslip, ensuring that it is completely covered. Surface tension should prevent the fixative from dispersing beyond the edges of the coverslip.
4. Leave to fix for 20 min at ambient temperature.
5. After this time, remove the fixative by aspiration.
6. Gently rinse the coverslip twice with PBS (1 mL {Solution 6}) by addition and aspiration. Immunofluorescent staining {Method 44} can proceed immediately from this point. If there is to be a delay before processing, then:
7. Gently add PBS/antibiotics (2 mL {Solution 67}) and replace the lid of the dish.
8. Store at 4 °C until required.

### **B.14 Methods for extraction**

#### **Precipitation of DNA with sodium acetate and isopropanol**

**Method 37**

The basis of the salt/alcohol method of nucleic acid precipitation lies in the use of a cation to neutralise the charge on the sugar-phosphate backbone, and the introduction of a low dielectric solvent to greatly enhance the mutual affinity of the polyanionic DNA and the cation in order that insoluble ion-pairs form. Isopropanol, having a lower dielectric constant, can provide the same effect as ethanol with lower volume, often allowing a precipitation to be performed in a 1.5 mL microcentrifuge tube. Although the dielectric constant falls further at low temperatures, it is usually unnecessary to refrigerate the mixture to achieve precipitation, although this can be useful where the concentration of DNA is low.

1. For each volume of DNA solution, add 0.1 volumes of sodium acetate (3 mol/L, pH 5.5 {Solution 55}).
2. For each volume of DNA solution, add 1 volume of isopropanol.
3. Mix by repeated inversion, during which the DNA should precipitate.
4. Where DNA content is high, the precipitate may be recoverable with a pipette tip or similar, in which case, transfer it to a new tube; otherwise, centrifuge ( $\sim 16\,000$  G, 10 min) to form a pellet, then carefully drain the supernatant.
5. Optionally, wash the DNA in ethanol (80% v/v, 1 mL {Solution 5}) for 10 min with gentle agitation, then either recover the DNA with a pipette tip or centrifuge as above.
6. Allow the residual alcohol to evaporate by standing the open tube inverted for 10 min. Do not over-dry.



7. Dissolve the DNA in an appropriate volume of a suitable buffer such as TE {Solution 20}. Agitation and heating (50 °C, 1 h) may be necessary to ensure complete dissolution.

#### **Activation of sodium vanadate for use as a phosphatase inhibitor**

**Method 38**

Sodium vanadate should be depolymerised to maximise its efficacy as an inhibitor of tyrosine phosphatases. The following method is intended to achieve this.

1. Dissolve sodium orthovanadate ( $\text{Na}_3\text{VO}_4$ , 920 mg) in water (~45 mL) to form a solution of concentration greater than 100 mmol/L.
2. Adjust to pH 10.0 with concentrated hydrochloric acid or sodium hydroxide as required. The solution should turn yellow.
3. Boil until the solution becomes colourless (~10 min).
4. Adjust to pH 10.0 with concentrated hydrochloric acid or sodium hydroxide as required.
5. Repeat the previous two steps until the solution remains colourless and the pH no longer requires adjustment.
6. Adjust the volume to 50 mL by the addition of water, forming a solution of 100 mmol/L concentration.
7. Divide into 9 portions of 5 mL and 5 portions of 1 mL, and store at -20 °C.
8. Thaw and use solution from successive 1 mL portions until they are exhausted, then thaw successive 5 mL portions and divide into 1 mL portions for further use.

#### **Protein extraction**

**Method 39**

All processing should be carried out on ice with chilled reagents. As far as is practicable, protein extracts should be maintained on ice while in use, and stored at -80 °C. This method is for the extraction of protein from a batch (1 – 10) of P100 tissue culture plates containing adherent cells.

1. Place on ice: ~500 mL of sterile PBS {Solution 6}, and twice as many autoclaved microcentrifuge tubes of 1.5 mL capacity as there are plates in the batch. Have available a large beaker to receive waste supernatant medium. Have available another beaker (~ 500 mL capacity) containing PBS (~ 250 mL) for cell scraper rinsing.
2. Calculate the volume of extraction buffer required for the batch on the basis of 1 mL for each densely occupied plate and 500  $\mu\text{L}$  for each sparsely occupied plate.
3. To this volume of chilled extraction buffer containing phosphatase inhibitors {Solution 66}, add 0.01 volumes of protease inhibitor cocktail {E.16}.
4. Remove plates to be harvested from incubation and place immediately on ice.
5. Decant culture medium from all plates into the large beaker and return the plates to ice.
6. Rinse each plate carefully with ice-cold PBS twice (~5 mL each rinse). After the last rinse, place the plates at an angle for ~ 1 min, embedded in ice, to allow any remain PBS to pool, and then remove this by aspiration.
7. For each plate in the batch, add half of the volume of extraction buffer containing phosphatase and protease inhibitors required for the plate, and distribute this across the surface. Allow the plate to sit on ice for 5 min.
8. Using a sterile cell scraper vigorously {E.16}, dislodge all visible cells from the plastic substrate and collect them at the lowest point of the plate, tilting this while still embedding it in ice to facilitate this.
9. Transfer the extract to a chilled microcentrifuge tube with a pipette and hold the tube on ice.

10. Repeat from step 7 using the other half of the designated buffer volume and collecting the new material in the same microcentrifuge tube. Discard the plate and vigorously rinse the cell scraper in the PBS prepared for this purpose above.
11. Repeat the necessary steps for each plate in the batch.
12. When all plates have been harvested, vigorously mix each extract by vortexing for ~ 30 s, then return to ice for a minimum of 5 min.
13. Centrifuge the extracts (16 000 G, 10 min, 4 °C) and transfer the supernatants to new chilled tubes. Optionally, retain the insoluble pellet and store at -80 °C.
14. Transfer the extracts to -80 °C storage.
15. Treat the contents of the beakers containing the waste culture medium and the PBS rinse with hypochlorite and discard.

### Protein concentration by ultrafiltration

### Method 40

This method is for the concentration of protein extracts of less than 500  $\mu\text{L}$  volume using centrifugally-driven membrane ultrafiltration devices [E.16] with a molecular weight cut-off of 3 kD.

1. Thaw protein samples on ice, and chill the appropriate number of devices and microcentrifuge tubes of 1.5 mL capacity.
2. Add a maximum of 500  $\mu\text{L}$  of each extract to be concentrated to the upper chamber of a device, keeping both extract stock and devices on ice as much as is practicably possible.
3. When all are loaded, centrifuge the devices (16 000 G; 1 h; 4 °C).
4. Transfer the retentates to new chilled tubes. To maximise recovery, wash the retentate across the filter membrane several times before transferring it to the new tube. If there is no visible retentate due to low initial protein concentration, use 20  $\mu\text{L}$  of chilled protein extraction buffer with added phosphatase and protease inhibitors {See Method 39, step 3} to dislodge protein from the surface of the membrane and transfer this to the new tube.
5. Discard eluates and used devices.
6. Transfer the retentates in their new tubes to -80 °C storage.

## B.15 Methods for quantitation

### Protein determination using the bicinchoninic acid method

### Method 41

Depending on the actual concentration of the protein solution to be quantitated, the dilution necessary to keep the resulting absorbance measurements on scale and in the linear range may vary. The dilution described here proved satisfactory for protein extracts after concentration by centrifugally-driven ultrafiltration {Method 40}. Standards and samples for quantitation should be run in at least duplicate, with triplicate being preferred. The format used is based on the 96-well tissue culture plate, so a suitable plate handling spectrophotometer is required. Ideally a set of standards should be included on each plate used.

Notes: Primary protein extracts should be held on ice to the greatest possible extent throughout the procedure. Pipetting should be done with care to prevent the generation of bubbles in the wells as these can interfere with the spectrophotometry. A multichannel pipette can be a useful tool in carrying out reagent additions, but is better avoided in the creation of the standard dilution series.

1. If necessary, thaw the protein extracts to be quantitated and the BSA standard [E.14] solution on ice.
2. Two or three columns per plate are reserved for protein standards. Into each well of these columns, place sodium hydroxide solution (1.0 mol/L, 50.0  $\mu\text{L}$  {Solution 58}).



3. Into each well to be used for quantitation of a protein extract, place sodium hydroxide solution (1.0 mol/L, 47.5  $\mu$ L {Solution 58}).
4. Into each of the two or three wells to be used for the highest standard protein concentration, add BSA standard solution (2.00 g/L, 50.0  $\mu$ L {E.14}), and mix gently.
5. Beginning with a well containing the highest standard concentration, draw up 50  $\mu$ L of liquid, transfer it to the well in the standard series to have the next lower concentration, and gently mix the well contents.
6. Repeat the previous step until protein has been transferred to the second to last well for the standard series, then withdraw and discard 50.0  $\mu$ L from this well. This leaves one well per standard series with no protein added to act as a blank.
7. Create the replicate standard dilution series similarly.
8. Add 2.50  $\mu$ L of each protein extract to be quantitated to replicate wells containing 47.5  $\mu$ L of 1.0 mol/L sodium hydroxide solution and mix carefully. Particular care must be taken with pipetting technique to ensure accuracy. This effects a 1 in 20 dilution of the protein sample.
9. Return primary protein extracts to  $-80^{\circ}\text{C}$  storage.
10. Each well, either standard or unknown, will require 100  $\mu$ L of prepared BCA reagent. Prepare a suitable volume by adding 1 volume of copper sulphate solution (4 % w/v {Solution 68}) to 49 volumes of BCA {E.15}, and mix gently but thoroughly. For one full 96-well plate, suitable volumes are 200  $\mu$ L of copper sulphate solution and 9.80 mL of BCA.
11. Add prepared BCA reagent to each well (100  $\mu$ L), using a multichannel pipette if preferred.
12. Incubate the plate(s) for 30 – 60 min at  $37^{\circ}\text{C}$ . Ensure that the spectrophotometer to be used is turned on so that it has time to stabilise before use.
13. After incubation, read and record the absorbance of each well, ideally at 562 nm, but any wavelength in the range 540 – 590 nm is satisfactory.
14. Construct a calibration curve from the readings for the replicate standards and blanks by determining the least-squares line of best fit for the standards. If the curve is not linear at high concentration, ignore those points when constructing the curve. Calculate the concentrations for the unknowns from the regression equation for the standard curve, adjusting for the dilution made during preparation of the plate. If any measured absorbances for unknowns fall outside the linear portion of the standard curve, the assay must be repeated for these samples using a different dilution factor.

### Membrane staining with Ponceau S

### Method 42

1. Place membranes to be stained flat in a dish.
2. Add sufficient Ponceau S stain {E.16} to cover the membranes.
3. Agitate by gentle rocking for 5 min.
4. Recover the stain, which can be reused many times.
5. Remove excess stain from each membrane with four brief washes in water.
6. Dry the membranes by placing them protein side uppermost on a paper towel, either at ambient temperature or at  $37^{\circ}\text{C}$  for 10 min.
7. Optionally, make a photographic record of the staining.
8. Destaining is often not specifically required, as this will usually happen spontaneously when next the membrane is used. If desired, membranes can be destained by gentle agitation in TBS {Solution 61}.

## B.16 Methods for Western blotting

### Chemiluminescent detection using the Fujifilm LAS-3000

Method 43

1. If thought necessary, make a booking to use the LAS-3000 imaging system.
2. Gather together: membranes to be imaged in TBS or TTBS, sufficient of each of the two components of the detection reagent {E.16} still unmixed, paper towels, P1000 pipette and tips, a timer, a clean forceps, and a transparent acetate sheet or similar, and proceed to the LAS-3000.
3. If, or when, the instrument is free, start the interface software and begin cooling the CCD camera. This will take ~5 min. Via the software, adjust the tray height as appropriate for the size and number of membranes to be imaged, and set the acquisition method for chemiluminescence and the capture mode to incremental with 10 s intervals and high sensitivity.
4. Combine the two components of the detection reagent.
5. With a forceps, drain the membranes by holding an edge against a paper towel, and arrange the membranes on the transparent sheet.
6. Apply the mixed detection reagents to the membranes. Surface tension should retain the reagents on the membranes. Start a 5 min timer.
7. On expiration of the 5 min period, gently drain the detection reagent from the membranes by drawing it off from an edge using a paper towel, and place the membranes still on the plastic sheet into the LAS-3000.
8. If the camera has not yet cooled to operating temperature and stabilised, wait until it has. Adjust the focus using the interface software and the positioning of the membranes under the camera.
9. Commence image capture. Monitor each image and stop acquisition when the signal is sufficiently strong, and certainly before it becomes oversaturated, as indicated by colour coding of pixels. Do not yet move the membranes.
10. Select from the images stored that which most appeals, and save it. If quantitation of bands is to be undertaken, this must be saved in the proprietary Fujifilm image format. Alternatively, or in addition, for downstream general image manipulation, the 8-bit TIFF format should be used.
11. If dye-conjugated markers have been used, change the acquisition method to "epi", and the capture mode to "precision" with an exposure time of 1/60 s. Capture and save a single image of the membranes. Since the membranes were not moved between the chemiluminescent capture and the epi-illumination capture, the images saved will be directly superimposable, and the marker images can be simply digitally added to the chemiluminescent image in their correct relative positions.

Note: If prolonged exposures prove to be required, a layer of plastic wrap can be placed over the membranes during exposure to prevent drying. Alternatively, TBS can be layered onto the membranes once they are in place under the camera.

## B.17 Methods for immunofluorescent labelling

### Immunofluorescent labelling of cells fixed on coverslips

Method 44

This procedure is for the fluorescent immunolabelling of cells for DNA,  $\alpha$ -tubulin, and pericentrin. Either of two methods of labelling for DNA may be used. In the first, the coverslips are initially incubated with Hoechst 33342. In the second, DNA labelling is achieved through the use of a mountant that contains DAPI. However, it was found that under the intense illumination associated with the 100x oil immersion objective lens in use, the DAPI-containing mountant rapidly discoloured, obliterating contrast with the stained DNA within a minute. It is thought that the unbound DAPI in the mountant



was oxidising either in response to the UVR or to the heat associated with the illumination. As a result, use of the DAPI mountant was abandoned, despite its marginally greater convenience, and the bulk of the work was performed using Hoechst staining, which provided better contrast and structural imaging.

Since fluorescent compounds are used, it is important to reduce the light levels of the work environment from the first step in which one is introduced, and to protect the samples from light as far as is practicable from that point.

1. If the coverslip has been stored at 4 °C, rather than processed immediately after fixation, then check by phase contrast microscopy to confirm cellular integrity and freedom from microbial growth. Proceed only if these are satisfactory.
2. Gently wash the coverslip twice in PBS (1 mL {Solution 6}) by addition and aspiration.
3. If mountant with DAPI is to be used, omit the next several steps, and resume at step 9.
4. Work in reduced lighting from this point on.
5. Add Hoechst 33342 (10 mg/L in saline, 100 µL {Solution 70}), ensuring that the coverslip is completely covered.
6. Allow to stand for 10 min.
7. After this time, remove the Hoechst 33342 solution by aspiration.
8. Wash twice gently with PBS (1 mL {Solution 6}) by addition and aspiration.
9. Permeabilise by adding KB buffer including 0.2% v/v Triton X-100 (100 µL {Solution 74}) and allow to stand for 5 min.
10. Rinse, by the addition of KB buffer (1 mL {Solution 72}) and aspiration.
11. Add KB buffer (1 mL {Solution 72}) and allow to stand for 5 min. This is a non-specific binding blocking step that utilises the BSA component of the KB buffer.
12. After this time, remove the KB buffer by aspiration.
13. Add mixed primary anti- $\alpha$ -tubulin and anti-pericentrin antibodies (100 µL {Solution 76}). Ensure that the entire coverslip is covered. Allow to stand at ambient temperature for 1 h. Alternatively, comparable results may be achieved more quickly by incubating at 37 °C for 30 min.
14. After this time, remove the primary antibodies by aspiration.
15. Rinse once with KB buffer (1 mL {Solution 72}) by addition and aspiration.
16. Add KB buffer (1 mL {Solution 72}) and allow to stand for 5 min. This is a further blocking step.
17. After this time, remove the KB buffer by aspiration.
18. If mountant with DAPI is to be used, reduced lighting must be used only from this point.
19. Add mixed secondary Alexa Fluor 488 conjugated anti-mouse and Alexa Fluor 594 conjugated anti-rabbit antibodies (100 µL {Solution 75}). Ensure that the entire coverslip is covered. Allow to stand for 30 min.
20. In anticipation of its use, remove the anti-fade mountant from -20 °C storage and allow it to warm to ambient temperature slowly. This is a requirement for its correct function.
21. After the 30 min secondary antibody incubation period, remove the supernatant secondary antibody mixture by aspiration.
22. Gently wash the coverslip three times with PBS (1 mL {Solution 6}) by addition and aspiration.
23. Add PBS (1 mL {Solution 6}). This is a fourth wash step, but rather than aspirate the PBS, it is easier to remove the coverslip in the next step with the PBS still present.
24. Using a forceps, or other pointed implement, carefully raise one edge of the coverslip until it can be grasped by the edges with a gloved hand.

25. Remove the coverslip from the PBS, drain briefly, and transfer it to a paper towel on a small tray, keeping the face with the cells attached uppermost.
26. Allow the coverslip to dry fully. This is an important requirement for correct function of the mountant.
27. When the coverslip has dried, apply a drop (~15 – 25  $\mu$ L) of mountant, with or without DAPI additive as appropriate, to the centre of a clean glass microscope slide, doing so without forming bubbles.
28. Handling the coverslip only by the edges, position one edge against the slide in such a way that when the opposite edge is lowered, the drop of mountant will come into contact with the centre of the face of coverslip to which the cells are attached.
29. Gently and slowly lower the coverslip. The mountant should move to fill the entire space between the slide and the coverslip. Experience is the best guide as to the size of drop required.
30. Apply a small drop of nail varnish to each corner of the coverslip so that when it dries it will hold the coverslip in place.
31. Return the mountant to  $-20\text{ }^{\circ}\text{C}$  storage.
32. Allow the mountant to cure for a period of 1 d in the dark at ambient temperature.
33. When cured, the edges of the coverslip should be sealed with nail varnish and this be allowed to dry.
34. Slides should be stored at  $4\text{ }^{\circ}\text{C}$  or  $-20\text{ }^{\circ}\text{C}$  in darkness until required.

### **B.18 Methods for immunofluorescent microscopy image processing**

#### **File format selection**

By far the most commonly used format for image files is that defined by the Joint Photographic Experts Group, known as JPEG. It allows variable compression of single layer image data, but does so in a lossy manner. An often overlooked aspect of this is that every time such a file is saved, the image quality degrades further, as existing compression artefacts contribute to further compression artefacts. JPEG format is therefore unacceptable for any file intended to be archived or modified, and that includes files in an image processing workflow. Its use should be limited to the distribution of images where greatly reduced file size is an overriding priority, usually in order to reduce the necessary data transmission bandwidth.

For routine storage of images during image processing, a lossless format is absolutely required, and it is questionable whether any compression mechanism is really necessary, as the processing overhead in compressing and decompressing images may be more of an issue than the modest increase in storage space needed for images while they are being manipulated. The TIFF format has many advantages in this respect. It supports multiple colour space models, such as RGB and CMYK, depths of up to 48 bits, and multipage or layered images. Furthermore, it does support a number of compression mechanisms, both lossless, notably LZW and ZIP, and lossy using the JPEG algorithm. On the other hand, because the TIFF format is extremely flexible, and indeed arbitrarily extensible, inter-application or cross-platform usage of TIFF files is not always without problems.

Once processed, a losslessly compressed format is the ideal, and where guaranteed cross-platform operation is desirable, and 24 bit single layer RGB is satisfactory, the Portable Network Graphic format, or PNG, is to be recommended highly.

In the general case then, images should be captured at source losslessly if possible, with TIFF and PNG being suitable formats. While being processed, TIFF format is best where multiple applications are to be



used, or the native format of the image processing application used if there is just one. For storage and distribution, PNG is the format of choice. Only where extremely high compression is needed and loss of detail is tolerable should JPEG be considered.

### **Image processing software**

Three software applications warrant specific mention: Adobe Photoshop, NIH ImageJ, and Lemkesoft GraphicConverter {Table E-18}.

Photoshop is an immensely powerful and stable program that is justifiably and indisputably the premier non-specialist image processing application available. It should be the first choice for any person considering more than casual editing or manipulation of images, and while relatively expensive, represents very good value. Of particular merit is the facility to work with multiple image layers in one document, and produce derivative images that comprise a blend of these superimposed according to simple or complex rules. In the current context of the processing of separately captured images of the same object excited by different wavelengths of light, the utility of this cannot be overstated. The first step in processing therefore is the importation of the individually captured images each into its own layer of a single Photoshop document. From there, image registration can be undertaken, simplified by the ability to modify blending, visibility and transparency of individual layers, and brightness and contrast can be adjusted for each layer independently, or coordinately. Addition of scale bars, image cropping, resizing, compositing, and compression as a final PNG product follow.

The freeware product ImageJ is also very powerful, but perhaps because it is free, it does not have the same polish and internal consistency as Photoshop. In particular, some important functions always operate on all open documents. If one should have the wrong size or format, the operation fails. If a currently open image is needed for further use, but needs to be excluded from an operation, then it must be saved as a disk file and closed until being reopened when needed. The additional steps required and the number of disk files that are generated this way can be annoying. ImageJ differs from Photoshop in one important respect: it does not support layering in quite the same way, but rather implements image stacks with only limited means for their combination. One of these, however, is not available in Photoshop: z-projection of multiple layers in a single operation {Method 48}, and this was used extensively here. Features implemented by way of plug-in modules for the rendering of three-dimensional data produced by confocal microscopy are also available for ImageJ and were used in the production of Figure 6-45.

One further software product deserves particular attention here, and that is GraphicConverter {E.9}, which does as its name implies, and is able to import about 200 graphic formats, and export about 80. It does far, far more than that, rivalling Photoshop in some respects, and it represents extraordinary value for the modest shareware fee asked. It is available only for the Macintosh platform.

### **Channel reassignment**

### **Method 45**

#### *Use of redundant data for Hoechst fluorescence*

For Hoechst or DAPI labelled DNA, a significant portion of the signal falls into the range of wavelengths recorded by the green channel of the digital camera employed. Both to prevent crosstalk with the signal from  $\alpha$ -tubulin, and to utilise all the available intensity information, this green component was merged into the blue channel to the extent that this subjectively enhanced contrast or detail.

This spectral overlap proved especially useful when it was found that owing to limitations in the image capture system, there was a tendency for the blue channel to be over-exposed. The rudimentary

intensity metering facility available during image capture does not provide individual intensity histograms for each colour channel, and the composite histogram that is provided has very low resolution, perhaps only eight brightness levels. This made it impossible to determine exposure quantitatively and necessitated a subjective approach based on a visual assessment of two full colour images displayed on monitors that were neither matched nor calibrated. Exposure was set at a point where saturation was not evident, that is, that trial increases in exposure were still resulting in greater image brightness. Unfortunately, this was an illusion, as it was often only the green channel that was not saturated, and in consequence, the blue channel was often over-exposed, and many captured pixels were at their saturation blue level of 255. However, by virtue of the redundant information present in the green channel, albeit with reduced dynamic range, eminently satisfactory images could be obtained by discarding the compromised blue channel data and replacing it with that from the green through use of the Photoshop "Channel mixer" function.

### *Enhancement of spectral differences - distinguishing ANABs*

With the discovery of the anomalous nucleic acid bodies in NZM10 cells came a problem: the difference in fluorescence colour that was so clear on direct observation proved very difficult to capture for the purposes of documentation (Figure B-1). To address this, a method based on colour channel reassignment was developed to bring about a greater visible difference between objects differing only relatively slightly colour.

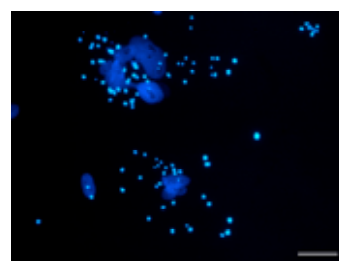


**Figure B-1: ANABs**

The process comprises three steps, of which the first is the key to the technique's utility. In this step, the green channel is subtracted from the blue, while simultaneously being added to the null red channel using the "Channel mixer" function. Since normal nuclear Hoechst labelling produces a fluorescence almost twice as bright in blue as it is in green, step one results in the reassignment of the typical nuclear fluorescence colour from greenish-blue to something approximating neutral grey since, an R:G:B ratio of 0:1:2 would become 1:1:1 after reassignment. For ANABs, which are greener, about 0:1.5:2, the result is a ratio of 1.5:1.5:0.5, a yellow-grey.

In the second step, the "Levels" function is used to make best use of the available brightness range, particularly important since the blue brightness was reduced as a result of step one. This is done for all channels coordinately so as not to alter the new colour ratios by too great an extent. These transformations are demonstrated in Figure B-2. The third and final step is a subjective increase of overall colour saturation to enhance the still subtle differences. While these changes destroy the original relative intensity information, the goal is to render more visible the minor differences present, and not numerical analysis.

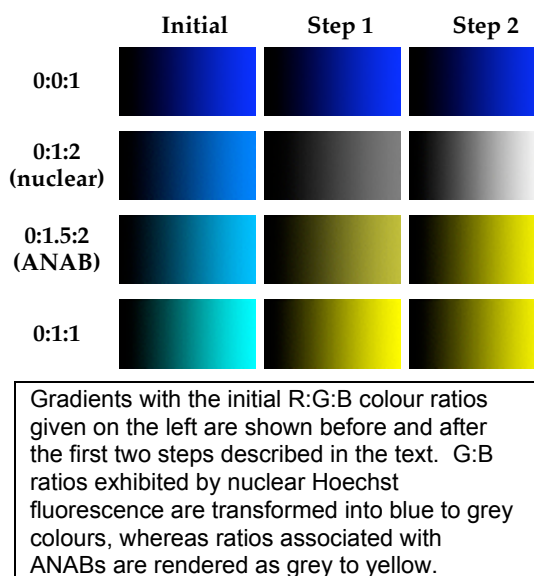


**Figure B-2: Colour reassignment process**

There is a problem with this approach, however, but fortunately not an insurmountable one. The tendency to over-expose the blue channel for reasons described above, distorts the recorded ratio of

green to blue: as the brightness of the ANAB increases, the blue level may be limited to 255 as a result of channel saturation, but the green can still increase. To compound the problem, since ANABs generally are brighter than nuclei, these are more likely to be subject to this effect. The problem is illustrated in Figure B-3, where the dramatic enhancement of ANAB visibility owes more to the saturation of the blue signal, and for most of the ANABs present the green signal also, than it does to the inherent difference in emission spectra.

The question then arises, is there actually any real difference in the emission spectra of the ANABs and normal nuclei or is the apparent change in colour seen simply an artefact caused by blue

channel saturation, or a similar physiological effect taking place in the eye? By sampling the intensity of green and blue signals for pixels where neither was saturated from nuclei and ANABs, it was established that the observed effect was physical, and not a perceptual or instrumental artefact. This study is described in the experimental chapter beginning on page 6-38.

### Level adjustment

Adjustment of brightness levels should not be undertaken without first considering the purpose intended for the image. Since this adjustment may distort both the absolute and the relative brightness of pixels in an image, these values cannot be used for quantitative purposes after level adjustment without the necessary corrections being made. For display purposes, adjustment linearly to maximise use of the available dynamic range, in effect a post-processing exposure compensation, and non-linearly, for example to compensate for the existence of features of interest at both very high and very low brightness levels, are both acceptable practices.

The particular instance of preparing multiple fluorescence photomicrographs representing different focal planes and using different fluorophores for assembly into a single composite image by z-projection {See 'Image projection'} falls between the extremes of preserving relative brightness and maximally enhancing contrast. Rather than simply adjusting each image independently, all images in a set for the same fluorophore should be adjusted to the same degree. In this way, the relative brightness relationship between objects in different focal planes is essentially maintained. In practice, this means determining the amount by which the most intense significant pixel in any of the images must be brightened to reach saturation, and the amount by which the intensity of the dimmest significant pixel in any image must be reduced to become zero, and adjusting images in the set by these amounts. The tonal range that results encompasses the darkest and brightest features present within the entire set, while no single image may use the entire dynamic range available.

There is a situation where this general rule should not be applied blindly, and this is where, despite having used the same exposure for all images in a fluorophore set, the intrinsic brightness of the signal changed between images being captured. The most likely situation where this can arise is in the bleaching of fluorophores. Here, there is a case for judicious subjective independent manipulation of

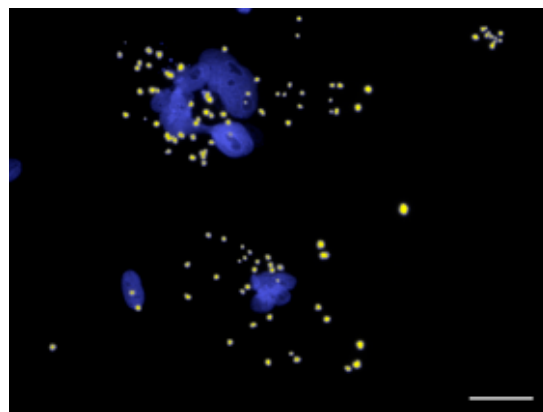


Figure 6-41 processed by colour reassignment. Here, the greater enhancement is partially artefactual due to overexposure of the ANABs causing saturation of the blue signal. Scale bar = 50  $\mu\text{m}$ .

**Figure B-3: Colour reassigned Figure 6-41**

### Method 46

component image brightness levels to restore the relationship that would have existed had not the fluorophore faded.

One issue that will result from the application of this rule is that the brightness of objects cannot be compared between different adjusted images, as the brightness range present in each will have been expanded to use the available dynamic range, irrespective of how broad that range was in the original: separate images of objects even with very different intrinsic brightness will end up being as bright as each other after adjustment. As a result, even qualitative assessments of relative brightness can only be made where the objects being compared are in the same image.

In the current work, this effect was seen mostly in the presentation of pericentrin data. In the great majority of cells, pericentrin labelling of centrosomes is very bright, and so the level of background cytoplasmic labelling appears dark in comparison. In telophase cells, however, centrosomal pericentrin labelling greatly diminishes, or even disappears, and after level adjustment the brightness of the cytoplasmic pericentrin labelling appears much greater.

### Image registration

### Method 47

When separate images for differently labelled fluorophores are captured there is often a need to combine these component images into a single image, a process termed "compositing". This may simply be to conserve space, but more frequently it is in order to demonstrate the spatial relationship between structures recorded in different component images as a result of differential fluorescent labelling. In the latter case, it is especially important that that spatial relationship is maintained in the compositing process.

When well designed and maintained microscopes are used, interchange of filter blocks in order to capture different fluorescence signals ought not to alter the optical path from a point on the specimen to the corresponding point on the camera sensor, but in practice this does occur to a greater or lesser degree. There is also the possibility that in the process of performing this operation, or of adjusting the focus, the microscope stage may be inadvertently disturbed between images intended to be of exactly the same field. To correct these problems, a means to align multiple images after their capture is needed, a process termed "registration".

The mainstay image processing software application, Photoshop, has no facility to perform this automatically. There is a plug-in extension for ImageJ named "Turboreg" that is able to register images that have well-defined points of similarity, but it cannot be used to register component images for different filter blocks, as these usually have very little in common since they are intended to record different structures through differential labelling. A registration method using available resources was developed that proved satisfactory, but being a painstaking computer-assisted manual process rather than a software tool, it was quite slow and accounted for about 75% of the time required to prepare each image.

The Photoshop document containing the channel reassigned {Method 45}, level adjusted {Method 46} component images on separate layers is opened, and for reasons that will be described below {See '*Image projection*'}, a new layer containing only black is created as a background and is locked. One component image is selected as the reference against which all of the others are to be registered, and this is locked for position.

If multiple component images exist for any fluorophore, these are first mutually registered, beginning with those for the same fluorophore as the reference layer. It is best to work one layer at a time, bringing it into register with the reference layer, or a previously registered layer. Layers containing component images for other fluorophores should be made invisible, as should other unregistered layers for the fluorophore being registered. Two methods are of value in bringing the subject layer into register with the reference. In the first, the visibility of the subject layer is repeatedly toggled on and off. Any misregistration is interpreted by the mind as movement, and the subject layer can be nudged so as to minimise this effect. This is analogous to the blink microscope technique used, among other things, in the discovery of Pluto by Tombaugh in 1930. The second method involves setting the blending mode for the upper layer of the two to "Difference". At each position in the resulting display, the difference between the corresponding positions in the two component images is shown; where these are identical, the result is black. Hence, in the result, only those places where there is a discord between the two are displayed. Again, by nudging the subject layer, the size of this difference signal can be minimised, but of course, not eliminated, as this would only be possible for identical component images. One technique is to align a structure that is in focus on one layer centrally within the out-of-focus halo of the same structure on the other (Figure B-4). Once registered, the blending mode should be returned to "Normal".

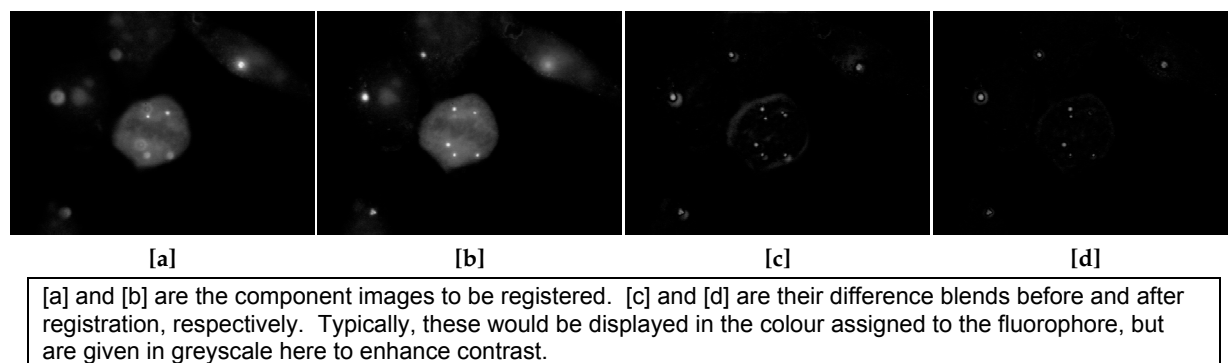


**Figure B-4: Image registration using difference blending**

As each successive layer for a fluorophore is brought into register, it is positionally linked to a previously registered layer for that fluorophore, or to the reference layer if it is for the same fluorophore. The end result of this stage will be three independent sets of mutually registered and positionally linked component images, one for each fluorophore. At this point, the layers for images associated with the fluorophore used in the reference image can be positionally locked.

The next step is to mutually register the two remaining sets of images against those for the reference fluorophore. Since each set is already internally registered and its layers are linked, it suffices to register just a single image from each against any of those for the reference set; the others will remain in register. The difference blending method can be used effectively here since the layers being operated on contain different colours, so the contents of both are present in the result. A slightly better approach that has a similar effect involves adjusting the advanced blending options for the layers to be registered. In particular, each layer's options should be set to blend only the channel for the fluorophore it depicts. These techniques allow the two layers to be seen superimposed, and the subject layer, and the invisible layers linked to it, can be nudged into place, as very often a structure present in one image will correspond to a structure or a void in another, and these features can be brought into alignment.

By exploring the various superimpositions available by altering the layer visibilities, any fine adjustment to individual layer positions can be made. All layers are then positionally locked and the file saved.

There is a useful technique that can help in registering images where the contrast in one or both is poor, as may occur where there are a few very bright structures while the bulk of the image is dark. By duplicating a layer and linking it to the original, it is possible to render invisible the original layer, alter the gamma setting of the duplicate layer to enhance the contrast, register both linked layers based on the duplicate, and then delete it, thus leaving the tonal settings of the original unchanged.

As an alternative to using layer difference blending, by inverting the upper layer and changing its opacity to 50%, a similar effect can be obtained, but with grey as an indication of identity and the colour displayed as an indication of which layer is contributing the signal. Once registered, the layer is inverted back to its original state, and its opacity returned to 100%.

### Image projection

### Method 48

At the magnification required to resolve the structures of interest, the optical depth of field is extremely limited. This can render it impossible to obtain a single clear image of multiple structures at different depths within a cell, so to record all such structures requires images to be captured from several focal planes. This can be true of each channel independently, so for a single observed cell, depending upon its depth and complexity, anywhere from three to eighteen images may be necessary to capture the information available to the observer at the microscope. The issue then arises of how best to present this information to provide an easily assimilable image showing all of the salient visible structures.

The approach developed for presentation of the current data relies upon the fact that an illuminated object, in this case a fluorescently labelled structure, will appear brighter when it is in focus than when it is not, thus, for each focal plane image, the brighter parts should correspond to objects in focus. Combining images from multiple focal planes in such a way that the brightest points of each are incorporated into a merged result achieves the effect of retaining all objects in focus from all focal planes. The term for this manipulation is a maximum intensity z-projection, and this function is available in ImageJ. It is not a perfect method though, as contrast can be lost, and artefactual halos around bright objects stemming from the contribution of out-of-focus images can be created. The benefits and deficiencies of the method can be judged from the example provided in Figure B-5, wherein images of pericentrin labelling for five focal planes, and the resultant z-projection are given.

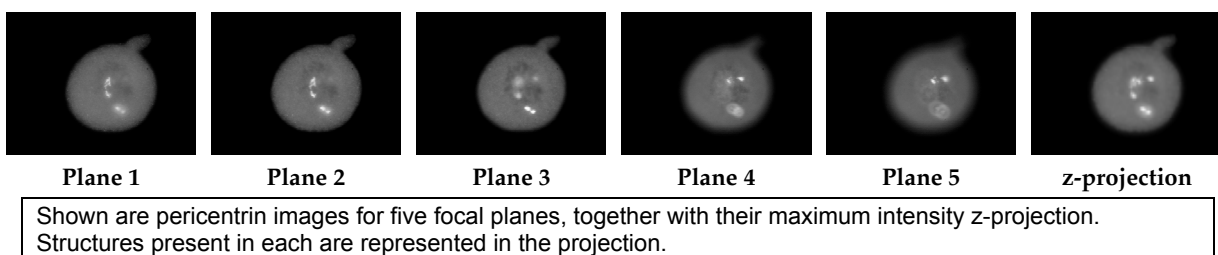


**Figure B-5: Z-projection of images**

No single focal plane image adequately portrays the true extent of the centrosomal aberrations present in this cell, whereas this is immediately clear from the z-projection image, and this economical and readily assimilable presentation more than compensates for the loss of the depth cues, the marginally reduced contrast, and the halo artefacts.

In practice, the multiple focal plane images for all channels were imported into a Photoshop document as separate layers, and after being spatially registered and adjusted for brightness and contrast, were exported as individual greyscale images. Here is where the incorporation of a black-filled layer mentioned above becomes significant. The registration process will probably have left transparent pixels



on some edges of a layer, and even if the entire layer is selected, if it is copied, the transparent pixels are not included in the copy. If a new document is created to receive this it will have the trimmed size; if the size of the new document is manually set and the image pasted, it will be centred and the registration lost. The solution is to set the layer visibilities in the source document so that only the layer to be exported and the black background layer are visible, to select all pixels, to select only the colour channel to be transferred and to do a merged copy. This will effectively fill the transparent pixels with black and maintain a constant image size. A new file is then created, which as a result of the merged copy will be correctly sized, and as a result of the colour channel selection will be greyscale, the merged copy is pasted in, and the file is saved, TIFF format being appropriate here. Each layer to be exported is treated similarly until one greyscale image for each layer is produced with the registration intact.

For each fluorophore or colour channel, image files for all focal planes are then opened in ImageJ and converted to an image stack, a step that would fail if the images had different sizes. A maximum intensity z-projection is performed on the stack, and the result saved. When all channels have been similarly processed, there will separate files for the three resultant projections and these can then be merged [Method 49].

### **Image merging**

**Method 49**

Image files should be maintained with registered layers separate, but derivative images with this information merged need to be produced for presentation. Where it transpires that only a single focal plane image is needed or is available for each fluorophore, the layers containing the three component images can simply be saved from Photoshop to a new file with layers merged. Where z-projection is carried out, it is expedient to use the ImageJ RGB merge function to perform this, after which the composite image is saved as a new file.

### **Sharpening and noise reduction**

**Method 50**

Occasionally, a median noise filter may need to be applied to images to eliminate artefactual speckles thought to be produced by the camera or image capture software. This filtering can be done in Photoshop or Image J, and performed on individual component images, projected images, or composite images. It is also an appropriate technique where there is a sparse speckled non-specific fluorescent background signal not associated with cells that detracts from image quality. On rare occasions, sharpening through the use of the unsharp mask filter in Photoshop may be warranted, but this should be used with discretion, as the introduction of artefacts can be troublesome. Typically, sharpening of only 2% to 5% should be considered.

### **Scaling and cropping**

**Method 51**

The relationship between physical distance and pixel size must be determined for each objective used, and the objective noted for each image. If this information is not available in the microscope or camera documentation it can be determined by capturing images of a haemocytometer grid: patterns do vary so care is needed.

Scale bars are easily added to Photoshop files by creating a separate layer and naming it appropriately, for example "10  $\mu\text{m}$  scale bar", constraining the rectangular selection tool to the size in pixels required to represent the desired physical distance, using this tool to select an arbitrary region of the desired size on the empty layer, and filling the selection, white being a good choice of fill colour for immunofluorescent imagery. The scale bar can then be moved independently by moving the entire layer. The master image file can then be saved with this new layer.

## Human metastatic melanoma in vitro

---

Cropping of unwanted areas can be achieved by moving the scale bar so that it is within the area to be retained, cropping the image, preferably using one of a set of fixed sizes rather than purely arbitrarily, and then repositioning the scale bar as needed. A merged copy can then be made or the file saved with merged layers to a new file, as appropriate. This will generally be an image that will be used for presentation, so a compressed format such as PNG is appropriate at this point.



# C

# Solutions

## C.1 General solutions

### Bromophenol blue (10% w/v)

Solution 1

To make 1.5 millilitres	Amount	Final concentration
Bromophenol blue	150 mg	10% w/v
Water	to 1.5 mL	
<b>Storage:</b>	-20 °C	

### Citrate-buffered saline

Solution 2

To make 5 litres	Amount	Final concentration
Sodium citrate (trisodium salt)	22.0 g	15 mmol/L
Potassium chloride	50.0 g	134 mmol/L
Water	to 4.8 L	
Hydrochloric acid (1 mol/L)		to pH 7.6
Water	to 5.0 L	
<b>Further treatment:</b>	Divide into 700 mL portions. Autoclave to sterilise.	
<b>Storage:</b>	Ambient temperature. Maintain sterility.	

### EDTA solution (500 mmol/L, pH 8.0)

Solution 3

To make 1 litre	Amount	Final concentration
EDTA	186.1 g	500 mmol/L
Water	to 900 mL	
Sodium hydroxide	~20 g	to pH 8.0
Water	to 1.00 L	
<b>Storage:</b>	Ambient temperature.	

### Ethanol (~70% v/v)

Solution 4

To make 1 litre	Amount	Final concentration
Ethanol	700 mL	~70% v/v
Water	to 1 L	
<b>Storage:</b>	Ambient temperature.	

### Ethanol (~80% v/v)

Solution 5

To make 1 litre	Amount	Final concentration
Ethanol	800 mL	~80% v/v
Water	to 1 L	
<b>Storage:</b>	Ambient temperature.	

### Phosphate-buffered saline (pH 7.4)

Solution 6

To make 1 litre	Amount	Final concentration
Sodium chloride	8.0 g	137 mmol/L
Potassium chloride	200 mg	14.9 mmol/L
Potassium phosphate (monobasic)	200 mg	27.7 mmol/L
Sodium phosphate (dibasic)	1.15 g	8.1 mmol/L
Water	to 900 mL	
Hydrochloric acid/Sodium hydroxide (1 – 6 mol/L)		to pH 7.4
Water	to 1.00 L	
<b>Further treatment:</b>	Autoclave to sterilise.	
<b>Storage:</b>	Ambient temperature. Maintain sterility.	

### SDS solution (10% w/v)

Solution 7

To make 1 litre	Amount	Final concentration
SDS	100 g	10.0% w/v
Water	to 1.00 L	
<b>Storage:</b>	Ambient temperature.	

**Tris buffer (100 mmol/L, pH 8.0)****Solution 8**

To make 1 litre	Amount	Final concentration
Tris buffer (500 mmol/L, pH 8.0) {Solution 9}	200 mL	100 mmol/L
Water	to 1.00 L	
<b>Storage:</b>	Ambient temperature.	

**Tris buffer (500 mmol/L, pH 8.0)****Solution 9**

To make 1 litre	Amount	Final concentration
Tris base	60.55 g	500 mmol/L
Water	to 900 mL	
Hydrochloric acid (1 – 6 mol/L)		pH 8.0
Water	to 1.00 L	
<b>Storage:</b>	Ambient temperature.	

**Xylene cyanol FF (10% w/v)****Solution 10**

To make 1.5 millilitres	Amount	Final concentration
Xylene cyanol FF	150 mg	10% w/v
Water	to 1.5 mL	
<b>Storage:</b>	-20 °C	

**C.2 Solutions for cell culture****αMEM/10% FCS/antibiotics****Solution 11**

To make ~450 millilitres	Amount	Final concentration
αMEM (sterile)	400 mL	
FCS	44.0 mL	10 % v/v
Antibiotic mixture {Solution 12}	4.0 mL	
<b>Storage:</b>	4 °C. Maintain sterility.	

**Antibiotic mixture for routine cell culture (112 x)****Solution 12**

To make 1 litre	Amount	Final concentration
Penicillin-G	1.12 x 10 <sup>7</sup> units	1.12 x 10 <sup>7</sup> units/L
Streptomycin sulphate	11.2 g	11.2 g/L
PBS {Solution 6}	to 1.0 L	
<b>Further treatment:</b>	Filter-sterilise. Dispense into 4.0 mL portions.	
<b>Storage:</b>	-20 °C. Maintain sterility.	
<b>Note:</b>	Final concentration given by 4 mL added to 400 mL medium supplemented with 10% v/v FCS will be 10 <sup>5</sup> units/L penicillin and 100 mg/L streptomycin.	

**Trypsin (0.06% w/v)****Solution 13**

To make ~700 millilitres	Amount	Final concentration
Trypsin	500 mg	0.06% w/v
Citrate-buffered saline {Solution 2}	10 mL	
<b>Filter-sterilise.</b>		
Citrate-buffered saline {Solution 2}	to 700 mL	
<b>Further treatment:</b>	Dispense into 10 mL portions.	
<b>Storage:</b>	-20 °C. Maintain sterility.	

**C.3 Solutions for extraction****Ammonium acetate solution (7.50 mol/L)****Solution 14**

To make 100 millilitres	Amount	Final concentration
Ammonium acetate	57.8 g	7.50 mol/L
Water	to 100 mL	
<b>Storage:</b>	Ambient temperature.	

**Guanidine hydrochloride solution (6.00 mol/L)****Solution 15**

To make 500 millilitres	Amount	Final concentration
Guanidine hydrochloride	287 g	6.00 mol/L
Water	to 500 mL	
<b>Storage:</b>	Ambient temperature.	

**Protease inhibitor cocktail (100 x)****Solution 16**

**Caution:** *PMSF is a potent acetylcholine esterase inhibitor and is extremely toxic. Suitable handling procedures must be used.*

To make 10 millilitres	Amount	Final concentration
PMSF	50.0 mg	0.50% w/v
Leupeptin	2.00 mg	0.02% w/v
Aprotinin	1.00 mg	0.01% w/v
Ethanol	10.0 mL	
<b>Storage:</b>	-20°C	

**Proteinase-K (20.0 g/L)****Solution 17**

To make 1 millilitre	Amount	Final concentration
Proteinase-K	20.0 mg	20.0 g/L
Water	to 1.00 mL	
<b>Storage:</b>	-20 °C	

**Sodium sarcosyl solution (20% w/v)****Solution 18**

To make 100 millilitres	Amount	Final concentration
Sodium sarcosyl	20.0 g	20.0% w/v
Water	to 100 mL	
<b>Storage:</b>	Ambient temperature.	

**C.4 Solutions for storage****Cell freezing solution (2 x)****Solution 19**

To make 9 millilitres	Amount	Final concentration
$\alpha$ MEM/10% FCS/antibiotics {Solution 11}	5.0 mL	
FCS	2.0 mL	28% v/v
DMSO	2.0 mL	22% v/v
<b>Further treatment:</b>	Mix well. Chill to 4 °C before use.	
<b>Storage:</b>	4 °C. Maintain sterility.	

**Tris/EDTA buffer (pH 8.0)****Solution 20**

To make 1 litre	Amount	Final concentration
Tris buffer (100 mmol/L, pH 8.0) {Solution 8}	100 mL	10 mmol/L
EDTA solution (500 mmol/L, pH 8.0) {Solution 3}	200 $\mu$ L	100 $\mu$ mol/L
Water	to 1 L	
<b>Storage:</b>	4 °C	

**C.5 Solutions for flow cytometry****EDTA/PBS (100  $\mu$ mol/L)****Solution 21**

To make 500 millilitres	Amount	Final concentration
EDTA (tetrasodium salt)	19.0 mg	100 $\mu$ mol/L
PBS (pH 7.4) {Solution 6}	to 500 mL	
<b>Note:</b>	Use of the tetrasodium EDTA salt minimises impact on the final pH.	
<b>Storage:</b>	Ambient temperature.	

**FCS/PBS (2% v/v)****Solution 22**

To make ~500 millilitres	Amount	Final concentration
PBS (pH 7.4) {Solution 6}	500 mL	
FCS	10 mL	2% v/v
<b>Storage:</b>	4 °C.	

## Propidium iodide solution (1.00 g/L)

Solution 23

**Caution:** *Propidium iodide is a mutagen.  
Suitable handling procedures must be used.*

To make 1 millilitre	Amount	Final concentration
Propidium iodide	1.00 mg	1.00 g/L
Methanol	500 $\mu$ L	50% v/v
<b>Dissolve.</b>		
Water	500 $\mu$ L	50% v/v
<b>Storage:</b>	4 °C, in a dark bottle.	

## RNase A (5.0 g/L)

Solution 24

To make 5 millilitres	Amount	Final concentration
RNase A	25.0 mg	5.0 g/L
Water	5 mL	
<b>Storage:</b>	4 °C.	

## C.6 Solutions for DNA electrophoresis

## Ethidium bromide (10.0 g/L)

Solution 25

**Caution:** *Ethidium bromide is a potent mutagen.  
Suitable handling and disposal procedures must be used.*

To make ~5 millilitres	Amount	Final concentration
Ethidium bromide	50.0 mg	10.0 g/L
Water	5.0 mL	
<b>Storage:</b>	4 °C, in a dark bottle.	

## Ethidium bromide stain (1.0 mg/L)

Solution 26

**Caution:** *Ethidium bromide is a potent mutagen.  
Suitable handling and disposal procedures must be used.*

To make 500 millilitres	Amount	Final concentration
TAE buffer (50 x) {Solution 29}	10.0 mL	1 x
Ethidium bromide (10.0 g/L) {Solution 25}	50 $\mu$ L	1.0 mg/L
Water	to 500 mL	
<b>Storage:</b>	Ambient temperature, in a dark bottle.	

## Formamide loading buffer (2 x)

Solution 27

To make ~50 millilitres	Amount	Final concentration
Formamide (deionised)	50.0 mL	
EDTA (disodium salt)	372 mg	20 mmol/L
Bromophenol blue (10% w/v) {Solution 1}	250 $\mu$ L	0.05% w/v
Xylene cyanol FF (10% w/v) {Solution 10}	250 $\mu$ L	0.05% w/v
<b>Further treatment:</b>	Divide into 1.5 mL portions	
<b>Storage:</b>	-20 °C.	

## TAE loading buffer (5 x)

Solution 28

To make ~2 millilitres	Amount	Final concentration
TAE buffer (50 x) {Solution 29}	200 $\mu$ L	5 x
Xylene cyanol FF (10% w/v) {Solution 10}	10 $\mu$ L	0.05% w/v
Glycerol	500 $\mu$ L	25% v/v
Water	1.3 mL	
<b>Storage:</b>	-20 °C.	

## Tris/acetic acid/EDTA buffer (TAE) (50 x)

Solution 29

To make 1 litre	Amount	Final concentration
Tris base	242.2 g	2.00 mol/L
Acetic acid (glacial)	57.2 mL	1.00 mol/L
EDTA solution (500 mmol/L) {Solution 3}	100.0 mL	50.0 mmol/L
Water	to 1.00 L	
<b>Further treatment:</b>	Autoclave to sterilise.	
<b>Storage:</b>	Ambient temperature.	

**Tris/borate/EDTA buffer (TBE) (10 x)****Solution 30**

To make 1 litre	Amount	Final concentration
Tris base	107.8 g	890 mmol/L
Boric acid	55.0 g	890 mmol/L
EDTA	7.44 g	20 mmol/L
Water	to 1.00 L	
<b>Storage:</b>	Ambient temperature.	
<b>Notes:</b>	pH will be ~8.3. May precipitate during storage. This can be prevented by autoclaving.	

**C.7 Solutions for protein electrophoresis****Protein sample loading buffer****Solution 31**

To make 100 millilitres	Amount	Final concentration
Tris-SDS buffer (pH 6.8, 4 x) {Solution 33}	12.5 mL	0.5 x
Glycerol	10.0 mL	10% v/v
2-mercaptoethanol	5.00 mL	5.0% v/v
Bromophenol blue (10%w/v) {Solution 1}	1.0 mL	0.1% w/v
SDS	2.00 g	2.0% w/v
Water	to 100 mL	
<b>Storage:</b>	-20 °C.	

**SDS-PAGE electrophoresis buffer****Solution 32**

To make 1 litre	Amount	Final concentration
Tris base	3.03 g	25 mmol/L
Glycine	14.4 g	192 mmol/L
SDS	1.00 g	0.1% w/v
Water	to 1.00 L	
<b>Note:</b>	pH ~8.3	
<b>Storage:</b>	Ambient temperature.	

**Tris/SDS buffer (pH 6.8, 4 x)****Solution 33**

To make 100 millilitres	Amount	Final concentration
Tris base	6.05 g	500 mmol/L
Water	~80 mL	
Hydrochloric acid (1 – 6 mol/L)		pH 6.8
Water	to 100.0 mL	
SDS	400 mg	0.4% w/v
<b>Storage:</b>	Ambient temperature.	

**Tris/SDS buffer (pH 8.8, 4 x)****Solution 34**

To make 100 millilitres	Amount	Final concentration
Tris base	18.2 g	1.5 mol/L
Water	~80 mL	
Hydrochloric acid (1 – 6 mol/L)		pH 8.8
Water	to 100.0 mL	
SDS	400 mg	0.4% w/v
<b>Storage:</b>	Ambient temperature.	

**C.8 Solutions for acrylamide gels****Ammonium persulphate solution (25% w/v)****Solution 35**

To make 1.5 millilitres	Amount	Final concentration
APS	375 mg	~25% w/v
Water	1.5 mL	
<b>Storage:</b>	-20 °C	
<b>Note:</b>	Storage life is ~1 month.	

## Gel solutions for SSCP analysis of DNA

Solution 36

**Caution:** *Acrylamide is a potent neurotoxin. Suitable handling procedures must be used.*

To make 10 millilitres (Sufficient for 2 x 4.5 mL gels)	14% acrylamide	14% acrylamide 10% glycerol
TBE buffer (10 x) {Solution 30}	500 $\mu$ L	500 $\mu$ L
Acrylamide : bis-acrylamide (37.5:1, 30%) or Acrylamide : bis-acrylamide (37.5:1, 40%)	4.67 mL or 3.50 mL	4.67 mL or 3.50 mL
Glycerol	nil	1.00 mL
Water: if 30% acrylamide used if 40% acrylamide used	4.83 mL or 6.00 mL	3.83 mL or 5.00 mL
<b>Mix gently and degas.</b>		
<b>Immediately prior to pouring:</b>		
TEMED	20 $\mu$ L	20 $\mu$ L
APS (25% w/v) {Solution 35}	20 $\mu$ L	20 $\mu$ L
<b>Mix gently and pour gels.</b>		

## Separating gel solutions for SDS-PAGE analysis of protein

Solution 37

**Caution:** *Acrylamide is a potent neurotoxin. Suitable handling procedures must be used.*

To make 7 millilitres (Sufficient for 2 x 3.2 mL gels)	6% v/v gel	15% v/v gel	20% v/v gel
Tris-SDS buffer (pH 8.8, 4 x) {Solution 34}	1.75 mL	1.75 mL	1.75 mL
Acrylamide : bis-acrylamide (37.5:1, 30%) or Acrylamide : bis-acrylamide (37.5:1, 40%)	1.40 mL or 1.05 mL	3.50 mL or 2.63 mL	4.67 mL or 3.50 mL
Water: if 30% acrylamide used if 40% acrylamide used	3.85 mL or 4.20 mL	1.75 mL or 2.63 mL	583 $\mu$ L or 1.75 mL
<b>Mix gently and degas.</b>			
<b>Immediately prior to pouring:</b>			
TEMED	15 $\mu$ L	15 $\mu$ L	15 $\mu$ L
APS (25% w/v) {Solution 35}	15 $\mu$ L	15 $\mu$ L	15 $\mu$ L
<b>Mix gently and pour gels.</b>			

## Stacking gel solution for SDS-PAGE analysis of protein (4% v/v)

Solution 38

**Caution:** *Acrylamide is a potent neurotoxin. Suitable handling procedures must be used.*

To make 3 millilitres (Sufficient for 2 stacking gels)	Amount
Tris-SDS buffer (pH 6.8, 4 x) {Solution 33}	750 $\mu$ L
Acrylamide : bis-acrylamide (37.5:1, 30%) or Acrylamide : bis-acrylamide (37.5:1, 40%)	400 $\mu$ L or 300 $\mu$ L
Water: if 30% acrylamide used or Water: if 40% acrylamide	1.85 mL or 1.95 mL
<b>Mix gently and degas.</b>	
<b>Immediately prior to pouring:</b>	
TEMED	10 $\mu$ L
APS (25% w/v) {Solution 35}	10 $\mu$ L
<b>Mix gently and pour gels.</b>	

## C.9 Solutions for silver staining of polyacrylamide gels

## Fixer A (80% Ethanol)

Solution 39

{See Solution 5}

## Fixer B (20% acetic acid)

Solution 40

To make 1 litre	Amount	Final concentration
Acetic acid (glacial)	200 mL	20% v/v
Water	to 1.00 L	
<b>Storage:</b>	Ambient temperature.	

**Oxidiser (10 x)****Solution 41**

To make 1 litre	Amount	Final concentration
Potassium dichromate	10.0 g	34 mmol/L
Nitric acid (65% solution) or Nitric acid (50% solution)	1.10 mL or 1.43 mL	0.072% v/v
Water	to 1.00 L	
<b>Storage:</b>	4 °C.	

**Silver stain (10 x)****Solution 42**

To make 1 litre	Amount	Final concentration
Silver nitrate	20.4 g	133 mmol/L
Water	to 1.00 L	
<b>Storage:</b>	4 °C, in a dark bottle.	

**Silver stain developer****Solution 43**

To make ~600 millilitres	Amount	Final concentration
Sodium carbonate	17.81 g	280 mmol/L
Water	to 600 mL	
<b>Immediately prior to use:</b>		
Formaldehyde solution (40%)	300 µL	0.0002% v/v
<b>Note:</b>	Use immediately.	

**C.10 Solutions for Western blotting****Amido black stain****Solution 44**

To make ~50 millilitres	Amount	Final concentration
Amido black	50 mg	0.1% w/v
Methanol	20 mL	40% v/v
Acetic acid	5 mL	10% v/v
Water	25 mL	50% v/v
<b>Note:</b>	Amido black powder is intensely coloured. Even minor spillage should be cleaned first by a dry process (brush, vacuum, tissues), and then with destaining solution {Solution 45}.	
<b>Storage:</b>	Ambient temperature.	

**Amido black destain****Solution 45**

To make ~500 millilitres	Amount	Final concentration
Methanol	200 mL	40% v/v
Acetic acid	50 mL	10% v/v
Water	250 mL	50% v/v
<b>Storage:</b>	Ambient temperature.	

**Blocking solution****Solution 46**

To make ~10 millilitres	Amount	Final concentration
Non-fat milk powder	1.0 g	~10% w/v
TTBS {Solution 49}	9 mL	
<b>Note:</b>	Always use fresh solution.	

**Buffer for electrotransfer of protein to PVDF membrane****Solution 47**

To make 1 litre	Amount	Final concentration
Tris base	3.03 g	25 mmol/L
Glycine	14.4 g	192 mmol/L
Water	to 1.00 L	
<b>Note:</b>	pH ~8.3 – 8.4	
<b>Storage:</b>	Ambient temperature.	

## Membrane stripping buffer

Solution 48

To make 1 litre	Amount	Final concentration
Tris base	9.85 g	62.5 mmol/L
Water	to 900 mL	
Hydrochloric acid (1 – 6 mol/L)		to pH 6.7
SDS	20.0 g	2.0% w/v
2-mercaptoethanol	7.0 mL	100 mmol/L
Water	to 1.0 L	
<b>Note:</b>	May precipitate during storage. Warm to re-dissolve.	
<b>Storage:</b>	4 °C.	

## Tween/Tris-buffered saline (pH 7.5)

Solution 49

To make 1 litre	Amount	Final concentration
Sodium chloride	9.00 g	154 mmol/L
Tris base	12.11 g	100 mmol/L
Water	to 950 mL	
Hydrochloric acid (1 – 6 mol/L)		to pH 7.5
Water	to 1.0 L	
Tween-20 detergent	nil, 500 $\mu$ L, or 1.00 mL	nil, 0.05% v/v, or 0.1% v/v
<b>Storage:</b>	Ambient temperature, or 4 °C if recurrent microbial growth occurs.	

## C.11 PCR composition

Solution 50

For each 25 $\mu$ L reaction	Amount	Final concentration
5x 'Q' PCR enhancer *	5.00 $\mu$ L	1 x
10x PCR buffer *	2.50 $\mu$ L	1 x
Magnesium chloride (25 mmol/L) *	1.50 $\mu$ L	3.00 mmol/L
Mixed dNTPs (5 mmol/L each dNTP)	500 nL	100 $\mu$ mol/L each dNTP
Taq enzyme *	100 nL	0.5 units
Sense or forward primer (20 $\mu$ mol/L)	250 nL	200 nmol/L
Antisense or reverse primer (20 $\mu$ mol/L)	250 nL	200 nmol/L
DNA-free water	12.9 $\mu$ L	
Template DNA (100 ng/ $\mu$ L)	2.00 $\mu$ L	200 ng
<b>Note:</b>	Items marked ** are from the Qiagen Taq DNA polymerase kit {Table E-2}.	





# Additional solutions (V3)

## C.12 General solutions

### $\beta$ -glycerophosphate solution (200 mmol/L)

Solution 51

To make 100 millilitres	Amount	Final concentration
$\beta$ -glycerophosphate (disodium salt)	4.32 g	200 mmol/L
Water	~90 mL	
<b>Dissolve.</b>		
Water	to 100 mL	
<b>Storage:</b>	Ambient temperature.	

### Dithiothreitol (500 mmol/L)

Solution 52

To make 50 millilitres	Amount	Final concentration
Dithiothreitol (DTT)	3.86 g	500 mmol/L
Water	~45 mL	
<b>Dissolve.</b>		
Water	to 50.0 mL	
<b>Storage:</b>	4 C.	

### PIPES (500 mmol/L, pH 6.9)

Solution 53

To make 20 millilitres	Amount	Final concentration
Piperazine-N,N'-bis(2-ethanesulfonic acid) (dipotassium salt) (PIPES)	3.79 g	500 mmol/L
Water	~18 mL	
<b>Dissolve.</b>		
Hydrochloric acid/Sodium hydroxide (1 – 6 mol/L)		to pH 6.9
Water	to 20 mL	
<b>Further treatment:</b>	Filter sterilise.	
<b>Storage:</b>	Ambient temperature.	

### Saline (0.9% w/v, sterile)

Solution 54

To make 400 millilitres	Amount	Final concentration
Sodium chloride	3.6 g	0.9% w/v
Water	~350 mL	
<b>Dissolve.</b>		
Water	to 400 mL	
<b>Further treatment:</b>	Autoclave to sterilise.	
<b>Storage:</b>	Ambient temperature.	

### Sodium acetate (3.0 mol/L, pH 5.5)

Solution 55

To make 75 millilitres	Amount	Final concentration
Sodium acetate	18.46 g	3.0 mol/L
Water	~60 mL	
<b>Dissolve.</b>		
Acetic acid, glacial		to pH 5.5
Water	to 75 mL	
<b>Further treatment:</b>	Autoclave to sterilise.	
<b>Storage:</b>	Ambient temperature.	

### Sodium chloride (5.0 mol/L)

Solution 56

To make 100 millilitres	Amount	Final concentration
Sodium chloride	27.7 g	5.0 mol/L
Water	~90 mL	
<b>Dissolve.</b>		
Water	to 100 mL	
<b>Storage:</b>	Ambient temperature.	

**Sodium hydroxide (10.0 mol/L)****Solution 57**

To make 100 millilitres	Amount	Final concentration
Sodium hydroxide	40.0 g	10.0 mol/L
Water	~90 mL	
<b>Dissolve.</b>		
Water	to 100 mL	
<b>Storage:</b>	Ambient temperature.	

**Sodium hydroxide (1.0 mol/L)****Solution 58**

To make 100 millilitres	Amount	Final concentration
Sodium hydroxide solution (10.0 mol/L) {Solution 57}	10.0 mL	1.0 mol/L
Water	to 100.0 mL	
<b>Storage:</b>	Ambient temperature.	

**Tris buffer (1.0 mol/L, pH 8.0)****Solution 59**

To make 200 millilitres	Amount	Final concentration
Tris base	24.23 g	1.0 mol/L
Water	to 180 mL	
Hydrochloric acid (1 – 6 mol/L)		pH 8.0
Water	to 100 mL	
<b>Storage:</b>	Ambient temperature.	

**Tris-buffered saline (pH 7.50, 5x)****Solution 60**

To make 1 litre	Amount	Final concentration
Sodium chloride	45.00 g	770 mmol/L
Tris base	60.55 g	500 mmol/L
Water	to ~900 mL	
Hydrochloric acid (1 – 6 mol/L)		to pH 7.50
Water	to 1.0 L	
<b>Storage:</b>	Ambient temperature.	

**Tris-buffered saline (pH 7.50)****Solution 61**

To make 2.0 litres	Amount	Final concentration
Tris-buffered saline (pH 7.50, 5x) {Solution 60}	400 mL	1x
Water	to 2.0 L	
<b>Storage:</b>	Ambient temperature.	

**C.13 Solutions for cell culture****αMEM/10% FCS (no antibiotics)****Solution 62**

To make ~440 millilitres	Amount	Final concentration
αMEM (sterile)	400 mL	
FCS	44.0 mL	10.0% v/v
<b>Storage:</b>	4 °C. Maintain sterility. Check for turbidity arising from microbial growth before each use.	

**αMEM/10% FCS/ciprofloxacin****Solution 63**

To make ~440 millilitres	Amount	Final concentration
Alpha MEM (sterile)	400 mL	
FCS	44.0 mL	10.0% v/v
Ciprofloxacin (2 g/L) {E.16}	4 mL	~20 mg/L
<b>Storage:</b>	4 °C. Maintain sterility.	



## C.14 Solutions for cell fixation

### Buffered formaldehyde fixative

Solution 64

**Caution:** *Paraformaldehyde is toxic by inhalation. Suitable handling procedures must be used.*

To make 50 millilitres	Amount	Final concentration
Paraformaldehyde	1.75 g	3.5% w/v
Water	~40 mL	
Sodium hydroxide (10.0 mol/L) {Solution 57}	20 $\mu$ L	
<b>Dissolve with gentle heat and stirring</b>		
PBS (10x, pH 7.4) {Solution 65}	5.0 mL	1x
PIPES (500 mmol/L, pH 6.9) {Solution 53}	2.0 mL	10 mmol/L
Hydrochloric acid (1 – 6 mol/L)		to pH 6.6 – 6.9
<b>Further treatment:</b>	Filter sterilise and divide into 2 mL portions.	
<b>Storage:</b>	–20 °C. Discard any unused fixative after three freeze/thaw cycles.	

### Phosphate-buffered saline (10x, pH 7.4)

Solution 65

To make 500 millilitres	Amount	Final concentration
Sodium chloride	40.0 g	1.37 mol/L
Potassium chloride	1.0 g	149 mmol/L
Potassium phosphate (monobasic)	1.0 g	277 mmol/L
Sodium phosphate (dibasic)	4.6 g	81 mmol/L
Hydrochloric acid/sodium hydroxide (1 – 6 mol/L)		to pH 7.4
Water	to 500 mL	
<b>Further treatment:</b>	Autoclave or filter sterilise.	
<b>Storage:</b>	Ambient temperature. Maintain sterility.	

## C.15 Solutions for extraction

### Protein lysis and extraction buffer

Solution 66

To make 100 millilitres	Amount	Final concentration
Tris buffer (1.0 mol/L, pH 8.0) {Solution 59}	5.0 mL	50 mmol/L
Sodium chloride (5.0 mol/L) {Solution 56}	2.4 mL	120 mmol/L
Sodium fluoride	83.98 mg	20 mmol/L
$\beta$ -glycerophosphate (200 mmol/L) {Solution 51}	10 mL	20 mmol/L
EDTA (500 mmol/L, pH 8.0) {Solution 3}	200 $\mu$ L	1 mmol/L
EGTA	228.24 mg	6 mmol/L
NP40 detergent	1 mL	1% v/v
Dithiothreitol (500 mmol/L) {Solution 52}	200 $\mu$ L	1 mmol/L
Sodium orthovanadate (activated) (100 mmol/L, pH 10) {Method 38}	250 $\mu$ L	250 $\mu$ mol/L
Water	to 100 mL	
<b>Further treatment:</b>	Filter sterilise.	
<b>Storage:</b>	4 °C	

## C.16 Solutions for storage

### PBS/antibiotics

Solution 67

To make ~400 millilitres	Amount	Final concentration
Phosphate-buffered saline (pH 7.4) {Solution 6}	400 mL	
Antibiotic mixture {Solution 12}	4.0 mL	
<b>Storage:</b>	4 °C. Maintain sterility.	

## C.17 Solutions for quantitation

### Copper sulphate (4.0 % w/v)

Solution 68

To make 100 millilitres	Amount	Final concentration
Copper (II) sulphate pentahydrate	4.0 g	4.0% w/v
Water	to ~90 mL	
<b>Dissolve.</b>		
Water	to 100 mL	
<b>Storage:</b>	Ambient temperature.	

**C.18 Solutions for immunofluorescent labelling****Hoechst 33342 (1.0 g/L)****Solution 69**

To make 50 millilitres	Amount	Final concentration
Hoechst 33342	50.0 mg	1.0 g/L
Saline (0.9% w/v, sterile) {Solution 54}	to 50.0 mL	
<b>Dissolve.</b>		
<b>Storage:</b>	4 °C	

**Hoechst 33342 (10 mg/L)****Solution 70**

To make 50 millilitres	Amount	Final concentration
Hoechst 33342 (1.0 g/L) {Solution 69}	500 µL	10 mg/L
Saline (0.9% w/v, sterile) {Solution 54}	to 50.0 mL	
<b>Storage:</b>	4 °C	

**KB buffer (10x)****Solution 71**

To make 200 millilitres	Amount	Final concentration
Tris base	2.42 g	100 mmol/L
Sodium chloride	17.53 g	1.5 mol/L
Water	~180 mL	
Hydrochloric acid (1 – 6 mol/L)		to pH 7.5
BSA	2.0 g	1.0% w/v
Water	to 200 mL	
<b>Storage:</b>	4 °C	

**KB buffer****Solution 72**

To make 50 millilitres	Amount	Final concentration
KB buffer (10x) {Solution 71}	5 mL	1x
Water	to 50 mL	
<b>Storage:</b>	4 °C	

**KB buffer/Triton X-100 (10x)****Solution 73**

To make 100 millilitres	Amount	Final concentration
KB buffer (10x) {Solution 71}	10 mL	1x
Triton X-100	2 mL	2.0% v/v
Water	to 100 mL	
<b>Storage:</b>	4 °C	

**KB buffer/Triton X-100****Solution 74**

To make 10 millilitres	Amount	Final concentration
KB buffer/Triton X-100 (10x) {Solution 73}	1 mL	1x
Water	to 10 mL	
<b>Storage:</b>	4 °C	

**Mixed fluorescent secondary antibodies****Solution 75**

To make 1 millilitre	Amount	Final concentration
KB buffer {Solution 72}	996 µL	
Alexa Fluor 488 F(ab'), fragment of goat anti-mouse IgG (H+L) {E.12}	2 µL	4 mg/L
Alexa Fluor 594 goat anti-rabbit IgG (H+L), highly cross-adsorbed {E.12}	2 µL	4 mg/L
<b>Storage:</b>	4 °C. Protect from light.	

**Mixed tubulin and pericentrin primary antibodies****Solution 76**

To make 1 millilitre	Amount	Final concentration
KB buffer {Solution 72}	997 µL	
Mouse monoclonal anti-bovine $\alpha$ -tubulin IgG {E.12}	2 µL	400 µg/L
Rabbit polyclonal anti-human pericentrin IgG {E.12}	1 µL	1 mg/L
<b>Storage:</b>	4 °C	



## C.19 Solutions for protein electrophoresis

### Separating gel solution for SDS-PAGE analysis of pRB

Solution 77

**Caution:** *Acrylamide is a potent neurotoxin. Suitable handling procedures must be used.*

To make 8.8 millilitres (Sufficient for 2 gels)	5% v/v gel
Tris-SDS buffer (pH 8.8, 4 x) {Solution 34}	2.2 mL
Bis-acrylamide (37.5:1, 40%)	1.1 mL
Water	5.5 mL
<b>Mix gently and degas.</b>	
<b>Immediately prior to pouring:</b>	
TEMED	20 $\mu$ L
APS (25% w/v) {Solution 35}	20 $\mu$ L
<b>Mix gently and pour gels.</b>	

## C.20 Solutions for Western blotting

### Buffer for electrotransfer to nitrocellulose membrane

Solution 78

To make 2.0 litres	Amount	Final concentration
Tris base	6.06 g	25 mmol/L
Glycine	28.8 g	192 mmol/L
Methanol	to 400 mL	20% v/v
Water	to 2.0 L	
<b>Note:</b>	pH ~8.3 – 8.4	
<b>Storage:</b>	Ambient temperature.	

## C.21 PCR composition

Solution 79

For each 25 $\mu$ L reaction	Amount	Final concentration
5x 'Q' PCR enhancer *	5.00 $\mu$ L	1 x
10x PCR buffer *	2.50 $\mu$ L	1 x
Magnesium chloride (25 mmol/L) *	1.50 $\mu$ L	3.00 mmol/L
BSA (10 g/L)	1.00 $\mu$ L	400 mg/L
Mixed dNTPs (5 mmol/L each dNTP)	500 nL	100 $\mu$ mol/L each dNTP
Taq enzyme *	100 nL	0.5 units
Sense or forward primer (20 $\mu$ mol/L)	250 nL	200 nmol/L
Antisense or reverse primer (20 $\mu$ mol/L)	250 nL	200 nmol/L
DNA-free water	11.9 $\mu$ L	
Template DNA (100 mg/L)	2.00 $\mu$ L	200 ng
<b>Note:</b>	Items marked '*' are from the Qiagen Taq DNA polymerase kit {Table E-2}.	



## D

## PCR primers

Product	Primer sequences (5' → 3')	Size	Reference
D9S274	TTG CTG TTC AAG TGA TCC TT TAC CTC ATG GCA ATT TCT TC	~141	RH13604
D9S156	ATC ACT TTT AAC TGA GGC GG AGA TGG TGG TGA ATA GAG GG	~134	RH15022
D9S157	CAT TTC ATC TGG TAG ACC CA TTT GAT TGG CTG GAA GTA GA	~205	RH13217
D9S162	TGA CCA GTT AAG GTT CCT TTC ATT CCC ACA ACA AAT CTC CT	~181	RH13250
D9S1749	AGG AGA GGG TAC GCT TGC AA TAC AGG GTG CGG GTG CAG ATA A	~140	GDB:595876
CDKN2A exon 3	CCG GTA GGG ACG GCA AGA GA CTG TAG GAC C <sup>C</sup> T CGG TGA CTG ATG A	169	Hussussian et al. <sup>559</sup>
CDKN2A exon 2C	TGG ACG TGC GCG ATG C GGA AGC TCT CAG GGT ACA AAT TC	189	Hussussian et al. <sup>559</sup>
CDKN2A exon 2B	AGC CCA ACT GCG CCG AC CCA GGT CCA CGG GCA GA	147	Hussussian et al. <sup>559</sup>
CDKN2A exon 2A	AGC TTC CTT TCC GTC ATG C GCA GCA CCA CCA CCG TG	203	Hussussian et al. <sup>559</sup>
CDKN2A exon 1	GGG AGC AGC ATG GAG CCG AGT CGC CCG CCA TCC CCT	203	Hussussian et al. <sup>559</sup>
D9S974	GAG CCT GGT CTG GAT CAT AA AAG CTT ACA GAA CCA GAC AG	~200	GDB:434853
D9S942	GCA AGA TTC CAA ACA GTA CTC ATC CTG CGG AAA CCA TT	~115	GDB:370738
D9S1748	CAC CTC AGA AGT CAG TGA GT GTG CTT GAA ATA CAC CTT TCC	~140	GDB:595589
CDKN2A exon 1β	TCC CAG TCT GCA GTT AAG G GTC TAA GTC GTT GTA ACC CG	440	Mao et al. <sup>839</sup>
CDKN2B exon 2	GGC CGG CAT CTC CCA TAC CTG TGT GGG CGG CTG GGG AAC CTG	345	Orlow et al. <sup>981</sup>
CDKN2B exon 1	AAG AGT GTC GTT AAG TTT ACG ACA TCG GCG ATC TAG GTT CCA	315	Orlow et al. <sup>981</sup>
D9S171	AGC TAA GTG AAC CTC ATC TCT GTC T ACC CTA GCA CTG ATG GTA TAG TCT	~159	RH15165
D9S161	GCT GCA TAA CAA ATT ACC ACA ATC CCC GGA AAC AGA TAA TA	~104	RH13232
D9S1853	GAT CCA GCC TCA CTG AA TTG GGC ATA GAA TTT TTA CTT T	~253	RH15594
HBB	GAA GAG CCA AGG ACA GGT AC CAA CTT CAT CCA CGT TCA CC	268	Dieffenbach <sup>273</sup>

Microsatellite product sizes are representative only as by their nature they are variable. It should be noted that the reverse primer for exon 3 of *CDKN2A* differs from the published sequence<sup>1181</sup> at position 11, highlighted in the table entry, with a C rather than a T present in the primer. No reason for this is given in the source paper, nor can any be reasonably inferred from primer stability analysis. In addition, the published sequence data predict 203 bp products for *CDKN2A* exons 1 and 2A, rather than the 204 bp indicated by Hussussian et al.<sup>559</sup>. These anomalies have no bearing on the success of amplification using these primers. An 'RH' reference denotes an entry in the Radiation Hybrid Database (<http://www.ebi.ac.uk/RHdb>), and a 'GDB' reference, an entry in the Genome Database (<http://www.gdb.org>). Primers were supplied by Invitrogen {E.8}.

Table D-1: PCR primers, products, and references





# E Apparatus, materials, and suppliers

## E.1 Apparatus

Item	Manufacturer	Model
Computer (principal)	Apple Computer	iMac DV Special Edition
DNA sequencer	ABI	Prism 377
Electronic particle counter	Coulter Electronics	ZF
Electrophoresis (agarose)	OWL	DNA sub-cell
Electrophoresis (PAGE)	Bio-Rad	Mini-PROTEAN II
Flow Cytometer	Becton Dickinson	FACScan
Gel drier	Bio-Rad	583
Gel imaging	Kodak	EDAS120
PCR thermal cycler	MJ Research	PTC100
Western blotting	Bio-Rad	Mini-PROTEAN II transfer module

Table E-1: Apparatus

## E.2 Commercial kits

Name	Use	From	ID
ECL™ Western Blotting Detection Reagents	Western blotting	Amersham	RPN2209
Taq DNA polymerase	PCR	Qiagen	201205
Vectastain ABC Elite Rabbit IgG	Western blotting	Vector Laboratories	PK6101
Wizard® PCR Preps DNA Purification System	DNA sequencing	Promega	A7170

Table E-2: Commercial kits

## E.3 Antibodies

Antibody	From	ID	Supplied @	Dilution	Used @	Incubation time
HRP-conjugated goat anti-mouse IgG	Pharmingen	554002	n.a.	1:250	n.a.	1 h
Mouse anti-human ARF <sup>CDKN2A</sup>	Neomarkers	MS-850-P1ABX	1 g/L	1:500	500 µg/L	2 h
Mouse anti-human p15 <sup>CDKN2B</sup>	Oncogene	NA33	100 mg/L	1:200	500 µg/L	1 h
Mouse anti-human p16 <sup>CDKN2A</sup>	Pharmingen	13381A	500 mg/L	1:1 000	500 µg/L	1 h
Rabbit anti-human pRB <sup>RB1</sup>	Santa Cruz	Rb (C-15) sc-50	200 mg/L	1:1 000	200 µg/L	1 h

Table E-3: Antibodies

## E.4 Enzymes

Enzyme	Use	From	ID
<i>Bst</i> N1	CDKN2A exon 2 PCR product cleavage prior to SSCP	New England Biolabs	R0168S
Proteinase K	Digestion of protein during genomic DNA extraction	Roche	1 000 144
RNase A	RNA digestion prior to flow cytometric DNA analysis	Boehringer Mannheim	109134
Trypsin	Detaching adherent cells during passaging	Difco	215320

Table E-4: Enzymes

## E.5 Standards

Standard	From	ID
Biotinylated protein MW standards	Bio-Rad	161-0319
DNA electrophoresis standard	New England Biolabs	N3231S
Dye-conjugated protein MW standards	Bio-Rad	161-0318
Positive control lysate for ARF antibody	Neomarkers	MS-850-PCL

Table E-5: Standards

## E.6 General reagents

Name	Formula	MW (d)	From
$\alpha$ MEM	n.a.	n.a.	Invitrogen
Acetic acid (glacial)	CH <sub>3</sub> COOH	60.05 (1.05 kg/L)	Scharlau
Acrylamide : bis-acrylamide (37.5:1)	n.a.	n.a.	Bio-Rad
Agarose	n.a.	n.a.	BioWhittaker
Amido black	n.a.	n.a.	Sigma
Ammonium acetate	CH <sub>3</sub> COONH <sub>4</sub>	77.08	BDH
Aprotinin	n.a.	n.a.	Sigma
APS	(NH <sub>4</sub> ) <sub>2</sub> S <sub>2</sub> O <sub>8</sub>	228.2	Sigma/Serva
5-aza-2'-deoxycytidine	C <sub>8</sub> H <sub>12</sub> N <sub>4</sub> O <sub>4</sub>	228.2	Sigma
Boric acid	H <sub>3</sub> BO <sub>3</sub>	61.83	Scharlau
Bromophenol blue	C <sub>19</sub> H <sub>9</sub> Br <sub>4</sub> O <sub>5</sub> SNa	691.9	Sigma
Carbon dioxide (5% v/v)	CO <sub>2</sub> /air	n.a.	BOC Gases
Chloroform	CHCl <sub>3</sub>	119.4 (1.49 kg/L)	BDH
DMSO	(CH <sub>3</sub> ) <sub>2</sub> SO	78.13 (1.10 kg/L)	Riedel de Haën
dNTPs	n.a.	n.a.	Boehringer Mannheim
EDTA (disodium salt)	C <sub>10</sub> H <sub>14</sub> N <sub>2</sub> O <sub>8</sub> Na <sub>2</sub> •2H <sub>2</sub> O	372.2	AppliChem
EDTA (tetrasodium salt)	C <sub>10</sub> H <sub>12</sub> N <sub>2</sub> O <sub>8</sub> Na <sub>4</sub> •2H <sub>2</sub> O	380.2	AppliChem
Ethanol	CH <sub>3</sub> CH <sub>2</sub> OH	46.07 (0.79 kg/L)	Nufarm
Ethidium bromide	C <sub>21</sub> H <sub>20</sub> N <sub>3</sub> Br	394.3	Sigma
FCS	n.a.	n.a.	Invitrogen
Formaldehyde (~37% solution)	CH <sub>2</sub> O	n.a.	BDH
Formamide	CH <sub>3</sub> NO	45.04 (1.13 kg/L)	BDH
Glycerol	CH <sub>2</sub> OHCHOHCH <sub>2</sub> OH	(d=1.25 kg/L)	Merck
$\beta$ -glycerophosphate (disodium salt)	(HOCH <sub>2</sub> ) <sub>2</sub> CHOP(O)(ONa) <sub>2</sub>	216	Sigma
Glycine	CH <sub>2</sub> NH <sub>2</sub> COOH	75.07	Scharlau
Guanidine hydrochloride	CH <sub>5</sub> N <sub>3</sub> •HCl	95.53	ICN Biomedicals
Hydrochloric acid	HCl	36.46	Ajax Chemicals
Isopropanol	CH <sub>3</sub> CHOHCH <sub>3</sub>	60.1 (0.78 kg/L)	LabScan
Leupeptin	n.a.	n.a.	Sigma
Methanol	CH <sub>3</sub> OH	32.04 (0.79 kg/L)	LabScan
2-mercaptoethanol	CH <sub>2</sub> OHCH <sub>2</sub> SH	78.13 (1.11 kg/L)	Riedel de Haën
Nitric acid	HNO <sub>3</sub>	n.a.	Ajax Chemicals
Non-fat milk powder	n.a.	n.a.	Anchor
Paclitaxel	n.a.	n.a.	Bristol-Myers Squibb
Penicillin-G	n.a.	n.a.	Sigma
PI	C <sub>27</sub> H <sub>34</sub> N <sub>4</sub> I <sub>2</sub>	668.4	Sigma
PMSF	C <sub>6</sub> H <sub>5</sub> CH <sub>2</sub> SO <sub>2</sub> F	174.2	Sigma
Potassium chloride	KCl	74.55	Riedel de Haën
Potassium dichromate	K <sub>2</sub> Cr <sub>2</sub> O <sub>7</sub>	294.2	Sigma
Potassium phosphate (monobasic)	KH <sub>2</sub> PO <sub>4</sub>	136.1	Ajax Chemicals
SDS	C <sub>12</sub> H <sub>25</sub> O <sub>4</sub> SNa	288.4	Serva
Silver nitrate	AgNO <sub>3</sub>	169.9	Scientific Supplies
Sodium carbonate	Na <sub>2</sub> CO <sub>3</sub>	106.0	Scharlau
Sodium chloride	NaCl	58.44	Scharlau/BDH
Sodium citrate (trisodium salt)	C <sub>6</sub> H <sub>5</sub> Na <sub>3</sub> O <sub>7</sub> •2H <sub>2</sub> O	294.1	Riedel de Haën
Sodium hydroxide	NaOH	40.00	Scharlau
Sodium phosphate (dibasic)	Na <sub>2</sub> HPO <sub>4</sub> •2H <sub>2</sub> O	156.01	BDH
Sodium sarcosyl	C <sub>15</sub> H <sub>28</sub> NO <sub>3</sub> Na	293.4	Sigma
Streptomycin sulphate	n.a.	n.a.	AppliChem
TEMED	(CH <sub>3</sub> ) <sub>2</sub> NCH <sub>2</sub> CH <sub>2</sub> N(CH <sub>3</sub> ) <sub>2</sub>	116.2 (0.77 kg/L)	Serva
Tris base	C <sub>4</sub> H <sub>11</sub> NO <sub>3</sub>	121.1	ICN Biomedicals
Tween-20 detergent	n.a.	n.a.	Serva
Xylene cyanol FF	C <sub>25</sub> H <sub>27</sub> N <sub>2</sub> O <sub>6</sub> S <sub>2</sub> Na	538.6	Sigma

Table E-6: General reagents

## E.7 Sundry materials

Item	ID	From
Autoradiography film	X-OMAT AR5	Kodak
Disposable syringe filters	Acrodisc	Pall Corporation
PCR primers	n.a.	Invitrogen
Plasticware	various	Falcon, Nunc
PVDF membrane	Immobilon-P	Millipore

Table E-7: Sundries



## E.8 Supplier data

Manufacturer or agent	Contact information
Adobe	<a href="http://www.adobe.com/">http://www.adobe.com/</a>
Ajax Chemicals	See APS Chemicals
Aldus	Now defunct: acquired by Adobe
Amersham Pharmacia Biotech	See AMRAD Pharmacia Biotech Ltd
AMRAD Pharmacia Biotech Ltd	Tel: 0800 733 893
Anchor	Tel: 09 296 3700 <a href="http://anchor.co.nz/">http://anchor.co.nz/</a>
Apple Computer	See Renaissance
AppliChem	See Scientific Supplies Ltd
Applied Biosystems	Tel: 0800 446 416 <a href="http://home.appliedbiosystems.com/">http://home.appliedbiosystems.com/</a>
APS Chemicals	<a href="http://www.apschem.com/">http://www.apschem.com/</a>
BDH Laboratory Supplies	See Biolab Ltd
Beckman Coulter	Tel: 0800 442 346
Becton Dickinson	Tel: 0800 572 468 <a href="http://www.bd.com/">http://www.bd.com/</a>
Biolab Ltd	Tel: 0800 933 966 <a href="http://www.biolab.co.nz/">http://www.biolab.co.nz/</a>
Bio-Rad Laboratories Pty Ltd	Tel: 09 415 2280 <a href="http://www.bio-rad.com/">http://www.bio-rad.com/</a>
BioWhittaker Molecular Applications	See Biolab Ltd
BOC Gases	Tel: 09 525 5600
Boehringer Mannheim	Tel: 0800 652 634
Coulter Electronics	See Beckman Coulter
Dade Behring	Tel: 0800 807 982
Difco	See Becton Dickinson
DNASTAR	<a href="http://www.dnastar.com/">http://www.dnastar.com/</a>
Edward Keller (NZ) Ltd	Tel: 09 414 5406
Falcon	See Becton Dickinson
G. A. Charters	Email: <a href="mailto:g.charters@auckland.ac.nz">g.charters@auckland.ac.nz</a>
Global Science and Technology Ltd	Tel: 09 443 5867
ICN Biomedicals	See Scientific Supplies Ltd
Immuno Chemical Products	Tel: 09 815 0624
In Vitro Technologies (NZ)	Tel: 09 573 0770 <a href="http://www.invitro.co.nz/">http://www.invitro.co.nz/</a>
Invitrogen	Tel: 09 579 3024 <a href="http://www.invitrogen.com/">http://www.invitrogen.com/</a>
Kodak	For gel imaging apparatus: See Invitrogen For X-ray film: See Radiographic Supplies Ltd
LabScan	See Scientific Supplies Ltd.
Merck (NZ) Ltd	Tel: 0800 426 252
Microsoft	<a href="http://www.microsoft.com/">http://www.microsoft.com/</a>
Millipore	See Biolab Ltd
MJ Research	See Biolab Ltd
Neomarkers	See Edward Keller (NZ) Ltd <a href="http://www.neomarkers.com/">http://www.neomarkers.com/</a>
New England Biolabs	See Biolab Ltd <a href="http://www.neb.com/">http://www.neb.com/</a>
Nufarm	Tel: 09 415 1750
Nunc	See Invitrogen
Oncogene	See Merck (NZ) Ltd <a href="http://www.apoptosis.com/">http://www.apoptosis.com/</a>
OWL	See Biolab Ltd
Pall Corporation	See Invitrogen
Pharmingen	See Becton Dickinson <a href="http://www.pharmingen.com/">http://www.pharmingen.com</a>
Promega	See Dade Behring
Qiagen	See Biolab Ltd
Radiographic Supplies Ltd	Tel: 0800 737 337
Renaissance	<a href="http://www.apple.co.nz/">http://www.apple.co.nz/</a>
Riedel-de Haën	See Scientific Supplies Ltd
Roche	Tel: 0800 652 634
Santa Cruz Biotechnology	See Global Science and Technology Ltd.
Scharlau	See Scientific Supplies Ltd
Scientific Supplies Ltd	Tel: 09 274 7579
Serva	See Scientific Supplies Ltd
Sigma	See Biolab Ltd
Thorsten Lemke	<a href="http://www.lemkesoft.de/">http://www.lemkesoft.de/</a>
Vector Laboratories	See In Vitro Technologies (NZ) <a href="http://www.vectorlabs.com/">http://www.vectorlabs.com/</a>
Verity House	See Becton Dickinson

Table E-8: Supplier data

**E.9 Software**

Software	Platform	Version	From	GAC rating
1D	Macintosh	2.0	Kodak	C+
Acrobat	Macintosh	5.0	Adobe	B-
Cellquest	Macintosh	3.1	Verity House	C-
Cn3D	Macintosh	3.0	NIH	A-
Editseq	Macintosh	3.8.7	DNASTAR Inc.	C
Editview	Macintosh	1.0.1	Applied Biosystems	C
Ghostscript	Macintosh	5.50	Aladdin	B
GraphicConverter	Macintosh	4.0.9	Thorsten Lemke	A+
Hypercard	Macintosh	2.4.1	Apple Computer	A
Intellidraw	Macintosh	1.1/2.01	Aldus/Adobe	A
Internet Explorer	Macintosh	5.0/5.1	Microsoft	C+
MacOS	Macintosh	10.2.2/9.2.2	Apple Computer	A-/A-
MapDraw	Macintosh	3.07	DNASTAR Inc.	C
Megalign	Macintosh	3.0.7	DNASTAR Inc.	C
Modfit LT	Macintosh	1.01	Verity House	E+
Molecular database	Macintosh	1.0	G. A. Charters	C
Office	Macintosh	98	Microsoft	C+
Photoshop	Macintosh	5.0	Adobe	A+
Referee	Macintosh	1.2	G. A. Charters	B-

The GAC rating represents the overall quality of the software as assessed by the author.  
A+ = essentially faultless; E = virtually useless.

**Table E-9: Software**



# Additional apparatus, materials, etc. (V3)

## E.10 Apparatus

Item	Manufacturer	Model
Computer (principal)	Apple Computer {E.8}	iMac G5 (iSight) 2.1 GHz 20"
Confocal laser scanning microscope	Leica	TCS SP2
Fluorescence microscope	Zeiss	Axioskop 2
Fluorescence microscope camera	Sony	DXC-S500
Fluorometer	Bio-Rad {E.8}	Versafluor
Gradient PCR thermal cycler	Bio-Rad {E.8}	iCycler
Luminescent image analyser	Fujifilm	LAS-3000
Nanodrop spectrophotometer	NanoDrop Technologies	ND-1000
Spectrophotometer (plate)	Biotek Instruments	ELx808

Table E-10: Additional apparatus (V3)

## E.11 Commercial kits

Name	Use	From	ID
DNA quantitation kit	DNA quantitation	Bio-Rad {E.8}	170-2480
Mycoplasma PCR ELISA detection kit	Mycoplasma detection	Roche {E.8}	11 663 925 910

Table E-11: Additional commercial kits (V3)

## E.12 Antibodies

Antibody	From	ID	Supplied @	Dilution	Used @	Incubation time
Alexa Fluor 488 F(ab') <sub>2</sub> fragment of goat anti-mouse IgG (H+L)	Molecular Probes	A11017	2 g/L	1:500	4 mg/L	30 min
Alexa Fluor 594 goat anti-rabbit IgG (H+L), highly cross-adsorbed	Molecular Probes	A11037	2 g/L	1:500	4 mg/L	30 min
Anti-GAPDH Mouse mAb (6C5)	Calbiochem	CB1001	8.6 g/L	1:5 000	1.7 mg/L	1 h
Anti-p16 (Ab-1) Mouse mAb (DCS-50.1/H4)	Calbiochem	NA29	100 mg/L	1:100	1 mg/L	1 h
Anti-Rb (Ab-11), Human (Mouse)	Calbiochem	OP136	100 mg/L	1:100	1 mg/L	1 h
HRP-conjugated rabbit polyclonal anti-mouse IgG (H+L)	Abcam	ab6728	2 g/L	1:5 000	400 µg/L	1 h
Mouse monoclonal anti-bovine α-tubulin IgG <sub>1</sub>	Molecular Probes	A11126	50 µg	–	400 µg/L	1 h
Rabbit polyclonal anti-human pericentrin IgG	Abcam	ab4448	500 mg/L	1:500	1 mg/L	1 h

Table E-12: Additional antibodies (V3)

## E.13 Enzyme

Enzyme	Use	From	ID
RNase, DNase-free	Removal of RNA from genomic DNA extracts	Roche {E.8}	11119915001

Table E-13: Additional enzyme (V3)

## E.14 Standards

Standard	From	ID
1Kb Plus DNA ladder	Invitrogen {E.8}	10787-018
BSA standard (2.00 mg/mL)	Pierce	23209
Precision plus kaleidoscope protein standards	Bio-Rad {E.8}	161-0375
Track-It 50 bp DNA ladder (not recommended)	Invitrogen {E.8}	10488-043

Table E-14: Additional standards (V3)

## E.15 General reagents

Name	Formula	MW (d)	From
BCA (Bicinchoninic acid) (2-(4-carboxyquinolin-2-yl)quinoline-4-carboxylic acid)	$(\text{HO}_2\text{CC}_9\text{H}_5\text{N})_2$	344.33	Sigma {E.8}
Bovine serum albumin (PCR additive)	n.a.	n.a.	New England Biolabs {E.8}
Copper (II) sulphate pentahydrate	$\text{CuSO}_4 \cdot 5\text{H}_2\text{O}$	249.69	Sigma {E.8}
Dithiothreitol	$\text{C}_4\text{H}_{10}\text{O}_2\text{S}_2$	154.25	Sigma {E.8}
EGTA (Ethylene glycol-bis(2-aminoethyl ether)-N,N,N',N'-tetraacetic acid)	$\text{C}_{14}\text{H}_{20}\text{N}_2\text{O}_{10}$	380.35	Sigma {E.8}
Hoechst 33342 (2'-(4-Ethoxyphenyl)-5-(4-methyl-1-piperazinyl)-2,5'-bis-1H-benzimidazole • 3HCl)	$\text{C}_{27}\text{H}_{28}\text{N}_6\text{O} \cdot 3\text{HCl}$	562.0	Scientific Supplies Ltd {E.8}
NP-40 (10 % w/v)	n.a.	n.a.	Roche {E.8}
Paraformaldehyde	$(\text{CH}_2\text{O})_n$	(1.3 kg/L)	Merck {E.8}
Piperazine-N,N'-bis(2-ethanesulfonic acid), dipotassium salt (PIPES)	$\text{C}_8\text{H}_{16}\text{N}_2\text{O}_6\text{S}_2\text{K}_2$	378.6	Sigma {E.8}
Sodium fluoride	NaF	41.99	Sigma {E.8}
Sodium orthovanadate	$\text{Na}_3\text{VO}_4$	183.91	Sigma {E.8}
Triton X-100	$\text{C}_{14}\text{H}_{22}\text{O}(\text{C}_2\text{H}_4\text{O})_n$	n.a.	Union Chemicals

Table E-15: Additional general reagents (V3)

## E.16 Sundry materials

Item	ID	From
Cell scrapers	353086	Falcon {E.8}
Ciprofloxacin	Ciproxin IV 200	Bayer
Fluorometer cuvettes	170-2415	Bio-Rad {E.8}
Laemmli sample buffer	161-0737	Bio-Rad {E.8}
Nanosep 3K centrifugal devices	OD003C34	Pall
Nitrocellulose membrane/filter paper sandwiches (0.45 $\mu\text{m}$ pore size)	162-0214	Bio-Rad {E.8}
PCR primers (6-FAM labelled)	n.a.	Applied Biosystems {E.8}
Ponceau S protein stain	P7170-1L	Sigma {E.8}
Prolong Gold antifade mountant	P36934	Invitrogen {E.8}
Prolong Gold antifade mountant/DAPI	P36935	Invitrogen {E.8}
Protease inhibitor cocktail (100x)	P-8340-5ML	Sigma {E.8}
Restore Western blot stripping buffer	21059	Pierce
Supersignal West Pico Chemiluminescent Substrate	34078	Pierce
SYBR-safe DNA gel stain	S33102	Invitrogen {E.8}

Table E-16: Additional sundries (V3)

## E.17 Supplier data

Manufacturer or agent	Contact information
A. Griekspoor and Tom Groothuis	<a href="http://mekentosj.com/4peaks/">http://mekentosj.com/4peaks/</a>
Abcam plc	<a href="http://www.abcam.com/">http://www.abcam.com/</a>
Alphatech	<a href="http://www.alphatech.co.nz/">http://www.alphatech.co.nz/</a>
Bayer	Tel: 09 443 3093 <a href="http://www.bayer.co.nz/">http://www.bayer.co.nz/</a>
Bio-strategy Ltd	Tel: 09 9969 9150 <a href="http://www.bio-strategy.com/">http://www.bio-strategy.com/</a>
BioTek Instruments	See Bio-strategy Ltd
Calbiochem	See Merck (NZ) Ltd {E.8}
Carl Zeiss (NZ) Ltd	Tel: 09 838 5626 <a href="http://www.zeiss.com.au/">http://www.zeiss.com.au/</a>
Fujifilm	<a href="http://www.fujifilm.co.nz/">http://www.fujifilm.co.nz/</a>
Leica	See Global Science and Technology {E.8}
Molecular Probes	See Invitrogen {E.8}
Nanodrop Technologies	See Biolab Ltd {E.8}
Pall	See Alphatech {E.8}
Pierce	See Global Science and Technology {E.8}
Sony	<a href="http://www.sony.co.nz/">http://www.sony.co.nz/</a>
Union Chemicals Ltd	Tel: 09 415 666 <a href="http://www.unionchemicals.co.nz/">http://www.unionchemicals.co.nz/</a>

Table E-17: Additional supplier data (V3)



## E.18 Software

Software	Platform	Version	From	GAC rating
4Peaks	Macintosh	1.7	A. Griekspoor and Tom Groothuis	B+
Cellquest Pro	Macintosh	4.0.2	Becton Dickinson	C+
ImageJ	Java	1.38j	NIH	B+
ImageReady CS	Macintosh	8.0	Adobe	A-
Mac OS X	Macintosh	10.4.9	Apple Inc.	A-
Office	Macintosh	V.x	Microsoft	C+
Photoshop CS	Macintosh	8.0	Adobe	A+
Primer3	web-based	v0.3.0	<a href="http://frodo.wi.mit.edu/">http://frodo.wi.mit.edu/</a>	B

The GAC rating represents the overall quality of the software as assessed by the author.  
A+ = essentially faultless; E = virtually useless.

Table E-18: Additional software (V3)





---

## **Reviews and supplementary material**

---



---

*While great advances have been made against many human diseases, cancer still challenges us, and remains a major contributor to human misery. The last 50 years have seen many improvements in treatment and survival, but we are still no better at preventing or curing cancer than in 1950.*

---

<b>cancer</b>	noun [mass noun] a disease caused by an uncontrolled division of abnormal cells in a part of the body. [count noun] a malignant growth or tumour resulting from such a division of cells.
<b>malignant</b>	adjective (of a tumour) tending to invade normal tissue or to recur after removal; cancerous. Contrasted with benign.
<b>tumour</b>	noun a swelling of a part of the body, generally without inflammation, caused by an abnormal growth of tissue, whether benign or malignant.

*The New Oxford Dictionary of English*<sup>1010</sup>

## F.1 The scourge of cancer

People are rare indeed who have not had their lives scarred by cancer in some way. It seems that every family has a member, and every person, a friend, who has been stricken by cancer, suffered and ultimately died. Those afflicted must face the shock of diagnosis, with its attendant confrontation with mortality, make difficult choices concerning treatment, endure sometimes protracted, painful, disfiguring, nauseating, and even dehumanising therapy with no certainty of cure, wait anxiously for destiny to deliver its verdict, and, ultimately, may have to accept that their only prospect is a relentless decline into death. Simultaneously, those who surround them must deal with the realities of assisting a friend to live, and possibly to die, desperately wishing things were otherwise but being powerless to alter them. Cancer is indeed a potent and multi-faceted contributor to human misery.

With the advent of improved sanitation and nutrition, the appreciation of antiseptics, and the development of drugs, antibiotics and vaccines, most of the diseases that have ravaged humanity over history can now be controlled. Smallpox has been declared extinct, and polio will soon join it. Bubonic plague, cholera, and typhus are no longer the threat they once were and exist not through a lack of understanding of their character or effective therapies, but due to poverty, politics, and the motivation for corporate profit. The impacts of influenza, diphtheria, and tuberculosis have been substantially reduced by immunisation. With mortality due to these causes declining, others such as heart disease, stroke, and diabetes take on greater importance. Here too, preventative, medicinal, and surgical procedures exist to limit their impact. Old foes may have temporary resurgence, as with antibiotic-resistant tuberculosis and new strains of influenza. New diseases may be recognised and rise to prominence or fall to new therapies: AIDS; Creutzfeldt-Jakob Disease; Alzheimer's Disease; Ebola. Throughout this, cancer remains. While advances have been made on some fronts, overall incidence and mortality rates are higher now than ever before {See 'Incidence, survival, and mortality', below}. The armamentarium of medical science has thus far failed to meet this challenge.

---

### F.2 The nature of cancer

#### Defining characteristics

Dictionary definitions provide a starting point and are entirely satisfactory for casual use, but here we must delve a little deeper. Cancer is not a disease in the sense that, for example, tuberculosis is a disease. No single causative agent exists and there is no classical set of symptoms at presentation that immediately identifies it; indeed, it can be entirely without symptoms until very late in its progression. It does not affect any particular cell-type, tissue, organ, individual, or even species, nor is any of these spared. It does not always progress at the same rate or in the same manner, nor is the outcome always the same. Cancer, rather than being a single disease, is a family of diseases that share a small set of common attributes.

Chief among these is the existence of an aberration of tissue homeostasis leading to inappropriate net cellular proliferation. Normally, this homeostasis is maintained by a metabolically regulated balance between cell division and cell death. In cancer, one, or more likely both, of these processes is disturbed. The second defining attribute, seen particularly in solid tumours, is the intrusion of these cells into adjoining tissue, termed local invasion. Together, these features form the minimum definition of cancer. A third characteristic is of relevance in animals that are more than ~1 cm in every dimension. Above this scale, it is unlikely that any tumour could grow to a troublesome size relying solely on diffusion for the supply of nutrients and the removal of waste. By presenting itself as a tissue under nutritive stress, a tumour can instigate the creation of new blood vessels to supply it, a process termed angiogenesis. These features together can cause sufficient deterioration in the function of both the tissue of origin and its environs as to be life-threatening. The final and most pernicious attribute of many cancers is their ability to cast cells into circulation that may lodge at distant sites and proliferate there, causing widespread secondary tumours. This process, metastasis, contributes most to the gravity of cancer as a disease, and greatly hinders effective therapy by requiring it to be systemic.

#### Incidence, survival, and mortality

Data from the National Cancer Institute of the USA for cancer incidence, survival and mortality<sup>1092</sup> {Table F-1} provide the sobering information that overall, both incidence and mortality rate have increased since 1950 [1]; we are no better now at preventing or curing cancer than we were then. While disturbing, this observation does not convey the dramatic improvements that have been made in five-year survival rates [2], or the greatly reduced mortality among those under 65 years of age, and in particular those under five {Table F-2}. Together with this, but more difficult to quantify, have come dramatic improvements in the quality of life enjoyed following therapy, with vastly improved pain control and the availability of extensive rehabilitation.



SUMMARY OF CHANGES IN CANCER INCIDENCE AND MORTALITY, 1950-98 AND

5-YEAR RELATIVE SURVIVAL RATES, 1950-97

Males and Females, By Primary Cancer Site

Primary Site	All Races		Whites				5-Year Relative Survival Rates (Percent)	
	Estimated Cancer Cases in 1998	Actual Cancer Deaths in 1998	Percent Change 1950-98					
			Incidence		U.S. Mortality			
			Total	EAPC	Total	EAPC	1950-54	1989-97
Oral cavity and Pharynx	30,100	7,965	-40.0	-0.7	-39.0	-1.0	46	58.4
Esophagus	13,200	11,764	-2.7	0.3	24.6	0.4	4	15.1
Stomach	21,700	12,957	-78.9	-2.6	-81.6	-3.5	12	20.7
Colon and Rectum	135,400	56,973	0.6	-0.1	-38.2	-0.9	37	62.0
Colon	98,200	48,814	15.1	0.1	-24.9	-0.4	41	62.1
Rectum	37,200	8,159	-23.3	-0.7	-68.3	-2.8	40	61.5
Liver and Intrahep	16,200	12,381	180.1	1.9	34.9	0.5	1	6.1
Pancreas	29,200	28,335	13.7	0.0	16.1	0.1	1	4.2
Larynx	10,000	3,866	20.0	0.1	-18.5	-0.3	52	66.1
Lung and Bronchus	169,500	154,472	248.2	2.2	252.5	2.8	6	14.8
Males	90,700	91,397	169.1	1.3	185.5	2.3	5	13.3
Females	78,800	63,075	598.0	4.3	617.2	5.2	9	16.8
Melanomas of skin	51,400	7,431	477.3	4.1	160.4	2.1	49	89.0
Breast(females)	192,200	41,736	63.1	1.3	-14.7	-0.1	60	86.8
Cervix uteri	12,900	4,340	-78.6	-2.8	-76.7	-3.5	59	71.5
Corpus and Uterus, NOS	38,300	6,421	3.7	-0.5	-68.2	-2.2	72	85.8
Ovary	23,400	13,390	0.7	0.2	-4.8	-0.3	30	51.5
Prostate	198,100	32,203	194.2	3.2	-1.4	0.3	43	97.0
Testis	7,200	370	124.6	1.9	-72.5	-3.2	57	95.4
Urinary bladder	54,300	11,757	53.8	0.9	-35.0	-1.1	53	81.9
Kidney and Renal pelvis	30,800	11,484	130.6	1.9	36.4	0.6	34	62.1
Brain and Other nervous	17,200	12,666	69.4	1.1	43.9	0.7	21	31.0
Thyroid	19,500	1,182	155.3	1.8	-48.8	-1.8	80	95.4
Hodgkin's disease	7,400	1,311	13.9	0.2	-75.1	-3.5	30	84.0
Non-Hodgkin's lymphomas	56,200	23,434	185.1	2.8	138.1	1.6	33	54.2
Multiple myeloma	14,400	10,311	222.8	1.7	199.0	2.1	6	28.0
Leukemias	31,500	20,469	11.0	0.2	-6.1	-0.4	10	46.0
Childhood(0-14 yrs)	8,800	1,456	35.1	0.8	-68.4	-2.8	20	78.5
All sites excluding Lung and Bronchus	1,098,500	387,047	46.3	0.8	-20.8	-0.4	38	70.4
All Sites	1,268,000	541,519	59.3	1.0	3.1	0.2	35	63.1

F: Cancer

EAPC = estimated annual percent change. Highlighting added.

Table F-1: Cancer incidence and survival rates in the USA (1950-1997/8)<sup>1092</sup>

All Primary Cancer Sites Combined

Age Group	1950	1975	1998	Estimated Annual Percent Change		Total Percent Change 1950-98
				1950-75	1975-98	
0-4	11.1	5.2	2.3	-2.8	-3.0	-77.5
5-14	6.6	4.7	2.6	-1.0	-2.8	-59.6
15-24	8.5	6.6	4.5	-0.7	-1.8	-48.2
25-34	19.8	14.6	10.9	-1.2	-1.1	-43.6
35-44	64.2	53.9	38.9	-0.4	-1.3	-38.4
45-54	175.2	179.2	134.2	0.2	-1.2	-22.6
55-64	394.0	423.2	385.9	0.3	-0.3	-0.7
65-74	700.0	769.8	830.2	0.4	0.4	19.4
75-84	1160.9	1156.0	1320.3	0.0	0.6	14.7
85+	1450.7	1437.9	1751.4	-0.2	0.9	21.5
All Ages	158.1	162.3	161.5	0.1	0.0	3.1

Mortality rates are per 100 000 of population. Highlighting added.

Table F-2: Cancer mortality rates in the USA (1950-1998)<sup>1092</sup>

### F.3 The cause of cancer

#### Scope of aetiology

Our understanding of cancer aetiology has advanced from ascribing it to an excess of black bile, to failure of the lymphatic system, to flaws in the biochemical control of cellular proliferation, to defects in the interplay between the genome and its environment. The current scope of our enquiry ranges mostly from the molecular to the organismic, but excursions to scales beyond these are sometimes made.

#### The prerequisites for cancer

The defining characteristics of cancer introduced above impose restrictions on the context in which cancer can develop. The characteristic of cellular proliferation implies the need both for regulated cellular growth, lest cells swell or dwindle in size as they increase in number, and the near-perfect transmission of modus operandi from one cellular generation to the next, lest the ability to survive and propagate be lost. To say this may seem to be no more than to say that life is a prerequisite for cancer, a fundamental notion indeed, but there are further implications. The first is that the organism must be multicellular for there to be any distinction between cellular proliferation and organismic replication. The second is that the life span of the organism as a whole must be considerably greater than that of its constituent cells, or it would die before aberrant cellular proliferation could be of any consequence. This further implies that there must be continual death and replacement of cells within the organism. The characteristic of local invasion requires that the organism be comprised of functionally distinct cell-types organised into tissues. Functional diversity implies a controlled mechanism of cellular differentiation, which implies an external agency by which the fates of cells can be independently determined. The relationship between incubation temperature and hatchling sex in many reptile species is one example<sup>S1426</sup>. The characteristic of angiogenesis implies that the proliferation rate of one cell-type can be influenced by another, as can tissue architecture. This leads to the formal requirement of a means of intercellular communication. Once this is granted, the possibilities for the control of cell differentiation are also expanded dramatically by allowing tissue patterning to be determined parentally, rather than physically, as exemplified by the role of morphogens in ontogenesis<sup>R1377</sup>. The characteristic of metastasis requires the presence of a transport mechanism within the organism, further reinforcing the need for tissue differentiation.

#### Human tumorigenesis

##### *Multi-step tumorigenesis*

Ultimately, all life processes are the result of the interaction of the genome and its environment within the bounds of physical laws, and this is therefore true of tumorigenesis. Current theory holds that cancer begins with a single cell sustaining a transmissible alteration that confers on it some growth advantage over its neighbours. It may reduce dependency on extracellular growth stimulation, or reduce sensitivity to extracellular growth repression. It may be something that increases the probability that the cell will divide, or reduces the probability that it will die. The alteration may interfere with its ability to maintain its genome, thus increasing the chance that further growth-advantageous alterations may occur and propagate. This leads directly to the concept of multi-step tumorigenesis, where cells gradually accumulate new attributes and become increasingly abnormal. A corollary of this is that tumours are clonal, a much-overworked term. Here, 'clonal' cannot be construed to mean that all cells comprising a tumour at any stage are genetically identical, indeed, as will be shown here, there is great genetic variability within tumours. It must instead be taken to mean that tumours ultimately originate from a single progenitor cell, but since this is true of any tissue in the body, it is hardly a distinction. What



makes this statement of value is that tumours may be derived from a cell already substantially differentiated and so have attributes that are characteristic of a particular cell-type.

As stated, each alteration that confers a growth advantage must be transmissible. This is generally taken to be synonymous with heritable, that is, transmitted by a cell to its descendants during cell division, but it need not be so. Transmission by viral infection also figures in tumorigenesis, as with human papillomavirus (HPV)<sup>®259</sup> and Epstein-Barr virus (EBV)<sup>®949</sup>. Whatever the mode, the nature of the alteration cannot be so disruptive as to prevent its transmission. Thus a tumorigenic virus cannot kill its host cell before replicating, a somatic gene mutation cannot prevent cell division, and, at a higher level, carriage of a germ-line mutation cannot have a phenotype that is invariably lethal during childhood.

#### *Tumour-suppressor genes and oncogenes*

The attempt to understand the interaction between genome and environment benefits greatly from the overlaps among epidemiology, biochemistry, molecular biology, and molecular genetics. Thus environmental factors implicated in causing the critical alteration, carcinogens, have been identified; the natures of the alterations made have been characterised at a molecular level; and the implications of these changes at the cellular level have been explored. In this way, many carcinogens have been found to be mutagens, that is, agencies of genetic alteration, as with  $\gamma$ -radiation and benzo[*a*]pyrene. An extremely valuable tool has been the study of hereditary syndromes in which predisposition toward cancer is prominent among the symptoms<sup>346</sup>. This has led to the identification of many genes that play important roles in the development of cancer, oncogenes, or its prevention, tumour-suppressor genes (Table F-3). Often, when the protein products of these genes are characterised, they are found to interact functionally with others similarly implicated in tumorigenesis. This has led to the identification of protein groups whose elements cooperate to perform a complex, often multi-step function, and this ability may be lost or degraded with the failure of any element. The functions performed by these subsystems are exactly those that would be expected given the prerequisites for the development of cancer. They participate in the control of cellular proliferation and differentiation, genome integrity, and intercellular communication. Those elements that are critical to a subsystem, that link subsystems together, that participate in multiple subsystems, or that can subvert function, are in general those considered to be tumour-suppressors or oncoproteins.

#### *The mutation versus aneuploidy debate*

A correlation between gross chromosomal defect and cancer was recognised at least as early as 1914, in which year Theodor Boveri stated that cancer cells contained '*...einen bestimmten, unrichtig kombinierten Chromosomenbestand*' (translation: '*...a certain set of incorrectly combined chromosomes*') and that '*Dieser ist die Ursache für die Wucherungstendenz, die auf alle Abkömmlinge der Urzelle [...] übergeht*' (translation: '*This is the origin of the tendency to rampant growth passed on to all descendants of the original cell*'<sup>127</sup>. In addition to changes in chromosome structure, such as translocations, abnormal chromosome numbers (aneuploidy) are frequently seen, and a loss or imbalance of gene expression may result. It has been proposed that this may be a driving force behind tumorigenesis. With advances in molecular genetics allowing the characterisation of the genome down to the individual nucleotide, oncogenes and tumour-suppressor genes have been recognised, and mutations in these proposed as causes of cancer. That chromosomal aberrations and mutations both occur is not in dispute. The issue is: which is the cause and which the effect?

## Human metastatic melanoma in vitro

<b>Familial adenomatous polyposis</b> <sup>739</sup> <b>Colorectal cancer, hepatoblastoma</b> <sup>415</sup> , <b>thyroid cancer</b> <sup>171 596</sup> , <b>brain tumours</b> <sup>470</sup>	
<i>APC</i> <sup>430 470</sup>	Mediates adhesion dependence: with $\beta$ -catenin <sup>1117 1210</sup> , E-cadherin <sup>571</sup> , GSK3 $\beta$ <sup>1528</sup> , WNT <sup>1040</sup> , and by regulating MYC <sup>492</sup> transcription. Involved in cell motility <sup>99</sup> , microtubule polymerisation <sup>931</sup> , and kinetochore function <sup>364</sup> .
<b>Turcot's syndrome</b> <sup>6603</sup> <b>Colorectal cancer, brain tumours</b>	
<i>APC</i> <sup>430 470</sup>	see above
<i>PMS2?</i> <sup>172 247</sup>	<b>DNA base mismatch detection</b> <sup>473 707</sup>
<b>HNPCC</b> <sup>636 1396</sup> ; <b>Muir-Torre syndrome</b> <b>Colorectal cancer, endometrial cancer, stomach cancer</b> <sup>1</sup>	
<i>PMS2</i> <sup>947</sup> (4)	see above
<i>PMS1</i> <sup>947</sup> (3)	<b>DNA base mismatch detection</b> <sup>473 707</sup>
<i>MLH1</i> <sup>797</sup> (2)	<b>DNA base mismatch detection</b> <sup>473 707</sup> Component of BASC
<i>MSH2</i> <sup>756 1274</sup> (1)	<b>DNA base mismatch detection</b> <sup>473 707</sup> Component of BASC. Forms a mismatch recognition complex with MSH6.
<i>MSH6</i> <sup>179 1441</sup> (5)	<b>DNA base mismatch detection</b> <sup>473 707</sup> Component of BASC. Forms a mismatch recognition complex with MSH2.
<i>TGFB2?</i> <sup>810</sup> (6)	<b>Growth factor receptor serine/threonine protein kinase</b> Growth factor responsiveness <sup>321</sup>
<b>Xeroderma pigmentosum</b> <sup>6715 6741</sup> <b>Trichothiodystrophy, neurological abnormalities, cutaneous carcinomas: melanoma</b> <sup>699</sup> , <b>squamous and basal cell carcinoma</b>	
<i>XPA</i> <sup>1303</sup> (A)	<b>Damaged DNA binding protein</b> <sup>1450</sup>
<i>ERCC3</i> <sup>1371</sup> (B)	<b>DNA helicase</b> <sup>822</sup>
<i>XPC</i> <sup>780</sup> (C)	<b>Damaged DNA binding protein</b> <sup>1450</sup>
<i>ERCC2</i> <sup>356</sup> (D)	<b>DNA helicase</b> <sup>1273</sup>
<i>DDB2</i> <sup>946</sup> (E)	<b>Damaged DNA binding protein</b> <sup>560</sup>
<i>ERCC4</i> <sup>1223</sup> (F)	<b>DNA repair endonuclease: with ERCC1</b> <sup>399</sup>
<i>ERCC5</i> <sup>959</sup> (G)	<b>DNA repair endonuclease</b> <sup>455</sup>
<i>POLH</i> <sup>1494</sup> (variant)	<b>DNA trans-lesion polymerase = DNA pol-<math>\eta</math></b> <sup>855</sup>
<i>ERCC6</i> <sup>215 835</sup> (CS)	<b>DNA-binding ATPase</b> <sup>1175</sup>
<b>Fanconi anaemia</b> Birth defects, bone marrow failure, pancytopenia, cancer predisposition: acute myeloid leukaemia <sup>1463</sup> , oral squamous cell carcinoma <sup>1058</sup> , myelodysplastic syndrome, breast cancer <sup>1496</sup>	
<i>FANCA</i> (A)	Dual incision prior to inter-strand cross link repair, with ERCC4 <sup>727</sup>
<i>FANCB</i> (B)	Unknown
<i>FANCC</i> (C)	Interferon- $\gamma$ signalling via STAT1 <sup>997</sup> , G <sub>2</sub> /M arrest via CDC2 <sup>721</sup> , CASP3 activation after ionising radiation <sup>449</sup> , mediates Fas-sponsored apoptosis <sup>703 1394</sup> .
<i>BRCA2</i> (D1)	Homologous recombination and DNA repair: with BRCA1 and RAD51 <sup>242</sup>
<i>FANCD2</i> <sup>1329</sup> (D2)	Unknown
<i>FANCE</i> <sup>251</sup> (E)	Unknown
<i>FANCF</i> (F)	Unknown
<i>FANCG</i> (G)	Unknown
<b>Wiskott-Aldrich syndrome</b> <sup>6963</sup> <b>Immunodeficiency, eczema, thrombocytopenia, lymphoreticular tumours, leukaemias, lymphomas</b> <sup>227 718</sup>	
<i>WAS</i> <sup>461</sup>	Signal transduction <sup>53 450 984</sup> : with EGFR <sup>1198</sup> , FYN <sup>769</sup> ; BTK <sup>450</sup> , modulated by CDC42 membrane GTPase <sup>669 706</sup> ; independent of actin polymerisation <sup>1226</sup> Cytoskeletal organisation <sup>1286</sup> : chemotaxis <sup>459</sup> , phagocytosis <sup>772 806</sup> Apoptosis <sup>1081</sup> Megakaryocyte differentiation <sup>890</sup>
<b>Ataxia telangiectasia</b> <sup>1212 1253</sup> <b>Immunodeficiency</b> <sup>1469</sup> , <b>lymphoma</b> <sup>661 786 1148</sup> , <b>leukaemia</b> <sup>886 1495</sup> , <b>breast cancer</b> <sup>599 621 1186</sup>	
<i>ATM</i> <sup>1111 1143</sup>	<b>Serine/threonine protein kinase</b> <sup>175</sup> Known substrates <sup>577</sup> : BRCA1 <sup>226 403</sup> , nibrin <sup>1458 1516</sup> , CHK2 <sup>858</sup> , p53 <sup>659</sup> , ABL <sup>76</sup> , MDM2 <sup>249</sup> DNA damage response <sup>153 528 1290</sup> : as component of BASC; with CHK1 <sup>193</sup> , CHK2 <sup>858 1333</sup> , MDM2 <sup>249</sup> , p53 <sup>659 906 1427</sup> DNA recombination: as component of BASC
<b>Nijmegen breakage syndrome</b> <sup>277 1212 1366</sup> <b>Immunodeficiency, lymphoma</b>	
<i>NBN</i> <sup>1365</sup>	DNA damage response: as component of BASC <sup>1458 1516</sup>
<b>Bloom's syndrome</b> <sup>6413</sup> <b>Growth deficiency, telangiectasia, diabetes mellitus, cancer predisposition: leukaemia, Hodgkin's lymphoma, oesophageal cancer</b>	
<i>BLM</i> <sup>317</sup>	<b>DNA helicase</b> <sup>637 791</sup> DNA damage response: as component of BASC

Table F-3: Hereditary conditions that predispose toward cancer (continues overleaf)

BASC, the BRCA1-associated genome surveillance complex, is reviewed in Appendix I.





<b>Hereditary retinoblastoma</b> <sup>10 320</sup> <b>Bilateral paediatric retinoblastoma, osteosarcoma</b> <sup>829</sup> , melanoma <sup>24 77 903</sup> , bladder cancer <sup>897</sup>	
<i>RB1</i> <sup>270 513 802 1177</sup>	<b>pRB-related 'pocket protein'</b> <sup>200</sup> Cell-cycle progression (G <sub>1</sub> ) <sup>479</sup> ; with E2F1 Control of differentiation <sup>194</sup>
<b>von Hippel-Lindau syndrome</b> <sup>211 218 @229 @375 977</sup> <b>Renal cell carcinoma, pheochromocytoma, CNS hemangioblastoma, pancreatic cancer</b> <sup>811</sup> , astrocytoma <sup>944</sup> , Hodgkin's disease <sup>265</sup>	
<i>VHL</i> <sup>1488 1502</sup>	<b>Transcription elongation inhibitor</b> <sup>922</sup> <b>Ubiquitin E3 ligase</b> <sup>213</sup> Growth factor response <sup>1007</sup> , via p27 <sup>674</sup>
<b>Wilms' tumour</b> <sup>1435</sup> ; <b>Denys-Drash syndrome</b> <sup>796</sup> <b>Paediatric kidney tumour, leukaemia</b> <sup>1060 1282</sup> , breast cancer <sup>1224</sup> , adult renal cell carcinoma <sup>151</sup>	
<i>WT1</i> <sup>454 878</sup>	<b>Transcription factor</b> <sup>297 765 1414</sup> Cell-cycle progression (G <sub>1</sub> ) <sup>723</sup> , via RBBP7 <sup>446</sup> , p21 <sup>323</sup> Apoptosis control via BCL2 <sup>862 878</sup>
<b>Multiple endocrine neoplasia</b> <sup>1323</sup> <b>Endocrine tumours: pituitary, parathyroid, pancreas, peptic ulcer disease, melanoma</b> <sup>957</sup>	
<i>MEN1</i> <sup>178</sup>	<b>Transcription co-factor</b> Specifically binds and inhibits the JUND transcription factor <sup>16</sup>
<b>Peutz-Jeghers syndrome</b> <sup>6867</sup> <b>Adenocarcinoma</b> <sup>107</sup> : colon <sup>282</sup> , breast, testis, ovary, biliary tract <sup>1271</sup> , pancreas <sup>1271</sup> , melanoma <sup>451 1114</sup>	
<i>STK11</i> <sup>499 604</sup>	<b>Serine/threonine kinase</b> <sup>1239</sup> Unknown function
<b>Li-Fraumeni syndrome</b> <sup>6328</sup> <b>Sarcoma, brain tumours</b> <sup>110</sup> , breast cancer	
<i>TP53</i> <sup>564</sup>	<b>Transcription factor</b> <sup>861</sup> Apoptotic control <sup>78 86 431</sup> : via BAX <sup>130</sup> , BCL2 <sup>895</sup> Cell-cycle progression: via CDKN1A <sup>313</sup> , GADD45 <sup>652</sup> Genomic stability <sup>129 1388</sup> DNA damage response <sup>1437</sup> : with ATM <sup>659 906 1427</sup> , ATR <sup>1327</sup> , CHK1 <sup>1208</sup> , CHK2 <sup>183 525 1208 1333</sup>
<i>CHEK2</i> <sup>85</sup>	<b>Serine/(threonine?) protein kinase</b> DNA damage response: with ATM, p53 <sup>525 1208 1333</sup> Cell-cycle progression: via CDC25 <sup>183</sup>
<b>Neurofibromatosis I</b> <sup>958</sup> <b>Fibromatous skin tumours, cafe au lait spots, pheochromocytoma, meningioma, glioma, astrocytoma</b> <sup>711 751</sup>	
<i>NF1</i> <sup>1455</sup>	<b>GTPase-activating protein</b> <sup>488</sup> Signal transduction: modulates RAS activity <sup>1514</sup>
<b>Neurofibromatosis II</b> <sup>6327</sup> <b>Bilateral acoustic schwannoma, meningioma</b> <sup>1352</sup>	
<i>NF2</i> <sup>693 865 1004</sup>	<b>Ezrin, radixin, moesin family (ERM) protein</b> <sup>135 541 876</sup> Cellular adhesion <sup>453 702</sup> and adhesion dependence <sup>1196</sup>
<b>Gorlin syndrome</b> <sup>6230</sup> <b>Multiple developmental defects, basal cell carcinoma, medulloblastoma</b>	
<i>PTCH</i> <sup>462 616</sup>	<b>Trans-membrane receptor protein: Sonic hedgehog signalling (with Smoothened)</b> <sup>1265</sup> Chromosomal stability <sup>1185</sup>
<b>Multiple hamartoma syndrome; Cowden syndrome</b> <sup>6319</sup> <b>Multiple hamartomas (skin, mucous membrane, breast, thyroid, intestine), brain tumours, prostate cancer, melanoma</b> <sup>170</sup>	
<i>PTEN</i> <sup>1231</sup>	<b>Dual specificity (Tyr, Ser/Thr) protein phosphatase; lipid phosphatase</b> Cell-cycle progression (G <sub>1</sub> ): via PI3K <sup>95 1368</sup> , cyclin-D1 <sup>1424</sup> , p21 <sup>1456</sup> and p27 <sup>775 1424</sup> Apoptotic control <sup>1423</sup> Cell adhesion migration <sup>1298</sup> : via FAK <sup>1297</sup>
<b>Melanoma-astrocytoma syndrome</b> <sup>646</sup> <b>Melanoma, neural tumours, commonly astrocytoma</b> <sup>58</sup>	
<i>CDKN2A</i> <sup>368</sup>	<b>ARF: Degradation targeting</b> <sup>1076</sup> Genome surveillance: with p53, MDM2 <sup>602</sup>
<b>Melanoma</b> <sup>484 1391</sup> , leukaemia <sup>18 975</sup> , mesothelioma <sup>1059 1465</sup> , pancreatic carcinoma <sup>149</sup>	
<i>CDKN2A</i> <sup>368</sup>	<b>p16: CDK4/6 cyclin-dependent kinase inhibitor</b> <sup>1180</sup> Cell-cycle progression (G <sub>1</sub> ): with pRB, cyclin-D, CDK4/6 <sup>1202 1373</sup> Cellular senescence <sup>557</sup>
<b>Melanoma</b> <sup>1250</sup>	
<i>CDK4</i> <sup>1529</sup>	<b>Cyclin-dependent kinase</b> <sup>480</sup> Cell-cycle progression (G <sub>1</sub> ): with pRB, Cyclin-D, p16 <sup>1202 1373</sup>

Table F-3 (continued)

<b>Gastric cancer<sup>448</sup>, colorectal cancer<sup>1091</sup>, lobular breast cancer (?)<sup>1072 1384</sup></b>	
<i>CDH1</i> <sup>93</sup>	<b>Calcium-dependent cell adhesion protein (epithelial): E-cadherin<sup>94</sup></b> Cell adhesion, tissue architecture, invasion suppression <sup>98</sup> , metastasis <sup>80</sup> Contact inhibition and adhesion dependence: with APC <sup>571</sup> , β-catenin, p27 <sup>1257</sup>
<b>Proximal colorectal cancer<sup>406 1519</sup>, myelodysplastic syndrome<sup>189</sup></b>	
<i>GSTT1</i> <sup>1267</sup>	<b>Glutathione S-transferase enzymes<sup>1130</sup></b> Chemical detoxification; free radical scavenging; tumour chemoresistance
<b>Ovarian cancer<sup>99</sup>, lung cancer<sup>1174</sup>, colorectal cancer<sup>1519</sup></b>	
<i>GSTM1</i> <sup>1011</sup>	<b>Glutathione S-transferase enzymes<sup>1130</sup></b> Chemical detoxification; free radical scavenging; tumour chemoresistance
<b>Breast cancer, ovarian cancer<sup>365</sup></b>	
<i>BRCA1</i> <sup>264 1403</sup>	DNA damage response: as component of BASC; with p53 <sup>987 1510</sup> , ATR <sup>1328</sup> Centrosome replication <sup>543</sup>
<b>Breast cancer<sup>1451</sup>, pancreatic cancer<sup>1160</sup></b>	
<i>BRCA2</i> <sup>1314</sup>	Homologous recombination and DNA repair: with BRCA1 and RAD51 <sup>242</sup>

Listed are hereditary diseases where: cancer predisposition is a facet of the symptomatology; an underlying gene has been identified; and there is some understanding of the function of the encoded protein.

Ordering is to allow juxtaposition of apparently distinct phenotypic manifestations with the same underlying cause (for example, *APC* mutation), or similar phenotypic manifestations with differing underlying causes (for example, Li-Fraumeni syndrome). Beyond that, syndromes are grouped into broad similarity of tumour type (for example, melanoma predisposition).

Parenthesised items following gene names denote recognised sub-classifications of the disease.

Bold entries among the associated diseases denote those typical of the syndrome. Others are those also reported in hereditary disease, or implicated by virtue of gene aberrations found in sporadic cases. Bold entries among the functions of encoded proteins denote the functional class to which the protein product belongs, where this is well defined.

**Table F-3 (concluded): Hereditary conditions that predispose toward cancer**

Proponents of aneuploidy as a cause<sup>@1178</sup> cite the inherently low basal mutation rate, suggesting that alone, it could not account for the number of aberrations seen in many tumours given the time over which they develop. If, however, an early mutation has the consequence of increasing this rate, this argument fails. Consistent with this, mutations in genes associated with DNA repair mechanisms are frequently observed, as are mutations in genes associated with the maintenance of chromosomal stability. A reasonable interpretation of current information is that mutation and aneuploidy are inextricably linked, and once either occurs, the rates of both increase. A mutation may affect the maintenance of chromosomal stability and euploidy as easily as gain or loss of a chromosome may affect basal mutation rate. It is a self-reinforcing cycle that is as likely to be initiated by a chance event affecting one aspect as the other. The search to identify which is the cause, and which the effect, is both misguided and irrelevant.

The material presented in Appendices I, J, K, and L is pertinent to this discussion.

**The immune system and cancer**

Many believe that the immune system has an important role in the prevention of cancer. That this is a fallacy becomes evident when it is appreciated that only in relatively few hereditary cancer predisposition syndromes is immunodeficiency present, and in the great majority of hereditary immunodeficiency syndromes, there is no associated predisposition toward cancer. This is discussed more fully in Appendix G.

**The progression of cancer**

However the progression from normality to malignancy is driven, it appears to proceed through a number of reasonably well defined stages. In tissues of epithelial lineage, it will often begin with hyperplasia: the presence of supernumerary cells not significantly morphologically different from the normal tissue. Dysplasia develops, during which the morphology of the cells diverges from the norm for the tissue of origin. With increasing dysplasia, the growing benign tumour ultimately will warrant the



designation of carcinoma in situ. With invasion into surrounding tissue, the tumour becomes malignant, and if it spreads to distant sites, it has become metastatic.

While these changes may be occurring at the level of the tissue there may or may not be any outward indication of this process. Where symptoms are sufficiently obvious to prompt the seeking of medical advice, they often include lumps or swelling (the origin of the word 'tumour'), pain, fatigue, unusual bleeding or discharge, gastric, intestinal or urinary obstruction, fever, unusual sweating, deficient wound healing, or neurological effects including alteration in sensation or motor control. It is not unusual for cancer to be asymptomatic and discovered through intentional screening, or fortuitously as a result of other medical procedures such as blood tests, X-rays, ultrasound examination, or surgery. When symptomatic however, it is likely that the cancer has been present undetected for some years, and, in the case of solid internal tumours, it is likely that a blood supply to the tumour has already been established. Once cancer is suspected, various diagnostic tools will be applied to verify if this is indeed the case, and if so, to identify the particular type and its stage of progression. From there, a strategy for treatment can be developed.

## **The treatment of cancer**

### *Conventional treatment*

Three major modalities have been the mainstays of cancer treatment since its recognition as a cellular disease: surgery, chemotherapy, and radiotherapy. Clinical experience has led to the development of particular treatment regimens for particular cancer types at various stages, the principal determinant being the degree to which the disease has metastasised, if at all. Where medical imaging and biopsies of the tumour and adjacent lymph nodes indicate that spread is unlikely, a purely local treatment may suffice, typically surgical resection of the tumour and marginal normal tissue, or targeted radiotherapy, delivered either from an external source, or by isotopic implantation.

Where metastasis is known or suspected, a systemic treatment is required. This is generally in the form of chemotherapy using cytotoxic or anti-proliferative drugs. Variations, such as isolated limb perfusion, and combined modalities, such as surgery with local radiotherapy may also be employed. In all cases, whether it depends on the surgeon's skill, the precision of conformant radiotherapy, or the pharmacological and biological attributes of drugs, the efficacy of treatment depends on the discrimination between cancerous and normal cells and the selective extirpation of the former.

### *Immune system modulation*

There is a school of thought that believes that the specificity of the immune system may be harnessed to provide the means of discrimination required. This process began long before the cellular basis of the immune system was known, with Coley's toxins in the nineteenth century. The late twentieth century saw the therapeutic use of recombinant cytokines, and today novel drugs that directly or indirectly affect immune system function are in clinical trial. Attempts have been made to create vaccines from mutated or over-expressed tumour antigens, with some success in animal models. Nevertheless, if no tumorigenic pathogen is present, these approaches may be limited.

### *The limitations of conventional therapies*

To refer to conventional therapies as 'cutting, poisoning, and burning' illustrates well how blunt are the tools of surgery, chemotherapy, and radiotherapy. The greatest obstacles to the success of conventional systemic treatment are the dispersed nature of cancer as a disease and the extremely close biological similarity between malignant and normal cells. To date, the major objective of chemotherapy has been

the selective destruction of proliferating cells, the rationale being that cancer cells are more likely to be dividing. As we learn more about cancer, we are finding that this is perhaps a poor distinction at best. Firstly, the situation is not that every cell in a tumour is dividing more frequently than normal, it is that overall, there is a net excess of cell proliferation over cell death. Alterations to apoptotic mechanisms may be as important as increased cellular proliferative capacity. Secondly, very many normal tissues, such as gut epithelium and haematopoietic precursor cells have an intrinsically high proliferation rate and are therefore detrimentally affected by these drugs, often to the extent of being dose-limiting for therapy. Thirdly, tumour vasculature is both spatially and temporally heterogeneous, with consequences for the uniform delivery of drugs, and hence their efficacy. To overcome these obstacles, ways must be found to exploit the aspects of tumour biology that do differ from the biology of normal cells and tissues.

### **Novel therapeutic strategies**

#### *Gene and anti-sense therapies*

In cases where tumour growth occurs only due to the functional failure of a tumour-suppressor, it may in future be possible to supply a replacement for a defective gene<sup>866</sup>, but there are immense problems in bringing such gene therapy to the clinic. In particular, delivery of the replacement gene specifically to tumour cells will be required where over-expression in normal cells is associated with toxicity. Even if delivery mechanisms can be developed, ensuring appropriate and sustained levels of gene expression are formidable obstacles.

Conversely, where tumour growth is supported by production of a mutant protein or over-production of a normal one, the possibility of specifically interfering with this exists. The most promising current approach to this is in the use of anti-sense agents<sup>231</sup>. These are multi-base nucleic acid analogues whose sequence is the complement of the mRNA of the target protein. When delivered or expressed intracellularly, they will avidly bind such mRNA and interfere with its translation. This technique works well in vitro, but therapeutically, it faces many of the same problems as gene therapy.

#### *Targeting signal transduction*

It is now widely appreciated that many of the molecular causes of disease are either components of, or exert their influence via, intracellular signal transduction channels<sup>495</sup>, and this may be particularly true of cancer. If drugs that interfere with spurious proliferative signalling can be found or developed, a therapeutic opportunity may exist in the treatment of some types of cancer.

As a class, receptor tyrosine kinases make excellent potential therapeutic targets since their function is often altered in cancer by erroneous expression, mutation, or over-expression of their specific ligand<sup>1530</sup>. Where this has the effect of stimulating net cellular proliferation, it can drive tumorigenesis. As an example, several novel drugs have been developed that target the epidermal growth factor receptor and a number are now in clinical trial<sup>515 1079</sup>.

Non-receptor kinases, both tyrosine and serine/threonine, also frequently participate in signal transduction channels and have been implicated in many cancer types. Among these are the cyclin-dependent kinases (CDKs) and other regulators of the cell division cycle, such as WEE1. Of particular interest is the recent FDA approval of imatinib mesylate for the treatment of chronic myelogenous leukaemia<sup>214</sup>. This drug is a tyrosine kinase inhibitor that counteracts the effects of the erroneous activation of the ABL kinase resulting from its expression as a BCR fusion protein after the chromosomal translocation characteristic of this cancer.



Another target is RAS, a signalling protein that is normally self-regulating. In many cancers however, this regulation is lost, and if triggered, RAS signalling remains active and can drive cellular proliferation. Its activation requires that it become associated with the cell membrane, and for this to occur, RAS must be post-translationally modified by farnesylation. Inhibitors of the farnesyltransferase enzyme that performs this may reduce or prevent aberrant RAS signalling. Compounds of this type are also in clinical trial<sup>638</sup>.

### *Anti-angiogenic agents*

In tissues produced by the normal processes of development and growth, the needs for nutrient and oxygen supply and waste removal are met by the co-establishment of a hierarchy of blood vessels and a network of lymphatic vessels. Since this is not the way in which tumours develop, this mechanism is not available to them. The manner in which cancers resolve this distinguishes them from almost all normal adult tissues: their continuing existence is dependent on their ability to induce angiogenesis {F-2}. Therefore, therapies that target the proliferation, but not the survival, of vascular endothelial cells should prevent the growth of tumours and probably cause their regression, and do so with minimal toxicity<sup>197</sup>. Two approaches to this exist, although in reality they may be different aspects of just one. Firstly, it should be possible to diminish or oppose the effect of growth factors that stimulate endothelial proliferation. This may entail the use of cytokine therapy, as has been used in the treatment of infant haemangioma with interferon- $\alpha$ , or of antagonistic antibodies directed against the receptors for critical growth factors, such as FGF2, VEGF, and angiogenin. Secondly, it may be possible to stimulate activity of the normal process that disables angiogenesis after wound healing and ovulation. Here, the anti-angiogenic properties of several small peptides that are cleavage products of proteins engaged in these processes may be extremely important. One such, angiostatin, a fragment of plasminogen, causes drastic regression of human breast, prostate, and colon tumours implanted into mice, and holds them in this state for the duration of treatment<sup>980</sup>. While no anti-angiogenic drugs have yet been approved for the treatment of human cancer, at least fifteen are in clinical trial, and there is a very real prospect that some, at least, will be efficacious.

### *Anti-metastatic agents*

Among the several hundred distinct normal human cell-types, only one, the leukocyte, has the ability to travel freely within and between tissues. Indeed, displacement of any other type of normal cell into an inappropriate context is generally sufficient to cause its immediate self-destruction through apoptosis, a process termed anoikis<sup>377</sup>. It is thought that this process is mediated through biochemical interactions between cells, and between a cell and the extracellular matrix. When the correct combination of signals is not available to a cell, that is, when it is displaced, it dies. In contrast, the most pernicious aspect of cancer, metastasis, implies that tumour cells can overcome these limitations. Clearly, there is more to metastasis than the fortuitous dislodgement of a cell or a clump of cells from a primary tumour, and some change in biological regulation must be taking place. To detach from the primary tumour, it must be able to decrease its intercellular affinity, and the proteins  $\beta$ -catenin and E-cadherin have been implicated in this role, particularly in gastric cancers<sup>956</sup>. To be able to survive in isolation during its travels, it must attain at least substrate-independence, and the integrins are implicated here<sup>725</sup>. In the case of individual cells, contact-independence must also be attained, and here again, E-cadherin or its signal transduction subsystem, has been implicated<sup>1447</sup>. To move within and between tissues requires that it have inherent motility, implicating cytoskeletal components<sup>593</sup> <sup>865</sup> and cytokine signalling, as with HGF/MET<sup>860</sup>. It must be able to pass both between other cells that may normally be strongly cohesive,

and possibly through the basement membrane, and here, matrix metalloproteinases have been implicated<sup>®1258</sup>. These processes must also work in reverse, in that the metastatic seed must be able either to adhere to, or exit through the vessel wall in order for a secondary tumour to form.

The possibility that these activities may be susceptible to modulation presents a therapeutic opportunity, and the search to elucidate the mechanisms governing metastasis, and for the means to influence it is now in progress. It is as yet too early to speculate on how successful this will be.

### *Pro-drugs*

One approach to resolving the issue of general, as opposed to tumour-specific cytotoxicity has been to separate the delivery of a drug from its activation<sup>®265</sup>. In this way, a biologically benign pro-drug can be administered systemically and subsequently, its latent therapeutic function activated locally. This approach is open to a great many variations. Higher tumour pro-drug concentration may be achieved by taking advantage of poor tumour vasculature. Systemic pro-drug levels can be allowed to rise until a steady-state is reached, whereupon the majority of the pro-drug can be removed from well-vascularised normal tissue immediately prior to activation. Drug activation may be triggered by radiolytic cleavage, by tumour hypoxia or pH, or by enzymatic activity. In the latter case, endogenous enzymes expressed in the tumour tissue type, or over-expressed in the tumour may be used. Alternatively, exogenous enzymes may be employed. In antibody-directed enzyme pro-drug therapy (ADEPT), such an enzyme is supplied and is targeted to the tumour by a linked antibody. Upon pro-drug delivery, activation only occurs within the tumour. In gene-directed enzyme pro-drug therapy (GDEPT), a gene for the enzyme may be introduced into the tumour, albeit with difficulty, that is subject to tissue-specific expression. Finally, while much of the early work with pro-drugs has employed traditional cytotoxins such as mustard derivatives, there is a great range of potentially suitable agents.

### *Genetic targeting*

A particularly cunning strategy to target tumour cells has been devised that harnesses two aspects of p53 molecular biology: its frequent functional loss in cancer cells, and its active disablement by many viruses as a prerequisite for productive infection. Onyx Pharmaceuticals have engineered an adenovirus, ONYX-015<sup>®1093</sup>, in which the gene responsible for disabling p53 upon infection is non-functional. In consequence, they believe, it will only be in cells where p53 is already non-functional that the virus can replicate, ultimately destroying the host cell in the process. Since all normal human tissues express functional p53, but it is mutated in most tumours, it will only be tumour cells that are destroyed. While attractive theoretically, our knowledge of p53 function is still incomplete, and opinion is divided on the soundness of the underlying premise and on what practical utility this approach will have. This issue will be clarified considerably with the completion of the clinical trials of ONYX-015 that are currently underway<sup>686</sup>. Also developed, but not yet to the same stage, is a similar virus that will target cells lacking the function of another tumour-suppressor, the retinoblastoma-associated protein, pRB {See Chapter 11}.

---

# G

# Immunodeficiency and cancer

---

*The theory of immune system surveillance as a general defence against cancer has many proponents, but little concrete evidence to support it. One of the telling arguments against this theory comes from the study of hereditary immunodeficiency syndromes. With very few exceptions, cancer is not a feature of these. Where it is, immunodeficiency and cancer predisposition are independent effects of a common molecular flaw, with no causal relationship existing between them. Similarly, arguments based on increased cancer incidence in those with suppressed immune system function do not stand up to close scrutiny. Consequently, suggested cancer therapies based on immune system modulation must be viewed with circumspection.*

---

## G.1 Introduction

There is a widely held theory that the immune system plays a role in the prevention of cancer, its rationale being essentially as follows. Where there is an operative immune system, cellular proteins are sampled and subjected to scrutiny by T-cells that will recognise foreign antigens. Any cells displaying such antigens elicit a cytotoxic response and are destroyed. Since cancer arises from events that often give rise to mutant proteins, there is a *prima facie* case that surveillance by the immune system has a significant role in the prevention of cancer. This hypothesis is amenable to testing since, if true, where the immune system is deficient, an abnormally high incidence of cancer should be seen.

Several lines of evidence are often raised in support of this. In AIDS, elevated rates of Kaposi's sarcoma (KS) and non-Hodgkin's lymphoma (NHL) are seen. Among the hereditary immunodeficiency diseases, increased cancer incidence is seen: lymphoma and breast cancer in ataxia telangiectasia (AT); lymphoma in Nijmegen breakage syndrome (NBS); and leukaemia in Bloom's syndrome (BS). Where the immune system has been depressed for therapeutic reasons, as in the case of organ transplantation or the treatment of autoimmune diseases, elevated cancer rates are also commonly reported. Taken together, the case in favour of a tumour-suppressive immune system function appears formidable. However, as this review will show, the increased cancer incidence seen is readily explicable without recourse to immunodeficiency as a cause.

## G.2 Acquired immunodeficiency syndrome

KS and NHL account for ~80% of cancers seen in patients with AIDS<sup>1100</sup>. Excluding these, cancer incidence in AIDS is only approximately twice that of the general population<sup>370</sup>. This bias and the relatively modest general increase in incidence are difficult to reconcile with the hypothesis of immune system tumour-suppression, under which a spectrum and incidence increase more akin to that seen in Li-Fraumeni syndrome (LFS) could be expected. Nevertheless, there is an association, and an explanation must be found.

The existence of tumorigenic viruses is well established. It is entirely possible that the Human Immunodeficiency Virus (HIV), generally accepted as the cause of AIDS, is yet another such, causing a tumorigenic transformation directly, and independently of its effects on the immune system. Once HIV infection is established, its suppressive effect on immune system function leaves the host vulnerable to opportunistic pathogens, notably *Pneumocystis carinii*, which causes pneumonia with a mortality rate of 37% within 12 months after diagnosis<sup>304</sup>. The host is similarly vulnerable to tumorigenic pathogens, and

---

## Human metastatic melanoma in vitro

these account for the overwhelming majority of AIDS-associated cancers, with Human Herpesvirus 8 leading to KS, Epstein-Barr virus (EBV) to NHL<sup>347</sup>, and Human Papilloma Virus (HPV) thought to lead to several other types<sup>257</sup>. Other as yet unrecognised tumorigenic pathogens may account for the balance.

Arguably, this supports the hypothesis of immune system tumour-suppression, but only in a very limited and indirect sense, that is, when the underlying cause is pathogenic infection. As for supporting a general role, it is negligible.

### G.3 Hereditary immunodeficiency syndromes

#### Introduction

Over 70 hereditary immune-deficiency syndromes are known, and in very many cases, the causes have been ascribed to specific genes, and this has been confirmed by the generation of knockout mice {Table G-1}.

Class	Genes
<b>Membrane proteins (receptors included)</b>	<i>C5R1, CD3E, CD4, CD5, CD8A, CD8B1, CD14, CD19, CD28, CD74, CD80, CR2, CTLA4, FAS, FCER2, FCGR2A FCGR2B, FCGR3A FCGR3B, FLT3, IFNGR1, IL2RA, IL2RB, IL2RG, IL5RA, IL7R, IL8RA IL8RB, LAG3, PTPRC, SPN, TACR1, TNFRSF1A, TNFRSF5, TNFRSF8</i> MHC class II genes at 6p21 T-cell receptor genes at 7q34 T-cell receptor alpha and delta genes at 14q11.2
<b>DNA-binding proteins (transcription factors included)</b>	<i>CEBPB, ETS1, FOS, GATA2, IRF1, IRF2, MYB, NFKB1, PAX5, POU2F2, RELA, SOX4, TCF3, TCF7, VAV1, ZNFN1A1</i>
<b>Cytokines and related proteins</b>	<i>CSF2, FASLG, IFNG, IL1B, IL2, IL4, IL5, IL6, IL7, IL10, IL12B, LTA, SDF1, TGFBI, TNFSF5</i>
<b>Signal transducers</b>	<i>BTK, CSK, FYN, ITK, JAK3, LCK, LYN, PIM1, PRKCB1, STAT6, SYK, ZAP70</i>
<b>Genome maintenance</b>	<i>ATM, DNMT1, POLB, PRKDC, RAG1, RAG2, XRCC5</i>
<b>Adhesion proteins</b>	<i>ICAM1, ITGB2, ITGB7, SELE, SELL</i>
<b>Apoptotic effectors</b>	<i>ABLI, BAX, BCL2</i>
<b>Proteasomal proteins</b>	<i>PSMB8, PSMB9</i>
<b>Other</b>	<i>ADA, B2M, C3, C4A C4B, CD2, CDKN1B, CHS1, GZMA, IGKC, PRF1, TAP1</i> Immunoglobulin heavy chain genes at 14q32.33 Immunoglobulin lambda genes at 22q11.1-q11.2

Classification is indicative only. Some proteins encoded may belong to multiple classes. Where closely linked related genes occur and it is not clear which is responsible for the phenotype, this is indicated, for example '*IL8RA|IL8RB*'.

**Table G-1: Genes implicated in hereditary immunodeficiency**

These diseases fall into five broad divisions: the severe combined immunodeficiencies (SCIDs), where both B-cell and T-cell function is compromised, onset is early, progression rapid, and outlook poor; the combined immunodeficiencies, affecting B-cell and T-cell function, but to a lesser degree; the B-cell immunodeficiencies, where T-cell function remains intact; the T-cell immunodeficiencies, where B-cell function remains intact; and the phagocytic immunodeficiencies. Representative diseases of each type where there is a significant body of literature are discussed briefly below, together with an assessment of the weight they add to the argument in favour of a tumour-suppressive immune system function.

#### Severe combined immunodeficiencies

##### *Class I: Flawed signal transduction*

The SCIDs can be further sub-divided for convenience, the first class being those where signal transduction is flawed. This includes genetic defects in *IL7R*, *JAK3*, *PTPRC*, *TNFSF5*, and *IL2RG*, the gene associated with X-linked SCID and accounting for ~50% of hereditary SCID. In these diseases, there are failures of lymphocyte proliferation and activation.





### ***Class II: Lymphocyte toxicity***

The second class involves lymphocyte cytotoxicity and is monotypic, with *ADA* being the only gene implicated. This accounts for 15%–30% of hereditary SCID. The encoded enzyme, adenosine deaminase, is involved in purine metabolism, and it could be thought that its mutation may cause deficiencies in nucleic acid synthesis that lead to the SCID phenotype. However, the basis for this disease is the selective cytotoxicity of unprocessed ADA substrates toward lymphocyte precursor cells.

### ***Class III: Flawed V(D)J recombination***

The third class involves flaws in V(D)J recombination, and includes *PRKDC*, *SCIDA*, *RAG1*, and *RAG2*. This destroys the immune system's greatest strength: its potential to produce a myriad of unique antigen receptors from a limited number of genes. It can also halt lymphocyte development, which stalls until this process completes.

### ***Class IV: Flawed antigen presentation***

The fourth class includes diseases where the processing and presentation of antigens is flawed and these are known collectively as 'bare lymphocyte syndrome'. The genes *MHC2TA*, *RFX5*, *RFXANK*, and *RFXAP* are implicated, and encode proteins that operate in both the HLA I and HLA II antigen presentation subsystems. Those involved in HLA II, the processing of antigens of extracellular origin, are the more prevalent.

### ***Cancer predisposition***

If the immune system served to prevent cancer, arguably it would be in these most severe diseases that this would show itself, but in none of these SCID syndromes, irrespective of their class, is there any significant predisposition to cancer. It may be argued that this is because death occurs due to infection before any tumour develops. Even if true, this can never be proven and must be considered speculation at best.

## **Combined immunodeficiencies**

### ***DiGeorge anomaly***

This is known best as a flaw in development, principally affecting the heart, often the palate, and in some cases, the thymus. It is in this last subset, about 20% of cases, that variable immunodeficiency is seen. While a region on chromosome 22, named 'Catch-22' has been implicated, no single gene has been identified as causative, and there is some suspicion that a deletion of contiguous genes may be necessary for development of the full disease phenotype. There is also evidence for a further susceptibility locus on chromosome 10. Occasional malignancies are reported, including B-cell lymphoma (BCL), neuroblastoma, glioma, and squamous cell carcinoma. Viral infection is suspected to play a part in some or all of these. Until the molecular basis of this disease is elucidated, to attribute increased cancer rates to immunosuppression is premature.

### ***Chediak-Higashi syndrome***

The symptomatology of Chediak-Higashi syndrome<sup>584</sup> includes immunodeficiency, abnormal pigmentation, and progressive neurological dysfunction. The associated *CHS1* gene encodes a protein involved in lysosomal trafficking<sup>1255</sup> and in this role it plays a part in Class II antigen presentation<sup>338</sup>. Although there are some reports of lymphoma associated with this disease, for the most part it is non-malignant lymphocyte proliferation that is seen.

The regulation of epidermal pigmentation is described more fully in Chapter 2

### **B-cell immunodeficiencies**

#### *X-linked agammaglobulinaemia*

The gene associated with X-linked agammaglobulinaemia (XLA)<sup>®1375</sup>, *BTK*, encodes a kinase that translocates to the nucleus<sup>902</sup> and is involved in the activation of the transcription factor NF $\kappa$ B via its inhibitor I $\kappa$ B kinase<sup>1022 1299</sup>. This in turn controls a variety of cellular processes relating to cytokine production and proliferation. BTK has an imperfectly understood role in the control of apoptosis in B-cells, inhibiting that induced by Fas<sup>1367</sup>, but promoting that induced by radiation<sup>1351</sup>. Despite this implication in the control of net cellular proliferation, there is no significant cancer predisposition seen. In the context of the increases seen in some immunodeficiencies, it is noteworthy that in XLA, anti-viral immune responses remain intact.

#### *Common variable immunodeficiency*

Common variable immunodeficiency (CVID)<sup>®1244</sup> is in essence a name given to all B-cell immunodeficiencies not otherwise classified. Not surprisingly therefore, it has a heterogeneous phenotype and multiple loci have been implicated. No candidate genes have been identified, and the underlying molecular causes are unknown, although flawed antigen presentation, apoptotic control, and IL12/IFN $\gamma$  signalling have been suggested. Some lymphoma and gastric cancer have been reported, but the incidence of the latter may not be significantly higher than expected<sup>909</sup>, and may be pathogen related, with *Helicobacter pylori* infection being suggested as a factor<sup>680 1527</sup>. Additionally, there are reports of lymphoproliferative disease, but upon investigation, these are found in the majority of cases to be benign<sup>1131</sup>. Since the mechanisms of CVID are various and unknown, the minor increase in cancer incidence cannot reliably be attributed to any cause, including immune system dysfunction.

### **T-cell immunodeficiencies**

#### *Duncan's disease (alias X-linked lymphoproliferative disorder)*

In this disease<sup>®908</sup>, the immune system has neither T-cell nor natural killer (NK) cell function. The implicated gene, *SH2D1A*, encodes a protein involved in the signal transduction of SLAM-family receptors. It is normally expressed only in T-cells and NK-cells and is required for their activation. Duncan's disease is usually asymptomatic prior to EBV infection, after which, expression of *SH2D1A* is also seen in B-cells and lymphoma develops in 20% – 60% of cases.

### **Phagocytic immunodeficiencies**

#### *Wiskott-Aldrich syndrome*

The symptomatology of Wiskott-Aldrich syndrome (WAS) includes immunodeficiency, eczema, and thrombocytopenia<sup>®963</sup>, and the median age at death, while improving, is now just ten years<sup>1020 1272</sup>. Among those who do not fall to uncontrollable infection, rates of lymphatic cancer are higher than expected, being seen in some 18% of cases. The functions of the protein product of the *WAS* gene, WASP, have been partially characterised. It is intimately associated with the organisation of the actin cytoskeleton, particularly in linking polymerisation to events at the cell surface. In so doing, it is critical for lymphocyte chemotaxis<sup>459</sup> and phagocytosis<sup>772 806 902</sup>. Secondly, WASP functions to inhibit apoptosis<sup>1081</sup>, and deregulation of this may contribute to lymphocyte depletion. Furthermore, it is necessary for differentiation of megakaryocytes into platelets. Loss of these functions is sufficient to account for the immunodeficiency seen. Three aspects of WASP biochemistry may account for the increased cancer incidence in WAS. It has a high affinity for the membrane-bound GTPase CDC42<sup>706</sup>, a RAS oncogene<sup>51 152 512</sup> homologue, once CDC42 has been activated<sup>669</sup> by E-cadherin<sup>675</sup>, a known tumour-suppressor<sup>448</sup>. When in this state, WASP is phosphorylated by BTK, the kinase described above in conjunction with XLA. As WASP is only normally expressed in cells of lymphoid lineage, effects of its



loss would only be seen in such cells, accounting for the different phenotypes of E-cadherin and WASP deficiencies. It physically associates with, and may be phosphorylated by, the epidermal growth factor receptor<sup>1198</sup>, deregulation of which is often seen in cancer, and it binds GRB2, a key mediator of RAS signal transduction. While there is more work to be done to reveal the full function of WASP, what is already known is sufficient to indicate that its role in tumour suppression does not depend upon its necessity for immune system integrity. The interrelationships among E-cadherin, CDC42, WASP, signal transduction, and cytoskeletal control warrant much greater discussion. They are, however, beyond the scope of this work.

### **An analogous myeloid disease**

#### ***Fanconi anaemia***

By way of comparison, it is edifying to consider a disease in which defects similar to those described above for lymphoid cells occur in cells of myeloid lineage, and Fanconi anaemia (FA)<sup>401</sup> provides an excellent example. In this disease, there is complete bone marrow failure resulting in severe anaemia. Growth retardation, infertility, and birth defects occur, and there is an increased risk of cancers, including leukaemias in 10% of cases, hepatocellular carcinoma in 10%, and squamous cell carcinoma and other cancers in about 5%. The interesting feature in the current context is that in FA, the immune system is intact. The cancer predisposition seen here results from the function of the FA-gene encoded proteins in co-operation with BASC in the detection and repair of genomic damage.

### **Chromosomal breakage syndromes**

There are three hereditary diseases in which immunodeficiency occurs where there is a clear increase in cancer predisposition: AT, NBS, and BS. They have features in common that distinguish them from other immunodeficiency diseases and indicate their close relationship. In all, an increased cellular vulnerability to radiation is seen that manifests as chromosomal breakage. The proteins encoded by the genes associated with them, ATM, nibrin, and BLM, are components of the BASC complex, explaining the overlapping characteristics of the associated disease syndromes. This complex is activated, among other things, by the presence of double-strand DNA breaks. In the majority of cells, these are indicative of genomic damage, so failure of BASC can dampen or eliminate the response to this, facilitating tumorigenesis. In cells of the immune system, double-strand DNA breakage is an essential part of the V(D)J recombination that is at the heart of the generation of antigen receptor diversity, and involvement of BASC in this should not be unexpected. There is certainly evidence that nibrin<sup>190</sup>, and possibly ATM<sup>186 687 801</sup>, may be necessary for accurate V(D)J recombination, although the data are somewhat equivocal<sup>481 542</sup>. Failure of V(D)J recombination is sufficient to produce immunodeficiency, as is seen in the form of SCID due to a defective catalytic subunit of DNA-dependent protein kinase, essential for this function<sup>667</sup>.

#### ***Ataxia telangiectasia***

In addition to the shared features of these diseases, AT also involves neuronal degeneration, progeria, and infertility. The associated protein, ATM<sup>753</sup>, encodes a serine/threonine kinase that is activated upon the detection of genomic damage and includes among its substrates p53, ABL, BRCA1, nibrin, CHK2, and, possibly indirectly, MDM2. It is a fundamental part of cellular processes including the DNA damage response, meiotic chromosomal synapsis, the mitotic spindle checkpoint, telomere maintenance, and apoptosis. In AT, lymphoma is frequently seen, perhaps due to the increased chromosomal breakage experienced in lymphoid cells during V(D)J recombination in the absence of functional BASC. Increased rates of breast cancer have also been reported.

### *Nijmegen breakage syndrome*

In addition to the common features, NBS<sup>®1361</sup> shares with AT the facet of neuronal degeneration. Its other symptoms include a shortness of stature, microcephaly, and a peculiar facial expression often described as 'bird-like'. The associated protein, nibrin, a substrate of ATM, participates in DNA double-strand break repair, modulates p53 induction after irradiation, is probably involved in assuring V(D)J recombination fidelity, and may influence DNA unwinding, possibly in conjunction with BLM. As with AT, lymphoma is a frequent concomitant of NBS.

### *Bloom's syndrome*

In addition to the common features, BS shares with AT telangiectasia and male infertility, and with NBS, growth retardation. Uniquely, an increased incidence of diabetes is a component of BS. The associated protein, BLM, is a DNA helicase that may modulate the p53 response after UVR and X-ray induced DNA damage, and mediates recombination in meiosis. As with AT and NBS, it is lymphoma that predominates among the cancers seen in BS, but leukaemias are also seen.

### **Summary**

In hereditary immunodeficiency diseases, an increased incidence of cancer is only rarely seen, and when it is, it is almost invariably lymphoma, that is, a cancer of precisely the cell-type that is by definition abnormal in these syndromes. Where non-lymphoma cancer does occur, the part played by pathogenic organisms unchallenged by a competent immune system may be the primary cause. Finally, in several syndromes, no molecular mechanism has been established and hence ascribing any increased cancer incidence to immunodeficiency is premature.

In the chromosomal breakage syndromes, there is a clear molecular basis to explain both the cancer predisposition and the immune deficiency seen, without needing to invoke the latter as a cause of the former. They are independent effects of a common cause. Furthermore, the cancer type seen is again predominantly lymphoma, and the comments above apply equally well here.

### **G.4 Therapeutic immunosuppression**

A great many immunosuppressive agents are used in the clinic for the treatment of autoimmune diseases and the management of organ transplantation. The most frequently used and best understood of these, together with their associated cancer risks are listed in Table G-2.

Where there are data, again, lymphoma predominates, but there is an interesting correlation between IL2 modulation and skin cancer occurrence that deserves further investigation. For the antimetabolites, the possibility of deleterious effects on DNA synthesis cannot readily be excluded, and in the case of cyclophosphamide, this, and its metabolites are well-known as potent mutagens.

### **G.5 The immune system and hereditary cancer syndromes**

The immune system is exquisitely sensitive and reactive to the presence of foreign antigens, that is, those not recognised as 'self'. It is particularly instructive to consider this in the context of hereditary cancer syndromes. On a population basis, the genetic variations that occur can be seen to be abnormal and hence deemed to be mutations. The immune system does not have the advantage of such a global perspective, and must interpret any mutant proteins as entirely bona fide, their antigens having been present through the entire process of negative selection of self-reactive lymphocytes. Any role for the immune system in the suppression of hereditary cancers is therefore forbidden to the same degree as other forms of autoimmune response.



Agent	Mode of action	Associated cancer risk
<b>T-cell activation</b>		
Muromonab CD3	CD3-TCR antibody	No data
<b>Steroid analogue</b>		
Prednisone	Gene activation	Probably no increased incidence
<b>IL2 activity modulation</b>		
Basiliximab	IL2R antibody	No data
Cyclosporine	IL2 production	Lymphoma, skin cancers (equivocal)
Sirolimus/rapamycin	IL2 signalling	Lymphoma, skin cancers
Tacrolimus	IL2 production	Lymphoma, skin cancers
<b>Antimetabolites</b>		
6-mercaptopurine	Purine analogue	Probably no increased incidence
Azathioprine	Purine analogue	Lymphoma, skin cancers, AML
Dapsone	DHFR inhibitor	Spleen and thyroid cancer in rats; limited human data
Methotrexate	Folate analogue	Inconclusive; chromosomal breakage seen
<b>Antiproliferative</b>		
Cyclophosphamide	Alkylator	Lymphoma, leukaemia, bladder cancer

**Table G-2: Cancer risks associated with therapeutic immunosuppressive agents**

## G.6 Limited potential for immune system tumour-suppression

Clearly, the arguments usually raised to support the notion of immune system tumour-suppression do not stand up to close scrutiny. In contrast, a single obvious and persuasive observation renders the proof of the contrary case trivial: the vast majority of people with cancer have a completely normal immune system. As an agent for the prevention of cancer, the immune system is clearly ineffective.

Is there then a basis on which to believe that there is any role at all for the immune system in the prevention of cancer? Surprisingly, the answer is that there may be. While excluded from responding to mutant proteins arising from inherited genes, no such restriction applies to mutant proteins arising somatically. As most cancer is sporadic, this is likely the majority. There is a significant caveat to this however. The principal role of the immune system is to combat infection, relying on the presence of foreign antigens, and its efficacy depends upon its sensitivity. However, cellular protein synthesis is not without error, even in the absence of genetic mutation. Messenger RNA may be incorrectly spliced, transfer RNAs may carry the wrong amino acid or match the wrong codon, and misfolding of nascent proteins may occur producing novel antigens. It seems likely that every cell will at some time display markers of abnormality. Hence, there must be a degree of tolerance that is in direct conflict with the need for sensitivity, and the process of evolution has determined the optimal compromise between these two objectives and defined a threshold of sensitivity. While xenobiotic proteins may appear sufficiently bizarre to an immune system so tuned as to elicit a response, those deriving from a subtle alteration to an intrinsic protein may fall below this threshold and so be tolerated. This is as it must be where the immune response is triggered by changes of structure, irrespective of their functional significance.

## G.7 Therapeutic immune system modulation

If the immune system does not normally serve to constrain tumorigenesis, there can be little hope of success for approaches to cancer treatment that seek to modulate this. It is a potent tool for the destruction of aberrant cells once identified, and where tumorigenic pathogens are present there is indeed scope to employ this through vaccination and modest enhancement of sensitivity. Unfortunately, the immune system's ability to distinguish host-derived tumour cells from normal tissue is extremely limited. If the sensitivity is therapeutically raised to the point where mildly aberrant cells are engaged with the same vigour as truly xenobiotic cells, there is a grave risk of provoking a serious autoimmune response. There may simply be too little structural abnormality and too little precision in the modulation feasible with therapeutic agents.

As an alternative, it may be possible to make a specific tumour protein more antigenic, perhaps through the use of engineered high-specificity antibodies that themselves elicit an immune response. However, to do so would simply be to employ the immune system as a cytotoxic effector mechanism, and medical science is already well endowed with such agents, for example, ricin. It is the targeting of the agent that has always been the sticking point and has led to the as yet fruitless search for a 'magic bullet' to direct it. The hope that the remarkable and exquisite selectivity of the immune system may provide this appears unlikely to be realised.

### **G.8 Conclusion**

It is difficult to embrace the notion that the immune system has any role in the prevention of cancer, except where a tumorigenic pathogen is the cause. Consequently, the utility of proposed therapies based on boosting this non-existent function must be viewed with circumspection, if not scepticism. The ability of the immune system to identify structurally aberrant proteins has not been able to be harnessed to target host-derived tumour antigens and is inherently limited by the need to avoid autoimmunity, nor is its cytotoxic function significantly better than that of existing agents. The immune system is an outstanding evolutionary achievement for the purposes of combating infection, but unfortunately, not cancer.

*Study of a rare hereditary paediatric cancer has led to the identification of pRB, a tumour-suppressor implicated in human cancer of many types. It plays a crucial role in embryogenesis, differentiation, cellular senescence, and proliferation. The manifold functions of pRB are mediated solely via interactions with over 100 proteins, both individually and in higher-order complexes. Its functions are modulated chiefly post-translationally, with regulated alterations in phosphorylation state being the best understood mechanism. Not surprisingly, many of the elements necessary for regulation of pRB function have themselves been implicated in tumour suppression or tumorigenesis, in particular, the cyclins, the CDKs, and the CKIs.*

*This appendix provides a general review of pRB structure, interaction, and regulation as a basis for a discussion of the mechanism by which pRB exerts control over cell-cycle progression. The relevance that this may have to tumorigenesis in general, and to melanoma in particular, is then addressed.*

---

## H.1 Retinoblastoma

Retinoblastoma is a paediatric intraocular tumour accounting for 5% of childhood blindness. It occurs as an inherited disease with autosomal dominant transmission<sup>117</sup> and 90% penetrance<sup>292</sup>, in which tumours are usually bilateral and multifocal. Sporadic cases are also known, but these differ from the typical hereditary disease in that they are usually unilateral and unifocal, although a hereditary low-penetrance unifocal phenotype has been described<sup>228</sup>. Several modes of treatment exist, including surgery and radiotherapy, and these are usually curative<sup>280</sup> and preserve vision. However, significant mortality still occurs after successful treatment of hereditary cases due to the increased incidence of subsequent primary tumours of various types {H.5}.

Since rodents infected with adenovirus often developed retinoblastoma-like symptoms<sup>920 921</sup> it was thought that human retinoblastoma may have a similar cause, but no trace of the adenovirus genome could be found in cells from patients<sup>1279 1353</sup>. A different interpretation began to emerge with the publication of a seminal paper by Knudson<sup>696</sup> that reported the results of a statistical analysis of retinoblastoma incidence. The clear inference to be drawn from the data was that retinoblastoma could develop after the occurrence of just two independent genetic events. In the case of the hereditary disease, one of these was presumed to be an inherited trait, while the second, and both in the case of the sporadic disease, were considered to be somatic changes. This is the 'two-hit' hypothesis. Although the two targets were not specifically identified in this work, given the diploid nature of the human genome, a reasonable working hypothesis was that a defect in only one gene was involved, with two events being required to disrupt both alleles. This was supported by loss-of-heterozygosity studies<sup>169</sup>.

## H.2 The retinoblastoma susceptibility gene, *RB1*

### Mapping

Cytogenetic analysis of retinoblastoma tumours led to the discovery of a frequently deleted chromosomal region at 13q14, and linkage analysis within kindreds displaying hereditary disease led to the identification of closely linked microsatellite markers which co-segregated with the disease phenotype. These efforts ultimately resulted in the identification of a candidate retinoblastoma susceptibility gene, *RB1*<sup>376 766</sup> and its authentication<sup>390</sup>.

---

### Gene structure and transcriptional regulation

*RB1* comprises 27 exons spanning over 200 kbp of genomic DNA<sup>117 1305</sup>, and is transcribed into an mRNA of 4.6 kb length<sup>766</sup>. No splice-variants appear to exist in normal tissue, but aberrant splicing resulting in truncation or skipped exons does occur in tumours<sup>802</sup>.

The initial *RB1* promoter characterisation<sup>1305</sup> was extended by Gill et al.<sup>416</sup>, who, by using a series of 5'-deletion constructs, discovered that a region spanning nucleotides –215 to –179, relative to the initiating methionine codon, contains the major functional determinants of transcriptional regulation. They identified putative SP1, CREB/ATF, and E2F binding sites, together with a potential hormone-response element. Surprisingly, the protein that they found to associate with the SP1 site was not SP1, but another protein they dubbed 'RBF-1'. Further work established that it is the GA-binding protein component of the E4TF1 Ets-family transcription factor complex that binds to this site<sup>1144</sup>. Mutation at this<sup>228</sup>, or the CREB/ATF site<sup>1126</sup> is associated with a mild, low-penetrance hereditary retinoblastoma phenotype.

A CpG island extends from the promoter into exon one<sup>1330</sup> and there is evidence that this can be methylated, preventing binding of E4TF1 and ATF/CREB and causing a 92% reduction in transcription rate<sup>970</sup>. Transcriptional silencing due to promoter methylation coupled with deletion or mutation of the alternate allele has been causally linked to over 9% of unilateral sporadic retinoblastomas<sup>438 969 970</sup>, and has been reported in oligodendroglial<sup>283</sup> tumours and glioblastoma<sup>930</sup>.

There is a consensus that pRB contributes to transcriptional regulation of its own gene, but there is less accord over the nature of this. Some opine that E2F transcription factors, regulated by pRB, function as repressors<sup>469 971 1188</sup>, but others have established that the E2F binding site is dispensable for auto-repression<sup>416</sup>. Positive auto-regulation via the ATF/CREB site has also been reported<sup>1000</sup>.

### H.3 The retinoblastoma-associated protein, pRB

#### Significance

Perhaps the best gauge of the importance of a protein is the consequence of its absence, as amply demonstrated in mouse knockout studies. A degree of perspective is afforded by comparing the effect of non-expression of two crucial tumour-suppressors: p53 and pRB. Mice engineered to be *Trp53*-null are born apparently normal, anatomically and physiologically. Only after about six months does their phenotype of increased tumour incidence emerge<sup>5281</sup>. *Trp53*, and by extension the human *TP53*, are tumour-suppressor genes, *par excellence*, but that is all they are. In contrast, mice engineered to be *Rb1*-null die before day 16 *in utero*, with major neural tube deformities, flaws in haematopoiesis, and liver and lens defects<sup>8759</sup>. Clearly, *Rb1*, and by extension *RB1*, have extremely important biological roles beyond tumour suppression. Perhaps the best generalisation of pRB function is to consider it as a key determiner of cellular fate. It profoundly influences proliferation, differentiation, senescence, and apoptosis<sup>6478 625</sup>. The retinoblastoma-associated protein is no less than the kismet of cells.

#### Translation

The *RB1* mRNA transcript contains an open reading frame encoding 928 amino acids, and SDS-PAGE immunoblotting detects at least five mobility variants with indicative molecular weights in the range 105 – 110 kD. These are believed to result from the adoption of multiple conformations determined by post-translational covalent modification, addressed further below. There is some evidence for translation from a second AUG start site resulting in an amino-terminally truncated variant seen by immunoblotting as a protein of 98 – 104 kD indicative molecular weight. The functional significance of this is unknown.





It has also been suggested that sequence variations in the 5' untranslated region may affect mRNA structure and thence translation efficiency<sup>384</sup>.

### Conservation and homology

Species including plants<sup>@§243 @§302</sup>, insects, fish, amphibians, birds, and other mammals have proteins clearly related to human pRB by sequence similarity {Table H-1}. Interestingly, no close homologues exist among unicellular organisms such as yeast. This is entirely in keeping with the principal biological functions of pRB being the constraint of proliferation and the implementation of differentiation, neither of which is of great relevance to such an organism.

See F.3 and J-20 for more discussion of the evolution of tumour-suppressors.

H: The pRB subsystem

Species	Common name	Homology length (amino acids)	Sequence comparison	
			Identity (%)	Similarity (%)
<i>Pan troglodytes</i>	Chimpanzee	882	98	98
<i>Mus musculus</i>	Mouse	928	89	93
<i>Rattus norvegicus</i>	Norway rat	900	89	94
<i>Gallus gallus</i>	Chicken	937	71	81
<i>Notophthalmus viridescens</i>	Eastern red-spotted newt	914	59	75
<i>Xenopus laevis</i>	African clawed frog	936	57	74
<i>Canis familiaris</i>	Dog	518	95	97
<i>Oncorhynchus mykiss</i>	Rainbow trout	944	54	70
<i>Oryzias latipes</i>	Japanese medaka fish	942	50	67
<i>Populus (hybrid)</i>	Aspen	790	24	40
<i>Chenopodium rubrum</i>	Red goosefoot	805	24	40
<i>Arabidopsis thaliana</i>	Mouse-ear cress	895	23	40
<i>Euphorbia esula</i>	Leafy spurge	528	25	44
<i>Zea mays</i>	Maize	765	24	40
<i>Drosophila melanogaster</i>	Fruit fly	709	23	40
<i>Pisum sativum</i>	Garden pea	792	24	40
<i>Caenorhabditis elegans</i>	A nematode worm	870	21	36

Data from NCBI/BLAST. Comparison is with *Homo sapiens* pRB. Similarity implies identity or a conservative amino acid substitution.

**Table H-1: pRB protein sequence conservation**

Within the human proteome, two proteins are sufficiently similar to pRB in terms of sequence conservation and function to support the notion of a 'pocket-protein' family {Table H-2}. Their degree of similarity to pRB is of the same order as that of the nearest plant pRB homologues. Whether this implies that pRB is strongly conserved and p107 and p130 are closely related, or precisely the opposite, is entirely subjective. It is telling, however, that while pRB has been established as a bona fide tumour-suppressor, there is insufficient evidence to support such a role for either p107 or p130<sup>@208</sup>.

Protein	Gene	Homology length (amino acids)	Sequence comparison	
			Identity (%)	Similarity (%)
p107	<i>RBL1</i>	559	27	44
p130	<i>RBL2</i>	703	24	41

Data from NCBI/BLAST. Comparison is with pRB. Similarity implies identity or a conservative amino acid substitution.

**Table H-2: Human proteins similar to pRB**

### Tissue-specificity of pRB expression

A comprehensive study of pRB expression in 53 human tissues was performed by Cordon-Cardo and Richon<sup>223</sup>. Expression was seen in all but interstitial matrix, which is essentially acellular. There was variability of expression between and within organs, however. In stratified epithelia, cells in the proliferating basal layer expressed low levels of pRB, while those in suprabasal layers expressed it strongly. In simple epithelia, expression was generally high, but where compartments differing in proliferation rate were distinguishable, an inverse correlation between expression and proliferation rate

was seen. Within the testis, this pattern was again repeated, with non-proliferating Sertoli cells having intense expression, while spermatogonial cells, spermatocytes, and spermatids had low or undetectable levels. Within tissues of the central nervous system, expression was low with the conspicuous exception of Purkinje cells, where it was intense. Intense staining was also seen in cells of the peripheral nervous system. Among haematopoietic cells, proliferating B-cells expressed high levels of pRB, while that seen in mature B-cells and in T-cells was much lower. It was the authors' overall conclusion that pRB regulated the proliferation of maturing cells.

### Sub-cellular disposition of pRB

The pRB protein is predominantly nuclear during interphase, being associated with low-density euchromatin. In metaphase and anaphase, it disperses to the cytoplasm eventually to reassociate with euchromatin during telophase<sup>1287</sup>. Hypophosphorylated pRB is tethered to the nucleus, but this linkage is weakened upon phosphorylation<sup>331 1317</sup>. Nevertheless, a confocal microscopic study of HL60 cells has shown that the ratio of nuclear to cytoplasmic pRB is stable both throughout the cell-cycle and during differentiation, independent of its phosphorylation status<sup>1485</sup>. However, these cells do not contain functional p16, an inhibitor of pRB phosphorylation, as they have only a single non-functional mutant *CDKN2A* allele<sup>1070</sup>. Consequently, pRB phosphorylation status may be abnormally high in these cells, and greater partitioning of pRB to the cytoplasm through reduced tethering may result.

pRB phosphorylation and the role of CDK4 and p16 are discussed more fully below.

### Turnover of pRB

In the normal course of events, pRB levels do not appear to be controlled by regulated proteolysis, although this does play a role in viral infection<sup>425</sup> and in apoptosis<sup>345 1300</sup>. It has been suggested by one group<sup>381</sup> that a cathepsin-like protease, dubbed SPase, may be involved in the cell-cycle dependent regulation of pRB, but this has not been confirmed. There is doubt also over the validity of their methodology in that, having synchronised cells first by isoleucine starvation, and then by aphidicolin treatment, the induction of this protease in response to this treatment cannot be excluded. More recently, a gene over-expressed in some hepatocellular carcinomas was found to encode a protein, gankyrin, that binds pRB and facilitates its 26S-proteasome-mediated destruction<sup>518</sup>. Data are as yet too sparse to conclude what the normal role of this protein may be, but the recent finding that it binds CDK4 in competition with p16, but does not inhibit it, suggests that this role may be significant<sup>778</sup>.

### Function of pRB

#### *Scope of review*

With such a broad range of functions, the molecular biology of pRB, and its attendant literature, are necessarily extensive and complex. A comprehensive review would fill several volumes, and given the burgeoning of knowledge in this area, would likely be obsolete before it reached publication. While many aspects of pRB are presented below, the emphasis is very much on the role it plays in tumour-suppression, and in particular, in the regulation of proliferation.

#### *Basis of pRB function*

The retinoblastoma-associated protein appears to contain no inherent enzymatic activity and the great weight of evidence is in favour of protein-protein interaction being its dominant operative mode<sup>6910</sup>. If so, its influence depends on its ability to modify the inter-molecular interactions of the bound protein. This may be achieved by one of four major mechanisms, given here in order of decreasing apparent relevance to pRB: masking of interaction domains; constraint of physical location; molecular matchmaking; and alteration of physical conformation.



Several domains within pRB have been implicated in mediating protein interactions, and conserved motifs in proteins that bind pRB have also been identified.

### *pRB-binding motifs*

#### **The LXCXE motif**

The basis for the retinoblastoma-like effects of adenovirus infection in rodents became clearer with the discovery that a viral protein, E1A, bound pRB in a step necessary for productive infection<sup>1433</sup>. Similar proteins were soon found to be produced by other small DNA viruses<sup>306</sup>. When the sequences of these were determined, many were found to contain a pentapeptide motif, LXCXE, including the adenovirus E1A protein (LVLDCPENP), the human papillomavirus E7 protein (VDLVCHQL), and the large-T proteins of SV40 (ENLFCSEEM) and polyomavirus (PDLFCYEPP). More recently, the sequence LPCAEE has been implicated in the pRB binding of the NSP90 non-structural protein from the teratogenic human rubella virus, *Rubivirus*<sup>367</sup>. The novelty here is that *Rubivirus* is not a DNA virus, but a positive-strand RNA virus. This attests to both the crucial role of pRB in mediating cellular affairs, and to the efficacy of the LXCXE motif in modulating this. Once identified, the LXCXE motif was found in many cellular proteins known to interact with pRB {Table H-3}, most notably the D-cyclins<sup>288 332</sup>.

#### **LXCXE relatives**

Two variations on the LXCXE motif have been suggested to operate similarly. The first, IXCXE has been identified in the transcriptional repressor HBP1, however it was shown that it was the LXCXE motif also present that mediated its association with p130<sup>1322</sup>. A stronger case for pRB binding by IXCXE exists with HEC<sup>1517</sup>, although it was not found to be essential for function. The second variant is LXSXE, suggested by Durfee et al.<sup>301</sup> as a possible basis for the binding of PPP1CA-2. They noted, however, that the domains of pRB associated with the binding of large-T and PPP1CA-2, while similar, were not identical, leaving open the possibility of a different mode of interaction. Further supportive evidence for a role for LXSXE comes from the directed-mutagenesis study in *Rubivirus* cited above<sup>367</sup>. In seeking to determine the importance of the LPCAEE motif, Fornig and Atreya altered the cysteine to arginine, and so showed that this was critical for proliferation. After approximately one generation time, however, the proliferation rate increased in correlation with a spontaneous mutation to LPSAEE in the motif of interest.

The LXSXE motif is present in the transcription factors JUN, MYC, BRCA1, E2F4, and E2F1 {Table H-3}, considered by many to be the most important pRB-interacting protein of all. Its presence in BRCA1 in addition to an LXCXE motif may account for the continuing ability of BRCA1 to bind pRB when this motif is disrupted<sup>340</sup>. In addition to these, it is present in ARID3B (ERLESSEPA), ELF1<sup>1393</sup> (VQLLSSEEL), ENC1 (VQLLSSEEL), GABPB1 (TGLVSSENS), lamin A/C (ALLNSKEAA, RKLESTESR), RBBP6<sup>1127</sup> (ALLESEHT), and TRIP11 (KKLSAEND, KLLSQEKE, QLSSNENF), all of which are known to bind pRB. Furthermore, it is present in p107 (KHLNSIEEQ) and in pRB itself (SMLKSEER), perhaps accounting for reports of oligomerisation *in vitro*<sup>505</sup>, and the reported ability of the C-terminus of pRB to block repression by the A/B pocket *in trans*<sup>480</sup>. The possibility that LXSXE may have a major role in pRB interactions does not appear to have been fully appreciated as there is very little reported in the literature.

#### **The DLXX(X)E motif**

While inspection of the viral protein sequences revealed the importance of LXCXE, a further potential binding motif may have been overlooked. The LXCXE motif within the adenovirus E1A protein CR2 region also conforms to the pattern DLXXE, as it does in polyomavirus large-T and HPV E7. In SV40 large-T, this overlap is absent, but a separate instance of DLXXE exists (QLMDLLGLERSA). A similar

## Human metastatic melanoma in vitro

motif, DLXXE, conserved among adenovirus strains, appears in the adjacent CE1 region. This composite motif, DLXX(X)E, is present in five of the proteins listed in {Table H-3}, including two with no other recognised binding motif, notably MDM2. It is present also in MYOD (DSPDLRFFEDLD), and TRIP11 (LKQDLNDEKKR), both of which bind pRB.

### pRB protein structure

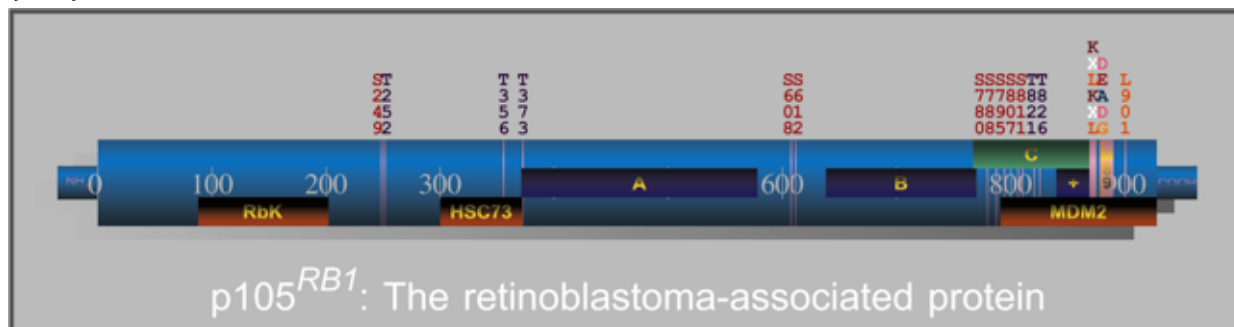


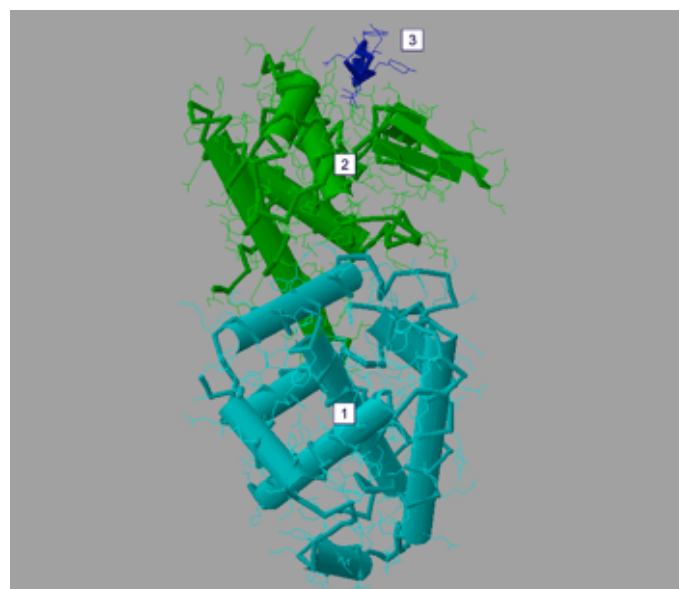
Figure H-1: Salient pRB features

### N-terminal domains

Sterner et al. have reported two related kinases, both referred to as RbK, that bind pRB within the 89 – 202 amino acid region, and phosphorylate pRB, and possibly the transactivation domain of MYC, in G<sub>2</sub>/M. The pRB domain implicated appears essential for pRB-mediated growth suppression and is altered in some retinoblastoma patients<sup>1260 1261</sup>. RbK does not appear to have been further characterised. In addition, the heat-shock protein HSP73 associates with the pRB 301 – 372 amino acid region<sup>583</sup>.

### The 'A' domain and the 'B' pocket

The investigation of viral protein binding led to the identification of two jointly required pRB domains {Figure H-2}: the 'A domain', spanning amino acids 372 – 578 [1], and the 'B pocket', spanning amino acids 639 – 770 [2]. These regions have also been shown to be necessary for nuclear tethering of pRB<sup>1318</sup>, but not for growth suppression<sup>271</sup>. Structural studies<sup>761</sup> suggest that the B pocket domain forms a lobe containing an apical cleft which is the principal binding site [3]. The conformation of B, and therefore of the binding cleft, seems to depend on the intact presence of the A domain. The functional combination of these domains is referred to as the 'small A/B pocket'<sup>1067</sup>, and it is from this feature that pRB, p107, and p130 derive their designation of 'pocket proteins'.



Key: pRB A domain = light blue; pRB B pocket = green; LXCXE-containing nonapeptide from HPV E7 = dark blue. Data from Lee et al. <sup>761</sup>. Rendered by Cn3D {E.9}.

Figure H-2: The pRB small A/B pocket

### The large A/B pocket and the C-pocket

The pRB small A/B pocket is also necessary for binding of members of the E2F transcription factor family<sup>1067</sup>, and, while this may be sufficient for binding in vitro<sup>626</sup>, it seems likely that an additional pRB C-terminal domain within the region spanning amino acids 841 – 870<sup>516</sup> is required in vivo<sup>551</sup>. Together with the small A/B pocket, this is referred to as the 'large A/B pocket'. This additional requirement may



in part be a consequence of the absence of the LXCXE motif from E2F. This further suggests that distinct domains within the A/B region may mediate interaction between LXCXE-bearers and E2F, and therefore, this binding need not be competitive. Indeed, simultaneous binding may be essential for function.

This additional domain intersects with the binding domain of the ABL tyrosine kinase, located at amino acids 768 – 869 and termed the ‘C-pocket’<sup>1420</sup>. Despite the overlap, it appears that simultaneous binding by pRB of ABL via the C-pocket and either E2F via the large, or cyclin-D2 via the small A/B pocket is possible<sup>1419</sup>. Within the C-pocket, at amino acid 792, begins a domain implicated in the binding of MDM2<sup>1461</sup>. This same region, albeit imprecisely defined, has also been shown to be necessary and sufficient for the binding of PPP1CA<sup>301</sup>.

At the extreme C-terminal end of the C-pocket, a motif 870KXLKXL875 exists that is believed to constitute the principal pRB–cyclin interaction domain for those that do not carry the LXCXE motif, that is, non-D-cyclins. It may also provide an alternative interaction mode for those that do<sup>12</sup>. One consequence of this is that it is required for effective targeting of pRB by CDK2, but not CDK4. Unlike the relatively stable and abiding interaction between the small A/B pocket and cyclin-D1, that between a cyclin and the KXLKXL motif appears to be transitory, serving more to direct and orient the associated kinase with respect to its substrate than to promote an on-going association.

#### **The C-terminal region: amino acids 876 – 928**

Driscoll et al.<sup>294</sup> have identified a region spanning amino acids 880 – 900, dubbed ‘M89’, that appears to be a critical determinant of C-terminal pRB conformation, and can significantly affect the accessibility of pRB targets to modifying enzymes, in particular, CDKs. Their work extended to the identification of other key determinants of pRB conformation, noted in Table H-5, and provided the first insight into the structural basis for the multiple electrophoretic species of pRB seen.

Cyclin-D1 may have a third mode of interaction with pRB. Pan et al.<sup>996</sup> report that pRB L901 mediates a productive cyclin-D1 interaction that appears to be distinct from that involving the nearby KXLKXL motif. Whether interaction here influences the role of the immediately adjacent M89 region is unknown.

Within M89 is a sequence 883DEADG887, that is a site for caspase-dependent cleavage of pRB during apoptosis<sup>1300</sup>. It seems likely that such cleavage would prevent both the association of MDM2, and that of cyclin-D1 mediated via L901.

#### ***pRB-binding proteins***

##### **Scope of pRB–protein interactions**

At least 129 proteins are believed to interact directly with pRB<sup>®910</sup>, and a selection of these that have been, or potentially may be, associated with tumorigenesis, is listed in Table H-3.

##### **Competition for pRB binding**

There appear to have been no definitive and comprehensive studies either of the mutual competition among potential pRB binding proteins for access, or of any precedence among any such competitors. In some cases, specific data are available, and in others, reasonable inferences can be drawn based on the apparent necessity of a single, well-defined pRB domain for binding of more than one protein, as with the B pocket. Slightly less robust implication of non-competition exists in the form of apparent spatial separation and non-intersection of binding requirements. The situation is extremely complicated, as there are undoubtedly multiple interactions among protein binding, covalent modification, and conformation. Such data as pertains to representative proteins interacting via the better-defined pRB domains is given in Table H-4.

## Human metastatic melanoma in vitro

See Appendix I for information about BRCA1 super-complexes.

Protein	Motif(s)	pRB domain(s)	Significance
AATF <sup>341</sup>	DDLGSSEEE LKDLDEEIFD	-	Binding prevents pRB repression of E2F <sup>341</sup> AATF also mediates apoptosis <sup>994</sup>
ABL <sup>1420</sup>	VVLDSTEAL	C <sup>1420</sup>	Binding inhibits ABL kinase <sup>1420</sup>
AHR <sup>1061</sup>	DMLYCAESH	Probably AB <sup>1061</sup>	Dioxin carcinogenesis <sup>1061</sup>
ATF2 <sup>1000</sup>	-	C-terminus <sup>1000</sup>	JUN induction <sup>1360</sup> pRB autoinduction <sup>1000</sup>
BRCA1 <sup>22 340</sup>	QKLPCEENP KKLESSEEN	1) A?B 2) Another <sup>340</sup>	BRCA1 regulates genome surveillance <sup>1403</sup>
Cyclin-A <sup>12</sup>	-	870KXLKXL <sup>12</sup>	Proliferation regulation <sup>@268</sup>
Cyclin-E <sup>12</sup>	-	870KXLKXL <sup>12</sup>	Proliferation regulation <sup>@658</sup>
Cyclin-D1 <sup>288</sup>	HQLLCCEVE	1) A?B <sup>288 332</sup> 2) C-terminus <sup>@996</sup>	Mitogen response; proliferation regulation <sup>@1204</sup>
Cyclin-D2 <sup>@332 1420</sup>	MELLCHEVT	A?B <sup>@332</sup>	Mitogen response; proliferation regulation <sup>@1204</sup>
Cyclin-D3 <sup>288</sup>	MELLCCGEGT	A?B <sup>288 @332</sup>	Mitogen response; proliferation regulation <sup>@1204</sup>
E2F1	QSLLSLEQE	AB+ <sup>516 1067</sup>	Proliferation regulation <sup>615</sup> ; apoptosis <sup>@1027</sup>
E2F4 <sup>779</sup>	EELMSSEVF	AB+?	Cell-cycle arrest <sup>405</sup>
HDAC1 <sup>831</sup>	KRIACEE?EF? <sup>5</sup> 55	1) AB? 2) indirect? <sup>734</sup>	Chromatin modelling <sup>831</sup> Modulation of p53 activity <sup>820</sup>
HSP75 <sup>185</sup>	EVLFCFEQF	AB <sup>185</sup>	pRB chaperone in M-phase and after heat shock <sup>185</sup>
ID2 <sup>748</sup>	-	AB <sup>567</sup>	Implicated in proliferation, differentiation, and apoptosis <sup>363 749</sup>
JUN <sup>941</sup>	LKLSPELE	1) A?B <sup>941</sup> 2) C-terminus <sup>941</sup>	Implicated in proliferation, oncogenic transformation, and apoptosis <sup>@1193</sup>
MCM7 <sup>1261</sup>	-	N-terminal to amino acid 380 <sup>1261</sup>	DNA replication licensing {Appendix K}
MDM2 <sup>1461</sup>	QKDLVQELQ	C-terminus <sup>1461</sup>	Regulation of p53 activity {J-21}
MYC <sup>1121</sup>	QKLISEEDL SLLSSTESS	B <sup>1121</sup>	Cellular growth, proliferation, and apoptosis <sup>1015</sup>
p21 <sup>933</sup>	-	1) AB <sup>933</sup> 2) C-terminus? <sup>933</sup>	Proliferation regulation; senescence {J-14}
POLD1 <sup>720</sup>	GKLPCLIEIS	AB <sup>720</sup>	Binding stimulates enzyme activity <sup>720</sup> Required for S-phase DNA synthesis <sup>@521</sup> Required for DNA mismatch <sup>803</sup> and UVR repair <sup>1505</sup>
PPP1CA <sup>301</sup>	PDLQSMEQI	C-terminus <sup>301 1295</sup>	Regulation of pRB by dephosphorylation <sup>@1296</sup>
PRDM2 <sup>147</sup>	VNDLGESEEE PEDLLEPK TEDLPKEPL GIDLPVENP	A?B <sup>146</sup>	Tumour-suppressing, proapoptotic methyltransferase <sup>@154</sup>
prohibitin <sup>1400</sup>	-	B <sup>1400</sup>	Inhibitor of E2F transactivation <sup>1400</sup>
RAF1 <sup>1399</sup>	QILSSIPELL	A?B <sup>1399</sup>	Major receptor tyrosine kinase signal transduction element <sup>@656</sup>
RBBP1 <sup>344</sup>	ETLVCHEVD	Probably AB <sup>344</sup>	Repression of E2F-dependent transcription <sup>735</sup>
RBBP4 <sup>1066</sup>	LKLHSFESH	1) A?B? <sup>1066</sup> 2) Indirect <sup>948</sup>	Chromatin remodelling <sup>948 1445</sup>
RBBP7 <sup>1066</sup>	-	Probably A?B <sup>550</sup>	Modulation of BRCA1 function <sup>187</sup>
RBBP8 <sup>396</sup>	AELECEEDV	1) Probably AB <sup>396</sup> 2) Another? <sup>271</sup>	Modulation of BRCA1 function {J-21}
RBBP9 <sup>1443</sup>	TELHCDEKT	Probably AB <sup>1443</sup>	Role in cellular transformation <sup>1443</sup>
RFC1 <sup>915</sup>	ASLVCQELG KALGSKEIP GVLESIERD	Probably AB <sup>1017</sup>	Component of replication factor C; necessary for processive DNA synthesis.
TAF1 <sup>1190</sup>	KVLSSTEVL SDLDSDE	1) C <sup>1190</sup> 2) AB+ <sup>1221</sup>	RNA polymerase II regulation <sup>@1406</sup>
UBTF <sup>168</sup>	YSLYCAELM	Probably AB <sup>168</sup>	RNA polymerase I (ribosomal RNA) regulation <sup>1382</sup>

Key: - = no recognised motif, or no binding domain data; B = B-pocket; C = C-pocket; AB = small A/B pocket; AB+ = large A/B pocket; ? = domain implicated, but not proven to be necessary. Binding motifs and domains are described in the text.

Table H-3: Selected pRB-interacting proteins



pRB	RbK	HSP73	Cyclin-D1 <sup>a</sup>	E2F	ABL	MDM2	PP1 $\alpha$	Cyclin-A
HSP73	–							
Cyclin-D1 <sup>a</sup>	(+)	(+)						
E2F1	(+)	(+)	+					
ABL	(+)	(+)	+	+				
MDM2	(+)	(+)	(+)	X	(X)			
PP1 $\alpha$	(+)	(+)	+	(X)	(X)	(X)		
Cyclin-A	(+)	(+)	(+)	+	–	–	–	
Cyclin-D1 <sup>b</sup>	(+)	(+)	(+)	(+)	–	–	–	–

<sup>a</sup> = binding via LXCXE motif and small A/B pocket. <sup>b</sup> = binding via pRB C-terminal domain

Key: X = compete for binding; + = can bind simultaneously; – = no data; (+), (X) = inferred

**Table H-4: Competition matrix for pRB binding**

### Phosphorylation of pRB

The earliest studies of the retinoblastoma-associated protein revealed that it was a nuclear phosphoprotein<sup>767</sup>, and that differences in phosphorylation status accounted for the multiplicity of electrophoretic species<sup>393</sup> seen. This observation facilitated the discovery that the phosphorylation state of pRB altered in synchrony with progression through the cell division cycle, with it being minimally phosphorylated upon synthesis and rapidly and sequentially phosphorylated at the G<sub>1</sub>-S transition<sup>888</sup>. The basis for this sequencing lies partly in subtle differences in substrate specificity of the relevant kinases<sup>1501</sup> and partly in their successive activation. It is also believed that conformational changes wrought by earlier phosphorylations are necessary to allow subsequent access to other sites. The significance of this sequential phosphorylation lies in the apparent independence of control of protein binding among the different interaction domains within pRB<sup>694</sup>. The proportion of phosphorylated pRB decreases at the beginning of anaphase<sup>812</sup>, indicating the existence of regulated phosphatase activity.

### pRB kinases

It was soon found that pRB was a substrate for the CDC2 kinase in vitro<sup>788</sup>, and of this<sup>768</sup>, or related kinases in vivo<sup>690</sup>. The latter possibility was confirmed with the discovery that pRB was a substrate of CDK2<sup>20</sup>, CDK4<sup>645</sup>, and the closely related CDK6<sup>885</sup>. Of the sixteen potential SER/THR-PRO CDK targets in pRB, thirteen have been found to be phosphorylated in vivo {Figure H-1} and considerable data concerning the timing, kinase-specificity and consequence of these phosphorylations have been gathered {Table H-5}.

Upon mitogen stimulation, pRB is phosphorylated by RAF1 before it is by cyclin-D-CDK4<sup>1399</sup>. This may provide an efficient link between RTK activation and the abrogation of pRB growth-suppression operative independently of that supplied by cyclin-D regulated kinases. This also places pRB downstream of RAS, and so may contribute to the oncogenic potential of the latter<sup>1014</sup>.

The RbK kinases of Sterner et al., also phosphorylate the pRB N-terminus during G<sub>2</sub>/M, and are apparently distinct from CDC2, CDK2, CDK4, MAPK1, and MAPK3<sup>1260</sup>.

### pRB phosphatases

Given the established importance of pRB phosphorylation, and the emerging biological importance of balanced antagonistic kinase/phosphatase pairs, there is a surprising dearth of data concerning the identity and regulation of pRB phosphatases. Using a system based upon the yeast two-hybrid screen of Fields and Song<sup>352</sup>, Durfee et al.<sup>301</sup> identified and cloned a protein that directly interacted with pRB, and was found to be the catalytic subunit of a type I protein phosphatase complex (PP1), PP1CA2. Through pRB immunoprecipitation of extracts of human cells at intervals after release from density-arrest, they found that the association of PP1CA2 with pRB was cell-cyclical, occurring in G<sub>1</sub>, diminishing

throughout S and G<sub>2</sub>, and returning in M-phase. By gel-mobility shift, PP1CA2 was inferred to bind the hypophosphorylated form of pRB, although binding to phosphorylated pRB was not ruled out. Ludlow et al.<sup>812 813</sup> have pursued the timing of dephosphorylation and found that it progresses sequentially.

The mode of physical interaction between pRB and PP1 has not been determined unequivocally. Several authors<sup>301 1296</sup> have suggested that the LXSXE sequences present imply association via the small A/B pocket, and therefore in competition with, and susceptible to the same regulation as, carriers of the LXCXE motif. Such an interaction is difficult to reconcile with the ability of PP1CA2 to bind a pRB construct that lacks the entire B domain, but the inability to bind one lacking only the region C-terminal to this<sup>301</sup>. More recent work has provided strong evidence that it is in fact the C-terminal region of pRB that associates with PP1, and in so doing, non-competitively inhibits its phosphatase function<sup>1295</sup>. This does not necessarily preclude the involvement of LXSXE, or the overlapping DLXXE, in this interaction [Table H-3], or that there may also be some affinity between PP1 and the small A/B pocket. It has been established that, as with other pRB-interacting proteins, the binding of PP1 is regulated by the phosphorylation state of pRB, specifically, that phosphorylation of S249, T373, S811, T821, or T826 prevents association at the C-terminus, while that of S608, S612, S780, or S807 does not<sup>1296</sup> [Table H-5].

On initial consideration, it appears paradoxical that an enzyme should be inhibited by its principal substrate: how could it ever function? Further reflection in the context of cyclical control of pRB phosphorylation, yields an attractive explanation for this. With PP1 bound to pRB and inhibited, any newly activated pRB kinase can phosphorylate pRB unopposed. In so doing, it may cause the release of proteins bound to pRB, with potentially far-reaching effect. In some cases, the particular pRB molecule that is phosphorylated may have been sequestering PP1, and this too would be released and disinhibited. If the kinase phosphorylated sites that also prevented re-association of PP1 with pRB, then it would be free to oppose the kinase and dephosphorylate pRB. This in turn may render pRB once again able to bind and inhibit PP1, completing the cycle. The net result of these interactions is to provide a limited period during which a variety of pRB regulated enzymes may be activated. This is consistent with the observed cell-cyclical nature of the pRB-PP1 association. In addition to being attractive from a mechanistic viewpoint, such a scenario also explains the otherwise problematic observation that despite inhibition of PP1 by pRB, the former is able to dephosphorylate the latter in vitro. The sequence of events would be that phosphorylated pRB, unable to bind and inhibit PP1, is dephosphorylated by it, whereupon it immediately proceeds to bind and inhibit it.

### *pRB acetylation*

Chan<sup>176</sup> et al. have established that pRB is also the subject of cell-cycle synchronised acetylation, and that this materially affects pRB function by hindering phosphorylation by CDKs and enhancing its affinity for MDM2. The ramifications of this novel aspect of pRB regulation remain to be explored.





S/T	Phosphorylation	Dephosphorylation	Relevance of phosphorylation
T5	In vivo phosphorylation not reported		
S230	In vivo phosphorylation not reported		
S249	Inaccessible when LXCXE bound <sup>1501</sup> Phosphorylated by cyclin-D1-CDK4, but may require prior T826 phosphorylation <sup>1501</sup>	Begins at M; complete by M+60 min <sup>S1116</sup> Dephosphorylated in response to TGFβ1 <sup>547</sup>	May prevent PP1α binding <sup>1296</sup>
T252	Inaccessible when LXCXE bound <sup>1501</sup> Phosphorylated by cyclin-D1-CDK4, but may require prior T826 phosphorylation <sup>1501</sup>	Begins at M; complete by M+60 min <sup>S1116</sup> Dephosphorylated in response to TGFβ1 <sup>547</sup>	No data available
T356	Phosphorylated by cyclin-D1-CDK4 <sup>1501</sup> Not phosphorylated by cyclin-A-CDK2 <sup>1501</sup>	Begins at M; complete by M+60 min <sup>S1116</sup>	Likely to affect pRB conformation <sup>294</sup>
T373	Phosphorylated by cyclin-D1-CDK4 <sup>1501</sup> Begins at M+30 min; complete by G <sub>1</sub> <sup>S1116</sup>	Begins at M; complete by M+30 min <sup>S1116</sup> Dephosphorylated in response to TGFβ1 <sup>547</sup>	May prevent PP1α binding <sup>1296</sup>
S567	No in vivo phosphorylation reported, but suggested based on in vitro data <sup>480</sup> . Not solvent accessible <sup>761</sup> . Mutation prevents pRB-mediated growth arrest and affects protein binding and phosphorylation <sup>1318</sup> .		
S608	Phosphorylated by cyclin-D1-CDK4 and cyclin-A-CDK2, but not cyclin-E-CDK2 <sup>1501</sup> Increases during M-phase, peaks at M+30 min <sup>S1116</sup>	Begins after M+30 min <sup>1296</sup> Complete after M+4 h <sup>S1116</sup> , that is, in G <sub>1</sub>	Probably prevents E2F binding <sup>695</sup>
S612	Phosphorylated by cyclin-A/E-CDK2 but not cyclin-D1-CDK4 <sup>1501</sup>	No data available	Probably prevents E2F binding <sup>695</sup>
S780	Phosphorylated by cyclin-D1-CDK4 but not cyclin-E-CDK2 <sup>689</sup> Increases during M-phase <sup>1296</sup> Peaks at M+30 min <sup>S1116</sup>	Begins after M+30 min; complete after M+6 h <sup>S1116</sup> , that is, in G <sub>1</sub> Dephosphorylated in response to TGFβ1 <sup>547</sup>	Probably prevents E2F binding <sup>689 695</sup>
S788	Phosphorylated by cyclin-D1-CDK4 <sup>1501</sup>	Begins at M; complete by M+ 60 min <sup>S1116</sup>	Probably prevents E2F binding <sup>695</sup>
S795	Phosphorylated by cyclin-D1-CDK4 and cyclin-A/E-CDK2 <sup>1501</sup> Inaccessible when LXCXE bound <sup>1501</sup> Begins at M+30 min; complete by G <sub>1</sub> <sup>S1116</sup>	Begins at M; complete by M+30 min <sup>S1116</sup>	Probably prevents E2F binding <sup>695</sup>
S807	Inaccessible when LXCXE bound <sup>1501</sup> Phosphorylation increases during early M-phase <sup>1296</sup>	Begins at M; complete by M+40 min <sup>S1116</sup> Dephosphorylated in response to TGFβ1 <sup>547</sup>	Likely to affect pRB conformation <sup>294</sup> Facilitates further pRB phosphorylation <sup>294</sup> Probably prevents E2F binding <sup>695</sup> Causes dissociation of pRB-ABL complex <sup>694</sup>
S811	Phosphorylated by cyclin-D1-CDK4 <sup>1501</sup>	Dephosphorylated in response to TGFβ1 <sup>547</sup>	Likely to affect pRB conformation <sup>294</sup> Facilitates further pRB phosphorylation <sup>294</sup> Probably prevents E2F binding <sup>695</sup> Causes dissociation of pRB-ABL complex <sup>694</sup> May prevent PP1α binding <sup>1296</sup>
T821	Phosphorylated by cyclin-A/E-CDK2 but not cyclin-D1-CDK4 <sup>1501</sup> Increases from soon after M-phase onset, peaks by M+40 min <sup>S1116</sup>	Never fully dephosphorylated <sup>S1116</sup> May not be a target of PP1 isoforms <sup>S1116</sup> Rapid, partial dephosphorylation begins at M <sup>S1116</sup> Second partial dephosphorylation begins at M+40 min <sup>S1116</sup>	Likely to affect pRB conformation <sup>294</sup> Probably <sup>1501</sup> prevents LXCXE binding, but some doubt exists <sup>S1116</sup> May prevent PP1α binding <sup>1296</sup> May dissociate preformed pRB-LXCXE <sup>1501</sup>
T826	Inaccessible when LXCXE bound <sup>1501</sup> Phosphorylated by cyclin-D1-CDK4 but not cyclin-A/E-CDK2 <sup>1501</sup>	Begins at M-phase onset; complete by M+10 min <sup>S1116</sup> Preferentially targeted by PP1δ <sup>1296</sup>	Prevents LXCXE binding <sup>1501</sup> May prevent PP1α binding <sup>1296</sup> Does not dissociate existing pRB-LXCXE <sup>1501</sup> Prerequisite for S249 and T252 phosphorylation <sup>1501</sup>

M = time of release of green monkey kidney fibroblast cells from nocodazole inhibition<sup>S1116</sup>.

Table H-5: pRB phosphorylation summary

## H.4 Phosphorylation-dependent regulation of proliferation by pRB

### A minimal proof

That pRB could influence the progression through the cell division cycle was unambiguously demonstrated by Goodrich et al., who injected purified pRB into proliferating cells and discovered that it prevented passage into S phase from G<sub>1</sub><sup>426</sup>. This effect could be overcome by the simultaneous expression of cyclin-A or cyclin-E<sup>522</sup>, suggesting that it was phosphorylation of pRB by a CDK that was critical, a possibility supported by the increased phosphorylation of pRB seen in this experiment. Co-expression of E2F1 was also able to overcome the G<sub>1</sub> arrest, and do so without influencing pRB phosphorylation<sup>615</sup>, establishing that E2F1 acted either downstream, or independently of pRB. The former appeared the more likely as E2F1 was known to bind pRB and thereby be functionally inhibited<sup>357</sup>. Further support came from the finding that E2F1 bound unphosphorylated pRB, but not that phosphorylated by cyclin-A-CDK2, cyclin-E-CDK2 or cyclin-D1-CDK4<sup>1281</sup>. The final link necessary to connect pRB with entry into S-phase, and therefore control of cellular proliferation, is provided by the preponderance of genes among the transcriptional targets of E2F1 whose encoded proteins are critical to this progression. Among these proteins are DNA pol- $\alpha$ , TS, PCNA, cyclin-E, cyclin-A, and CDC2<sup>253</sup>. Therefore, it can reasonably be concluded that the phosphorylation-dependent release of E2F1 from pRB inhibition regulates progression from G<sub>1</sub> to S phase. As a corollary, whatever influences the phosphorylation status of pRB is likely to influence progression through the cell-cycle<sup>252</sup>.

See J-12 for an overview of CDK activation.

### A model scenario

#### Caveat lector

The enormous complexity of pRB interactions defies exposition in any readily assimilable manner. Nevertheless, a 'thought experiment' involving a model system, wherein cells arrested in G<sub>1</sub> by virtue of an absence of mitogens are stimulated to proliferate, can provide a basis from which a possible sequence of events can be deduced from experimental observations. Of necessity, simplifying assumptions have been made. For each of the proteins cited, multiple close relatives with overlapping but distinct characteristics exist, and their expression and interactions may vary with organism, cell-type, and physiological context. As a result, the scenario presented may be neither generally applicable, nor even applicable in any particular case.

#### G<sub>1</sub> arrest

When cells arrest in G<sub>1</sub> for want of mitogenic stimulation, pRB is essentially unphosphorylated and therefore competent to bind proteins via any of its interaction domains. E2F1/2/3-DP1/2/3 transcription factors, able to associate via the pRB large A/B pocket are favoured candidates, and in this way pRB is localised to the promoter of E2F-regulated genes. The interaction between these molecules involves the transactivation domain of E2F, and this is thought to contribute to gene repression.

This binding does not prevent pRB interacting with additional proteins through other domains. There is general agreement<sup>131 831</sup> that pRB is able to recruit active HDAC1 to E2F, but opinion is divided over how this occurs. Much of the controversy centres on the putative binding of the HDAC1 IXCXE sequence to the pRB small A/B pocket. Magnaghi-Jaulin et al.<sup>831</sup> found that deletion of this sequence strongly decreased binding, as did the presence of a synthetic IXCXE peptide, while an LXCXE peptide was an even better competitor. Consistent with this, Dahiya et al.<sup>234</sup> found that mutation of the pRB LXCXE binding cleft prevented HDAC1 association. Conversely, two groups have arrived at precisely the opposite conclusion<sup>271 655</sup>. The second area of controversy is over whether the interaction between pRB and HDAC1 is direct or mediated by an additional protein. The results of Magnaghi-Jaulin et al.<sup>831</sup>



support the notion of a direct interaction between the two, involving the A/B pocket, but not the C-terminal region of pRB. Others have proposed a matchmaking role for RBBP1<sup>734</sup> or RBBP4<sup>655</sup>. These apparently contradictory results are perhaps most easily reconciled by assuming that all of these interaction modes occur, and that differences in experimental conditions are responsible for the discordant results.

However HDAC1 binds pRB, it does so coincidentally with pRB dephosphorylation<sup>1064</sup>, being bound in early G<sub>1</sub>. At that time, it deacetylates amino-terminal lysine amino acids of nucleosomal core histones, reinstating the positive charge there. This is thought to enhance the affinity of the core for DNA, and thereby deny access to the promoter by the transcriptional apparatus and thus repress the gene. It is released at the transition to S-phase<sup>1064</sup>, coincident with the observed acetylation of histone H4<sup>350</sup> and nucleosomal relaxation.

With many genes whose transcription is necessary for S-phase progression having E2F binding sites in their promoters, unphosphorylated pRB, will cause cell-cycle arrest at this point.

### *Release from inhibition*

#### **Cyclin-D1 elevation**

There is a low level of constitutive expression of *CCND1* mediated through CREs in its promoter<sup>929</sup>, but in the absence of mitogenic stimulus, cyclin-D1 is rapidly degraded via the ubiquitin-directed proteasomal subsystem<sup>274 412</sup>, its half-life being of the order of ten minutes. This situation changes abruptly upon mitogen stimulation, when cyclin-D1 levels rise dramatically<sup>814</sup>. Two mechanisms are thought to be involved in this elevation.

Firstly, the rate of transcription of *CCND1* is increased. While studies in a variety of cell-types have uncovered elements of the signal transduction path leading to this activation, no overall pattern of general applicability has yet emerged, and apparent contradictions exist. The transcription factor MYC directly induces cyclin-D2<sup>124</sup>, and probably also cyclin-D1<sup>1018</sup>, and consistent with this, the level of cyclin-D1 expression closely parallels the activation of MYC. The transcription factor LEF1 has also been shown to contribute to *CCND1* expression<sup>1216</sup>. Strongly implicated are proteins with homology to RAS. RAS itself may initiate multiple independent molecular cascades leading to increased *CCND1* transcription. When activated by ectopic expression<sup>353</sup>, or by PDGF<sup>995</sup> stimulation, it can increase *CCND1* transcription via MEK1, MAPK1, and ultimately SP1 sites<sup>929</sup> in the promoter. Additionally, it may operate via MAPK3 and JUN, ultimately via an AP-1 promoter site<sup>23</sup>. The role of the different MAPK enzymes is not entirely clear as p38MAPK has been reported both to enhance *CCND1* transcription via ATF2 promoter sites in response to HGF stimulation<sup>1083</sup>, but also to cause a reduction in this rate<sup>754</sup>. Two RAS homologues, Rac1<sup>5624</sup> and Ral<sup>5504</sup> have been shown to influence *CCND1* transcription, apparently via the NF-κB subsystem.

The second mechanism of cyclin-D1 elevation is the enhancement of protein stability, and here, members of the PI3K family are involved. In addition to possible activation by RAS, PI3K is also downstream of G-protein-coupled membrane receptors<sup>1162</sup>, providing a further link between extracellular conditions and cyclin-D1 regulation. However activated, PI3K, probably via AKT1<sup>417</sup> or another protein kinase B, can inhibit the GSK3β enzyme that is responsible for phosphorylation of cyclin-D1 T286<sup>274</sup> which would otherwise mark it for nuclear export<sup>30</sup> and accelerated degradation<sup>275</sup>. Without this proteolysis, the half-life of cyclin-D1 rises to over one hour.

The mechanisms of enhanced cyclin-D1 expression are very complex, with multiple inter-links among the RAS, MYC, MAPK, and PI3K subsystems, multiple binding sites in the promoter, and multiple independent degradative pathways<sup>417 @1169</sup>.

### CDK4 activation

With cyclin-D1 levels elevated, and its cellular disposition increasingly nuclear, the opportunity for interaction with CDK4 increases. With three provisos, this will enable the CDK4 kinase function. Firstly, the association of cyclin-D1 with CDK4 is dependent on a serum-inducible assembly factor<sup>859</sup>, possibly p21<sup>1003</sup> [J-17]. Secondly, CDK4 activity depends on its phosphorylation state, which in turn depends on the relative activities of CAK and CDC25A, which is itself subject to upstream regulation. Finally, complex assembly and kinase activation are both subject to inhibition by CKIs, particularly p16<sup>CDKN2A</sup> and its relatives, and this may be further influenced by gankyrin {See 'Turnover of pRB', above}. Clearly, CDK4 is at a major regulatory node.

See J-12 for a discussion of the analogous situation with respect to CDK2.

### Initial pRB phosphorylation

Cyclin-D1, in this case, with its attendant activated CDK4 partner, can bind pRB either via the latter's small A/B pocket and its own LXCXE motif, or via an additional C-terminal pRB domain {Table H-3}. Within the constraints of the model scenario being explored, only the second docking mode is available since the small A/B pocket is hypothesised to be occupied by HDAC1 or its linking protein. This has important implications for the functional scope of CDK4 since when docking is via the pRB C-terminus, S807 and S811 cannot be phosphorylated<sup>996</sup>. Furthermore, a number of pRB CDK4 target sites are inaccessible when a protein is occupying the B pocket<sup>1501</sup>. Phosphorylation at one of these, T826, appears to be a prerequisite for subsequent phosphorylation at S249 and T252, possibly influencing the regulation of N-terminal interacting proteins. These phosphorylations cannot therefore proceed at this time. Of the thirteen in vivo phosphorylation targets within pRB, given the substrate specificities, pRB conformation and steric constraints, the immediate CDK4 targets available in the model scenario are T356, T373, S608, S780, and S788.

### Persistence of small A/B pocket interactions

These initial phosphorylations do not appear to suffice to cause the general dissociation of proteins interacting with pRB via the small A/B pocket as phosphorylation of T821 may be essential for this, and it is not a substrate for CDK4<sup>1501</sup>. While T826 is a potential CDK4 target, phosphorylation here may not cause dissociation of existing complexes, even if it can prevent their formation<sup>1501</sup>. This may be moot in this instance since T826 appears to be inaccessible when any protein is occupying the B pocket, as is assumed here. Hence, proteins interacting with pRB via their LXCXE motif and the small A/B pocket are immune to eviction by cyclin-D1-CDK4.

The situation is less clear with respect to HDAC1, as the mode of its attachment is uncertain. It has been suggested by Harbour et al.<sup>480</sup> that phosphorylation of pRB by CDK4 is sufficient to cause dissociation of pRB-HDAC1 complexes, but some doubt exists over this. Certainly, in co-transfection experiments they were able to establish that the ability of HDAC1 to bind via the pRB small A/B pocket is disrupted in the presence of cyclin-D2. Simultaneously, they found that a co-expressed pRB C-terminal fragment became phosphorylated, and that irrespective of its phosphorylation state, it was able to bind the pRB small A/B pocket, even when HDAC1 could not. However, their conclusion that the C-terminal domain is involved in inhibiting binding of HDAC1 is questionable. They appear to have given no consideration to the ability of co-expressed cyclin-D2 to interact directly with the small A/B pocket via its LXCXE motif. Within the context of a co-transfection, expressed cyclin-D2 could simply have out-competed HDAC1 or



its linking protein for binding. Nor did they address the possibility that cyclin-D2-dependent phosphorylation of the small A/B pocket itself may have inhibited HDAC1 binding. Unfortunately, based on this report, the suggestion that cyclin-D-CDK4 can displace HDAC1 from pRB has entered the literature and been adopted<sup>1296</sup>.

### Transcriptional activation

Notwithstanding this uncertainty, a mechanism exists whereby HDAC1 can be removed from the proximity of the promoter in consequence of CDK4 phosphorylation. It depends not on the severance of the link between pRB and HDAC1, but on that between pRB-HDAC1 and E2F. Phosphorylation at S608, S780, or S788 is sufficient to prevent binding of E2F to pRB<sup>695</sup>, and while there appear to have been no definitive studies, it is assumed to suffice to dissociate existing complexes. If so, an early consequence of CDK4 activation will be the detachment of pRB, with its attendant histone deacetylase complex, from the promoter-bound E2F transcription factor. With the local deacetylase concentration reduced, acetylation of the core histones becomes possible, and with it, a loosening of the nucleosomal structure and the granting of access for the transcription apparatus to the E2F-regulated gene. This process has been reported recently in some detail by Morrison et al. with respect to the gene for cyclin-E1<sup>891</sup>.

Interestingly, TAF1, a component of the RNA polymerase II complex with serine kinase<sup>279</sup>, histone acetyltransferase<sup>898</sup>, and ubiquitin ligase capacity<sup>81025</sup>, also binds pRB via the large A/B pocket, resulting in the inhibition of its kinase, but not its acetyltransferase function<sup>1221</sup>. While it has not been established experimentally, the apparent coincidence of pRB domains mediating E2F and TAF1 interaction suggests that TAF1 may also be evicted from pRB complexes by activated CDK4. This would be consistent with the reported ability of cyclin-D1 to bind TAF1 independently of pRB and prevent the inhibition of its kinase function by the latter<sup>1222</sup>. This interaction may also affect transcription from promoters containing SP1 binding sites<sup>15</sup>. This modulation of TAF1 function may well influence RNA polymerase II transcriptional rate or specificity at exactly the time when such a control is required: the onset of S-phase<sup>1406</sup>.

Following the de-repression of E2F-regulated genes, many of which encode proteins essential for the synthesis and repair of DNA<sup>1039</sup>, there follows a period of active transcription and protein synthesis in preparation for S-phase. It is at some point during this period that entry into S-phase becomes inevitable.

### Passage through the restriction point into S-phase

The term 'restriction point' was coined by Arthur B. Pardee<sup>999</sup> to describe:

...a single switching point in  $G_1$  ... that regulates the reentry [sic] of a cell into a new round of the cell cycle.

*Proceedings of the National Academy of Sciences of the USA*, 71:1286-90, 1974

Factors that cells may encounter in vivo, such as 'high cell density, nutrient or serum insufficiency, or high cAMP [levels]' would cause an arrest at this point, while 'non-physiological agents such as hydroxyurea or colchicine' would not. The reference to cAMP as a cause of arrest in its own right reveals that its role in signal transduction was then unrecognised. The principle that Pardee wished to establish was that stimuli of diverse origins converged at a unique, crucial, biochemical decision point. If passed, a cell would be committed to continuing through the cell-cycle.

For a time, it was thought that passage beyond this point signified a commitment to execute a complete cellular division, and that it was the only physiological determinant of this progression. This has proven not to be the case, nor was it ever suggested by Pardee, who proposed only that it controlled re-entry to the cycle. The restriction point must be considered only as a point of commitment to enter S-phase, but this is still a very significant function that is now recognised to contribute not only to the integration of extracellular growth signals, but also to purely internal signals, particularly those related to differentiation and senescence. From this definition, it is reasonable to conclude that it is the de-repression of E2F that is the crucial step that constitutes this transition. CDK4-sponsored release of E2F from pRB may be an initial step, but it does not suffice. As described, phosphorylation of pRB by CDK4 may lead to the release and disinhibition of PP1, an antagonistic phosphatase, and the phosphorylation state of pRB becomes dependent on which of the two predominates. If mitogen stimulation continues, cyclin-D continues to be elevated, and CDK4 remains active. If mitogen stimulation abates, or a CDK4 inhibitor is induced, the phosphatase will prevail and E2F will be again sequestered. To this point, the process remains reversible, and the restriction point has not been passed.

Under these conditions, there will be some transcription of E2F targets, although this may be intermittent. Among these is *CCNE1*, the gene for one isoform of cyclin-E<sup>409</sup>. *CCNE2*, the second cyclin-E gene may also be under E2F regulation, but this has not yet been established conclusively<sup>840</sup>. In time, with continuing CDK4-dependent partial activation of E2F, production of cyclin-E will outpace its degradation, and activated CDK2 will enter the equation. Two properties of cyclin-E-CDK2 are of note at this point. Firstly, it is not subject to inhibition by a major class of CDK4 inhibitors, the p16-related CKIs. Thus, if activation of CDK4 had been being constrained by the presence of such inhibitors, but still had managed to rise to a level sufficient to allow the accumulation of cyclin-E, the inhibitors immediately lose any ability to constrain further progression. The second salient feature is that activation of CDK2 by ectopic expression of cyclin-E is sufficient to promote S-phase entry, and, most importantly, do so even in the presence of a non-phosphorylatable form of pRB<sup>815</sup>. The inference therefore is that the only critical target of E2F may be cyclin-E. The production of other proteins from E2F-regulated genes may be rate-limiting for DNA synthesis, but it seems that even constitutive levels of expression are sufficient to allow its commencement.

While immune to inhibition by p16-related CKIs, CDK2 is subject to regulation by p21-related CKIs, in particular, p27. Cyclin-D1-CDK4 also binds and is inhibited by p27<sup>1336</sup>, and an interesting dynamism exists in the inter-relationships among p16, p27, cyclin-E-CDK2, and cyclin-D1-CDK4. When p16-related inhibitors are absent, whatever p27 is present in the cell will bind cyclin-D1-CDK4 as it is produced, delaying the onset of pRB phosphorylation. However, once it starts, and cyclin-E-CDK2 begins to accumulate, it will do so in the absence of competition from p27. Furthermore, p27 is itself a CDK2 substrate, and when phosphorylated, becomes the subject of ubiquitin-directed proteolysis<sup>1379</sup>, further enhancing CDK2 activity. Conversely, if p16-related inhibitors are present, such p27 as exists is free to inhibit the low levels of activated CDK2 that may be produced under these circumstances, and thus forestall the self-reinforcing accumulation of CDK2. The apparent induction of p16 upon pRB phosphorylation would contribute to this<sup>783</sup>.

See J-14 for more on p27 regulation.

See Appendix K for a discussion of DNA replication licensing, including the role of CDC6.

While the critical CDK2 target has not been identified, a strong candidate is CDC6, a component of the DNA replication licensing subsystem. CDC6 is an excellent in vitro substrate for cyclin-E-CDK2, with the same pattern of phosphorylation as is seen in vivo, and this phosphorylation is required for the



initiation of DNA synthesis<sup>609</sup>. In serum-deprived cells, ectopically expressed CDC6, in conjunction with cyclin-E-CDK2, but not cyclin-A-CDK2, results in the commencement of DNA replication<sup>S220</sup>.

### Further pRB phosphorylation

Within the model scenario under consideration, the activation of CDK2 assures entry into S-phase, and synchronisation with the centrosomal division cycle. If these functions were considered insufficiently noteworthy, it has yet another role: further phosphorylation of pRB, probably mediated via the pRB C-terminal KXLKXL sequence<sup>12</sup>. Immediate CDK2 targets include S612 and T821. The significance of the first is unknown, but the second is thought to bring about a conformation change<sup>294</sup> that reduces the affinity of the small A/B pocket for LXCXE-bearing proteins, and probably causes dissociation of such complexes<sup>1501</sup>. With their departure, other sites previously masked from the cyclin-D1-CDK4 complex docked at the C-terminus become available including S795, also a target of CDK2, and T826. Phosphorylation at the latter then renders S249 and T252 available to cyclin-D1-CDK4<sup>1501</sup>. In the final step, cyclin-D1-CDK4 complexes can now dock via the vacant small A/B pocket, even if only transiently, and effect the phosphorylation of S807 and S811, inaccessible from the C-terminus. In consequence of these alterations, ABL is released and disinhibited whereupon it is thought to take part in the monitoring of genomic integrity in conjunction with ATM and p53<sup>662</sup>. There is a functional parallel here with the simultaneous induction of ARF by E2F1 resulting in increased levels of p53 [J-21].

Phosphorylation at all of the sites where it is seen in vivo has now been completed. Interestingly, it occurred in five stages, the same as the number of major pRB electrophoretic species discernible in Western blots of asynchronous populations<sup>294</sup>. The functional consequences of these final phosphorylations have yet to be fully explored, and given the very large number of proteins that interact with pRB, this will be no small feat.

### Maintenance of pRB phosphorylation

The reign of cyclin-E-CDK2 is relatively short-lived. By activating CDK2, cyclin-E has been the author of its own demise since its phosphorylation at T380 by CDK2 results in its degradation via ubiquitin-directed proteolysis<sup>1446</sup>. The preferred model has it that this phosphorylation causes the dissociation of cyclin-E from CDK2, rendering it subject to the ubiquitin-ligase function of CUL3<sup>1233</sup>. Nevertheless, phosphorylation of pRB can be maintained as rising cyclin-A, another E2F1 target, continues to activate CDK2.

### Dephosphorylation of pRB

This too comes to an end in metaphase, when cyclin-A also becomes a target of proteasomal degradation, here at the instigation of the cyclosome. Only then does the driving force behind pRB phosphorylation abate sufficiently to allow the opposing phosphatase any opportunity to reverse the process. Like its phosphorylation, the dephosphorylation of pRB is synchronised with the cell-cycle and appears to be incremental<sup>S1116</sup>.

### Variations on the theme

#### *Continuous cycling*

The extent of dephosphorylation depends in large measure on the cellular context at the time. In particular, if mitogens are still present and p16-related inhibitors absent, cyclin-D1-CDK4 will still be active, although RAS stimulation of *CCND1* may only be operative in G<sub>2</sub><sup>S527</sup>. Not only will this prevent complete dephosphorylation of pRB by antagonising PP1 activity, it may modify PP1 directly through phosphorylation<sup>689</sup>. In any case, cyclin-D1-CDK4 can only oppose PP1 with respect to sites that are substrates for both. Thus, the initial dephosphorylation may be limited to S612 and T821. However,

See Appendix J for a discussion of centrosome molecular biology.

transient dephosphorylation of T826 may occur, and during the period when both T821 and T826 are dephosphorylated, pRB again has the capacity to interact via the small A/B pocket. Subsequent re-phosphorylation of T826 by cyclin-D1–CDK4 may be insufficient to dissociate such a newly formed complex. One consequence of this that S249 and T252 may also be subject to dephosphorylation as access by cyclin-D1–CDK4 here depends on prior T826 phosphorylation and is hindered by B-pocket occupancy, unless, presumably, the occupant is cyclin-D1 itself. This raises a further distinction between the situation that pertains in cells released from mitogen deprivation and those cycling continuously. In the latter case, this mode of docking is available to cyclin-D1, whereas in the former, it is denied access by the presence of HDAC1 or its linking protein. Now, the tables are turned, and cyclin-D1 is in the position to prevent the recruitment of the deacetylase complex. In addition, S807 and S811 will be subject to phosphorylation, albeit transiently, and can partially impede re-sequestration of ABL. Finally, the continuing phosphorylation of S795 probably suffices to prevent re-association between pRB and E2F.

In all probability then, in the continuing presence of mitogenic stimulation, all of the recognised means by which pRB constrains proliferation are disabled. This does not imply that such cells can cycle freely. Requirements of chromatin decondensation, E2F production, CDK2 activation, and DNA replication licensing must still be met. A change in cyclin-D1 status before the next passage through the restriction point would alter the situation markedly.

### *Inhibitory cytokines*

Inhibitory cytokines have the capacity to prevent cellular proliferation even in the presence of mitogens. One of the better studied and understood of these is TGF $\beta$ , a potent inhibitor of epithelial cell division. It has been found to operate through several signal transduction channels including SMAD<sup>594</sup>, MAPK<sup>546</sup>, and PI3K<sup>62</sup> subsystems, and several mechanisms of engendering cell-cycle arrest in G<sub>1</sub> have been identified. It depresses MYC transcription<sup>1473</sup> and possibly via this, reduces cyclin-D1 expression<sup>697</sup> and induces p15<sup>CDKN2B1179</sup>, an inhibitor of CDK4; it induces p21<sup>CDKN1A998</sup>, an inhibitor of CDK2; it decreases the activity of both CDC25A<sup>565 566</sup> and CAK<sup>928</sup>, contributing to the inactivation of existing CDKs; and it may interfere with the translation of CDK4 mRNA<sup>893</sup>. These results suggest very strongly that modulation of the pRB subsystem is an important component of the growth inhibitory effect of TGF $\beta$ .

### *Cellular senescence*

Observations by Leonard Hayflick<sup>538 @1197</sup> revealed that cultured human fibroblasts could sustain only a limited number of population doublings prior to undergoing a phenotypic change and ceasing to proliferate. In contrast, cultures derived from tumours appeared to be immortal. This established as the norm the concept of cellular, or replicative, senescence, an inherent proliferative limitation, and its defeat as a feature of neoplastic transformation. Its existence implies a cellular memory that survives mitosis, but the molecular basis of this memory is still a subject of experiment and debate.

An extremely attractive candidate mechanism involves the maintenance of the distinctive base sequences found at the termini of chromosomal DNA, known as telomeres<sup>@1263</sup>. The normal process of DNA replication cannot access these final bases since new bases are appended at the trailing edge of the polymerase as it proceeds along the template strand. When it reaches the terminus and dissociates, the single-stranded sequence to which it had been binding must remain unreplicated. This is a progressive process, and in most tissues, telomeres are seen to shorten with each round of DNA synthesis<sup>28</sup>. In some tissues however, the enzyme telomerase is expressed that has the capacity to concatenate telomere





sequences onto these termini using an inherent RNA template; it is, therefore, a reverse-transcriptase, the first found in eukaryotes. Such tissues include the germ-line and those with an extremely high cellular turnover rate, such as haematopoietic cells and cells of the intestinal lining. Aberrant expression of telomerase is also a feature of cancer cells<sup>532</sup>. An alternative explanation of this cellular memory may involve the simple mechanism of gradual accumulation of a regulatory protein due to a slight bias in favour of expression over degradation<sup>415</sup>. It is also entirely possible, and suggested by many<sup>617 925</sup>, that several independent mechanisms of replicative senescence exist, and that the relative importance of these may differ among cell-types.

While the details of replicative senescence remain elusive, a number of critical elements have been characterised. These include the telomerase reverse-transcriptase, TERT<sup>272</sup>, ATM<sup>884</sup>, p53<sup>113</sup>, CDC25A<sup>1133</sup>, CDK4<sup>1077</sup>, p16<sup>296</sup>, p21<sup>1145</sup>, p27<sup>26</sup>, and pRB<sup>691</sup>. There is thus very strong circumstantial evidence that modulation of pRB subsystem activity, probably through altered phosphorylation, is involved in the regulation of senescence.

### *Viral infection*

Viruses are able to carry out their vital and defining functions utilising a genome of tens of genes, in stark contrast to all other classes of organism, where thousands to hundreds of thousands are more usual. They are able to do so by usurping cellular regulation and perverting the host cell metabolism to their own ends. It is therefore of great interest that in many DNA and retroviruses, a large proportion of the reduced viral genome is dedicated to the nullification of the pRB subsystem. Typically, this is achieved by carrying a gene that encodes a protein that binds to the pRB small A/B pocket via an LXCXE motif. This is often portrayed as a means of defeating the pRB-dependent constraint on cellular proliferation, but there is no reason why this should be required for viral infection to proceed, nor is it sufficient to achieve this. To do so would require that the binding of a viral protein to pRB interfered with the constraint of E2F activity. This is not the case, however, as it is insufficient to disrupt pRB-E2F complexes<sup>1499</sup> and furthermore, the ability of pRB to bind such proteins and to impose a cell-cycle arrest are functionally separable<sup>177 271</sup>.

What then is the function served, from the viewpoint of the virus, or defeated, from the viewpoint of the cell, by such binding? By binding in the small A/B pocket, a viral protein will prevent the recruitment of the histone deacetylase complex to gene promoters and so diminish the ability of pRB to repress transcription of genes used in the synthesis of DNA, something beneficial to the virus. When bound there, it will also deny this docking mode to cyclin-D1, and thereby prevent phosphorylation of S807 and S811, as these are not accessible from the C-terminal docking domain<sup>1501</sup>. In consequence, ABL will not dissociate from pRB<sup>694</sup> and it will remain inhibited<sup>1420</sup>. One substrate of the ABL kinase is MDM2, and its phosphorylation prevents it binding to, and directing the degradation of p53<sup>420</sup>. Therefore, on-going inhibition of ABL by pRB may contribute to the suppression of the p53-dependent apoptotic response that could otherwise be triggered during the infection of mitogen-stimulated cells. ABL can also promote apoptosis via p73<sup>1395</sup>, and this effect is also nullified by the continuing association of ABL with pRB. While the suppression of apoptosis may be required in order to give the infecting virus the opportunity to replicate, this interpretation is difficult to reconcile with the general observation that expression of a viral pRB-binding protein such as E7<sup>1266</sup>, E1A<sup>1319</sup>, or large-T<sup>219</sup>, promotes rather than inhibits apoptosis, especially where p53 is not disabled by an additional viral protein<sup>1319</sup>.

### Complications

As noted above, the model scenario presented incorporates many simplifying assumptions, particularly regarding the multiplicity of related proteins of each type involved. At last count, there are three pRB-related pocket proteins<sup>@208 @1264</sup>, six E2F transcription factors<sup>@1339</sup> that may dimerise with one of three DP co-factors<sup>@1479</sup>, three D-cyclins<sup>@1204</sup>, two E-cyclins<sup>1009 @1141</sup>, two A-cyclins<sup>@100 @268</sup>, perhaps four CDKs implicated in G<sub>1</sub>-S transition regulation<sup>@502</sup>, four CKIs related to p16<sup>@1113 @1326</sup>, and three related to p21<sup>@936</sup>. This discussion could not be complete without some indication of the distinctions among these.

Generally, depending on their lineage, cells express cyclin-D2 and either cyclin-D1 or cyclin-D3. All contain the LXCXE motif {Table H-3} and all are thought to bind pRB. All can bind CDK2, CDK4, and CDK6, and all can activate them, except in the case of cyclin-D1-CDK2<sup>517</sup>. This may well account for the biphasic response seen with ectopic expression of cyclin-D1, wherein a small increment of expression accelerates S-phase entry, but a larger increment causes a G<sub>1</sub> arrest. In the first instance, increased CDK4 activity would cause the acceleration, but when the available CDK4 is saturated, additional cyclin-D1 would act as a competitive inhibitor of CDK2<sup>386</sup>, preventing its activation by cyclin-E.

E2F1, -2, and -3 associate with pRB, rather than p107 or p130; have an N-terminal domain that binds cyclin-A, but not cyclin-E, that is essential for phosphorylation of the DP co-factor; and are exclusively nuclear. E2F4 and -5 associate with p107 and, particularly so in the case of E2F5, p130. An association between E2F4 and pRB has also been reported commencing at the G<sub>1</sub>-S transition<sup>899</sup> and in the growth-suppressive response to TGFβ<sup>779</sup>. E2F4 is the predominant form found in quiescent cells, when it is essentially nuclear, this localisation depending on DP2, and p107 or p130, but not pRB. As cells approach S-phase, it becomes increasingly cytoplasmic<sup>790</sup>, and when engineered to remain nuclear, is functionally indistinguishable from E2F1<sup>924</sup>. E2F6 has no transactivation domain or pocket-protein-binding domain and may be a natural inhibitor of the other E2Fs<sup>160</sup>.

The CKI p15<sup>CDKN2B</sup> has a more polarised tissue-dependent expression than p16, being present at high levels in lung, but scarce or absent in kidney. Also unlike p16, its expression is not regulated by pRB, nor is its mRNA level different in proliferating versus quiescent cells, but it does increase some thirty-fold in response to TGFβ treatment of epithelial cells<sup>471</sup>. Like *CDKN2A*, it has been reported to be subject to transcriptional silencing through promoter methylation<sup>509</sup>. The p18<sup>CDKN2C</sup> inhibitor has greatest expression in skeletal muscle, and may<sup>1326</sup> be a better inhibitor of CDK6 than of CDK4<sup>445 955</sup>. The p19<sup>CDKN2D</sup> inhibitor has expression linked to the cell-cycle that peaks at the G<sub>1</sub>-S transition and then declines until mitosis.

See J-14 for a comparison of p21 and p27.

Protein levels of the pRB-relatives, p107 and p130 vary cell-cyclically, and at least in the case of p130, this is due to alteration of protein translation or stability as the mRNA level stays essentially constant. Interestingly, their patterns of expression are mutually inverted. Levels of p107 are low in quiescent cells as a consequence of repression via E2F4, and rise during G<sub>1</sub>, while those of p130 are high in quiescent cells and low during proliferation<sup>1240</sup>. Both are subject to cell-cyclical phosphorylation, and while both are substrates for CDK4, neither is a substrate for CDK2<sup>82</sup>. Indeed, they are either inhibitors of CDK2<sup>163 1449</sup>, or influence its substrate specificity<sup>489</sup>. Consistent with this, phosphorylation of both begins in mid-G<sub>1</sub> coincidentally with CDK4 activation<sup>1462</sup>. In the case of p130, this proceeds rapidly and completes before that of pRB<sup>863</sup>.



## H.5 The pRB subsystem and cancer

### The pRB-related pocket proteins

While homozygous mutant *Rb1* mice die *in utero* with severe developmental flaws, the corresponding heterozygotes are viable, but spontaneously develop pituitary tumours<sup>5545</sup>. In the analogous human situation, it is of course predisposition to retinoblastoma that is seen. It is widely reported that despite having been cured of their initial tumour, survivors of hereditary retinoblastoma are at increased risk of developing second and subsequent primary tumours<sup>8 9 266 291 300 320 903 1440</sup>, notably osteosarcoma<sup>472</sup>, and often die during childhood or adolescence as a result. While there may be an iatrogenic component to this, as with increased bladder leiomyosarcoma after cyclophosphamide treatment<sup>649 917</sup>, the major effect is thought to be due to the functional loss of pRB upon mutation of the intact allele in other tissues. The nature of subsequent primary tumours is probably a joint reflection of the vulnerability to mutation, and the importance of the tumour-suppressor function of pRB in different tissues. Among tumours other than, or as sequelae of retinoblastoma, alterations of *RB1* or expression of pRB are also widely reported, instances being in breast carcinoma<sup>428</sup>, chondrosarcoma<sup>46</sup>, glioma<sup>491</sup>, small-cell lung cancer<sup>1493</sup>, non-small-cell lung cancer<sup>429</sup>, oesophageal squamous cell carcinoma<sup>644</sup>, pituitary adenoma<sup>1230</sup>, hepatocellular carcinoma<sup>555</sup>, osteosarcoma<sup>87</sup>, thymic carcinoma<sup>524</sup>, and head and neck squamous cell carcinoma<sup>736</sup>. In addition, aberrant over-expression of pRB has been reported in bladder carcinoma<sup>90</sup> and hepatocellular carcinoma<sup>555</sup>.

In contrast, the other members of the pRB-related pocket protein family appear to be less important in tumour suppression. *Rbl1*-null mice are viable, and are reported to be either phenotypically normal<sup>8763</sup>, or growth-impaired and exhibiting myeloid hyperplasia<sup>8757</sup>. A similar disparity exists for *Rbl2*-null mice, with both apparent normality<sup>8212</sup> and embryonic lethality<sup>8758</sup> being reported. It has been suggested that the particular genetic backgrounds of the differing mouse strains used in these experiments may account for this phenomenon. Nevertheless, even in the more permissive C57BL/6 strain the double, *Rbl1/Rbl2* homozygous knockout results in early neonatal death<sup>8212 @8436</sup>, indicating that they may have overlapping abilities to perform a function critical for survival. Alterations affecting p130 have been reported in a few human tumour types, including vulvar squamous cell carcinoma<sup>1500</sup>, nasopharyngeal carcinoma<sup>209</sup>, Burkitt's lymphoma<sup>205</sup>, and small-cell lung cancer<sup>496</sup>. Alterations affecting p107 appear to be very rare<sup>1294</sup>.

### The D-cyclins

The oncogenic potential of cyclin-D1 is well established<sup>@286</sup>, indeed it was the search for an 11q13 oncogene associated with BCL and parathyroid adenoma that led to its identification<sup>1107</sup>. In the case of BCL, it was found that chromosomal translocation resulted in aberrant expression of cyclin-D1, not normally produced by B or T lymphocytes. Moderate over-expression has been reported in many carcinomas including hepatocellular (58%)<sup>622</sup>, lung non-small-cell (37%)<sup>1476</sup>, head and neck squamous cell (48%)<sup>74</sup>, and those of the breast (35%)<sup>1526</sup>, and bladder (31%)<sup>983</sup>.

Over-expression of cyclin-D2 has been reported in a number of myeloid malignancies<sup>261</sup>, sometimes as a consequence of BCR-ABL activity<sup>255</sup>. It is seen in male germ-cell tumours<sup>539</sup>; and in gastric cancer, it correlates with progression, while over-expression of cyclin-D1 does not<sup>1292</sup>. Conversely, loss of expression due to promoter methylation has been reported in breast carcinoma<sup>330</sup>.

Chromosomal translocations resulting in the aberrant expression of cyclin-D3 have been found in a subset of multiple myeloma cell-lines and tumours<sup>1194</sup> and *CCND3* has been found to be amplified in a

glioblastoma<sup>722</sup>. Over-expression has been reported in pancreatic adenocarcinoma<sup>590</sup>, non-Hodgkin's lymphoma<sup>905</sup>, and breast carcinoma<sup>75</sup>.

### The cyclin-dependent kinases

There is no strong case to support a direct role for CDK2 in tumorigenesis, although some over-expression and increased activity have been reported<sup>672 843 889</sup>. While the same is true for CDK6<sup>740</sup>, the corresponding case for CDK4 is very substantial. A germ-line *CDK4* R24C mutation that prevents binding and inhibition by p16 has been found in melanoma<sup>1444</sup>, and mice engineered to be homozygous for this allele spontaneously develop multiple tumours<sup>1248</sup>, particularly invasive melanoma<sup>1249</sup>. A mutation in the corresponding position in *CDK6* has been sought, but not found<sup>1200</sup>. *CDK4* is amplified in cervical carcinoma<sup>198</sup>, osteosarcoma<sup>1416</sup>, breast carcinoma<sup>32</sup>, glioblastoma<sup>1104</sup>, and Ewing's sarcoma<sup>733</sup>; and *CDK4* is over-expressed in oral and pharyngeal carcinoma<sup>709</sup>, glioblastoma<sup>740</sup>, cervical carcinoma<sup>198</sup>, breast carcinoma<sup>32</sup>, hepatoblastoma<sup>671</sup>, and ovarian carcinoma<sup>853</sup>.

### The cyclin-dependent kinase inhibitors

#### *p16 and relatives*

Three proteins structurally similar to p16<sup>CDKN2A</sup> and with overlapping function are known: p15<sup>CDKN2B</sup>, p18<sup>CDKN2C</sup>, and p19<sup>CDKN2D</sup>. Assessing the contributions toward tumour suppression of the closely-linked 9p21 genes *CDKN2A* and *CDKN2B* and their encoded proteins ARF, p16, p15, and its p10<sup>1345</sup> and p15.5<sup>398</sup> splice variants is no simple task. Co-deletion of the genes is commonly reported, as is simultaneous transcriptional silencing due to methylation, but combined inactivation by different mechanisms is also known. In consequence, it is difficult to determine if only one, either, or both are the functional targets, and what, if any, tissue specificity there may be among these alternatives.

*CDKN2A* is undoubtedly a tumour-suppressor gene of stature rivalling *TP53*. It seems likely that the two proteins it encodes, p16<sup>6368</sup> and ARF, contribute independently toward this<sup>61203</sup>. This is perhaps best demonstrated by the phenotypes of mice engineered to be functionally deficient in each of these proteins without compromise of the function of the other. When ARF was selectively ablated, mice displayed a cancer-prone phenotype, with spontaneous tumour development in 19 of 24 animals, the most common type being sarcoma<sup>6631</sup>. Similar results were seen for p16, with spontaneous tumour development in 10 of 39 homozygotes, with the predominant type being sarcoma, while lymphoma and melanoma were also seen<sup>61192</sup>. Interestingly, a melanoma kindred has been reported wherein two members are homozygous for a non-functional *CDKN2A* allele: one has melanoma, the other is unaffected<sup>442</sup>. Clearly, while loss of p16 function may predispose toward the development of melanoma, it does not guarantee it. Other genetic or environmental factors must be involved {See Chapter 1, 'The cause of melanoma'}.

See J-21 for more about ARF.

In contrast, the *Cdkn2b* knockout mouse has a relatively mild phenotype, with an 8% tumour incidence after 18 months<sup>6750</sup>. Nevertheless, there is probably a sufficient weight of evidence to suggest that it is a tumour-suppressor in its own right, albeit relatively minor. In particular, homozygous deletion of *CDKN2B*, but not *CDKN2A* has been reported in bladder cancer<sup>312</sup>, multiple myeloma<sup>1311</sup>, and non-Hodgkin's lymphoma<sup>1220</sup>; and methylation of *CDKN2B*, without alteration of p16 expression is almost universal in adult acute myelogenous leukaemia, and very common in adult acute lymphocytic leukaemia, paediatric acute myelogenous leukaemia, and in glioma<sup>508 509</sup>. This same pattern is seen in radiation-induced murine T-cell lymphomas<sup>6836</sup>. Other data supports a joint role for these tumour-suppressors. Simultaneous functional loss of p15 and p16 may be important in the development of T-cell acute lymphoblastic leukaemia<sup>586 978</sup>, glioma<sup>1227</sup>, and multiple myeloma<sup>945</sup>. In oesophageal squamous



carcinoma, promoter methylation of *CDKN2A* is seen either alone, or in combination with methylation of *CDKN2B*, but the latter rarely occurs alone<sup>1464</sup>.

The p18<sup>*Cdkn2c*</sup> knockout mouse exhibited pituitary hyperplasia leading to the formation of primary tumours that were fatal due to their large size. They appeared to have little invasive or metastatic propensity however. Other tumour types were also seen, including lymphoma, and renal, adrenal and testicular tumours<sup>8750</sup>. There is evidence to support a tumour-suppressor function for p18 in humans, particularly in multiple myeloma<sup>724</sup>, and perhaps acute lymphoblastic leukaemia<sup>585</sup>, meningioma<sup>122</sup>, and breast cancer, where a *CDKN2C* mutation leading to a p18 unable to bind CDK6 has been reported<sup>746</sup>.

An extensive study of human haematopoietic malignancies found only very few instances of p19 alteration<sup>293</sup>, nor is it implicated in other tumour types. The phenotype of the p19-deficient mouse supports the hypothesis that it is not a tumour-suppressor, but rather, regulates testicular development<sup>81524</sup>.

### ***p21 and relatives***

The initial report of the p21<sup>*Cdkn1a*</sup>-null mouse<sup>8262</sup> concluded that while aberrations of G<sub>1</sub>-arrest were evident in cell cultures, there was no significant disposition toward spontaneous tumour formation by six months of age. However, when such mice were followed for an extended period it was found that spontaneous tumours did arise at a mean age of sixteen months, the predominant type being haematopoietic<sup>8850</sup>. Among human tumours, mutations of *CDKN1A* are known, but in general, are infrequent<sup>1320</sup>. Among 81 gliomas<sup>784</sup>, 28 pituitary adenomas<sup>569</sup>, and 20 gastric carcinomas<sup>1001</sup>, no mutation was detected by PCR-SSCP or sequencing. Intragenic deletions or point mutations have been found in adrenocortical adenoma<sup>568</sup>, 5 of 40 thyroid carcinomas<sup>1206</sup>, 3 of 28 brain tumours<sup>1347</sup>, and 7 of 102 tumours of assorted types<sup>1408</sup>. Interestingly, a polymorphism that may affect the ability of p21 to interact with PCNA was identified in 42 of 50 cases of oesophageal squamous cell carcinoma in contrast to only 8 of 50 in putatively normal individuals<sup>57</sup>.

The most evident characteristic of the p27<sup>*Cdkn1b*</sup> knockout mouse is that it is significantly larger than its wild-type litter-mates, an apparent consequence of increased general cellular proliferation resulting in enlarged organs<sup>8349 8934</sup>. Spontaneous development of pituitary tumours is seen, a feature also present in the phenotype of *Cdkn2c*-null<sup>8372</sup> and *Rb1*+/- animals, suggesting an important functional overlap in this tissue. In human solid tumours, reduced expression of p27 is frequently associated with rapid tumour progression and poor prognosis<sup>548 854 1155</sup>, while the converse may be true in some lymphomas<sup>8904</sup>. *CDKN1B* alterations are only rarely seen in tumours<sup>648</sup>, however a mutation with simultaneous loss of heterozygosity at 12p13 has been found in 1 of 36 breast carcinomas<sup>1254</sup>.

Mice lacking *Cdkn1c* had cleft palates and skeletal deformities and usually died neonatally. In the ~10% of instances where they survived beyond weaning, their growth was markedly retarded and developmental flaws in reproductive organs become apparent in both males and females. While no increased cancer predisposition was detected during the five months of the study, increased incidence with later onset cannot be excluded<sup>81291</sup>. Mutation of *CDKN1C* has not been reported in human tumours, but loss of expression and loss of heterozygosity at 11p15.5 has been seen in thyroid<sup>592</sup>, bladder<sup>991</sup>, and hepatocellular<sup>589</sup> carcinomas, and in pancreatic adenocarcinoma<sup>591</sup>. *CDKN1C* is a strong candidate for the Beckwith-Wiedemann syndrome gene<sup>162</sup>, a disease in which there is a mild predisposition toward cancer, particularly Wilms' tumour. While mutation has been found in some cases<sup>486</sup>, conclusive proof is

proving difficult to obtain, not least because the implicated locus also contains *IGF2*, an equally viable candidate, and both are subject to parental imprinting<sup>614</sup>.

### The E2F transcription factors

The E2F transcription factors are involved in both the induction and repression of genes, and mediate both proliferation and apoptosis, hence, it is not possible to predict, a priori, whether their normal role is tumour-suppressive, excessive function oncogenic, neither, or even both for different E2F types or under different circumstances<sup>1477</sup>. The very real nature of this difficulty is demonstrated by the case of E2F1, one of the better studied E2Fs. *E2F1* is amplified in the HEL erythroleukaemia cell-line<sup>1124</sup>, E2F1 was over-expressed in 24 of 26 small-cell lung cancers<sup>333</sup>, and its expression correlated with invasiveness in head and neck carcinoma<sup>1511</sup>, all suggesting a role in tumorigenesis. However, the *E2f1*-null mouse has an elevated rate of spontaneous tumour formation, particularly reproductive tract sarcomas<sup>1480</sup>, suggesting a role in tumour suppression. How these effects come about is unknown, but it seems unlikely to involve interaction with pRB since no mutations in the pRB interaction domain of E2F1 were found in a survey of 406 human tumours<sup>932</sup>, and concurrent ablation of *E2f1* reduces tumour incidence and increases the longevity of *Rb1* +/- heterozygous mice<sup>1478</sup>.

E2F4 appears to influence tumour development significantly, seemingly due to the presence of an unstable (CAG)<sub>13-18</sub> trinucleotide repeat that encodes a polyserine tract. Alterations have been found here in various digestive<sup>856 1161 1252 1448 1520</sup> and haematological<sup>1708</sup> tumours. It has been suggested that at least in some instances, this instability is due to a mutation within *MSH3*, whose encoded protein plays a prominent role in DNA mismatch repair<sup>570</sup>.

There is little if any evidence to suggest a role for the other E2F transcription factors in tumorigenesis, with the possible exception of E2F5, which has been found to be amplified and over-expressed in some breast cancers<sup>1041</sup>.

## H.6 The pRB subsystem and melanoma

See F.3 for more about hereditary cancer syndromes.

The genetic analysis of hereditary tumour kindreds is a rich source of information pertinent to the molecular aetiology of cancer, and this is the case with melanoma<sup>134 164</sup>. In some syndromes, melanoma occurs as the only, first, or predominant tumour type, notably when the disease phenotype is linked to 9p21<sup>484 1391</sup>, 12q14<sup>1250</sup>, or 1p36<sup>64</sup>. Here, the implicated genes are, respectively, *CDKN2A*<sup>355 1076</sup>, *CDK4*<sup>1529</sup>, and possibly *CDC2L1*<sup>942</sup> or even *PINK1*<sup>1355</sup>, but probably not *TP73*<sup>719 1156 1344</sup>. In others, melanoma is just one component of a more complex cancer predisposition as in xeroderma pigmentosum<sup>699</sup>, with multiple linkage groups; hereditary retinoblastoma<sup>24 77 903 1337</sup>, implicating *RB1*; type I multiple endocrine neoplasia<sup>957</sup>, implicating *MEN1*; multiple hamartoma syndrome, implicating *PTEN*<sup>170</sup>; and melanoma-astrocytoma syndrome, implicating *CDKN2A* exon 1 $\beta$ <sup>1076</sup>. Among these, alterations in *RB1*, *CDKN2A*, and *CDK4* may be expected to affect the pRB subsystem directly<sup>468</sup>.

Most interestingly, extensive surveys have failed to provide any evidence for a role for *CDK2*<sup>1390</sup> or *CDK6*<sup>1200</sup> in the tumorigenesis of melanoma, and there appears to be no report of amplification or mutation of *CCNE1*. Deregulated phosphorylation of pRB, per se, may therefore be insufficient to predispose toward melanoma. This hints that the critical role for pRB is modulated by *CDK4*, but not *CDK2*, and that it may be inconsequential in tissues where the dominant cyclin-D-associated CDK is *CDK6*. Heretical though it may seem, this is consistent with the possibility that the ability of pRB to repress E2F activity may not be the critical aspect. The disparity between incidences of *CDK4* and *CDKN2A* mutations in hereditary melanoma<sup>421</sup> further suggests that there may be partial functional



overlap between CDK4 and another kinase less susceptible to p16 inhibition, or that some function other than inhibition of CDK4 may also be involved.

See 9–8, where results that relate to this are presented.

Hence, suspicion must fall upon ARF as a further, possibly subordinate, contributor to melanoma tumorigenesis. Fitzgerald et al. reported finding no *CDKN2A* mutations that would alter ARF, but not p16, in 33 consecutive melanoma patients who had one or more first or second-degree affected relations<sup>355</sup>, nor were any sequence alterations found in *CDKN2A* exon 1 $\beta$  among ten 9p21-linked melanoma kindreds by Fagnoli et al.<sup>343</sup>. However, one melanoma-astrocytoma syndrome kindred has been reported in which there is a germ-line mutation in *CDKN2A* exon 1 $\beta$ . More data are required before a definitive assessment can be made of what role, if any, is played by ARF in the tumorigenesis of melanoma.

See 8–10, where results that relate to this are presented.

The hypothesis has been raised that it is the integrity of the pRB subsystem as a functional whole that protects against melanoma, and hence, failure of any critical component predisposes toward it. The strongest evidence to support this is the common finding that in melanomas, there is very often a functional defect in a single element of the subsystem, generally p16, pRB, or CDK4<sup>73 828 1391</sup>. Nevertheless, multiple flaws have been found in individual cases, with amplification of *CCND1* or mutation of *CDK4* being seen in conjunction with *CDKN2A* deletion<sup>1095 1391</sup>. Clearly, pRB cannot be the only significant target of alterations affecting cyclin-D1 or CDK4, and some additional advantage is conferred by their presence. The basis for this advantage is unknown, but the most probable explanation is that further, as yet uncharacterised, substrates for cyclin-D1–CDK4 exist. The rationale for this is that the implicated CDK4 mutation involves its escape from inhibition by p16. For this to be significant in a cellular context where p16 or pRB are absent, the necessity of a substrate other than pRB, and an inhibitor other than p16 is implied. Potentially, where p16 is absent, some degree of constraint may still operate through induction of p15, unless CDK4 is impervious to this. Furthermore, if the amplification of cyclin-D1 were serving some purpose other than increasing CDK4 activity, then it could be expected to act as an inhibitor of CDK2 activation, hindering, rather than helping proliferation. As to the identity of such a substrate, nothing is known with certainty. There is one report of a cytoplasmic p88 CDK4 substrate<sup>730</sup>, but this does not appear to have been confirmed. It is also possible that it corresponds to a product of caspase cleavage of pRB. The cited report relies on the lack of recognition of p88 by the pRB monoclonal antibody employed to exclude this, but it is quite possible that upon cleavage, the necessary epitope is lost or its conformation modified. The particular antibody is not defined sufficiently well in the report to establish if this may be the case. While the principal caspase degradation products of pRB are p44 and p68, there is evidence of the early production of larger, and the subsequent production of smaller products<sup>345</sup>.

H: The pRB subsystem





---

# BRCA1 super-complexes

---

*BRCA1, the tumour-suppressor associated with hereditary early-onset breast and ovarian cancer is instrumental in genome maintenance, and yet has no recognised enzymatic activity. Immunoprecipitation studies using antibodies against it have revealed that it associates with an array of other proteins involved in the replication and repair of DNA, many of them known tumour-suppressors. These complexes, containing, and perhaps nucleated by BRCA1, may hold a central position in the early stages of many and diverse molecular operations on DNA.*

---

Many functional aspects of BASC are described in Appendix J. The relevant material, beginning on J-17, should be read in conjunction with this appendix.

## I.1 BRCA1

The tumour-suppressor BRCA1<sup>1397</sup> was identified by virtue of its frequent mutation in kindreds that experienced elevated incidence of early-onset breast and ovarian cancers. Analysis of its primary sequence revealed few clues to its function, the chief inference being that it probably bound DNA directly. It appears to have no intrinsic enzymatic activity suggesting that its principal functional mode is that of a scaffold protein, co-factor, or inhibitor. Studies of human cell-lines and in mouse models established that BRCA1 was required for normal DNA repair functions, particularly with respect to the repair of double-strand breaks by homologous end-joining.

## I.2 BRCA1 super-complexes

In order to elucidate the molecular mechanisms of BRCA1 function, Wang et al. performed immunoprecipitation studies with a number of anti-BRCA1 antibodies and detected some forty interacting protein species<sup>1403</sup>. They established that all cellular BRCA1 exists in protein super-complexes of ~2 MD, and that these are composed of lower-order complexes that in many cases had been independently implicated in detection and repair of DNA anomalies. Associated also was the kinase ATM, known to be activated soon after the advent of DNA damage, and an important regulator of the cellular response to this. It is likely that the composition of these super-complexes is dynamic, and that not all components detected in the immunoprecipitates necessarily co-exist within the same super-complex. This would provide the flexibility needed for BRCA1 to mediate the coupling of common enzyme systems to diverse classes of DNA structure.

The intimate association of proteins with these functions led Wang et al. to propose that these super-complexes serve to integrate the processes of DNA damage detection and repair and coined the phrase 'BRCA1-associated genome surveillance complexes' (BASC) to describe them.

## I.3 BASC composition, inherent function, and assembly

### MSH2–MSH6, and MLH1

Among the proteins identified were critical components of the DNA mismatch repair (MMR) subsystem, in particular the MSH2–MSH6 dimer, and MLH1. The dimer has a weak intrinsic affinity for DNA, but this is greatly enhanced under certain circumstances, most notably in the presence of mismatched DNA or extrahelical bases<sup>563</sup>. MLH1, in conjunction with its dimerisation partner PMS, when complexed with MSH2–MSH6 also enhances this affinity<sup>547</sup>. The MSH2–MSH6 dimer is a DNA-dependent ATPase activated in the presence of anomalous DNA<sup>432</sup>. When binding ATP, its affinity for DNA is weaker, but that for MLH1 is stronger<sup>546</sup>. It is therefore likely that some form of self-regulation occurs<sup>432</sup>. In addition

---

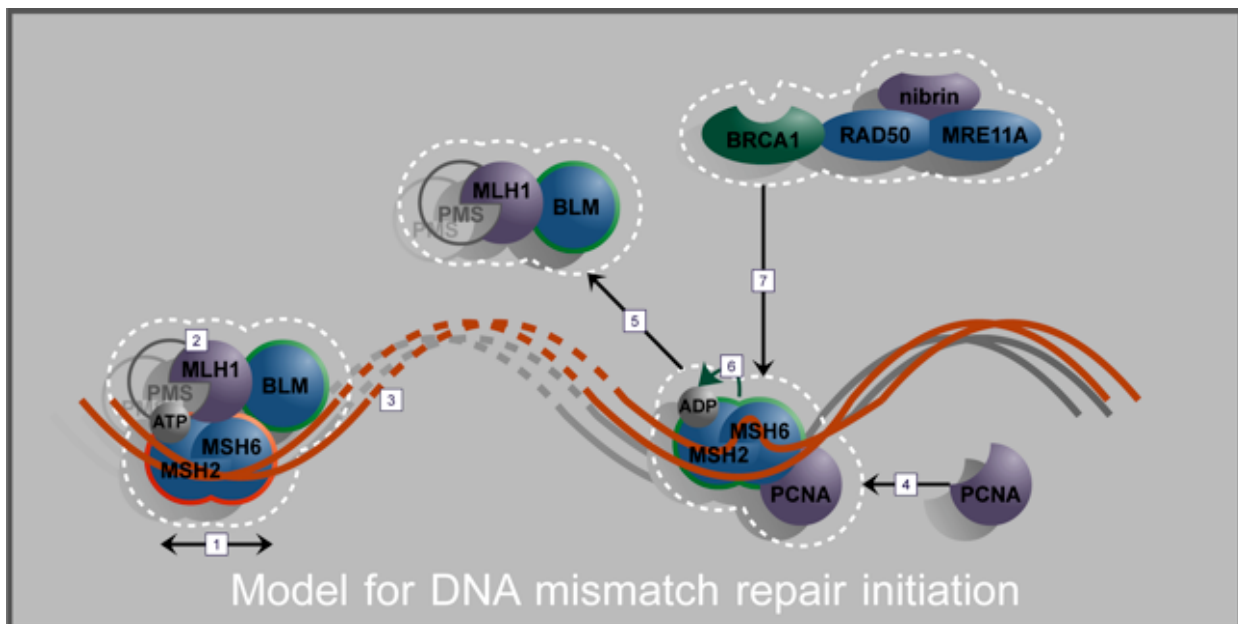


**Figure I-1: Model for DNA mismatch repair initiation**

to these interactions, MLH1 binds the helicase BLM, but the functional significance of this is unclear. MSH6 can recruit PCNA, but doing so dislodges MLH1 from the complex<sup>128</sup>.

The consideration of two further experimental observations allows the construction of a model for the temporal sequence of protein interactions during the initiation of mismatch repair. It is the presence of ATP, not the act of its hydrolysis, that reduces the affinity of the MSH2–MSH6 dimer for DNA<sup>562</sup>; and, even in the presence of ATP, MSH2–MSH6 cannot disengage from DNA that is circular or end-capped<sup>433</sup>, implying mobility of the complex along the DNA helix<sup>433</sup>.

The model {Figure I-1} postulates that it is the ATPase-inactive, ATP-binding form of MSH2–MSH6 that is mobile upon the DNA helix [1], and that it carries with it MLH1 and its dimerisation partner, PMS [2], enhancing its affinity for DNA mismatches. It is possible that the attendant BLM helicase assists in complex mobility [3]. Upon encountering a DNA anomaly, MSH6 recruits PCNA [4], and at this time, the MLH1 complex is dislodged [5], the ATPase activated, and the ATP hydrolysed [6]. The reduced DNA-affinity resulting from the loss of MLH1–PMS would be compensated for by that bestowed by association with ADP. MSH2–MSH6 becomes immobile at the location of the mismatch and serves as a clamp loader for PCNA in preparation for the assembly of the synthetic DNA repair subsystem<sup>207</sup>. The presence of PCNA enhances complex mismatch-affinity further<sup>362</sup>. In the absence of MLH1–PMS, the recruitment of BRCA1 and its retinue to MSH2–MSH6 may then occur<sup>1398</sup> [7].

For the theoretical reason given above, MSH2–MSH6 cannot be involved in DSB repair, since it would simply disengage from the DNA at the break. This suggests that ATM is unlikely to be activated as a result of MMR, and consistent with this there is no great overlap in the phenotypic consequences of ATM and mismatch repair dysfunction, although there is evidence that ATM status may influence the phenotype where MMR is dysfunctional<sup>833</sup>. In practice, ATM activation during MMR does not appear to have been studied directly or reported. If ATM is not activated, and presuming a need for signalling of the presence of DNA mismatches beyond the local level, an alternative mechanism must exist. What this may be is unknown, but the similarity between the molecular switch effected by the MSH2–MSH6 ATPase, and that effected by RAS-homology GTPases may prove significant.

## Replication factor C

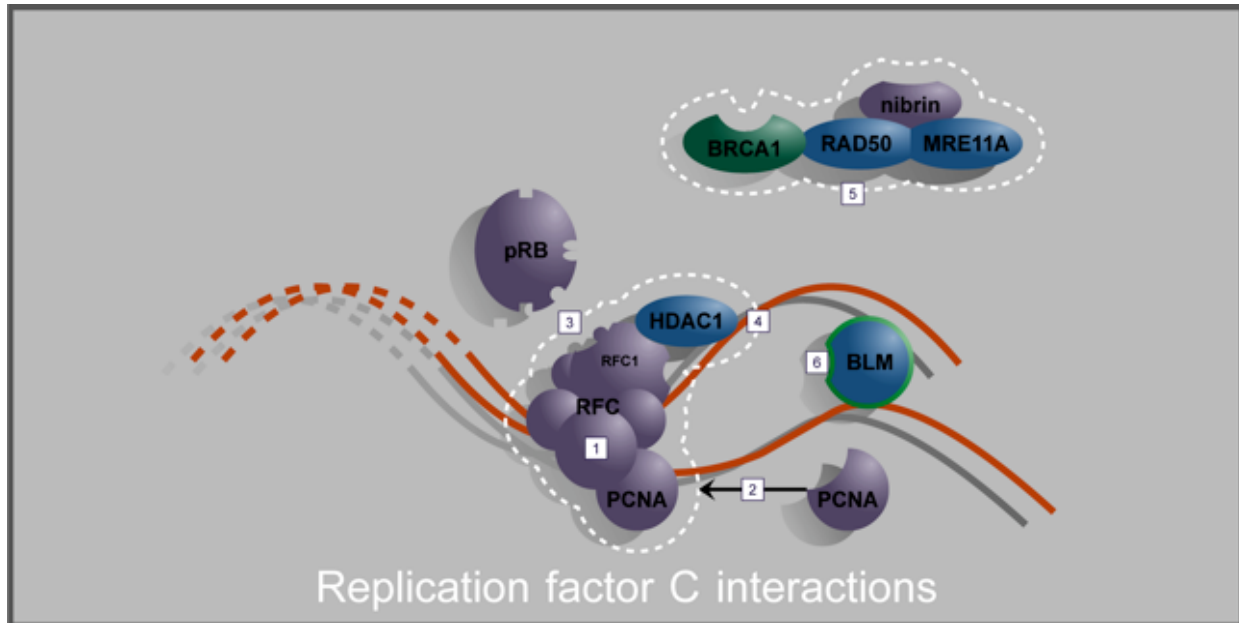


**Figure I-2: Replication factor C interactions**

Three of the elements of the replication factor C (RFC) heteropentamer<sup>6915</sup> were detected in the BRCA1 immunoprecipitates [Figure I-2] [1]. This complex is critical for processive DNA synthesis, both at replication forks and during repair. Its best understood function is as a clamp loader for PCNA<sup>916</sup> [2], but it also mediates the switch from the initial usage of DNA pol- $\alpha$  to DNA pol- $\delta$ <sup>830</sup>. Once this has been achieved, PCNA itself acts as the anchor for other elements of the DNA synthetic subsystem and RFC dissociates<sup>1037</sup>. The recruitment of PCNA to replication forks by RFC is analogous to that to sites of mismatched base-pairs by MSH6. The p145 RFC sub-unit, RFC1, associates with pRB via an LXCXE motif<sup>1017</sup> [3], and this may be a means by which its functionality or location are synchronised with the commencement of S-phase. RFC1 also binds the histone deacetylase HDAC1<sup>35</sup>, and this may enable it to repress transcription in the vicinity of its operation [4]. The role of BRCA1 in association with RFC is not clear, but it may serve as a bridge between RFC and the MRE11A–RAD50–nibrin complex in the event of replication fork collapse<sup>371</sup> [5], a process that also requires BLM<sup>371</sup> [6].

### MRE11A–RAD50–nibrin

Consistent with this, the MRE11A–RAD50–nibrin complex<sup>6233</sup> was also detected in the BRCA1 immunoprecipitation study of Wu et al. This is an ATP-dependent<sup>534</sup> single-stranded DNA endonuclease and 3' DNA exonuclease<sup>1341</sup>. It participates in several aspects of DNA biochemistry including homologous and non-homologous<sup>549</sup> DNA end-joining, meiotic recombination, and telomere maintenance<sup>1523</sup>. Its homologue in yeast is required for the activation of Rad53 and Chk1 after DNA double-strand breakage (DSB)<sup>549</sup>, implicating it in the cellular response to genomic damage in addition to its maintenance role. The nuclease function is provided by the MRE11A component and is regulated both by the RAD50 ATPase and by phosphorylation by ATM after DNA damage<sup>284</sup> such as the double-strand breakage caused by ionising radiation<sup>239</sup>. This phosphorylation, and nuclear accumulation of the complex, both require the prior phosphorylation of the nibrin component by ATM<sup>144</sup>. Direct association between BRCA1 and RAD50 has also been shown<sup>1518</sup>, and this may provide an additional mode of regulation of the MRE11A nuclease<sup>534</sup> §1342.

**BLM**

BLM, referred to above, was also detected in the immunoprecipitates. This is a DNA helicase<sup>637 791</sup> that, in conjunction with nibrin, may serve to unwind damaged DNA to facilitate its repair. Like nibrin, it contributes to the repair of IR-damaged DNA, but it also participates in the repair of UVR-induced damage<sup>573</sup>. Under these circumstances, BLM is phosphorylated in an ATM-dependent manner<sup>2</sup>. In addition, BLM is required for recruitment of the MRE11A–RAD50–nibrin complex to stalled replication forks<sup>371</sup>. Although BLM and MLH1 bind, there is preliminary evidence to suggest that BLM plays no part in mismatch repair<sup>1013</sup>, and may participate in other MLH1-mediated functions<sup>371</sup>. This is supported by the significant differences in the phenotypes seen where BLM is non-functional in comparison to those where components of MMR are defective.

**ATM**

An extremely significant finding was the presence of the ATM kinase in BRCA1-associated complexes. ATM participates in meiotic chromosome synapsis<sup>1033</sup>, the mitotic spindle checkpoint<sup>1209</sup>, and in telomere maintenance<sup>688</sup>. Its most important function may be in the early response to genomic damage, as it is rapidly activated when this is sustained<sup>153</sup>. Its direct and indirect substrates include BRCA1, BLM, and nibrin within the BASC, and p53, CDC25C, CHK2, MDM2, RBBP8, and E2F, beyond it. Via these channels, it initiates the cellular response to genomic damage that may include cell-cycle arrest or apoptosis. The mechanism by which ATM is activated in response to DNA damage is unknown and its discovery will be welcomed by many.

**I.4 BASC failure and disease**

The critical nature of BASC is exemplified by the phenotypes that emerge with the loss of function of any of its components, and these are shown in Table I–1. The predominance of cancer and immunodeficiency syndromes is particularly noteworthy. The absence of diseases associated with loss of function of RAD50 is probably due to an embryogenic requirement for two functional alleles. In mice, complete ablation of either *Rad50*<sup>S818</sup> or *Nbs1*<sup>S1522</sup> is embryonically lethal, and in the case of RAD50, this may also apply in humans, while a single functional *NBN* allele may satisfy embryogenic requirements. A similar argument may apply to components of RFC.

Bloom's syndrome, Ataxia telangiectasia and Nijmegen breakage syndrome are also discussed in Appendix G.

Component	Syndrome	Characteristics
ATM	Ataxia telangiectasia	Immunodeficiency; lymphoma; breast cancer
BLM	Bloom's syndrome <sup>@413</sup>	Immunodeficiency; growth deficiency; telangiectasia; diabetes; leukaemia; lymphoma
BRCA1	Hereditary breast/ovarian cancer <sup>@1422</sup>	Breast cancer; ovarian cancer
MLH1 MSH2 MSH6	Hereditary non-polyposis colorectal cancer <sup>@923</sup>	Colorectal cancer; gastric cancer; endometrial cancer
MRE11A	Ataxia telangiectasia-like disorder <sup>1262</sup>	Immunodeficiency; colorectal cancer
Nibrin	Nijmegen breakage syndrome <sup>@1361</sup>	Immunodeficiency; lymphoma

**Table I–1: Diseases associated with failure of BASC components**

# J

# Genome partitioning

*The critical process of spatially aligning replicated genomes during cell division is the province of the centrosome. Where this fails, the maintenance of stable ploidy is compromised, often with adverse consequences for the newly divided cells. Where they are viable, their genetic complement may be imbalanced and in consequence, their inherent activities and their sensitivity and responsiveness to external influences may be aberrant. If this leads to a dysregulation of proliferation, there can be dire consequences for the organism as a whole. The very frequent observation of centrosomal anomalies and ploidy changes in cancer attests to this.*

## J.1 Introduction

The maintenance of cellular viability and of species identity in diploid organisms depends on the reliable partitioning of the replicated genome between the two cells that result from cellular division. Without this, tissue differentiation and function could not be maintained, nor would the reliable hereditary transmission of beneficial genetic changes be possible. Failure of the first would make survival of a multi-cellular diploid organism impossible, and failure of the second would remove a critical component of the evolutionary process. Without evolution, there would be no basis for the generation of distinct species. Clearly, much hinges on the fidelity of this partitioning.

For any process involving the study or control of motion, whether of stars or chromosomes, a frame of reference is essential. The establishment of the mitotic spindle provides this within the dividing cell, laying down the spatial context of the coming events. It defines the axis of chromosomal motion during anaphase and the location of the division during cytokinesis. In multicellular organisms, where the fidelity of genome partitioning is vital, a supervisory subsystem is present that orchestrates this: the centrosome<sup>@290</sup>.

## J.2 Centrosome structure

### Morphology

The centrosome is a cytoplasmic structure comprising two centrioles, interconnecting fibres, and associated amorphous pericentriolar material (Figure J-1). Each centriole, measuring ~200 nm by ~500 nm, is composed of nine triplets of parallel coplanar microtubules arranged parallel to a common axis. One end of the centriole appears from electron-microscopic studies to be closed, and one to be open. There is evidence of a central structure aligned with the axis and connected to the middle microtubule of each triplet, and adjacent triplets are also connected. When viewed

This appendix deals with the spatial regulation of genome partitioning. The temporal regulation is covered in Appendix L.

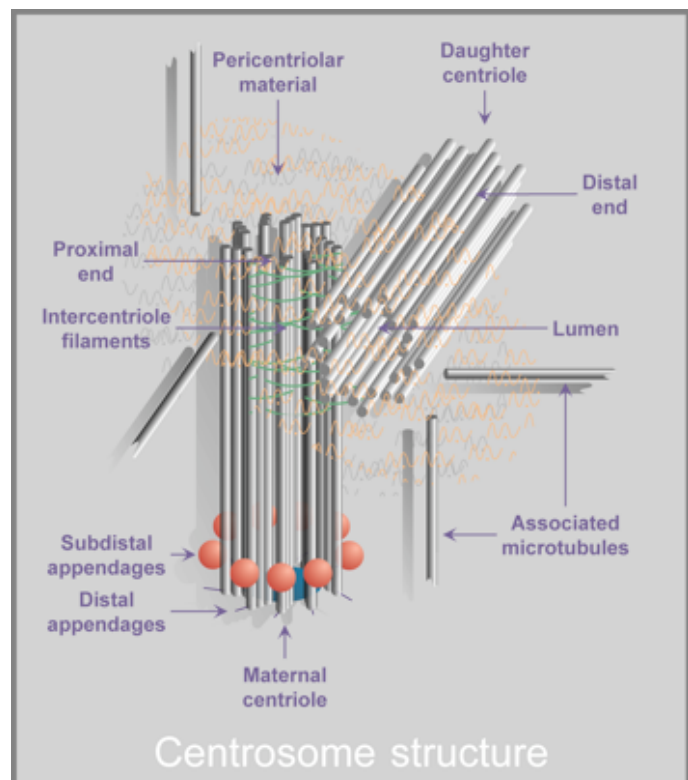


Figure J-1: Centrosome structure

from the open end, each triplet is oriented at a rotation of  $\sim 30^\circ$  clockwise to the tangential. The centrioles generally lie perpendicular to one another, with the open ends in proximity, hence their designation as proximal, and that of the other ends as distal. The two centrioles are distinguishable in that one, referred to as maternal, has both distal and subdistal appendages, lacking in the daughter centriole. The entire structure is associated with the slower-growing, minus-ends of cytoplasmic microtubules, connected chiefly via the pericentriolar material.

### Composition

Investigations in yeast, *Drosophila*, *Xenopus*, mouse, and human cells have brought to light a number of probable molecular components of the centrosome and its regulators, many listed in Table J-1. The investigation of the functions and interactions of these proteins is at present developing rapidly and many have been implicated in specific steps of the centrosome cycle {See 'The centrosome cycle', below}. However, given the inchoate state of our knowledge, any mechanistic analysis requires a degree of speculation to compensate for an economy of data.

### J.3 Centrosome function and dysfunction

Despite a century of investigation, the precise role of the centrosome is yet to be determined. Our understanding is based mainly on inferences drawn from coincidences of position and timing with visible cellular events. The association of centrosomes with the foci of the spindle microtubules at the cell poles during mitosis is strong circumstantial evidence for involvement in anaphase. The nature of this involvement has been difficult to investigate as micromanipulative removal of centrosomes was possible only during interphase, and cells so treated did not enter mitosis, in itself an interesting observation. Alternatives, such as antibody injection, could not be guaranteed to obliterate all function.

This changed with the work of Khodjakov et al.<sup>520 §663 §664</sup>, who, by incorporating green fluorescent protein into centrosomes, were able to ablate one or both with laser microsurgery at various points in the cell-cycle and observe the consequences\*. Their innovative approach led to results that have laid the cornerstone for our current understanding of centrosome function. Firstly, they found that destruction of one or both centrosomes in prophase did not interfere with the assembly of the mitotic spindle or, directly, with the process of anaphase. Where one centrosome was left intact, cytokinesis was essentially normal, but where both were ablated, 30% – 50% of cytokineses failed. The proximal cause of this was the failure of the mitotic spindle to maintain its orientation perpendicular to the cellular equator. In consequence, the segregation of chromatids was at times constrained by a reduced cellular diameter; misalignment caused incorrect chromosomal partitioning, even to the extent of generating one binuclear and one anuclear daughter cell; and obstruction of cleavage furrow propagation sometimes caused total failure of cytokinesis, also resulting in polyploidy. They went on to follow the fate of the acentrosomal daughter cell that resulted from the division of a cell in which one centrosome had been destroyed. Quite unexpectedly, they discovered that such cells never again commenced the synthesis of DNA, being trapped forever in a pseudo-G<sub>1</sub> state. Khodjakov et al. have therefore defined a two-fold function for the centrosome: to guide the process of anaphase, and to endow the daughter cell with proliferative potential. This is an extremely elegant method for ensuring that cells which would otherwise suffer a failure of cytokinesis, never get the opportunity to do so. There is also some poetry in the way this recapitulates the contribution by the sperm to the ovum of a functional centriole<sup>1138</sup>.

---

\* Khodjakov et al. provided an excellent video supplement to their seminal paper that demonstrates graphically the consequences of centrosome dysfunction. It is available at: <http://www.jcb.org/cgi/content/full/153/1/237/DC1>



Protein	Observations
14-3-3	Stratifin and 14-3-3 $\gamma$ are centrosomal. They are lost from the centrosome upon serum starvation <sup>S1031</sup>
AKAP9	Associates with centrosomes and the cleavage furrow <sup>1154</sup>
ATR	ATR duplication is associated with centrosome amplification and aneuploidy <sup>1242</sup>
BRCA1	Mutation is associated with excess centrosomes, unequal chromosome segregation, and aneuploidy <sup>263</sup>
BRCA2	Mutation is associated with excess centrosomes and micronucleation <sup>1349</sup>
CDC16	Centrosomal throughout the cell-cycle <sup>1348</sup>
CDC2	Centrosomal throughout the cell-cycle. Present within the pericentriolar material and on centrioles themselves <sup>1035</sup>
CDC20	Required for centriole splitting <sup>S1374</sup>
CDC25	Required for daughter centriole assembly <sup>S1374</sup>
CDC27	Centrosomal throughout the cell-cycle <sup>1348</sup>
CDK2	Function essential for centrosome duplication <sup>S857 879</sup> Critical centrosomal regulator <sup>@1438</sup>
CEP2	Target of NEK2; important in centriole cohesion <sup>379</sup>
CUL1	SCFC component associated with the centrosome; essential for centriole separation <sup>S373</sup>
Cyclin-A	Centrosomal from preprophase to metaphase <sup>59</sup> Function is essential for centrosome duplication <sup>S879</sup> Necessary for microtubule nucleation <sup>S142</sup>
Cyclin-E	Over-expression is associated with chromosomal instability <sup>1256</sup> Over-expression cooperates synergistically with TP53 deletion <sup>927</sup>
Dynein proteins	Interaction with dynactin is necessary for centrosome duplication and separation <sup>S823</sup> Dominant negative dynein allows spontaneous centrosome assembly, decoupling nuclear and centrosomal cell-cycles <sup>S84</sup> With dynactin, involved in delivery of $\gamma$ -tubulin and pericentrin for microtubule nucleation <sup>S1492</sup>
E2F2, E2F3	Function is essential for centrosome duplication <sup>S879</sup>
GADD45	Deletion is associated with aneuploidy, chromosome aberrations, gene amplification, and excess centrosomes <sup>S530</sup>
HRAS	Ectopic expression results in excess centrosomes, chromosome misalignment, and micronucleation <sup>1122</sup>
HSP90	Core centrosomal protein <sup>S745</sup>
MDM2	Over-expression is associated with excess centrosomes and chromosomal instability <sup>159</sup>
MEK1	Ectopic expression results in excess centrosomes, chromosome misalignment, and micronucleation <sup>1122</sup>
MRE11A	Non-expression results in excess centrosomes <sup>S1474</sup>
NEDD8	Modifier of centrosomal SKP1 <sup>S373</sup>
NEK2	Centrosomal throughout the cell-cycle; over-expression causes centrosome splitting and dispersal <sup>380</sup> . Binds and inhibits PP1 <sup>497</sup> . Probably anchors CEP2 to centrosome during interphase <sup>379</sup>
NM23	Centrosomal disposition <sup>S1115</sup>
NPM1	Associates with unduplicated centrosome; target of CDK2 causing loss of association; detachment is required for centrosome duplication <sup>974 1332</sup>
NUMA1	Associates with separating centrosomes in early mitosis <sup>S1504</sup>
p21	Reduction is associated with excess centrosomes and polyploidy <sup>S38 1309</sup>
p27	Injection of p27 inhibits centrosome duplication <sup>S731</sup>
p53	Deletion is associated with excess centrosomes, aneuploidy, gene amplification, and apoptosis <sup>388</sup> Cooperates synergistically with cyclin-E over-expression <sup>927</sup>
PARP	Centrosomal disposition <sup>633</sup>
PLK	Required for centrosome maturation <sup>951</sup>
PP1	PP1 $\alpha$ is a target of CDK2 <sup>798</sup> , and PP1 $\gamma$ is a target of NEK2 <sup>497</sup> . PP1 $\alpha$ <sup>880</sup> and PP1 $\gamma$ <sup>497</sup> are centrosomal
SKP1	Centrosomal throughout the cell-cycle <sup>443</sup> SCFC component associated with the centrosome; essential for centriole separation <sup>S373</sup>
SKP2	Targeted disruption results in excess centrosomes, polyploidy, enlarged nuclei, and apoptosis <sup>S935</sup>
STK15	Gene amplification is associated with excess chromosomes and aneuploidy <sup>1521</sup>
STX8	Associates with centrosomes and mitotic spindle. Binds cyclin-B1 and p21 <sup>870</sup>
TTK	Mouse homologue Mps1p is required for centrosome duplication; target of CDK2; associates with centrosomes beginning in S-phase; over-expression is associated with excess centrosomes <sup>S354</sup> . Human protein is not implicated <sup>1269</sup>
XRCC2	Deletion is associated with centrosome fragmentation and chromosome missegregation <sup>440</sup>
XRCC3	Deletion is associated with centrosome fragmentation and chromosome missegregation <sup>440</sup>
zyg-1	Required for daughter centriole formation <sup>S964</sup>

Table J-1: Proteins implicated in centrosomal regulation

The centrosome may yet prove to have a further indispensable cellular function. As a cell divides, the last physical link between nascent daughter cells is an intercellular bridge that derives from the spindle midbody. In what appears to be a final, critical step in their separation<sup>1029</sup>, this bridge is visited by a maternal centriole<sup>824</sup>, very likely implementing the last checkpoint on cell division. Its arrival signals that it has been released from its duty in anchoring the mitotic spindle by the breakdown of the latter in telophase, and that no impediment remains to the culmination of cytokinesis.

While loss of centrosomal function has dire consequences for cellular propagation, excessive functionality, in the form of supernumerary centrosomes, is no less deleterious. This is principally because despite their being unnecessary for spindle formation, they are not without influence on its structure. When, for whatever reason, excess centrosomes are present, the centrosome's microtubule organising capacity overrides the default bipolar spindle geometry rather than reinforcing it. In consequence, multipolar spindles can form, and at anaphase, two sets of chromosomes will attempt to segregate in three or more directions with resultant chaos. With the number of pronuclei at odds with the normal two-fold symmetry of cleavage furrow propagation, cytokinesis is also chaotic. With three centrosomes, the cell may well divide into three, and such behaviour has been observed in CHO cells<sup>8657</sup>, with the production of cells of unequal size accompanied by micronucleation<sup>1159</sup>. Thus, the failure of centrosome numerical control may well lead to the generation of cells likely to contain one or two thirds of the normal chromosome complement. Coupled with the possibility of aborted cytokinesis, centrosome functional failure can readily account for triploidy and derivatives thereof, as reported here, and previously by others in human melanoma tumours<sup>81 912 988</sup> and cell-lines<sup>245 668 787</sup>.

### J.4 The centrosome cycle

#### Overview

The centrosome and the nucleus share the distinction of being under numerical control during cell division. Each is duplicated exactly once every cell-cycle<sup>1237</sup>, and each daughter cell receives exactly one of each. In either case, were this not a fundamental requirement for the survival of the cell or its descendants, it is unlikely that this degree of control would have come into existence, or if it did, have endured. Why this is so for the nucleus is well established, but the critical role of the centrosome remains enigmatic.

The centrosome derives its name from its predominantly perinuclear location, but as implied above, this alters in synchrony with the cell-cycle. With the commencement of S-phase, centrosome duplication begins, and is essentially complete by late G<sub>2</sub>. Immediately prior to the onset of mitosis, the now duplicated centrosomes separate and migrate to opposite poles of the cell associating closely with the forming mitotic spindle. Each remains at this location until late in telophase, when, with the disassembly of the mitotic spindle, a single centriole moves to the midbody that connects the two incipient daughter cells. When cytokinesis is complete, the centriole returns to a perinuclear location.

#### Molecular biology

##### *Interphase*

During interphase, the centrosome is to be found in its perinuclear location {Figure J-2}. The centriole pair is tethered closely by NPM1 [1], a ribonuclease<sup>974</sup> better known as a nucleolar ribosome assembly factor<sup>523</sup>. The pair is more loosely attached via the NEK2 kinase and the CEP2 protein [2]. Of these, only NEK2 remains centrosomal throughout the cell-cycle<sup>380</sup>. They are closely associated with a catalytic subunit of the PP1 protein phosphatase<sup>497</sup>. Both the alpha<sup>880</sup> and gamma<sup>497</sup> isoforms have been reported to be centrosomal, but nothing appears to be known of which regulatory subunits may be involved. At



this stage, PP1 is unphosphorylated and therefore active [3], inhibiting the aurora-family kinase, STK15. NEK2 may also be a PP1 substrate, but whether or not this is the case, it is inactive for want of phosphorylation.

### Initiation of centriole replication

The activation of CDK2 {Figure J-3} [1] at the G<sub>1</sub>-S-phase transition appears to be the critical event triggering the onset of centrosome duplication<sup>857</sup>, and provides synchronisation between the nuclear and centrosomal cell-cycles<sup>1438</sup>. Whether the activating partner for CDK2 is cyclin-E, cyclin-A, or either, is not clear. There is strong evidence from *Xenopus* that cyclin-E is critical<sup>8519</sup>, and this is supported by a role for p27 in regulating duplication, and the association seen between cyclin-E over-expression and genomic instability<sup>1256</sup>. However, in mammalian cells, cyclin-A has been strongly implicated<sup>8879</sup>.

Activated CDK2 phosphorylates NPM1, dislodging it from the centrosome and breaking the close association between centrioles [2] in a step critical for the progression of centrosome replication<sup>1332</sup>. The NEK2-CEP2 linkage remains intact, however, keeping the separated centrioles in proximity. A second CDK2 substrate, at least in the mouse<sup>8354</sup>, is the Mps1p kinase. While phosphorylation increases protein stability and allows Mps1p to associate with the centrosome, the consequences for Mps1p enzyme function, and what its substrates may be are yet to be determined. Recent work has suggested that its homologue in humans, TTK, while being necessary for the spindle assembly checkpoint, is dispensable for centrosome duplication<sup>1269</sup>. Finally, the apparent requirement for E2F-dependent transcription to support centrosome duplication<sup>879</sup> implies that the well-characterised role of CDK2 phosphorylation of pRB [3] may have consequences beyond fostering S-phase entry.

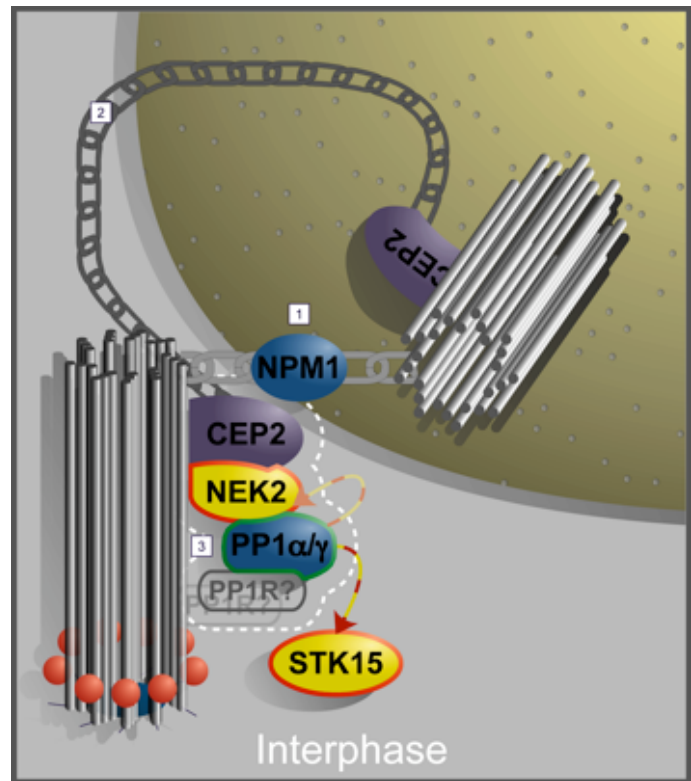


Figure J-2: The centrosome in interphase

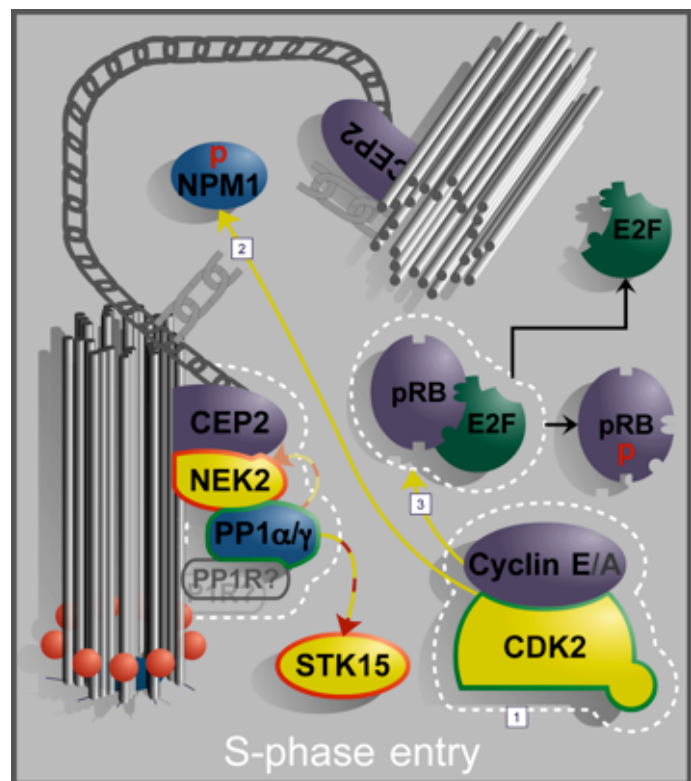
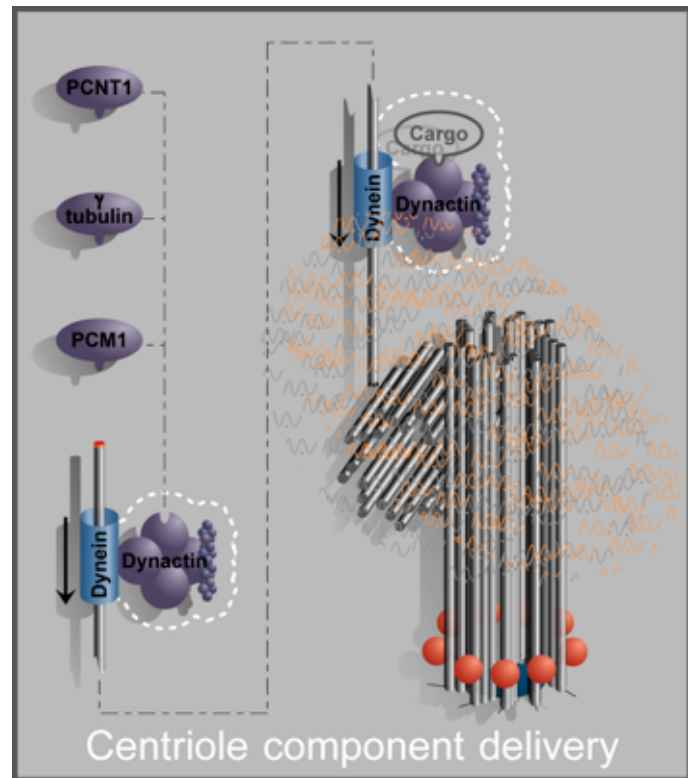


Figure J-3: The centrosome at S-phase entry

## Human metastatic melanoma in vitro

At this point, centriole replication can commence. Whether the disruption of the strict orthogonal geometry of the centriole pair attendant upon the departure of NPM1 represents the limiting factor in this process is unclear, as are the details of procentriole establishment and growth. Given that centrioles can assemble *de novo* in cells where no maternal centriole is present, albeit in *Chlamydomonas*<sup>847</sup>, an attractive hypothesis is that the component molecules are able to self-assemble, ultimately achieving the lowest energy state with the effective co-crystallisation of a new centriole. If so, where a maternal centriole was present, it may act as a centre of nucleation, accelerating the process and dictating the place at which it occurs.



**Figure J-4: Centriole component delivery**

A more active role for a pre-existing centriole relates to supply logistics. Functional and immunocytochemical studies have established that the minus-end directed cytoplasmic dynein/dynactin microtubule motor is required for centriole assembly<sup>823</sup>. Its role appears to be as a transport system for delivery of centriole components including PCM1<sup>63</sup>, pericentrin<sup>1492</sup>,  $\gamma$ -tubulin<sup>1492</sup>, and dynactin itself {Figure J-4}. By increasing the local concentration of these by virtue of being at the hub of a microtubule network, the maternal centriole would greatly enhance the rate of daughter centriole assembly. The other, and possibly preferred theory, is that the maternal centriole acts as a template, but nothing has been established concerning how this may occur.

Once started, centriole assembly continues until halted by the onset of mitosis. There does not appear to be any inherent mechanism arresting assembly after one round of duplication. One consequence of this is that where S-phase is extended, centrosome amplification can occur<sup>863</sup>. This is normally prevented by a mechanism involving p53 and BRCA1 {See 'p53: Guardian of the centrosome?', below}, but where this is defective, or not triggered by the particular event, a failure of numerical control can occur. The mechanism is not fail-safe. The recent implication of the *Caenorhabditis elegans* *zyg-1* gene<sup>964</sup> in this numerical control may lead to a greater understanding of this, as it encodes a kinase that appears to inhibit procentriole establishment until after centriole separation.

### **Centrosome severance**

Late in G<sub>2</sub>, the centrosomes separate and migrate to the cell poles to form the prophase asters. This is one of the points in the molecular regulation of centrosome replication where only fragmentary information is available and inference and speculation must serve instead. Centrosome severance appears to be linked to the commitment to enter mitosis since the study cited above involving an extended S-phase found that under these circumstances the centrosomes remained linked.

What is clear is that at or about this time, PP1 is phosphorylated and deactivated. Two kinases are known to be able to perform this: STK15<sup>643</sup> and NEK2<sup>497</sup>. An intriguing relationship therefore exists

between PP1 and STK15 in that each is able to inactivate the other<sup>643</sup> [Figure J-5] [1]. The consequence of this functional antagonism is that at any time, one of the pair will be dominant, suppressing the function of the other, and this state will endure in the absence of any external perturbation. To borrow a term from digital electronics, this could be said to form a bi-stable kinase-phosphatase oscillator. This fosters the suggestion that PP1 and NEK2 may form another such bi-stable element [2],

particularly in light of their direct physical association and the ability of NEK2 homodimers to effect reciprocal trans-phosphorylation<sup>497</sup>, thereby maintaining dominance. This would be a logical inference from a mechanistic viewpoint, but its proof must await the demonstration of an inactivating dephosphorylation of NEK2 by PP1.

Also to be determined is the nature of the external perturbation that triggers the state change. This may take the form of a kinase targeting NEK2 or STK15 and thereby opposing their deactivation by PP1. Conceivably, PP1 may itself be the kinase target if the inherent autophosphorylation capacity of NEK2 were sufficiently strong. An obvious candidate kinase is activated CDK2 [3]. As centrosome separation usually occurs late in G<sub>2</sub>, cyclin-A presents a more attractive choice of activating partner for CDK2 than does cyclin-E. Such a change may hold significance for substrate preference, allowing events to be initiated in their proper sequence. This model is lent some credence by the reported ability of CDK2 to phosphorylate and inhibit the PP1 alpha<sup>798</sup> catalytic subunit, although this has not been demonstrated in a centrosomal context. CDK2 could therefore serve to prime the state transition, being the external perturbation necessary to upset the status quo, and STK15 and NEK2 maintain this state beyond the inactivation of CDK2 upon the loss of its cyclin partner during mitosis. It seems likely that PP1 is targeted by multiple kinases, ensuring that it remains inhibited until the last of them becomes inactive. Ultimately, a prime target of this control mechanism is CEP2, as it is a substrate of both NEK2 and PP1<sup>497</sup> [4]. The significance of this becomes clear when it is recalled that CEP2 is a critical component in the linkage between duplicating centrosomes<sup>864</sup>.

Upon activation of NEK2 [Figure J-6] [1], CEP2 is phosphorylated causing it to dissociate from NEK2, thereby severing its

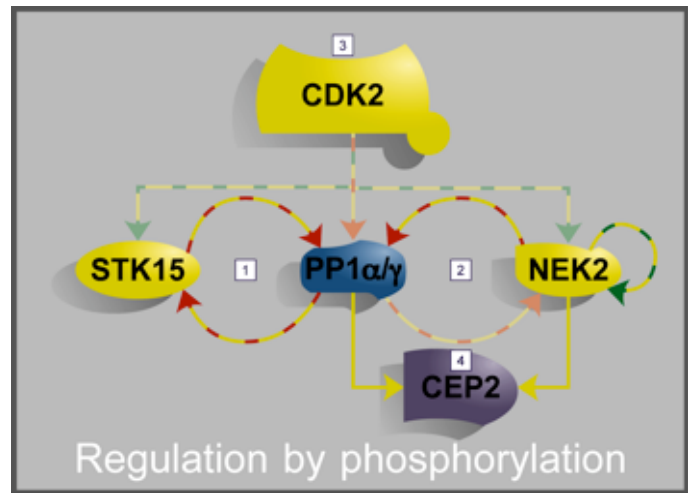


Figure J-5: Centrosomal regulatory phosphorylations

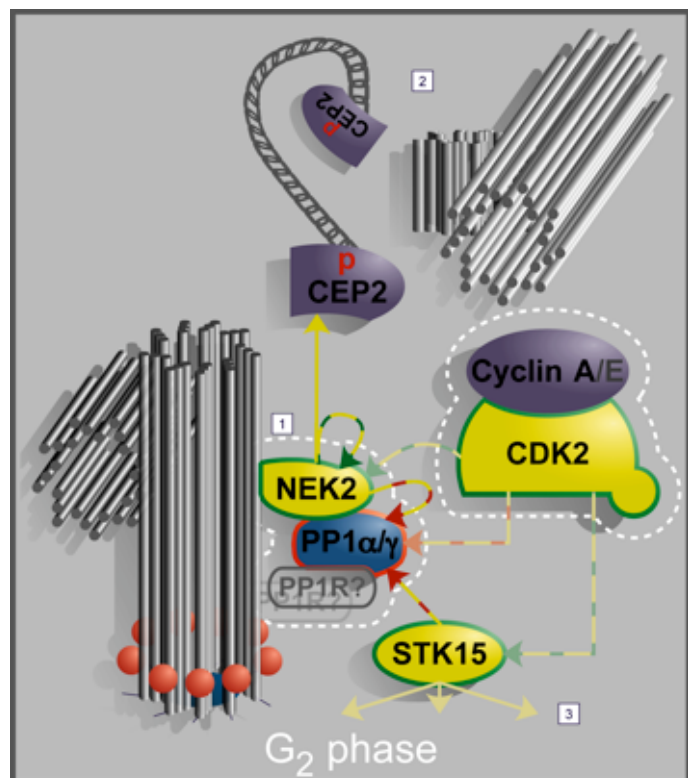
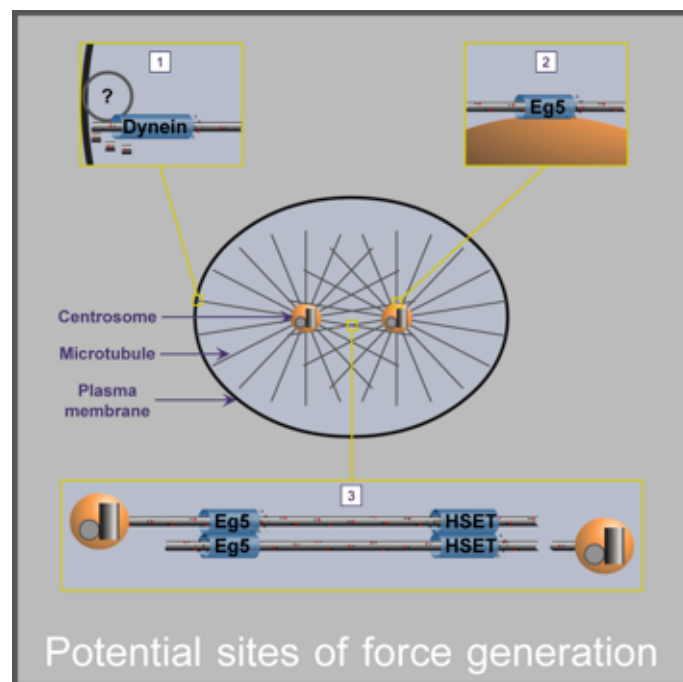


Figure J-6: Centrosomes in G<sub>2</sub>

centrosomal link and triggering centrosome separation [2]. There are probably additional STK15 substrates yet to be identified, providing scope for further consequences of its activation [3].

### Centrosome separation

Once the centrosomes are fully detached, they are free to relocate to the cell poles. This is an active process that is dependent on cytoplasmic microtubules and motor proteins, but there is as yet no broad agreement on how these elements contribute to the process. Consideration of the known activities and spatio-temporal associations of these components suggests a number of possible mechanisms to generate the required separative force {Figure J-7}. Cytoplasmic dynein, perhaps the most common minus-end directed microtubule motor protein<sup>44</sup>, has been shown to be essential for centrosome migration in *Drosophila melanogaster*<sup>51098</sup> and *Caenorhabditis elegans*<sup>5424</sup>. In both cases, the observation was



**Figure J-7: Generation of inter-centrosome force**

that centrosomes failed to become diametrically opposed at the nuclear surface prior to nuclear envelope breakdown (NEB), and that this asymmetry resulted in poor spindle alignment. However, the centrosomes did separate substantially after NEB, even if the geometry was imperfect. Therefore, while dynein may be important in centrosomal positioning prior to separation, it does not appear to provide the major separative force. As it is a minus-end directed motor, and microtubules are arranged radially around centrosomes with the minus-ends in the pericentrosomal material, the only direction that dynein could travel with respect to a centrosome would be towards it. For this to result in separation of centrosomes implies that it must be anchored at the cellular cortex, and act to pull the centrosomes outward [1]. In support of this model, 'astral-pulling' has been reported<sup>50 1410</sup>, there is evidence that dynein participates in cortical microtubule anchoring<sup>145</sup>, and disassembly of microtubules, particularly at their plus end, is well established. The NUMA1 protein<sup>1504</sup> could play a role here as it associates with both microtubule minus-ends and the dynein minus-end directed motor protein. In so doing it can organise randomly oriented microtubule into asters with minus foci, and concentrate dynein at their centres, precisely what is seen at the spindle pole. As it stands, this model cannot account for specific bipolarity or separation of centrosomes beginning prior to the extension of microtubules to the cortex. It is in the resolution of the first that centrosomes come into their own as microtubule organising centres.

A more likely candidate to provide motive force is the plus-end directed kinesin-like protein, Eg5. By its nature, it distances itself from the centrosome anchoring the microtubule to which it is attached, and it is known to be required for centrosome separation<sup>951</sup>. To harness the force generated by Eg5 to promote separation requires only that it be physically coupled to the centrosome that is not anchoring the microtubule on which it travels. An obvious mechanism for this is the direct attachment of Eg5 to one centrosome where it engages a microtubule radiating from the other centrosome [2]. Studies of Eg5 location during mitosis show, however, that it does not remain centrosomal, but rather associates with

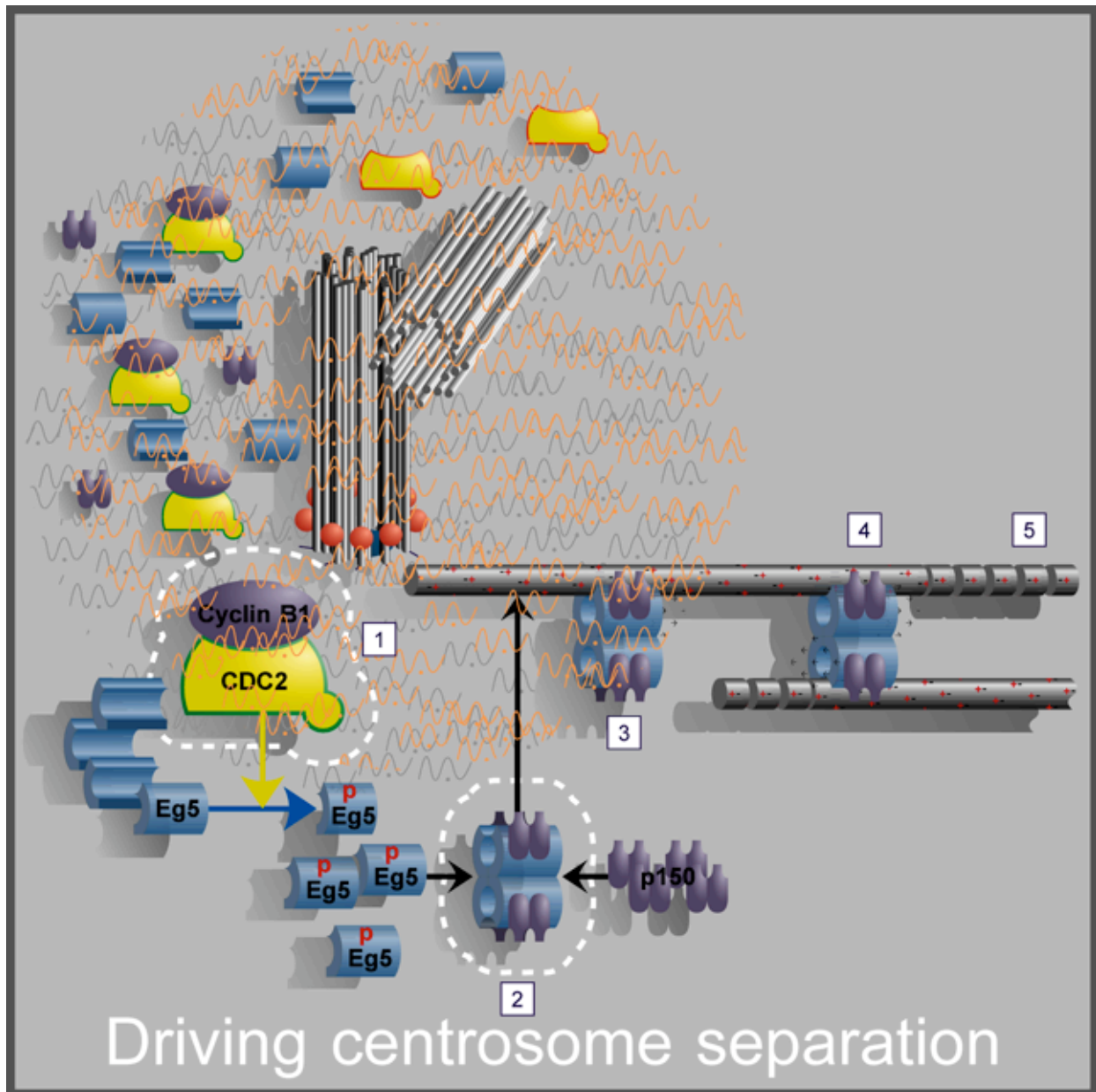


**Figure J-8: Centrosome separation**

the full length of the microtubules of the forming mitotic spindle<sup>1356</sup>, and furthermore, moves upon them<sup>1436</sup>. This leads to the third, and most favoured model of centrosomal force generation, wherein Eg5 promotes the relative motion of antiparallel microtubules, with each being translated in the minus direction [3]. However, not all workers find this to be consistent with experimental observations<sup>1410</sup>. A particularly attractive aspect of this model is that it spontaneously gives rise to bipolar symmetry since the net force generated will be directed along a line linking the centrosomes. The situation is complicated by the existence of a related kinesin-like motor protein, HSET, which has been demonstrated to cross-link microtubules directly, but is minus-end directed<sup>918</sup>, and therefore works in opposition to Eg5. The net effect is therefore likely to depend on the relative activities of the various elements, and this balance is likely to be under an active control that is still to be characterised.

The synchronisation of the commencement of centrosome separation with the start of mitosis parallels the mechanism that synchronises centrosome replication with S-phase: the activation of a CDK. In this case {Figure J-8}, it is CDC2, most probably in conjunction with cyclin-B1 [1]. CDC2 is a constitutive part of the centrosome, being distributed throughout the pericentriolar material and present at the surface of

centrioles<sup>1035</sup>. Phosphorylation of Eg5 by activated CDC2 dramatically affects its cellular disposition and binding properties causing it to accumulate in prophase at the centrosomes from a state of cytoplasmic dispersal<sup>1431</sup>. This is probably due to an increased affinity for the p150 subunit of dynactin<sup>101 102</sup> [2], already there as a result of dynein mediated component delivery. In conjunction with dynein, dynactin is thought to act as an adaptor, linking the dynein motor to its cargo.

In addition to domains mediating interactions with dynein and cargo, each component of the usual p150 dimer contains one that binds microtubules. These domains are thought to augment the affinity of the attached motor unit, be it dynein or Eg5, for microtubules and possibly maintain contact during any temporary detachment of the motor during procession. Eg5 most probably adopts a conformation similar to its *Drosophila melanogaster* homologue Krp130, that of a bipolar homotetramer<sup>S640</sup>, ideally suited for the interlinking of antiparallel microtubules. Whether as dimers or tetramers, the assembled Eg5 complex, with its associated p150, is then able to form a stable association with the centrosomally anchored microtubule, and it begins its motion toward the plus-end [3]. During its progression, it may encounter a microtubule of opposite polarity to which the available Eg5/p150 site can bind. More symmetrically, dimeric unipolar Eg5 motors may form at each centrosome, and upon encountering one another, engage to bring about the same structure. Once the cross-link is in place, and assuming that the microtubules are rigid and non-compressible, a force tending to separate the centrosomes will be developed [4]. During this period, microtubule growth at the plus-end is also favoured [5], providing increasingly long connecting rods that the Eg5 complex can use to displace the attached centrosomes.

Ultimately, separation must be constrained by the physical size, flexibility, and strength of the plasma membrane in order to prevent its rupture, but the manner in which this is regulated is unknown. Ideally, once the maximal tolerable extension has been reached, further extension should be suppressed, but this should not be at the expense of the stability of the assembled mitotic spindle. Two simple mechanisms for achieving this goal would be the modulation of Eg5 activity or of plus-end microtubule extension. Both may occur via active mechanisms, and physical contact with the forming metaphase plate would constitute a suitable synchronising trigger. Alternatively, the Eg5 motor may simply stall when the translational force it is able to exert on a microtubule is counter-balanced by the compressive force ultimately generated by plasma membrane containment, and defined by its elasticity and cohesiveness.

### ***Post-mitotic relocation***

As telophase is completing, the advancing cleavage furrow constricts the equator of the dividing cell resulting in the formation of a bridge interconnecting the incipient daughter cells. The mitotic spindle and polar microtubules have been disassembled, and the centrosome is no longer required at the cell pole. The fate of the centrosome at this stage has best been described by Piel et al.<sup>1029</sup>, who followed events with fluorescently tagged centrosomes and time-lapse video phase-contrast microscopy. They found that one, and occasionally both centrosomes split into their separate centrioles once again, that the maternal centriole moved rapidly across the cell to the intercellular bridge, and upon its arrival, a narrowing of the bridge was observed. They demonstrated that the arrival of the maternal centriole at the bridge, and its subsequent departure, were both necessary precursors to cellular abscission, and, by synchronised nocodazole addition, that movement in both directions was microtubule dependent. By serial-section electron microscopy, they determined that it was the subdistal appendages of the centriole that were implicated in the bridge interaction. The motive force behind this relocation is unknown, but the presence of dynein and dynactin at the cleavage furrow and midbody<sup>636</sup> may go some way toward an explanation. In 70% of cells observed, only one centrosome split, and only one maternal centriole visited

the bridge. This raises the question of the basis for this asymmetry, an aspect not addressed in their paper.

It seems unlikely that there could be any communication between centrosomes located at opposite sides of nearly completely separated cells, so the distinction in abscission mediating function must be inherent within each, and normally exist in only one. A plausible model to explain this can be developed from the hypothesis that centrioles progress through three stages of functional maturity. The first is the partially or newly formed nascent centriole, incapable of either fostering further centriole assembly or of sponsoring cellular abscission. In the second stage, the centriole achieves a fully active status, being able to perform both functions. Finally, the centriole becomes cytokinetically passive, being able to promote centriole assembly, but not mediate abscission. The first corresponds to the current definition of a daughter centriole, and the last two to subdivisions of maternal status. The established involvement of the maternal subdistal appendages with cellular abscission suggests that this may be the site where the distinction between active and passive states is made. If the appendages possessed a one-time abscission mediating function, the transition from nascent to active could correspond to its synthesis, and from active to passive, to its use and disablement. The transitions between these stages and their associations with cellular events are depicted in Figure J-9. Early in  $G_1$  [1], the cell has a single centrosome consisting of one nascent centriole, and one which for the moment is assumed to be passive, having been the agency behind the recent abscission. During  $G_1$  [2], the nascent centriole achieves active status, and in S-phase, the centrosome splits, and new nascent centrioles are formed [3]. During mitosis [4], the centrosomes separate and move to the cell poles where they reside until the completion of telophase. At this time, the single active centriole separates from its partner and moves to the inter-cellular bridge [5] where it stimulates abscission, and in so doing, loses its active status and becomes passive. Cytokinesis completes [6] with two daughter cells each containing centrosomes that are again in their initial state, ready for the next cycle.

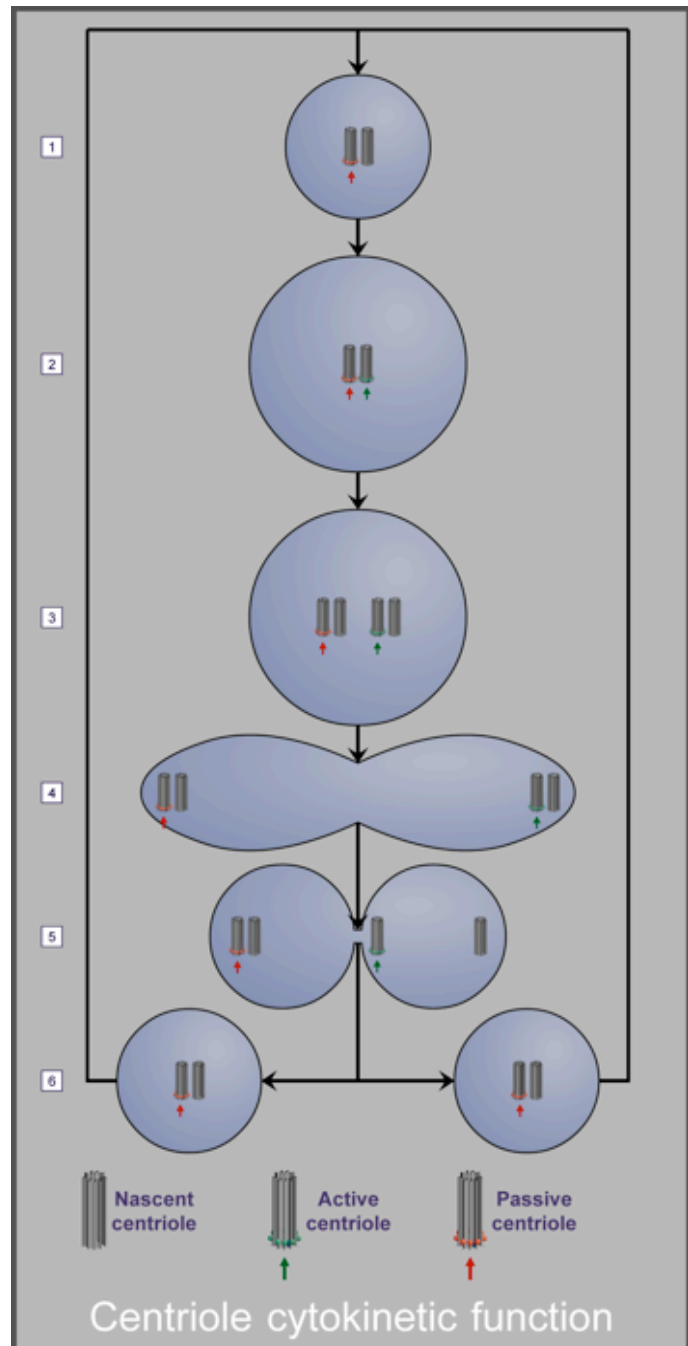


**Figure J-9: Centriole peregrination**

This model neatly accounts for the activation of a single centriole during each cytokinesis. How then are the 30% of cases where two centrioles are activated to be accounted for? One possibility rests with the experimental system in which the key observations were made: the HeLa human cervical adenocarcinoma cell-line. This line is aneuploid<sup>31</sup>, contains HPV18 DNA sequences<sup>427</sup>, and possibly as a result, only weakly expresses p53. This suggests that centrosomal regulation may be abnormal in this cell-line, and the 30% incidence of multiple maternal centriole activation may simply be a consequence of this {See 'p53: Guardian of the centrosome?', below}. Examination of this scenario within the context of the model just described brings to light a further aspect worthy of consideration. If each centrosome contains an active centriole at the completion of telophase, then both will detach and migrate to the intercellular bridge, and both will then become inactive. Irrespective of whether one or two centrioles were active, after cytokinesis the disposition of the centrioles in the daughter cells is identical. The system spontaneously reverts to generating exactly one active centriole per cytokinesis.

### **Upstream regulation – the cyclin-dependent kinases CDK2 and CDC2**

A tacit assumption in the preceding discussion was that the regulation of the synchronising kinases CDK2 and CDC2 was being performed correctly. However, given their crucial role, this must be expanded upon, as flaws in this process can and do influence centrosome regulation and may therefore impact on the maintenance of euploidy. Three major modes of regulating CDK kinase activity are known<sup>1008</sup>.

#### *Regulation by cyclin association*

The first mode of CDK regulation provided the basis for the name of the class to which they belong: cyclin-dependency. Only with the cooperation of an activating partner can any CDK function as a kinase. In the case of CDK2, activation has been reported in conjunction with cyclins A<sup>315</sup>, B1<sup>267</sup>, D2<sup>1285</sup>, and E<sup>701</sup>. Interestingly, while it binds to cyclin-D1, it is inhibited, rather than activated by it<sup>386 517</sup>, and opinion is divided over the effect of cyclin-D3 binding<sup>202 332</sup>. The most important physiological CDK2 cyclin partners appear to be cyclin-A and cyclin-E. A non-cyclin activating partner, RINGO, has recently been identified in *Xenopus laevis*, and CDK2 so activated is less susceptible to the other regulatory modes<sup>635</sup>. In the case of CDC2, the activating cyclin must be either a cyclin-A or cyclin-B isoform.

One central theme of this dependency is that it lays down the broad sequence of CDK activation during the cell-cycle. With the disinhibition of E2F1 late in G<sub>1</sub>, synthesis of cyclin-E commences and the activation of CDK2 becomes possible. Later, in a poorly understood process involving E2F and pRB-related pocket proteins, cyclin-A expression increases. The availability of a second activating cyclin for CDK2 may have implications for kinase substrate specificity<sup>892</sup>. When levels of cyclin-A grow beyond that of its preferred partner CDK2, the excess may commence the activation of CDC2 late in S-phase or in G<sub>2</sub>. This is soon overtaken by the increasing availability of cyclin-B1, which in conjunction with CDC2 mediates the majority of M-phase activities.

#### *Regulation by alteration of phosphorylation status*

The second mode of CDK regulation involves alterations to the phosphorylation status of three residues conserved both evolutionarily and among the CDKs. Representative proteins with close homology to CDK2 or CDC2 are shown in Table J-2.

In general, the effect of phosphorylation of <T14> or <Y15> inhibits kinase function<sup>91</sup>, whereas phosphorylation of <T160> is mandatory for activity<sup>444</sup>. The kinases and phosphatases responsible for regulation of these sites in vivo have not been identified unequivocally, but in some cases, very good



Species	Protein	<T14>	<Y15>	<T160>
<i>Saccharomyces cerevisiae</i>	Cdc28	T18	Y19	T169
<i>Schizosaccharomyces pombe</i>	CDC2	T14	Y15	T167
<i>Dictyostelium discoideum</i>	crp	T14	Y15	S159
<i>Arabidopsis thaliana</i>	p34(cdc2)	T14	Y15	T161
<i>Caenorhabditis elegans</i>	p34cdc2	T32	Y33	T179
<i>Drosophila melanogaster</i>	cdc2c (cdk2)	T18	Y19	T162
	cdc2	T14	Y15	T161
<i>Xenopus laevis</i>	CDK2 (Eg1)	T14	Y15	T160
	CDC2	T14	Y15	T161
<i>Mus musculus</i>	Cdk2	T14	Y15	T160
	Cdc2A	T14	Y15	T161
<i>Homo sapiens</i>	CDK2*	T14	Y15	T160
	CDC2	T14	Y15	T161

\* Multiple splice variants exist, including an N-terminal extension with T17/Y18 (XP\_049150).

**Table J-2: Conservation of CDK regulatory phosphorylation sites**

candidates have been suggested. For the most part, these too share a high degree of homology among species.

From structural studies, it is known that the <T14> or <Y15> residues are positioned within the catalytic cleft of the kinase domain, and inhibition is probably through exclusion of ATP by the resident phosphate groups {See 'Regulation by inhibition', below}. The kinase responsible for <Y15> phosphorylation may be <WEE1><sup>1453</sup>, but that for <T14> has not been established with any certainty and may be *PKMYT1*<sup>116</sup>. In both cases however, the associated phosphatase appears to be CDC25. In vertebrates, where multiple CDC25s and CDKs exist, CDC25A<sup>120 1170 @952</sup> appears to participate predominantly in the regulation of CDK2, and CDC25C, that of CDC2.

Despite the similarities among CDKs, differences in regulation by phosphorylation are known<sup>116 1046</sup>, and generalisations must be viewed with caution. Indeed, studies in *Drosophila melanogaster* have suggested that the phosphorylation state of T14 and Y15 of cdc2c is functionally irrelevant<sup>874</sup>, and a paradoxical Cdk2 Y15 phosphorylation in conjunction with stimulus to proliferate has been reported in mouse cells expressing human CDC25A<sup>8184</sup>.

The critical T-loop T160 phosphorylation significantly alters CDK2 conformation and thereby facilitates substrate binding<sup>138 531 1120</sup>, and a similar situation almost certainly prevails in the case of CDC2<sup>1048</sup>. In vivo, the CAK complex, or a related kinase, performs the activating phosphorylation of <T160><sup>629</sup>, but there is evidence that significant differences exist in this function between yeast and vertebrates<sup>628</sup>, with the possibility in the latter of an influence by p53<sup>1157</sup>. The identity of the antagonistic phosphatase is unresolved, with PP2<sup>195</sup> and KAP<sup>1047</sup> being implicated.

The presence of multiple phosphorylation sites, potentially independently regulated, implies numerous unique combinations and transmutations {Figure J-10}. Some patterns and transitions have been detected

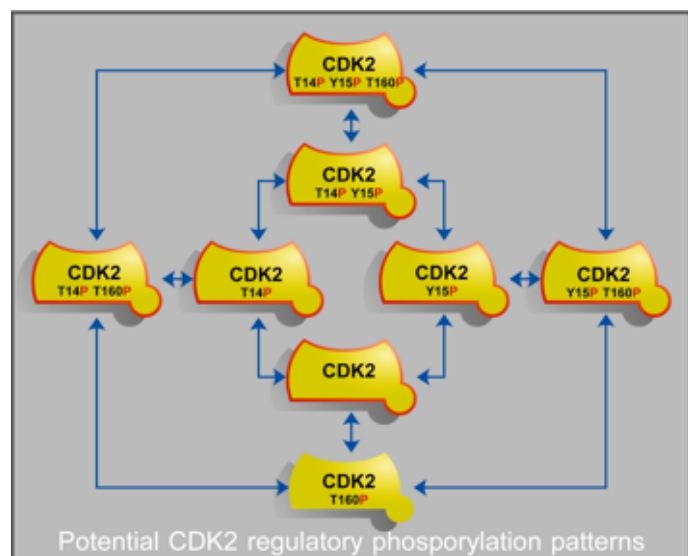


**Figure J-10: CDK2 phosphorylation states**

## Human metastatic melanoma in vitro

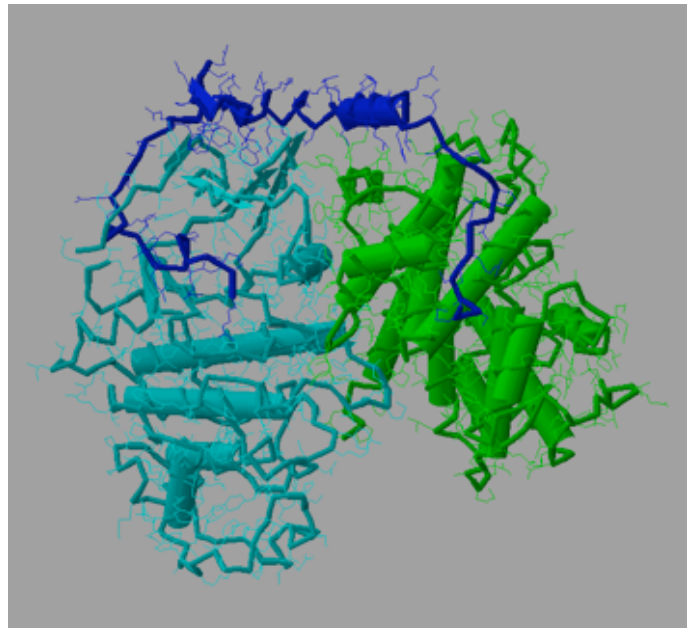
experimentally and some can be inferred to exist. A thorough analysis of possible interactions among these states is yet to be reported. What does seem to be clear is that only that molecular species phosphorylated on <T160> alone has the potential to become active.

### Regulation by inhibition

The third mode of CDK regulation is via the actions of inhibitory proteins. Members of one class, the p16-related family, are specific inhibitors of CDK4/6, and so have no direct role in the regulation of CDK2 or CDC2, or consequently, centrosome regulation. In contrast, members of a second class, characterised by homology to the p21<sup>CDKN1A@125</sup> protein, are of direct relevance, particularly p27<sup>CDKN1B</sup>.

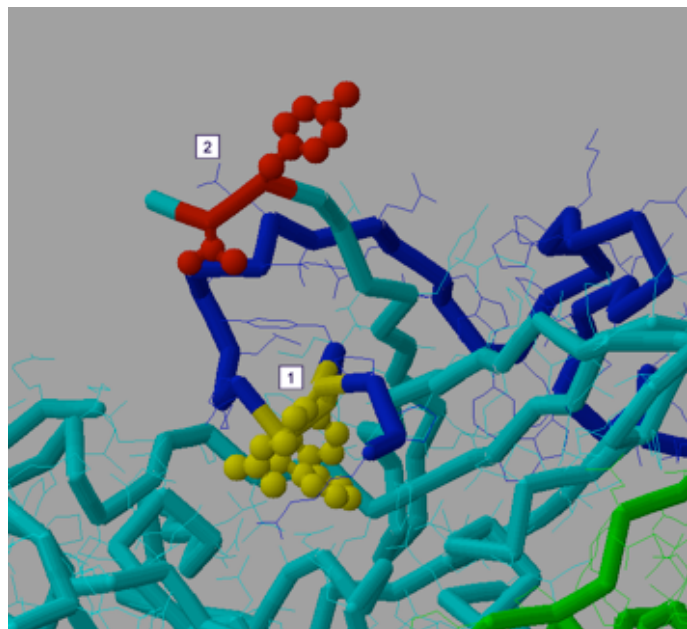
p27 has been implicated in cell-cycle arrest in response to the presence of inhibitory cytokines (IL4<sup>799 1386</sup>, TGFβ<sup>1089</sup>, IL1-α<sup>1503</sup>), the absence of stimulatory cytokines (PDGF<sup>1189</sup>, FGF2<sup>1189</sup>, IL2<sup>1386</sup>, IL3<sup>1069</sup>, IL10<sup>1386</sup>), hypoxia<sup>402</sup>, and in anchorage dependency<sup>490 716 1217</sup>, contact inhibition<sup>276 503 610 771 1045 1257</sup>, and myeloid cell differentiation<sup>244</sup>. It can bind CDK2 and cyclin-A or cyclin-E either individually, or in a ternary structure {Figure J-11} through multiple protein interaction domains. Its major inhibitory function {Figure J-12} is mediated by the insertion into the kinase catalytic site of three amino acids, F87, Y88 and R90 [1], which mimic the interactions of ATP. This model is supported by studies of the related p57 protein<sup>485</sup>. The immediate adjacency of the CDK2 T14 and Y15 regulatory sites [2], displaced by the presence of p27, suggests that the same underlying inhibitory mechanism is employed by both: the occupation of the ATP binding site.

The level and functionality of p27 are under post-transcriptional control via at least three degradative mechanisms, operative in different cell-cycle phases and physiological conditions<sup>834 1215</sup>. The first, which dominates in G<sub>1</sub>, involves the ATP-dependent proteolytic cleavage of the N-terminal cyclin-binding domain, resulting in a reduced affinity of p27 for cyclin-CDK



Key: CDK2 = light blue; cyclin-A = green; p27 (N-terminal 69 amino acids) = dark blue. Data from Russo et al.<sup>1119</sup> Rendered by Cn3D {E.9}.

Figure J-11: Complex of cyclin-A, CDK2, and p27



Key: as for Figure J-11. p27 amino acids shown in yellow mimic ATP binding. CDK2 amino acids shown in red are those subject to regulatory phosphorylation.

Figure J-12: Mechanism of CDK2 inhibition by p27

complexes<sup>1215</sup>. The second, operative in S and G<sub>2</sub>, hinges on T187 phosphorylation by CDK2 and ubiquitin-directed proteolysis<sup>1379</sup>.

This presents an apparent conundrum in that p27 is a substrate of the very enzyme it inhibits. One mechanism that could account for this would require that p27 be phosphorylated by a CDK2 other than that to which it is bound, and therefore inhibiting. One implication of this would be that a possibly large fraction of CDK2 would be bound and inhibited by unphosphorylated p27, there being an increasing scarceness of active kinase. This does not accord well with the efficient degradation of p27 at the appropriate time. The likely resolution of this paradox is both simpler and more elegant (Figure J-13). The key lies in the physical and temporal separation of the binding event and the inhibition event. Avid binding of p27 depends on its interaction with both the cyclin and the CDK in a complex [1]. It does not, however, appear to depend on any interaction between its inhibitory domain and the ATP-binding site of the CDK. Furthermore, there is no evidence, nor does it appear likely, that p27 could displace a resident ATP. Particularly in light of the extended, flexible structure of p27, it is reasonable to infer that p27 binds an active cyclin-CDK2 complex, already charged with ATP, and merely awaiting the docking of a substrate [2]. The C-terminal region of p27 provides an immediate target [3]. Thus, with the execution of its function, CDK2 discharges the resultant ADP molecule freeing the docking site. This vacancy is then rapidly filled by the p27 inhibitory domain that is immediately available [4], completing the process.

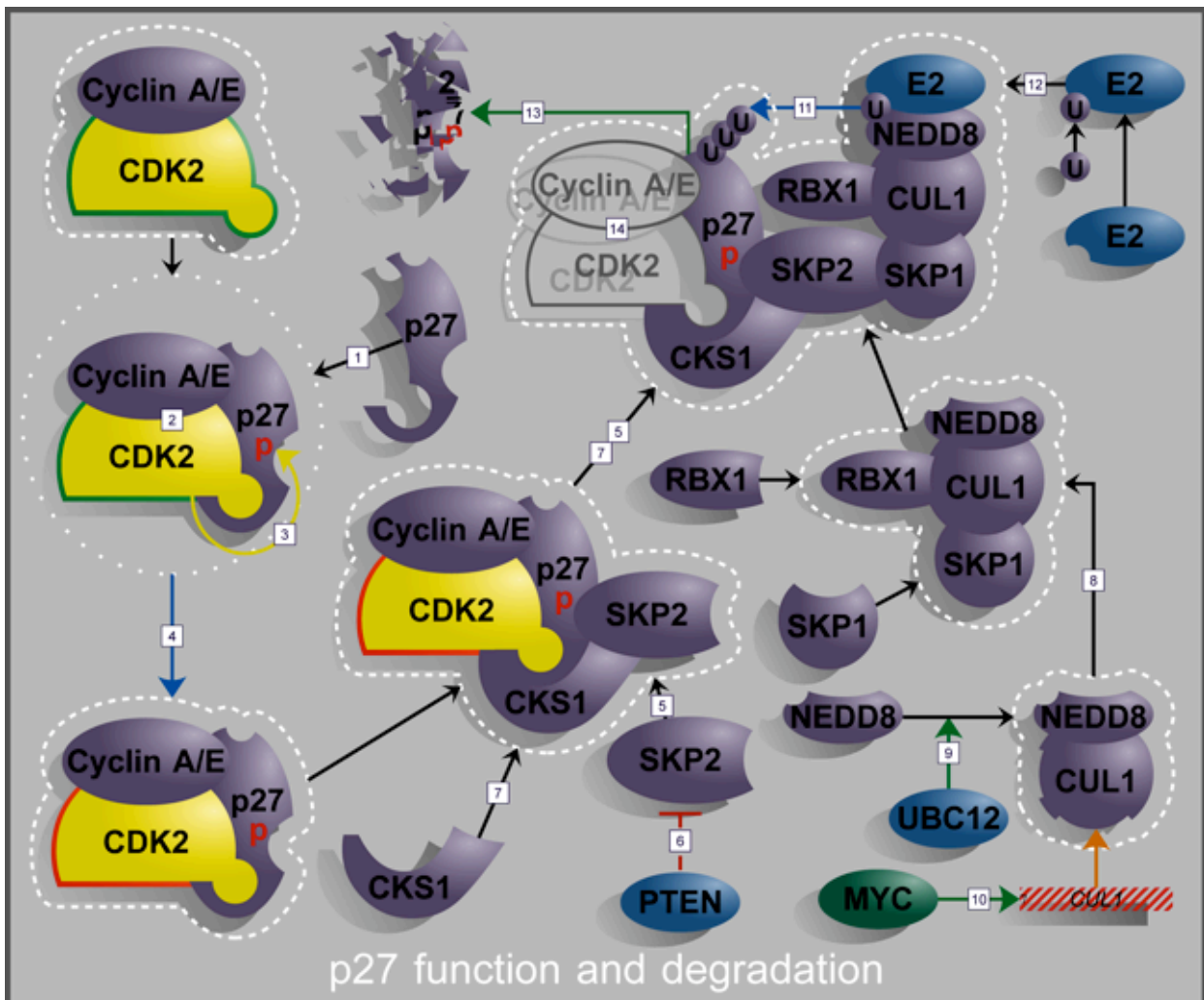


Figure J-13: p27 function and degradations

The subtleties of this proposed mechanism extend further. For the phosphorylation of p27 to occur, the kinase must be active, implying that p27 is joining a cyclin-CDK2 complex, rather than either element alone, and that the T14/Y15/T160 phosphorylation state necessary for kinase activity exists. If the first condition is not met, the joining of the remaining partner is unlikely to result in p27 phosphorylation. If the second is not met, then the subsequent modification of CDK2 phosphorylation status will not be sufficient to activate it, indeed in the presence of p27 the activating kinase, CAK, is thought to be denied access to the T160 site<sup>1078</sup>. Overall, the implication is that the inhibition of an active CDK2 is easier to reverse by ubiquitin-directed proteolysis than is the inhibition of an inactive CDK2. While it may be a pedantic distinction, it would be more accurate and potentially less misleading, to refer to p27 and its kin not as inhibitors, but rather as activational repressors.

The third mechanism for post-translational modification of p27 function involves the caspase-dependent cleavage of the C-terminal region of p27, which includes both the nuclear-localisation signal (NLS) and the T187 residue whose phosphorylation triggers ubiquitin-directed degradation<sup>807</sup>. The combined consequences of this are unclear. Loss of T187 should render p27 immune to ubiquitin-directed degradation, making it a more effective repressor of CDK2, and potentially other CDKs. However, the loss of the NLS may constrain it to the cytoplasm. CDKs may therefore be differentially repressed depending upon their cellular location. This is particularly noteworthy considering the role played by CDK2 in centrosome regulation. The caspase-dependency also suggests a role in apoptosis, but this too is unclear as p27 is considered to have anti-apoptotic properties, even after cleavage<sup>335</sup>.

Consignment of p27 for degradation by the proteasome is achieved by the ubiquitin ligase action of the SKP1–Cullin–F-box complex (SCFC) (Figure J–13). The best characterised mechanism for delivery of p27 to the SCFC for ubiquitylation is mediation by the F-box protein SKP2, although a SKP2-independent mechanism is known<sup>477</sup>. SKP2 is able to bind both T187-phosphorylated p27 and SKP1 simultaneously [5], and, notably, SKP2 levels are modulated via the PTEN/PI3K signal transduction channel<sup>837</sup> [6], often perturbed in cancer<sup>6155</sup>. The affinity of SKP2 for p27 is significantly enhanced by the accessory protein CKS1<sup>400</sup> [7], better known for its CDK-binding ability<sup>1380</sup>. Efficient recruitment of CUL1 to SCFC [8], and therefore enhanced p27 degradation, depends upon its conjugation to the NEDD8 ubiquitin-like protein, a process possibly catalysed by UBC12<sup>1036</sup> [9]. *CUL1*, the gene for the third core component of the SCFC is itself a transcriptional target of MYC<sup>967</sup> [10], linking oncogenic transformation to the activation of the SCFC. SCFC acts as an E3 ubiquitin ligase, assisting the transfer of activated ubiquitin from an E2 ubiquitin-conjugating enzyme [11] to the target protein [12]. The identity of the E2 enzyme has not been established unequivocally, with one report showing that either UBC2 or CDC34 could perform this function in vitro, while UBC4 is inactive<sup>993</sup>, and a second making a strong case for UBC4, particularly in conjunction with NEDD8<sup>647</sup>. By whichever mechanism it is achieved, once p27 has been ubiquitylated, it becomes eligible for proteasomal degradation [13]. In light of the context of this discussion, it is noteworthy that the SCFC complex is centrosomal<sup>373 443</sup>, associates directly with the 26S proteasome, also possibly via NEDD8<sup>632</sup>, and most conclusively, that centrosomes associate with functional 20S and 26S proteasomes<sup>337</sup>. It appears that monomeric p27 is not a subject of this process, and that it is the trimeric complex that is the target<sup>1468</sup>. Whether this is a substrate specificity, or simply due to phosphorylated p27 only existing in these complexes is unclear. Little is known of the fate of the complex. It may be degraded *in toto*, or a de-repressed cyclin–CDK complex may survive [14].

The similarity between p21 and p27 is strongest in the N-terminal regions, implicated, as discussed, in cyclin and CDK interaction. Like p27, p21 also prevents access to the critical T160 residue by CAK<sup>1078</sup>,



but whether p21 also directly interferes with ATP binding is not known. Of the three residues implicated in ATP mimicry in p27, only that corresponding to Y88 is conserved in p21, so until the analogous crystal structure for p21 is reported, the question remains open. The C-terminal regions of the two proteins are quite dissimilar. In p21, there is a domain that binds and inhibits PCNA, and a further cyclin-binding domain homologous to that near the N-terminus, neither present in p27. The critical p27 T187 phosphorylation site governing SKP2 binding and thence degradation has no analogue in p21. Notwithstanding this, p21 is phosphorylated on T145, with consequences for its PCNA inhibitory function<sup>1109</sup>, however, it seems unlikely that CDK2 is the responsible kinase. Interestingly, while p21 is labile in vivo, and is both ubiquitinated and degraded via the proteasome, its degradation is independent of its ubiquitination status<sup>1199</sup>. The manner and biological significance of this ubiquitination are yet to be elucidated.

With respect to their interaction with CDKs, the salient functional distinctions between p21 and p27 appear to be fourfold. Firstly, p27 can repress <T160>-enabled CDKs through ATP-mimicry, enabling it to modulate CDK activity efficiently even after this phosphorylation. On the other hand, p21 may lack this ability, and would be restricted to the role of inhibition through competitive binding to the cyclin, rendering it less potent at curbing CDKs once activated. Secondly, repression of activated CDK2 by p27 is inherently self-limiting by virtue of T187 phosphorylation and degradation targeting, while p21 is not subject to this. Thirdly, p21 has alternative modes of cyclin binding not available to p27. Binding via the N-terminal domain may result in CDK inhibition, while binding via the C-terminal domain may not, and rather serve to target the CDK kinase function to particular substrates. This 'adaptor' role has been demonstrated with respect to CDK2 and DNA ligase I<sup>713</sup>, but the precise mode of p21-CDK2 interaction has not been explored. This model also neatly resolves the continuing controversy in the literature over the stoichiometry of p21 inhibition of CDKs<sup>482 501</sup>. Studies into this aspect have generally involved immunoprecipitations and relative quantitation, and consequently, can provide only a population average of the complexes present. If the p21-CDK interactions were randomly distributed between the two binding modes, only half would result in inhibition, consistent both with the presence of active CDK in immunoprecipitates, extinguishable by the addition of excess p21, observed by some, and the ability of a single p21 to effect inhibition, observed by others. Finally, while the level of p27 appears to be regulated principally by changes in protein stability, that of p21 is under a much greater degree of transcriptional control, and is among the proteins induced by p53<sup>313</sup>. This distinction is of particular interest as it directly links cellular stress responses to centrosome regulation.

### **Upstream regulation: the response to genomic damage**

#### *Overview*

In *Schizosaccharomyces pombe*, the need to delay cell-cycle progression in the event of genomic damage is addressed by the regulation of Cdc2 activity<sup>S1090</sup>. The presence of DNA damage causes the activation of the Rad3 kinase, which phosphorylates and activates the Cds1 kinase<sup>S1302</sup>. This phosphorylates Cdc25 creating a binding site for a 14-3-3 protein, either Rad24 or Rad25<sup>S366</sup>, and promoting its exclusion from the nucleus. While this separates Cdc25 from its Cdc2 substrate, the principal means of regulation seems to be direct inhibition<sup>S392 S805</sup>. Cds1 also phosphorylates Wee1, activating its kinase function, at least in vitro<sup>S108</sup>. This achieves a result that complements the deactivation of Cdc25 as they are antagonistic enzymes that both target Cdc2.

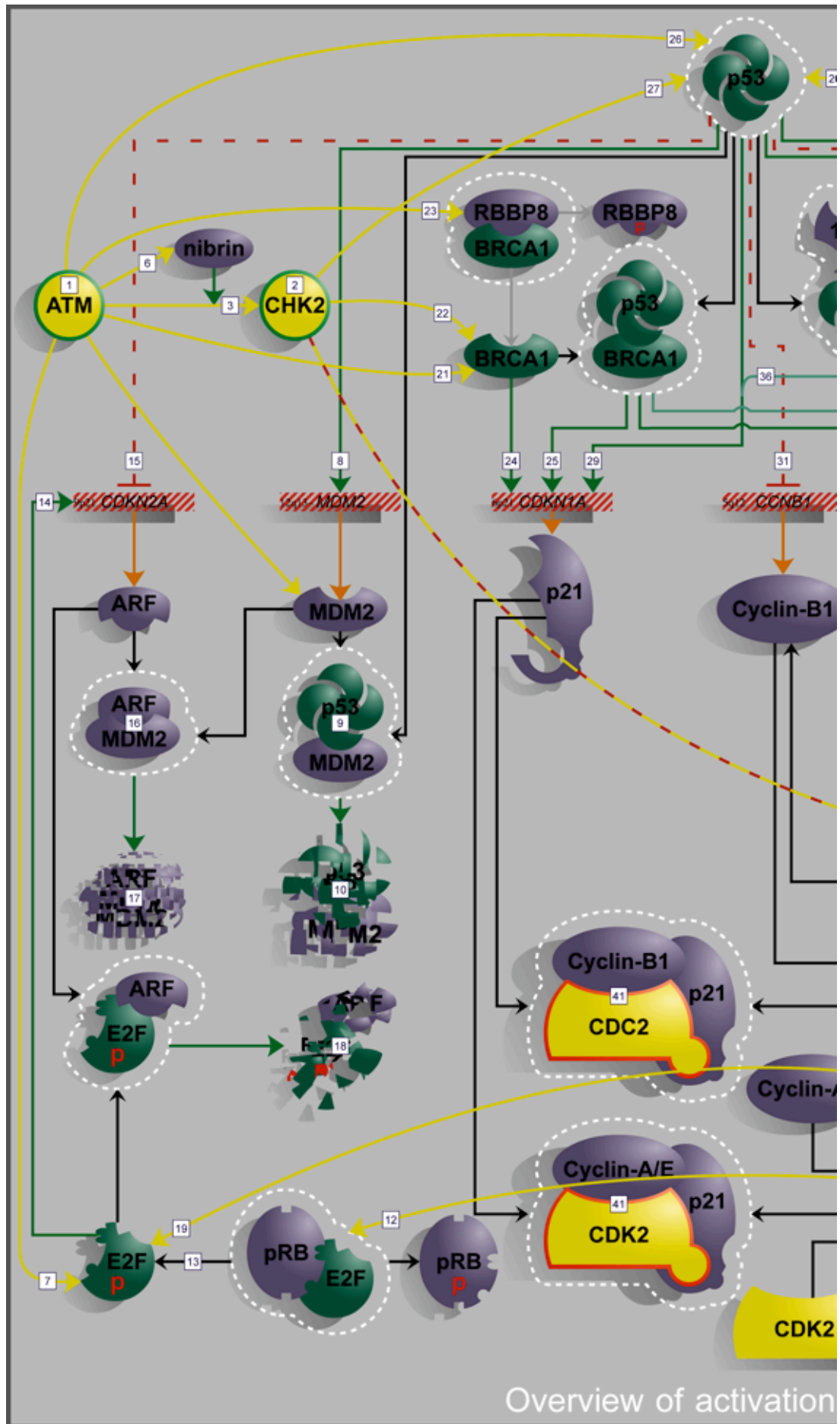
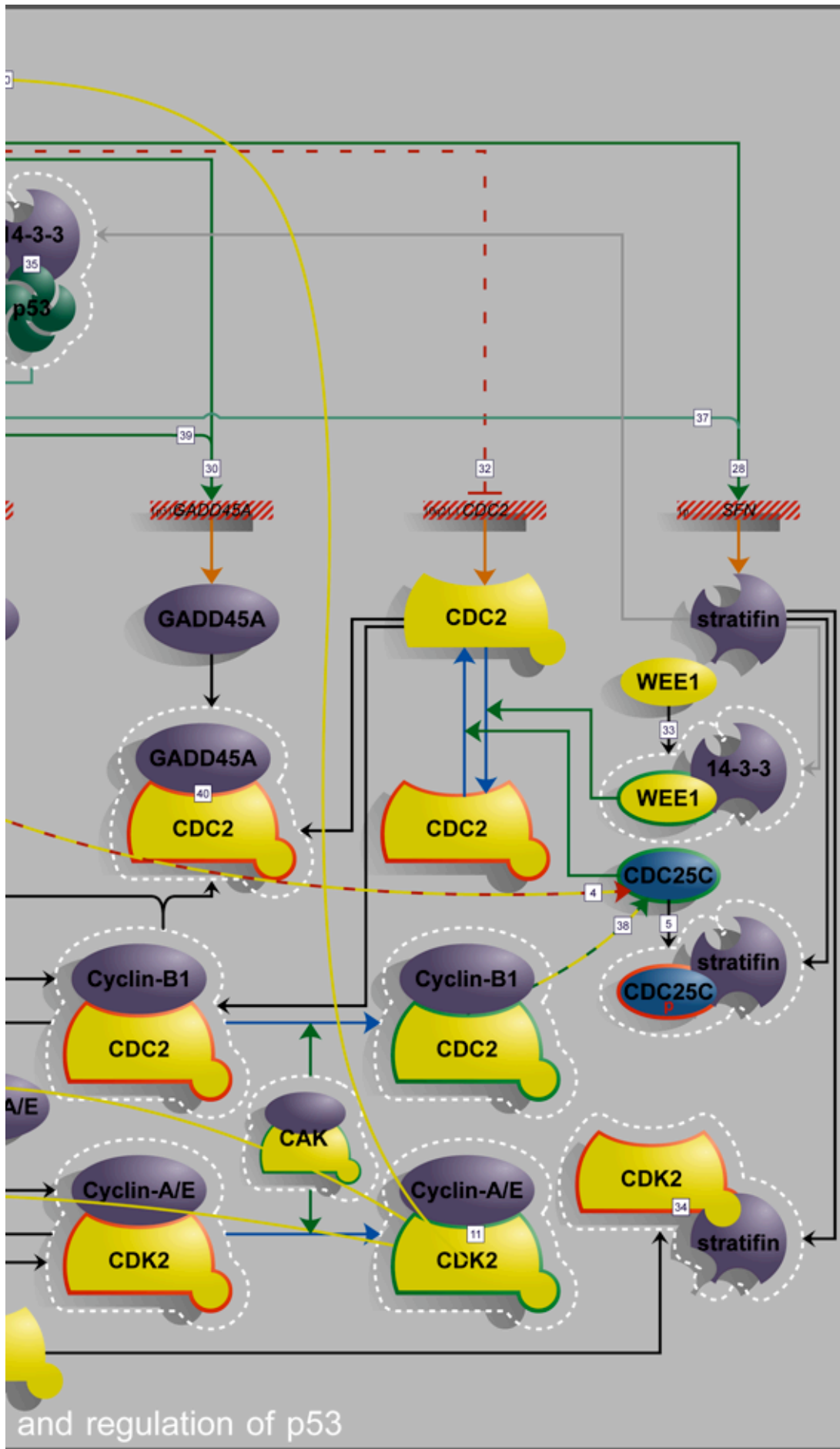


Figure J-14: Activation and effect of p53 pertaining to centrosome regulation



J: Genome partitioning

Figure J-14 continued

This mechanism is conserved essentially in its entirety in humans {Figure J–14}, the homologues of Rad3 and Cds1 being, respectively, ATM [1], the principal kinase of the BRCA1-associated genome surveillance complex (BASC)<sup>®641</sup>, and CHK2 [2]. The manner of its activation in humans is not fully understood, but by analogy with DNA-dependent protein kinase, is thought to be triggered by the presence of double-strand DNA breaks<sup>660</sup>. Paralleling the yeast mechanism, ATM phosphorylates T68<sup>19</sup> of CHK2<sup>858</sup> [3], activating its kinase function and allowing it to propagate the effects of ATM activity to downstream targets, including both CDC25A<sup>339</sup> and CDC25C S16<sup>181</sup> [4], with similar consequences: inhibition, association with stratifin, and nuclear exclusion [5]. The phosphorylation of CHK2 occurs only at DNA breaks<sup>1404</sup> and depends upon the prior phosphorylation by ATM of nibrin<sup>144</sup> [6], another component of BASC. Direct phosphorylation of WEE1 in humans is yet to be demonstrated for ATM or CHK2, but that by Chk1, a structurally distinct kinase with overlapping function, is suspected in *Xenopus laevis*<sup>§760</sup>. This phosphorylation is necessary for 14-3-3 association, and this significantly enhances kinase activity<sup>1110</sup>, so the prospect of phosphorylation by ATM or CHK2 seems likely. A further target of activated ATM is the transcription factor E2F1 resulting in its stabilisation and accumulation prior to apoptosis<sup>§789</sup> [7].

The situation is, however, a great deal more complex in humans than in yeast. In addition to the proteins with close yeast homologues, such as ATM, CHK2, MLH1, MSH2, MHS6, RAD50, and MRE11A, BASC contains, or affects evolutionarily new proteins, including BLM, BRCA1, p53, and nibrin. The existence of an additional control layer is a likely evolutionary concomitant of the transition to multicellular, organ-based animals, with its attendant increased requirement for mitotic fidelity. It seems that the process is not yet complete as the failure of these late additions is often associated with a disease unique to such organisms: cancer. Chief among these evolutionary newcomers is that model tumour-suppressor, p53.

The importance of p53 dysfunction to the process of tumorigenesis may well be the best researched and most widely accepted phenomenon in the field of cancer molecular biology. The regulation of p53 function is therefore of great interest as it may have major and wide-ranging therapeutic implications. This regulation is also among the most complex yet perceived, and while its full elucidation is an enormous challenge, there is potential scope for interventions ranging from the indiscriminate to the extremely subtle. Recent emphasis has been on its roles in facilitating repair of genomic damage and inducing apoptosis. Less well studied is the interaction between p53 activation and centrosome regulation, the aspect of concern here. The brief review that follows bears only on this aspect of p53 function, enabling a causal link to be established. It therefore omits a great deal of p53 molecular biology, but these omissions have been extensively reviewed elsewhere<sup>®66 @217</sup>.

### *Inferred characteristics of p53*

The results of *Trp53* knockout studies in the mouse<sup>§281</sup> have established that p53 function is dispensable for normal development and survival. However, natural or engineered <*TP53*> defect leads to a disease of general cancer predisposition: in humans, LFS<sup>328</sup>. The variable onset and spectrum of tumours associated with LFS suggests that p53 defects are not directly causative of cancer, in contrast to the situation with, for example, *RB1*. It seems instead that there is a failure to intervene in the progression toward cancer resulting from arbitrary tumorigenic events. From this can be inferred two characteristics of p53 molecular biology: firstly, that it is continuously active in a monitoring role without adversely affecting cellular physiology; and secondly, that its function is modified in response to a tumorigenic event.





### *Watchful waiting by p53*

In its continuous monitoring role, cellular p53 is maintained at a relatively low level by virtue of having a short half-life<sup>1087</sup>. This appears to be mediated principally by the induction of MDM2 by p53 [8] resulting in the formation of p53–MDM2 complexes [9] that are proteolytically degraded [10]. In this way, p53 expression is self-governing, with the actual level being determined by the kinetics of transcription and degradation. It was the failure of this mechanism that caused p53 to be misidentified originally as an oncogene since increased expression was seen to correlate with malignancy. The point of equilibrium of this dynamic balance is sensitive to any external alteration. A relevant example of this occurs with the activation of CDK2 on entry to S-phase [11]. By phosphorylating pRB [12], cyclin-E–CDK2 disrupts its association with E2F1, releasing it from inhibition [13]. In addition to many targets associated with proliferation and apoptosis, E2F1 also induces the beta transcript of *CDKN2A* [14], whose expression is normally held at a low level by p53-dependent repression<sup>1097</sup> [15]. The protein product of this expression is ARF, which bears the same relationship to MDM2 as MDM2 does to p53 [16], that is, it hastens its degradation [17]. ARF also binds and inhibits the transactivational capacity of E2F1<sup>334</sup> and may contribute<sup>8848</sup> to its proteasome-dependent degradation once it has been dissociated from pRB<sup>150</sup> [18]. Inversely, MDM2 binds and augments the activity of E2F1<sup>849</sup>, perhaps contributing to its own demise by stimulating ARF production. Overall, the entry to S-phase is accompanied by augmented p53 levels, consistent with an increased state of vigilance being appropriate during the critical process of genome replication. The status quo is regained with the deactivation of E2F1 through the elimination of its DNA-binding ability consequent upon phosphorylation by cyclin-A–CDK2<sup>1467</sup> [19]. SER315 of p53 is also a target of CDK2<sup>1053</sup> [20], and its phosphorylation results in localisation of p53 to the centrosome<sup>241</sup>  
<sup>1310</sup>.

The inter-relationships among p53, E2F1, ARF, and MDM2 are complex, and, coupled with the mechanisms for p53 activation, form an extremely dynamic and responsive regulatory network with the potential to support fine nuances of control under a variety of circumstances. The elucidation of these relationships will likely form the core of a new model for cell-cycle regulation.

### *p53: Guardian of the centrosome?*

The activation of p53 from its dormant, surveillance mode to full functionality is mediated in large part by post-translational modification<sup>@39</sup>, and can be triggered by diverse environmental stresses<sup>45 793 1034</sup>, the best-characterised stimulus being the presence of genomic damage. Neatly conforming to the evolutionary progression presented above is the fact that perhaps the two most important ‘new’ components, BRCA1 and p53, are each targets of both of the most highly conserved ‘old’ components, ATM and CHK2. This delineates the interface between the old and the new.

Phosphorylation of BRCA1 by ATM after exposure to ionising radiation occurs on S1387, S1423, and S1457<sup>403</sup> [21]; the functional significance of these modifications is unknown. Consistent with the possibility of selective response, different phosphorylation patterns, mediated by the ATM-relative ATR, are observed after UVR<sup>404</sup> exposure. CHK2 and BRCA1 coincide at nuclear foci, but after gamma-irradiation, they separate. This process depends upon S988 phosphorylation of BRCA1 by CHK2 [22]<sup>762</sup>. It will be interesting to learn whether this process is ATM-dependent, and whether it has consequences for transcriptional activation, with or without the involvement of p53. ATM also phosphorylates the BRCA1-binding protein RBBP8 [23], another evolutionary newcomer. The significance of this is currently hotly disputed. On the one hand, Li et al. assert that phosphorylation of RBBP8 S664 and S745 by ATM causes dissociation of the BRCA1–RBBP8 complex allowing BRCA1 to participate in

transcription<sup>782</sup>. On the other hand, Wu-Baer and Baer found that this complex remained intact after irradiation<sup>803</sup>. Notwithstanding this controversy, BRCA1 participates in the induction of *CDKN1A*, either independently<sup>1245</sup> [24], or in conjunction with p53<sup>174</sup> [25].

In the case of p53, phosphorylation of S15 [26] by ATM<sup>659</sup> augments its transactivational capacity by increasing its affinity for the p300 co-activator<sup>299</sup>, while phosphorylation of S20 by CHK2<sup>1208</sup> [27] stabilises it by preventing its association with MDM2<sup>183</sup>. Simultaneously, MDM2 is phosphorylated in an ATM-dependent manner, possibly directly<sup>666</sup>. The phosphorylation of p53 directly by ATM, and indirectly via CHK2 would allow the triggering of a subset of subsidiary mechanisms through the activation of CHK2 independently of ATM<sup>1213</sup>.

The mainstream of the p53-response is mediated by its influence on gene transcription upon activation. The target genes involved in centrosome regulation are essentially the same as those that bring about cell-cycle arrest since both activities are driven by CDKs. Among these genes are some whose expression is enhanced by virtue of containing specific p53-binding sites<sup>1381</sup>, such as *SFN* [28], *CDKN1A* [29], and *GADD45A* [30]. Others have their expression reduced, such as *CCNB1* [31] and *CDC2* [32], and this is achieved indirectly, dependent on the prior induction of p21<sup>CDKN1A250</sup>. The favoured explanation, at least in the case of *CDC2*, is that the repression is performed by the binding of p130–E2F4 to the promoter. In the normal course of events, this would be released upon phosphorylation of p130 by a CDK, but this is prevented by the p53-mediated expression of p21<sup>1315</sup>. A similar situation may prevail with respect to repression of *CDKN2A*. By whatever mechanism it is achieved, the repression of *CCNB1* and *CDC2* is an important contribution to the reduction of CDC2 kinase activity.

The *SFN* gene encodes the 14-3-3 protein, stratifin, introduced above as part of the 'old' DNA damage response system in which it binds and inhibits CDC25C [5] after phosphorylation of the latter by CHK2. 14-3-3 proteins also participate in the activation of WEE1 [33], and while stratifin has not been specifically identified in this capacity, this is an attractive scenario as p53 could then influence both arms of a major mechanism of CDC2 activation. In tandem with this, stratifin has been implicated in the regulation of CDK2 activity by direct inhibitory binding<sup>747</sup> [34]. Increased expression of 14-3-3 by the 'new' p53 bolsters these useful effects. Furthermore, 14-3-3 proteins are known to associate with p53 [35] and enhance sequence-specific DNA binding<sup>1409</sup>. This positively influences transcription of *CDKN1A*<sup>1259</sup> [36], and possibly other genes. Assuming stratifin has this capacity, p53 would induce a co-factor that enhances and possibly directs its own function. The 'new' system may modify the 'old' in yet another way as mouse studies suggest that p53-sponsored transcription of *SFN*<sup>8511</sup> may also benefit from BRCA1 activity<sup>841</sup> [37].

While these mechanisms suffice to reduce the level of activation of existing or new CDC2, they do not address the presence of previously activated kinase, and without this, inhibition of CDC2 kinase activity would not be absolute. This is particularly true since CDC25C is itself activated by cyclin-B1–CDC2 phosphorylation<sup>529</sup> [38] forming a self-reinforcing system that facilitates the rapid activation of CDC2 at the entry to M-phase, and so, even a small residual CDC2 activity could soon be amplified. This possibility is prevented by the induction of *GADD45A*, or possibly either of its close relatives, by p53<sup>642</sup> [30] assisted by BRCA1<sup>613</sup> [39], as it has the capacity to disrupt cyclin-B1–CDC2 complexes and sequester CDC2 in an inactive state<sup>1507</sup> [40]. Other interactions of *GADD45* with p21<sup>652</sup> and PCNA<sup>52</sup> are known, but the significance of these is unclear.



Finally, the induction of p21, in addition to mediating the repression of *CDC2* and *CCNB1*, also provides a potent direct activational repressor of CDKs. By binding preformed cyclin-A/E-CDK2 or cyclin-A/B-CDC2 complexes, p21 prevents CDK activation by CAK [41].

Together, these p53-mediated effects expunge all CDC2 and CDK2 activity and prevent its reappearance while p53 remains active. Hence, since these are critical mediators of the centrosome cycle, the case is made that aberrations of p53 regulation may adversely affect centrosome regulation.

### **Interdependence of nuclear and centrosomal cycle regulation**

The need to synchronise commitment to the nuclear and centrosomal cell-cycles is addressed by employing the same key activators: CDK2 and CDC2. Under ideal circumstances that is all that would be required. Unfortunately, there are times when the nuclear cycle either stalls for want of some limiting factor, or must be delayed due to the presence of genomic damage. If this occurs, synchronisation with the centrosome cycle must still be maintained. Due to the commonality of control between the two cycles, no additional provision is required to achieve this. Whatever delays the nuclear cycle by modulating CDK2 and CDC2 activity will perforce delay the centrosome cycle to a corresponding degree.

The converse condition may also prevail, wherein centrosome duplication is stalled, for example, by the presence of a microtubule toxin. Fittingly, a mechanism exists for such an event to trigger an arrest of the nuclear cycle. It has been found that after only a brief treatment with nocodazole, a tubulin depolymerising agent, p53 is released from its centrosomal association and activated<sup>204</sup>. In consequence, the daughter cells arrest in  $G_1$  after cytokinesis with elevated p21 levels. In addition, the activating Y15 dephosphorylation of CDC2 has been shown to occur first at the centrosome before propagating to the nucleus<sup>248</sup>. If this were the catalyst that commences the self-reinforcing activation of nuclear CDC2, then any delay at the centrosome would delay the onset of mitosis.

### **Evolution in action**

In the present epoch, mechanisms for the organisation of the mitotic spindle appear to be in a state of evolutionary transition. In plants, the odd aberrant mitosis may not be too dramatic. While they engage in fluid transportation, they lack a bona fide circulatory system, and while they have specialised tissues, they have few specialised organs. Their vulnerability to cancer-like disease is limited and a centrosomal system or its equivalent is not required. Yeast, being unicellular, are more vulnerable to failed mitosis in that one fault wipes out an entire lineage. In consequence, they possess a mechanism to improve mitotic fidelity, the spindle pole body. Multi-cellular animals, with complex circulatory and organ systems, whose corporeal life-span far exceeds that of their constituent cells, require still greater control over mitotic fidelity, hence the centrosome. It acts to manage an otherwise error-prone system in order to increase its reliability. For similar reasons, an evolutionary need to enhance the accuracy of genome duplication at the genetic level exists, hence p53.

Each of these systems normally performs well in isolation, but where they interact, or under abnormal circumstances, the few vulnerabilities become manifest. Evolution has brought life to the point where these mechanisms work adequately, but they do not always fail gracefully.



# K

# DNA replication licensing

*The replication of DNA exactly once during each cell division cycle is absolutely required for the maintenance of cellular viability and identity. Molecular events occurring at DNA replication origins orchestrate this in a process called DNA replication licensing. Were this to fail, gene amplifications and hyperploidy would result. However, it is not a likely cause of integral changes of cellular ploidy.*

## K.1 Introduction

The accurate transmission of genetic information during cell division depends absolutely on its precise duplication prior to cytokinesis. Each DNA nucleotide must be used as a template in the creation of a complementary strand exactly once, and this replication process must be in synchrony with the cell division cycle. The regulation of this, known as DNA replication licensing, involves two transitions. The first occurs after commitment to cytokinesis at the end of mitosis, when replication can be allowed. The second occurs simultaneously with the beginning of replication from a point of origin in S-phase, when and whence, any further commencement must be forbidden.

## K.2 Enabling DNA replication

The molecular basis for the first transition is illustrated in Figure K-1. The association of HCDH1 with the cyclosome both activates the latter's ubiquitin ligase function and provides substrate specificity<sup>1024</sup> [1]. Once activated, it is able to consign target proteins to the proteasome for degradation. One such target is geminin<sup>868</sup> [2], a protein that binds CDT1 with high affinity. Freed from geminin, CDT1 can assist in the direction of preformed DNA licensing complexes, composed of the mini-chromosome maintenance (MCM) proteins, to DNA-bound origin recognition complexes (ORC)<sup>1442</sup> [3]. This assembly is also dependent on the presence of CDC6 [4], providing a further control input. With the addition of the MCM complex to the ORC, DNA replication is licensed to commence [5], but does not actually begin until the recruitment and activation of the DNA polymerase complex. Activation of an inherent DNA helicase function of the MCM is probably also required. Failure to control this transition correctly could result from the absence of geminin, the mutation of either geminin or CDT1 preventing their interaction, or from over-expression of CDT1. No studies addressing the possible involvement of either geminin or CDT1 in tumorigenesis have yet been reported.

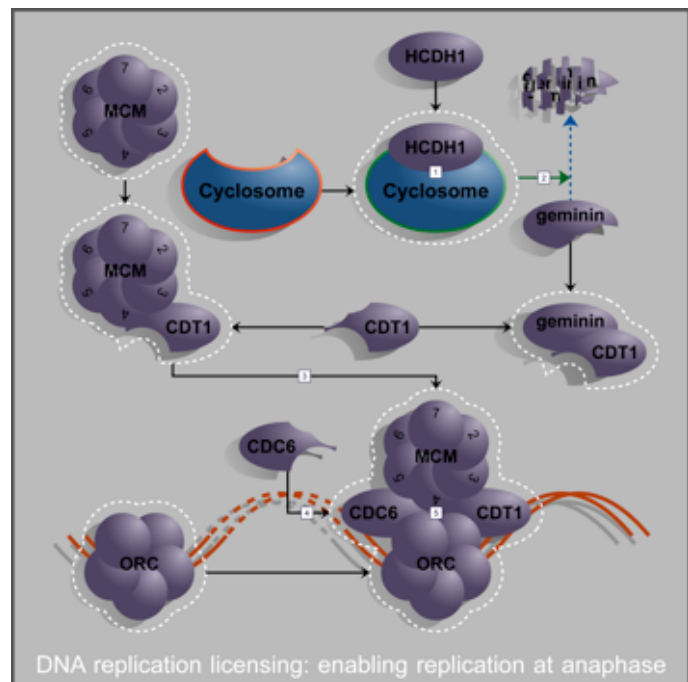


**Figure K-1: Enabling DNA replication at anaphase**

### K.3 Disabling DNA replication

The molecular basis of the second transition, the revocation of the DNA replication licence at the onset of S-phase, is illustrated in Figure K-2. The activation of CDK2 by newly synthesised cyclin-A [1] results in the phosphorylation of the CDC6 component of the protein complex at a replication origin<sup>1021</sup> [2]. Consequently, CDC6 translocates to the nucleolus where it is detained [3]. Since its presence at the ORC is essential for binding of the MCM complex, its removal greatly diminishes the possibility of reformation, once the MCM is detached. A second target of CDK2 is the cyclosome activator HCDH1, which, when phosphorylated, undergoes a conformational change that renders it unable to associate with the cyclosome [4]. The

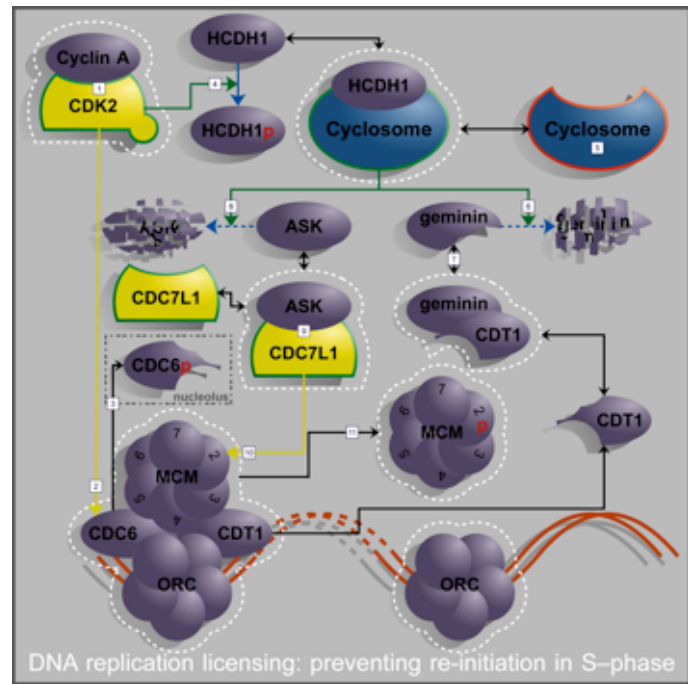


**Figure K-2: Disabling DNA replication at G<sub>1</sub>-S**

resultant inactivation of the ubiquitin-ligase function of the cyclosome [5] means that it is no longer able to direct the degradation of geminin [6]. As described above, geminin interacts with CDT1 [7] and prevents its binding to the MCM complex, a prerequisite for its recruitment to the ORC. The inhibition of this function due to rising geminin levels as a result of a dampening of degradation represents the second mechanism for the prevention of replication relicensing. A second protein escaping degradation by virtue of the inactivation of the cyclosome is ASK [8]. In a manner analogous to the activation of CDKs by cyclins<sup>851</sup>, ASK activates the kinase CDC71L [9], which is then able to phosphorylate elements of the MCM complex, notably MCM2 [10]. When phosphorylated, the MCM complex detaches from the ORC [11], completing the process of de-licensing replication for this origin. Without CDC6, relegated to the nucleolus, or CDT1, inhibited by geminin, there is no opportunity for reattachment.

Dysfunction of this mechanism could potentially be caused by the same spectrum of alterations to geminin or CDT1 outlined above; by alteration of CDC6 preventing its phosphorylation by CDK2 or translocation; or by increased activity of the CDC71L kinase. There have been apparently conflicting results concerning the effects of CDC6 mutation. In accord with the model presented above, Liang and Stillman<sup>785</sup> reported a CDC6 mutant that retains MCM attachment to ORCs throughout the cell-cycle and engages in promiscuous DNA replication resulting in hyperploidy. Subsequently, using site-directed mutagenesis against the conserved CDK phosphorylation site of *Xenopus* CDC6, Pelizon et al.<sup>§1016</sup> did find that CDC6 remained nuclear. Nevertheless, only one round of DNA synthesis was supported, reinforcing the notion that multiple controls are in place. Over-expression of CDC71L or ASK in tumours is suggested by some authors<sup>1168</sup>, with one limited study reporting that there may be differences in incidence among various tumour types<sup>514</sup>.

### K.4 Failure of licensing as a cause of genomic heterogeneity

Failure of DNA licensing involves a loss of synchronisation between genomic replication and cytokinesis. Hence, it is not a plausible mechanism for the generation of integral changes in ploidy, but rather, is a likely contributor to gene amplification, another recognised path of tumour progression.

# L

# Synchronisation of cytokinesis

While the physical separation and positioning of replicated genomes is an essential prerequisite for the accurate trans-generational transmission of genetic information, the synchronisation of this separation with the physical division of the dividing cell is no less important. The key to this synchronisation lies in proteins normally associated with the centromeres. Upon the commencement of chromosome separation, they migrate to the equatorial cortex and signal that anaphase has commenced and that cytokinesis may proceed.

## L.1 Cytokinesis

The physical process of division of a cell, cytokinesis, begins at the completion of mitosis when an equatorial contractile ring commences to constrict, creating the cleavage furrow. Constriction continues until the leading edge of the furrow reaches the central spindle, forming the spindle midbody. The membranes of the daughter cells are sealed and they are detached from the midbody, achieving independent existence. Clearly, cytokinesis cannot safely be allowed to commence until the replicated chromosomes have separated, implying that some synchronisation mechanism must be in place.

## L.2 Synchronising cytokinesis initiation

One thread of this mechanism hinges on the fate of proteins intimately associated with the centromeres of metaphase chromosomes [Figure L-1] [1], particularly the inner centromere protein, INCENP, the aurora-family kinase STK12, and survivin<sup>1428</sup>. All are essential for the completion of cytokinesis<sup>191 627 825</sup>.

Their status as chromosomal passenger proteins changes at anaphase, when they are left behind at the spindle plate after the departure of the chromatids<sup>221</sup>. Some of each remains there, but a significant amount migrates to the equatorial cortex [2]

in a dynamic, microtubule-dependent manner. INCENP is critical for this translocation<sup>13</sup> and in this respect, its ability to bind  $\beta$ -tubulin is probably essential<sup>1429</sup>. In so doing, it conveys to the site where the constriction of the cell membrane will commence the information that chromosome separation has begun, and consistent with this, INCENP appears at the cortex prior to the formation of the cleavage furrow<sup>307</sup>. On arrival, STK12 phosphorylates the myosin light chain<sup>926</sup> [3], a prerequisite for its interaction with actin necessary to produce relative motion [4]. The role of survivin in cytokinesis remains enigmatic, and it is better characterised in terms of its involvement in apoptosis<sup>1370</sup>.

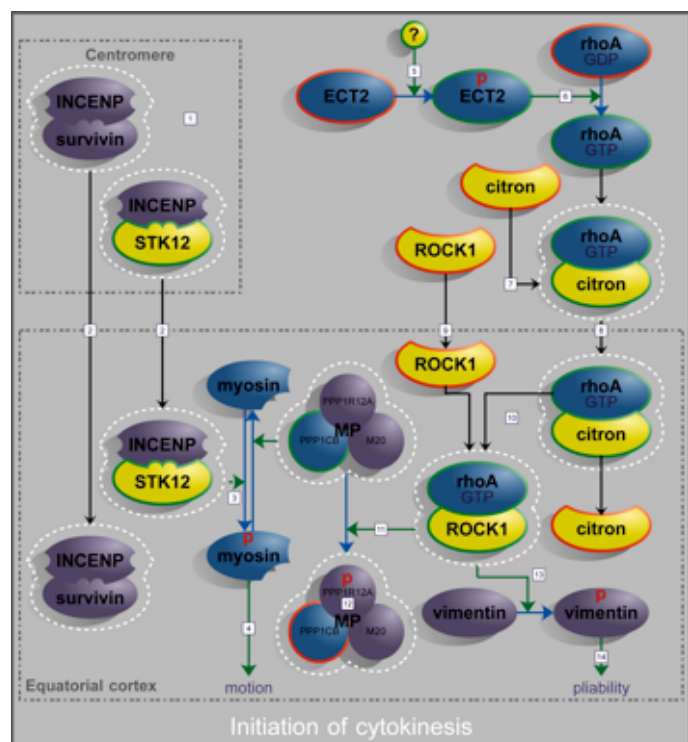


Figure L-1: Initiation of cytokinesis

In the second thread leading to cytokinesis initiation, the earliest characterised event is the phosphorylation of ECT2 by an unknown kinase [5]. Cyclin-A-CDK2 is an ideal candidate for this function given the timing of its activation. ECT2 is a guanine nucleoside exchange factor for RAS-related GTPases<sup>1313</sup> and its expression levels are synchronised with the cell-cycle, increasing from S to M-phase<sup>1128</sup>. Its function is essential for the increase in rhoA-GTP seen with progression toward telophase [6], and this is critical for cytokinesis<sup>679</sup>. In the absence of an activating partner, the GTPase activity of rho enzymes is weak and so the GTP-associated form is relatively stable. In this form, rhoA is able to bind and presumably activate the kinase citron<sup>826</sup> [7], which it then transports to the equatorial cortex<sup>309</sup> [8]. In a manner not yet understood, the rho-associated kinase ROCK1 also accumulates here [9], but until the arrival of rhoA, it is inactive. The interactions between rhoA and its two potential associates, ROCK1 and citron are not clear [10]. There may be an ongoing redistribution of rhoA between the two kinases allowing them to have temporally overlapping activity. Another possibility is that upon arrival, citron comes into contact with its substrate, and after causing its phosphorylation, detaches from rhoA leaving it free to activate ROCK1. This would result in sequential activation of the kinases. The relationship between the two kinases will be clearer once the in vivo substrates of citron have been identified. Substrates for ROCK1, on the other hand, have been identified. ROCK1 phosphorylates the larger regulatory subunit of the myosin phosphatase complex (MP), PPP1R12A<sup>650</sup> [11]. This probably inactivates the bound catalytic subunit, but the mechanism is unclear<sup>483</sup>. By inactivating the phosphatase [12], the balance is moved in favour of myosin phosphorylation, being performed by STK12 [3]. An additional substrate for ROCK1 is the intermediate filament (IF) protein vimentin [13]. This is of particular interest since melanocytes and melanomas appear to express only this class of IF protein<sup>161 1218</sup>. When phosphorylated, vimentin molecules lose their ability to cohere, with the result that this extremely durable skeletal structure becomes locally pliable [14]. An interesting aside to this is that ROCK1 is a target for caspase-3 cleavage during apoptosis. The removal of a carboxyl-terminal domain renders ROCK1 constitutively active. Under these circumstances, it mediates the membrane blebbing seen in apoptosis<sup>1171</sup>.

Thus, the essence of cytokinesis initiation is the softening of the vimentin cytoskeleton together with the activation of the actomyosin motor system in a manner that depends upon the release of chromosomally bound proteins at anaphase. The multiple independent threads leading to the initiation of cytokinesis provide an excellent mechanism for preventing early division, something that would be disastrous for the cell. This is not without risk however, as it makes it more likely that a single failure may prevent cytokinesis, a consequence hardly less severe. Millennia of evolution have probably settled upon the optimal compromise between these conflicting objectives, but the bias does seem to be in favour of preventing the former, at the possible expense of the latter. Nevertheless, failures may still occur in either direction.

### L.3 Cytokinesis regulators and cancer

On the basis of the model presented, interference with the binding of STK12 to INCENP, or in their joint transport to the cortex, loss of STK12 function, over-expression or aberrant activation of the ECT2 kinase, constitutively active ECT2 or rhoA, or loss of ROCK1 function could each sponsor failure of cytokinesis, and so may potentially contribute to polyploidy and tumorigenesis.

INCENP is over-expressed in several colorectal cancer cell-lines<sup>13</sup>, an observation superficially difficult to reconcile with the model presented above. While it may be expected that this would increase the transport of STK12 to the cortex, the reverse is also distinctly possible. An excess of INCENP could





either sequester STK12, or saturate the transport mechanism. Also within this functional thread, Tatsuka et al.<sup>1312</sup> found over-expression of STK12 (AIM-1) in colorectal and other cancer cell-lines. Their observations included multi-nuclearity, consistent with expectation. By yet another name, AIK1, STK12 over-expression was also reported in 94% of invasive ductal carcinomas of the breast<sup>1304</sup>.

Over-expression of rhoA in vitro causes cellular transformation in a ROCK1-dependent manner<sup>1123</sup> and has been reported in colon, breast, lung, and testicular germ-cell tumours<sup>378 630</sup>. On the other hand, mutation of rhoA in cancer cell-lines appears to be rare<sup>914</sup>. These observations suggest that intact rhoA function is necessary, but not sufficient for tumour progression. There is a strong case that rhoA is important in RAS-mediated oncogenic transformation<sup>665 1052</sup>, probably through its role in membrane dynamics. It has been implicated in adhesion<sup>329</sup>, migration<sup>919</sup>, invasion<sup>1490</sup>, and metastasis<sup>258</sup>. Additionally, a more direct role for rhoA is beginning to surface: it appears that it can stimulate the transcription of *JUN* via MAPK12<sup>842</sup>. The participation in these abnormal processes of its dependent kinase, ROCK1, has been confirmed<sup>600</sup> with reports of involvement in metastatic cell migration in breast cancer<sup>126</sup>, and a retardation in migration and dissemination of prostate cancer cells in vivo<sup>1246</sup> being seen in response to a specific inhibitor. One further link between rhoA–ROCK1 and cancer is the observation that in melanoma, co-expression of vimentin, a ROCK1 substrate, and keratin augment cell motility<sup>203</sup> and correlate with invasion and metastasis<sup>500</sup>.



---

# M

# The autocrine effect

---

## M.1 Introduction

In multicellular organisms, cells may produce substances that affect the phenotype, survival, and tendency to replicate of adjacent cells: the paracrine effect. A special case of this is where a cell-type both produces, and responds to these substances: the autocrine effect. This is of particular importance where cells are cultured in vitro in monoculture. Under these circumstances, it should be possible to develop a mathematical basis to describe the autocrine effect on population growth.

## M.2 Assumptions

Several simplifying assumptions are made in the construction of this theory. The primary assumption is that all cells within the culture are phenotypically equivalent, that is, they all produce the same suite and volume of growth factors, respond identically to them, and proliferate and die for identical reasons, with identical probability. In practice, there may be minor random variations from such behaviour, but in monoculture, by definition, this assumption should be valid. It is assumed that soluble factors in the medium disperse uniformly, and that cultural conditions, such as pH, nutrient availability, and temperature are identical for all cells.

## M.3 Exponential growth

That cell cultures grow numerically exponentially is not an assumption of the model, but is readily derived from it. Under the assumed conditions, the destinies of each cell to divide or die at any time are both mutually independent, and independent of context. Where  $N_t$  is the population at time  $t$ ,  $p_{division}$  is the inherent probability that a cell will divide during the interval  $[t, t+1]$ , and  $p_{death}$  is the probability that a cell will die in that interval, the population size at time  $t+1$  is given by the equation:

$$N_{t+1} = N_t + N_t(p_{division} - p_{death})$$

### Equation M-1: Independent growth

This equation has an inherently exponential character. That such growth is indeed observed supports the validity of the underlying assumptions.

## M.4 Incorporating a reflexive effect

If, however, we wish to include an influence on population growth that stems from the presence of the cells themselves, we must modify this equation. Assuming that all cells contribute equally to the effect, and do so at the same magnitude from the time they achieve independent existence until the time they die, and further, that no other factor influences this, the following set of equations can be derived, where  $f$  is the effect each cell having lived ( $\omega_t$ ) will have on the fate of those extant:

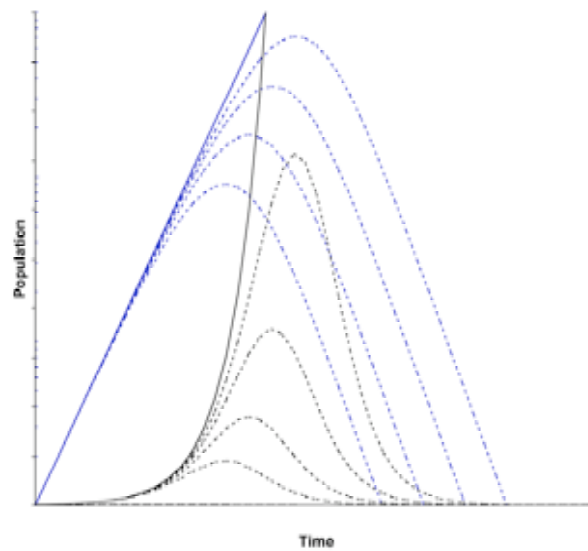
$$i) \quad \omega_t = \sum_{u=0}^{t-1} N_u$$

$$ii) \quad N_{t+1} = N_t(1 + \max\{p_{division} + \omega_t f_{stimulus}, 0\} - \max\{p_{death} + \omega_t f_{inhibition}, 0\})$$

### Equation M-2: Theoretical growth with reflexive influence

---

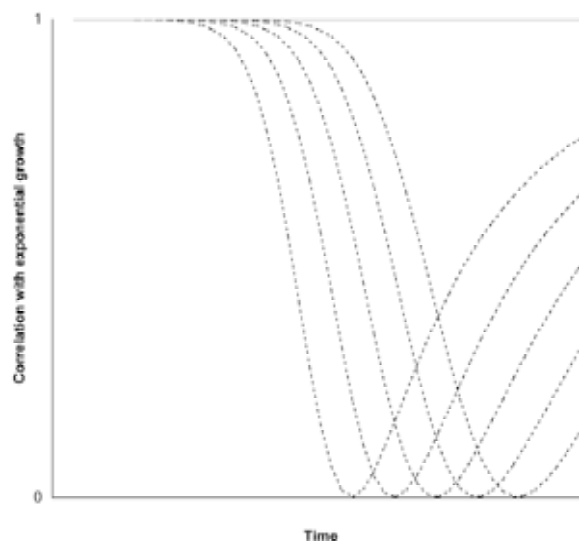
To illustrate this, the effect on population size over time of an anti-proliferative reflexive influence affecting only the rate of division is shown graphically in Figure M-1.



This graph shows the theoretical growth of a population subject to an anti-proliferative reflexive influence. Black lines are plotted on a linear y-axis, blue lines on a logarithmic y-axis. Solid lines denote unaffected cultures, dashed lines, progressively more affected. Units are arbitrary. The cells are assumed to have a non-negative inherent rate of cell death smaller than their inherent rate of division.

**Figure M-1: Anti-proliferative reflexive effect**

Clearly, the production of even small quantities of an anti-proliferative autocrine factor can bring about an arrest of population growth, and most likely, a decline. While the inhibitory effect is growing to its maximum magnitude, where it entirely offsets the inherent proliferative potential, an increasing departure from exponential growth with time will be seen. Once this maximum is attained and the population begins to decline due to its inherent rate of cell death, the change in population with time will again begin to approximate the exponential. The theory can be demonstrated graphically by observing the predicted change in correlation to an exponential function over time {Figure M-2}.



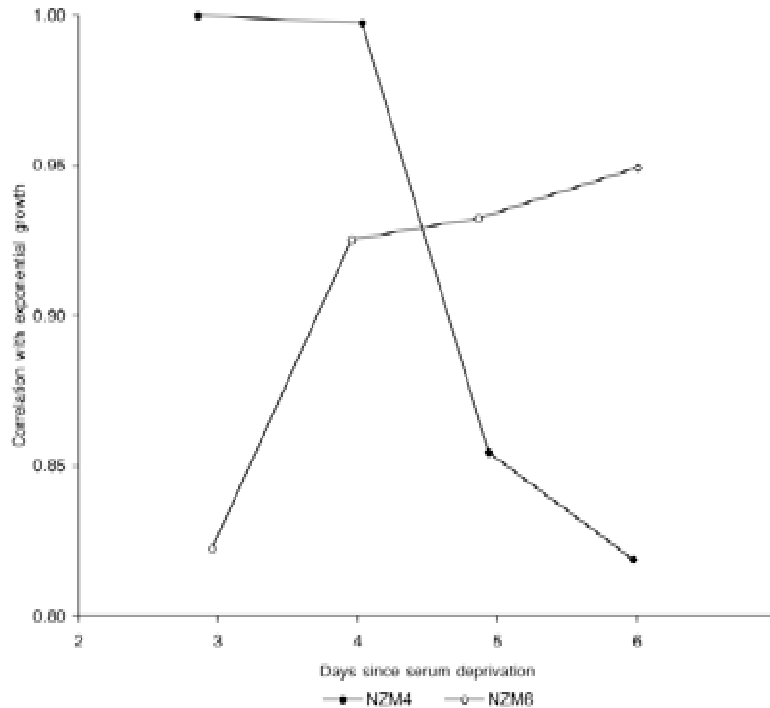
This graph shows the theoretical deviation of growth from exponential in consequence of the production of an anti-proliferative factor. The solid line indicates the complete correlation seen in the absence of an effect; the dashed lines show the successively greater deviation with greater effect. The y-axis is the correlation coefficient,  $R^2$ ; time units are arbitrary.

**Figure M-2: Theoretical growth rate deviation due to a reflexive anti-proliferative effect**

In practice, the initial approximation may be poor due to experimental error, and a period where the correlation improves may be expected.

### M.5 Agreement with observations

Using the data presented in Chapter 7, particularly the exemplar cell-lines NZM4 and NZM6, an assessment of the utility of this model can be made {Figure M-3}.



This graph shows the actual deviation of growth from exponential observed in vitro. The y-axis is the correlation coefficient,  $R^2$ , for the exponential line of best fit for the data from inception to the time point.

**Figure M-3: Measured deviation from exponential growth in exemplar NZM cell-lines**

For NZM4, where spontaneous cell-cycle phase redistribution was seen and the instantaneous proliferation rate (IPR) declined with time in culture, an increasing departure from exponential growth is seen as is predicted for the production of an anti-proliferative factor. In contrast, for NZM6, where no such redistribution was seen, and the IPR did not alter significantly with time, the approximation to exponential growth improves with the addition of more data points and the reduction in the effect of experimental error.

### M.6 Limitations of the model

Doubtless the real situation is more complex, with the effects of factor degradation, receptor expression, saturation, and turnover, and likely many more, in operation. More complex again would be the situation in vivo, where there is an interplay among numerous distinct cellular phenotypes and biological factors such as tissue architecture and vasculature will have major effects.

M: The autocrine effect



---

# References and bibliography

---

Items marked '†' are not specifically referred to in this edition but are included to maintain consistency of numbering between editions.

- 1 Aarnio M, Salovaara R, Aaltonen LA, Mecklin JP and Jarvinen HJ  
Features of gastric cancer in hereditary non-polyposis colorectal cancer syndrome  
*International Journal of Cancer* **74**:551–5 1997 [Abstract](#)
  - 2 Ababou M, Dutertre S, Lecluse Y, Onclercq R, Chatton B and Amor-Gueret M  
ATM-dependent phosphorylation and accumulation of endogenous BLM protein in response to ionizing radiation  
*Oncogene* **19**:5955–63 2000 [Abstract](#)
  - 3 Abal M, Souto AA, Amat-Guerri F, Acuna AU, Andreu JM and Barasoain I  
Centrosome and spindle pole microtubules are main targets of a fluorescent taxoid inducing cell death  
*Cell Motility and the Cytoskeleton* **49**:1–15 2001 [Abstract](#)
  - 4 Abdel-Malek Z, Scott MC, Suzuki I, Tada A, Im S, Lamoreux L, Ito S, Barsh G and Hearing VJ  
The melanocortin-1 receptor is a key regulator of human cutaneous pigmentation  
*Pigment Cell Research* **13 Suppl 8**:156–62 2000 [Abstract](#)
  - 5 Abdel-Malek Z, Suzuki I, Tada A, Im S and Akcali C  
The melanocortin-1 receptor and human pigmentation  
*Annals of the New York Academy of Sciences* **885**:117–33 1999 [Abstract](#)
  - 6 Aberdam E, Bertolotto C, Sviderskaya EV, de Thillot V, Hemesath TJ, Fisher DE, Bennett DC, Ortonne JP and Ballotti R  
Involvement of microphthalmia in the inhibition of melanocyte lineage differentiation and of melanogenesis by agouti signal protein  
*Journal of Biological Chemistry* **273**:19560–5 1998 [Abstract](#)
  - 7 Aberle H, Bauer A, Stappert J, Kispert A and Kemler R  
beta-catenin is a target for the ubiquitin-proteasome pathway  
*EMBO Journal* **16**:3797–804 1997 [Abstract](#)
  - 8 Abramson DH, Ellsworth RM and Zimmerman LE  
Nonocular cancer in retinoblastoma survivors  
*Transactions - American Academy of Ophthalmology & Otolaryngology* **81**:454–7 1976 [Abstract](#)
  - 9 Abramson DH, Ronner HJ and Ellsworth RM  
Second tumors in nonirradiated bilateral retinoblastoma  
*American Journal of Ophthalmology* **87**:624–7 1979 [Abstract](#)
  - 10 Abramson DH and Servodidio CA  
Retinoblastoma  
*Optometry Clinics* **3**:49–61 1993 [Abstract](#)
  - 11 Acharya S, Wilson T, Gradia S, Kane MF, Guerrette S, Marsischky GT, Kolodner R and Fishel R  
hMSH2 forms specific mismatch-binding complexes with hMSH1 and hMSH6  
*Proceedings of the National Academy of Sciences of the USA* **93**:13629–34 1996 [Abstract](#)
  - 12 Adams PD, Li X, Sellers WR, Baker KB, Leng X, Harper JW, Taya Y and Kaelin WG Jr  
Retinoblastoma protein contains a C-terminal motif that targets it for phosphorylation by cyclin-cdk complexes  
*Molecular and Cellular Biology* **19**:1068–80 1999 [Abstract](#)
  - 13 Adams RR, Wheatley SP, Gouldsworthy AM, Kandels-Lewis SE, Carmena M, Smythe C, Gerloff DL and Earnshaw WC  
INCENP binds the Aurora-related kinase AIRK2 and is required to target it to chromosomes, the central spindle and cleavage furrow  
*Current Biology* **10**:1075–8 2000 [Abstract](#)
  - 14 Adesanya OO, Zhou J, Samathanam C, Powell-Braxton L and Bondy CA  
Insulin-like growth factor 1 is required for G2 progression in the estradiol-induced mitotic cycle  
*Proceedings of the National Academy of Sciences of the USA* **96**:3287–91 1999 [Abstract](#)
  - 15 Adnane J, Shao Z and Robbins PD  
Cyclin D1 associates with the TBP-associated factor TAF(II)250 to regulate Sp1-mediated transcription  
*Oncogene* **18**:239–47 1999 [Abstract](#)
  - 16 Agarwal SK, Guru SC, Heppner C, Erdos MR, Collins RM, Park SY, Saggari S, Chandrasekharappa SC, Collins FS, Spiegel AM, Marx SJ and Burns AL  
Menin interacts with the AP1 transcription factor JunD and represses JunD-activated transcription  
*Cell* **96**:143–52 1999 [Abstract](#)
  - 17 Agarwala SS and Kirkwood JM  
Temozolomide, a novel alkylating agent with activity in the central nervous system, may improve the treatment of advanced metastatic melanoma  
*Oncologist* **5**:144–51 2000 [Abstract](#)
  - 18 Aguiar RC, Sill H, Goldman JM and Cross NC  
The commonly deleted region at 9p21-22 in lymphoblastic leukemias spans at least 400 kb and includes p16 but not p15 or the IFN gene cluster  
*Leukemia* **11**:233–8 1997 [Abstract](#)
  - 19 Ahn JY, Schwarz JK, Piwnicka-Worms H and Canman CE  
Threonine 68 phosphorylation by ataxia telangiectasia mutated is required for efficient activation of Chk2 in response to ionizing radiation  
*Cancer Research* **60**:5934–6 2000 [Abstract](#)
  - 20 Akiyama T, Ohuchi T, Sumida S, Matsumoto K and Toyoshima K  
Phosphorylation of the retinoblastoma protein by cdk2  
*Proceedings of the National Academy of Sciences of the USA* **89**:7900–4 1992 [Abstract](#)
  - 21 Akslen LA, Monstad SE, Larsen B, Straume O and OGREID D  
Frequent mutations of the p53 gene in cutaneous melanoma of the nodular type  
*International Journal of Cancer* **79**:91–5 1998 [Abstract](#)
-

## Human metastatic melanoma in vitro

- 22 al-Aoukaty A, Rolstad B and Maghazachi AA  
Recruitment of pleckstrin and phosphoinositide 3-kinase gamma into the cell membranes, and their association with G beta gamma after activation of NK cells with chemokines  
*Journal of Immunology* **162**:3249–55 1999 [Abstract](#)
- 23 Albanese C, D'Amico M, Reutens AT, Fu M, Watanabe G, Lee RJ, Kitsis RN, Henglein B, Avantaggiati M, Somasundaram K, Thimmapaya B and Pestell RG  
Activation of the cyclin D1 gene by the E1A-associated protein p300 through AP-1 inhibits cellular apoptosis  
*Journal of Biological Chemistry* **274**:34186–95 1999 [Abstract](#)
- 24 Albert LS, Sober AJ and Rhodes AR  
Cutaneous melanoma and bilateral retinoblastoma  
*Journal of the American Academy of Dermatology* **23**:1001–4 1990 [Abstract](#)
- 25 Alcorta DA, Xiong Y, Phelps D, Hannon G, Beach D and Barrett JC  
Involvement of the cyclin-dependent kinase inhibitor p16 (INK4a) in replicative senescence of normal human fibroblasts  
*Proceedings of the National Academy of Sciences of the USA* **93**:13742–7 1996 [Abstract](#)
- 26 Alexander K and Hinds PW  
Requirement for p27(KIP1) in retinoblastoma protein-mediated senescence  
*Molecular and Cellular Biology* **21**:3616–31 2001 [Abstract](#)
- 27 Alessi DR, James SR, Downes CP, Holmes AB, Gaffney PR, Reese CB and Cohen P  
Characterization of a 3-phosphoinositide-dependent protein kinase which phosphorylates and activates protein kinase Balpha  
*Current Biology* **7**:261–9 1997 [Abstract](#)
- 28 Allsopp RC, Chang E, Kashefi-Aazam M, Rogaev EI, Piatyszek MA, Shay JW and Harley CB  
Telomere shortening is associated with cell division in vitro and in vivo  
*Experimental Cell Research* **220**:194–200 1995 [Abstract](#)
- 29 Almasan A, Yin Y, Kelly RE, Lee EY, Bradley A, Li W, Bertino JR and Wahl GM  
Deficiency of retinoblastoma protein leads to inappropriate S-phase entry, activation of E2F-responsive genes, and apoptosis  
*Proceedings of the National Academy of Sciences of the USA* **92**:5436–40 1995 [Abstract](#)
- 30 Alt JR, Cleveland JL, Hannink M and Diehl JA  
Phosphorylation-dependent regulation of cyclin D1 nuclear export and cyclin D1-dependent cellular transformation  
*Genes and Development* **14**:3102–14 2000 [Abstract](#)
- 31 American Type Culture Collection Catalogue Item # CCL-2 <http://www.atcc.org/>
- 32 An HX, Beckmann MW, Reifenberger G, Bender HG and Niederacher D  
Gene amplification and overexpression of CDK4 in sporadic breast carcinomas is associated with high tumor cell proliferation  
*American Journal of Pathology* **154**:113–8 1999 [Abstract](#)
- 33 Ancans J, Tobin DJ, Hoogduijn MJ, Smit NP, Wakamatsu K and Thody AJ  
Melanosomal pH controls rate of melanogenesis, eumelanin/phaeomelanin ratio and melanosome maturation in melanocytes and melanoma cells  
*Experimental Cell Research* **268**:26–35 2001 [Abstract](#)
- 34 Andegeko Y, Moyal L, Mittelman L, Tsarfaty I, Shiloh Y and Rotman G  
Nuclear retention of ATM at sites of DNA double strand breaks  
*Journal of Biological Chemistry* **276**:38224–30 2001 [Abstract](#)
- 35 Anderson LA and Perkins ND  
The large subunit of replication factor C interacts with the histone deacetylase, HDAC1  
*Journal of Biological Chemistry* **277**:29550–4 2002 [Abstract](#)
- 36 Anwar S, Hall C, White J, Deakin M, Farrell W and Elder JB  
Hereditary non-polyposis colorectal cancer: an updated review  
*European Journal of Surgical Oncology* **26**:635–45 2000 [Abstract](#)
- 37 Aoki E, Uchida T, Ohashi H, Nagai H, Murase T, Ichikawa A, Yamao K, Hotta T, Kinoshita T, Saito H and Murate T  
Methylation status of the p15INK4B gene in hematopoietic progenitors and peripheral blood cells in myelodysplastic syndromes  
*Leukemia* **14**:586–93 2000 [Abstract](#)
- 38 Apfel R, Lottspeich F, Hoppe J, Behl C, Durr G and Bogdahn U  
Purification and analysis of growth regulating proteins secreted by a human melanoma cell line  
*Melanoma Research* **2**:327–36 1992 [Abstract](#)
- 39 Appella E and Anderson CW  
Post-translational modifications and activation of p53 by genotoxic stresses  
*European Journal of Biochemistry* **268**:2764–72 2001 [Abstract](#)
- 40 Aprelikova ON, Fang BS, Meissner EG, Cotter S, Campbell M, Kuthiala A, Bessho M, Jensen RA and Liu ET  
BRCA1-associated growth arrest is RB-dependent  
*Proceedings of the National Academy of Sciences of the USA* **96**:11866–71 1999 [Abstract](#)
- 41 Aprelikova O, Pace AJ, Fang B, Koller BH and Liu ET  
BRCA1 is a selective co-activator of 14–3-3 sigma gene transcription in mouse embryonic stem cells  
*Journal of Biological Chemistry* **276**:25647–50 2001 [Abstract](#)
- 42 Araujo SJ and Wood RD  
Protein complexes in nucleotide excision repair  
*Mutation Research* **435**:23–33 1999 [Abstract](#)
- 43 Arita Y, Santiago-Schwarz F and Coppock DL  
Survival mechanisms induced by 12-O-tetradecanoylphorbol-13-acetate in normal human melanocytes include inhibition of apoptosis and increased Bcl-2 expression  
*Melanoma Research* **10**:412–20 2000 [Abstract](#)
- 44 Asai DJ and Koonce MP  
The dynein heavy chain: structure, mechanics and evolution  
*Trends in Cell Biology* **11**:196–202 2001 [Abstract](#)
- 45 Ashcroft M, Taya Y and Vousden KH  
Stress signals utilize multiple pathways to stabilize p53  
*Molecular and Cellular Biology* **20**:3224–33 2000 [Abstract](#)
- 46 Asp J, Inerot S, Block JA and Lindahl A  
Alterations in the regulatory pathway involving p16, pRb and cdk4 in human chondrosarcoma  
*Journal of Orthopaedic Research* **19**:149–54 2001 [Abstract](#)
- 47 Athar M, Kim AL, Ahmad N, Mukhtar H, Gautier J and Bickers DR  
Mechanism of ultraviolet B-induced cell cycle arrest in G2/M phase in immortalized skin keratinocytes with defective p53  
*Biochemical and Biophysical Research Communications* **277**:107–11 2000 [Abstract](#)





- 48 Atkins MB  
The treatment of metastatic melanoma with chemotherapy and biologics  
*Current Opinion in Oncology* 9:205–13 1997 [Abstract](#)
- 49 Atkins MB, Kunkel L, Sznol M and Rosenberg SA  
High-dose recombinant interleukin-2 therapy in patients with metastatic melanoma: long-term survival update  
*Cancer Journal from Scientific American* 6 Suppl 1:S11–4 2000 [Abstract](#)
- 50 Ault JG and Rieder CL  
Centrosome and kinetochore movement during mitosis  
*Current Opinion in Cell Biology* 6:41–9 1994 [Abstract](#)
- 51 Ayllon V and Rebollo A  
Ras-induced cellular events  
*Molecular Membrane Biology* 17:65–73 2000 [Abstract](#)
- 52 Azam N, Vairapandi M, Zhang W, Hoffman B and Liebermann DA  
Interaction of CR6 (GADD45gamma) with proliferating cell nuclear antigen impedes negative growth control  
*Journal of Biological Chemistry* 276:2766–74 2001 [Abstract](#)
- 53 Baba Y, Nonoyama S, Matsushita M, Yamadori T, Hashimoto S, Imai K, Arai S, Kunikata T, Kurimoto M, Kurosaki T, Ochs HD, Yata Ji, Kishimoto T and Tsukada S  
Involvement of wiskott-aldrich syndrome protein in B-cell cytoplasmic tyrosine kinase pathway  
*Blood* 93:2003–12 1999 [Abstract](#)
- 54 Bachman KE, Herman JG, Corn PG, Merlo A, Costello JF, Cavenee WK, Baylin SB and Graff JR  
Methylation-associated silencing of the tissue inhibitor of metalloproteinase-3 gene suggest a suppressor role in kidney, brain, and other human cancers  
*Cancer Research* 59:798–802 1999 [Abstract](#)
- 55 Baeg GH, Matsumine A, Kuroda T, Bhattacharjee RN, Miyashiro I, Toyoshima K and Akiyama T  
The tumour suppressor gene product APC blocks cell cycle progression from G0/G1 to S phase  
*EMBO Journal* 14:5618–25 1995 [Abstract](#)
- 56 Bahadoran P, Aberdam E, Mantoux F, Busca R, Bille K, Yalman N, de Saint Basile G, Casaroli-Marano R, Ortonne JP and Ballotti R  
Rab27a: A key to melanosome transport in human melanocytes  
*Journal of Cell Biology* 152:843–50 2001 [Abstract](#)
- 57 Bahl R, Arora S, Nath N, Mathur M, Shukla NK and Ralhan R  
Novel polymorphism in p21(waf1/cip1) cyclin dependent kinase inhibitor gene: association with human esophageal cancer  
*Oncogene* 19:323–8 2000 [Abstract](#)
- 58 Bahua M, Vidaud D, Jenkins RB, Bieche I, Kimmel DW, Assouline B, Smith JS, Alderete B, Cayuela JM, Harpey JP, Caille B and Vidaud M  
Germ-line deletion involving the INK4 locus in familial proneness to melanoma and nervous system tumors  
*Cancer Research* 58:2298–303 1998 [Abstract](#)
- 59 Bailly E, Pines J, Hunter T and Bornens M  
Cytoplasmic accumulation of cyclin B1 in human cells: association with a detergent-resistant compartment and with the centrosome  
*Journal of Cell Science* 101:529–45 1992 [Abstract](#)
- 60 Bailly M, Bertrand S and Dore JF  
Increased spontaneous mutation rates and prevalence of karyotype abnormalities in highly metastatic human melanoma cell lines  
*Melanoma Research* 3:51–61 1993 [Abstract](#)
- 61 Bailly M and Dore JF  
Clonal drift and role of chromosome dosage in human melanoma metastatic cell lines: a statistical analysis  
*Anticancer Research* 12:1163–72 1992 [Abstract](#)
- 62 Bakin AV, Tomlinson AK, Bhowmick NA, Moses HL and Arteaga CL  
Phosphatidylinositol 3-kinase function is required for transforming growth factor beta-mediated epithelial to mesenchymal transition and cell migration  
*Journal of Biological Chemistry* 275:36803–10 2000 [Abstract](#)
- 63 Balczon R, Varden CE and Schroer TA  
Role for microtubules in centrosome doubling in Chinese hamster ovary cells  
*Cell Motility and the Cytoskeleton* 42:60–72 1999 [Abstract](#)
- 64 Bale SJ, Dracopoli NC, Tucker MA, Clark WH Jr, Fraser MC, Stanger BZ, Green P, Donis-Keller H, Housman DE and Greene MH  
Mapping the gene for hereditary cutaneous malignant melanoma-dysplastic nevus to chromosome 1p  
*New England Journal of Medicine* 320:1367–72 1989 [Abstract](#)
- 65 Bales ES, Dietrich C, Bandyopadhyay D, Schwahn DJ, Xu W, Didenko V, Leiss P, Conrad N, Pereira-Smith O, Orengo I and Medrano EE  
High levels of expression of p27KIP1 and cyclin E in invasive primary malignant melanomas  
*Journal of Investigative Dermatology* 113:1039–46 1999 [Abstract](#)
- 66 Balint E E and Vousden KH  
Activation and activities of the p53 tumour suppressor protein  
*British Journal of Cancer* 85:1813–1823 2001 [Abstract](#)
- 67 Bandyopadhyay D and Medrano EE  
Melanin accumulation accelerates melanocyte senescence by a mechanism involving p16INK4a/CDK4/pRB and E2F1  
*Annals of the New York Academy of Sciences* 908:71–84 2000 [Abstract](#)
- 68 Bandyopadhyay D, Timchenko N, Suwa T, Hornsby PJ, Campisi J and Medrano EE  
The human melanocyte: a model system to study the complexity of cellular aging and transformation in non-fibroblastic cells  
*Experimental Gerontology* 36:1265–75 2001 [Abstract](#)
- 69 Banin S, Gout I and Brickell P  
Interaction between Wiskott-Aldrich Syndrome protein (WASP) and the Fyn protein-tyrosine kinase  
*Molecular Biology Reports* 26:173–7 1999 [Abstract](#)
- 70 Baroja A, de la Hoz C, Alvarez A, Ispizua A, Bilbao J and de Gandarias JM  
Genesis and evolution of high-ploidy tumour cells evaluated by means of the proliferation markers p34(cdc2), cyclin B1, PCNA and 3[H]-thymidine  
*Cell Proliferation* 29:89–100 1996 [Abstract](#)
- 71 Barth H, Hoffmann I, Klein S, Kaszkin M, Richards J and Kinzel V  
Role of cdc25-C phosphatase in the immediate G2 delay induced by the exogenous factors epidermal growth factor and phorbol ester  
*Journal of Cellular Physiology* 168:589–99 1996 [Abstract](#)

## Human metastatic melanoma in vitro

72	Barth H and Kinzel V Epidermal growth factor rapidly impairs activation of p34cdc2 protein kinase in HeLa cells at the G2-M boundary <i>Journal of Cellular Physiology</i>	162:44–51	1995	<a href="#">Abstract</a>
73	Bartkova J, Lukas J, Guldberg P, Alnsner J, Kirkin AF, Zeuthen J and Bartek J The p16-cyclin D/Cdk4-pRb pathway as a functional unit frequently altered in melanoma pathogenesis <i>Cancer Research</i>	56:5475–83	1996	<a href="#">Abstract</a>
74	Bartkova J, Lukas J, Muller H, Strauss M, Gusterson B and Bartek J Abnormal patterns of D-type cyclin expression and G1 regulation in human head and neck cancer <i>Cancer Research</i>	55:949–56	1995	<a href="#">Abstract</a>
75	Bartkova J, Zemanova M and Bartek J Abundance and subcellular localisation of cyclin D3 in human tumours <i>International Journal of Cancer</i>	65:323–7	1996	<a href="#">Abstract</a>
76	Baskaran R, Wood LD, Whitaker LL, Canman CE, Morgan SE, Xu Y, Barlow C, Baltimore D, Wynshaw-Boris A, Kastan MB and Wang JY Ataxia telangiectasia mutant protein activates c-Abl tyrosine kinase in response to ionizing radiation <i>Nature</i>	387:516–9	1997	<a href="#">Abstract</a>
77	Bataille V, Hiles R and Bishop JA Retinoblastoma, melanoma and the atypical mole syndrome <i>British Journal of Dermatology</i>	132:134–8	1995	<a href="#">Abstract</a>
78	Bates S and Vousden KH Mechanisms of p53-mediated apoptosis <i>Cellular and Molecular Life Sciences</i>	55:28–37	1999	<a href="#">Abstract</a>
79	Baxter SW, Thomas EJ and Campbell IG GSTM1 null polymorphism and susceptibility to endometriosis and ovarian cancer <i>Carcinogenesis</i>	22:63–66	2001	<a href="#">Abstract</a>
80	Beavon IR The E-cadherin-catenin complex in tumour metastasis: structure, function and regulation <i>European Journal of Cancer</i>	36:1607–20	2000	<a href="#">Abstract</a>
81	Becher R, Gibas Z, Karakousis C and Sandberg AA Nonrandom chromosome changes in malignant melanoma <i>Cancer Research</i>	43:5010–6	1983	<a href="#">Abstract</a>
82	Beijersbergen RL, Carlee L, Kerkhoven RM and Bernards R Regulation of the retinoblastoma protein-related p107 by G1 cyclin complexes <i>Genes and Development</i>	9:1340–53	1995	<a href="#">Abstract</a>
83	Belcheva MM and Coscia CJ Diversity of G Protein-Coupled Receptor Signaling Pathways to ERK/MAP Kinase <i>Neurosignals</i>	11:34–44	2002	<a href="#">Abstract</a>
84	Belec I, Gonzalez C, Puro J and Szabad J Dominant-negative mutant dynein allows spontaneous centrosome assembly, uncouples chromosome and centrosome cycles <i>Current Biology</i>	11:136–40	2001	<a href="#">Abstract</a>
85	Bell DW, Varley JM, Szydlo TE, Kang DH, Wahrer DC, Shannon KE, Lubratovich M, Verselis SJ, Isselbacher KJ, Fraumeni JF, Birch JM, Li FP, Garber JE and Haber DA Heterozygous germ line hCHK2 mutations in Li-Fraumeni syndrome <i>Science</i>	286:2528–31	1999	<a href="#">Abstract</a>
86	Bellamy CO p53 and apoptosis <i>British Medical Bulletin</i>	53:522–38	1997	<a href="#">Abstract</a>
87	Benassi MS, Molendini L, Gamberi G, Ragazzini P, Sollazzo MR, Merli M, Asp J, Magagnoli G, Balladelli A, Bertoni F and Picci P Alteration of pRb/p16/cdk4 regulation in human osteosarcoma <i>International Journal of Cancer</i>	84:489–93	1999	<a href="#">Abstract</a>
88	Benathan M and Labidi F Cysteine-dependent 5-S-cysteinyl-dopa formation and its regulation by glutathione in normal epidermal melanocytes <i>Archives of Dermatological Research</i>	288:697–702	1996	<a href="#">Abstract</a>
89	Benathan M, Virador V, Furumura M, Kobayashi N, Panizzon RG and Hearing VJ Co-regulation of melanin precursors and tyrosinase in human pigment cells: roles of cysteine and glutathione <i>Cellular and Molecular Biology (Noisy-le-grand)</i>	45:981–90	1999	<a href="#">Abstract</a>
90	Benedict WF, Lerner SP, Zhou J, Shen X, Tokunaga H and Czerniak B Level of retinoblastoma protein expression correlates with p16 (MTS-1/INK4A/CDKN2) status in bladder cancer <i>Oncogene</i>	18:1197–203	1999	<a href="#">Abstract</a>
91	Berry LD and Gould KL Regulation of Cdc2 activity by phosphorylation at T14/Y15 <i>Progress in Cell Cycle Research</i>	2:99–105	1996	<a href="#">Abstract</a>
92	Bertolotto C, Abbe P, Hemesath TJ, Bille K, Fisher DE, Ortonne JP and Ballotti R Microphthalmia gene product as a signal transducer in cAMP-induced differentiation of melanocytes <i>Journal of Cell Biology</i>	142:827–35	1998	<a href="#">Abstract</a>
93	Berx G, Becker KF, Hofler H and van Roy F Mutations of the human E-cadherin (CDH1) gene <i>Human Mutation</i>	12:226–37	1998	<a href="#">Abstract</a>
94	Berx G, Staes K, van Hengel J, Molemans F, Bussemakers MJ, van Bokhoven A and van Roy F Cloning and characterization of the human invasion suppressor gene E-cadherin (CDH1) <i>Genomics</i>	26:281–9	1995	<a href="#">Abstract</a>
95	Besson A, Robbins SM and Yong VW PTEN/MMAC1/TEP1 in signal transduction and tumorigenesis <i>European Journal of Biochemistry</i>	263:605–11	1999	<a href="#">Abstract</a>
96	Biden K, Young J, Buttenshaw R, Searle J, Cooksley G, Xu DB and Leggett B Frequency of mutation and deletion of the tumor suppressor gene CDKN2A (MTS1/p16) in hepatocellular carcinoma from an Australian population <i>Hepatology</i>	25:593–7	1997	<a href="#">Abstract</a>
97	Bilodeau ML, Greulich JD, Hullinger RL, Bertolotto C, Ballotti R and Andrisani OM BMP-2 stimulates tyrosinase gene expression and melanogenesis in differentiated melanocytes <i>Pigment Cell Research</i>	14:328–36	2001	<a href="#">Abstract</a>



- 98 Birchmeier W, Hulsken J and Behrens J  
E-cadherin as an invasion suppressor  
*Ciba Foundation Symposium* **189**:124–36 1995 [Abstract](#)
- 99 Birchmeier W, Hulsken J and Behrens J  
Adherens junction proteins in tumour progression  
*Cancer Surveys* **24**:129–40 1995 [Abstract](#)
- 100 Blanchard JM  
Cyclin A2 transcriptional regulation: modulation of cell cycle control at the G1/S transition by peripheral cues  
*Biochemical Pharmacology* **60**:1179–84 2000 [Abstract](#)
- 101 Blangy A, Arnaud L and Nigg EA  
Phosphorylation by p34cdc2 protein kinase regulates binding of the kinesin-related motor HsEg5 to the dynactin subunit p150  
*Journal of Biological Chemistry* **272**:19418–24 1997 [Abstract](#)
- 102 Blangy A, Lane HA, d'Herin P, Harper M, Kress M and Nigg EA  
Phosphorylation by p34cdc2 regulates spindle association of human Eg5, a kinesin-related motor essential for bipolar spindle formation in vivo  
*Cell* **83**:1159–69 1995 [Abstract](#)
- 103 Blesch A, Bosserhoff AK, Apfel R, Behl C, Hessdoerfer B, Schmitt A, Jachimczak P, Lottspeich F, Buettner R and Bogdahn U  
Cloning of a novel malignant melanoma-derived growth-regulatory protein, MIA  
*Cancer Research* **54**:5695–701 1994 [Abstract](#)
- 104 Blume-Jensen P, Janknecht R and Hunter T  
The kit receptor promotes cell survival via activation of PI 3-kinase and subsequent Akt-mediated phosphorylation of Bad on Ser136  
*Current Biology* **8**:779–82 1998 [Abstract](#)
- 105 Blume-Jensen P and Hunter T  
Oncogenic kinase signalling  
*Nature* **411**:355–65 2001 [Abstract](#)
- 106 Blume-Jensen P, Wernstedt C, Heldin CH and Ronnstrand L  
Identification of the major phosphorylation sites for protein kinase C in kit/stem cell factor receptor in vitro and in intact cells  
*Journal of Biological Chemistry* **270**:14192–200 1995 [Abstract](#)
- 107 Boardman LA, Thibodeau SN, Schaid DJ, Lindor NM, McDonnell SK, Burgart LJ, Ahlquist DA, Podratz KC, Pittelkow M and Hartmann LC  
Increased risk for cancer in patients with the Peutz-Jeghers syndrome  
*Annals of Internal Medicine* **128**:896–9 1998 [Abstract](#)
- 108 Boddy MN, Furnari B, Mondesert O and Russell P  
Replication checkpoint enforced by kinases Cds1 and Chk1  
*Science* **280**:909–12 1998 [Abstract](#)
- 109 Bogdahn U, Apfel R, Hahn M, Gerlach M, Behl C, Hoppe J and Martin R  
Autocrine tumor cell growth-inhibiting activities from human malignant melanoma  
*Cancer Research* **49**:5358–63 1989 [Abstract](#)
- 110 Bogler O, Huang HJ, Kleihues P and Cavenee WK  
The p53 gene and its role in human brain tumors  
*Glia* **15**:308–27 1995 [Abstract](#)
- 111 Boissy RE, Sakai C, Zhao H, Kobayashi T and Hearing VJ  
Human tyrosinase related protein-1 (TRP-1) does not function as a DHICA oxidase activity in contrast to murine TRP-1  
*Experimental Dermatology* **7**:198–204 1998 [Abstract](#)
- 112 Bolognia JL and Orlow SJ  
Melanocyte biology  
In: *Dermatology* Bolognia et al. (eds) Elsevier Science, Cambridge, England ISBN 072343234 in press [Abstract](#)
- 113 Bond J, Haughton M, Blaydes J, Gire V, Wynford-Thomas D and Wyllie F  
Evidence that transcriptional activation by p53 plays a direct role in the induction of cellular senescence  
*Oncogene* **13**:2097–104 1996 [Abstract](#)
- 114 Bondurand N, Pingault V, Goerich DE, Lemort N, Sock E, Caignec CL, Wegner M and Goossens M  
Interaction among SOX10, PAX3 and MITF, three genes altered in Waardenburg syndrome  
*Human Molecular Genetics* **9**:1907–17 2000 [Abstract](#)
- 115 Boni R, Vortmeyer AO, Burg G, Hofbauer G and Zhuang Z  
The PTEN tumour suppressor gene and malignant melanoma  
*Melanoma Research* **8**:300–2 1998 [Abstract](#)
- 116 Booher RN, Holman PS and Fattaey A  
Human Myt1 is a cell cycle-regulated kinase that inhibits Cdc2 but not Cdk2 activity  
*Journal of Biological Chemistry* **272**:22300–6 1997 [Abstract](#)
- 117 Bookstein R, Lee EY, To H, Young LJ, Sery TW, Hayes RC, Friedmann T and Lee WH  
Human retinoblastoma susceptibility gene: genomic organization and analysis of heterozygous intragenic deletion mutants  
*Proceedings of the National Academy of Sciences of the USA* **85**:2210–4 1988 [Abstract](#)
- 118 Bordon R, Fine R, Murray D and Richmond A  
Characterization of the role of melanoma growth stimulatory activity (MGSA) in the growth of normal melanocytes, nevocytes, and malignant melanocytes  
*Journal of Cellular Biochemistry* **44**:207–19 1990 [Abstract](#)
- 119 Borg A, Johannsson U, Johannsson O, Hakansson S, Westerdahl J, Masback A, Olsson H and Ingvar C  
Novel germline p16 mutation in familial malignant melanoma in southern Sweden  
*Cancer Research* **56**:2497–500 1996 [Abstract](#)
- 120 Borgne A and Meijer L  
Sequential dephosphorylation of p34(cdc2) on Thr-14 and Tyr-15 at the prophase/metaphase transition  
*Journal of Biological Chemistry* **271**:27847–54 1996 [Abstract](#)
- 121 Bosserhoff AK, Echtenacher B, Hein R and Buettner R  
Functional role of melanoma inhibitory activity in regulating invasion and metastasis of malignant melanoma cells in vivo  
*Melanoma Research* **11**:417–21 2001 [Abstract](#)
- 122 Bostrom J, Meyer-Puttitz B, Wolter M, Blaschke B, Weber RG, Lichter P, Ichimura K, Collins VP and Reifenberger G  
Alterations of the tumor suppressor genes CDKN2A (p16(INK4a)), p14(ARF), CDKN2B (p15(INK4b)), and CDKN2C (p18(INK4c)) in atypical and anaplastic meningiomas  
*American Journal of Pathology* **159**:661–9 2001 [Abstract](#)

## Human metastatic melanoma in vitro

- 123 Boukamp P, Popp S, Bleuel K, Tomakidi E, Burkle A and Fusenig NE  
Tumorigenic conversion of immortal human skin keratinocytes (HaCaT) by elevated temperature  
*Oncogene* **18**:5638–45 1999 [Abstract](#)
- 124 Bouchard C, Thieke K, Maier A, Saffrich R, Hanley-Hyde J, Ansorge W, Reed S, Sicinski P, Bartek J and Eilers M  
Direct induction of cyclin D2 by Myc contributes to cell cycle progression and sequestration of p27  
*EMBO Journal* **18**:5321–33 1999 [Abstract](#)
- 125 Boulaire J, Fotadar A and Fotadar R  
The functions of the cdk-cyclin kinase inhibitor p21WAF1  
*Pathologie Biologie* **48**:190–202 2000 [Abstract](#)
- 126 Bourguignon LY, Zhu H, Shao L, Zhu D and Chen YW  
Rho-kinase (ROK) promotes CD44v(3,8–10)-ankyrin interaction and tumor cell migration in metastatic breast cancer cells  
*Cell Motility and the Cytoskeleton* **43**:269–87 1999 [Abstract](#)
- 127 Boveri T  
Gustav Fischer Verlag Jena, Germany 1914
- 128 Bowers J, Tran PT, Joshi A, Liskay RM and Alani E  
MSH-MLH complexes formed at a DNA mismatch are disrupted by the PCNA sliding clamp  
*Journal of Molecular Biology* **306**:957–68 2001 [Abstract](#)
- 129 Boyle JM, Mitchell EL, Greaves MJ, Roberts SA, Tricker K, Burt E, Varley JM and Scott D  
Chromosome instability is a predominant trait of fibroblasts from Li-Fraumeni families  
*British Journal of Cancer* **77**:2181–92 1998 [Abstract](#)
- 130 Brady HJ and Gil Gomez G  
Bax. The pro-apoptotic Bcl-2 family member, Bax  
*International Journal of Biochemistry and Cell Biology* **30**:647–50 1998 [Abstract](#)
- 131 Brehm A, Miska EA, McCance DJ, Reid JL, Bannister AJ and Kouzarides T  
Retinoblastoma protein recruits histone deacetylase to repress transcription  
*Nature* **391**:597–601 1998 [Abstract](#)
- 132 Bremner R, Du DC, Connolly-Wilson MJ, Bridge P, Ahmad KF, Mostachfi H, Rushlow D, Dunn JM and Gallie BL  
Deletion of RB exons 24 and 25 causes low-penetrance retinoblastoma  
*American Journal of Human Genetics* **61**:556–70 1997 [Abstract](#)
- 133 Breslow A  
Tumor thickness, level of invasion and node dissection in stage I cutaneous melanoma  
*Annals of Surgery* **182**:572–5 1975 [Abstract](#)
- 134 Bressac de Paillerets B, Avril MF, Chompret A and Demenais F  
Genetic and environmental factors in cutaneous malignant melanoma  
*Biochimie* **84**:67–74 2002 [Abstract](#)
- 135 Bretscher A, Chambers D, Nguyen R and Reczek D  
ERM-Merlin and EBP50 protein families in plasma membrane organization and function  
*Annual Review of Cell and Developmental Biology* **16**:113–43 2000 [Abstract](#)
- 136 Brilliant MH  
The mouse p (pink-eyed dilution) and human P genes, oculocutaneous albinism type 2 (OCA2), and melanosomal pH  
*Pigment Cell Research* **14**:86–93 2001 [Abstract](#)
- 137 Brizzi MF, Dentelli P, Rosso A, Yarden Y and Pegoraro L  
STAT protein recruitment and activation in c-Kit deletion mutants  
*Journal of Biological Chemistry* **274**:16965–72 1999 [Abstract](#)
- 138 Brown NR, Noble ME, Endicott JA and Johnson LN  
The structural basis for specificity of substrate and recruitment peptides for cyclin-dependent kinases  
*Nature Cell Biology* **1**:438–43 1999 [Abstract](#)
- 139 Bruch-Gerharz D, Ruzicka T and Kolb-Bachofen V  
Nitric oxide in human skin: current status and future prospects  
*Journal of Investigative Dermatology* **110**:1–7 1998 [Abstract](#)
- 140 Brunet A, Bonni A, Zigmond MJ, Lin MZ, Juo P, Hu LS, Anderson MJ, Arden KC, Blenis J and Greenberg ME  
Akt promotes cell survival by phosphorylating and inhibiting a Forkhead transcription factor  
*Cell* **96**:857–68 1999 [Abstract](#)
- 141 Buchner T, Hiddemann W, Wormann B, Kleinemeier B, Schumann J, Gohde W, Ritter J, Muller KM, von Bassewitz DB, Roessner A et al  
Differential pattern of DNA-aneuploidy in human malignancies  
*Pathology, Research and Practice* **179**:310–7 1985 [Abstract](#)
- 142 Buendia B, Draetta G and Karsenti E  
Regulation of the microtubule nucleating activity of centrosomes in *Xenopus* egg extracts: role of cyclin A-associated protein kinase  
*Journal of Cell Biology* **116**:1431–42 1992 [Abstract](#)
- 143 Bulavin DV, Higashimoto Y, Popoff IJ, Gaarde WA, Basrur V, Potapova O, Appella E and Fornace AJ Jr  
Initiation of a G2/M checkpoint after ultraviolet radiation requires p38 kinase  
*Nature* **411**:102–7 2001 [Abstract](#)
- 144 Buscemi G, Savio C, Zannini L, Micciche F, Masnada D, Nakanishi M, Tauchi H, Komatsu K, Mizutani S, Khanna K, Chen P, Concannon P, Chessa L and Delia D  
Chk2 activation dependence on Nbs1 after DNA damage  
*Molecular and Cellular Biology* **21**:5214–22 2001 [Abstract](#)
- 145 Busson S, Dujardin D, Moreau A, Dompierre J and De Mey JR  
Dynein and dyactin are localized to astral microtubules and at cortical sites in mitotic epithelial cells  
*Current Biology* **8**:541–4 1998 [Abstract](#)
- 146 Buyse IM and Huang S  
In vitro analysis of the E1A-homologous sequences of RIZ  
*Journal of Virology* **71**:6200–3 1997 [Abstract](#)
- 147 Buyse IM, Shao G and Huang S  
The retinoblastoma protein binds to RIZ, a zinc-finger protein that shares an epitope with the adenovirus E1A protein  
*Proceedings of the National Academy of Sciences of the USA* **92**:4467–71 1995 [Abstract](#)
- 148 Cai H, Smola U, Wixler V, Eisenmann-Tappe I, Diaz-Meco MT, Moscat J, Rapp U and Cooper GM  
Role of diacylglycerol-regulated protein kinase C isoforms in growth factor activation of the Raf-1 protein kinase  
*Molecular and Cellular Biology* **17**:732–41 1997 [Abstract](#)



- 149 Caldas C, Hahn SA, da Costa LT, Redston MS, Schutte M, Seymour AB, Weinstein CL, Hruban RH, Yeo CJ and Kern SE  
Frequent somatic mutations and homozygous deletions of the p16 (MTS1) gene in pancreatic adenocarcinoma [published erratum  
appears in *Nature Genetics* 8:410]  
*Nature Genetics* 8:27–32 1994 [Abstract](#)
- 150 Campanero MR and Flemington EK  
Regulation of E2F through ubiquitin-proteasome-dependent degradation: stabilization by the pRB tumor suppressor protein  
*Proceedings of the National Academy of Sciences of the USA* 94:2221–6 1997 [Abstract](#)
- 151 Campbell CE, Kuriyan NP, Rackley RR, Caulfield MJ, Tubbs R, Finke J and Williams BR  
Constitutive expression of the Wilms tumor suppressor gene (WT1) in renal cell carcinoma  
*International Journal of Cancer* 78:182–8 1998 [Abstract](#)
- 152 Campbell SL, Khosravi-Far R, Rossman KL, Clark GJ and Der CJ  
Increasing complexity of Ras signaling  
*Oncogene* 17:1395–413 1998 [Abstract](#)
- 153 Canman CE and Lim DS  
The role of ATM in DNA damage responses and cancer  
*Oncogene* 17:3301–8 1998 [Abstract](#)
- 154 Canote R, Du Y, Carling T, Tian F, Peng Z and Huang S  
The tumor suppressor gene RIZ in cancer gene therapy  
*Oncology Reports* 9:57–60 2002 [Abstract](#)
- 155 Cantley LC and Neel BG  
New insights into tumor suppression: PTEN suppresses tumor formation by restraining the phosphoinositide 3-kinase/AKT pathway  
*Proceedings of the National Academy of Sciences of the USA* 96:4240–5 1999 [Abstract](#)
- 156 Carreira S, Dexter TJ, Yavuzer U, Easty DJ and Goding CR  
Brachyury-related transcription factor Tbx2 and repression of the melanocyte-specific TRP-1 promoter  
*Molecular and Cellular Biology* 18:5099–108 1998 [Abstract](#)
- 157 Carreira S, Liu B and Goding CR  
The gene encoding the T-box factor Tbx2 is a target for the microphthalmia-associated transcription factor in melanocytes  
*Journal of Biological Chemistry* 275:21920–7 2000 [Abstract](#)
- 158 Carroll MP and May WS  
Protein kinase C-mediated serine phosphorylation directly activates Raf-1 in murine hematopoietic cells  
*Journal of Biological Chemistry* 269:1249–56 1994 [Abstract](#)
- 159 Carroll PE, Okuda M, Horn HF, Biddinger P, Stambrook PJ, Gleich LL, Li YQ, Tarapore P and Fukasawa K  
Centrosome hyperamplification in human cancer: chromosome instability induced by p53 mutation and/or Mdm2 overexpression  
*Oncogene* 18:1935–44 1999 [Abstract](#)
- 160 Cartwright P, Muller H, Wagener C, Holm K and Helin K  
E2F-6: a novel member of the E2F family is an inhibitor of E2F-dependent transcription  
*Oncogene* 17:611–23 1998 [Abstract](#)
- 161 Caselitz J, Janner M, Breitbart E, Weber K and Osborn M  
Malignant melanomas contain only the vimentin type of intermediate filaments  
*Virchows Archiv. A: Pathological Anatomy and Histopathology* 400:43–51 1983 [Abstract](#)
- 162 Caspary T, Cleary MA, Perlman EJ, Zhang P, Elledge SJ and Tilghman SM  
Oppositely imprinted genes p57(Kip2) and igf2 interact in a mouse model for Beckwith-Wiedemann syndrome  
*Genes and Development* 13:3115–24 1999 [Abstract](#)
- 163 Castano E, Kleyner Y and Dynlacht BD  
Dual cyclin-binding domains are required for p107 to function as a kinase inhibitor  
*Molecular and Cellular Biology* 18:5380–91 1998 [Abstract](#)
- 164 Castellano M and Parmiani G  
Genes involved in melanoma: an overview of INK4a and other loci  
*Melanoma Research* 9:421–32 1999 [Abstract](#)
- 165 Castellano M, Pollock PM, Walters MK, Sparrow LE, Down LM, Gabrielli BG, Parsons PG and Hayward NK  
CDKN2A/p16 is inactivated in most melanoma cell lines  
*Cancer Research* 57:4868–75 1997 [Abstract](#)
- 166 Catania A, Airaghi L, Colombo G and Lipton JM  
Alpha-melanocyte-stimulating hormone in normal human physiology and disease states  
*Trends in Endocrinology and Metabolism* 11:304–8 2000 [Abstract](#)
- 167 Catteau A, Harris WH, Xu CF and Solomon E  
Methylation of the BRCA1 promoter region in sporadic breast and ovarian cancer: correlation with disease characteristics  
*Oncogene* 18:1957–65 1999 [Abstract](#)
- 168 Cavanaugh AH, Hempel WM, Taylor LJ, Rogalsky V, Todorov G and Rothblum LI  
Activity of RNA polymerase I transcription factor UBF blocked by Rb gene product  
*Nature* 374:177–80 1995 [Abstract](#)
- 169 Cavenee WK, Dryja TP, Phillips RA, Benedict WF, Godbout R, Gallie BL, Murphree AL, Strong LC and White RL  
Expression of recessive alleles by chromosomal mechanisms in retinoblastoma  
*Nature* 305:779–84 1983 [Abstract](#)
- 170 Celebi JT, Shendrik I, Silvers DN and Peacocke M  
Identification of PTEN mutations in metastatic melanoma specimens  
*Journal of Medical Genetics* 37:653–7 2000 [Abstract](#)
- 171 Cetta F, Olschwang S, Petracchi M, Montalto G, Baldi C, Zuckermann M, Costantini RM, Fusco A  
Genetic alterations in thyroid carcinoma associated with familial adenomatous polyposis: clinical implications and suggestions for  
early detection  
*World Journal of Surgery* 22:1231–6 1998 [Abstract](#)
- 172 Chadwick RB, Meek JE, Prior TW, Peltomaki P and de La Chapelle A  
Polymorphisms in a pseudogene highly homologous to PMS2  
*Human Mutation* 16:530 2000 [Abstract](#)
- 173 Chakraborty AK, Platt JT, Kim KK, Kwon BS, Bennett DC and Pawelek JM  
Polymerization of 5,6-dihydroxyindole-2-carboxylic acid to melanin by the pmel 17/silver locus protein  
*European Journal of Biochemistry* 236:180–8 1996 [Abstract](#)
- 174 Chai YL, Cui J, Shao N, Shyam E, Reddy P and Rao VN  
The second BRCT domain of BRCA1 proteins interacts with p53 and stimulates transcription from the p21WAF1/CIP1 promoter  
*Oncogene* 18:263–8 1999 [Abstract](#)

## Human metastatic melanoma in vitro

- 175 Chan DW, Son SC, Block W, Ye R, Khanna KK, Wold MS, Douglas P, Goodarzi AA, Pelley J, Taya Y, Lavin MF and Lees Miller SP  
Purification and characterization of ATM from human placenta. A manganese-dependent, wortmannin-sensitive serine/threonine protein kinase  
*Journal of Biological Chemistry* **275**:7803–10 2000 [Abstract](#)
- 176 Chan HM, Krstic-Demonacos M, Smith L, Demonacos C and La Thangue NB  
Acetylation control of the retinoblastoma tumour-suppressor protein  
*Nature Cell Biology* **3**:667–74 2001 [Abstract](#)
- 177 Chan HM, Smith L and La Thangue NB  
Role of LXCXE motif-dependent interactions in the activity of the retinoblastoma protein  
*Oncogene* **20**:6152–63 2001 [Abstract](#)
- 178 Chandrasekharappa SC, Guru SC, Manickam P, Olufemi SE, Collins FS, Emmert-Buck MR, Debelenko LV, Zhuang Z, Lubensky IA, Liotta LA, Crabtree JS, Wang Y, Roe BA, Weisemann J, Boguski MS, Agarwal SK, Kester MB, Kim YS, Heppner C, Dong Q, Spiegel AM, Burns AL and Marx SJ  
Positional cloning of the gene for multiple endocrine neoplasia-type 1  
*Science* **276**:404–7 1997 [Abstract](#)
- 179 Charames GS, Millar AL, Pal T, Narod S and Bapat B  
Do MSH6 mutations contribute to double primary cancers of the colorectum and endometrium?  
*Human Genetics* **107**:623–9 2000 [Abstract](#)
- 180 Charters GA  
Aspects of growth regulation in cultured human melanoma cells  
The University of Auckland, New Zealand MSc. thesis 1997
- 181 Chaturvedi P, Eng WK, Zhu Y, Mattern MR, Mishra R, Hurler MR, Zhang X, Annan RS, Lu Q, Faucette LF, Scott GF, Li X, Carr SA, Johnson RK, Winkler JD and Zhou BB  
Mammalian Chk2 is a downstream effector of the ATM-dependent DNA damage checkpoint pathway  
*Oncogene* **18**:4047–54 1999 [Abstract](#)
- 182 Chedekel MR and Zeise L  
Sunlight, melanogenesis and radicals in the skin  
*Lipids* **23**:587–91 1988 [Abstract](#)
- 183 Chehab NH, Malikzay A, Appel M and Halazonetis TD  
Chk2/hCds1 functions as a DNA damage checkpoint in G(1) by stabilizing p53  
*Genes and Development* **14**:278–88 2000 [Abstract](#)
- 184 Chehab NH, Malikzay A, Stavridi ES and Halazonetis TD  
Phosphorylation of Ser-20 mediates stabilization of human p53 in response to DNA damage  
*Proceedings of the National Academy of Sciences of the USA* **96**:13777–82 1999 [Abstract](#)
- 185 Chen CF, Chen Y, Dai K, Chen PL, Riley DJ and Lee WH  
A new member of the hsp90 family of molecular chaperones interacts with the retinoblastoma protein during mitosis and after heat shock  
*Molecular and Cellular Biology* **16**:4691–9 1996 [Abstract](#)
- 186 Chen G and Lee EYHP  
The product of the ATM gene is a 370-kDa nuclear phosphoprotein  
*Journal of Biological Chemistry* **271**:33693–7 1996 [Abstract](#)
- 187 Chen GC, Guan LS, Yu JH, Li GC, Choi-Kim HR and Wang ZY  
Rb-associated protein 46 (RbAp46) inhibits transcriptional transactivation mediated by BRCA1  
*Biochemical and Biophysical Research Communications* **284**:507–14 2001 [Abstract](#)
- 188 Chen H, Salopek TG and Jimbow K  
The role of phosphoinositide 3-kinase in the sorting and transport of newly synthesized tyrosinase-related protein-1 (TRP-1)  
*Journal of Investigative Dermatology Symposium Proceedings* **6**:105–14 2001 [Abstract](#)
- 189 Chen H, Sandler DP, Taylor JA, Shore DL, Liu E, Bloomfield CD, Bell DA  
Increased risk for myelodysplastic syndromes in individuals with glutathione transferase theta 1 (GSTT1) gene defect  
*Lancet* **347**:295–7 1996 [Abstract](#)
- 190 Chen HT, Bhandoola A, Difilippantonio MJ, Zhu J, Brown MJ, Tai X, Rogakou EP, Brotz TM, Bonner WM, Ried T and Nussenzweig A  
Response to RAG-mediated VDJ cleavage by NBS1 and gamma-H2AX  
*Science* **290**:1962–5 2000 [Abstract](#)
- 191 Chen J, Wu W, Tahir SK, Kroeger PE, Rosenberg SH, Cowser LM, Bennett F, Krajewski S, Krajewska M, Welsh K, Reed JC and Ng SC  
Down-regulation of survivin by antisense oligonucleotides increases apoptosis, inhibits cytokinesis and anchorage-independent growth  
*Neoplasia* **2**:235–41 2000 [Abstract](#)
- 192 Chen MJ, Lin YT, Lieberman HB, Chen G and Lee EY  
ATM-dependent phosphorylation of human Rad9 is required for ionizing radiation-induced checkpoint activation  
*Journal of Biological Chemistry* **276**:16580–6 2001 [Abstract](#)
- 193 Chen P, Gate M, O'Connell MJ, Khanna KK, Bugg SJ, Hogg A, Scott SP, Hobson K and Lavin MF  
Chk1 complements the G2/M checkpoint defect and radiosensitivity of ataxia-telangiectasia cells  
*Oncogene* **18**:249–56 1999 [Abstract](#)
- 194 Chen PL, Riley DJ and Lee WH  
The retinoblastoma protein as a fundamental mediator of growth and differentiation signals  
*Critical Reviews in Eukaryotic Gene Expression* **5**:79–95 1995 [Abstract](#)
- 195 Cheng A, Kaldis P and Solomon MJ  
Dephosphorylation of human cyclin-dependent kinases by protein phosphatase type 2C alpha and beta 2 isoforms  
*Journal of Biological Chemistry* **275**:34744–9 2000 [Abstract](#)
- 196 Cheng M, Sexl V, Sherr CJ and Roussel MF  
Assembly of cyclin D-dependent kinase and titration of p27Kip1 regulated by mitogen-activated protein kinase kinase (MEK1)  
*Proceedings of the National Academy of Sciences of the USA* **95**:1091–6 1998 [Abstract](#)
- 197 Cherrington JM, Strawn LM and Shawver LK  
New paradigms for the treatment of cancer: the role of anti-angiogenesis agents  
*Advances in Cancer Research* **79**:1–38 2000 [Abstract](#)
- 198 Cheung TH, Yu MM, Lo KW, Yim SF, Chung TK and Wong YF  
Alteration of cyclin D1 and CDK4 gene in carcinoma of uterine cervix  
*Cancer Letters* **166**:199–206 2001 [Abstract](#)



199	Christophers AJ Melanoma is not caused by sunlight <i>Mutation Research</i>	422:113–7	1998	<a href="#">Abstract</a>
200	Chow KN and Dean DC Domains A and B in the Rb pocket interact to form a transcriptional repressor motif <i>Molecular and Cellular Biology</i>	16:4862–8	1996	<a href="#">Abstract</a>
201	Chowdhury S, Vaughan MM and Gore ME New approaches to the systemic treatment of melanoma <i>Cancer Treatment Reviews</i>	25:259–70	1999	<a href="#">Abstract</a>
202	Chu CY and Lim RW Involvement of p27(kip1) and cyclin D3 in the regulation of cdk2 activity during skeletal muscle differentiation <i>Biochimica et Biophysica Acta</i>	1497:175–85	2000	<a href="#">Abstract</a>
203	Chu YW, Seftor EA, Romer LH and Hendrix MJ Experimental coexpression of vimentin and keratin intermediate filaments in human melanoma cells augments motility <i>American Journal of Pathology</i>	148:63–9	1996	<a href="#">Abstract</a>
204	Ciciarello M, Mangiacasale R, Casenghi M, Zaira-Limongi M, D'Angelo M, Soddu S, Lavia P and Cundari E p53 displacement from centrosomes and p53-mediated G1 arrest following transient inhibition of the mitotic spindle <i>Journal of Biological Chemistry</i>	276:19205–13	2001	<a href="#">Abstract</a>
205	Cinti C, Leoncini L, Nyongo A, Ferrari F, Lazzi S, Bellan C, Vatti R, Zamparelli A, Cevenini G, Tosi GM, Claudio PP, Maraldi NM, Tosi P and Giordano A Genetic alterations of the retinoblastoma-related gene RB2/p130 identify different pathogenetic mechanisms in and among Burkitt's lymphoma subtypes <i>American Journal of Pathology</i>	156:751–60	2000	<a href="#">Abstract</a>
206	Citterio E, Van Den Boom V, Schnitzler G, Kanaar R, Bonte E, Kingston RE, Hoeijmakers JH, Vermeulen W, Lipkin SM, Wang V, Jacoby R, Banerjee Basu S, Baxevanis AD, Lynch HT, Elliott RM and Collins FS ATP-dependent chromatin remodeling by the Cockayne syndrome B DNA repair-transcription-coupling factor <i>Nature Genetics</i>	24:27–35	2000	<a href="#">Abstract</a>
207	Clark AB, Valle F, Drotschmann K, Gary RK and Kunkel TA Functional interaction of proliferating cell nuclear antigen with MSH2-MSH6 and MSH2-MSH3 complexes <i>Journal of Biological Chemistry</i>	275:36498–501	2000	<a href="#">Abstract</a>
208	Classon M and Dyson N p107 and p130: versatile proteins with interesting pockets <i>Experimental Cell Research</i>	264:135–47	2001	<a href="#">Abstract</a>
209	Claudio PP, Howard CM, Fu Y, Cinti C, Califano L, Micheli P, Mercer EW, Caputi M and Giordano A Mutations in the retinoblastoma-related gene RB2/p130 in primary nasopharyngeal carcinoma <i>Cancer Research</i>	60:8–12	2000	<a href="#">Abstract</a>
210	Cleaver JE, Thompson LH, Richardson AS and States JC A summary of mutations in the UV-sensitive disorders: xeroderma pigmentosum, Cockayne syndrome, and trichothiodystrophy <i>Human Mutation</i>	14:9–22	1999	<a href="#">Abstract</a>
211	Clifford SC, Prowse AH, Affara NA, Buys CH and Maher ER Inactivation of the von Hippel-Lindau (VHL) tumour suppressor gene and allelic losses at chromosome arm 3p in primary renal cell carcinoma: evidence for a VHL-independent pathway in clear cell renal tumourigenesis <i>Genes, Chromosomes and Cancer</i>	22:200–9	1998	<a href="#">Abstract</a>
212	Cobrinik D, Lee MH, Hannon G, Mulligan G, Bronson RT, Dyson N, Harlow E, Beach D, Weinberg RA and Jacks T Shared role of the pRB-related p130 and p107 proteins in limb development <i>Genes and Development</i>	10:1633–44	1996	<a href="#">Abstract</a>
213	Cockman ME, Masson N, Mole DR, Jaakkola P, Chang GW, Clifford SC, Maher ER, Pugh CW, Ratcliffe PJ and Maxwell PH Hypoxia inducible factor-alpha binding and ubiquitylation by the von Hippel-Lindau tumor suppressor protein <i>Journal of Biological Chemistry</i>	275:25733–41	2000	<a href="#">Abstract</a>
214	Cohen MH, Williams G, Johnson JR, Duan J, Gobburu J, Rahman A, Benson K, Leighton J, Kim SK, Wood R, Rothmann M, Chen G, U KM, Staten AM and Pazdur R Approval summary for imatinib mesylate capsules in the treatment of chronic myelogenous leukemia <i>Clin Cancer Research</i>	8:935–42	2002	<a href="#">Abstract</a>
215	Colella S, Nardo T, Botta E, Lehmann AR and Stefanini M Identical mutations in the CSB gene associated with either Cockayne syndrome or the DeSanctis-cacchione variant of xeroderma pigmentosum <i>Human Molecular Genetics</i>	9:1171–5	2000	<a href="#">Abstract</a>
216	†Collins Concise Dictionary (4ed) HarperCollins Publishers ISBN 0–00–472396–1	Glascow, United Kingdom	1999	
217	Colman MS, Afshari CA and Barrett JC Regulation of p53 stability and activity in response to genotoxic stress <i>Mutation Research</i>	462:179–88	2000	<a href="#">Abstract</a>
218	Conway JE, Chou D, Clatterbuck RE, Brem H, Long DM and Rigamonti D Hemangioblastomas of the central nervous system in von Hippel-Lindau syndrome and sporadic disease <i>Neurosurgery</i>	48:55–62	2001	<a href="#">Abstract</a>
219	Conzen SD, Snay CA and Cole CN Identification of a novel antiapoptotic functional domain in simian virus 40 large T antigen <i>Journal of Virology</i>	71:4536–43	1997	<a href="#">Abstract</a>
220	Cook JG, Park CH, Burke TW, Leone G, DeGregori J, Engel A and Nevins JR Analysis of Cdc6 function in the assembly of mammalian prereplication complexes <i>Proceedings of the National Academy of Sciences of the USA</i>	99:1347–52	2002	<a href="#">Abstract</a>
221	Cooke CA, Heck MM and Earnshaw WC The inner centromere protein (INCENP) antigens: movement from inner centromere to midbody during mitosis <i>Journal of Cell Biology</i>	105:2053–67	1987	<a href="#">Abstract</a>
222	Corcoran EE and Means AR Defining Ca <sup>2+</sup> /calmodulin-dependent protein kinase cascades in transcriptional regulation <i>Journal of Biological Chemistry</i>	276:2975–8	2001	<a href="#">Abstract</a>
223	Cordon-Cardo C and Richon VM Expression of the retinoblastoma protein is regulated in normal human tissues <i>American Journal of Pathology</i>	144:500–10	1994	<a href="#">Abstract</a>

## Human metastatic melanoma in vitro

- 224 Corn PG, Kuerbitz SJ, van Noesel MM, Esteller M, Compitello N, Baylin SB and Herman JG  
Transcriptional silencing of the p73 gene in acute lymphoblastic leukemia and Burkitt's lymphoma is associated with 5' CpG island methylation  
*Cancer Research* **59**:3352–6 1999 [Abstract](#)
- 225 Cory GO, MacCarthy-Morrogh L, Banin S, Gout I, Brickell PM, Levinsky RJ, Kinnon C and Lovering RC  
Evidence that the Wiskott-Aldrich syndrome protein may be involved in lymphoid cell signaling pathways  
*Journal of Immunology* **157**:3791–5 1996 [Abstract](#)
- 226 Cortez D, Wang Y, Qin J and Elledge SJ  
Requirement of ATM-dependent phosphorylation of brca1 in the DNA damage response to double-strand breaks  
*Science* **286**:1162–6 1999 [Abstract](#)
- 227 Cotelingam JD, Witebsky FG, Hsu SM, Blaese RM and Jaffe ES  
Malignant lymphoma in patients with the Wiskott-Aldrich syndrome  
*Cancer Investigation* **3**:515–22 1985 [Abstract](#)
- 228 Cowell JK, Bia B and Akoulitchev A  
A novel mutation in the promotor region in a family with a mild form of retinoblastoma indicates the location of a new regulatory domain for the RB1 gene  
*Oncogene* **12**:431–6 1996 [Abstract](#)
- 229 Couch V, Lindor NM, Karnes PS and Michels VV  
von Hippel-Lindau disease  
*Mayo Clin Proc* **75**:265–72 2000 [Abstract](#)
- 230 Crean SJ and Cunningham SJ  
Gorlin's syndrome: main features and recent advances  
*British Journal of Hospital Medicine* **56**:392–7 1996 [Abstract](#)
- 231 Crooke ST  
Potential roles of antisense technology in cancer chemotherapy  
*Oncogene* **19**:6651–9 2000 [Abstract](#)
- 232 Cross DA, Alessi DR, Cohen P, Andjelkovich M and Hemmings BA  
Inhibition of glycogen synthase kinase-3 by insulin mediated by protein kinase B  
*Nature* **378**:785–9 1995 [Abstract](#)
- 233 D'Amours D and Jackson SP  
The mre11 complex: at the crossroads of dna repair and checkpoint signalling  
*Nature Reviews: Molecular Cell Biology* **3**:317–27 2002 [Abstract](#)
- 234 Dahiya A, Gavin MR, Luo RX and Dean DC  
Role of the LXCXE binding site in Rb function  
*Molecular and Cellular Biology* **20**:6799–805 2000 [Abstract](#)
- 235 Dai CY and Enders GH  
p16 INK4a can initiate an autonomous senescence program  
*Oncogene* **19**:1613–22 2000 [Abstract](#)
- 236 Daksis JI, Lu RY, Facchini LM, Marhin WW and Penn LJ  
Myc induces cyclin D1 expression in the absence of de novo protein synthesis and links mitogen-stimulated signal transduction to the cell cycle  
*Oncogene* **9**:3635–45 1994 [Abstract](#)
- 237 Dammann R, Yang G and Pfeifer GP  
Hypermethylation of the cpG island of Ras association domain family 1A (RASSF1A), a putative tumor suppressor gene from the 3p21.3 locus, occurs in a large percentage of human breast cancers  
*Cancer Research* **61**:3105–9 2001 [Abstract](#)
- 238 Danen EH, de Vries TJ, Morandini R, Ghanem GG, Ruiters DJ and van Muijen GN  
E-cadherin expression in human melanoma  
*Melanoma Research* **6**:127–31 1996 [Abstract](#)
- 239 Dasika GK, Lin SC, Zhao S, Sung P, Tomkinson A and Lee EY  
DNA damage-induced cell cycle checkpoints and DNA strand break repair in development and tumorigenesis  
*Oncogene* **18**:7883–99 1999 [Abstract](#)
- 240 Danska JS and Guidos CJ  
Essential and perilous: V(D)J recombination and DNA damage checkpoints in lymphocyte precursors.  
*Seminars in Immunology* **9**:199–206 1997 [Abstract](#)
- 241 David-Pfeuty T  
Potent inhibitors of cyclin-dependent kinase 2 induce nuclear accumulation of wild-type p53 and nucleolar fragmentation in human untransformed and tumor-derived cells  
*Oncogene* **18**:7409–22 1999 [Abstract](#)
- 242 Davies AA, Masson JY, Mcllwraith MJ, Stasiak AZ, Stasiak A, Venkiteraman AR and West SC  
Role of BRCA2 in control of the RAD51 recombination and DNA repair protein  
*Molecular Cell* **7**:273–82 2001 [Abstract](#)
- 243 de Jager SM and Murray JA  
Retinoblastoma proteins in plants.  
*Plant Molecular Biology* **41**:295–9 1999 [Abstract](#)
- 244 de Koning JP, Soede-Bobok AA, Ward AC, Schelen AM, Antonissen C, van Leeuwen D, Lowenberg B and Touw IP  
STAT3-mediated differentiation and survival of myeloid cells in response to granulocyte colony-stimulating factor: role for the cyclin-dependent kinase inhibitor p27(Kip1)  
*Oncogene* **19**:3290–8 2000 [Abstract](#)
- 245 de Lucca EJ, Pathak S and Cheung MC  
Stability of cytogenetic alterations in a human melanoma cell line and five clonal derivatives  
*International Journal of Cancer* **41**:297–304 1988 [Abstract](#)
- 246 DePina AS and Langford GM  
Vesicle transport: the role of actin filaments and myosin motors  
*Microscopy Research and Technique* **47**:93–106 1999 [Abstract](#)
- 247 De Rosa M, Fasano C, Panariello L, Scarano MI, Belli G, Iannelli A, Ciciliano F and Izzo P  
Evidence for a recessive inheritance of Turcot's syndrome caused by compound heterozygous mutations within the PMS2 gene  
*Oncogene* **19**:1719–23 2000 [Abstract](#)
- 248 De Souza CP, Ellem KA and Gabrielli BG  
Centrosomal and cytoplasmic Cdc2/cyclin B1 activation precedes nuclear mitotic events  
*Experimental Cell Research* **257**:11–21 2000 [Abstract](#)





- 249 de Toledo SM, Azzam EI, Dahlberg WK, Gooding TB and Little JB  
ATM complexes with HDM2 and promotes its rapid phosphorylation in a p53-independent manner in normal and tumor human cells exposed to ionizing radiation  
*Oncogene* **19**:6185–6193 2000 [Abstract](#)
- 250 de Toledo SM, Azzam EI, Keng P, Laffrenier S and Little JB  
Regulation by ionizing radiation of CDC2, cyclin A, cyclin B, thymidine kinase, topoisomerase IIalpha, and RAD51 expression in normal human diploid fibroblasts is dependent on p53/p21Waf1  
*Cell Growth and Differentiation* **9**:887–96 1998 [Abstract](#)
- 251 de Winter JP, Leveille F, van Berkel CG, Roomians MA, van Der Weel L, Steltenpool J, Demuth I, Morgan NV, Alon N, Bosnoyan-Collins L, Lightfoot J, Leegwater PA, Waisfisz Q, Komatsu K, Arwert F, Pronk JC, Mathew CG, Digweed M, Buchwald M and Joenje H  
Isolation of a cDNA representing the Fanconi anemia complementation group E gene  
*American Journal of Human Genetics* **67**:1306–8 2000 [Abstract](#)
- 252 DeCaprio JA, Ludlow JW, Lynch D, Furukawa Y, Griffin J, Piwnica-Worms H, Huang CM and Livingston DM  
The product of the retinoblastoma susceptibility gene has properties of a cell cycle regulatory element  
*Cell* **58**:1085–95 1989 [Abstract](#)
- 253 DeGregori J, Kowalik T and Nevins JR  
Cellular targets for activation by the E2F1 transcription factor include DNA synthesis- and G1/S-regulatory genes [published erratum appears in *Molecular and Cellular Biology* **15**:5846–7]  
*Molecular and Cellular Biology* **15**:4215–24 1995 [Abstract](#)
- 254 de Grujil FR  
Skin cancer and solar UV radiation  
*European Journal of Cancer* **35**:2003–9 1999 [Abstract](#)
- 255 Deininger MW, Vieira SA, Parada Y, Banerji L, Lam EW, Peters G, Mahon FX, Kohler T, Goldman JM and Melo JV  
Direct relation between BCR-ABL tyrosine kinase activity and cyclin D2 expression in lymphoblasts  
*Cancer Research* **61**:8005–13 2001 [Abstract](#)
- 256 del Marmol V, Ito S, Jackson I, Vachtenheim J, Berr P, Ghanem G, Morandini R, Wakamatsu K and Huez G  
TRP-1 expression correlates with eumelanogenesis in human pigment cells in culture  
*FEBS Letters* **327**:307–10 1993 [Abstract](#)
- 257 Del Mistro A and Chieco-Bianchi L  
HPV-related neoplasias in HIV-infected individuals  
*European Journal of Cancer* **37**:1227–35 2001 [Abstract](#)
- 258 del Peso L, Hernandez-Alcoceba R, Embade N, Carnero A, Esteve P, Paje C and Lacal JC  
Rho proteins induce metastatic properties in vivo  
*Oncogene* **15**:3047–57 1997 [Abstract](#)
- 259 Dell G and Gaston K  
Human papillomaviruses and their role in cervical cancer  
*Cellular and Molecular Life Sciences* **58**:1923–42 2001 [Abstract](#)
- 260 Dell'Angelica EC, Mullins C, Caplan S and Bonifacino JS  
Lysosome-related organelles  
*FASEB Journal* **14**:1265–78 2000 [Abstract](#)
- 261 Delmer A, Ajchenbaum-Cymbalista F, Tang R, Ramond S, Faussat AM, Marie JP and Zittoun R  
Overexpression of cyclin D2 in chronic B-cell malignancies  
*Blood* **85**:2870–6 1995 [Abstract](#)
- 262 Deng C, Zhang P, Harper JW, Elledge SJ and Leder P  
Mice lacking p21CIP1/WAF1 undergo normal development, but are defective in G1 checkpoint control  
*Cell* **82**:675–84 1995 [Abstract](#)
- 263 Deng CX  
Tumorigenesis as a consequence of genetic instability in Brca1 mutant mice  
*Mutation Research* **477**:183–9 2001 [Abstract](#)
- 264 Deng CX and Brodie SG  
Roles of BRCA1 and its interacting proteins  
*Bioessays* **22**:728–37 2000 [Abstract](#)
- 265 Denny WA  
Prodrug strategies in cancer therapy  
*European Journal of Medical Chemistry* **36**:577–95 2001 [Abstract](#)
- 266 DerKinderen DJ, Koten JW, Nagelkerke NJ, Tan KE, Beemer FA and Den Otter W  
Non-ocular cancer in patients with hereditary retinoblastoma and their relatives  
*International Journal of Cancer* **41**:499–504 1988 [Abstract](#)
- 267 Desai D, Gu Y and Morgan DO  
Activation of human cyclin-dependent kinases in vitro  
*Molecular Biology of the Cell* **3**:571–82 1992 [Abstract](#)
- 268 Desdouets C, Sobczak-Thépot J, Murphy M and Brechot C  
Cyclin A: function and expression during cell proliferation.  
*Progress in Cell Cycle Research* **1**:115–23 1995 [Abstract](#)
- 269 D'hondt R, Thomas J, Van Oosterom AT and Dewolf-Peeters C  
Hodgkin's disease in a patient with Von Hippel-Lindau disease. A case report  
*Acta Clinica Belgica* **55**:276–8 2000 [Abstract](#)
- 270 DiCiommo D, Gallie BL and Bremner R  
Retinoblastoma: the disease, gene and protein provide critical leads to understand cancer  
*Seminars in Cancer Biology* **10**:255–69 2000 [Abstract](#)
- 271 Dick FA, Sailhamer E and Dyson NJ  
Mutagenesis of the pRB pocket reveals that cell cycle arrest functions are separable from binding to viral oncoproteins  
*Molecular and Cellular Biology* **20**:3715–27 2000 [Abstract](#)
- 272 Dickson MA, Hahn WC, Ino Y, Ronfard V, Wu JY, Weinberg RA, Louis DN, Li FP and Rheinwald JG  
Human keratinocytes that express hTERT and also bypass a p16(INK4a)-enforced mechanism that limits life span become immortal yet retain normal growth and differentiation characteristics  
*Molecular and Cellular Biology* **20**:1436–47 2000 [Abstract](#)
- 273 Dieffenbach CW and Dveksler GS (eds)  
PCR Primer: A laboratory manual  
Cold Spring Harbour Press, New York, USA ISBN 0–87969–447–5 1995

## Human metastatic melanoma in vitro

274	Diehl JA, Cheng M, Roussel MF and Sherr CJ Glycogen synthase kinase-3beta regulates cyclin D1 proteolysis and subcellular localization <i>Genes and Development</i>	12:3499-511	1998	<a href="#">Abstract</a>
275	Diehl JA, Zindy F and Sherr CJ Inhibition of cyclin D1 phosphorylation on threonine-286 prevents its rapid degradation via the ubiquitin-proteasome pathway <i>Genes and Development</i>	11:957-72	1997	<a href="#">Abstract</a>
276	Dietrich C, Wallenfang K, Oesch F and Wieser R Differences in the mechanisms of growth control in contact-inhibited and serum-deprived human fibroblasts <i>Oncogene</i>	15:2743-7	1997	<a href="#">Abstract</a>
277	Digweed M, Reis A and Sperling K Nijmegen breakage syndrome: consequences of defective DNA double strand break repair <i>Bioessays</i>	21:649-56	1999	<a href="#">Abstract</a>
278	Dikic I, Tokiwa G, Lev S, Courtneidge SA and Schlessinger J A role for Pyk2 and Src in linking G-protein-coupled receptors with MAP kinase activation <i>Nature</i>	383:547-50	1996	<a href="#">Abstract</a>
279	Dikstein R, Ruppert S and Tjian R TAFII250 is a bipartite protein kinase that phosphorylates the base transcription factor RAP74 <i>Cell</i>	84:781-90	1996	<a href="#">Abstract</a>
280	Donaldson SS and Smith LM Retinoblastoma: biology, presentation, and current management <i>Oncology</i>	3:45-51	1989	<a href="#">Abstract</a>
281	Donehower LA, Harvey M, Slagle BL, McArthur MJ, Montgomery CA Jr, Butel JS and Bradley A Mice deficient for p53 are developmentally normal but susceptible to spontaneous tumours <i>Nature</i>	356:215-21	1992	<a href="#">Abstract</a>
282	Dong SM, Kim KM, Kim SY, Shin MS, Na EY, Lee SH, Park WS, Yoo NJ, Jang JJ, Yoon CY, Kim JW, Kim SY, Yang YM, Kim SH, Kim CS and Lee JY Frequent somatic mutations in serine/threonine kinase 11/Peutz-Jeghers syndrome gene in left-sided colon cancer <i>Cancer Research</i>	58:3787-90	1998	<a href="#">Abstract</a>
283	Dong SM, Pang JC, Poon WS, Hu J, To KF, Chang AR and Ng HK Concurrent hypermethylation of multiple genes is associated with grade of oligodendroglial tumors <i>Journal of Neuropathology and Experimental Neurology</i>	60:808-16	2001	<a href="#">Abstract</a>
284	Dong Z, Zhong Q and Chen PL The Nijmegen breakage syndrome protein is essential for Mre11 phosphorylation upon DNA damage <i>Journal of Biological Chemistry</i>	274:19513-6	1999	<a href="#">Abstract</a>
285	Donjerkovic D and Scott DW Regulation of the G1 phase of the mammalian cell cycle <i>Cell Research</i>	10:1-16	2000	<a href="#">Abstract</a>
286	Donnellan R and Chetty R Cyclin D1 and human neoplasia <i>Molecular Pathology</i>	51:1-7	1998	<a href="#">Abstract</a>
287	Douville E and Downward J EGF induced SOS phosphorylation in PC12 cells involves P90 RSK-2 <i>Oncogene</i>	15:373-83	1997	<a href="#">Abstract</a>
288	Dowdy SF, Hinds PW, Louie K, Reed SI, Arnold A and Weinberg RA Physical interaction of the retinoblastoma protein with human D cyclins <i>Cell</i>	73:499-511	1993	<a href="#">Abstract</a>
289	Downward J The GRB2/Sem-5 adaptor protein <i>FEBS Letters</i>	338:113-7	1994	<a href="#">Abstract</a>
290	Doxsey S Re-evaluating centrosome function <i>Nature Reviews: Molecular Cell Biology</i>	2:688-98	2001	<a href="#">Abstract</a>
291	Draper GJ, Sanders BM and Kingston JE Second primary neoplasms in patients with retinoblastoma <i>British Journal of Cancer</i>	53:661-71	1986	<a href="#">Abstract</a>
292	Draper GJ, Sanders BM, Brownbill PA and Hawkins MM Patterns of risk of hereditary retinoblastoma and applications to genetic counselling <i>British Journal of Cancer</i>	66:211-9	1992	<a href="#">Abstract</a>
293	Drexler HG Review of alterations of the cyclin-dependent kinase inhibitor INK4 family genes p15, p16, p18 and p19 in human leukemia-lymphoma cells <i>Leukemia</i>	12:845-59	1998	<a href="#">Abstract</a>
294	Driscoll B, T'Ang A, Hu YH, Yan CL, Fu Y, Luo Y, Wu KJ, Wen S, Shi XH, Barsky L, Weinberg K, Murphree AL and Fung YK Discovery of a regulatory motif that controls the exposure of specific upstream cyclin-dependent kinase sites that determine both conformation and growth suppressing activity of pRb <i>Journal of Biological Chemistry</i>	274:9463-71	1999	<a href="#">Abstract</a>
295	Du K and Montminy M CREB is a regulatory target for the protein kinase Akt/PKB <i>Journal of Biological Chemistry</i>	273:32377-9	1998	<a href="#">Abstract</a>
296	Duan J, Zhang Z and Tong T Senescence delay of human diploid fibroblast induced by anti-sense p16INK4a expression <i>Journal of Biological Chemistry</i>	276:48325-31	2001	<a href="#">Abstract</a>
297	Duarte A, Caricasole A, Graham CF and Ward A Wilms' tumour-suppressor protein isoforms have opposite effects on Igf2 expression in primary embryonic cells, independently of p53 genotype <i>British Journal of Cancer</i>	77:253-9	1998	<a href="#">Abstract</a>
298	Dufner A and Thomas G Ribosomal S6 kinase signaling and the control of translation <i>Experimental Cell Research</i>	253:100-9	1999	<a href="#">Abstract</a>
299	Dumaz N and Meek DW Serine15 phosphorylation stimulates p53 transactivation but does not directly influence interaction with HDM2 <i>EMBO Journal</i>	18:7002-10	1999	<a href="#">Abstract</a>



- 300 Dunkel IJ, Gerald WL, Rosenfield NS, Strong EW, Abramson DH and Ghavimi F  
Outcome of patients with a history of bilateral retinoblastoma treated for a second malignancy: the Memorial Sloan-Kettering experience  
*Medical and Pediatric Oncology* 30:59–62 1998 [Abstract](#)
- 301 Durfee T, Becherer K, Chen PL, Yeh SH, Yang Y, Kilburn AE, Lee WH and Elledge SJ  
The retinoblastoma protein associates with the protein phosphatase type 1 catalytic subunit  
*Genes and Development* 7:555–69 1993 [Abstract](#)
- 302 Durfee T, Feiler HS and Grissem W  
Retinoblastoma-related proteins in plants: homologues or orthologues of their metazoan counterparts?  
*Plant Molecular Biology* 43:635–42 2000 [Abstract](#)
- 303 Dutil EM, Tokar A and Newton AC  
Regulation of conventional protein kinase C isozymes by phosphoinositide-dependent kinase 1 (PDK-1)  
*Current Biology* 8:1366–75 1998 [Abstract](#)
- 304 Dworkin MS, Hanson DL and Navin TR  
Survival of patients with AIDS, after diagnosis of *Pneumocystis carinii* pneumonia, in the United States  
*Journal of Infectious Diseases* 183:1409–12 2001 [Abstract](#)
- 305 Dyer MA and Cepko CL  
p57(Kip2) regulates progenitor cell proliferation and amacrine interneuron development in the mouse retina  
*Development* 127:3593–605 2000 [Abstract](#)
- 306 Dyson N, Buchkovich K, Whyte P and Harlow E  
Cellular proteins that are targeted by DNA tumor viruses for transformation  
*Princess Takamatsu Symposia* 20:191–8 1989 [Abstract](#)
- 307 Earnshaw WC and Cooke CA  
Analysis of the distribution of the INCENPs throughout mitosis reveals the existence of a pathway of structural changes in the chromosomes during metaphase and early events in cleavage furrow formation  
*Journal of Cell Science* 98 ( Pt 4):443–61 1991 [Abstract](#)
- 308 Eberle J, Weitmann S, Thieck O, Pech H, Paul M and Orfanos CE  
Downregulation of endothelin B receptor in human melanoma cell lines parallel to differentiation genes  
*Journal of Investigative Dermatology* 112:925–32 1999 [Abstract](#)
- 309 Eda M, Yonemura S, Kato T, Watanabe N, Ishizaki T, Madaule P and Narumiya S  
Rho-dependent transfer of Citron-kinase to the cleavage furrow of dividing cells  
*Journal of Cell Science* 114:3273–84 2001 [Abstract](#)
- 310 Edgar AJ and Bennett JP  
Inhibition of dendrite formation in mouse melanocytes transiently transfected with antisense DNA to myosin Va  
*Journal of Anatomy* 195 ( Pt 2):173–84 1999 [Abstract](#)
- 311 Egan SE, Giddings BW, Brooks MW, Buday L, Sizeland AM and Weinberg RA  
Association of Sos Ras exchange protein with Grb2 is implicated in tyrosine kinase signal transduction and transformation  
*Nature* 363:45–51 1993 [Abstract](#)
- 312 Eissa S, Ali Labib R and Khalifa A  
Deletion of p16 and p15 genes in schistosomiasis-associated bladder cancer (SABC)  
*Clinica Chimica Acta* 300:159–69 2000 [Abstract](#)
- 313 el-Deiry WS, Tokino T, Velculescu VE, Levy DB, Parsons R, Trent JM, Lin D, Mercer WE, Kinzler KW and Vogelstein B  
WAF1, a potential mediator of p53 tumor suppression  
*Cell* 75:817–25 1993 [Abstract](#)
- 314 Elenitoba-Johnson KS and Jaffe ES  
Lymphoproliferative disorders associated with congenital immunodeficiencies  
*Seminars in Diagnostic Pathology* 14:35–47 1997 [Abstract](#)
- 315 Elledge SJ, Richman R, Hall FL, Williams RT, Lodgson N and Harper JW  
CDK2 encodes a 33-kDa cyclin A-associated protein kinase and is expressed before CDC2 in the cell cycle  
*Proceedings of the National Academy of Sciences of the USA* 89:2907–11 1992 [Abstract](#)
- 316 Eller MS, Ostrom K and Gilchrist BA  
DNA damage enhances melanogenesis  
*Proceedings of the National Academy of Sciences of the USA* 93:1087–92 1996 [Abstract](#)
- 317 Ellis NA, Groden J, Ye TZ, Straughen J, Lennon DJ, Cioffi S, Proytcheva M and German J  
The Bloom's syndrome gene product is homologous to RecQ helicases  
*Cell* 83:655–66 1995 [Abstract](#)
- 318 Emi M, Matsushima M, Katagiri T, Yoshimoto M, Kasumi F, Yokota T, Nakata T, Miki Y and Nakamura Y  
Multiplex mutation screening of the BRCA1 gene in 1000 Japanese breast cancers  
*Japanese Journal of Cancer Research* 89:12–6 1998 [Abstract](#)
- 319 Eng C  
Genetics of Cowden syndrome: through the looking glass of oncology  
*International Journal of Oncology* 12:701–10 1998 [Abstract](#)
- 320 Eng C, Li FP, Abramson DH, Ellsworth RM, Wong FL, Goldman MB, Seddon J, Tarbell N and Boice JD Jr  
Mortality from second tumors among long-term survivors of retinoblastoma  
*Journal of the National Cancer Institute* 85:1121–8 1993 [Abstract](#)
- 321 Engel ME, Datta PK and Moses HL  
Signal transduction by transforming growth factor-beta: a cooperative paradigm with extensive negative regulation  
*Journal of Cellular Biochemistry. Supplement* 30–31:111–22 1998 [Abstract](#)
- 322 England NL, Cuthbert AP, Trott DA, Jezzard S, Nobori T, Carson DA and Newbold RF  
Identification of human tumour suppressor genes by monochromosome transfer: rapid growth-arrest response mapped to 9p21 is mediated solely by the cyclin-D-dependent kinase inhibitor gene, CDKN2A (p16INK4A)  
*Carcinogenesis* 17:1567–75 1996 [Abstract](#)
- 323 Englert C, Maheswaran S, Garvin AJ, Kreidberg J and Haber DA  
Induction of p21 by the Wilms' tumor suppressor gene WT1  
*Cancer Research* 57:1429–34 1997 [Abstract](#)
- 324 Escarceller M, Buchwald M, Singleton BK, Jeggo PA, Jackson SP, Moustacchi E and Papadopoulou D  
Fanconi anemia C gene product plays a role in the fidelity of blunt DNA end-joining  
*Journal of Molecular Biology* 279:375–85 1998 [Abstract](#)

## Human metastatic melanoma in vitro

- 325 Esteller M, Sparks A, Toyota M, Sanchez-Cespedes M, Capella G, Peinado MA, Gonzalez S, Tarafa G, Sidransky D, Meltzer SJ, Baylin SB and Herman JG  
Analysis of adenomatous polyposis coli promoter hypermethylation in human cancer  
*Cancer Research* **60**:4366–71 2000 [Abstract](#)
- 326 Esteller M, Tortola S, Toyota M, Capella G, Peinado MA, Baylin SB and Herman JG  
Hypermethylation-associated inactivation of p14(ARF) is independent of p16(INK4a) methylation and p53 mutational status  
*Cancer Research* **60**:129–33 2000 [Abstract](#)
- 327 Evans DG, Sainio M and Baser ME  
Neurofibromatosis type 2  
*Journal of Medical Genetics* **37**:897–904 2000 [Abstract](#)
- 328 Evans SC and Lozano G  
The Li-Fraumeni syndrome: an inherited susceptibility to cancer  
*Molecular Medicine Today* **3**:390–5 1997 [Abstract](#)
- 329 Evers EE, Zondag GC, Malliri A, Price LS, ten Klooster JP, van der Kammen RA and Collard JG  
Rho family proteins in cell adhesion and cell migration  
*European Journal of Cancer* **36**:1269–74 2000 [Abstract](#)
- 330 Evron E, Umbricht CB, Korz D, Raman V, Loeb DM, Niranjana B, Buluwela L, Weitzman SA, Marks J and Sukumar S  
Loss of cyclin D2 expression in the majority of breast cancers is associated with promoter hypermethylation  
*Cancer Research* **61**:2782–7 2001 [Abstract](#)
- 331 Ewen ME  
The cell cycle and the retinoblastoma protein family  
*Cancer and Metastasis Reviews* **13**:45–66 1994 [Abstract](#)
- 332 Ewen ME, Sluss HK, Sherr CJ, Matsushime H, Kato J and Livingston DM  
Functional interactions of the retinoblastoma protein with mammalian D-type cyclins  
*Cell* **73**:487–97 1993 [Abstract](#)
- 333 Eymin B, Gazzeri S, Brambilla C and Brambilla E  
Distinct pattern of E2F1 expression in human lung tumours: E2F1 is upregulated in small cell lung carcinoma  
*Oncogene* **20**:1678–87 2001 [Abstract](#)
- 334 Eymin B, Karayan L, Seite P, Brambilla C, Brambilla E, Larsen CJ and Gazzeri S  
Human ARF binds E2F1 and inhibits its transcriptional activity  
*Oncogene* **20**:1033–41 2001 [Abstract](#)
- 335 Eymin B, Sordet O, Droin N, Munsch B, Haug M, Van de Craen M, Vandenaabeele P and Solary E  
Caspase-induced proteolysis of the cyclin-dependent kinase inhibitor p27Kip1 mediates its anti-apoptotic activity  
*Oncogene* **18**:4839–47 1999 [Abstract](#)
- 336 Ezhevsky SA, Ho A, Becker-Hapak M, Davis PK and Dowdy SF  
Differential regulation of retinoblastoma tumor suppressor protein by G(1) cyclin-dependent kinase complexes in vivo  
*Molecular and Cellular Biology* **21**:4773–84 2001 [Abstract](#)
- 337 Fabunmi RP, Wigley WC, Thomas PJ and DeMartino GN  
Activity and regulation of the centrosome-associated proteasome  
*Journal of Biological Chemistry* **275**:409–13 2000 [Abstract](#)
- 338 Faigle W, Raposo G, Tenza D, Pinet V, Vogt AB, Kropshofer H, Fischer A, de Saint Basile G and Amigorena S  
Deficient peptide loading and MHC class II endosomal sorting in a human genetic immunodeficiency disease: the Chediak-Higashi syndrome  
*Journal of Cell Biology* **141**:1121–34 1998 [Abstract](#)
- 339 Falck J, Mailand N, Syljuasen RG, Bartek J and Lukas J  
The ATM-Chk2-Cdc25A checkpoint pathway guards against radioresistant DNA synthesis  
*Nature* **410**:842–7 2001 [Abstract](#)
- 340 Fan S, Yuan R, Ma YX, Xiong J, Meng Q, Erdos M, Zhao JN, Goldberg ID, Pestell RG and Rosen EM  
Disruption of BRCA1 LXCXE motif alters BRCA1 functional activity and regulation of RB family but not RB protein binding  
*Oncogene* **20**:4827–41 2001 [Abstract](#)
- 341 Fanciulli M, Bruno T, Di Padova M, De Angelis R, Iezzi S, Iacobini C, Floridi A and Passananti C  
Identification of a novel partner of RNA polymerase II subunit 11, Che-1, which interacts with and affects the growth suppression function of Rb  
*FASEB Journal* **14**:904–12 2000 [Abstract](#)
- 342 Fang X, Yu S, Eder A, Mao M, Bast RC Jr, Boyd D and Mills GB  
Regulation of BAD phosphorylation at serine 112 by the Ras-mitogen-activated protein kinase pathway  
*Oncogene* **18**:6635–40 1999 [Abstract](#)
- 343 Fargnoli MC, Chimenti S, Keller G, Soyer HP, Dal Pozzo V, Hofler H and Peris K  
CDKN2a/p16INK4a mutations and lack of p19ARF involvement in familial melanoma kindreds  
*Journal of Investigative Dermatology* **111**:1202–6 1998 [Abstract](#)
- 344 Fattaey AR, Helin K, Dembski MS, Dyson N, Harlow E, Vuocolo GA, Hanobik MG, Haskell KM, Oliff A, Defeo-Jones D et al  
Characterization of the retinoblastoma binding proteins RBP1 and RBP2  
*Oncogene* **8**:3149–56 1993 [Abstract](#)
- 345 Fattman CL, Delach SM, Dou QP and Johnson DE  
Sequential two-step cleavage of the retinoblastoma protein by caspase-3/-7 during etoposide-induced apoptosis  
*Oncogene* **20**:2918–26 2001 [Abstract](#)
- 346 Fearon ER  
Human cancer syndromes: clues to the origin and nature of cancer  
*Science* **278**:1043–50 1997 [Abstract](#)
- 347 Feigal EG  
AIDS-associated malignancies: research perspectives  
*Biochimica et Biophysica Acta* **1423**:C1–9 1999 [Abstract](#)
- 348 Ferguson AT, Evron E, Umbricht CB, Pandita TK, Chan TA, Hermeking H, Marks JR, Lambers AR, Futreal PA, Stampfer MR and Sukumar S  
High frequency of hypermethylation at the 14–3–3 sigma locus leads to gene silencing in breast cancer  
*Proceedings of the National Academy of Sciences of the USA* **97**:6049–54 2000 [Abstract](#)
- 349 Fero ML, Rivkin M, Tasch M, Porter P, Carow CE, Firpo E, Polyak K, Tsai LH, Broudy V, Perlmutter RM, Kaushansky K and Roberts JM  
A syndrome of multiorgan hyperplasia with features of gigantism, tumorigenesis, and female sterility in p27(Kip1)-deficient mice  
*Cell* **85**:733–744 1996 [Abstract](#)



- 350 Ferreira R, Naguibneva I, Mathieu M, Ait Si Ali S, Robin P, Pritchard LL and Harel-Bellan A  
Cell cycle-dependent recruitment of HDAC-1 correlates with deacetylation of histone H4 on an Rb-E2F target promoter  
*EMBO Reports* 2:794–9 2001 [Abstract](#)
- 351 Ficari F, Cama A, Valanzano R, Curia MC, Palmirotta R, Aceto G, Esposito DL, Crognale S, Lombardi A, Messerini L, Mariani-Costantini R, Tonelli F and Battista P  
APC gene mutations and colorectal adenomatosis in familial adenomatous polyposis  
*British Journal of Cancer* 82:348–53 2000 [Abstract](#)
- 352 Fields S and Song O  
A novel genetic system to detect protein-protein interactions  
*Nature* 340:245–6 1989 [Abstract](#)
- 353 Filmus J, Robles AI, Shi W, Wong MJ, Colombo LL and Conti CJ  
Induction of cyclin D1 overexpression by activated ras  
*Oncogene* 9:3627–33 1994 [Abstract](#)
- 354 Fisk HA and Winey M  
The mouse Mps1p-like kinase regulates centrosome duplication  
*Cell* 106:95–104 2001 [Abstract](#)
- 355 FitzGerald MG, Harkin DP, Silva-Arrieta S, MacDonald DJ, Lucchina LC, Unsal H, O'Neill E, Koh J, Finkelstein DM, Isselbacher KJ, Sober AJ and Haber DA  
Prevalence of germ-line mutations in p16, p19ARF, and CDK4 in familial melanoma: analysis of a clinic-based population  
*Proceedings of the National Academy of Sciences of the USA* 93:8541–5 1996 [Abstract](#)
- 356 Flejter WL, McDaniel LD, Johns D, Friedberg EC and Schultz RA  
Correction of xeroderma pigmentosum complementation group D mutant cell phenotypes by chromosome and gene transfer: involvement of the human ERCC2 DNA repair gene  
*Proceedings of the National Academy of Sciences of the USA* 89:261–5 1992 [Abstract](#)
- 357 Flemington EK, Speck SH and Kaelin WG Jr  
E2F-1-mediated transactivation is inhibited by complex formation with the retinoblastoma susceptibility gene product  
*Proceedings of the National Academy of Sciences of the USA* 90:6914–8 1993 [Abstract](#)
- 358 Florenes VA, Bhattacharya N, Bani MR, Ben-David Y, Kerbel RS and Slingerland JM  
TGF-beta mediated G1 arrest in a human melanoma cell line lacking p15INK4B: evidence for cooperation between p21Cip1/WAF1 and p27Kip1  
*Oncogene* 13:2447–57 1996 [Abstract](#)
- 359 Florenes VA, Maeldandsmo GM, Kerbel RS, Slingerland JM, Nesland JM and Holm R  
Protein expression of the cell-cycle inhibitor p27Kip1 in malignant melanoma: inverse correlation with disease-free survival  
*American Journal of Pathology* 153:305–12 1998 [Abstract](#)
- 360 Flores ER, Allen-Hoffmann BL, Lee D and Lambert PF  
The human papillomavirus type 16 E7 oncogene is required for the productive stage of the viral life cycle  
*Journal of Virology* 74:6622–31 2000 [Abstract](#)
- 361 Flores JF, Walker GJ, Glendening JM, Haluska FG, Castresana JS, Rubio MP, Pastoride GC, Boyer LA, Kao WH, Bulyk mL, Barnhill RL, Hayward NK, Housman DE and Fountain JW  
Loss of the p16INK4a and p15INK4b genes, as well as neighboring 9p21 markers, in sporadic melanoma  
*Cancer Research* 56:5023–32 1996 [Abstract](#)
- 362 Flores-Rozas H, Clark D and Kolodner RD  
Proliferating cell nuclear antigen and Msh2p-Msh6p interact to form an active mismatch recognition complex  
*Nature Genetics* 26:375–8 2000 [Abstract](#)
- 363 Florio M, Hernandez MC, Yang H, Shu HK, Cleveland JL and Israel MA  
Id2 promotes apoptosis by a novel mechanism independent of dimerization to basic helix-loop-helix factors  
*Molecular and Cellular Biology* 18:5435–44 1998 [Abstract](#)
- 364 Fodde R, Kuipers J, Rosenberg C, Smits R, Kielman M, Gaspar C, van Es JH, Breukel C, Wiegant J, Giles RH and Clevers H  
Mutations in the APC tumour suppressor gene cause chromosomal instability  
*Nature Cell Biology* 3:433–8 2001 [Abstract](#)
- 365 Ford D, Easton DF and Peto J  
Estimates of the gene frequency of BRCA1 and its contribution to breast and ovarian cancer incidence  
*American Journal of Human Genetics* 57:1457–62 1995 [Abstract](#)
- 366 Ford JC, al-Khodairy F, Fotou E, Sheldrick KS, Griffiths DJ and Carr AM  
14–3-3 protein homologs required for the DNA damage checkpoint in fission yeast  
*Science* 265:533–5 1994 [Abstract](#)
- 367 Forng RY and Atreya CD  
Mutations in the retinoblastoma protein-binding LXCXE motif of rubella virus putative replicase affect virus replication  
*Journal of General Virology* 80:327–32 1999 [Abstract](#)
- 368 Foulkes WD, Flanders TY, Pollock PM and Hayward NK  
The CDKN2A (p16) gene and human cancer  
*Molecular Medicine* 3:5–20 1997 [Abstract](#)
- 369 Fountain JW, Bale SJ, Housman DE and Dracopoli NC  
Genetics of melanoma  
*Cancer Surveys* 9:645–71 1990 [Abstract](#)
- 370 Franceschi S, Dal Maso L, Amiani S, Crosignani P, VerCELLI M, Simonato L, Falcini F, Zanetti R, Barchielli A, Serraino D and Rezza G  
Risk of cancer other than Kaposi's sarcoma and non-Hodgkin's lymphoma in persons with AIDS in Italy. Cancer and AIDS Registry Linkage Study  
*British Journal of Cancer* 78:966–70 1998 [Abstract](#)
- 371 Franchitto A and Pichierri P  
Bloom's syndrome protein is required for correct relocalization of RAD50/MRE11/NBS1 complex after replication fork arrest  
*Journal of Cell Biology* 157:19–30 2002 [Abstract](#)
- 372 Franklin DS, Godfrey VL, Lee H, Kovalev GI, Schoonhoven R, Chen-Kiang S, Su L and Xiong Y  
CDK inhibitors p18(INK4c) and p27(Kip1) mediate two separate pathways to collaboratively suppress pituitary tumorigenesis  
*Genes and Development* 12:2899–911 1998 [Abstract](#)
- 373 Freed E, Lacey KR, Huie P, Lyapina SA, Deshaies RJ, Stearns T and Jackson PK  
Components of an SCF ubiquitin ligase localize to the centrosome and regulate the centrosome duplication cycle  
*Genes and Development* 13:2242–57 1999 [Abstract](#)
- 374 Friedmann PS, Wren F, Buffey J and Macneil S  
Alpha-MSH causes a small rise in cAMP but has no effect on basal or ultraviolet-stimulated melanogenesis in human melanocytes  
*British Journal of Dermatology* 123:145–51 1990 [Abstract](#)

## Human metastatic melanoma in vitro

375	Friedrich CA Von Hippel-Lindau syndrome. A pleomorphic condition <i>Cancer</i>	<b>86:2478–82</b>	1999	<a href="#">Abstract</a>
376	Friend SH, Bernards R, Rogelj S, Weinberg RA, Rapaport JM, Albert DM and Dryja TP A human DNA segment with properties of the gene that predisposes to retinoblastoma and osteosarcoma <i>Nature</i>	<b>323:643–6</b>	1986	<a href="#">Abstract</a>
377	Frisch SM and Screaton RA Anoikis mechanisms <i>Current Opinion in Cell Biology</i>	<b>13:555–62</b>	2001	<a href="#">Abstract</a>
378	Fritz G, Just I and Kaina B Rho GTPases are over-expressed in human tumors <i>International Journal of Cancer</i>	<b>81:682–7</b>	1999	<a href="#">Abstract</a>
379	Fry AM, Mayor T, Meraldi P, Stierhof YD, Tanaka K and Nigg EA C-Nap1, a novel centrosomal coiled-coil protein and candidate substrate of the cell cycle-regulated protein kinase Nek2 <i>Journal of Cell Biology</i>	<b>141:1563–74</b>	1998	<a href="#">Abstract</a>
380	Fry AM, Meraldi P and Nigg EA A centrosomal function for the human Nek2 protein kinase, a member of the NIMA family of cell cycle regulators <i>EMBO Journal</i>	<b>17:470–81</b>	1998	<a href="#">Abstract</a>
381	Fu YH, Nishinaka T, Yokoyama K and Chiu R A retinoblastoma susceptibility gene product, RB, targeting protease is regulated through the cell cycle <i>FEBS Letters</i>	<b>421:89–93</b>	1998	<a href="#">Abstract</a>
382	Fujimori A, Hoki Y, Popescu NC and Pommier Y Silencing and selective methylation of the normal topoisomerase I gene in camptothecin-resistant CEM/C2 human leukemia cells <i>Oncology Research</i>	<b>8:295–301</b>	1996	<a href="#">Abstract</a>
383	Fujita N, Sato S, Ishida A and Tsuruo T Involvement of Hsp90 in signaling and stability of 3-phosphoinositide-dependent kinase-1 <i>Journal of Biological Chemistry</i>	<b>277:10346–53</b>	2002	<a href="#">Abstract</a>
384	Fujita T, Ohtani-Fujita N and Sakai T Identification of an RB-responsive region in the 5' untranslated region of the RB gene <i>Cancer Letters</i>	<b>101:149–57</b>	1996	<a href="#">Abstract</a>
385	Fuller BB and Meyskens FL Jr Endocrine responsiveness in human melanocytes and melanoma cells in culture <i>Journal of the National Cancer Institute</i>	<b>66:799–802</b>	1981	<a href="#">Abstract</a>
386	Fukami-Kobayashi J and Mitsui Y Cyclin D1 inhibits cell proliferation through binding to PCNA and cdk2 <i>Experimental Cell Research</i>	<b>246:338–47</b>	1999	<a href="#">Abstract</a>
387	Fukasawa K, Choi T, Kuriyama R, Rulong S and Vande Woude GF Abnormal centrosome amplification in the absence of p53 <i>Science</i>	<b>271:1744–7</b>	1996	<a href="#">Abstract</a>
388	Fukasawa K, Wiener F, Vande-Woude GF and Mai S Genomic instability and apoptosis are frequent in p53 deficient young mice <i>Oncogene</i>	<b>15:1295–302</b>	1997	<a href="#">Abstract</a>
389	Funasaka Y, Chakraborty AK, Hayashi Y, Komoto M, Ohashi A, Nagahama M, Inoue Y, Pawelek J and Ichihashi M Modulation of melanocyte-stimulating hormone receptor expression on normal human melanocytes: evidence for a regulatory role of ultraviolet B, interleukin-1alpha, interleukin-1beta, endothelin-1 and tumour necrosis factor-alpha <i>British Journal of Dermatology</i>	<b>139:216–24</b>	1998	<a href="#">Abstract</a>
390	Fung YK, Murphree AL, T'Ang A, Qian J, Hinrichs SH and Benedict WF Structural evidence for the authenticity of the human retinoblastoma gene <i>Science</i>	<b>236:1657–61</b>	1987	<a href="#">Abstract</a>
391	Funk JO, Schiller PI, Barrett MT, Wong DJ, Kind P and Sander CA p16INK4a expression is frequently decreased and associated with 9p21 loss of heterozygosity in sporadic melanoma <i>Journal of Cutaneous Pathology</i>	<b>25:291–6</b>	1998	<a href="#">Abstract</a>
392	Furnari B, Blasina A, Boddy MN, McGowan CH and Russell P Cdc25 inhibited in vivo and in vitro by checkpoint kinases Cds1 and Chk1 <i>Molecular Biology of the Cell</i>	<b>10:833–45</b>	1999	<a href="#">Abstract</a>
393	Furukawa Y, DeCaprio JA, Freedman A, Kanakura Y, Nakamura M, Ernst TJ, Livingston DM and Griffin JD Expression and state of phosphorylation of the retinoblastoma susceptibility gene product in cycling and noncycling human hematopoietic cells <i>Proceedings of the National Academy of Sciences of the USA</i>	<b>87:2770–4</b>	1990	<a href="#">Abstract</a>
394	Furumura M, Poterf SB, Toyofuku K, Matsunaga J, Muller J and Hearing VJ Involvement of ITF2 in the transcriptional regulation of melanogenic genes <i>Journal of Biological Chemistry</i>	<b>276:28147–54</b>	2001	<a href="#">Abstract</a>
395	Furumura M, Sakai C, Poterf SB, Vieira WD, Barsh GS and Hearing VJ Characterization of genes modulated during pheomelanogenesis using differential display <i>Proceedings of the National Academy of Sciences of the USA</i>	<b>95:7374–8</b>	1998	<a href="#">Abstract</a>
396	Fusco C, Raymond A and Zervos AS Molecular cloning and characterization of a novel retinoblastoma-binding protein <i>Genomics</i>	<b>51:351–8</b>	1998	<a href="#">Abstract</a>
397	Futaki M, Watanabe S, Kajigaya S and Liu JM Fanconi anemia protein, FANCG, is a phosphoprotein and is upregulated with FANCA after TNF-alpha treatment <i>Biochemical and Biophysical Research Communications</i>	<b>281:347–51</b>	2001	<a href="#">Abstract</a>
398	Fuxe J, Raschperger E and Pettersson RF Translation of p15.INK4B, an N-terminally extended and fully active form of p15INK4B, is initiated from an upstream GUG codon <i>Oncogene</i>	<b>19:1724–8</b>	2000	<a href="#">Abstract</a>
399	Gaillard PH and Wood RD Activity of individual ERCC1 and XPF subunits in DNA nucleotide excision repair <i>Nucleic Acids Research</i>	<b>29:872–879</b>	2001	<a href="#">Abstract</a>
400	Ganoth D, Bornstein G, Ko TK, Larsen B, Tyers M, Pagano M and Hershko A The cell-cycle regulatory protein Cks1 is required for SCF(Skp2)-mediated ubiquitinylation of p27 <i>Nature Cell Biology</i>	<b>3:321–4</b>	2001	<a href="#">Abstract</a>



- 401 Garcia-Higuera I, Taniguchi T, Ganesan S, Meyn MS, Timmers C, Hejna J, Grompe M and D'Andrea AD  
Interaction of the Fanconi anemia proteins and BRCA1 in a common pathway  
*Molecular Cell* 7:249–62 2001 [Abstract](#)
- 402 Gardner LB, Li Q, Park MS, Flanagan WM, Semenza GL and Dang CV  
Hypoxia inhibits G1/S transition through regulation of p27 expression  
*Journal of Biological Chemistry* 276:7919–26 2001 [Abstract](#)
- 403 Gatei M, Scott SP, Filippovitch I, Soronika N, Lavin MF, Weber B and Khanna KK  
Role for ATM in DNA damage-induced phosphorylation of BRCA1  
*Cancer Research* 60:3299–304 2000 [Abstract](#)
- 404 Gatei M, Zhou BB, Hobson K, Scott S, Young D and Khanna KK  
Ataxia telangiectasia mutated (ATM) kinase and ATM and Rad3 related kinase mediate phosphorylation of Brca1 at distinct and overlapping sites. In vivo assessment using phospho-specific antibodies  
*Journal of Biological Chemistry* 276:17276–80 2001 [Abstract](#)
- 405 Gaubatz S, Lindeman GJ, Ishida S, Jakoi L, Nevins JR, Livingston DM and Rempel RE  
E2F4 and E2F5 play an essential role in pocket protein-mediated G1 control  
*Molecular Cell* 6:729–35 2000 [Abstract](#)
- 406 Gawronska-Szklarz B, Lubinski J, Kladny J, Kurzawski G, Bielicki D, Wojcicki M, Sych Z and Musial HD  
Polymorphism of GSTM1 gene in patients with colorectal cancer and colonic polyps  
*Experimental and Toxicologic Pathology* 51:321–5 1999 [Abstract](#)
- 407 Gene Map <http://www.ncbi.nlm.nih.gov/genemap/>
- 408 Généthon [http://www.genethon.fr/genethon\\_en.html](http://www.genethon.fr/genethon_en.html)
- 409 Geng Y, Eaton EN, Picon M, Roberts JM, Lundberg AS, Gifford A, Sardet C and Weinberg RA  
Regulation of cyclin E transcription by E2Fs and retinoblastoma protein  
*Oncogene* 12:1173–80 1996 [Abstract](#)
- 410 Geng Y, Yu Q, Whoriskey W, Dick F, Tsai KY, Ford HL, Biswas DK, Pardee AB, Amati B, Jacks T, Richardson A, Dyson N and Sicinski P  
Expression of cyclins E1 and E2 during mouse development and in neoplasia  
*Proceedings of the National Academy of Sciences of the USA* 98:13138–43 2001 [Abstract](#)
- 411 Georgieva J, Sinha P and Schadendorf D J  
Expression of cyclins and cyclin dependent kinases in human benign and malignant melanocytic lesions  
*Clinical Pathology* 54:229–35 2001 [Abstract](#)
- 412 Germain D, Russell A, Thompson A and Hendley J  
Ubiquitination of free cyclin D1 is independent of phosphorylation on threonine 286  
*Journal of Biological Chemistry* 275:12074–9 2000 [Abstract](#)
- 413 German J  
Bloom's syndrome  
*Dermatologic Clinics* 13:7–18 1995 [Abstract](#)
- 414 Ghadimi BM, Sackett DL, Difilippantonio MJ, Schrock E, Neumann T, Jauho A, Auer G and Ried T  
Centrosome amplification and instability occurs exclusively in aneuploid, but not in diploid colorectal cancer cell lines, and correlates with numerical chromosomal aberrations  
*Genes, Chromosomes and Cancer* 27:183–90 2000 [Abstract](#)
- 415 Giardiello FM, Petersen GM, Brensinger JD, Luce MC, Cayouette MC, Bacon J, Booker SV and Hamilton SR  
Hepatoblastoma and APC gene mutation in familial adenomatous polyposis  
*Gut* 39:867–9 1996 [Abstract](#)
- 416 Gill RM, Hamel PA, Zhe J, Zacksenhaus E, Gallie BL and Phillips RA  
Characterization of the human RB1 promoter and of elements involved in transcriptional regulation  
*Cell Growth and Differentiation* 5:467–74 1994 [Abstract](#)
- 417 Gille H and Downward J  
Multiple ras effector pathways contribute to G(1) cell cycle progression  
*Journal of Biological Chemistry* 274:22033–40 1999 [Abstract](#)
- 418 Glendening JM, Flores JF, Walker GJ, Stone S, Albino AP and Fountain JW  
Homozygous loss of the p15INK4B gene (and not the p16INK4 gene) during tumor progression in a sporadic melanoma patient  
*Cancer Research* 55:5531–5 1995 [Abstract](#)
- 419 Goding CR  
Mitf from neural crest to melanoma: signal transduction and transcription in the melanocyte lineage  
*Genes and Development* 14:1712–28 2000
- 420 Goldberg Z, Vogt Sionov R, Berger M, Zwang Y, Perets R, Van Etten RA, Oren M, Taya Y and Haupt Y  
Tyrosine phosphorylation of Mdm2 by c-Abl: implications for p53 regulation  
*EMBO Journal* 21:3715–27 2002 [Abstract](#)
- 421 Goldstein AM, Chidambaram A, Halpern A, Holly EA, Guerry IV D, Sagebiel R, Elder DE and Tucker MA  
Rarity of CDK4 germline mutations in familial melanoma  
*Melanoma Research* 12:51–5 2002 [Abstract](#)
- 422 Goldstein AM, Struewing JP, Chidambaram A, Fraser MC and Tucker MA  
Genotype-phenotype relationships in U.S. melanoma-prone families with CDKN2A and CDK4 mutations  
*Journal of the National Cancer Institute* 92:1006–10 2000 [Abstract](#)
- 423 Gomez PF, Luo D, Hirosaki K, Shinoda K, Yamashita T, Suzuki J, Otsu K, Ishikawa K and Jimbow K  
Identification of rab7 as a melanosome-associated protein involved in the intracellular transport of tyrosinase-related protein 1  
*Journal of Investigative Dermatology* 117:81–90 2001 [Abstract](#)
- 424 Gonczy P, Pichler S, Kirkham M and Hyman AA  
Cytoplasmic dynein is required for distinct aspects of MTOC positioning, including centrosome separation, in the one cell stage *Caenorhabditis elegans* embryo  
*Journal of Cell Biology* 147:135–50 1999 [Abstract](#)
- 425 Gonzalez SL, Stremiau M, He X, Basile JR and Munger K  
Degradation of the retinoblastoma tumor suppressor by the human papillomavirus type 16 E7 oncoprotein is important for functional inactivation and is separable from proteasomal degradation of E7  
*Journal of Virology* 75:7583–91 2001 [Abstract](#)
- 426 Goodrich DW, Wang NP, Qian YW, Lee EY and Lee WH  
The retinoblastoma gene product regulates progression through the G1 phase of the cell cycle  
*Cell* 67:293–302 1991 [Abstract](#)

## Human metastatic melanoma in vitro

- 427 Goodwin EC and DiMaio D  
Repression of human papillomavirus oncogenes in HeLa cervical carcinoma cells causes the orderly reactivation of dormant tumor suppressor pathways  
*Proceedings of the National Academy of Sciences of the USA* **97**:12513–8 2000 [Abstract](#)
- 428 Gorgoulis VG, Koutroumbi EN, Kotsinas A, Zacharatos P, Markopoulos C, Giannikos L, Kyriakou V, Voulgaris Z, Gogas I and Kittas C  
Alterations of p16-pRb pathway and chromosome locus 9p21–22 in sporadic invasive breast carcinomas  
*Molecular Medicine* **4**:807–22 1998 [Abstract](#)
- 429 Gorgoulis VG, Zacharatos P, Kotsinas A, Mariatos G, Liloglou T, Vogiatzi T, Foukas P, Rassidakis G, Garinis G, Ioannides T, Zoumpourlis V, Bramis J, Michail PO, Asimacopoulos PJ, Field JK and Kittas C  
Altered expression of the cell cycle regulatory molecules pRb, p53 and MDM2 exert a synergetic effect on tumor growth and chromosomal instability in non-small cell lung carcinomas (NSCLCs)  
*Molecular Medicine* **6**:208–37 2000 [Abstract](#)
- 430 Goss KH and Groden J  
Biology of the adenomatous polyposis coli tumor suppressor  
*Journal of Clinical Oncology* **18**:1967–79 2000 [Abstract](#)
- 431 Gottlieb TM and Oren M  
p53 and apoptosis  
*Seminars in Cancer Biology* **8**:359–68 1998 [Abstract](#)
- 432 Gradia S, Acharya S and Fishel R  
The human mismatch recognition complex hMSH2-hMSH6 functions as a novel molecular switch  
*Cell* **91**:995–1005 1997 [Abstract](#)
- 433 Gradia S, Subramanian D, Wilson T, Acharya S, Makhov A, Griffith J and Fishel R  
hMSH2-hMSH6 forms a hydrolysis-independent sliding clamp on mismatched DNA  
*Molecular Cell* **3**:255–61 1999 [Abstract](#)
- 434 Graham A, Wakamatsu K, Hunt G, Ito S and Thody AJ  
Agouti protein inhibits the production of eumelanin and pheomelanin in the presence and absence of alpha-melanocyte stimulating hormone  
*Pigment Cell Research* **10**:298–303 1997 [Abstract](#)
- 435 Gray RJ, Pockaj BA and Kirkwood JM  
An update on adjuvant interferon for melanoma  
*Cancer Control* **9**:16–21 2002 [Abstract](#)
- 436 Grana X, Garriga J and Mayol X  
Role of the retinoblastoma protein family, pRb, p107 and p130 in the negative control of cell growth  
*Oncogene* **17**:3365–83 1998 [Abstract](#)
- 437 Granholm DE, Reese RN and Granholm NH  
Agouti alleles influence thiol concentrations in hair follicles and extrafollicular tissues of mice (Ay/a, AwJ/AwJ, a/a)  
*Pigment Cell Research* **8**:302–6 1995 [Abstract](#)
- 438 Greger V, Debus N, Lohmann D, Hopping W, Passarge E and Horsthemke B  
Frequency and parental origin of hypermethylated RB1 alleles in retinoblastoma  
*Human Genetics* **94**:491–6 1994 [Abstract](#)
- 439 Grenon M, Gilbert C and Lowndes NF  
Checkpoint activation in response to double-strand breaks requires the Mre11/Rad50/Xrs2 complex  
*Nature Cell Biology* **3**:844–7 2001 [Abstract](#)
- 440 Griffin CS, Simpson PJ, Wilson CR and Thacker J  
Mammalian recombination-repair genes XRCC2 and XRCC3 promote correct chromosome segregation  
*Nature Cell Biology* **2**:757–61 2000 [Abstract](#)
- 441 Grimes CA and Jope RS  
CREB DNA binding activity is inhibited by glycogen synthase kinase-3 beta and facilitated by lithium  
*Journal of Neurochemistry* **78**:1219–32 2001 [Abstract](#)
- 442 Gruis NA, van der Velden PA, Sandkuijl LA, Prins DE, Weaver-Feldhaus J, Kamb A, Bergman W and Frants RR  
Homozygotes for CDKN2 (p16) germline mutation in Dutch familial melanoma kindreds  
*Nature Genetics* **10**:351–3 1995 [Abstract](#)
- 443 Gstaiger M, Marti A and Krek W  
Association of human SCF(SKP2) subunit p19(SKP1) with interphase centrosomes and mitotic spindle poles  
*Experimental Cell Research* **247**:554–62 1999 [Abstract](#)
- 444 Gu Y, Rosenblatt J and Morgan DO  
Cell cycle regulation of CDK2 activity by phosphorylation of Thr160 and Tyr15  
*EMBO Journal* **11**:3995–4005 1992 [Abstract](#)
- 445 Guan KL, Jenkins CW, Li Y, Nichols MA, Wu X, O'Keefe CL, Matera AG and Xiong Y  
Growth suppression by p18, a p16INK4/MTS1- and p14INK4B/MTS2-related CDK6 inhibitor, correlates with wild-type pRb function  
*Genes and Development* **8**:2939–52 1994 [Abstract](#)
- 446 Guan LS, Rauchman M and Wang ZY  
Induction of Rb-associated protein (RbAp46) by Wilms' tumor suppressor WT1 mediates growth inhibition  
*Journal of Biological Chemistry* **273**:27047–50 1998 [Abstract](#)
- 447 Gudermann T  
Multiple pathways of ERK activation by G protein-coupled receptors  
*Novartis Foundation Symposium* **239**:68–79 2001 [Abstract](#)
- 448 Guilford PJ, Hopkins JB, Grady WM, Markowitz SD, Willis J, Lynch H, Rajput A, Wiesner GL, Lindor NM, Burgart LJ, Toro TT, Lee D, Limacher JM, Shaw DW, Findlay MP and Reeve AE  
E-cadherin germline mutations define an inherited cancer syndrome dominated by diffuse gastric cancer  
*Human Mutation* **14**:249–55 1999 [Abstract](#)
- 449 Guillouf C, Vit JP and Rosselli F  
Loss of the Fanconi anemia group C protein activity results in an inability to activate caspase-3 after ionizing radiation  
*Biochimie* **82**:51–8 2000 [Abstract](#)
- 450 Guinamard R, Aspenstrom P, Fougereau M, Chavier P and Guillemot JC  
Tyrosine phosphorylation of the Wiskott-Aldrich syndrome protein by Lyn and Btk is regulated by CDC42  
*FEBS Letters* **434**:431–6 1998 [Abstract](#)
- 451 Guldberg P, thor Straten P, Ahrenkiel V, Seremet T, Kirkin AF and Zeuthen J  
Somatic mutation of the Peutz-Jeghers syndrome gene, LKB1/STK11, in malignant melanoma  
*Oncogene* **18**:1777–80 1999 [Abstract](#)





- 452 Guo Z, Kumagai A, Wang SX and Dunphy WG  
Requirement for Atr in phosphorylation of Chk1 and cell cycle regulation in response to DNA replication blocks and UV-damaged DNA in *Xenopus* egg extracts  
*Genes and Development* 14:2745–56 2000 [Abstract](#)
- 453 Gutmann DH, Sherman L, Seftor L, Haipek C, Hoang-Lu K and Hendrix M  
Increased expression of the NF2 tumor suppressor gene product, merlin, impairs cell motility, adhesion and spreading  
*Human Molecular Genetics* 8:267–75 1999 [Abstract](#)
- 454 Haber DA and Buckler AJ  
WT1: a novel tumor suppressor gene inactivated in Wilms' tumor  
*New Biologist* 4:97–106 1992 [Abstract](#)
- 455 Habraken Y, Sung P, Prakash L and Prakash S  
Human xeroderma pigmentosum group G gene encodes a DNA endonuclease  
*Nucleic Acids Research* 22:3312–6 1994 [Abstract](#)
- 456 Habraken Y, Sung P, Prakash L and Prakash S  
ATP-dependent assembly of a ternary complex consisting of a DNA mismatch and the yeast MSH2-MSH6 and MLH1-PMS1 protein complexes  
*Journal of Biological Chemistry* 273:9837–41 1998 [Abstract](#)
- 457 Habraken Y, Sung P, Prakash L and Prakash S  
Enhancement of MSH2-MSH3-mediated mismatch recognition by the yeast MLH1-PMS1 complex  
*Current Biology* 7:790–3 1997 [Abstract](#)
- 458 Hachiya A, Kobayashi A, Ohuchi A, Takema Y and Imokawa G  
The paracrine role of stem cell factor/c-kit signaling in the activation of human melanocytes in ultraviolet-B-induced pigmentation  
*Journal of Investigative Dermatology* 116:578–86 2001 [Abstract](#)
- 459 Haddad E, Zugaza JL, Louache F, Debili N, Crouin C, Schwarz K, Fischer A, Vainchenker W and Bertoglio J  
The interaction between Cdc42 and WASP is required for SDF-1-induced T-lymphocyte chemotaxis  
*Blood* 97:33–8 2001 [Abstract](#)
- 460 Haddad MM, Xu W, Schwahn DJ, Liao F and Medrano EE  
Activation of a cAMP pathway and induction of melanogenesis correlate with association of p16(INK4) and p27(KIP1) to CDKs, loss of E2F-binding activity, and premature senescence of human melanocytes  
*Experimental Cell Research* 253:561–72 1999 [Abstract](#)
- 461 Hagemann TL and Kwan SP  
The identification and characterization of two promoters and the complete genomic sequence for the Wiskott-Aldrich syndrome gene  
*Biochemical and Biophysical Research Communications* 256:104–9 1999 [Abstract](#)
- 462 Hahn H, Wicking C, Zaphiropoulos PG, Gailani MR, Shanley S, Chidambaram A, Vorechovsky I, Holmberg E, Unden AB, Gillies S, Negus K, Smyth I, Pressman C, Leffell DJ, Gerrard B, Goldstein AM, Dean M, Toftgard R, Chenevix-Trench G, Wainwright B and Bale AE  
Mutations of the human homolog of *Drosophila* patched in the nevoid basal cell carcinoma syndrome  
*Cell* 85:841–51 1996 [Abstract](#)
- 463 Halaban R  
The regulation of normal melanocyte proliferation  
*Pigment Cell Research* 13:4–14 2000 [Abstract](#)
- 464 Halaban R  
Growth factors and melanomas  
*Seminars in Oncology* 23:673–81 1996 [Abstract](#)
- 465 Halaban R, Cheng E, Smicun Y and Germino J  
Deregulated E2F transcriptional activity in autonomously growing melanoma cells  
*Journal of Experimental Medicine* 191:1005–16 2000 [Abstract](#)
- 466 Halaban R, Langdon R, Birchall N, Cuono C, Baird A, Scott G, Moellmann G and McGuire J  
Basic fibroblast growth factor from human keratinocytes is a natural mitogen for melanocytes  
*Journal of Cell Biology* 107:1611–9 1988 [Abstract](#)
- 467 Halaban R, Rubin JS and White W  
met and HGF-SF in normal melanocytes and melanoma cells  
*EXS* 65:329–39 1993 [Abstract](#)
- 468 Haluska FG and Hodi FS  
Molecular genetics of familial cutaneous melanoma  
*Journal of Clinical Oncology* 16:670–82 1998 [Abstract](#)
- 469 Hamel PA, Gill RM, Phillips RA and Gallie BL  
Transcriptional repression of the E2-containing promoters E1aE, c-myc, and RB1 by the product of the RB1 gene  
*Molecular and Cellular Biology* 12:3431–8 1992 [Abstract](#)
- 470 Hamilton SR, Liu B, Parsons RE, Papadopoulos N, Jen J, Powell SM, Krush AJ, Berk T, Cohen Z, Tetu B et al  
The molecular basis of Turcot's syndrome  
*New England Journal of Medicine* 332:839–47 1995 [Abstract](#)
- 471 Hannon GJ and Beach D  
p15INK4B is a potential effector of TGF-beta-induced cell cycle arrest  
*Nature* 371:257–61 1994 [Abstract](#)
- 472 Hansen MF, Koufos A, Gallie BL, Phillips RA, Fodstad O, Brogger A, Gedde-Dahl T and Cavenee WK  
Osteosarcoma and retinoblastoma: a shared chromosomal mechanism revealing recessive predisposition  
*Proceedings of the National Academy of Sciences of the USA* 82:6216–20 1985 [Abstract](#)
- 473 Hansen WK and Kelley MR  
Review of mammalian DNA repair and translational implications  
*Journal of Pharmacology and Experimental Therapeutics* 295:1–9 2000 [Abstract](#)
- 474 Hara E, Smith R, Parry D, Tahara H, Stone S and Peters G  
Regulation of p16CDKN2 expression and its implications for cell immortalization and senescence  
*Molecular and Cellular Biology* 16:859–67 1996 [Abstract](#)
- 475 Hara M, Yaar M and Gilchrist BA  
Endothelin-1 of keratinocyte origin is a mediator of melanocyte dendricity  
*Journal of Investigative Dermatology* 105:744–8 1995 [Abstract](#)
- 476 Hara M, Yaar M, Byers HR, Goukassian D, Fine RE, Gonsalves J and Gilchrist BA  
Kinesin participates in melanosomal movement along melanocyte dendrites  
*Journal of Investigative Dermatology* 114:438–43 2000 [Abstract](#)

## Human metastatic melanoma in vitro

477	Hara T, Kamura T, Nakayama K, Oshikawa K, Hatakeyama S and Nakayama K Degradation of p27(Kip1) at the G(0)-G(1) transition mediated by a Skp2-independent ubiquitination pathway <i>Journal of Biological Chemistry</i>	276:48937-43	2001	<a href="#">Abstract</a>
478	Harbour JW and Dean DC Rb function in cell-cycle regulation and apoptosis <i>Nature Cell Biology</i>	2:E65-7	2000	<a href="#">Abstract</a>
479	Harbour JW and Dean DC The Rb/E2F pathway: expanding roles and emerging paradigms <i>Genes and Development</i>	14:2393-409	2000	<a href="#">Abstract</a>
480	Harbour JW, Luo RX, Dei-Santi A, Postigo AA and Dean DC Cdk phosphorylation triggers sequential intramolecular interactions that progressively block Rb functions as cells move through G1 <i>Cell</i>	98:859-69	1999	<a href="#">Abstract</a>
481	Harfst E, Cooper S, Neubauer S, Distel L and Grawunder U Normal V(D)J recombination in cells from patients with Nijmegen breakage syndrome <i>Molecular Immunology</i>	37:915-29	2000	<a href="#">Abstract</a>
482	Harper JW, Elledge SJ, Keyomarsi K, Dynlacht B, Tsai LH, Zhang P, Dobrowolski S, Bai C, Connell-Crowley L, Swindell E et al Inhibition of cyclin-dependent kinases by p21 <i>Molecular Biology of the Cell</i>	6:387-400	1995	<a href="#">Abstract</a>
483	Hartshorne DJ, Ito M and Erdodi F Myosin light chain phosphatase: subunit composition, interactions and regulation <i>Journal of Muscle Research and Cell Motility</i>	19:325-41	1998	<a href="#">Abstract</a>
484	Hashemi J, Platz A, Ueno T, Stierner U, Ringborg U and Hansson J CDKN2A germ-line mutations in individuals with multiple cutaneous melanomas <i>Cancer Research</i>	60:6864-7	2000	<a href="#">Abstract</a>
485	Hashimoto Y, Kohri K, Kaneko Y, Morisaki H, Kato T, Ikeda K and Nakanishi M Critical role for the 310 helix region of p57(Kip2) in cyclin-dependent kinase 2 inhibition and growth suppression <i>Journal of Biological Chemistry</i>	273:16544-50	1998	<a href="#">Abstract</a>
486	Hatada I, Ohashi H, Fukushima Y, Kaneko Y, Inoue M, Komoto Y, Okada A, Ohishi S, Nabetani A, Morisaki H, Nakayama M, Niikawa N and Mukai T An imprinted gene p57KIP2 is mutated in Beckwith-Wiedemann syndrome <i>Nature Genetics</i>	14:171-3	1996	<a href="#">Abstract</a>
487	Hatakeyama M and Weinberg RA The role of RB in cell cycle control <i>Progress in Cell Cycle Research</i>	1:9-19	1995	<a href="#">Abstract</a>
488	Hattori S, Maekawa M and Nakamura S Identification of neurofibromatosis type I gene product as an insoluble GTPase-activating protein toward ras p21 <i>Oncogene</i>	7:481-5	1992	<a href="#">Abstract</a>
489	Hauser PJ, Agrawal D, Chu B and Pledger WJ p107 and p130 associated cyclin A has altered substrate specificity <i>Journal of Biological Chemistry</i>	272:22954-9	1997	<a href="#">Abstract</a>
490	Hauser PJ, Agrawal D and Pledger WJ Primary keratinocytes have an adhesion dependent S phase checkpoint that is absent in immortalized cell lines <i>Oncogene</i>	17:3083-92	1998	<a href="#">Abstract</a>
491	He J, Olson JJ and James CD Lack of p16INK4 or retinoblastoma protein (pRb), or amplification-associated overexpression of cdk4 is observed in distinct subsets of malignant glial tumors and cell lines <i>Cancer Research</i>	55:4833-6	1995	<a href="#">Abstract</a>
492	He TC, Sparks AB, Rago C, Hermeking H, Zawel L, da Costa LT, Morin PJ, Vogelstein B and Kinzler KW Identification of c-MYC as a target of the APC pathway <i>Science</i>	281:1509-12	1998	<a href="#">Abstract</a>
493	Hearing VJ, Tsukamoto K, Urabe K, Kameyama K, Montague PM and Jackson IJ Functional properties of cloned melanogenic proteins <i>Pigment Cell Research</i>	5:264-70	1992	<a href="#">Abstract</a>
494	Heidenreich A, Gaddipati JP, Moul JW and Srivastava S Molecular analysis of P16(Ink4)/CDKN2 and P15(INK4B)/MTS2 genes in primary human testicular germ cell tumors <i>Journal of Urology</i>	159:1725-30	1998	<a href="#">Abstract</a>
495	Heldin CH Signal transduction: multiple pathways, multiple options for therapy <i>Stem Cells</i>	19:295-303	2001	<a href="#">Abstract</a>
496	Helin K, Holm K, Niebuhr A, Eiberg H, Tommerup N, Hougaard S, Poulsen HS, Spang-Thomsen M and Norgaard P Loss of the retinoblastoma protein-related p130 protein in small cell lung carcinoma <i>Proceedings of the National Academy of Sciences of the USA</i>	94:6933-8	1997	<a href="#">Abstract</a>
497	Helps NR, Luo X, Barker HM and Cohen PT NIMA-related kinase 2 (Nek2), a cell-cycle-regulated protein kinase localized to centrosomes, is complexed to protein phosphatase 1 <i>Biochemical Journal</i>	349:509-18	2000	<a href="#">Abstract</a>
498	Hemesath TJ, Price ER, Takemoto C, Badalian T and Fisher DE MAP kinase links the transcription factor Microphthalmia to c-Kit signalling in melanocytes <i>Nature</i>	391:298-301	1998	<a href="#">Abstract</a>
499	Hemminki A, Markie D, Tomlinson I, Avizienyte E, Roth S, Loukola A, Bignell G, Warren W, Aminoff M, Hoglund P, Jarvinen H, Kristo P, Pelin K, Ridanpaa M, Salovaara R, Toro T, Bodmer W, Olschwang S, Olsen AS, Stratton MR, de la Chapelle A and Aaltonen LA A serine/threonine kinase gene defective in Peutz-Jeghers syndrome <i>Nature</i>	391:184-7	1998	<a href="#">Abstract</a>
500	Hendrix MJ, Seftor EA, Chu YW, Seftor RE, Nagle RB, McDaniel KM, Leong SP, Yohem KH, Leibovitz AM, Meyskens FL Jr et al Coexpression of vimentin and keratins by human melanoma tumor cells: correlation with invasive and metastatic potential <i>Journal of the National Cancer Institute</i>	84:165-74	1992	<a href="#">Abstract</a>
501	Hengst L, Gopfert U, Lashuel HA and Reed SI Complete inhibition of Cdk/cyclin by one molecule of p21(Cip1) <i>Genes and Development</i>	12:3882-8	1998	<a href="#">Abstract</a>



- 502 Hengstschlager M, Braun K, Soucek T, Miloloza A and Hengstschlager Otnad E  
Cyclin-dependent kinases at the G1-S transition of the mammalian cell cycle  
*Mutation Research* **436**:1–9 1999 [Abstract](#)
- 503 Henriet P, Zhong ZD, Brooks PC, Weinberg KI and DeClerck YA  
Contact with fibrillar collagen inhibits melanoma cell proliferation by up-regulating p27KIP1  
*Proceedings of the National Academy of Sciences of the USA* **97**:10026–31 2000 [Abstract](#)
- 504 Henry DO, Moskalenko SA, Kaur KJ, Fu M, Pestell RG, Camonis JH and White MA  
Ral GTPases contribute to regulation of cyclin D1 through activation of NF-kappaB  
*Molecular and Cellular Biology* **20**:8084–92 2000 [Abstract](#)
- 505 Hensey CE, Hong F, Durfee T, Qian YW, Lee EY and Lee WH  
Identification of discrete structural domains in the retinoblastoma protein. Amino-terminal domain is required for its oligomerization  
*Journal of Biological Chemistry* **269**:1380–7 1994 [Abstract](#)
- 506 Herlyn M, Berking C, Li G and Satyamoorthy K  
Lessons from melanocyte development for understanding the biological events in naevus and melanoma formation  
*Melanoma Research* **10**:303–12 2000 [Abstract](#)
- 507 Herlyn M, Mancianti ML, Jambrosic J, Bolen JB and Koprowski H  
Regulatory factors that determine growth and phenotype of normal human melanocytes  
*Experimental Cell Research* **179**:322–31 1988 [Abstract](#)
- 508 Herman JG, Civin CI, Issa JP, Collector MI, Sharkis SJ and Baylin SB  
Distinct patterns of inactivation of p15INK4B and p16INK4A characterize the major types of hematological malignancies  
*Cancer Research* **57**:837–41 1997 [Abstract](#)
- 509 Herman JG, Jen J, Merlo A and Baylin SB  
Hypermethylation-associated inactivation indicates a tumor suppressor role for p15INK4B  
*Cancer Research* **56**:722–7 1996 [Abstract](#)
- 510 Herman JG, Latif F, Weng Y, Lerman MI, Zbar B, Liu S, Samid D, Duan DS, Gnarr JR, Linehan WM et al  
Silencing of the VHL tumor-suppressor gene by DNA methylation in renal carcinoma  
*Proceedings of the National Academy of Sciences of the USA* **91**:9700–4 1994 [Abstract](#)
- 511 Hermeking H, Lengauer C, Polyak K, He TC, Zhang L, Thiagalingam S, Kinzler KW and Vogelstein B  
14–3–3 sigma is a p53-regulated inhibitor of G2/M progression  
*Molecular Cell* **1**:3–11 1997 [Abstract](#)
- 512 Hernandez-Alcoceba R, del Peso L and Lacal JC  
The Ras family of GTPases in cancer cell invasion  
*Cellular and Molecular Life Sciences* **57**:65–76 2000 [Abstract](#)
- 513 Herwig S and Strauss M  
The retinoblastoma protein: a master regulator of cell cycle, differentiation and apoptosis.  
*European Journal of Biochemistry* **246**:581–601 1997 [Abstract](#)
- 514 Hess GF, Drong RF, Weiland KL, Slightom JL, Sclafani RA and Hollingsworth RE  
A human homolog of the yeast CDC7 gene is overexpressed in some tumors and transformed cell lines  
*Gene* **211**:133–40 1998 [Abstract](#)
- 515 Hidalgo M, Siu LL, Nemunaitis J, Rizzo J, Hammond LA, Takimoto C, Eckhardt SG, Tolcher A, Britten CD, Denis L, Ferrante K, Von Hoff DD, Silberman S and Rowinsky EK  
Phase I and pharmacologic study of OSI-774, an epidermal growth factor receptor tyrosine kinase inhibitor, in patients with advanced solid malignancies  
*Journal of Clinical Oncology* **19**:3267–79 2001 [Abstract](#)
- 516 Hiebert SW  
Regions of the retinoblastoma gene product required for its interaction with the E2F transcription factor are necessary for E2 promoter repression and pRb-mediated growth suppression  
*Molecular and Cellular Biology* **13**:3384–91 1993 [Abstract](#)
- 517 Higashi H, Suzuki-Takahashi I, Saitoh S, Segawa K, Taya Y, Okuyama A, Nishimura S and Kitagawa M  
Cyclin-dependent kinase-2 (Cdk2) forms an inactive complex with cyclin D1 since Cdk2 associated with cyclin D1 is not phosphorylated by Cdk7-cyclin-H  
*European Journal of Biochemistry* **237**:460–7 1996 [Abstract](#)
- 518 Higashitsuji H, Itoh K, Nagao T, Dawson S, Nonoguchi K, Kido T, Mayer RJ, Arai S and Fujita J  
Reduced stability of retinoblastoma protein by gankyrin, an oncogenic ankyrin-repeat protein overexpressed in hepatomas  
*Nature Medicine* **6**:96–9 2000 [Abstract](#)
- 519 Hinchcliffe EH, Li C, Thompson EA, Maller JL and Sluder G  
Requirement of Cdk2-cyclin E activity for repeated centrosome reproduction in *Xenopus* egg extracts  
*Science* **283**:851–4 1999 [Abstract](#)
- 520 Hinchcliffe EH, Miller FJ, Cham M, Khodjakov A and Sluder G  
Requirement of a centrosomal activity for cell cycle progression through G1 into S phase  
*Science* **291**:1547–50 2001 [Abstract](#)
- 521 Hindges R and Hubscher U  
DNA polymerase delta, an essential enzyme for DNA transactions  
*Biological Chemistry* **378**:345–62 1997 [Abstract](#)
- 522 Hinds PW, Mittnacht S, Dulic V, Arnold A, Reed SI and Weinberg RA  
Regulation of retinoblastoma protein functions by ectopic expression of human cyclins  
*Cell* **70**:993–1006 1992 [Abstract](#)
- 523 Hingorani K, Szebeni A and Olson MO  
Mapping the functional domains of nucleolar protein B23  
*Journal of Biological Chemistry* **275**:24451–7 2000 [Abstract](#)
- 524 Hirabayashi H, Fujii Y, Sakaguchi M, Tanaka H, Yoon HE, Komoto Y, Inoue M, Miyoshi S and Matsuda H  
p16INK4, pRB, p53 and cyclin D1 expression and hypermethylation of CDKN2 gene in thymoma and thymic carcinoma  
*International Journal of Cancer* **73**:639–44 1997 [Abstract](#)
- 525 Hirao A, Kong YY, Matsuoka S, Wakeham A, Ruland J, Yoshida H, Liu D, Elledge SJ and Mak TW  
DNA damage-induced activation of p53 by the checkpoint kinase Chk2  
*Science* **287**:1824–7 2000 [Abstract](#)
- 526 Hirobe T  
Endothelins are involved in regulating the proliferation and differentiation of mouse epidermal melanocytes in serum-free primary culture  
*Journal of Investigative Dermatology Symposium Proceedings* **6**:25–31 2001 [Abstract](#)

## Human metastatic melanoma in vitro

527	Hitomi M and Stacey DW Cyclin D1 production in cycling cells depends on ras in a cell-cycle-specific manner <i>Current Biology</i>	9:1075–84	1999	<a href="#">Abstract</a>
528	Hoekstra MF Responses to DNA damage and regulation of cell cycle checkpoints by the ATM protein kinase family <i>Current Opinion in Genetics and Development</i>	7:170–5	1997	<a href="#">Abstract</a>
529	Hoffmann I, Clarke PR, Marcote MJ, Karsenti E and Draetta G Phosphorylation and activation of human cdc25-C by cdc2--cyclin B and its involvement in the self-amplification of MPF at mitosis <i>EMBO Journal</i>	12:53–63	1993	<a href="#">Abstract</a>
530	Hollander MC, Sheikh MS, Bulavin DV, Lundgren K, Augeri-Henmueller L, Shehee R, Molinaro TA, Kim KE, Tolosa E, Ashwell JD, Rosenberg MP, Zhan Q, Fernandez-Salguero PM, Morgan WF, Deng CX and Fornace AJ Jr Genomic instability in Gadd45a-deficient mice <i>Nature Genetics</i>	23:176–84	1999	<a href="#">Abstract</a>
531	Holmes JK and Solomon MJ The role of Thr160 phosphorylation of Cdk2 in substrate recognition <i>European Journal of Biochemistry</i>	268:4647–52	2001	<a href="#">Abstract</a>
532	Holt SE and Shay JW Role of telomerase in cellular proliferation and cancer <i>Journal of Cellular Physiology</i>	180:10–8	1999	<a href="#">Abstract</a>
533	Honda R and Yasuda H Association of p19(ARF) with Mdm2 inhibits ubiquitin ligase activity of Mdm2 for tumor suppressor p53 <i>EMBO Journal</i>	18:22–7	1999	<a href="#">Abstract</a>
534	Hopfner KP, Karcher A, Craig L, Woo TT, Carney JP and Tainer JA Structural biochemistry and interaction architecture of the DNA double-strand break repair Mre11 nuclease and Rad50-ATPase <i>Cell</i>	105:473–85	2001	<a href="#">Abstract</a>
535	Horikawa T, Norris DA, Yohn JJ, Zekman T, Travers JB and Morelli JG Melanocyte mitogens induce both melanocyte chemokinesis and chemotaxis <i>Journal of Investigative Dermatology</i>	104:256–9	1995	<a href="#">Abstract</a>
536	Hornyak TJ, Hayes DJ, Chiu LY and Ziff EB Transcription factors in melanocyte development: distinct roles for Pax-3 and Mitf <i>Mechanisms of Development</i>	101:47–59	2001	<a href="#">Abstract</a>
537	Hou L, Panthier JJ and Arnheiter H Signaling and transcriptional regulation in the neural crest-derived melanocyte lineage: interactions between KIT and MITF <i>Development</i>	127:5379–89	2000	<a href="#">Abstract</a>
538	Houck JC, Sharma VK and Hayflick L Functional failures of cultured human diploid fibroblasts after continued population doublings <i>Proceedings of the Society for Experimental Biology and Medicine</i>	137:331–3	1971	<a href="#">Abstract</a>
539	Houldsworth J, Reuter V, Bosl GJ and Chaganti RS Aberrant expression of cyclin D2 is an early event in human male germ cell tumorigenesis <i>Cell Growth and Differentiation</i>	8:293–9	1997	<a href="#">Abstract</a>
540	Houlston RS and Damato BE Genetic predisposition to ocular melanoma <i>Eye</i>	13:43–6	1999	<a href="#">Abstract</a>
541	Hovens CM and Kaye AH The tumour suppressor protein NF2/merlin: the puzzle continues <i>Journal of Clinical Neuroscience</i>	8:4–7	2001	<a href="#">Abstract</a>
542	Hsieh CL, Arlett CF and Lieber MR V(D)J recombination in ataxia telangiectasia, Bloom's syndrome, and a DNA ligase I-associated immunodeficiency disorder <i>Journal of Biological Chemistry</i>	268:20105–9	1993	<a href="#">Abstract</a>
543	Hsu LC and White RL BRCA1 is associated with the centrosome during mitosis <i>Proceedings of the National Academy of Sciences of the USA</i>	95:12983–8	1998	<a href="#">Abstract</a>
544	Hsu MY, Wheelock MJ, Johnson KR and Herlyn M Shifts in cadherin profiles between human normal melanocytes and melanomas <i>Journal of Investigative Dermatology Symposium Proceedings</i>	1:188–94	1996	<a href="#">Abstract</a>
545	Hu N, Gutschmann A, Herbert DC, Bradley A, Lee WH and Lee EY Heterozygous Rb-1 delta 20/+mice are predisposed to tumors of the pituitary gland with a nearly complete penetrance <i>Oncogene</i>	9:1021–7	1994	<a href="#">Abstract</a>
546	Hu PP, Shen X, Huang D, Liu Y, Counter C and Wang XF The MEK pathway is required for stimulation of p21(WAF1/CIP1) by transforming growth factor-beta <i>Journal of Biological Chemistry</i>	274:35381–7	1999	<a href="#">Abstract</a>
547	Hu X, Cress WD, Zhong Q and Zuckerman KS Transforming growth factor beta inhibits the phosphorylation of pRB at multiple serine/threonine sites and differentially regulates the formation of pRB family-E2F complexes in human myeloid leukemia cells <i>Biochemical and Biophysical Research Communications</i>	276:930–9	2000	<a href="#">Abstract</a>
548	Hu YX, Watanabe H, Li P, Wang Y, Ohtsubo K, Yamaguchi Y and Sawabu N An immunohistochemical analysis of p27 expression in human pancreatic carcinomas <i>Pancreas</i>	21:226–30	2000	<a href="#">Abstract</a>
549	Huang J and Dynan WS Reconstitution of the mammalian DNA double-strand break end-joining reaction reveals a requirement for an Mre11/Rad50/NBS1-containing fraction <i>Nucleic Acids Research</i>	30:667–74	2002	<a href="#">Abstract</a>
550	Huang S, Lee WH and Lee EY A cellular protein that competes with SV40 T antigen for binding to the retinoblastoma gene product <i>Nature</i>	350:160–2	1991	<a href="#">Abstract</a>
551	Huang S, Shin E, Sheppard KA, Chokroverty L, Shan B, Qian YW, Lee EY and Yee AS The retinoblastoma protein region required for interaction with the E2F transcription factor includes the T/E1A binding and carboxy-terminal sequences <i>DNA and Cell Biology</i>	11:539–48	1992	<a href="#">Abstract</a>
552	Huizing M, Sarangarajan R, Strovel E, Zhao Y, Gahl WA and Boissy RE AP-3 mediates tyrosinase but not TRP-1 trafficking in human melanocytes <i>Molecular Biology of the Cell</i>	12:2075–85	2001	<a href="#">Abstract</a>



- 553 Huncharek M, Caubet JF and McGarry R  
Single-agent DTIC versus combination chemotherapy with or without immunotherapy in metastatic melanoma: a meta-analysis of 3273 patients from 20 randomized trials  
*Melanoma Research* **11**:75–81 2001 [Abstract](#)
- 554 HUGO nomenclature database  
<http://www.gene.ucl.ac.uk/nomenclature/>
- 555 Hui AM, Li X, Makuuchi M, Takayama T and Kubota K  
Over-expression and lack of retinoblastoma protein are associated with tumor progression and metastasis in hepatocellular carcinoma  
*International Journal of Cancer* **84**:604–8 1999 [Abstract](#)
- 556 Hur EM and Kim KT  
G protein-coupled receptor signalling and cross-talk. Achieving rapidity and specificity  
*Cellular Signalling* **14**:397–405 2002 [Abstract](#)
- 557 Huschtscha LI and Reddel RR  
p16(INK4a) and the control of cellular proliferative life span  
*Carcinogenesis* **20**:921–6 1999 [Abstract](#)
- 558 Huschtscha LI, Noble JR, Neumann AA, Moy EL, Barry P, Melki JR, Clark SJ and Reddel RR  
Loss of p16INK4 expression by methylation is associated with lifespan extension of human mammary epithelial cells  
*Cancer Research* **58**:3508–12 1998 [Abstract](#)
- 559 Hussussian CJ, Struewing JP, Goldstein AM, Higgins PA, Ally DS, Sheahan MD, Clark WH Jr, Tucker MA and Dracopoli NC  
Germline p16 mutations in familial melanoma  
*Nature Genetics* **8**:15–21 1994 [Abstract](#)
- 560 Hwang BJ and Chu G  
Purification and characterization of a human protein that binds to damaged DNA  
*Biochemistry* **32**:1657–66 1993 [Abstract](#)
- 561 Hwu WJ  
New approaches in the treatment of metastatic melanoma: thalidomide and temozolomide  
*Oncology (Huntington)* **14**:25–8 2000 [Abstract](#)
- 562 Iaccarino I, Marra G, Palombo F and Jiricny J  
hMSH2 and hMSH6 play distinct roles in mismatch binding and contribute differently to the ATPase activity of hMutSalpha  
*EMBO Journal* **17**:2677–86 1998 [Abstract](#)
- 563 Iaccarino I, Palombo F, Drummond J, Totty NF, Hsuan JJ, Modrich P and Jiricny J  
MSH6, a *Saccharomyces cerevisiae* protein that binds to mismatches as a heterodimer with MSH2  
*Current Biology* **6**:484–6 1996 [Abstract](#)
- 564 IARC p53 mutation database  
<http://www.iarc.fr/p53/Index.html>
- 565 Iavarone A and Massague J  
E2F and histone deacetylase mediate transforming growth factor beta repression of cdc25A during keratinocyte cell cycle arrest  
*Molecular and Cellular Biology* **19**:916–22 1999 [Abstract](#)
- 566 Iavarone A and Massague J  
Repression of the CDK activator Cdc25A and cell-cycle arrest by cytokine TGF-beta in cells lacking the CDK inhibitor p15  
*Nature* **387**:417–22 1997 [Abstract](#)
- 567 Iavarone A, Garg P, Lasorella A, Hsu J and Israel MA  
The helix-loop-helix protein Id-2 enhances cell proliferation and binds to the retinoblastoma protein  
*Genes and Development* **8**:1270–84 1994 [Abstract](#)
- 568 Iida S, Fujii H and Moriwaki K  
A somatic mutation of the p21(Waf1/Cip1) gene in a human adrenocortical adenoma  
*Anticancer Research* **17**:633–6 1997 [Abstract](#)
- 569 Ikeda H, Yoshimoto T and Shida N  
Molecular analysis of p21 and p27 genes in human pituitary adenomas  
*British Journal of Cancer* **76**:1119–23 1997 [Abstract](#)
- 570 Ikeda M, Orimo H, Moriyama H, Nakajima E, Matsubara N, Mibu R, Tanaka N, Shimada T, Kimura A and Shimizu K  
Close correlation between mutations of E2F4 and hMSH3 genes in colorectal cancers with microsatellite instability  
*Cancer Research* **58**:594–8 1998 [Abstract](#)
- 571 Ilyas M and Tomlinson IP  
The interactions of APC, E-cadherin and beta-catenin in tumour development and progression  
*Journal of Pathology* **182**:128–37 1997 [Abstract](#)
- 572 Imada K and Leonard WJ  
The Jak-STAT pathway  
*Molecular Immunology* **37**:1–11 2000 [Abstract](#)
- 573 Imamura O, Fujita K, Shimamoto A, Tanabe H, Takeda S, Furuichi Y and Matsumoto T  
Bloom helicase is involved in DNA surveillance in early S phase in vertebrate cells  
*Oncogene* **20**:1143–51 2001 [Abstract](#)
- 574 Imayama S, Furumura M and Hori Y  
Deposition of basic fibroblast growth factor on surface of epidermal melanocytes suggesting the stromal control of epidermal pigmentation  
*Pigment Cell Research* **7**:170–4 1994 [Abstract](#)
- 575 Imokawa G, Kobayasi T and Miyagishi M  
Intracellular signaling mechanisms leading to synergistic effects of endothelin-1 and stem cell factor on proliferation of cultured human melanocytes. Cross-talk via trans-activation of the tyrosine kinase c-kit receptor  
*Journal of Biological Chemistry* **275**:33321–8 2000 [Abstract](#)
- 576 Imokawa G, Miyagishi M and Yada Y  
Endothelin-1 as a new melanogen: coordinated expression of its gene and the tyrosinase gene in UVB-exposed human epidermis  
*Journal of Investigative Dermatology* **105**:32–7 1995 [Abstract](#)
- 577 Imokawa G, Yada Y and Kimura M  
Signalling mechanisms of endothelin-induced mitogenesis and melanogenesis in human melanocytes  
*Biochemical Journal* **314**:305–12 1996 [Abstract](#)
- 578 Imokawa G, Yada Y and Miyagishi M  
Endothelins secreted from human keratinocytes are intrinsic mitogens for human melanocytes  
*Journal of Biological Chemistry* **267**:24675–80 1992 [Abstract](#)

## Human metastatic melanoma in vitro

- 579 Imokawa G, Yada Y, Kimura M and Morisaki N  
Granulocyte/macrophage colony-stimulating factor is an intrinsic keratinocyte-derived growth factor for human melanocytes in UVA-induced melanosis  
*Biochemical Journal* **313**:625–31 1996 [Abstract](#)
- 580 Imokawa G, Yada Y, Morisaki N and Kimura M  
Biological characterization of human fibroblast-derived mitogenic factors for human melanocytes  
*Biochemical Journal* **330**:1235–9 1998 [Abstract](#)
- 581 Inazu M and Mishima Y  
Detection of eumelanogenic and pheomelanogenic melanosomes in the same normal human melanocyte  
*Journal of Investigative Dermatology* **100**:172S-175S 1993 [Abstract](#)
- 582 Ingley E and Hemmings BA  
Pleckstrin homology (PH) domains in signal transduction  
*Journal of Cellular Biochemistry* **56**:436–43 1994 [Abstract](#)
- 583 Inoue A, Torigoe T, Sogahata K, Kamiguchi K, Takahashi S, Sawada Y, Saijo M, Taya Y, Ishii S, Sato N et al  
70-kDa heat shock cognate protein interacts directly with the N-terminal region of the retinoblastoma gene product pRb. Identification of a novel region of pRb-mediated protein interaction  
*Journal of Biological Chemistry* **270**:22571–6 1995 [Abstract](#)
- 584 Introne W, Boissy RE and Gahl WA  
Clinical, molecular, and cell biological aspects of Chediak-Higashi syndrome  
*Molecular Genetics and Metabolism* **68**:283–303 1999 [Abstract](#)
- 585 Iolascon A, Faienza MF, Coppola B, della Ragione F, Schettini F and Biondi A  
Homozygous deletions of cyclin-dependent kinase inhibitor genes, p16(INK4A) and p18, in childhood T cell lineage acute lymphoblastic leukemias  
*Leukemia* **10**:255–60 1996 [Abstract](#)
- 586 Irvani M, Dhat R and Price CM  
Methylation of the multi tumor suppressor gene-2 (MTS2, CDKN1, p15INK4B) in childhood acute lymphoblastic leukemia  
*Oncogene* **15**:2609–14 1997 [Abstract](#)
- 587 Issa JP, Ottaviano YL, Celano P, Hamilton SR, Davidson NE and Baylin SB  
Methylation of the oestrogen receptor CpG island links ageing and neoplasia in human colon  
*Nature Genetics* **7**:536–40 1994 [Abstract](#)
- 588 Ito M, Kawa Y, Ono H, Okura M, Baba T, Kubota Y, Nishikawa SI and Mizoguchi M  
Removal of stem cell factor or addition of monoclonal anti-c-KIT antibody induces apoptosis in murine melanocyte precursors  
*Journal of Investigative Dermatology* **112**:796–801 1999 [Abstract](#)
- 589 Ito Y, Takeda T, Sakon M, Tsujimoto M, Monden M and Matsuura N  
Expression of p57/Kip2 protein in hepatocellular carcinoma  
*Oncology* **61**:221–5 2001 [Abstract](#)
- 590 Ito Y, Takeda T, Wakasa K, Tsujimoto M and Matsuura N  
Expression and possible role of cyclin D3 in human pancreatic adenocarcinoma  
*Anticancer Research* **21**:1043–8 2001 [Abstract](#)
- 591 Ito Y, Takeda T, Wakasa K, Tsujimoto M and Matsuura N  
Expression of p57/Kip2 protein in pancreatic adenocarcinoma  
*Pancreas* **23**:246–50 2001 [Abstract](#)
- 592 Ito Y, Yoshida H, Nakano K, Kobayashi K, Yokozawa T, Hirai K, Matsuzuka F, Matsuura N, Kuma K and Miyauchi A  
Expression of p57/Kip2 protein in normal and neoplastic thyroid tissues  
*International Journal of Molecular Medicine* **9**:373–6 2002 [Abstract](#)
- 593 Itoh K, Yoshioka K, Akedo H, Uehata M, Ishizaki T and Narumiya S  
An essential part for Rho-associated kinase in the transcellular invasion of tumor cells  
*Nature Medicine* **5**:221–5 1999 [Abstract](#)
- 594 Itoh S, Itoh F, Goumans MJ and Ten Dijke P  
Signaling of transforming growth factor-beta family members through Smad proteins  
*European Journal of Biochemistry* **267**:6954–67 2000 [Abstract](#)
- 595 Ivanova K, Le Poole IC, Gerzer R, Westerhof W and Das PK  
Effect of nitric oxide on the adhesion of human melanocytes to extracellular matrix components  
*Journal of Pathology* **183**:469–76 1997 [Abstract](#)
- 596 Iwama T, Konishi M, Iijima T, Yoshinaga K, Tominaga T, Koike M and Miyaki M  
Somatic mutation of the APC gene in thyroid carcinoma associated with familial adenomatous polyposis  
*Japanese Journal of Cancer Research* **90**:372–6 1999 [Abstract](#)
- 597 Iyengar B  
UV guided dendritic growth patterns and the networking of melanocytes  
*Experientia* **50**:669–72 1994 [Abstract](#)
- 598 Iyengar B  
The role of melanocytes in the repair of UV related DNA damage in keratinocytes  
*Pigment Cell Research* **11**:110–3 1998 [Abstract](#)
- 599 Izatt L, Greenman J, Hodgson S, Ellis D, Watts S, Scott G, Jacobs C, Liebmann R, Zvelebil MJ, Mathew C and Solomon E  
Identification of germline missense mutations and rare allelic variants in the ATM gene in early-onset breast cancer  
*Genes, Chromosomes and Cancer* **26**:286–94 1999 [Abstract](#)
- 600 Izawa I, Amano M, Chihara K, Yamamoto T and Kaibuchi K  
Possible involvement of the inactivation of the Rho-Rho-kinase pathway in oncogenic Ras-induced transformation  
*Oncogene* **17**:2863–71 1998 [Abstract](#)
- 601 Jacobs JJ, Keblusek P, Robanus-Maandag E, Kristel P, Lingbeek M, Nederlof PM, van Welsem T, van de Vijver MJ, Koh EY, Daley GQ and van Lohuizen M  
Senescence bypass screen identifies TBX2, which represses Cdkn2a (p19(ARF)) and is amplified in a subset of human breast cancers  
*Nature Genetics* **26**:291–9 2000 [Abstract](#)
- 602 James MC and Peters G  
Alternative product of the p16/CKDN2A locus connects the Rb and p53 tumor suppressors  
*Progress in Cell Cycle Research* **4**:71–81 2000 [Abstract](#)
- 603 Jarvis L, Bathurst N, Mohan D and Beckly D  
Turcot's syndrome. A review  
*Diseases of the Colon and Rectum* **31**:907–14 1988 [Abstract](#)



604	Jenne DE, Reimann H, Nezu J, Friedel W, Loff S, Jeschke R, Muller O, Back W and Zimmer M Peutz-Jeghers syndrome is caused by mutations in a novel serine threonine kinase <i>Nature Genetics</i>	18:38–43	1998	<a href="#">Abstract</a>
605	Jensen CJ, Buch MB, Krag TO, Hemmings BA, Gammeltoft S and Frodin M 90-kDa ribosomal S6 kinase is phosphorylated and activated by 3-phosphoinositide-dependent protein kinase-1 <i>Journal of Biological Chemistry</i>	274:27168–76	1999	<a href="#">Abstract</a>
606	Jergil B, Lindblad C, Rorsman H and Rosengren E Dopa oxidation and tyrosine oxygenation by human melanoma tyrosinase <i>Acta Dermato-Venereologica</i>	63:468–75	1983	<a href="#">Abstract</a>
607	Jhun BH, Rivnay B, Price D and Avraham H The MATK tyrosine kinase interacts in a specific and SH2-dependent manner with c-Kit <i>Journal of Biological Chemistry</i>	270:9661–6	1995	<a href="#">Abstract</a>
608	Ji TH, Grossmann M and Ji I G protein-coupled receptors. I. Diversity of receptor-ligand interactions <i>Journal of Biological Chemistry</i>	273:17299–302	1998	<a href="#">Abstract</a>
609	Jiang W, Wells NJ and Hunter T Multistep regulation of DNA replication by Cdk phosphorylation of HsCdc6 <i>Proceedings of the National Academy of Sciences of the USA</i>	96:6193–8	1999	<a href="#">Abstract</a>
610	Jiang Y, Prosper F and Verfaillie CM Opposing effects of engagement of integrins and stimulation of cytokine receptors on cell cycle progression of normal human hematopoietic progenitors <i>Blood</i>	95:846–54	2000	<a href="#">Abstract</a>
611	Jimbow K, Hua C, Gomez PF, Hirosaki K, Shinoda K, Salopek TG, Matsusaka H, Jin HY and Yamashita T Intracellular vesicular trafficking of tyrosinase gene family protein in eu- and pheomelanosome biogenesis <i>Pigment Cell Research</i>	13 Suppl 8:110–7	2000	<a href="#">Abstract</a>
612	Jimbow K, Park JS, Kato F, Hirosaki K, Toyofuku K, Hua C and Yamashita T Assembly, target-signaling and intracellular transport of tyrosinase gene family proteins in the initial stage of melanosome biogenesis <i>Pigment Cell Research</i>	13:222–9	2000	<a href="#">Abstract</a>
613	Jin S, Zhao H, Fan F, Blanck P, Fan W, Colchagie AB, Fornace AJ Jr and Zhan Q BRCA1 activation of the GADD45 promoter <i>Oncogene</i>	19:4050–7	2000	<a href="#">Abstract</a>
614	John RM, Ainscough JF, Barton SC and Surani MA Distant cis-elements regulate imprinted expression of the mouse p57( Kip2) (Cdkn1c) gene: implications for the human disorder, Beckwith–Wiedemann syndrome <i>Human Molecular Genetics</i>	10:1601–9	2001	<a href="#">Abstract</a>
615	Johnson DG, Schwarz JK, Cress WD and Nevins JR Expression of transcription factor E2F1 induces quiescent cells to enter S phase <i>Nature</i>	365:349–52	1993	<a href="#">Abstract</a>
616	Johnson RL, Rothman AL, Xie J, Goodrich LV, Bare JW, Bonifas JM, Quinn AG, Myers RM, Cox DR, Epstein EH and Scott MP Human homolog of patched, a candidate gene for the basal cell nevus syndrome <i>Science</i>	272:1668–71	1996	<a href="#">Abstract</a>
617	Jones CJ, Kipling D, Morris M, Hepburn P, Skinner J, Bounacer A, Wyllie FS, Ivan M, Bartek J, Wynford-Thomas D and Bond JA Evidence for a telomere-independent "clock" limiting RAS oncogene-driven proliferation of human thyroid epithelial cells <i>Molecular and Cellular Biology</i>	20:5690–9	2000	<a href="#">Abstract</a>
618	Jones PA DNA methylation and cancer <i>Cancer Research</i>	46:461–6	1986	<a href="#">Abstract</a>
619	Jones PA, Rideout WM 3rd, Shen JC, Spruck CH and Tsai YC Methylation, mutation and cancer <i>Bioessays</i>	14:33–6	1992	<a href="#">Abstract</a>
620	Jones WO, Harman CR, Ng AK and Shaw JH Incidence of malignant melanoma in Auckland, New Zealand: highest rates in the world <i>World Journal of Surgery</i>	23:732–5	1999	<a href="#">Abstract</a>
621	Jongmans W and Hall J Cellular responses to radiation and risk of breast cancer <i>European Journal of Cancer</i>	35:540–8	1999	<a href="#">Abstract</a>
622	Joo M, Kang YK, Kim MR, Lee HK and Jang JJ Cyclin D1 overexpression in hepatocellular carcinoma <i>Liver</i>	21:89–95	2001	<a href="#">Abstract</a>
623	Jordan SA and Jackson IJ MGF (KIT ligand) is a chemokinetic factor for melanoblast migration into hair follicles <i>Developmental Biology</i>	225:424–36	2000	<a href="#">Abstract</a>
624	Joyce D, Bouzahzah B, Fu M, Albanese C, D'Amico M, Steer J, Klein JU, Lee RJ, Segall JE, Westwick JK, Der CJ and Pestell RG Integration of Rac-dependent regulation of cyclin D1 transcription through a nuclear factor-kappaB-dependent pathway <i>Journal of Biological Chemistry</i>	274:25245–9	1999	<a href="#">Abstract</a>
625	Kaelin WG Jr Functions of the retinoblastoma protein <i>Bioessays</i>	21:950–8	1999	<a href="#">Abstract</a>
626	Kaelin WG Jr, Krek W, Sellers WR, DeCaprio JA, Ajchenbaum F, Fuchs CS, Chittenden T, Li Y, Farnham PJ, Blunar MA et al Expression cloning of a cDNA encoding a retinoblastoma-binding protein with E2F-like properties <i>Cell</i>	70:351–64	1992	<a href="#">Abstract</a>
627	Kaitna S, Mendoza M, Jantsch-Plunger V and Glotzer M Incpn and an aurora-like kinase form a complex essential for chromosome segregation and efficient completion of cytokinesis <i>Current Biology</i>	10:1172–81	2000	<a href="#">Abstract</a>
628	Kaldis P, Russo AA, Chou HS, Pavletich NP and Solomon M Human and yeast cdk-activating kinases (CAKs) display distinct substrate specificities <i>Journal of Molecular Biology Cell</i>	9:2545–60	1998	<a href="#">Abstract</a>
629	Kaldis P and Solomon MJ Analysis of CAK activities from human cells <i>European Journal of Biochemistry</i>	267:4213–21	2000	<a href="#">Abstract</a>

## Human metastatic melanoma in vitro

- 630 Kamai T, Arai K, Tsujii T, Honda M and Yoshida K  
Overexpression of RhoA mRNA is associated with advanced stage in testicular germ cell tumour  
*BJU International* **87**:227–31 2001 [Abstract](#)
- 631 Kamijo T, Bodner S, van de Kamp E, Randle DH and Sherr CJ  
Tumor spectrum in ARF-deficient mice  
*Cancer Research* **59**:2217–22 1999 [Abstract](#)
- 632 Kamitani T, Kito K, Fukuda-Kamitani T and Yeh ET  
Targeting of NEDD8 and Its Conjugates for Proteasomal Degradation by NUB1  
*Journal of Biological Chemistry* **276**:46655–60 2001 [Abstract](#)
- 633 Kanai M, Uchida M, Hanai S, Uematsu N, Uchida K and Miwa M  
Poly(ADP-ribose) polymerase localizes to the centrosomes and chromosomes  
*Biochemical and Biophysical Research Communications* **278**:385–9 2000 [Abstract](#)
- 634 Kanter-Lewensohn L, Dricu A, Girnita L, Wejde J and Larsson O  
Expression of insulin-like growth factor-1 receptor (IGF-1R) and p27Kip1 in melanocytic tumors: a potential regulatory role of IGF-1 pathway in distribution of p27Kip1 between different cyclins  
*Growth Factors* **17**:193–202 2000 [Abstract](#)
- 635 Karaiskou A, Perez LH, Ferby I, Ozon R, Jessus C and Nebreda AR  
Differential regulation of Cdc2 and Cdk2 by RINGO and cyclins  
*Journal of Biological Chemistry* **276**:36028–34 2001 [Abstract](#)
- 636 Karki S, LaMonte B and Holzbaur EL  
Characterization of the p22 subunit of dynactin reveals the localization of cytoplasmic dynein and dynactin to the midbody of dividing cells  
*Journal of Cell Biology* **142**:1023–34 1998 [Abstract](#)
- 637 Karow JK, Chakraverty RK and Hickson ID  
The Bloom's syndrome gene product is a 3'-5' DNA helicase  
*Journal of Biological Chemistry* **272**:30611–4 1997 [Abstract](#)
- 638 Karp JE, Kaufmann SH, Adjei AA, Lancet JE, Wright JJ and End DW  
Current status of clinical trials of farnesyltransferase inhibitors  
*Current Opinion in Oncology* **13**:470–6 2001 [Abstract](#)
- 639 Kasahara S, Aizawa K, Okamiya M, Kazuno N, Mutoh S, Fugo H, Cooper EL and Wago H  
UVB irradiation suppresses cytokine production and innate cellular immune functions in mice  
*Cytokine* **14**:104–11 2001 [Abstract](#)
- 640 Kashina AS, Baskin RJ, Cole DG, Wedaman KP, Saxton WM and Scholey JM  
A bipolar kinesin  
*Nature* **379**:270–2 1996 [Abstract](#)
- 641 Kastan MB and Lim DS Nat Rev  
The many substrates and functions of ATM  
*Molecular and Cellular Biology* **1**:179–86 2000 [Abstract](#)
- 642 Kastan MB, Zhan Q, el-Deiry WS, Carrier F, Jacks T, Walsh WV, Plunkett BS, Vogelstein B and Fornace AJ Jr  
A mammalian cell cycle checkpoint pathway utilizing p53 and GADD45 is defective in ataxia-telangiectasia  
*Cell* **71**:587–97 1992 [Abstract](#)
- 643 Katayama H, Zhou H, Li Q, Tatsuka M and Sen S  
Interaction and feedback regulation between STK15/BTAK/Aurora-A kinase and protein phosphatase 1 through mitotic cell division cycle  
*Journal of Biological Chemistry* in press 2001 [Abstract](#)
- 644 Kato H, Yoshikawa M, Fukai Y, Tajima K, Masuda N, Tsukada K, Kuwano H and Nakajima T  
An immunohistochemical study of p16, pRb, p21 and p53 proteins in human esophageal cancers  
*Anticancer Research* **20**:345–9 2000 [Abstract](#)
- 645 Kato J, Matsushime H, Hiebert SW, Ewen ME and Sherr CJ  
Direct binding of cyclin D to the retinoblastoma gene product (pRb) and pRb phosphorylation by the cyclin D-dependent kinase CDK4  
*Genes and Development* **7**:331–42 1993 [Abstract](#)
- 646 Kaufman DK, Kimmel DW, Parisi JE and Michels VV  
A familial syndrome with cutaneous malignant melanoma and cerebral astrocytoma  
*Neurology* **43**:1728–31 1993 [Abstract](#)
- 647 Kawakami T, Chiba T, Suzuki T, Iwai K, Yamanaka K, Minato N, Suzuki H, Shimbara N, Hidaka Y, Osaka F, Omata M and Tanaka K  
NEDD8 recruits E2-ubiquitin to SCF E3 ligase  
*EMBO Journal* **20**:4003–12 2001 [Abstract](#)
- 648 Kawamata N, Morosetti R, Miller CW, Park D, Spirin KS, Nakamaki T, Takeuchi S, Hatta Y, Simpson J, Wilczynski S et al  
Molecular analysis of the cyclin-dependent kinase inhibitor gene p27/Kip1 in human malignancies  
*Cancer Research* **55**:2266–9 1995 [Abstract](#)
- 649 Kawamura J, Sakurai M, Tsukamoto K and Tochigi H  
Leiomyosarcoma of the bladder eighteen years after cyclophosphamide therapy for retinoblastoma  
*Urologia Internationalis* **51**:49–53 1993 [Abstract](#)
- 650 Kawano Y, Fukata Y, Oshiro N, Amano M, Nakamura T, Ito M, Matsumura F, Inagaki M and Kaibuchi K  
Phosphorylation of myosin-binding subunit (MBS) of myosin phosphatase by Rho-kinase in vivo  
*Journal of Cell Biology* **147**:1023–38 1999 [Abstract](#)
- 651 Kazanietz MG  
Eyes wide shut: protein kinase C isozymes are not the only receptors for the phorbol ester tumor promoters  
*Molecular Carcinogenesis* **28**:5–11 2000 [Abstract](#)
- 652 Kearsley JM, Coates PJ, Prescott AR, Warbrick E and Hall PA  
Gadd45 is a nuclear cell cycle regulated protein which interacts with p21Cip1  
*Oncogene* **11**:1675–83 1995 [Abstract](#)
- 653 Kedzierski RM and Yanagisawa M  
Endothelin system: the double-edged sword in health and disease  
*Annual Review of Pharmacology and Toxicology* **41**:851–76 2001 [Abstract](#)
- 654 Keller-Melchior R, Schmidt R and Piepkorn M  
Expression of the tumor suppressor gene product p16INK4 in benign and malignant melanocytic lesions  
*Journal of Investigative Dermatology* **110**:932–8 1998 [Abstract](#)





- 655 Kennedy BK, Liu OW, Dick FA, Dyson N, Harlow E and Vidal M  
Histone deacetylase-dependent transcriptional repression by pRB in yeast occurs independently of interaction through the LXCXE binding cleft  
*Proceedings of the National Academy of Sciences of the USA* 98:8720–5 2001 [Abstract](#)
- 656 Kerkhoff E and Rapp UR  
Cell cycle targets of Ras/Raf signalling  
*Oncogene* 17:1457–62 1998 [Abstract](#)
- 657 Keryer G, Ris H and Borisy GG  
Centriole distribution during tripolar mitosis in Chinese hamster ovary cells  
*Journal of Cell Biology* 98:2222–9 1984 [Abstract](#)
- 658 Keyomarsi K and Herliczek TW  
The role of cyclin E in cell proliferation, development and cancer  
*Progress in Cell Cycle Research* 3:171–91 1997 [Abstract](#)
- 659 Khanna KK, Keating KE, Kozlov S, Scott S, Gatei M, Hobson K, Taya Y, Gabrielli B, Chan D, Lees-Miller SP and Lavin MF  
ATM associates with and phosphorylates p53: mapping the region of interaction  
*Nature Genetics* 20:398–400 1998 [Abstract](#)
- 660 Khanna KK and Jackson SP  
DNA double-strand breaks: signaling, repair and the cancer connection  
*Nature Genetics* 27:247–54 2001 [Abstract](#)
- 661 Khanna KK  
Cancer risk and the ATM gene: a continuing debate  
*Journal of the National Cancer Institute* 92:795–802 2000 [Abstract](#)
- 662 Kharbanda S, Yuan ZM, Weichselbaum R and Kufe D  
Determination of cell fate by c-Abl activation in the response to DNA damage  
*Oncogene* 17:3309–18 1998 [Abstract](#)
- 663 Khodjakov A, Cole RW, Oakley BR and Rieder CL  
Centrosome-independent mitotic spindle formation in vertebrates  
*Current Biology* 10:59–67 2000 [Abstract](#)
- 664 Khodjakov A and Rieder CL  
Centrosomes enhance the fidelity of cytokinesis in vertebrates and are required for cell cycle progression  
*Journal of Cell Biology* 153:237–42 2001 [Abstract](#)
- 665 Khosravi Far R, Solski PA, Clark GJ, Kinch MS and Der CJ  
Activation of Rac1, RhoA, and mitogen-activated protein kinases is required for Ras transformation  
*Molecular and Cellular Biology* 15:6443–53 1995 [Abstract](#)
- 666 Khosravi R, Maya R, Gottlieb T, Oren M, Shiloh Y and Shkedy D  
Rapid ATM-dependent phosphorylation of MDM2 precedes p53 accumulation in response to DNA damage  
*Proceedings of the National Academy of Sciences of the USA* 96:14973–7 1999 [Abstract](#)
- 667 Kienker LJ, Shin EK and Meek K  
Both V(D)J recombination and radioresistance require DNA-PK kinase activity, though minimal levels suffice for V(D)J recombination  
*Nucleic Acids Research* 28:2752–61 2000 [Abstract](#)
- 668 Kiguchi K, Ishiwata I, Ishiwata C, Tokieda Y, Iguchi M, Suzuki R, Saga M and Ishikawa H  
Establishment and characterization of melanoma cell line derived from malignant melanoma of human uterine cervix  
*Human Cell* 11:93–100 1998 [Abstract](#)
- 669 Kim AS, Kakalis LT, Abdul-Manan N, Liu GA and Rosen MK  
Autoinhibition and activation mechanisms of the Wiskott-Aldrich syndrome protein  
*Nature* 404:151–8 2000 [Abstract](#)
- 670 Kim CJ, Reintgen DS and Balch CM  
The new melanoma staging system  
*Cancer Control* 9:9–15 2002 [Abstract](#)
- 671 Kim H, Ham EK, Kim YI, Chi JG, Lee HS, Park SH, Jung YM, Myung NK, Lee MJ and Jang JJ  
Overexpression of cyclin D1 and cdk4 in tumorigenesis of sporadic hepatoblastomas  
*Cancer Letters* 131:177–83 1998 [Abstract](#)
- 672 Kim JH, Kang MJ, Park CU, Kwak HJ, Hwang Y and Koh GY  
Amplified CDK2 and cdc2 activities in primary colorectal carcinoma  
*Cancer* 85:546–53 1999 [Abstract](#)
- 673 Kim JH, Kiefer LL, Woychik RP, Wilkison WO, Truesdale A, Ittoop O, Willard D, Nichols J and Zemel MB  
Agouti regulation of intracellular calcium: role of melanocortin receptors  
*American Journal of Physiology* 272:E379–84 1997 [Abstract](#)
- 674 Kim M, Katayose Y, Li Q, Rakkar AN, Li Z, Hwang SG, Katayose D, Trepel J, Cowan KH and Seth P  
Recombinant adenovirus expressing Von Hippel-Lindau-mediated cell cycle arrest is associated with the induction of cyclin-dependent kinase inhibitor p27Kip1  
*Biochemical and Biophysical Research Communications* 253:672–7 1998 [Abstract](#)
- 675 Kim SH, Li Z and Sacks DB  
E-cadherin-mediated cell-cell attachment activates Cdc42  
*Journal of Biological Chemistry* 275:36999–7005 2000 [Abstract](#)
- 676 Kim SK, Ro JY, Kemp BL, Lee JS, Kwon TJ, Fong KM, Sekido Y, Minna JD, Hong WK and Mao L  
Identification of three distinct tumor suppressor loci on the short arm of chromosome 9 in small cell lung cancer  
*Cancer Research* 57:400–3 1997 [Abstract](#)
- 677 Kim ST, Lim DS, Canman CE and Kastan MB  
Substrate specificities and identification of putative substrates of ATM kinase family members  
*Journal of Biological Chemistry* 274:37538–43 1999 [Abstract](#)
- 678 Kim YG, Kim HJ, Kim DS, Kim SD, Han WS, Kim KH, Chung JH and Park KC  
Up-Regulation and redistribution of Bax in ultraviolet B-irradiated melanocytes  
*Pigment Cell Research* 13:352–7 2000 [Abstract](#)
- 679 Kimura K, Tsuji T, Takada Y, Miki T and Narumiya S  
Accumulation of GTP-bound RhoA during cytokinesis and a critical role of ECT2 in this accumulation  
*Journal of Biological Chemistry* 275:17233–6 2000 [Abstract](#)
- 680 Kinlen LJ, Webster AD, Bird AG, Haile R, Peto J, Sothhill JF and Thompson RA  
Prospective study of cancer in patients with hypogammaglobulinaemia  
*Lancet* 1:263–6 1985 [Abstract](#)

## Human metastatic melanoma in vitro

- 681 Kinoshita H, Shi Y, Sandefur C, Meisner LF, Chang C, Choon A, Reznikoff CR, Bova GS, Friedl A and Jarrard DF  
Methylation of the androgen receptor minimal promoter silences transcription in human prostate cancer  
*Cancer Research* **60**:3623–30 2000 [Abstract](#)
- 682 Kinzel V, Kaszkin M, Blume A and Richards J  
Epidermal growth factor inhibits transiently the progression from G2-phase to mitosis: a receptor-mediated phenomenon in various cells  
*Cancer Research* **50**:7932–6 1990 [Abstract](#)
- 683 Kippenberger S, Bernd A, Bereiter-Hahn J, Ramirez-Bosca A and Kaufmann R  
The mechanism of melanocyte dendrite formation: the impact of differentiating keratinocytes  
*Pigment Cell Research* **11**:34–7 1998 [Abstract](#)
- 684 Kippenberger S, Bernd A, Loitsch S, Muller J, Guschel M and Kaufmann R  
Cyclic stretch up-regulates proliferation and heat shock protein 90 expression in human melanocytes  
*Pigment Cell Research* **12**:246–51 1999 [Abstract](#)
- 685 Kippenberger S, Loitsch S, Muller J, Guschel M, Ramirez-Bosca A, Kaufmann R and Bernd A  
Melanocytes respond to mechanical stretch by activation of mitogen-activated protein kinases (MAPK)  
*Pigment Cell Research* **13**:278–80 2000 [Abstract](#)
- 686 Kirn D  
Oncolytic virotherapy for cancer with the adenovirus dl1520 (Onyx-015): results of phase I and II trials  
*Expert Opinion on Biological Therapy* **1**:525–38 2001 [Abstract](#)
- 687 Kirsch IR  
V(D)J recombination and ataxia-telangiectasia: a review  
*International Journal of Radiation Biology* **66**:S97–108 1994 [Abstract](#)
- 688 Kishi S, Zhou XZ, Ziv Y, Khoo C, Hill DE, Shiloh Y and Lu KP  
Telomeric protein Pin2/TRF1 as an important ATM target in response to double strand DNA breaks  
*Journal of Biological Chemistry* **276**:29282–91 2001 [Abstract](#)
- 689 Kitagawa M, Higashi H, Jung HK, Suzuki-Takahashi I, Ikeda M, Tamai K, Kato J, Segawa K, Yoshida E, Nishimura S and Taya Y  
The consensus motif for phosphorylation by cyclin D1-Cdk4 is different from that for phosphorylation by cyclin A/E-Cdk2  
*EMBO Journal* **15**:7060–9 1996 [Abstract](#)
- 690 Kitagawa M, Saitoh S, Ogino H, Okabe T, Matsumoto H, Okuyama A, Tamai K, Ohba Y, Yasuda H, Nishimura S et al  
cdc2-like kinase is associated with the retinoblastoma protein  
*Oncogene* **7**:1067–74 1992 [Abstract](#)
- 691 Kiyono T, Foster SA, Koop JI, McDougall JK, Galloway DA and Klingelutz AJ  
Both Rb/p16INK4a inactivation and telomerase activity are required to immortalize human epithelial cells  
*Nature* **396**:84–8 1998 [Abstract](#)
- 692 Klein-Parker HA, Warshawski L and Tron VA  
Melanocytes in human skin express bcl-2 protein  
*Journal of Cutaneous Pathology* **21**:297–301 1994 [Abstract](#)
- 693 Kluwe L, Bayer S, Baser ME, Hazim W, Haase W, Funsterer C, Mautner VF  
Identification of NF2 germ-line mutations and comparison with neurofibromatosis 2 phenotypes [published erratum appears in *Human Genetics* **99**:292]  
*Human Genetics* **98**:534–8 1996 [Abstract](#)
- 694 Knudsen ES and Wang JY  
Differential regulation of retinoblastoma protein function by specific Cdk phosphorylation sites  
*Journal of Biological Chemistry* **271**:8313–20 1996 [Abstract](#)
- 695 Knudsen ES and Wang JY  
Dual mechanisms for the inhibition of E2F binding to RB by cyclin-dependent kinase-mediated RB phosphorylation  
*Molecular and Cellular Biology* **17**:5771–83 1997 [Abstract](#)
- 696 Knudson AG Jr  
Mutation and cancer: statistical study of retinoblastoma  
*Proceedings of the National Academy of Sciences of the USA* **68**:820–3 1971 [Abstract](#)
- 697 Ko TC, Sheng HM, Reisman D, Thompson EA and Beauchamp RD  
Transforming growth factor-beta 1 inhibits cyclin D1 expression in intestinal epithelial cells  
*Oncogene* **10**:177–84 1995 [Abstract](#)
- 698 Kobayashi T, Urabe K, Winder A, Jimenez-Cervantes C, Imokawa G, Brewington T, Solano F, Garcia-Borrón JC and Hearing VJ  
Tyrosinase related protein 1 (TRP1) functions as a DHICA oxidase in melanin biosynthesis  
*EMBO Journal* **13**:5818–25 1994 [Abstract](#)
- 699 Kocabalkan O, Ozgur F, Erk Y, Gursu KG and Gungen Y  
Malignant melanoma in xeroderma pigmentosum patients: report of five cases  
*European Journal of Surgical Oncology* **23**:43–7 1997 [Abstract](#)
- 700 Koehler MR, Bosserhoff A, von Beust G, Bauer A, Blesch A, Buettner R, Schlegel J, Bogdahn U and Schmid M  
Assignment of the human melanoma inhibitory activity gene (MIA) to 19q13.32-q13.33 by fluorescence in situ hybridization (FISH)  
*Genomics* **35**:265–7 1996 [Abstract](#)
- 701 Koff A, Giordano A, Desai D, Yamashita K, Harper JW, Elledge S, Nishimoto T, Morgan DO, Franza BR and Roberts JM  
Formation and activation of a cyclin E-cdk2 complex during the G1 phase of the human cell cycle  
*Science* **257**:1689–94 1992 [Abstract](#)
- 702 Koga H, Araki N, Takeshima H, Nishi T, Hirota T, Kimura Y, Nakao M and Saya H  
Impairment of cell adhesion by expression of the mutant neurofibromatosis type 2 (NF2) genes which lack exons in the ERM-homology domain  
*Oncogene* **17**:801–10 1998 [Abstract](#)
- 703 Koh PS, Hughes GC, Faulkner GR, Keeble WW and Bagby GC  
The Fanconi anemia group C gene product modulates apoptotic responses to tumor necrosis factor-alpha and Fas ligand but does not suppress expression of receptors of the tumor necrosis factor receptor superfamily  
*Experimental Hematology* **27**:1–8 1999 [Abstract](#)
- 704 Kolch W  
Meaningful relationships: the regulation of the Ras/Raf/MEK/ERK pathway by protein interactions  
*Biochemical Journal* **351**:289–305 2000 [Abstract](#)
- 705 Kolch W, Heidecker G, Kochs G, Hummel R, Vahidi H, Mischak H, Finkenzeller G, Marme D and Rapp UR  
Protein kinase C alpha activates RAF-1 by direct phosphorylation  
*Nature* **364**:249–52 1993 [Abstract](#)
- 706 Kolluri R, Toliás KF, Carpenter CL, Rosen FS and Kirchhausen T  
Direct interaction of the Wiskott-Aldrich syndrome protein with the GTPase Cdc42  
*Proceedings of the National Academy of Sciences of the USA* **93**:5615–8 1996 [Abstract](#)



707	Kolodner RD and Marsischky GT Eukaryotic DNA mismatch repair <i>Current Opinion in Genetics and Development</i>	9:89–96	1999	<a href="#">Abstract</a>
708	Komatsu N, Takeuchi S, Ikezoe T, Tasaka T, Hata Y, Machida H, Williamson IK, Bartram CR, Koeffler HP and Taguchi H Mutations of the E2F4 gene in hematological malignancies having microsatellite instability <i>Blood</i>	95:1509–10	2000	<a href="#">Abstract</a>
709	Koontongkaew S, Chareonkitkajorn L, Chanvitan A, Leelakriangsak M and Amornphimoltham P Alterations of p53, pRb, cyclin D(1) and cdk4 in human oral and pharyngeal squamous cell carcinomas <i>Oral Oncology</i>	36:334–9	2000	<a href="#">Abstract</a>
710	Korabiowska M, Brinck U, Kotthaus I, Berger H and Droese M Comparative study of the expression of DNA mismatch repair genes, the adenomatous polyposis coli gene and growth arrest DNA damage genes in melanoma recurrences and metastases <i>Melanoma Research</i>	10:537–44	2000	<a href="#">Abstract</a>
711	Korf BR Malignancy in neurofibromatosis type 1 <i>Oncologist</i>	5:477–85	2000	<a href="#">Abstract</a>
712	Kos L, Aronson A, Takayama H, Maina F, Ponzetto C, Merlino G and Pavan W Hepatocyte growth factor/scatter factor-MET signaling in neural crest-derived melanocyte development <i>Pigment Cell Research</i>	12:13–21	1999	<a href="#">Abstract</a>
713	Koundrioukoff S, Jonsson ZO, Hasan S, de Jong RN, van der Vliet PC, Hottiger MO and Hubscher U A direct interaction between proliferating cell nuclear antigen (PCNA) and Cdk2 targets PCNA-interacting proteins for phosphorylation <i>Journal of Biological Chemistry</i>	275:22882–7	2000	<a href="#">Abstract</a>
714	Kraehn GM, Utikal J, Udart M, Greulich KM, Bezold G, Kaskel P, Leiter U and Peter RU Extra c-myc oncogene copies in high risk cutaneous malignant melanoma and melanoma metastases <i>British Journal of Cancer</i>	84:72–9	2001	<a href="#">Abstract</a>
715	Kraemer KH, Lee MM and Scotto J Xeroderma pigmentosum. Cutaneous, ocular, and neurologic abnormalities in 830 published cases <i>Archives of Dermatology</i>	123:241–50	1987	<a href="#">Abstract</a>
716	Kramer A, Horner S, Willer A, Fruehauf S, Hochhaus A, Hallek M and Hehlmann R Adhesion to fibronectin stimulates proliferation of wild-type and bcr/abl-transfected murine hematopoietic cells <i>Proceedings of the National Academy of Sciences of the USA</i>	96:2087–92	1999	<a href="#">Abstract</a>
717	Krasagakis K, Garbe C, Zouboulis CC and Orfanos CE Growth control of melanoma cells and melanocytes by cytokines <i>Recent Results in Cancer Research</i>	139: 169–82	1995	<a href="#">Abstract</a>
718	Kroft SH, Finn WG, Singleton TP, Ross CW, Sheldon S and Schnitzer B Follicular large cell lymphoma with immunoblastic features in a child with Wiskott-Aldrich syndrome: an unusual immunodeficiency-related neoplasm not associated with Epstein-Barr virus <i>American Journal of Clinical Pathology</i>	110:95–9	1998	<a href="#">Abstract</a>
719	Kroiss MM, Bosserhoff AK, Vogt T, Buettner R, Bogenrieder T, Landthaler M and Stolz W Loss of expression or mutations in the p73 tumour suppressor gene are not involved in the pathogenesis of malignant melanomas <i>Melanoma Research</i>	8:504–9	1998	<a href="#">Abstract</a>
720	Krucher NA, Zygmunt A, Mazloum N, Tamrakar S, Ludlow JW and Lee MY Interaction of the retinoblastoma protein (pRb) with the catalytic subunit of DNA polymerase delta (p125) <i>Oncogene</i>	19:5464–70	2000	<a href="#">Abstract</a>
721	Kruyt FA, Dijkmans LM, Arwert F and Joenje H Involvement of the Fanconi's anemia protein FAC in a pathway that signals to the cyclin B/cdc2 kinase <i>Cancer Research</i>	57:2244–51	1997	<a href="#">Abstract</a>
722	Kuchiki H, Saino M, Nobukuni T, Yasuda J, Maruyama T, Kayama T, Murakami Y and Sekiya T Detection of amplification of a chromosomal fragment at 6p21 including the cyclin D3 gene in a glioblastoma cell line by arbitrarily primed polymerase chain reaction <i>International Journal of Cancer</i>	85:113–6	2000	<a href="#">Abstract</a>
723	Kudoh T, Ishidate T, Moriyama M, Toyoshima K and Akiyama T G1 phase arrest induced by Wilms tumor protein WT1 is abrogated by cyclin/CDK complexes <i>Proceedings of the National Academy of Sciences of the USA</i>	92:4517–21	1995	<a href="#">Abstract</a>
724	Kulkarni MS, Daggett JL, Bender TP, Kuehl WM, Bergsagel PL and Williams ME Frequent inactivation of the cyclin-dependent kinase inhibitor p18 by homozygous deletion in multiple myeloma cell lines: ectopic p18 expression inhibits growth and induces apoptosis <i>Leukemia</i>	16:127–34	2002	<a href="#">Abstract</a>
725	Kumar CC Signaling by integrin receptors <i>Oncogene</i>	17:1365–73	1998	<a href="#">Abstract</a>
726	Kumar R, Smeds J, Berggren P, Straume O, Rozell BL, Akslen LA and Hemminki K A single nucleotide polymorphism in the 3'untranslated region of the CDKN2A gene is common in sporadic primary melanomas but mutations in the CDKN2B, CDKN2C, CDK4 and p53 genes are rare <i>International Journal of Cancer</i>	95:388–93	2001	<a href="#">Abstract</a>
727	Kumaresan KR and Lambert MW Fanconi anemia, complementation group A, cells are defective in ability to produce incisions at sites of psoralen interstrand cross-links <i>Carcinogenesis</i>	21:741–51	2000	<a href="#">Abstract</a>
728	Kuo KK, Sato N, Mizumoto K, Maehara N, Yonemasu H, Ker CG, Sheen PC and Tanaka M Centrosome abnormalities in human carcinomas of the gallbladder and intrahepatic and extrahepatic bile ducts <i>Hepatology</i>	31:59–64	2000	<a href="#">Abstract</a>
729	Kurokawa K and Kato J Cyclic AMP delays G2 progression and prevents efficient accumulation of cyclin B1 proteins in mouse macrophage cells <i>Cell Structure and Function</i>	23:357–65	1998	<a href="#">Abstract</a>
730	Kwon TK, Buchholz MA, Gabrielson EW and Nordin AA A novel cytoplasmic substrate for cdk4 and cdk6 in normal and malignant epithelial derived cells <i>Oncogene</i>	11:2077–83	1995	<a href="#">Abstract</a>
731	Lacey KR, Jackson PK and Stearns T Cyclin-dependent kinase control of centrosome duplication <i>Proceedings of the National Academy of Sciences of the USA</i>	96:2817–22	1999	<a href="#">Abstract</a>

## Human metastatic melanoma in vitro

- 732 Lackinger D, Ruppitsch W, Ramirez MH, Hirsch-Kauffmann M and Schweiger M  
Involvement of the Fanconi anemia protein FA-C in repair processes of oxidative DNA damages  
*FEBS Letters* **440**:103–6 1998 [Abstract](#)
- 733 Ladanyi M, Lewis R, Jhanwar SC, Gerald W, Huvos AG and Healey JH  
MDM2 and CDK4 gene amplification in Ewing's sarcoma  
*Journal of Pathology* **175**:211–7 1995 [Abstract](#)
- 734 Lai A, Lee JM, Yang WM, DeCaprio JA, Kaelin WG Jr, Seto E and Branton PE  
RBP1 recruits both histone deacetylase-dependent and -independent repression activities to retinoblastoma family proteins  
*Molecular and Cellular Biology* **19**:6632–41 1999 [Abstract](#)
- 735 Lai A, Marcellus RC, Corbell HB and Branton PE  
RBP1 induces growth arrest by repression of E2F-dependent transcription  
*Oncogene* **18**:2091–100 1999 [Abstract](#)
- 736 Lai S and El Naggar AK  
Differential expression of key cell cycle genes (p16/cyclin D1/pRb) in head and neck squamous carcinomas  
*Laboratory Investigation* **79**:255–60 1999 [Abstract](#)
- 737 Lai Z, Ferry KV, Diamond MA, Wee KE, Kim YB, Ma J, Yang T, Benfield PA, Copeland RA and Auger KR  
Human mdm2 mediates multiple mono-ubiquitination of p53 by a mechanism requiring enzyme isomerization  
*Journal of Biological Chemistry* **276**:31357–67 2001 [Abstract](#)
- 738 Laird PW and Jaenisch R  
DNA methylation and cancer  
*Human Molecular Genetics* **3 Spec No**:1487–95 1994 [Abstract](#)
- 739 Lal G and Gallinger S  
Familial adenomatous polyposis  
*Seminars in Surgical Oncology* **18**:314–23 2000 [Abstract](#)
- 740 Lam PY, Di Tomaso E, Ng HK, Pang JC, Roussel MF and Hjelm NM  
Expression of p19INK4d, CDK4, CDK6 in glioblastoma multiforme  
*British Journal of Neurosurgery* **14**:28–32 2000 [Abstract](#)
- 741 Lambert WC, Kuo HR and Lambert MW  
Xeroderma pigmentosum  
*Dermatologic Clinics* **13**:169–209 1995 [Abstract](#)
- 742 Lambert J, Onderwater J, Vander Haeghen Y, Vancoillie G, Koerten HK, Mommaas AM and Naeyaert JM  
Myosin V colocalizes with melanosomes and subcortical actin bundles not associated with stress fibers in human epidermal melanocytes  
*Journal of Investigative Dermatology* **111**:835–40 1998 [Abstract](#)
- 743 Land EJ and Riley PA  
Spontaneous redox reactions of dopaquinone and the balance between the eumelanin and pheomelanin pathways  
*Pigment Cell Research* **13**:273–7 2000 [Abstract](#)
- 744 Lane ME, Elend M, Heidmann D, Herr A, Marzodko S, Herzig A and Lehner CF  
A screen for modifiers of cyclin E function in *Drosophila melanogaster* identifies Cdk2 mutations, revealing the insignificance of putative phosphorylation sites in Cdk2  
*Genetics* **155**:233–44 2000 [Abstract](#)
- 745 Lange BM, Bachi A, Wilm M and Gonzalez C  
Hsp90 is a core centrosomal component and is required at different stages of the centrosome cycle in *Drosophila* and vertebrates  
*EMBO Journal* **19**:1252–62 2000 [Abstract](#)
- 746 Lapointe J, Lachance Y, Labrie Y, Labrie C, Lapointe J, Lachance Y, Labrie Y, Labrie C, Lapointe J, Lachance Y, Labrie Y and Labrie C  
A p18 mutant defective in CDK6 binding in human breast cancer cells  
*Cancer Research* **56**:4586–9 1996 [Abstract](#)
- 747 Laronga C, Yang HY, Neal C and Lee MH  
Association of the cyclin-dependent kinases and 14–3-3 sigma negatively regulates cell cycle progression  
*Journal of Biological Chemistry* **275**:23106–12 2000 [Abstract](#)
- 748 Lasorella A, Iavarone A and Israel MA  
Id2 specifically alters regulation of the cell cycle by tumor suppressor proteins  
*Molecular and Cellular Biology* **16**:2570–8 1996 [Abstract](#)
- 749 Lasorella A, Noseda M, Beyna M, Yokota Y and Iavarone A  
Id2 is a retinoblastoma protein target and mediates signalling by Myc oncoproteins  
*Nature* **407**:592–8 2000 [Abstract](#)
- 750 Latres E, Malumbres M, Sotillo R, Martin J, Ortega S, Martin-Caballero J, Flores JM, Cordon-Cardo C and Barbacid M  
Limited overlapping roles of P15(INK4b) and P18(INK4c) cell cycle inhibitors in proliferation and tumorigenesis  
*EMBO Journal* **19**:3496–506 2000 [Abstract](#)
- 751 Lau N, Feldkamp MM, Roncari L, Loehr AH, Shannon P, Gutmann DH and Guha A  
Loss of neurofibromin is associated with activation of RAS/MAPK and PI3-K/AKT signaling in a neurofibromatosis 1 astrocytoma  
*Journal of Neuropathology and Experimental Neurology* **59**:759–67 2000 [Abstract](#)
- 752 Laux DE, Curran EM, Welshons WV, Lubahn DB and Huang TH  
Hypermethylation of the Wilms' tumor suppressor gene CpG island in human breast carcinomas  
*Breast Cancer Research and Treatment* **56**:35–43 1999 [Abstract](#)
- 753 Lavin MF and Khanna KK  
ATM: the protein encoded by the gene mutated in the radiosensitive syndrome ataxia-telangiectasia.  
*International Journal of Radiation Biology* **75**:1201–14 1999 [Abstract](#)
- 754 Lavoie JN, L'Allemain G, Brunet A, Muller R and Pouyssegur J  
Cyclin D1 expression is regulated positively by the p42/p44MAPK and negatively by the p38/HOGMAPK pathway  
*Journal of Biological Chemistry* **271**:20608–16 1996 [Abstract](#)
- 755 Lazebnik YA, Medvedeva ND and Zenin VV  
Reversible G2 block in the cell cycle of Ehrlich ascites carcinoma cells  
*Experimental Cell Research* **195**:247–54 1991 [Abstract](#)
- 756 Leach FS, Nicolaides NC, Papadopoulos N, Liu B, Jen J, Parsons R, Peltomaki P, Sistonen P, Aaltonen LA, Nystrom-Lahti M et al  
Mutations of a mutS homolog in hereditary nonpolyposis colorectal cancer  
*Cell* **75**:1215–25 1993 [Abstract](#)
- 757 LeCouter JE, Kablar B, Hardy WR, Ying C, Megeney LA, May LL and Rudnicki MA  
Strain-dependent myeloid hyperplasia, growth deficiency, and accelerated cell cycle in mice lacking the Rb-related p107 gene  
*Molecular and Cellular Biology* **18**:7455–65 1998 [Abstract](#)



758	LeCouter JE, Kablar B, Whyte PF, Ying C and Rudnicki MA Strain-dependent embryonic lethality in mice lacking the retinoblastoma-related p130 gene <i>Development</i>	125:4669–79	1998	<a href="#">Abstract</a>
759	Lee EY, Chang CY, Hu N, Wang YC, Lai CC, Herrup K, Lee WH and Bradley A Mice deficient for Rb are nonviable and show defects in neurogenesis and haematopoiesis <i>Nature</i>	359:288–94	1992	<a href="#">Abstract</a>
760	Lee J, Kumagai A and Dunphy WG Positive regulation of Wee1 by Chk1 and 14–3-3 proteins <i>Molecular Biology of the Cell</i>	12:551–63	2001	<a href="#">Abstract</a>
761	Lee JO, Russo AA and Pavletich NP Structure of the retinoblastoma tumour-suppressor pocket domain bound to a peptide from HPV E7 <i>Nature</i>	391:859–65	1998	<a href="#">Abstract</a>
762	Lee JS, Collins KM, Brown AL, Lee CH and Chung JH hCds1-mediated phosphorylation of BRCA1 regulates the DNA damage response <i>Nature</i>	404:201–4	2000	<a href="#">Abstract</a>
763	Lee MH, Williams BO, Mulligan G, Mukai S, Bronson RT, Dyson N, Harlow E and Jacks T Targeted disruption of p107: functional overlap between p107 and Rb <i>Genes and Development</i>	10:1621–32	1996	<a href="#">Abstract</a>
764	Lee ST, Nicholls RD, Jong MT, Fukai K and Spritz RA Organization and sequence of the human P gene and identification of a new family of transport proteins <i>Genomics</i>	26:354–63	1995	<a href="#">Abstract</a>
765	Lee TH, Moffett P and Pelletier J The Wilms' tumor suppressor gene (wt1) product represses different functional classes of transcriptional activation domains <i>Nucleic Acids Research</i>	27:2889–97	1999	<a href="#">Abstract</a>
766	Lee WH, Bookstein R, Hong F, Young LJ, Shew JY and Lee EY Human retinoblastoma susceptibility gene: cloning, identification, and sequence <i>Science</i>	235:1394–9	1987	<a href="#">Abstract</a>
767	Lee WH, Shew JY, Hong FD, Sery TW, Donoso LA, Young LJ, Bookstein R and Lee EY The retinoblastoma susceptibility gene encodes a nuclear phosphoprotein associated with DNA binding activity <i>Nature</i>	329:642–5	1987	<a href="#">Abstract</a>
768	Lees JA, Buchkovich KJ, Marshak DR, Anderson CW and Harlow E The retinoblastoma protein is phosphorylated on multiple sites by human cdc2 <i>EMBO Journal</i>	10:4279–90	1991	<a href="#">Abstract</a>
769	Lennartsson J, Blume-Jensen P, Hermanson M, Ponten E, Carlberg M and Ronnstrand L Phosphorylation of Shc by Src family kinases is necessary for stem cell factor receptor/c-kit mediated activation of the Ras/MAP kinase pathway and c-fos induction <i>Oncogene</i>	18:5546–53	1999	<a href="#">Abstract</a>
770	Leteurtre F, Li X, Guardiola P, Le Roux G, Sergere JC, Richard P, Carosella ED and Gluckman E Accelerated telomere shortening and telomerase activation in Fanconi's anaemia <i>British Journal of Haematology</i>	105:883–93	1999	<a href="#">Abstract</a>
771	Levenberg S, Yarden A, Kam Z and Geiger B p27 is involved in N-cadherin-mediated contact inhibition of cell growth and S-phase entry <i>Oncogene</i>	18:869–76	1999	<a href="#">Abstract</a>
772	Leverrier Y, Lorenzi R, Blundell MP, Brickell P, Kinnon C, Ridley AJ and Thrasher AJ Cutting Edge: The Wiskott-Aldrich Syndrome Protein Is Required for Efficient Phagocytosis of Apoptotic Cells <i>Journal of Immunology</i>	166:4831–4834	2001	<a href="#">Abstract</a>
773	Levy C, Nechushtan H and Razin E A new role for the STAT3 inhibitor, PIAS3: a repressor of microphthalmia transcription factor <i>Journal of Biological Chemistry</i>	277:1962–6	2002	<a href="#">Abstract</a>
774	Lewis DC, Warren N, Shukla VK, Grimshaw D, Laidler P and Padua RA Gross rearrangements and deletions of the retinoblastoma gene are rare in malignant melanoma <i>Acta Dermato-Venereologica</i>	73:236	1993	<a href="#">Abstract</a>
775	Li DM and Sun H PTEN/MMAC1/TEP1 suppresses the tumorigenicity and induces G1 cell cycle arrest in human glioblastoma cells <i>Proceedings of the National Academy of Sciences of the USA</i>	95:15406–11	1998	<a href="#">Abstract</a>
776	Li G, Satyamoorthy K and Herlyn M N-cadherin-mediated intercellular interactions promote survival and migration of melanoma cells <i>Cancer Research</i>	61:3819–25	2001	<a href="#">Abstract</a>
777	Li G, Schaidler H, Satyamoorthy K, Hanakawa Y, Hashimoto K and Herlyn M Downregulation of E-cadherin and Desmoglein 1 by autocrine hepatocyte growth factor during melanoma development <i>Oncogene</i>	20:8125–35	2001	<a href="#">Abstract</a>
778	Li J and Tsai MD Novel insights into the INK4-CDK4/6-Rb pathway: counter action of gankyrin against INK4 proteins regulates the CDK4-mediated phosphorylation of Rb <i>Biochemistry</i>	41:3977–83	2002	<a href="#">Abstract</a>
779	Li JM, Hu PP, Shen X, Yu Y and Wang XF E2F4-RB and E2F4-p107 complexes suppress gene expression by transforming growth factor beta through E2F binding sites <i>Proceedings of the National Academy of Sciences of the USA</i>	94:4948–53	1997	<a href="#">Abstract</a>
780	Li L, Bales ES, Peterson CA and Legerski RJ Characterization of molecular defects in xeroderma pigmentosum group C <i>Nature Genetics</i>	5:413–7	1993	<a href="#">Abstract</a>
781	Li Q, Ahuja N, Burger PC and Issa JP Methylation and silencing of the Thrombospondin-1 promoter in human cancer <i>Oncogene</i>	18:3284–9	1999	<a href="#">Abstract</a>
782	Li S, Ting NS, Zheng L, Chen PL, Ziv Y, Shiloh Y, Lee EY and Lee WH Functional link of BRCA1 and ataxia telangiectasia gene product in DNA damage response <i>Nature</i>	406:210–5	2000	<a href="#">Abstract</a>
783	Li Y, Nichols MA, Shay JW and Xiong Y Transcriptional repression of the D-type cyclin-dependent kinase inhibitor p16 by the retinoblastoma susceptibility gene product pRb <i>Cancer Research</i>	54:6078–82	1994	<a href="#">Abstract</a>

## Human metastatic melanoma in vitro

- 784 Li YJ, Hoang-Xuan K, Zhou XP, Sanson M, Mokhtari K, Faillot T, Cornu P, Poisson M, Thomas G and Hamelin R  
Analysis of the p21 gene in gliomas  
*Journal of Neuro-Oncology* 40:107–11 1998 [Abstract](#)
- 785 Liang C and Stillman B  
Persistent initiation of DNA replication and chromatin-bound MCM proteins during the cell cycle in cdc6 mutants  
*Genes and Development* 11:3375–86 1997 [Abstract](#)
- 786 Liao MJ and Van Dyke T  
Critical role for Atm in suppressing V(D)J recombination-driven thymic lymphoma  
*Genes and Development* 13:1246–50 1999 [Abstract](#)
- 787 Limon J, Dal Cin P, Sait SN, Karakousis C and Sandberg AA  
Chromosome changes in metastatic human melanoma  
*Cancer Genetics and Cytogenetics* 30:201–11 1988 [Abstract](#)
- 788 Lin BT, Gruenwald S, Morla AO, Lee WH and Wang JY  
Retinoblastoma cancer suppressor gene product is a substrate of the cell cycle regulator cdc2 kinase  
*EMBO Journal* 10:857–64 1991 [Abstract](#)
- 789 Lin WC, Lin FT and Nevins JR  
Selective induction of E2F1 in response to DNA damage, mediated by ATM-dependent phosphorylation  
*Genes and Development* 15:1833–44 2001 [Abstract](#)
- 790 Lindeman GJ, Gaubatz S, Livingston DM and Ginsberg D  
The subcellular localization of E2F-4 is cell-cycle dependent  
*Proceedings of the National Academy of Sciences of the USA* 94:5095–100 1997 [Abstract](#)
- 791 Lindor NM, Furuichi Y, Kitao S, Shimamoto A, Arndt C and Jalal S Am  
Rothmund-Thomson syndrome due to RECQ4 helicase mutations: report and clinical and molecular comparisons with Bloom syndrome and Werner syndrome  
*Journal of Medical Genetics* 90:223–8 2000 [Abstract](#)
- 792 Lingle WL and Salisbury JL  
Altered centrosome structure is associated with abnormal mitoses in human breast tumors  
*American Journal of Pathology* 155:1941–51 1999 [Abstract](#)
- 793 Linke SP, Clarkin KC, Di Leonardo A, Tsou A and Wahl GM  
A reversible, p53-dependent G0/G1 cell cycle arrest induced by ribonucleotide depletion in the absence of detectable DNA damage  
*Genes and Development* 10:934–47 1996 [Abstract](#)
- 794 Linnekin D  
Early signaling pathways activated by c-Kit in hematopoietic cells  
*International Journal of Biochemistry and Cell Biology* 31:1053–74 1999 [Abstract](#)
- 795 Linnekin D, Mou S, Deberry CS, Weiler SR, Keller JR, Ruscetti FW and Longo DL  
Stem cell factor, the JAK-STAT pathway and signal transduction  
*Leukemia and Lymphoma* 27:439–44 1997 [Abstract](#)
- 796 Little M, Holmes G, Bickmore W, van Heyningen V, Hastie N and Wainwright B  
DNA binding capacity of the WT1 protein is abolished by Denys-Drash syndrome WT1 point mutations  
*Human Molecular Genetics* 4:351–8 1995 [Abstract](#)
- 797 Liu B, Parsons R, Papadopoulos N, Nicolaides NC, Lynch HT, Watson P, Jass JR, Dunlop M, Wyllie A, Peltomaki P, de la Chapelle A, Hamilton SR, Vogelstein B and Kinzler KW  
Analysis of mismatch repair genes in hereditary non-polyposis colorectal cancer patients  
*Nature Medicine* 2:169–74 1996 [Abstract](#)
- 798 Liu CW, Wang RH, Dohadwala M, Schonthal AH, Villa-Moruzzi E and Berndt N  
Inhibitory phosphorylation of PP1alpha catalytic subunit during the G(1)/S transition  
*Journal of Biological Chemistry* 274:29470–5 1999 [Abstract](#)
- 799 Liu J, Flanagan WM, Drazba JA, Estes ML, Barnett GH, Haqqi T, Kondo S and Barna BP  
The CDK inhibitor, p27Kip1, is required for IL-4 regulation of astrocyte proliferation  
*Journal of Immunology* 159:812–9 1997 [Abstract](#)
- 800 Liu Q, Guntuku S, Cui XS, Matsuoka S, Cortez D, Tamai K, Luo G, Carattini-Rivera S, DeMayo F, Bradley A, Donehower LA and Elledge SJ  
Chk1 is an essential kinase that is regulated by Atr and required for the G(2)/M DNA damage checkpoint  
*Genes and Development* 14:1448–59 2000 [Abstract](#)
- 801 Liyanage M, Weaver Z, Barlow C, Coleman A, Pankratz DG, Anderson S, Wynshaw-Boris A and Ried T  
Abnormal rearrangement within the alpha/delta T-cell receptor locus in lymphomas from Atm-deficient mice  
*Blood* 96:1940–6 2000 [Abstract](#)
- 802 Lohmann DR  
RB1 gene mutations in retinoblastoma  
*Human Mutation* 14:283–8 1999 [Abstract](#)
- 803 Longley MJ, Pierce AJ and Modrich P  
DNA polymerase delta is required for human mismatch repair in vitro  
*Journal of Biological Chemistry* 272:10917–21 1997 [Abstract](#)
- 804 Longstreth J  
Cutaneous malignant melanoma and ultraviolet radiation: a review  
*Cancer and Metastasis Reviews* 7:321–33 1988 [Abstract](#)
- 805 Lopez-Girona A, Kanoh J and Russell P  
Nuclear exclusion of Cdc25 is not required for the DNA damage checkpoint in fission yeast  
*Current Biology* 11:50–4 2001 [Abstract](#)
- 806 Lorenzi R, Brickell PM, Katz DR, Kinnon C and Thrasher AJ  
Wiskott-Aldrich syndrome protein is necessary for efficient IgG-mediated phagocytosis  
*Blood* 95:2943–6 2000 [Abstract](#)
- 807 Loubat A, Rochet N, Turchi L, Rezzonico R, Far DF, Auberger P, Rossi B and Ponzio G  
Evidence for a p23 caspase-cleaved form of p27[KIP1] involved in G1 growth arrest  
*Oncogene* 18:3324–33 1999 [Abstract](#)
- 808 Loughheed JC, Holton JM, Alber T, Bazan JF and Handel TM  
Structure of melanoma inhibitory activity protein, a member of a recently identified family of secreted proteins  
*Proceedings of the National Academy of Sciences of the USA* 98:5515–20 2001 [Abstract](#)
- 809 Lu D, Willard D, Patel IR, Kadwell S, Overton L, Kost T, Luther M, Chen W, Woychik RP, Wilkison WO et al  
Agouti protein is an antagonist of the melanocyte-stimulating-hormone receptor  
*Nature* 371:799–802 1994 [Abstract](#)



- 810 Lu SL, Kawabata M, Imamura T, Akiyama Y, Nomizu T, Miyazono K and Yuasa Y  
HNPCC associated with germline mutation in the TGF-beta type II receptor gene  
*Nature Genetics* **19**:17–8 1998 [Abstract](#)
- 811 Lubensky IA, Pack S, Ault D, Vortmeyer AO, Libutti SK, Choyke PL, Walther MM, Linehan WM and Zhuang Z  
Multiple neuroendocrine tumors of the pancreas in von Hippel-Lindau disease patients: histopathological and molecular genetic analysis  
*American Journal of Pathology* **153**:223–31 1998 [Abstract](#)
- 812 Ludlow JW, Glendening CL, Livingston DM and DeCarprio JA  
Specific enzymatic dephosphorylation of the retinoblastoma protein  
*Molecular and Cellular Biology* **13**:367–72 1993 [Abstract](#)
- 813 Ludlow JW, Shon J, Pipas JM, Livingston DM and DeCaprio JA  
The retinoblastoma susceptibility gene product undergoes cell cycle-dependent dephosphorylation and binding to and release from SV40 large T  
*Cell* **60**:387–96 1990 [Abstract](#)
- 814 Lukas J, Bartkova J and Bartek J  
Convergence of mitogenic signalling cascades from diverse classes of receptors at the cyclin D-cyclin-dependent kinase-pRb-controlled G1 checkpoint  
*Molecular and Cellular Biology* **16**:6917–25 1996 [Abstract](#)
- 815 Lukas J, Herzinger T, Hansen K, Moroni MC, Resnitzky D, Helin K, Reed SI and Bartek J  
Cyclin E-induced S phase without activation of the pRb/E2F pathway  
*Genes and Development* **11**:1479–92 1997 [Abstract](#)
- 816 Lukas J, Parry D, Aagaard L, Mann DJ, Bartkova J, Strauss M, Peters G and Bartek J  
Retinoblastoma-protein-dependent cell-cycle inhibition by the tumour suppressor p16  
*Nature* **375**:503–6 1995 [Abstract](#)
- 817 Lundberg R, Mavinakere M and Campbell C  
Deficient dna end joining activity in extracts from fanconi anemia fibroblasts  
*Journal of Biological Chemistry* **276**:9543–9 2001 [Abstract](#)
- 818 Luo G, Yao MS, Bender CF, Mills M, Bladl AR, Bradley A and Petriani JH  
Disruption of mRad50 causes embryonic stem cell lethality, abnormal embryonic development, and sensitivity to ionizing radiation  
*Proceedings of the National Academy of Sciences of the USA* **96**:7376–81 1999 [Abstract](#)
- 819 Luttrell LM and Lefkowitz RJ  
The role of beta-arrestins in the termination and transduction of G-protein-coupled receptor signals  
*Journal of Cell Science* **115**:455–65 2002 [Abstract](#)
- 820 Luo J, Su F, Chen D, Shiloh A and Gu W  
Deacetylation of p53 modulates its effect on cell growth and apoptosis  
*Nature* **408**:377–81 2000 [Abstract](#)
- 821 Ma C, Papermaster D and Cepko CL  
A unique pattern of photoreceptor degeneration in cyclin D1 mutant mice  
*Proceedings of the National Academy of Sciences of the USA* **95**:9938–43 1998 [Abstract](#)
- 822 Ma L, Siemssen ED, Noteborn HM and van der Eb AJ  
The xeroderma pigmentosum group B protein ERCC3 produced in the baculovirus system exhibits DNA helicase activity  
*Nucleic Acids Research* **22**:4095–102 1994 [Abstract](#)
- 823 Ma S, Trivinos-Lagos L, Graf R and Chisholm RL  
Dynein intermediate chain mediated dynein-dynactin interaction is required for interphase microtubule organization and centrosome replication and separation in Dictyostelium  
*Journal of Cell Biology* **147**:1261–74 1999 [Abstract](#)
- 824 Mack G and Rattner JB  
Centrosome repositioning immediately following karyokinesis and prior to cytokinesis  
*Cell Motility and the Cytoskeleton* **26**:239–47 1993 [Abstract](#)
- 825 Mackay AM, Ainsztein AM, Eckley DM and Earnshaw WC  
A dominant mutant of inner centromere protein (INCENP), a chromosomal protein, disrupts prometaphase congression and cytokinesis  
*Journal of Cell Biology* **140**:991–1002 1998 [Abstract](#)
- 826 Madaule P, Eda M, Watanabe N, Fujisawa K, Matsuoka T, Bito H, Ishizaki T and Narumiya S  
Role of citron kinase as a target of the small GTPase Rho in cytokinesis  
*Nature* **394**:491–4 1998 [Abstract](#)
- 827 Maeda K, Naganuma M, Fukuda M, Matsunaga J and Tomita Y  
Effect of pituitary and ovarian hormones on human melanocytes in vitro  
*Pigment Cell Research* **9**:204–12 1996 [Abstract](#)
- 828 Maelandsmo GM, Florenes VA, Hovig E, Oyjord T, Engebraaten O, Holm R, Borresen AL and Fodstad O  
Involvement of the pRb/p16/cdk4/cyclin D1 pathway in the tumorigenesis of sporadic malignant melanomas  
*British Journal of Cancer* **73**:909–16 1996 [Abstract](#)
- 829 Maes P, Brichard B, Vermeylen C, Cornu G and Ninane J  
Primary and secondary osteosarcoma of the face: a rare childhood malignancy  
*Medical and Pediatric Oncology* **30**:170–4 1998 [Abstract](#)
- 830 Maga G, Stucki M, Spadari S and Hubscher U  
DNA polymerase switching: I. Replication factor C displaces DNA polymerase alpha prior to PCNA loading  
*Journal of Molecular Biology* **295**:791–801 2000 [Abstract](#)
- 831 Magnaghi-Jaulin L, Groisman R, Naguibneva I, Robin P, Lorain S, Le Villain JP, Troalen F, Trouche D and Harel Bellan A  
Retinoblastoma protein represses transcription by recruiting a histone deacetylase  
*Nature* **391**:601–5 1998 [Abstract](#)
- 832 Mailand N, Falck J, Lukas C, Syljuasen RG, Welcker M, Bartek J and Lukas J  
Rapid destruction of human Cdc25A in response to DNA damage  
*Science* **288**:1425–9 2000 [Abstract](#)
- 833 Maillet P, Chappuis PO, Vaudan G, Dobbie Z, Muller H, Hutter P and Sappino AP  
A polymorphism in the ATM gene modulates the penetrance of hereditary non-polyposis colorectal cancer  
*International Journal of Cancer* **88**:928–31 2000 [Abstract](#)
- 834 Malek NP, Sundberg H, McGrew S, Nakayama K, Kyriakidis TR and Roberts JM  
A mouse knock-in model exposes sequential proteolytic pathways that regulate p27Kip1 in G1 and S phase  
*Nature* **413**:323–7 2001 [Abstract](#)

## Human metastatic melanoma in vitro

- 835 Mallery DL, Tanganelli B, Colella S, Steingrimsdottir H, van Gool AJ, Troelstra C, Stefanini M and Lehmann AR  
Molecular analysis of mutations in the CSB (ERCC6) gene in patients with Cockayne syndrome  
*American Journal of Human Genetics* **62**:77–85 1998 [Abstract](#)
- 836 Malumbres M, Perez de Castro I, Santos J, Melendez B, Mangués R, Serrano M, Pellicer A and Fernández Piqueras J  
Inactivation of the cyclin-dependent kinase inhibitor p15INK4b by deletion and de novo methylation with independence of p16INK4a alterations in murine primary T-cell lymphomas  
*Oncogene* **14**:1361–70 1997 [Abstract](#)
- 837 Mamillapalli R, Gavrilova N, Mihaylova VT, Tsvetkov LM, Wu H, Zhang H and Sun H  
PTEN regulates the ubiquitin-dependent degradation of the CDK inhibitor p27(KIP1) through the ubiquitin E3 ligase SCF(SKP2)  
*Current Biology* **11**:263–7 2001 [Abstract](#)
- 838 Mantel C, Braun SE, Reid S, Henegariu O, Liu L, Hangoc G and Broxmeyer HE  
p21(cip-1/waf-1) deficiency causes deformed nuclear architecture, centriole overduplication, polyploidy, and relaxed microtubule damage checkpoints in human hematopoietic cells  
*Blood* **93**:1390–8 1999 [Abstract](#)
- 839 Mao L, Merlo A, Bedi G, Shapiro GI, Edwards CD, Rollins BJ and Sidransky D  
A novel p16INK4A transcript  
*Cancer Research* **55**:2995–7 1995 [Abstract](#)
- 840 Marchand M, Brichard V, van Baren N and Coulié PG  
Biological and clinical developments in melanoma vaccines  
*Expert Opinion on Biological Therapy* **1**:497–510 2001 [Abstract](#)
- 841 Mariatos G, Gorgoulis VG, Zacharatos P, Kotsinas A, Vogiatzi T, Rassidakis G, Foukas P, Liloglou T, Tiniakos D, Angelou N, Manolis EN, Veslemes M, Field JK and Kittas C  
Expression of p16(INK4A) and alterations of the 9p21–23 chromosome region in non-small-cell lung carcinomas: relationship with tumor growth parameters and ploidy status  
*International Journal of Cancer* **89**:133–41 2000 [Abstract](#)
- 842 Marinissen MJ, Chiariello M and Gutkind JS  
Regulation of gene expression by the small GTPase Rho through the ERK6 (p38 gamma) MAP kinase pathway  
*Genes and Development* **15**:535–53 2001 [Abstract](#)
- 843 Marone M, Scambia G, Giannitelli C, Ferrandina G, Masciullo V, Bellacosa A, Benedetti-Panici P and Mancuso S  
Analysis of cyclin E and CDK2 in ovarian cancer: gene amplification and RNA overexpression  
*International Journal of Cancer* **75**:34–9 1998 [Abstract](#)
- 844 Marshall ES, Finlay GJ, Matthews JH, Shaw JH, Nixon J and Baguley BC  
Microculture-based chemosensitivity testing: a feasibility study comparing freshly explanted human melanoma cells with human melanoma cell lines  
*Journal of the National Cancer Institute* **84**: 340–5 1992 [Abstract](#)
- 845 Marshall ES, Holdaway KM, Shaw JH, Finlay GJ, Matthews JH and Baguley BC  
Anticancer drug sensitivity profiles of new and established melanoma cell lines  
*Oncology Research* **5**: 301–9 1993 [Abstract](#)
- 846 Marshall ES, Matthews JH, Shaw JH, Nixon J, Tumewu P, Finlay GJ, Holdaway KM and Baguley BC  
Radiosensitivity of new and established human melanoma cell lines: comparison of [3H]thymidine incorporation and soft agar clonogenic assays  
*European Journal of Cancer* **30A**:1370–6 1994 [Abstract](#)
- 847 Marshall WF, Vucica Y and Rosenbaum JL  
Kinetics and regulation of de novo centriole assembly. Implications for the mechanism of centriole duplication  
*Current Biology* **11**:308–17 2001 [Abstract](#)
- 848 Martelli F, Hamilton T, Silver DP, Sharpless NE, Bardeesy N, Rokas M, DePinho RA, Livingston DM and Grossman SR  
p19ARF targets certain E2F species for degradation  
*Proceedings of the National Academy of Sciences of the USA* **98**:4455–60 2001 [Abstract](#)
- 849 Martin K, Trouche D, Hagemeyer C, Sorensen TS, La Thangue NB and Kouzarides T  
Stimulation of E2F1/DP1 transcriptional activity by MDM2 oncoprotein  
*Nature* **375**:691–4 1995 [Abstract](#)
- 850 Martin-Caballero J, Flores JM, Garcia-Palencia P and Serrano M  
Tumor susceptibility of p21(Waf1/Cip1)-deficient mice  
*Cancer Research* **61**:6234–8 2001 [Abstract](#)
- 851 Masai H and Arai K  
Dbf4 motifs: conserved motifs in activation subunits for Cdc7 kinases essential for S-phase  
*Biochemical and Biophysical Research Communications* **275**:228–32 2000 [Abstract](#)
- 852 Masaki T, Ninomiya H, Sakamoto A and Okamoto Y  
Structural basis of the function of endothelin receptor  
*Molecular and Cell Biochemistry* **190**:153–6 1999 [Abstract](#)
- 853 Masciullo V, Scambia G, Marone M, Giannitelli C, Ferrandina G, Bellacosa A, Benedetti-Panici P and Mancuso S  
Altered expression of cyclin D1 and CDK4 genes in ovarian carcinomas  
*International Journal of Cancer* **74**:390–5 1997 [Abstract](#)
- 854 Masciullo V, Sgambato A, Pacilio C, Pucci B, Ferrandina G, Palazzo J, Carbone A, Cittadini A, Mancuso S, Scambia G and Giordano A  
Frequent loss of expression of the cyclin-dependent kinase inhibitor p27 in epithelial ovarian cancer  
*Cancer Research* **59**:3790–4 1999 [Abstract](#)
- 855 Masutani C, Kusumoto R, Yamada A, Dohmae N, Yokoi M, Yuasa M, Araki M, Iwai S, Takio K and Hanaoka F  
The XPV (xeroderma pigmentosum variant) gene encodes human DNA polymerase eta  
*Nature* **399**:700–4 1999 [Abstract](#)
- 856 Matsubara N, Yoshitaka T, Matsuno T, Ikeda M, Isozaki H, Tanaka N and Shimizu K  
Multiple tumors and a novel E2F-4 mutation. A case report  
*Digestion* **62**:213–6 2000 [Abstract](#)
- 857 Matsumoto Y, Hayashi K and Nishida E  
Cyclin-dependent kinase 2 (Cdk2) is required for centrosome duplication in mammalian cells  
*Current Biology* **9**:429–32 1999 [Abstract](#)
- 858 Matsuoka S, Rotman G, Ogawa A, Shiloh Y, Tamai K and Elledge SJ  
Ataxia telangiectasia-mutated phosphorylates Chk2 in vivo and in vitro  
*Proceedings of the National Academy of Sciences of the USA* **97**:10389–94 2000 [Abstract](#)
- 859 Matsushime H, Quelle DE, Shurtleff SA, Shibuya M, Sherr CJ and Kato JY  
D-type cyclin-dependent kinase activity in mammalian cells  
*Molecular and Cellular Biology* **14**:2066–76 1994 [Abstract](#)





860	Maulik G, Shrikhande A, Kijima T, Ma PC, Morrison PT and Salgia R Role of the hepatocyte growth factor receptor, c-Met, in oncogenesis and potential for therapeutic inhibition <i>Cytokine and Growth Factor Reviews</i>	13:41–59	2002	<a href="#">Abstract</a>
861	May P and May E Twenty years of p53 research: structural and functional aspects of the p53 protein <i>Oncogene</i>	18:7621–36	1999	<a href="#">Abstract</a>
862	Mayo MW, Wang CY, Drouin SS, Madrid LV, Marshall AF, Reed JC, Weissman BE and Baldwin AS WT1 modulates apoptosis by transcriptionally upregulating the bcl-2 proto-oncogene <i>EMBO Journal</i>	18:3990–4003	1999	<a href="#">Abstract</a>
863	Mayol X, Garriga J and Grana X Cell cycle-dependent phosphorylation of the retinoblastoma-related protein p130 <i>Oncogene</i>	11:801–8	1995	<a href="#">Abstract</a>
864	Mayor T, Stierhof YD, Tanaka K, Fry AM and Nigg EA The centrosomal protein C-Nap1 is required for cell cycle-regulated centrosome cohesion <i>Journal of Cell Biology</i>	151:837–46	2000	<a href="#">Abstract</a>
865	McClatchey AI, Saotome I, Mercer K, Crowley D, Gusella JF, Bronson RT and Jacks T Mice heterozygous for a mutation at the Nf2 tumor suppressor locus develop a range of highly metastatic tumors <i>Genes and Development</i>	12:1121–33	1998	<a href="#">Abstract</a>
866	McCormick F Cancer gene therapy: fringe or cutting edge? <i>Nature Rev Cancer</i>	1:130–41	2001	<a href="#">Abstract</a>
867	McGarrity TJ, Kulin HE and Zaino RJ Peutz-Jeghers syndrome <i>American Journal of Gastroenterology</i>	95:596–604	2000	<a href="#">Abstract</a>
868	McGarry TJ and Kirschner MW Geminin, an inhibitor of DNA replication, is degraded during mitosis <i>Cell</i>	93:1043–53	1998	<a href="#">Abstract</a>
869	McGovern VJ, Mihm MC Jr, Bailly C, Booth JC, Clark WH Jr, Cochran AJ, Hardy EG, Hicks JD, Levene A, Lewis MG, Little JH and Milton GW The classification of malignant melanoma and its histologic reporting <i>Cancer</i>	32:1446–57	1973	<a href="#">Abstract</a>
870	McShea A, Samuel T, Eppel JT, Galloway DA and Funk JO Identification of CIP-1-associated regulator of cyclin B (CARB), a novel p21-binding protein acting in the G2 phase of the cell cycle <i>Journal of Biological Chemistry</i>	275:23181–6	2000	<a href="#">Abstract</a>
871	Mead LJ, Gillespie MT, Hung JY, Rane US, Rayeroux KC, Irving LB and Campbell LJ Frequent loss of heterozygosity in early non-small cell lung cancers at chromosome 9p21 proximal to the CDKN2a gene <i>International Journal of Cancer</i>	71:213–7	1997	<a href="#">Abstract</a>
872	Medrano EE, Im S, Yang F and Abdel-Malek ZA Ultraviolet B light induces G1 arrest in human melanocytes by prolonged inhibition of retinoblastoma protein phosphorylation associated with long-term expression of the p21Waf-1/SDI-1/Cip-1 protein <i>Cancer Research</i>	55:4047–52	1995	<a href="#">Abstract</a>
873	Meek DW The role of p53 in the response to mitotic spindle damage <i>Pathologie Biologie</i>	48:246–54	2000	<a href="#">Abstract</a>
874	Meier F, Nesbit M, Hsu MY, Martin B, Van Belle P, Elder DE, Schaumburg-Lever G, Garbe C, Walz TM, Donatien P, Crombleholme TM and Herlyn M Human melanoma progression in skin reconstructs : biological significance of bFGF <i>American Journal of Pathology</i>	156:193–200	2000	<a href="#">Abstract</a>
875	Menasche G, Pastural E, Feldmann J, Certain S, Ersoy F, Dupuis S, Wulffraat N, Bianchi D, Fischer A, Le Deist F and de Saint Basile G Mutations in RAB27A cause Griscelli syndrome associated with haemophagocytic syndrome <i>Nature Genetics</i>	25:173–6	2000	<a href="#">Abstract</a>
876	Meng JJ, Lowrie DJ, Sun H, Dorsey E, Pelton PD, Bashour AM, Groden J, Ratner N and Ip W Interaction between two isoforms of the NF2 tumor suppressor protein, merlin, and between merlin and ezrin, suggests modulation of ERM proteins by merlin <i>Journal of Neuroscience Research</i>	62:491–502	2000	<a href="#">Abstract</a>
877	Menke AL, Shvarts A, Riteco N, van Ham RC, van der Eb AJ and Jochemsen AG Wilms' tumor 1-KTS isoforms induce p53-independent apoptosis that can be partially rescued by expression of the epidermal growth factor receptor or the insulin receptor <i>Cancer Research</i>	57:1353–63	1997	<a href="#">Abstract</a>
878	Menke AL, van der Eb AJ and Jochemsen AG The Wilms' tumor 1 gene: oncogene or tumor suppressor gene? <i>International Review of Cytology</i>	181:151–212	1998	<a href="#">Abstract</a>
879	Meraldi P, Lukas J, Fry AM, Bartek J and Nigg EA Centrosome duplication in mammalian somatic cells requires E2F and Cdk2-cyclin A <i>Nature Cell Biology</i>	1:88–93	1999	<a href="#">Abstract</a>
880	Meraldi P and Nigg EA Centrosome cohesion is regulated by a balance of kinase and phosphatase activities <i>Journal of Cell Science</i>	114:3749–57	2001	<a href="#">Abstract</a>
881	Merbs SL and Sidransky D Analysis of p16 (CDKN2/MTS-1/INK4A) alterations in primary sporadic uveal melanoma <i>Investigative Ophthalmology and Visual Science</i>	40:779–83	1999	<a href="#">Abstract</a>
882	Merienne K, Jacquot S, Zeniou M, Pannetier S, Sassone-Corsi P and Hanauer A Activation of RSK by UV-light: phosphorylation dynamics and involvement of the MAPK pathway <i>Oncogene</i>	19:4221–9	2000	<a href="#">Abstract</a>
883	Merlo A, Herman JG, Mao L, Lee DJ, Gabrielson E, Burger PC, Baylin SB and Sidransky D 5' CpG island methylation is associated with transcriptional silencing of the tumour suppressor p16/CDKN2/MTS1 in human cancers <i>Nature Medicine</i>	1:686–92	1995	<a href="#">Abstract</a>
884	Metcalfe JA, Parkhill J, Campbell L, Stacey M, Biggs P, Byrd PJ and Taylor AM Accelerated telomere shortening in ataxia telangiectasia <i>Nature Genetics</i>	13:350–3	1996	<a href="#">Abstract</a>

## Human metastatic melanoma in vitro

885	Meyerson M and Harlow E Identification of G1 kinase activity for cdk6, a novel cyclin D partner <i>Molecular and Cellular Biology</i>	14:2077-86	1994	<a href="#">Abstract</a>
886	Meyn MS Ataxia-telangiectasia, cancer and the pathobiology of the ATM gene <i>Clinical Genetics</i>	55:289-304	1999	<a href="#">Abstract</a>
887	Mian IS and Moser MJ The Fanconi anemia complementation group A protein contains a peroxidase domain <i>Molecular Genetics and Metabolism</i>	63:230-4	1998	<a href="#">Abstract</a>
888	Mihara K, Cao XR, Yen A, Chandler S, Driscoll B, Murphree AL, T'Ang A and Fung YK Cell cycle-dependent regulation of phosphorylation of the human retinoblastoma gene product <i>Science</i>	246:1300-3	1989	<a href="#">Abstract</a>
889	Mihara M, Shintani S, Nakahara Y, Kiyota A, Ueyama Y, Matsumura T and Wong DT Overexpression of CDK2 is a prognostic indicator of oral cancer progression <i>Japanese Journal of Cancer Research</i>	92:352-60	2001	<a href="#">Abstract</a>
890	Miki H, Nonoyama S, Zhu Q, Aruffo A, Ochs HD and Takenawa T Tyrosine kinase signaling regulates Wiskott-Aldrich syndrome protein function, which is essential for megakaryocyte differentiation <i>Cell Growth and Differentiation</i>	8:195-202	1997	<a href="#">Abstract</a>
891	Miller MB and Bassler BL Quorum sensing in bacteria <i>Annual Review of Microbiology</i>	55:165-99	2001	<a href="#">Abstract</a>
892	Miller ME and Cross FR Cyclin specificity: how many wheels do you need on a unicycle? <i>Journal of Cell Science</i>	114:1811-20	2001	<a href="#">Abstract</a>
893	Miller SJ, Suthiphongchai T, Zambetti GP and Ewen ME p53 binds selectively to the 5' untranslated region of cdk4, an RNA element necessary and sufficient for transforming growth factor beta- and p53-mediated translational inhibition of cdk4 <i>Molecular and Cellular Biology</i>	20:8420-31	2000	<a href="#">Abstract</a>
894	Miranti CK, Ohno S and Brugge JS Protein kinase C regulates integrin-induced activation of the extracellular regulated kinase pathway upstream of Shc <i>Journal of Biological Chemistry</i>	274:10571-81	1999	<a href="#">Abstract</a>
895	Miyashita T, Krajewski S, Krajewska M, Wang HG, Lin HK, Liebermann DA, Hoffman B and Reed JC Tumor suppressor p53 is a regulator of bcl-2 and bax gene expression in vitro and in vivo <i>Oncogene</i>	9:1799-805	1994	<a href="#">Abstract</a>
896	Miyaki M, Iijima T, Ishii R, Hishima T, Mori T, Yoshinaga K, Takami H, Kuroki T and Iwama T Molecular evidence for multicentric development of thyroid carcinomas in patients with familial adenomatous polyposis <i>American Journal of Pathology</i>	157:1825-7	2000	<a href="#">Abstract</a>
897	Miyamoto H, Shuin T, Torigoe S, Iwasaki Y and Kubota Y Retinoblastoma gene mutations in primary human bladder cancer <i>British Journal of Cancer</i>	71:831-5	1995	<a href="#">Abstract</a>
898	Mizzen CA, Yang XJ, Kokubo T, Brownell JE, Bannister AJ, Owen-Hughes T, Workman J, Wang L, Berger SL, Kouzarides T, Nakatani Y and Allis CD The TAF(II)250 subunit of TFIID has histone acetyltransferase activity <i>Cell</i>	87:1261-70	1996	<a href="#">Abstract</a>
899	Moberg K, Starz MA and Lees JA E2F-4 switches from p130 to p107 and pRB in response to cell cycle reentry <i>Molecular and Cellular Biology</i>	16:1436-49	1996	<a href="#">Abstract</a>
900	Modiano, JF Personal communication			
901	Modiano JF, Ritt MG, Wojcieszyn J and Smith R 3rd Growth arrest of melanoma cells is differentially regulated by contact inhibition and serum deprivation <i>DNA and Cell Biology</i>	18:357-67	1999	<a href="#">Abstract</a>
902	Mohamed AJ, Vargas L, Nore BF, Backesjo CM, Christensson B and Smith CI Nucleocytoplasmic shuttling of Bruton's tyrosine kinase <i>Journal of Biological Chemistry</i>	275:40614-9	2000	<a href="#">Abstract</a>
903	Moll AC, Imhof SM, Bouter LM and Tan KE Second primary tumors in patients with retinoblastoma. A review of the literature <i>Ophthalmic Genetics</i>	18:27-34	1997	<a href="#">Abstract</a>
904	Moller MB P27 in cell cycle control and cancer <i>Leukemia and Lymphoma</i>	39:19-27	2000	<a href="#">Abstract</a>
905	Moller MB, Nielsen O and Pedersen NT Cyclin D3 expression in non-Hodgkin lymphoma. Correlation with other cell cycle regulators and clinical features <i>American Journal of Clinical Pathology</i>	115:404-12	2001	<a href="#">Abstract</a>
906	Morgan SE and Kastan MB p53 and ATM: cell cycle, cell death, and cancer <i>Advances in Cancer Research</i>	71:1-25	1997	<a href="#">Abstract</a>
907	Morita E, Lee DG, Sugiyama M and Yamamoto S Expression of c-kit ligand in human keratinocytes <i>Archives of Dermatological Research</i>	286:273-7	1994	<a href="#">Abstract</a>
908	Morra M, Howie D, Grande MS, Sayos J, Wang N, Wu C, Engel P and Terhorst C X-linked lymphoproliferative disease: a progressive immunodeficiency <i>Annual Review of Immunology</i>	19:657-82	2001	<a href="#">Abstract</a>
909	Morrell D, Chase CL and Swift M Cancer and autoimmune disease in families with common variable immune deficiency <i>Genetic Epidemiology</i>	3:17-26	1986	<a href="#">Abstract</a>
910	Morris EJ and Dyson NJ Retinoblastoma protein partners (See also <a href="http://www.mgh.harvard.edu/depts/cancercenter/binding.html">http://www.mgh.harvard.edu/depts/cancercenter/binding.html</a> ) <i>Advances in Cancer Research</i>	82:1-54	2001	<a href="#">Abstract</a>
911	Morrison AJ, Sardet C and Herrera RE Retinoblastoma protein transcriptional repression through histone deacetylation of a single nucleosome <i>Molecular and Cellular Biology</i>	22:856-65	2002	<a href="#">Abstract</a>



- 912 Morse HG, Moore GE, Ortiz LM, Gonzalez R and Robinson WA  
Malignant melanoma: from subcutaneous nodule to brain metastasis  
*Cancer Genetics and Cytogenetics* 72:16–23 1994 [Abstract](#)
- 913 Morvillo V, Bover L and Mordoh J  
Identification and characterization of a 14 kDa immunosuppressive protein derived from IIB-MEL-J, a human melanoma cell line  
*Cellular and Molecular Biology* 42:779–795 1996 [Abstract](#)
- 914 Moscow JA, He R, Gnarr JR, Knutsen T, Weng Y, Zhao WP, Whang-Peng J, Linehan WM and Cowan KH  
Examination of human tumors for rhoA mutations  
*Oncogene* 9:189–94 1994 [Abstract](#)
- 915 Mossi R and Hubscher U  
Clamping down on clamps and clamp loaders--the eukaryotic replication factor C  
*European Journal of Biochemistry* 254:209–16 1998 [Abstract](#)
- 916 Mossi R, Jonsson ZO, Allen BL, Hardin SH and Hubscher U  
Replication factor C interacts with the C-terminal side of proliferating cell nuclear antigen  
*Journal of Biological Chemistry* 272:1769–76 1997 [Abstract](#)
- 917 Motta L, Porcaro AB, Ficarra V, D'Amico A, Piubello Q and Comunale L  
Leiomyosarcoma of the bladder fourteen years after cyclophosphamide therapy for retinoblastoma  
*Scandinavian Journal of Urology and Nephrology* 35:248–9 2001 [Abstract](#)
- 918 Mountain V, Simerly C, Howard L, Ando A, Schatten G and Compton DA  
The kinesin-related protein, HSET, opposes the activity of Eg5 and cross-links microtubules in the mammalian mitotic spindle  
*Journal of Cell Biology* 147:351–66 1999 [Abstract](#)
- 919 Mukai M, Nakamura H, Tatsuta M, Iwasaki T, Togawa A, Imamura F and Akeido H  
Hepatoma cell migration through a mesothelial cell monolayer is inhibited by cyclic AMP-elevating agents via a Rho-dependent pathway  
*FEBS Letters* 484:69–73 2000 [Abstract](#)
- 920 Mukai N, Kobayashi S and Oguri M  
Ultrastructural studies of human adenovirus-produced retinoblastoma-like neoplasms in Sprague-Dawley rats  
*Investigative Ophthalmology* 13:593–601 1974 [Abstract](#)
- 921 Mukai N, Nakajima T, Freddo T, Jacobson M and Dunn M  
Retinoblastoma-like neoplasm induced in C3H/BifB/Ki strain mice by human adenovirus serotype 12  
*Acta Neuropathologica* 39:147–55 1977 [Abstract](#)
- 922 Mukhopadhyay D, Knebelmann B, Cohen HT, Ananth S, Sukhatme VP  
The von Hippel-Lindau tumor suppressor gene product interacts with Sp1 to repress vascular endothelial growth factor promoter activity  
*Molecular and Cellular Biology* 17:5629–39 1997 [Abstract](#)
- 923 Muller A and Fishel R  
Mismatch repair and the hereditary non-polyposis colorectal cancer syndrome (HNPCC)  
*Cancer Investigation* 20:102–9 2002 [Abstract](#)
- 924 Muller H, Moroni MC, Vigo E, Petersen BO, Bartek J and Helin K  
Induction of S-phase entry by E2F transcription factors depends on their nuclear localization  
*Molecular and Cellular Biology* 17:5508–20 1997 [Abstract](#)
- 925 Munro J, Stott FJ, Vousden KH, Peters G and Parkinson EK  
Role of the alternative INK4A proteins in human keratinocyte senescence: evidence for the specific inactivation of p16INK4A upon immortalization  
*Cancer Research* 59:2516–21 1999 [Abstract](#)
- 926 Murata Hori M, Fumoto K, Fukuta Y, Iwasaki T, Kikuchi A, Tatsuka M and Hosoya H  
Myosin II regulatory light chain as a novel substrate for AIM-1, an aurora/Ipl1p-related kinase from rat  
*Journal of Biochemistry (Tokyo)* 128:903–7 2000 [Abstract](#)
- 927 Mussman JG, Horn HF, Carroll PE, Okuda M, Tarapore P, Donehower LA and Fukasawa K  
Synergistic induction of centrosome hyperamplification by loss of p53 and cyclin E overexpression  
*Oncogene* 19:1635–46 2000 [Abstract](#)
- 928 Nagahara H, Ezhevsky SA, Vocero-Akbani AM, Kaldis P, Solomon MJ and Dowdy SF  
Transforming growth factor beta targeted inactivation of cyclin E: cyclin-dependent kinase 2 (Cdk2) complexes by inhibition of Cdk2 activating kinase activity  
*Proceedings of the National Academy of Sciences of the USA* 96:14961–6 1999 [Abstract](#)
- 929 Nagata D, Suzuki E, Nishimatsu H, Satonaka H, Goto A, Omata M and Hirata Y  
Transcriptional activation of the cyclin D1 gene is mediated by multiple cis-elements, including SP1 sites and a cAMP-responsive element in vascular endothelial cells  
*Journal of Biological Chemistry* 276:662–9 2001 [Abstract](#)
- 930 Nakamura M, Yonekawa Y, Kleihues P and Ohgaki H  
Promoter hypermethylation of the RB1 gene in glioblastomas  
*Laboratory Investigation* 81:77–82 2001 [Abstract](#)
- 931 Nakamura M, Zhou XZ and Lu KP  
Critical role for the EB1 and APC interaction in the regulation of microtubule polymerization  
*Current Biology* 11:1062–7 2001 [Abstract](#)
- 932 Nakamura T, Monden Y, Kawashima K, Naruke T and Nishimura S  
Failure to detect mutations in the retinoblastoma protein-binding domain of the transcription factor E2F-1 in human cancers  
*Japanese Journal of Cancer Research* 87:1204–9 1996 [Abstract](#)
- 933 Nakanishi M, Kaneko Y, Matsushima H and Ikeda K  
Direct interaction of p21 cyclin-dependent kinase inhibitor with the retinoblastoma tumor suppressor protein  
*Biochemical and Biophysical Research Communications* 263:35–40 1999 [Abstract](#)
- 934 Nakayama K, Ishida N, Shirane M, Inomata A, Inoue T, Shishido N, Horii I, Loh DY and Nakayama K  
Mice lacking p27(Kip1) display increased body size, multiple organ hyperplasia, retinal dysplasia, and pituitary tumors  
*Cell* 85:707–20 1996 [Abstract](#)
- 935 Nakayama K, Nagahama H, Minamishima YA, Matsumoto M, Nakamichi I, Kitagawa K, Shirane M, Tsunematsu R, Tsukiyama T, Ishida N, Kitagawa M, Nakayama K and Hatakeyama S  
Targeted disruption of Skp2 results in accumulation of cyclin E and p27(Kip1), polyploidy and centrosome overduplication  
*EMBO Journal* 19:2069–81 2000 [Abstract](#)
- 936 Nakayama K and Nakayama K  
Cip/Kip cyclin-dependent kinase inhibitors: brakes of the cell cycle engine during development  
*Bioessays* 20:1020–9 1998 [Abstract](#)

## Human metastatic melanoma in vitro

- 937 Nakazawa K, Sahuc F, Damour O, Collombel C and Nakazawa H  
Regulatory effects of heat on normal human melanocyte growth and melanogenesis: comparative study with UVB  
*Journal of Investigative Dermatology* **110**:972–7 1998 [Abstract](#)
- 938 Nataraj AJ, Olivos-Glander I, Kusukawa N and Highsmith WE Jr  
Single-strand conformation polymorphism and heteroduplex analysis for gel-based mutation detection  
*Electrophoresis* **20**:1177–85 1999 [Abstract](#)  
<http://physics.nist.gov/cuu/Units/index.html>
- 939 National Institute of Science and Technology, USA
- 940 Napolitano A, Memoli S, Crescenzi O and Prota G  
Oxidative Polymerization of the Pheomelanin Precursor 5-Hydroxy-1,4-benzothiazinylalanine: A New Hint to the Pigment Structure  
*Journal of Organic Chemistry* **61**:598–604 1996 [Abstract](#)
- 941 Nead MA, Baglia LA, Antinore MJ, Ludlow JW and McCance DJ  
Rb binds c-Jun and activates transcription  
*EMBO Journal* **17**:2342–52 1998 [Abstract](#)
- 942 Nelson MA, Ariza ME, Yang JM, Thompson FH, Taetle R, Trent JM, Wymer J, Massey-Brown K, Broome-Powell M, Easton J, Lahti JM and Kidd VJ  
Abnormalities in the p34cdc2-related PITSLRE protein kinase gene complex (CDC2L) on chromosome band 1p36 in melanoma  
*Cancer Genetics and Cytogenetics* **108**:91–9 1999 [Abstract](#)
- 943 Newell-Price J, King P and Clark AJ  
The CpG island promoter of the human proopiomelanocortin gene is methylated in nonexpressing normal tissue and tumors and represses expression  
*Molecular Endocrinology* **15**:338–48 2001 [Abstract](#)
- 944 Ng HK, Tse JY and Poon WS  
Cerebellar astrocytoma associated with von Hippel-Lindau disease: case report with molecular findings  
*British Journal of Neurosurgery* **13**:504–7 1999 [Abstract](#)
- 945 Ng MH, Chung YF, Lo KW, Wickham NW, Lee JC and Huang DP  
Frequent hypermethylation of p16 and p15 genes in multiple myeloma  
*Blood* **89**:2500–6 1997 [Abstract](#)
- 946 Nichols AF, Ong P and Linn S  
Mutations specific to the xeroderma pigmentosum group E Ddb- phenotype  
*Journal of Biological Chemistry* **271**:24317–20 1996 [Abstract](#)
- 947 Nicolaides NC, Papadopoulos N, Liu B, Wei YF, Carter KC, Ruben SM, Rosen CA, Haseltine WA, Fleischmann RD, Fraser CM et al  
Mutations of two PMS homologues in hereditary nonpolyposis colon cancer  
*Nature* **371**:75–80 1994 [Abstract](#)
- 948 Nicolas E, Morales V, Magnaghi-Jaulin L, Harel-Bellan A, Richard-Foy H and Trouche D  
RbAp48 belongs to the histone deacetylase complex that associates with the retinoblastoma protein  
*Journal of Biological Chemistry* **275**:9797–804 2000 [Abstract](#)
- 949 Niedobitek G, Meru N and Delecluse HJ  
Epstein-Barr virus infection and human malignancies  
*International Journal of Experimental Pathology* **82**:149–70 2001 [Abstract](#)
- 950 Nigg EA Nat Rev  
Mitotic kinases as regulators of cell division and its checkpoints  
*Molecular and Cellular Biology* **2**:21–32 2001 [Abstract](#)
- 951 Nigg EA, Blangy A and Lane HA  
Dynamic changes in nuclear architecture during mitosis: on the role of protein phosphorylation in spindle assembly and chromosome segregation  
*Experimental Cell Research* **229**:174–80 1996 [Abstract](#)
- 952 Nilsson I and Hoffmann I  
Cell cycle regulation by the Cdc25 phosphatase family  
*Progress in Cell Cycle Research* **4**:107–14 2000 [Abstract](#)
- 953 Nishimura EK, Yoshida H, Kunisada T and Nishikawa SI  
Regulation of E- and P-cadherin expression correlated with melanocyte migration and diversification  
*Developmental Biology* **215**:155–66 1999 [Abstract](#)
- 954 Nishioka E, Funasaka Y, Kondoh H, Chakraborty AK, Mishima Y and Ichihashi M  
Expression of tyrosinase, TRP-1 and TRP-2 in ultraviolet-irradiated human melanomas and melanocytes: TRP-2 protects melanoma cells from ultraviolet B induced apoptosis  
*Melanoma Research* **9**:433–43 1999 [Abstract](#)
- 955 Noh SJ, Li Y, Xiong Y and Guan KL  
Identification of functional elements of p18INK4C essential for binding and inhibition of cyclin-dependent kinase (CDK) 4 and CDK6  
*Cancer Research* **59**:558–64 1999 [Abstract](#)
- 956 Nollet F, Bex G and van Roy F  
The role of the E-cadherin/catenin adhesion complex in the development and progression of cancer  
*Molecular and Cellular Biology Research Communications* **2**:77–85 1999 [Abstract](#)
- 957 Nord B, Platz A, Smoczyński K, Kytola S, Robertson G, Calender A, Murat A, Weintraub D, Burgess J, Edwards M, Skogseid B, Owen D, Lassam N, Hogg D, Larsson C and Teh BT  
Malignant melanoma in patients with multiple endocrine neoplasia type 1 and involvement of the MEN1 gene in sporadic melanoma  
*International Journal of Cancer* **87**:463–7 2000 [Abstract](#)
- 958 North K Am  
Neurofibromatosis Type 1  
*Journal of Medical Genetics* **97**:119–127 2000 [Abstract](#)
- 959 Nospikel T and Clarkson SG  
Mutations that disable the DNA repair gene XPG in a xeroderma pigmentosum group G patient  
*Human Molecular Genetics* **3**:963–7 1994 [Abstract](#)
- 960 Novak A and Dedhar S  
Signaling through beta-catenin and Lef/Tcf  
*Cellular and Molecular Life Sciences* **56**:523–37 1999 [Abstract](#)
- 961 Nozaki S, Abrams JS, Pearce MK and Sauder DN  
Augmentation of granulocyte/macrophage colony-stimulating factor expression by ultraviolet irradiation is mediated by interleukin 1 in Pam 212 keratinocytes  
*Journal of Investigative Dermatology* **97**:10–4 1991 [Abstract](#)



- 962 Oakeley EJ  
DNA methylation analysis: a review of current methodologies  
*Pharmacology and Therapeutics* **84**:389–400 1999 [Abstract](#)
- 963 Ochs HD  
The Wiskott-Aldrich syndrome  
*Clinical Reviews in Allergy and Immunology* **20**:61–86 2001 [Abstract](#)
- 964 O'Connell KF, Caron C, Kopish KR, Hurd DD, Kempfues KJ, Li Y and White JG  
The *C. elegans* zyg-1 gene encodes a regulator of centrosome duplication with distinct maternal and paternal roles in the embryo  
*Cell* **105**:547–58 2001 [Abstract](#)
- 965 O'Connell MJ, Walworth NC and Carr AM  
The G2-phase DNA-damage checkpoint  
*Trends in Cell Biology* **10**:296–303 2000 [Abstract](#)
- 966 Oei P  
Personal communication
- 967 O'Hagan RC, Ohh M, David G, de Alboran IM, Alt FW, Kaelin WG Jr and DePinho RA  
Myc-enhanced expression of Cul1 promotes ubiquitin-dependent proteolysis and cell cycle progression  
*Genes and Development* **14**:2185–91 2000 [Abstract](#)
- 968 Ohta Y, Haire RN, Litman RT, Fu SM, Nelson RP, Kratz J, Kornfeld SJ, de la Morena M, Good RA and Litman GW  
Genomic organization and structure of Bruton agammaglobulinemia tyrosine kinase: localization of mutations associated with varied clinical presentations and course in X chromosome-linked agammaglobulinemia  
*Proceedings of the National Academy of Sciences of the USA* **91**:9062–6 1994 [Abstract](#)
- 969 Ohtani-Fujita N, Dryja TP, Rapaport JM, Fujita T, Matsumura S, Ozasa K, Watanabe Y, Hayashi K, Maeda K, Kinoshita S, Matsumura T, Ohnishi Y, Hotta Y, Takahashi R, Kato MV, Ishizaki K, Sasaki MS, Horsthemke B, Minoda K and Sakai T  
Hypermethylation in the retinoblastoma gene is associated with unilateral, sporadic retinoblastoma  
*Cancer Genetics and Cytogenetics* **98**:43–9 1997 [Abstract](#)
- 970 Ohtani-Fujita N, Fujita T, Aoike A, Osifchin NE, Robbins PD and Sakai T  
CpG methylation inactivates the promoter activity of the human retinoblastoma tumor-suppressor gene  
*Oncogene* **8**:1063–7 1993 [Abstract](#)
- 971 Ohtani-Fujita N, Fujita T, Takahashi R, Robbins PD, Dryja TP and Sakai T  
A silencer element in the retinoblastoma tumor-suppressor gene  
*Oncogene* **9**:1703–11 1994 [Abstract](#)
- 972 Ohtani N, Zebedee Z, Huot TJ, Stinson JA, Sugimoto M, Ohashi Y, Sharrocks AD, Peters G and Hara E  
Opposing effects of Ets and Id proteins on p16INK4a expression during cellular senescence  
*Nature* **409**:1067–70 2001 [Abstract](#)
- 973 Okazaki K, Uzuka M, Morikawa F, Toda K and Seiji M  
Transfer mechanism of melanosomes in epidermal cell culture  
*Journal of Investigative Dermatology* **67**:541–7 1976 [Abstract](#)
- 974 Okuda M, Horn HF, Tarapore P, Tokuyama Y, Smulian AG, Chan PK, Knudsen ES, Hofmann IA, Snyder JD, Bove KE and Fukasawa K  
Nucleophosmin/B23 is a target of CDK2/cyclin E in centrosome duplication  
*Cell* **103**:127–40 2000 [Abstract](#)
- 975 Okuda T, Shurtleff SA, Valentine MB, Raimondi SC, Head DR, Behm F, Curcio-Brint AM, Liu Q, Pui CH, Sherr CJ et al  
Frequent deletion of p16INK4a/MTS1 and p15INK4b/MTS2 in pediatric acute lymphoblastic leukemia  
*Blood* **85**:2321–30 1995 [Abstract](#)
- 976 Ollmann MM, Lamoreux ML, Wilson BD and Barsh GS  
Interaction of Agouti protein with the melanocortin 1 receptor in vitro and in vivo  
*Genes and Development* **12**:316–30 1998 [Abstract](#)
- 977 Olschwang S, Richard S, Boisson C, Giraud S, Laurent-Puig P, Resche F and Thomas G  
Germline mutation profile of the VHL gene in von Hippel-Lindau disease and in sporadic hemangioblastoma  
*Human Mutation* **12**:424–30 1998 [Abstract](#)
- 978 Omura-Minamisawa M, Diccianni MB, Batova A, Chang RC, Bridgeman LJ, Yu J, Pullen J, Bowman WP and Yu AL  
Universal inactivation of both p16 and p15 but not downstream components is an essential event in the pathogenesis of T-cell acute lymphoblastic leukemia  
*Clin Cancer Research* **6**:1219–28 2000 [Abstract](#)
- 979 Opdecamp K, Nakayama A, Nguyen MT, Hodgkinson CA, Pavan WJ and Arnheiter H  
Melanocyte development in vivo and in neural crest cell cultures: crucial dependence on the Mitf basic-helix-loop-helix-zipper transcription factor  
*Development* **124**:2377–86 1997 [Abstract](#)
- 980 O'Reilly MS, Holmgren L, Chen C and Folkman J  
Angiostatin induces and sustains dormancy of human primary tumors in mice  
*Nature Medicine* **2**:689–92 1996 [Abstract](#)
- 981 Orlov I, Lacombe L, Hannon GJ, Serrano M, Pellicer I, Dalbagni G, Reuter VE, Zhang ZF, Beach D and Cordon Cardo C  
Deletion of the p16 and p15 genes in human bladder tumors  
*Journal of the National Cancer Institute* **87**:1524–9 1995 [Abstract](#)
- 982 Omer CA, Miller PJ, Diehl RE and Kral AM  
Identification of Tcf4 residues involved in high-affinity beta-catenin binding  
*Biochemical and Biophysical Research Communications* **256**:584–90 1999 [Abstract](#)
- 983 Osman I, Scher H, Zhang ZF, Soos TJ, Hamza R, Eissa S, Khaled H, Koff A and Cordon Cardo C  
Expression of cyclin D1, but not cyclins E and A, is related to progression in bilharzial bladder cancer  
*Clin Cancer Research* **3**:2247–51 1997 [Abstract](#)
- 984 O'Sullivan E, Kinnon C and Brickell P  
Wiskott-Aldrich syndrome protein, WASP  
*International Journal of Biochemistry and Cell Biology* **31**:383–7 1999 [Abstract](#)
- 985 Ottaviano YL, Issa JP, Parl FF, Smith HS, Baylin SB and Davidson NE  
Methylation of the estrogen receptor gene CpG island marks loss of estrogen receptor expression in human breast cancer cells  
*Cancer Research* **54**:2552–5 1994 [Abstract](#)
- 986 Otterson GA, Khleif SN, Chen W, Coxon AB and Kaye FJ  
CDKN2 gene silencing in lung cancer by DNA hypermethylation and kinetics of p16INK4 protein induction by 5-aza 2'deoxytidine  
*Oncogene* **11**:1211–6 1995 [Abstract](#)
- 987 Ouchi T, Monteiro AN, August A, Aaronson SA and Hanafusa H  
BRCA1 regulates p53-dependent gene expression  
*Proceedings of the National Academy of Sciences of the USA* **95**:2302–6 1998 [Abstract](#)

## Human metastatic melanoma in vitro

- 988 Ohyashiki JH, Ohyashiki K, Gibas Z, Karakousis C and Sandberg AA  
Cytogenetic findings in a malignant melanoma and its derived cell line  
*Cancer Genetics and Cytogenetics* **23**:77–85 1986 [Abstract](#)
- 989 Olivares C, Jimenez-Cervantes C, Lozano JA, Solano F and Garcia Borrón JC  
The 5,6-dihydroxyindole-2-carboxylic acid (DHICA) oxidase activity of human tyrosinase  
*Biochemical Journal* **354**:131–9 2001 [Abstract](#)
- 990 Ono H, Kawa Y, Asano M, Ito M, Takano A, Kubota Y, Matsumoto J and Mizoguchi M  
Development of melanocyte progenitors in murine Steel mutant neural crest explants cultured with stem cell factor, endothelin-3, or TPA  
*Pigment Cell Research* **11**:291–8 1998 [Abstract](#)
- 991 Oya M and Schulz WA  
Decreased expression of p57(KIP2)mRNA in human bladder cancer  
*British Journal of Cancer* **83**:626–31 2000 [Abstract](#)
- 992 Pagano M and Gauvreau K  
Principles of Biostatistics  
Duxbury Press, Belmont, California, USA ISBN 0–534–14069–6 1993
- 993 Pagano M, Tam SW, Theodoras AM, Beer-Romero P, Del Sal G, Chau V, Yew PR, Draetta GF and Rolfe M  
Role of the ubiquitin-proteasome pathway in regulating abundance of the cyclin-dependent kinase inhibitor p27  
*Science* **269**:682–5 1995 [Abstract](#)
- 994 Page G, Lodige I, Kogel D and Scheidtmann KH  
AATF, a novel transcription factor that interacts with Dlk/ZIP kinase and interferes with apoptosis  
*FEBS Letters* **462**:187–91 1999 [Abstract](#)
- 995 Page K, Li J and Hershenson MB  
Platelet-derived growth factor stimulation of mitogen-activated protein kinases and cyclin D1 promoter activity in cultured airway smooth-muscle cells. Role of Ras  
*American Journal of Respiratory Cell and Molecular Biology* **20**:1294–302 1999 [Abstract](#)
- 996 Pan W, Cox S, Hoess RH and Grafstrom RH  
A cyclin D1/cyclin-dependent kinase 4 binding site within the C domain of the retinoblastoma protein  
*Cancer Research* **61**:2885–91 2001 [Abstract](#)
- 997 Pang Q, Fagerlie S, Christianson TA, Keeble W, Faulkner G, Diaz J, Rathbun RK and Bagby GC  
The Fanconi anemia protein FANCC binds to and facilitates the activation of STAT1 by gamma interferon and hematopoietic growth factors  
*Molecular and Cellular Biology* **20**:4724–35 2000 [Abstract](#)
- 998 Pardali K, Kurisaki A, Moren A, ten Dijke P, Kardassis D and Moustakas A  
Role of Smad proteins and transcription factor Sp1 in p21(Waf1/Cip1) regulation by transforming growth factor-beta  
*Journal of Biological Chemistry* **275**:29244–56 2000 [Abstract](#)
- 999 Pardee AB  
A restriction point for control of normal animal cell proliferation  
*Proceedings of the National Academy of Sciences of the USA* **71**:1286–90 1974 [Abstract](#)
- 1000 Park K, Choe J, Osifchin NE, Templeton DJ, Robbins PD and Kim SJ  
The human retinoblastoma susceptibility gene promoter is positively autoregulated by its own product  
*Journal of Biological Chemistry* **269**:6083–8 1994 [Abstract](#)
- 1001 Park YE, Choi KC and Choi YH  
p21 expression and mutation in gastric carcinoma: analysis by immunohistochemistry and PCR-SSCP  
*Journal of Korean Medical* **13**:507–12 1998 [Abstract](#)
- 1002 Parmar J, Marshall ES, Charters GA, Holdaway KM, Shelling AN and Baguley BC  
Radiation-induced cell cycle delays and p53 status of early passage melanoma cell lines  
*Oncology Research* **12**:149–55 2000 [Abstract](#)
- 1003 Parry D, Mahony D, Wills K and Lees E  
Cyclin D-CDK subunit arrangement is dependent on the availability of competing INK4 and p21 class inhibitors  
*Molecular and Cellular Biology* **19**:1775–83 1999 [Abstract](#)
- 1004 Parry DM, MacCollin MM, Kaiser-Kupfer MI, Pulaski K, Nicholson HS, Bolesta M, Eldridge R and Gusella JF  
Germ-line mutations in the neurofibromatosis 2 gene: correlations with disease severity and retinal abnormalities  
*American Journal of Human Genetics* **59**:529–39 1996 [Abstract](#)
- 1005 Parry D and Peters G  
Temperature-sensitive mutants of p16CDKN2 associated with familial melanoma  
*Molecular and Cellular Biology* **16**:3844–3852 1996 [Abstract](#)
- 1006 Pastural E, Ersoy F, Yalman N, Wulffraat N, Grillo E, Ozkinay F, Tezcan I, Gedikoglu G, Philippe N, Fischer A and de Saint Basile G  
Two genes are responsible for Griscelli syndrome at the same 15q21 locus  
*Genomics* **63**:299–306 2000 [Abstract](#)
- 1007 Pause A, Lee S, Lonergan KM and Klausner RD  
The von Hippel-Lindau tumor suppressor gene is required for cell cycle exit upon serum withdrawal  
*Proceedings of the National Academy of Sciences of the USA* **95**:993–8 1998 [Abstract](#)
- 1008 Pavletich NP  
Mechanisms of cyclin-dependent kinase regulation: structures of Cdks, their cyclin activators, and Cip and INK4 inhibitors  
*Journal of Molecular Biology* **287**:821–8 1999 [Abstract](#)
- 1009 Payton M and Coats S  
Cyclin E2, the cycle continues  
*International Journal of Biochemistry and Cell Biology* **34**:315–20 2002 [Abstract](#)
- 1010 Pearsall J (ed)  
The New Oxford Dictionary of English  
Oxford University Press, Oxford, England ISBN 0–19–861263-X 1998
- 1011 Pearson WR, Vorachek WR, Xu SJ, Berger R, Hart I, Vannais D and Patterson D  
Identification of class-mu glutathione transferase genes GSTM1-GSTM5 on human chromosome 1p13  
*American Journal of Human Genetics* **53**:220–33 1993 [Abstract](#)
- 1012 Pedeux R, Al-Irani N, Marteau C, Pellicier F, Branche R, Ozturk M, Franchi J and Dore JF  
Thymidine dinucleotides induce S phase cell cycle arrest in addition to increased melanogenesis in human melanocytes  
*Journal of Investigative Dermatology* **111**:472–7 1998 [Abstract](#)
- 1013 Pedrazzi G, Perrera C, Blaser H, Kuster P, Marra G, Davies SL, Ryu GH, Freire R, Hickson ID, Jiricny J and Stagljar I  
Direct association of Bloom's syndrome gene product with the human mismatch repair protein MLH1  
*Nucleic Acids Research* **29**:4378–86 2001 [Abstract](#)



- 1014 Peeper DS, Upton TM, Ladha MH, Neuman E, Zalvide J, Bernards R, DeCaprio JA and Ewen ME  
Ras signalling linked to the cell-cycle machinery by the retinoblastoma protein  
*Nature* **386**:177–81 1997 [Abstract](#)
- 1015 Pelengaris S, Rudolph B and Littlewood T  
Action of Myc in vivo - proliferation and apoptosis  
*Current Opinion in Genetics and Development* **10**:100–5 2000 [Abstract](#)
- 1016 Pelizon C, Madine MA, Romanowski P and Laskey RA  
Unphosphorylatable mutants of Cdc6 disrupt its nuclear export but still support DNA replication once per cell cycle  
*Genes and Development* **14**:2526–33 2000 [Abstract](#)
- 1017 Pennaneach V, Salles-Passador I, Munshi A, Brickner H, Regazzoni K, Dick F, Dyson N, Chen TT, Wang JY, Fotedar R and Fotedar A  
The large subunit of replication factor C promotes cell survival after DNA damage in an LxCxE motif- and Rb-dependent manner  
*Molecular Cell* **7**:715–27 2001 [Abstract](#)
- 1018 Perez-Roger I, Kim SH, Griffiths B, Sewing A and Land H  
Cyclins D1 and D2 mediate myc-induced proliferation via sequestration of p27(Kip1) and p21(Cip1)  
*EMBO Journal* **18**:5310–20 1999 [Abstract](#)
- 1019 Perry A, Nobori T, Ru N, Anderl K, Borell TJ, Mohapatra G, Feuerstein BG, Jenkins RB and Carson DA  
Detection of p16 gene deletions in gliomas: a comparison of fluorescence in situ hybridization (FISH) versus quantitative PCR  
*Journal of Neuro pathology and Experimental Neurology* **56**:999–1008 1997 [Abstract](#)
- 1020 Perry GS 3rd, Spector BD, Schuman LM, Mandel JS, Anderson VE, McHugh RB, Hanson MR, Fahlstrom SM, Krivit W and Kersey JH  
The Wiskott-Aldrich syndrome in the United States and Canada (1892–1979)  
*Journal of Pediatrics* **97**:72–8 1980 [Abstract](#)
- 1021 Petersen BO, Lukas J, Sorensen CS, Bartek J and Helin K  
Phosphorylation of mammalian CDC6 by cyclin A/CDK2 regulates its subcellular localization  
*EMBO Journal* **18**:396–410 1999 [Abstract](#)
- 1022 Petro JB, Rahman SM, Ballard DW and Khan WN  
Bruton's tyrosine kinase is required for activation of I $\kappa$ B kinase and nuclear factor  $\kappa$ B in response to B cell receptor engagement  
*Journal of Experimental Medicine* **191**:1745–54 2000 [Abstract](#)
- 1023 Pfahlberg A, Kolmel KF and Gefeller O  
Timing of excessive ultraviolet radiation and melanoma: epidemiology does not support the existence of a critical period of high susceptibility to solar ultraviolet radiation- induced melanoma  
*British Journal of Dermatology* **144**:471–5 2001 [Abstract](#)
- 1024 Pflieger CM, Lee E and Kirschner MW  
Substrate recognition by the Cdc20 and Cdh1 components of the anaphase-promoting complex  
*Genes and Development* **15**:2396–407 2001 [Abstract](#)
- 1025 Pham AD and Sauer F  
Ubiquitin-activating/conjugating activity of TAFII250, a mediator of activation of gene expression in Drosophila  
*Science* **289**:2357–60 2000 [Abstract](#)
- 1026 Research Products Catalogue 1996  
PharMingen  
San Diego, California, U.S.A 1997
- 1027 Phillips AC and Vousden KH  
E2F-1 induced apoptosis  
*Apoptosis* **6**:173–82 2001 [Abstract](#)
- 1028 Philo JS, Wen J, Wypych J, Schwartz MG, Mendiaz EA and Langley KE  
Human stem cell factor dimer forms a complex with two molecules of the extracellular domain of its receptor, Kit  
*Journal of Biological Chemistry* **271**:6895–902 1996 [Abstract](#)
- 1029 Piel M, Nordberg J, Euteneuer U and Bornens M  
Centrosome-dependent exit of cytokinesis in animal cells  
*Science* **291**:1550–3 2001 [Abstract](#)
- 1030 Pierce KL, Luttrell LM and Lefkowitz RJ  
New mechanisms in heptahelical receptor signaling to mitogen activated protein kinase cascades  
*Oncogene* **20**:1532–9 2001 [Abstract](#)
- 1031 Pietromonaco SF, Seluja GA, Aitken A and Elias L  
Association of 14–3–3 proteins with centrosomes  
*Blood Cells, Molecules, and Diseases* **22**:225–37 1996 [Abstract](#)
- 1032 Planque N, Leconte L, Coquelle FM, Martin P and Saule S  
Specific Pax-6/microphthalmia transcription factor interactions involve their DNA-binding domains and inhibit transcriptional properties of both proteins  
*Journal of Biological Chemistry* **276**:29330–7 2001 [Abstract](#)
- 1033 Plug AW, Peters AH, Xu Y, Keegan KS, Hoekstra MF, Baltimore D, de Boer P and Ashley T  
ATM and RPA in meiotic chromosome synapsis and recombination  
*Nature Genetics* **17**:457–61 1997 [Abstract](#)
- 1034 Pluquet O and Hainaut P  
Genotoxic and non-genotoxic pathways of p53 induction  
*Cancer Letters* **174**:1–15 2001 [Abstract](#)
- 1035 Pockwinse SM, Krockmalnic G, Doxsey SJ, Nickerson J, Lian JB, van Wijnen AJ, Stein JL, Stein GS and Penman S  
Cell cycle independent interaction of CDC2 with the centrosome, which is associated with the nuclear matrix-intermediate filament scaffold  
*Proceedings of the National Academy of Sciences of the USA* **94**:3022–7 1997 [Abstract](#)
- 1036 Podust VN, Brownell JE, Gladysheva TB, Luo RS, Wang C, Coggins MB, Pierce JW, Lightcap ES and Chau V  
A Nedd8 conjugation pathway is essential for proteolytic targeting of p27Kip1 by ubiquitination  
*Proceedings of the National Academy of Sciences of the USA* **97**:4579–84 2000 [Abstract](#)
- 1037 Podust VN, Tiwari N, Stephan S and Fanning E  
Replication factor C disengages from proliferating cell nuclear antigen (PCNA) upon sliding clamp formation, and PCNA itself tethers DNA polymerase delta to DNA  
*Journal of Biological Chemistry* **273**:31992–9 1998 [Abstract](#)
- 1038 Poetsch M, Dittberner T and Woenckhaus C  
PTEN/MMAC1 in malignant melanoma and its importance for tumor progression  
*Cancer Genetics and Cytogenetics* **125**:21–6 2001 [Abstract](#)

## Human metastatic melanoma in vitro

- |      |   |                 |      |                          |
|------|---|-----------------|------|--------------------------|
| 1039 | Polager S, Kalma Y, Berkovich E and Ginsberg D<br>E2Fs up-regulate expression of genes involved in DNA replication, DNA repair and mitosis<br><i>Oncogene</i>   | 21:437–46       | 2002 | <a href="#">Abstract</a> |
| 1040 | Polakis P<br>Wnt signaling and cancer<br><i>Genes and Development</i>   | 14:1837–51      | 2000 | <a href="#">Abstract</a> |
| 1041 | Polanowska J, Le Cam L, Orsetti B, Valles H, Fabbriozzi E, Fajas L, Taviaux S, Theillet C and Sardet C<br>Human E2F5 gene is oncogenic in primary rodent cells and is amplified in human breast tumors<br><i>Genes, Chromosomes and Cancer</i>                              | 28:126–30       | 2000 | <a href="#">Abstract</a> |
| 1042 | Pollock PM, Welch J and Hayward NK<br>Evidence for three tumor suppressor loci on chromosome 9p involved in melanoma development<br><i>Cancer Research</i>  | 61:1154–61      | 2001 | <a href="#">Abstract</a> |
| 1043 | Polsky D, Bastian BC, Hazan C, Melzer K, Pack J, Houghton A, Busam K, Cordon-Cardo C and Osman I<br>HDM2 protein overexpression, but not gene amplification, is related to tumorigenesis of cutaneous melanoma<br><i>Cancer Research</i>                                    | 61:7642–6       | 2001 | <a href="#">Abstract</a> |
| 1044 | Polsky D, Young AZ, Busam KJ and Alani RM<br>The transcriptional repressor of p16/Ink4a, Id1, is up-regulated in early melanomas<br><i>Cancer Research</i>  | 61:6008–11      | 2001 | <a href="#">Abstract</a> |
| 1045 | Polyak K, Kato JY, Solomon MJ, Sherr CJ, Massague J, Roberts JM and Koff A<br>p27Kip1, a cyclin-Cdk inhibitor, links transforming growth factor-beta and contact inhibition to cell cycle arrest<br><i>Genes and Development</i>  | 8:9–22          | 1994 | <a href="#">Abstract</a> |
| 1046 | Poon RY, Jiang W, Toyoshima H and Hunter T<br>Cyclin-dependent kinases are inactivated by a combination of p21 and THR-14/TYR-15 phosphorylation after UV-induced DNA damage<br><i>Journal of Biological Chemistry</i>  | 271:13283–13291 | 1996 | <a href="#">Abstract</a> |
| 1047 | Poon RY and Hunter T<br>Dephosphorylation of Cdk2 Thr160 by the cyclin-dependent kinase-interacting phosphatase KAP in the absence of cyclin<br><i>Science</i>  | 270:90–3        | 1995 | <a href="#">Abstract</a> |
| 1048 | Poon RY, Yamashita K, Adamczewski JP, Hunt T and Shuttleworth J<br>The cdc2-related protein p40MO15 is the catalytic subunit of a protein kinase that can activate p33cdk2 and p34cdc2<br><i>EMBO Journal</i>   | 12:3123–32      | 1993 | <a href="#">Abstract</a> |
| 1049 | Potterf SB, Furumura M, Dunn KJ, Arnheiter H and Pavan WJ<br>Transcription factor hierarchy in Waardenburg syndrome: regulation of MITF expression by SOX10 and PAX3<br><i>Human Genetics</i>   | 107:1–6         | 2000 | <a href="#">Abstract</a> |
| 1050 | Potterf SB, Mollaaghababa R, Hou L, Southard-Smith EM, Hornyak TJ, Arnheiter H and Pavan WJ<br>Analysis of SOX10 function in neural crest-derived melanocyte development: SOX10-dependent transcriptional control of dopachrome tautomerase<br><i>Developmental Biology</i> | 237:245–57      | 2001 | <a href="#">Abstract</a> |
| 1051 | Potterf SB, Virador V, Wakamatsu K, Furumura M, Santis C, Ito S and Hearing VJ<br>Cysteine transport in melanosomes from murine melanocytes<br><i>Pigment Cell Research</i>   | 12:4–12         | 1999 | <a href="#">Abstract</a> |
| 1052 | Prendergast GC, Khosravi-Far R, Solski PA, Kurzawa H, Lebowitz PF and Der CJ<br>Critical role of Rho in cell transformation by oncogenic Ras<br><i>Oncogene</i>   | 10:2289–96      | 1995 | <a href="#">Abstract</a> |
| 1053 | Price BD, Hughes-Davies L and Park SJ<br>Cdk2 kinase phosphorylates serine 315 of human p53 in vitro<br><i>Oncogene</i>   | 11:73–80        | 1995 | <a href="#">Abstract</a> |
| 1054 | Price DJ, Rivnay B and Avraham H<br>CHK down-regulates SCF/KL-activated Lyn kinase activity in Mo7e megakaryocytic cells<br><i>Biochemical and Biophysical Research Communications</i>  | 259:611–6       | 1999 | <a href="#">Abstract</a> |
| 1055 | Price DJ, Rivnay B, Fu Y, Jiang S, Avraham S and Avraham H<br>Direct association of Csk homologous kinase (CHK) with the diphosphorylated site Tyr568/570 of the activated c-KIT in megakaryocytes<br><i>Journal of Biological Chemistry</i>                                | 272:5915–20     | 1997 | <a href="#">Abstract</a> |
| 1056 | Price ER, Ding HF, Badalian T, Bhattacharya S, Takemoto C, Yao TP, Hemesath TJ and Fisher DE<br>Lineage-specific signaling in melanocytes. C-kit stimulation recruits p300/CBP to microphthalmia<br><i>Journal of Biological Chemistry</i>                                  | 273:17983–6     | 1998 | <a href="#">Abstract</a> |
| 1057 | Price ER, Horstmann MA, Wells AG, Weillbaeher KN, Takemoto CM, Landis MW and Fisher DE<br>alpha-Melanocyte-stimulating hormone signaling regulates expression of microphthalmia, a gene deficient in Waardenburg syndrome<br><i>Journal of Biological Chemistry</i>         | 273:33042–7     | 1998 | <a href="#">Abstract</a> |
| 1058 | Prime SS, Thakker NS, Pring M, Guest PG and Paterson IC<br>A review of inherited cancer syndromes and their relevance to oral squamous cell carcinoma<br><i>Oral Oncology</i>   | 37:1–16         | 2001 | <a href="#">Abstract</a> |
| 1059 | Prins JB, Williamson KA, Kamp MM, Van Hezik EJ, Van der Kwast TH, Hagemeyer A and Versnel MA<br>The gene for the cyclin-dependent-kinase-4 inhibitor, CDKN2A, is preferentially deleted in malignant mesothelioma<br><i>International Journal of Cancer</i>                 | 75:649–53       | 1998 | <a href="#">Abstract</a> |
| 1060 | Pritchard Jones K and King Underwood L<br>The Wilms tumour gene WT1 in leukaemia<br><i>Leukemia and Lymphoma</i>  | 27:207–20       | 1997 | <a href="#">Abstract</a> |
| 1061 | Puga A, Barnes SJ, Dalton TP, Chang Cy, Knudsen ES and Maier MA<br>Aromatic hydrocarbon receptor interaction with the retinoblastoma protein potentiates repression of E2F-dependent transcription and cell cycle arrest<br><i>Journal of Biological Chemistry</i>          | 275:2943–50     | 2000 | <a href="#">Abstract</a> |
| 1062 | Pugazhenth S, Nesterova A, Sable C, Heidenreich KA, Boxer LM, Heasley LE and Reusch JE<br>Akt/protein kinase B up-regulates Bcl-2 expression through cAMP-response element-binding protein<br><i>Journal of Biological Chemistry</i>  | 275:10761–6     | 2000 | <a href="#">Abstract</a> |
| 1063 | Pullen N, Dennis PB, Andjelkovic M, Dufner A, Kozma SC, Hemmings BA and Thomas G<br>Phosphorylation and activation of p70s6k by PDK1<br><i>Science</i>  | 279:707–10      | 1998 | <a href="#">Abstract</a> |





- 1064 Puri PL, Iezzi S, Stiegler P, Chen TT, Schiltz RL, Muscat GE, Giordano A, Kedes L, Wang JY and Sartorelli V  
Class I histone deacetylases sequentially interact with MyoD and pRb during skeletal myogenesis  
*Molecular Cell* 8:885–97 2001 [Abstract](#)
- 1065 Qian X, Jin L, Kulig E and Lloyd RV  
DNA methylation regulates p27kip1 expression in rodent pituitary cell lines  
*American Journal of Pathology* 153:1475–82 1998 [Abstract](#)
- 1066 Qian YW and Lee EY  
Dual retinoblastoma-binding proteins with properties related to a negative regulator of ras in yeast  
*Journal of Biological Chemistry* 270:25507–13 1995 [Abstract](#)
- 1067 Qin XQ, Chittenden T, Livingston DM and Kaelin WG Jr  
Identification of a growth suppression domain within the retinoblastoma gene product  
*Genes and Development* 6:953–64 1992 [Abstract](#)
- 1068 Qin XQ, Livingston DM, Kaelin WG Jr and Adams PD  
Deregulated transcription factor E2F-1 expression leads to S-phase entry and p53-mediated apoptosis  
*Proceedings of the National Academy of Sciences of the USA* 91:10918–22 1994 [Abstract](#)
- 1069 Quentmeier H, Zaborski M and Drexler HG  
Effects of thrombopoietin, interleukin-3 and the kinase inhibitor K-252a on growth and polyploidization of the megakaryocytic cell line M-07e  
*Leukemia* 12:1603–11 1998 [Abstract](#)
- 1070 Quesnel B, Preudhomme C, Lepelley P, Hetuin D, Vanrumbeke M, Bauters F, Velu T and Fenaux P  
Transfer of p16INKA/CDKN2 gene in leukaemic cell lines inhibits cell proliferation  
*British Journal of Haematology* 95:291–8 1996 [Abstract](#)
- 1071 Radhi JM  
Malignant melanoma arising from nevi, p53, p16, and Bcl-2: expression in benign versus malignant components  
*Journal of Cutaneous Medicine and Surgery* 3:293–7 1999 [Abstract](#)
- 1072 Rahman N, Stone JG, Coleman G, Gusterson B, Seal S, Marossy A, Lakhani SR, Ward A, Nash A, McKinna A, A'Hern R, Stratton MR and Houlston RS  
Lobular carcinoma in situ of the breast is not caused by constitutional mutations in the E-cadherin gene  
*British Journal of Cancer* 82:568–70 2000 [Abstract](#)
- 1073 Raleigh JM and O'Connell MJ  
The G(2) DNA damage checkpoint targets both Wee1 and Cdc25  
*Journal of Cell Science* 113:1727–36 2000 [Abstract](#)
- 1074 Ram PT and Iyengar R  
G protein coupled receptor signaling through the Src and Stat3 pathway: role in proliferation and transformation  
*Oncogene* 20:1601–6 2001 [Abstract](#)
- 1075 Ramsay J, Birrell G, Baumann K, Boderio A, Parsons P and Lavin M  
Radiosensitive melanoma cell line with mutation of the gene for ataxia telangiectasia  
*British Journal of Cancer* 77:11–4 1998 [Abstract](#)
- 1076 Randerson-Moor JA, Harland M, Williams S, Cuthbert-Heavens D, Sheridan E, Aveyard J, Sibley K, Whitaker L, Knowles M, Bishop JN and Bishop DT  
A germline deletion of p14(ARF) but not CDKN2A in a melanoma-neural system tumour syndrome family  
*Human Molecular Genetics* 10:55–62 2001 [Abstract](#)
- 1077 Rane SG, Cosenza SC, Mettus RV and Reddy EP  
Germ line transmission of the Cdk4(R24C) mutation facilitates tumorigenesis and escape from cellular senescence  
*Molecular and Cellular Biology* 22:644–56 2002 [Abstract](#)
- 1078 Rank KB, Evans DB and Sharma SK  
The N-terminal domains of cyclin-dependent kinase inhibitory proteins block the phosphorylation of cdk2/Cyclin E by the CDK-activating kinase  
*Biochemical and Biophysical Research Communications* 271:469–73 2000 [Abstract](#)
- 1079 Ranson M, Hammond LA, Ferry D, Kris M, Tullo A, Murray PI, Miller V, Averbuch S, Ochs J, Morris C, Feyereislova A, Swaisland H and Rowinsky EK  
ZD1839, a selective oral epidermal growth factor receptor-tyrosine kinase inhibitor, is well tolerated and active in patients with solid, malignant tumors: results of a phase I trial  
*Journal of Clinical Oncology* 20:2240–50 2002 [Abstract](#)
- 1080 Rapin I, Lindenbaum Y, Dickson DW, Kraemer KH and Robbins JH  
Cockayne syndrome and xeroderma pigmentosum  
*Neurology* 55:1442–9 2000 [Abstract](#)
- 1081 Rawlings SL, Crooks GM, Bockstoce D, Barsky LW, Parkman R and Weinberg KI  
Spontaneous apoptosis in lymphocytes from patients with Wiskott-Aldrich syndrome: correlation of accelerated cell death and attenuated bcl-2 expression  
*Blood* 94:3872–82 1999 [Abstract](#)
- 1082 Razzini G, Brancaccio A, Lemmon MA, Guarnieri S and Falasca M  
The role of the pleckstrin homology domain in membrane targeting and activation of phospholipase Cbeta(1)  
*Journal of Biological Chemistry* 275:14873–81 2000 [Abstract](#)
- 1083 Recio JA and Merlino G  
Hepatocyte growth factor/scatter factor activates proliferation in melanoma cells through p38 MAPK, ATF-2 and cyclin D1  
*Oncogene* 21:1000–8 2002 [Abstract](#)
- 1084 Reed AL, Califano J, Cairns P, Westra WH, Jones RM, Koch W, Ahrendt S, Eby Y, Sewell D, Nawroz H, Bartek J and Sidransky D  
High frequency of p16 (CDKN2/MTS-1/INK4A) inactivation in head and neck squamous cell carcinoma  
*Cancer Research* 56:3630–3 1996 [Abstract](#)
- 1085 Reed JA, Loganzo F Jr, Shea CR, Walker GJ, Flores JF, Glendening JM, Bogdany JK, Shiel MJ, Haluska FG, Fountain JW et al  
Loss of expression of the p16/cyclin-dependent kinase inhibitor 2 tumor suppressor gene in melanocytic lesions correlates with invasive stage of tumor progression  
*Cancer Research* 55:2713–8 1995 [Abstract](#)
- 1086 Reed RJ and Martin P  
Variants of melanoma  
*Seminars in Cutaneous Medicine and Surgery* 16:137–58 1997 [Abstract](#)
- 1087 Reich NC, Oren M and Levine AJ  
Two distinct mechanisms regulate the levels of a cellular tumor antigen, p53  
*Molecular and Cellular Biology* 3:2143–50 1983 [Abstract](#)

## Human metastatic melanoma in vitro

- |      |  |   |      |                          |
|------|--|---|------|--------------------------|
| 1088 | Reid K, Turnley AM, Maxwell GD, Kurihara Y, Kurihara H, Bartlett PF and Murphy M<br>Multiple roles for endothelin in melanocyte development: regulation of progenitor number and stimulation of differentiation<br><i>Development</i>                                  | 122:3911–9  | 1996 | <a href="#">Abstract</a> |
| 1089 | Reynisdottir I, Polyak K, Iavarone A and Massague J<br>Kip/Cip and Ink4 Cdk inhibitors cooperate to induce cell cycle arrest in response to TGF-beta<br><i>Genes and Development</i>   | 9:1831–45   | 1995 | <a href="#">Abstract</a> |
| 1090 | Rhind N, Furnari B and Russell P<br>Cdc2 tyrosine phosphorylation is required for the DNA damage checkpoint in fission yeast<br><i>Genes and Development</i>   | 11:504–11   | 1997 | <a href="#">Abstract</a> |
| 1091 | Richards FM, McKee SA, Rajpar MH, Cole TR, Evans DG, Jankowski JA, McKeown C, Sanders DS and Maher ER<br>Germline E-cadherin gene (CDH1) mutations predispose to familial gastric cancer and colorectal cancer<br><i>Human Molecular Genetics</i>                      | 8:607–10  | 1999 | <a href="#">Abstract</a> |
| 1092 | Ries LAG, Eisner MP, Kosary CL, Hankey BF, Miller BA, Clegg L, Edwards BK (eds)<br>SEER Cancer Statistics Review 1973–1998<br>National Cancer Institute, Bethesda, Maryland, USA   | <a href="http://seer.cancer.gov/Publications/CSR1973_1998/">http://seer.cancer.gov/Publications/CSR1973_1998/</a> | 2001 |                          |
| 1093 | Ries S and Korn WM<br>ONYX-015: mechanisms of action and clinical potential of a replication-selective adenovirus<br><i>British Journal of Cancer</i>  | 86:5–11   | 2002 | <a href="#">Abstract</a> |
| 1094 | Riley PA<br>Melanin<br><i>International Journal of Biochemistry and Cell Biology</i>   | 29:1235–9   | 1997 | <a href="#">Abstract</a> |
| 1095 | Rizos H, Darmanian AP, Indsto JO, Shannon JA, Kefford RF and Mann GJ<br>Multiple abnormalities of the p16INK4a-pRb regulatory pathway in cultured melanoma cells<br><i>Melanoma Research</i>   | 9:10–9  | 1999 | <a href="#">Abstract</a> |
| 1096 | Rizos H, Puig S, Badenas C, Malvey J, Darmanian AP, Jimenez L, Mila M and Kefford RF<br>A melanoma-associated germline mutation in exon 1beta inactivates p14ARF<br><i>Oncogene</i>  | 20:5543–7   | 2001 | <a href="#">Abstract</a> |
| 1097 | Robertson KD and Jones PA<br>The human ARF cell cycle regulatory gene promoter is a CpG island which can be silenced by DNA methylation and down-regulated by wild-type p53<br><i>Molecular and Cellular Biology</i>   | 18:6457–73  | 1998 | <a href="#">Abstract</a> |
| 1098 | Robinson JT, Wojcik EJ, Sanders MA, McGrail M and Hays TS<br>Cytoplasmic dynein is required for the nuclear attachment and migration of centrosomes during mitosis in <i>Drosophila</i><br><i>Journal of Cell Biology</i>  | 146:597–608   | 1999 | <a href="#">Abstract</a> |
| 1099 | Robinson WA, Elefanty AG and Hersey P<br>Expression of the tumour suppressor genes p15 and p16 in malignant melanoma<br><i>Melanoma Research</i>   | 6:285–9   | 1996 | <a href="#">Abstract</a> |
| 1100 | Roche LM, Weinstein RB, Paul SM and Costa SJ<br>Cancer in people with AIDS in New Jersey<br><i>New Jersey Medicine</i>   | 98:27–36  | 2001 | <a href="#">Abstract</a> |
| 1101 | Rodeck U, Bossler A, Graeven U, Fox FE, Nowell PC, Knabbe C and Kari C<br>Transforming growth factor beta production and responsiveness in normal human melanocytes and melanoma cells<br><i>Cancer Research</i>   | 54: 575–81  | 1994 | <a href="#">Abstract</a> |
| 1102 | Rodriguez-Ayerbe C and Smith Zubiaga I<br>Effect of serum withdrawal on the proliferation of B16F10 melanoma cells<br><i>Cell Biology International</i>  | 24:279–83   | 2000 | <a href="#">Abstract</a> |
| 1103 | Rodriguez-Viciana P, Warne PH, Dhand R, Vanhaesebroeck B, Gout I, Fry MJ, Waterfield MD and Downward J<br>Phosphatidylinositol-3-OH kinase as a direct target of Ras<br><i>Nature</i>  | 370:527–32  | 1994 | <a href="#">Abstract</a> |
| 1104 | Rollbrocker B, Waha A, Louis DN, Wiestler OD and von Deimling A<br>Amplification of the cyclin-dependent kinase 4 (CDK4) gene is associated with high cdk4 protein levels in glioblastoma multiforme<br><i>Acta Neuropathologica</i>                                   | 92:70–4   | 1996 | <a href="#">Abstract</a> |
| 1105 | Romero-Graillet C, Aberdam E, Biagoli N, Massabni W, Ortonne JP and Ballotti R<br>Ultraviolet B radiation acts through the nitric oxide and cGMP signal transduction pathway to stimulate melanogenesis in human melanocytes<br><i>Journal of Biological Chemistry</i> | 271:28052–6   | 1996 | <a href="#">Abstract</a> |
| 1106 | Romero-Graillet C, Aberdam E, Clement M, Ortonne JP and Ballotti R<br>Nitric oxide produced by ultraviolet-irradiated keratinocytes stimulates melanogenesis<br><i>Journal of Clinical Investigation</i>   | 99:635–42   | 1997 | <a href="#">Abstract</a> |
| 1107 | Rosenberg CL, Wong E, Petty EM, Bale AE, Tsujimoto Y, Harris NL and Arnold A<br>PRAD1, a candidate BCL1 oncogene: mapping and expression in centrocytic lymphoma<br><i>Proceedings of the National Academy of Sciences of the USA</i>                                  | 88:9638–42  | 1991 | <a href="#">Abstract</a> |
| 1108 | Ross DA and Wilson GD<br>Flow cytometric analysis of p53 oncoprotein expression in cutaneous melanoma<br><i>British Journal of Surgery</i>   | 84:803–7  | 1997 | <a href="#">Abstract</a> |
| 1109 | Rossig L, Jadidi AS, Urbich C, Badorf C, Zeiher AM and Dimmeler S<br>Akt-dependent phosphorylation of p21(Cip1) regulates PCNA binding and proliferation of endothelial cells<br><i>Molecular and Cellular Biology</i>   | 21:5644–57  | 2001 | <a href="#">Abstract</a> |
| 1110 | Rothblum Oviatt CJ, Ryan CE and Piwnica-Worms H<br>14–3-3 binding regulates catalytic activity of human wee1 kinase<br><i>Cell Growth and Differentiation</i>  | 12:581–9  | 2001 | <a href="#">Abstract</a> |
| 1111 | Rotman G and Shiloh Y<br>ATM: from gene to function<br><i>Human Molecular Genetics</i>   | 7:1555–63   | 1998 | <a href="#">Abstract</a> |
| 1112 | Rountree MR, Bachman KE, Herman JG and Baylin SB<br>DNA methylation, chromatin inheritance, and cancer<br><i>Oncogene</i>  | 20:3156–65  | 2001 | <a href="#">Abstract</a> |
| 1113 | Roussel MF<br>The INK4 family of cell cycle inhibitors in cancer<br><i>Oncogene</i>  | 18:5311–7   | 1999 | <a href="#">Abstract</a> |



- 1114 Rowan A, Bataille V, MacKie R, Healy E, Bicknell D, Bodmer W and Tomlinson I  
Somatic mutations in the Peutz-Jeghers (LKB1/STK11) gene in sporadic malignant melanomas  
*Journal of Investigative Dermatology* **112**:509–11 1999 [Abstract](#)
- 1115 Roymans D, Vissenberg K, De Jonghe C, Willems R, Engler G, Kimura N, Grobden B, Claes P, Verbelen JP, Van Broeckhoven C and Slegers H  
Identification of the tumor metastasis suppressor Nm23-H1/Nm23-R1 as a constituent of the centrosome  
*Experimental Cell Research* **262**:145–53 2001 [Abstract](#)
- 1116 Rubin E, Mittnacht S, Villa-Moruzzi E and Ludlow JW  
Site-specific and temporally-regulated retinoblastoma protein dephosphorylation by protein phosphatase type 1  
*Oncogene* **20**:3776–85 2001 [Abstract](#)
- 1117 Rubinfeld B, Souza B, Albert I, Muller O, Chamberlain SH, Masiarz FR, Munemitsu S and Polakis P  
Association of the APC gene product with beta-catenin  
*Science* **262**:1731–4 1993 [Abstract](#)
- 1118 Ruiz A, Puig S, Lynch M, Castel T and Estivill X  
Retention of the CDKN2A locus and low frequency of point mutations in primary and metastatic cutaneous malignant melanoma  
*International Journal of Cancer* **76**:312–6 1998 [Abstract](#)
- 1119 Russo AA, Jeffrey PD, Patten AK, Massague J and Pavletich NP  
Crystal structure of the p27Kip1 cyclin-dependent-kinase inhibitor bound to the cyclin A-Cdk2 complex  
*Nature* **382**:325–31 1996 [Abstract](#)
- 1120 Russo AA, Jeffrey PD and Pavletich NP  
Structural basis of cyclin-dependent kinase activation by phosphorylation  
*Nature Structural Biology* **3**:696–700 1996 [Abstract](#)
- 1121 Rustgi AK, Dyson N and Bernards R  
Amino-terminal domains of c-myc and N-myc proteins mediate binding to the retinoblastoma gene product  
*Nature* **352**:541–4 1991 [Abstract](#)
- 1122 Saavedra HI, Knauf JA, Shirokawa JM, Wang J, Ouyang B, Elisei R, Stambrook PJ and Fagin JA  
The RAS oncogene induces genomic instability in thyroid PCCL3 cells via the MAPK pathway  
*Oncogene* **19**:3948–54 2000 [Abstract](#)
- 1123 Sahai E, Ishizaki T, Narumiya S and Treisman R  
Transformation mediated by RhoA requires activity of ROCK kinases  
*Current Biology* **9**:136–45 1999 [Abstract](#)
- 1124 Saito M, Helin K, Valentine MB, Griffith BB, Willman CL, Harlow E and Look AT  
Amplification of the E2F1 transcription factor gene in the HEL erythroleukemia cell line  
*Genomics* **25**:130–8 1995 [Abstract](#)
- 1125 Sakaguchi M, Fujii Y, Hirabayashi H, Yoon HE, Komoto Y, Oue T, Kusafuka T, Okada A and Matsuda H  
Inversely correlated expression of p16 and Rb protein in non-small cell lung cancers: an immunohistochemical study  
*International Journal of Cancer* **65**:442–5 1996 [Abstract](#)
- 1126 Sakai T, Ohtani N, McGee TL, Robbins PD and Dryja TP  
Oncogenic germ-line mutations in Sp1 and ATF sites in the human retinoblastoma gene  
*Nature* **353**:83–6 1991 [Abstract](#)
- 1127 Sakai Y, Saijo M, Coelho K, Kishino T, Niikawa N and Taya Y  
cDNA sequence and chromosomal localization of a novel human protein, RBQ-1 (RBBP6), that binds to the retinoblastoma gene product  
*Genomics* **30**:98–101 1995 [Abstract](#)
- 1128 Sakata H, Rubin JS, Taylor WG and Miki T  
A Rho-specific exchange factor Ect2 is induced from S to M phases in regenerating mouse liver  
*Hepatology* **32**:193–9 2000 [Abstract](#)
- 1129 Sala Trepat M, Rouillard D, Escarceller M, Laquerbe A, Moustacchi E and Papadopoulos D  
Arrest of S-phase progression is impaired in Fanconi anemia cells  
*Experimental Cell Research* **260**:208–15 2000 [Abstract](#)
- 1130 Salinas AE and Wong MG  
Glutathione S-transferases—a review  
*Current Medicinal Chemistry* **6**:279–309 1999 [Abstract](#)
- 1131 Sander CA, Medeiros LJ, Weiss LM, Yano T, Sneller MC and Jaffe ES  
Lymphoproliferative lesions in patients with common variable immunodeficiency syndrome  
*American Journal of Surgical Pathology* **16**:1170–82 1992 [Abstract](#)
- 1132 Sanders DS, Blessing K, Hassan GA, Bruton R, Marsden JR and Jankowski J  
Alterations in cadherin and catenin expression during the biological progression of melanocytic tumours  
*Molecular Pathology* **52**:151–7 1999 [Abstract](#)
- 1133 Sandhu C, Donovan J, Bhattacharya N, Stampfer M, Worland P and Slingerland J  
Reduction of Cdc25A contributes to cyclin E1-Cdk2 inhibition at senescence in human mammary epithelial cells  
*Oncogene* **19**:5314–23 2000 [Abstract](#)
- 1134 Sandhu C, Garbe J, Bhattacharya N, Dakis J, Pan CH, Yaswen P, Koh J, Slingerland JM and Stampfer MR  
Transforming growth factor beta stabilizes p15INK4B protein, increases p15INK4B-cdk4 complexes, and inhibits cyclin D1-cdk4 association in human mammary epithelial cells  
*Molecular and Cellular Biology* **17**:2458–67 1997 [Abstract](#)
- 1135 Saridaki Z, Koumantaki E, Liloglou T, Sourvinos G, Papadopoulos O, Zoras O and Spandidos DA  
High frequency of loss of heterozygosity on chromosome region 9p21-p22 but lack of p16INK4a/p19ARF mutations in greek patients with basal cell carcinoma of the skin  
*Journal of Investigative Dermatology* **115**:719–25 2000 [Abstract](#)
- 1136 Sasaki M, Dharia A, Oh BR, Tanaka Y, Fujimoto S and Dahiya R  
Progesterone receptor B gene inactivation and CpG hypermethylation in human uterine endometrial cancer  
*Cancer Research* **61**:97–102 2001 [Abstract](#)
- 1137 Sasaki M, Horikoshi T, Uchiwa H and Miyachi Y  
Up-regulation of tyrosinase gene by nitric oxide in human melanocytes  
*Pigment Cell Research* **13**:248–52 2000 [Abstract](#)
- 1138 Sathananthan AH, Ratnam SS, Ng SC, Tarin JJ, Gianaroli L and Trounson A  
The sperm centriole: its inheritance, replication and perpetuation in early human embryos  
*Human Reproduction* **11**:345–56 1996 [Abstract](#)

## Human metastatic melanoma in vitro

- |      |   |              |      |                          |
|------|---|--------------|------|--------------------------|
| 1139 | Sato N, Mizumoto K, Nakamura M, Maehara N, Minamishima YA, Nishio S, Nagai E and Tanaka M<br>Correlation between centrosome abnormalities and chromosomal instability in human pancreatic cancer cells<br><i>Cancer Genetics and Cytogenetics</i>   | 126:13–9     | 2001 | <a href="#">Abstract</a> |
| 1140 | Sato S, Fujita N and Tsuruo T<br>Modulation of Akt kinase activity by binding to Hsp90<br><i>Proceedings of the National Academy of Sciences of the USA</i>   | 97:10832–7   | 2000 | <a href="#">Abstract</a> |
| 1141 | Sauer K and Lehner CF<br>The role of cyclin E in the regulation of entry into S phase<br><i>Progress in Cell Cycle Research</i>   | 1:125–39     | 1995 | <a href="#">Abstract</a> |
| 1142 | Sauvaigo S, Fretts RE, Riopelle RJ and Lagarde AE<br>Autonomous proliferation of MeWo human melanoma cell lines in serum-free medium: secretion of growth-stimulating activities<br><i>International Journal of Cancer</i>  | 37:123–32    | 1986 | <a href="#">Abstract</a> |
| 1143 | Savitsky K, Bar-Shira A, Gilad S, Rotman G, Ziv Y, Vanagaite L, Tagle DA, Smith S, Uziel T, Sfez S et al<br>A single ataxia telangiectasia gene with a product similar to PI-3 kinase<br><i>Science</i>   | 268:1749–53  | 1995 | <a href="#">Abstract</a> |
| 1144 | Savoysky E, Mizuno T, Sowa Y, Watanabe H, Sawada J, Nomura H, Ohsugi Y, Handa H and Sakai T<br>The retinoblastoma binding factor 1 (RBF-1) site in RB gene promoter binds preferentially E4TF1, a member of the Ets transcription factors family<br><i>Oncogene</i>   | 9:1839–46    | 1994 | <a href="#">Abstract</a> |
| 1145 | Sayama K, Shirakata Y, Midorikawa K, Hanakawa Y and Hashimoto K<br>Possible involvement of p21 but not of p16 or p53 in keratinocyte senescence<br><i>Journal of Cellular Physiology</i>  | 179:40–4     | 1999 | <a href="#">Abstract</a> |
| 1146 | Schadendorf D, Moller A, Algermissen B, Worm M, Sticherling M and Czarnetzki BM<br>IL-8 produced by human malignant melanoma cells in vitro is an essential autocrine growth factor<br><i>Journal of Immunology</i>   | 151:2667–75  | 1993 | <a href="#">Abstract</a> |
| 1147 | Schaffer JV and Bologna JL<br>The melanocortin-1 receptor: red hair and beyond<br><i>Archives of Dermatology</i>  | 137:1477–85  | 2001 | <a href="#">Abstract</a> |
| 1148 | Schaffner C, Idler I, Stilgenbauer S, Dohner H and Lichter P<br>Mantle cell lymphoma is characterized by inactivation of the ATM gene<br><i>Proceedings of the National Academy of Sciences of the USA</i>  | 97:2773–8    | 2000 | <a href="#">Abstract</a> |
| 1149 | Scharnhorst V, Dekker P, van der Eb AJ and Jochemsen AG<br>Internal translation initiation generates novel WT1 protein isoforms with distinct biological properties<br><i>Journal of Biological Chemistry</i>   | 274:23456–62 | 1999 | <a href="#">Abstract</a> |
| 1150 | Schauer E, Trautinger F, Kock A, Schwarz A, Bhardwaj R, Simon M, Ansel JC, Schwarz T and Luger TA<br>Proopiomelanocortin-derived peptides are synthesized and released by human keratinocytes<br><i>Journal of Clinical Investigation</i>   | 93:2258–62   | 1994 | <a href="#">Abstract</a> |
| 1151 | Scheid MP, Schubert KM and Duronio V<br>Regulation of bad phosphorylation and association with Bcl-x(L) by the MAPK/Erk kinase<br><i>Journal of Biological Chemistry</i>  | 274:31108–13 | 1999 | <a href="#">Abstract</a> |
| 1152 | Scherschun L and Lim HW Am<br>Photoprotection by sunscreens<br><i>Journal of Clinical Dermatology</i>   | 2:131–4      | 2001 | <a href="#">Abstract</a> |
| 1153 | Schlaepfer DD, Jones KC and Hunter T<br>Multiple Grb2-mediated integrin-stimulated signaling pathways to ERK2/mitogen-activated protein kinase: summation of both c-Src- and focal adhesion kinase-initiated tyrosine phosphorylation events<br><i>Molecular and Cellular Biology</i>   | 18:2571–85   | 1998 | <a href="#">Abstract</a> |
| 1154 | Schmidt PH, Dransfield DT, Claudio JO, Hawley RG, Trotter KW, Milgram SL and Goldenring JR<br>AKAP350, a multiply spliced protein kinase A-anchoring protein associated with centrosomes<br><i>Journal of Biological Chemistry</i>  | 274:3055–66  | 1999 | <a href="#">Abstract</a> |
| 1155 | Schmitz MJ, Hendricks DT, Farley J, Taylor RR, Geradts J, Rose GS and Birrer MJ<br>p27 and cyclin D1 abnormalities in uterine papillary serous carcinoma<br><i>Gynecologic Oncology</i>   | 77:439–45    | 2000 | <a href="#">Abstract</a> |
| 1156 | Schittek B, Sauer B and Garbe C<br>Lack of p73 mutations and late occurrence of p73 allelic deletions in melanoma tissues and cell lines<br><i>International Journal of Cancer</i>  | 82:583–6     | 1999 | <a href="#">Abstract</a> |
| 1157 | Schneider E, Montenarh M and Wagner P<br>Regulation of CAK kinase activity by p53<br><i>Oncogene</i>  | 17:2733–41   | 1998 | <a href="#">Abstract</a> |
| 1158 | Scholes AG, Liloglou T, Maloney P, Hagan S, Nunn J, Hiscott P, Damato BE, Grierson I and Field JK<br>Loss of heterozygosity on chromosomes 3, 9, 13, and 17, including the retinoblastoma locus, in uveal melanoma<br><i>Investigative Ophthalmology and Visual Science</i>   | 42:2472–7    | 2001 | <a href="#">Abstract</a> |
| 1159 | Schultz N and Onfelt A<br>Video time-lapse study of mitosis in binucleate V79 cells: chromosome segregation and cleavage<br><i>Mutagenesis</i>  | 9:117–23     | 1994 | <a href="#">Abstract</a> |
| 1160 | Schutte M, da Costa LT, Hahn SA, Moskaluk C, Hoque AT, Rozenblum E, Weinstein CL, Bittner M, Meltzer PS, Trent JM et al<br>Identification by representational difference analysis of a homozygous deletion in pancreatic carcinoma that lies within the BRCA2 region<br><i>Proceedings of the National Academy of Sciences of the USA</i> | 92:5950–4    | 1995 | <a href="#">Abstract</a> |
| 1161 | Schwemmle S and Pfeifer GP<br>Genomic structure and mutation screening of the E2F4 gene in human tumors<br><i>International Journal of Cancer</i>   | 86:672–7     | 2000 | <a href="#">Abstract</a> |
| 1162 | Schwindinger WF and Robishaw JD<br>Heterotrimeric G-protein betagamma-dimers in growth and differentiation<br><i>Oncogene</i>   | 20:1653–60   | 2001 | <a href="#">Abstract</a> |
| 1163 | Scott G, Cassidy L and Abdel-Malek Z<br>Alpha-melanocyte-stimulating hormone and endothelin-1 have opposing effects on melanocyte adhesion, migration, and pp125FAK phosphorylation<br><i>Experimental Cell Research</i>  | 237:19–28    | 1997 | <a href="#">Abstract</a> |
| 1164 | Scott G, Deng A, Rodriguez-Burford C, Seiberg M, Han R, Babiarz L, Grizzle W, Bell W and Pentland A<br>Protease-activated receptor 2, a receptor involved in melanosome transfer, is upregulated in human skin by ultraviolet irradiation<br><i>Journal of Investigative Dermatology</i>  | 117:1412–20  | 2001 | <a href="#">Abstract</a> |



- 1165 Scott G, Liang H and Luthra D  
Stem cell factor regulates the melanocyte cytoskeleton  
*Pigment Cell Research* 9:134–41 1996 [Abstract](#)
- 1166 Scott G and Zhao Q  
Rab3a and SNARE proteins: potential regulators of melanosome movement  
*Journal of Investigative Dermatology* 116:296–304 2001 [Abstract](#)
- 1167 Scott GA and Cassidy L  
Rac1 mediates dendrite formation in response to melanocyte stimulating hormone and ultraviolet light in a murine melanoma model  
*Journal of Investigative Dermatology* 111:243–50 1998 [Abstract](#)
- 1168 Sclafani RA  
Cdc7p-Dbf4p becomes famous in the cell cycle  
*Journal of Cell Science* 113:2111–7 2000 [Abstract](#)
- 1169 Sears RC and Nevins JR  
Signaling networks that link cell proliferation and cell fate  
*Journal of Biological Chemistry* in press 2002 [Abstract](#)
- 1170 Sebastian B, Kakizuka A and Hunter T  
Cdc25M2 activation of cyclin-dependent kinases by dephosphorylation of threonine-14 and tyrosine-15  
*Proceedings of the National Academy of Sciences of the USA* 90:3521–4 1993 [Abstract](#)
- 1171 Sebbagh M, Renvoize C, Hamelin J, Riche N, Bertoglio J and Breard J  
Caspase-3-mediated cleavage of ROCK I induces MLC phosphorylation and apoptotic membrane blebbing  
*Nature Cell Biology* 3:346–52 2001 [Abstract](#)
- 1172 Seiberg M  
Keratinocyte-melanocyte interactions during melanosome transfer  
*Pigment Cell Research* 14:236–42 2001 [Abstract](#)
- 1173 Seiberg M, Paine C, Sharlow E, Andrade-Gordon P, Costanzo M, Eisinger M and Shapiro SS  
The protease-activated receptor 2 regulates pigmentation via keratinocyte-melanocyte interactions  
*Experimental Cell Research* 254:25–32 2000 [Abstract](#)
- 1174 Seidegard J, Pero RW, Markowitz MM, Roush G, Miller DG and Beattie EJ  
Isoenzyme(s) of glutathione transferase (class Mu) as a marker for the susceptibility to lung cancer: a follow up study  
*Carcinogenesis* 11:33–6 1990 [Abstract](#)
- 1175 Selby CP and Sancar A  
Human transcription-repair coupling factor CSB/ERCC6 is a DNA-stimulated ATPase but is not a helicase and does not disrupt the ternary transcription complex of stalled RNA polymerase II  
*Journal of Biological Chemistry* 272:1885–90 1997 [Abstract](#)
- 1176 Sellers WR, Novitch BG, Miyake S, Heith A, Otterson GA, Kaye FJ, Lassar AB and Kaelin WG Jr  
Stable binding to E2F is not required for the retinoblastoma protein to activate transcription, promote differentiation, and suppress tumor cell growth  
*Genes and Development* 12:95–106 1998 [Abstract](#)
- 1177 Sellers WR and Kaelin WG Jr  
Role of the retinoblastoma protein in the pathogenesis of human cancer  
*Journal of Clinical Oncology* 15:3301–12 1997 [Abstract](#)
- 1178 Sen S  
Aneuploidy and cancer  
*Current Opinion in Oncology* 12:82–8 2000 [Abstract](#)
- 1179 Seoane J, Pouponnot C, Staller P, Schader M, Eilers M and Massague J  
TGFbeta influences Myc, Miz-1 and Smad to control the CDK inhibitor p15INK4b  
*Nature Cell Biology* 3:400–8 2001 [Abstract](#)
- 1180 Serrano M  
The tumor suppressor protein p16INK4a  
*Experimental Cell Research* 237:7–13 1997 [Abstract](#)
- 1181 Serrano M, Hannon GJ and Beach D  
A new regulatory motif in cell-cycle control causing specific inhibition of cyclin D/CDK4  
*Nature* 366:704–7 1993 [Abstract](#)
- 1182 Serrone L and Hersey P  
The chemoresistance of human malignant melanoma: an update  
*Melanoma Research* 9:51–8 1999 [Abstract](#)
- 1183 Serve H, Hsu YC and Besmer P  
Tyrosine residue 719 of the c-kit receptor is essential for binding of the P85 subunit of phosphatidylinositol (PI) 3-kinase and for c-kit-associated PI 3-kinase activity in COS-1 cells  
*Journal of Biological Chemistry* 269:6026–30 1994 [Abstract](#)
- 1184 Sexl V, Diehl JA, Sherr CJ, Ashmun R, Beach D and Roussel MF  
A rate limiting function of cdc25A for S phase entry inversely correlates with tyrosine dephosphorylation of Cdk2  
*Oncogene* 18:573–82 1999 [Abstract](#)
- 1185 Shafei-Benaissa E, Savage JR, Babin P, Larregue M, Papworth D, Tanzer J, Bonnetblanc JM and Huret JL  
The naevoid basal-cell carcinoma syndrome (Gorlin syndrome) is a chromosomal instability syndrome  
*Mutation Research* 397:287–92 1998 [Abstract](#)
- 1186 Shafman TD, Levitz S, Nixon AJ, Gibans LA, Nichols KE, Bell DW, Ishioka C, Isselbacher KJ, Gelman R, Garber J, Harris JR and Haber DA  
Prevalence of germline truncating mutations in ATM in women with a second breast cancer after radiation therapy for a contralateral tumor  
*Genes, Chromosomes and Cancer* 27:124–9 2000 [Abstract](#)
- 1187 Sharma S, Wagh S and Govindarajan R  
Melanosomal proteins—role in melanin polymerization  
*Pigment Cell Research* 15:127–33 2002 [Abstract](#)
- 1188 Shan B, Chang CY, Jones D and Lee WH  
The transcription factor E2F-1 mediates the autoregulation of RB gene expression  
*Molecular and Cellular Biology* 14:299–309 1994 [Abstract](#)
- 1189 Shankland SJ, Pippin J, Flanagan M, Coats SR, Nangaku M, Gordon KL, Roberts JM, Couser WG and Johnson RJ  
Mesangial cell proliferation mediated by PDGF and bFGF is determined by levels of the cyclin kinase inhibitor p27Kip1  
*Kidney International* 51:1088–99 1997 [Abstract](#)

## Human metastatic melanoma in vitro

- 1190 Shao Z, Ruppert S and Robbins PD  
The retinoblastoma-susceptibility gene product binds directly to the human TATA-binding protein-associated factor TAFII250  
*Proceedings of the National Academy of Sciences of the USA* **92**:3115–9 1995 [Abstract](#)
- 1191 Sharlow ER, Paine CS, Babiartz L, Eisinger M, Shapiro S and Seiberg M  
The protease-activated receptor-2 upregulates keratinocyte phagocytosis  
*Journal of Cell Science* **113**:3093–101 2000 [Abstract](#)
- 1192 Sharpless NE, Bardeesy N, Lee KH, Carrasco D, Castrillon DH, Aguirre AJ, Wu EA, Horner JW and DePinho RA  
Loss of p16Ink4a with retention of p19Arf predisposes mice to tumorigenesis  
*Nature* **413**:86–91 2001 [Abstract](#)
- 1193 Shaulian E and Karin M  
AP-1 in cell proliferation and survival  
*Oncogene* **20**:2390–400 2001 [Abstract](#)
- 1194 Shaughnessy J Jr, Gabrea A, Qi Y, Brents L, Zhan F, Tian E, Sawyer J, Barlogie B, Bergsagel PL and Kuehl M  
Cyclin D3 at 6p21 is dysregulated by recurrent chromosomal translocations to immunoglobulin loci in multiple myeloma  
*Blood* **98**:217–23 2001 [Abstract](#)
- 1195 Shaw M, Cohen P and Alessi DR  
Further evidence that the inhibition of glycogen synthase kinase-3beta by IGF-1 is mediated by PDK1/PKB-induced phosphorylation of Ser-9 and not by dephosphorylation of Tyr-216  
*FEBS Letters* **416**:307–11 1997 [Abstract](#)
- 1196 Shaw RJ, McClatchey AI and Jacks T  
Regulation of the neurofibromatosis type 2 tumor suppressor protein, merlin, by adhesion and growth arrest stimuli  
*Journal of Biological Chemistry* **273**:7757–64 1998 [Abstract](#)
- 1197 Shay JW and Wright WE  
Hayflick, his limit, and cellular ageing  
*Molecular and Cellular Biology* **1**:72–6 2000 [Abstract](#)
- 1198 She HY, Rockow S, Tang J, Nishimura R, Skolnik EY, Chen M, Margolis B and Li W  
Wiskott-Aldrich syndrome protein is associated with the adapter protein Grb2 and the epidermal growth factor receptor in living cells  
*Molecular Biology of the Cell* **8**:1709–21 1997 [Abstract](#)
- 1199 Sheaff RJ, Singer JD, Swanger J, Smitherman M, Roberts JM and Clurman BE  
Proteasomal turnover of p21Cip1 does not require p21Cip1 ubiquitination  
*Molecular Cell* **5**:403–10 2000 [Abstract](#)
- 1200 Shennan MG, Badin AC, Walsh S, Summers A, From L, McKenzie M, Goldstein AM, Tucker MA, Hogg D and Lassam N  
Lack of germline CDK6 mutations in familial melanoma  
*Oncogene* **19**:1849–52 2000 [Abstract](#)
- 1201 Sherr CJ and Weber JD  
The ARF/p53 pathway  
*Current Opinion in Genetics and Development* **10**:94–9 2000 [Abstract](#)
- 1202 Sherr CJ  
The Pezcoller lecture: cancer cell cycles revisited.  
*Cancer Research* **60**:3689–95 2000 [Abstract](#)
- 1203 Sherr CJ  
The INK4a/ARF network in tumour suppression  
*Molecular and Cellular Biology* **2**:731–7 2001 [Abstract](#)
- 1204 Sherr CJ  
D-type cyclins.  
*Trends in Biochemical Sciences* **20**:187–90 1995 [Abstract](#)
- 1205 Shew JY, Lin BT, Chen PL, Tseng BY, Yang-Feng TL and Lee WH  
C-terminal truncation of the retinoblastoma gene product leads to functional inactivation  
*Proceedings of the National Academy of Sciences of the USA* **87**:6–10 1990 [Abstract](#)
- 1206 Shi Y, Zou M, Farid NR and al Sedairy ST  
Evidence of gene deletion of p21 (WAF1/CIP1), a cyclin-dependent protein kinase inhibitor, in thyroid carcinomas  
*British Journal of Cancer* **74**:1336–41 1996 [Abstract](#)
- 1207 Shibahara S, Takeda K, Yasumoto K, Udono T, Watanabe K, Saito H and Takahashi K  
Microphthalmia-associated transcription factor (MITF): multiplicity in structure, function, and regulation  
*Journal of Investigative Dermatology Symposium Proceedings* **6**:99–104 2001 [Abstract](#)
- 1208 Shieh SY, Ahn J, Tamai K, Taya Y and Prives C  
The human homologs of checkpoint kinases Chk1 and Cds1 (Chk2) phosphorylate p53 at multiple DNA damage-inducible sites [published erratum appears in *Genes and Development* **14**:750]  
*Genes and Development* **14**:289–300 2000 [Abstract](#)
- 1209 Shigeta T, Takagi M, Delia D, Chessa L, Iwata S, Kanke Y, Asada M, Eguchi M and Mizutani S  
Defective control of apoptosis and mitotic spindle checkpoint in heterozygous carriers of ATM mutations  
*Cancer Research* **59**:2602–7 1999 [Abstract](#)
- 1210 Shih IM, Yu J, He TC, Vogelstein B and Kinzler KW  
The beta-catenin binding domain of adenomatous polyposis coli is sufficient for tumor suppression  
*Cancer Research* **60**:1671–6 2000 [Abstract](#)
- 1211 Shih YC, Kerr J, Liu J, Hurst T, Khoo SK, Ward B, Wainwright B and Chenevix Trench G  
Rare mutations and no hypermethylation at the CDKN2A locus in epithelial ovarian tumours  
*International Journal of Cancer* **70**:508–11 1997 [Abstract](#)
- 1212 Shiloh Y  
Ataxia-telangiectasia and the Nijmegen breakage syndrome: related disorders but genes apart.  
*Annual Review of Genetics* **31**:635–62 1997 [Abstract](#)
- 1213 Shiloh Y  
ATM and ATR: networking cellular responses to DNA damage  
*Current Opinion in Genetics and Development* **11**:71–77 2001 [Abstract](#)
- 1214 Shimamura A, Ballif BA, Richards SA and Blenis J  
Rsk1 mediates a MEK-MAP kinase cell survival signal  
*Current Biology* **10**:127–35 2000 [Abstract](#)
- 1215 Shirane M, Harumiya Y, Ishida N, Hirai A, Miyamoto C, Hatakeyama S, Nakayama K and Kitagawa M  
Down-regulation of p27(Kip1) by two mechanisms, ubiquitin-mediated degradation and proteolytic processing  
*Journal of Biological Chemistry* **274**:13886–93 1999 [Abstract](#)



- 1216 Shtutman M, Zhurinsky J, Simcha I, Albanese C, D'Amico M, Pestell R and Ben Ze'ev A  
The cyclin D1 gene is a target of the beta-catenin/LEF-1 pathway  
*Proceedings of the National Academy of Sciences of the USA* **96**:5522-7 1999 [Abstract](#)
- 1217 Shulze A, Zeffass-Thome K, Berges J, Middendorp S, Jansen-Durr P and Henglein B  
Anchorage-dependent transcription of the cyclin A gene  
*Molecular and Cellular Biology* **16**:4632-8 1996 [Abstract](#)
- 1218 Si SP, Tsou HC, Lee X and Peacocke M  
Cultured human melanocytes express the intermediate filament vimentin  
*Journal of Investigative Dermatology* **101**:383-6 1993 [Abstract](#)
- 1219 Sideras P, Muller S, Shiels H, Jin H, Khan WN, Nilsson L, Parkinson E, Thomas JD, Branden L, Larsson I et al  
Genomic organization of mouse and human Bruton's agammaglobulinemia tyrosine kinase (Btk) loci  
*Journal of Immunology* **153**:5607-17 1994 [Abstract](#)
- 1220 Siebert R, Willers CP, Schramm A, Fossa A, Dresen IM, Uppenkamp M, Nowrousian MR, Seeber S and Opalka B  
Homozygous loss of the MTS1/p16 and MTS2/p15 genes in lymphoma and lymphoblastic leukaemia cell lines  
*British Journal of Haematology* **91**:350-4 1995 [Abstract](#)
- 1221 Siegert JL and Robbins PD  
Rb inhibits the intrinsic kinase activity of TATA-binding protein-associated factor TAFII250  
*Molecular and Cellular Biology* **19**:846-54 1999 [Abstract](#)
- 1222 Siegert JL, Rushton JJ, Sellers WR, Kaelin WG Jr and Robbins PD  
Cyclin D1 suppresses retinoblastoma protein-mediated inhibition of TAFII250 kinase activity  
*Oncogene* **19**:5703-11 2000 [Abstract](#)
- 1223 Sijbers AM, de Laat WL, Ariza RR, Biggerstaff M, Wei YF, Moggs JG, Carter KC, Shell BK, Evans E, de Jong MC, Rademakers S, de Rooij J, Jaspers NG, Hoeijmakers JH and Wood RD  
Xeroderma pigmentosum group F caused by a defect in a structure-specific DNA repair endonuclease  
*Cell* **86**:811-22 1996 [Abstract](#)
- 1224 Silberstein GB, Van Horn K, Strickland P, Roberts CT Jr and Daniel CW  
Altered expression of the WT1 Wilms tumor suppressor gene in human breast cancer  
*Proceedings of the National Academy of Sciences of the USA* **94**:8132-7 1997 [Abstract](#)
- 1225 Sill H, Aguiar CT, Schmidt H, Hochhaus A, Goldman JM and Cross NC  
Mutational analysis of the p15 and p16 genes in acute leukaemias  
*British Journal of Haematology* **92**:681-3 1996 [Abstract](#)
- 1226 Silvin C, Belisle B and Abo A  
A role for WASP in TCR-mediated transcriptional activation independent of actin polymerization  
*Journal of Biological Chemistry* **276**:21450-7 2001 [Abstract](#)
- 1227 Simon M, Koster G, Menon AG and Schramm J  
Functional evidence for a role of combined CDKN2A (p16-p14(ARF))/CDKN2B (p15) gene inactivation in malignant gliomas  
*Acta Neuropathologica* **98**:444-52 1999 [Abstract](#)
- 1228 Simons A, Melamed-Bessudo C, Wolkowicz R, Sperling J, Sperling R, Eisenbach L and Rotter V  
PACT: cloning and characterization of a cellular p53 binding protein that interacts with Rb  
*Oncogene* **14**:145-55 1997 [Abstract](#)
- 1229 Simpkins SB, Bocker T, Swisher EM, Mutch DG, Gersell DJ, Kovatich AJ, Palazzo JP, Fishel R and Goodfellow PJ  
MLH1 promoter methylation and gene silencing is the primary cause of microsatellite instability in sporadic endometrial cancers  
*Human Molecular Genetics* **8**:661-6 1999 [Abstract](#)
- 1230 Simpson DJ, Hibberts NA, McNicol AM, Clayton RN and Farrell WE  
Loss of pRb expression in pituitary adenomas is associated with methylation of the RB1 CpG island  
*Cancer Research* **60**:1211-6 2000 [Abstract](#)
- 1231 Simpson L and Parsons R  
PTEN: Life as a Tumor Suppressor  
*Experimental Cell Research* **264**:29-41 2001 [Abstract](#)
- 1232 Singal R, van Wert J and Bashambu M  
Cytosine methylation represses glutathione S-transferase P1 (GSTP1) gene expression in human prostate cancer cells  
*Cancer Research* **61**:4820-6 2001 [Abstract](#)
- 1233 Singer JD, Gurian-West M, Clurman B and Roberts JM  
Cullin-3 targets cyclin E for ubiquitination and controls S phase in mammalian cells  
*Genes and Development* **13**:2375-87 1999 [Abstract](#)
- 1234 Singh RK, Varney ML, Bucana CD and Johansson SL  
Expression of interleukin-8 in primary and metastatic malignant melanoma of the skin  
*Melanoma Research* **9**:383-7 1999 [Abstract](#)
- 1235 Skyldberg B, Fujioka K, Hellstrom AC, Sylven L, Moberger B and Auer G  
Human papillomavirus infection, centrosome aberration, and genetic stability in cervical lesions  
*Modern Pathology* **14**:279-84 2001 [Abstract](#)
- 1236 Slawinska D and Slawinski J  
Ultraweak photon emission in model reactions of the in vitro formation of eumelanins and pheomelanins  
*Pigment Cell Research* **1**:171-5 1987 [Abstract](#)
- 1237 Sluder G and Hinchcliffe EH  
Control of centrosome reproduction: the right number at the right time  
*Biology of the Cell* **91**:413-27 1999 [Abstract](#)
- 1238 Smit NP, Van der Meulen H, Koerten HK, Kolb RM, Mommaas AM, Lentjes EG and Pavel S  
Melanogenesis in cultured melanocytes can be substantially influenced by L-tyrosine and L-cysteine  
*Journal of Investigative Dermatology* **109**:796-800 1997 [Abstract](#)
- 1239 Smith DP, Spicer J, Smith A, Swift S and Ashworth A  
The mouse Peutz-Jeghers syndrome gene Lkb1 encodes a nuclear protein kinase  
*Human Molecular Genetics* **8**:1479-85 1999 [Abstract](#)
- 1240 Smith EJ, Leone G and Nevins JR  
Distinct mechanisms control the accumulation of the Rb-related p107 and p130 proteins during cell growth  
*Cell Growth and Differentiation* **9**:297-303 1998 [Abstract](#)
- 1241 Smith J, Andrau JC, Kallenbach S, Laquerbe A, Doyen N and Papadopoulou D  
Abnormal rearrangements associated with V(D)J recombination in Fanconi anemia  
*Journal of Molecular Biology* **281**:815-25 1998 [Abstract](#)

## Human metastatic melanoma in vitro

- 1242 Smith L, Liu SJ, Goodrich L, Jacobson D, Degnin C, Bentley N, Carr A, Flaggs G, Keegan K, Hoekstra M and Thayer MJ  
Duplication of ATR inhibits MyoD, induces aneuploidy and eliminates radiation-induced G1 arrest  
*Nature Genetics* **19**:39–46 1998 [Abstract](#)
- 1243 Smits VA, van Peer MA, Essers MA, Klompmaker R, Rijksen G and Medema RH  
Negative growth regulation of SK-N-MC cells by bFGF defines a growth factor-sensitive point in G2  
*Journal of Biological Chemistry* **275**:19375–81 2000 [Abstract](#)
- 1244 Sneller MC  
Common variable immunodeficiency  
*American Journal of Medical Science* **321**:42–8 2001 [Abstract](#)
- 1245 Somasundaram K, Zhang H, Zeng YX, Houvras Y, Peng Y, Zhang H, Wu GS, Licht JD, Weber BL and El-Deiry WS  
Arrest of the cell cycle by the tumour-suppressor BRCA1 requires the CDK-inhibitor p21WAF1/Cip1  
*Nature* **389**:187–90 1997 [Abstract](#)
- 1246 Somlyo AV, Bradshaw D, Ramos S, Murphy C, Myers CE and Somlyo AP  
Rho-kinase inhibitor retards migration and in vivo dissemination of human prostate cancer cells  
*Biochemical and Biophysical Research Communications* **269**:652–9 2000 [Abstract](#)
- 1247 Song SH, Jong HS, Choi HH, Inoue H, Tanabe T, Kim NK and Bang YJ  
Transcriptional silencing of Cyclooxygenase-2 by hyper-methylation of the 5' CpG island in human gastric carcinoma cells  
*Cancer Research* **61**:4628–35 2001 [Abstract](#)
- 1248 Sotillo R, Dubus P, Martin J, de la Cueva E, Ortega S, Malumbres M and Barbacid M  
Wide spectrum of tumors in knock-in mice carrying a Cdk4 protein insensitive to INK4 inhibitors  
*EMBO Journal* **20**:6637–47 2001 [Abstract](#)
- 1249 Sotillo R, Garcia JF, Ortega S, Martin J, Dubus P, Barbacid M and Malumbres M  
Invasive melanoma in Cdk4-targeted mice  
*Proceedings of the National Academy of Sciences of the USA* **98**:13312–7 2001 [Abstract](#)
- 1250 Soufir N, Avril MF, Chompret A, Demenais F, Bombléd J, Spatz A, Stoppa-Lyonnet D, Benard J and Bressac de Paillerets B  
Prevalence of p16 and CDK4 germline mutations in 48 melanoma-prone families in France. The French Familial Melanoma Study Group  
*Human Molecular Genetics* **7**:209–16 1998 [Abstract](#)
- 1251 Soufir N, Moles JP, Vilmer C, Moch C, Verola O, Rivet J, Tesniere A, Dubertret L and Basset Seguin N  
P16 UV mutations in human skin epithelial tumors  
*Oncogene* **18**:5477–81 1999 [Abstract](#)
- 1252 Souza RF, Yin J, Smolinski KN, Zou TT, Wang S, Shi YQ, Rhyu MG, Cottrell J, Abraham JM, Biden K, Simms L, Leggett B, Bova GS, Frank T, Powell SM, Sugimura H, Young J, Harpaz N, Shimizu K, Matsubara N and Meltzer SJ  
Frequent mutation of the E2F-4 cell cycle gene in primary human gastrointestinal tumors  
*Cancer Research* **57**:2350–3 1997 [Abstract](#)
- 1253 Spacey SD, Gatti RA and Bebb G  
The molecular basis and clinical management of ataxia telangiectasia  
*Canadian Journal of Neurological Sciences* **27**:184–91 2000 [Abstract](#)
- 1254 Spirin KS, Simpson JF, Takeuchi S, Kawamata N, Miller CW and Koeffler HP  
p27/Kip1 mutation found in breast cancer  
*Cancer Research* **56**:2400–4 1996 [Abstract](#)
- 1255 Spritz RA  
Multi-organellar disorders of pigmentation: tied up in traffic  
*Clinical Genetics* **55**:309–17 1999 [Abstract](#)
- 1256 Spruck CH, Won KA and Reed SI  
Deregulated cyclin E induces chromosome instability  
*Nature* **401**:297–300 1999 [Abstract](#)
- 1257 St Croix B, Sheehan C, Rak JW, Florenes VA, Slingerland JM and Kerbel RS  
E-Cadherin-dependent growth suppression is mediated by the cyclin-dependent kinase inhibitor p27(KIP1)  
*Journal of Cell Biology* **142**:557–71 1998 [Abstract](#)
- 1258 Stamenkovic I  
Matrix metalloproteinases in tumor invasion and metastasis  
*Seminars in Cancer Biology* **10**:415–33 2000 [Abstract](#)
- 1259 Stavridi ES, Chehab NH, Malikzay A and Halazonetis TD  
Substitutions that compromise the ionizing radiation-induced association of p53 with 14–3-3 proteins also compromise the ability of p53 to induce cell cycle arrest  
*Cancer Research* **61**:7030–3 2001 [Abstract](#)
- 1260 Sterner JM, Murata Y, Kim HG, Kennett SB, Templeton DJ and Horowitz JM  
Detection of a novel cell cycle-regulated kinase activity that associates with the amino terminus of the retinoblastoma protein in G2/M phases  
*Journal of Biological Chemistry* **270**:9281–8 1995 [Abstract](#)
- 1261 Sterner JM, Tao Y, Kennett SB, Kim HG and Horowitz JM  
The amino terminus of the retinoblastoma (Rb) protein associates with a cyclin-dependent kinase-like kinase via Rb amino acids required for growth suppression  
*Cell Growth and Differentiation* **7**:53–64 1996 [Abstract](#)
- 1262 Stewart GS, Maser RS, Stankovic T, Bressan DA, Kaplan MI, Jaspers NG, Raams A, Byrd PJ, Petrini JH and Taylor AM  
The DNA double-strand break repair gene hMRE11 is mutated in individuals with an ataxia-telangiectasia-like disorder  
*Cell* **99**:577–87 1999 [Abstract](#)
- 1263 Stewart SA and Weinberg RA  
Senescence: does it all happen at the ends?  
*Oncogene* **21**:627–30 2002 [Abstract](#)
- 1264 Stiegler P and Giordano A  
The family of retinoblastoma proteins  
*Critical Reviews in Eukaryotic Gene Expression* **11**:59–76 2001 [Abstract](#)
- 1265 Stone DM, Hynes M, Armanini M, Swanson TA, Gu Q, Johnson RL, Scott MP, Pennica D, Goddard A, Phillips H, Noll M, Hooper JE, de Sauvage F and Rosenthal A  
The tumour-suppressor gene patched encodes a candidate receptor for Sonic hedgehog  
*Nature* **384**:129–34 1996 [Abstract](#)
- 1266 Stoppler H, Stoppler MC, Johnson E, Simbulan Rosenthal CM, Smulson ME, Iyer S, Rosenthal DS and Schlegel R  
The E7 protein of human papillomavirus type 16 sensitizes primary human keratinocytes to apoptosis  
*Oncogene* **17**:1207–14 1998 [Abstract](#)





- 1267 Strange RC and Fryer AA  
Chapter 19. The glutathione S-transferases: influence of polymorphism on cancer susceptibility  
*IARC Scientific Publications (Lyon)* **148**:231–49 1999 [Abstract](#)
- 1268 Strom M, Hume AN, Tarafder AK, Barkagianni E and Seabra MC  
A family of Rab27-binding proteins: Melanophilin links Rab27a and myosin Va function in melanosome transport  
*Journal of Biological Chemistry* in press 2002 [Abstract](#)
- 1269 Stucke VM, Sillje HH, Arnaud L and Nigg EA  
Human Mps1 kinase is required for the spindle assembly checkpoint but not for centrosome duplication  
*EMBO Journal* **21**:1723–32 2002 [Abstract](#)
- 1270 Sturm RA, Teasdale RD and Box NF  
Human pigmentation genes: identification, structure and consequences of polymorphic variation  
*Gene* **277**:49–62 2001 [Abstract](#)
- 1271 Su GH, Hruban RH, Bansal RK, Bova GS, Tang DJ, Shekher MC, Westerman AM, Entius MM, Goggins M, Yeo CJ and Kern SE  
Germline and somatic mutations of the STK11/LKB1 Peutz-Jeghers gene in pancreatic and biliary cancers  
*American Journal of Pathology* **154**:1835–40 1999 [Abstract](#)
- 1272 Sullivan KE, Mullen CA, Blaese RM and Winkelstein JA  
A multiinstitutional survey of the Wiskott-Aldrich syndrome  
*Journal of Pediatrics* **125**:876–85 1994 [Abstract](#)
- 1273 Sung P, Bailly V, Weber C, Thompson LH, Prakash L and Prakash S  
Human xeroderma pigmentosum group D gene encodes a DNA helicase  
*Nature* **365**:852–5 1993 [Abstract](#)
- 1274 Suspiro A, Fidalgo P, Cravo M, Albuquerque C, Ramalho E, Leitao CN and Costa Mira F  
The Muir-Torre syndrome: a rare variant of hereditary nonpolyposis colorectal cancer associated with hMSH2 mutation  
*American Journal of Gastroenterology* **93**:1572–4 1998 [Abstract](#)
- 1275 Suzuki E, Nagata D, Kakoki M, Hayakawa H, Goto A, Omata M and Hirata Y  
Molecular mechanisms of endothelin-1-induced cell-cycle progression: involvement of extracellular signal-regulated kinase, protein kinase C, and phosphatidylinositol 3-kinase at distinct points  
*Circulation Research* **84**:611–9 1999 [Abstract](#)
- 1276 Suzuki I, Im S, Tada A, Scott C, Akcali C, Davis MB, Barsh G, Hearing V and Abdel-Malek Z  
Participation of the melanocortin-1 receptor in the UV control of pigmentation  
*Journal of Investigative Dermatology Symposium Proceedings* **4**:29–34 1999 [Abstract](#)
- 1277 Suzuki I, Tada A, Ollmann MM, Barsh GS, Im S, Lamoreux ML, Hearing VJ, Nordlund JJ and Abdel-Malek ZA  
Agouti signaling protein inhibits melanogenesis and the response of human melanocytes to alpha-melanotropin  
*Journal of Investigative Dermatology* **108**:838–42 1997 [Abstract](#)
- 1278 Suzuki K, Kodama S and Watanabe M  
Recruitment of ATM protein to double strand DNA irradiated with ionizing radiation  
*Journal of Biological Chemistry* **274**:25571–5 1999 [Abstract](#)
- 1279 Suzuki N, Ueno T, Kaneko A, Fujii S and Fujinaga K  
Analysis of retinoblastoma for human adenovirus type 12 genome  
*Graefes Archive for Clinical and Experimental Ophthalmology* **220**:167–70 1983 [Abstract](#)
- 1280 Suzuki S, Katagiri T and Takeuchi T  
Macrophages release melanocyte dendrite extension factor in response to ultra-violet ray  
*In Vitro Cellular and Developmental Biology. Animal* **29A**:419–26 1993 [Abstract](#)
- 1281 Suzuki-Takahashi I, Kitagawa M, Saijo M, Higashi H, Ogino H, Matsumoto H, Taya Y, Nishimura S and Okuyama A  
The interactions of E2F with pRB and with p107 are regulated via the phosphorylation of pRB and p107 by a cyclin-dependent kinase  
*Oncogene* **10**:1691–8 1995 [Abstract](#)
- 1282 Svedberg H, Chylicki K, Baldetorp B, Rauscher FJ 3rd and Gullberg U  
Constitutive expression of the Wilms' tumor gene (WT1) in the leukemic cell line U937 blocks parts of the differentiation program  
*Oncogene* **16**:925–32 1998 [Abstract](#)
- 1283 Svecizer A, Novak B and Mitchison JM  
The size control of fission yeast revisited  
*Journal of Cell Science* **109**:2947–57 1996 [Abstract](#)
- 1284 Sviderskaya EV, Hill SP, Evans-Whipp TJ, Chin L, Orlow SJ, Easty DJ, Cheong SC, Beach D, DePinho RA and Bennett DC  
p16(Ink4a) in melanocyte senescence and differentiation  
*Journal of the National Cancer Institute* **94**:446–54 2002 [Abstract](#)
- 1285 Sweeney KJ, Sarcevic B, Sutherland RL and Musgrove EA  
Cyclin D2 activates Cdk2 in preference to Cdk4 in human breast epithelial cells  
*Oncogene* **14**:1329–40 1997 [Abstract](#)
- 1286 Symons M, Derry JM, Karlak B, Jiang S, Lemahieu V, McCormick F, Francke U and Abo A  
Wiskott-Aldrich syndrome protein, a novel effector for the GTPase CDC42Hs, is implicated in actin polymerization  
*Cell* **84**:723–34 1996 [Abstract](#)
- 1287 Szekeley L, Jin P, Jiang WQ, Rosen A, Wiman KG, Klein G and Ringertz N  
Position-dependent nuclear accumulation of the retinoblastoma (RB) protein during in vitro myogenesis  
*Journal of Cellular Physiology* **155**:313–22 1993 [Abstract](#)
- 1288 Tachibana M, Takeda K, Nobukuni Y, Urabe K, Long JE, Meyers KA, Aaronson SA and Miki T  
Ectopic expression of MITF, a gene for Waardenburg syndrome type 2, converts fibroblasts to cells with melanocyte characteristics  
*Nature Genetics* **14**:50–4 1996 [Abstract](#)
- 1289 Tada A, Suzuki I, Im S, Davis MB, Cornelius J, Babcock G, Nordlund JJ and Abdel-Malek ZA  
Endothelin-1 is a paracrine growth factor that modulates melanogenesis of human melanocytes and participates in their responses to ultraviolet radiation  
*Cell Growth and Differentiation* **9**:575–84 1998 [Abstract](#)
- 1290 Takagi M, Delia D, Chessa L, Iwata S, Shigeta T, Kanke Y, Goi K, Asada M, Eguchi M, Kodama C and Mizutani S  
Defective control of apoptosis, radiosensitivity, and spindle checkpoint in ataxia telangiectasia  
*Cancer Research* **58**:4923–9 1998 [Abstract](#)
- 1291 Takahashi K, Nakayama Ki and Nakayama K  
Mice lacking a CDK inhibitor, p57Kip2, exhibit skeletal abnormalities and growth retardation  
*Journal of Biochemistry* **127**:73–83 2000 [Abstract](#)
- 1292 Takano Y, Kato Y, Masuda M, Ohshima Y and Okayasu I  
Cyclin D2, but not cyclin D1, overexpression closely correlates with gastric cancer progression and prognosis  
*Journal of Pathology* **189**:194–200 1999 [Abstract](#)

## Human metastatic melanoma in vitro

- 1293 Takeda K, Takemoto C, Kobayashi I, Watanabe A, Nobukuni Y, Fisher DE and Tachibana M  
Ser298 of MITF, a mutation site in Waardenburg syndrome type 2, is a phosphorylation site with functional significance  
*Human Molecular Genetics* **9**:125–32 2000 [Abstract](#)
- 1294 Takimoto H, Tsukuda K, Ichimura K, Hanafusa H, Nakamura A, Oda M, Harada M and Shimizu K  
Genetic alterations in the retinoblastoma protein-related p107 gene in human hematologic malignancies  
*Biochemical and Biophysical Research Communications* **251**:264–8 1998 [Abstract](#)
- 1295 Tamrakar S and Ludlow JW  
The carboxyl-terminal region of the retinoblastoma protein binds non-competitively to protein phosphatase type 1alpha and inhibits catalytic activity  
*Journal of Biological Chemistry* **275**:27784–9 2000 [Abstract](#)
- 1296 Tamrakar S, Rubin E and Ludlow JW  
Role of pRB dephosphorylation in cell cycle regulation  
*Frontiers in Bioscience* **5**:D121–37 2000 [Abstract](#)
- 1297 Tamura M, Gu J, Danen EH, Takino T, Miyamoto S and Yamada KM  
PTEN interactions with focal adhesion kinase and suppression of the extracellular matrix-dependent phosphatidylinositol 3-kinase/Akt cell survival pathway  
*Journal of Biological Chemistry* **274**:20693–703 1999 [Abstract](#)
- 1298 Tamura M, Gu J, Tran H and Yamada KM  
PTEN gene and integrin signaling in cancer  
*Journal of the National Cancer Institute* **91**:1820–8 1999 [Abstract](#)
- 1299 Tan JE, Wong SC, Gan SK, Xu S and Lam KP  
The adaptor protein BLNK is required for B cell antigen receptor-induced activation of NFk-B and cell cycle entry and survival of B lymphocytes  
*Journal of Biological Chemistry* in press 2001 [Abstract](#)
- 1300 Tan X and Wang JY  
The caspase-RB connection in cell death  
*Trends in Cell Biology* **8**:116–20 1998 [Abstract](#)
- 1301 Tan Y, Demeter MR, Ruan H and Comb MJ  
BAD Ser-155 phosphorylation regulates BAD/Bcl-XL interaction and cell survival  
*Journal of Biological Chemistry* **275**:25865–9 2000 [Abstract](#)
- 1302 Tanaka K, Boddy MN, Chen XB, McGowan CH and Russell P  
Threonine-11, phosphorylated by Rad3 and atm in vitro, is required for activation of fission yeast checkpoint kinase Cds1  
*Molecular and Cellular Biology* **21**:3398–404 2001 [Abstract](#)
- 1303 Tanaka K, Miura N, Satokata I, Miyamoto I, Yoshida MC, Satoh Y, Kondo S, Yasui A, Okayama H and Okada Y  
Analysis of a human DNA excision repair gene involved in group A xeroderma pigmentosum and containing a zinc-finger domain  
*Nature* **348**:73–6 1990 [Abstract](#)
- 1304 Tanaka T, Kimura M, Matsunaga K, Fukada D, Mori H and Okano Y  
Centrosomal kinase AIK1 is overexpressed in invasive ductal carcinoma of the breast  
*Cancer Research* **59**:2041–4 1999 [Abstract](#)
- 1305 T'Ang A, Wu KJ, Hashimoto T, Liu WY, Takahashi R, Shi XH, Mihara K, Zhang FH, Chen YY, Du C et al  
Genomic organization of the human retinoblastoma gene  
*Oncogene* **4**:401–7 1989 [Abstract](#)
- 1306 Tang A, Eller MS, Hara M, Yaar M, Hirohashi S and Gilchrist BA  
E-cadherin is the major mediator of human melanocyte adhesion to keratinocytes in vitro  
*Journal of Cell Science* **107**:983–92 1994 [Abstract](#)
- 1307 Tang L, Li G, Tron VA, Trotter MJ and Ho VC  
Expression of cell cycle regulators in human cutaneous malignant melanoma  
*Melanoma Research* **9**:148–54 1999 [Abstract](#)
- 1308 Tang Q, Gonzales M, Inoue H and Bowden GT  
Roles of Akt and glycogen synthase kinase 3beta in the ultraviolet B induction of cyclooxygenase-2 transcription in human keratinocytes  
*Cancer Research* **61**:4329–32 2001 [Abstract](#)
- 1309 Tarapore P, Horn HF, Tokuyama Y and Fukasawa K  
Direct regulation of the centrosome duplication cycle by the p53-p21Waf1/Cip1 pathway  
*Oncogene* **20**:3173–84 2001 [Abstract](#)
- 1310 Tarapore P, Tokuyama Y, Horn HF and Fukasawa K  
Difference in the centrosome duplication regulatory activity among p53 'hot spot' mutants: potential role of Ser 315 phosphorylation-dependent centrosome binding of p53  
*Oncogene* **20**:6851–63 2001 [Abstract](#)
- 1311 Tasaka T, Berenson J, Vescio R, HIRAMA T, Miller CW, Nagai M, Takahara J and Koeffler HP  
Analysis of the p16INK4A, p15INK4B and p18INK4C genes in multiple myeloma  
*British Journal of Haematology* **96**:98–102 1997 [Abstract](#)
- 1312 Tatsuka M, Katayama H, Ota T, Tanaka T, Odashima S, Suzuki F and Terada Y  
Multinuclearity and increased ploidy caused by overexpression of the aurora- and lpl1-like midbody-associated protein mitotic kinase in human cancer cells  
*Cancer Research* **58**:4811–6 1998 [Abstract](#)
- 1313 Tatsumoto T, Xie X, Blumenthal R, Okamoto I and Miki T  
Human ECT2 is an exchange factor for Rho GTPases, phosphorylated in G2/M phases, and involved in cytokinesis  
*Journal of Cell Biology* **147**:921–8 1999 [Abstract](#)
- 1314 Tavtigian SV, Simard J, Rommens J, Couch F, Shattuck-Eidens D, Neuhausen S, Merajver S, Thorlacius S, Offit K, Stoppa-Lyonnet D, Belanger C, Bell R, Berry S, Bogden R, Chen Q, Davis T, Dumont M, Frye C, Hattier T, Jammulapati S, Janecki T, Jiang P, Kehrer R, Leblanc JF, Goldgar DE et al  
The complete BRCA2 gene and mutations in chromosome 13q-linked kindreds  
*Nature Genetics* **12**:333–7 1996 [Abstract](#)
- 1315 Taylor WR, Schonthal AH, Galante J and Stark GR  
p130/E2F4 binds to and represses the cdc2 promoter in response to p53  
*Journal of Biological Chemistry* **276**:1998–2006 2001 [Abstract](#)
- 1316 Teitz T, Wei T, Valentine MB, Vanin EF, Grenet J, Valentine VA, Behm FG, Look AT, Lahti JM and Kidd VJ  
Caspase 8 is deleted or silenced preferentially in childhood neuroblastomas with amplification of MYCN  
*Nature Medicine* **6**:529–35 2000 [Abstract](#)



- 1317 Templeton DJ  
Nuclear binding of purified retinoblastoma gene product is determined by cell cycle-regulated phosphorylation  
*Molecular and Cellular Biology* 12:435–43 1992 [Abstract](#)
- 1318 Templeton DJ, Park SH, Lanier L and Weinberg RA  
Nonfunctional mutants of the retinoblastoma protein are characterized by defects in phosphorylation, viral oncoprotein association, and nuclear tethering  
*Proceedings of the National Academy of Sciences of the USA* 88:3033–7 1991 [Abstract](#)
- 1319 Teodoro JG, Shore GC and Branton PE  
Adenovirus E1A proteins induce apoptosis by both p53-dependent and p53-independent mechanisms  
*Oncogene* 11:467–74 1995 [Abstract](#)
- 1320 Terry LA, Boyd J, Alcorta D, Lyon T, Solomon G, Hannon G, Berchuck A, Beach D and Barrett JC  
Mutational analysis of the p21/WAF1/CIP1/SDI1 coding region in human tumor cell lines  
*Molecular Carcinogenesis* 16:221–8 1996 [Abstract](#)
- 1321 Teschauer W, Mussack T, Braun A, Waldner H and Fink E  
Conditions for single strand conformation polymorphism (SSCP) analysis with broad applicability: a study on the effects of acrylamide, buffer and glycerol concentrations in SSCP analysis of exons of the p53 gene)  
*European Journal of Clinical Chemistry and Clinical Biochemistry* 34:125–31 1996 [Abstract](#)
- 1322 Tevosian SG, Shih HH, Mendelson KG, Sheppard KA, Paulson KE and Yee AS  
HBP1: a HMG box transcriptional repressor that is targeted by the retinoblastoma family  
*Genes and Development* 11:383–96 1997 [Abstract](#)
- 1323 Thakker RV  
Multiple endocrine neoplasia—syndromes of the twentieth century  
*Journal of Clinical Endocrinology and Metabolism* 83:2617–20 1998 [Abstract](#)
- 1324 Thody AJ  
alpha-MSH and the regulation of melanocyte function  
*Annals of the New York Academy of Sciences* 885:217–29 1999 [Abstract](#)
- 1325 Thommes K, Lennartsson J, Carlberg M and Ronnstrand L  
Identification of Tyr-703 and Tyr-936 as the primary association sites for Grb2 and Grb7 in the c-Kit/stem cell factor receptor  
*Biochemical Journal* 341:211–6 1999 [Abstract](#)
- 1326 Thullberg M, Bartkova J, Khan S, Hansen K, Ronnstrand L, Lukas J, Strauss M and Bartek J  
Distinct versus redundant properties among members of the INK4 family of cyclin-dependent kinase inhibitors  
*FEBS Letters* 470:161–6 2000 [Abstract](#)
- 1327 Tibbetts RS, Brumbaugh KM, Williams JM, Sarkaria JN, Cliby WA, Shieh SY, Taya Y, Prives C and Abraham RT  
A role for ATR in the DNA damage-induced phosphorylation of p53  
*Genes and Development* 13:152–7 1999 [Abstract](#)
- 1328 Tibbetts RS, Cortez D, Brumbaugh KM, Scully R, Livingston D, Elledge SJ and Abraham RT  
Functional interactions between BRCA1 and the checkpoint kinase ATR during genotoxic stress  
*Genes and Development* 14:2989–3002 2000 [Abstract](#)
- 1329 Timmers C, Taniguchi T, Hejna J, Reifsteck C, Lucas L, Bruun D, Thayer M, Cox B, Olson S, D'Andrea AD, Moses R and Grompe M  
Positional cloning of a novel Fanconi anemia gene, FANCD2  
*Molecular Cell* 7:241–8 2001 [Abstract](#)
- 1330 Toguchida J, McGee TL, Paterson JC, Eagle JR, Tucker S, Yandell DW and Dryja TP  
Complete genomic sequence of the human retinoblastoma susceptibility gene  
*Genomics* 17:535–43 1993 [Abstract](#)
- 1331 Toker A and Newton AC  
Akt/protein kinase B is regulated by autophosphorylation at the hypothetical PDK-2 site  
*Journal of Biological Chemistry* 275:8271–4 2000 [Abstract](#)
- 1332 Tokuyama Y, Horn HF, Kawamura K, Tarapore P and Fukasawa K  
Specific phosphorylation of nucleophosmin on Thr(199) by cyclin-dependent kinase 2-cyclin E and its role in centrosome duplication  
*Journal of Biological Chemistry* 276:21529–37 2001 [Abstract](#)
- 1333 Tominaga K, Morisaki H, Kaneko Y, Fujimoto A, Tanaka T, Ohtsubo M, Hirai M, Okayama H, Ikeda K and Nakanishi M  
Role of human Cds1 (Chk2) kinase in DNA damage checkpoint and its regulation by p53  
*Journal of Biological Chemistry* 274:31463–7 1999 [Abstract](#)
- 1334 Touhara K, Inglese J, Pitcher JA, Shaw G and Lefkowitz RJ  
Binding of G protein beta gamma-subunits to pleckstrin homology domains  
*Journal of Biological Chemistry* 269:10217–20 1994 [Abstract](#)
- 1335 Toyooka KO, Toyooka S, Virmani AK, Sathyanarayana UG, Euhus DM, Gilcrease M, Minna JD and Gazdar AF  
Loss of expression and aberrant methylation of the CDH13 (H-cadherin) gene in breast and lung carcinomas  
*Cancer Research* 61:4556–60 2001 [Abstract](#)
- 1336 Toyoshima H and Hunter T  
p27, a novel inhibitor of G1 cyclin-Cdk protein kinase activity, is related to p21  
*Cell* 78:67–74 1994 [Abstract](#)
- 1337 Traboulsi EI, Zimmerman LE and Manz HJ  
Cutaneous malignant melanoma in survivors of heritable retinoblastoma  
*Archives of Ophthalmology* 106:1059–61 1988 [Abstract](#)
- 1338 Tran TA, Ross JS, Carlson JA and Mihm MC Jr  
Mitotic cyclins and cyclin-dependent kinases in melanocytic lesions  
*Human Pathology* 29:1085–90 1998 [Abstract](#)
- 1339 Trimarchi JM and Lees JA Nat Rev  
Sibling rivalry in the E2F family  
*Molecular and Cellular Biology* 3:11–20 2002 [Abstract](#)
- 1340 Trotter MJ, Tang L and Tron VA  
Overexpression of the cyclin-dependent kinase inhibitor p21(WAF1/CIP1) in human cutaneous malignant melanoma  
*Journal of Cutaneous Pathology* 24:265–71 1997 [Abstract](#)
- 1341 Trujillo KM, Yuan SS, Lee EY and Sung P  
Nuclease activities in a complex of human recombination and DNA repair factors Rad50, Mre11, and p95  
*Journal of Biological Chemistry* 273:21447–50 1998 [Abstract](#)

## Human metastatic melanoma in vitro

- |      |  |              |      |                          |
|------|--|--------------|------|--------------------------|
| 1342 | Trujillo KM and Sung P<br>DNA structure-specific nuclease activities in the <i>Saccharomyces cerevisiae</i> Rad50*Mrp11 complex<br><i>Journal of Biological Chemistry</i>  | 276:35458-64 | 2001 | <a href="#">Abstract</a> |
| 1343 | Tsao H, Benoit E, Sober AJ, Thiele C and Haluska FG<br>Novel mutations in the p16/CDKN2A binding region of the cyclin-dependent kinase-4 gene<br><i>Cancer Research</i>  | 58:109-13    | 1998 | <a href="#">Abstract</a> |
| 1344 | Tsao H, Zhang X, Majewski P and Haluska FG<br>Mutational and expression analysis of the p73 gene in melanoma cell lines<br><i>Cancer Research</i>  | 59:172-4     | 1999 | <a href="#">Abstract</a> |
| 1345 | Tsubari M, Tiihonen E and Laiho M<br>Cloning and characterization of p10, an alternatively spliced form of p15 cyclin-dependent kinase inhibitor<br><i>Cancer Research</i>   | 57:2966-73   | 1997 | <a href="#">Abstract</a> |
| 1346 | Tsujimura T, Morii E, Nozaki M, Hashimoto K, Moriyama Y, Takebayashi K, Kondo T, Kanakura Y and Kitamura Y<br>Involvement of transcription factor encoded by the mi locus in the expression of c-kit receptor tyrosine kinase in cultured mast cells of mice<br><i>Blood</i>   | 88:1225-33   | 1996 | <a href="#">Abstract</a> |
| 1347 | Tsumanuma I, Tanaka R, Abe S, Kawasaki T, Washiyama K and Kumanishi T<br>Infrequent mutation of Waf1/p21 gene, a CDK inhibitor gene, in brain tumors<br><i>Neurologia Medico-Chirurgica</i>  | 37:150-6     | 1997 | <a href="#">Abstract</a> |
| 1348 | Tugendreich S, Tomkiel J, Earnshaw W and Hieter P<br>CDC27Hs colocalizes with CDC16Hs to the centrosome and mitotic spindle and is essential for the metaphase to anaphase transition<br><i>Cell</i>   | 81:261-8     | 1995 | <a href="#">Abstract</a> |
| 1349 | Tutt A, Gabriel A, Bertwistle D, Connor F, Paterson H, Peacock J, Ross G and Ashworth A<br>Absence of Brca2 causes genome instability by chromosome breakage and loss associated with centrosome amplification<br><i>Current Biology</i>   | 9:1107-10    | 1999 | <a href="#">Abstract</a> |
| 1350 | Tzivion G, Shen YH and Zhu J<br>14-3-3 proteins; bringing new definitions to scaffolding<br><i>Oncogene</i>  | 20:6331-8    | 2001 | <a href="#">Abstract</a> |
| 1351 | Uckun FM<br>Bruton's tyrosine kinase (BTK) as a dual-function regulator of apoptosis<br><i>Biochemical Pharmacology</i>  | 56:683-91    | 1998 | <a href="#">Abstract</a> |
| 1352 | Ueki K, Wen-Bin C, Narita Y, Asai A and Kirino T<br>Tight association of loss of merlin expression with loss of heterozygosity at chromosome 22q in sporadic meningiomas<br><i>Cancer Research</i>   | 59:5995-8    | 1999 | <a href="#">Abstract</a> |
| 1353 | Ueno T, Suzuki N, Kaneko A and Fujinaga K<br>Analysis of retinoblastoma for human adenovirus and human JC virus genome integration<br><i>Japanese Journal of Ophthalmology</i>   | 31:274-83    | 1987 | <a href="#">Abstract</a> |
| 1354 | Uings IJ and Farrow SN<br>Cell receptors and cell signalling<br><i>Molecular Pathology</i>   | 53:295-9     | 2000 | <a href="#">Abstract</a> |
| 1355 | Unoki M and Nakamura Y<br>Growth-suppressive effects of BPOZ and EGR2, two genes involved in the PTEN signaling pathway<br><i>Oncogene</i>   | 20:4457-65   | 2001 | <a href="#">Abstract</a> |
| 1356 | Uzbekov R, Prigent C and Arlot Bonnemains Y<br>Cell cycle analysis and synchronization of the <i>Xenopus laevis</i> XL2 cell line: study of the kinesin related protein XIg5<br><i>Microscopy Research and Technique</i>   | 45:31-42     | 1999 | <a href="#">Abstract</a> |
| 1357 | Vainio H, Miller AB and Bianchini F<br>An international evaluation of the cancer-preventive potential of sunscreens<br><i>International Journal of Cancer</i>  | 88:838-42    | 2000 | <a href="#">Abstract</a> |
| 1358 | Valyi-Nagy IT, Murphy GF, Mancianti ML, Whitaker D and Herlyn M<br>Phenotypes and interactions of human melanocytes and keratinocytes in an epidermal reconstruction model<br><i>Laboratory Investigation</i>  | 62:314-24    | 1990 | <a href="#">Abstract</a> |
| 1359 | Van Belle P, Rodeck U, Nuamah I, Halpern AC and Elder DE<br>Melanoma-associated expression of transforming growth factor-beta isoforms<br><i>American Journal of Pathology</i>   | 148:1887-94  | 1996 | <a href="#">Abstract</a> |
| 1360 | van Dam H, Duyndam M, Rottier R, Bosch A, de Vries Smits L, Herrlich P, Zantema A, Angel P and van der Eb AJ<br>Heterodimer formation of cJun and ATF-2 is responsible for induction of c-jun by the 243 amino acid adenovirus E1A protein<br><i>EMBO Journal</i>  | 12:479-87    | 1993 | <a href="#">Abstract</a> |
| 1361 | van der Burgt I, Chrzanowska KH, Smeets D and Weemaes C<br>Nijmegen breakage syndrome<br><i>Journal of Medical Genetics</i>  | 33:153-6     | 1996 | <a href="#">Abstract</a> |
| 1362 | van Vugt MA, Smits VA, Klompmaker R and Medema RH<br>Inhibition of Polo-like kinase-1 by DNA damage occurs in an ATM- or ATR-dependent fashion<br><i>Journal of Biological Chemistry</i>   | 276:41656-60 | 2001 | <a href="#">Abstract</a> |
| 1363 | Vancoillie G, Lambert J, Haeghen YV, Westbroek W, Mulder A, Koerten HK, Mommaas AM, Van Oostveldt P and Naeyaert JM<br>Colocalization of dynactin subunits P150Glued and P50 with melanosomes in normal human melanocytes<br><i>Pigment Cell Research</i>  | 13:449-57    | 2000 | <a href="#">Abstract</a> |
| 1364 | Vancoillie G, Lambert J and Nayaert JM<br>Melanocyte biology and its implications for the clinician<br><i>European Journal of Dermatology</i>  | 9:241-51     | 1999 | <a href="#">Abstract</a> |
| 1365 | Varon R, Vissinga C, Platzer M, Cersaletti KM, Chrzanowska KH, Saar K, Beckmann G, Seemanova E, Cooper PR, Nowak NJ, Stumm M, Weemaes CM, Gatti RA, Wilson RK, Digweed M, Rosenthal A, Sperling K, Concannon P and Reis A<br>Nibrin, a novel DNA double-strand break repair protein, is mutated in Nijmegen breakage syndrome<br><i>Cell</i> | 93:467-76    | 1998 | <a href="#">Abstract</a> |
| 1366 | van der Burgt I, Chrzanowska KH, Smeets D and Weemaes C<br>Nijmegen breakage syndrome<br><i>Journal of Medical Genetics</i>  | 33:153-6     | 1996 | <a href="#">Abstract</a> |
| 1367 | Vassilev A, Ozer Z, Navara C, Mahajan S and Uckun FM<br>Bruton's tyrosine kinase as an inhibitor of the Fas/CD95 death-inducing signaling complex<br><i>Journal of Biological Chemistry</i>  | 274:1646-56  | 1999 | <a href="#">Abstract</a> |



- 1368 Vazquez F and Sellers WR  
The PTEN tumor suppressor protein: an antagonist of phosphoinositide 3-kinase signaling  
*Biochimica et Biophysica Acta* **1470**:M21–35 2000 [Abstract](#)
- 1369 Verastegui C, Bille K, Ortonne JP and Ballotti R  
Regulation of the microphthalmia-associated transcription factor gene by the Waardenburg syndrome type 4 gene, SOX10  
*Journal of Biological Chemistry* **275**:30757–60 2000 [Abstract](#)
- 1370 Verhagen AM, Coulson EJ and Vaux DL  
Inhibitor of apoptosis proteins and their relatives: IAPs and other BIRPs  
*Genome Biology* **2**:REVIEWS3009 2001 [Abstract](#)
- 1371 Vermeulen W, Scott RJ, Rodgers S, Muller HJ, Cole J, Ariet CF, Kleijer WJ, Bootsma D, Hoeijmakers JH and Weeda G  
Clinical heterogeneity within xeroderma pigmentosum associated with mutations in the DNA repair and transcription gene ERCC3  
*American Journal of Human Genetics* **54**:191–200 1994 [Abstract](#)
- 1372 Veronesi U and Cascinelli N  
Narrow excision (1-cm margin). A safe procedure for thin cutaneous melanoma  
*Archives of Surgery* **126**:438–41 1991 [Abstract](#)
- 1373 Vidal A and Koff A  
Cell-cycle inhibitors: three families united by a common cause  
*Gene* **247**:1–15 2000 [Abstract](#)
- 1374 Vidwans SJ, Wong ML and O'Farrell PH  
Mitotic regulators govern progress through steps in the centrosome duplication cycle  
*Journal of Cell Biology* **147**:1371–8 1999 [Abstract](#)
- 1375 Vihinen M, Mattsson PT and Smith CI  
Bruton tyrosine kinase (BTK) in X-linked agammaglobulinemia (XLA)  
*Frontiers in Bioscience* **5**:D917–28 2000 [Abstract](#)
- 1376 Villuendas R, Sanchez-Beato M, Martinez JC, Saez AI, Martinez-Delgado B, Garcia JF, Mateo MS, Sanchez-Verde L, Benitez J, Martinez P and Piris MA  
Loss of p16/INK4A protein expression in non-Hodgkin's lymphomas is a frequent finding associated with tumor progression  
*American Journal of Pathology* **153**:887–97 1998 [Abstract](#)
- 1377 Vincent JP and Briscoe J  
Morphogens  
*Current Biology* **11**:R851–4 2001 [Abstract](#)
- 1378 Virador VM, Muller J, Wu X, Abdel-Malek ZA, Yu ZX, Ferrans VJ, Kobayashi N, Wakamatsu K, Ito S, Hammer JA and Hearing VJ  
Influence of alpha-melanocyte-stimulating hormone and ultraviolet radiation on the transfer of melanosomes to keratinocytes  
*FASEB Journal* **16**:105–7 2002 [Abstract](#)
- 1379 Vlach J, Hennecke S and Amati B  
Phosphorylation-dependent degradation of the cyclin-dependent kinase inhibitor p27  
*EMBO Journal* **16**:5334–44 1997 [Abstract](#)
- 1380 Vogel L and Baratte B  
Suc1: cdc2 affinity reagent or essential cdk adaptor protein?  
*Progress in Cell Cycle Research* **2**:129–35 1996 [Abstract](#)
- 1381 Vogelstein B and Kinzler KW  
p53 function and dysfunction  
*Cell* **70**:523–6 1992 [Abstract](#)
- 1382 Voit R, Schafer K and Grummt I  
Mechanism of repression of RNA polymerase I transcription by the retinoblastoma protein  
*Molecular and Cellular Biology* **17**:4230–7 1997 [Abstract](#)
- 1383 Volarevic S and Thomas G  
Role of S6 phosphorylation and S6 kinase in cell growth  
*Progress in Nucleic Acid Research and Molecular Biology* **65**:101–27 2001 [Abstract](#)
- 1384 Vos CB, Cleton-Jansen AM, Berx G, de Leeuw WJ, ter Haar NT, van Roy F, Cornelisse CJ, Peterse JL and van de Vijver MJ  
E-cadherin inactivation in lobular carcinoma in situ of the breast: an early event in tumorigenesis  
*British Journal of Cancer* **76**:1131–3 1997 [Abstract](#)
- 1385 Wagh S, Ramaiah A, Subramanian R and Govindarajan R  
Melanosomal proteins promote melanin polymerization  
*Pigment Cell Research* **13**:442–8 2000 [Abstract](#)
- 1386 Wagner EF, Hleb M, Hanna N and Sharma S  
A pivotal role of cyclin D3 and cyclin-dependent kinase inhibitor p27 in the regulation of IL-2-, IL-4-, or IL-10-mediated human B cell proliferation  
*Journal of Immunology* **161**:1123–31 1998 [Abstract](#)
- 1387 Wagner M, Hampel B, Hutter E, Pfister G, Krek W, Zwerschke W and Jansen Durr P  
Metabolic stabilization of p27 in senescent fibroblasts correlates with reduced expression of the F-box protein Skp2  
*Experimental Gerontology* **37**:41–55 2001 [Abstract](#)
- 1388 Wahl GM, Linke SP, Paulson TG and Huang LC  
Maintaining genetic stability through TP53 mediated checkpoint control  
*Cancer Surveys* **29**:183–219 1997 [Abstract](#)
- 1389 Waldman T, Kinzler KW and Vogelstein B  
p21 is necessary for the p53-mediated G1 arrest in human cancer cells  
*Cancer Research* **55**:5187–90 1995 [Abstract](#)
- 1390 Walker G and Hayward N  
No evidence of a role for activating CDK2 mutations in melanoma  
*Melanoma Research* **11**:343–8 2001 [Abstract](#)
- 1391 Walker GJ, Flores JF, Glendening JM, Lin AH, Markl ID and Fountain JW  
Virtually 100% of melanoma cell lines harbor alterations at the DNA level within CDKN2A, CDKN2B, or one of their downstream targets  
*Genes, Chromosomes and Cancer* **22**:157–63 1998 [Abstract](#)
- 1392 †Wallace D and Hughes J  
Style Book: A Guide for New Zealand Writers and Editors  
GP Publications, Wellington, NZ ISBN 1–86956–123–6 1995
- 1393 Wang CY, Petryniak B, Thompson CB, Kaelin WG and Leiden JM  
Regulation of the Ets-related transcription factor Elf-1 by binding to the retinoblastoma protein  
*Science* **260**:1330–5 1993 [Abstract](#)

## Human metastatic melanoma in vitro

1394	Wang J, Otsuki T, Youssoufian H, Foe JL, Kim S, Devetten M, Yu J, Li Y, Dunn D and Liu JM Overexpression of the fanconi anemia group C gene (FAC) protects hematopoietic progenitors from death induced by Fas-mediated apoptosis <i>Cancer Research</i>	58:3538-41	1998	<a href="#">Abstract</a>
1395	Wang JY Regulation of cell death by the Abl tyrosine kinase <i>Oncogene</i>	19:5643-50	2000	<a href="#">Abstract</a>
1396	Wang Q, Lasset C, Desseigne F, Saurin JC, Maugard C, Navarro C, Ruano E, Descos L, Trillet-Lenoir V, Bosset JF and Puisieux A Prevalence of germline mutations of hMLH1, hMSH2, hPMS1, hPMS2, and hMSH6 genes in 75 French kindreds with nonpolyposis colorectal cancer <i>Human Genetics</i>	105:79-85	1999	<a href="#">Abstract</a>
1397	Wang Q, Zhang H, Fishel R and Greene MI BRCA1 and cell signaling <i>Oncogene</i>	19:6152-8	2000	<a href="#">Abstract</a>
1398	Wang Q, Zhang H, Guerrette S, Chen J, Mazurek A, Wilson T, Slupianek A, Skorski T, Fishel R and Greene MI Adenosine nucleotide modulates the physical interaction between hMSH2 and BRCA1 <i>Oncogene</i>	20:4640-9	2001	<a href="#">Abstract</a>
1399	Wang S, Ghosh RN and Chellappan SP Raf-1 physically interacts with Rb and regulates its function: a link between mitogenic signaling and cell cycle regulation <i>Molecular and Cellular Biology</i>	18:7487-98	1998	<a href="#">Abstract</a>
1400	Wang S, Nath N, Adlam M and Chellappan S Prohibitin, a potential tumor suppressor, interacts with RB and regulates E2F function <i>Oncogene</i>	18:3501-10	1999	<a href="#">Abstract</a>
1401	Wang SQ, Setlow R, Berwick M, Polsky D, Marghoob AA, Kopf AW and Bart RS Ultraviolet A and melanoma: a review <i>Journal of the American Academy of Dermatology</i>	44:837-46	2001	<a href="#">Abstract</a>
1402	Wang T, Dowal L, El-Maghrabi MR, Rebecchi M and Scarlata S The pleckstrin homology domain of phospholipase C-beta(2) links the binding of gbetagamma to activation of the catalytic core <i>Journal of Biological Chemistry</i>	275:7466-9	2000	<a href="#">Abstract</a>
1403	Wang Y, Cortez D, Yazdi P, Neff N, Elledge SJ and Qin J BASC, a super complex of BRCA1-associated proteins involved in the recognition and repair of aberrant DNA structures <i>Genes and Development</i>	14:927-39	2000	<a href="#">Abstract</a>
1404	Ward IM, Wu X and Chen J Threonine 68 of Chk2 Is Phosphorylated at Sites of DNA Strand Breaks <i>Journal of Biological Chemistry</i>	276:47755-47758	2001	<a href="#">Abstract</a>
1405	Warner BJ, Blain SW, Seoane J and Massague J Myc downregulation by transforming growth factor beta required for activation of the p15(Ink4b) G(1) arrest pathway <i>Molecular and Cellular Biology</i>	19:5913-22	1999	<a href="#">Abstract</a>
1406	Wassarman DA and Sauer F TAF(II)250: a transcription toolbox <i>Journal of Cell Science</i>	114:2895-902	2001	<a href="#">Abstract</a>
1407	Watanabe A, Takeda K, Ploplis B and Tachibana M Epistatic relationship between Waardenburg syndrome genes MITF and PAX3 <i>Nature Genetics</i>	18:283-6	1998	<a href="#">Abstract</a>
1408	Watanabe H, Fukuchi K, Takagi Y, Tomoyasu S, Tsuruoka N and Gomi K Molecular analysis of the Cip1/Waf1 (p21) gene in diverse types of human tumors <i>Biochimica et Biophysica Acta</i>	1263:275-80	1995	<a href="#">Abstract</a>
1409	Waterman MJ, Stavridi ES, Waterman JL and Halazonetis TD ATM-dependent activation of p53 involves dephosphorylation and association with 14-3-3 proteins <i>Nature Genetics</i>	19:175-8	1998	<a href="#">Abstract</a>
1410	Waters JC, Cole RW and Rieder CL The force-producing mechanism for centrosome separation during spindle formation in vertebrates is intrinsic to each aster <i>Journal of Cell Biology</i>	122:361-72	1993	<a href="#">Abstract</a>
1411	Watt PM, Kumar R and Kees UR Promoter demethylation accompanies reactivation of the HOX11 proto-oncogene in leukemia <i>Genes, Chromosomes and Cancer</i>	29:371-7	2000	<a href="#">Abstract</a>
1412	Weber JD, Taylor LJ, Roussel MF, Sherr CJ and Bar Sagi D Nucleolar Arf sequesters Mdm2 and activates p53 <i>Nature Cell Biology</i>	1:20-6	1999	<a href="#">Abstract</a>
1413	Weber RG, Bridger JM, Benner A, Weisenberger D, Ehemann V, Reifemberger G and Lichter P Centrosome amplification as a possible mechanism for numerical chromosome aberrations in cerebral primitive neuroectodermal tumors with TP53 mutations <i>Cytogenetics and Cell Genetics</i>	83:266-9	1998	<a href="#">Abstract</a>
1414	Webster NJ, Kong Y, Sharma P, Haas M, Sukumar S and Seely BL Differential effects of Wilms tumor WT1 splice variants on the insulin receptor promoter <i>Biochemical and Molecular Medicine</i>	62:139-50	1997	<a href="#">Abstract</a>
1415	Wehrle-Haller B, Meller M and Weston JA Analysis of melanocyte precursors in Nf1 mutants reveals that MGF/KIT signaling promotes directed cell migration independent of its function in cell survival <i>Developmental Biology</i>	232:471-83	2001	<a href="#">Abstract</a>
1416	Wei G, Lonardo F, Ueda T, Kim T, Huvos AG, Healey JH and Ladanyi M CDK4 gene amplification in osteosarcoma: reciprocal relationship with INK4A gene alterations and mapping of 12q13 amplicons <i>International Journal of Cancer</i>	80:199-204	1999	<a href="#">Abstract</a>
1417	Weilbach FX, Bogdahn U, Poot M, Apfel R, Behl C, Drenkard D, Martin R and Hoehn H Melanoma-inhibiting activity inhibits cell proliferation by prolongation of the S-phase and arrest of cells in the G2 compartment <i>Cancer Research</i>	50:6981-6	1990	<a href="#">Abstract</a>
1418	Weiler SR, Mou S, DeBerry CS, Keller JR, Ruscetti FW, Ferris DK, Longo DL and Linnekin D JAK2 is associated with the c-kit proto-oncogene product and is phosphorylated in response to stem cell factor <i>Blood</i>	87:3688-93	1996	<a href="#">Abstract</a>
1419	Welch PJ and Wang JY Disruption of retinoblastoma protein function by coexpression of its C pocket fragment <i>Genes and Development</i>	9:31-46	1995	<a href="#">Abstract</a>



- 1420 Welch PJ and Wang JY  
A C-terminal protein-binding domain in the retinoblastoma protein regulates nuclear c-Abl tyrosine kinase in the cell cycle  
*Cell* **75**:779–90 1993 [Abstract](#)
- 1421 Welch PJ and Wang JY  
Abrogation of retinoblastoma protein function by c-Abl through tyrosine kinase-dependent and -independent mechanisms  
*Molecular and Cellular Biology* **15**:5542–51 1995 [Abstract](#)
- 1422 Welch PL and King MC  
BRCA1 and BRCA2 and the genetics of breast and ovarian cancer  
*Human Molecular Genetics* **10**:705–13 2001 [Abstract](#)
- 1423 Weng LP, Brown JL and Eng C  
PTEN induces apoptosis and cell cycle arrest through phosphoinositol-3-kinase/Akt-dependent and -independent pathways  
*Human Molecular Genetics* **10**:237–242 2001 [Abstract](#)
- 1424 Weng LP, Brown JL and Eng C  
PTEN coordinates G(1) arrest by down-regulating cyclin D1 via its protein phosphatase activity and up-regulating p27 via its lipid phosphatase activity in a breast cancer model  
*Human Molecular Genetics* **10**:599–604 2001 [Abstract](#)
- 1425 Westerdahl J, Olsson H and Ingvar C  
At what age do sunburn episodes play a crucial role for the development of malignant melanoma  
*European Journal of Cancer* **30A**:1647–54 1994 [Abstract](#)
- 1426 Western PS and Sinclair AH  
Sex, genes, and heat: triggers of diversity  
*Journal of Experimental Zoology* **290**:624–31 2001 [Abstract](#)
- 1427 Westphal CH, Rowan S, Schmaltz C, Elson A, Fisher DE and Leder P  
atm and p53 cooperate in apoptosis and suppression of tumorigenesis, but not in resistance to acute radiation toxicity  
*Nature Genetics* **16**:397–401 1997 [Abstract](#)
- 1428 Wheatley SP, Carvalho A, Vagnarelli P and Earnshaw WC  
INCENP is required for proper targeting of Survivin to the centromeres and the anaphase spindle during mitosis  
*Current Biology* **11**:886–90 2001 [Abstract](#)
- 1429 Wheatley SP, Kandels-Lewis SE, Adams RR, Ainsztein AM and Earnshaw WC  
INCENP binds directly to tubulin and requires dynamic microtubules to target to the cleavage furrow  
*Experimental Cell Research* **262**:122–7 2001 [Abstract](#)
- 1430 White E  
Tumour biology. p53, guardian of Rb  
*Nature* **371**:21–2 1994 [Abstract](#)
- 1431 Whitehead CM and Rattner JB  
Expanding the role of HsEg5 within the mitotic and post-mitotic phases of the cell cycle  
*Journal of Cell Science* **111**:2551–61 1998 [Abstract](#)
- 1432 Whiteman DC, Parsons PG and Green AC  
p53 expression and risk factors for cutaneous melanoma: a case-control study  
*International Journal of Cancer* **77**:843–8 1998 [Abstract](#)
- 1433 Whyte P, Buchkovich KJ, Horowitz JM, Friend SH, Raybuck M, Weinberg RA and Harlow E  
Association between an oncogene and an anti-oncogene: the adenovirus E1A proteins bind to the retinoblastoma gene product  
*Nature* **334**:124–9 1988 [Abstract](#)
- 1434 Widschwendter M, Berger J, Hermann M, Muller HM, Amberger A, Zeschnigk M, Widschwendter A, Abendstein B, Zeimet AG, Daxenbichler G and Marth C  
Methylation and silencing of the retinoic acid receptor-beta2 gene in breast cancer  
*Journal of the National Cancer Institute* **92**:826–32 2000 [Abstract](#)
- 1435 Wiener JS, Coppes MJ and Ritchey ML  
Current concepts in the biology and management of Wilms tumor  
*Journal of Urology* **159**:1316–25 1998 [Abstract](#)
- 1436 Wilde A, Lizarraga SB, Zhang L, Wiese C, Gliksman NR, Walczak CE and Zheng Y  
Ran stimulates spindle assembly by altering microtubule dynamics and the balance of motor activities  
*Nature Cell Biology* **3**:221–7 2001 [Abstract](#)
- 1437 Williams KJ, Boyle JM, Birch JM, Norton JD and Scott D  
Cell cycle arrest defect in Li-Fraumeni Syndrome: a mechanism of cancer predisposition?  
*Oncogene* **14**:277–82 1997 [Abstract](#)
- 1438 Winey M  
Cell cycle: driving the centrosome cycle  
*Current Biology* **9**:R449–52 1999 [Abstract](#)
- 1439 Winters ZE, Hunt NC, Bradburn MJ, Royds JA, Turley H, Harris AL and Norbury CJ  
Subcellular localisation of cyclin B, Cdc2 and p21(WAF1/CIP1) in breast cancer. association with prognosis  
*European Journal of Cancer* **37**:2405–12 2001 [Abstract](#)
- 1440 Winther J and Olsen JH  
Non-ocular cancer in retinoblastoma survivors  
*Acta Ophthalmologica - Supplement* **182**:144–7 1987 [Abstract](#)
- 1441 Wijnen J, de Leeuw W, Vasen H, van der Klift H, Moller P, Stormorken A, Meijers-Heijboer H, Lindhout D, Menko F, Vossen S, Moslein G, Tops C, Brocker-Vriends A, Wu Y, Hofstra R, Sijmons R, Cornelisse C, Morreau H and Fodde R  
Familial endometrial cancer in female carriers of MSH6 germline mutations  
*Nature Genetics* **23**:142–4 1999 [Abstract](#)
- 1442 Wohlschlegel JA, Dwyer BT, Dhar SK, Cvetic C, Walter JC and Dutta A  
Inhibition of eukaryotic DNA replication by geminin binding to Cdt1  
*Science* **290**:2309–12 2000 [Abstract](#)
- 1443 Woitach JT, Zhang M, Niu CH and Thorgeirsson SS  
A retinoblastoma-binding protein that affects cell-cycle control and confers transforming ability  
*Nature Genetics* **19**:371–4 1998 [Abstract](#)
- 1444 Wolfel T, Hauer M, Schneider J, Serrano M, Wolfel C, Klehmannhieb E, Deplaen E, Hankeln T, Zumbuschfelde KHM and Beach D  
A p16(INK4a)-insensitive CDK4 mutant targeted by cytolytic T lymphocytes in a human melanoma  
*Science* **269**:1281–1284 1995 [Abstract](#)

## Human metastatic melanoma in vitro

- |      |  |              |      |                          |
|------|--|--------------|------|--------------------------|
| 1445 | Wolffe AP, Urnov FD and Guschin D<br>Co-repressor complexes and remodelling chromatin for repression<br><i>Biochemical Society Transactions</i>  | 28:379–86    | 2000 | <a href="#">Abstract</a> |
| 1446 | Won KA and Reed SI<br>Activation of cyclin E/CDK2 is coupled to site-specific autophosphorylation and ubiquitin-dependent degradation of cyclin E<br><i>EMBO Journal</i>   | 15:4182–93   | 1996 | <a href="#">Abstract</a> |
| 1447 | Woo DK, Kim HS, Lee HS, Kang YH, Yang HK and Kim WH<br>Altered expression and mutation of beta-catenin gene in gastric carcinomas and cell lines<br><i>International Journal of Cancer</i>   | 95:108–13    | 2001 | <a href="#">Abstract</a> |
| 1448 | Woo DK, Lee WA, Kim YI and Kim WH<br>Microsatellite instability and alteration of E2F-4 gene in adenosquamous and squamous cell carcinomas of the stomach<br><i>Pathology International</i>  | 50:690–5     | 2000 | <a href="#">Abstract</a> |
| 1449 | Woo MS, Sanchez I and Dynlacht BD<br>p130 and p107 use a conserved domain to inhibit cellular cyclin-dependent kinase activity<br><i>Molecular and Cellular Biology</i>  | 17:3566–79   | 1997 | <a href="#">Abstract</a> |
| 1450 | Wood RD<br>DNA damage recognition during nucleotide excision repair in mammalian cells<br><i>Biochimie</i>   | 81:39–44     | 1999 | <a href="#">Abstract</a> |
| 1451 | Wooster R, Bignell G, Lancaster J, Swift S, Seal S, Mangion J, Collins N, Gregory S, Gumbs C and Micklem G<br>Identification of the breast cancer susceptibility gene BRCA2 [published erratum appears in <i>Nature</i> 379:749]<br><i>Nature</i>          | 378:789–92   | 1995 | <a href="#">Abstract</a> |
| 1452 | Worm J, Bartkova J, Kirkin AF, Straten P, Zeuthen J, Bartek J and Guldberg P<br>Aberrant p27Kip1 promoter methylation in malignant melanoma<br><i>Oncogene</i>   | 19:5111–5    | 2000 | <a href="#">Abstract</a> |
| 1453 | Wu CL, Kirley SD, Xiao H, Chuang Y, Chung DC and Zukerberg LR<br>Cables enhances cdk2 tyrosine 15 phosphorylation by Wee1, inhibits cell growth, and is lost in many human colon and squamous cancers<br><i>Cancer Research</i>                            | 61:7325–32   | 2001 | <a href="#">Abstract</a> |
| 1454 | Wu M, Hemesath TJ, Takemoto CM, Horstmann MA, Wells AG, Price ER, Fisher DZ and Fisher DE<br>c-Kit triggers dual phosphorylations, which couple activation and degradation of the essential melanocyte factor Mi<br><i>Genes and Development</i>           | 14:301–12    | 2000 | <a href="#">Abstract</a> |
| 1455 | Wu R, Lopez-Correa C, Rutkowski JL, Baumbach LL, Glover TW and Legius E<br>Germline mutations in NF1 patients with malignancies<br><i>Genes, Chromosomes and Cancer</i>  | 26:376–80    | 1999 | <a href="#">Abstract</a> |
| 1456 | Wu RC, Li X and Schonthal AH<br>Transcriptional activation of p21WAF1 by PTEN/MMAC1 tumor suppressor<br><i>Molecular and Cell Biochemistry</i>   | 203:59–71    | 2000 | <a href="#">Abstract</a> |
| 1457 | Wu X, Bowers B, Rao K, Wei Q and Hammer JA3rd<br>Visualization of melanosome dynamics within wild-type and dilute melanocytes suggests a paradigm for myosin V function In vivo<br><i>Journal of Cell Biology</i>  | 143:1899–918 | 1998 | <a href="#">Abstract</a> |
| 1458 | Wu X, Ranganathan V, Weisman DS, Heine WF, Ciccone DN, O'Neill TB, Crick KE, Pierce KA, Lane WS, Rathbun G, Livingston DM and Weaver DT<br>ATM phosphorylation of Nijmegen breakage syndrome protein is required in a DNA damage response<br><i>Nature</i> | 405:477–82   | 2000 | <a href="#">Abstract</a> |
| 1459 | Wu X, Rao K, Bowers MB, Copeland NG, Jenkins NA and Hammer JA 3rd<br>Rab27a enables myosin Va-dependent melanosome capture by recruiting the myosin to the organelle<br><i>Journal of Cell Science</i>   | 114:1091–100 | 2001 | <a href="#">Abstract</a> |
| 1460 | Wu-Baer F and Baer R<br>Effect of DNA damage on a BRCA1 complex<br><i>Nature</i>   | 414:36       | 2001 | <a href="#">Abstract</a> |
| 1461 | Xiao ZX, Chen J, Levine AJ, Modjtahedi N, Xing J, Sellers WR and Livingston DM<br>Interaction between the retinoblastoma protein and the oncoprotein MDM2<br><i>Nature</i>   | 375:694–8    | 1995 | <a href="#">Abstract</a> |
| 1462 | Xiao ZX, Ginsberg D, Ewen M and Livingston DM<br>Regulation of the retinoblastoma protein-related protein p107 by G1 cyclin-associated kinases<br><i>Proceedings of the National Academy of Sciences of the USA</i>  | 93:4633–7    | 1996 | <a href="#">Abstract</a> |
| 1463 | Xie Y, de Winter JP, Waisfisz Q, Nieuwint AW, Scheper RJ, Arwert F, Hoatlin ME, Ossenkoppele GJ, Schuurhuis GJ and Joenje H<br>Aberrant Fanconi anaemia protein profiles in acute myeloid leukaemia cells<br><i>British Journal of Haematology</i>         | 111:1057–64  | 2000 | <a href="#">Abstract</a> |
| 1464 | Xing EP, Nie Y, Song Y, Yang GY, Cai YC, Wang LD and Yang CS<br>Mechanisms of inactivation of p14ARF, p15INK4b, and p16INK4a genes in human esophageal squamous cell carcinoma<br><i>Clin Cancer Research</i>  | 5:2704–13    | 1999 | <a href="#">Abstract</a> |
| 1465 | Xio S, Li D, Vijn J, Sugarbaker DJ, Corson JM and Fletcher JA<br>Codeletion of p15 and p16 in primary malignant mesothelioma<br><i>Oncogene</i>  | 11:511–5     | 1995 | <a href="#">Abstract</a> |
| 1466 | Xu HJ, Hu SX, Hashimoto T, Takahashi R and Benedict WF<br>The retinoblastoma susceptibility gene product: a characteristic pattern in normal cells and abnormal expression in malignant cells<br><i>Oncogene</i>   | 4:807–12     | 1989 | <a href="#">Abstract</a> |
| 1467 | Xu M, Sheppard KA, Peng CY, Yee AS and Piwnicka-Worms H<br>Cyclin A/CDK2 binds directly to E2F-1 and inhibits the DNA-binding activity of E2F-1/DP-1 by phosphorylation<br><i>Molecular and Cellular Biology</i>   | 14:8420–31   | 1994 | <a href="#">Abstract</a> |
| 1468 | Xu X, Nakano T, Wick S, Dubay M and Brizuela L<br>Mechanism of Cdk2/Cyclin E inhibition by p27 and p27 phosphorylation<br><i>Biochemistry</i>  | 38:8713–22   | 1999 | <a href="#">Abstract</a> |
| 1469 | Xu Y, Ashley T, Brainerd EE, Bronson RT, Meyn MS and Baltimore D<br>Targeted disruption of ATM leads to growth retardation, chromosomal fragmentation during meiosis, immune defects, and thymic lymphoma<br><i>Genes and Development</i>                  | 10:2411–22   | 1996 | <a href="#">Abstract</a> |
| 1470 | Yaar M, Eller MS, DiBenedetto P, Reenstra WR, Zhai S, McQuaid T, Archambault M and Gilchrist BA<br>The trk family of receptors mediates nerve growth factor and neurotrophin-3 effects in melanocytes<br><i>Journal of Clinical Investigation</i>          | 94:1550–62   | 1994 | <a href="#">Abstract</a> |





- 1471 Yaar M, Grossman K, Eller M and Gilchrist BA  
Evidence for nerve growth factor-mediated paracrine effects in human epidermis  
*Journal of Cell Biology* **115**:821–8 1991 [Abstract](#)
- 1472 Yada Y, Higuchi K and Imokawa G  
Effects of endothelins on signal transduction and proliferation in human melanocytes  
*Journal of Biological Chemistry* **266**:18352–7 1991 [Abstract](#)
- 1473 Yagi K, Furuhashi M, Aoki H, Goto D, Kuwano H, Sugamura K, Miyazono K and Kato M  
c-myc is a downstream target of the Smad pathway  
*Journal of Biological Chemistry* **277**:854–61 2002 [Abstract](#)
- 1474 Yamaguchi Iwai Y, Sonoda E, Sasaki MS, Morrison C, Haraguchi T, Hiraoka Y, Yamashita YM, Yagi T, Takata M, Price C, Kakazu N and Takeda S  
Mre11 is essential for the maintenance of chromosomal DNA in vertebrate cells  
*EMBO Journal* **18**:6619–29 1999 [Abstract](#)
- 1475 Yamamoto O and Bhawan J  
Three modes of melanosome transfers in Caucasian facial skin: hypothesis based on an ultrastructural study  
*Pigment Cell Research* **7**:158–69 1994 [Abstract](#)
- 1476 Yamanouchi H, Furihata M, Fujita J, Murakami H, Yoshinouchi T, Takahara J and Ohtsuki Y  
Expression of cyclin E and cyclin D1 in non-small cell lung cancers  
*Lung Cancer* **31**:3–8 2001 [Abstract](#)
- 1477 Yamasaki L  
Balancing proliferation and apoptosis in vivo: the Goldilocks theory of E2F/DP action  
*Biochimica et Biophysica Acta* **1423**:M9–15 1999 [Abstract](#)
- 1478 Yamasaki L, Bronson R, Williams BO, Dyson NJ, Harlow E and Jacks T  
Loss of E2F-1 reduces tumorigenesis and extends the lifespan of Rb1(+/-)mice  
*Nature Genetics* **18**:360–4 1998 [Abstract](#)
- 1479 Yamasaki L  
Growth regulation by the E2F and DP transcription factor families  
*Results and Problems in Cell Differentiation* **22**:199–227 1998 [Abstract](#)
- 1480 Yamasaki L, Jacks T, Bronson R, Goillot E, Harlow E and Dyson NJ  
Tumor induction and tissue atrophy in mice lacking E2F-1  
*Cell* **85**:537–48 1996 [Abstract](#)
- 1481 Yarden RI and Brody LC  
BRCA1 interacts with components of the histone deacetylase complex  
*Proceedings of the National Academy of Sciences of the USA* **96**:4983–8 1999 [Abstract](#)
- 1482 Yasumoto K, Yokoyama K, Takahashi K, Tomita Y and Shibahara S  
Functional analysis of microphthalmia-associated transcription factor in pigment cell-specific transcription of the human tyrosinase family genes  
*Journal of Biological Chemistry* **272**:503–9 1997 [Abstract](#)
- 1483 Yavuzer U, Keenan E, Lowings P, Vachtenheim J, Currie G and Goding CR  
The Microphthalmia gene product interacts with the retinoblastoma protein in vitro and is a target for deregulation of melanocyte-specific transcription  
*Oncogene* **10**:123–34 1995 [Abstract](#)
- 1484 Yee NS, Hsiau CW, Serve H, Vosseller K and Besmer P  
Mechanism of down-regulation of c-kit receptor. Roles of receptor tyrosine kinase, phosphatidylinositol 3'-kinase, and protein kinase C  
*Journal of Biological Chemistry* **269**:31991–8 1994 [Abstract](#)
- 1485 Yen A, Coder D and Varvayanis S  
Concentration of RB protein in nucleus vs. cytoplasm is stable as phosphorylation of RB changes during the cell cycle and differentiation  
*European Journal of Cell Biology* **72**:159–65 1997 [Abstract](#)
- 1486 Yim CY, Bastian NR, Smith JC, Hibbs JB Jr and Samlowski WE  
Macrophage nitric oxide synthesis delays progression of ultraviolet light-induced murine skin cancers  
*Cancer Research* **53**:5507–11 1993 [Abstract](#)
- 1487 Yoshida H, Kunisada T, Grimm T, Nishimura EK, Nishioka E and Nishikawa SI  
Review: melanocyte migration and survival controlled by SCF/c-kit expression  
*Journal of Investigative Dermatology Symposium Proceedings* **6**:1–5 2001 [Abstract](#)
- 1488 Yoshida M, Ashida S, Kondo K, Kobayashi K, Kanno H, Shinohara N, Shitara N, Kishida T, Kawakami S, Baba M, Yamamoto I, Hosaka M, Shuin T and Yao M  
Germ-line mutation analysis in patients with von Hippel-Lindau disease in Japan: an extended study of 77 families  
*Japanese Journal of Cancer Research* **91**:204–12 2000 [Abstract](#)
- 1489 Yoshikawa H, Matsubara K, Qian GS, Jackson P, Groopman JD, Manning JE, Harris CC and Herman JG  
SOCS-1, a negative regulator of the JAK/STAT pathway, is silenced by methylation in human hepatocellular carcinoma and shows growth-suppression activity  
*Nature Genetics* **28**:29–35 2001 [Abstract](#)
- 1490 Yoshioka K, Nakamori S and Itoh K  
Overexpression of small GTP-binding protein RhoA promotes invasion of tumor cells  
*Cancer Research* **59**:2004–10 1999 [Abstract](#)
- 1491 Yoshiura K, Kanai Y, Ochiai A, Shimoyama Y, Sugimura T and Hirohashi S  
Silencing of the E-cadherin invasion-suppressor gene by CpG methylation in human carcinomas  
*Proceedings of the National Academy of Sciences of the USA* **92**:7416–9 1995 [Abstract](#)
- 1492 Young A, Dichtenberg JB, Purohit A, Tuft R and Doxsey S  
Cytoplasmic dynein-mediated assembly of pericentriar and gamma tubulin onto centrosomes  
*Journal of Molecular Biology Cell* **11**:2047–56 2000 [Abstract](#)
- 1493 Yuan J, Knorr J, Altmannsberger M, Goeckenjan G, Ahr A, Scharl A and Strebhardt K  
Expression of p16 and lack of pRB in primary small cell lung cancer  
*Journal of Pathology* **189**:358–62 1999 [Abstract](#)
- 1494 Yuasa M, Masutani C, Eki T and Hanaoka F  
Genomic structure, chromosomal localization and identification of mutations in the xeroderma pigmentosum variant (XPV) gene  
*Oncogene* **19**:4721–8 2000 [Abstract](#)
- 1495 Yuille MA and Coignet LJ  
The ataxia telangiectasia gene in familial and sporadic cancer  
*Recent Results in Cancer Research* **154**:156–73 1998 [Abstract](#)

## Human metastatic melanoma in vitro

1496	Youssoufian H Fanconi anemia and breast cancer: what's the connection? <i>Nature Genetics</i>	27:352-3	2001	<a href="#">Abstract</a>
1497	Zachary I Focal adhesion kinase <i>International Journal of Biochemistry and Cell Biology</i>	29:929-34	1997	<a href="#">Abstract</a>
1498	Zaitzu H and Kimura G Serum-dependent regulation of proliferation of cultured rat fibroblasts in G1 and G2 phases <i>Experimental Cell Research</i>	174:146-55	1988	<a href="#">Abstract</a>
1499	Zalvide J, Stubdal H and DeCaprio JA The J domain of simian virus 40 large T antigen is required to functionally inactivate RB family proteins <i>Molecular and Cellular Biology</i>	18:1408-15	1998	<a href="#">Abstract</a>
1500	Zamparelli A, Masciullo V, Bovicelli A, Santini D, Ferrandina G, Minimo C, Terzano P, Costa S, Cinti C, Ceccarelli C, Mancuso S, Scambia G, Bovicelli L and Giordano A <i>Human Pathology</i>	32:4-9	2001	<a href="#">Abstract</a>
1501	Zarkowska T and Mitnacht S Expression of cell-cycle-associated proteins pRB2/p130 and p27kip in vulvar squamous cell carcinomas <i>Journal of Biological Chemistry</i>	272:12738-46	1997	<a href="#">Abstract</a>
1502	Zbar B Von Hippel-Lindau disease and sporadic renal cell carcinoma. <i>Cancer Surveys</i>	25:219-32	1995	<a href="#">Abstract</a>
1503	Zeki K, Morimoto I, Arao T, Eto S and Yamashita U Interleukin-1alpha regulates G1 cell cycle progression and arrest in thyroid carcinoma cell lines NIM1 and NPA <i>Journal of Endocrinology</i>	160:67-73	1999	<a href="#">Abstract</a>
1504	Zeng C NuMA: a nuclear protein involved in mitotic centrosome function <i>Microscopy Research and Technique</i>	49:467-77	2000	<a href="#">Abstract</a>
1505	Zeng XR, Jiang Y, Zhang SJ, Hao H and Lee MY DNA polymerase delta is involved in the cellular response to UV damage in human cells <i>Journal of Biological Chemistry</i>	269:13748-51	1994	<a href="#">Abstract</a>
1506	Zerp SF, van Elsas A, Peltenburg LT and Schrier PI p53 mutations in human cutaneous melanoma correlate with sun exposure but are not always involved in melanomagenesis <i>British Journal of Cancer</i>	79:921-6	1999	<a href="#">Abstract</a>
1507	Zhan Q, Antinore MJ, Wang XW, Carrier F, Smith ML, Harris CC and Fornace AJ Jr Association with Cdc2 and inhibition of Cdc2/Cyclin B1 kinase activity by the p53-regulated protein Gadd45 <i>Oncogene</i>	18:2892-900	1999	<a href="#">Abstract</a>
1508	Zhang H and Rosdahl I Expression of oncogenes, tumour suppressor, mismatch repair and apoptosis-related genes in primary and metastatic melanoma cells <i>International Journal of Oncology</i>	19:1149-53	2001	<a href="#">Abstract</a>
1509	Zhang H, Shepherd AT, Eason DD, Wei S, Diaz JI, Djeu JY, Wu GD and Blanck G Retinoblastoma protein expression leads to reduced Oct-1 DNA binding activity and enhances interleukin-8 expression <i>Cell Growth and Differentiation</i>	10:457-65	1999	<a href="#">Abstract</a>
1510	Zhang H, Somasundaram K, Peng Y, Tian H, Zhang H, Bi D, Weber BL and el-Deiry WS BRCA1 physically associates with p53 and stimulates its transcriptional activity <i>Oncogene</i>	16:1713-21	1998	<a href="#">Abstract</a>
1511	Zhang SY, Liu SC, Johnson DG and Klein Szanto AJ E2F-1 gene transfer enhances invasiveness of human head and neck carcinoma cell lines <i>Cancer Research</i>	60:5972-6	2000	<a href="#">Abstract</a>
1512	Zhang Y, Ma WY, Kaji A, Bode AM and Dong Z Requirement of ATM in UVA-induced signaling and apoptosis <i>Journal of Biological Chemistry</i>	in press	2001	<a href="#">Abstract</a>
1513	Zhang Y, Xiong Y and Yarbrough WG ARF promotes MDM2 degradation and stabilizes p53: ARF-INK4a locus deletion impairs both the Rb and p53 tumor suppression pathways <i>Cell</i>	92:725-34	1998	<a href="#">Abstract</a>
1514	Zhang YY, Vik TA, Ryder JW, Srour EF, Jacks T, Shannon K and Clapp DW Nf1 regulates hematopoietic progenitor cell growth and ras signaling in response to multiple cytokines <i>Journal of Experimental Medicine</i>	187:1893-902	1998	<a href="#">Abstract</a>
1515	Zhao H, Zhao Y, Nordlund JJ and Boissy RE Human TRP-1 has tyrosine hydroxylase but no dopa oxidase activity <i>Pigment Cell Research</i>	7:131-40	1994	<a href="#">Abstract</a>
1516	Zhao S, Weng YC, Yuan SS, Lin YT, Hsu HC, Lin SC, Gerbino E, Song MH, Zdzienicka MZ, Gatti RA, Shay JW, Ziv Y, Shiloh Y and Lee EY Functional link between ataxia-telangiectasia and Nijmegen breakage syndrome gene products <i>Nature</i>	405:473-7	2000	<a href="#">Abstract</a>
1517	Zheng L, Chen Y, Riley DJ, Chen PL and Lee WH Retinoblastoma protein enhances the fidelity of chromosome segregation mediated by hsHec1p <i>Molecular and Cellular Biology</i>	20:3529-37	2000	<a href="#">Abstract</a>
1518	Zhong Q, Chen CF, Li S, Chen Y, Wang CC, Xiao J, Chen PL, Sharp ZD and Lee WH Association of BRCA1 with the hRad50-hMre11-p95 complex and the DNA damage response <i>Science</i>	285:747-50	1999	<a href="#">Abstract</a>
1519	Zhong S, Wyllie AH, Barnes D, Wolf CR and Spurr NK Relationship between the GSTM1 genetic polymorphism and susceptibility to bladder, breast and colon cancer <i>Carcinogenesis</i>	14:1821-4	1993	<a href="#">Abstract</a>
1520	Zhong X, Hemmi H, Koike J, Tsujita K and Shimatake H Various AGC repeat numbers in the coding region of the human transcription factor gene E2F-4 <i>Human Mutation</i>	15:296-7	2000	<a href="#">Abstract</a>
1521	Zhou H, Kuang J, Zhong L, Kuo WL, Gray JW, Sahin A, Brinkley BR and Sen S Tumour amplified kinase STK15/BTAK induces centrosome amplification, aneuploidy and transformation <i>Nature Genetics</i>	20:189-93	1998	<a href="#">Abstract</a>



1522	Zhu J, Petersen S, Tessarollo L and Nussenzweig A Targeted disruption of the Nijmegen breakage syndrome gene NBS1 leads to early embryonic lethality in mice <i>Current Biology</i>	11:105–9	2001	<a href="#">Abstract</a>
1523	Zhu XD, Kuster B, Mann M, Petrini JH and Lange T Cell-cycle-regulated association of RAD50/MRE11/NBS1 with TRF2 and human telomeres <i>Nature Genetics</i>	25:347–52	2000	<a href="#">Abstract</a>
1524	Zindy F, van Deursen J, Grosveld G, Sherr CJ and Roussel MF INK4d-deficient mice are fertile despite testicular atrophy <i>Molecular and Cellular Biology</i>	20:372–8	2000	<a href="#">Abstract</a>
1525	Zochbauer-Muller S, Fong KM, Maitra A, Lam S, Geradts J, Ashfaq R, Virmani AK, Milchgrub S, Gazdar AF and Minna JD 5' CpG island methylation of the FHIT gene is correlated with loss of gene expression in lung and breast cancer <i>Cancer Research</i>	61:3581–5	2001	<a href="#">Abstract</a>
1526	Zuckerberg LR, Yang WI, Gadd M, Thor AD, Koerner FC, Schmidt EV and Arnold A Cyclin D1 (PRAD1) protein expression in breast cancer: approximately one-third of infiltrating mammary carcinomas show overexpression of the cyclin D1 oncogene <i>Modern Pathology</i>	8:560–7	1995	<a href="#">Abstract</a>
1527	Zullo A, Romiti A, Rinaldi V, Vecchione A, Tomao S, Aiuti F, Frati L and Luzi G Gastric pathology in patients with common variable immunodeficiency <i>Gut</i>	45:77–81	1999	<a href="#">Abstract</a>
1528	Zumbrunn J, Kinoshita K, Hyman AA and Nathke IS Binding of the adenomatous polyposis coli protein to microtubules increases microtubule stability and is regulated by GSK3beta phosphorylation <i>Current Biology</i>	11:44–49	2001	<a href="#">Abstract</a>
1529	Zuo L, Weger J, Yang Q, Goldstein AM, Tucker MA, Walker GJ, Hayward N and Dracopoli NC Germline mutations in the p16INK4a binding domain of CDK4 in familial melanoma <i>Nature Genetics</i>	12:97–9	1996	<a href="#">Abstract</a>
1530	Zwick E, Bange J and Ullrich A Receptor tyrosine kinases as targets for anticancer drugs <i>Trends in Molecular Medicine</i>	8:17–23	2002	<a href="#">Abstract</a>

## References and bibliography (V3)

1531	Amend KL, Elder JT, Tomsho LP, Bonner JD, Johnson TM, Schwartz J, Berwick M and Gruber SB EGF gene polymorphism and the risk of incident primary melanoma <i>Cancer Research</i>	64:2668–72	2004	<a href="#">Abstract</a>
1532	Balaban GB, Herlyn M, Clark WH Jr and Nowell PC Karyotypic evolution in human malignant melanoma <i>Cancer Genetics and Cytogenetics</i>	19:113–22	1986	<a href="#">Abstract</a>
1533	Bar-Eli M Gene regulation in melanoma progression by the AP-2 transcription factor <i>Pigment Cell Research</i>	14:78–85	2001	<a href="#">Abstract</a>
1534	Barlogie B, Gohde W, Johnston DA, Smallwood L, Schumann J, Drewinko B and Freireich EJ Determination of ploidy and proliferative characteristics of human solid tumors by pulse cytophotometry <i>Cancer Research</i>	38:3333–9	1978	<a href="#">Abstract</a>
1535	Begg CB, Orlow I, Hummer AJ, Armstrong BK, Kricker A, Marrett LD, Millikan RC, Gruber SB, Anton Culver H, Zanetti R, Gallagher RP, Dwyer T, Rebbeck TR, Mitra N, Busam K, From L and Berwick M Lifetime risk of melanoma in CDKN2A mutation carriers in a population-based sample <i>Journal of the National Cancer Institute</i>	97:1507–15	2005	<a href="#">Abstract</a>
1536	Bello-Fernandez C, Packham G and Cleveland JL The ornithine decarboxylase gene is a transcriptional target of c-Myc <i>Proceedings of the National Academy of Sciences of the USA</i>	90:7804–8	1993	<a href="#">Abstract</a>
1537	Bertram CG, Gaut RM, Barrett JH, Randerson-Moor J, Whitaker L, Turner F, Bataille V, dos Santos Silva I, Swerdlow AJ, Bishop DT and Newton Bishop JA An assessment of a variant of the DNA repair gene XRCC3 as a possible nevus or melanoma susceptibility genotype <i>Journal of Investigative Dermatology</i>	122:429–32	2004	<a href="#">Abstract</a>
1538	Beuret L, Flori E, Denoyelle C, Bille K, Busca R, Picardo M, Bertolotto C and Ballotti R Up-regulation of MET expression by alpha-melanocyte stimulating hormone and MITF allows HGF to protect melanocytes and melanoma cells from apoptosis <i>Journal of Biological Chemistry</i>	Mar 19 (in press)	2007	<a href="#">Abstract</a>
1539	Bhatt KV, Spofford LS, Aram G, McMullen M, Pumiglia K and Aplin AE Adhesion control of cyclin D1 and p27Kip1 levels is deregulated in melanoma cells through BRAF-MEK-ERK signaling <i>Oncogene</i>	24:3459–71	2005	<a href="#">Abstract</a>
1540	Björnhagen V, Erhardt K, Lagerlöf B and Auer G Comparison of nuclear DNA content in primary and metastatic malignant melanoma <i>Analytical &amp; Quantitative Cytology &amp; Histology</i>	13:343–50	1991	<a href="#">Abstract</a>
1541	Blankenburg S, König IR, Moessner R, Laspe P, Thoms KM, Krueger U, Khan SG, Westphal G, Berking C, Volkenandt M, Reich K, Neumann C, Ziegler A, Kraemer KH and Emmert S Assessment of 3 xeroderma pigmentosum group C gene polymorphisms and risk of cutaneous melanoma: a case-control study <i>Carcinogenesis</i>	26:1085–90	2005	<a href="#">Abstract</a>

## Human metastatic melanoma in vitro

- 1542 Calin GA, di Iasio MG, Caprini E, Vorechovsky I, Natali PG, Sozzi G, Croce CM, Barbanti Brodano G, Russo G and Negrini M  
Low frequency of alterations of the alpha (PPP2R1A) and beta (PPP2R1B) isoforms of the subunit A of the serine-threonine phosphatase 2A in human neoplasms  
*Oncogene* **19**:1191–5 2000 [Abstract](#)
- 1543 Campos EI, Martinka M, Mitchell DL, Dai DL and Li G  
Mutations of the ING1 tumor suppressor gene detected in human melanoma abrogate nucleotide excision repair  
*International Journal of Oncology* **25**:73–80 2004 [Abstract](#)
- 1544 Castiglia D, Pagani E, Alvino E, Vernole P, Marra G, Cannavo E, Jiricny J, Zambruno G and D'Atri S  
Biallelic somatic inactivation of the mismatch repair gene MLH1 in a primary skin melanoma  
*Genes Chromosomes and Cancer* **37**:165–75 2003 [Abstract](#)
- 1545 Casula M, Colombino M, Satta MP, Cossu A, Ascierio PA, Bianchi Scarra G, Castiglia D, Budroni M, Rozzo C, Manca A, Lissia A, Carboni A, Petretto E, Satriano SM, Botti G, Mantelli M, Ghiorzo P, Stratton MR, Tanda F and Palmieri G J  
BRAF gene is somatically mutated but does not make a major contribution to malignant melanoma susceptibility: the Italian Melanoma Intergroup Study  
*Clinical Oncology* **22**:286–92 2004 [Abstract](#)
- 1546 Chang F, Steelman LS, Shelton JG, Lee JT, Navolanic PM, Blalock WL, Franklin R and McCubrey JA  
Regulation of cell cycle progression and apoptosis by the Ras/Raf/MEK/ERK pathway  
*International Journal of Oncology* **22**:469–80 2003 [Abstract](#)
- 1547 Chin L, Garraway LA and Fisher DE  
Malignant melanoma: genetics and therapeutics in the genomic era  
*Genes and Development* **20**:2149–82 2006 [Abstract](#)
- 1548 Curtin JA, Busam K, Pinkel D and Bastian BC  
Somatic activation of KIT in distinct subtypes of melanoma  
*Journal of Clinical Oncology* **24**:4340–6 2006 [Abstract](#)
- 1549 Debniak T, Gorski B, Cybulski C, Jakubowska A, Kurzawski G, Lener M, Mierzejewski M, Masojc B, Medrek K, Kladny J, Zaluga E, Maleszka R, Chosia M and Lubinski J  
Germline 657/del5 mutation in the NBS1 gene in patients with malignant melanoma of the skin  
*Melanoma Research* **13**:365–70 2003 [Abstract](#)
- 1550 Debniak T, Scott RJ, Huzarski T, Byrski T, Masojc B, van de Wetering T, Serrano-Fernandez P, Gorski B, Cybulski C, Gronwald J, Debniak B, Maleszka R, Kladny J, Bieniek A, Nagay L, Haus O, Grzybowska E, Wandzel P, Niepsuj S, Narod SA and Lubinski J  
XPD common variants and their association with melanoma and breast cancer risk  
*Breast Cancer Research and Treatment* **98**:209–15 2006 [Abstract](#)
- 1551 Demunter A, Stas M, Degreef H, De Wolf Peeters C and van den Oord JJ  
Analysis of N- and K-ras mutations in the distinctive tumor progression phases of melanoma  
*Journal of Investigative Dermatology* **117**:1483–9 2001 [Abstract](#)
- 1552 Dhomen N and Marais R  
New insight into BRAF mutations in cancer  
*Current Opinion in Genetics and Development* **17**:3–9 2007 [Abstract](#)
- 1553 Dichtenberg JB, Zimmerman W, Sparks CA, Young A, Vidair C, Zheng Y, Carrington W, Fay FS and Doxsey SJ  
Pericentrin and gamma-tubulin form a protein complex and are organized into a novel lattice at the centrosome  
*Journal of Cell Biology* **141**:163–74 1998 [Abstract](#)
- 1554 Doxsey SJ, Stein P, Evans L, Calarco PD and Kirschner M  
Pericentrin, a highly conserved centrosome protein involved in microtubule organization  
*Cell* **76**:639–50 1994 [Abstract](#)
- 1555 Eckhart L, Bach J, Ban J and Tschachler E  
Melanin binds reversibly to thermostable DNA polymerase and inhibits its activity  
*Biochemical and Biophysical Research Communications* **271**:726–30 2000 [Abstract](#)
- 1556 Ehlers JP, Worley L, Onken MD and Harbour JW  
DDEF1 is located in an amplified region of chromosome 8q and is overexpressed in uveal melanoma  
*Clinical Cancer Research* **11**:3609–13 2005 [Abstract](#)
- 1557 EMD Chemicals/Calbiochem technical support  
Personal communication
- 1558 Feng X, Hara Y and Riabowol K  
Different HATS of the ING1 gene family  
*Trends in Cell Biology* **12**:532–8 2002 [Abstract](#)
- 1559 Feng XH, Liang YY, Liang M, Zhai W and Lin X  
Direct interaction of c-Myc with Smad2 and Smad3 to inhibit TGF-beta-mediated induction of the CDK inhibitor p15(Ink4B)  
*Molecular Cell* **9**:133–43 2002 [Abstract](#)
- 1560 Feng Y, Shi J, Goldstein AM, Tucker MA and Nelson MA  
Analysis of mutations and identification of several polymorphisms in the putative promoter region of the P34CDC2-related CDC2L1 gene located at 1P36 in melanoma cell lines and melanoma families  
*International Journal of Cancer* **99**:834–8 2002 [Abstract](#)
- 1561 Ferraro D, Corso S, Fasano E, Panieri E, Santangelo R, Borrello S, Giordano S, Pani G and Galeotti T  
Pro-metastatic signaling by c-Met through RAC-1 and reactive oxygen species (ROS)  
*Oncogene* **25**:3689–98 2006 [Abstract](#)
- 1562 Fujikawa-Yamamoto K, Ohdoi C, Yamagishi H, Zong ZP, Murakami M and Yamaguchi N  
Lack of synchrony among multiple nuclei induces partial DNA fragmentation in V79 cells polyploidized by demecolcine  
*Cell Proliferation* **32**:337–49 1999 [Abstract](#)
- 1563 Galaktionov K, Chen X and Beach D  
Cdc25 cell-cycle phosphatase as a target of c-myc  
*Nature* **382**:511–7 1996 [Abstract](#)
- 1564 Garnett MJ and Marais R  
Guilty as charged: B-RAF is a human oncogene  
*Cancer Cell* **6**:313–9 2004 [Abstract](#)
- 1565 Garraway LA, Widlund HR, Rubin MA, Getz G, Berger AJ, Ramaswamy S, Beroukhir R, Milner DA, Granter SR, Du J, Lee C, Wagner SN, Li C, Golub TR, Rimm DL, Meyerson ML, Fisher DE and Sellers WR  
Integrative genomic analyses identify MITF as a lineage survival oncogene amplified in malignant melanoma  
*Nature* **436**:117–22 2005 [Abstract](#)
- 1566 Giehl K  
Oncogenic Ras in tumour progression and metastasis  
*Biological Chemistry* **386**:193–205 2005 [Abstract](#)



- 1567 Gil J and Peters G  
Regulation of the INK4b-ARF-INK4a tumour suppressor locus: all for one or one for all  
*Nature Reviews Molecular Cell Biology* 7:667–77 2006 [Abstract](#)
- 1568 Goldstein AM, Chan M, Harland M, Gillanders EM, Hayward NK, Avril MF, Azizi E, Bianchi Scarra G, Bishop DT, Bressac de Paillerets B, Bruno W, Calista D, Cannon Albright LA, Demenais F, Elder DE, Ghiorzo P, Gruis NA, Hansson J, Hogg D, Holland EA, Kanetsky PA, Kefford RF, Landi MT, Lang J, Leachman SA, Mackie RM, Magnusson V, Mann GJ, Niendorf K, Newton Bishop J, Palmer JM, Puig S, Puig Butille JA, de Snoo FA, Stark M, Tsao H, Tucker MA, Whitaker L and Yakobson E  
High-risk melanoma susceptibility genes and pancreatic cancer, neural system tumors, and uveal melanoma across GenoMEL  
*Cancer Research* 66:9818–28 2006 [Abstract](#)
- 1569 Govindarajan B, Sligh JE, Vincent BJ, Li M, Canter JA, Nickoloff BJ, Rodenburg RJ, Smeitink JA, Oberley L, Zhang Y, Slingerland J, Arnold RS, Lambeth JD, Cohen C, Hilenski L, Griendling K, Martinez Diez M, Cuezva JM and Arbiser JL  
Overexpression of Akt converts radial growth melanoma to vertical growth melanoma  
*Journal of Clinical Investigation* 117:719–29 2007 [Abstract](#)
- 1570 Guidotti JE, Bregerie O, Robert A, Debey P, Brechot C and Desdouets C  
Liver cell polyploidization: a pivotal role for binuclear hepatocytes  
*Journal of Biological Chemistry* 278:19095–101 2003 [Abstract](#)
- 1571 Guillot B, Dalac S, Delaunay M, Baccard M, Chevrand Breton J, Dereure O, Machel L, Sassolas B, Zeller J, Bernard P, Bedane C and Wolkenstein P  
Cutaneous malignant melanoma and neurofibromatosis type 1  
*Melanoma Research* 14:159–63 2004 [Abstract](#)
- 1572 Hamby CV, Mendola CE, Potla L, Stafford G and Backer JM  
Differential expression and mutation of NME genes in autologous cultured human melanoma cells with different metastatic potentials  
*Biochemical and Biophysical Research Communications* 211:579–85 1995 [Abstract](#)
- 1573 Han J, Colditz GA, Liu JS and Hunter DJ  
Genetic variation in XPD, sun exposure, and risk of skin cancer  
*Cancer Epidemiology Biomarkers & Prevention* 14:1539–44 2005 [Abstract](#)
- 1574 Hewitt C, Lee Wu C, Evans G, Howell A, Elles RG, Jordan R, Sloan P, Read AP and Thakker N  
Germline mutation of ARF in a melanoma kindred  
*Human Molecular Genetics* 11:1273–9 2002 [Abstract](#)
- 1575 Howell WM, Bateman AC, Turner SJ, Collins A and Theaker JM  
Influence of vascular endothelial growth factor single nucleotide polymorphisms on tumour development in cutaneous malignant melanoma  
*Genes and Immunity* 3:229–32 2002 [Abstract](#)
- 1576 Howell WM, Rose Zerilli MJ, Theaker JM and Bateman AC  
ICAM-1 polymorphisms and development of cutaneous malignant melanoma  
*International Journal of Immunogenetics* 32:367–73 2005 [Abstract](#)
- 1577 Hussein MR  
Genetic pathways to melanoma tumorigenesis  
*Journal of Clinical Pathology* 57:797–801 2004 [Abstract](#)
- 1578 Iscovich J, Abdulrazik M, Cour C, Fischbein A, Pe'er J and Goldgar DE  
Prevalence of the BRCA2 6174 del T mutation in Israeli uveal melanoma patients  
*International Journal of Cancer* 98:42–4 2002 [Abstract](#)
- 1579 Ishihara T, Sasaki M, Oshimura M, Kamada N, Yamada K, Okada M, Sakurai M, Sugiyama T, Shiraishi Y and Kohno S  
A summary of cytogenetic studies on 534 cases of chronic myelocytic leukemia in Japan  
*Cancer Genetics and Cytogenetics* 9:81–91 1983 [Abstract](#)
- 1580 James MR, Dumeni T, Stark MS, Duffy DL, Montgomery GW, Martin NG and Hayward NK  
Rapid screening of 4000 individuals for germ-line variations in the BRAF gene  
*Clinical Chemistry* 52:1675–8 2006 [Abstract](#)
- 1581 Jannot AS, Meziani R, Bertrand G, Gerard B, Descamps V, Archimbaud A, Picard C, Ollivaud L, Basset Seguin N, Kerob D, Lanternier G, Lebbe C, Saiag P, Crickx B, Clerget Darpoux F, Grandchamp B, Soufir N and Melan Cohort  
Allele variations in the OCA2 gene (pink-eyed-dilution locus) are associated with genetic susceptibility to melanoma  
*European Journal of Human Genetics* 13:913–20 2005 [Abstract](#)
- 1582 Jansen-Durr P, Meichle A, Steiner P, Pagano M, Finke K, Botz J, Wessbecher J, Draetta G and Eilers M  
Differential modulation of cyclin gene expression by MYC  
*Proceedings of the National Academy of Sciences of the USA* 90:3685–9 1993 [Abstract](#)
- 1583 Jonsson G, Dahl C, Staaf J, Sandberg T, Bendahl PO, Ringnér M, Guldborg P and Borg Å  
Genomic profiling of malignant melanoma using tiling-resolution arrayCGH  
*Oncogene* online publication Jan 29 2007 [Abstract](#)
- 1584 Kamino H, Kiryu H and Ratech H  
Small malignant melanomas: clinicopathologic correlation and DNA ploidy analysis  
*Journal of the American Academy of Dermatology* 22:1032–8 1990 [Abstract](#)
- 1585 Karlsson M, Boeryd B, Carstensen J, Kagedal B, Bratel AT and Wingren S  
DNA ploidy and S-phase in primary malignant melanoma as prognostic factors for stage III disease  
*British Journal of Cancer* 67:134–8 1993 [Abstract](#)
- 1586 Kawamura K, Moriyama M, Shiba N, Ozaki M, Tanaka T, Nojima T, Fujikawa Yamamoto K, Ikeda R and Suzuki K  
Centrosome hyperamplification and chromosomal instability in bladder cancer  
*European Urology* 43:505–15 2003 [Abstract](#)
- 1587 Kennedy C, ter Huurne J, Berkhout M, Gruis N, Bastiaens M, Bergman W, Willemze R and Bavinck JN  
Melanocortin 1 receptor (MC1R) gene variants are associated with an increased risk for cutaneous melanoma which is largely independent of skin type and hair color  
*Journal of Investigative Dermatology* 117:294–300 2001 [Abstract](#)
- 1588 Kheir SM, Bines SD, Vonroenn JH, Soong SJ, Urist MM and Coon JS  
Prognostic significance of DNA aneuploidy in stage I cutaneous melanoma  
*Annals of Surgery* 207:455–61 1988 [Abstract](#)
- 1589 Kim M, Gans JD, Nogueira C, Wang A, Paik JH, Feng B, Brennan C, Hahn WC, Cordon Cardo C, Wagner SN, Flotte TJ, Duncan LM, Granter SR and Chin L  
Comparative oncogenomics identifies NEDD9 as a melanoma metastasis gene  
*Cell* 125:1269–81 2006 [Abstract](#)
- 1590 Korabiowska M, Brinck U, Brinkmann U, Berger H, Ruschenburg I and Droese M  
Prognostic significance of newly defined ploidy related parameters in melanoma  
*Anticancer Research* 20:1685–90 2000 [Abstract](#)

## Human metastatic melanoma in vitro

- 1591 Korabiowska M, Brinck U, Stachura J, Jawien J, Hasse FM, Cordon-Cardos C and Fischer G  
Exonic deletions of mismatch repair genes MLH1 and MSH2 correlate with prognosis and protein expression levels in malignant melanomas  
*Anticancer Research* **26**:1231–5 2006 [Abstract](#)
- 1592 Korner H, Epanchintsev A, Berking C, Schuler Thurner B, Speicher MR, Menssen A and Hermeking H  
Digital karyotyping reveals frequent inactivation of the dystrophin/DMD gene in malignant melanoma  
*Cell Cycle* **6**:189–98 2007 [Abstract](#)
- 1593 Koynova D, Jordanova E, Kukutsch N, van der Velden P, Toncheva D and Gruis N  
Increased C-MYC copy numbers on the background of CDKN2A loss is associated with improved survival in nodular melanoma  
*Journal of Cancer Research and Clinical Oncology* **133**:117–23 2007 [Abstract](#)
- 1594 Landi MT, Bauer J, Pfeiffer RM, Elder DE, Hulley B, Minghetti P, Calista D, Kanetsky PA, Pinkel D and Bastian BC  
MC1R germline variants confer risk for BRAF-mutant melanoma  
*Science* **313**:521–2 2006 [Abstract](#)
- 1595 Landi MT, Kanetsky PA, Tsang S, Gold B, Munroe D, Rebbeck T, Swoyer J, Ter Minassian M, Hedayati M, Grossman L, Goldstein AM, Calista D and Pfeiffer RM  
MC1R, ASIP, and DNA repair in sporadic and familial melanoma in a Mediterranean population  
*Journal of the National Cancer Institute* **97**:998–1007 2005 [Abstract](#)
- 1596 Langdon SP (ed)  
Cancer cell culture : methods and protocols  
Humana Press, Totowa, New Jersey, USA ISBN 1–58829–079–4 2003
- 1597 Larue L and Delmas V  
The WNT/Beta-catenin pathway in melanoma  
*Frontiers in Bioscience* **11**:733–42 2006 [Abstract](#)
- 1598 Leone G, DeGregori J, Sears R, Jakoi L and Nevins JR  
Myc and Ras collaborate in inducing accumulation of active cyclin E/Cdk2 and E2F  
*Nature* **387**:422–6 1997 [Abstract](#)
- 1599 Leung AK and Lamond AI  
The dynamics of the nucleolus  
*Critical Reviews in Eukaryotic Gene Expression* **13**:39–54 2003 [Abstract](#)
- 1600 Levy C, Khaled M and Fisher DE  
MITF: master regulator of melanocyte development and melanoma oncogene  
*Trends in Molecular Medicine* **12**:406–14 2006 [Abstract](#)
- 1601 Li C, Hu Z, Liu Z, Wang LE, Gershenwald JE, Lee JE, Prieto VG, Duvic M, Grimm EA and Wei Q  
Polymorphisms of the neuronal and inducible nitric oxide synthase genes and the risk of cutaneous melanoma: a case-control study  
*Cancer* **109**:1570–8 2007 [Abstract](#)
- 1602 Li C, Hu Z, Liu Z, Wang LE, Strom SS, Gershenwald JE, Lee JE, Ross MI, Mansfield PF, Cormier JN, Prieto VG, Duvic M, Grimm EA and Wei Q  
Polymorphisms in the DNA repair genes XPC, XPD, and XPG and risk of cutaneous melanoma: a case-control analysis  
*Cancer Epidemiology Biomarkers & Prevention* **15**:2526–32 2006 [Abstract](#)
- 1603 Li C, Larson D, Zhang Z, Liu Z, Strom SS, Gershenwald JE, Prieto VG, Lee JE, Ross MI, Mansfield PF, Cormier JN, Duvic M, Grimm EA and Wei Q  
Polymorphisms of the FAS and FAS ligand genes associated with risk of cutaneous malignant melanoma  
*Pharmacogenetics and Genomics* **16**:253–63 2006 [Abstract](#)
- 1604 Li W, Sanki A, Karim RZ, Thompson JF, Soon Lee C, Zhuang L, McCarthy SW and Scolyer RA  
The role of cell cycle regulatory proteins in the pathogenesis of melanoma  
*Pathology* **38**:287–301 2006 [Abstract](#)
- 1605 Liao SK, Dent PB and McCulloch PB  
Characterization of human malignant melanoma cell lines. I. Morphology and growth characteristics in culture  
*Journal of the National Cancer Institute* **54**:1037–44 1975 [Abstract](#)
- 1606 Libra M, Malaponte G, Navolanic PM, Gangemi P, Bevelacqua V, Proietti L, Bruni B, Stivala F, Mazzarino MC, Travali S and McCubrey JA  
Analysis of BRAF mutation in primary and metastatic melanoma  
*Cell Cycle* **4**:1382–4 2005 [Abstract](#)
- 1607 Lieman JH, Worley LA and Harbour JW  
Loss of Rb-E2F repression results in caspase-8-mediated apoptosis through inactivation of focal adhesion kinase  
*Journal of Biological Chemistry* **280**:10484–90 2005 [Abstract](#)
- 1608 Marabese M, Vikhanskaya F and Brogini M  
p73: A chiaroscuro gene in cancer  
*European Journal of Cancer* Apr 9 (in press) 2007 [Abstract](#)
- 1609 McCulloch PB, Dent PB, Hayes PR and Liao SK  
Common and individually specific chromosomal characteristics of cultured human melanoma  
*Cancer Research* **36**:398–404 1976 [Abstract](#)
- 1610 McDermott KM, Zhang J, Holst CR, Kozakiewicz BK, Singla V and Tlsty TD  
p16(INK4a) prevents centrosome dysfunction and genomic instability in primary cells  
*PLoS Biology* **4**:e51 2006 [Abstract](#)
- 1611 McGill GG, Haq R, Nishimura EK and Fisher DE  
c-Met expression is regulated by Mitf in the melanocyte lineage  
*Journal of Biological Chemistry* **281**:10365–73 2006 [Abstract](#)
- 1612 Menssen A and Hermeking H  
Characterization of the c-MYC-regulated transcriptome by SAGE: identification and analysis of c-MYC target genes  
*Proceedings of the National Academy of Sciences of the USA* **99**:6274–9 2002 [Abstract](#)
- 1613 Michaloglou C, Vredeveld LC, Soengas MS, Denoyelle C, Kuilman T, van der Horst CM, Majoor DM, Shay JW, Mooi WJ and Peeper DS  
BRAF<sup>E600</sup>-associated senescence-like cell cycle arrest of human naevi  
*Nature* **436**:720–4 2005 [Abstract](#)
- 1614 Mikule K, Delaval B, Kaldis P, Jurczyk A, Hergert P and Doxsey S  
Loss of centrosome integrity induces p38—p53—p21-dependent G1—S arrest  
*Nature Cell Biology* **9**:160–70 2006 [Abstract](#)



- 1615 Millikan RC, Hummer A, Begg C, Player J, de Cotret AR, Winkel S, Mohrenweiser H, Thomas N, Armstrong B, Krickler A, Marrett LD, Gruber SB, Culver HA, Zanetti R, Gallagher RP, Dwyer T, Rebbeck TR, Busam K, From L, Mujumdar U and Berwick M  
Polymorphisms in nucleotide excision repair genes and risk of multiple primary melanoma: the Genes Environment and Melanoma Study  
*Carcinogenesis* 27:610–8 2006 [Abstract](#)
- 1616 Mirmohammadsadeh A, Marini A, Nambiar S, Hassan M, Tannapfel A, Ruzicka T and Hengge UR  
Epigenetic silencing of the PTEN gene in melanoma  
*Cancer Research* 66:6546–52 2006 [Abstract](#)
- 1617 Mitnacht S  
The retinoblastoma protein—from bench to bedside  
*European Journal of Cell Biology* 84:97–107 2005 [Abstract](#)
- 1618 Molven A, Grimstvedt MB, Steine SJ, Harland M, Avril MF, Hayward NK and Akslen LA  
A large Norwegian family with inherited malignant melanoma, multiple atypical nevi, and CDK4 mutation  
*Genes Chromosomes and Cancer* 44:10–8 2005 [Abstract](#)
- 1619 Moritz M, Braunfeld MB, Sedat JW, Alberts B and Agard DA  
Microtubule nucleation by gamma-tubulin-containing rings in the centrosome  
*Nature* 378:638–40 1995 [Abstract](#)
- 1620 Morse HG and Moore GE  
Cytogenetic homogeneity in eight independent sites in a case of malignant melanoma  
*Cancer Genetics and Cytogenetics* 69:108–12 1993 [Abstract](#)
- 1621 Mossner R, Anders N, Konig IR, Kruger U, Schmidt D, Berking C, Ziegler A, Brockmoller J, Kaiser R, Volkenandt M, Westphal GA and Reich K  
Variations of the melanocortin-1 receptor and the glutathione-S transferase T1 and M1 genes in cutaneous malignant melanoma  
*Archives of Dermatological Research* 298:371–9 2007 [Abstract](#)
- 1622 Muhonen T, Pyrhonen S, Laasonen A, Asko-Seljavaara S and Franssila K  
DNA aneuploidy and low S-phase fraction as favourable prognostic signs in metastatic melanoma  
*British Journal of Cancer* 64:749–52 1991 [Abstract](#)
- 1623 Muir PD and Gunz FW  
A cytogenetic study of eight human melanoma cell lines  
*Pathology* 11:597–606 1979 [Abstract](#)
- 1624 Muthusamy V, Hobbs C, Nogueira C, Cordon Cardo C, McKee PH, Chin L and Bosenberg MW  
Amplification of CDK4 and MDM2 in malignant melanoma  
*Genes Chromosomes and Cancer* 45:447–54 2006 [Abstract](#)
- 1625 Natali PG, Nicotra MR, Di Renzo MF, Prat M, Bigotti A, Cavaliere R and Comoglio PM  
Expression of the c-Met/HGF receptor in human melanocytic neoplasms: demonstration of the relationship to malignant melanoma tumour progression  
*British Journal of Cancer* 68:746–50 1993 [Abstract](#)
- 1626 Nelson MA, Radmacher MD, Simon R, Aickin M, Yang J, Panda L, Emerson J, Roe D, Adair L, Thompson F, Bangert J, Leong SP, Taetle R, Salmon S and Trent J  
Chromosome abnormalities in malignant melanoma: clinical significance of nonrandom chromosome abnormalities in 206 cases  
*Cancer Genetics and Cytogenetics* 122:101–9 2000 [Abstract](#)
- 1627 Nelson MA, Reynolds SH, Rao UN, Goulet AC, Feng Y, Beas A, Honchak B, Averill J, Lowry DT, Senft JR, Jefferson AM, Johnson RC and Sargent LM  
Increased gene copy number of the transcription factor E2F1 in malignant melanoma  
*Cancer Biology and Therapy* 5:407–12 2006 [Abstract](#)
- 1628 Okamoto I, Krogler J, Endler G, Kaufmann S, Mustafa S, Exner M, Mannhalter C, Wagner O and Pehamberger H  
A microsatellite polymorphism in the heme oxygenase-1 gene promoter is associated with risk for melanoma  
*International Journal of Cancer* 119:1312–5 2006 [Abstract](#)
- 1629 Okamoto I, Roka F, Krogler J, Endler G, Kaufmann S, Tockner S, Marsik C, Jilma B, Mannhalter C, Wagner O and Pehamberger H  
The EGF A61G polymorphism is associated with disease-free period and survival in malignant melanoma  
*Journal of Investigative Dermatology* 126:2242–6 2006 [Abstract](#)
- 1630 Omholt K, Platz A, Kanter L, Ringborg U and Hansson J  
NRAS and BRAF mutations arise early during melanoma pathogenesis and are preserved throughout tumor progression  
*Clinical Cancer Research* 9:6483–8 2003 [Abstract](#)
- 1631 Osborne JE and Hutchinson PE  
Vitamin D and systemic cancer: is this relevant to malignant melanoma?  
*British Journal of Dermatology* 147:197–213 2002 [Abstract](#)
- 1632 Otsuka T, Takayama H, Sharp R, Celli G, LaRochelle WJ, Bottaro DP, Ellmore N, Vieira W, Owens JW, Anver M and Merlino G  
c-Met autocrine activation induces development of malignant melanoma and acquisition of the metastatic phenotype  
*Cancer Research* 58:5157–67 1998 [Abstract](#)
- 1633 Palmer JS, Duffy DL, Box NF, Aitken JF, O’Gorman LE, Green AC, Hayward NK, Martin NG and Sturm RA  
Melanocortin-1 receptor polymorphisms and risk of melanoma: is the association explained solely by pigmentation phenotype?  
*American Journal of Human Genetics* 6:176–86 2000 [Abstract](#)
- 1634 Pedersen MI and Wang N  
Chromosomal evolution in the progression and metastasis of human malignant melanoma. A multiple lesion study  
*Cancer Genetics and Cytogenetics* 41:185–201 1989 [Abstract](#)
- 1635 Perez-Roger I, Solomon DL, Sewing A and Land H  
Myc activation of cyclin E/Cdk2 kinase involves induction of cyclin E gene transcription and inhibition of p27(Kip1) binding to newly formed complexes  
*Oncogene* 14:2373–81 1997 [Abstract](#)
- 1636 Pihan GA, Purohit A, Wallace J, Knecht H, Woda B, Quesenberry P and Doxsey SJ  
Centrosome defects and genetic instability in malignant tumors  
*Cancer Research* 58:3974–85 1998 [Abstract](#)
- 1637 Pihan GA, Purohit A, Wallace J, Malhotra R, Liotta L and Doxsey SJ  
Centrosome defects can account for cellular and genetic changes that characterize prostate cancer progression  
*Cancer Research* 61:2212–9 2001 [Abstract](#)
- 1638 Pilch H, Gunzel S, Schaffer U, Tanner B and Heine M  
Evaluation of DNA ploidy and degree of DNA abnormality in benign and malignant melanocytic lesions of the skin using video imaging  
*Cancer* 88:1370–7 2000 [Abstract](#)

## Human metastatic melanoma in vitro

- 1639 Pope JH, Morrison L, Moss DJ, Parsons PG and Regius Mary Sister  
Human malignant melanoma cell lines  
*Pathology* 11:191–5 1979 [Abstract](#)
- 1640 Povey JE, Darakhshan F, Robertson K, Bisset Y, Mekky M, Rees J, Doherty V, Kavanagh G, Anderson N, Campbell H, Mackie RM and Melton DW  
DNA repair gene polymorphisms and genetic predisposition to cutaneous melanoma  
*Carcinogenesis* Jan 8 2007 [Abstract](#)
- 1641 Puri N, Ahmed S, Janamanchi V, Tretiakova M, Zumba O, Krausz T, Jagadeeswaran R and Salgia R  
c-Met Is a Potentially New Therapeutic Target for Treatment of Human Melanoma  
*Clinical Cancer Research* 13:2246–53 2007 [Abstract](#)
- 1642 Rao PN and Johnson RT  
Mammalian cell fusion: studies on the regulation of DNA synthesis and mitosis  
*Nature* 225:159–64 1970 [Abstract](#)
- 1643 Reifenberger J, Knobbe CB, Wolter M, Blaschke B, Schulte KW, Pietsch T, Ruzicka T and Reifenberger G  
Molecular genetic analysis of malignant melanomas for aberrations of the WNT signaling pathway genes CTNNB1, APC, ICAT and BTRC  
*International Journal of Cancer* 100:549–56 2002 [Abstract](#)
- 1644 Rode J, Williams RA, Charlton IG, Dhillon AP and Moss E  
Nuclear DNA profiles in primary melanomas and their metastases  
*Cancer* 67:2333–6 1991 [Abstract](#)
- 1645 Rotolo S, Diotti R, Gordon RE, Qiao RF, Yao Z, Phelps RG and Dong J  
Effects on proliferation and melanogenesis by inhibition of mutant BRAF and expression of wild-type INK4A in melanoma cells  
*International Journal of Cancer* 20;115:164–9 2005 [Abstract](#)
- 1646 Roy B, Beamon J, Balint E and Reisman D  
Transactivation of the human p53 tumor suppressor gene by c-Myc/Max contributes to elevated mutant p53 expression in some tumors  
*Molecular and Cellular Biology* 14:7805–15 1994 [Abstract](#)
- 1647 Rubben A, Bausch B and Nikkels A  
Somatic deletion of the NF1 gene in a neurofibromatosis type 1-associated malignant melanoma demonstrated by digital PCR  
*Molecular Cancer* 5:36 2006 [Abstract](#)
- 1648 Rubinfeld B, Robbins P, El Gamil M, Albert I, Porfiri E and Polakis P  
Stabilization of beta-catenin by genetic defects in melanoma cell lines  
*Science* 275:1790–2 1997 [Abstract](#)
- 1649 Salisbury JL, Baron AT and Sanders MA  
The centrin-based cytoskeleton of *Chlamydomonas reinhardtii*: distribution in interphase and mitotic cells  
*Journal of Cell Biology* 107:635–41 1988 [Abstract](#)
- 1650 Sauter ER, Yeo UC, von Stemm A, Zhu W, Litwin S, Tichansky DS, Pistrutto G, Nesbit M, Pinkel D, Herlyn M and Bastian BC  
Cyclin D1 is a candidate oncogene in cutaneous melanoma  
*Cancer Research* 62:3200–6 2002 [Abstract](#)
- 1651 Schmidt B, Weinberg DS, Hollister K and Barnhill RL  
Analysis of melanocytic lesions by DNA image cytometry  
*Cancer* 73:2971–7 1994 [Abstract](#)
- 1652 Seckinger D, Sugarbaker E, and Frankfurt O  
DNA content in human cancer. Application in pathology and clinical medicine  
*Archives of Pathology & Laboratory Medicine* 113:619–26 1989 [Abstract](#)
- 1653 Seoane J, Le HV and Massague J  
Myc suppression of the p21(Cip1) Cdk inhibitor influences the outcome of the p53 response to DNA damage  
*Nature* 419:729–34 2002 [Abstract](#)
- 1654 Shan B, Durfee T and Lee WH  
Disruption of RB/E2F-1 interaction by single point mutations in E2F-1 enhances S-phase entry and apoptosis  
*Proceedings of the National Academy of Sciences of the USA* 93:679–84 1996 [Abstract](#)
- 1655 Sharpless E and Chin L  
The INK4a/ARF locus and melanoma  
*Oncogene* 22:3092–8 2003 [Abstract](#)
- 1656 Sheehy PF, Wakonig Vaartaja T, Winn R and Clarkson BD  
Asynchronous DNA synthesis and asynchronous mitosis in multinuclear ovarian cancer cells  
*Cancer Research* 34:991–6 1974 [Abstract](#)
- 1657 Shen H, Liu Z, Strom SS, Spitz MR, Lee JE, Gershenwald JE, Ross MI, Mansfield PF, Duvic M, Ananthaswamy HN and Wei Q  
p53 codon 72 Arg homozygotes are associated with an increased risk of cutaneous melanoma  
*Journal of Investigative Dermatology* 121:1510–4 2003 [Abstract](#)
- 1658 Shibuya H, Kato A, Kai N, Fujiwara S and Goto M  
A case of Werner syndrome with three primary lesions of malignant melanoma  
*Journal of Dermatology* 32:737–44 2005 [Abstract](#)
- 1659 Shtromas I, White BN, Holden JJ, Reimer DL and Roder JC  
DNA amplification and tumorigenicity of the human melanoma cell line MeWo  
*Cancer Research* 45:642–7 1985 [Abstract](#)
- 1660 Sidwell RU, Sandison A, Wing J, Fawcett HD, Seet JE, Fisher C, Nardo T, Stefanini M, Lehmann AR and Cream JJ  
A novel mutation in the XPA gene associated with unusually mild clinical features in a patient who developed a spindle cell melanoma  
*British Journal of Dermatology* 155:81–8 2006 [Abstract](#)
- 1661 Siniinikova OM, Egan KM, Quinn JL, Boutrand L, Lenoir GM, Stoppa-Lyonnet D, Desjardins L, Levy C, Goldgar D and Gragoudas ES  
Germline BRCA2 sequence variants in patients with ocular melanoma  
*International Journal of Cancer* 82:325–8 1999 [Abstract](#)
- 1662 Slater SD, Cook MG, Fisher C, Wright NA and Foster CS  
A comparative study of proliferation indices and ploidy in dysplastic naevi and malignant melanomas using flow cytometry  
*Histopathology* 19:337–44 1991 [Abstract](#)
- 1663 Soto Martinez JL, Cabrera Morales CM, Serrano Ortega S and Lopez Nevot MA  
Mutation and homozygous deletion analyses of genes that control the G1/S transition of the cell cycle in skin melanoma: p53, p21, p16 and p15  
*Clinical and Translational Oncology* 7:156–64 2005 [Abstract](#)





- 1664 Soufir N, Meziani R, Lacapere JJ, Bertrand G, Fumeron F, Bourillon A, Gerard B, Descamps V, Crickx B, Ollivaud L, Archimbaud A, Lebbe C, Basset Seguin N, Saiag P and Grandchamp B  
Association between endothelin receptor B nonsynonymous variants and melanoma risk  
*Journal of the National Cancer Institute* **97**:1297–301 2005 [Abstract](#)
- 1665 Sphyris N and Harrison DJ  
p53 deficiency exacerbates pleiotropic mitotic defects, changes in nuclearity and polyploidy in transdifferentiating pancreatic acinar cells  
*Oncogene* **24**:2184–94 2005 [Abstract](#)
- 1666 Stark M and Hayward N  
Genome-wide loss of heterozygosity and copy number analysis in melanoma using high-density single-nucleotide polymorphism arrays  
*Cancer Research* **67**:2632–42 2007 [Abstract](#)
- 1667 Stark M, Puig Butille JA, Walker G, Badenas C, Malveyh J, Hayward N and Puig S  
Mutation of the tumour suppressor p33ING1b is rare in melanoma  
*British Journal of Dermatology* **155**:94–9 2006 [Abstract](#)
- 1668 Stones C  
Personal communication
- 1669 Strano S, Dell'Orso S, Di Agostino S, Fontemaggi G, Sacchi A and Blandino G  
Mutant p53: an oncogenic transcription factor  
*Oncogene* **26**:2212–9 2007 [Abstract](#)
- 1670 Streit M and Detmar M  
Angiogenesis, lymphangiogenesis, and melanoma metastasis  
*Oncogene* **22**:3172–9 2003 [Abstract](#)
- 1671 Sung H, Kang SH, Bae YJ, Hong JT, Chung YB, Lee CK and Song S  
PCR-based detection of Mycoplasma species  
*Journal of Microbiology* **44**:42–9 2006 [Abstract](#)
- 1672 Talve LA, Collan YU and Ekfors TO  
Primary malignant melanoma of the skin. Relationships of nuclear DNA content, nuclear morphometric variables, Clark level and tumor thickness  
*Analytical & Quantitative Cytology & Histology* **19**:62–74 1997 [Abstract](#)
- 1673 The Breast Cancer Linkage Consortium  
Cancer risks in BRCA2 mutation carriers  
*Journal of the National Cancer Institute* **91**:1310–6 1999 [Abstract](#)
- 1674 Thompson FH, Emerson J, Olson S, Weinstein R, Leavitt SA, Leong SP, Emerson S, Trent JM, Nelson MA, Salmon SE and Taelle R  
Cytogenetics of 158 patients with regional or disseminated melanoma. Subset analysis of near-diploid and simple karyotypes.  
*Cancer Genetics and Cytogenetics* **83**:93–104 1995 [Abstract](#)
- 1675 Tuve S, Wagner SN, Schittek B and Putzer BM  
Alterations of DeltaTA-p 73 splice transcripts during melanoma development and progression  
*International Journal of Cancer* **108**:162–6 2004 [Abstract](#)
- 1676 Udart M, Utikal J, Krahn GM and Peter RU  
Chromosome 7 aneusomy. A marker for metastatic melanoma? Expression of the epidermal growth factor receptor gene and chromosome 7 aneusomy in nevi, primary malignant melanomas and metastases  
*Neoplasia* **3**:245–5 2001 [Abstract](#)
- 1677 Uphoff CC and Drexler HG  
Detection of mycoplasma contaminations in cell cultures by PCR analysis  
*Human Cell* **12**:229–36 1999 [Abstract](#)
- 1678 Uphoff CC  
Personal communication
- 1679 Uphoff CC, Meyer C and Drexler HG  
Elimination of mycoplasma from leukemia-lymphoma cell lines using antibiotics  
*Leukemia* **16**:284–8 2002 [Abstract](#)
- 1680 Uzawa M, Grams J, Madden B, Toft D and Salisbury JL  
Identification of a complex between centrin and heat shock proteins in CSF-arrested Xenopus oocytes and dissociation of the complex following oocyte activation  
*Developmental Biology* **17**:51–9 1995 [Abstract](#)
- 1681 van Oven MW, Baas PC, Oosterhuis JW, Schraffordt Koops H and Dam-Meirring A  
Significance of aneuploidy in melanoma of the extremity  
*Cancer* **70**:109–13 1992 [Abstract](#)
- 1682 Vinceti M, Pellacani G, Casali B, Malagoli C, Nicoli D, Farnetti E, Bassissi S, Bergomi M and Seidenari S  
High risk of cutaneous melanoma amongst carriers of the intercellular adhesion molecule-1 R241 allele  
*Melanoma Research* **16**:93–6 2006 [Abstract](#)
- 1683 von Roenn JH, Kheir SM, Wolter JM and Coon JS  
Significance of DNA abnormalities in primary malignant melanoma and nevi, a retrospective flow cytometric study  
*Cancer Research* **46**:3192–5 1986 [Abstract](#)
- 1684 Wanzel M, Herold S and Eilers M  
Transcriptional repression by Myc  
*Trends in Cell Biology* **13**:146–50 2003 [Abstract](#)
- 1685 Wass J, Zbroja RA, Young GA, Vincent PC, Joyce RM and Croaker G  
Malignant melanoma: analysis by DNA flow cytometry  
*Pathology* **17**:475–80 1985 [Abstract](#)
- 1686 Wiemer EA, Ofman R, Middelkoop E, de Boer M, Wanders RJ and Tager MJ  
Production and characterisation of monoclonal antibodies against native and disassembled human catalase  
*Journal of Immunological Methods* **151**:165–75 1992 [Abstract](#)
- 1687 Wilkins RJ  
Personal communication
- 1688 Willmore-Payne C, Holden JA, Tripp S and Layfield LJ  
Human malignant melanoma: detection of BRAF- and c-kit-activating mutations by high-resolution amplicon melting analysis  
*Human Pathology* **36**:486–93 2005 [Abstract](#)
- 1689 Winsey SL, Haldar NA, Marsh HP, Bunce M, Marshall SE, Harris AL, Wojnarowska F and Welsh KI  
A variant within the DNA repair gene XRCC3 is associated with the development of melanoma skin cancer  
*Cancer Research* **60**:5612–6 2000 [Abstract](#)

## Human metastatic melanoma in vitro

---

- 1690 Woenckhaus C, Fenic I, Giebel J, Hauser S, Failing K, Woenckhaus J, Dittberner T and Poetsch M  
Loss of heterozygosity at 12p13 and loss of p27KIP1 protein expression contribute to melanoma progression  
*Virchows Archiv* **445**:491–7 2004 [Abstract](#)
- 1691 Woenckhaus C, Giebel J, Failing K, Fenic I, Dittberner T and Poetsch M  
Expression of AP-2alpha, c-kit, and cleaved caspase-6 and -3 in naevi and malignant melanomas of the skin. A possible role for caspases in melanoma progression?  
*Journal of Pathology* **201**:278–87 2003 [Abstract](#)
- 1692 Worm J, Christensen C, Gronbaek K, Tulchinsky E and Guldberg P  
Genetic and epigenetic alterations of the APC gene in malignant melanoma  
*Oncogene* **23**:5215–26 2004 [Abstract](#)
- 1693 Wu KJ, Grandori C, Amacker M, Simon Vermot N, Polack A, Lingner J and Dalla-Favera R  
Direct activation of TERT transcription by c-MYC  
*Nature Genetics* **21**:220–4 1999 [Abstract](#)
- 1694 Yamaura M, Takata M, Miyazaki A and Saida T  
Specific dermoscopy patterns and amplifications of the cyclin D1 gene to define histopathologically unrecognizable early lesions of acral melanoma in situ  
*Archives of Dermatology* **141**:1413–8 2005 [Abstract](#)
- 1695 Zar JH  
Biostatistical Analysis (2nd Edition)  
Prentice Hall, New Jersey, USA ISBN 0–13077–925–3 1984
- 1696 Zebisch A, Czernilofsky AP, Keri G, Smigelskaite J, Sill H and Troppmair J  
Signaling through RAS-RAF-MEK-ERK: from basics to bedside  
*Current Medicinal Chemistry* **14**:601–23 2007 [Abstract](#)
- 1697 Zhu C, Zhao J, Bibikova M, Levenson JD, Bossy-Wetzel E, Fan JB, Abraham RT and Jiang W  
Functional analysis of human microtubule-based motor proteins, the kinesins and dyneins, in mitosis/cytokinesis using RNA interference  
*Molecular Biology of the Cell* **16**:3187–99 2005 [Abstract](#)
- 1698 Zhu J, Woods D, McMahon M and Bishop JM  
Senescence of human fibroblasts induced by oncogenic Raf  
*Genes and Development* **12**:2997–3007 1998 [Abstract](#)
- 1699 Zimmerman WC, Sillibourne J, Rosa J and Doxsey SJ  
Mitosis-specific anchoring of gamma tubulin complexes by pericentrin controls spindle organization and mitotic entry  
*Molecular Biology of the Cell* **15**:3642–57 2004 [Abstract](#)

